Studies in Penetration of Charged Particles in Matter (1964)

Pages
405

Size
7 x 10

ISBN
0309336589

Subcommittee on Penetration of Charged Particles in Matter; Committee on Nuclear Science; National Research Council

Nuclear Science Series
Report Number 39

STUDIES IN PENETRATION OF CHARGED PARTICLES IN MATTER

National Academy of Sciences—
National Research Council

Publication 1133

COMMITTEE ON NUCLEAR SCIENCE

SAMUEL K. ALLISON, *Chairman*
Enrico Fermi Institute, University of Chicago
Chicago 37, Illinois

Robley D. Evans, *Vice Chairman*
Mass. Institute of Technology
Cambridge 39, Mass.

E. C. Anderson
Los Alamos Scientific Lab.
Los Alamos, New Mexico

Nathan Ballou
U. S. Naval Rad. Defense Labs
San Francisco, California

C. J. Borkowski
Oak Ridge National Laboratory
Oak Ridge, Tennessee

Robert G. Cochran
Dept. of Nuclear Engineering
A & M College of Texas
College Station.

U. Fano
National Bureau of Standards
Washington 25, D. C.

Herbert Goldstein
Columbia University
New York, New York

Bernd Kahn
Taft Engineering Center
Cincinnati 26, Ohio

Jerry Marion
University of Maryland
College Park, Maryland

R. L. Platzman
Argonne National Laboratory
Lemont, Illinois

Ernest C. Pollard
Penn. State University
University Park, Penna.

Lewis Slack, Secretary
National Research Council
Washington, D. C.

Katharine Way
Oak Ridge National Laboratory
Oak Ridge, Tennessee

George W. Wetherill
Institute for Geophysics
University of California
Los Angeles, California

Liaison

Paul C. Aebersold
Division of Civilian Applications
Atomic Energy Commission
Washington 25, D. C.

J. Howard McMillen
National Science Foundation
Washington 25, D. C.

Subcommittee on
PENETRATION OF CHARGED PARTICLES IN MATTER

U. Fano, *Chairman*
National Bureau of Standards
Washington 25, D. C.

Samuel K. Allison
University of Chicago
Chicago 37, Illinois

Walter H. Barkas
University of California
Berkeley, California

Martin J. Berger
National Bureau of Standards
Washington 25, D. C.

Hans A. Bethe
Cornell University
Ithaca, New York

Hans Bichsel
University of Southern Calif.
Los Angeles 7, California

R. L. Gluckstern
Department of Physics
Yale University
New Haven 11, Conn.

William P. Jesse
St. Procopius College
Lisle, Illinois

Jens Linhard
Aarhus University
Aarhus, Denmark

L. C. Northcliffe
Department of Physics
Yale University
New Haven, Conn.

Robert L. Platzman
Argonne National Laboratory
Lemont, Illinois

R. H. Ritchie
Oak Ridge National Laboratory
Oak Ridge, Tennessee

Rudolph Sternheimer
Brookhaven National Laboratory
Upton, Long Island, New York

James E. Turner
Oak Ridge National Laboratory
Oak Ridge, Tennessee

Nuclear Science Series
Report Number 39
Committee on Nuclear Science

STUDIES IN
PENETRATION OF CHARGED PARTICLES IN MATTER

Subcommittee on Penetration of Charged Particles
Committee on Nuclear Science
National Academy of Sciences—National Research Council

Publication 1133
NATIONAL ACADEMY OF SCIENCES—NATIONAL RESEARCH COUNCIL
Washington, D. C.
1964

Available from
Printing & Publishing Office
National Academy of Sciences
2101 Constitution Ave., N.W.
Washington, D. C. 20418

Price $7.00

Library of Congress
Catalog Card Number: 64-60027

PREFACE

The study of the passage of charged particles through matter was under way at the beginning of this century and was advanced particularly by Lenard, Bragg and Rutherford. It turned out to be a most effective tool for exploring the structure of matter. By 1913, Bohr's theory of the slowing down of charged particles had given a quantitative account of the essential features of the process, on the basis of Rutherford's model. Quantum mechanics later confirmed most details of Bohr's analysis and developed them further, particularly owing to Bethe's efforts.

After this initial burst of progress, the desire to acquire greater mastery of the details of the penetration process and to calculate the parameters of the main formulas from first principles have continued to attract attention. This attention stems, in part, from the subsidiary but ever-present role of particle penetration in most experiments of nuclear and high-energy physics as well as in radiation chemistry, radiation biology, and certain aspects of solid-state physics. Experiments in these fields require accurate reference data on particle penetration, and, conversely, they feed back new information on the penetration process itself. A recent example of this feed-back is the discovery of difference in the penetration of particles of opposite charge.[1] The continued attention given to the process also derives from the intrinsic interest of the effect of the passage of particles upon atoms and atomic aggregates, and of the cumulative effect that the many collisions have upon the particles themselves. The study of these complex processes in increasing depth and detail constitutes a never-ending task.

The National Research Council Committee on Nuclear Science has long maintained a Subcommittee on the Penetration of Charged Particles in Matter. This Subcommittee, which is responsible for following, and stimulating, progress in this field, has operated slowly, at times through informal discussions among its members and then through the organization of an international conference organized at Gatlinburg, Tenn., in 1958.[2] More recently the Subcommittee has stimulated the preparation of a series of "state of the art" reports, which are presented in this volume.

A review of the subject of particle penetration has revealed that development in this field has been much more rapid that this writer, at least, had anticipated. Part of the activity has resulted from the very decision to undertake the review of this process. Many new lines of advance have opened up in the last two years—as this volume should convey—and they have not yet been brought to even momentary conclusions. For this reason, no serious attempt was made to give these reports even a mildly uniform or editorially integrated character. The scope of the present operation is limited severely by the extreme scarcity of persons who are prepared to devote to the subject of particle penetration a major portion of their activity for several years. Since only a small minority of the Subcommittee is so prepared, it was deemed unrealistic to expect its members to provide a sustained effort for a

---

[1] See p. 23 of Appendix A, and Phys. Rev. Letters, 11, 26 (1963).

[2] The Conference proceedings are available as NAS-NRC Publication 752, Nuclear Science Series Report 29 (1960).

time sufficient to bring currently open questions to a conclusion and to integrate their several contributions adequately.

The Subcommittee met at Cornell University in June 1963 to review the material prepared by its members and to arrange for the publication of this volume. Actually, much of the material presented here has been developed, or at least reworked deeply, as a result of the Cornell meeting. Therefore, neither the whole Subcommittee nor its Chairman, as an editor, has had adequate opportunity to examine the reports in their final form. Here again, expeditiousness suggested that the reports be circulated as they stand under the responsibility of their individual authors.

Part of the Subcommittee's effort has consisted in the preparation of two survey articles that have been published in the Annual Review of Nuclear Science (vol. 13). These articles, which serve as background to several of the present reports, are reprinted here (as Appendixes A and B) with the permission of the publishers of the Annual Review of Nuclear Science.

The subjects of the reports reflect to some extent the interests of the individual authors rather than a preconceived organization plan. Their arrangement in the volume begins with a study by J. Lindhard (based on the Thomas-Fermi model) of the role of similarity considerations in establishing over-all quantitative features of the stopping-power process. This approach also yields basic elements of a theory of the ion-atom collisions prevalent at low ion velocities. Both of the next two reports, by H. Bichsel and by J. E. Turner, deal with the experimental verification of stopping-power theory and with the determination of parameters of this theory from experimental results. These reports are complementary inasmuch as Bichsel's focuses on details of the analysis and significance of experimental data, whereas Turner's focuses on the broader aspects of the relationship between experiment and theory and on the role of various experiments in providing key items of information. Report No. 4, by U. Fano and J. E. Turner, amplifies the treatment of shell corrections in Appendix A. Report No. 5, by M. J. Berger and S. M. Seltzer, analyzes the effects of scattering and of energy loss fluctuations on the penetration of protons and the resulting difficulties in the interpretation of experiments.

The initial group of reports of general character is followed by five reports that provide specific data on the penetration of charged particles, including extensive tabulations and graphs. This second group of reports constitutes the core of the volume for most of its intended users. The user who requires accuracy of the order of 10 percent may generally draw information directly from the tables. However, maximum utilization of the available accuracy, which generally approaches 1 percent, requires an adequate understanding of relevant circumstances; reference to the accompanying text is recommended for this purpose.

In Report No. 11, S. K. Allison contributes new experimental methods and results. His report describes a technique for observing the slowing down of neutral atoms and of ions while their charge state remains unchanged, and it presents results of such observations in hydrogen gas. The volume terminates with an outline that lists currently unsolved problems.

At its Cornell meeting, the Subcommittee agreed to recommend the following definitions and nomenclature for related concepts of particle range and of mean excitation energy:

> "Range" of a particle should indicate its "mean (rectified) path-length" from its relevant point of departure to the point where it comes to rest; that is, where further displacement is not detectable.

The term "c.s.d.a. range" is introduced to indicate the quantity $\int_0^{E_0} (dE/ds)^{-1} dE$, which represents the range in the continuous slowing down approximation (see Appendix A, pp. 16 and 45).

"Projected range" should indicate the mean depth of penetration into a material; that is, the mean projection of a particle's path on its direction of incidence on the material.

"Mean excitation energy" should indicate the quantity I of stopping-power theory defined in terms of absorption frequencies E_n/h and oscillator strengths f_n by $I = \exp \Sigma_n f_n \ln E_n$.[3]

"Adjusted mean excitation energy," $I_{adj.}$, should indicate the quantity related to I but determined from experimental values of the stopping power under the assumption that shell corrections vanish in the high-energy limit (see Report No. 6).

Thanks are given to the various authors of this volume for their special efforts to supply contributions on a tight schedule. Subcommittee members who have not contributed reports have supported the preparation of this volume with information, data, and valuable advice; among these, particular thanks are due Dr. R. L. Platzman of the Argonne National Laboratory. Dr. J. E. Turner of the Oak Ridge National Laboratory has devoted special efforts to the whole undertaking. Dr. L. Slack, of the staff of the National Academy of Sciences—National Research Council, has effectively undertaken the task of arranging for the publication of the volume.

The Subcommittee membership currently consists of S. K. Allison, Walter Barkas, Martin J. Berger, H. A. Bethe, Hans Bichsel, U. Fano, R. L. Gluckstern, William P. Jesse, Jens Lindhard, L. C. Northcliffe, Robert L. Platzman, R. H. Ritchie, R. M. Sternheimer, and James E. Turner.

U. Fano,
Subcommittee Chairman

Washington, D. C., January 1964

[3] In this formula (as in Appendix A, pp. 14, 17, and 19) the f_n are normalized so that $\Sigma_n f_n = 1$; an adjustment is required for the more common normalization $\Sigma_n f_n = Z$.

1. THOMAS-FERMI APPROACH AND SIMILARITY IN ATOMIC COLLISIONS

Jens Lindhard[1]

Abstract

This paper concerns the significance of similarity in atomic collisions and stopping problems. Similarity properties are primarily connected with dynamic Thomas-Fermi treatments. The discussion deals mainly with the basic physical picture, but not with details as regards measurements and applications. Deviations from similarity are treated, as well as possibilities of improving our incomplete description of collision processes.

Collisions between ions and atoms are analyzed roughly, and are divided into two major groups. One group relates to the quantal perturbation case, where the phenomena may be described in terms of properties of the medium only. This case is discussed in some detail. Significant properties are, for example, dipole spectra of atomic systems, behavior of stopping at lower velocities, and applicability of free electron gas picture in atomic dynamics.

The second group of collisions relates to ions of relatively low velocity, where collisions between ions and atoms may become nearly elastic, the energy loss being largely kinetic energy of recoil atoms. For such collisions, classical mechanics may be used; similarity properties are based on this circumstance, and become different from those of the first group. Inelastic effects are also of importance and may be roughly estimated, as discussed briefly.

1. Introduction

In the theory of slowing-down of charged particles it has often turned out that approximate results came out rather easily; yet, it could be exceedingly difficult to obtain high accuracy. With one or two exceptions, attempts at precise calculations in any specified case were hardly promising. Alternatively, it can be useful to establish a simple comprehensive theoretical description.

It is clear, moreover, that, unlike chemical reactions, atomic collision processes are quite violent disturbances of atoms, so that effects due to shell structure, chemical properties, etc., should normally be of minor importance. Thus, it is indicated that Thomas-Fermi methods can be desirable in a study of ion-atom

[1]Institute of Physics, University of Aarhus, Aarhus, Denmark.

collisions. In a well-known paper by F. Bloch (3), the Thomas-Fermi approach to atomic dynamics was studied for the first time.

This paper is mainly an attempt to present the case for the Thomas-Fermi approach. The Thomas-Fermi approach, as used in the static atomic model (Ref. 27), is based on self-consistent potentials and on local connection between density and zero-point energy of a degenerate electron gas. However, its most important consequence is similarity in properties of atoms, all atoms being contained in one case. The similarity is lost in more detailed descriptions, as in the Thomas-Fermi-Dirac model or even the Hartree model. In comprehensive treatments of atomic phenomena the property of similarity is the most important feature of the model. When mentioning the Thomas-Fermi approach, I therefore primarily mean an attempt to explore similarity features as far as possible, rather than the actual approximation procedure itself. In this sense, the Lenz-Jensen treatment may be superior to the normal Thomas-Fermi treatment because it retains similarity and better describes the outer parts of atoms.

One advantage of a similarity description is that it gives a standard with which to compare experiments. It is important, of course, that this standard, considered as a first approximation, is fairly accurate. It is also desirable that corrections for individual deviations from similarity may be made when necessary (e.g., corrections due to atomic shell structure). In fact, an approximation is well-defined only if deviations from it can be accounted for. The description asked for is thus of the type of similarity methods in other branches of physics, e.g., the van der Waals' equation of state.

In the following discussion, collisions and stopping are treated for all kinds of ions and at any velocity. It can hardly be expected that general similarity holds for all such cases. Some type of simplification of the basic quantal treatment should be permissible in order that similarity might apply. In point of fact, it turns out that, for many purposes, stopping problems may be crudely divided into two simple cases. One case is where quantal perturbation methods are applicable; the other is where classical mechanics may be used. In both of these cases the resulting simplifications turn out to permit similarity, though not of the same kind.

Connected to the Thomas-Fermi model is one feature that should be emphasized here—the use of statistical methods. The system of electrons is compared to a gas of free electrons, in some respect even with neglect of the variation in space of the gas density. I believe that this gas picture is useful also when one goes beyond the simple static Thomas-Fermi model. It makes possible calculations of numerous collision effects in cases where other methods fail. The electron gas and its generalization, the dielectric approach, is referred to repeatedly in the following discussion.

After a preliminary analysis of basic approximations in Section 2, the discussion is divided into two parts. The first part is the perturbation approximation treated in Section 3, and the second part concerns quasi-elastic collisions, discussed in Section 4. In both cases, similarity properties and statistical methods are of importance. Apart from similarity, there are several other questions at issue, in particular the single-particle and dielectric approaches. These questions are connected to the perturbation case in Section 3, where the accuracy attained is fairly high.

The entire discussion is meant partly as an account of results obtained and partly as a program or framework for further research. I do not attempt to analyze or discuss experimental results, but treat only their influence on the main ideas of the present aspects of atomic collisions.

Reference is made several times to the survey article by N. Bohr (1), whose terminology is followed here to a large extent. The reader is also referred to the other papers in this volume, in particular to the review by Fano relating to the perturbation approximation in Section 3, and the experimental review by Northcliffe, relating to Section 4.

2. Criteria for Basic Approximations

Instead of studying only the basic ion-atom collisions, it has been customary to pay special attention to more indirect effects, such as the average energy loss per cm by a swift ion, or its range. In the present treatment of atomic collisions, I shall not discuss finer details of each collision. We need mainly such averages over cross sections as are important in slowing-down. One important example is the stopping cross section, $S = \int T d\sigma$, where T is the energy loss and $d\sigma$ the differential cross section.

There may be said to be two distinctly different mechanisms of slowing-down for nonrelativistic particles—one being electronic stopping, i.e., energy loss spent as excitation or ejection of atomic electrons, and the other nuclear stopping, by which is meant the transfer of energy to translatory motion of an atom as a whole. The former is an inelastic process, and the latter an elastic collision. As discussed below, a closer scrutiny shows that this separation between two types of collisions is usually a fairly good approximation, though not always a very accurate one.

There are essentially three important parameters in slowing-down, the velocity v of the particle and the atomic numbers Z_1 of the particle and Z_2 of substance. The masses M_1 and M_2 are normally less significant parameters. M_1 usually enters in a trivial way, and M_2 is often unimportant. Moreover, the masses are not independent of the atomic numbers. If we study details of collision processes, further parameters may enter, as, for example, the classical impact parameter or the exchange of momentum in a collision.

At high particle-velocities the energy loss is nearly exclusively electronic stopping, and nuclear collisions are exceedingly rare. For the classification into high and low velocities, we take as a starting point the simple analysis given by N. Bohr (1). When a swift particle of velocity v and charge q_1 collides with another one at rest and with charge q_2, quantum mechanical perturbation methods may be used if (according to Bohr)

$$\varkappa = \frac{2q_1 q_2}{\hbar v} < 1 \ , \tag{2.1}$$

whereas a classical treatment would be proper when $\varkappa > 1$.

For the many-particle collision problems occurring in penetration phenomena, where, for example, two atomic nuclei and a number of electrons are involved, the application of Equation 2.1 is not always immediately clear. One useful supplement to Equation 2.1 is the result that the ion starts carrying electrons to an appreciable extent when its velocity becomes $v < v_0 Z_1^{2/3}$, where $v_0 = e^2/\hbar$. Its average charge q_1 will then actually be of order of (cf. Ref. 1)

$$q_1 = Z_1^* e \cong e\nu_1 \frac{v}{v_0} \cong e Z_1^{1/3} \frac{v}{v_0} \ , \tag{2.2}$$

in not-too-close collisions. Z_1 is the atomic number of the incoming particle, and $\nu_1 \sim Z_1^{1/3}$ is an effective quantum number of electrons carried by the ion. This corresponds to the circumstance that the majority of the electrons attached to the ion have orbital velocities $\sim v_1 = v_0 Z_1^{2/3}$. Already used here are Thomas-Fermi estimates of effective quantum numbers and orbital velocities of electrons, though only in a qualitative way.

Let us consider a collision between the ion and an electron at rest. It is apparent from Equation 2.2 that if the ion velocity exceeds

$$v \gtrsim 2Z_1 v_0 , \tag{2.3a}$$

the charge becomes $q_1 \approx Z_1 e$, and the inequality (Eq. 2.1) is seen to be fulfilled, so that quantal perturbation methods are valid. Then, quantities such as cross sections, average stopping, etc., are nearly proportional to Z_1^2, the square of the charge number of the particle.

Perturbation methods hold more widely than is suggested by Condition 2.3a. The atomic electrons are not at rest, as supposed in Condition 2.3a, but have orbital velocities v_j between v_0 and $Z_2 v_0$; for the majority of the electrons v_j is of order of $v_2 = v_0 Z_2^{2/3}$. If now, for a collision with an atomic electron

$$v_j \gtrsim 2Z_1 v_0 , \tag{2.3b}$$

perturbation methods may be used for any ion velocity, v, since the relative velocity in the collision remains large, independently of v. It may be noted that Conditions 2.3a and 2.3b are the outcome of a single inequality involving an average relative velocity of ion and electron, i.e., $(v^2 + v_j^2)^{1/2} \gtrsim 2Z_1 v_0$.

Quantities such as total stopping are obtained by summing over all electrons. For such purposes, Condition 2.3a is a more important restriction than Condition 2.3b. Indeed, at low ion velocities the atomic electrons no longer contribute nearly equally to energy loss; each loosely bound electron contributes much more than a strongly bound one. Therefore, the important v_j elements in Condition 2.3b are small, and cannot be expected to change drastically the Condition 2.3a.

As mentioned above, another characteristic velocity is $v_1 = v_0 \cdot Z_1^{2/3}$. When v is small compared to v_1, the balance charge of the ion, given by Equation 2.2, is small, and we are concerned with nearly neutral systems colliding with each other. If v is less than v_1, the electronic stopping must increase with v, since, e.g., in the Bethe stopping formula S is proportional to (q_1^2/v^2) times an increasing function of v. On the other hand, if v is large compared to v_1, the ion carries relatively few electrons and q_1 is fairly constant, so that the electronic stopping decreases with increasing v. Maximum in stopping therefore occurs in the neighborhood of v_1.

In any case v_1 gives a separation between high and low velocities, and is for several purposes a more important criterion than Condition 2.3a or Condition 2.3b. We therefore consider separately a low-velocity region

$$0 < v < v_1 = v_0 Z_1^{2/3} \tag{2.4}$$

As we shall see, this velocity region is also the one in which quasi-elastic ion-atom collisions of nearly classical type become important, and where electronic excitation is simple but is not always tractable by quantal perturbation methods.

If one of the above three inequalities (Conditions 2.3a and 2.3b and in Eq. 2.4) holds, special simplifications appear. The fulfillment of either of the conditions permits perturbation methods, as, in either, a perturbation treatment can be of interest for all velocities v. However, since Equation 2.4 indicates the velocities $v<v_0$ may always require special approximations, we need investigate perturbation for $v>v_0$ at least, i.e., protons with energies larger than 25 kev. If, as an auxiliary, we study stopping by electron gases, or by one of the electrons bound in an atom, it is proper to consider all velocities, i.e., also $v<v_0$.

3. Perturbation Approximation

One result in the preceding section is that the perturbation approximation, at any velocity of the penetrating particle, is an important standard and must be investigated. In this approximation, stopping is proportional to $Z_1^2e^2$, the square of the charge of the particle. The great simplification contained in the perturbation approximation is that we are concerned with properties of the medium only, and, in fact, linear properties. The number of significant parameters is reduced from three to two, v and Z_2.

We apply, of course, the perturbation approximation primarily in the case of a proton. Many authors have expressed misgivings about the simple theory of stopping for protons with energies of several hundred kev or less, because of capture and loss effects. Such misgivings are contrary to the spirit of the Thomas-Fermi description. I return to the justification of the perturbation approximation for protons, with such questions in view. Other questions of proton stopping are treated in the accompanying article by Fano (2). In the remainder of this section the penetrating particle may be imagined to be a proton, if any specification is desirable.

High Velocities ($x \gg 1$)

When separating now into several velocity regions, we measure the particle velocity in terms of critical velocities belonging to the medium. Since electronic orbital velocities in atoms are $\sim v_2 = Z_2^{2/3} v_0$, we might at first demand that v is large compared to v_2, corresponding to the high-velocity region, but a better measure of velocities is given in Equation 3.4. Relativistic corrections will not be included, although most of these are quite simple (cf., e.g., Ref. 2). The omission is made for simplicity, and also because the corrections are small except in extreme relativistic cases. The customary stopping cross section per atom may be written as

$$S_e = \frac{4\pi Z_1^2 e^4}{mv^2} Z_2 \cdot L \,, \tag{3.1}$$

where L is a function of two variables in the perturbation approximation; we write $L = L(v, Z_2)$. In the region of high velocities, the dimensionless quantity L is asymptotically connected to an average excitation potential I, as shown by Bethe (19),

$$L = \log \frac{2mv^2}{I} \,, \quad Z_2 \log I = \sum_i f_{0i} \log \hbar\omega_{0i} \tag{3.2}$$

where f_{0i} are the dipole oscillator strengths of the transition frequencies ω_{0i} for the atomic system.

The Thomas-Fermi demand in this case is simple. In fact, the unit of time of the Thomas-Fermi atom is proportional to Z_2^{-1}, and since an energy in a perturbation treatment behaves as Planck's constant times a frequency, the energy I in Equation 3.2 must be given by Bloch's relation (3, 7),

$$I = I_0 \cdot Z_2 , \tag{3.3}$$

where I_0 is a constant. This result gives a good approximation to experimental results for proton stopping, a sensible empirical estimate of I_0 being ~10 ev. Thus, while Equation 3.3 is a good approximation for high Z_2 values, vis. $Z_2 \gtrsim 15$, considerable deviations remain in several substances. Some of these deviations clearly are due to shell effects, but others are systematic, with the ratio I/Z_2 on the average increasing with decreasing Z_2 and attaining values above 15 ev in the lightest substances.

Intermediate Velocities ($x \gtrsim 1$)

Before entering into these questions, we may consider the straightforward Thomas-Fermi extension of Bloch's relations to somewhat lower, though still fairly high, velocities. The logarithm in Equation 3.2, as well as the stopping cross section (Eq. 3.1), are according to Equation 3.3, functions of the variable $x = v^2/v_0^2 Z_2$. Here $x^{1/2}$ may be said to be the reduced velocity of a Thomas-Fermi similarity treatment. At lower velocities, where the contributions to L are no longer of logarithmic type, we may still tentatively introduce a standard similarity corresponding to x (Ref. 7),

$$L = L(x) , \quad x = \frac{v^2}{v_0^2 Z_2} , \tag{3.4}$$

and can then discuss which kinds of deviations may occur. The achievement of similarity is that the two variables in Equation 3.1 are reduced to one variable in Equation 3.4.

One application of Equation 3.4 consists in semi-empirical comparisons. By means of Equation 3.1, and measurements of the stopping cross section S_e, empirical values of L may be obtained. A plot of such values of L against x for measurements in any substance is a convenient Thomas-Fermi comparison of the results. This method of comparison may be expected to be sensible, at least at such relatively large velocities where x is considerably larger than 1.

I return to deviations from Bloch's relation (Eq. 3.3). They afford an opportunity to discuss what is meant by a Thomas-Fermi treatment of atoms. The systematic increase of the ratio I/Z_2 with decreasing Z_2 has given rise to several suggestions. On various grounds (e.g., Refs. 5, 6, 18) it has been suggested that the scaling unit of the frequency spectrum is not proportional to Z_2 but that it increases more slowly with Z_2. In this connection, reference has been made to the variation of energy with Z_2 in a Thomas-Fermi-Dirac model. It appears to me that these surmises are not very promising.

What one needs is an approximate physical picture, primarily as regards the dipole oscillator strength distribution for atoms and molecules. The following picture is perhaps adequate. Complete validity of the Thomas-Fermi model means that the density of oscillator strength is always $g(\omega/Z_2\omega_R)$, where ω_R is the Rydberg frequency. Deviations from this density must occur in all atoms and molecules. One type of

deviation should appear at frequencies of order of $Z_2^2\omega_R$; i.e., K-shell binding energies. In most cases this deviation is hardly important because little oscillator strength remains at such high frequencies. In the intermediate region, too, where $\omega \sim Z_2\omega_R$, deviations from the Thomas-Fermi spectrum must occur, connected to inner electron shells; but these deviations also should be of less direct importance than those at the lowest frequencies. In fact, the density of oscillator strength increases for decreasing ω, but there must be some kind of gap in the spectrum up to a frequency of order of ω_R; i.e., for $(\omega/Z_2\omega_R) \sim Z_2^{-1}$. This clear-cut departure from Thomas-Fermi scaling of the spectrum is the more predominant the lower the atomic number. Since the gap implies a shift (in the low-frequency region) of oscillator strength density towards higher ω-values, as compared to the Thomas-Fermi spectrum, it follows directly that I-values must increase above Bloch's result for decreasing atomic number.[2] As to chemical bindings, polarization in solids or phase changes, the resulting effects on oscillator strength distribution should be confined to quite low transition frequencies.

If the simple picture presented here is a fair approximation to distribution of dipole oscillator strength, several important conclusions may be drawn from it. A few conclusions of this type are discussed below. However, simplifications other than those mentioned above will be made in order to arrive at some of the results.

The first conclusion is that curves of experimental L against x will, at high values of x, be a set of rather closely lying and nearly parallel lines; separation between curves is caused primarily by deviations from Bloch's relation (Eq. 3.3). Although the curves do not vary exactly as const. + log x in the upper region, the deviations from the logarithmic curve should remain comparatively small. In the present formulation they are given by a Thomas-Fermi equivalent of K-, L-, M-, ... shell corrections.

Next, we are interested in continuing the curve farther down, to velocities where $x \lesssim 1$. The corrections to (Eq. 3.2) may be said to be of two kinds. First, L is a sum of logarithmic terms corresponding to various transition frequencies; none of these terms can be negative. This implies a cut-off, at least when the arguments inside logarithms become less than 1, and therefore a positive correction to L. Second, when $2mv^2$ is large compared to the transition energy $\hbar\omega$, there is a downward correction, of the kind mentioned above. This may be called the asymptotic correction.

We are thus confronted with three theoretical problems: Computations of I-values, estimation of individual asymptotic corrections, and estimation of cut-off corrections. Computation of I-values should be the simplest of these problems, yet it is not readily solved because of the fact that direct theoretical computations have not been made, except in atomic hydrogen and helium. For this reason alone, the Bloch relation (Eq. 3.3) is useful. The difficulties in estimating I is one of the

---

[2] The gap may be thought of as rather constant, and less dependent on atomic shells than would appear from purely energetic considerations. Thus, in inert gases the energy gap is large. In other gases the gap is small, but the dipole oscillator strengths are pushed upwards in frequency. (The upward shift of the oscillator strength is due to a polarization effect within the electron cloud; see p. 9). Therefore, the net result for the total oscillator strength distribution is about the same in these two cases.

reasons why the original attempts at estimating the more involved inner shell corrections may not give accurate results.

As I see it, previous estimates of I-values and corrections to Equation 3.2 were hampered mainly by disregard both of polarization effects within an atom as a whole and of important corrections due to the less strongly bound electrons. Both of these effects are included, to a considerable extent, in a Thomas-Fermi scheme and may be estimated in various approximations within this scheme (e.g., the simple compressible liquid of Bloch). Particularly concerning the question of polarization, there have been differences of opinion in recent literature (cf. e.g., Ref. 12). I return to polarization and correction effects below.

Low Velocities ($x<1$)

Let us consider the third type of quantities, the cut-off correction which appears at low x-values. It is often maintained that for stopping in this region (i.e., protons with energy below several hundred kev) systematics no longer prevail, particularly because of capture and loss of electrons, and the associated energy transfers to electrons and screening of the field around the proton. Since I argue the case for the Thomas-Fermi description, let me discuss here the opposite point of view (Ref. 8) where, e.g., screening effects are due to the medium only. It seems important to check the degree of accuracy of the Thomas-Fermi perturbation treatment at low velocities. If such treatment applies here with any accuracy at all, it should be more accurate and better understood at high velocities.

For an approximate treatment at low velocities, two of the previous assumptions are needed—one is the cut-off corresponding to L having no negative contributions, and the other is that deviations from Thomas-Fermi spectrum $g(\omega/Z_2\omega_R)$ occur only below a certain frequency $\gtrsim \omega_R$, in a manner characteristic of the atom in question. At low velocities, high frequencies in the atom contribute little to stopping, because of the cut-off effect. The increase in stopping (Eq. 3.1), therefore, is essentially of Thomas-Fermi type, i.e., common to all atoms. In the L-curves there still remains the effect giving deviations of the I-value from Bloch's relation. The spreading of L-curves at low x-values should roughly be like that at high x-values in an absolute measure, and therefore larger in a relative measure. Note that L-curves may possibly cross each other, due to effects of successive inner atomic shells.

Maximum in stopping cross section, S_{max}, for protons occurs at widely different energies, E_{max}, of order of 100 kev. The above considerations were utilized tentatively, in order to derive from measured values of S_{max} and x_{max} the correlated I-value of the substance in question. This appears to give I-values in fair accord with those found at high velocities. Furthermore, check of an approximate statistical model of oscillator strength is obtained (Ref. 8).

The question may be asked why it should be at all possible to look apart from electron capture, loss, and screening; i.e., why the proton may be treated in the perturbation approximation. In this connection the simplest case that can be studied theoretically with considerable accuracy is that of a proton of arbitrary velocity in an electron gas of comparatively high density. In this case the question of capture, loss, and screening is solved automatically. Stopping is closely proportional to the proton charge squared, and screening is nearly independent of the charge. In a dilute electron gas with low kinetic energies of electrons, stopping effects are no longer proportional to Z_1^2 at low velocities, but statistical methods of the Thomas-Fermi type are still applicable.

In a substance with $Z_2 > 1$, the greater part of the atom corresponds to an electron gas of comparatively high density, but a certain fraction corresponds to a gas of relatively low density. To a large extent, stopping of protons by atoms is therefore within the perturbation approximation; but at quite low velocities ($v < v_0$), where loosely bound electrons give large stopping contributions, the approximation fails. In any case, the stopping effect remains little influenced by differences in capture and loss phenomena.

For α-particles the situation is, of course, different, since screening effects occur at considerably higher velocities. Directly, α-particles are of little use in the analysis of linear properties of matter. Instead, α-particles and the heavier ions mentioned in Section 4 may (e. g., by Thomas-Fermi scaling) serve to estimate deviations from stopping being proportional to Z_1^2 in the case of protons (cf. also Eq. 4.12). In this connection, the highly interesting problem of stopping of negative heavy particles at low velocities should be mentioned. As to intermediate velocities ($v \sim 20 v_0$) it has been suggested by Barkas et al. (24) that there is a large difference between ranges for negative and positive baryons.

Comparison with Electron Gas

A useful example seems to be the stopping of charged particles in a free electron gas, where relatively high accuracy is possible and important theoretical features are illustrated. The linear dynamic properties of the electron gas are contained in the dielectric constants $\epsilon^l(k, \omega)$ and $\epsilon^{tr}(k, \omega)$, which depend on wave number and frequency of the field. In the first approximation the dynamics is equivalent to a dynamic self-consistent perturbation treatment. A most conspicuous feature in such stopping phenomena is the polarization effect. From the results for the free electron gas it appears that polarization within an atom also is important (Ref. 7). The influence of polarization on the levels of the static model may be disregarded in first approximation, but the dipole oscillator strengths of the various transitions are strongly affected. The effect is most pronounced in an electron gas where all of the dipole oscillator strength is pushed upwards and collected in the plasma frequency, $\omega_0 = (4\pi n\, e^2/m)^{1/2}$. This effect of polarization should remain appreciable in atomic systems.

In the absence of more precise calculations, a qualitative estimate of atomic oscillator strength distribution in atomic systems has been made by merely assuming a local modified plasma frequency, $\chi \omega_0$, where $\chi \sim 2^{1/2}$. This assumption gives easy estimates for both Thomas-Fermi and Hartree density distributions, and seems useful for exploratory purposes at least (cf. Refs. 7, 8, 2).

Other interesting results obtainable in an electron gas are summation rules as expressed by the dielectric constant. Besides the familiar Bethe sum rule for generalized oscillator strengths may be mentioned the equipartition rule, according to which the stopping contribution from close collisions and from resonance collisions are exactly equal (Ref. 16). This result implies that, for an electron gas, e. g., the asymptotic corrections to Equation 3.2 are contributed equally from close collisions and resonance collisions, so that only one of the two need be calculated. It turns out that also in atoms the asymptotic shell corrections obey the equipartition rule, as far as present computations go (cf. Refs. 2, 25, 26). Moreover, the electron gas picture leads to asymptotic corrections in fair agreement with more direct calculations on atoms. It therefore seems feasible, within a Thomas-Fermi description, to compute the velocity-dependent corrections to the Bethe-Bloch formula (Eq. 3.2).

4. Quasi-Elastic Collisions

In the perturbation case, the stopping cross section depends on two parameters, v and Z_2, but it depends on only one parameter if similarity applies. The present case of low velocities is considerably more complicated. Not only is stopping initially a function of at least three parameters (i.e., v, Z_1 and Z_2), but there are two different stopping mechanisms, electronic and nuclear stopping, with the latter, moreover, leading to sizable fluctuation effects.

Both experimentally and theoretically there is a vast number of cases to be investigated. The field is much less explored than is that of stopping of protons, and the relative accuracy is less by perhaps an order of magnitude. Two major groups of problems arise. One group concerns stopping and range problems, i.e., the fate of the particle; the other group concerns radiation damage in the medium, i.e, the fate of the substance. In the latter group of problems the competition between electronic and nuclear stopping is particularly important. From these brief comments it would appear that similarity considerations, if applicable, can be of great value.

The perturbation case corresponds to high velocities. In the following is treated velocities v less than the critical velocity v_1 (cf. Eq. 2.4). The electronic stopping decreases when velocity is diminished, as mentioned in Section 2. The direct quasi-elastic collisions between the ion and atoms, giving rise to atomic recoils, then become of increasing significance in the energy loss of the ion, and they dominate completely at quite low velocities (1). When treating the case $v < v_1$ — still from a Thomas-Fermi similarity point of view—I therefore consider primarily the recoil of atoms, which so far has been disregarded. Since velocities are comparatively low, the ions are nearly neutral, i.e., $Z_1^*/Z_1 \ll 1$; as an extreme case it should be noted that nearly neutral might correspond to, e.g., $Z_1^* \sim 15$, for heavy ions. The simplest starting-point for quasi-elastic collisions is that of very low velocities ($v \ll v_0$). The phenomena occurring here may be described as a neutralized heavy ion moving slowly past an atom in a classical orbit determined by the repulsive force. This collision is not completely elastic, and, in an approximately continuous way, energy is transferred to atomic and ionic electrons.

I shall now attempt to indicate, in a tentative and simple way, how similarity may be applicable in quasi-elastic collisions. The first question is a computation of static ion-atom interactions on the basis of the Thomas-Fermi treatment of a cloud of electrons belonging to two nuclei, Z_1 and Z_2, at a distance R. The potential energy must behave as $Z_1 Z_2 e^2/R$ times a function of two variables, depending on R, Z_1 and Z_2, e.g., the two variables R/a and (Z_1/Z_2),

$$U = \frac{Z_1 Z_2 e^2}{R} \cdot u \,, \tag{4.1}$$

where $u = u(R/a,\ Z_1/Z_2)$, and $a = a_0 \cdot 0.8853(Z_1^{2/3} + Z_2^{2/3})^{-1/2}$. In a comprehensive description where similarity is used, it would be preferable to be able to express u as a function of one variable only. In fact, Bohr (1) made an assumption of this kind by putting $u = \exp\{-R \cdot 0.8853/a\}$. Estimates of actual potentials for various values of (Z_1/Z_2) have been made by Firsov (15) and many others. It is apparent that, within a fair approximation, one may assume u to be a function of one variable only, but the exponential function in the Bohr potential decreases much too rapidly at large distances. The other natural choice,

$$u = \varphi_0(R/a) \,, \tag{4.2}$$

with φ_0 being the Fermi function (Ref. 27) belonging to the Thomas-Fermi atom, turns out to be a good approximation.

So far, there is similarity in ion-atom interactions, the unit of length being a. Then, Equation 4.1 implies that the unit of energy is $Z_1Z_2e^2/a$. With this in mind, consider the possibility of similarity in ion-atom collisions. Let the atom be at rest in the laboratory system, whereas the ion has the energy E. In the center-of-gravity system the energy is $E\,M_2/(M_1 + M_2)$, and when this is measured in reduced units a dimensionless parameter

$$\epsilon = E \cdot \frac{aM_2}{Z_1Z_2e^2\,(M_1+M_2)} \tag{4.3}$$

is obtained. Similarly, the impact parameter p is p/a in reduced units. Since the reduced mass is $M_0 = M_1M_2/(M_1 + M_2)$, we also have a unit of velocity, w, given by

$$w = \left(\frac{2Z_1Z_2e^2}{M_0a}\right)^{1/2} \tag{4.4}$$

By means of reduced energy, ϵ, reduced length, $\xi = R/a$, and reduced time, $\tau = t\,w/a$, one is able to solve all scattering problems by solving one case, for arbitrary ϵ and ξ. Thus

$$d\sigma = \pi a^2\, f(\epsilon,\ \sin^2\frac{\theta}{2})\,d\Omega\ . \tag{4.5}$$

This description may be carried a little further. Consider possible generalizations of the static force. The velocity-dependent forces are due to irreversible excitation of the electron clouds of the colliding systems. Let v(R) be the relative velocity of the heavy centers at the distance of separation R. The excitations depend on a competition between v(R) and the electron velocities $\sim v_0Z^{2/3}$, i.e., on the dimensionless variable $v(R)/v_0Z^{2/3}$. The force is then expected to be of type of

$$K = \frac{Z_1Z_2e^2}{R^2}\,k\left(\frac{R}{a},\ \frac{v(R)}{v_0Z^{2/3}}\right) \tag{4.6}$$

Here, the function tends to 1 for $R/a \to 0$. Consider scattering when Equation 4.6 applies. Similarity between two collisions demands also that the new collision variable $v(R)/v_0Z^{2/3}$ is the same in the two collisions. The demand would appear to be in contradiction to Equation 4.4. Only if $\lambda = (w/v_0Z^{2/3})$ is a constant, similarity can be obtained in the present case too. This holds quite well, because for the stable isotopes $A_1 \cong 2Z_1$, $A_2 \cong 2Z_2$, and for most values of Z_1 and Z_2 the constancy of λ is remarkable. One clear exception occurs when either the atom or the ion is a proton, because λ then increases by a factor of $2^{1/2}$. Still, since the dependence on the last variable in Equation 4.6 is not a strong one, and since in most collisions deflection angles θ are small, fixed values of ϵ and p/a may be expected to imply corresponding collisions, so that Equation 4.5 remains valid.

Even though the result (Eq. 4.5) is not particularly complicated, it is not easily applicable to direct comparisons. It is possible to compute (from Eq. 4.5) averages of powers of $\sin\theta/2$, and, although this is useful, one may obtain instead an important simplification already in the differential cross section (Eq. 4.5). Consider, e.g.,

the Rutherford scattering where $f(\epsilon, \sin^2\frac{\theta}{2})d\Omega = Cdt/t^2$, so that f becomes a function of one parameter only, viz.

$$t = \epsilon^2 \sin^2\frac{\theta}{2} \quad . \tag{4.7}$$

In classical perturbation treatments too, where $\theta \ll 1$, $d\sigma$ will for any potential be a function of only $\epsilon^2\theta^2/4 \sim t$, multiplied by πa^2. For screened Coulomb fields, but not generally for all types of interaction, the extrapolation where $\epsilon^2\theta^2/4$ from the perturbation results is replaced by t turns out to be quite accurate (Ref. 9), and comprehensive approximation procedures may be developed along these lines. In place of Equation 4.5 we now get a much simpler result, conveniently written as

$$d\sigma = \pi a^2 \cdot \frac{dt}{2t^{3/2}} f(t^{1/2}) \, . \tag{4.8}$$

The function f(y) is shown in Figure 1 as computed from the potential (Eq. 4.1 and Eq. 4.2), using the extrapolated perturbation treatment. For Rutherford scattering $f(y) = 1/(2y)$.

In analogy to Equation 4.5, the formula (Eq. 4.8) may embrace both the elastic case (Eq. 4.2) and the quasi-elastic case (Eq. 4.6), the latter when constancy of λ is fulfilled. We are normally concerned with an incoming ion of energy E colliding with a free atom at rest. In this case, elastic collisions correspond to $(T/T_m) = \sin^2\theta/2$, where $T_m = \gamma E = E \cdot 4M_1M_2/(M_1+M_2)^2$ is the maximum energy transfer. It may be noted that a useful simplification for exploratory purposes is a power law scattering, where f(y) in Equation 4.8 is proportional to $t^{1/2-1/s}$, corresponding approximately to interaction potentials proportional to R^{-s}.

For many purposes all inelastic effects (Refs. 10, 11) from distant and not-so-distant collisions may be summarily considered as a continuous slowing-down, given

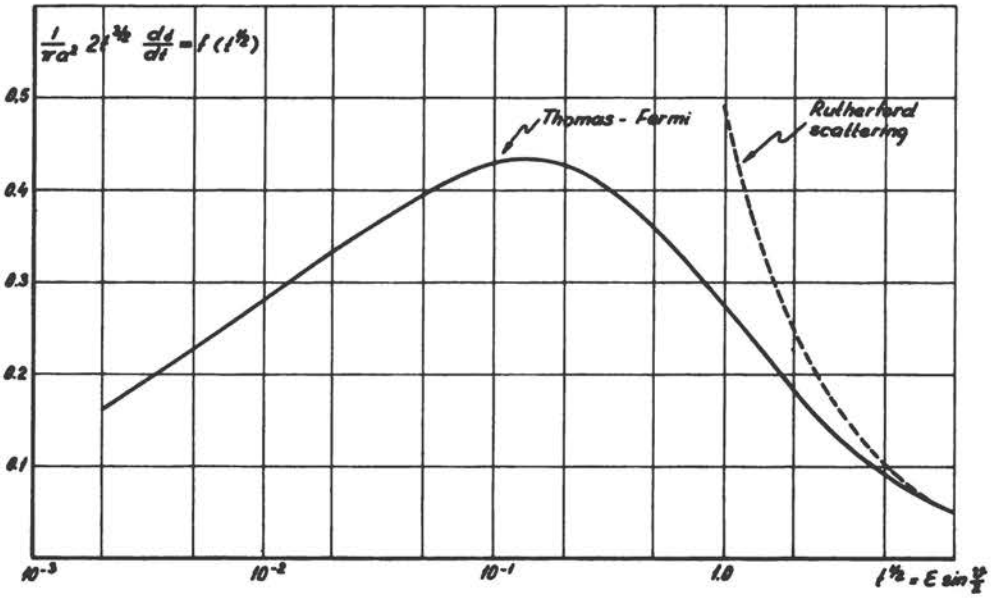

Figure 1. Universal differential scattering cross section for elastic nuclear collisions (Eq. 3.8) based on a Thomas-Fermi type potential. At high values of $t^{1/2}$ this cross section joins smoothly with the Rutherford scattering cross section.

by the electronic stopping cross section (Eq. 4.12). Besides electronic stopping should then be considered separately elastic collisions as described by Equation 4.8 and as shown in Figure 1.

The above theoretical picture has similarity features that are contained in corresponding collisions and also in the universal cross section (Eq. 4.8). Many of its details may be checked. Theoretically, the present scattering method applied to exponentially screened fields is in good agreement with accurate calculations by Everhart, Stone, and Carbone (22). Experimentally, and as regards inelastic effects, the studies of quasi-elastic collisions by Fedorenko (17) and by Everhart, et al. (23), are in fair agreement with the present scattering method.

Ranges and Stopping Cross Sections

The similarity property of cross sections has interesting consequences. In the case of the elastic collisions described by Equation 4.8, the stopping cross section becomes

$$S_n = \int d\sigma T = \pi a^2 \gamma E \int_0^{\epsilon} dy\, f(y) \,. \tag{4.9}$$

Therefore, the dimensionless quantity

$$\rho = RNM_2\, 4\pi a^2 \frac{M_1}{(M_1+M_2)^2} \,, \tag{4.10}$$

where R is distance along path, is the reduced path length as long as elastic collisions dominate. From Equations 4.9 and 4.10 is obtained a reduced stopping cross section,

$$s = S \cdot N \cdot (M_1 + M_2)/(Z_1 Z_2 4\pi e^2\, a\, M_1) \,,$$

where the part due to nuclear collisions, $s_n = s_n(\epsilon)$, is a function of ϵ only (cf. Fig. 2). Thus, the three variables in the stopping cross section have been reduced to one, and it becomes possible to make simple comparisons between theory and experiments on slowing-down and ranges (Ref. 10). By means of the cross section (Eq. 4.8), range quantities other than the mean path range may be studied, as well as fluctuations in range. It should be mentioned that, also Equation 4.5, without the simplification (Eq. 4.8), implies that s_n becomes a function of ϵ only, as in Equation 4.9.

If electronic stopping is proportional to velocity (cf. Eq. 4.12), it will be of type of

$$s_e = k \cdot \epsilon^{1/2} \,, \tag{4.11}$$

where k is independent of velocity but may depend on Z_1 and Z_2. Therefore, Equation 4.11 contains one variable besides ϵ. It so happens that in many cases k has approximately the same value, ~0.15 (cf. Fig. 2). On the basis of Equations 4.8 and 4.11, a comprehensive description of stopping has been attempted (Ref. 10) in the velocity region $v < v_1$ given by Equation 2.4, or $\epsilon < \epsilon_1 \sim 10^3$. With recent measurements, comparison may be made both for low ϵ-values, $\epsilon < 1$, where nuclear stopping dominates, and for high ϵ-values, $\epsilon \gg 1$, where Equation 4.11 or 4.12 may be studied. Further application of Equations 4.8 and 4.11 has been made in the studies of the division of energy between electrons and recoil atoms, which is important in damage effects by particle radiations (Ref. 11).

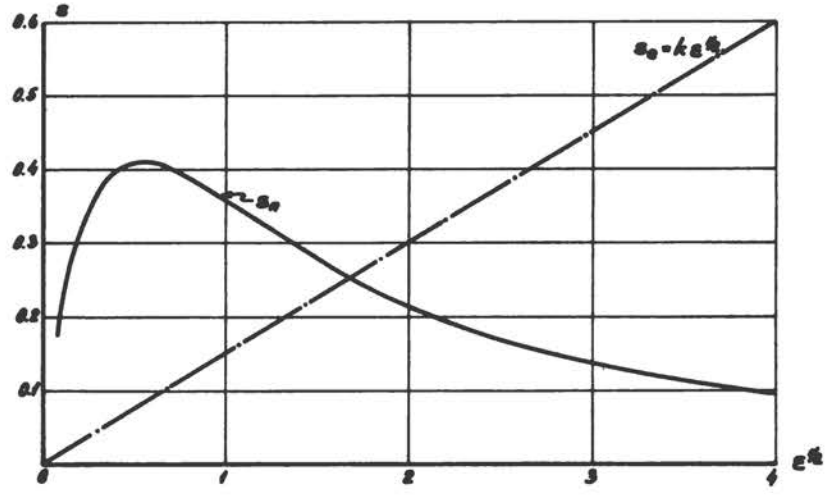

Figure 2. Theoretical nuclear stopping cross sections in ρ - ϵ variables. The abscissa is $\epsilon^{1/2}$; i.e., proportional to v. The fulldrawn curve is $s_n(\epsilon)$, computed from Figure 1. The dot-and-dash line is s_e for k = 0.15.

A rough estimate of electronic stopping at low velocities, where Equation 2.4 applies, is given in References 7 and 9. It appears that adiabatic arguments, suggesting vanishing electronic stopping by atoms for $v < v_0$ (Refs. 1, 21), are hardly applicable. In fact, comparisons either with motions through gases and liquids, or with electron scattering by screened Coulomb fields, indicate that electronic stopping is proportional to ion velocity, and that supposed differences between freely moving metallic electrons and more strongly bound ones should not exist. This is clearly indicated in the quasi-elastic collisions, where the motion may be quite slow, but the electron clouds are forced through each other, and the kinetic energy is ample for the production of electron excitations.

The calculation of electronic stopping is complicated by the occurrence of excitation in close collisions as well as in distant ones, and by the circumstance that loosely bound electrons contribute relatively more to the stopping than do the strongly bound ones. Semiclassical Thomas-Fermi reasoning would lead to a stopping behaving as $Z^{5/3}$ times a function of $v/v_0 Z^{2/3}$. More accurate studies of stopping for ions of low velocity in free electron gases have been made (Refs. 13, 16). They may be used in estimating the contributions from electrons of different binding for various values of Z_1 and Z_2. In this way a simplified comprehensive formula of Thomas-Fermi type was obtained (Ref. 9),

$$S_e = \xi_e 8\pi e^2 a_0 \frac{Z_1 Z_2}{Z} \frac{v}{v_0} , \qquad (4.12)$$

where $\xi_e \approx Z_1^{1/6}$. The formula seems to be in fair accordance with observations (Ref. 29). Of course, there are fluctuations about the average smooth dependence on atomic number, and these are due to shell effects of the ion (cf. Ref. 28). It may be noted that, e.g., for protons, Equation 4.12 is not proportional to Z_1^2, and thus does not correspond to the perturbation case.

References

1. N. Bohr, Mat. Fys. Medd. Dan. Vid. Selsk. 18, no. 8 (1948).

2. U. Fano, accompanying paper, also published in Ann. Rev. Nucl. Sci. 13 (1963).

3. F. Bloch, Z. Physik 81, 363 (1933).

4. F. Bloch, Ann. d. Physik 16, 285 (1933).

5. H. Jensen, Z. d. Physik 106, 620 (1937).

6. W. Brandt, Phys. Rev. 111, 1042, and ibid. 112, 1624 (1958).

7. J. Lindhard and M. Scharff, Mat. Fys. Medd. Dan. Vid. Selsk. 27, no. 15 (1953).

8. J. Lindhard and M. Scharff, Natl. Acad. Sci. - NRC Publ. 752, p. 49 (1960).

9. J. Lindhard and M. Scharff, Phys. Rev. 124, 128 (1962), and Notes on Atomic Collisions I and IV (in preparation).

10. J. Lindhard, M. Scharff and H. E. Schiøtt, Mat. Fys. Medd. Dan. Vid. Selsk. 33, no. 14 (1963). Contains reference to recent range measurements for heavy ions.

11. J. Lindhard, V. Nielsen, M. Scharff and P. V. Thomsen, Mat. Fys. Medd. Dan. Vid. Selsk. 33, no. 10 (1963); J. Lindhard and V. Nielsen, Physics Letters 2, 209 (1963).

12. Report on Conference on Penetration of Atomic Particles, Gatlinburg 1958, Natl. Acad. Sci. - NRC Publ. 752, (1960).

13. E. Fermi and E. Teller, Phys. Rev. 72, 399 (1947).

14. B. G. Harvey, Ann. Rev. Nucl. Sci. 10, 235 (1960).

15. O. B. Firsov, JETP 5, 1192 (1957); ibid. 7, 308 (1958); ibid. 9, 1076 (1959).

16. Aa. Winther and J. Lindhard, Mat. Fys. Medd. Dan. Vid. Selsk. 34, no. 4 (1964); J. Lindhard, Mat. Fys. Medd. Dan. Vid. Selsk. 28, no. 8 (1954).

17. N. V. Fedorenko, Sovjet Phys. Uspekhi 2, 526 (1959).

18. Do In Seb, JETP 16, 87 (1963).

19. H. A. Bethe, Ann. d. Physik 5, 325 (1930).

20. A. Russek and M. T. Thomas, Phys. Rev. 109, 2015 (1958).

21. F. Seitz, Disc. Far. Soc. 5, 271 (1949).

22. E. Everhart, G. Stone and R. J. Carbone, Phys. Rev. 99, 1287 (1955).

23. G. H. Morgan and E. Everhart, Phys. Rev. 128, 667 (1962); E. N. Fuls, P. R. Jones, F. P. Ziemba and E. Everhart, Phys. Rev. 107, 704 (1957).

24. W. H. Barkas, J. N. Dyer and H. H. Heckman, Phys. Rev. Letters 11, 1381 (1963).

25. M. C. Walske, Phys. Rev. 88, 1283 (1952); ibid. 10, 940 (1956).

26. U. Fano and J. E. Turner, cf. ref. 2.

27. P. Gombás, Hdb. d. Phys. XXXVI, 109 (1956).

28. J. H. Ormrod and H. E. Duckworth, Can. J. Phys. 41, 1424 (1963).

29. L. C. Northcliffe, accompanying paper, also published in Ann. Rev. Nucl. Sci. 13, (1963).

2. A CRITICAL REVIEW OF EXPERIMENTAL STOPPING POWER AND RANGE DATA

H. Bichsel[1]

Abstract

Of the many experimental data available, a few have been selected as being especially comprehensive or accurate for an evaluation in terms of the Bethe theory. The choice has been restricted to data pertaining to the penetration of hydrogen and helium ions. The discrepancies found in the experimental data discourage reliance on a single data point for the determination of the parameters necessary for the theory (e. g. , the I-value) and also make it appear highly desirable to encourage further intensive experimental study of the charged particle interaction.

A short discussion is given of the theory, including some comments about the shell corrections. This discussion is followed by detailed discussion of several experiments and a detailed treatment of aluminum and copper data.

1. Introduction

It is the purpose of this paper to extract from the vast amount of information available in the field of stopping power and range data some of the most reliable experiments and to determine whether it is possible to give a consistent evaluation of these measurements in terms of the complete Bethe theory.

In some instances it is possible to intercompare experimental data directly (see "Comparison with Range Data" in Section 4; Section 5; and "Stopping Power at High Energies" in Section 6), but mostly it is necessary to extract a set of parameters occurring in the theory (I-value, shell corrections) and to compare the sets obtained in different experiments.

No low velocity data are considered because charge exchange effects become important (roughly below 0. 5 Mev for protons, below 2 Mev for alphas).

In this report I have tried to treat the data in such a way as to obtain a quantity which is approximately constant (see, for example, "Preliminary Analysis" in Section 4). Obviously, the quantity ξ_{exp}/ξ_{th} as a function of particle energy would be approximately unity (ξ_{exp} represents an experimental stopping-power result, ξ_{th} the stopping power computed from the Bethe theory). If this ratio is not constant, deviations can be caused by (a) accidental errors in the measurements, (b) systematic errors in the measurements, and (c) systematic errors of the theory.

[1]Physics Department, University of Southern California, Los Angeles.

In general, no attempt was made to discuss the error evaluation given by an author (for example, no thought has been given to the claims for the accuracy of a given foil thickness determination; it will be remembered that considerable discrepancies occurred for commercial and evaporated gold foils), but it will be quite easy to see whether the quoted accuracy is in agreement with the actual facts.

For charged particles (charge z, velocity $\beta = v/c$) with negligible charge-exchange effects, the complete theoretical expression will be found in Reference 1. For the analysis of experimental data, the stopping power ξ in an element (Z, A) can conveniently be written in the form (Ref. 2)

$$\xi = -dE/\rho dx = (z^2 Z/A) \cdot K(\beta)[f(\beta) - \ln I - (\Sigma C_i/Z)]$$

$$K(\beta) = 4\pi e^4 N_0/mc^2\beta^2 \qquad (1)$$

$$f(\beta) = \ln [2mc^2\beta^2/(1-\beta^2)] - \beta^2$$

where I is the average excitation energy of the stopping atoms, and C_i represents the shell corrections. In this report, the shell corrections are computed as nonvanishing for $\beta \rightarrow 1$, so that the I-values obtained are the "optical I." In Reference 2 the C_i are assumed to vanish for $\beta \rightarrow 1$. This expression is valid for protons of energies above 0.5 Mev and below about 1000 Mev. Density corrections are neglected. In this paper, I is defined as constant (see first part of Section 2 for a different approach).

If an experimental test of the theory is desired, the following points have to be considered: (a) the velocity dependences $K(\beta)$ and $f(\beta)$ will have to be tested; (b) experimental and theoretical values of I will have to be compared; (c) the importance of the shell corrections will have to be investigated; and (d) the correctness of the factor z^2Z/A will have to be established. Each point is considered in turn:

(a) Both $K(\beta)$ and $f(\beta)$ are well-defined and well-known functions of the velocity. Until a complete theory of the shell corrections is developed, it is sensible to include deviations of $K(\beta)$ and $f(\beta)$ from their mathematical form as part of the shell corrections.

(b) Very few theoretical I-values are known (H, He, etc., Ref. 26), and the agreement between theory and experiment is within the estimated errors, which are at least 5 percent. For most other elements it will be necessary to use experimentally determined I-values. These values will be strongly influenced by the magnitudes of the shell corrections, especially at low energies. General theoretical guidelines for the dependence of I on Z are available (Bloch theory, I = kZ, or Jensen theory, see Sec. 3 of Ref. 1), but experimental data are necessary to find the constants of these expressions.

(c) Only K- and L-shell corrections have been computed theoretically. Unfortunately, owing to departures of the atomic field from the Coulomb law, these corrections are most unreliable for the light elements, where they could be tested most accurately. The work for aluminum (Ref. 3 and Sec. 7 of this report) seems to indicate that the theory is essentially correct. For the heavier elements (Z > 20), the higher shell corrections become quite important at moderate energies (1 to 20 Mev for protons), amounting to several percent in the stopping power. No theory is available at present and it has to be understood that a <u>whole function</u> of the velocity is thus not known.

(d) The ratio Z/A represents the number of electrons in the material per unit chemical atomic weight and thus is not subject to appreciable error.

The charge state represented by z of the incident particle is discussed in the papers by Northcliffe and Allison (see Reports 8 and 11 and Appendix B). The present paper is mainly concerned with protons above 0.5 Mev, and discussion for charge-state effects is therefore unnecessary.

2. General Comments on Shell Corrections

The shell-correction term in Equation 1 can be merged with ln I by introducing a single energy-dependent parameter I' defined by:

$$\ln I' = \ln I + (\Sigma C_i/Z) \quad . \tag{2}$$

Instead of having as an unknown function the shell corrections, we will have the unknown function $I'(\beta)$. An approach of this type, being investigated by G. F. Williamson at the University of Washington, is presented in References 5 and 14.

The fundamental hope would be that $I'(\beta)$ can be represented by a reasonably simple function of β and Z. It would appear, though, that difficulties will be experienced by any theory that will not take into account the systematic trends in the behavior of electron shells for different atoms. The change in such quantities as the ionization potential of individual shells shows a different Z dependence for each shell; and, while the exact correlation between the magnitude of shell corrections and the ionization potentials of electron shells may not be clear, it appears unlikely that the shell corrections will show a simple behavior if the ionization potentials do not.

To this author it appears to be more desirable to introduce shell corrections explicitly. As mentioned above, this is possible for the inner two shells with the theory developed by Walske (Ref. 4). For the outer shells, no theory is available, and a first approach would be to measure the stopping power for many elements over a large range of velocities and extract the shell corrections as the difference between experimental and theoretical values without higher shell corrections. This has been done for copper (Ref. 5). At present there are not enough experimental data available to allow this approach to be carried out very dependably for the heavier elements (Ag, Au).

In a second approach, also used in Reference 5, it is assumed that the higher shell corrections have approximately the same velocity dependence as the L-shell correction.[2] While this may be expected to be reasonably successful for the velocity range where C_i is positive, it may be a fairly bad approximation for smaller velocities. An additional difficulty appears, in that presumably it will be necessary to introduce a separate correction for each subshell, so that up to ten C_i may be necessary. Since for each C_i two parameters will be required for the scaling, this approach could lose significance just as well as the first approach. It appears possible to reduce the number of parameters used through the arguments presented in Reference 5.

---

[2] It has lately come to my attention that a similar scaling procedure has been used (upon Bethe's suggestion) by Hirschfelder and Magee (Phys. Rev. 73, 207, 1948), using B_K.

On the whole, the situation is very unsatisfactory. New measurements are a very definite necessity, and further semitheoretical speculation with present data seems to be rather hopeless. For any satisfactory discussion of stopping power to an accuracy of 1 percent or better, the shell corrections are absolutely essential, and at present it appears that they will have to be approached from the experimental side, especially for the low energies.

The theoretical approach presented in Report No. 4 of this publication eventually may provide theoretical guidance.

3. Treatment of Experimental Data

Classification

It will be reasonable to classify experimental measurements according to the following parameters: (a) atomic number of stopping material, (b) energy of incident particle, (c) charge of incident particle, and (d) type of measurement (range, stopping power, fractional energy loss in thick absorbers, with various ways of determining left-over energy). While measurements are available for many combinations of these parameters, very few data overlap within the possible range of the parameters in such a way as to allow consistency checks.

The analysis is made difficult by the range of quoted experimental errors (from 0. 1 to 10 percent), and by the fact that (as will be shown) errors have not been estimated accurately by many authors. Both underestimates and overestimates of errors occur.

A practice convenient for an over-all representation of data is the use of logarithmic plots, but this practice is quite unsuitable for a careful analysis of data because it will tend to cover up discrepancies rather than to point them out.

Reduction of Original Data

Experimental data usually cover a certain range of one or two of the experimental parameters mentioned above. For example, the measurements by MacKenzie and his collaborators at University of California, Los Angeles (U. C. L. A.), measure the stopping power for many different elements, but for fixed particle charge and energy. Nielsen, on the other hand, measures the energy dependence of ξ for six different elements and two different particles.

As a preliminary step of analysis, the raw data of certain sets of experiments have been reduced so as to eliminate the influence of physical factors that are either constant in the whole set or theoretically well known; for example, Equation 4 (in Sec. 4) replaces measured stopping-power values ξ_{exp} with values X of a more nearly energy-independent variable.

Adjustment of Parameters and Errors of Fitting

Equation 1 contains the parameter I and other parameters that help specify the dependence of the shell corrections C_i upon the properties of the incident particle and the stopping material. The following sections make repeated reference to analysis of experimental data directed simultaneously to the determination of these

parameters and to estimating the accuracy of this determination and, more generally, the over-all agreement of the theory with the experimental results. To this end the following procedure was generally employed.

Call $\tau_{exp}^{(i)}$ the result of a certain measurement, of stopping power or range, and $\tau_{th}^{(i)}$ the corresponding theoretical expression which is a function of I and of other parameters. Some of these parameters, like the particle velocity β_i, are regarded as known with sufficient accuracy, the others are still undetermined. Construct, for a set of n such results, the expression

$$S = \sum_{i}^{n} \left(\frac{\tau_{exp}^{(i)} - \tau_{th}^{(i)}}{\tau_{exp}^{(i)}} \right)^2 \quad . \tag{3}$$

The expression implies that one attributes to each experimental result a statistical weight proportional to $1/\tau_{exp}^{(i)\,2}$.

For the given set of experimental results $\tau_{exp}^{(i)}$, S is a known mathematical function of I and of the other parameters $\lambda_1, \lambda_2, \ldots$ to be adjusted. This function is then calculated by a computer program which locates the parameter values that yield a minimum

$$S\,(I, \lambda_1, \lambda_2, \ldots) = S_{min} \quad . \tag{3a}$$

The set of parameter values $(I, \lambda_1, \ldots)$ obtained by solving this equation is adopted as the "best fit" solution extracted from the given set of experimental data.

An estimate of the errors of these values—due to the occurrence of accidental experimental errors only—is obtained as follows: The error ΔI of I is obtained by finding on the computer the value $I + \Delta I$ such that

$$S\,(I+\Delta I, \lambda_1, \lambda_2, \ldots) = S_{min}\,(1+1/n) \quad , \tag{3b}$$

where n is the number of experimental measurements in the set. If $n > 10$, the factor for S_{min} is chosen to be 1.10. In Equation 3b the best-fit value of the other parameters $\lambda_1, \ldots$ (if any) is utilized. The errors $\Delta\lambda_1, \ldots$ are obtained by the same procedure. This procedure implies several approximations which are fairly realistic in the present application. The chief assumption is that the $\tau_{th}^{(i)}$ depend on I and on each of the other parameters (if any) through separate additive terms, which are independent of the index i, i. e., which are constant for the whole set of measurements under consideration. This assumption is clearly valid for I if the quantities τ have been suitably reduced in advance, and in particular if they are values of the variable X defined by Equation 4 (in Sec. 4). Another assumption is that the number of experiments in the set, n, is sufficiently large to be properly entered in Equation 3b instead of $n-\mu$ where μ is the number of parameters $I, \lambda_1, \lambda_2, \ldots$ fitted by Equation 3a.

4. Evaluation of Nielsen's Data

Preliminary Analysis

Nielsen's measurements of stopping power of protons and deuterons in beryllium, aluminum, nickel, copper, silver, and gold cover the energy range from about

1 Mev to about 4.5 Mev (Ref. 6). This energy range is not sufficient to give information about I and the shell corrections separately, but valuable information can nevertheless be obtained.

Under the circumstances, it is appropriate to compute the quantity

$$X = f(\beta) - (A/Z) \cdot (\xi_{exp}/K(\beta)) . \tag{4}$$

A typical plot of X versus particle energy is given for silver in Figure 1. The values for deuterons are plotted together with the proton data. It is immediately obvious that X is not a constant (in fact, X is just the energy dependent ln I′ of Williamson's representation and a measurement of the quantity $\ln I + \Sigma C_i/Z$ of Eq. 1). The order of magnitude of the accidental errors in the measurement is indicated by the scatter of the points about a smooth curve. Of course, any systematic errors in the measurement could not be discerned in this representation. (However, errors in the energy determination or other systematic errors might be responsible for the dip of the two deuteron values at about 4.4 Mev, indicated by the dotted line; but similar deviations do not appear for the other elements. Here it is obvious why it would be valuable to have independent overlapping data.)

To obtain an index of the accidental errors of the data, a "theoretical" value of ξ was obtained from

$$\xi_{th} = (Z/A) \cdot K(\beta) \cdot [f(\beta) - \overline{X}] , \tag{4a}$$

where $\overline{X}$ represents the value of X for the smooth curve fitted visually to the points. The fractional root mean square deviation of ξ was then computed and found to be 0.8 percent in the case of silver. For nickel, the result was 1.4 percent, and for aluminum, 0.7 percent. It thus appears that the statistical uncertainties in these measurements are somewhat smaller than estimated by Nielsen (1 to 3 percent).

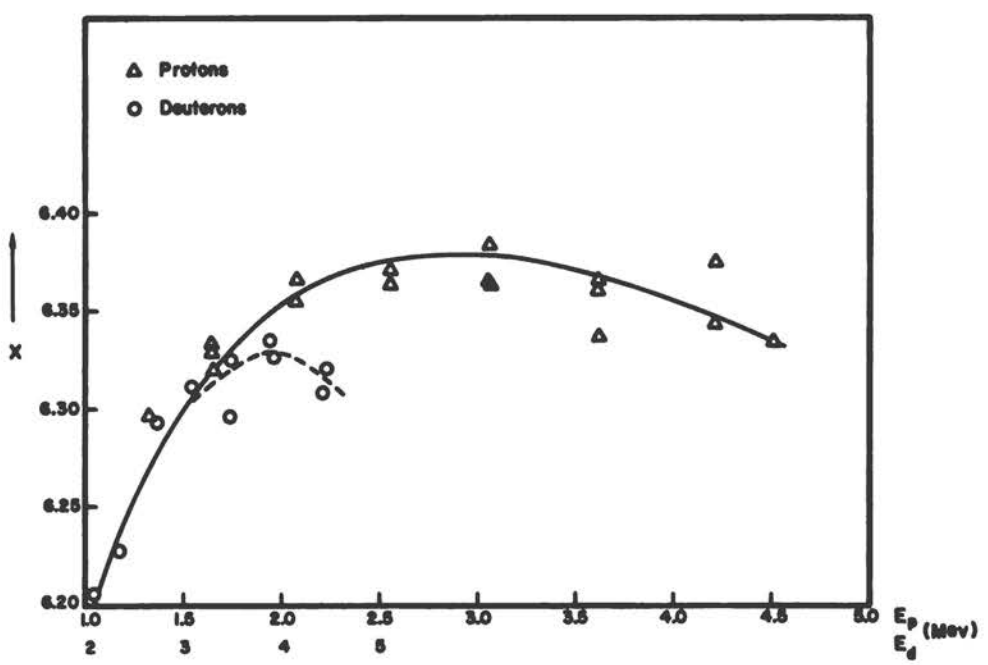

Figure 1. Nielsen's low-energy stopping-power data for silver. The quantity X is defined in Equation 4. The smooth curve is fitted visually.

It must be pointed out once more that no systematic errors are included in the above numbers; also, it has been assumed that equal weight can be given to each point.

Comparison with Range Data

Experimental range data for particle energies and materials comparable to those in Nielsen's experiment have been obtained at Rice Institute (Ref. 7). The absolute experimental accuracy was estimated by the authors to be about 0. 5 percent (including estimates of systematic errors), while internal consistency observations indicate accidental errors of about 0. 2 percent for aluminum, less than 0. 5 percent for nickel, and about 0. 1 percent for silver. The experimental ranges were corrected for multiple scattering. Since range differences ΔR are compared with the integrated reciprocal stopping-power values (the theoretical c. s. d. a. range),

$$\Delta R = R(E_p) - R(2\ \text{Mev}) = \int_{2\,\text{Mev}}^{E_p} 1/\xi\ dE\ , \tag{5}$$

where ξ represents the smoothed Nielsen data, several of the difficulties of range measurements thus are eliminated or reduced (e. g. , correction for final energy of proton, exact magnitude of multiple-scattering correction for the end of the range, asymmetry of distribution function).

In Table 1, the fractional differences between experimental range differences and the integrated stopping-power values are given. While the agreement for the two types of measurements is good for aluminum and nickel, the differences for silver are larger than the experimental errors.

TABLE 1

Comparison of Experimental Range Differences with Computed Differences Obtained from Nielsen's Stopping-Power Data

E_p Mev	Al	Ni	Ag	
2	0	0	0	Normalization
3	-0. 1%	0. 2%	1. 35%	
4	-0. 4%	0. 1%	1. 47%	
5	-0. 3%	0. 5%	1. 7%	

Use of Higher Shell Corrections

In an earlier paper (Ref. 5), it has been speculated that it should be possible to approximate the exact higher shell corrections by scaling the L-shell correction of Walske (Ref. 4). For nickel, for example, which has only a few electrons in the M-shell, an approximation with only one additional function should give satisfactory results. For gold, on the other hand, it may be necessary to use three or more functions, one or two for the M-shell, one or two for the N-shell, etc.

In a plot of shell corrections versus the squared velocity β^2 of the incident particle, let us call the scaling factor for the abscissa V, the one for the ordinate A (this corresponds to the factors 1/A1, B3, etc., in Reference 5, but is not identical with them). A computer program has been written which computes the quantity S defined in Equation 3 as a function of V, A, and the I-value. The smallest value of S for the Nielsen data is found, and the corresponding theoretical table is produced.

The result for nickel is the following: I = 307.5 ev; V = 6.0; and A = 1.2. This is in close agreement with the evaluation presented in Reference 5 for copper. It is noteworthy that the k = I/Z = 11.0 ev value obtained in this way is rather close to the value k = 11.2 ev obtained at high energies for copper (where the influence of the M-shell correction is quite small).

A similar evaluation for silver, using only one scaled L-shell correction (rather than 3 or 4 as was done in Ref. 5) gives I = 447.5 ev, V = 5.6, A = 3.0. It would appear that this approach is not too suitable for silver; in particular, the I-value is quite different from the high-energy value (presumably around 470 ev). In addition, the decrease in the I-value could be partly overcome by an increase in A. Anyway, the whole procedure has limited significance for silver because the experimental data only cover a small velocity range, and no separate fitting for the M-shell and N-shell has been carried out.

The two evaluations based on visual fitting of X and on scaling of shell corrections are compared in Table 2. It is seen that the agreement between the two approaches is excellent. Extrapolation of the values of $\overline{X}$ beyond the measured energy range would be inaccurate; e.g., notice the disagreements at 1 Mev and 5 Mev in Table 2. This also points out that any experimental approach to the determination of higher shell corrections requires very extensive measurements. On the other hand, the method using shell corrections would be expected to extrapolate quite well.

TABLE 2

Comparison of Stopping Power (in Mev/g cm^{-2}) Computed from Bethe Theory, Using a Two-Parameter Function for C_M (or C_L for Aluminum) with the Smoothed Experimental Function ($\overline{X}$) of Figure 1.

	Al		Ni		Ag	
E_p	($\overline{X}$) Mev	(C_L) Mev	($\overline{X}$) Mev	(C_M) Mev	($\overline{X}$) Mev	(C_M) Mev
1	172.4	171.9	126.8	127.5	93.7	93.3
1.5	133.3	132.4	100.8	100.6	74.8	74.9
2	109.9	109.5	84.6	84.8	64.0	64.1
2.5	94.2	94.0	73.5	73.7	56.4	56.6
3	82.8	82.7	65.4	65.7	50.7	50.9
3.5	74.2	74.1	59.3	59.5	46.4	46.3
4	67.4	67.3	54.4	54.4	42.9	42.6
4.5	62.0	61.8	50.5	50.3	40.0	39.6
5	57.4	57.2	47.4	46.8	37.5	37.0

5. Evaluation of MacKenzie's Data

Three sets of measurements are available from MacKenzie's work (Ref. 8): for proton energies of about 12, 20, and 29 Mev. The stopping-power ratio $S_e = \xi/\xi_{Al}$ is given for many elements. The computed quantity

$$Y = f(\beta) - S_e \left(f(\beta) - \ln 163 - (C_K + C_L)_{Al}/13 \right) - \ln Z \qquad (6)$$

should be almost a constant (it corresponds to the logarithm of the Bloch constant k, added to the shell corrections $\Sigma C_i/Z$ of each element).

The intercomparison between elements at different energies could be affected by errors in the assumed I-value and shell corrections for aluminum. The possible influence of these numbers can be seen in the following tabulation:

E_p	$f(\beta)$	$(C_K + C_L)/13$	$f(\beta) - \ln 163 - (C_K + C_L)/13$
12.0	10.153	0.068	4.991
19.8	10.641	0.046	5.501
28.7	11.000	0.033	5.873

The shell corrections for aluminum amount to only about 1 percent, and any inaccuracy will therefore not influence the intercomparision very much.

In Figure 2 the results are plotted, and, for comparison, the experiment by Bakker and Segrè (9) is included. The scatter of the Burkig and MacKenzie data approximates the error estimates of these authors and is far lower than that of the other authors.

One could, of course, regard the fluctuations in the figure as the expression of true fluctuations in atomic properties. This would seem an extreme point of view, but at present there is inadequate evidence to dismiss it altogether.

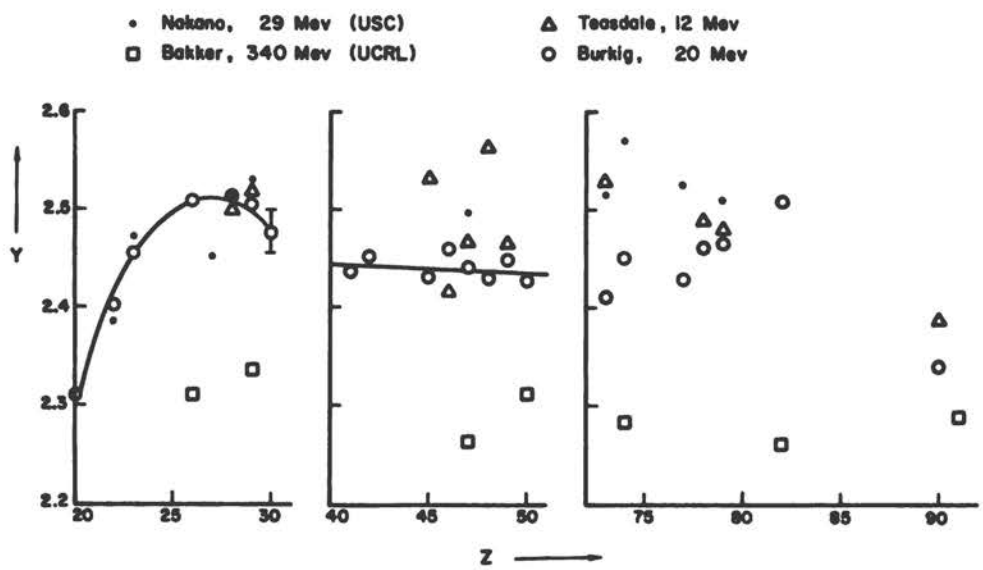

Figure 2. Evaluation of the relative stopping power for elements of atomic number Z. Plotted is the quantity Y defined in Equation 6.

A systematic dependence of Y on Z seems to exist for the light elements, since e^Y increases from about 10 to about 12.2 as Z increases from 20 to 27.

The results do not resolve any dependence of the shell corrections on energy between 10 and 30 Mev. For silver, the total shell corrections used in Reference 5 are 0.20, 0.15, and 0.13 for 12, 20, and 29 Mev, respectively. If k = 10.0 ev were used, the "experimental" shell corrections C_e for silver would be

$$C_e = Y - \ln 10 = Y - 2.303 \ ,$$

giving the result 0.162, 0.137, and 0.194 for the three energies. Since the quoted experimental error amounts to an error of about ±0.015 in Y, the agreement is satisfactory only for the 20-Mev measurement.

The values of Y at 300 Mev lie very decidedly below those obtained at lower energies, indicating a considerable reduction in the shell corrections with increasing energy. The shell correction for silver at 300 Mev is smaller than at the lower energies by a factor of 5 or 10. The spread between the points for silver and tin would indicate an accuracy of about ±1/2 percent in the measurements of S_e at 300 Mev.

6. Copper

Stopping Power at High Energies

In keeping with the general idea of this paper, to present data in a way which points up their inherent inconsistency, with minimum reference to theory, the stopping-power measurements for protons in copper at high energies (above 100 Mev) are given in Figure 3. The measured ratio of stopping power for copper and aluminum is plotted (Refs. 14-16) as a function of proton energy. It is unfortunate that the discrepancies amount to several times the quoted errors. For comparison, the corresponding ratio for theoretical values is given as a solid line. For aluminum, an I-value of 163 ev is chosen; for copper, I = 326 ev.

It should be pointed out that Reference 14 gives absolute values of stopping power for copper, and the I-values presented there (at 650 Mev, I = 300 ± 12 ev for Cu, and I = 136 ± 8 ev for Al) are therefore absolute.

Further comments are given in the conclusion of this section.

It has been noticed (in Ref. 16) that there is a discrepancy between the "total range" measurements and the "difference" measurements of this experiment. Consult Table 5 of Reference 16, where the theoretical value of the ratio of stopping powers (using the I-value found from the range measurement) is about 1 percent smaller than the experimental value.

Ranges

Since quite a few range measurements are available, including several absolute values, it may be appropriate to use for this problem the approach using the full Bethe theory. It is assumed that the aluminum range curve is correct, and relative total range measurements (Refs. 16,17) are converted into absolute ranges. It should be pointed out that in Reference 17 a discrepancy exists in the table entry of 75.8 mg cm^{-2} for copper and 65.8 mg cm^{-2} for aluminum (the same numbers appear

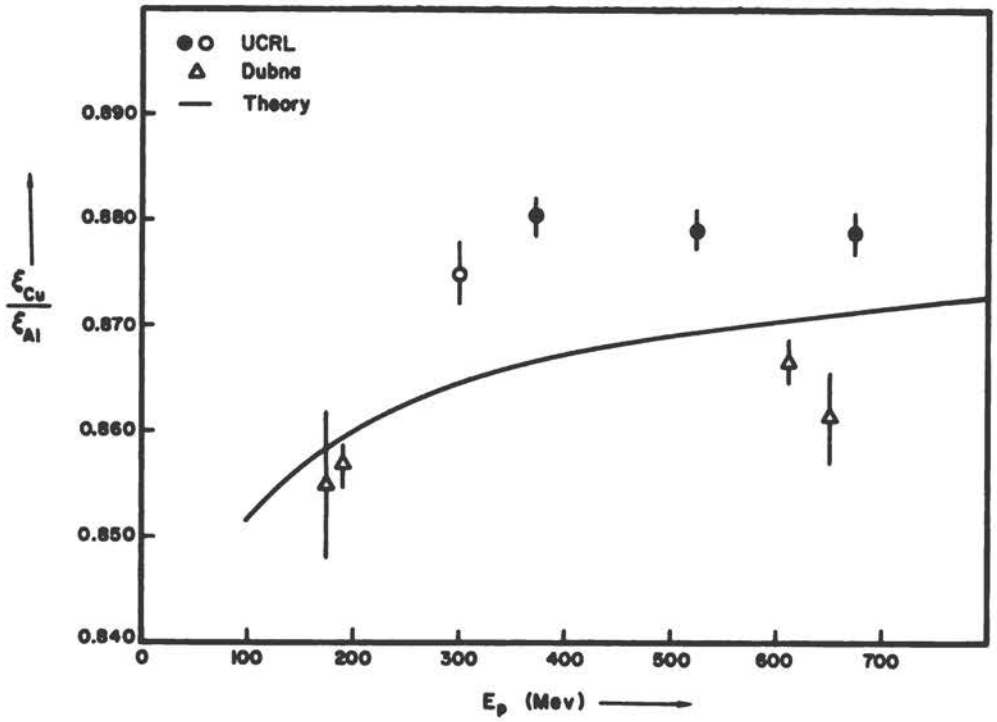

Figure 3. Relative stopping power for high-energy protons in copper and aluminum. The theoretical values are computed with I = 163 for Aluminum and I = 326 ev for copper.

in the Russian original). This value will be disregarded for the present purposes. Not considering any other results, the I-value and the two parameters for the M-shell correction are allowed considerable leeway for the computation of S. The minimum appears for I = 326 ev with an uncertainty of about ±3 ev, with $1/V = 7 \pm 1$, $A = 1.3 \pm 0.4$. For these parameters, $S_{min} = 5.46 \times 10^{-4}$, which gives an average standard error of ±0.6 percent for the individual measurements. The comparison of experimental and theoretical best-fit data is given in Table 3. It will be noticed that the over-all accuracy is influenced considerably by the measurements at 150 and 200 Mev.

The measurements by Bloembergen (Ref. 18) corrected for multiple scattering—using the same scaling factors for C_M as above—give a best fit for I = 349 ± 5 ev (accidental error only!). The average error for each measurement is ±0.7 percent. A systematic deviation seems to exist: the eight measurements between 76 and 102 Mev are all larger than the theoretical values (by ~ 0.4 percent on the average); the seven measurements from 44 to 73 Mev and from 108 to 114 Mev are smaller than theoretical values for I = 349 ev. This is a rather marginal effect, of course.

If the data are compared with a theoretical curve with I = 330 ev, the experimental ranges are on the average larger than the theoretical ones by 1.2 percent.

This deviation lies somewhat outside of the quoted experimental error.

These data are very insensitive to the choice of V and A.

TABLE 3

Comparison of Experimental and Theoretical Proton Ranges in Copper (I = 326 ev)

E_p Mev	R_{exp} (g cm^{-2})	R_{th} (g cm^{-2})	$\frac{R_{th}-R_{exp}}{R_{exp}}$ (%)
2	0.0164	-	-
3	0.0308	0.03084	0.1
4	0.0486	0.04873	0.3
5	0.0698	0.06987	0.1
6	0.0937	0.0941	0.4
7	0.1207	0.1213	0.5
10	0.2200	0.2201	0.0
18	0.5995	0.5985	-0.2
148.6	23.8	23.53	-1.1
190.1	36.4	35.78	-1.7
279.9	68.6	68.22	-0.6
340	93.4	93.61	0.2
473.3	157.9	157.9	0
658	258.3	259.7	0.6
663	263.0	262.6	-0.1
750	313.66	314.3	0.2

Low-Energy Stopping Power

For the measurements between 0.5 and 4.5 Mev (Refs. 20, 6) and at 12, 20, and 29 Mev, a least-squares fit has been made. The minimum S appears for I = 320 ± 2 ev, 1/V = 7.0 ± 0.7, A = 1.3 ± 0.1. It is to be expected that A (the amplitude of the M-shell correction) will be determined quite accurately; on the other hand, the dependence on V is rather insensitive.

Here, $S_{min} = 6.7 \times 10^{-4}$, $\sigma = 0.5$ percent. A secondary minimum appears at I = 310, 1/V ~ 6.1, A ~ 1.5. Here, $S = 10.6 \times 10^{-4}$.

For the 31 stopping-power values (raw data) of Nielsen (6), the smallest S is obtained for I = 310 ev, 1/V = 6.0, A = 1.5, and $S = 4.46 \times 10^{-3}$ for an average error per measurement $\sigma = \pm 1.2$ percent, with no systematic deviations apparent. For 1/V = 7.0, A = 1.3, and I = 320 ev, a value $S = 4.85 \times 10^{-3}$ is obtained; thus, the fit is almost as good.

Conclusion

Stopping-power results below 30 Mev and ranges at all energies (with exception of those of Ref. 18) give I-values separated by approximately the arithmetic sum of their accidental errors.

On the whole, the situation is rather unsatisfactory. The Dubna report (Ref. 14) does not describe well enough the method used for one to judge its merits. If the errors quoted are taken at face value, the discrepancy between the Dubna and the Berkeley measurements is considerable.

It appears that an I-value of 326 ev will be most satisfactory at this moment. This approximately splits the difference between the high-energy stopping-power data. It is not satisfactory for the stopping power from 0. 5 to 4. 5 Mev (systematically off by about 0. 8 percent), but it works out all right for the stopping power at 20 and 29 Mev (±0. 4 percent), and for most of the ranges discussed.

7. Aluminum

Range Measurements

Above a proton energy of 1. 4 Mev, the experimental information about stopping power and ranges for aluminum is fairly satisfactory. The range measurements between 3 and 18 Mev are quite accurate (Ref. 3) and allow the determination of the I-value with reasonable accuracy. The values below 3 Mev have not been used for the present calculation; their inaccuracy may be slightly larger, and the uncertainty in the L-shell correction would increase the uncertainty in I.

The least-squares fit gives I = 163. 2 ev with a statistical error of ±0. 7 ev. The average accidental error of each measurement amounts to 0. 2 percent. This is in close agreement with the result of Reference 3. The ranges are given in Table 4.

The range data by Bloembergen and Van Heerden (18) would yield S_{min} for I = 166 ev, with an accidental error of about ±3 ev. The average error σ per data point is about 0. 86 percent. For I = 163 ev, σ = 0. 91 percent, the results are given in Table 5.

The alpha particle measurements in aluminum at Yale (Ref. 13) give an error of about ±0. 8 percent for each data point and agree with the computed curve for I = 163 ev to within 0. 3 percent on the average, but no S analysis has been made so far.

The difference between the computed value corresponding to Table 4 and the single range measurement at U. C. L. A. (Ref. 19) amounts to 0. 7 percent and is at least twice the sum of quoted errors. The measurements of currents of this work could conceivably cause some error, otherwise the discrepancy is unexplained.

The measurement by Simmons (23) is about 0. 5 ± 0. 5 percent lower than the entry in the present table. No check has been made for the underlying assumptions in Reference 23.

TABLE 4

Proton Ranges in Aluminum for 3 to 18 Mev, I = 163. 2 ev

E_p Mev	R_{exp} (g cm^{-2})	R_{th} (g cm^{-2})	Δ (%)
3. 062	0. 02296	. 02289	-0. 3
4. 023	0. 03590	. 03590	-
5. 038	0. 05254	. 05236	-0. 3
5. 504	0. 06076	. 06081	+0. 1
6. 150	0. 0733	. 07345	+0. 2
11. 820	0. 22712	. 22704	-0. 03
14. 971	0. 34376	. 34350	-0. 08
17. 836	0. 46844	. 46756	-0. 19

TABLE 5

Proton Ranges in Aluminum (Bloembergen Data), I = 163 ev

E_p Mev	R_{exp} (g cm^{-2})	R_{th} (g cm^{-2})	Δ (%)
34.96	1.547	1.543	-0.3
37.16	1.757	1.720	-2.1
39.66	1.928	1.931	0.2
42.57	2.198	2.191	-0.3
44.86	2.402	2.405	0.1
47.67	2.634	2.680	1.7
52.08	3.189	3.137	-1.6
52.33	3.188	3.164	-0.8
56.68	3.687	3.647	-1.1
56.96	3.784	3.679	-0.7
61.79	4.258	4.252	-0.1
62.10	4.280	4.290	0.2
65.78	4.756	4.753	-0.1
66.10	4.786	4.794	0.2
72.94	5.773	5.709	-1.1
73.05	5.714	5.724	0.2
75.70	6.141	6.098	-0.7
75.84	6.078	6.118	0.7

The range at 340 Mev measured in Berkeley (Ref. 15) is smaller by about 1.15 percent than the computed value for I = 163 ev. Unpublished estimates of diffraction (or shadow) scattering indicate that this effect has reduced the experimental range by approximately 0.5 ± 0.25 percent. If this correction were applied, the difference (0.65 percent) would be only slightly larger than the experimental error (0.5 percent or maybe somewhat more). Further accurate, absolute measurements at high energies evidently would be desirable.

The very small I-value for aluminum obtained at Dubna (Ref. 14) is related to the small I-value for copper, and it appears preferable to neglect this result at this time.

Stopping-Power Measurements

The measurement of absolute stopping power for protons of 17.8 Mev at U. C. L. A. (Ref. 21) gives an I-value of 163 ev, with a fairly small error (unpublished evaluation by H. Bichsel). The measurements for the other elements of this reference seem to be unreliable.

The only other set of measurements with fairly good accuracy is found in Reference 6, for protons between 1.4 and 4.5 Mev. While the table for aluminum presented in Allison's summary article (Ref. 24) agrees with the data of Reference 6 to within about ±2 percent, the situation at lower energies is described aptly by Whaling (Ref. 20, p. 197): "The experimental values are in poor agreement and do not fix the position of the curve." Whaling also omits a set of data lying 15 percent below his adopted curve. This makes a comparison with Bethe's theory difficult.

The Shell Corrections

While Walske's K-shell corrections presumably are reliable, his L-shell corrections are not valid for $Z < 30$, and thus would not apply for aluminum. An attempt has nevertheless been made to scale the L-shell correction given by Walske for $Z = 30$ to the use for aluminum. It is expected that the maximum for C_L occurs for a proton energy between 0.25 and 0.5 Mev. Since there are essentially two sets of data for this energy range (Refs. 22, 24), differing by about 20 percent, it is quite impossible to determine C_L experimentally. For the measurements above 1.4 Mev, any change in the energy-scaling parameter for C_L can be compensated by a corresponding change in the scale of magnitude of C_L. A satisfactory fit to the Nielsen data can be obtained by using an unchanged energy scale for C_L, i.e., by setting $Z = 13$ in the computation of η_L (the Walske parameter) and reducing C_L by 30 percent. This fit is shown in Table 6.

TABLE 6

Nielsen's Stopping-Power Data for Aluminum. I = 163 ev, Stopping Power in Mev g^{-1} cm^2

E_p Mev	ξ_{exp}	ξ_{th}	Δ (%)
1.487	134.2	134.0	-0.2
1.596	127.9	128.1	0.1
1.610	127.3	127.3	0.0
1.689	123.3	123.3	0.0
1.697	122.8	122.9	0.1
1.913	112.5	113.2	0.7
1.922	112.9	112.9	0.0
1.990	110.9	110.3	-0.6
2.032	108.2	108.7	0.5
2.052	107.8	108.0	0.2
2.161	103.2	104.2	1.0
2.173	103.2	103.8	0.6
2.473	95.1	94.96	-0.1
2.495	95.8	94.38	-1.5
2.524	93.0	93.62	0.7
3.017	82.6	82.56	-0.1
3.024	82.1	82.42	0.4
3.043	82.3	82.05	-0.3
3.547	73.8	73.52	-0.4
3.574	72.9	73.13	0.3
3.587	72.3	72.93	0.9
4.142	66.2	65.70	-0.8
4.150	65.7	65.60	-0.1
4.175	66.0	65.32	-1.0
4.187	64.4	65.18	1.2
4.188	65.4	65.17	-0.4
4.436	63.0	62.48	-0.8
4.508	61.6	61.74	0.2

Conclusion

While the I-value for aluminum would appear to be reasonably close to 163 ev at the moment, it is by no means certain that it will not change again. Three approaches are possible to obtain a more definite result:

(a) Measure stopping power or range differences at fairly large energies (protons between 100 and 1000 Mev) with an absolute accuracy of about 0. 1 percent, and for many different energies.

(b) Measure the stopping power below 1. 4 Mev absolutely with an accuracy of 1 percent or better, or measure relative stopping power below 2. 5 Mev with the same accuracy.

(c) Measure range differences (or stopping power) with very high accuracy at intermediate energies.

8. Measurements with Tritons below 3 Mev

Range-difference measurements with tritons of energy 2. 736 Mev, using thin foils to reduce the particle energy and detecting the reduced energy with a silicon detector, have been made at Oak Ridge (Ref. 25). For nitrogen, air, aluminum, argon, and nickel, the results of a least-squares analysis, according to Equation 3, are presented in Table 7. The average accidental error $\sigma = \sqrt{S/n}$ of each of n data points is given. A second analysis using the best values I' for I obtained in other measurements (Secs. 7, 9) has been made. The error σ' obtained is much larger, and it would appear that considerable systematic errors are present (possible sources of systematic errors might be surface effects on the aluminum foil, details of self-absorption in the source foil, etc.). The present analysis was made with the points of Figure 3 of Reference 25.[3] Measurements for energies below 1. 4 Mev were not evaluated because of charge-state effects, but they might supply useful information in this connection.

TABLE 7

Least-Squares Fits for Triton Measurements.
I' is the Best Value for I Found in Other Measurements.

Element	I(ev)	σ(%)	I'(ev)	σ'(%)
N_2	90	±0. 36	78	±2. 3
Air	94	±0. 4	84	±2. 0
Al	155	±0. 2	163	±0. 9
Ar	212	±0. 3	184	±3. 5
Ni	310	±0. 4	307. 5	±1. 0
Kr	380	±0. 3	360	~±1

[3] I am grateful to Dr. Bishop for supplying me with the raw data of Figure 3 of his paper.

9. Measurements in Gases

Measurements with Natural Alpha Particles

The experimental data used for this evaluation are shown in Tables 8 and 9. While the range measurements are fairly old (Ref. 10), the energy determinations are recent (Ref. 11). In an analysis of both alpha and proton data it was found that a small L-shell correction has to be introduced (Ref. 12). One can write approximately $C_L = 2.5 \times 10^{-4}/\beta^2$ for nitrogen, oxygen, and air. For the K-shell, the full value given by Walske has been used. For nitrogen and oxygen, the comparison of experimental and theoretical data for the best fit is given in Table 8. It is seen that the accidental errors are very small for nitrogen, while they are slightly larger for oxygen. The experimental accuracy is quoted to be around 0.1 percent.

TABLE 8

Ranges in mg cm^{-2} of Alpha Particles in Nitrogen and Oxygen

E_α Mev	N_2			O_2		
	R_{exp}	R_{th} (I=76.8 ev)	%	R_{exp}	R_{th} (I=99)	%
5.305	4.58	4.580	-	4.90	4.900	-
6.062	5.64	5.636	-0.07	6.05	6.033	-0.28
7.687	8.23	8.232	+0.03	8.83	8.812	-0.20
8.785	10.23	10.231	+0.01	10.92	10.948	+0.26

The associated errors from statistics for the I-value for nitrogen and oxygen are ±0.2 ev and ±1.2 ev, respectively. It will be noticed that the theoretical ranges were normalized at $E_\alpha = 5.305$ Mev, so charge-state effects should have very little influence. There is a discrepancy between the k-values (I/Z ratios) for nitrogen and oxygen: 11.0 ev and 12.4 ev. It is not clear whether this is a true difference or whether it is due to systematic errors.

For air, a total of 17 experimental range values are available. The best fit is obtained for I = 84.0 ev with $\sigma = 1.35 \times 10^{-3}$, and the estimated statistical error for I is about ±0.25 ev. The data used are given in Table 9.

The value for Z used in the calculation for air is 7.22, according to Bethe's suggestion, and the atomic mass A = 14.485. It should be pointed out that the combination of theoretical stopping power obtained here for nitrogen, oxygen, and argon is larger by about 0.5 percent than the stopping power for air. No obvious explanation comes to mind.

Measurements at Yale

Differential range measurements with accelerated helium ions of energies up to about 44 Mev were made by Martin and Northcliffe (13). For nitrogen, the best I-value was 77.7 ev, with an error of about ±0.5 ev. This is in good agreement with the data for natural alphas.

TABLE 9

Ranges of Natural Alpha Particles in Air

E_α Mev	R_{exp} (cm)	R_{th} (I=84.0 ev) (cm)	%
5.305	3.842	3.842	-
5.482	4.051	4.042	-0.23
5.996	4.657	4.646	-0.23
6.062	4.730	4.727	-0.06
6.278	4.984	4.995	+0.22
6.278	5.004	4.995	-0.18
6.622	5.429	5.435	+0.10
6.775	5.638	5.636	-0.04
6.818	5.692	5.693	+0.01
7.384	6.457	6.468	+0.17
7.687	6.907	6.902	-0.08
8.277	7.792	7.781	-0.14
8.785	8.570	8.574	+0.05
9.065	9.040	9.027	-0.14
9.492	9.724	9.737	+0.13
10.506	11.51	11.517	+0.06
10.543	11.58	11.584	+0.04

For argon, the best fit was obtained for I = 183 ev ± 2 ev, using both C_K and C_L. This compares well with the natural alphas, where I = 185 ev, using the Walske theoretical values of C_L.

Stopping-Power Measurements for Protons

Except for one measurement (Ref. 27) at about 4.5 Mev, all data are obtained for energies below 1 Mev. Also, the errors given by the authors are usually quite large, so that the following determination of I-values, etc., is not very reliable. While the I-value for argon for the alpha particles was about 184 ev, the best fit for the protons appears at 205 ev, and for the triton data from Oak Ridge a value somewhat above 210 ev is required (see Section 8).

For protons in nitrogen, the best fit is obtained for I = 92 ev, which is substantially higher than the value for alphas.

It thus appears that there is a fairly large inconsistency between measurements for protons and alpha particles, and the usual conclusion is reached—more measurements will have to be made, if definite information is desired.

10. Conclusion

Of all the experimental data that have come to my attention, only those discussed in the preceding sections have been analyzed completely. The remaining data

have been examined sufficiently to indicate the absence of major disagreements (other than those discussed in this report) and to indicate little prospect of obtaining a better determination of I and of the shell corrections.

While it appears on the whole that the Bethe theory describes the stopping phenomena satisfactorily, it must also be understood that only for aluminum is it possible to give information with an accuracy of about one-half of 1 percent. For all other elements the accuracy is not much better than 5 percent except in some isolated regions. Uncertainties are encountered both for the I-values and for the shell corrections.

To obtain stopping power and range energy information with an accuracy of 1 percent or better, it will be necessary to obtain accurate measurements over an extended energy region for several different elements. It is hoped that neighboring elements will show I-values and shell corrections which vary smoothly with Z (or at least the observed electron excitation potentials). This is by no means certain; for example, the ratio of stopping power of copper and nickel below 1 Mev changes considerably. For the light elements ($Z < 36$) it should be possible to obtain a fairly good understanding of the behavior of the stopping power once the I-values are determined well. The scaling procedure used to obtain M-shell corrections seems to work satisfactorily, even though it would be desirable to have a more reliable check for krypton (see Fig. 5 of Ref. 5). It is not even clear whether any reliable information is available about the I-value of krypton. It appears undesirable to determine the I-value of a material based on one measurement at a single energy. Also, the discrepancy between the I-values obtained for some gases for protons (stopping power with only fair accuracy) and alphas (ranges with good accuracy) is rather discouraging.

For the heavier elements, it will be necessary to obtain extensive, accurate information for a better understanding of the shell corrections. I believe that for gold (or another element with $Z > 70$) it will be necessary to make measurements over an energy range of 1 to 30 Mev (the Nielsen measurements cover some of this); and for the medium-weight elements ($Z \sim 50$), measurements from 1 to 15 Mev will be necessary. For these elements it would also be desirable to have absolute measurements at many energies with protons between 50 and 200 Mev in order to be able to determine the I-values. The hope is that the higher shell corrections in this energy region could be represented by

$$\sum_{i=M}^{P} C_i = K_c/\beta^2 ,$$

so that only two parameters would have to be determined (the I-value and K_c).

There are so many free parameters in the theory that many measurements are required to determine all of them reliably. This is, of course, the reason why our present knowledge is rather unsatisfactory.

11. Acknowledgments

Support by the Atomic Energy Commission for the research of this report is gratefully acknowledged. The facilities of the Western Data Processing Center at U. C. L. A. (IBM 7090 and 7094 computers) and of the Computer Center of the University of Southern California (H-800 computer) have been used for the computations

of this report, and their availability is gratefully acknowledged. In the final preparation of the manuscript, Dr. Fano was very helpful, and I am grateful for his cooperation.

Drs. Sternheimer, Platzman, and Turner contributed greatly to my understanding of the subject, and I thank them for their help.

12. Appendix

The parameters determined in this report are influenced by the values of the fundamental atomic constants. It may be of interest to note that the famous value I = 80.5 ev for air apparently was computed with $e = 4.77 \cdot 10^{-10}$ esu, so that the present-day value of 84 ev shows a change mainly for this reason. For the computer program used for the evaluations of this report, the following values of basic constants were used (mainly from Cohen et al., Rev. Mod. Phys. 27, 363, 1955):

Electron radius	$e^4/m^2c^4 = r_0^2 = 7.94030 \cdot 10^{-26}$ cm^2
Avogadro's number	$N_0 = 6.02486 \cdot 10^{23}$ g/mole
Electron mass	$m_0 = 0.510976$ Mev
Proton mass	M = 938.213 Mev
Deuteron mass	1875.496 Mev
Triton mass	2808.7 Mev
Alpha mass	3727.147 Mev

The following is a list of the atomic weights used:

Element	Z	A
Beryllium	4	9.013
Nitrogen	7	14.008
Air	7.22	14.485
Oxygen	8	16.000
Aluminum	13	26.98
Argon	18	39.944
Nickel	28	58.71
Copper	29	63.54
Silver	47	107.880
Gold	79	197.0
Lead	82	207.21

References

1. U. Fano, Am. Rev. Nucl. Sci. 13, 1963. Reprinted as Appendix A to the present volume.

2. Hans Bichsel, Section 8c (pages 8-20 to 8-47) of American Institute of Physics Handbook, 2nd ed., (McGraw Hill, New York, 1963).

3. H. Bichsel and E. A. Uehling, Phys. Rev. 119, 1670 (1960).

4. M. C. Walske, Phys. Rev. 88, 1283 (1952); and 101, 940 (1956).

5. Hans Bichsel, Tech. Report No. 3, Physics Department, University of Southern California (June 21, 1961), and Appendix.

6. L. P. Nielsen, Kgl. Danske Videnskab. Selskab. Mat. Fys. Medd 33 (6) (1961).

7. H. Bichsel and B. J. Farmer, Bull. Am. Phys. Soc. 5, 263 (1960).

8. V. C. Burkig and K. R. MacKenzie, Phys. Rev. 106, 848 (1957); G. H. Nakano, H. Bichsel, and K. R. MacKenzie, Phys. Rev. 132, 291 (1963); and J. G. Teasdale, Tech. Report No. 3, Department of Physics. University of California, Los Angeles (Dec. 20, 1949).

9. C. J. Bakker and E. Segrè, Phys. Rev. 81, 489 (1951).

10. Bogaardt and Koudijs, Physica 17, 703 (1951).

11. A. Rytz, Helv. Phys. Acta 34, 240 (1961).

12. H. Bichsel, Bull. Am. Phys. Soc. 6, 519 (1961).

13. F. Martin and L. C. Northcliffe, Phys. Rev. 128, 1166 (1962), and earlier papers.

14. Prokoshkin and Vasilevsky, Report D566 of the Laboratory of Nuclear Problems, Dubna, U. S. S. R. (1960).

15. R. Mather and E. Segrè, Phys. Rev. 84, 191 (1951).

16. S. Von Friesen and W. H. Barkas, Nuovo Cim. Suppl. 19, 41 (1961).

17. B. V. Rybakov, J. Exp. Theor. Phys. (U. S. S. R.) 28, 651 (1955). Transl. JETP 1, 435 (1955).

18. Bloembergen and Van Heerden, Phys. Rev. 83, 561 (1951).

19. E. L. Hubbard and K. R. MacKenzie, Phys. Rev. 85, 107 (1952).

20. W. Whaling, Handbuch der Physik, 34, p. 202, Springer Verlag, Berlin (1958).

21. Sachs and Richardson, Phys. Rev. 83, 834 (1951).

22. Bader, Pixley, Mozer, and Whaling, Phys. Rev. 103, 32 (1956).

23. D. H. Simmons, Proc. Phys. Soc. (London) A65, 454 (1952).

24. S. K. Allison and S. D. Warshaw, Rev. Mod. Phys. 25, 779 (1953).

25. Wolke, Bishop, Eichler, Johnson, and O'Kelley, Phys. Rev. 129, 2591 (1963).

26. A. Dalgarno, Proc. Phys. Soc. 76, 422 (1960).

27. J. E. Brolley and F. L. Ribe, Phys. Rev. 98, 1112 (1955).

3. ON THE EXPERIMENTAL VERIFICATION AND DETERMINATION OF PARAMETERS OF STOPPING-POWER THEORY

J. E. Turner[1]

Abstract

Stopping power and range measurements are reviewed from the standpoint of general verification of stopping-power theory and the determination of the parameters of the theory. Certain experiments stand out in this respect in providing coverage of a wide range of chemical elements and/or incident particle energies. Experiments are analyzed on the basis of information they furnish, particularly with respect to mean excitation energies, I, and shell corrections. The value I = 163±1 ev for aluminum appears to be well established in the literature, and is taken as an anchor point in the analysis of data. In general, high-energy experiments (e. g., with protons of several hundred Mev) furnish direct information about mean excitation energies. Experiments at lower energies provide information on the variation of shell corrections with incident particle energy and with atomic number. The information provided collectively by the experiments discussed is displayed in summary form.

1. General Considerations

Understanding of the passage of charged particles through matter is based on the theory presented in Appendix A of this volume. The theory can be tested experimentally, in principle, by direct measurement of the rate of energy loss and range that it predicts in specific cases. In practice, however, only a relatively small number of physical systems are amenable to exact or nearly exact theoretical treatment in terms of universal constants, even within the bounds of the theory itself, and practical considerations limit the number of materials with which experimental work is feasible. As a consequence of this situation, whereas the theory as a whole rests on a firm experimental basis, verification of details and determination of the parameters of the theory are by no means exhaustive.

It is the purpose of this report to review in a general way the over-all picture with respect to the experimental information now available on stopping power. More detailed analyses of data for various stopping materials, with respect to energy and charge of incident particle and the kinds of measurements available, are given in the reports of Bichsel (Report No. 2) and Northcliffe (Report No. 8, and Appendix B) in this volume. The present report complements that of Bichsel in regarding the data from the general point of view of verification of the theory and determination of parameters. The important questions of consistency of the data and best numerical values available are treated in Bichsel's report. For other detailed reviews the reader is referred to References 10 and 17.

[1]Oak Ridge National Laboratory, Oak Ridge, Tenn.

In the literature experimental values are reported for stopping power, range, and/or mean excitation energies. For a given stopping material these quantities are related by theory, so that values reported for one quantity can generally be expressed alternatively in terms of values for the others.[2] In cases in which mean excitation energies, I, are reported, it should be noted that the quantity I defined by Equation 34 of Appendix A is not determined directly by measurement.[3] Where an experimental value of I is reported, the value has been inferred from measurements of stopping power and/or range. In order to obtain I from these measurements one has to evaluate all quantities, except I, that appear in Equation 38 of Appendix A. The main uncertainty in doing this usually lies in the evaluation of the shell-correction term, C/Z. The significance of this evaluation is discussed more fully with respect to specific experiments in the following pages.

2. Data for the Chemical Elements

For the lighest elements, theory and experiment are in agreement. The data reported in Table 1 of Appendix A show that, to within experimental uncertainties (which are of the order of 5-10 percent), calculated and observed mean excitation energies for hydrogen, helium, lithium, and beryllium[4] are the same. Calculations of mean excitation energies for more complex stopping materials are in progress at the present time (Ref. 13).

Measurements are available for most light elements in pure form or in compounds. The mean excitation energies for the light elements depend upon the state of chemical combination of the atom.[5] It is notable that, except for the work of Thompson (16), systematic stopping-power measurements, at least at high energies, do not appear to have been made on light atoms in various states of chemical binding. Thompson reported proton stopping-power measurements made with hydrogen, carbon, nitrogen, oxygen, and chlorine in compounds. With the exception of chlorine, the mean excitation energies reported for these elements showed a wide variation (for example, over 20 percent in the case of nitrogen), which was attributed to different chemical binding of the atom in different molecules. Presumably for chlorine and heavier elements chemical binding effects are negligible. Thompson's measurements are now over a decade old and could be profitably repeated and extended.

Extensive stopping-power measurements have been carried out with aluminum. Probably the most reliable value of the mean excitation energy for an element with an atomic number greater than 10 is that for aluminum. Shell corrections for that element are not large, and their contribution to stopping power can be estimated with sufficient accuracy. The value I = 163±1 ev for aluminum is well established through

---

[2]The reader is cautioned, however, that there is nonuniformity in the literature with respect to both terminology and the handling of the theory itself. For example, some authors treat the mean excitation energy, I, as an energy-dependent parameter of the theory rather than as the constant defined by Equation 34 in Appendix A.

[3]See Report No. 6 of this volume for a more detailed discussion of this point.

[4]In the case of Be, however, reported I-values range from 56 ev (Ref. 11) to 64 ev (Ref. 7).

[5]See Report No. 6.

many measurements appearing in the literature (Ref. 4). Support of this value also comes from the bulk of the evidence summarized in Reference 10, showing that the average of the absolute measurements cited there yields I = 163 ev.[6]

Next to aluminum, the most extensively investigated heavier element is copper, but at present there is uncertainty about the exact value of the mean excitation energy of this element. The two most important recent experiments with copper are those of Barkas and von Friesen (2) and of Zrelov and Stoletov (18). These investigators report, respectively, the values I = 323 ev and I = 305 ev. In a plot of the ratio of mean excitation energy and atomic number as a function of the latter,[7] these experimental values are seen to lie on either side of the line describing the general trend of the elements. This suggests that the actual value for copper is probably close to the average of 323 and 305, i.e., close to 314 ev.

Less extensive data exist for many other elements throughout the periodic table. Stopping-power measurements have been made for a number of elements relative to aluminum and copper. Much of the data is summarized and evaluated in the reviews already cited (Refs. 5,10,12,17).

3. Data for Other Materials

Stopping-power measurements have been made with a large number of compounds and mixtures. The most extensively studied substances other than pure elements are air and emulsion. The National Bureau of Standards Handbook 79 (Ref. 10) adopts a value of 85 ev for the mean excitation energy for air, which is in essential agreement with Brolley and Ribe's proton stopping-power measurements (Ref. 6) and with the result I = 84 ev of Bichsel's analysis of alpha particle range data (Ref. 5). The value 84-85 ev is also compatible with an estimation (Ref. 10) based on the weighted average of Thompson's I-values for nitrogen and oxygen. However, this value does not appear to be in good agreement with other proton data. As discussed in Report No. 2, the I-values for nitrogen and argon determined from available proton measurements at energies below that of the Brolley-Ribe experiment are some 10 percent larger than the I-values obtained from the alpha particle data. These discrepancies are unexplained at the present time.

From range measurements with protons, Barkas and von Friesen (2) reported the experimental value 328 ev for the mean excitation energy of photographic emulsion. From the chemical composition given for the emulsion used, and from the I-values of the individual elements, one would expect on the basis of the Bragg rule that the mean excitation energy for emulsion would be very close to 300 ev. This discrepancy is also unexplained at the present time.

4. Key Experiments

From the wealth of information available, certain experiments play a key role from the standpoint of the verification of stopping-power theory itself and the

---

[6] Low values for Al (I = 136±8 ev) and for Cu (300±12 ev) were reported from high-energy measurements at Dubna. Bichsel has analyzed these results in comparison with independent experiments in Report No. 2 of this volume. His analysis suggests that the Dubna values not be accepted at face value without further evaluation of the experimental method.

[7] See Figure 1 in Report No. 6 of this volume.

determination of parameters of the theory. Estimates of shell corrections over a wide range of energies for a number of elements are shown in Figure 6 of Appendix A. From these curves and the error bars shown (corresponding to 1 percent uncertainty in the stopping power) one sees that shell corrections are not very significant for the light elements at high energies, but that this is not the case for heavy elements. For example, with protons in aluminum, Figure 6 in Appendix A shows that, above about 15 Mev, shell corrections contribute less than 1 percent to stopping power. For protons in lead, on the other hand, the corresponding energy is about 320 Mev. In the following pages, experiments will be considered on the basis of the knowledge they provide about stopping power and, more particularly, on the basis of the information they provide specifically about I and about shell corrections.

Thompson (16) measured the stopping power for protons with a mean energy of 270 Mev in hydrogen, carbon, nitrogen, oxygen, and chlorine relative to copper. With reference to what has just been said, the shell corrections for these elements for 270 Mev protons have a negligible effect on stopping power, so that Thompson's measurements represent a direct determination of I. In making relative stopping-power measurements, part of a standard absorber, say copper, is replaced by a thickness of the substance under investigation that gives the same amount of slowing down in a given incident particle energy range as the removed copper. From Equation 38 in Appendix A, with negligible shell corrections and density effect, one can express the stopping power per electron, ϵ, of a substance in the form

$$\epsilon = -\frac{1}{NZ}\left(\frac{dE}{ds}\right) = f(v)\,\{\,F(v) - \ln I\,\}\ ,$$

where f and F are the known functions of the incident particle speed v given by Equation 38 in Appendix A. Measurement of the thickness of a substance equivalent to a given thickness of copper at a given incident particle speed yields directly the ratio of the stopping power per electron in the material relative to that in copper at the given speed. Using the subscripts 1 and 0 to denote, respectively, the material under investigation and the copper or other standard absorber, one can write for this ratio

$$\frac{\epsilon_1}{\epsilon_0} = \frac{F(v) - \ln I_1}{F(v) - \ln I_0}\ .$$

Determining ϵ_1 / ϵ_0 experimentally thus provides a value of I_1 in terms of the mean excitation energy I_0 of the standard substance.

Probably the most significant result of Thompson's work, as already noted, is the recognition of the variation in values of I found for a given element in different chemical compounds. Some absolute values of I and ranges of variation reported by Thompson are shown in Figure 1 of Report No. 6. The values shown there have been adjusted from Thompson's data to give a mean excitation energy for copper of 314 ev, rather than the value I_0 = 279 ev used by Thompson for this element.

The light elements have also been studied systematically by Brolley and Ribe (6). In these experiments protons and deuterons of a single low velocity were used, and stopping powers of a number of elements and compounds and of air were obtained. Specifically, Brolley and Ribe measured the stopping powers of hydrogen, air, and and krypton for 4.43 Mev protons (averaged between 5.0 Mev and 3.8 Mev). With 8.86 Mev deuterons they also measured the stopping power of a number of gases (H_2, He, N_2, O_2, Ne, Ar, Kr, Xe, CH_4 and CO_2) relative to that of air. Several of the Brolley-Ribe I-values are shown in Figure 1 of Report No. 6. Taken collectively, the data show consistent trends from substance to substance and represent a base

point for systematic studies of stopping power among the light elements. Since there is no variation in the incident particle energies in the Brolley-Ribe measurements, they do not give any information on the variation of shell corrections, C/Z, with particle energy. However, with the knowledge of I obtained from high-energy measurements, such as those of Thompson (16) and of Bakker and Segrè (1), the Brolley-Ribe data do show the absolute contribution of shell corrections to the stopping power at 1 proton energy for the light elements. This is discussed below in connection with other data relevant to shell corrections.

Bakker and Segrè (1) measured stopping powers relative to copper for protons with a mean energy of 300 Mev in a number of elements spread throughout the periodic system (H, Li, Be, C, Al, Fe, Cu, Ag, Sn, W, Pb, and U). Some of their data, renormalized to give the value I = 163 ev for aluminum, discussed above, are also shown in Figure 1 of Report No. 6. Figure 6 of Appendix A indicates that for tungsten, lead, and uranium the shell corrections for 300 Mev protons amount to 1 percent or more of the stopping power. Therefore, the Bakker and Segrè experiments furnish direct determinations of the mean excitation energies I for the lighter elements in the series (through Sn). For the heavier elements, tungsten, lead, and uranium, the Bakker-Segrè data can be used directly to obtain the adjusted mean excitation energy, I_{adj}, under the approximation that the residual part of C/Z for protons at an energy of 300 Mev is negligible. (Report No. 6.)

Since the measurements of Bakker and Segrè encompass the entire periodic system, they also furnish a rather complete picture of the adjusted mean excitation energies, I_{adj}, as a function of atomic number Z. In the experimental arrangement of Bakker and Segrè a copper absorber was used as a standard to bring incident protons to rest. The incident proton energy was about 340 Mev, and approximately 94 gm/cm^2 of copper absorber was needed to stop the protons. In the experiments, approximately the first 30 gm/cm^2 of the copper absorber was replaced by the material being investigated, through which the incident protons then slowed down from 340 Mev to about 265 Mev. Since most of the range is covered while the proton energy is still high, and since the materials being investigated were substituted in the first portion of the proton range, the ratio of I-values from the Bakker-Segrè experiments should not depend much on the actual absolute range determinations made in copper.[8] The dependence of I_{adj} on Z as demonstrated by the Bakker-Segrè data is evident from Figure 1 in Report No. 6.

Another set of measurements made with elements spread throughout a wide portion of the periodic table is that of Zrelov and Stoletov (18). Range measurements were made with 660 Mev protons in copper, and stopping-power measurements relative to copper were carried out for hydrogen, beryllium, carbon, iron, cadmium, and tungsten. These measurements, like those of Bakker and Segrè, give direct information on I_{adj}.

The same is true of the measurements of Barkas and von Friesen (2) with 750 Mev protons. These authors measured the stopping powers of aluminum, lead, and uranium and photographic emulsion relative to copper in the energy ranges 750-600 Mev, 600-450 Mev, and 450-300 Mev.[9] They also made range determinations in the

---

[8] As shown in Figure 2 of Report No. 2, the scatter of the Bakker-Segrè data tends to indicate that the error estimated by the authors may be too small.

[9] Questions of the internal consistency of the data in different energy ranges are discussed by Bichsel (5).

substances mentioned, and thereby determined the mean excitation energies for copper, lead, uranium and emulsion, assuming the value I = 163 ev for aluminum. Some of the results are shown in Figure 1 of Report No. 6. As already mentioned, there is a discrepancy between the value of I thus determined for emulsion and the value that one expects from the given chemical composition of the emulsion.

In the experiments discussed until now—with the exception of the measurements of Brolley and Ribe at one value of energy—shell corrections have not played a major role in the interpretation of results. We next consider experimental information available for protons at lower energies in materials of medium and high Z, where shell corrections are large. Several extensive series of measurements have been made. At fixed values of proton energy there are, in addition to the Brolley and Ribe data (Ref. 6) for the light elements, the measurements of Sachs and Richardson (15) and of Burkig and MacKenzie (7) that include heavier elements. Sachs and Richardson made absolute measurements of the stopping power for 17.8 Mev protons (with energy losses in the range ~.15 Mev to ~2 Mev for foils of various thicknesses) in aluminum, nickel, copper, rhodium, silver, cadmium, tin, tantalum, tungsten, and gold. Burkig and MacKenzie measured the stopping power of 23 elements (from Be through Th) relative to aluminum for 19.8 Mev protons. The three sets of measurements (Refs. 6, 15, 7) provide stopping-power measurements at proton energies of 4.45 Mev, 18 Mev, and 19.8 Mev.

Bichsel, Mozley, and Aron (3) made range measurements of 6 to 18 Mev protons in beryllium, aluminum, copper, silver, and gold. Since the theoretical expression for stopping power, Equation 38 of Appendix A, is not valid down to arbitrarily small energies, one usually expresses the range of a proton of energy E in the form

$$R(E) = R_0(E_0) + \int_{E_0}^{E} \left(\frac{dE}{ds}\right)^{-1} dE \ .$$

Here E_0 is a value of energy large enough to satisfy the conditions under which the theory is applicable. $R_0(E_0)$ is an experimentally determined value of the range at E_0, and plays the role of a constant of integration. The range expressed by the above equation is the c.s.d.a. (continuous slowing down approximation) range as defined in connection with Equation 39 of Appendix A.

If one wishes to study the quantity $\ln I + C/Z$ from range measurements, then the above expression for R(E) implies that a minimum of two range measurements (one at E_0 and one at $E > E_0$) are required in order that the constant of integration $R_0(E_0)$ can be evaluated. In practice, a series of range measurements is made in an energy interval, as in the Bichsel, Mozley, and Aron work. With I as an adjustable parameter and with estimated values of C/Z as a function of energy, range-energy relations are calculated and normalized to give the observed range $R_0(E_0)$ at one energy. The particular range-energy relation that best fits all of the observed ranges in the experiment is selected, and this determines I. This procedure for determining I is dependent on knowing C/Z as a function of energy.

Alternatively, one can handle the data in the following way to extract information on shell corrections. The range-energy curves can be differentiated to obtain the stopping power as a function of energy. One can then calculate the quantity L(v, Z) (defined by Equation 53a in Appendix A) as a function of energy and write

$$\frac{C}{Z} + \ln I = \ln 2mv^2 - L(v, Z) \ .$$

One obtains in this way an experimental curve for $C/Z + \ln I$ as a function of energy. Since I is independent of energy, this curve shows the variation of C/Z as a function of energy and also gives the absolute value of C/Z to the extent that I is known, e.g., from high-energy data. Thus the low-energy experiments for a range of energies give directly the variation of C/Z with energy.

Other experiments at low energies have been conducted by Nielsen (11) and by Rybakov (14). Nielsen measured stopping power for protons and deuterons in the energy range from 1.5 Mev to 4.5 Mev in beryllium, aluminum, nickel, copper, silver, and gold. Rybakov measured proton ranges at several energies between 1 and 7.3 Mev in aluminum, iron, copper, molybdenum, cadmium, tin, tantalum, and lead. These two sets of data show the variation of C/Z with bombarding particle energy and also the variation of C/Z with Z at fixed energy.

The most recent stopping-power measurements are those of Nakano, MacKenzie, and Bichsel (9). In these experiments the stopping power for protons of average energy 28.7 Mev (over an energy loss interval of $\sim$2 Mev) was measured relative to aluminum in beryllium, titanium, vanadium, cobalt, nickel, copper, silver, tantalum, tungsten, iridium, and gold. The data show relative stopping powers as a function of Z and furnish an additional set of stopping-power values for a number of elements at one proton energy.

The data cited above have been tabulated in Figure 1 with respect to atomic number, energy, and energy-interval represented by the measurements. Experiments at a single energy are indicated by the smaller rectangles, and the other studies by the larger rectangles. The dashed line represents the approximate locus of points at which the total shell correction contributes about 1 percent to stopping power for various atomic numbers. The location of this line has been estimated directly from the curves in Figure 6 of Appendix A. Taken collectively, the data represent measurements for a large number of the chemical elements, some measurements being available in three decades of incident particle energy. From Figure 6 in Appendix A, it can be seen that, except for the lightest elements, the measurements tabulated in Figure 1 give data for many elements over ranges of energy in which shell corrections vary from their maximum values to close to their limiting values at $\beta = 1$. From these data our understanding of stopping power is verified in large measure. This understanding takes the form of knowledge of (1) the actual numerical values of the parameters of the theory and (2) the variation of these parameters with incident particle energy and with atomic number.

5. Acknowledgments

The author is indebted to Dr. U. Fano for valuable comments and discussion about many of the items considered here. Thanks are also due Drs. H. Bichsel and R. H. Ritchie for helpful discussions.

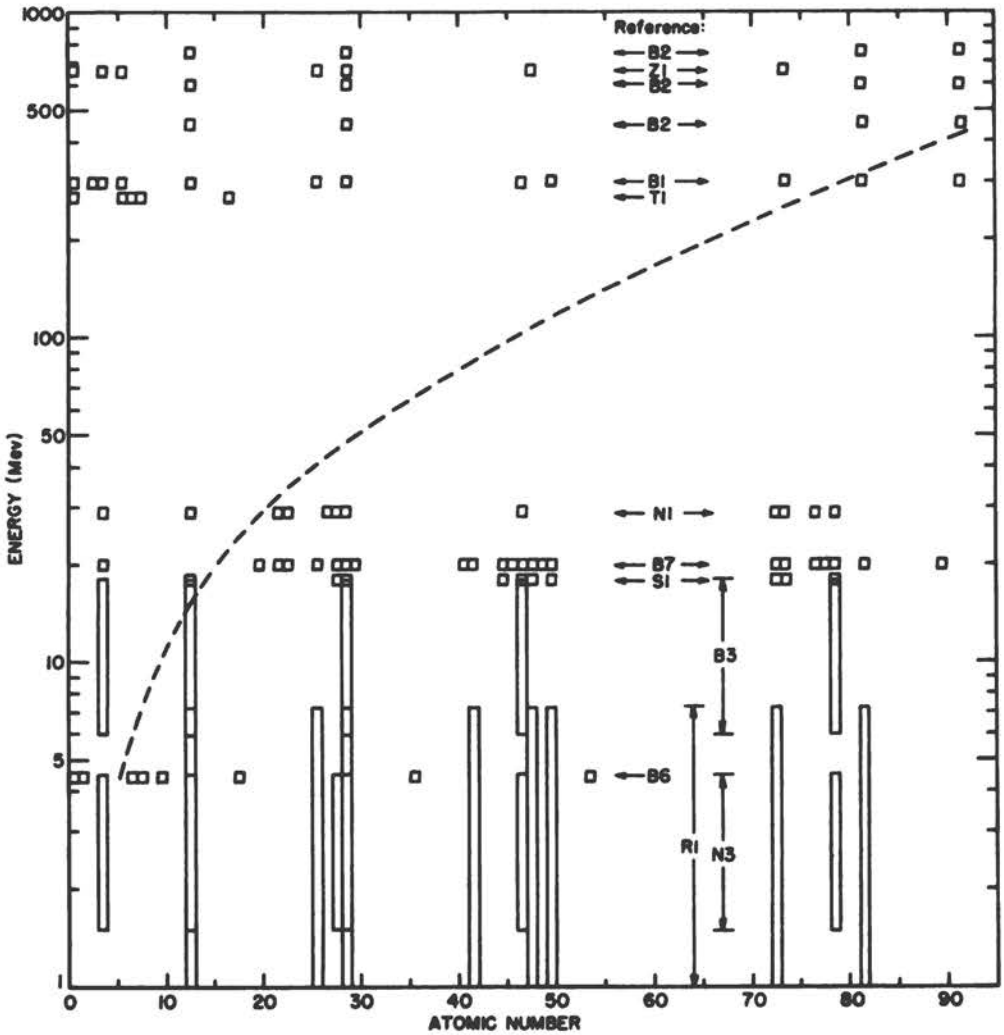

Figure 1. Tabulation of experiments cited.

References

1. C. J. Bakker and E. Segrè, Phys. Rev. 81, 489 (1951).

2. W. H. Barkas and S. von Friesen, Nuovo Cimento Suppl. 19, 41 (1961).

3. H. Bichsel, R. F. Mozley, and W. A. Aron, Phys. Rev. 105, 1788 (1957).

4. H. Bichsel and E. A. Uehling, Phys. Rev. 119, 1670 (1960).

5. H. Bichsel, Report No. 2 of this volume.

6. J. R. Brolley and F. L. Ribe, Phys. Rev. 98, 1112 (1955).

7. V. C. Burkig and K. R. MacKenzie, Phys. Rev. 106, 848 (1957).

8. U. Fano, Ann. Rev. Nucl. Sci., 13, 1 (1963). Reprinted as Appendix A to the present volume.

9. G. H. Nakano, K. R. MacKenzie, and H. Bichsel, Phys. Rev. 132, 291 (1963).

10. National Bureau of Standards Handbook 79, Washington, D. C. (1961).

11. L. P. Nielsen, Mat. Fys. Medd. Dan. Vid. Selsk. 33, no. 6 (1961).

12. L. C. Northcliffe, Ann. Rev. Nuc. Sci., 13, 67 (1963). Reprinted as Appendix B to the present volume. See also the supplementary Paper No. 8 of this volume.

13. R. L. Platzman, private communication.

14. B. V. Rybakov, J. Exp. Theor. Phys. (USSR) 28, 651 (1955). Transl. JETP 1, 435 (1955).

15. D. C. Sachs and J. R. Richardson, Phys. Rev. 89, 1163 (1953).

16. T. J. Thompson, University of California Radiation Laboratory Report UCRL-1910 (1952).

17. W. Whaling, Encyclopedia of Physics, 34, 193 (Springer, Berlin, 1958).

18. V. P. Zrelov and G. D. Stoletov, J. Exp. Theor. Phys. (USSR) 36, 658 (1959). Transl. JETP 9, 461 (1959).

4. CONTRIBUTIONS TO THE THEORY OF SHELL CORRECTIONS

U. Fano[1] and J. E. Turner[2]

Abstract

Sum rules pertaining to the inelastic form factor $F_n(\underline{q})$ are calculated and applied to the evaluation of shell corrections to the stopping-power formula, to order $1/v^4$ in the velocity of the incident particle. Details are given pertaining to the evaluation of the shell corrections in the paper reproduced as Appendix A to this volume. Comments are presented regarding the possible generality of a Lindhard-Winther equipartition rule.

1. Introduction

This report complements the treatment of shell corrections given in Section 4 of the article reproduced as Appendix A of this volume. The following topics are developed further: (a) the low-Q approximation is improved by working out the expansion into powers of $1/v^2$ in greater detail and calculating explicitly the contribution of electron correlations to the coefficient K_1; (b) the high-Q approximation is improved by obtaining the relevant expansion into powers of $1/v^2$ (this expansion is shown to coincide with the low-Q expansion to order $(1/v^2)^2$, except for possible electron correlation effects that have not been calculated, and the result confirms a surmise introduced in Appendix A); (c) some comments are made on the possible generality of an equipartition sum rule developed recently by Lindhard and Winther (1);[3] (d) the numerical evaluation of the shell corrections in the high-energy limit, which have been utilized in Appendix A and in Report No. 6, are described in some detail. None of these four topics has been developed as far as one would wish but it seems desirable to present the matters as they stand.

2. Sum Rules over Inelastic Form Factors

Equations 56 and 57 of Appendix A[4] reduce the calculation of the low-Q contribution to the stopping power, to order $(1/v^2)^2$, to the calculation of the sums

$$S_r = \Sigma_n E_n{}^r \, |F_n(\underline{q})|^2 \tag{1}$$

for r = 1, 3, and 5. Here, as in Appendix A, the Σ_n extends over all excited and

---

[1]National Bureau of Standards, Washington, D. C.

[2]Oak Ridge National Laboratory, Oak Ridge, Tenn.

[3]We are greatly indebted to Prof. Lindhard for early communication of his results.

[4]Henceforth in this paper the numbers for equations, references, and figures, preceded by the letter A refer to equations, references, and figures in Appendix A.

ionized stationary states of a material, and E_n is the energy level of each of these states measured from the energy of the ground state 0. Moreover, according to Equation A17, $F_n(\underline{q})$ is the matrix element

$$F_n(\underline{q}) = Z^{-1/2}(n \,|\, \Sigma_j^{Z} A_j(\underline{q}) \,|\, 0) \,, \tag{2}$$

with

$$A_j(\underline{q}) = \exp(i\underline{q} \cdot \underline{r}_j / \hbar) \tag{3}$$

where $\underline{r}_j$ indicates the position of the j-th electron, and a limiting process for $Z = \infty$, in the sense of Equation A41, is implied where relevant. Averaging of Equation 1 over the direction of $\underline{q}$ is also implied, in keeping with the assumed isotropy of the ground state of the material.

The expression $|F_n(\underline{q})|^2$ in Equation 1 represents the probability of eventual excitation of a system to its n-th state as a result of the momentary absorption of the momentum $\underline{q}$ by one of its particles. Therefore, S_r represents the r-th moment of the absorbed energy averaged over the probability distribution $|F_n(\underline{q})|^2$. The quantities S_r are of importance in a variety of problems and therefore deserve some general study. An effort in this direction has been undertaken in the past by Placzek in connection with neutron scattering (Ref. A95). A nonrelativistic approximation will be used, as in the relevant part of Appendix A. The odd moments of the energy distribution, represented by odd values of r in Equation 1, exhibit simple features which will be emphasized here. This section deals with the calculation of the S_r. The application to the calculation of the low-Q contribution to the stopping power will be described in the next section.

The calculation of the S_r is straightforward in principle but meets a practical difficulty in the occurrence of a large number of terms, except for r = 1 or 2. Most of these terms can be shown to vanish, but a considerable advantage accrues from arranging the calculation so as to minimize the number of separate terms to be considered and to facilitate the identification of the terms that vanish. These considerations guided the selection of the procedure adopted here, which makes use of a moment generating function G. The same procedure serves also for the calculation of the high-Q contribution in Section 4.

The quantity (Eq. 1) has the alternative form

$$\begin{aligned} S_r &= \left\{ \left(\frac{d}{dx}\right)^r \Sigma_n e^{xE_n} |F_n(\underline{q})|^2 \right\}_{x=0} \\ &= \left\{ \left(\frac{d}{dx}\right)^r G(x, \underline{q}) \right\}_{x=0} . \end{aligned} \tag{4}$$

From the definitions of Equations 2 and 3 and the definition of E_n, we have

$$\begin{aligned} G(x, \underline{q}) &= \Sigma_n \Sigma_{i,j} Z^{-1} (0 | A_i^*(\underline{q}) | n) e^{xE_n} (n | A_j(\underline{q}) | 0) \\ &= Z^{-1} \Sigma_{i,j} \Sigma_n (0 | A_i^*(\underline{q}) | n) (n | e^{xH} A_j(\underline{q}) e^{-xH} | 0) \,, \\ &= \Sigma_r \frac{1}{r!} S_r x^r \end{aligned} \tag{5}$$

where H indicates the Hamiltonian of the material

$$H = \Sigma_j \frac{p_j^2}{2m} + \Sigma_{j,N} U(|\underline{r}_j - \underline{R}_N|) + \frac{1}{2} \overset{i\neq j}{\Sigma_{i,j}} V(|\underline{r}_i - \underline{r}_j|)$$

$$= \Sigma_j \frac{p_j^2}{2m} - \Sigma_{j,N} \frac{Z_N e^2}{|\underline{r}_j - \underline{R}_N|} + \frac{1}{2} \overset{i\neq j}{\Sigma_{i,j}} \frac{e^2}{|\underline{r}_i - \underline{r}_j|} \quad . \tag{6}$$

Here m is the electron mass, $\underline{p}_j = m\underline{v}_j$ is the momentum of the j-th electron, $U(|\underline{r}_j - \underline{R}_N|)$ its potential energy due to the attraction by a nucleus at $\underline{R}_N$, and $V(|\underline{r}_i - \underline{r}_j|)$ the potential energy of two electrons due to their repulsion. The completeness of the set of states n, as represented by the closure rule $\Sigma_n |n)(n| = 1$ can now be utilized to yield

$$G(x,\underline{q}) = Z^{-1} \Sigma_{i,j} (0|A_i(\underline{q})^* e^{xH} A_j(\underline{q}) e^{-xH}|0) \quad . \tag{7}$$

Thus we have to evaluate the mean value of a somewhat complex operator for the ground state of the material, without explicit reference to its excited states.

The operator can be simplified by utilizing the commutation rule, which follows from Equations 6 and 3:

$$[H, A_j(\underline{q})] = \frac{1}{2} [\underline{q} \cdot \underline{v}_j A_j(\underline{q}) + A_j(\underline{q}) \underline{q} \cdot \underline{v}_j]$$

$$= A_j(\underline{q}) (Q + \underline{q} \cdot \underline{v}_j) \quad , \tag{8}$$

where $Q = q^2/2m$. From Equation 8 there follows in turn

$$\exp(xH) A_j(\underline{q}) = A_j(\underline{q}) \exp[x(H + Q + \underline{q} \cdot \underline{v}_j)] \quad , \tag{9}$$

so that

$$G(x,\underline{q}) = Z^{-1} \Sigma_{i,j} (0|A_i(\underline{q})^* A_j(\underline{q}) e^{x(H+Q+\underline{q}\cdot\underline{v}_j)} e^{-xH}|0) \quad . \tag{10}$$

The factors exp(xH) and exp(-xH) do not quite cancel out because H does not commute with $\underline{v}_j$, but Feynman's operator calculus (Ref. 2) shows that one can write

$$\exp[x(H + Q + \underline{q} \cdot \underline{v}_j)] \exp(-xH) = \exp \int_0^x [Q + \underline{q} \cdot \underline{v}_j(x')] dx' \quad , \tag{11}$$

where

$$\underline{v}_j(x) = e^{xH} \underline{v}_j e^{-xH} = \underline{v}_j + [H, \underline{v}_j] x + \frac{1}{2} [H, [H, \underline{v}_j]] x^2 + \ldots\ldots \tag{12}$$

The notation utilized in Equation 11 implies that in any product of operators $\underline{v}_j(x')$, $\underline{v}_j(x'')$,... these operators are ordered from left to right in the order of increasing values of $x', x'', \ldots$. Equation 10 now becomes

$$G(x,\underline{q}) = Z^{-1} \Sigma_{i,j} (0|A_i(\underline{q})^* A_j(\underline{q}) \exp\left\{\int_0^x [Q + \underline{q} \cdot \underline{v}_j(x')] dx'\right\}|0) \quad , \tag{13}$$

and one can proceed to expand the exponential into powers of x, so that the coefficient of each term will represent one of the S_r, according to Equation 5.[5]

The exponential operator (Eq. 11) is in fact defined by its expansion

$$\exp \int_0^x [Q+\underline{q}\cdot\underline{v}_j(x')]\,dx' = 1 + \int_0^x dx'[Q+\underline{q}\cdot\underline{v}_j(x')] + \\ + \int_0^x dx' \int_0^{x'} dx''[Q+\underline{q}\cdot\underline{v}_j(x'')][Q+\underline{q}\cdot\underline{v}_j(x')] + \ldots . \tag{14}$$

Substitution of the definition (Eq. 12) of $\underline{v}_j(x)$ into Equation 14 enables one to carry out the multiple integrations over x', x''... so that Equation 14 takes the form

$$\exp \int_0^x [Q+\underline{q}\cdot\underline{v}_j(x')]\,dx' = \Sigma_r \frac{1}{r!} H_j^{(r)}(\underline{q})x^r . \tag{14a}$$

Further substitution into Equation 13 and comparison with Equation 5 yields then

$$S_r = Z^{-1}\Sigma_{i,j}(0|A_i(\underline{q})^* A_j(\underline{q})H_j^{(r)}(\underline{q})|0) . \tag{15}$$

We are left at this point with the tasks of calculating the $H_j^{(r)}(\underline{q})$ explicitly for r = 1, 3, and 5, and then of calculating the mean values $(0|A_i^* A_j H_j^{(r)}|0)$.

To express the $H_j^{(r)}$ conveniently, we introduce for an arbitrary operator O the notation

$$O' = [H,O] = -i\hbar\, dO/dt . \tag{16}$$

We obtain, then, from Equations 12, 14, and 14a

$$\begin{aligned}
H_j^{(0)} &= 1, \qquad H_j^{(1)} = Q+\underline{q}\cdot\underline{v}_j \\
H_j^{(2)} &= \underline{q}\cdot\underline{v}_j' + (Q+\underline{q}\cdot\underline{v}_j)^2 \\
H_j^{(3)} &= \underline{q}\cdot\underline{v}_j'' + [\underline{q}\cdot\underline{v}_j'(Q+\underline{q}\cdot\underline{v}_j) + 2(Q+\underline{q}\cdot\underline{v}_j)\underline{q}\cdot\underline{v}_j'] + (Q+\underline{q}\cdot\underline{v}_j)^3 , \\
H_j^{(4)} &= \underline{q}\cdot\underline{v}_j''' + 3(\underline{q}\cdot\underline{v}_j')^2 + \underline{q}\cdot\underline{v}_j''(Q+\underline{q}\cdot\underline{v}_j) + 3(Q+\underline{q}\cdot\underline{v}_j)\,\underline{q}\cdot\underline{v}_j'' \\
&\quad + \underline{q}\cdot\underline{v}_j'(Q+\underline{q}\cdot\underline{v}_j)^2 + 2(Q+\underline{q}\cdot\underline{v}_j)\underline{q}\cdot\underline{v}_j'(Q+\underline{q}\cdot\underline{v}_j) + 3(Q+\underline{q}\cdot\underline{v}_j)^2\,\underline{q}\cdot\underline{v}_j' + (Q+\underline{q}\cdot\underline{v}_j)^4 \\
H_j^{(5)} &= \underline{q}\cdot\underline{v}_j'''' + \underline{q}\cdot\underline{v}_j'''(Q+\underline{q}\cdot\underline{v}_j) + 4(Q+\underline{q}\cdot\underline{v}_j)\underline{q}\cdot\underline{v}_j''' + 4\underline{q}\cdot\underline{v}_j''\,\underline{q}\cdot\underline{v}_j' + 6\underline{q}\cdot\underline{v}_j'\,\underline{q}\cdot\underline{v}_j'' \\
&\quad + \underline{q}\cdot\underline{v}_j''(Q+\underline{q}\cdot\underline{v}_j)^2 + 3(Q+\underline{q}\cdot\underline{v}_j)\underline{q}\cdot\underline{v}_j''(Q+\underline{q}\cdot\underline{v}_j) + 6(Q+\underline{q}\cdot\underline{v}_j)^2\,\underline{q}\cdot\underline{v}_j'' \\
&\quad + 3(\underline{q}\cdot\underline{v}_j')^2(Q+\underline{q}\cdot\underline{v}_j) + 4\underline{q}\cdot\underline{v}_j'(Q+\underline{q}\cdot\underline{v}_j)\underline{q}\cdot\underline{v}_j' + 8(Q+\underline{q}\cdot\underline{v}_j)(\underline{q}\cdot\underline{v}_j')^2 + \underline{q}\cdot\underline{v}_j'(Q+\underline{q}\cdot\underline{v}_j)^3 \\
&\quad + 2(Q+\underline{q}\cdot\underline{v}_j)\underline{q}\cdot\underline{v}_j'(Q+\underline{q}\cdot\underline{v}_j)^2 + 3(Q+\underline{q}\cdot\underline{v}_j)^2\,\underline{q}\cdot\underline{v}_j'(Q+\underline{q}\cdot\underline{v}_j) + 4(Q+\underline{q}\cdot\underline{v}_j)^3\,\underline{q}\cdot\underline{v}_j' \\
&\quad + (Q+\underline{q}\cdot\underline{v}_j)^5 .
\end{aligned} \tag{17}$$

---

[5] It might be of great advantage to express Equation 13 as an exponential function of matrix elements rather than as the matrix element of an exponential operator; i. e., to delay the expansion into powers of x until the mean value over the ground state has been taken.

Calculation of S_1

To calculate the mean values of the quantities $A_i^* A_j H_j^{(r)}$ in Equation 15, beginning with r = 1, we start by symmetrizing them. From the commutation rule (Eq. 8) and from the fact that A_i and $\underline{v}_j$ commute for $i \neq j$ it follows that

$$A_i(\underline{q})^* A_j(\underline{q})(Q + \underline{q}\cdot\underline{v}_j) = Q\delta_{ij} + \frac{1}{2}(\underline{q}\cdot\underline{v}_j A_i^* A_j + A_i^* A_j \underline{q}\cdot\underline{v}_j) \quad . \tag{18}$$

The operator $A_i^* A_j = \exp[-i\underline{q}\cdot(\underline{r}_i - \underline{r}_j)/\hbar]$ is not Hermitian but can be expanded into a power series of Hermitian time-even operators $[\underline{q}\cdot(\underline{r}_i - \underline{r}_j)]^n$. Therefore, the second term on the right in Equation 18 can be expanded into a series of symmetric terms,

$$\underline{q}\cdot\underline{v}_j[\underline{q}\cdot(\underline{r}_i - \underline{r}_j)]^n + [\underline{q}\cdot(\underline{r}_i - \underline{r}_j)]^n \underline{q}\cdot\underline{v}_j \quad , \tag{19}$$

each of which is Hermitian and time-odd and has, therefore, mean value zero, provided only that the ground state is stationary and isotropic. This term drops out, then, and we obtain the well-known result (Eq. A27)

$$S_1 = Q \quad . \tag{20}$$

Calculation of S_3

The last term of $H_j^{(3)}$ in Equation 17 is found (by repeated application of Equation 18) to contribute

$$(0|A_i^* A_j(Q + \underline{q}\cdot\underline{v}_j)^3|0) = [Q^3 + 3Q(0|(\underline{q}\cdot\underline{v}_j)^2|0)]\delta_{ij} \quad . \tag{21}$$

As noted above, we must still average over the direction of $\underline{q}$. This averaging yields

$$\langle(\underline{q}\cdot\underline{v}_j)^2\rangle_{\hat{q}} = \frac{1}{3}q^2 v_j^2 = \frac{1}{3}Q\,2mv_j^2 \tag{22}$$

so that

$$\langle(0|A_i^* A_j(Q + \underline{q}\cdot\underline{v}_j)^3|0)\rangle_{\hat{q}} = [Q^3 + Q^2\,2m\langle v_j^2\rangle]\delta_{ij} \quad . \tag{23}$$

To evaluate the contribution of the first two terms of $H_j^{(3)}$ a symmetrization procedure is required. Considering that $\underline{v}_j'$ commutes with both A_i^* and A_j, we have

$$\begin{aligned} &A_i^* A_j[\underline{q}\cdot\underline{v}_j'' + \underline{q}\cdot\underline{v}'(Q + \underline{q}\cdot\underline{v}_j) + 2(Q + \underline{q}\cdot\underline{v}_j)\underline{q}\cdot\underline{v}_j'] \\ &= \frac{1}{2}(A_i^* A_j \underline{q}\cdot\underline{v}_j'' + \underline{q}\cdot\underline{v}_j'' A_i^* A_j) + \frac{1}{2}[A_i^* A_j, \underline{q}\cdot\underline{v}_j''] \\ &+ \frac{3}{2}[\underline{q}\cdot\underline{v}_j' A_i^* A_j(Q + \underline{q}\cdot\underline{v}_j) + A_i^* A_j(Q + \underline{q}\cdot\underline{v}_j)\underline{q}\cdot\underline{v}_j'] + \frac{1}{2}A_i^* A_j[\underline{q}\cdot\underline{v}_j, \underline{q}\cdot\underline{v}_j'] \quad , \end{aligned} \tag{24}$$

where [B,C] = BC-CB.

The first term on the right in Equation 24 reduces to Hermitian time-odd operators so that its contribution vanishes. Application of Equation 18 to the third term on the right of Equation 24 splits it into a term $3Q\underline{q}\cdot\underline{v}_j\,\delta_{ij}$, which vanishes upon averaging over the direction of $\underline{q}$, and another term which reduces again to Hermitian time-odd

terms and thus yields no contribution. The second term on the right in Equation 24 can be transformed as follows

$$\begin{aligned}\tfrac{1}{2}[A_i^* A_j, \underline{q}\cdot\underline{v}_j''\,] &= \tfrac{1}{2}[A_i^* A_j, [H, \underline{q}\cdot\underline{v}_j']] \\ &= \tfrac{1}{2}[[A_i^* A_j, H], \underline{q}\cdot\underline{v}_j'\,] \\ &= -\tfrac{1}{2}[A_i^* A_j (2Q + \underline{q}\cdot\underline{v}_j - \underline{q}\cdot\underline{v}_i),\ \underline{q}\cdot\underline{v}_j'\,] \\ &= -\tfrac{1}{2} A_i^* A_j [(\underline{q}\cdot\underline{v}_j - \underline{q}\cdot\underline{v}_i), \underline{q}\cdot\underline{v}_j'\,] \ .\end{aligned} \tag{25}$$

Of the two terms on the right in Equation 25, the first one cancels the last term of Equation 24, so that the second one alone is left to contribute to the mean value of Equation 24. This mean value is, then,

$$\tfrac{1}{2}\,(0\,|\,A_i^*(\underline{q})A_j(\underline{q})[\underline{q}\cdot\underline{v}_i, \underline{q}\cdot\underline{v}_j'\,]\,|\,0) \ . \tag{26}$$

To calculate $[\underline{q}\cdot\underline{v}_i, \underline{q}\cdot\underline{v}_j'\,]$ explicitly, set $\underline{v}_j = (\hbar/im)\underline{\nabla}_j$, where $\underline{\nabla}$ indicates the gradient operator, and apply Equations 16 and 6. This gives

$$[\underline{q}\cdot\underline{v}_i, \underline{q}\cdot\underline{v}_j'\,] = \frac{\hbar^2}{m^2}\,\underline{q}\cdot\underline{\nabla}_i q\cdot\underline{\nabla}_j \left\{\Sigma_{k,N}\, U(|\underline{r}_k - \underline{R}_N|) + \tfrac{1}{2}\Sigma_{k,\ell}^{k\neq\ell}\, V(|\underline{r}_k - \underline{r}_\ell|)\right\} \tag{27}$$

$$= \frac{\hbar^2}{m^2}\,(\underline{q}\cdot\underline{\nabla}_j)^2 \left\{[\Sigma_N U(|\underline{r}_j - \underline{R}_N|) + \Sigma_\ell^{\ell\neq j} V(|\underline{r}_j - \underline{r}_\ell|)]\delta_{ij} - V(|\underline{r}_j - \underline{r}_i|)(1-\delta_{ij})\right\},$$

taking into account that $\underline{q}\cdot\underline{\nabla}_i q\cdot\underline{\nabla}_j U = 0$ for $i \neq j$ and that $\underline{\nabla}_i V(|\underline{r}_j - \underline{r}_i|) = -\underline{\nabla}_j V(|\underline{r}_j - \underline{r}_i|)$. Upon introduction of the Coulomb form of the potentials, as given in Equation 6, Equation 27 becomes

$$\begin{aligned}[\underline{q}\cdot\underline{v}_i, \underline{q}\cdot\underline{v}_j'\,] = \tfrac{1}{3}q^2\,\frac{4\pi\hbar^2 e^2}{m^2} &\left\{[\Sigma_N Z_N \delta(\underline{r}_j - \underline{R}_N) - \Sigma_\ell^{\ell\neq j}\delta(\underline{r}_j - \underline{r}_\ell)]\,\delta_{ij}\right. \\ &\left. + \delta(\underline{r}_j - \underline{r}_i)\,(1-\delta_{ij})\right\} + \frac{\hbar^2 e^2}{m^2}\left\{\Sigma_\ell^{\ell\neq j}\,\frac{3[\underline{q}\cdot(\underline{r}_j - \underline{r}_\ell)]^2 - q^2\,|\underline{r}_j - \underline{r}_\ell|^2}{|\underline{r}_j - \underline{r}_\ell|^5}\,\delta_{ij}\right. \\ &\left. - \frac{3[\underline{q}\cdot(\underline{r}_j - \underline{r}_i)]^2 - q^2\,|\underline{r}_j - \underline{r}_i|^2}{|\underline{r}_j - \underline{r}_i|^5}\,(1-\delta_{ij})\right\} .\end{aligned} \tag{28}$$

Notice that the contribution of the first brace on the right in Equation 28 is independent of the direction of $\underline{q}$, and that of the second brace depends on the Legendre polynominal P_2 of the angle between $\underline{q}$ and another vector; the separation into two such terms holds for any central potential law.

Upon multiplication of $[\underline{q}\cdot\underline{v}_i, \underline{q}\cdot\underline{v}_j'\,]$ by $A_i^* A_j$, to calculate Equation 26, the factor $A_i^* A_j$ reduces to unity when multiplied by δ_{ij} or by $\delta(\underline{r}_j - \underline{r}_i)$, that is, by each term on the right in Equation 28 except the last one. The next-to-last term of Equation 28 vanishes when averaged over the direction of $\underline{q}$. The second and third

terms on the right in Equation 28 cancel later, upon summation over i and j. Thus, one finds the average value

$$Z^{-1}\Sigma_{i,j}\frac{1}{2}\langle(0|A_i^*(\underline{q})A_j(\underline{q})[\underline{q}\cdot\underline{v}_i,\underline{q}\cdot\underline{v}_j']|0)\rangle_q$$

$$= Q\frac{4\pi\hbar^2e^2}{3m}\,Z^{-1}\Sigma_{jN}Z_N(0|\delta(\underline{r}_j-\underline{R}_N)|0) - \tag{29}$$

$$-\frac{\hbar^2e^2}{2m^2}\,Z^{-1}\sum_{i,j}^{i\neq j}\left(0\left|\left\langle\exp\left[i\frac{\underline{q}\cdot(\underline{r}_j-\underline{r}_i)}{\hbar}\right]\frac{3[\underline{q}\cdot(\underline{r}_j-\underline{r}_i)]^2-q^2|\underline{r}_j-\underline{r}_i|^2}{|\underline{r}_j-\underline{r}_i|^5}\right\rangle_{\hat{q}}\right|0\right).$$

The averaging process over the direction of $\hat{q}$ in the last term of Equation 29 is equivalent to the calculation of the coefficient of $P_2(\cos\theta)$ in the Legendre expansion of $\exp(iz\cos\theta)$; one can write

$$\frac{1}{2}\int_0^{\pi}\sin\theta d\theta\exp(iz\cos\theta)\frac{3(z\cos\theta)^2-z^2}{z^5} = -\frac{2}{15}\,g_2(z)\ , \tag{30}$$

where

$$g_2(z) = \frac{j_2(z)}{z^2/15} = 15\sqrt{\frac{\pi}{2z^5}}\,J_{5/2}(z) = 1+0(z^2) \tag{30a}$$

reduces to unity at $z = 0$. Application of Equation 30 reduces Equation 29 to

$$Z^{-1}\Sigma_{i,j}\frac{1}{2}\langle(0|A_i^*A_j[\underline{q}\cdot\underline{v}_i,\underline{q}\cdot\underline{v}_j']|0)\rangle_{\hat{q}} \tag{31}$$

$$= Q\frac{4\pi\hbar^2e^2}{3m}\,\Sigma_NZ_N(0|\delta(\underline{r}_j-\underline{R}_N)|0) + Q^2\frac{4}{15}\sum_i^{i\neq j}\left(0\left|\frac{e^2}{|\underline{r}_j-\underline{r}_i|}\,g_2\left(q\frac{|\underline{r}_j-\underline{r}_i|}{\hbar}\right)\right|0\right)$$

where $Z^{-1}\Sigma_j$ has been suppressed in consideration that all electrons are identical.

Finally, S_3 is obtained by combining Equations 23 and 31 in accordance with Equations 15 and 17. The index j can now be dropped, with the understanding that all quantities refer to an average electron under consideration, and that Σ_i' excludes this electron from the sum over i. We also indicate the mean values over the ground state by $\langle\ \rangle_0$ instead of $(0|..|0)$. Thus, one finds

$$S_3 = Q^3 + Q^2 2m\langle v^2\rangle_0 + Q\ \frac{4\pi\hbar^2e^2}{3m}\,\Sigma_NZ_N\langle\delta(\underline{r}-\underline{R}_N)\rangle_0 \tag{32}$$

$$+ Q^2\frac{4}{15}\left\langle\Sigma_i'\frac{e^2}{|\underline{r}-\underline{r}_i|}\,g_2(q|\underline{r}-\underline{r}_i|/\hbar)\right\rangle_0\ .$$

Calculation of S_5

This calculation should proceed by analogy with the calculation of S_3, but it involves a larger number of terms, some of which are more complicated than those treated above. We have calculated only a selection of terms that appear most important for our immediate application. In the first place, the application of Section 3 requires only terms of S_5 which are proportional to Q^3. Secondly, the effect of electron-electron correlations on S_5 will be disregarded as negligibly small; notice that the corresponding effect on S_3 will be seen in Section 3 to be even smaller than had been anticipated in Appendix A. To disregard electron-electron correlations, one cancels not only all terms of Equation 15 with $i \neq j$ but also all contributions to $H_j^{(5)}$ which arise explicitly from the interaction potential $V(|\underline{r}_j - \underline{r}_i|)$.

Because $A_i^* A_j$ reduces to unity, irrespective of q, for $i = j$, we can drop all terms of $H_j^{(5)}$ in Equation 17 of other than third degree in Q, that is, with factors $Q^a q^b$ with $a + b/2 \neq 3$. The residual terms, arising from the last five terms of $H_j^{(5)}$, are

$$\begin{aligned}(H_j^{(5)})_{\sim Q^3} &= 10Q^2\,(\underline{q}\cdot\underline{v}_j'\,\underline{q}\cdot\underline{v}_j + 2\underline{q}\cdot\underline{v}_j\underline{q}\cdot\underline{v}_j') + 5Q(\underline{q}\cdot\underline{v}_j)^4 \\ &= 15Q^2\,(\underline{q}\cdot\underline{v}_j\underline{q}\cdot\underline{v}_j' + \underline{q}\cdot\underline{v}_j'\underline{q}\cdot\underline{v}_j) + 5Q^2[\underline{q}\cdot\underline{v}_j, \underline{q}\cdot\underline{v}_j'] + 5Q(\underline{q}\cdot\underline{v}_j)^4 .\end{aligned} \tag{33}$$

The first term on the right in Equation 33 is Hermitian and time-odd; hence its contribution vanishes. The contribution of the second term is proportional to the first term on the right in Equation 29 when electron-electron correlations are disregarded. The third term reduces, upon averaging over the direction of $\underline{q}$, to $Q^3 4m^2 v_j^4$.

Thus, one finds, with the notation of Equation 32,

$$(S_5)_{\sim Q^3,\ \text{no corr.}} = Q^3 \left\{ 4m^2 \langle v^4 \rangle_0 + 10 \frac{4\pi\hbar^2 e^2}{3m} \Sigma_N Z_N \langle \delta(\underline{r} - \underline{R}_N) \rangle_0 \right\} . \tag{34}$$

3. Shell Corrections for Low-Q Collisions

The treatment of shell corrections on page 35 of Appendix A separates these corrections into two contributions, called C_1 and C_2. These contributions correspond respectively, though somewhat loosely, to collisions with low momentum and energy transfer and to collisions with high momentum and energy transfer. Equation A56 expresses C_1 as

$$\frac{C_1}{Z} = \frac{1}{2}\Sigma_n^{(1)} \sum_{r=1}^{\infty} \frac{1}{r!} \left[\frac{d^r f_n(Q)}{dQ^r} \right]_{Q=0} \frac{E_n{}^{2r}}{(2mv^2)^r} , \tag{35}$$

where

$$f_n(Q) = \frac{E_n}{Q} |F_n(\underline{q})|^2 , \tag{36}$$

v is the velocity of the incident particle, and the $\Sigma_n^{(1)}$ is limited to states with $E_n \lesssim mv^2$.

However, it is understood, according to Walske's original analysis (Ref. A134), that this restriction to Σ_n may be removed if it is simultaneously agreed to discard terms of Equation 35 with $r > 2$. Therefore we take

$$\frac{C_1}{Z} \sim \frac{1}{2} \sum_{r=1}^{2} \frac{1}{r!r} \frac{1}{(2mv^2)^r} \left[\left(\frac{d}{dQ} \right)^r \Sigma_n E_n^{2r} f_n(Q) \right]_{Q=0} . \tag{37}$$

According to the definitions (Eq. 36 and Eq. 1), the $\Sigma_n E_n^{2r} f_n(Q)$ in Equation 37 is just S_{2r+1}/Q, so that

$$\frac{C_1}{Z} \sim \frac{1}{2} \sum_{r=1}^{2} \frac{1}{r!r} \frac{1}{(2mv^2)^r} \left[\left(\frac{d}{dQ} \right)^r \frac{S_{2r+1}}{Q} \right]_{Q=0} . \tag{38}$$

The operator indicated by the brackets of Equation 38 selects the terms of degree r+1 in the expansion of S_{2r+1} into powers of Q. For r=1, a full expression of S_3 is given by Equation 32. For r=2, the relevant term of the expansion of S_5 is given by Equation 34, except for effects of electron-electron correlations. Substitution of these formulas into Equation 38 yields

$$\frac{C_1}{Z} \sim \frac{1}{2} \left\{ \frac{2m\langle v^2 \rangle_0 + \frac{4}{15} \Sigma_i' \langle e^2/|\underline{r} - \underline{r}_i| \rangle_0}{2mv^2} + \frac{4m^2 \langle v^4 \rangle_0 + (40\pi\hbar^2 e^2/3m) \Sigma_N Z_N \langle \delta(\underline{r} - \underline{R}_n) \rangle_0}{2(2mv^2)^2} \right\} . \tag{39}$$

(Notice that the factor g_2 in the last term of Equation 32 reduces to unity in the present application.)

This result coincides with Equations A58, A58a, and A58b with the understanding that the "correlation terms," which are merely indicated in Equation A58a, are explicitly represented by $(2/15)\Sigma_i' \langle e^2/|\underline{r} - \underline{r}_i| \rangle_0$ in Equation 39, and those indicated in Equation A58b are still missing in Equation 39. The term $(4/15)\Sigma' \langle e^2/|\underline{r} - \underline{r}'| \rangle_0$ is clearly much smaller than $2m\langle v^2 \rangle_0$ as expected; its influence will be calculated below.

For the purpose of evaluating the mean values of the properties of atomic electrons in Equation 39, let us introduce the symbols.

$T = \Sigma_j \frac{p_j^2}{2m}$	=	kinetic energy of all electrons in the system.
$U = \Sigma_{j,N} U(\lvert \underline{r}_j - \underline{R}_N \rvert)$	=	nuclear attraction energy of all electrons in the system.
$V = \frac{1}{2} \Sigma_{i,j}^{i \neq j} \frac{e^2}{\lvert \underline{r}_i - \underline{r}_j \rvert}$	=	mutual repulsion energy of all electrons in the system.
$\rho(\underline{R}) = \Sigma_j \langle \delta(\underline{r}_j - \underline{R}) \rangle_0 a^3$	=	density at $\underline{R}$ of all electrons in the system expressed in electrons per cubic Bohr radius a.

$B = -[\langle T\rangle_0 + \langle U\rangle_0 + \langle V\rangle_0]$ = total binding energy of all electrons in the system.

$Ry = \hbar^2/2ma^2 = e^2/2a$ = (Rydberg) binding energy of electron in H atom.

Equation 39 can now be written

$$C_1 \sim \frac{\langle T\rangle_0 + \frac{1}{15}\langle V\rangle_0}{mv^2} + \frac{\langle T^2\rangle_0 + (10\pi/3)Ry^2 \Sigma_N Z_N \rho(\underline{R}_N)}{(mv^2)^2} \quad . \tag{40}$$

The virial theorem

$$\langle T\rangle_0 = -\frac{1}{2}(\langle U\rangle_0 + \langle V\rangle_0) = B \tag{41}$$

can be utilized to express $\langle T\rangle_0$ and $\langle V\rangle_0$ in terms of B and $\langle U\rangle_0$, which are more easily evaluated. Thereby, Equation 40 becomes

$$C_1 \sim \frac{13B - \langle U\rangle_0}{15mv^2} + \frac{\langle T^2\rangle_0 + (10\pi/3)Ry^2 \Sigma_N Z_N \rho(\underline{R}_N)}{(mv^2)^2} \quad . \tag{42}$$

Values of B, obtained in various ways, are tabulated (Ref. A52, p. 183) for a number of atoms throughout the periodic system. The "empirical" data in this table are approximated rather closely by

$$B_{emp} \sim Z^{2.4}\, Ry \quad . \tag{43}$$

The Thomas-Fermi model, in its basic form, yields, instead,

$$B_{TF} \sim 1.54\, Z^{7/3}\, Ry \quad . \tag{43a}$$

The value of $\langle U\rangle_0$ is calculated, for a single atom, by integrating the product of $-Ze^2/r$ and of the electron density $\rho(r)$ over the whole atomic volume. A calculation by J. W. Cooper for aluminum, argon, silver, and copper, utilizing a Hartree-Fock ρ yields values fitted by

$$\langle U\rangle_{0\ HF} \sim -2.4\, Z^{2.4}\, Ry \quad . \tag{44}$$

The Thomas-Fermi model yields, instead,

$$\langle U\rangle_{0\ TF} \sim -3.32\, Z^{7/3}\, Ry \quad . \tag{44a}$$

Notice that, according to these results, $13B - \langle U\rangle_0$ differs by <3 percent from the corresponding "no correlation" expression 15B. As noted in Appendix A, page 36, successive shells of an atom contributed comparable amounts to B and $\langle U\rangle_0$.

On the other hand, the quantities $\langle T^2\rangle_0$ and $\rho(\underline{R}_N)$ in the second term of Equation 42 depend primarily on the contribution of K-shell electrons. For the H atom $\langle T^2\rangle$ amounts to 5 Ry^2. For the hydrogenic approximation of a single K electron, the contribution increases in proportion to Z^4; when screening is considered, the

contribution increases in proportion to $(Z-0.3)^4$. Thus, the whole K-shell contributes

$$\langle T^2 \rangle_{OK} \sim 10(Z-0.3)^4 \ \mathrm{Ry}^2 \ . \tag{45}$$

With regard to the electron density at the nucleus of a single atom ($\underline{R}_N = 0$), the screened hydrogenic approximation yields for the K-shell contribution

$$[\rho(0)]_K = \frac{2}{\pi} (Z-0.3)^3 \ . \tag{46}$$

Hartree data for argon agree with this value very well, and they show that outer shells contribute an additional 10 percent, approximately. Assuming that the outer electron contribution to be added to Equation 45 is also of the same order, it is suggested that calculation of the second term of Equation 42 utilizing Equations 45 and 46 with a 10-percent allowance for other shells will be correct to within a few percent.

4. Expansion of the High-Q Contribution into Powers of $1/v^2$

In this section we replace the treatment of Section 2.7 of Appendix A by a more-accurate though nonrelativistic procedure. This procedure is designed to calculate the contribution to stopping power from the region $(Q, E_n) \sim Q_{max}$, including corrections whose need is pointed out at the beginning of Section 4 of Appendix A but which have been taken into account previously only for atomic H (Ref. A134) and for an electron gas (Ref. 1).

We start then from the nonrelativistic approximation (Eq. A16a) to the inelastic cross section and replace the expression (Eq. A37) of the high-Q contribution to the stopping power by

$$\int_{Q_2}^{\infty} \Sigma_n E_n \, d\sigma_n \, \mathrm{St}(qv-E_n) = \frac{2\pi z^2 e^4}{mv^2} Z \int_{Q_2}^{\infty} \frac{dQ}{Q^2} \Sigma_n E_n |F_n(\underline{q})|^2 \, \mathrm{St}(qv-E_n) \ . \tag{47}$$

In this formula the integration over Q has been extended to its actual limit $Q = \infty$, and the step function has been introduced in the integrand to specify that the integration over Q and sum over n extend only over combinations of these variables that fulfill the condition of Equation A18. (The step function St(x) equals 1 for positive x, and 0 for negative x; since $Q = q^2/2m$, $\mathrm{St}(qv-E_n)$ vanishes when Equation A18 is violated.) The upper limit Q_{max} to the integral in Equation A37 served to fulfill Equation A18 approximately. The lower limit to the integral, Q_2, is the same as in Equation A37.

We utilize here the integral representation

$$\mathrm{St}(x) = \frac{1}{2\pi i} \int_{-i\infty+\epsilon}^{i\infty+\epsilon} dy \ \frac{e^{yx}}{y} \tag{48}$$

and wish to calculate the expression

$$\begin{aligned} \Sigma_n E_n |F_n(\underline{q})|^2 \, \mathrm{St}(qv-E_n) &= \frac{1}{2\pi i} \int_{-i\infty+\epsilon}^{i\infty+\epsilon} dy \, \frac{e^{yqv}}{y} \, \Sigma_n e^{-yE_n} E_n |F_n(\underline{q})|^2 \\ &= \frac{1}{2\pi i} \int_{-i\infty+\epsilon}^{i\infty+\epsilon} dy \, \frac{e^{yqv}}{y} \left(-\frac{d}{dy}\right) G(-y, \underline{q}) \end{aligned} \tag{49}$$

to be entered in Equation 47. The function G in this formula is the same as defined by Equations 4 and 5 in Section 2.

In section 2, the expansion of $G(x,\underline{q})$ into powers of x has been relevant. However, this expansion is seen (for example, from Eq. 13 and Eq. 14) to involve simultaneously an expansion into powers of q and Q. These quantities are large in the high-Q range, with which we are concerned. Therefore, a modified expansion should be sought which is appropriate to our problem.

Notice that the operator on the right side of Equation 13 contains a factor $\exp\int_0^x Q dx' = \exp(Qx)$, which is actually a number rather than an operator and can be factored out of the mean value operation. Since, in our range of interest, Q is of the order of $qv \gg \underline{q}\cdot\underline{v}_j$ (v is the incident particle's velocity and v_j an atomic electron velocity), the factor $\exp(Qx)$ contains that part of the dependence of G on x which is not suitably expanded into powers of x. Accordingly we define, with analogy to Equations 13, 14a, 15, and 4,

$$\bar{G}(x,\underline{q}) = \exp(-Qx)\, G(x,\underline{q}) = Z^{-1}\Sigma_{i,j}\,(0|A_i^*(\underline{q})A_j(\underline{q})\exp\textstyle\int_0^x \underline{q}\cdot\underline{v}_j(x')dx'|0)$$

$$= \Sigma_r \frac{1}{r!}\, x^r Z^{-1}\Sigma_{i,j}\,(0|A_i^*(\underline{q})A_j(\underline{q})\bar{H}_j^{(r)}(\underline{q})|0) = \Sigma_r \frac{1}{r!}\, x^r \bar{S}_r \quad , \tag{50}$$

where each of the operators $\bar{H}_j^{(r)}$ is to be obtained from the corresponding $H^{(r)}$ in Equation 17 by deleting the terms that contain Q explicitly. It will be verified later that the expansion utilized here reduces eventually to an expansion into powers of v_j/v.

We substitute now in Equation 49

$$G(-y,\underline{q}) = e^{-yQ}\,\Sigma_r \frac{1}{r!}\,(-y)^r\,\bar{S}_r \tag{51}$$

and, more specifically,

$$-\frac{d}{dy}\,G(-y,\underline{q}) = e^{-yQ}Q\,\Sigma_r\,(1-\frac{r}{yQ})\frac{(-y)^r}{r!}\,\bar{S}_r$$

$$= e^{-yQ}\,Q\,\Sigma_r\left[\frac{(-yQ)^r}{r!} + \frac{(-yQ)^{r-1}}{(r-1)!}\right]\frac{\bar{S}_r}{Q^r} \quad . \tag{52}$$

Since $Q > Q_2 > 0$, we can replace y as an independent variable by

$$w = yQ \quad . \tag{53}$$

We shall also set, where suitable,

$$u = \frac{2mv}{q} \quad , \qquad Q = \frac{q^2}{2m} = \frac{2mv^2}{u^2} \quad . \tag{54}$$

Equation 49 yields, then,

$$\frac{1}{Q}\,\Sigma_n E_n\,|F_n(\underline{q})|^2\,St(qv-E_n) = \Sigma_n f_n(Q)\,St(qv-E_n)$$

$$= \frac{1}{2\pi i}\int_{-i\infty+\epsilon}^{i\infty+\epsilon} dw\,\frac{e^{w(u-1)}}{w}\,\Sigma_r\left[\frac{(-w)^r}{r!}+\frac{(-w)^{r-1}}{(r-1)!}\right]\frac{\bar{S}_r}{Q^r}\ . \tag{55}$$

The integration over w reduces now to application of Equation 48 and of the related formula

$$\frac{1}{2\pi i}\int_{-i\infty+\epsilon}^{i\infty+\epsilon} dw\,\frac{e^{w(u-1)}}{w}w^r = \left(\frac{d}{du}\right)^r St(u-1) = \left(\frac{d}{du}\right)^{r-1}\delta(u-1) = \delta^{(r-1)}(u-1), \tag{56}$$

with the result

$$\frac{1}{Q}\Sigma_n E_n\,|F_n(q)|^2\,St(qv-E_n) = \Sigma_n f_n(Q)\,St(qv-E_n)$$

$$= St(u-1)\left(\bar{S}_0+\frac{\bar{S}_1}{Q}\right)+\left[\Sigma_{r=1}\frac{(-1)^r}{r!}\,\delta^{(r-1)}(u-1)+\Sigma_{r=2}\frac{(-1)^{r-1}}{(r-1)!}\,\delta^{(r-2)}(u-1)\right]\frac{\bar{S}_r}{Q^r}\ . \tag{57}$$

Substitution into Equation 47, taking into account Equation 54 and, in particular, $dQ/Q = -2du/u$, yields now

$$\int_{Q_2}^{\infty}\Sigma_n E_n\,d\sigma_n\,St(qv-E_n) = \frac{2\pi z^2e^4}{mv^2}Z\left\{\bar{S}_0\ell n\,\frac{2mv^2}{Q_2}+\int_{Q_2}^{2mv^2}\frac{dQ}{Q^2}\,\bar{S}_1\right.$$

$$\left.-2\left[\left(\Sigma_{r=1}\,\frac{1}{r!}\left(\frac{d}{du}\right)^{r-1}+\Sigma_{r=2}\,\frac{1}{(r-1)!}\left(\frac{d}{du}\right)^{r-2}\right)\frac{\bar{S}_r}{uQ^r}\right]_{u=1}\right\}\ . \tag{58}$$

We proceed now to the evaluation of the coefficients $\bar{S}_r$ (defined by Equation 50), taking into account that they appear in Equation 58 in the combination $\bar{S}_r/Q^r$ and that $q = 2mv$ and $Q = 2mv^2$ at $u = 1$. For simplicity, we disregard here again the effects of electron-electron correlation, as we did in the evaluation of S_5 in Section 2. In the present instance correlation effects should be particularly small because the large value of q causes the products $A_i^*(\underline{q})A_j(\underline{q}) = \exp[i\underline{q}\cdot(\underline{r}_j-\underline{r}_i)/\hbar]$ to oscillate very rapidly. We set, then, $i = j$, that is, $A_i^*A_j = 1$, so that

$$\bar{S}_r = Z^{-1}\Sigma_j\langle 0|\bar{H}_j^{(r)}(\underline{q})|0\rangle\ , \tag{59}$$

and agree to disregard all effects of electron-electron interaction.

Terms of $\bar{H}_j^{(r)}(\underline{q})$ of order s in q will yield, upon division by Q^r and setting $q = 2mv$, contributions to $\bar{S}_r/Q^r$ of order $2r-s$ in $1/v$. We are interested here in calculating to order $1/v^4$ and shall accordingly consider only terms of order $s \geq 2r-4$. We obtain, then, from Equation 17,

$$\bar{H}_j^{(0)} = 1 \ , \quad \bar{H}_j^{(1)} = \underline{q}\cdot\underline{v}_j \ , \quad \bar{H}_j^{(2)} = \underline{q}\cdot\underline{v}_j' + (\underline{q}\cdot\underline{v}_j)^2 \ ,$$
$$\bar{H}_j^{(3)} = \frac{3}{2}(\underline{q}\cdot\underline{v}_j' \ \underline{q}\cdot\underline{v}_j + \underline{q}\cdot\underline{v}_j \underline{q}\cdot\underline{v}_j') + \frac{1}{2}[\underline{q}\cdot\underline{v}_j, \underline{q}\cdot\underline{v}_j'] + (\underline{q}\cdot\underline{v}_j)^3 + O(q^{2r-5}) \ , \qquad (60)$$
$$\bar{H}_j^{(4)} = (\underline{q}\cdot\underline{v}_j)^4 + O(q^{2r-5}) \ , \quad \bar{H}_j^{(r)} = O(q^{2r-5}) \text{ for } r \geq 5 \ .$$

The process of averaging over the direction of $\underline{q}$, discussed in Section 2, cancels the contributions of $\bar{H}_j^{(1)}$, of the $\underline{q}\cdot\underline{v}_j'$ term of $\bar{H}_j^{(2)}$, and of the $(\underline{q}\cdot\underline{v}_j)^3$ term of $\bar{H}_j^{(3)}$. The first term of $\bar{H}_j^{(3)}$ has mean value zero because it is Hermitian and time-odd (see Sec. 2). The mean value of the remainder of $\bar{H}_j^{(3)}$ is given by Equation 29, with i = j; the mean values of $\bar{H}_j^{(2)}$ and $\bar{H}_j^{(4)}$ are elementary. After averaging over the direction of $\underline{q}$ we obtain, in the notation of Equation 32,

$$\bar{S}_0 = 1 \ , \quad \bar{S}_1 = 0 \ , \quad \bar{S}_2/Q^2 = \frac{2}{3} m \langle v^2\rangle_0/Q \ ,$$
$$\bar{S}_3/Q^3 = (4\pi\hbar^2 e^2/3mQ^2)\Sigma_N Z_N \langle \delta(\underline{r}-\underline{R}_N)\rangle_0 \ , \quad \bar{S}_4/Q^4 = 4m^2 \langle v^4\rangle_0/5Q^2 \ . \qquad (61)$$

Upon substitution of Equation 61 in Equation 58, the residual operations over u are straightforward and yield our final result, in the notation of Equation 40

$$\int_{Q_2}^{\infty} \Sigma_n E_n \, d\sigma_n \, St(qv - E_n)$$
$$= \frac{4\pi z^2 e^4}{mv^2} Z \left\{ \ln \frac{2mv}{q_2} - \frac{1}{Z}\left[\frac{\langle T\rangle_0}{mv^2} + \frac{\langle T^2\rangle_0 + (10\pi/3)Ry^2 \Sigma_N Z_N \rho(\underline{R}_N)}{(mv^2)^2} + \ldots \right] \right\} \qquad (62)$$

This formula should be compared with the complete stopping-power formula (Eq. A38) and with the expression (Eq. 40) of the low-Q contribution to the shell correction C. The comparison shows that the square bracket represents a high-Q contribution to the shell correction which is identical with the low-Q contribution to order $1/v^4$, to within the correlation term $(1/15)\langle V\rangle_0$ whose counterpart in Equation 62 has not been evaluated. The approximate equality of the high- and low-Q contributions which has thus been established confirms the surmise made on page 37 of Appendix A.

However, the treatment developed in this section for the high-Q contributions does not follow exactly the same line as that presented on pages 31 and 35 of Appendix A, which underlies the low-Q calculation of Section 3. It is likely, but has not been demonstrated, that the two treatments are in fact consistent and their results comparable to the stated order of accuracy. A new unified treatment of the low- and high-Q contributions to shell corrections would be desirable. Such a treatment might perhaps start from Equation 47 with its lower integration limit set at Q = 0, and then utilize Equation 49 with alternative expansions of $G(x, \underline{q})$ appropriate to different ranges of Q.

5. Comments on Equipartition Sum Rules

A curious aspect of stopping-power theory—which is still ill-understood and somewhat ill-defined but has attracted renewed attention in recent months—appears from the following remarks:

(a) In Bohr's initial theory of the energy loss (Ref. A25, and pp. 4, 8 of

Appendix A), where collisions are classified according to the impact parameter b, values of b larger and smaller than the atomic radius contributes equal aggregate amounts to the stopping power.

(b) In Bethe's theory the equivalent statement is that the leading term $\ln[(2mv^2)^2/I^2]$ in the center braces of Equation A38 arises in equal portions from $\int_{Q_{min}}^{I} dQ/Q$ and $\int_{I}^{Q_{max}} dQ/Q$.

(c) The energy-loss contribution of transverse excitations, which arises only from values of Q and E_n near the limit $Q = Q_{min}$ (see Appendix A, fig. 2 on p. 10), stems in equal amounts from low-Q and high-Q collisions as noted in Section 2.8 of Appendix A. The intermediate range of Q does not contribute an appreciable amount of transverse excitations because energy and momentum cannot be conserved in this range at $Q \sim Q_{min}$ (see Appendix A, Sec. 2.4). However, the density effect appears to destroy the equality of low-Q and high-Q contributions because it reduces only the probability of low-Q transverse collisions.

(d) The stopping-power's variation, as a function of the incident particle's velocity, arises from the factor $1/v^2$ in Equation A38 and from the factor in the braces. The latter variation stems from the shift of the line $Q = Q_{min}$, which limits the values of Q and E_n consistent with energy conservation. Since this line intersects the dotted area of Figure A2 in two separate regions, of low Q and high Q, two separate contributions to the variations of stopping power can be distinguished here rather clearly. As noted above (in Sec. 4), these two contributions are equal, at least to within electron correlation effects that have not been analyzed completely and to order $(1/v^2)^2$.

(e) Lindhard and Winther (1) have recently studied in detail the stopping power of an electron gas. In this model, the region of Q and E_n consistent with momentum conservation has a sharp limit on the low-Q side, in contrast to the general case shown in Figure A2 where the dotted area fades out. This limit crosses the energy conservation limit $Q = Q_{min}$ at two exactly defined points, and thus distinguishes low-Q and high-Q contributions sharply, provided only that the particle velocity is sufficiently high. The two contributions to the variations of stopping power are shown to be exactly equal, irrespective of any expansion into powers of $1/v^2$.

The preceding remarks and special results might have a common origin in a single general equipartition theorem. It would, of course, be of interest, particularly for the shell-correction problem, to establish such a theorem. The theorem should define a line in the (Q, E_n) plane of Figure A2, or in an equivalent representation, such that the two regions of the plane on either side of the line contribute equally to the stopping power. Insofar as there exists an "empty crescent" in the map of Figure A2—that is, insofar as there is an intermediate range of values of Q for which momentum conservation restricts the possible values of E_n more stringently than energy conservation—it is sufficient to state that the desired line crosses the line $Q = Q_{min}$ somewhere within the empty crescent. Items (d) and (e) above involve such a statement. However, one should like to define the line more precisely and independently of the existence of an approximately empty crescent.

The following remark, which originates from Reference 1, is also of interest. Energy conservation requires the projection of the momentum transfer q along the

direction of the incident particle to equal E_n/v. With reference to the angle ψ between $\underline{q}$ and this direction (see Fig. A1), the condition is

$$E_n = qv \cos\psi \ . \tag{63}$$

The line $Q = Q_{min}$ in Figure A2, which sets the energy conservation limit to the integration over E_n and Q, represents Equation 63 for $\psi = 0$ and a given v, but a whole family of nonintersecting lines can be considered in the (Q, E_n) or equivalent representations, which correspond to alternative values of the parameter $v\cos\psi$. For a given v, the points on one such line correspond to momentum transfers $\underline{q}$ with a constant obliquity ψ and with different magnitudes q. Any of these lines that intersects the empty crescent contains two separate classes of points, with large q (i.e., large Q) and small q. The high-q collisions yield (for $\psi < 45°$) ejected electrons which are faster than the incident particle. On the contrary, the low-q collisions yield excitations with properties nearly independent of q and, therefore, with very small group velocity, much lower than the velocity v of the incident particle. Thus a criterion might be sought for classifying high-q and low-q excitations depending on whether their group velocity is higher than v. An equipartition theorem could then perhaps state that for each direction of $\underline{q}$ equal amounts of energy are spent in producing excitations that propagate ahead of the incident particle and in excitations that trail it.

However, the concept of excitation velocity does not appear to have been established in general. In the electron gas model of Reference 1, the final state of each excitation process, and therefore its energy E_n, is identified by the momentum transfer $\underline{q}$ and by the statement that either it is a state of collective excitation or that it removes an electron of given momentum from the initial ground state. This special circumstance permits the definition of the group velocity $\partial E_n/\partial q$, in that it specifies which characteristics of the excitation are kept constant in the operation $\partial/\partial q$. The same circumstance plays an important role in the proof of the equipartition theorem for the electron gas, so that the proof does not apply immediately in its absence.

The following energy-momentum relationship for the excitations of a material, which relates to the basic sum rule

$$\Sigma_n E_n |F_n(q)|^2/Q = \Sigma_n f_n(Q) = 1 \tag{64}$$

equivalent to Equation 20, might conceivably lead to a suitable definition of excitation velocity. Consider for each value of Q an excitation energy E such that

$$\begin{aligned} &E_n < E \\ &\Sigma_n f_n(Q) = g \ , \quad 0 < g < 1 \ . \end{aligned} \tag{65}$$

Equation 65 defines a set of curves

$$g(E_n, Q) = \bar{g}(q, E_n) = \text{const.} \tag{66}$$

in the (E_n, Q) or in the (q, E_n) representation. The slope of the curve that passes through a given point (q, E_n),

$$\left(\frac{dE_n}{dq}\right)_{\text{constant } \bar{g}} = - \frac{\partial\bar{g}/\partial q}{\partial\bar{g}/\partial E_n} \ , \tag{67}$$

defines a velocity pertaining to an excitation with the given values of E_n and q. For high-Q collisions all the curves of Equation 66 lie in a narrow bundle along the line $E_n = Q$ of Figure A2, and the value of Equation 67 coincides with the velocity of the ejected electron. For low-Q collisions, the curves of Equation 66 tend to become vertical in the representation of Figure A2, and horizontal in a (q, E_n) plot, so that the value of Equation 67 vanishes.[6] Through each point, (q, E_n) or (E_n, Q), one can draw one line of the family of curves for Equation 66 and one line of the family of curves for Equation 63 with the appropriate value of $v \cos\psi$. One might then classify a collision with given (q, E_n) as a low-q or high-q collision depending on whether the velocity (Eq. 67) is lower or higher than $v \cos\psi$. Each line of Equation 63, $E_n = qv \cos\psi$, should have a point at which it is tangent to one of the lines of Equation 66; this point might conceivably be significant for equipartition.

6. Discussion of Numerical Values

The relationship of the foregoing theoretical developments to the employment of actual numerical values for shell corrections elsewhere in these reports (notably in Reports 2, 6, 7 and in Appendix A) is next considered. Although the shell corrections may be based on different points of departure for different purposes, the numerical values arrived at are in essential agreement throughout these reports within the ranges of applicability stated by the authors.

Estimates of the high-energy limiting values of the total shell corrections based on the expressions developed in this report are given in Table 1, where relevant quantities from Section 3 are evaluated for the determination of C_1 by means of Equation 42, including correlation terms to order $1/v^2$. A 10-percent addition to the K-shell contribution to the coefficient $1/v^4$ was also made. From the result of Section 4, the total atomic shell correction C due to both the high-Q and low-Q contributions was taken simply to be $C \sim 2C_1$. The resulting numerical values for C/Z at $\beta = 1$ are given in the last column of Table 1. It was found that the final values of C/Z were essentially the same, whether the Hartree-Fock or the Thomas-Fermi model estimations from Section 3 were employed for the coefficient of $1/v^2$. The values of C/Z from Table 1 are just the high-energy limiting values of the proton shell-correction curves constructed as described in Section 4.5 of Appendix A and shown in Figure A6. As discussed in Appendix A, these curves were drawn to represent smoothed stopping-power results obtained by Bichsel. (These results were based on a scaling procedure for representing shell corrections akin to that described in Report No. 2 except that C vanished for $\beta = 1$ and I_{adj} was used in it instead of I. The values in Table 1 are also the ones utilized in Report No. 6). Therefore, this report, Appendix A, and Report No. 6 employ a unified treatment of shell corrections to be used in conjunction with the mean excitation energy I. Report No. 2 is also consistent with these reports, whereas Bichsel's earlier work utilized a different procedure, as noted above.

With respect to the numerical consistency of the shell corrections in the above-mentioned reports and in Report No. 7, the following is the situation. For computational purposes, the formula shown as Equation 16 in Report No. 7 was used to obtain shell corrections for the tables presented there. The velocity parameter was restricted to values $\eta > 0.13$ when this formula was applied. This corresponds to a proton energy > 8 Mev. The authors of Report No. 7 state that checks were made,

[6] Figure A2 fails to show that the upper edge of the shaded area bends downward on the left side of the graph since E_n never vanishes for quantum systems. In the low-energy discrete portion of the excitation spectrum, the shaded area breaks into a number of near-vertical strips corresponding to discrete levels.

TABLE 1

Estimated Shell Corrections for $\beta = 1$

Element	Z	B_{emp} (Ry) (Eq. 42)	$-\langle U\rangle_{0HF}$ (Ry) (Eq. 44)	$-\langle U\rangle_{0TF}$ (Ry) (Eq. 44a)	$\langle T^2\rangle_{\overline{0K}}$ (Ry^2) (Eq. 45)	$\frac{10}{3}\pi Z[\rho(0)]_K$ (Ry^2) (Eq. 46)	$\left(\frac{C}{Z}\right)_{\beta=1}$
Be	4	27.8	66.7	84.6	1.85×10^3	1.35×10^3	.000
Al	13	4.72×10^2	1.13×10^3	1.32×10^3	2.59×10^5	1.78×10^5	.002
Ar	18	1.01×10^3	2.42×10^3	2.82×10^3	9.85×10^5	6.67×10^5	.003
Cu	29	3.20×10^3	7.68×10^3	8.50×10^3	6.81×10^6	4.56×10^6	.007
Ag	47	1.01×10^4	2.42×10^4	2.63×10^4	4.77×10^7	3.20×10^7	.014
Pb	82	3.88×10^4	9.31×10^4	9.60×10^4	4.52×10^8	2.98×10^8	.039
U	92	5.20×10^4	1.25×10^5	1.29×10^5	7.16×10^8	4.74×10^8	.051

and that good numerical agreement was found between their results and results obtained by Bichsel using the scaling procedure described in Report No. 2. In Report No. 7, the shell corrections are regarded as becoming vanishingly small in the high-energy limit, $\beta = 1$. As discussed in Report No. 6, it is threfore appropriate to use the adjusted mean excitation energy, I_{adj}, with these shell corrections.

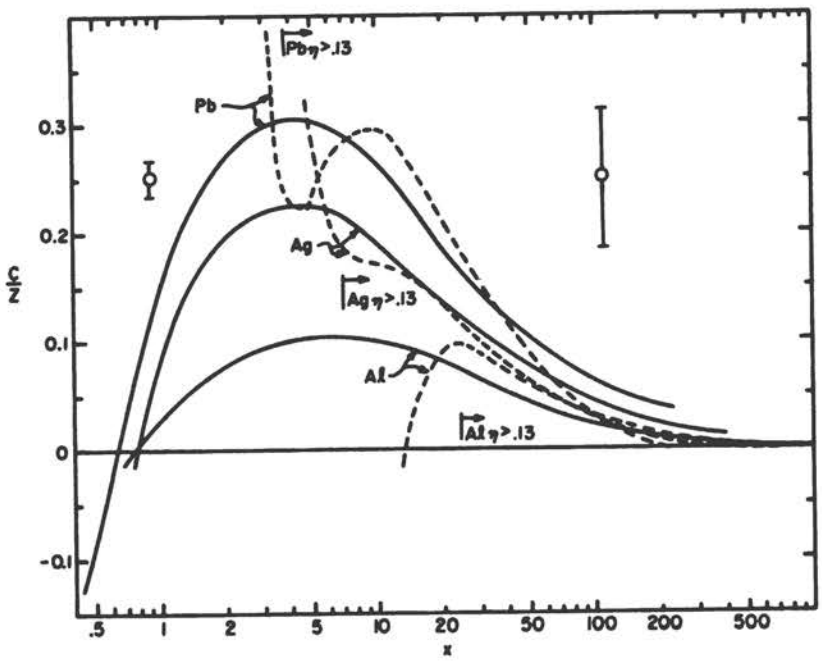

Figure 1. Comparison of shell corrections. The solid curves are taken from Figure A6 and the dashed curves were calculated from Equation 16 in Report No. 7 of the present volume.

Based on these considerations, then, a final appraisal of the consistency of numerical shell corrections used in the various reports of this volume can be made by comparing numerical values obtained from Equation 16 in Report No. 7 with the curves in Figure A6. This has been done, and the results are shown in Figure 1 for aluminum, silver, and lead. The solid curves were taken directly from Figure A6 and the dashed lines show the corresponding curves as calculated from the formula in Report No. 7. For each element the range of x corresponding to $\eta > 0.13$ is indicated. It is seen that the two sets of curves agree numerically to well within 1 percent of the total stopping power (the amount indicated by the error bars) in the regions $\eta > 0.13$, except in the case of lead when η gets close to the limiting value 0.13. There, the discrepancy is of the order of 1 percent where it is largest. Except perhaps for details of structure of this kind, the various shell-correction estimations in the reports in this volume should make very little numerical difference in stopping-power and range calculations.

References

1. J. Lindhard and A. Winther, Kgl. Danske Videnskab. Selskab. Math. Fys. Medd. 34 (4), (1964).

2. R. P. Feynman, Phys. Rev. 84, 108 (1951).

5. MULTIPLE-SCATTERING CORRECTIONS FOR PROTON RANGE MEASUREMENTS[1]

Martin J. Berger[2] and Stephen M. Seltzer[2]

Abstract

Three approximate methods are described that may be used to calculate differential and integral distributions of projected range, median ranges, and curves of ionization versus depth (Bragg curves) for protons traversing thick absorbers. One of the methods is based on the application of a multiple-scattering detour distribution obtained by Yang; the second method is due to Bichsel and Uehling; and the third makes use of random sampling. Two types of statistical fluctuations are taken into account: energy loss straggling in collisions with atomic electrons, and the "wiggliness" of the track (detours) due to multiple Coulomb scattering by atoms. All three methods were used to extract the values of the proton c.s.d.a. range, r, and of the mean excitation energy, I_{adj}, of the medium from Bragg curves in lead and copper measured by Mather and Segre and by Zrelov and Stoletov. They give results for r and I_{adj} that are in good agreement with each other, but do not account entirely for shape of the measured Bragg curves.

1. Introduction

The analysis of proton range measurements requires corrections which take into account energy loss straggling as well as deviations of the proton tracks from a straight-line path due to multiple Coulomb scattering. These corrections, although relatively small, are significant if one wants to extract accurate values of the mean excitation energy of the medium from range measurements.

The purpose of this report is to discuss and compare a few methods of correction that have been proposed, including those of Mather and Segrè (1) and of Bichsel and Uehling (2), the application of a multiple-scattering detour distribution of Yang (3), and Monte Carlo calculations of Barkas and von Friesen (4) and of Berger (5). The theoretical background for the topics treated here is discussed by U. Fano in Appendix A of this volume under the headings "Energy Straggling" and "Multiple Scattering Effects on Penetration."

Range measurements have been made in a variety of experimental arrangements; here we shall consider only the schematic, and somewhat oversimplified, situation sketched in Figure 1. A beam of monoenergetic particles of energy T_0 is incident

[1]Supported by the National Aeronautics and Space Administration under contract R-80 with the National Bureau of Standards.

[2]National Bureau of Standards, Washington, D. C.

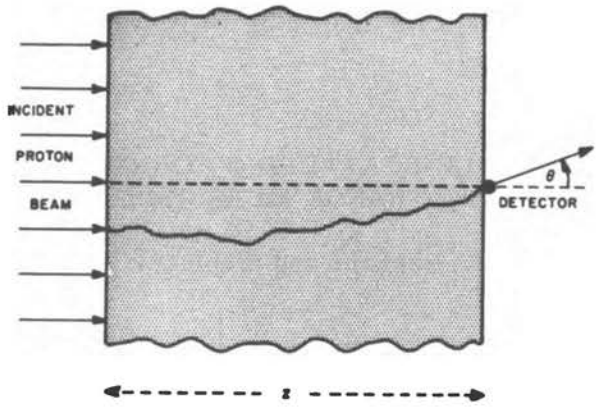

Figure 1. Assumed source-target-detector configuration for range measurements.

perpendicularly, in the z-direction, on a slab of thickness z. In a "poor geometry" experiment, the slab is unbounded in the x- and y-directions. In "good geometry" it is laterally bounded, which reduces the magnitude of the multiple-scattering corrections but complicates their evaluation. A proton detector is placed immediately behind the slab and is assumed to be characterized by a response $R(T, \theta)$ to individual protons emerging from the exit face of the slab with energy T and obliquity θ.

Let $J(z, T, \theta)\sin\theta d\theta dT$ represent the probability that a proton is transmitted through the slab and emerges through the exit face with an energy between T and T+dT and with an obliquity between θ and $\theta+d\theta$. The reading of the detector as a function of slab thickness, to be denoted by $Q(z)$, is given by

$$Q(z) = Q_0 \int_0^{T_0} dT \int_0^{\pi/2} \sin\theta d\theta J(z, T, \theta) R(T, \theta) , \qquad (1)$$

where Q_0 is a normalization constant which depends on the source strength and, at sufficiently high energies, also on the possible loss of protons from the beam due to nuclear interactions. For convenience, it will be assumed that $Q(z)$ is normalized so that its maximum value is unity, and Q_0 will be omitted from subsequent equations.

We shall have occasion to consider two types of detectors with the following response functions:

(a) Proton counter (e.g., a Faraday cup) that measures the current of protons across the exit face of the target slab. The response of such a device is independent of the proton energy and direction,[3] so that

$$R(T, \theta) = 1 . \qquad (2)$$

The corresponding detector reading, to be denoted as $Q_{IR}(z)$, is called the integral distribution of projected range because it is proportional to the number of protons that penetrate to a depth greater than z.

[3] In an actual experimental situation there may be a limitation on the proton energies and obliquities which the detector will accept; this complication is disregarded in our schematization.

(b) Ionization chamber. The response of such an instrument is proportional to the stopping power of the gas in the chamber and to the pathlength in the chamber which is, in turn, inversely proportional to $\cos\theta$.[4]

Thus,

$$R(T,\theta) = -\frac{1}{\rho}\left[\frac{dE}{dx}(T)\right]_{gas}\frac{1}{\cos\theta} \cdot \tag{3}$$

The corresponding detector reading, to be denoted as $Q_{BR}(z)$, is usually called a curve of ionization versus depth or Bragg ionization curve.

2. Statement of the Problem

Let us suppose, for a moment, that the protons travel in a straight line within the target and that their energy loss at each point on their track is equal to the mean loss corresponding to their instantaneous energy. In this case, the integral distribution of projected range would be a step function,

$$Q_{IR}(z) = \begin{cases} 1 & z \le r \\ 0 & z > r \end{cases}, \tag{4}$$

where

$$r = \int_0^{T_0} \frac{dT}{-\frac{1}{\rho}\frac{dE}{dx}(T)} \tag{5}$$

is the mean range in the continuous-slowing-down approximation (the c.s.d.a. range defined in the preface to this volume). From the location of the step of an experimental integral range curve one could immediately deduce the c.s.d.a. range and, from the latter, the mean excitation energy of the medium. Because of energy loss fluctuations and multiple-scattering detours, some protons will travel farther, others less far, than the c.s.d.a. range, so that the integral range distribution does not have the shape of an abrupt step but is rounded off. To extract from an experimental range distribution the value of the c.s.d.a. range one must therefore establish a parametric relation of some kind between the shape of $Q_{IR}(z)$ and the value of r, taking into account the proton energy and the characteristics of the medium.[5] For example, one may calculate, as a function of r, the median projected range,[6] i.e., the target thickness $z_{1/2}$ such that $Q_{IR}(z_{1/2}) = 0.5$ (50 percent transmission). Analogous criteria have been developed relating the c.s.d.a. range to the shape of Bragg ionization curves, which will be discussed in Section 7.

The evaluation of $Q_{IR}(z)$ or $Q_{BR}(z)$ requires the calculation of the transmitted proton current $J(z, T, \theta)$. This is a difficult problem of transport theory which so far

[4]Again, this is true only for a limited range of exit obliquities.

[5]It is also possible to relate the shape of $Q_{IR}(z)$ directly to the value of the mean excitation energy, avoiding the use of the c.s.d.a. range as auxiliary variable.

[6]The concept of the median projected range is useful only when the loss of protons from the beam due to nuclear interactions is insignificant.

has been solved only in various approximations. An exact solution is difficult to obtain for several reasons. The problem involves at least three independent variables (position, direction, energy), none of which can be suppressed; the underlying single-scattering cross sections have very strong peaks corresponding to the small deflections or energy losses; one must calculate penetration to very great depths, under conditions where the use of simplified cross sections or other approximations have serious consequences.

Approximate solutions can be obtained through the use of results for restricted problems combined in a suitable manner. The combination can be done either analytically, or numerically by random sampling. In the analytical approach, energy loss fluctuations are taken into account indirectly through the use of a probability distribution for pathlengths which relates the actual pathlength to the c.s.d.a. range. This distribution is then folded into a conditional probability distribution which describes multiple-scattering detours (shortening of the projected range) for a particle with given pathlength. The multiple-scattering detours can be readily calculated only in the continuous-slowing-down approximation, and the use of the convolution implies that the small correlation between energy loss (or pathlength) fluctuations and multiple-scattering detours is not taken into account.

In the Monte Carlo approach a random-walk model is employed in which each step of the walk takes into account the effects of many successive single-scattering events. The transition probabilities for the random walk are derived from the appropriate transport-theoretic results (pathlength distribution, multiple deflections). The grouping of single-scattering events into steps of an artificial random walk is made necessary by their enormous number, which makes direct analog computation too expensive. The grouping introduces a certain systematic error which is superimposed on the statistical error. The Monte Carlo calculation is more laborious and gives less insight into the problem than analytical approximations, but is capable, with sufficient effort, of giving more accurate results. Moreover, the Monte Carlo method is the only one now available which can be used to treat laterally bounded targets for which the sideways escape of protons is important.

3. Outline of Analytical Approximation Scheme

We may assume as known, and shall describe below in more detail, the following probability distributions:[7]

$G(s)ds$ = probability that a proton with initial energy T_0 will have traveled a pathlength between s and s+ds when it has been slowed down to a stop. G(s) is determined by energy-loss fluctuations.

$F(z;\varepsilon)dz$ = conditional probability that a proton with initial energy T_0 and pathlength s will come to rest at a depth between z and z+dz. F(z;s) is determined by detours resulting from multiple Coulomb scattering. In principle, the detours depend on the detailed history of the proton. In practice, one is limited to computing them in the continuous-slowing-down approximation.

[7] These distributions pertain to protons slowing down in an unbounded homogeneous medium. The multiple-scattering angular deflections are usually small enough so that one can disregard the probability that the proton direction will be completely reversed. Therefore, one need not distinguish between a slab of finite thickness and an unbounded medium.

The convolution of these two distributions yields the probability

$$H(z)dz = \int_z^\infty G(s)F(z;s)dsdz \tag{6}$$

that a proton with initial energy T_0 will come to rest at a depth between z and z+dz. The integral distribution of projected range is then given by

$$Q_{IR}(z) = \int_z^\infty H(z')dz' \ . \tag{7}$$

This equation states that the proton current through the exit face of a slab of thickness z is proportional to the fraction of the protons which, in an unbounded medium, would have come to a stop at depths $z' > z$. This relation holds only if the protons move in the direction of increasing z along their entire track, never suffering a reversal of direction.

The Bragg ionization curve can similarly be expressed as

$$Q_{BR}(z) = \int_z^\infty H(z')R^*(z',z)dz' \ . \tag{8}$$

For a proton that eventually comes to a stop at a depth $z' > z$, we do not know the energy and direction that it had when crossing the exit plane at z. As will be shown below, it is possible to make an estimate of these quantities adequate for the analysis of Bragg ionization curves. We shall denote the response function based on such an estimate as $R^*(z',z)$.

4. Pathlength Distribution

The pathlength distribution is approximately Gaussian,

$$G(s) = \frac{1}{\sqrt{2\pi}\,\sigma} \, e^{-(s-r)^2/2\sigma^2} \tag{9}$$

with a mean r equal to the c.s.d.a. range defined by Equation 5 and a variance

$$\sigma^2 = 0.1570 \frac{Z}{A} \int_0^{T_0} \frac{1-1/2\beta^2}{(1-\beta^2)\left[1+2\frac{m}{M}(1-\beta^2)^{-1/2}\right]} \left[-\frac{1}{\rho}\frac{dE}{dx}(T)\right]^{-3} KdT \tag{10}$$

Z, A and ρ are the atomic number, atomic weight, and density of the medium, βc is the proton velocity, and m/M the ratio of the electron mass to the proton mass; r and σ are in units of g cm^{-2}, $-\frac{1}{\rho}\frac{dE}{dx}(T)$ in Mev/g cm^{-2} (see also p. 42 of Appendix A of this volume). K is a correction factor taking into account the binding of the atomic electrons and is important only at low energies. The most comprehensive evaluation of σ has been made by Sternheimer (6), who tabulated the so-called percentage range straggling

$$p = 100\frac{\sigma}{r} \tag{11}$$

for beryllium, carbon, aluminum, copper, lead, and air (assuming mean excitation energies[8] I_{adj} = 64, 78, 166, 371, 1071, and 94 ev, respectively) at energies between 2 and 10^5 Mev. At constant energy, p is almost independent of Z, showing only a very small increase from beryllium to lead, and can be considered a function of $\log I_{adj}$ only. Table 1 gives p-values taken directly from Sternheimer for beryllium and

TABLE 1

Percentage Range-straggling Parameter p for Protons
(according to Sternheimer)

T (Mev)	Be I_{adj} = 64ev	C I_{adj} = 78ev	Al I_{adj} = 163ev	Cu I_{adj} = 314ev	Sn I_{adj} = 516ev	Pb I_{adj} = 826ev
1000	0.879	0.886	0.921	0.956	0.988	1.025
800	0.897	0.904	0.943	0.980	1.015	1.055
600	0.924	0.932	0.974	1.016	1.055	1.099
500	0.942	0.952	0.996	1.039	1.080	1.129
400	0.966	0.976	1.023	1.071	1.116	1.167
350	0.980	0.991	1.040	1.089	1.136	1.190
300	0.997	1.009	1.060	1.111	1.161	1.218
250	1.017	1.029	1.084	1.139	1.191	1.251
200	1.041	1.054	1.112	1.172	1.229	1.293
160	1.065	1.078	1.140	1.205	1.267	1.334
140	1.078	1.093	1.157	1.225	1.288	1.358
120	1.094	1.109	1.178	1.250	1.316	1.388
100	1.112	1.128	1.201	1.278	1.347	1.420
80	1.135	1.152	1.231	1.315	1.389	1.463
70	1.149	1.166	1.249	1.338	1.415	1.492
60	1.165	1.183	1.271	1.364	1.445	1.527
50	1.183	1.203	1.297	1.397	1.483	1.570
40	1.206	1.230	1.330	1.437	1.531	1.623
30	1.238	1.263	1.377	1.493	1.592	1.689
25	1.259	1.285	1.408	1.529	1.630	1.728
20	1.286	1.315	1.450	1.575	1.677	1.774
15	1.322	1.357	1.507	1.634	1.731	1.819
10	1.382	1.424	1.597	1.717	1.815	1.923
8	1.419	1.466	1.649	1.751	1.845	1.977
6	1.469	1.526	1.720	1.842	1.949	2.087
4	1.550	1.631	1.814	1.984	2.123	2.257
2	1.704	1.867	1.968	2.219	2.436	2.602

[8] In accordance with the definition adopted by the Subcommittee (see preface and Paper No. 6 of this volume), we shall use the symbol I_{adj} in place of the customary I to indicate the mean excitation energy derived from experimental data on the assumption that shell corrections vanish in the high-energy limit.

aluminum, and p-values for copper, tin, and lead, adjusted to 314, 516 and 826 ev, respectively, by interpolation with respect to $\log I_{adj}$.[9] Table 2 gives selected values of the correction factor K used by Sternheimer.

TABLE 2

Binding-effect Correction Factor K in Formula for σ^2
(according to Sternheimer)

T (Mev)	Be	Al	Pb
1	1.37		
2	1.24	1.33	
5	1.12	1.27	1.31
10	1.07	1.19	1.22
50	1.02	1.06	1.19
100		1.04	1.16
200			1.11

A more accurate pathlength distribution derived by Lewis (7) is expressed as the product of a Gaussian times a correction factor $L\left(\frac{s-r}{\sigma}\right)$. The latter is evaluated as an Edgeworth series consisting of Hermite polynomials $H_n\left(\frac{s-r}{\sigma}\right)$ accompanied by coefficients which depend on the cumulants (certain combination of moments) of the pathlength distribution. The Lewis distribution is no longer symmetric; the most probable value of the pathlength is longer than the mean value. Lewis also found that the mean pathlength is slightly shorter than the c.s.d.a. range. The range, the difference being negligibly small for protons, however; for example, it amounts to only 0.02 percent for 340-Mev protons in lead.

The distribution of pathlengths which protons travel as their energy falls from T_0 to $T_f \neq 0$ may also be of interest. In the Gaussian approximation, one must use a mean value $r(T_0, T_f) = r(T_0) - r(T_f)$ and a variance $\sigma^2(T_0, T_f) = \sigma^2(T_0) - \sigma^2(T_f)$. The cumulants which enter into the Lewis correction factor can similarly be obtained by taking the difference of the cumulants evaluated for energies T_0 and T_f.

Table 3 shows $L\left(\frac{s-r}{\sigma}\right)$ for lead, $T_0 = 340$ Mev and various final energies T_f between 339 Mev and 1 Mev. It can be seen that only for very small $(T_0 - T_f)$-differences is there a significant departure from a Gaussian distribution. Table 4 shows $L\left(\frac{s-r}{\sigma}\right)$ for $T_0 = 340$ Mev and $T_f = 339$ Mev, as function of the atomic number of the medium.

[9] It would have been desirable to recompute p, using a more recent stopping-power table (Paper No. 7 of this volume). Because of the deadline for this publication, we were unable to do this and to adjust the remaining calculations in this paper accordingly.

TABLE 3

Lewis Correction Factor $L(\frac{s-r}{\sigma})$ for Pathlength Distribution in Lead, as Function of the Final Energy T_f, for an Initial Energy T_0 = 340 Mev

$\frac{s-r}{\sigma}$	T_f (Mev)							
	339	338	336	332	324	308	276	1
-1.0	0.75	0.83	0.88	0.91	0.93	0.95	0.97	0.98
-0.8	0.76	0.83	0.88	0.91	0.94	0.95	0.97	0.98
-0.6	0.78	0.84	0.89	0.92	0.94	0.96	0.97	0.98
-0.4	0.80	0.86	0.91	0.94	0.96	0.97	0.98	0.99
-0.2	0.84	0.90	0.94	0.96	0.97	0.98	0.99	0.99
0.0	0.89	0.95	0.97	0.99	0.99	1.00	1.00	1.00
0.2	0.98	1.01	1.02	1.02	1.02	1.01	1.01	1.01
0.4	1.10	1.09	1.07	1.05	1.04	1.03	1.02	1.01
0.6	1.25	1.17	1.12	1.08	1.06	1.04	1.03	1.02
0.8	1.40	1.25	1.16	1.10	1.07	1.05	1.03	1.02
1.0	1.52	1.31	1.19	1.13	1.08	1.06	1.04	1.02

TABLE 4

Lewis Correction Factor $L(\frac{s-r}{\sigma})$ for Pathlength Distribution for Different Media. T_0 = 340 Mev, T_f = 339 Mev

$\frac{s-r}{\sigma}$	C I_{adj} = 78.4ev	Al I_{adj} = 163ev	Cu I_{adj} = 314ev	Ag I_{adj} = 487ev	Pb I_{adj} = 826ev
-1.0	0.59	0.64	0.68	0.71	0.75
-0.8	0.62	0.66	0.70	0.73	0.76
-0.6	0.66	0.70	0.73	0.75	0.78
-0.4	0.71	0.74	0.76	0.78	0.80
-0.2	0.77	0.79	0.81	0.82	0.84
0.0	0.86	0.87	0.88	0.89	0.89
0.2	0.99	0.99	0.99	0.98	0.98
0.4	1.19	1.16	1.14	1.12	1.10
0.6	1.42	1.37	1.32	1.29	1.25
0.8	1.67	1.58	1.51	1.46	1.40
1.0	1.85	1.75	1.66	1.60	1.52

5. Multiple Scattering Detours

Theory of Yang

Yang (3) has given a prescription for calculating the joint distribution of the depth of penetration z and of the multiple-scattering deflection θ for a charged particle that has traveled a pathlength s. He explicitly evaluated the distribution of z for two cases: integrating over all possible values of θ, and for $\theta = 0°$. The first of these distributions will be used here.

Yang's derivation is based on an approximate form of the transport equation which makes use of the small-angle approximation and leads to a Gaussian distribution of multiple-scattering deflections instead of the more exact Molière distribution when all other variables are integrated out. The energy loss of the particle along its track is disregarded. At first sight, these restrictive assumptions would seem to preclude the use of Yang's distribution in the present problem. However, Monte Carlo calculations for protons, which will be described below, indicate that the applicability of the Yang distribution can be greatly extended, at least approximately, by the following adjustment: the one parameter that occurs in the distribution (the average difference $\langle s-z \rangle$ between pathlength and depth of penetration) is to be calculated with the use of rigorous transport theory, without resort to the small-angle approximation, and with inclusion of energy loss according to the continuous-slowing-down approximation. The Yang distribution is expressed in terms of the scaled variable

$$v = 2 \frac{s-z}{\langle s-z \rangle} \tag{12}$$

and has the form

$$F(z;s)dz = Y(v)dv$$

$$Y(v) = \begin{cases} 2\pi^{-1/2} v^{-3/2} \left[\exp(-1/v) - 3\exp(-9/v)\right] , & v \le 2 \\ \frac{\pi}{4} \exp(-\pi^2 v/16) , & v > 2 . \end{cases} \tag{13}$$

The percentage detour factor

$$D = \frac{100 \langle s-z \rangle}{s} \tag{14}$$

is shown in Figure 2 for beryllium, aluminum, copper, and lead as function of the initial proton energy T_0. These results are obtained by the transport calculation outlined in Section 8, which uses as input the Rutherford single-scattering cross

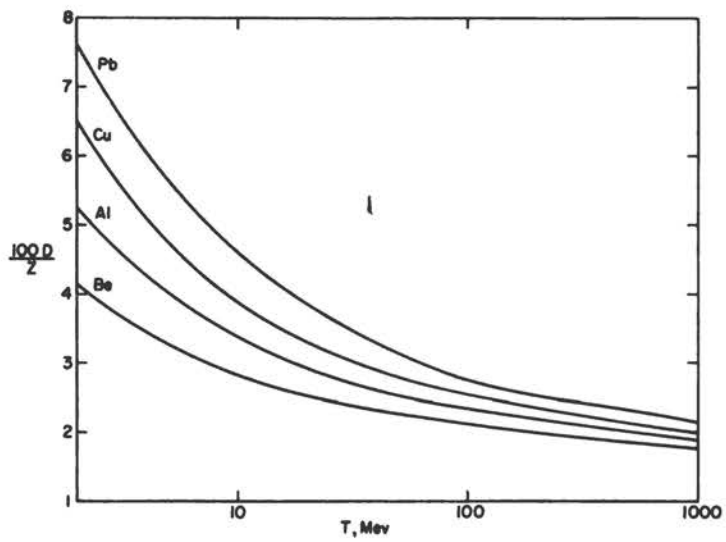

Figure 2. Ratio of percentage detour parameter, D, to the atomic number of the medium.

section modified for screening according to the prescription of Molière. The calculation is expected to be quite accurate at high energies, but there is some doubt whether the screening corrections are adequate for protons with energies as low as a few Mev.

Barkas (Paper No. 7 of this volume) has measured percentage detour factors in photographic emulsion and has then derived corresponding factors for other materials, assuming that the quantity $(1-n)(X_0/s)D$ is independent of the material (X_0 = radiation length, n a parameter that is close to 0.63 for all substances except those of lowest atomic number). Table 5 shows that Barkas' scaling procedure yields values of D, at energies between 1 and 8 Mev, which are somewhat lower than the calculated values, the discrepancies being greatest for low-Z materials.

TABLE 5

Comparison of Percentage Detour Factors D Obtained by Calculation and by the Scaling of Experimental Emulsion Data

T	Pb		Sn		Cu		Al	
(Mev)	Exp.	Cal.	Exp.	Cal.	Exp.	Cal.	Exp.	Cal.
1	7.2	7.6	3.9	4.6	2.0	2.5	0.7	0.9
2	5.9	6.2	3.1	3.6	1.6	1.9	0.6	0.7
3	5.2	5.4	2.7	3.1	1.4	1.6	0.5	0.6
4	4.7	5.0	2.5	2.8	1.3	1.5	0.5	0.6
5	4.4	4.6	2.3	2.6	1.2	1.4	0.4	0.5
6	4.2	4.4	2.2	2.5	1.1	1.3	0.4	0.5
7	4.0	4.2	2.1	2.3	1.0	1.2	0.4	0.5
8	3.8	4.0	2.0	2.3	1.0	1.2	0.4	0.5

Theory of Bichsel and Uehling

Bichsel and Uehling (2) based their considerations on the use of the angular multiple-scattering distributions of Molière (8),

$$f_M(\theta, B)\theta d\theta = \theta d\theta \{2\exp(-\theta^2) + f^{(1)}/B + f^{(2)}/B^2 + \dots\} , \qquad (15)$$

where

$$\theta = \Theta/\chi_c\sqrt{B}$$

and where Θ is the deflection angle.[10] Bichsel and Uehling start by assuming "smoothed-out" trajectories, along which the scaled Molière scattering angle θ is constant. The difference between pathlength and depth of penetration, in the small-angle approximation, is then expressed as

$$s - z = \frac{1}{2}\int_0^s \Theta^2 ds' = \frac{1}{2}\int_0^s \theta^2 \chi_c^2 B ds \qquad (16)$$

[10] The functions $f^{(1)}$ and $f^{(2)}$ have been tabulated by Molière (8), Bethe (9), and Scott (10). The prescription of Molière for evaluating χ_c and B, with energy loss accounted for in the continuous-slowing-down approximation, is summarized in Section 8.

For a smoothed-out trajectory, s-z is then proportional to θ^2, the proportionality constant being

$$\Delta_{BU} = \tfrac{1}{2} \int_0^s \chi_c^2 \, B \, ds' \, . \tag{17}$$

With this assumption, the distribution of s-z can be immediately derived from the Molière distribution, and is found to be

$$F(z;s)dz = \frac{dv}{4\sqrt{\frac{v}{2}}} f_M\left(\sqrt{\frac{v}{2}}, B\right) \tag{18}$$

with $v = 2 \, \frac{s-z}{\Delta_{BU}}$

Bichsel and Uehling attempted to account for the difference between actual proton paths and smoothed-out paths by a "wiggliness correction" based on the use of results in the paper of Yang. They estimate that s-z should, on the average, be increased by an additional amount $\frac{2}{15} \Delta_{BU}$ due to the wiggliness of the track. They then suggest that when folding the distribution F into the pathlength distribution G, this correction can be taken into account by using an F as calculated for a smoothed-out path but changing the mean of G from r to $r - \frac{2}{15} \Delta_{BU}$ and its variance from σ^2 to $\sigma^2 + \left(\frac{2}{15} \Delta_{BU}\right)^2$. This procedure is expected to be reasonably accurate because the required percentage change in mean and variance is usually rather small. Bichsel (private communication) suggested that even when the distribution F is of interest rather than its convolution with G, the same procedure can still be followed, the folding in this case being done with a Gaussian with mean $r - \frac{2}{15} \Delta_{BU}$ and variance $\left(\frac{2}{15} \Delta_{BU}\right)^2$. The peak of the distribution then occurs no longer at z = s but, more correctly, at a value of z slightly smaller than s (see Fig. 5).

Monte Carlo Detour Calculations

Barkas and von Friesen (4) made range measurements on 750-Mev protons, using a thin target rod with a 1" x 1" cross section in order to minimize the required multiple-scattering corrections, and carried out parallel Monte Carlo calculations. The protons were assumed to be incident along the axis of the rod. The entire track-length was divided into 102 intervals of gradually decreasing size, and the angular and lateral multiple-scattering deflections in each successive interval were sampled from a bivariate Gaussian distribution (Ref. 11). In this manner, tracks were followed until the proton escaped from the rod. The following information was extracted from the sampled tracks: (a) the escape of protons through the lateral surfaces of the rod, as a function of the depth of penetration; (b) the detour distribution for protons that passed through the entire length of the rod and emerged with an obliquity $\theta \leq 45°$ with respect to the rod axis.

Berger (5) calculated detour distributions for 338.5-Mev protons in lead and copper targets assumed laterally unbounded. The proton track-length (assumed equal to the c.s.d.a. range) was divided into 30 intervals, and the multiple-scattering deflection in each interval was sampled from the Molière distribution. The displacement in the z-direction in a section of path of length Δs is given by $\Delta z = u_x \Delta\xi + u_y \Delta\eta + u_z \Delta\zeta$, where $\underline{u}$ is the direction of motion at the beginning of the section, and where $\Delta\xi$, $\Delta\eta$, and $\Delta\zeta$ are the displacements expressed in a Cartesian coordinate system whose ζ-axis coincides with $\underline{u}$. In Berger's calculation, since u_x and u_y are

usually much smaller than u_z, the lateral multiple-scattering deflections were disregarded ($\Delta\xi = \Delta\eta = 0$) and $\Delta\zeta$ was calculated in three different approximations. In Model 1 the ratio $\frac{\Delta\zeta}{\Delta s}$ was set equal to unity, in Model 2 equal to $(1-\cos\omega)/2$, and in Model 3 equal to $1-\cos\omega$. Models 1 and 3 would seem to bracket the correct value, and Model 2 may come closest to representing the actual situation. The model error could be reduced by a subdivision of the proton track into more intervals or by an application of the Yang detour distribution within each interval. The effect of disregarding the lateral multiple-scattering deflections, $\Delta\xi$ and $\Delta\eta$, should be examined more carefully.

Comparisons

In Figure 3, detour distributions for 338.5-Mev protons in lead and copper are shown as determined (a) with the use of the Yang distribution and the percentage detour factor D, and (b) by the Monte Carlo method. Both calculations pertain to

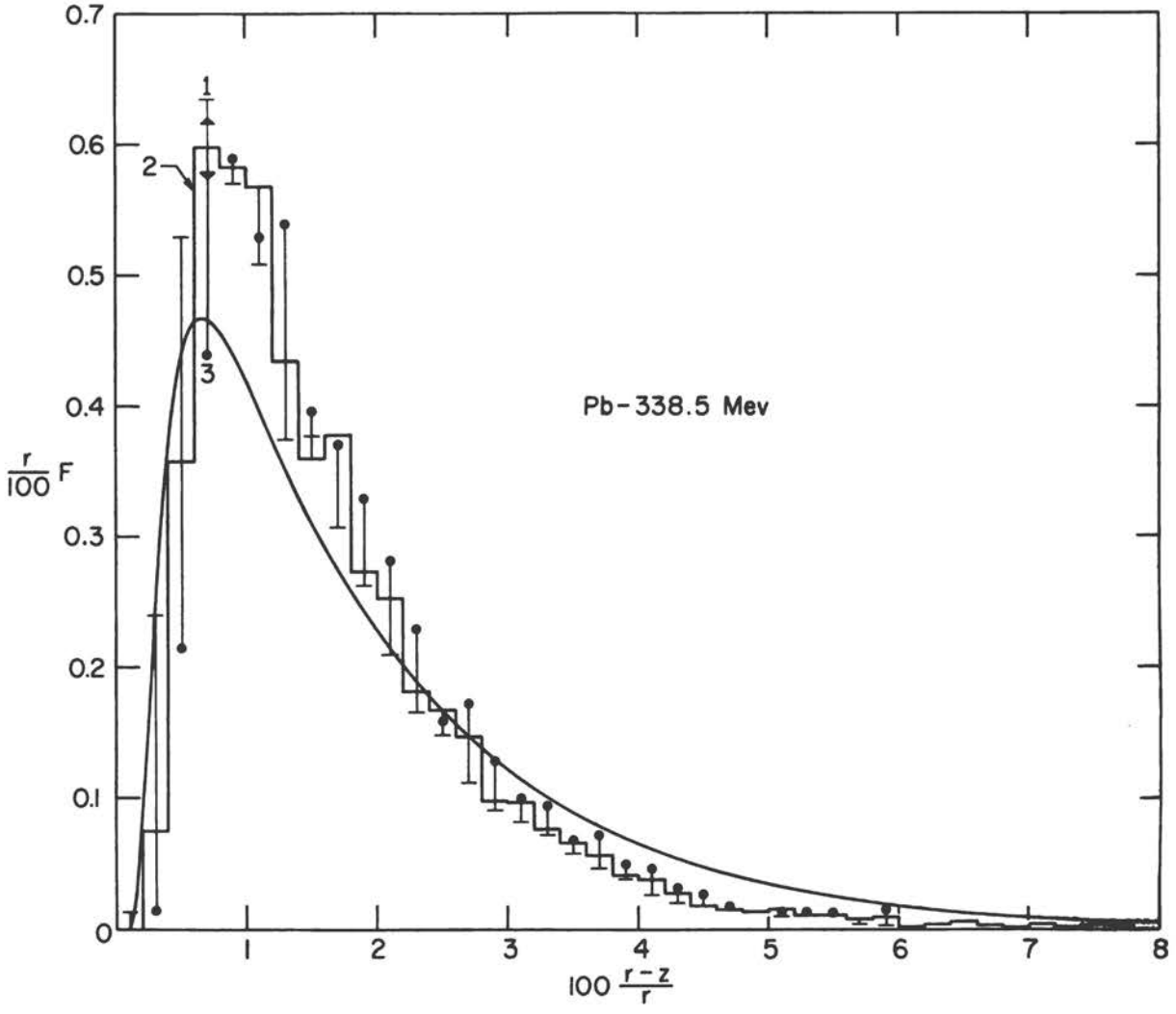

Figure 3(a). Lead (I_{adj} = 826 ev)

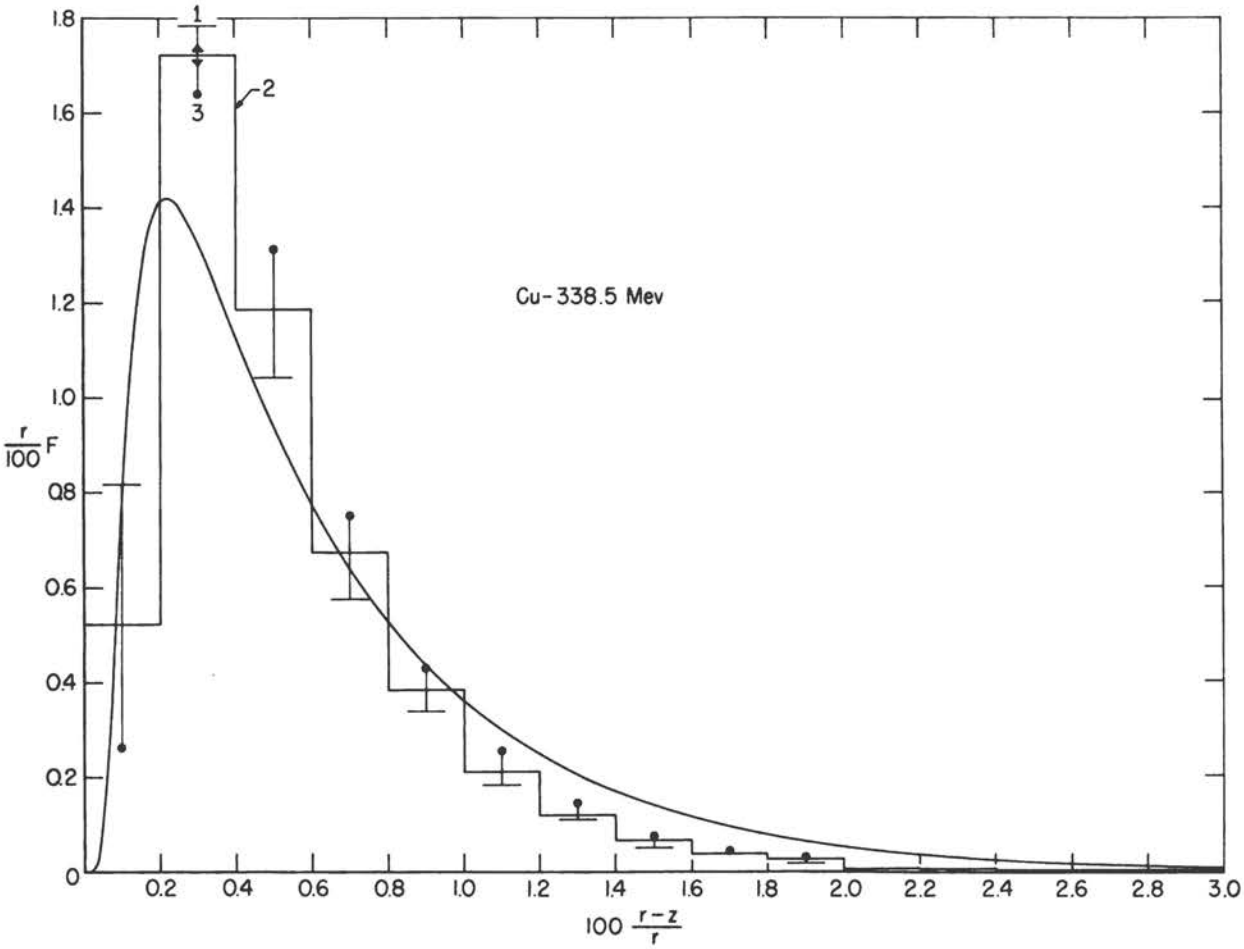

Figure 3(b). Copper (I_{adj} = 314 ev)

Figure 3(a) and (b). Detour distribution for protons slowed down from 338.5 Mev to 2 Mev. Solid curve obtained with the Yang distribution and the detour parameter D. Histograms are based on 5000 Monte Carlo histories (Models 1, 2, and 3 as indicated; arrowheads indicate statistical error).

protons slowed down to an energy of 2 Mev in a slab that is laterally unbounded. The agreement between the two methods is fairly good. However, the Monte Carlo distribution has a higher peak, corresponding to small detours, and a lower tail. The origin of this discrepancy is not entirely clear to us. The application of the Yang distribution, derived originally in a one-velocity, small-angle, diffusion-type approximation, is obviously an oversimplification in the present instance. Not only is there a drastic energy change from 338.5 to 2 Mev, but the associated angular multiple-scattering deflections, as shown in Figure 4, are not very small. Also, the Monte Carlo results, based on 5000 histories, are subject to considerable statistical fluctuations, particularly in the tail of the distributions corresponding to large detours. However, neither statistical errors nor systematic errors due to the uncertainty as to the Monte Carlo model that should be used seem to us large enough to account for the discrepancy with respect to the Yang distribution.

Figure 5 compares the Yang detour distribution for 338.5-Mev proton in lead with the corresponding result of the theory of Bichsel and Uehling. There is fairly good agreement provided the "wiggliness correction" is applied to the distribution for smoothed-out tracks.

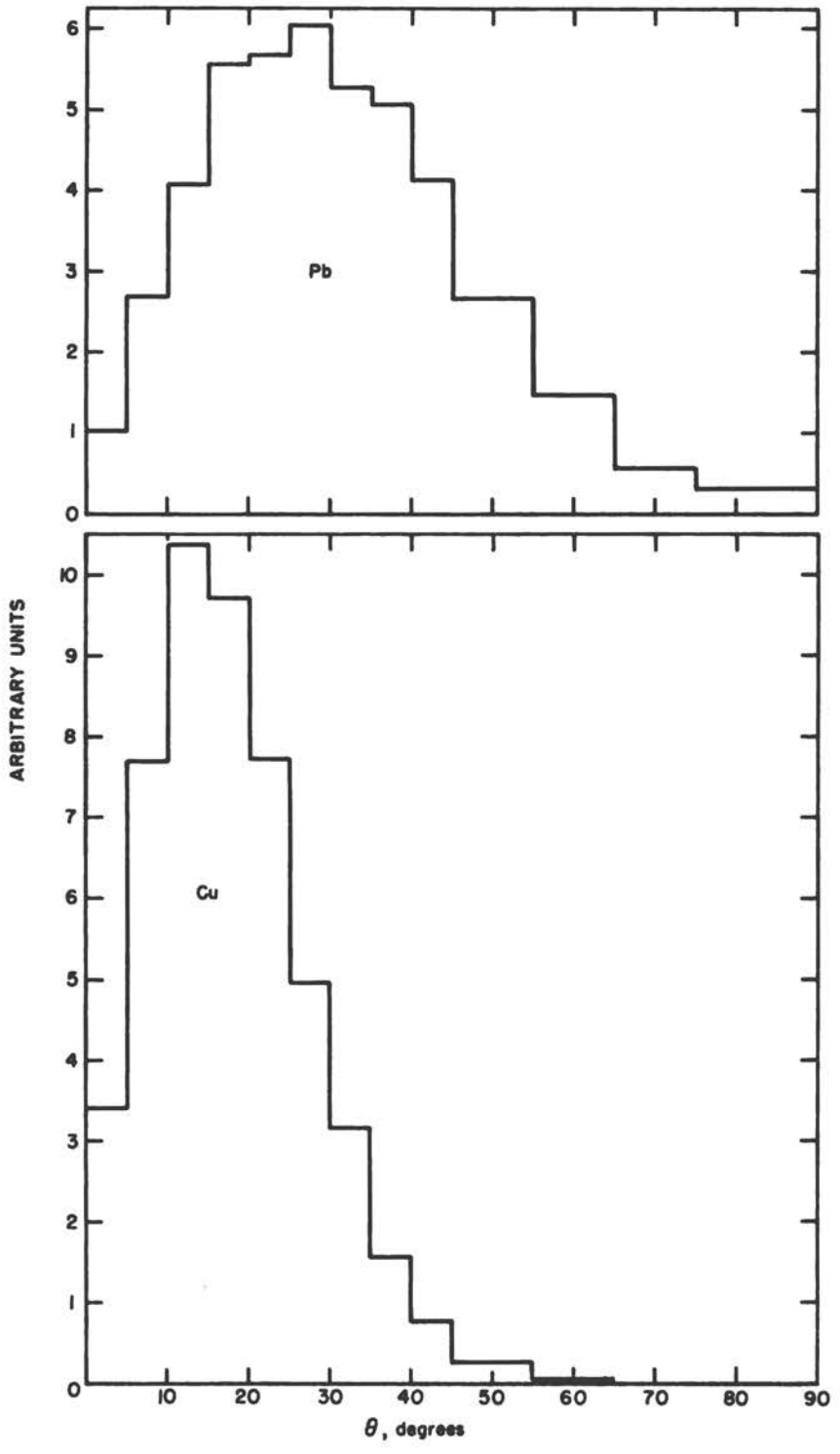

Figure 4. Angular distribution of protons slowed down from 338.5 Mev to 2 Mev in lead or copper, based on 5000 Monte Carlo histories. θ is the obliquity with respect to the initial direction of motion.

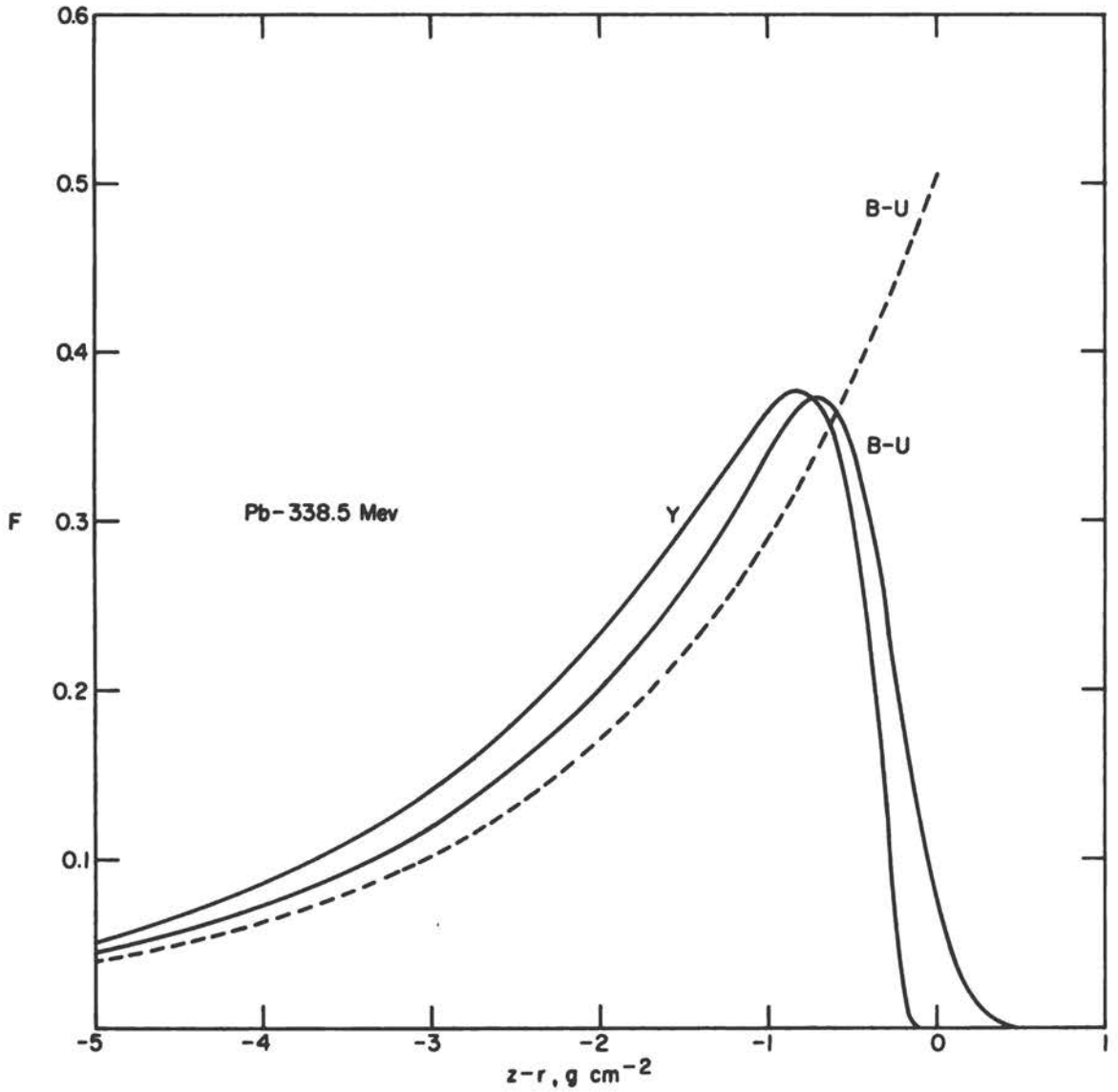

Figure 5. Comparison of the Yang and Bichsel-Uehling detour distributions for protons slowed down in lead from 338.5 to 2 Mev. The dotted curve is the Bichsel-Uehling result without the "wiggliness correction."

Figure 6 shows the Monte Carlo results of Barkas and von Friesen for 750-Mev protons in lead and copper rods. For comparison, corresponding detour distributions for laterally unbounded targets are also shown (based on the Yang distribution). The ratio of the areas under the distributions for good and poor geometry represents the loss of protons through side-walls of the rod.

From the available evidence, we would conclude that the various calculational techniques provide reasonable approximations for the detour distribution. In Section 7 it will further be shown that the degree of approximation is adequate for the

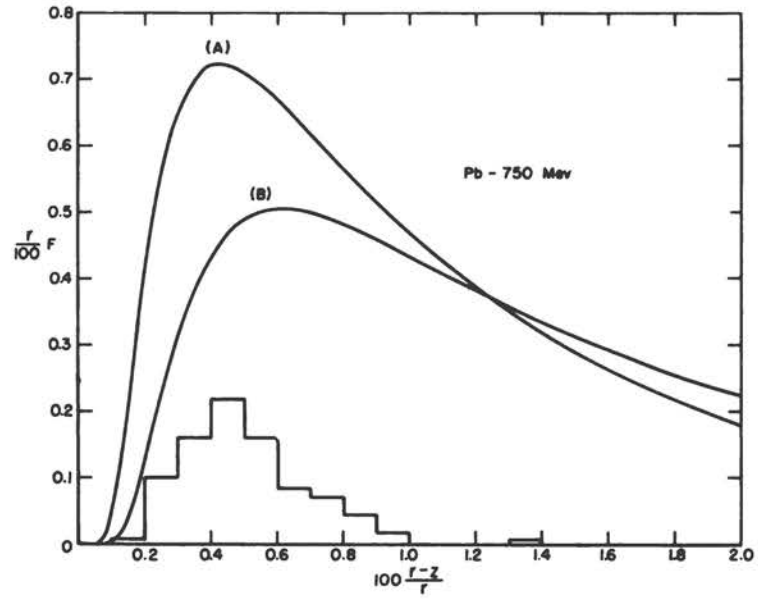

Figure 6(a). Lead

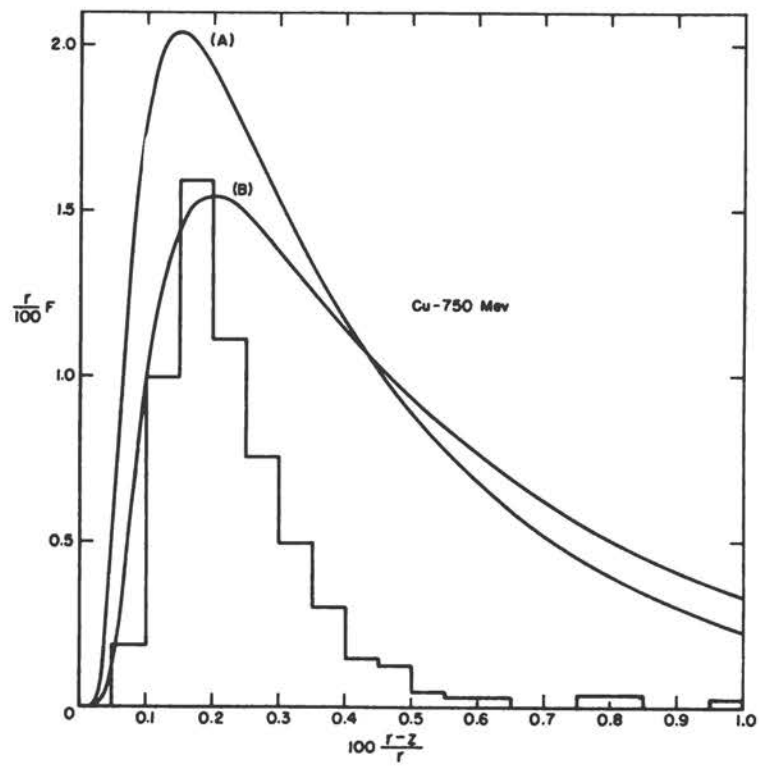

Figure 6(b). Copper

Figure 6. Detour distributions for 750-Mev protons. The histograms represent the Monte Carlo results of Barkas and von Friesen for an absorber rod with a 1" x 1" cross section. The curves were calculated according to Yang for a laterally unbounded absorber: (A) with a detour factor corresponding to the approximation of Barkas and von Friesen, and (B) with a detour factor according to the prescription in Section 8 (Eqs. 40-44).

determination of mean excitation energies from range measurements. If exact detour distributions are considered to be of interest by themselves, further work is required.[11]

6. Differential and Integral Range Distributions

In this section it will be convenient to use instead of z the scaled variable

$$x = \frac{z-r}{\sigma} \tag{19}$$

and the corresponding distribution of projected range,

$$h(x)dx = H(z)dz \ . \tag{20}$$

By folding the pathlength distribution (Eq. 9) into the Yang detour distribution (Eq. 13), one finds that

$$h_Y(x) = \frac{1}{\sqrt{2\pi}} \int_0^\infty \exp\left[-(\frac{vt}{2} + x)^2/2\right] Y(v)dv \tag{21}$$

with

$$t = \frac{\langle s-z \rangle}{\sigma} = \frac{D}{p} \ . \tag{22}$$

The distribution $h_Y(x)$ thus depends only on a single parameter t, which expresses the relative importance of multiple-scattering detours and pathlength straggling. In first approximation, t is proportional to the atomic number Z of the medium. In Figure 7, the ratio t/Z is plotted versus energy for beryllium, aluminum, copper, and lead.

$$h_Y(x) = \frac{\sqrt{2}}{\pi} \int_0^2 \exp\left[-(\frac{vt}{2} + x)^2/2\right] v^{-3/2} \left[\exp(-1/v) - 3\exp(-9/v)\right] dv$$

$$+ \frac{\pi}{8\sqrt{2}} e^{-\frac{b^2-4ac}{a}} \left[1 - \Phi(\frac{b}{\sqrt{a}})\right] \tag{23}$$

where:

$$a = t^2/8$$

$$b = (t^2 + tx + \pi^2/8)/4$$

$$c = (t+x)^2/2 + \pi^2/8$$

$$\Phi(u) = \frac{2}{\sqrt{\pi}} \int_0^u e^{-y^2} dy \quad \text{(error integral)} \ .$$

The integral distribution of projected range,

$$Q_{IR}^{Y}(x) = \int_x^\infty h_Y(x')dx' \ , \tag{24}$$

---

[11] A manuscript by L. V. Spencer (private communication) lays out the general framework for an accurate analytical calculation. See earlier work by Spencer and Coyne (12).

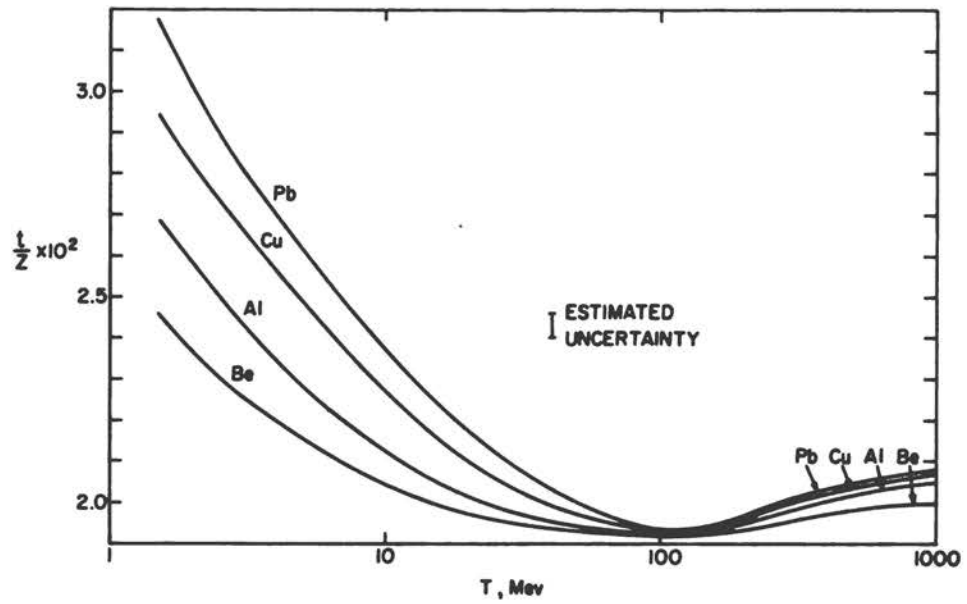

Figure 7. Ratio of characteristic parameter, t, of projected range distribution to the atomic number of medium.

has been obtained through numerical integration and is presented in Table 6 for a set of t-values sufficient to describe protons with energies between 1 and 1000 Mev in all substances.

In some experiments, the median projected range is measured; i.e., the target thickness $z_{1/2}$ such that 50 percent of the incident protons are transmitted. Let $x_{1/2}$ be the corresponding scaled median thickness. Then

$$z_{1/2} = r + \sigma x_{1/2} \ , \tag{25}$$

and

$$100 \ \frac{r - z_{1/2}}{r} = D \left(- \frac{x_{1/2}}{t} \right) \ . \tag{26}$$

Thus, the percent deviation of the median range from the c.s.d.a. range is equal to the percentage detour factor D multiplied by an additional correction factor $\left(- \frac{x_{1/2}}{t} \right)$.

Values of $x_{1/2}$ and $\left(\frac{x_{1/2}}{t} \right)$ as functions of t are given in Table 7.

The use of the Bichsel-Uehling detour distribution results in a differential range distribution

$$h_{BU}(x) = \frac{1}{4\sqrt{\pi}} \int_0^\infty \exp \left[- \left(\frac{vt}{2} + x \right)^2 / 2 \right] f_M \left(\sqrt{\frac{v}{2}}, B \right) dv \ , \tag{27}$$

with f_M given by Equation 15. In this case there are two parameters which characterize the distribution: the variable B of the Molière theory, and the ratio

$$t = \frac{\Delta_{BU}}{\sigma} \ . \tag{28}$$

TABLE 6

Integral Distribution of Projected Range, $Q_{IR}(x)$

x \ t	0.0	0.5	1.0	1.5	2.0	2.5	3.0
-6.0	1.0000	1.0000	.9983	.9872	.9620	.9255	.8825
-5.0	1.0000	.9999	.9943	.9708	.9295	.8780	.8227
-4.0	1.0000	.9987	.9804	.9335	.8694	.8003	.7326
-3.0	.9987	.9873	.9341	.8498	.7593	.6743	.5984
-2.5	.9938	.9654	.8826	.7773	.6761	.5872	.5112
-2.0	.9773	.9167	.7995	.6773	.5714	.4839	.4121
-1.5	.9332	.8254	.6789	.5504	.4489	.3697	.3075
-1.0	.8413	.6842	.5264	.4071	.3202	.2560	.2074
-0.5	.6915	.5060	.3627	.2672	.2025	.1569	.1238
0.0	.5000	.3245	.2165	.1520	.1109	.0833	.0639
0.5	.3085	.1762	.1097	.0734	.0516	.0376	.0281
1.0	.1587	.0795	.0463	.0296	.0201	.0142	.0103
1.5	.0668	.0294	.0161	.0098	.0064	.0044	.0031
2.0	.0228	.0088	.0045	.0027	.0017	.0011	.0008
2.5	.0062	.0021	.0010	.0006	.0004	.0002	.0002
3.0	.0014	.0004	.0002	.0001	.0001	.0000	.0000

TABLE 7

Scaled Median Range $x_{1/2}$ and Correction Factor $\left(\frac{x_{1/2}}{t}\right)$ for Computing Percentage Deviation of Median from c.s.d.a. Range

t	$x_{1/2}$	$x_{1/2}/t$
0.0	0.0	-1.0
0.1	-0.09988	-0.9988
0.15	-0.1495	-0.9965
0.2	-0.1987	-0.9936
0.3	-0.2959	-0.9862
0.4	-0.3910	-0.9774
0.5	-0.4839	-0.9677
0.6	-0.5747	-0.9578
0.8	-0.7504	-0.9380
1.0	-0.9194	-0.9194
1.2	-1.083	-0.9025
1.5	-1.321	-0.8803
2.0	-1.702	-0.8511
2.5	-2.074	-0.8295
3.0	-2.440	-0.8135

(If the "wiggliness correction" is applied, σ must be replaced by $[\sigma^2 + (\frac{2}{15}\Delta_{BU})^2]^{1/2}$). The integral range distribution obtained from Equation 27 by numerical integration has been tabulated (Ref. 2) for B = 10 and $\xi = 1/t = 0.0,\ 0.69,\ 1.20,\ 2.0$, and 4.0. The percentage deviation of the median projected range from the c.s.d.a. range has been presented by Bichsel (13) for gold, silver, nickel, and aluminum in the form of graphs covering energies between 1 and 1000 Mev.

7. Analysis of Bragg Ionization Curves

We now turn to the evaluation of the Bragg ionization curve,

$$Q_{BR}(z) = \int_{\frac{z-r}{\sigma}}^{\infty} h(x')\, R^*(x', x)\, dx' , \tag{29}$$

obtained with an ionization chamber. As pointed out in Section 1, the value of Q is proportional to a constant factor which represents the fraction of the protons that have not been scattered out of the beam by large angular deflections due to nuclear interactions. This reduction factor need not be known for the determination of the c.s.d.a. range or mean excitation energy. It is sufficient to know the shape of the Bragg curve; that is, the relative variations of Q, near the end of the range. The evaluation of Equation 29 requires a choice of a differential range distribution and an estimate of the detector response.

Procedure of Mather and Segrè

The procedure adopted by Mather and Segrè in the analysis of their data was particularly simple and turns out to be quite adequate for the determination of the mean excitation energy. Only in regard to predicting the shape of the Bragg curve is it inferior to the other more elaborate procedures discussed below. Mather and Segrè assumed, in effect, that the detour distribution is given as a delta function,

$$F(z;s) = \delta(z - s + \Delta_{MS}) , \tag{30}$$

where Δ_{MS} is the shortening of the projected range compared to the pathlength due to multiple-scattering detours. For Δ_{MS} they derived the simple approximation[12]

$$\Delta_{MS} = r\,\frac{Z}{6400} \quad (Z = \text{atomic number}) . \tag{31}$$

The corresponding differential range distribution is

$$h_{MS}(x) = \frac{1}{\sqrt{2\pi}}\, e^{-(x+t)^2/2} \tag{32}$$

with $t = \Delta_{MS}/\sigma$.

Mather and Segrè further assumed that the response of their argon-filled ionization chamber could be represented with sufficient accuracy by

---

[12] This result is somewhat smaller than the detour predicted by Equations 40-44 of Section 8. Concerning the nature of the Mather-Segrè approximation, see also page 47 of Appendix A of this volume.

$$R^*(z', z) = \text{const} \cdot (z'-z)^{-0.46} . \quad (33)$$

The resulting Bragg curve, normalized to unit peak height, is shown in Table 8.

TABLE 8

Bragg Ionization Curve Computed According to the Prescription of Mather and Segrè

$\frac{z-(r-\Delta_{MS})}{\sigma}$	Q_{BR}
-4.0	0.552
-3.5	0.592
-3.0	0.647
-2.5	0.721
-2.0	0.817
-1.5	0.923
-1.0	0.995
-0.5	0.970
0.0	0.819
0.5	0.578
1.0	0.333
1.5	0.155
2.0	0.057
2.5	0.017
3.0	0.004

Estimate of the Detector Response

When evaluating Equation 29 with the use of the differential range distributions $h_Y(x)$ and $h_{BU}(x)$, we have made a crude estimate of $R^*(z', z)$, corresponding essentially to that of Mather and Segrè, as well as a more elaborate estimate, according to the following procedure:

Crude Estimate:

a. Assume that the residual c.s.d.a. range of the proton, upon leaving the target, is equal to $r_z = z'-z$.

b. Determine the corresponding proton energy $T(r_z)$ by interpolation in a range-energy table.

c. Determine $-\frac{1}{\rho}\frac{dE}{dx}(T)$ in argon by interpolation in a stopping-power table.

d. Let $R^*(z', z) = -\frac{1}{\rho}\frac{dE}{dx}(T)$.

More Elaborate Estimate:

1. Carry out steps, a, b, and c as in the crude estimate.

2. Estimate the proton direction at the time of emergence from the target, using a mean obliquity cosine $\langle \cos\theta | T_0 \rightarrow T \rangle$ calculated according to Equations 40-44 of Section 8.

3. Make an improved estimate of the residual range, $r_z = (z'-z)/\langle \cos\theta \rangle$.

4. With this improved value of r_z, repeat steps 1 and 2 and obtain new values of T, $\langle \cos\theta \rangle$ and $-\frac{1}{\rho}\frac{dE}{dx}(T)$.

5. Make an improved response estimate $R^*(z', z) = -\frac{1}{\rho}\frac{dE}{dx}(T)/\langle \cos\theta \rangle$. If the change in R^* is sufficiently small (less than, say, 0.5 percent), the calculation is finished; if it is not, iterate the procedure until convergence is achieved.

The difference between Bragg curves calculated with the crude estimate and with the more elaborate estimate of the detector response serves to indicate the error inherent in such estimates.

Monte Carlo Calculation of Bragg Ionization Curves

A very simple elaboration is needed of the procedures indicated in Section 5 (under "Monte Carlo Detour Calculations"). Instead of pre-selecting for each proton track a set of pathlength intervals, one divides the energy history of the proton into intervals and samples the pathlength in each interval. Once this is done, the remainder of the calculation of trajectories proceeds as in the calculation of path detours. There is no difficulty in estimating the detector response because the energy and direction of the proton are known at all times.

In a calculation of this type by Berger (5), the energy region between 338.5 and 2 Mev was divided into 30 intervals of gradually decreasing size, and the pathlength in each interval was sampled from a Gaussian distribution with mean $r(T') - r(T'')$ and variance $\sigma(T') - \sigma(T'')$, T' and T'' being the energies at the beginning and the end of the interval. This was an approximation. However, the departure of the actual distribution from a Gaussian, as predicted by the Lewis theory, amounts only to a few percent (see, e.g., Table 3). Moreover, the Bragg curve needs to be evaluated only for large z, so that the cumulative pathlength of the protons is long enough for the Gaussian approximation to be very close.

Determination of the Range and Mean Excitation Energy

The required analysis is as follows:

1. a. Assume a value for the mean excitation energy, say I^0_{adj}.

   b. Determine the corresponding values of the c.s.d.a. range and pathlength straggling parameters, r_0 and σ_0.

   c. Evaluate the parameter t with the use of the chosen multiple-scattering theory.

   d. Compute the theoretical Bragg curve $Q_{BR}(z)$, either analytically or by a Monte Carlo calculation, and normalize it so that its peak value is unity.

e. Find the ordinate P of the theoretical curve corresponding to a depth equal to the assumed c.s.d.a. range r_0.

2. a. Normalize the experimental Bragg curve so that its peak value is unity.

b. Determine the depth on the experimental curve for which the ordinate has the value P. This depth is an estimate of the experimental c.s.d.a. range r.

c. With the use of a range-energy table, determine the corresponding experimental value of the mean excitation energy, I_{adj}.

3. In principle, it is necessary to repeat the entire procedure with a new theoretical Bragg curve corresponding to I_{adj}. However, the value of P is very insensitive to the value of the mean excitation energy, so that with any reasonably close initial value I^0_{adj} no new calculation is required.

The analysis according to Mather and Segrè is simpler, requiring only the determination (from the normalized experimental Bragg curve) of the absorber thickness at which the ordinate has fallen to a value to 82 percent of the peak value. As can be seen from Table 8, this thickness provides an estimate of the experimental c.s.d.a. range minus the projected range shortening, $r - \Delta_{MS}$.

Table 9 compares values of the mean excitation energy derived by various methods[13] from ionization curves in lead and copper measured by Mather and Segrè (1)[14] and by Zrelov and Stoletov (14). The following points emerge: (1) There appears to be no significant difference between the I_{adj}-values derived by the different methods. The differences in I_{adj} from one run of an experiment to another are greater than those due to the use of different methods of analysis. (2) The values of I_{adj} for lead in Table 9 are systematically lower than those deduced by the experimenters in their original publications. This is due to the use of a new range-energy table based on improved estimates of shell corrections (Report No. 7 of this volume).

Shape of the Bragg Ionization Curve near the End of the Range

Mather and Segrè pointed out that their experimental Bragg curves agreed with the curves predicted by their simple analysis only in the region beyond the peak but not in the region preceding it (see Fig. 9a). They thought that nuclear interactions were the most likely cause for this discrepancy. Later Bichsel (15) examined this question and pointed out that on the basis of his multiple-scattering corrections, and assuming plausible values for the relevant parameters, he could account very well for the shape of the Mather-Segrè curve for 340-Mev protons in lead without having to invoke the effect of nuclear interactions. We have once more looked at this question and have reached the conclusion that there are aspects to it which are not fully explained.

[13] The values in Table 9 were obtained with "elaborate" estimates of the detector response. However, the use of "crude" estimates would have changed the I_{adj}-values by at most one or two units in the third significant figure.

[14] We are indebted to Dr. R. Mather for placing at our disposal detailed experimental data not given explicitly in his paper.

TABLE 9

C.s.d.a. Ranges and Corresponding Mean Excitation Energies Obtained by the Methods Indicated in Section 7 (p. 88). The Experimental Value of r is that Absorber Thickness to the Right of the Maximum at which the Normalized Bragg Curve has Fallen to a Value P. Values of I_{adj} in Parentheses are Those Deduced by the Experimenters in their Original Publications with the Use of Older Range-energy Tables

Source of data	Method of analysis	P	r (g/cm^2)	I_{adj} (ev)
Mather and Segrè:				
Pb - 338.5 Mev	Yang	0.320	123.12	756
	Bichsel-Uehling	0.385	122.85	747
	Monte Carlo #1	0.320	123.12	756
	Monte Carlo #2	0.290	123.25	760
	Monte Carlo #3	0.252	123.42	766
	Mather and Segrè	0.82	122.76	744(793)
Pb - 339.7 Mev	Yang	0.320	124.61	782
	Mather and Segrè	0.82	124.37	774(829)
Cu - 337.9 Mev	Yang	0.543	92.05	314
	Mather and Segrè	0.82	91.84	309(312)
Cu - 338.5 Mev	Yang	0.543	92.04	308
	Monte Carlo #1	0.535	92.03	308
	Monte Carlo #2	0.517	92.07	308
	Monte Carlo #3	0.497	92.11	309
	Mather and Segrè	0.82	91.77	302(304)
Cu - 339.7 Mev	Yang	0.543	92.98	317
	Mather and Segrè	0.82	92.69	310(313)
Zrelov and Stoletov:				
Cu - 658 Mev	Yang	0.551	258.54	317
	Monte Carlo #1	0.558	258.49	317
	Monte Carlo #2	0.530	258.70	319
	Monte Carlo #3	0.512	258.83	320
	Mather and Segrè	0.82	257.6	309(305)

To begin with, we compare (in Figs. 8a-8c), the Bragg curves resulting from use of the Yang distribution, the Bichsel-Uehling theory, and Monte Carlo calculations (based on I_{adj} = 826 ev for lead and 314 ev for copper). At 338.5 Mev and 658.0 Mev for copper, there is good agreement. At 338.5 Mev in lead, there are noticeable differences; in particular, the Monte Carlo results in the region preceding the peak are somewhat lower than the other two curves.

In making comparisons with experiment in regard to curve shape, we have from the start eliminated possible discrepancies due to a different value of the c.s.d.a. range. For each method, we recalculated the theoretical curves with

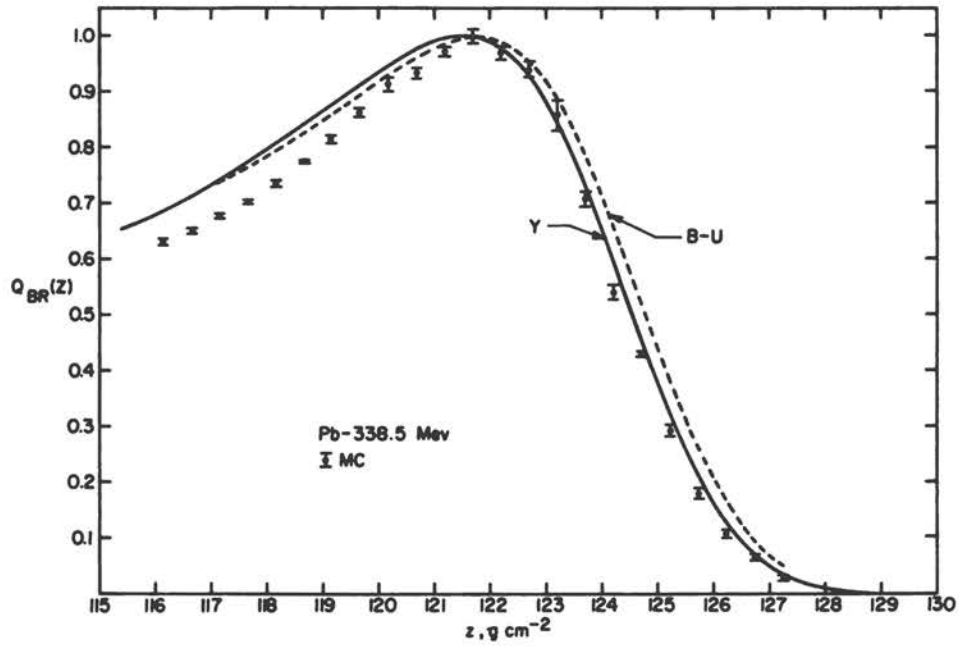

Figure 8(a)

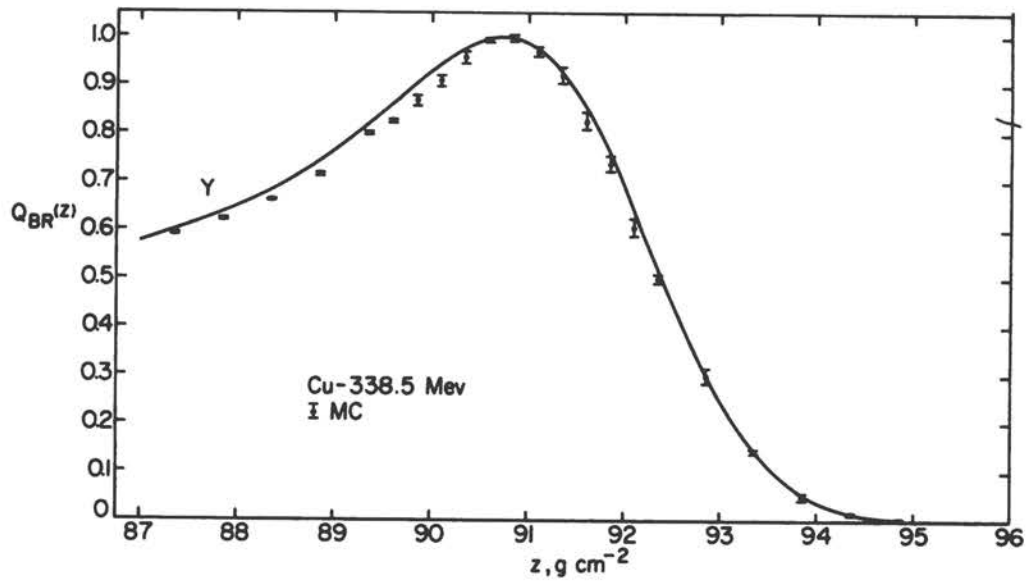

Figure 8(b)

Figure 8. Theoretical Bragg ionization curves near the end of the proton range, derived with the use of the Yang distribution (Y), from the Bichsel-Uehling theory (B-U), and by the Monte Carlo method (MC). (a) 338.5-Mev protons in lead (I_{adj} = 826 ev): solid curve, Y; dotted curve, B-U; points, MC (Model 2). (b) 338.5-Mev protons in copper (I_{adj} = 314 ev): solid curve, Y; points, MC (Model 2).

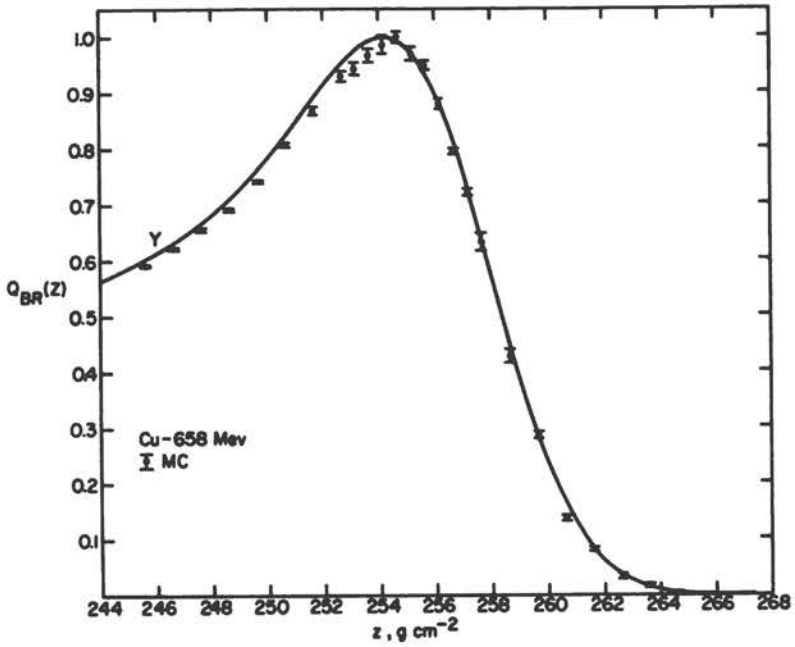

Figure 8(c)

Figure 8. Theoretical Bragg ionization curves near the end of the proton range, derived with the use of the Yang distribution (Y), from the Bichsel-Uehling theory (B-U), and by the Monte Carlo method (MC). (c) 658-Mev protons in copper (I_{adj} = 314 ev): solid curve, Y; points, MC (Model 2).

exactly those values of r and I_{adj} which had been obtained from the analysis of the experimental data described in Section 7 (under "Determination of the Range and Mean Excitation Energy") and summarized in Table 9. The subsequent comparison (Fig. 9a) with the lead data of Mather and Segrè indicates that there is good agreement with the Yang and Bichsel-Uehling curves everywhere, and that to the left of the peak the Monte Carlo curve still lies a little below the experimental curve. For copper (Figs. 9b and 9c), the situation is worse. All three theoretical predictions, to the left of the peak, are below the Mather-Segrè points at 338.5 Mev and the Zrelov-Stoletov points at 658 Mev, for which the discrepancies are much greater.

There are at least two ways of accounting for the discrepancies between the predicted and observed curve shapes:

(1) By subtracting the calculated from the experimental Bragg curves, one obtains residual curves that have themselves the shape of terminal sections of Bragg curves for protons with energies lower than the nominal source energy. This suggests the possibility that the incident proton beam in the Mather-Segrè and Zrelov-Stoletov experiments may have had a more complicated structure than expected. Some plausibility is given to this suggestion by the finding of Barkas and von Friesen that the nominal 750-Mev proton beam in their experiment contained an admixture of protons with a 10-percent lower mean range.

(2) The second possible explanation is the shortening of the projected range by nuclear interactions involving small deflections and energy losses.

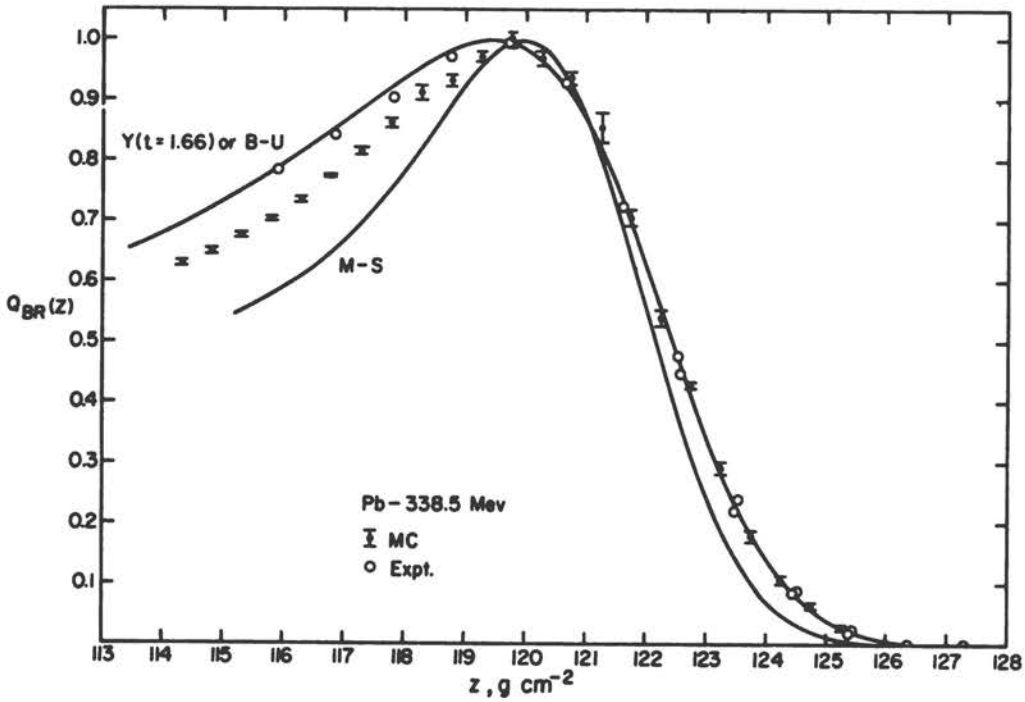

Figure 9(a)

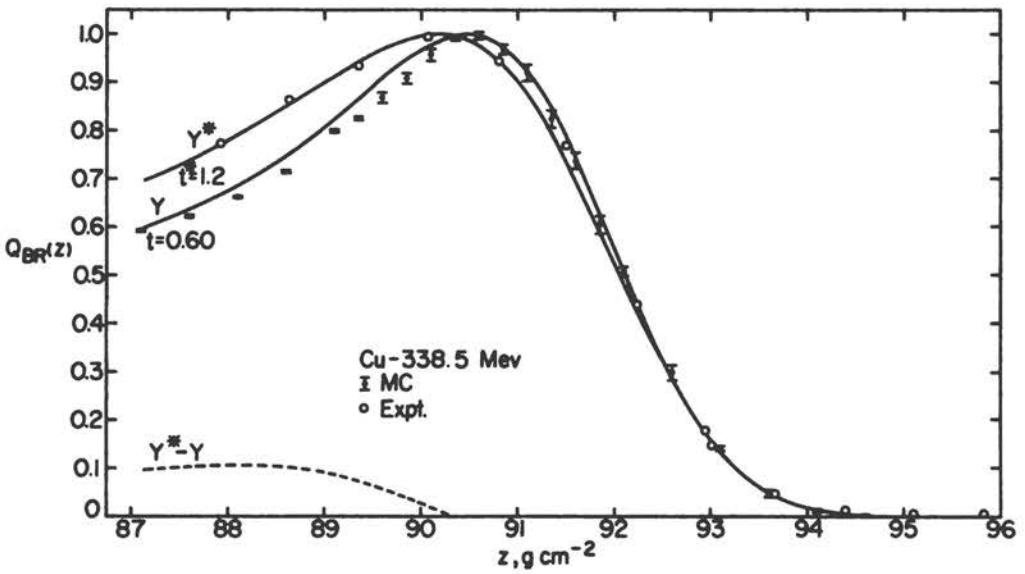

Figure 9(b)

Figure 9. Comparison of theoretical and experimental Bragg ionization curves near the end of the proton range. (a) Comparison with the experimental data of Mather and Segrè for 338.5-Mev protons in lead: Y, Yang, I_{adj} = 756 ev, t = 1.66; B-U, Bichsel-Uehling, I_{adj} = 747 ev; M-S, Mather-Segrè (theoretical), I_{adj} = 744 ev; MC, Monte Carlo, Model 2, I_{adj} = 760 ev. (b) Comparison with the experimental data of Mather and Segrè for 338.5-Mev protons in copper: Y, Yang, I_{adj} = 308 ev, t = 0.60; Y^*, Yang, I_{adj} = 308 ev, t^* = 1.2; MC, Monte Carlo, Model 2, I_{adj} = 308 ev; dotted curve, difference between Yang curves with t^* = 1.2 and t = 0.60.

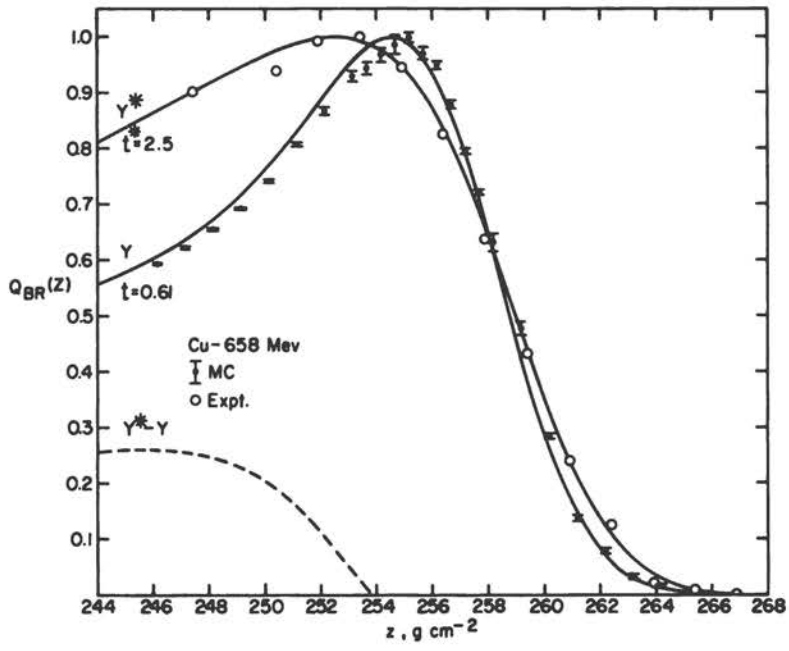

Figure 9(c)

Figure 9. Comparison of theoretical and experimental Bragg ionization curves near the end of the proton range. (c) Comparison with the experimental data of Zrelov and Stoletov for 658-Mev protons in copper: Y, Yang, I_{adj} = 317 ev, t = 0.61; Y*, Yang, I_{adj} = 317 ev, t^* = 2.5; MC, Monte Carlo, Model 2, I_{adj} = 319 ev; dotted curve, difference between Yang curves with t^* = 2.5 and t = 0.61.

We have found that, when the Yang distribution is used, the replacement of the parameter t by a quantity $t^* > t$ is sufficient to produce theoretical Bragg curves in copper that are in very close agreement with experiment. The corresponding shortening of the mean projected range, $(t^* - t)\sigma$, is equal to 0.6 g cm^{-2} at 338.5 Mev and to 4.9 g cm^{-2} at 658 Mev. No attempt as yet has been made to account for such effects on the basis of nuclear theory. To judge from the available data on nuclear energy levels the probability of small nuclear excitations would be much greater for copper than for lead, which is consistent with the observed multiple-scattering effects.

8. Appendix

Evaluation of the Bichsel-Uehling Detour Parameter

The quantity Δ_{BU}, defined by Equation 17, must be evaluated according to the theory of Molière, taking into account energy loss in the continuous slowing-down approximation. For convenient reference we list here the final form of the equations after insertion of numerical values for the various constants. The various symbols have the following meaning: τ = kinetic energy in units of the rest mass; βc = proton velocity; Z, A = atomic number and weight of the medium.

$$\chi_c'^2 = 1.783 \times 10^{-7} \frac{Z^2}{A} \left[\frac{\tau+1}{\tau(\tau+2)}\right]^2 \tag{34}$$

$$\chi_a^2 = 2.017 \times 10^{-11} \frac{Z^{2/3}}{\tau(\tau+2)} \left[1.13 + 3.76\left(\frac{Z}{137\beta}\right)^2\right] \tag{35}$$

$$\chi_c^2 = \int_T^{T_0} \chi_c'^2 (T') \frac{dT'}{-\frac{1}{\rho}\frac{dE}{dx}(T')} \tag{36}$$

$$\log \overline{\chi_a^2} = (1/\chi_c^2) \int_T^{T_0} \chi_c'^2(T') \log \chi_a^2 \frac{dT'}{-\frac{1}{\rho}\frac{dE}{dx}(T')} \tag{37}$$

$$\frac{eB}{B} = \frac{\chi_c^2}{1.167\,\overline{\chi_a^2}} \tag{38}$$

$$\Delta_{BU} = \frac{1}{2} \int_0^{T_0} \chi_c^2 (T') B(T') \frac{dT'}{-\frac{1}{\rho}\frac{dE}{dx}(T')} (g/cm^2) \ . \tag{39}$$

Transport-Theoretical Evaluation of the Detour Factor

The percentage detour factor is given by

$$D = \frac{100}{r} \int_0^{T_0} \{1 - \langle \cos\theta | T \rightarrow T' \rangle\} \frac{dT'}{-\frac{1}{\rho}\frac{dE}{dx}(T')} \ , \tag{40}$$

where $\langle \cos\theta | T_0 \rightarrow T \rangle$ is the mean obliquity cosine of a proton which started out in the z-direction with energy T_0 and has been slowed down to energy T. It has been shown by Lewis (16) and Spencer (17) that

$$\langle \cos\theta | T_0 \rightarrow T \rangle = \exp \left\{ - \int_T^{T_0} C(T') \frac{dT'}{-\frac{1}{\rho}\frac{dE}{dx}(T')} \right\} \ , \tag{41}$$

where

$$C(T) = 2\pi N \int_0^{\pi} \sin\theta \, d\theta \, \sigma(\theta, T) (1 - \cos\theta) \ , \tag{42}$$

and where N is the number of atoms per unit volume and $\sigma(\theta, T)$ the single-scattering cross section for a proton of energy T.

Following Spencer, we have used for $\sigma(\theta, T)$ the Rutherford cross section modified to take into account screening. Then

$$N\sigma(\theta, T) = \frac{1}{2}\chi_c'^2 \frac{1}{\left(1-\cos\theta+\frac{\chi_a^2}{2}\right)^2} , \tag{43}$$

where $\chi_c'^2$ and χ_a^2 are defined by Equations 34 and 35. When this cross section is substituted into Equation 42, the result is

$$C(T) = \frac{1}{2}\chi_c'^2 \left\{ \log\left(1+\frac{4}{\chi_a^2}\right) - \frac{1}{1+\frac{\chi_a^2}{4}} \right\} \tag{44}$$

References

1. R. Mather and E. Segrè, Phys. Rev. 84, 191 (1951).
2. H. Bichsel and E. A. Uehling, Phys. Rev. 119, 1670 (1960).
3. C. N. Yang, Phys. Rev. 84, 599 (1951).
4. W. H. Barkas and S. von Friesen, Nuovo Cimento Suppl. 19, 41 (1961).
5. M. J. Berger, Methods in Computational Physics, vol. 1, p. 135 (Academic Press, New York, 1963).
6. R. M. Sternheimer, Phys. Rev. 117, 485 (1960).
7. H. W. Lewis, Phys. Rev. 85, 20 (1952).
8. G. Molière, Z. Naturforschung, 3a, 78 (1948).
9. H. A. Bethe, Phys. Rev. 89, 1256 (1953).
10. W. T. Scott, Revs. Mod. Phys. 35, 231 (1963).
11. B. Rossi, "High-Energy Particles," (Prentice-Hall, Englewood Cliffs, N.J., 1952).
12. L. V. Spencer and J. Coyne, Phys. Rev. 128, 2230 (1962).
13. H. Bichsel, in "American Institute of Physics Handbook," 2nd ed., section 8C, pp. 8-20 to 8-47, (McGraw-Hill, New York, 1963).
14. V. P. Zrelov and G. D. Stoletov, Soviet. Phys. Transl. JETP 36, 461 (1959).
15. H. Bichsel, Phys. Rev. 120, 1012 (1960).
16. H. W. Lewis, Phys. Rev. 78, 526 (1950).
17. L. V. Spencer, Phys. Rev. 98, 1507 (1955).

6. VALUES OF I AND I_{adj} SUGGESTED BY THE SUBCOMMITTEE

J. E. Turner[1]

Abstract

Values of I/Z and I_{adj}/Z are suggested for the chemical elements in the form of graphs representing these quantities as functions of Z.

The quantity I, the mean excitation energy, that enters the theoretical expression for stopping power is a well-defined parameter of the theory. The definition of I for a material is given by Equation 34 in Appendix A: $\ln I = \sum_n f_n \ln E_n$.[2] From its definition, I depends only upon the ground- and excited-state wave functions of a stopping material, and hence is a property of that material, independent of the energy and other characteristics of an incident particle. The determination of I from its definition for a given material presents serious difficulties, since the oscillator strengths f_n are generally not well known in the range of the most important excitation energies E_n. Theoretical values of I have been calculated only for the elements through beryllium, although calculations for more complicated systems are in progress at the present time (R. L. Platzman, private communication). For a general discussion of I and matters related to its determination the reader is referred to Section 3 of Appendix A.

In practice, I is determined empirically from stopping power and/or range measurements. To do this one has to evaluate all of the terms in Equation 38 of Appendix A except I, which is thereby determined. Except at very high energies (e.g., ~1 Gev for protons), the density effect term δ is either negligible or else it can be estimated with relatively good accuracy. Therefore, if the incident particle energy and stopping power have been determined in an experiment, then the quantity $\ln I + C/Z$ can be evaluated to within the experimental uncertainties of the experiment. To determine I itself, an estimate must be made of C/Z, and this introduces further uncertainties unless this quantity is small. In addition, since only the logarithm of I enters the theory directly, a small uncertainty in stopping power introduces a relatively large uncertainty in I. As a result of these circumstances, precise values of I for most of the chemical elements cannot be given at the present time.

In many applications one needs the value of I for a material through which charged particles pass. Accordingly, the Subcommittee considered it desirable to recommend a "best" set of I values for the chemical elements, insofar as the present uncertainties just described would allow. Such a set is presented in summary form in Figure 1, which has been constructed on the basis of numerous discussions and recommendations from individual Subcommittee members. Because of the present state of the art, such a figure is necessarily tentative and uncertain in many respects. It should be made clear that compromises have been made in a number of places in the figure in order to try to make it reflect as accurately as possible the general consensus of the Subcommittee.

---

[1] Oak Ridge National Laboratory, Oak Ridge, Tenn.

[2] For the meaning of f_n and E_n see pp. 17 and 19 of Appendix A.

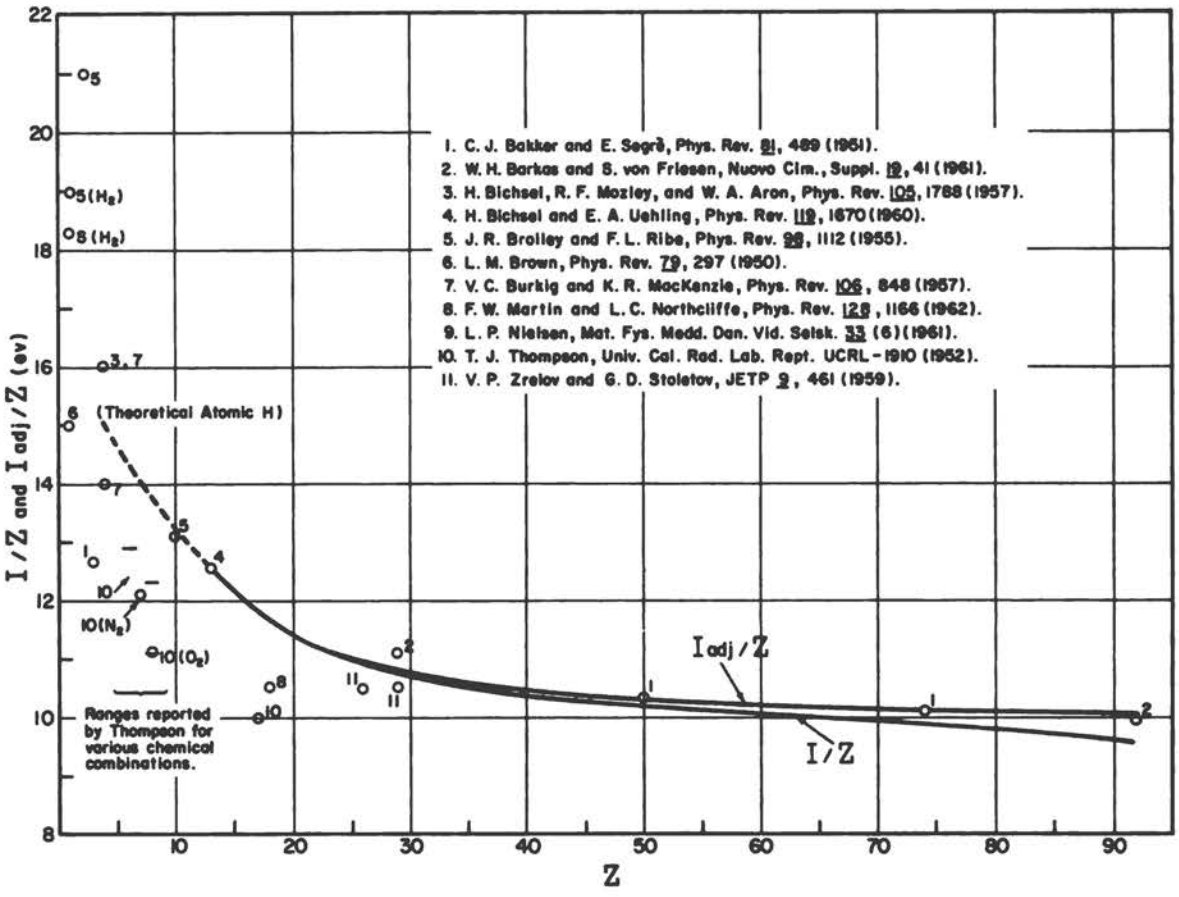

Figure 1. Values of I/Z and I_{adj}/Z in electron-volts for various atomic numbers Z, showing selected experimental points. For $Z \geq 13$ (Al) it is suggested that the smooth curves be used to obtain I/Z and I_{adj}/Z. For $Z < 13$ one can use experimental values where given or use the dashed curve to estimate I/Z. The region of low Z is populated with scattered experimental points, presumably reflecting the dependence of I/Z on the state of chemical combination of an element, as well as experimental uncertainties. The values of I/Z in this figure can be used with the shell-correction curves of Figure 6 in Appendix A of this volume.

The value I = 163 ev for aluminum is probably reliable to within ±1 ev,[3] and this value was made an anchor point of the figure. For elements heavier than aluminum, it was felt that present knowledge warrants drawing the solid curve in the figure for I/Z as a function of Z. The extent of uncertainties introduced by doing this is indicated by the scatter of the selected data shown for $Z > 13$. For the elements lighter than aluminum, experiment shows a variation in the value of I found for a given element, depending on the chemical state of the element in a stopping material.[4] To represent the situation for the light elements, the dashed curve was drawn to indicate only a very general trend for elements below aluminum. The reported variation of I/Z due to different chemical binding is shown for carbon, nitrogen, and oxygen. Some experimental values of I/Z for other light elements are also shown.

[3] See Reports No. 2 and No. 3 in this volume.

[4] See Section 3 in Appendix A; also, Report No. 3 in this volume.

In addition to the mean excitation energy, I, values of a related quantity called the adjusted mean excitation energy, I_{adj}, are also shown in the figure.[5] This quantity is determined from experimental measurements under the assumption that shell corrections vanish when the speed of the incident particle approaches the speed of light ($\beta \to 1$). Since, as mentioned above, stopping-power measurements determine directly $\ln I + C/Z$, it follows that the relationship between I_{adj} and I is given by

$$\ln I_{adj} = \ln I + \left(\frac{C}{Z}\right)_{\beta=1} \tag{1}$$

or

$$I_{adj} = I \exp(C/Z)_{\beta=1} \ , \tag{2}$$

where $(C/Z)_{\beta=1}$ is the high-energy limit of the shell-correction term.[6] In the literature, high-energy measurements are frequently analyzed with the assumption that $C/Z \to 0$ as $\beta \to 1$, in which case the quantity here called I_{adj} is given.

Although I and I_{adj} differ conceptually, the difference in their numerical values is of little practical importance except for the heaviest elements. Table 1 summarizes the actual extent of differences. The numbers in the table were calculated from Equation 1, utilizing for C/Z the first two terms of the series expansion in powers of $1/\beta^2$ developed and evaluated as described in Section 6 of Report No. 4, and the value of I_{adj} as determined from the figure. Since the shell-correction curves in Figure 6 of Appendix A are adjusted to give this high-energy limit, it is appropriate to use these curves with the value of I from the graph shown here.

TABLE 1

Values of I_{adj}, I, and $\Delta I \equiv I_{adj} - I$, in electron volts, for several elements

Element	Z	I_{adj}	$(C/Z)_{\beta=1}$	I	ΔI
Be	4	60	.000	60	0
Al	13	163	.002	163	0
Ar	18	210	.003	210	0
Cu	29	314	.007	312	2
Ag	47	487	.014	480	7
Pb	82	827	.039	796	31
U	92	922	.051	877	45

Particular thanks are due Dr. R. M. Sternheimer for making available to the Subcommittee the results of many of his own analyses and for providing valuable suggestions during the development of the final form of the figure.

[5] See preface of this volume for the background of the terminology concerning I and I_{adj} used in these reports.

[6] See Section 6 of Paper No. 4.

7. TABLES OF ENERGY LOSSES AND RANGES OF HEAVY CHARGED PARTICLES

Walter H. Barkas[1] and Martin J. Berger[2]

Abstract

Two-variable proton stopping-power and range tables are given as functions of the particle energy τ and of the mean excitation energy I_{adj} of the medium, for 160 values of τ between 1 and 5000 Mev, and for 36 values of I_{adj}. These tables can be applied to any medium with specified mean excitation energy. By simple scaling, they can also be applied to other heavy particles with mass and charge different from that of the proton. The tabulated values below 8 Mev are based on experimental stopping-power and range data as summarized by a 9-parameter least-squares range formula. Above 8 Mev they are based on the Bethe stopping-power theory, except for the shell corrections which are calculated by an empirical formula in the variables τ and I_{adj} derived from the analysis of experimental data. The two-variable tables do not include the density effect correction which begins to be appreciable when the kinetic energy of the particle is approximately equal to the rest mass. Stopping-power and range tables which include the density effect correction are given for protons, kaons, pions, and muons, for 36 elements and compounds.

1. Introduction

In this paper we tabulate stopping powers and particle ranges. Making use of the available empirical data we first express the electronic stopping power as a universal function of two variables, particle energy and mean excitation energy. With these variables we are able to systematize the calculation of ranges in all materials. The work is further generalized so as to apply to all charged particles.

When the particle velocity exceeds about 0.87c, the density of the stopping material becomes an additional parameter affecting the stopping power, so that the two-variable tables then apply only for stopping materials at low densities. Moreover, the ranges in this energy interval may greatly exceed the geometrical free path for nuclear interaction, and become largely meaningless except for muons. For selected materials, stopping-power and range tables are given which take the density effect into account. Some of the tables were prepared not only for protons but also for various kinds of mesons for which the density effect, at a given kinetic energy, is more important. If a need should arise for data pertaining to materials not included here, our computer program (IBM 7094) is available to prepare other tables similar to those in the present report.

---

[1]Lawrence Radiation Laboratory, University of California, Berkeley.

[2]National Bureau of Standards, Washington, D. C.; work supported by National Aeronautics and Space Administration under Contract R-80.

The tables throughout most of the energy range are reliable to about 1 percent. In the few-Mev region, however, the stopping power becomes increasingly sensitive to the assumed mean excitation energy and there is also a lack of reliable theory, at least for the heavy elements.

The very low velocity region ($\beta < 0.05$) is not a part of this report but is treated in the review articles of Allison and Warshaw (1), Whaling (2), and Northcliffe (3).

2. Assumptions from Theory

We assume that the mean energy loss per unit pathlength ι of a particle heavy compared with an electron and of unit positive charge, can be calculated from the expression

$$\iota = \frac{2\pi n r_0^2 mc^2}{\beta^2}\left[\ln\left(\frac{2mc^2}{I^2}\,\eta^2\,W_{max}\right) - 2\beta^2 - \frac{2C}{Z} - \delta\right]. \qquad (1)$$

When the moving particle is a positive point-charge of magnitude, ze, its average rate of energy loss, $-\left\langle\frac{dT}{ds}\right\rangle$, is assumed to be equal to $z^2\iota$, T being its kinetic energy and ds an element of path. In Equation 1, $r_0 = e^2/(mc^2)$ cm, and n is the number of electrons per cm^2 per unit of path (expressed usually in cm or in g/cm^2). We also express pathlengths in units of electrons/cm^2.

The particle velocity in units of the velocity of light is symbolized by β, and $\eta \equiv \beta/(1-\beta^2)^{1/2}$. The quantity

$$W_{max} = \frac{2mc^2\eta^2}{1+2r(1+\eta^2)^{1/2}+r^2} \qquad (2)$$

is the maximum energy that can be transferred to a stationary unbound electron by the moving particle when the electron-to-particle mass ratio is r. For particles heavier than electrons this expression for W_{max} is approximated by $2mc^2\eta^2$. In fact, when the particle momentum is so great that this approximation fails, the moving particle also probably cannot be treated as a point-charge. An electromagnetic form-factor for the particle then also ought to be introduced (Ref. 4).

The mean excitation energy, I, is an atomic parameter, namely the logarithmic average over the excitation energies weighted by the oscillator strengths (Ref. 5). With few exceptions, the oscillator strengths are not known with sufficient accuracy to calculate I-values, and they must be determined by stopping-power or range measurements.

The shell-correction[3] term, $\frac{C}{Z}$, is required when the velocities of atomic electrons are not small compared with the particle velocity. It has in the past been assumed to vanish in the limit $\eta \to \infty$. Stopping-power experiments at high energies have been used to determine I, the only remaining parameter. Recently Fano (5) has

[3]We are somewhat unsystematic in this paper and use the expressions "shell correction" and "tight-binding correction" to denote the same concept. In Ref. 5, the expression "inner shell correction" is used.

studied shell corrections in more detail in the high energy limit, and has pointed out that $\frac{C}{Z}$ has a finite but small value when $\eta \to \infty$. It is therefore convenient to introduce adjusted quantities I_{adj} and C_{adj} such that

$$\ln I + \frac{C}{Z} = \ln I_{adj} + \frac{C_{adj}}{Z} \quad , \tag{3}$$

and to require that $C_{adj} \to 0$ as the particle velocity approached that of light. Then in a large energy-interval where the particle velocity is well above that of the most tightly bound electron, C_{adj} may be neglected. At lower velocities C_{adj} is the operationally defined quantity replacing C while I_{adj} replaces I so as to maintain Equation 1 exact.

In Equation 1 the density-correction term of Sternheimer (6) is, as usual, symbolized by δ. It is assumed that for a mixture of elements with mean excitation energies $I_1, I_2, \ldots, I_k$ the effective mean excitation energy I is given by

$$\ln I = \sum_{1}^{k} a_i \ln I_i \quad , \tag{4}$$

where a_i is the fraction of the electron population belonging to the ith element. This equation is based on additivity of stopping effects—a rule that is reliable for physical mixtures but accurate to no better than a few percent for compounds. The mean excitation energy of a compound is best found from measurements made on it. Averages similar to Equation 4 can be made for the shell corrections and for the density effect.

Attempts to describe the stopping power of matter at low velocities have been made by Bohr (7), Lindhard and Scharff (8), and others; however, the accuracy required for energy determination from range measurements has not been achieved by pure theory, and this remains the most challenging problem of current stopping-power theory. The work of Walske (9) on C, in which he extends the usefulness of Equation 1 to lower velocities by estimating the effect of the K and L electronic shells, is deemed to be most useful in a practical sense. Because at low particle velocities the shell corrections become large, and for heavy elements relativistic effects and higher shell corrections not included in Walske's calculations are present, it is probably unwise to depend on them at low velocities. We use empirical data in this region, demanding, however, that such data be smooth with respect to both particle energy and mean excitation energy. The fundamental assumption of smoothness in I_{adj} is discussed below. At high velocities we use the asymptotic form of Walske's corrections.

The energy loss of heavy particles by radiation and the energy transmitted in collisions—elastic and inelastic—to nuclei is omitted from consideration. Neglect of energy loss in elastic collisions with nuclei is generally justified except for particles penetrating a stopping material of low atomic number (Ref. 7). Inelastic collisions are excluded in our definition of range (see Sec. 3).

3. Definition of Range

Although the "range" as a loose concept of the distance a particle goes in being brought to rest is rather generally understood, its precise definition requires some care, and it cannot be made with complete satisfaction.

On the one hand, the range of a heavy particle is only well-defined when it is determined solely by energy loss to electrons, because this loss is never very large in a single collision. In the measurement of the range, then, particles that have suffered catastrophic energy losses to nuclei must be excluded, and secondary particles that are products of such nuclear interactions also must be eliminated. Practically, the effects of nuclear interactions can be largely avoided in "good geometry" experiments, although some remaining corrections may need to be applied. On the other hand, a theoretical estimate of the distance that a charged particle of energy T_0 goes in coming to rest is most simply carried out by the integration

$$R_0 = \int_0^{T_0} \left\langle \frac{dT}{ds} \right\rangle^{-1} dT \ . \tag{5}$$

Here $\left\langle \frac{dT}{ds} \right\rangle$, found from Equation 1, is the mean energy loss to electrons per unit pathlength. The particle is brought to rest, however, by a series of electron collisions, each of finite energy transfer. When a detailed analysis of this process is made, Equation 5 is found to underestimate the range. The average pathlength R of the particle is given by $R = R_0 (1 + \epsilon)$. At low energies, $\epsilon \approx 2r/B$. Here B is the bracketed quantity in Equation 1 evaluated at $T = T_0$, and r is the mass ratio defined above (Refs. 10, 11). The correction is most important for the lightest particles, but seldom exceeds 0.001. The stochastic nature of the process leads to a dispersion of the energy losses experienced in traversing an absorber, and is the cause of "range straggling." R_0, then, is not the range but rather a quantity, differing but little from it, which we shall call the c.s.d.a. (continuous slowing down approximation) range. The tables of this report are based on this definition, but we also define the range, $R(T_0)$ of a particle with initial energy T_0, as the average length of the paths of many such particles which are brought to rest without experiencing nuclear interactions.

Often a median range, R_m, has been defined as the thickness of material through which one-half of the incident monoenergetic charged particles are transmitted. We do not adopt this range definition for the following reasons:

(a) Our range R is the one more closely related to the quantity R_0 calculated from stopping theory.

(b) This median range depends not only on interactions with electrons but also on multiple-scattering detours due to nuclear interactions, both elastic and inelastic. These multiple-scattering effects are sensitive to the arrangement of source and detector, and the correction is peculiar to that geometry.

(c) The median range is defined with respect to a transmission curve. At high energies, however, the range becomes greater than the mean free path for nuclear interaction, and the median range then measures a nuclear attenuation distance.

When the path of the particle in the stopping material is not visible, the effects of scattering and nuclear interactions require difficult corrections. In such visual instruments as bubble and cloud chambers, as well as in emulsion, the whole particle path is seen. Such visual ranges are distinctly better than the nonvisual ones. In emulsion, for example, the range-straggling curve is obtained without scattering error, and formulas for scattering effects can be checked experimentally. The gas of the cloud chamber can bring to rest only quite slow particles, however, while low energies cannot be measured in a bubble chamber because the bubble size then may

be comparable to the range. An uncertainty regarding the liquid density may also exist under the thermodynamic conditions of bubble-track formation. Nevertheless, bubble-chamber ranges are potentially of great value; in this report range and stopping-power data for bubble-chamber liquids are given in Printout Table IV.[4]

4. Scaling of the Range

It is convenient to separate the range-energy problem into two parts: (a) Given four of the five quantities—energy, mass, charge, range, and mean excitation energy—find the fifth; and (b) for a specified material, calculate the mean excitation energy from the material's physical and chemical state. It was found possible to carry out part (a) provided certain approximations were made. Part (b) is not treated here, but it is the subject of accompanying reports.

Ranges most frequently are tabulated for protons, but when both range and energy are normalized by the appropriate mass ratio, the range-energy relation is the same for all heavy singly-charged positive particles provided that the weak mass-dependence of the energy-loss rate is neglected. We find the ranges of muons, pions, kaons, and hyperons in this way. Ranges of heavy hydrogen nuclei, multiply-charged nuclei, and hypernuclei can also be considered within the scope of this report. Many range-energy relationships, therefore, correspond to each stopping material. We encompass them all by writing, for each particle range, $R(\beta)$, its relation to the ideal proton range:

$$R(\beta) = \frac{M}{z^2}\left[\lambda(\beta) + B_z(\beta)\right] \quad . \tag{6}$$

(An "ideal" proton is a particle of protonic mass and charge which does not capture electrons or interact strongly with nuclei.) In Equation 6, M and z are the particle mass and charge in units of the proton. The quantity $\lambda(\beta)$ is the range of the ideal proton as a function of its velocity β. The term B_z is added to evaluate the range extension caused by the capture of electrons by a positive particle of charge ze. The expression $\lambda + B_1$ is the range of a real proton. Practically, it is hardly distinguishable from λ.

If the particle charge is negative, and the velocity is not very high, there is evidence (Ref. 12) that its energy-loss rate is lower than that of a positive particle. While more study of this effect will be necessary for its full evaluation, its influence can be included formally in Equation 6 by introducing a range extension B_{-1}.

We evaluate B_z for multiply-charged ions as follows (Refs. 13, 4):

$$B_z(\beta) = \int_0^{\beta}\left[\left(\frac{z}{z^*}\right)^2 - 1\right]\frac{d\lambda}{d\beta}\, d\beta \quad , \tag{7}$$

where z^*e is the charge effective for energy loss of an ion of atomic number z. Stated otherwise, z^{*2} is equal to $\mathcal{J}/\iota$, where $\mathcal{J}$ is the rate of energy loss of the ion and ι is the rate of energy loss of an ideal proton at the same velocity. There is considerable

[4] In this paper, text tables bear Arabic numerals and the printout tables bear Roman numerals.

evidence (Ref. 14) that in high-density materials, and at not too low velocities, z* is almost independent of the material. We take an approximate result from the emulsion measurements (Ref. 4)

$$\left[\left(\frac{z}{z^*}\right)^2 - 1\right] \approx 1.3 \times 10^{-5}\, z^{5/3}/\beta^{7/3} \text{ for } \frac{137\beta}{z} < 2 \quad , \tag{8}$$

together with a simple low-velocity proton range-energy relation,

$$\lambda \approx (11.1 + 1.34\, I_{adj}^{5/8})\frac{A\beta^{10/3}}{Z} \text{ g/cm}^2 \quad . \tag{9}$$

From these formulas we obtain an estimate of the range extension in a material of mean excitation energy I_{adj}, atomic weight A, and atomic number Z. It is found to be proportional to β:

$$B_z(I_{adj},\beta) \approx (48.0 + 5.8\, I_{adj}^{5/8})\frac{A}{Z} \times 10^{-5}\, z^{5/3}\,\beta \text{ g/cm}^2 \quad . \tag{10}$$

This rather crude formula approximates the range extension for $\beta < 2z/137$. For $\beta > 2z/137$ the ion is completely stripped of electrons and the range extension becomes an additive constant of magnitude:

$$B_z(I_{adj}) \approx (7.0 + 0.85\, I_{adj}^{5/8})\frac{A}{Z}\, 10^{-6}\, z^{8/3} \text{ g/cm}^2 \text{ (z positive)} \quad . \tag{11}$$

B_{-1} (asymptotic) in emulsion is at least $35 \times 10^{-4}\frac{A}{Z}$ g/cm^2 (Ref. 12).

More experimental study of the range extension, B_z, especially for heavy-element absorbers and for very heavy ions would be desirable, of course. The above formulas are based largely on emulsion data for a few ions of light elements. When the ion is of high atomic number, a finite pathlength may be traversed before the ion attains an equilibrium charge. Then B_z and R will depend also on the initial charge-state of the ion.

An estimate of the reliability of Equation 6 could reasonably be demanded. Experimentally the mass dependence has been tested for muons, pions, kaons, protons, Σ^+ hyperons, deuterons, and tritons, as well as hydrogen-3 and hydrogen-4 hyperfragments (Refs. 13-21). The mass dependence of Equation 6 at nonrelativistic velocities appears to be reliable to about one part in 1000, but it is not thought to be exact. According to Equation 2, particle mass enters when the electron mass is not strictly negligible compared with it. Especially for mesons, a small effect of the electron/particle mass ratio, r, remains. Effects of the particle/nucleus mass ratio also exist. Checks that have been made used emulsion as the stopping material and did not adequately test the form of Equation 6 for a stopping material of such light atoms as hydrogen. Here a mass-dependent contribution to the stopping is expected (Ref. 4).

Although electron ranges are not a part of this paper (they are treated separately in Paper No. 10), it is of interest to observe that emulsion ranges of electrons with tens and hundreds of kev energy seem to be found as well from Equation 6 as from formulas specifically developed for electrons, but the large scattering, straggling, and radiation energy-loss of electrons reduces the usefulness of electron range data.

In view of the tests cited, the dependence at moderate energies of the range on neglected particle structure-characteristics (form factors) also cannot be more than a few tenths of a percent.

The influences mentioned are all small, so that we shall assume that the purpose of our work will have been served when the range λ of an ideal proton as a function of particle velocity, β, is known. For other positive particles, the quantity M/z^2 is given in Table 1.

TABLE 1

The Quantity M/z^2 for Particles of One and Two Units of Charge

Particle	z	M/z^2
e^+	+1	0.00054463
μ^+	+1	0.11261
π^+	+1	0.14878
K^+	+1	0.5264
p	+1	1.0000
Σ^+	+1	1.2677
d	+1	1.99901
t	+1	2.99372
He^3	+2	0.74829
He^4	+2	0.99315
He^6	+2	1.4935
ΛH^3	+1	3.1877
ΛH^4	+1	4.1802
ΛHe^4	+2	1.0449
ΛHe^5	+2	1.2896
ΛHe^7	+2	1.7899

5. Sources and Use of Experimental Data

In order to prepare this report, it was needed to know quite well the mean excitation energy and low-energy ranges for only certain key elements. For these, empirical data were available, but more and better information would have been very useful. The final tables, however, are insensitive to errors in the estimated mean excitation energies except at low energies.

The available compilation of information includes the following items. Early measurements were reviewed in the report titled, "Index and Annotated Bibliography

of Range and Stopping Cross-Section Data" by Brown and Jarmie (22). This work contains a comprehensive bibliography of early measurements. The low-energy region was thoroughly reviewed most recently by Whaling (2). The previous review by Allison and Warshaw (1), however, remains valuable for stopping-power information. Heavy ion data are reviewed by Northcliffe (3) and by Allison (23) as part of the current work. The National Bureau of Standards Handbook No. 79 contains useful information, and many references. R. M. Sternheimer's (24) review of energy-loss formulas, I-values, and ionization-loss experiments is relevant to all these problems. Bethe and Ashkin's (25) and Uehling's (26, 27) works and the accompanying article (Appendix A) by Fano summarize the useful theory. The older work of Bohr (7) as well as the work of Lindhard and Scharff (8) and of Brandt (28) contribute to the theory but these works are not immediately useful for accurate range calculations.

For the present report we have referred to the following experimental data: (a) measurements quoted in the review articles cited above; (b) the range measurements by Zrelov and Stoletov (30); (c) corrected relative range measurements by Rybakov (31); (d) energy loss and range measurements made in emulsion, aluminum, copper, lead, and uranium by Barkas, et al. (32-34); and (e) the measurements by MacKenzie and his collaborators (35) and those by Nielsen (36). Important aid in this task was obtained from the measurements and extensive calculations of Bichsel (37), based in part on his own work and on the theoretical work of Walske (9). Earlier, Sternheimer (38, 39) calculated proton ranges in several elements and also gave an interpolation prescription based on the smoothness as a function of Z of the electronic stopping cross section.

For particle velocities comparable to or higher than that of the K electrons of the stopping material, C_{adj} is small and may be estimated from theory. The mean excitation energy can be determined then by measuring ι and solving Equation 1 for I_{adj}. With it one is able to make limited extrapolations and to interpolate energy-loss rates by means of the theory. At lower velocities more reliance must be placed on the correction for tight binding, and the resulting value of I_{adj} is less reliable. The difficulty is aggravated as the atomic number rises because the shell corrections become larger.

In the intermediate-velocity region, one observes deviations from Equation 1 if C_{adj} is set equal to zero. The theory here can act as a guide; one demands that the deviation be a smooth function of velocity (Ref. 34). Since the calculations of C_{adj} are inadequate for heavy elements, at the lower energies only empirical data seem reliable. Improved efficiency is believed to have been attained in the utilization of such measurements in the present paper. The observations, of course, are the anchor points of the theoretical calculations. It has been usual to demand that the measurements define a smooth range-energy curve for a given stopping material. Now it is further assumed that, with certain reservations, the range measured in electrons per cm^2 is also a smooth function of mean excitation energy for each proton energy. An effort has been made to fit, with theoretical interpolation, a smooth surface to the two-parameter range data. The requirement of smoothness in both parameters is a powerful means for resolving inconsistencies in empirical data.

In order rationally to employ smoothness of energy-loss rate with I_{adj}, the basis for and limitations of such a postulate must be discussed. First, one notes that when the ranges (in electrons per cm^2) for a series of similar elements at a given energy are graphed as a function of Z, they define a smooth curve. Thus, for example, the ranges at 8 Mev given by Whaling (2) for the noble gases behave in this way. A series of metals (Be, Al, Cu, Ag, Au, Pb, and U) is found to define a smooth locus somewhat

below that of the noble gases. The effective mean excitation energy of typical metals is perhaps 6 percent less than one would predict from their atomic numbers on using the noble gas curve. On correctly choosing I_{adj}-values and replotting the data as a function of I_{adj}, one finds that the curves almost coincide. Were C_{adj}, which depends on Z, strictly a function of I_{adj}, the curves would coincide. Conceptually the shell corrections could be extended to the valence and conduction electrons. Then it is maintained that C_{adj} would be closely a function only of I_{adj} and η.

Thompson (29) first detected apparent differences in stopping powers that depend on molecular binding in a series of selected materials. There is known to be a dependence of the mean excitation energy on the average electron density in the stopping material, as predicted by Lindhard and Scharff (8). If the electron density in a series of elements were not to increase smoothly with increasing atomic number, one could not expect a smooth variation of stopping power per electron with Z. Burkig and MacKenzie (35) observed deviations from a smooth dependence on atomic number of electronic stopping power in a systematic study of many elements. The elements calcium, titanium, vanadium, and thorium, as well as the noble gases appear to be anomalous.

Chemical binding effects are limited primarily to light elements and low particle energies. The valence electrons in these cases constitute a large fraction of all those participating in the stopping. In the light elements, tight-binding corrections are small, so that the stopping behavior of a compound of such elements is almost entirely determined by the mean excitation energy even if, for a given element, it varies from compound to compound.

When I_{adj} is determined by the high-velocity stopping behavior of the material, the rates of energy loss calculated from Equation 1 for high velocities are exact by definition. In order to express ι everywhere as a function of I_{adj} and η, C_{adj} must remain expressible as a function of them, even at low velocities where C_{adj} becomes more than a mere correction. As indicated above, such an expression of C_{adj} is only approximate. Nevertheless, when the correct mean excitation energy for an element is used, the error introduced on expressing the shell correction as a function of I_{adj} and η is, at worst, that arising from the use of a shell correction that is more appropriate for a neighboring element—an error of second order.

For a composite material the use of the same value of I_{adj} in the shell-correction formula as that derived from the high-velocity energy-loss rate also is justified only as an approximation. Such materials as animal tissue or hydrocarbons are chiefly composed of light elements for which the shell corrections are small in any case. The most extreme example of practical importance is nuclear research emulsion, which consists of crystals of heavy elements embedded in a light-element matrix. The range curve here corresponds well to no single mean excitation energy at all velocities (Ref. 4). A simpler way to treat this case is to note that the range, R, in an n-component material is found with good accuracy from the formula (Ref. 4)

$$\frac{1}{R} = \sum_{i=1}^{n} f_i/R_i \ . \qquad (12)$$

Here R_i is the calculated range in the ith component and, if the ranges are expressed in g/cm^2, f_i is the fraction by weight of that constituent of the stopping material. This formula, while not rigorously derivable, is very accurate, and integration is avoided.

At low velocities our data are entirely empirical, but have been subjected to a systematic smoothing. The requirement that the stopping power be a function of both variables, I_{adj} and η, tends to make every point on the range or stopping-power surface depend on all the data used to construct the surface. The smoothing procedure made use of the experimental values of the stopping power as well as of the range.

Shell corrections for media of low atomic number, at energies below 8 Mev, were estimated using the nomogram of Fano's article (Fig. 6 of Appendix A), which, in turn, is based on the analysis of the available experimental data. These estimates were adjusted to be consistent with our shell corrections (Eq. 16) at 8 Mev. The magnitude of these shell corrections is small, so that even our necessarily rather rough estimates are adequate. Inserting the shell corrections into the stopping-power formula, ranges were then calculated numerically for hydrogen, beryllium, and aluminum, assuming the ranges at 1 Mev to be those given in Whaling's (2) compilation of experimental data. The calculated ranges agree well with those of Whaling at 2, 3,.. 8 Mev, and the latter were used in the subsequent analysis. The range data of Rybakov (31) for iron, copper, tin, and lead, smoothed in energy and corrected for multiple scattering as described in Section 7, were used to obtain, by interpolation, range values at 1, 2,.. 8 Mev.

The entire body of range data for energies $1 \leq \tau \leq 9$ Mev was summarized by the formula

$$\log \lambda = \log \frac{A}{Z} + \sum_{n=0}^{2} \sum_{m=0}^{2} a_{mn} (\log I_{adj})^m (\log \tau)^n \quad , \tag{13}$$

the coefficients a_{mn} being obtained by a least-squares analysis (λ in g cm^{-2}). To provide a smooth transition to energies above 8 Mev, the input data were enlarged to include not only the Whaling and Rybakov ranges but also ranges at 9 Mev. The latter were derived from an incremental range calculation based on stopping-power theory. Table 2 gives the input data for the least-squares analysis. The assignment of I_{adj}-values to particular elements agrees with the recommendations of the subcommittee (Paper No. 6). Table 3 contains the least-squares coefficients, and Table 4 the percentage deviations between the fitted and input ranges. The root-mean square error of the fit is 2 percent.

TABLE 2

Ranges (mg/cm^2), Multiplied by $\frac{Z}{A}$, That Were Used as Input Data to Produce the Least-Squares Formula (Eq. 13)

Proton Energy Mev	H_2 I_{adj}= 19 ev	Be I_{adj}= 60 ev	Al I_{adj}= 163 ev	Fe I_{adj}= 285 ev	Cu I_{adj}= 314 ev	Sn I_{adj}= 516 ev	Pb I_{adj}= 826 ev
1	0.830	1.290	1.870	2.700	2.793	3.791	4.749
2	2.840	3.920	5.400	6.843	7.166	8.846	12.27
3	5.900	7.780	10.46	13.27	13.83	16.43	22.36
4	9.930	12.79	16.80	20.95	21.91	26.12	34.43
5	14.90	18.90	24.60	29.79	31.95	37.49	48.28
6	20.77	25.70	33.73	40.50	43.36	50.55	63.32
7	27.53	33.79	44.09	52.14	55.68	65.29	79.94
8	35.16	42.88	55.41	66.11	69.37	81.30	98.14
9	43.38	53.14	67.99	80.57	84.23	98.55	118.4

TABLE 3

Coefficients a_{mn} in Equation 13

m \ n	0	1	2
0	-7.5265×10^{-1}	2.5398	-2.4598×10^{-1}
1	7.3736×10^{-2}	-3.1200×10^{-1}	1.1548×10^{-1}
2	4.0556×10^{-2}	1.8664×10^{-2}	-9.9661×10^{-3}

TABLE 4

Percentage Deviation of Ranges Computed with Equation 13 from the Input Ranges in Table 2

Proton Energy Mev	H_2 I_{adj}= 19 ev	Be I_{adj}= 60 ev	Al I_{adj}= 163 ev	Fe I_{adj}= 285 ev	Cu I_{adj}= 314 ev	Sn I_{adj}= 516 ev	Pb I_{adj}= 826 ev
1	0.2	-2.5	5.1	-3.3	-1.5	-4.3	1.4
2	1.2	-1.6	2.4	3.1	3.0	6.7	-0.5
3	0.9	-2.0	0.5	-1.1	-1.1	4.5	-2.5
4	0.7	-2.1	0.4	-1.0	-1.5	2.2	-2.9
5	0.4	-2.0	-0.2	0.3	-2.9	1.3	-2.7
6	0.2	-0.3	-0.4	0.1	-3.1	0.8	-1.4
7	-0.1	0.1	-0.2	1.1	-2.0	0.5	0.3
8	-0.3	0.5	0.6	0.5	-1.1	0.8	0.7
9	0.1	0.6	1.2	1.3	0.0	1.5	1.0

From Equation 13 one can derive, by differentiation, a stopping-power formula,

$$\frac{d\tau}{d\lambda} = \frac{\tau}{\lambda} \left\{ \sum_{n=1}^{2} \sum_{m=0}^{2} n a_{mn} (\log I_{adj})^m (\log \tau)^{n-1} \right\}^{-1} \qquad (14)$$

As a final check, the stopping-power values computed according to Equation 14 were compared with the compilation of experimental values by Bichsel (37). As shown in Table 5, the agreement is generally close, although occasional discrepancies up to 4 percent occur. This is not incompatible with the experimental errors.

6. The Tight-Binding Corrections

The quantity C in Equation 1 is the sum of corrections for each electron shell of the atom. Thus

$$C = C_K + C_L + C_M + \ldots\ldots .$$

The variations of C_K and C_L with velocity and atomic number have been calculated (Ref. 9). Each is large and negative at very low velocities, but, as the velocity

TABLE 5

Proton Stopping Power (Mev/g cm^{-2}). L.SQ., Derived from the Least-Squares Formula (Eq. 14). B, Experimental Values Compiled by Bichsel (37)

Proton Energy (Mev)	H_2, I_{adj} = 19 ev		Be, I_{adj} = 60 ev		Al, I_{adj} = 163 ev	
	L.SQ.	B	L.SQ.	B	L.SQ.	B
1	669	676	223_5	220	170	173
2	385	393	138_5	137	112	110.7
3	278	282	102	101	85.9	83.2
4	220	222	81.5	81	68.7	67.6
5	183	184	67.9	67	57.8	57.3
6	158	158	58.3	58	49.9	50.0

Proton Energy (Mev)	Cu, I_{adj} = 314 ev		Sn, I_{adj} = 516 ev		Pb, I_{adj} = 826 ev	
	L.SQ.	B	L.SQ.	B	L.SQ.	B
1	121	121	87.5	89	63.6	63
2	82.9	80	61.8	61	46.3	44.5
3	64.2	62	48.7	48	37.2	36.5
4	52.7	51	40.6	40	31.5	31.8
5	44.8	44	34.9	35	27.4	27.9
6	39.1	39	30.7	31	24.3	25.0

increases, the sign of every C changes. Each passes through a maximum and subsequently falls. Each C_{adj} should approach zero as η^{-2} for large η. At reasonably high velocities, the velocity dependence for each element is expressible in the same form as Walske's asymptotic expressions:

$$C_{adj} \approx \frac{\alpha}{\eta^2} + \frac{\beta}{\eta^4} + \frac{\gamma}{\eta^6} + \ldots\ldots \qquad (15)$$

C_{adj} also varies rapidly with I_{adj}. At a particular value of η, the form $A(\eta)I_{adj}^2 + B(\eta)I_{adj}^3$ is capable of fitting the data to its present accuracy.

Bichsel (37) has extended the work of Walske semi-empirically. He makes allowance for the numbers and binding energies of electrons in each subshell of the atom. The form of C_{adj} for each higher shell was assumed to be obtainable by scaling the correction that Walske calculated for the L shell. When applied to all the shells of such heavy elements as lead and uranium, the corrections were successful in predicting the measured ranges and energy losses at both high and low velocities. At the same time, each I_{adj} remained constant at a value close to that found by Barkas and von Friesen. Bichsel's procedure is completely numerical, however, and must be carried out in detail for each stopping material.

We have thought it better to express C_{adj} analytically. As mentioned above, it was also considered wiser not to attempt to carry the calculations down to very low velocities. For $\eta < 0.13$ it was necessary only to smooth the empirical ranges (expressed in electrons per square centimeter) as functions of I_{adj} and of η separately.

Then, by trial, the data were expressed in a semi-empirical formula. Above $\eta = 0.13$, the shell-correction term was assumed to have the dependence on η and I_{adj} given above. The available information then was used to determine the coefficients in the formula (which is not valid for $\eta < 0.13$)

$$C_{adj}(I,\eta) = (0.422377\eta^{-2} + 0.0304043\eta^{-4} - 0.00038106\eta^{-6})\,10^{-6}\,I_{adj}^2 + (3.858019\eta^{-2} - 0.1667989\eta^{-4} + 0.00157955\eta^{-6})\,10^{-9}\,I_{adj}^3 \quad (16)$$

These coefficients doubtless can be improved, and the functional form can be refined as more reliable data become available. A great advantage of such an expression is that it provides an analytic energy-loss formula for all materials applicable over a wide range of velocities. It also summarizes the bulk of what is known about the energy losses of fast particles in matter. Expression 16 is consistent, within the limits of experimental error, with the shell corrections used by other authors in this volume (see Fig. 1 in Paper No. 4).

The shell correction enters the stopping-power formula not as C_{adj} but as C_{adj}/Z. To establish the necessary relation between I_{adj} and Z, we have used the expressions

$$I_{adj}/Z = 12 + 7/Z \text{ ev}, \qquad I_{adj} < 163 \text{ ev} \quad (17a)$$

$$I_{adj}/Z = 9.76 + 58.8Z^{-1.19} \text{ ev}, \qquad I_{adj} \geq 163 \text{ ev}. \quad (17b)$$

The assumed straight-line relationship for small values of I_{adj} is an oversimplification that is permissible because the shell corrections are quite small. The relation (Eq. 17b), due to Sternheimer (private communication), yields mean excitation energies of 163 ev, 314 ev and 826 ev for aluminum, copper, and lead, respectively, and has been recommended by the subcommittee as "best smooth curve" (see Paper No. 6 of this volume).

7. Multiple-Scattering Corrections

The definition of the range given in Section 3 of this paper prescribes in effect how its measurement is to be carried out. The experimental technique must be such as to insure that the true rectified pathlength has been determined, and that nuclear interactions do not influence the results of the measurement. Difficult problems in the interpretation of incorrectly performed measurements may arise in separating the effects of energy loss to electrons, nuclear influences, and the effects of scattering on the range and on the range-straggling. One may attempt to correct the measurements if the geometry of the experimental arrangement is known. This topic is treated more extensively in Paper No. 5 in this volume.

Here we discuss a simple correction procedure that often may be satisfactory. It is noted first that scattering corrections can be measured in emulsion because the whole particle trajectory can be seen. Any desired range-distribution function can be obtained by measurements on randomly sampled tracks. In addition, we know—from Rossi (42), for example—that in any material the increment of the mean-square angle of multiple scattering, multiplied by the radiation length and divided by the increment in pathlength, has the same magnitude, approximately $(21.2/p\beta)^2$, for a singly-charged particle of momentum p and velocity β. In this expression $p\beta$ is measured in Mev/c. To apply this rule, of course, account must be taken of the fact that $p\beta$ falls as the particle loses energy.

Suppose the particle starts parallel to the x-axis from an origin of rectangular coordinates x, y, and z in the stopping material. Then if θ is the instantaneous angle between the x-axis and the particle direction and ds is an element of its path we define

$$S_p = \int_0^S ds \cos\theta \ , \tag{18}$$

where S is the distance traversed by the particle in being brought to rest at a depth of penetration, S_p. We call the average value of S_p the projected range, R_p. The expectation value of S is the range, R; S is a random variable of variance $\sigma^2(R)$.

For making the multiple-scattering correction, suppose the quantity to be evaluated is $\Delta R = R - R_p$. It is

$$\Delta R = \int_0^R \langle 1 - \cos\theta \rangle \, ds \approx \frac{1}{2} \int_0^R \langle \theta^2 \rangle \, ds \ . \tag{19}$$

The fractional correction, $\Delta R/R$, therefore, is one-half of the mean-square scattering angle.

The scattering in emulsion is well known empirically. We note that one can compensate for the use of the small-angle approximation by measuring ΔR on tracks in emulsion, and thus one can replace the number 21.2 Mev/c by an empirically determined quantity, k. Then

$$\frac{d\langle \theta^2 \rangle}{ds} = \frac{1}{X_0} \left(\frac{zk}{p\beta} \right)^2 \ , \tag{20}$$

where X_0 is the radiation length in the stopping material. Measurements (Ref. 4) made on tracks of protons and muons indicate, moreover, that the best value to use for k is about 19.7 Mev/c, if the radiation length is taken to be 2.91 cm. This evaluation should be studied more exhaustively, but for the present purpose of making a small correction, such an estimate nevertheless may be accurate enough. To carry out the calculation of $\langle \theta^2 \rangle$, we first write $p\beta$ as a function of distance s along the average trajectory. In the low-energy region this is

$$p\beta = aM^{1-n} z^{2n} (R-s)^n \ ,$$

where, to good approximation, a is a constant determined by I_{adj}, and n is close to 0.63 for all materials except those of lowest atomic number (for which the correction is small). Now, from Equations 16 and 15 we find that the expression $(1-n)X_0\Delta R/R^2$ at a given energy is independent of the material. Since n varies very little, $(X_0/R)(\Delta R/R)$ also will not vary much from one material to another.

The statistical variable S_p has a skewed distribution, especially in stopping materials of high atomic number. Its expectation value or mean, R_p, is smaller than the median range R_m defined in Section 3. Some experimenters, notably Rybakov (31), whose data we use, compared median ranges in various metals with the median range in aluminum. The correction, which is evaluated by Berger (41) is somewhat less than ΔR. In Table 6 we list the percentage corrections we applied to Rybakov's ranges.

TABLE 6

Percent Range Corrections for Scattering, $\frac{100(R-R_m)}{R}$

Proton Energy (Mev)	Emulsion	Al	Fe	Cu	Cd	Sn	Pb
1	2.07	0.72	1.55	1.80	3.18	3.36	5.96
2	1.67	0.59	1.26	1.48	2.65	2.76	4.92
3	1.47	0.52	1.10	1.32	2.32	2.43	4.34
4	1.34	0.47	1.01	1.18	2.12	2.22	3.98
5	1.24	0.43	0.93	1.10	2.00	2.07	3.73
6	1.18	0.41	0.88	1.03	1.88	1.96	3.54
7	1.11	0.39	0.85	0.99	1.79	1.87	3.37
8	1.07	0.37	0.81	0.94	1.72	1.79	3.23

8. The Two-Variable Stopping Power and Range Tables[5]

Method of Presentation

The proton stopping power (Mev/g cm^{-2}) divided by Z/A and the proton range (g cm^{-2}) multiplied by Z/A are given as functions of the proton kinetic energy τ(Mev) and the mean excitation energy I_{adj} (ev) in Printout Tables I and II. The advantages of this method of presentation are as follows:

(1) Through elimination of the factors Z/A, i.e., through the use of electrons per cm^2 as unit of distance, the main dependence of stopping power and range on the nature of the medium has been removed. The residual dependence is in the mean excitation energy; only interpolation in I_{adj} is necessary for application to any particular substance.

(2) A close grid in I_{adj} is provided, so that linear interpolation is adequate. This makes it easy to estimate the range or stopping-power uncertainty caused by a known uncertainty in I_{adj}, or vice versa.

(3) The tables will retain their validity and usefulness even when, as seems probable, the preferred I_{adj}-values for various materials will undergo changes in the future.

(4) The uniform method of presentation permits easy detection of measurement errors, or of anomalies that may have significance.

(5) Because of the scaling properties of stopping power and range for particles with different mass and charge, even a single measurement of range or stopping power in a material of unknown stopping behavior can be used to obtain range-energy curves for all types of particles.

Method of Computation

For proton kinetic energies below 7.9 Mev, the stopping power was evaluated with the use of the empirical formula (Eq. 14). Above 8.1 Mev it was evaluated

[5]Without the density-effect correction.

theoretically according to Equation 1, with shell corrections given by Equations 16 and 17 and with the density effect disregarded. Between 7.9 and 8.1 Mev, the arithmetic average of the results of the two procedures was used.

The calculation of the c.s.d.a. range was made from the integral

$$\lambda(\tau) = \lambda_1 + \int_{\tau_1}^{\tau} \frac{dt}{\iota} \quad . \tag{21}$$

Here λ_1 is an empirical range given by Equation 13 and corresponding to kinetic energy $\tau_1 = 1$ Mev. The upper limit $\tau = 938.213\,[(1-\beta^2)^{-1/2} - 1]$ Mev is the proton kinetic energy corresponding to velocity $\beta = \eta/(1+\eta^2)^{1/2}$.

Units

The units of stopping power in Printout Table I are Mev per 6.0249×10^{23} (Avogadro's number[6]) of electrons cm^{-2}. The units of range in Printout Table II are 6.0249×10^{23} electrons cm^{-2}. For any particular material, the stopping power is readily converted to Mev/g cm^{-2} through multiplication by Z/A, and the range to g cm^{-2} through multiplication by A/Z. To obtain the range in cm, one must further divide by the density ρ in g cm^{-3}. The quantity A/Z is given in Table 7 for various materials. To apply Printout Tables I and II for a particle of mass M and charge z in units of the proton, the energies in the left-most column must be multiplied by M, and the ranges (after adding B_z if necessary) by M/z^2. This factor is given in Table 1.

Significant Figures

The stopping power and range are given to five figures, whereas the physical input data and method of calculation are such that, at most, three figures are significant. The other two figures are included to allow differencing of the tabulated data. Such differencing is required when one is interpolating with respect to I_{adj}. It may also be required for the computation of partial ranges between two given energies.

Sample computations, which are summarized in Table 8, indicate that with linear interpolation in I_{adj} or τ one can achieve at least three-figure accuracy.

Application to Particular Materials

The choice of the value of the mean excitation energy I_{adj} is at the reader's discretion. Some suggested I_{adj}-values are listed in Table 7. They are not definitive but are based on the present, tentative consensus of the subcommittee (see Report No. 6 of this volume). For $Z \geq 13$ they are based on the semiempirical formula (Eq. 17b).

For compounds and mixtures, provided one assumes that the contribution of various constituents is additive (Bragg's rule), one must replace Z/A by an average value

$$\left\langle \frac{Z}{A} \right\rangle = \frac{1}{\rho} \sum_i \frac{Z_i}{A_i} \rho_i \quad , \tag{22}$$

[6] The use of this value for Avogadro's number implies that atomic weights must be expressed according to the old mass scale in which the atomic weight of O^{16} is exactly 16, rather than according to the new scale in which the atomic weight of C^{12} is exactly 12.

TABLE 7

A/Z and an Estimate of I_{adj} for Some Elemental Absorbers

Element	I_{adj}(ev)	A/Z
$_{1}H$	19	1.0080
$_{4}Be$	60	2.2533
$_{13}Al$	163	2.0754
$_{26}Fe$	285	2.1481
$_{28}Ni$	304	2.0961
$_{29}Cu$	314	2.1910
$_{47}Ag$	487	2.2953
$_{50}Sn$	516	2.3740
$_{74}W$	748	2.4854
$_{78}Pt$	787	2.5029
$_{79}Au$	797	2.4937
$_{82}Pb$	826	2.5270
$_{83}Bi$	835	2.5181
$_{92}U$	923	2.5877

where Z_i/A_i corresponds to the i'th constituent with partial density ρ_i ($\sum_i \rho_i = \rho$). The corresponding average value of the mean excitation energy is, according to Equation 4,

$$\log \langle I_{adj} \rangle = \left\langle \frac{Z}{A} \right\rangle^{-1} \frac{1}{\rho} \sum_i \frac{Z_i}{A_i} \rho_i \log I_{adj\ i} \ . \tag{23}$$

It should be recalled that one must expect departures from additivity due to chemical binding effects, particularly for media of low average atomic number. It is therefore preferable, if possible, to use a value of $\langle I_{adj} \rangle$ derived directly, by experiment or calculation, for the substance in question.

The use of Printout Tables I and II for mixtures and compounds introduces a small error in regard to shell corrections. In effect, one first selects a value of $\langle I_{adj} \rangle$ and then, by implication, uses an average atomic number $\langle Z \rangle$ given by Equation 17, whereas the correct method of averaging is

$$\left\langle \frac{C}{Z} \right\rangle = \left\langle \frac{Z}{A} \right\rangle^{-1} \frac{1}{\rho} \sum_i \frac{Z_i}{A_i} \rho_i \frac{C_i}{A_i} \ . \tag{24}$$

The error is largest for substances in which both high-Z and low-Z components are present. For example, for photographic emulsion, the maximum error in the proton stopping power occurs at ~ 20 Mev (0.6 percent too high) and the maximum error in the range at ~ 30 Mev (0.5 percent too low).

TABLE 8a

Accuracy of Interpolation in Printout Tables I and II.
Linear Interpolation with Respect to Mean Excitation Energy I_{adj}:
(H_2O, from 60 and 70 to 65.1 ev; Cu, from 300 and 320 to 314 ev;
Pb, from 800 and 850 to 826 ev).

Medium	(Mev)	Stopping Power, Mev/g cm^{-2}		Range, g cm^{-2}	
		Interpolated	Direct	Interpolated	Direct
H_2O	10	46.812	46.796	0.11827	0.11830
	100	7.4245	7.4215	7.5664	7.5687
	1000	2.2452	2.2445	320.36	320.44
Cu	10	27.317	27.315	2.1819	2.1820
	100	4.8845	4.8839	11.771	11.772
	1000	1.5573	1.5572	468.40	468.41
Pb	10	17.501	17.497	0.35605	0.35607
	100	3.5318	3.5315	16.821	16.821
	1000	1.1956	1.1955	618.98	618.99

TABLE 8b

Accuracy of Interpolation in Printout Tables I and II.
Linear Interpolation with Respect to Proton Energy T,
from 320 and 330 to 324 Mev.

I_{adj} (ev)	Stopping Power (Mev/g cm^{-2}) $\times \frac{A}{Z}$		Range (g cm^{-2}) $\times \frac{Z}{A}$	
	Interpolated	Direct	Interpolated	Direct
60	6.2364	6.2356	31.574	31.571
300	5.1276	5.1270	38.996	38.993
800	4.4354	4.4349	45.954	45.950

Approximation Formula

The stopping power is available in terms of a formula (Eqs. 1, 16, and 17). It is convenient also to have an analytical representation for the range which precludes the necessity of always having to rely on a large table of numbers. We have not made an exhaustive search for an optimum formula, but have found it convenient to represent the proton range between 7 Mev and 1200 Mev by the following expression:

$$\log \lambda = \log \frac{A}{Z} + \sum_{n=0}^{3} \sum_{m=0}^{3} \alpha_{mn} (\log I_{adj})^m (\log T)^n , \qquad (25)$$

where λ is measured in g cm^{-2}. The coefficients in this expression, given in Table 9 were obtained through a least-squares adjustment based on 600 range values (at 30 energies and 20 values of I_{adj}). The root mean square percentage deviation between the input data and fitted values at these 600 points is 0.6 percent. The worst error occurs for T = 7 Mev, and I_{adj} = 15 ev, and it amounts to 2.8 percent, but in most

TABLE 9

Coefficients α_{mn} in Equation 25

m \ n	0	1	2	3
0	-8.0155	1.8371	4.5233×10^{-2}	-5.9898×10^{-3}
1	3.6916×10^{-1}	-1.4520×10^{-2}	-9.5873×10^{-4}	-5.2315×10^{-4}
2	-1.4307×10^{-2}	-3.0142×10^{-2}	7.1303×10^{-3}	-3.3802×10^{-4}
3	3.4718×10^{-3}	2.3603×10^{-3}	-6.8538×10^{-4}	3.9405×10^{-5}

regions of the table the error is much smaller than 1 percent. It is interesting to note that if one differentiates Equation 25 to obtain an analytical expression for the stopping power analogous to Equation 14, the resulting root mean square percentage error is still only 1.3 percent.

The 12,960 numbers contained in Printout Tables I and II have also been compressed into a deck of 648 binary IBM-cards, copies of which can be made available to interested parties.

9. Density Effect

The density effect, i.e., the reduction of the ionization loss due to the polarization of the medium, has been systematically evaluated by Sternheimer (6) for many elements and compounds, and we shall use his results. Sternheimer expresses the density effect correction δ (which enters into Equation 1 for the stopping power) as a function of the particle velocity with the use of the semi-empirical formula

$$\delta(\eta) = \begin{cases} 0 & X < X_0 \\ \log \eta^2 + \delta_0 + \delta_1 (X_1 - X)^{\delta_2} & X_0 \le X < X_1 \\ \log \eta^2 + \delta_0 & X \ge X_1 \end{cases} \qquad (26)$$

where $X = (\log_{10} e) \log \eta = 0.43429 \log \eta$.

The quantities δ_0, δ_1, δ_2, X_0 and X_1 depend on the characteristics of the medium.[7] Sternheimer made, at different times (1952, 1956), two evaluations of these parameters for various media, using different values of the mean excitation energy I. Neither of

[7] In Sternheimer's notation, δ_0, δ_1 and δ_2 are called C, a, and m. The parameter δ_0 is given by $\delta_0 = -2 \log (I/h\nu_p) - 1$ where $\nu_p = c(nr_0/\pi)^{1/2}$ is the plasma frequency of the medium. In addition to his published values, Sternheimer has communicated additional parameter values for Cu and Pb to U. Fano (letter, May 2, 1962) which we have also used; these values are:

	I	δ_0	δ_1	δ_2	X_0	X_1
Cu	323 ev	-4.43	0.109	3.39	0.2	3.0
Pb	826 ev	-6.21	0.355	2.64	0.4	3.0

his two I-values coincides in general to the I_{adj}-value adopted in the present work. Following his suggestion, we have made the appropriate adjustment through logarithmic interpolation. Let $\delta^{(1)}$ and $\delta^{(2)}$ denote the density effect corrections for a given medium and energy, evaluated with mean excitation energies I_1 and I_2. The desired value, corresponding to mean excitation energy I_{adj} is obtained as

$$\delta = \alpha\,\delta^{(1)} + (1 - \alpha)\delta^{(2)} \quad , \tag{27}$$

with

$$\alpha = \log (I_2/I_{adj}) / \log (I_2/I_1) \quad .$$

Sternheimer's density-effect parameters for gases pertain to normal pressure. To obtain δ for any other pressure, one must insert into Equation 26 the argument $\eta\sqrt{P}$ instead of η, where P is the pressure in atmospheres.

The percentage reductions of the stopping power and increases of the range caused by the density effect are indicated in Table 10 for protons, kaons, pions, and muons in beryllium, copper, and lead.

10. Stopping Powers and Ranges for Protons and Mesons in Selected Materials

Printout Tables IIIa-d contain stopping powers and ranges for protons, kaons, pions, and muons in 27 substances. Density-effect corrections are included. The assumed values of I_{adj} are in agreement with the recommendations of the Subcommittee (see Report No. 6 in this volume). For mixtures and compounds, an average value of I_{adj} was computed according to Equation 23, and shell corrections were averaged according to Equation 24. Meson stopping powers were obtained by scaling proton stopping powers. Meson ranges were obtained by numerical integration, using a base point at 1 Mev calculated by scaling the corresponding proton range. The accuracy of the computed stopping powers and ranges is expected to be of the order of 1 percent. Five significant figures are given in Printout Table III in order to facilitate interpolation.

There are a number of substances of interest for which the density-effect correction has not yet been evaluated. In the absence of such a correction, the universal Printout Tables I and II are adequate. Nevertheless, we have thought it useful to present (in Printout Table IV) proton stopping powers and ranges of nine substances of complicated composition, at energies up to 1000 Mev. With this limitation, the lack of density-effect correction will introduce only a very small error, as indicated in Table 10.

11. Acknowledgments

We are grateful to Marilyn Gode-von Aesch and to Stephen M. Seltzer for assistance with programming. Earlier, Peter Trower and Herbert Yoshida participated in this work, and to them also we owe thanks. We are particularly obligated to Prof. Hans Bichsel not only for his published reports but also for correspondence and consultation in connection with the tight-binding corrections. We thank Dr. R. M. Sternheimer for advice on the density effect and on numerous other topics.

TABLE 10a

Percent Reduction of Stopping Power Due to Density Effect

Energy	Protons			Kaons			Pions			Muons		
(Mev)	Be	Cu	Pb	Be	Cu	Pb	Be	Cu	Pb	Be	Cu	Pb
5000	6.2	4.1	1.5	9.4	6.6	3.2	16.6	12.6	7.9	18.2	14.1	9.1
4000	5.2	3.4	1.1	8.2	5.7	2.6	15.3	11.5	6.9	16.9	12.9	8.1
3200	4.2	2.7	0.7	7.1	4.8	2.0	14.0	10.4	6.0	15.6	11.8	7.2
2400	3.2	2.0	0.4	5.7	3.8	1.4	12.4	9.0	5.0	14.0	10.3	6.0
1600	1.9	1.1	0.2	4.0	2.6	0.7	10.1	7.2	3.6	11.6	8.4	4.5
1000	0.8	0.5		2.4	1.5	0.3	7.6	5.2	2.3	9.1	6.3	3.0
800	0.5	0.3		1.8	1.0	0.1	6.5	4.4	1.7	7.9	5.4	2.4
600	0.2	0.1		1.1	0.7		5.2	3.4	1.1	6.5	4.4	1.7
500				0.7	0.5		4.4	2.9	0.8	5.6	3.7	1.3
400				0.4	0.2		3.6	2.2	0.5	4.7	3.0	0.9
300				0.1	0.1		2.6	1.6	0.3	3.5	2.2	0.5
200							1.5	0.9		2.2	1.3	0.2
150							0.8	0.5		1.4	0.8	
100							0.3	0.2		0.6	0.4	
80							0.1	0.1		0.3	0.2	
60										0.1	0.1	

TABLE 10b

Percent Increase of Range Due to Density Effect

Energy	Protons			Kaons			Pions			Muons		
(Mev)	Be	Cu	Pb	Be	Cu	Pb	Be	Cu	Pb	Be	Cu	Pb
5000	3.3	2.1	0.6	5.5	3.7	1.4	11.1	8.1	4.4	12.5	9.2	5.3
4000	2.7	1.7	0.4	4.7	3.1	1.1	10.0	7.2	3.8	11.4	8.3	4.6
3200	2.1	1.3	0.2	3.9	2.5	0.8	9.0	6.3	3.2	10.3	7.4	3.9
2400	1.5	0.9	0.1	3.0	1.9	0.5	7.7	5.3	2.5	8.9	6.3	3.1
1600	0.8	0.5		2.0	1.2	0.2	6.0	4.0	1.7	7.1	4.9	2.2
1000	0.3	0.2		1.0	0.6		4.2	2.8	0.9	5.2	3.5	1.3
800	0.1	0.1		0.7	0.4		3.5	2.3	0.7	4.4	2.9	1.0
600				0.4	0.2		2.7	1.7	0.4	3.5	2.2	0.6
500				0.2	0.1		2.2	1.4	0.3	3.0	1.9	0.5
400				0.1			1.7	1.0	0.2	2.4	1.5	0.3
300							1.2	0.7	0.1	1.7	1.0	0.2
200							0.6	0.3		0.9	0.6	
150							0.3	0.2		0.5	0.3	
100							0.1	0.1		0.2	0.1	
80										0.1	0.1	

References

1. S. K. Allison and S. D. Warshaw, Rev. Mod. Phys. 25, 779 (1953).

2. Ward Whaling, in "Encyclopedia of Physics," 34 (1), 193 (S. Fluegge, ed., Springer-Verlag, Berlin, 1958).

3. L. C. Northcliffe, Paper No. 8 and Appendix B of the present volume.

4. Walter H. Barkas, "Nuclear Research Emulsions" (Academic Press, New York, 1963).

5. U. Fano, Ann. Rev. Nucl. Sci. 13 (1963). Reprinted as Appendix A of the present volume.

6. R. M. Sternheimer, Phys. Rev. 88, 851 (1952); 91, 256 (1953); and 103, 511 (1956).

7. N. Bohr, Kgl. Danske Videnskab. Selskab. Mat.-Fys. Medd. 18 (8), (1948).

8. J. Lindhard and M. Scharff, Kgl. Danske Videnskab. Selskab Mat.-Fys. Medd. 27 (15), (1953).

9. M. C. Walske, Phys. Rev. 88, 1283 (1952); 101, 940 (1956).

10. H. W. Lewis, Phys. Rev. 85, 20 (1952).

11. U. Fano, Phys. Rev. 92, 328 (1953).

12. Walter H. Barkas, John N. Dyer, and Harry H. Heckman, Phys. Rev. Lett. 11, 26 (1963).

13. W. H. Barkas, Phys. Rev. 89, 1019 (1953).

14. H. H. Heckman, B. L. Perkins, W. G. Simon, F. M. Smith, and W. H. Barkas, Phys. Rev. 117, 544 (1960).

15. W. H. Barkas, W. Birnbaum, and F. M. Smith, Phys. Rev. 101, 778 (1956); H. H. Heckman, F. M. Smith, and W. H. Barkas, Nuovo Cimento 3, 85 (1956).

16. W. H. Barkas and H. Tyren, Phys. Rev. 89, 1 (1953).

17. R. W. Deutsch, Phys. Rev. 97, 1110 (1955).

18. L. E. Bailey, Univ. California Radiation Laboratory Report UCRL-3334 (March 1956).

19. J. N. Dyer, W. H. Barkas, H. H. Heckman, C. J. Mason, N. A. Nickols, and F. M. Smith, Bull. Am. Phys. Soc. 5, 224 (1960).

20. W. E. Slater, Nuovo Cimento Suppl. 10, 1 (1958).

21. Fred W. Inman, Univ. California Radiation Laboratory Report UCRL-3815 (June 1957).

22. Ronald E. Brown and Nelson Jarmie, Los Alamos Scientific Laboratory Report LA-2156 (1958).

23. S. K. Allison, Paper No. 11 of the present volume.

24. R. M. Sternheimer, in "Nuclear Physics," edited by L. C. L. Yuan and C. S. Wu, (Academic Press, New York, 1961).

25. H. A. Bethe and J. Ashkin, "Experimental Nuclear Physics," pt. 2, vol. 1, edited by E. Segrè (John Wiley and Sons, New York, 1952).

26. E. A. Uehling, Ann. Rev. Nucl. Sci. 4 (1954).

27. Report No. 29, Nuclear Science Series, National Academy of Sciences—National Research Council Publ. 752.

28. W. Brandt, Phys. Rev. 104, 691 (1956); and "Energy Loss and Range of Charged Particles in Compounds," Dupont Report (July 1960).

29. T. J. Thompson, Univ. California Radiation Laboratory Report UCRL-1910 (August 1952).

30. V. P. Zrelov and G. D. Stoletov, J. Exp. Theor. Phys. (USSR). Transl. JETP 9, 461 (1959).

31. B. V. Rybakov, J. Exp. Theor. Phys. (USSR) 28, 651 (1955). Transl. JETP 1, 435 (1955).

32. W. H. Barkas, P. H. Barrett, P. Cüer, H. H. Heckman, F. M. Smith, and H. K. Ticho, Nuovo Cimento 8, 185 (1958).

33. W. H. Barkas and S. von Friesen, Nuovo Cimento Suppl. 19, 41 (1961).

34. W. H. Barkas, Nuovo Cimento 8, 201 (1958).

35. V. C. Burkig and K. R. MacKenzie, Phys. Rev. 106, 848 (1957); see also K. R. MacKenzie (Ref. 27), pp. 13-20.

36. L. P. Nielsen, Kgl. Danske Videnskab. Selskab Mat.-Fys. Medd. 33 (6), (1961).

37. Hans Bichsel, in "American Institute of Physics Handbook," ed. 2, section 8c, (McGraw-Hill, New York, 1963).

38. R. M. Sternheimer, Phys. Rev. 115, 137 (1959). The values of I used in this paper in the calculations for Be, Cu, and Pb are appreciably larger than the currently accepted values, and therefore these tables cannot be used for these elements. Of course, these reservations do not apply for the tables pertaining to C, Al, and air. See also the erratum in Phys. Rev. 124, 2051 (1958) and revised tables for Cu and Pb in "High Energy and Nuclear Physics Handbook" of the Rutherford High Energy Laboratory, Clinton (1963).

39. R. M. Sternheimer, Phys. Rev. 118, 1045 (1960).

40. U. Fano and J. E. Turner, Paper No. 4 of the present volume.

41. M. J. Berger and S. M. Seltzer, Paper No. 5 of this volume.

42. B. Rossi, High Energy Particles (Prentice Hall, New York, 1952).

43. M. J. Berger and S. M. Seltzer, Paper No. 10 of the present volume.

PRINTOUT TABLE I

TWO-VARIABLE STOPPING-POWER TABLE

Calculated stopping power, ι, as a function of the proton kinetic energy T and the mean excitation energy I_{adj}. (Because of typographical limitations, I_{adj} is indicated as I in the table headings. The units of I_{adj} are ev.) The entries, when multiplied by Z/A, give the stopping power in units of Mev/g cm^{-2}. Powers of ten are indicated by the symbol E; thus 1.2345E 02 means 1.2345×10^2. Since energy/mass is a function only of the velocity, the column labeled energy is also to be interpreted as the particle kinetic energy divided by the mass in units of the proton mass. More figures are tabulated than are significant in order to facilitate interpolation.

STOPPING POWER

ENERGY MEV	I= 15.0	I= 17.5	I= 20.0	I= 30.0	I= 40.0	I= 50.0	I= 60.0	I= 70.0	I= 80.0
1.0	7.0488E 02	6.8506E 02	6.6719E 02	6.0975E 02	5.6685E 02	5.3285E 02	5.0483E 02	4.8112E 02	4.6064E 02
2.0	3.9916E 02	3.9212E 02	3.8540E 02	3.6179E 02	3.4254E 02	3.2649E 02	3.1279E 02	3.0088E 02	2.9039E 02
3.0	2.8701E 02	2.8256E 02	2.7827E 02	2.6295E 02	2.5028E 02	2.3962E 02	2.3045E 02	2.2245E 02	2.1537E 02
4.0	2.2742E 02	2.2382E 02	2.2040E 02	2.0839E 02	1.9861E 02	1.9044E 02	1.8344E 02	1.7735E 02	1.7196E 02
5.0	1.8999E 02	1.8675E 02	1.8371E 02	1.7339E 02	1.6519E 02	1.5842E 02	1.5268E 02	1.4771E 02	1.4334E 02
6.0	1.6411E 02	1.6103E 02	1.5820E 02	1.4886E 02	1.4164E 02	1.3579E 02	1.3087E 02	1.2664E 02	1.2293E 02
7.0	1.4505E 02	1.4204E 02	1.3934E 02	1.3064E 02	1.2410E 02	1.1887E 02	1.1453E 02	1.1082E 02	1.0759E 02
8.0	1.2929E 02	1.2639E 02	1.2385E 02	1.1598E 02	1.1029E 02	1.0582E 02	1.0215E 02	9.9029E 01	9.6322E 01
9.0	1.1604E 02	1.1353E 02	1.1134E 02	1.0468E 02	9.9918E 01	9.6204E 01	9.3153E 01	9.0560E 01	8.8302E 01
10.0	1.0614E 02	1.0387E 02	1.0191E 02	9.5902E 01	9.1615E 01	8.8272E 01	8.5526E 01	8.3193E 01	8.1162E 01
12.0	9.0951E 01	8.9058E 01	8.7415E 01	8.2404E 01	7.8829E 01	7.6043E 01	7.3755E 01	7.1813E 01	7.0122E 01
14.0	7.9816E 01	7.8189E 01	7.6777E 01	7.2474E 01	6.9407E 01	6.7017E 01	6.5057E 01	6.3392E 01	6.1944E 01
16.0	7.1279E 01	6.9852E 01	6.8613E 01	6.4841E 01	6.2153E 01	6.0060E 01	5.8344E 01	5.6887E 01	5.5620E 01
18.0	6.4515E 01	6.3242E 01	6.2138E 01	5.8777E 01	5.6384E 01	5.4521E 01	5.2994E 01	5.1698E 01	5.0572E 01
20.0	5.9014E 01	5.7866E 01	5.6870E 01	5.3837E 01	5.1679E 01	5.0000E 01	4.8623E 01	4.7456E 01	4.6441E 01
22.0	5.4449E 01	5.3402E 01	5.2494E 01	4.9730E 01	4.7764E 01	4.6234E 01	4.4980E 01	4.3918E 01	4.2994E 01
24.0	5.0596E 01	4.9633E 01	4.8798E 01	4.6258E 01	4.4451E 01	4.3046E 01	4.1895E 01	4.0919E 01	4.0071E 01
26.0	4.7298E 01	4.6406E 01	4.5634E 01	4.3283E 01	4.1611E 01	4.0311E 01	3.9246E 01	3.8343E 01	3.7559E 01
28.0	4.4441E 01	4.3611E 01	4.2891E 01	4.0702E 01	3.9146E 01	3.7936E 01	3.6945E 01	3.6105E 01	3.5376E 01
30.0	4.1942E 01	4.1165E 01	4.0491E 01	3.8442E 01	3.6986E 01	3.5854E 01	3.4926E 01	3.4141E 01	3.3459E 01
32.0	3.9735E 01	3.9005E 01	3.8371E 01	3.6445E 01	3.5076E 01	3.4012E 01	3.3141E 01	3.2403E 01	3.1762E 01
34.0	3.7773E 01	3.7083E 01	3.6485E 01	3.4667E 01	3.3375E 01	3.2371E 01	3.1549E 01	3.0853E 01	3.0248E 01
36.0	3.6015E 01	3.5362E 01	3.4796E 01	3.3074E 01	3.1850E 01	3.0899E 01	3.0121E 01	2.9462E 01	2.8889E 01
38.0	3.4432E 01	3.3811E 01	3.3273E 01	3.1637E 01	3.0474E 01	2.9571E 01	2.8832E 01	2.8205E 01	2.7662E 01
40.0	3.2997E 01	3.2405E 01	3.1893E 01	3.0334E 01	2.9227E 01	2.8366E 01	2.7662E 01	2.7066E 01	2.6548E 01
42.0	3.1691E 01	3.1126E 01	3.0636E 01	2.9147E 01	2.8090E 01	2.7268E 01	2.6595E 01	2.6026E 01	2.5532E 01
44.0	3.0497E 01	2.9956E 01	2.9487E 01	2.8062E 01	2.7049E 01	2.6262E 01	2.5619E 01	2.5074E 01	2.4601E 01
46.0	2.9400E 01	2.8881E 01	2.8431E 01	2.7064E 01	2.6093E 01	2.5338E 01	2.4721E 01	2.4198E 01	2.3745E 01
48.0	2.8390E 01	2.7891E 01	2.7459E 01	2.6145E 01	2.5211E 01	2.4486E 01	2.3893E 01	2.3391E 01	2.2955E 01
50.0	2.7456E 01	2.6976E 01	2.6559E 01	2.5294E 01	2.4395E 01	2.3697E 01	2.3126E 01	2.2643E 01	2.2223E 01
55.0	2.5402E 01	2.4962E 01	2.4581E 01	2.3422E 01	2.2599E 01	2.1960E 01	2.1438E 01	2.0995E 01	2.0611E 01
60.0	2.3673E 01	2.3266E 01	2.2914E 01	2.1844E 01	2.1085E 01	2.0495E 01	2.0012E 01	1.9604E 01	1.9249E 01
65.0	2.2196E 01	2.1818E 01	2.1490E 01	2.0496E 01	1.9789E 01	1.9241E 01	1.8792E 01	1.8413E 01	1.8083E 01
70.0	2.0919E 01	2.0565E 01	2.0259E 01	1.9329E 01	1.8668E 01	1.8155E 01	1.7736E 01	1.7381E 01	1.7073E 01
75.0	1.9804E 01	1.9472E 01	1.9184E 01	1.8309E 01	1.7688E 01	1.7206E 01	1.6812E 01	1.6478E 01	1.6189E 01
80.0	1.8822E 01	1.8508E 01	1.8236E 01	1.7410E 01	1.6824E 01	1.6368E 01	1.5996E 01	1.5681E 01	1.5408E 01
85.0	1.7949E 01	1.7652E 01	1.7394E 01	1.6611E 01	1.6055E 01	1.5624E 01	1.5271E 01	1.4973E 01	1.4714E 01
90.0	1.7169E 01	1.6887E 01	1.6641E 01	1.5897E 01	1.5368E 01	1.4957E 01	1.4622E 01	1.4338E 01	1.4092E 01
95.0	1.6468E 01	1.6198E 01	1.5964E 01	1.5253E 01	1.4749E 01	1.4357E 01	1.4037E 01	1.3766E 01	1.3532E 01
100.0	1.5833E 01	1.5575E 01	1.5351E 01	1.4671E 01	1.4189E 01	1.3814E 01	1.3508E 01	1.3249E 01	1.3024E 01
105.0	1.5257E 01	1.5009E 01	1.4794E 01	1.4142E 01	1.3679E 01	1.3320E 01	1.3026E 01	1.2778E 01	1.2562E 01
110.0	1.4730E 01	1.4492E 01	1.4285E 01	1.3659E 01	1.3214E 01	1.2868E 01	1.2586E 01	1.2347E 01	1.2140E 01
115.0	1.4247E 01	1.4018E 01	1.3819E 01	1.3215E 01	1.2787E 01	1.2454E 01	1.2182E 01	1.1952E 01	1.1753E 01
120.0	1.3803E 01	1.3582E 01	1.3390E 01	1.2807E 01	1.2394E 01	1.2073E 01	1.1810E 01	1.1588E 01	1.1396E 01
125.0	1.3393E 01	1.3179E 01	1.2993E 01	1.2430E 01	1.2031E 01	1.1720E 01	1.1467E 01	1.1252E 01	1.1066E 01
130.0	1.3013E 01	1.2806E 01	1.2626E 01	1.2081E 01	1.1694E 01	1.1394E 01	1.1148E 01	1.0941E 01	1.0761E 01
135.0	1.2660E 01	1.2460E 01	1.2285E 01	1.1757E 01	1.1382E 01	1.1090E 01	1.0852E 01	1.0651E 01	1.0477E 01
140.0	1.2332E 01	1.2137E 01	1.1968E 01	1.1455E 01	1.1090E 01	1.0808E 01	1.0577E 01	1.0381E 01	1.0212E 01
145.0	1.2025E 01	1.1836E 01	1.1671E 01	1.1173E 01	1.0819E 01	1.0544E 01	1.0319E 01	1.0129E 01	9.9645E 00
150.0	1.1738E 01	1.1554E 01	1.1394E 01	1.0909E 01	1.0564E 01	1.0297E 01	1.0078E 01	9.8932E 00	9.7329E 00
155.0	1.1469E 01	1.1290E 01	1.1134E 01	1.0661E 01	1.0325E 01	1.0065E 01	9.8518E 00	9.6717E 00	9.5156E 00
160.0	1.1217E 01	1.1041E 01	1.0889E 01	1.0428E 01	1.0101E 01	9.8468E 00	9.6391E 00	9.4635E 00	9.3113E 00
165.0	1.0979E 01	1.0808E 01	1.0659E 01	1.0209E 01	9.8895E 00	9.6415E 00	9.4389E 00	9.2674E 00	9.1189E 00
170.0	1.0754E 01	1.0587E 01	1.0442E 01	1.0002E 01	9.6902E 00	9.4479E 00	9.2499E 00	9.0824E 00	8.9373E 00
175.0	1.0542E 01	1.0379E 01	1.0237E 01	9.8071E 00	9.5018E 00	9.2650E 00	9.0714E 00	8.9076E 00	8.7657E 00
180.0	1.0342E 01	1.0182E 01	1.0043E 01	9.6223E 00	9.3236E 00	9.0918E 00	8.9024E 00	8.7421E 00	8.6033E 00
185.0	1.0152E 01	9.9952E 00	9.8595E 00	9.4473E 00	9.1547E 00	8.9277E 00	8.7422E 00	8.5853E 00	8.4493E 00
190.0	9.9716E 00	9.8181E 00	9.6851E 00	9.2811E 00	8.9944E 00	8.7720E 00	8.5902E 00	8.4364E 00	8.3031E 00
195.0	9.8004E 00	9.6498E 00	9.5194E 00	9.1232E 00	8.8421E 00	8.6240E 00	8.4457E 00	8.2949E 00	8.1642E 00
200.0	9.6375E 00	9.4897E 00	9.3618E 00	8.9731E 00	8.6972E 00	8.4832E 00	8.3082E 00	8.1603E 00	8.0321E 00
210.0	9.3344E 00	9.1919E 00	9.0685E 00	8.6936E 00	8.4275E 00	8.2211E 00	8.0524E 00	7.9097E 00	7.7860E 00
220.0	9.0584E 00	8.9206E 00	8.8013E 00	8.4389E 00	8.1817E 00	7.9822E 00	7.8191E 00	7.6812E 00	7.5617E 00
230.0	8.8059E 00	8.6725E 00	8.5569E 00	8.2059E 00	7.9569E 00	7.7636E 00	7.6057E 00	7.4721E 00	7.3564E 00
240.0	8.5741E 00	8.4446E 00	8.3325E 00	7.9920E 00	7.7504E 00	7.5629E 00	7.4097E 00	7.2801E 00	7.1678E 00
250.0	8.3605E 00	8.2348E 00	8.1258E 00	7.7949E 00	7.5601E 00	7.3779E 00	7.2291E 00	7.1031E 00	6.9940E 00
260.0	8.1632E 00	8.0408E 00	7.9348E 00	7.6128E 00	7.3843E 00	7.2070E 00	7.0621E 00	6.9396E 00	6.8334E 00
270.0	7.9804E 00	7.8611E 00	7.7578E 00	7.4440E 00	7.2213E 00	7.0485E 00	6.9073E 00	6.7879E 00	6.6845E 00
280.0	7.8106E 00	7.6942E 00	7.5933E 00	7.2871E 00	7.0698E 00	6.9013E 00	6.7635E 00	6.6470E 00	6.5460E 00
290.0	7.6524E 00	7.5387E 00	7.4402E 00	7.1410E 00	6.9288E 00	6.7641E 00	6.6295E 00	6.5157E 00	6.4171E 00
300.0	7.5047E 00	7.3935E 00	7.2972E 00	7.0047E 00	6.7971E 00	6.6360E 00	6.5044E 00	6.3931E 00	6.2967E 00
310.0	7.3666E 00	7.2577E 00	7.1634E 00	6.8771E 00	6.6738E 00	6.5162E 00	6.3874E 00	6.2784E 00	6.1840E 00
320.0	7.2371E 00	7.1304E 00	7.0380E 00	6.7574E 00	6.5583E 00	6.4039E 00	6.2776E 00	6.1709E 00	6.0784E 00
330.0	7.1155E 00	7.0109E 00	6.9203E 00	6.6451E 00	6.4498E 00	6.2984E 00	6.1746E 00	6.0699E 00	5.9792E 00
340.0	7.0012E 00	6.8985E 00	6.8095E 00	6.5394E 00	6.3478E 00	6.1991E 00	6.0776E 00	5.9748E 00	5.8858E 00
350.0	6.8934E 00	6.7925E 00	6.7052E 00	6.4399E 00	6.2516E 00	6.1056E 00	5.9862E 00	5.8853E 00	5.7979E 00
360.0	6.7917E 00	6.6926E 00	6.6067E 00	6.3459E 00	6.1609E 00	6.0173E 00	5.9000E 00	5.8008E 00	5.7148E 00
370.0	6.6956E 00	6.5981E 00	6.5136E 00	6.2571E 00	6.0751E 00	5.9339E 00	5.8185E 00	5.7209E 00	5.6364E 00
380.0	6.6046E 00	6.5087E 00	6.4255E 00	6.1731E 00	5.9939E 00	5.8549E 00	5.7414E 00	5.6453E 00	5.5621E 00
390.0	6.5184E 00	6.4239E 00	6.3420E 00	6.0934E 00	5.9170E 00	5.7801E 00	5.6683E 00	5.5737E 00	5.4918E 00
400.0	6.4367E 00	6.3435E 00	6.2629E 00	6.0179E 00	5.8440E 00	5.7091E 00	5.5989E 00	5.5057E 00	5.4250E 00

STOPPING POWER

ENERGY MEV	I= 15.0	I= 17.5	I= 20.0	I= 30.0	I= 40.0	I= 50.0	I= 60.0	I= 70.0	I= 80.0
410.0	6.3590E 00	6.2672E 00	6.1876E 00	5.9461E 00	5.7747E 00	5.6417E 00	5.5331E 00	5.4412E 00	5.3616E 00
420.0	6.2851E 00	6.1946E 00	6.1161E 00	5.8778E 00	5.7088E 00	5.5776E 00	5.4704E 00	5.3798E 00	5.3013E 00
430.0	6.2148E 00	6.1254E 00	6.0480E 00	5.8129E 00	5.6460E 00	5.5166E 00	5.4108E 00	5.3214E 00	5.2439E 00
440.0	6.1478E 00	6.0596E 00	5.9831E 00	5.7510E 00	5.5862E 00	5.4584C 00	5.3540E 00	5.2657E 00	5.1892E 00
450.0	6.0839E 00	5.9968E 00	5.9212E 00	5.6919E 00	5.5292E 00	5.4030E 00	5.2998E 00	5.2126E 00	5.1371E 00
460.0	6.0229E 00	5.9368E 00	5.8622E 00	5.6356E 00	5.4748E 00	5.3501E 00	5.2481E 00	5.1619E 00	5.0873E 00
470.0	5.9646E 00	5.8795E 00	5.8057E 00	5.5817E 00	5.4228E 00	5.2995C 00	5.1987E 00	5.1135E 00	5.0397E 00
480.0	5.9089E 00	5.8247E 00	5.7517E 00	5.5302E 00	5.3730E 00	5.2511E 00	5.1515E 00	5.0672E 00	4.9942E 00
490.0	5.8555E 00	5.7722E 00	5.7001E 00	5.4809E 00	5.3255E 00	5.2048E 00	5.1063E 00	5.0229E 00	4.9507E 00
500.0	5.8044E 00	5.7220E 00	5.6506E 00	5.4338E 00	5.2799E 00	5.1605E 00	5.0630E 00	4.9805E 00	4.9091E 00
510.0	5.7555E 00	5.6739E 00	5.6032E 00	5.3885E 00	5.2362E 00	5.1180E 00	5.0215E 00	4.9399E 00	4.8691E 00
520.0	5.7085E 00	5.6277E 00	5.5577E 00	5.3451E 00	5.1943E 00	5.0773E 00	4.9817E 00	4.9009E 00	4.8308E 00
530.0	5.6634E 00	5.5834E 00	5.5140E 00	5.3035E 00	5.1541E 00	5.0382E 00	4.9435E 00	4.8635E 00	4.7941E 00
540.0	5.6201E 00	5.5408E 00	5.4721E 00	5.2635E 00	5.1155E 00	5.0007E 00	4.9069E 00	4.8275E 00	4.7588E 00
550.0	5.5785E 00	5.4999E 00	5.4318E 00	5.2251E 00	5.0784E 00	4.9646E 00	4.8716E 00	4.7930E 00	4.7249E 00
560.0	5.5385E 00	5.4606E 00	5.3931E 00	5.1882E 00	5.0427E 00	4.9300E 00	4.8378E 00	4.7598E 00	4.6923E 00
570.0	5.5000E 00	5.4227E 00	5.3558E 00	5.1526E 00	5.0084E 00	4.8966E 00	4.8052E 00	4.7279E 00	4.6610E 00
580.0	5.4629E 00	5.3863E 00	5.3199E 00	5.1184E 00	4.9754E 00	4.8645E 00	4.7739E 00	4.6972E 00	4.6308E 00
590.0	5.4272E 00	5.3512E 00	5.2854E 00	5.0855E 00	4.9436E 00	4.8336E 00	4.7437E 00	4.6676E 00	4.6018E 00
600.0	5.3928E 00	5.3174E 00	5.2521E 00	5.0537E 00	4.9130E 00	4.8038E 00	4.7146E 00	4.6391E 00	4.5738E 00
610.0	5.3596E 00	5.2848E 00	5.2200E 00	5.0231E 00	4.8834E 00	4.7751E 00	4.6866E 00	4.6117E 00	4.5468E 00
620.0	5.3276E 00	5.2534E 00	5.1890E 00	4.9936E 00	4.8550E 00	4.7474E 00	4.6595E 00	4.5852E 00	4.5208E 00
630.0	5.2968E 00	5.2230E 00	5.1591E 00	4.9651E 00	4.8275E 00	4.7207E 00	4.6334E 00	4.5597E 00	4.4957E 00
640.0	5.2670E 00	5.1937E 00	5.1303E 00	4.9376E 00	4.8009E 00	4.6949E 00	4.6083E 00	4.5350E 00	4.4715E 00
650.0	5.2382E 00	5.1654E 00	5.1024E 00	4.9111E 00	4.7753E 00	4.6700E 00	4.5840E 00	4.5112E 00	4.4482E 00
660.0	5.2103E 00	5.1381E 00	5.0755E 00	4.8854E 00	4.7506E 00	4.6460E 00	4.5605E 00	4.4882E 00	4.4256E 00
670.0	5.1834E 00	5.1116E 00	5.0495E 00	4.8606E 00	4.7267E 00	4.6227E 00	4.5378E 00	4.4660E 00	4.4038E 00
680.0	5.1574E 00	5.0861E 00	5.0243E 00	4.8367E 00	4.7035E 00	4.6002E 00	4.5159E 00	4.4445E 00	4.3827E 00
690.0	5.1323E 00	5.0614E 00	5.0000E 00	4.8135E 00	4.6812E 00	4.5785E 00	4.4946E 00	4.4237E 00	4.3623E 00
700.0	5.1079E 00	5.0374E 00	4.9764E 00	4.7910E 00	4.6595E 00	4.5575E 00	4.4741E 00	4.4036E 00	4.3426E 00
710.0	5.0843E 00	5.0143E 00	4.9536E 00	4.7693E 00	4.6386E 00	4.5371E 00	4.4543E 00	4.3842E 00	4.3235E 00
720.0	5.0615E 00	4.9918E 00	4.9315E 00	4.7483E 00	4.6183E 00	4.5174E 00	4.4350E 00	4.3654E 00	4.3050E 00
730.0	5.0394E 00	4.9701E 00	4.9101E 00	4.7279E 00	4.5986E 00	4.4984E 00	4.4164E 00	4.3472E 00	4.2871E 00
740.0	5.0179E 00	4.9490E 00	4.8894E 00	4.7082E 00	4.5796E 00	4.4799E 00	4.3984E 00	4.3295E 00	4.2698E 00
750.0	4.9971E 00	4.9286E 00	4.8693E 00	4.6891E 00	4.5612E 00	4.4620E 00	4.3809E 00	4.3124E 00	4.2530E 00
760.0	4.9770E 00	4.9088E 00	4.8498E 00	4.6705E 00	4.5433C 00	4.4446E 00	4.3640E 00	4.2958E 00	4.2368E 00
770.0	4.9574E 00	4.8896E 00	4.8309E 00	4.6525E 00	4.5260E 00	4.4278E 00	4.3476E 00	4.2798E 00	4.2210E 00
780.0	4.9385E 00	4.8710E 00	4.8126E 00	4.6351E 00	4.5092E 00	4.4115E 00	4.3317E 00	4.2642E 00	4.2057E 00
790.0	4.9201E 00	4.8529E 00	4.7948E 00	4.6182E 00	4.4929E 00	4.3956E 00	4.3162E 00	4.2491E 00	4.1909E 00
800.0	4.9022E 00	4.8354E 00	4.7775E 00	4.6017E 00	4.4770E 00	4.3803E 00	4.3012E 00	4.2344E 00	4.1765E 00
810.0	4.8849E 00	4.8184E 00	4.7607E 00	4.5858E 00	4.4617E 00	4.3654E 00	4.2867E 00	4.2202E 00	4.1625E 00
820.0	4.8680E 00	4.8018E 00	4.7445E 00	4.5703E 00	4.4467E 00	4.3509E 00	4.2726E 00	4.2064E 00	4.1490E 00
830.0	4.8516E 00	4.7857E 00	4.7286E 00	4.5553E 00	4.4323E 00	4.3368E 00	4.2589E 00	4.1929E 00	4.1358E 00
840.0	4.8357E 00	4.7701E 00	4.7133E 00	4.5407E 00	4.4182E 00	4.3232E 00	4.2456E 00	4.1799E 00	4.1231E 00
850.0	4.8203E 00	4.7549E 00	4.6983E 00	4.5265E 00	4.4045E 00	4.3099E 00	4.2326E 00	4.1673E 00	4.1107E 00
860.0	4.8053E 00	4.7402E 00	4.6838E 00	4.5127E 00	4.3912E 00	4.2970E 00	4.2201E 00	4.1550E 00	4.0986E 00
870.0	4.7906E 00	4.7258E 00	4.6697E 00	4.4993E 00	4.3783E 00	4.2845E 00	4.2079E 00	4.1431E 00	4.0869E 00
880.0	4.7764E 00	4.7119E 00	4.6560E 00	4.4862E 00	4.3658E 00	4.2723E 00	4.1960E 00	4.1314E 00	4.0755E 00
890.0	4.7626E 00	4.6983E 00	4.6426E 00	4.4736E 00	4.3536E 00	4.2605E 00	4.1845E 00	4.1202E 00	4.0645E 00
900.0	4.7492E 00	4.6851E 00	4.6297E 00	4.4612E 00	4.3417E 00	4.2490E 00	4.1732E 00	4.1092E 00	4.0537E 00
910.0	4.7361E 00	4.6723E 00	4.6170E 00	4.4492E 00	4.3302E 00	4.2378E 00	4.1623E 00	4.0985E 00	4.0433E 00
920.0	4.7233E 00	4.6598E 00	4.6047E 00	4.4375E 00	4.3189E 00	4.2269E 00	4.1517E 00	4.0882E 00	4.0331E 00
930.0	4.7109E 00	4.6476E 00	4.5928E 00	4.4262E 00	4.3080E 00	4.2163E 00	4.1414E 00	4.0781E 00	4.0232E 00
940.0	4.6989E 00	4.6358E 00	4.5811E 00	4.4151E 00	4.2974E 00	4.2060E 00	4.1314E 00	4.0683E 00	4.0136E 00
950.0	4.6871E 00	4.6242E 00	4.5697E 00	4.4044E 00	4.2870E 00	4.1960E 00	4.1216E 00	4.0587E 00	4.0042E 00
960.0	4.6756E 00	4.6130E 00	4.5587E 00	4.3939E 00	4.2769E 00	4.1862E 00	4.1121E 00	4.0494E 00	3.9951E 00
970.0	4.6645E 00	4.6020E 00	4.5479E 00	4.3837E 00	4.2671E 00	4.1767E 00	4.1028E 00	4.0404E 00	3.9863E 00
980.0	4.6536E 00	4.5914E 00	4.5374E 00	4.3737E 00	4.2576E 00	4.1674E 00	4.0938E 00	4.0316E 00	3.9776E 00
990.0	4.6430E 00	4.5810E 00	4.5272E 00	4.3640E 00	4.2482E 00	4.1584E 00	4.0850E 00	4.0230E 00	3.9692E 00
1000.0	4.6327E 00	4.5709E 00	4.5173E 00	4.3546E 00	4.2392E 00	4.1496E 00	4.0765E 00	4.0146E 00	3.9610E 00
1100.0	4.5426E 00	4.4825E 00	4.4305E 00	4.2724E 00	4.1603E 00	4.0733E 00	4.0022E 00	3.9421E 00	3.8901E 00
1200.0	4.4720E 00	4.4134E 00	4.3626E 00	4.2083E 00	4.0989E 00	4.0140E 00	3.9446E 00	3.8859E 00	3.8351E 00
1300.0	4.4162E 00	4.3588E 00	4.3090E 00	4.1579E 00	4.0507E 00	3.9675E 00	3.8996E 00	3.8421E 00	3.7924E 00
1400.0	4.3719E 00	4.3155E 00	4.2666E 00	4.1181E 00	4.0128E 00	3.9311E 00	3.8643E 00	3.8079E 00	3.7590E 00
1500.0	4.3366E 00	4.2810E 00	4.2329E 00	4.0867E 00	3.9829E 00	3.9025E 00	3.8367E 00	3.7811E 00	3.7330E 00
1600.0	4.3084E 00	4.2536E 00	4.2061E 00	4.0618E 00	3.9594E 00	3.8800E 00	3.8152E 00	3.7603E 00	3.7128E 00
1800.0	4.2683E 00	4.2147E 00	4.1682E 00	4.0271E 00	3.9269E 00	3.8493E 00	3.7858E 00	3.7322E 00	3.6857E 00
2000.0	4.2438E 00	4.1911E 00	4.1454E 00	4.0067E 00	3.9083E 00	3.8320E 00	3.7696E 00	3.7169E 00	3.6712E 00
2200.0	4.2301E 00	4.1781E 00	4.1330E 00	3.9962E 00	3.8992E 00	3.8239E 00	3.7624E 00	3.7104E 00	3.6654E 00
2400.0	4.2239E 00	4.1725E 00	4.1279E 00	3.9927E 00	3.8967E 00	3.8223E 00	3.7615E 00	3.7101E 00	3.6655E 00
2600.0	4.2231E 00	4.1722E 00	4.1281E 00	3.9941E 00	3.8990E 00	3.8253E 00	3.7651E 00	3.7141E 00	3.6700E 00
2800.0	4.2264E 00	4.1758E 00	4.1320E 00	3.9991E 00	3.9048E 00	3.8316E 00	3.7719E 00	3.7213E 00	3.6776E 00
3000.0	4.2325E 00	4.1823E 00	4.1388E 00	4.0068E 00	3.9131E 00	3.8404E 00	3.7810E 00	3.7308E 00	3.6873E 00
3200.0	4.2408E 00	4.1909E 00	4.1476E 00	4.0163E 00	3.9232E 00	3.8509E 00	3.7919E 00	3.7419E 00	3.6987E 00
3400.0	4.2507E 00	4.2010E 00	4.1580E 00	4.0273E 00	3.9346E 00	3.8627E 00	3.8039E 00	3.7543E 00	3.7112E 00
3600.0	4.2618E 00	4.2123E 00	4.1695E 00	4.0393E 00	3.9470E 00	3.8754E 00	3.8169E 00	3.7674E 00	3.7246E 00
3800.0	4.2737E 00	4.2244E 00	4.1818E 00	4.0521E 00	3.9601E 00	3.8888E 00	3.8305E 00	3.7812E 00	3.7385E 00
4000.0	4.2863E 00	4.2372E 00	4.1946E 00	4.0654E 00	3.9737E 00	3.9026E 00	3.8445E 00	3.7954E 00	3.7528E 00
4500.0	4.3195E 00	4.2707E 00	4.2284E 00	4.1000E 00	4.0090E 00	3.9383E 00	3.8806E 00	3.8318E 00	3.7895E 00
5000.0	4.3537E 00	4.3051E 00	4.2630E 00	4.1353E 00	4.0447E 00	3.9744E 00	3.9169E 00	3.8684E 00	3.8263E 00

STOPPING POWER

ENERGY MEV	I= 90.0	I= 100.0	I= 120.0	I= 140.0	I= 160.0	I= 180.0	I= 200.0	I= 220.0	I= 240.0
1.0	4.4266E 02	4.2670E 02	3.9939E 02	3.7672E 02	3.5743E 02	3.4074E 02	3.2609E 02	3.1308E 02	3.0140E 02
2.0	2.8102E 02	2.7258E 02	2.5790E 02	2.4548E 02	2.3475E 02	2.2535E 02	2.1701E 02	2.0953E 02	2.0276E 02
3.0	2.0902E 02	2.0328E 02	1.9326E 02	1.8473E 02	1.7734E 02	1.7084E 02	1.6505E 02	1.5984E 02	1.5512E 02
4.0	1.6714E 02	1.6278E 02	1.5518E 02	1.4871E 02	1.4310E 02	1.3816E 02	1.3376E 02	1.2980E 02	1.2621E 02
5.0	1.3943E 02	1.3591E 02	1.2979E 02	1.2459E 02	1.2008E 02	1.1613E 02	1.1260E 02	1.0943E 02	1.0655E 02
6.0	1.1964E 02	1.1668E 02	1.1154E 02	1.0720E 02	1.0345E 02	1.0016E 02	9.7237E 01	9.4607E 01	9.2224E 01
7.0	1.0473E 02	1.0218E 02	9.7755E 01	9.4033E 01	9.0830E 01	8.8024E 01	8.5534E 01	8.3300E 01	8.1277E 01
8.0	9.3931E 01	9.1791E 01	8.8086E 01	8.4956E 01	8.2246E 01	7.9887E 01	7.7785E 01	7.5886E 01	7.4156E 01
9.0	8.6301E 01	8.4503E 01	8.1370E 01	7.8700E 01	7.6368E 01	7.4343E 01	7.2527E 01	7.0872E 01	6.9354E 01
10.0	7.9363E 01	7.7745E 01	7.4929E 01	7.2528E 01	7.0432E 01	6.8610E 01	6.6974E 01	6.5485E 01	6.4117E 01
12.0	6.8625E 01	6.7280E 01	6.4938E 01	6.2941E 01	6.1198E 01	5.9679E 01	5.8314E 01	5.7070E 01	5.5927E 01
14.0	6.0662E 01	5.9511E 01	5.7506E 01	5.5798E 01	5.4306E 01	5.3003E 01	5.1832E 01	5.0764E 01	4.9782E 01
16.0	5.4499E 01	5.3492E 01	5.1740E 01	5.0246E 01	4.8943E 01	4.7802E 01	4.6776E 01	4.5840E 01	4.4980E 01
18.0	4.9575E 01	4.8680E 01	4.7122E 01	4.5796E 01	4.4638E 01	4.3623E 01	4.2710E 01	4.1878E 01	4.1113E 01
20.0	4.5543E 01	4.4737E 01	4.3335E 01	4.2142E 01	4.1100E 01	4.0186E 01	3.9363E 01	3.8614E 01	3.7925E 01
22.0	4.2177E 01	4.1444E 01	4.0169E 01	3.9083E 01	3.8136E 01	3.7304E 01	3.6556E 01	3.5874E 01	3.5247E 01
24.0	3.9321E 01	3.8648E 01	3.7479E 01	3.6483E 01	3.5614E 01	3.4851E 01	3.4164E 01	3.3539E 01	3.2964E 01
26.0	3.6866E 01	3.6244E 01	3.5163E 01	3.4243E 01	3.3441E 01	3.2735E 01	3.2101E 01	3.1523E 01	3.0991E 01
28.0	3.4731E 01	3.4152E 01	3.3147E 01	3.2292E 01	3.1546E 01	3.0890E 01	3.0300E 01	2.9763E 01	2.9269E 01
30.0	3.2856E 01	3.2315E 01	3.1375E 01	3.0576E 01	2.9879E 01	2.9266E 01	2.8714E 01	2.8212E 01	2.7751E 01
32.0	3.1195E 01	3.0687E 01	2.9804E 01	2.9054E 01	2.8400E 01	2.7824E 01	2.7307E 01	2.6835E 01	2.6402E 01
34.0	2.9714E 01	2.9235E 01	2.8402E 01	2.7695E 01	2.7078E 01	2.6536E 01	2.6048E 01	2.5604E 01	2.5195E 01
36.0	2.8383E 01	2.7930E 01	2.7142E 01	2.6473E 01	2.5890E 01	2.5376E 01	2.4915E 01	2.4495E 01	2.4109E 01
38.0	2.7182E 01	2.6751E 01	2.6003E 01	2.5368E 01	2.4815E 01	2.4327E 01	2.3889E 01	2.3491E 01	2.3125E 01
40.0	2.6091E 01	2.5680E 01	2.4969E 01	2.4364E 01	2.3837E 01	2.3373E 01	2.2956E 01	2.2577E 01	2.2229E 01
42.0	2.5095E 01	2.4704E 01	2.4024E 01	2.3447E 01	2.2945E 01	2.2502E 01	2.2104E 01	2.1742E 01	2.1410E 01
44.0	2.4183E 01	2.3809E 01	2.3158E 01	2.2606E 01	2.2126E 01	2.1702E 01	2.1322E 01	2.0976E 01	2.0658E 01
46.0	2.3344E 01	2.2985E 01	2.2362E 01	2.1833E 01	2.1372E 01	2.0966E 01	2.0601E 01	2.0270E 01	1.9965E 01
48.0	2.2570E 01	2.2225E 01	2.1626E 01	2.1118E 01	2.0675E 01	2.0285E 01	1.9935E 01	1.9617E 01	1.9325E 01
50.0	2.1853E 01	2.1521E 01	2.0945E 01	2.0456E 01	2.0030E 01	1.9655E 01	1.9318E 01	1.9012E 01	1.8731E 01
55.0	2.0272E 01	1.9968E 01	1.9441E 01	1.8994E 01	1.8605E 01	1.8262E 01	1.7954E 01	1.7674E 01	1.7417E 01
60.0	1.8937E 01	1.8656E 01	1.8170E 01	1.7757E 01	1.7399E 01	1.7082E 01	1.6798E 01	1.6540E 01	1.6304E 01
65.0	1.7792E 01	1.7532E 01	1.7080E 01	1.6697E 01	1.6364E 01	1.6070E 01	1.5806E 01	1.5567E 01	1.5347E 01
70.0	1.6801E 01	1.6558E 01	1.6135E 01	1.5777E 01	1.5466E 01	1.5191E 01	1.4945E 01	1.4721E 01	1.4516E 01
75.0	1.5933E 01	1.5704E 01	1.5308E 01	1.4971E 01	1.4679E 01	1.4421E 01	1.4190E 01	1.3980E 01	1.3787E 01
80.0	1.5167E 01	1.4951E 01	1.4576E 01	1.4259E 01	1.3983E 01	1.3740E 01	1.3522E 01	1.3324E 01	1.3142E 01
85.0	1.4485E 01	1.4280E 01	1.3926E 01	1.3625E 01	1.3364E 01	1.3133E 01	1.2927E 01	1.2739E 01	1.2567E 01
90.0	1.3874E 01	1.3680E 01	1.3343E 01	1.3057E 01	1.2808E 01	1.2589E 01	1.2393E 01	1.2215E 01	1.2051E 01
95.0	1.3324E 01	1.3139E 01	1.2817E 01	1.2544E 01	1.2307E 01	1.2099E 01	1.1911E 01	1.1741E 01	1.1586E 01
100.0	1.2826E 01	1.2648E 01	1.2341E 01	1.2080E 01	1.1853E 01	1.1654E 01	1.1475E 01	1.1312E 01	1.1164E 01
105.0	1.2372E 01	1.2202E 01	1.1907E 01	1.1657E 01	1.1440E 01	1.1248E 01	1.1077E 01	1.0921E 01	1.0779E 01
110.0	1.1957E 01	1.1794E 01	1.1510E 01	1.1270E 01	1.1062E 01	1.0878E 01	1.0713E 01	1.0563E 01	1.0426E 01
115.0	1.1577E 01	1.1419E 01	1.1146E 01	1.0915E 01	1.0714E 01	1.0537E 01	1.0378E 01	1.0234E 01	1.0103E 01
120.0	1.1226E 01	1.1074E 01	1.0811E 01	1.0588E 01	1.0394E 01	1.0223E 01	1.0070E 01	9.9313E 00	9.8042E 00
125.0	1.0902E 01	1.0755E 01	1.0501E 01	1.0285E 01	1.0098E 01	9.9329E 00	9.7850E 00	9.6508E 00	9.5281E 00
130.0	1.0602E 01	1.0460E 01	1.0213E 01	1.0005E 01	9.8234E 00	9.6636E 00	9.5205E 00	9.3907E 00	9.2719E 00
135.0	1.0323E 01	1.0185E 01	9.9459E 00	9.7436E 00	9.5681E 00	9.4132E 00	9.2744E 00	9.1487E 00	9.0336E 00
140.0	1.0062E 01	9.9285E 00	9.6967E 00	9.5003E 00	9.3300E 00	9.1797E 00	9.0450E 00	8.9229E 00	8.8112E 00
145.0	9.8192E 00	9.6891E 00	9.4638E 00	9.2730E 00	9.1074E 00	8.9613E 00	8.8305E 00	8.7119E 00	8.6034E 00
150.0	9.5915E 00	9.4649E 00	9.2457E 00	9.0600E 00	8.8989E 00	8.7568E 00	8.6295E 00	8.5141E 00	8.4086E 00
155.0	9.3778E 00	9.2545E 00	9.0410E 00	8.8601E 00	8.7032E 00	8.5648E 00	8.4408E 00	8.3285E 00	8.2257E 00
160.0	9.1770E 00	9.0567E 00	8.8485E 00	8.6722E 00	8.5192E 00	8.3842E 00	8.2634E 00	8.1538E 00	8.0536E 00
165.0	8.9877E 00	8.8704E 00	8.6671E 00	8.4951E 00	8.3458E 00	8.2141E 00	8.0961E 00	7.9892E 00	7.8914E 00
170.0	8.8092E 00	8.6946E 00	8.4960E 00	8.3279E 00	8.1821E 00	8.0534E 00	7.9382E 00	7.8338E 00	7.7383E 00
175.0	8.6404E 00	8.5284E 00	8.3342E 00	8.1699E 00	8.0273E 00	7.9016E 00	7.7889E 00	7.6869E 00	7.5935E 00
180.0	8.4807E 00	8.3710E 00	8.1811E 00	8.0203E 00	7.8808E 00	7.7578E 00	7.6476E 00	7.5477E 00	7.4564E 00
185.0	8.3293E 00	8.2219E 00	8.0359E 00	7.8785E 00	7.7419E 00	7.6214E 00	7.5135E 00	7.4157E 00	7.3263E 00
190.0	8.1856E 00	8.0803E 00	7.8981E 00	7.7438E 00	7.6100E 00	7.4919E 00	7.3862E 00	7.2904E 00	7.2028E 00
195.0	8.0489E 00	7.9457E 00	7.7670E 00	7.6158E 00	7.4846E 00	7.3688E 00	7.2652E 00	7.1713E 00	7.0854E 00
200.0	7.9189E 00	7.8177E 00	7.6423E 00	7.4939E 00	7.3652E 00	7.2516E 00	7.1499E 00	7.0578E 00	6.9736E 00
210.0	7.6769E 00	7.5793E 00	7.4102E 00	7.2670E 00	7.1429E 00	7.0334E 00	6.9354E 00	6.8466E 00	6.7653E 00
220.0	7.4562E 00	7.3619E 00	7.1985E 00	7.0601E 00	6.9402E 00	6.8344E 00	6.7396E 00	6.6538E 00	6.5754E 00
230.0	7.2543E 00	7.1629E 00	7.0046E 00	6.8707E 00	6.7546E 00	6.6521E 00	6.5604E 00	6.4773E 00	6.4014E 00
240.0	7.0688E 00	6.9801E 00	6.8266E 00	6.6967E 00	6.5840E 00	6.4847E 00	6.3957E 00	6.3151E 00	6.2414E 00
250.0	6.8978E 00	6.8116E 00	6.6625E 00	6.5362E 00	6.4268E 00	6.3302E 00	6.2438E 00	6.1655E 00	6.0940E 00
260.0	6.7397E 00	6.6559E 00	6.5107E 00	6.3879E 00	6.2814E 00	6.1875E 00	6.1034E 00	6.0272E 00	5.9576E 00
270.0	6.5932E 00	6.5115E 00	6.3700E 00	6.2504E 00	6.1466E 00	6.0551E 00	5.9731E 00	5.8989E 00	5.8311E 00
280.0	6.4570E 00	6.3773E 00	6.2393E 00	6.1225E 00	6.0213E 00	5.9320E 00	5.8520E 00	5.7796E 00	5.7135E 00
290.0	6.3301E 00	6.2522E 00	6.1174E 00	6.0034E 00	5.9045E 00	5.8173E 00	5.7392E 00	5.6685E 00	5.6039E 00
300.0	6.2116E 00	6.1354E 00	6.0036E 00	5.8921E 00	5.7954E 00	5.7101E 00	5.6338E 00	5.5647E 00	5.5015E 00
310.0	6.1007E 00	6.0262E 00	5.8972E 00	5.7880E 00	5.6934E 00	5.6099E 00	5.5351E 00	5.4675E 00	5.4057E 00
320.0	5.9968E 00	5.9237E 00	5.7973E 00	5.6904E 00	5.5977E 00	5.5159E 00	5.4427E 00	5.3764E 00	5.3158E 00
330.0	5.8991E 00	5.8275E 00	5.7036E 00	5.5987E 00	5.5078E 00	5.4276E 00	5.3558E 00	5.2908E 00	5.2314E 00
340.0	5.8073E 00	5.7370E 00	5.6153E 00	5.5124E 00	5.4232E 00	5.3445E 00	5.2740E 00	5.2102E 00	5.1519E 00
350.0	5.7207E 00	5.6517E 00	5.5322E 00	5.4311E 00	5.3435E 00	5.2661E 00	5.1970E 00	5.1343E 00	5.0771E 00
360.0	5.6390E 00	5.5712E 00	5.4537E 00	5.3543E 00	5.2682E 00	5.1922E 00	5.1242E 00	5.0627E 00	5.0064E 00
370.0	5.5618E 00	5.4951E 00	5.3795E 00	5.2818E 00	5.1971E 00	5.1224E 00	5.0555E 00	4.9949E 00	4.9396E 00
380.0	5.4887E 00	5.4230E 00	5.3093E 00	5.2132E 00	5.1298E 00	5.0562E 00	4.9904E 00	4.9308E 00	4.8764E 00
390.0	5.4195E 00	5.3548E 00	5.2428E 00	5.1481E 00	5.0660E 00	4.9936E 00	4.9288E 00	4.8701E 00	4.8165E 00
400.0	5.3538E 00	5.2900E 00	5.1797E 00	5.0864E 00	5.0055E 00	4.9341E 00	4.8703E 00	4.8124E 00	4.7596E 00

STOPPING POWER

ENERGY MEV	I= 90.0	I= 100.0	I= 120.0	I= 140.0	I= 160.0	I= 180.0	I= 200.0	I= 220.0	I= 240.0
410.0	5.2914E 00	5.2285E 00	5.1198E 00	5.0278E 00	4.9480E 00	4.8777E 00	4.8147E 00	4.7577E 00	4.7056E 00
420.0	5.2320E 00	5.1700E 00	5.0628E 00	4.9720E 00	4.8933E 00	4.8240E 00	4.7619E 00	4.7057E 00	4.6543E 00
430.0	5.1755E 00	5.1144E 00	5.0085E 00	4.9189E 00	4.8413E 00	4.7729E 00	4.7116E 00	4.6561E 00	4.6054E 00
440.0	5.1217E 00	5.0613E 00	4.9568E 00	4.8684E 00	4.7918E 00	4.7242E 00	4.6637E 00	4.6089E 00	4.5589E 00
450.0	5.0704E 00	5.0107E 00	4.9075E 00	4.8202E 00	4.7445E 00	4.6777E 00	4.6180E 00	4.5639E 00	4.5145E 00
460.0	5.0214E 00	4.9625E 00	4.8604E 00	4.7742E 00	4.6994E 00	4.6334E 00	4.5744E 00	4.5209E 00	4.4721E 00
470.0	4.9746E 00	4.9163E 00	4.8155E 00	4.7302E 00	4.6563E 00	4.5911E 00	4.5327E 00	4.4799E 00	4.4316E 00
480.0	4.9298E 00	4.8722E 00	4.7725E 00	4.6882E 00	4.6151E 00	4.5506E 00	4.4929E 00	4.4406E 00	4.3929E 00
490.0	4.8870E 00	4.8300E 00	4.7314E 00	4.6479E 00	4.5756E 00	4.5118E 00	4.4548E 00	4.4031E 00	4.3559E 00
500.0	4.8460E 00	4.7896E 00	4.6920E 00	4.6094E 00	4.5379E 00	4.4748E 00	4.4183E 00	4.3671E 00	4.3204E 00
510.0	4.8067E 00	4.7509E 00	4.6543E 00	4.5725E 00	4.5017E 00	4.4392E 00	4.3833E 00	4.3327E 00	4.2865E 00
520.0	4.7690E 00	4.7138E 00	4.6181E 00	4.5372E 00	4.4670E 00	4.4052E 00	4.3498E 00	4.2997E 00	4.2539E 00
530.0	4.7329E 00	4.6781E 00	4.5834E 00	4.5032E 00	4.4337E 00	4.3725E 00	4.3176E 00	4.2680E 00	4.2227E 00
540.0	4.6982E 00	4.6439E 00	4.5500E 00	4.4706E 00	4.4018E 00	4.3411E 00	4.2868E 00	4.2376E 00	4.1927E 00
550.0	4.6648E 00	4.6111E 00	4.5180E 00	4.4393E 00	4.3711E 00	4.3109E 00	4.2571E 00	4.2084E 00	4.1639E 00
560.0	4.6328E 00	4.5795E 00	4.4872E 00	4.4092E 00	4.3416E 00	4.2820E 00	4.2286E 00	4.1803E 00	4.1362E 00
570.0	4.6019E 00	4.5491E 00	4.4576E 00	4.3803E 00	4.3132E 00	4.2541E 00	4.2012E 00	4.1533E 00	4.1096E 00
580.0	4.5722E 00	4.5198E 00	4.4291E 00	4.3524E 00	4.2859E 00	4.2273E 00	4.1748E 00	4.1273E 00	4.0840E 00
590.0	4.5437E 00	4.4917E 00	4.4017E 00	4.3256E 00	4.2597E 00	4.2015E 00	4.1494E 00	4.1023E 00	4.0593E 00
600.0	4.5161E 00	4.4646E 00	4.3753E 00	4.2998E 00	4.2344E 00	4.1766E 00	4.1250E 00	4.0783E 00	4.0356E 00
610.0	4.4896E 00	4.4384E 00	4.3498E 00	4.2749E 00	4.2100E 00	4.1527E 00	4.1014E 00	4.0551E 00	4.0127E 00
620.0	4.4640E 00	4.4132E 00	4.3253E 00	4.2509E 00	4.1865E 00	4.1296E 00	4.0787E 00	4.0327E 00	3.9906E 00
630.0	4.4394E 00	4.3889E 00	4.3016E 00	4.2278E 00	4.1638E 00	4.1073E 00	4.0568E 00	4.0111E 00	3.9694E 00
640.0	4.4155E 00	4.3655E 00	4.2788E 00	4.2054E 00	4.1419E 00	4.0858E 00	4.0357E 00	3.9903E 00	3.9489E 00
650.0	4.3926E 00	4.3428E 00	4.2567E 00	4.1839E 00	4.1208E 00	4.0651E 00	4.0153E 00	3.9702E 00	3.9291E 00
660.0	4.3703E 00	4.3209E 00	4.2354E 00	4.1631E 00	4.1004E 00	4.0451E 00	3.9956E 00	3.9508E 00	3.9100E 00
670.0	4.3489E 00	4.2998E 00	4.2148E 00	4.1430E 00	4.0807E 00	4.0257E 00	3.9766E 00	3.9321E 00	3.8915E 00
680.0	4.3282E 00	4.2794E 00	4.1949E 00	4.1235E 00	4.0616E 00	4.0071E 00	3.9582E 00	3.9140E 00	3.8737E 00
690.0	4.3081E 00	4.2596E 00	4.1757E 00	4.1047E 00	4.0432E 00	3.9890E 00	3.9405E 00	3.8965E 00	3.8564E 00
700.0	4.2887E 00	4.2405E 00	4.1571E 00	4.0866E 00	4.0254E 00	3.9715E 00	3.9233E 00	3.8796E 00	3.8397E 00
710.0	4.2699E 00	4.2220E 00	4.1391E 00	4.0690E 00	4.0082E 00	3.9546E 00	3.9067E 00	3.8633E 00	3.8236E 00
720.0	4.2518E 00	4.2041E 00	4.1217E 00	4.0520E 00	3.9916E 00	3.9383E 00	3.8906E 00	3.8474E 00	3.8080E 00
730.0	4.2342E 00	4.1868E 00	4.1048E 00	4.0355E 00	3.9754E 00	3.9224E 00	3.8750E 00	3.8321E 00	3.7929E 00
740.0	4.2172E 00	4.1700E 00	4.0885E 00	4.0196E 00	3.9598E 00	3.9071E 00	3.8600E 00	3.8173E 00	3.7783E 00
750.0	4.2006E 00	4.1538E 00	4.0727E 00	4.0041E 00	3.9447E 00	3.8923E 00	3.8454E 00	3.8029E 00	3.7642E 00
760.0	4.1847E 00	4.1380E 00	4.0574E 00	3.9892E 00	3.9300E 00	3.8779E 00	3.8312E 00	3.7890E 00	3.7505E 00
770.0	4.1692E 00	4.1228E 00	4.0425E 00	3.9747E 00	3.9158E 00	3.8640E 00	3.8176E 00	3.7756E 00	3.7372E 00
780.0	4.1541E 00	4.1080E 00	4.0281E 00	3.9606E 00	3.9021E 00	3.8505E 00	3.8043E 00	3.7625E 00	3.7243E 00
790.0	4.1396E 00	4.0936E 00	4.0142E 00	3.9470E 00	3.8887E 00	3.8374E 00	3.7914E 00	3.7498E 00	3.7119E 00
800.0	4.1254E 00	4.0797E 00	4.0006E 00	3.9338E 00	3.8758E 00	3.8247E 00	3.7789E 00	3.7376E 00	3.6998E 00
810.0	4.1117E 00	4.0662E 00	3.9875E 00	3.9209E 00	3.8633E 00	3.8124E 00	3.7669E 00	3.7257E 00	3.6880E 00
820.0	4.0984E 00	4.0531E 00	3.9748E 00	3.9085E 00	3.8511E 00	3.8004E 00	3.7551E 00	3.7141E 00	3.6767E 00
830.0	4.0855E 00	4.0404E 00	3.9624E 00	3.8964E 00	3.8393E 00	3.7888E 00	3.7437E 00	3.7029E 00	3.6656E 00
840.0	4.0729E 00	4.0280E 00	3.9504E 00	3.8847E 00	3.8278E 00	3.7776E 00	3.7327E 00	3.6920E 00	3.6549E 00
850.0	4.0607E 00	4.0160E 00	3.9387E 00	3.8733E 00	3.8167E 00	3.7667E 00	3.7220E 00	3.6815E 00	3.6445E 00
860.0	4.0489E 00	4.0044E 00	3.9274E 00	3.8623E 00	3.8058E 00	3.7561E 00	3.7115E 00	3.6712E 00	3.6345E 00
870.0	4.0374E 00	3.9931E 00	3.9164E 00	3.8515E 00	3.7953E 00	3.7458E 00	3.7014E 00	3.6613E 00	3.6247E 00
880.0	4.0262E 00	3.9821E 00	3.9057E 00	3.8411E 00	3.7851E 00	3.7358E 00	3.6916E 00	3.6516E 00	3.6151E 00
890.0	4.0153E 00	3.9714E 00	3.8953E 00	3.8310E 00	3.7752E 00	3.7261E 00	3.6821E 00	3.6423E 00	3.6059E 00
900.0	4.0048E 00	3.9610E 00	3.8852E 00	3.8211E 00	3.7656E 00	3.7166E 00	3.6728E 00	3.6331E 00	3.5969E 00
910.0	3.9945E 00	3.9509E 00	3.8754E 00	3.8115E 00	3.7562E 00	3.7074E 00	3.6638E 00	3.6243E 00	3.5882E 00
920.0	3.9845E 00	3.9411E 00	3.8658E 00	3.8022E 00	3.7471E 00	3.6985E 00	3.6550E 00	3.6157E 00	3.5798E 00
930.0	3.9748E 00	3.9315E 00	3.8566E 00	3.7932E 00	3.7383E 00	3.6899E 00	3.6465E 00	3.6073E 00	3.5715E 00
940.0	3.9654E 00	3.9222E 00	3.8475E 00	3.7844E 00	3.7297E 00	3.6814E 00	3.6383E 00	3.5992E 00	3.5635E 00
950.0	3.9562E 00	3.9132E 00	3.8388E 00	3.7758E 00	3.7213E 00	3.6732E 00	3.6302E 00	3.5913E 00	3.5557E 00
960.0	3.9472E 00	3.9044E 00	3.8302E 00	3.7675E 00	3.7132E 00	3.6653E 00	3.6224E 00	3.5836E 00	3.5482E 00
970.0	3.9385E 00	3.8958E 00	3.8219E 00	3.7594E 00	3.7053E 00	3.6575E 00	3.6148E 00	3.5761E 00	3.5408E 00
980.0	3.9301E 00	3.8875E 00	3.8138E 00	3.7515E 00	3.6976E 00	3.6500E 00	3.6074E 00	3.5689E 00	3.5337E 00
990.0	3.9218E 00	3.8794E 00	3.8060E 00	3.7439E 00	3.6901E 00	3.6426E 00	3.6002E 00	3.5618E 00	3.5267E 00
1000.0	3.9138E 00	3.8715E 00	3.7983E 00	3.7364E 00	3.6828E 00	3.6355E 00	3.5932E 00	3.5549E 00	3.5199E 00
1100.0	3.8441E 00	3.8031E 00	3.7320E 00	3.6718E 00	3.6198E 00	3.5738E 00	3.5327E 00	3.4955E 00	3.4616E 00
1200.0	3.7903E 00	3.7502E 00	3.6808E 00	3.6222E 00	3.5713E 00	3.5265E 00	3.4864E 00	3.4501E 00	3.4169E 00
1300.0	3.7485E 00	3.7092E 00	3.6412E 00	3.5837E 00	3.5340E 00	3.4900E 00	3.4507E 00	3.4152E 00	3.3827E 00
1400.0	3.7159E 00	3.6773E 00	3.6105E 00	3.5540E 00	3.5051E 00	3.4620E 00	3.4234E 00	3.3884E 00	3.3565E 00
1500.0	3.6905E 00	3.6525E 00	3.5867E 00	3.5311E 00	3.4830E 00	3.4405E 00	3.4025E 00	3.3681E 00	3.3367E 00
1600.0	3.6709E 00	3.6334E 00	3.5685E 00	3.5136E 00	3.4661E 00	3.4242E 00	3.3867E 00	3.3527E 00	3.3218E 00
1800.0	3.6447E 00	3.6080E 00	3.5445E 00	3.4909E 00	3.4444E 00	3.4034E 00	3.3667E 00	3.3335E 00	3.3032E 00
2000.0	3.6309E 00	3.5949E 00	3.5325E 00	3.4797E 00	3.4341E 00	3.3937E 00	3.3577E 00	3.3251E 00	3.2953E 00
2200.0	3.6256E 00	3.5901E 00	3.5286E 00	3.4765E 00	3.4315E 00	3.3917E 00	3.3562E 00	3.3240E 00	3.2947E 00
2400.0	3.6263E 00	3.5911E 00	3.5303E 00	3.4789E 00	3.4343E 00	3.3950E 00	3.3599E 00	3.3281E 00	3.2990E 00
2600.0	3.6311E 00	3.5963E 00	3.5360E 00	3.4851E 00	3.4410E 00	3.4020E 00	3.3672E 00	3.3357E 00	3.3069E 00
2800.0	3.6389E 00	3.6044E 00	3.5446E 00	3.4941E 00	3.4503E 00	3.4117E 00	3.3771E 00	3.3459E 00	3.3173E 00
3000.0	3.6490E 00	3.6147E 00	3.5553E 00	3.5051E 00	3.4616E 00	3.4232E 00	3.3889E 00	3.3578E 00	3.3295E 00
3200.0	3.6606E 00	3.6264E 00	3.5674E 00	3.5175E 00	3.4742E 00	3.4361E 00	3.4019E 00	3.3711E 00	3.3429E 00
3400.0	3.6733E 00	3.6393E 00	3.5806E 00	3.5309E 00	3.4878E 00	3.4499E 00	3.4159E 00	3.3852E 00	3.3572E 00
3600.0	3.6868E 00	3.6530E 00	3.5945E 00	3.5450E 00	3.5021E 00	3.4643E 00	3.4305E 00	3.3999E 00	3.3720E 00
3800.0	3.7009E 00	3.6672E 00	3.6089E 00	3.5596E 00	3.5169E 00	3.4792E 00	3.4455E 00	3.4151E 00	3.3872E 00
4000.0	3.7153E 00	3.6817E 00	3.6236E 00	3.5745E 00	3.5319E 00	3.4944E 00	3.4608E 00	3.4304E 00	3.4027E 00
4500.0	3.7522E 00	3.7188E 00	3.6611E 00	3.6123E 00	3.5700E 00	3.5327E 00	3.4994E 00	3.4692E 00	3.4416E 00
5000.0	3.7892E 00	3.7560E 00	3.6986E 00	3.6500E 00	3.6079E 00	3.5708E 00	3.5376E 00	3.5076E 00	3.4802E 00

STOPPING POWER

ENERGY MEV	I= 260.0	I= 280.0	I= 300.0	I= 320.0	I= 340.0	I= 380.0	I= 420.0	I= 460.0	I= 500.0
1.0	2.9086E 02	2.8125E 02	2.7246E 02	2.6437E 02	2.5688E 02	2.4346E 02	2.3172E 02	2.2134E 02	2.1208E 02
2.0	1.9660E 02	1.9096E 02	1.8575E 02	1.8094E 02	1.7646E 02	1.6838E 02	1.6125E 02	1.5489E 02	1.4918E 02
3.0	1.5081E 02	1.4685E 02	1.4319E 02	1.3979E 02	1.3663E 02	1.3091E 02	1.2584E 02	1.2131E 02	1.1722E 02
4.0	1.2292E 02	1.1990E 02	1.1711E 02	1.1452E 02	1.1211E 02	1.0772E 02	1.0384E 02	1.0036E 02	9.7222E 01
5.0	1.0392E 02	1.0150E 02	9.9270E 01	9.7195E 01	9.5260E 01	9.1748E 01	8.8634E 01	8.5844E 01	8.3322E 01
6.0	9.0047E 01	8.8047E 01	8.6199E 01	8.4483E 01	8.2884E 01	7.9981E 01	7.7407E 01	7.5101E 01	7.3016E 01
7.0	7.9431E 01	7.7736E 01	7.6172E 01	7.4720E 01	7.3367E 01	7.0913E 01	6.8738E 01	6.6790E 01	6.5030E 01
8.0	7.2568E 01	7.1102E 01	6.9740E 01	6.8469E 01	6.7279E 01	6.5105E 01	6.3160E 01	6.1404E 01	5.9806E 01
9.0	6.7950E 01	6.6645E 01	6.5425E 01	6.4281E 01	6.3202E 01	6.1218E 01	5.9427E 01	5.7797E 01	5.6303E 01
10.0	6.2853E 01	6.1676E 01	6.0576E 01	5.9543E 01	5.8570E 01	5.6776E 01	5.5154E 01	5.3675E 01	5.2316E 01
12.0	5.4870E 01	5.3885E 01	5.2962E 01	5.2095E 01	5.1276E 01	4.9762E 01	4.8387E 01	4.7127E 01	4.5962E 01
14.0	4.8873E 01	4.8025E 01	4.7231E 01	4.6483E 01	4.5775E 01	4.4465E 01	4.3270E 01	4.2170E 01	4.1149E 01
16.0	4.4183E 01	4.3439E 01	4.2742E 01	4.2085E 01	4.1462E 01	4.0308E 01	3.9253E 01	3.8279E 01	3.7372E 01
18.0	4.0403E 01	3.9741E 01	3.9120E 01	3.8534E 01	3.7980E 01	3.6949E 01	3.6007E 01	3.5134E 01	3.4321E 01
20.0	3.7285E 01	3.6689E 01	3.6129E 01	3.5601E 01	3.5101E 01	3.4172E 01	3.3321E 01	3.2532E 01	3.1796E 01
22.0	3.4666E 01	3.4123E 01	3.3614E 01	3.3133E 01	3.2678E 01	3.1832E 01	3.1057E 01	3.0339E 01	2.9667E 01
24.0	3.2430E 01	3.1933E 01	3.1466E 01	3.1025E 01	3.0608E 01	2.9832E 01	2.9121E 01	2.8461E 01	2.7845E 01
26.0	3.0499E 01	3.0039E 01	2.9608E 01	2.9201E 01	2.8816E 01	2.8099E 01	2.7442E 01	2.6834E 01	2.6264E 01
28.0	2.8811E 01	2.8384E 01	2.7984E 01	2.7606E 01	2.7248E 01	2.6583E 01	2.5973E 01	2.5408E 01	2.4879E 01
30.0	2.7324E 01	2.6925E 01	2.6551E 01	2.6198E 01	2.5864E 01	2.5243E 01	2.4674E 01	2.4147E 01	2.3654E 01
32.0	2.6001E 01	2.5627E 01	2.5276E 01	2.4945E 01	2.4632E 01	2.4050E 01	2.3517E 01	2.3023E 01	2.2561E 01
34.0	2.4818E 01	2.4465E 01	2.4135E 01	2.3823E 01	2.3528E 01	2.2980E 01	2.2479E 01	2.2014E 01	2.1580E 01
36.0	2.3751E 01	2.3418E 01	2.3106E 01	2.2812E 01	2.2533E 01	2.2015E 01	2.1542E 01	2.1103E 01	2.0693E 01
38.0	2.2786E 01	2.2470E 01	2.2174E 01	2.1894E 01	2.1630E 01	2.1140E 01	2.0691E 01	2.0276E 01	1.9888E 01
40.0	2.1906E 01	2.1606E 01	2.1324E 01	2.1059E 01	2.0808E 01	2.0342E 01	1.9916E 01	1.9521E 01	1.9153E 01
42.0	2.1102E 01	2.0816E 01	2.0547E 01	2.0295E 01	2.0055E 01	1.9611E 01	1.9205E 01	1.8830E 01	1.8479E 01
44.0	2.0364E 01	2.0090E 01	1.9834E 01	1.9592E 01	1.9364E 01	1.8940E 01	1.8552E 01	1.8194E 01	1.7859E 01
46.0	1.9684E 01	1.9421E 01	1.9176E 01	1.8944E 01	1.8725E 01	1.8320E 01	1.7949E 01	1.7606E 01	1.7287E 01
48.0	1.9054E 01	1.8803E 01	1.8567E 01	1.8345E 01	1.8135E 01	1.7746E 01	1.7390E 01	1.7062E 01	1.6756E 01
50.0	1.8471E 01	1.8229E 01	1.8002E 01	1.7789E 01	1.7587E 01	1.7213E 01	1.6871E 01	1.6556E 01	1.6262E 01
55.0	1.7180E 01	1.6959E 01	1.6752E 01	1.6557E 01	1.6373E 01	1.6033E 01	1.5722E 01	1.5435E 01	1.5168E 01
60.0	1.6085E 01	1.5882E 01	1.5691E 01	1.5512E 01	1.5343E 01	1.5030E 01	1.4744E 01	1.4481E 01	1.4236E 01
65.0	1.5145E 01	1.4956E 01	1.4779E 01	1.4613E 01	1.4457E 01	1.4166E 01	1.3902E 01	1.3658E 01	1.3432E 01
70.0	1.4327E 01	1.4151E 01	1.3986E 01	1.3831E 01	1.3685E 01	1.3415E 01	1.3168E 01	1.2942E 01	1.2731E 01
75.0	1.3610E 01	1.3444E 01	1.3290E 01	1.3145E 01	1.3008E 01	1.2754E 01	1.2523E 01	1.2311E 01	1.2114E 01
80.0	1.2975E 01	1.2819E 01	1.2673E 01	1.2537E 01	1.2407E 01	1.2169E 01	1.1952E 01	1.1752E 01	1.1567E 01
85.0	1.2409E 01	1.2261E 01	1.2123E 01	1.1994E 01	1.1872E 01	1.1646E 01	1.1441E 01	1.1252E 01	1.1078E 01
90.0	1.1901E 01	1.1761E 01	1.1630E 01	1.1507E 01	1.1391E 01	1.1177E 01	1.0982E 01	1.0803E 01	1.0638E 01
95.0	1.1442E 01	1.1309E 01	1.1184E 01	1.1067E 01	1.0957E 01	1.0753E 01	1.0568E 01	1.0398E 01	1.0240E 01
100.0	1.1026E 01	1.0899E 01	1.0780E 01	1.0668E 01	1.0562E 01	1.0368E 01	1.0191E 01	1.0029E 01	9.8785E 00
105.0	1.0647E 01	1.0525E 01	1.0411E 01	1.0304E 01	1.0203E 01	1.0016E 01	9.8473E 00	9.6921E 00	9.5484E 00
110.0	1.0300E 01	1.0183E 01	1.0073E 01	9.9704E 00	9.8735E 00	9.6946E 00	9.5323E 00	9.3835E 00	9.2458E 00
115.0	9.9811E 00	9.8683E 00	9.7629E 00	9.6640E 00	9.5707E 00	9.3987E 00	9.2427E 00	9.0996E 00	8.9673E 00
120.0	9.6870E 00	9.5782E 00	9.4766E 00	9.3812E 00	9.2914E 00	9.1256E 00	8.9753E 00	8.8376E 00	8.7102E 00
125.0	9.4149E 00	9.3098E 00	9.2117E 00	9.1196E 00	9.0328E 00	8.8728E 00	8.7278E 00	8.5949E 00	8.4720E 00
130.0	9.1624E 00	9.0607E 00	8.9658E 00	8.8767E 00	8.7928E 00	8.6381E 00	8.4979E 00	8.3694E 00	8.2507E 00
135.0	8.9274E 00	8.8289E 00	8.7370E 00	8.6507E 00	8.5694E 00	8.4196E 00	8.2838E 00	8.1595E 00	8.0446E 00
140.0	8.7083E 00	8.6127E 00	8.5235E 00	8.4398E 00	8.3610E 00	8.2157E 00	8.0840E 00	7.9635E 00	7.8522E 00
145.0	8.5033E 00	8.4105E 00	8.3238E 00	8.2425E 00	8.1660E 00	8.0249E 00	7.8971E 00	7.7801E 00	7.6721E 00
150.0	8.3113E 00	8.2210E 00	8.1367E 00	8.0577E 00	7.9832E 00	7.8460E 00	7.7218E 00	7.6081E 00	7.5032E 00
155.0	8.1309E 00	8.0430E 00	7.9609E 00	7.8840E 00	7.8115E 00	7.6780E 00	7.5571E 00	7.4465E 00	7.3444E 00
160.0	7.9612E 00	7.8755E 00	7.7956E 00	7.7206E 00	7.6500E 00	7.5199E 00	7.4021E 00	7.2944E 00	7.1949E 00
165.0	7.8013E 00	7.7177E 00	7.6397E 00	7.5665E 00	7.4976E 00	7.3707E 00	7.2559E 00	7.1509E 00	7.0539E 00
170.0	7.6503E 00	7.5686E 00	7.4925E 00	7.4210E 00	7.3538E 00	7.2299E 00	7.1178E 00	7.0153E 00	6.9207E 00
175.0	7.5075E 00	7.4277E 00	7.3532E 00	7.2834E 00	7.2177E 00	7.0967E 00	6.9872E 00	6.8870E 00	6.7947E 00
180.0	7.3722E 00	7.2942E 00	7.2213E 00	7.1531E 00	7.0888E 00	6.9704E 00	6.8634E 00	6.7655E 00	6.6752E 00
185.0	7.2440E 00	7.1675E 00	7.0963E 00	7.0294E 00	6.9665E 00	6.8507E 00	6.7459E 00	6.6502E 00	6.5619E 00
190.0	7.1221E 00	7.0473E 00	6.9774E 00	6.9120E 00	6.8504E 00	6.7369E 00	6.6343E 00	6.5406E 00	6.4541E 00
195.0	7.0063E 00	6.9329E 00	6.8645E 00	6.8003E 00	6.7399E 00	6.6287E 00	6.5282E 00	6.4363E 00	6.3517E 00
200.0	6.8960E 00	6.8240E 00	6.7569E 00	6.6939E 00	6.6347E 00	6.5257E 00	6.4271E 00	6.3370E 00	6.2540E 00
210.0	6.6905E 00	6.6211E 00	6.5564E 00	6.4958E 00	6.4387E 00	6.3337E 00	6.2387E 00	6.1520E 00	6.0721E 00
220.0	6.5031E 00	6.4361E 00	6.3736E 00	6.3150E 00	6.2599E 00	6.1584E 00	6.0667E 00	5.9830E 00	5.9059E 00
230.0	6.3314E 00	6.2665E 00	6.2060E 00	6.1493E 00	6.0960E 00	5.9978E 00	5.9092E 00	5.8282E 00	5.7536E 00
240.0	6.1736E 00	6.1107E 00	6.0520E 00	5.9970E 00	5.9453E 00	5.8502E 00	5.7642E 00	5.6858E 00	5.6135E 00
250.0	6.0281E 00	5.9669E 00	5.9100E 00	5.8566E 00	5.8064E 00	5.7140E 00	5.6305E 00	5.5544E 00	5.4842E 00
260.0	5.8935E 00	5.8340E 00	5.7786E 00	5.7267E 00	5.6778E 00	5.5880E 00	5.5068E 00	5.4328E 00	5.3646E 00
270.0	5.7686E 00	5.7107E 00	5.6567E 00	5.6061E 00	5.5586E 00	5.4711E 00	5.3921E 00	5.3200E 00	5.2536E 00
280.0	5.6525E 00	5.5961E 00	5.5434E 00	5.4941E 00	5.4477E 00	5.3624E 00	5.2853E 00	5.2150E 00	5.1504E 00
290.0	5.5443E 00	5.4892E 00	5.4378E 00	5.3896E 00	5.3443E 00	5.2610E 00	5.1858E 00	5.1172E 00	5.0541E 00
300.0	5.4433E 00	5.3894E 00	5.3391E 00	5.2920E 00	5.2477E 00	5.1663E 00	5.0928E 00	5.0258E 00	4.9641E 00
310.0	5.3487E 00	5.2959E 00	5.2468E 00	5.2007E 00	5.1573E 00	5.0777E 00	5.0058E 00	4.9402E 00	4.8799E 00
320.0	5.2600E 00	5.2083E 00	5.1601E 00	5.1150E 00	5.0726E 00	4.9945E 00	4.9241E 00	4.8599E 00	4.8009E 00
330.0	5.1767E 00	5.1260E 00	5.0788E 00	5.0345E 00	4.9929E 00	4.9164E 00	4.8474E 00	4.7845E 00	4.7266E 00
340.0	5.0983E 00	5.0485E 00	5.0022E 00	4.9588E 00	4.9180E 00	4.8429F 00	4.7752E 00	4.7135E 00	4.6567E 00
350.0	5.0244E 00	4.9755E 00	4.9300E 00	4.8876E 00	4.8473E 00	4.7736E 00	4.7072E 00	4.6466E 00	4.5909E 00
360.0	4.9546E 00	4.9066E 00	4.8619E 00	4.8200E 00	4.7806E 00	4.7082E 00	4.6429E 00	4.5834E 00	4.5287E 00
370.0	4.8887E 00	4.8415E 00	4.7975E 00	4.7563E 00	4.7176E 00	4.6464E 00	4.5822E 00	4.5237E 00	4.4699E 00
380.0	4.8263E 00	4.7798E 00	4.7365E 00	4.6960E 00	4.6579E 00	4.5879E 00	4.5247E 00	4.4671E 00	4.4142E 00
390.0	4.7671E 00	4.7214E 00	4.6788E 00	4.6389E 00	4.6014E 00	4.5324E 00	4.4702E 00	4.4135E 00	4.3614E 00
400.0	4.7110E 00	4.6660E 00	4.6240E 00	4.5847E 00	4.5477E 00	4.4798E 00	4.4185E 00	4.3627E 00	4.3114E 00

STOPPING POWER

ENERGY MEV	I= 260.0	I= 280.0	I= 300.0	I= 320.0	I= 340.0	I= 380.0	I= 420.0	I= 460.0	I= 500.0
410.0	4.6577E 00	4.6133E 00	4.5719E 00	4.5332E 00	4.4967E 00	4.4298E 00	4.3694E 00	4.3144E 00	4.2638E 00
420.0	4.6070E 00	4.5632E 00	4.5224E 00	4.4842E 00	4.4483E 00	4.3823E 00	4.3227E 00	4.2685E 00	4.2186E 00
430.0	4.5588E 00	4.5156E 00	4.4753E 00	4.4376E 00	4.4021E 00	4.3370E 00	4.2783E 00	4.2248E 00	4.1756E 00
440.0	4.5128E 00	4.4702E 00	4.4304E 00	4.3932E 00	4.3582E 00	4.2939E 00	4.2359E 00	4.1831E 00	4.1346E 00
450.0	4.4690E 00	4.4269E 00	4.3876E 00	4.3508E 00	4.3163E 00	4.2528E 00	4.1956E 00	4.1434E 00	4.0955E 00
460.0	4.4272E 00	4.3855E 00	4.3467E 00	4.3104E 00	4.2763E 00	4.2136E 00	4.1570E 00	4.1055E 00	4.0582E 00
470.0	4.3872E 00	4.3461E 00	4.3077E 00	4.2718E 00	4.2381E 00	4.1761E 00	4.1202E 00	4.0693E 00	4.0225E 00
480.0	4.3490E 00	4.3083E 00	4.2704E 00	4.2349E 00	4.2016E 00	4.1403E 00	4.0850E 00	4.0347E 00	3.9885E 00
490.0	4.3125E 00	4.2722E 00	4.2347E 00	4.1996E 00	4.1666E 00	4.1060E 00	4.0513E 00	4.0016E 00	3.9559E 00
500.0	4.2775E 00	4.2376E 00	4.2005E 00	4.1658E 00	4.1332E 00	4.0732E 00	4.0191E 00	3.9699E 00	3.9247E 00
510.0	4.2439E 00	4.2045E 00	4.1678E 00	4.1334E 00	4.1011E 00	4.0417E 00	3.9882E 00	3.9395E 00	3.8948E 00
520.0	4.2118E 00	4.1728E 00	4.1364E 00	4.1024E 00	4.0704E 00	4.0116E 00	3.9586E 00	3.9104E 00	3.8661E 00
530.0	4.1809E 00	4.1423E 00	4.1063E 00	4.0726E 00	4.0409E 00	3.9827E 00	3.9302E 00	3.8825E 00	3.8386E 00
540.0	4.1513E 00	4.1131E 00	4.0774E 00	4.0440E 00	4.0126E 00	3.9550E 00	3.9030E 00	3.8557E 00	3.8122E 00
550.0	4.1229E 00	4.0850E 00	4.0496E 00	4.0165E 00	3.9854E 00	3.9283E 00	3.8768E 00	3.8299E 00	3.7869E 00
560.0	4.0956E 00	4.0580E 00	4.0229E 00	3.9901E 00	3.9593E 00	3.9027E 00	3.8517E 00	3.8052E 00	3.7626E 00
570.0	4.0693E 00	4.0320E 00	3.9973E 00	3.9648E 00	3.9342E 00	3.8781E 00	3.8275E 00	3.7814E 00	3.7391E 00
580.0	4.0440E 00	4.0071E 00	3.9726E 00	3.9404E 00	3.9101E 00	3.8544E 00	3.8042E 00	3.7586E 00	3.7166E 00
590.0	4.0197E 00	3.9830E 00	3.9489E 00	3.9169E 00	3.8868E 00	3.8316E 00	3.7819E 00	3.7366E 00	3.6950E 00
600.0	3.9963E 00	3.9599E 00	3.9260E 00	3.8943E 00	3.8644E 00	3.8097E 00	3.7603E 00	3.7154E 00	3.6741E 00
610.0	3.9737E 00	3.9376E 00	3.9039E 00	3.8725E 00	3.8429E 00	3.7885E 00	3.7395E 00	3.6950E 00	3.6540E 00
620.0	3.9519E 00	3.9161E 00	3.8827E 00	3.8515E 00	3.8221E 00	3.7681E 00	3.7195E 00	3.6753E 00	3.6347E 00
630.0	3.9310E 00	3.8954E 00	3.8622E 00	3.8312E 00	3.8020E 00	3.7485E 00	3.7002E 00	3.6563E 00	3.6160E 00
640.0	3.9107E 00	3.8754E 00	3.8425E 00	3.8117E 00	3.7827E 00	3.7295E 00	3.6816E 00	3.6380E 00	3.5980E 00
650.0	3.8912E 00	3.8561E 00	3.8234E 00	3.7928E 00	3.7641E 00	3.7113E 00	3.6637E 00	3.6204E 00	3.5806E 00
660.0	3.8723E 00	3.8375E 00	3.8050E 00	3.7746E 00	3.7461E 00	3.6936E 00	3.6464E 00	3.6034E 00	3.5639E 00
670.0	3.8541E 00	3.8195E 00	3.7872E 00	3.7570E 00	3.7287E 00	3.6766E 00	3.6296E 00	3.5869E 00	3.5477E 00
680.0	3.8365E 00	3.8021E 00	3.7701E 00	3.7401E 00	3.7119E 00	3.6601E 00	3.6135E 00	3.5710E 00	3.5321E 00
690.0	3.8195E 00	3.7853E 00	3.7535E 00	3.7237E 00	3.6956E 00	3.6442E 00	3.5979E 00	3.5557E 00	3.5170E 00
700.0	3.8031E 00	3.7691E 00	3.7374E 00	3.7078E 00	3.6799E 00	3.6288E 00	3.5828E 00	3.5409E 00	3.5024E 00
710.0	3.7872E 00	3.7534E 00	3.7219E 00	3.6925E 00	3.6648E 00	3.6140E 00	3.5682E 00	3.5265E 00	3.4883E 00
720.0	3.7718E 00	3.7382E 00	3.7069E 00	3.6776E 00	3.6501E 00	3.5996E 00	3.5541E 00	3.5126E 00	3.4746E 00
730.0	3.7569E 00	3.7235E 00	3.6924E 00	3.6633E 00	3.6359E 00	3.5857E 00	3.5404E 00	3.4992E 00	3.4614E 00
740.0	3.7425E 00	3.7092E 00	3.6783E 00	3.6494E 00	3.6222E 00	3.5722E 00	3.5272E 00	3.4862E 00	3.4487E 00
750.0	3.7285E 00	3.6955E 00	3.6647E 00	3.6359E 00	3.6088E 00	3.5592E 00	3.5144E 00	3.4737E 00	3.4363E 00
760.0	3.7150E 00	3.6821E 00	3.6515E 00	3.6229E 00	3.5960E 00	3.5465E 00	3.5020E 00	3.4615E 00	3.4243E 00
770.0	3.7019E 00	3.6692E 00	3.6388E 00	3.6103E 00	3.5835E 00	3.5343E 00	3.4900E 00	3.4497E 00	3.4127E 00
780.0	3.6892E 00	3.6567E 00	3.6264E 00	3.5980E 00	3.5714E 00	3.5225E 00	3.4784E 00	3.4383E 00	3.4015E 00
790.0	3.6769E 00	3.6445E 00	3.6144E 00	3.5862E 00	3.5597E 00	3.5110E 00	3.4672E 00	3.4273E 00	3.3907E 00
800.0	3.6650E 00	3.6328E 00	3.6028E 00	3.5747E 00	3.5483E 00	3.4999E 00	3.4563E 00	3.4166E 00	3.3801E 00
810.0	3.6534E 00	3.6214E 00	3.5915E 00	3.5636E 00	3.5373E 00	3.4891E 00	3.4457E 00	3.4062E 00	3.3699E 00
820.0	3.6422E 00	3.6103E 00	3.5806E 00	3.5528E 00	3.5266E 00	3.4786E 00	3.4354E 00	3.3961E 00	3.3600E 00
830.0	3.6313E 00	3.5996E 00	3.5700E 00	3.5423E 00	3.5163E 00	3.4685E 00	3.4255E 00	3.3863E 00	3.3504E 00
840.0	3.6208E 00	3.5892E 00	3.5597E 00	3.5321E 00	3.5062E 00	3.4587E 00	3.4158E 00	3.3769E 00	3.3411E 00
850.0	3.6105E 00	3.5790E 00	3.5497E 00	3.5223E 00	3.4965E 00	3.4491E 00	3.4065E 00	3.3677E 00	3.3321E 00
860.0	3.6006E 00	3.5692E 00	3.5400E 00	3.5127E 00	3.4870E 00	3.4399E 00	3.3974E 00	3.3588E 00	3.3233E 00
870.0	3.5909E 00	3.5597E 00	3.5306E 00	3.5034E 00	3.4778E 00	3.4309E 00	3.3886E 00	3.3501E 00	3.3148E 00
880.0	3.5816E 00	3.5505E 00	3.5215E 00	3.4944E 00	3.4689E 00	3.4222E 00	3.3801E 00	3.3417E 00	3.3066E 00
890.0	3.5725E 00	3.5415E 00	3.5126E 00	3.4856E 00	3.4603E 00	3.4137E 00	3.3718E 00	3.3336E 00	3.2986E 00
900.0	3.5636E 00	3.5328E 00	3.5040E 00	3.4771E 00	3.4519E 00	3.4055E 00	3.3637E 00	3.3257E 00	3.2908E 00
910.0	3.5550E 00	3.5243E 00	3.4957E 00	3.4689E 00	3.4437E 00	3.3975E 00	3.3559E 00	3.3180E 00	3.2833E 00
920.0	3.5467E 00	3.5161E 00	3.4875E 00	3.4609E 00	3.4358E 00	3.3897E 00	3.3483E 00	3.3106E 00	3.2760E 00
930.0	3.5386E 00	3.5081E 00	3.4796E 00	3.4531E 00	3.4281E 00	3.3822E 00	3.3409E 00	3.3033E 00	3.2689E 00
940.0	3.5307E 00	3.5003E 00	3.4720E 00	3.4455E 00	3.4206E 00	3.3749E 00	3.3337E 00	3.2963E 00	3.2619E 00
950.0	3.5230E 00	3.4927E 00	3.4645E 00	3.4381E 00	3.4133E 00	3.3678E 00	3.3268E 00	3.2895E 00	3.2552E 00
960.0	3.5156E 00	3.4854E 00	3.4573E 00	3.4310E 00	3.4062E 00	3.3609E 00	3.3200E 00	3.2828E 00	3.2487E 00
970.0	3.5083E 00	3.4782E 00	3.4502E 00	3.4240E 00	3.3994E 00	3.3542E 00	3.3134E 00	3.2764E 00	3.2424E 00
980.0	3.5013E 00	3.4713E 00	3.4434E 00	3.4172E 00	3.3927E 00	3.3476E 00	3.3070E 00	3.2701E 00	3.2362E 00
990.0	3.4944E 00	3.4646E 00	3.4367E 00	3.4107E 00	3.3862E 00	3.3413E 00	3.3008E 00	3.2640E 00	3.2303E 00
1000.0	3.4878E 00	3.4580E 00	3.4302E 00	3.4043E 00	3.3799E 00	3.3351E 00	3.2948E 00	3.2581E 00	3.2245E 00
1100.0	3.4303E 00	3.4014E 00	3.3744E 00	3.3492E 00	3.3255E 00	3.2820E 00	3.2429E 00	3.2073E 00	3.1746E 00
1200.0	3.3864E 00	3.3582E 00	3.3319E 00	3.3073E 00	3.2842E 00	3.2418E 00	3.2036E 00	3.1688E 00	3.1369E 00
1300.0	3.3529E 00	3.3252E 00	3.2994E 00	3.2754E 00	3.2527E 00	3.2112E 00	3.1738E 00	3.1397E 00	3.1085E 00
1400.0	3.3272E 00	3.3000E 00	3.2747E 00	3.2511E 00	3.2288E 00	3.1880E 00	3.1513E 00	3.1179E 00	3.0872E 00
1500.0	3.3078E 00	3.2810E 00	3.2561E 00	3.2328E 00	3.2109E 00	3.1707E 00	3.1345E 00	3.1016E 00	3.0715E 00
1600.0	3.2933E 00	3.2669E 00	3.2423E 00	3.2193E 00	3.1977E 00	3.1580E 00	3.1223E 00	3.0899E 00	3.0601E 00
1800.0	3.2753E 00	3.2495E 00	3.2254E 00	3.2030E 00	3.1818E 00	3.1431E 00	3.1082E 00	3.0764E 00	3.0473E 00
2000.0	3.2679E 00	3.2425E 00	3.2189E 00	3.1968E 00	3.1761E 00	3.1380E 00	3.1037E 00	3.0725E 00	3.0439E 00
2200.0	3.2676E 00	3.2426E 00	3.2193E 00	3.1975E 00	3.1771E 00	3.1395E 00	3.1057E 00	3.0750E 00	3.0468E 00
2400.0	3.2723E 00	3.2476E 00	3.2246E 00	3.2030E 00	3.1828E 00	3.1457E 00	3.1122E 00	3.0819E 00	3.0540E 00
2600.0	3.2805E 00	3.2560E 00	3.2332E 00	3.2118E 00	3.1918E 00	3.1550E 00	3.1219E 00	3.0918E 00	3.0642E 00
2800.0	3.2911E 00	3.2668E 00	3.2441E 00	3.2230E 00	3.2031E 00	3.1666E 00	3.1338E 00	3.1039E 00	3.0765E 00
3000.0	3.3034E 00	3.2793E 00	3.2568E 00	3.2358E 00	3.2160E 00	3.1798E 00	3.1471E 00	3.1175E 00	3.0903E 00
3200.0	3.3170E 00	3.2930E 00	3.2706E 00	3.2497E 00	3.2301E 00	3.1940E 00	3.1616E 00	3.1321E 00	3.1051E 00
3400.0	3.3314E 00	3.3075E 00	3.2852E 00	3.2644E 00	3.2449E 00	3.2090E 00	3.1767E 00	3.1474E 00	3.1205E 00
3600.0	3.3463E 00	3.3225E 00	3.3004E 00	3.2797E 00	3.2602E 00	3.2245E 00	3.1924E 00	3.1631E 00	3.1364E 00
3800.0	3.3616E 00	3.3379E 00	3.3159E 00	3.2952E 00	3.2758E 00	3.2403E 00	3.2083E 00	3.1791E 00	3.1525E 00
4000.0	3.3772E 00	3.3536E 00	3.3316E 00	3.3110E 00	3.2917E 00	3.2562E 00	3.2243E 00	3.1953E 00	3.1687E 00
4500.0	3.4163E 00	3.3928E 00	3.3710E 00	3.3505E 00	3.3313E 00	3.2961E 00	3.2644E 00	3.2356E 00	3.2092E 00
5000.0	3.4549E 00	3.4316E 00	3.4099E 00	3.3895E 00	3.3704E 00	3.3354E 00	3.3038E 00	3.2751E 00	3.2489E 00

STOPPING POWER

ENERGY MEV	I= 550.0	I= 600.0	I= 650.0	I= 700.0	I= 750.0	I= 800.0	I= 850.0	I= 900.0	I= 950.0
1.0	2.0178E 02	1.9265E 02	1.8449E 02	1.7713E 02	1.7045E 02	1.6436E 02	1.5877E 02	1.5362E 02	1.4885E 02
2.0	1.4279E 02	1.3708E 02	1.3195E 02	1.2729E 02	1.2304E 02	1.1915E 02	1.1556E 02	1.1223E 02	1.0914E 02
3.0	1.1263E 02	1.0852E 02	1.0481E 02	1.0144E 02	9.8353E 01	9.5515E 01	9.2892E 01	9.0458E 01	8.8191E 01
4.0	9.3688E 01	9.0519E 01	8.7652E 01	8.5041E 01	8.2648E 01	8.0444E 01	7.8405E 01	7.6509E 01	7.4741E 01
5.0	8.0484E 01	7.7935E 01	7.5627E 01	7.3523E 01	7.1593E 01	6.9814E 01	6.8166E 01	6.6633E 01	6.5201E 01
6.0	7.0669E 01	6.8560E 01	6.6650E 01	6.4908E 01	6.3310E 01	6.1835E 01	6.0468E 01	5.9196E 01	5.8008E 01
7.0	6.3048E 01	6.1267E 01	5.9655E 01	5.8183E 01	5.6833E 01	5.5587E 01	5.4432E 01	5.3357E 01	5.2352E 01
8.0	5.7994E 01	5.6358E 01	5.4869E 01	5.3508E 01	5.2258E 01	5.1106E 01	5.0042E 01	4.9056E 01	4.8141E 01
9.0	5.4601E 01	5.3054E 01	5.1642E 01	5.0349E 01	4.9160E 01	4.8066E 01	4.7058E 01	4.6127E 01	4.5269E 01
10.0	5.0762E 01	4.9345E 01	4.8046E 01	4.6849E 01	4.5743E 01	4.4718E 01	4.3766E 01	4.2881E 01	4.2058E 01
12.0	4.4619E 01	4.3384E 01	4.2238E 01	4.1171E 01	4.0171E 01	3.9231E 01	3.8344E 01	3.7505E 01	3.6710E 01
14.0	3.9965E 01	3.8867E 01	3.7842E 01	3.6877E 01	3.5965E 01	3.5099E 01	3.4273E 01	3.3482E 01	3.2723E 01
16.0	3.6317E 01	3.5333E 01	3.4409E 01	3.3535E 01	3.2703E 01	3.1908E 01	3.1145E 01	3.0409E 01	2.9697E 01
18.0	3.3371E 01	3.2483E 01	3.1646E 01	3.0852E 01	3.0093E 01	2.9365E 01	2.8663E 01	2.7983E 01	2.7322E 01
20.0	3.0935E 01	3.0129E 01	2.9367E 01	2.8642E 01	2.7948E 01	2.7281E 01	2.6635E 01	2.6008E 01	2.5397E 01
22.0	2.8882E 01	2.8145E 01	2.7448E 01	2.6784E 01	2.6147E 01	2.5533E 01	2.4938E 01	2.4360E 01	2.3795E 01
24.0	2.7123E 01	2.6446E 01	2.5805E 01	2.5194E 01	2.4607E 01	2.4041E 01	2.3492E 01	2.2957E 01	2.2435E 01
26.0	2.5598E 01	2.4972E 01	2.4380E 01	2.3814E 01	2.3272E 01	2.2748E 01	2.2239E 01	2.1744E 01	2.1260E 01
28.0	2.4260E 01	2.3679E 01	2.3129E 01	2.2604E 01	2.2100E 01	2.1614E 01	2.1141E 01	2.0681E 01	2.0230E 01
30.0	2.3077E 01	2.2535E 01	2.2022E 01	2.1533E 01	2.1063E 01	2.0609E 01	2.0168E 01	1.9739E 01	1.9319E 01
32.0	2.2020E 01	2.1513E 01	2.1033E 01	2.0575E 01	2.0135E 01	1.9711E 01	1.9299E 01	1.8897E 01	1.8504E 01
34.0	2.1072E 01	2.0595E 01	2.0144E 01	1.9714E 01	1.9301E 01	1.8902E 01	1.8516E 01	1.8139E 01	1.7771E 01
36.0	2.0214E 01	1.9765E 01	1.9340E 01	1.8934E 01	1.8545E 01	1.8170E 01	1.7806E 01	1.7452E 01	1.7105E 01
38.0	1.9435E 01	1.9010E 01	1.8608E 01	1.8225E 01	1.7858E 01	1.7503E 01	1.7160E 01	1.6825E 01	1.6498E 01
40.0	1.8723E 01	1.8320E 01	1.7939E 01	1.7576E 01	1.7228E 01	1.6893E 01	1.6568E 01	1.6251E 01	1.5942E 01
42.0	1.8070E 01	1.7687E 01	1.7325E 01	1.6980E 01	1.6650E 01	1.6331E 01	1.6023E 01	1.5723E 01	1.5430E 01
44.0	1.7469E 01	1.7104E 01	1.6759E 01	1.6431E 01	1.6116E 01	1.5813E 01	1.5520E 01	1.5235E 01	1.4957E 01
46.0	1.6914E 01	1.6565E 01	1.6235E 01	1.5922E 01	1.5622E 01	1.5333E 01	1.5054E 01	1.4782E 01	1.4517E 01
48.0	1.6398E 01	1.6065E 01	1.5749E 01	1.5450E 01	1.5163E 01	1.4888E 01	1.4621E 01	1.4362E 01	1.4109E 01
50.0	1.5920E 01	1.5599E 01	1.5297E 01	1.5010E 01	1.4736E 01	1.4472E 01	1.4217E 01	1.3969E 01	1.3727E 01
55.0	1.4857E 01	1.4566E 01	1.4292E 01	1.4033E 01	1.3785E 01	1.3546E 01	1.3316E 01	1.3093E 01	1.2876E 01
60.0	1.3951E 01	1.3685E 01	1.3434E 01	1.3197E 01	1.2971E 01	1.2754E 01	1.2544E 01	1.2341E 01	1.2144E 01
65.0	1.3169E 01	1.2923E 01	1.2693E 01	1.2474E 01	1.2266E 01	1.2067E 01	1.1875E 01	1.1689E 01	1.1508E 01
70.0	1.2486E 01	1.2258E 01	1.2045E 01	1.1842E 01	1.1650E 01	1.1465E 01	1.1287E 01	1.1116E 01	1.0949E 01
75.0	1.1885E 01	1.1673E 01	1.1473E 01	1.1284E 01	1.1105E 01	1.0933E 01	1.0768E 01	1.0609E 01	1.0454E 01
80.0	1.1352E 01	1.1152E 01	1.0965E 01	1.0788E 01	1.0620E 01	1.0460E 01	1.0305E 01	1.0157E 01	1.0012E 01
85.0	1.0875E 01	1.0687E 01	1.0510E 01	1.0344E 01	1.0186E 01	1.0035E 01	9.8902E 00	9.7506E 00	9.6154E 00
90.0	1.0446E 01	1.0268E 01	1.0101E 01	9.9437E 00	9.7945E 00	9.6521E 00	9.5156E 00	9.3840E 00	9.2567E 00
95.0	1.0058E 01	9.8883E 00	9.7301E 00	9.5810E 00	9.4397E 00	9.3048E 00	9.1756E 00	9.0512E 00	8.9310E 00
100.0	9.7045E 00	9.5434E 00	9.3927E 00	9.2509E 00	9.1165E 00	8.9884E 00	8.8657E 00	8.7477E 00	8.6337E 00
105.0	9.3821E 00	9.2282E 00	9.0844E 00	8.9490E 00	8.8209E 00	8.6988E 00	8.5820E 00	8.4697E 00	8.3613E 00
110.0	9.0865E 00	8.9390E 00	8.8014E 00	8.6719E 00	8.5494E 00	8.4328E 00	8.3212E 00	8.2140E 00	8.1107E 00
115.0	8.8143E 00	8.6728E 00	8.5407E 00	8.4166E 00	8.2992E 00	8.1875E 00	8.0807E 00	7.9782E 00	7.8793E 00
120.0	8.5630E 00	8.4268E 00	8.2999E 00	8.1806E 00	8.0678E 00	7.9606E 00	7.8581E 00	7.7598E 00	7.6651E 00
125.0	8.3301E 00	8.1989E 00	8.0766E 00	7.9617E 00	7.8532E 00	7.7501E 00	7.6516E 00	7.5571E 00	7.4662E 00
130.0	8.1137E 00	7.9870E 00	7.8690E 00	7.7582E 00	7.6536E 00	7.5542E 00	7.4593E 00	7.3684E 00	7.2809E 00
135.0	7.9120E 00	7.7896E 00	7.6755E 00	7.5685E 00	7.4674E 00	7.3715E 00	7.2799E 00	7.1923E 00	7.1079E 00
140.0	7.7238E 00	7.6051E 00	7.4947E 00	7.3911E 00	7.2934E 00	7.2006E 00	7.1122E 00	7.0275E 00	6.9460E 00
145.0	7.5475E 00	7.4325E 00	7.3254E 00	7.2250E 00	7.1304E 00	7.0405E 00	6.9549E 00	6.8730E 00	6.7942E 00
150.0	7.3821E 00	7.2704E 00	7.1665E 00	7.0691E 00	6.9773E 00	6.8902E 00	6.8072E 00	6.7278E 00	6.6516E 00
155.0	7.2267E 00	7.1161E 00	7.0171E 00	6.9225E 00	6.8333E 00	6.7488E 00	6.6682E 00	6.5912E 00	6.5173E 00
160.0	7.0803E 00	6.9747E 00	6.8764E 00	6.7844E 00	6.6976E 00	6.6154E 00	6.5372E 00	6.4624E 00	6.3906E 00
165.0	6.9423E 00	6.8393E 00	6.7436E 00	6.6540E 00	6.5695E 00	6.4896E 00	6.4135E 00	6.3407E 00	6.2709E 00
170.0	6.8118E 00	6.7114E 00	6.6180E 00	6.5307E 00	6.4484E 00	6.3705E 00	6.2964E 00	6.2256E 00	6.1577E 00
175.0	6.6883E 00	6.5903E 00	6.4992E 00	6.4140E 00	6.3338E 00	6.2578E 00	6.1856E 00	6.1166E 00	6.0504E 00
180.0	6.5713E 00	6.4755E 00	6.3865E 00	6.3033E 00	6.2250E 00	6.1509E 00	6.0804E 00	6.0131E 00	5.9486E 00
185.0	6.4602E 00	6.3665E 00	6.2796E 00	6.1983E 00	6.1217E 00	6.0493E 00	5.9805E 00	5.9148E 00	5.8519E 00
190.0	6.3546E 00	6.2630E 00	6.1779E 00	6.0984E 00	6.0235E 00	5.9528E 00	5.8855E 00	5.8213E 00	5.7598E 00
195.0	6.2542E 00	6.1644E 00	6.0812E 00	6.0033E 00	5.9301E 00	5.8608E 00	5.7950E 00	5.7323E 00	5.6722E 00
200.0	6.1585E 00	6.0706E 00	5.9890E 00	5.9127E 00	5.8410E 00	5.7732E 00	5.7088E 00	5.6474E 00	5.5886E 00
210.0	5.9801E 00	5.8955E 00	5.8170E 00	5.7437E 00	5.6748E 00	5.6097E 00	5.5479E 00	5.4890E 00	5.4326E 00
220.0	5.8172E 00	5.7356E 00	5.6599E 00	5.5893E 00	5.5229E 00	5.4602E 00	5.4007E 00	5.3441E 00	5.2898E 00
230.0	5.6678E 00	5.5890E 00	5.5159E 00	5.4477E 00	5.3836E 00	5.3231E 00	5.2657E 00	5.2111E 00	5.1588E 00
240.0	5.5304E 00	5.4541E 00	5.3833E 00	5.3173E 00	5.2553E 00	5.1968E 00	5.1414E 00	5.0886E 00	5.0381E 00
250.0	5.4036E 00	5.3296E 00	5.2610E 00	5.1970E 00	5.1369E 00	5.0802E 00	5.0265E 00	4.9754E 00	4.9265E 00
260.0	5.2863E 00	5.2143E 00	5.1477E 00	5.0855E 00	5.0272E 00	4.9722E 00	4.9201E 00	4.8705E 00	4.8232E 00
270.0	5.1774E 00	5.1074E 00	5.0425E 00	4.9821E 00	4.9254E 00	4.8720E 00	4.8213E 00	4.7732E 00	4.7272E 00
280.0	5.0761E 00	5.0079E 00	4.9447E 00	4.8858E 00	4.8306E 00	4.7786E 00	4.7294E 00	4.6825E 00	4.6378E 00
290.0	4.9816E 00	4.9150E 00	4.8534E 00	4.7960E 00	4.7422E 00	4.6915E 00	4.6435E 00	4.5979E 00	4.5544E 00
300.0	4.8933E 00	4.8283E 00	4.7682E 00	4.7121E 00	4.6596E 00	4.6101E 00	4.5633E 00	4.5188E 00	4.4763E 00
310.0	4.8106E 00	4.7471E 00	4.6883E 00	4.6335E 00	4.5822E 00	4.5339E 00	4.4881E 00	4.4447E 00	4.4032E 00
320.0	4.7331E 00	4.6709E 00	4.6133E 00	4.5598E 00	4.5096E 00	4.4623E 00	4.4176E 00	4.3751E 00	4.3346E 00
330.0	4.6602E 00	4.5993E 00	4.5429E 00	4.4904E 00	4.4413E 00	4.3950E 00	4.3512E 00	4.3097E 00	4.2701E 00
340.0	4.5916E 00	4.5318E 00	4.4766E 00	4.4252E 00	4.3770E 00	4.3317E 00	4.2888E 00	4.2481E 00	4.2093E 00
350.0	4.5269E 00	4.4683E 00	4.4141E 00	4.3636E 00	4.3164E 00	4.2719E 00	4.2299E 00	4.1900E 00	4.1520E 00
360.0	4.4659E 00	4.4083E 00	4.3551E 00	4.3055E 00	4.2591E 00	4.2155E 00	4.1743E 00	4.1351E 00	4.0978E 00
370.0	4.4081E 00	4.3515E 00	4.2992E 00	4.2506E 00	4.2050E 00	4.1622E 00	4.1217E 00	4.0832E 00	4.0466E 00
380.0	4.3535E 00	4.2978E 00	4.2464E 00	4.1986E 00	4.1538E 00	4.1117E 00	4.0719E 00	4.0341E 00	3.9981E 00
390.0	4.3017E 00	4.2469E 00	4.1963E 00	4.1493E 00	4.1052E 00	4.0638E 00	4.0246E 00	3.9875E 00	3.9522E 00
400.0	4.2526E 00	4.1986E 00	4.1488E 00	4.1025E 00	4.0591E 00	4.0183E 00	3.9798E 00	3.9433E 00	3.9085E 00

STOPPING POWER

ENERGY MEV	I= 550.0	I= 600.0	I= 650.0	I= 700.0	I= 750.0	I= 800.0	I= 850.0	I= 900.0	I= 950.0
410.0	4.2059E 00	4.1527E 00	4.1037E 00	4.0580E 00	4.0153E 00	3.9752E 00	3.9372E 00	3.9013E 00	3.8671E 00
420.0	4.1615E 00	4.1091E 00	4.0607E 00	4.0157E 00	3.9737E 00	3.9341E 00	3.8968E 00	3.8613E 00	3.8276E 00
430.0	4.1192E 00	4.0676E 00	4.0199E 00	3.9755E 00	3.9340E 00	3.8950E 00	3.8582E 00	3.8233E 00	3.7901E 00
440.0	4.0790E 00	4.0280E 00	3.9809E 00	3.9372E 00	3.8963E 00	3.8578E 00	3.8215E 00	3.7871E 00	3.7543E 00
450.0	4.0406E 00	3.9903E 00	3.9438E 00	3.9006E 00	3.8602E 00	3.8223E 00	3.7865E 00	3.7525E 00	3.7202E 00
460.0	4.0039E 00	3.9542E 00	3.9084E 00	3.8657E 00	3.8258E 00	3.7884E 00	3.7530E 00	3.7195E 00	3.6876E 00
470.0	3.9689E 00	3.9198E 00	3.8745E 00	3.8324E 00	3.7930E 00	3.7560E 00	3.7211E 00	3.6880E 00	3.6565E 00
480.0	3.9355E 00	3.8870E 00	3.8422E 00	3.8005E 00	3.7616E 00	3.7251E 00	3.6906E 00	3.6579E 00	3.6268E 00
490.0	3.9035E 00	3.8555E 00	3.8112E 00	3.7700E 00	3.7316E 00	3.6954E 00	3.6613E 00	3.6290E 00	3.5983E 00
500.0	3.8728E 00	3.8254E 00	3.7816E 00	3.7409E 00	3.7028E 00	3.6671E 00	3.6334E 00	3.6015E 00	3.5711E 00
510.0	3.8435E 00	3.7965E 00	3.7532E 00	3.7129E 00	3.6753E 00	3.6399E 00	3.6066E 00	3.5750E 00	3.5450E 00
520.0	3.8153E 00	3.7689E 00	3.7260E 00	3.6861E 00	3.6489E 00	3.6139E 00	3.5809E 00	3.5497E 00	3.5200E 00
530.0	3.7884E 00	3.7423E 00	3.6999E 00	3.6604E 00	3.6236E 00	3.5890E 00	3.5563E 00	3.5254E 00	3.4960E 00
540.0	3.7625E 00	3.7169E 00	3.6748E 00	3.6358E 00	3.5993E 00	3.5650E 00	3.5327E 00	3.5021E 00	3.4730E 00
550.0	3.7376E 00	3.6924E 00	3.6508E 00	3.6121E 00	3.5759E 00	3.5420E 00	3.5100E 00	3.4797E 00	3.4509E 00
560.0	3.7137E 00	3.6689E 00	3.6277E 00	3.5893E 00	3.5535E 00	3.5199E 00	3.4882E 00	3.4582E 00	3.4297E 00
570.0	3.6907E 00	3.6464E 00	3.6054E 00	3.5674E 00	3.5320E 00	3.4986E 00	3.4672E 00	3.4375E 00	3.4093E 00
580.0	3.6686E 00	3.6246E 00	3.5841E 00	3.5464E 00	3.5112E 00	3.4782E 00	3.4471E 00	3.4176E 00	3.3896E 00
590.0	3.6473E 00	3.6037E 00	3.5635E 00	3.5262E 00	3.4913E 00	3.4586E 00	3.4277E 00	3.3985E 00	3.3707E 00
600.0	3.6269E 00	3.5836E 00	3.5437E 00	3.5067E 00	3.4721E 00	3.4396E 00	3.4090E 00	3.3801E 00	3.3526E 00
610.0	3.6071E 00	3.5642E 00	3.5247E 00	3.4879E 00	3.4536E 00	3.4214E 00	3.3910E 00	3.3623E 00	3.3351E 00
620.0	3.5881E 00	3.5456E 00	3.5063E 00	3.4698E 00	3.4358E 00	3.4038E 00	3.3737E 00	3.3452E 00	3.3182E 00
630.0	3.5698E 00	3.5276E 00	3.4886E 00	3.4524E 00	3.4186E 00	3.3869E 00	3.3570E 00	3.3288E 00	3.3019E 00
640.0	3.5522E 00	3.5102E 00	3.4715E 00	3.4356E 00	3.4021E 00	3.3706E 00	3.3410E 00	3.3129E 00	3.2863E 00
650.0	3.5351E 00	3.4935E 00	3.4551E 00	3.4194E 00	3.3861E 00	3.3549E 00	3.3254E 00	3.2976E 00	3.2711E 00
660.0	3.5187E 00	3.4773E 00	3.4392E 00	3.4038E 00	3.3707E 00	3.3397E 00	3.3105E 00	3.2828E 00	3.2566E 00
670.0	3.5028E 00	3.4617E 00	3.4238E 00	3.3887E 00	3.3558E 00	3.3250E 00	3.2960E 00	3.2686E 00	3.2425E 00
680.0	3.4875E 00	3.4466E 00	3.4090E 00	3.3741E 00	3.3415E 00	3.3109E 00	3.2820E 00	3.2548E 00	3.2289E 00
690.0	3.4726E 00	3.4321E 00	3.3947E 00	3.3600E 00	3.3276E 00	3.2972E 00	3.2686E 00	3.2415E 00	3.2158E 00
700.0	3.4583E 00	3.4180E 00	3.3809E 00	3.3464E 00	3.3142E 00	3.2840E 00	3.2555E 00	3.2286E 00	3.2031E 00
710.0	3.4445E 00	3.4044E 00	3.3675E 00	3.3332E 00	3.3012E 00	3.2712E 00	3.2430E 00	3.2162E 00	3.1909E 00
720.0	3.4311E 00	3.3913E 00	3.3546E 00	3.3205E 00	3.2887E 00	3.2589E 00	3.2308E 00	3.2042E 00	3.1790E 00
730.0	3.4182E 00	3.3786E 00	3.3421E 00	3.3082E 00	3.2766E 00	3.2470E 00	3.2190E 00	3.1926E 00	3.1676E 00
740.0	3.4056E 00	3.3663E 00	3.3300E 00	3.2963E 00	3.2649E 00	3.2354E 00	3.2077E 00	3.1814E 00	3.1565E 00
750.0	3.3935E 00	3.3544E 00	3.3183E 00	3.2848E 00	3.2536E 00	3.2242E 00	3.1966E 00	3.1706E 00	3.1458E 00
760.0	3.3818E 00	3.3428E 00	3.3070E 00	3.2737E 00	3.2426E 00	3.2134E 00	3.1860E 00	3.1601E 00	3.1354E 00
770.0	3.3704E 00	3.3317E 00	3.2960E 00	3.2629E 00	3.2320E 00	3.2030E 00	3.1757E 00	3.1499E 00	3.1254E 00
780.0	3.3594E 00	3.3209E 00	3.2854E 00	3.2524E 00	3.2217E 00	3.1929E 00	3.1657E 00	3.1400E 00	3.1157E 00
790.0	3.3487E 00	3.3104E 00	3.2751E 00	3.2423E 00	3.2117E 00	3.1831E 00	3.1560E 00	3.1305E 00	3.1063E 00
800.0	3.3384E 00	3.3003E 00	3.2651E 00	3.2325E 00	3.2021E 00	3.1736E 00	3.1467E 00	3.1213E 00	3.0972E 00
810.0	3.3284E 00	3.2905E 00	3.2555E 00	3.2230E 00	3.1927E 00	3.1644E 00	3.1376E 00	3.1124E 00	3.0884E 00
820.0	3.3187E 00	3.2809E 00	3.2461E 00	3.2138E 00	3.1837E 00	3.1554E 00	3.1288E 00	3.1037E 00	3.0798E 00
830.0	3.3093E 00	3.2717E 00	3.2371E 00	3.2049E 00	3.1749E 00	3.1468E 00	3.1203E 00	3.0953E 00	3.0716E 00
840.0	3.3002E 00	3.2628E 00	3.2283E 00	3.1963E 00	3.1664E 00	3.1384E 00	3.1121E 00	3.0872E 00	3.0636E 00
850.0	3.2913E 00	3.2541E 00	3.2197E 00	3.1879E 00	3.1582E 00	3.1303E 00	3.1041E 00	3.0793E 00	3.0558E 00
860.0	3.2828E 00	3.2457E 00	3.2115E 00	3.1798E 00	3.1502E 00	3.1224E 00	3.0963E 00	3.0717E 00	3.0483E 00
870.0	3.2744E 00	3.2375E 00	3.2034E 00	3.1719E 00	3.1424E 00	3.1148E 00	3.0888E 00	3.0642E 00	3.0409E 00
880.0	3.2664E 00	3.2296E 00	3.1957E 00	3.1642E 00	3.1349E 00	3.1074E 00	3.0815E 00	3.0571E 00	3.0339E 00
890.0	3.2585E 00	3.2219E 00	3.1881E 00	3.1568E 00	3.1276E 00	3.1002E 00	3.0744E 00	3.0501E 00	3.0270E 00
900.0	3.2509E 00	3.2144E 00	3.1808E 00	3.1496E 00	3.1205E 00	3.0933E 00	3.0676E 00	3.0433E 00	3.0203E 00
910.0	3.2435E 00	3.2072E 00	3.1737E 00	3.1426E 00	3.1137E 00	3.0865E 00	3.0609E 00	3.0368E 00	3.0139E 00
920.0	3.2364E 00	3.2001E 00	3.1668E 00	3.1358E 00	3.1070E 00	3.0799E 00	3.0545E 00	3.0304E 00	3.0076E 00
930.0	3.2294E 00	3.1933E 00	3.1601E 00	3.1293E 00	3.1005E 00	3.0736E 00	3.0482E 00	3.0242E 00	3.0015E 00
940.0	3.2226E 00	3.1867E 00	3.1536E 00	3.1229E 00	3.0942E 00	3.0674E 00	3.0421E 00	3.0183E 00	2.9956E 00
950.0	3.2161E 00	3.1803E 00	3.1473E 00	3.1167E 00	3.0881E 00	3.0614E 00	3.0362E 00	3.0124E 00	2.9899E 00
960.0	3.2097E 00	3.1740E 00	3.1411E 00	3.1107E 00	3.0822E 00	3.0556E 00	3.0305E 00	3.0068E 00	2.9843E 00
970.0	3.2035E 00	3.1679E 00	3.1352E 00	3.1048E 00	3.0765E 00	3.0499E 00	3.0249E 00	3.0013E 00	2.9790E 00
980.0	3.1975E 00	3.1620E 00	3.1294E 00	3.0991E 00	3.0709E 00	3.0444E 00	3.0195E 00	2.9960E 00	2.9737E 00
990.0	3.1916E 00	3.1563E 00	3.1238E 00	3.0936E 00	3.0655E 00	3.0391E 00	3.0143E 00	2.9909E 00	2.9686E 00
1000.0	3.1859E 00	3.1507E 00	3.1183E 00	3.0883E 00	3.0602E 00	3.0339E 00	3.0092E 00	2.9858E 00	2.9637E 00
1100.0	3.1372E 00	3.1031E 00	3.0716E 00	3.0424E 00	3.0152E 00	2.9897E 00	2.9657E 00	2.9431E 00	2.9216E 00
1200.0	3.1005E 00	3.0672E 00	3.0365E 00	3.0080E 00	2.9815E 00	2.9567E 00	2.9333E 00	2.9113E 00	2.8904E 00
1300.0	3.0728E 00	3.0402E 00	3.0102E 00	2.9824E 00	2.9564E 00	2.9321E 00	2.9092E 00	2.8877E 00	2.8672E 00
1400.0	3.0522E 00	3.0202E 00	2.9907E 00	2.9633E 00	2.9379E 00	2.9140E 00	2.8916E 00	2.8704E 00	2.8504E 00
1500.0	3.0370E 00	3.0055E 00	2.9764E 00	2.9495E 00	2.9245E 00	2.9010E 00	2.8789E 00	2.8581E 00	2.8384E 00
1600.0	3.0261E 00	2.9950E 00	2.9664E 00	2.9399E 00	2.9151E 00	2.8920E 00	2.8703E 00	2.8497E 00	2.8303E 00
1800.0	3.0141E 00	2.9837E 00	2.9557E 00	2.9298E 00	2.9056E 00	2.8830E 00	2.8618E 00	2.8417E 00	2.8227E 00
2000.0	3.0112E 00	2.9814E 00	2.9539E 00	2.9284E 00	2.9047E 00	2.8825E 00	2.8616E 00	2.8420E 00	2.8233E 00
2200.0	3.0146E 00	2.9851E 00	2.9580E 00	2.9330E 00	2.9096E 00	2.8877E 00	2.8672E 00	2.8478E 00	2.8294E 00
2400.0	3.0222E 00	2.9931E 00	2.9663E 00	2.9415E 00	2.9184E 00	2.8968E 00	2.8765E 00	2.8573E 00	2.8392E 00
2600.0	3.0327E 00	3.0039E 00	2.9774E 00	2.9528E 00	2.9299E 00	2.9085E 00	2.8884E 00	2.8694E 00	2.8515E 00
2800.0	3.0452E 00	3.0167E 00	2.9904E 00	2.9660E 00	2.9433E 00	2.9221E 00	2.9021E 00	2.8833E 00	2.8655E 00
3000.0	3.0592E 00	3.0308E 00	3.0047E 00	2.9805E 00	2.9580E 00	2.9369E 00	2.9171E 00	2.8984E 00	2.8807E 00
3200.0	3.0742E 00	3.0459E 00	3.0200E 00	2.9959E 00	2.9735E 00	2.9526E 00	2.9329E 00	2.9143E 00	2.8967E 00
3400.0	3.0897E 00	3.0617E 00	3.0358E 00	3.0119E 00	2.9896E 00	2.9688E 00	2.9492E 00	2.9307E 00	2.9132E 00
3600.0	3.1057E 00	3.0778E 00	3.0521E 00	3.0282E 00	3.0061E 00	2.9853E 00	2.9658E 00	2.9474E 00	2.9300E 00
3800.0	3.1220E 00	3.0941E 00	3.0685E 00	3.0448E 00	3.0227E 00	3.0020E 00	2.9826E 00	2.9642E 00	2.9469E 00
4000.0	3.1383E 00	3.1105E 00	3.0850E 00	3.0613E 00	3.0393E 00	3.0187E 00	2.9994E 00	2.9811E 00	2.9638E 00
4500.0	3.1790E 00	3.1514E 00	3.1260E 00	3.1026E 00	3.0807E 00	3.0602E 00	3.0410E 00	3.0229E 00	3.0057E 00
5000.0	3.2188E 00	3.1914E 00	3.1661E 00	3.1428E 00	3.1210E 00	3.1007E 00	3.0815E 00	3.0635E 00	3.0464E 00

PRINTOUT TABLE II

TWO-VARIABLE RANGE TABLE

Calculated range, λ, as a function of the proton kinetic energy τ and the mean excitation energy I_{adj}. (Because of typographical limitations, I_{adj} is indicated as I in the table headings. The units of I_{adj} are ev.) The entries, when multiplied by A/Z, give the range in units of g cm^{-2}. Powers of ten are indicated by the symbol E; thus 1.2345E-02 means 1.2345×10^{-2}. Since energy/mass is a function only of the velocity, the column labeled energy is also to be interpreted as the particle kinetic energy divided by the mass in units of the proton mass. The range is then given by Equation 6. More figures are tabulated than are significant in order to facilitate interpolation and differencing. Example of use: Suppose it is required to find the energy of a He^3 beam which has a range of 300 gm/cm^2 in iron (I_{adj} = 285 ev). On dividing by A/Z (=2.1481), from Table 9, this range is 139.66 $(Z/A)g/cm^2$. Then, using Equation 6, we find $\lambda + B_2 = 186.64$ $(Z/A)g/cm^2$. Now B_2 is found from Equation 11 to be only 0.0003 in these units so that $\lambda = 186.64$ $(Z/A)g/cm^2$. From Table 8 we find $\tau = 915$ Mev. Then using Printout Table I, $T = M\tau = 4.(0.74829)915 = 2738$ Mev.

RANGE

ENERGY MEV	I= 15.0	I= 17.5	I= 20.0	I= 30.0	I= 40.0	I= 50.0	I= 60.0	I= 70.0	I= 80.0
1.0	7.7449E-04	8.1110E-04	8.4553E-04	9.6783E-04	1.0738E-03	1.1694E-03	1.2575E-03	1.3400E-03	1.4180E-03
2.0	2.7486E-03	2.8278E-03	2.9036E-03	3.1804E-03	3.4257E-03	3.6491E-03	3.8563E-03	4.0508E-03	4.2352E-03
3.0	5.7500E-03	5.8785E-03	6.0035E-03	6.4686E-03	6.8872E-03	7.2710E-03	7.6280E-03	7.9638E-03	8.2821E-03
4.0	9.6951E-03	9.8860E-03	1.0073E-02	1.0772E-02	1.1405E-02	1.1985E-02	1.2525E-02	1.3032E-02	1.3513E-02
5.0	1.4529E-02	1.4800E-02	1.5066E-02	1.6057E-02	1.6950E-02	1.7768E-02	1.8526E-02	1.9237E-02	1.9909E-02
6.0	2.0210E-02	2.0585E-02	2.0950E-02	2.2301E-02	2.3508E-02	2.4607E-02	2.5622E-02	2.6571E-02	2.7465E-02
7.0	2.6706E-02	2.7212E-02	2.7700E-02	2.9488E-02	3.1068E-02	3.2495E-02	3.3808E-02	3.5031E-02	3.6179E-02
8.0	3.3995E-02	3.4664E-02	3.5302E-02	3.7611E-02	3.9624E-02	4.1430E-02	4.3082E-02	4.4614E-02	4.6049E-02
9.0	4.2198E-02	4.3049E-02	4.3855E-02	4.6715E-02	4.9170E-02	5.1352E-02	5.3335E-02	5.5166E-02	5.6876E-02
10.0	5.1218E-02	5.2268E-02	5.3253E-02	5.6707E-02	5.9633E-02	6.2215E-02	6.4550E-02	6.6699E-02	6.8701E-02
12.0	7.1642E-02	7.3132E-02	7.4513E-02	7.9278E-02	8.3243E-02	8.6703E-02	8.9811E-02	9.2655E-02	9.5293E-02
14.0	9.5172E-02	9.7156E-02	9.8984E-02	1.0522E-01	1.1034E-01	1.1478E-01	1.1875E-01	1.2236E-01	1.2571E-01
16.0	1.2174E-01	1.2427E-01	1.2659E-01	1.3444E-01	1.4085E-01	1.4636E-01	1.5127E-01	1.5572E-01	1.5984E-01
18.0	1.5127E-01	1.5440E-01	1.5726E-01	1.6689E-01	1.7468E-01	1.8136E-01	1.8728E-01	1.9265E-01	1.9760E-01
20.0	1.8372E-01	1.8750E-01	1.9094E-01	2.0248E-01	2.1177E-01	2.1971E-01	2.2672E-01	2.3307E-01	2.3891E-01
22.0	2.1903E-01	2.2351E-01	2.2758E-01	2.4116E-01	2.5206E-01	2.6134E-01	2.6953E-01	2.7692E-01	2.8370E-01
24.0	2.5717E-01	2.6239E-01	2.6713E-01	2.8289E-01	2.9550E-01	3.0620E-01	3.1563E-01	3.2413E-01	3.3192E-01
26.0	2.9808E-01	3.0409E-01	3.0954E-01	3.2762E-01	3.4203E-01	3.5425E-01	3.6499E-01	3.7466E-01	3.8351E-01
28.0	3.4173E-01	3.4857E-01	3.5477E-01	3.7530E-01	3.9161E-01	4.0542E-01	4.1754E-01	4.2844E-01	4.3841E-01
30.0	3.8807E-01	3.9579E-01	4.0278E-01	4.2588E-01	4.4420E-01	4.5967E-01	4.7324E-01	4.8543E-01	4.9656E-01
32.0	4.3708E-01	4.4573E-01	4.5354E-01	4.7934E-01	4.9975E-01	5.1697E-01	5.3205E-01	5.4558E-01	5.5794E-01
34.0	4.8873E-01	4.9833E-01	5.0702E-01	5.3562E-01	5.5822E-01	5.7726E-01	5.9392E-01	6.0886E-01	6.2249E-01
36.0	5.4297E-01	5.5358E-01	5.6317E-01	5.9471E-01	6.1958E-01	6.4052E-01	6.5882E-01	6.7522E-01	6.9017E-01
38.0	5.9978E-01	6.1144E-01	6.2196E-01	6.5655E-01	6.8380E-01	7.0671E-01	7.2671E-01	7.4462E-01	7.6093E-01
40.0	6.5913E-01	6.7188E-01	6.8338E-01	7.2113E-01	7.5083E-01	7.7578E-01	7.9755E-01	8.1702E-01	8.3476E-01
42.0	7.2100E-01	7.3487E-01	7.4737E-01	7.8841E-01	8.2065E-01	8.4771E-01	8.7130E-01	8.9240E-01	9.1159E-01
44.0	7.8534E-01	8.0038E-01	8.1393E-01	8.5835E-01	8.9322E-01	9.2246E-01	9.4794E-01	9.7070E-01	9.9141E-01
46.0	8.5215E-01	8.6839E-01	8.8302E-01	9.3094E-01	9.6852E-01	1.0000E 00	1.0274E 00	1.0519E 00	1.0742E 00
48.0	9.2139E-01	9.3887E-01	9.5461E-01	1.0061E 00	1.0465E 00	1.0803E 00	1.1097E 00	1.1360E 00	1.1599E 00
50.0	9.9304E-01	1.0118E 00	1.0287E 00	1.0839E 00	1.1272E 00	1.1634E 00	1.1948E 00	1.2229E 00	1.2484E 00
55.0	1.1825E 00	1.2047E 00	1.2245E 00	1.2895E 00	1.3403E 00	1.3827E 00	1.4196E 00	1.4524E 00	1.4822E 00
60.0	1.3866E 00	1.4123E 00	1.4354E 00	1.5107E 00	1.5695E 00	1.6186E 00	1.6612E 00	1.6991E 00	1.7334E 00
65.0	1.6049E 00	1.6343E 00	1.6608E 00	1.7472E 00	1.8145E 00	1.8705E 00	1.9191E 00	1.9624E 00	2.0016E 00
70.0	1.8370E 00	1.8705E 00	1.9006E 00	1.9985E 00	2.0747E 00	2.1382E 00	2.1932E 00	2.2421E 00	2.2863E 00
75.0	2.0828E 00	2.1205E 00	2.1543E 00	2.2645E 00	2.3500E 00	2.4212E 00	2.4829E 00	2.5376E 00	2.5872E 00
80.0	2.3419E 00	2.3840E 00	2.4218E 00	2.5446E 00	2.6400E 00	2.7193E 00	2.7879E 00	2.8488E 00	2.9039E 00
85.0	2.6140E 00	2.6607E 00	2.7026E 00	2.8387E 00	2.9443E 00	3.0320E 00	3.1079E 00	3.1752E 00	3.2361E 00
90.0	2.8989E 00	2.9504E 00	2.9966E 00	3.1465E 00	3.2627E 00	3.3592E 00	3.4426E 00	3.5166E 00	3.5834E 00
95.0	3.1964E 00	3.2528E 00	3.3034E 00	3.4677E 00	3.5949E 00	3.7005E 00	3.7917E 00	3.8726E 00	3.9456E 00
100.0	3.5061E 00	3.5677E 00	3.6229E 00	3.8020E 00	3.9407E 00	4.0556E 00	4.1549E 00	4.2429E 00	4.3224E 00
105.0	3.8279E 00	3.8948E 00	3.9548E 00	4.1492E 00	4.2996E 00	4.4243E 00	4.5319E 00	4.6273E 00	4.7133E 00
110.0	4.1615E 00	4.2339E 00	4.2988E 00	4.5091E 00	4.6716E 00	4.8063E 00	4.9225E 00	5.0254E 00	5.1183E 00
115.0	4.5067E 00	4.5848E 00	4.6547E 00	4.8813E 00	5.0563E 00	5.2013E 00	5.3264E 00	5.4371E 00	5.5370E 00
120.0	4.8633E 00	4.9472E 00	5.0224E 00	5.2657E 00	5.4536E 00	5.6092E 00	5.7433E 00	5.8620E 00	5.9691E 00
125.0	5.2311E 00	5.3210E 00	5.4015E 00	5.6620E 00	5.8631E 00	6.0296E 00	6.1730E 00	6.2999E 00	6.4144E 00
130.0	5.6099E 00	5.7059E 00	5.7919E 00	6.0701E 00	6.2847E 00	6.4623E 00	6.6153E 00	6.7506E 00	6.8726E 00
135.0	5.9995E 00	6.1018E 00	6.1934E 00	6.4897E 00	6.7182E 00	6.9072E 00	7.0699E 00	7.2139E 00	7.3436E 00
140.0	6.3997E 00	6.5085E 00	6.6058E 00	6.9206E 00	7.1633E 00	7.3639E 00	7.5367E 00	7.6894E 00	7.8271E 00
145.0	6.8103E 00	6.9257E 00	7.0289E 00	7.3626E 00	7.6198E 00	7.8323E 00	8.0153E 00	8.1771E 00	8.3228E 00
150.0	7.2312E 00	7.3533E 00	7.4625E 00	7.8156E 00	8.0875E 00	8.3123E 00	8.5057E 00	8.6766E 00	8.8306E 00
155.0	7.6622E 00	7.7911E 00	7.9065E 00	8.2793E 00	8.5663E 00	8.8035E 00	9.0075E 00	9.1878E 00	9.3502E 00
160.0	8.1030E 00	8.2390E 00	8.3606E 00	8.7535E 00	9.0560E 00	9.3058E 00	9.5206E 00	9.7105E 00	9.8814E 00
165.0	8.5536E 00	8.6968E 00	8.8248E 00	9.2382E 00	9.5563E 00	9.8190E 00	1.0045E 01	1.0244E 01	1.0424E 01
170.0	9.0138E 00	9.1642E 00	9.2987E 00	9.7330E 00	1.0067E 01	1.0343E 01	1.0580E 01	1.0789E 01	1.0978E 01
175.0	9.4835E 00	9.6413E 00	9.7824E 00	1.0238E 01	1.0588E 01	1.0877E 01	1.1126E 01	1.1345E 01	1.1543E 01
180.0	9.9623E 00	1.0128E 01	1.0276E 01	1.0753E 01	1.1119E 01	1.1422E 01	1.1682E 01	1.1912E 01	1.2119E 01
185.0	1.0450E 01	1.0623E 01	1.0778E 01	1.1277E 01	1.1661E 01	1.1977E 01	1.2249E 01	1.2489E 01	1.2705E 01
190.0	1.0947E 01	1.1128E 01	1.1290E 01	1.1811E 01	1.2212E 01	1.2542E 01	1.2826E 01	1.3077E 01	1.3302E 01
195.0	1.1453E 01	1.1642E 01	1.1810E 01	1.2354E 01	1.2772E 01	1.3117E 01	1.3413E 01	1.3675E 01	1.3909E 01
200.0	1.1968E 01	1.2164E 01	1.2340E 01	1.2907E 01	1.3343E 01	1.3702E 01	1.4010E 01	1.4282E 01	1.4527E 01
210.0	1.3022E 01	1.3235E 01	1.3426E 01	1.4040E 01	1.4511E 01	1.4899E 01	1.5233E 01	1.5527E 01	1.5792E 01
220.0	1.4110E 01	1.4340E 01	1.4545E 01	1.5207E 01	1.5715E 01	1.6134E 01	1.6493E 01	1.6810E 01	1.7095E 01
230.0	1.5230E 01	1.5477E 01	1.5698E 01	1.6409E 01	1.6955E 01	1.7405E 01	1.7790E 01	1.8131E 01	1.8436E 01
240.0	1.6381E 01	1.6646E 01	1.6882E 01	1.7644E 01	1.8229E 01	1.8710E 01	1.9123E 01	1.9487E 01	1.9814E 01
250.0	1.7562E 01	1.7845E 01	1.8098E 01	1.8911E 01	1.9535E 01	2.0049E 01	2.0489E 01	2.0877E 01	2.1226E 01
260.0	1.8773E 01	1.9074E 01	1.9343E 01	2.0210E 01	2.0874E 01	2.1420E 01	2.1889E 01	2.2302E 01	2.2673E 01
270.0	2.0012E 01	2.0332E 01	2.0618E 01	2.1538E 01	2.2243E 01	2.2824E 01	2.3321E 01	2.3759E 01	2.4153E 01
280.0	2.1279E 01	2.1618E 01	2.1921E 01	2.2896E 01	2.3643E 01	2.4257E 01	2.4784E 01	2.5248E 01	2.5665E 01
290.0	2.2572E 01	2.2931E 01	2.3252E 01	2.4282E 01	2.5072E 01	2.5721E 01	2.6278E 01	2.6768E 01	2.7208E 01
300.0	2.3892E 01	2.4271E 01	2.4609E 01	2.5697E 01	2.6529E 01	2.7214E 01	2.7801E 01	2.8317E 01	2.8781E 01
310.0	2.5237E 01	2.5636E 01	2.5992E 01	2.7137E 01	2.8014E 01	2.8735E 01	2.9352E 01	2.9896E 01	3.0384E 01
320.0	2.6607E 01	2.7026E 01	2.7401E 01	2.8605E 01	2.9526E 01	3.0283E 01	3.0932E 01	3.1503E 01	3.2015E 01
330.0	2.8000E 01	2.8441E 01	2.8834E 01	3.0097E 01	3.1063E 01	3.1858E 01	3.2538E 01	3.3137E 01	3.3674E 01
340.0	2.9417E 01	2.9879E 01	3.0290E 01	3.1614E 01	3.2626E 01	3.3458E 01	3.4170E 01	3.4797E 01	3.5359E 01
350.0	3.0857E 01	3.1340E 01	3.1770E 01	3.3155E 01	3.4214E 01	3.5084E 01	3.5828E 01	3.6484E 01	3.7071E 01
360.0	3.2318E 01	3.2823E 01	3.3273E 01	3.4719E 01	3.5825E 01	3.6734E 01	3.7511E 01	3.8195E 01	3.8809E 01
370.0	3.3801E 01	3.4328E 01	3.4797E 01	3.6306E 01	3.7460E 01	3.8407E 01	3.9218E 01	3.9931E 01	4.0571E 01
380.0	3.5305E 01	3.5854E 01	3.6343E 01	3.7916E 01	3.9117E 01	4.0104E 01	4.0948E 01	4.1691E 01	4.2357E 01
390.0	3.6829E 01	3.7400E 01	3.7910E 01	3.9546E 01	4.0797E 01	4.1823E 01	4.2701E 01	4.3474E 01	4.4166E 01
400.0	3.8373E 01	3.8967E 01	3.9497E 01	4.1198E 01	4.2497E 01	4.3564E 01	4.4477E 01	4.5279E 01	4.5999E 01

RANGE

ENERGY MEV	I= 15.0	I= 17.5	I= 20.0	I= 30.0	I= 40.0	I= 50.0	I= 60.0	I= 70.0	I= 80.0
410.0	3.9936E 01	4.0553E 01	4.1103E 01	4.2869E 01	4.4219E 01	4.5326E 01	4.6273E 01	4.7106E 01	4.7853E 01
420.0	4.1518E 01	4.2158E 01	4.2729E 01	4.4561E 01	4.5960E 01	4.7109E 01	4.8091E 01	4.8955E 01	4.9729E 01
430.0	4.3118E 01	4.3782E 01	4.4373E 01	4.6272E 01	4.7722E 01	4.8912E 01	4.9929E 01	5.0824E 01	5.1625E 01
440.0	4.4736E 01	4.5423E 01	4.6035E 01	4.8002E 01	4.9503E 01	5.0734E 01	5.1787E 01	5.2713E 01	5.3542E 01
450.0	4.6371E 01	4.7082E 01	4.7716E 01	4.9749E 01	5.1302E 01	5.2575E 01	5.3664E 01	5.4622E 01	5.5479E 01
460.0	4.8023E 01	4.8758E 01	4.9413E 01	5.1515E 01	5.3120E 01	5.4435E 01	5.5561E 01	5.6549E 01	5.7435E 01
470.0	4.9692E 01	5.0451E 01	5.1127E 01	5.3298E 01	5.4955E 01	5.6314E 01	5.7475E 01	5.8496E 01	5.9410E 01
480.0	5.1376E 01	5.2160E 01	5.2858E 01	5.5098E 01	5.6808E 01	5.8209E 01	5.9408E 01	6.0460E 01	6.1404E 01
490.0	5.3076E 01	5.3884E 01	5.4604E 01	5.6914E 01	5.8677E 01	6.0122E 01	6.1357E 01	6.2443E 01	6.3415E 01
500.0	5.4792E 01	5.5624E 01	5.6366E 01	5.8747E 01	6.0563E 01	6.2052E 01	6.3324E 01	6.4442E 01	6.5443E 01
510.0	5.6522E 01	5.7379E 01	5.8144E 01	6.0595E 01	6.2465E 01	6.3998E 01	6.5307E 01	6.6458E 01	6.7489E 01
520.0	5.8267E 01	5.9149E 01	5.9936E 01	6.2458E 01	6.4382E 01	6.5959E 01	6.7307E 01	6.8491E 01	6.9551E 01
530.0	6.0025E 01	6.0933E 01	6.1742E 01	6.4337E 01	6.6315E 01	6.7936E 01	6.9322E 01	7.0539E 01	7.1629E 01
540.0	6.1798E 01	6.2731E 01	6.3563E 01	6.6229E 01	6.8263E 01	6.9929E 01	7.1352E 01	7.2603E 01	7.3723E 01
550.0	6.3584E 01	6.4543E 01	6.5397E 01	6.8136E 01	7.0225E 01	7.1936E 01	7.3398E 01	7.4682E 01	7.5831E 01
560.0	6.5383E 01	6.6367E 01	6.7244E 01	7.0057E 01	7.2201E 01	7.3957E 01	7.5458E 01	7.6775E 01	7.7959E 01
570.0	6.7195E 01	6.8205E 01	6.9105E 01	7.1991E 01	7.4191E 01	7.5993E 01	7.7532E 01	7.8883E 01	8.0094E 01
580.0	6.9019E 01	7.0055E 01	7.0979E 01	7.3938E 01	7.6194E 01	7.8042E 01	7.9620E 01	8.1005E 01	8.2246E 01
590.0	7.0856E 01	7.1918E 01	7.2864E 01	7.5898E 01	7.8210E 01	8.0104E 01	8.1721E 01	8.3141E 01	8.4412E 01
600.0	7.2704E 01	7.3793E 01	7.4762E 01	7.7871E 01	8.0239E 01	8.2179E 01	8.3836E 01	8.5290E 01	8.6592E 01
610.0	7.4564E 01	7.5679E 01	7.6672E 01	7.9856E 01	8.2281E 01	8.4267E 01	8.5963E 01	8.7452E 01	8.8785E 01
620.0	7.6436E 01	7.7577E 01	7.8594E 01	8.1853E 01	8.4335E 01	8.6367E 01	8.8103E 01	8.9627E 01	9.0991E 01
630.0	7.8318E 01	7.9486E 01	8.0527E 01	8.3861E 01	8.6400E 01	8.8480E 01	9.0255E 01	9.1814E 01	9.3209E 01
640.0	8.0212E 01	8.1406E 01	8.2470E 01	8.5881E 01	8.8478E 01	9.0604E 01	9.2420E 01	9.4013E 01	9.5439E 01
650.0	8.2115E 01	8.3337E 01	8.4425E 01	8.7911E 01	9.0566E 01	9.2740E 01	9.4595E 01	9.6224E 01	9.7682E 01
660.0	8.4030E 01	8.5278E 01	8.6390E 01	8.9953E 01	9.2666E 01	9.4887E 01	9.6783E 01	9.8446E 01	9.9935E 01
670.0	8.5954E 01	8.7229E 01	8.8365E 01	9.2005E 01	9.4776E 01	9.7044E 01	9.8981E 01	1.0068E 02	1.0220E 02
680.0	8.7888E 01	8.9191E 01	9.0351E 01	9.4067E 01	9.6897E 01	9.9213E 01	1.0119E 02	1.0292E 02	1.0448E 02
690.0	8.9832E 01	9.1162E 01	9.2346E 01	9.6140E 01	9.9028E 01	1.0139E 02	1.0341E 02	1.0518E 02	1.0676E 02
700.0	9.1785E 01	9.3142E 01	9.4351E 01	9.8222E 01	1.0117E 02	1.0358E 02	1.0564E 02	1.0745E 02	1.0906E 02
710.0	9.3747E 01	9.5132E 01	9.6365E 01	1.0031E 02	1.0332E 02	1.0578E 02	1.0788E 02	1.0972E 02	1.1137E 02
720.0	9.5718E 01	9.7131E 01	9.8388E 01	1.0242E 02	1.0548E 02	1.0799E 02	1.1013E 02	1.1201E 02	1.1369E 02
730.0	9.7699E 01	9.9138E 01	1.0042E 02	1.0453E 02	1.0765E 02	1.1021E 02	1.1239E 02	1.1430E 02	1.1602E 02
740.0	9.9687E 01	1.0115E 02	1.0246E 02	1.0665E 02	1.0983E 02	1.1244E 02	1.1466E 02	1.1661E 02	1.1835E 02
750.0	1.0168E 02	1.0318E 02	1.0451E 02	1.0877E 02	1.1202E 02	1.1467E 02	1.1694E 02	1.1892E 02	1.2070E 02
760.0	1.0369E 02	1.0521E 02	1.0657E 02	1.1091E 02	1.1421E 02	1.1692E 02	1.1922E 02	1.2125E 02	1.2305E 02
770.0	1.0570E 02	1.0725E 02	1.0863E 02	1.1306E 02	1.1642E 02	1.1917E 02	1.2152E 02	1.2358E 02	1.2542E 02
780.0	1.0772E 02	1.0930E 02	1.1071E 02	1.1521E 02	1.1863E 02	1.2143E 02	1.2382E 02	1.2592E 02	1.2779E 02
790.0	1.0975E 02	1.1136E 02	1.1279E 02	1.1737E 02	1.2086E 02	1.2371E 02	1.2614E 02	1.2827E 02	1.3017E 02
800.0	1.1179E 02	1.13^2E 02	1.1488E 02	1.1954E 02	1.2309E 02	1.2598E 02	1.2846E 02	1.3063E 02	1.3257E 02
810.0	1.1383E 02	1.1550E 02	1.1698E 02	1.2172E 02	1.2532E 02	1.2827E 02	1.3079E 02	1.3299E 02	1.3496E 02
820.0	1.1588E 02	1.1757E 02	1.1908E 02	1.2390E 02	1.2757E 02	1.3057E 02	1.3312E 02	1.3536E 02	1.3737E 02
830.0	1.1794E 02	1.1966E 02	1.2119E 02	1.2609E 02	1.2982E 02	1.3287E 02	1.3547E 02	1.3775E 02	1.3978E 02
840.0	1.2001E 02	1.2175E 02	1.2331E 02	1.2829E 02	1.3208E 02	1.3518E 02	1.3782E 02	1.4013E 02	1.4221E 02
850.0	1.2208E 02	1.2385E 02	1.2544E 02	1.3050E 02	1.3435E 02	1.3749E 02	1.4018E 02	1.4253E 02	1.4463E 02
860.0	1.2415E 02	1.2596E 02	1.2757E 02	1.3271E 02	1.3662E 02	1.3982E 02	1.4254E 02	1.4493E 02	1.4707E 02
870.0	1.2624E 02	1.2807E 02	1.2971E 02	1.3493E 02	1.3890E 02	1.4215E 02	1.4492E 02	1.4734E 02	1.4951E 02
880.0	1.2833E 02	1.3019E 02	1.3185E 02	1.3716E 02	1.4119E 02	1.4449E 02	1.4730E 02	1.4976E 02	1.5196E 02
890.0	1.3043E 02	1.3232E 02	1.3400E 02	1.3939E 02	1.4348E 02	1.4683E 02	1.4968E 02	1.5218E 02	1.5442E 02
900.0	1.3253E 02	1.3445E 02	1.3616E 02	1.4163E 02	1.4578E 02	1.4918E 02	1.5208E 02	1.5462E 02	1.5689E 02
910.0	1.3464E 02	1.3659E 02	1.3832E 02	1.4387E 02	1.4809E 02	1.5154E 02	1.5448E 02	1.5705E 02	1.5936E 02
920.0	1.3675E 02	1.3873E 02	1.4049E 02	1.4612E 02	1.5040E 02	1.5390E 02	1.5688E 02	1.5950E 02	1.6183E 02
930.0	1.3887E 02	1.4088E 02	1.4266E 02	1.4838E 02	1.5272E 02	1.5627E 02	1.5929E 02	1.6194E 02	1.6431E 02
940.0	1.4100E 02	1.4303E 02	1.4484E 02	1.5064E 02	1.5504E 02	1.5864E 02	1.6171E 02	1.6440E 02	1.6680E 02
950.0	1.4313E 02	1.4519E 02	1.4703E 02	1.5291E 02	1.5737E 02	1.6102E 02	1.6413E 02	1.6686E 02	1.6930E 02
960.0	1.4526E 02	1.4736E 02	1.4922E 02	1.5518E 02	1.5971E 02	1.6341E 02	1.6656E 02	1.6933E 02	1.7180E 02
970.0	1.4740E 02	1.4953E 02	1.5142E 02	1.5746E 02	1.6205E 02	1.6580E 02	1.6900E 02	1.7180E 02	1.7430E 02
980.0	1.4955E 02	1.5170E 02	1.5362E 02	1.5974E 02	1.6440E 02	1.6820E 02	1.7144E 02	1.7428E 02	1.7681E 02
990.0	1.5170E 02	1.5388E 02	1.5582E 02	1.6203E 02	1.6675E 02	1.7060E 02	1.7388E 02	1.7676E 02	1.7933E 02
1000.0	1.5386E 02	1.5607E 02	1.5804E 02	1.6433E 02	1.6910E 02	1.7301E 02	1.7633E 02	1.7925E 02	1.8185E 02
1100.0	1.7567E 02	1.7817E 02	1.8040E 02	1.8752E 02	1.9292E 02	1.9734E 02	2.0110E 02	2.0439E 02	2.0734E 02
1200.0	1.9786E 02	2.0066E 02	2.0315E 02	2.1111E 02	2.1715E 02	2.2208E 02	2.2628E 02	2.2995E 02	2.3324E 02
1300.0	2.2037E 02	2.2346E 02	2.2622E 02	2.3502E 02	2.4170E 02	2.4714E 02	2.5178E 02	2.5584E 02	2.5946E 02
1400.0	2.4313E 02	2.4653E 02	2.4955E 02	2.5919E 02	2.6650E 02	2.7247E 02	2.7754E 02	2.8199E 02	2.8595E 02
1500.0	2.6610E 02	2.6980E 02	2.7308E 02	2.8357E 02	2.9152E 02	2.9800E 02	3.0352E 02	3.0834E 02	3.1265E 02
1600.0	2.8924E 02	2.9323E 02	2.9678E 02	3.0812E 02	3.1671E 02	3.2370E 02	3.2966E 02	3.3487E 02	3.3952E 02
1800.0	3.3589E 02	3.4049E 02	3.4457E 02	3.5759E 02	3.6744E 02	3.7547E 02	3.8230E 02	3.8827E 02	3.9360E 02
2000.0	3.8290E 02	3.8808E 02	3.9269E 02	4.0739E 02	4.1851E 02	4.2756E 02	4.3526E 02	4.4198E 02	4.4798E 02
2200.0	4.3011E 02	4.3589E 02	4.4102E 02	4.5738E 02	4.6975E 02	4.7982E 02	4.8837E 02	4.9585E 02	5.0251E 02
2400.0	4.7743E 02	4.8379E 02	4.8945E 02	5.0746E 02	5.2106E 02	5.3214E 02	5.4154E 02	5.4976E 02	5.5708E 02
2600.0	5.2479E 02	5.3173E 02	5.3790E 02	5.5754E 02	5.7238E 02	5.8444E 02	5.9469E 02	6.0364E 02	6.1162E 02
2800.0	5.7213E 02	5.7965E 02	5.8633E 02	6.0759E 02	6.2364E 02	6.3669E 02	6.4777E 02	6.5744E 02	6.6606E 02
3000.0	6.1942E 02	6.2751E 02	6.3469E 02	6.5755E 02	6.7481E 02	6.8883E 02	7.0073E 02	7.1112E 02	7.2038E 02
3200.0	6.6663E 02	6.7528E 02	6.8297E 02	7.0741E 02	7.2585E 02	7.4084E 02	7.5355E 02	7.6465E 02	7.7453E 02
3400.0	7.1374E 02	7.2295E 02	7.3113E 02	7.5714E 02	7.7676E 02	7.9269E 02	8.0621E 02	8.1801E 02	8.2852E 02
3600.0	7.6073E 02	7.7050E 02	7.7916E 02	8.0673E 02	8.2751E 02	8.4439E 02	8.5870E 02	8.7119E 02	8.8231E 02
3800.0	8.0759E 02	8.1791E 02	8.2706E 02	8.5616E 02	8.7810E 02	8.9591E 02	9.1101E 02	9.2418E 02	9.3591E 02
4000.0	8.5432E 02	8.6518E 02	8.7482E 02	9.0544E 02	9.2851E 02	9.4725E 02	9.6312E 02	9.7698E 02	9.8930E 02
4500.0	9.7053E 02	9.8272E 02	9.9354E 02	1.0279E 03	1.0538E 03	1.0748E 03	1.0926E 03	1.1081E 03	1.1219E 03
5000.0	1.0858E 03	1.0993E 03	1.1113E 03	1.1493E 03	1.1780E 03	1.2012E 03	1.2208E 03	1.2380E 03	1.2532E 03

RANGE

ENERGY MEV	I= 90.0	I= 100.0	I= 120.0	I= 140.0	I= 160.0	I= 180.0	I= 200.0	I= 220.0	I= 240.0
1.0	1.4923E-03	1.5636E-03	1.6988E-03	1.8259E-03	1.9468E-03	2.0625E-03	2.1739E-03	2.2816E-03	2.3861E-03
2.0	4.4111E-03	4.5799E-03	4.8999E-03	5.2010E-03	5.4369E-03	5.7605E-03	6.0236E-03	6.2778E-03	6.5243E-03
3.0	8.5859E-03	8.8773E-03	9.4293E-03	9.9480E-03	1.0440E-02	1.0910E-02	1.1361E-02	1.1797E-02	1.2218E-02
4.0	1.3971E-02	1.4410E-02	1.5240E-02	1.6018E-02	1.6755E-02	1.7457E-02	1.8130E-02	1.8779E-02	1.9405E-02
5.0	2.0549E-02	2.1161E-02	2.2315E-02	2.3394E-02	2.4413E-02	2.5382E-02	2.6309E-02	2.7200E-02	2.8060E-02
6.0	2.8314E-02	2.9125E-02	3.0650E-02	3.2071E-02	3.3410E-02	3.4679E-02	3.5892E-02	3.7055E-02	3.8174E-02
7.0	3.7267E-02	3.8303E-02	4.0247E-02	4.2052E-02	4.3747E-02	4.5351E-02	4.6879E-02	4.8342E-02	4.9747E-02
8.0	4.7404E-02	4.8691E-02	5.1099E-02	5.3328E-02	5.5415E-02	5.7389E-02	5.9256E-02	6.1045E-02	6.2760E-02
9.0	5.8487E-02	6.0015E-02	6.2868E-02	6.5504E-02	6.7970E-02	7.0288E-02	7.2490E-02	7.4593E-02	7.6611E-02
10.0	7.0583E-02	7.2365E-02	7.5687E-02	7.8753E-02	8.1618E-02	8.4303E-02	8.6851E-02	8.9285E-02	9.1621E-02
12.0	9.7766E-02	1.0010E-01	1.0444E-01	1.0844E-01	1.1217E-01	1.1565E-01	1.1894E-01	1.2209E-01	1.2511E-01
14.0	1.2883E-01	1.3178E-01	1.3724E-01	1.4226E-01	1.4693E-01	1.5128E-01	1.5540E-01	1.5932E-01	1.6309E-01
16.0	1.6367E-01	1.6728E-01	1.7397E-01	1.8009E-01	1.8579E-01	1.9108E-01	1.9608E-01	2.0085E-01	2.0542E-01
18.0	2.0220E-01	2.0653E-01	2.1452E-01	2.2184E-01	2.2863E-01	2.3493E-01	2.4088E-01	2.4655E-01	2.5198E-01
20.0	2.4433E-01	2.4943E-01	2.5883E-01	2.6741E-01	2.7537E-01	2.8274E-01	2.8970E-01	2.9633E-01	3.0268E-01
22.0	2.9001E-01	2.9592E-01	3.0680E-01	3.1673E-01	3.2593E-01	3.3444E-01	3.4247E-01	3.5011E-01	3.5743E-01
24.0	3.3915E-01	3.4592E-01	3.5839E-01	3.6973E-01	3.8023E-01	3.8995E-01	3.9910E-01	4.0781E-01	4.1614E-01
26.0	3.9171E-01	3.9939E-01	4.1351E-01	4.2635E-01	4.3822E-01	4.4919E-01	4.5953E-01	4.6935E-01	4.7875E-01
28.0	4.4764E-01	4.5627E-01	4.7212E-01	4.8653E-01	4.9983E-01	5.1212E-01	5.2369E-01	5.3468E-01	5.4519E-01
30.0	5.0687E-01	5.1650E-01	5.3417E-01	5.5020E-01	5.6500E-01	5.7867E-01	5.9152E-01	6.0373E-01	6.1540E-01
32.0	5.6937E-01	5.8004E-01	5.9960E-01	6.1733E-01	6.3369E-01	6.4878E-01	6.6297E-01	6.7644E-01	6.8931E-01
34.0	6.3508E-01	6.4683E-01	6.6836E-01	6.8786E-01	7.0583E-01	7.2241E-01	7.3799E-01	7.5277E-01	7.6688E-01
36.0	7.0397E-01	7.1685E-01	7.4042E-01	7.6175E-01	7.8139E-01	7.9951E-01	8.1652E-01	8.3266E-01	8.4805E-01
38.0	7.7599E-01	7.9004E-01	8.1572E-01	8.3895E-01	8.6032E-01	8.8002E-01	8.9852E-01	9.1606E-01	9.3278E-01
40.0	8.5112E-01	8.6636E-01	8.9423E-01	9.1941E-01	9.4257E-01	9.6392E-01	9.8395E-01	1.0029E 00	1.0210E 00
42.0	9.2930E-01	9.4578E-01	9.7591E-01	1.0031E 00	1.0281E 00	1.0511E 00	1.0728E 00	1.0932E 00	1.1127E 00
44.0	1.0105E 00	1.0283E 00	1.0607E 00	1.0900E 00	1.1169E 00	1.1417E 00	1.1649E 00	1.1869E 00	1.2078E 00
46.0	1.0947E 00	1.1138E 00	1.1486E 00	1.1800E 00	1.2089E 00	1.2354E 00	1.2603E 00	1.2839E 00	1.3063E 00
48.0	1.1818E 00	1.2023E 00	1.2396E 00	1.2732E 00	1.3040E 00	1.3324E 00	1.3590E 00	1.3842E 00	1.4082E 00
50.0	1.2719E 00	1.2937E 00	1.3336E 00	1.3694E 00	1.4023E 00	1.4326E 00	1.4610E 00	1.4878E 00	1.5133E 00
55.0	1.5097E 00	1.5352E 00	1.5816E 00	1.6233E 00	1.6616E 00	1.6968E 00	1.7297E 00	1.7608E 00	1.7904E 00
60.0	1.7650E 00	1.7944E 00	1.8478E 00	1.8958E 00	1.9397E 00	1.9800E 00	2.0178E 00	2.0534E 00	2.0873E 00
65.0	2.0376E 00	2.0710E 00	2.1318E 00	2.1863E 00	2.2362E 00	2.2820E 00	2.3248E 00	2.3652E 00	2.4035E 00
70.0	2.3269E 00	2.3646E 00	2.4331E 00	2.4945E 00	2.5506E 00	2.6022E 00	2.6503E 00	2.6957E 00	2.7387E 00
75.0	2.6327E 00	2.6749E 00	2.7514E 00	2.8200E 00	2.8826E 00	2.9401E 00	2.9938E 00	3.0443E 00	3.0923E 00
80.0	2.9545E 00	3.0013E 00	3.0863E 00	3.1624E 00	3.2317E 00	3.2955E 00	3.3549E 00	3.4108E 00	3.4639E 00
85.0	3.2919E 00	3.3436E 00	3.4373E 00	3.5212E 00	3.5976E 00	3.6678E 00	3.7332E 00	3.7948E 00	3.8530E 00
90.0	3.6447E 00	3.7014E 00	3.8043E 00	3.8962E 00	3.9799E 00	4.0568E 00	4.1284E 00	4.1957E 00	4.2594E 00
95.0	4.0125E 00	4.0745E 00	4.1867E 00	4.2870E 00	4.3783E 00	4.4620E 00	4.5400E 00	4.6133E 00	4.6827E 00
100.0	4.3951E 00	4.4624E 00	4.5844E 00	4.6933E 00	4.7923E 00	4.8832E 00	4.9678E 00	5.0473E 00	5.1225E 00
105.0	4.7921E 00	4.8650E 00	4.9969E 00	5.1147E 00	5.2218E 00	5.3200E 00	5.4114E 00	5.4972E 00	5.5784E 00
110.0	5.2033E 00	5.2819E 00	5.4241E 00	5.5510E 00	5.6664E 00	5.7721E 00	5.8705E 00	5.9628E 00	6.0501E 00
115.0	5.6283E 00	5.7128E 00	5.8656E 00	6.0019E 00	6.1257E 00	6.2392E 00	6.3448E 00	6.4438E 00	6.5374E 00
120.0	6.0670E 00	6.1575E 00	6.3212E 00	6.4671E 00	6.5996E 00	6.7211E 00	6.8339E 00	6.9398E 00	7.0398E 00
125.0	6.5190E 00	6.6157E 00	6.7905E 00	6.9463E 00	7.0877E 00	7.2173E 00	7.3377E 00	7.4506E 00	7.5572E 00
130.0	6.9842E 00	7.0872E 00	7.2734E 00	7.4393E 00	7.5898E 00	7.7277E 00	7.8558E 00	7.9759E 00	8.0893E 00
135.0	7.4622E 00	7.5717E 00	7.7696E 00	7.9458E 00	8.1056E 00	8.2520E 00	8.3880E 00	8.5154E 00	8.6357E 00
140.0	7.9528E 00	8.0690E 00	8.2788E 00	8.4655E 00	8.6349E 00	8.7900E 00	8.9340E 00	9.0689E 00	9.1962E 00
145.0	8.4559E 00	8.5788E 00	8.8008E 00	8.9983E 00	9.1773E 00	9.3413E 00	9.4935E 00	9.6360E 00	9.7705E 00
150.0	8.9712E 00	9.1010E 00	9.3354E 00	9.5438E 00	9.7328E 00	9.9058E 00	1.0066E 01	1.0217E 01	1.0358E 01
155.0	9.4984E 00	9.6353E 00	9.8823E 00	1.0102E 01	1.0301E 01	1.0483E 01	1.0652E 01	1.0810E 01	1.0960E 01
160.0	1.0037E 01	1.0181E 01	1.0441E 01	1.0672E 01	1.0882E 01	1.1073E 01	1.1251E 01	1.1417E 01	1.1574E 01
165.0	1.0588E 01	1.0739E 01	1.1012E 01	1.1255E 01	1.1475E 01	1.1676E 01	1.1862E 01	1.2037E 01	1.2201E 01
170.0	1.1150E 01	1.1309E 01	1.1595E 01	1.1850E 01	1.2080E 01	1.2291E 01	1.2486E 01	1.2669E 01	1.2841E 01
175.0	1.1723E 01	1.1889E 01	1.2189E 01	1.2456E 01	1.2697E 01	1.2917E 01	1.3122E 01	1.3313E 01	1.3493E 01
180.0	1.2307E 01	1.2481E 01	1.2795E 01	1.3073E 01	1.3326E 01	1.3556E 01	1.3770E 01	1.3970E 01	1.4158E 01
185.0	1.2902E 01	1.3084E 01	1.3412E 01	1.3702E 01	1.3966E 01	1.4206E 01	1.4430E 01	1.4638E 01	1.4835E 01
190.0	1.3508E 01	1.3697E 01	1.4039E 01	1.4343E 01	1.4617E 01	1.4868E 01	1.5101E 01	1.5318E 01	1.5523E 01
195.0	1.4124E 01	1.4322E 01	1.4678E 01	1.4994E 01	1.5280E 01	1.5541E 01	1.5783E 01	1.6010E 01	1.6223E 01
200.0	1.4750E 01	1.4956E 01	1.5327E 01	1.5656E 01	1.5953E 01	1.6225E 01	1.6477E 01	1.6713E 01	1.6934E 01
210.0	1.6033E 01	1.6255E 01	1.6656E 01	1.7011E 01	1.7332E 01	1.7626E 01	1.7897E 01	1.8151E 01	1.8390E 01
220.0	1.7355E 01	1.7594E 01	1.8025E 01	1.8407E 01	1.8753E 01	1.9068E 01	1.9360E 01	1.9633E 01	1.9890E 01
230.0	1.8715E 01	1.8972E 01	1.9434E 01	1.9843E 01	2.0213E 01	2.0552E 01	2.0865E 01	2.1157E 01	2.1432E 01
240.0	2.0112E 01	2.0386E 01	2.0880E 01	2.1318E 01	2.1713E 01	2.2074E 01	2.2409E 01	2.2721E 01	2.3014E 01
250.0	2.1544E 01	2.1837E 01	2.2363E 01	2.2830E 01	2.3251E 01	2.3635E 01	2.3991E 01	2.4323E 01	2.4636E 01
260.0	2.3011E 01	2.3322E 01	2.3882E 01	2.4377E 01	2.4825E 01	2.5233E 01	2.5611E 01	2.5964E 01	2.6295E 01
270.0	2.4511E 01	2.4841E 01	2.5435E 01	2.5960E 01	2.6434E 01	2.6867E 01	2.7268E 01	2.7641E 01	2.7992E 01
280.0	2.6044E 01	2.6393E 01	2.7021E 01	2.7577E 01	2.8078E 01	2.8536E 01	2.8959E 01	2.9354E 01	2.9725E 01
290.0	2.7608E 01	2.7977E 01	2.8640E 01	2.9226E 01	2.9756E 01	3.0239E 01	3.0685E 01	3.1101E 01	3.1492E 01
300.0	2.9203E 01	2.9592E 01	3.0290E 01	3.0908E 01	3.1465E 01	3.1974E 01	3.2444E 01	3.2882E 01	3.3294E 01
310.0	3.0828E 01	3.1236E 01	3.1971E 01	3.2620E 01	3.3206E 01	3.3741E 01	3.4235E 01	3.4695E 01	3.5127E 01
320.0	3.2481E 01	3.2910E 01	3.3681E 01	3.4363E 01	3.4978E 01	3.5539E 01	3.6057E 01	3.6540E 01	3.6993E 01
330.0	3.4162E 01	3.4612E 01	3.5420E 01	3.6135E 01	3.6779E 01	3.7366E 01	3.7909E 01	3.8415E 01	3.8889E 01
340.0	3.5871E 01	3.6342E 01	3.7187E 01	3.7935E 01	3.8609E 01	3.9223E 01	3.9791E 01	4.0320E 01	4.0816E 01
350.0	3.7606E 01	3.8098E 01	3.8982E 01	3.9763E 01	4.0467E 01	4.1108E 01	4.1701E 01	4.2253E 01	4.2771E 01
360.0	3.9367E 01	3.9880E 01	4.0802E 01	4.1617E 01	4.2351E 01	4.3021E 01	4.3639E 01	4.4215E 01	4.4755E 01
370.0	4.1153E 01	4.1688E 01	4.2649E 01	4.3498E 01	4.4263E 01	4.4960E 01	4.5604E 01	4.6203E 01	4.6766E 01
380.0	4.2963E 01	4.3520E 01	4.4520E 01	4.5404E 01	4.6199E 01	4.6925E 01	4.7595E 01	4.8218E 01	4.8803E 01
390.0	4.4796E 01	4.5376E 01	4.6415E 01	4.7334E 01	4.8161E 01	4.8915E 01	4.9611E 01	5.0259E 01	5.0867E 01
400.0	4.6653E 01	4.7255E 01	4.8335E 01	4.9288E 01	5.0147E 01	5.0930E 01	5.1652E 01	5.2325E 01	5.2956E 01

RANGE

ENERGY MEV	I= 90.0	I= 100.0	I= 120.0	I= 140.0	I= 160.0	I= 180.0	I= 200.0	I= 220.0	I= 240.0
410.0	4.8532E 01	4.9156E 01	5.0276E 01	5.1266E 01	5.2157E 01	5.2968E 01	5.3718E 01	5.4415E 01	5.5069E 01
420.0	5.0432E 01	5.1080E 01	5.2241E 01	5.3266E 01	5.4189E 01	5.5030E 01	5.5806E 01	5.6528E 01	5.7206E 01
430.0	5.2354E 01	5.3024E 01	5.4227E 01	5.5288E 01	5.6244E 01	5.7114E 01	5.7917E 01	5.8665E 01	5.9366E 01
440.0	5.4297E 01	5.4990E 01	5.6234E 01	5.7332E 01	5.8320E 01	5.9220E 01	6.0051E 01	6.0824E 01	6.1548E 01
450.0	5.6259E 01	5.6976E 01	5.8261E 01	5.9396E 01	6.0417E 01	6.1348E 01	6.2206E 01	6.3004E 01	6.3753E 01
460.0	5.8241E 01	5.8981E 01	6.0309E 01	6.1481E 01	6.2535E 01	6.3496E 01	6.4381E 01	6.5206E 01	6.5978E 01
470.0	6.0242E 01	6.1006E 01	6.2376E 01	6.3585E 01	6.4673E 01	6.5664E 01	6.6578E 01	6.7428E 01	6.8224E 01
480.0	6.2261E 01	6.3049E 01	6.4462E 01	6.5709E 01	6.6830E 01	6.7852E 01	6.8794E 01	6.9670E 01	7.0491E 01
490.0	6.4299E 01	6.5111E 01	6.6567E 01	6.7851E 01	6.9006E 01	7.0059E 01	7.1029E 01	7.1932E 01	7.2777E 01
500.0	6.6353E 01	6.7190E 01	6.8689E 01	7.0012E 01	7.1201E 01	7.2284E 01	7.3283E 01	7.4212E 01	7.5082E 01
510.0	6.8425E 01	6.9286E 01	7.0829E 01	7.2190E 01	7.3414E 01	7.4528E 01	7.5555E 01	7.6511E 01	7.7406E 01
520.0	7.0514E 01	7.1399E 01	7.2986E 01	7.4385E 01	7.5644E 01	7.6790E 01	7.7846E 01	7.8828E 01	7.9748E 01
530.0	7.2619E 01	7.3529E 01	7.5160E 01	7.6598E 01	7.7891E 01	7.9068E 01	8.0153E 01	8.1162E 01	8.2107E 01
540.0	7.4740E 01	7.5674E 01	7.7349E 01	7.8827E 01	8.0154E 01	8.1363E 01	8.2478E 01	8.3514E 01	8.4484E 01
550.0	7.6876E 01	7.7835E 01	7.9555E 01	8.1071E 01	8.2434E 01	8.3675E 01	8.4819E 01	8.5882E 01	8.6878E 01
560.0	7.9027E 01	8.0012E 01	8.1776E 01	8.3332E 01	8.4730E 01	8.6003E 01	8.7176E 01	8.8266E 01	8.9287E 01
570.0	8.1193E 01	8.2203E 01	8.4012E 01	8.5607E 01	8.7041E 01	8.8346E 01	8.9548E 01	9.0666E 01	9.1713E 01
580.0	8.3373E 01	8.4408E 01	8.6263E 01	8.7897E 01	8.9366E 01	9.0704E 01	9.1936E 01	9.3081E 01	9.4154E 01
590.0	8.5567E 01	8.6627E 01	8.8527E 01	9.0202E 01	9.1707E 01	9.3077E 01	9.4339E 01	9.5512E 01	9.6610E 01
600.0	8.7775E 01	8.8861E 01	9.0806E 01	9.2521E 01	9.4062E 01	9.5464E 01	9.6756E 01	9.7957E 01	9.9081E 01
610.0	8.9995E 01	9.1107E 01	9.3098E 01	9.4853E 01	9.6430E 01	9.7865E 01	9.9187E 01	1.0042E 02	1.0157E 02
620.0	9.2229E 01	9.3367E 01	9.5404E 01	9.7199E 01	9.8812E 01	1.0028E 02	1.0163E 02	1.0289E 02	1.0406E 02
630.0	9.4476E 01	9.5639E 01	9.7722E 01	9.9558E 01	1.0121E 02	1.0271E 02	1.0409E 02	1.0537E 02	1.0658E 02
640.0	9.6734E 01	9.7923E 01	1.0005E 02	1.0193E 02	1.0362E 02	1.0515E 02	1.0656E 02	1.0787E 02	1.0910E 02
650.0	9.9005E 01	1.0022E 02	1.0240E 02	1.0431E 02	1.0604E 02	1.0760E 02	1.0905E 02	1.1039E 02	1.1164E 02
660.0	1.0129E 02	1.0253E 02	1.0475E 02	1.0671E 02	1.0847E 02	1.1007E 02	1.1154E 02	1.1291E 02	1.1419E 02
670.0	1.0358E 02	1.0485E 02	1.0712E 02	1.0912E 02	1.1091E 02	1.1255E 02	1.1405E 02	1.1545E 02	1.1676E 02
680.0	1.0589E 02	1.0718E 02	1.0950E 02	1.1154E 02	1.1337E 02	1.1504E 02	1.1657E 02	1.1800E 02	1.1933E 02
690.0	1.0820E 02	1.0952E 02	1.1189E 02	1.1397E 02	1.1584E 02	1.1754E 02	1.1910E 02	1.2056E 02	1.2192E 02
700.0	1.1053E 02	1.1188E 02	1.1429E 02	1.1641E 02	1.1832E 02	1.2005E 02	1.2165E 02	1.2313E 02	1.2452E 02
710.0	1.1287E 02	1.1424E 02	1.1670E 02	1.1886E 02	1.2081E 02	1.2257E 02	1.2420E 02	1.2571E 02	1.2713E 02
720.0	1.1521E 02	1.1661E 02	1.1912E 02	1.2132E 02	1.2331E 02	1.2511E 02	1.2677E 02	1.2831E 02	1.2975E 02
730.0	1.1757E 02	1.1900E 02	1.2155E 02	1.2380E 02	1.2582E 02	1.2765E 02	1.2934E 02	1.3091E 02	1.3238E 02
740.0	1.1994E 02	1.2139E 02	1.2399E 02	1.2628E 02	1.2834E 02	1.3021E 02	1.3193E 02	1.3353E 02	1.3502E 02
750.0	1.2231E 02	1.2379E 02	1.2644E 02	1.2877E 02	1.3087E 02	1.3277E 02	1.3452E 02	1.3615E 02	1.3767E 02
760.0	1.2470E 02	1.2620E 02	1.2890E 02	1.3128E 02	1.3341E 02	1.3535E 02	1.3713E 02	1.3879E 02	1.4034E 02
770.0	1.2709E 02	1.2862E 02	1.3137E 02	1.3379E 02	1.3596E 02	1.3793E 02	1.3974E 02	1.4143E 02	1.4301E 02
780.0	1.2949E 02	1.3105E 02	1.3385E 02	1.3631E 02	1.3851E 02	1.4052E 02	1.4237E 02	1.4408E 02	1.4569E 02
790.0	1.3191E 02	1.3349E 02	1.3634E 02	1.3884E 02	1.4108E 02	1.4312E 02	1.4500E 02	1.4675E 02	1.4838E 02
800.0	1.3433E 02	1.3594E 02	1.3883E 02	1.4137E 02	1.4366E 02	1.4573E 02	1.4764E 02	1.4942E 02	1.5107E 02
810.0	1.3675E 02	1.3840E 02	1.4133E 02	1.4392E 02	1.4624E 02	1.4835E 02	1.5029E 02	1.5210E 02	1.5378E 02
820.0	1.3919E 02	1.4086E 02	1.4385E 02	1.4648E 02	1.4883E 02	1.5098E 02	1.5295E 02	1.5478E 02	1.5650E 02
830.0	1.4163E 02	1.4333E 02	1.4637E 02	1.4904E 02	1.5143E 02	1.5361E 02	1.5562E 02	1.5748E 02	1.5922E 02
840.0	1.4408E 02	1.4581E 02	1.4889E 02	1.5161E 02	1.5404E 02	1.5626E 02	1.5829E 02	1.6019E 02	1.6195E 02
850.0	1.4654E 02	1.4830E 02	1.5143E 02	1.5419E 02	1.5666E 02	1.5891E 02	1.6098E 02	1.6290E 02	1.6469E 02
860.0	1.4901E 02	1.5079E 02	1.5397E 02	1.5677E 02	1.5928E 02	1.6157E 02	1.6367E 02	1.6562E 02	1.6744E 02
870.0	1.5148E 02	1.5329E 02	1.5652E 02	1.5936E 02	1.6191E 02	1.6423E 02	1.6637E 02	1.6835E 02	1.7020E 02
880.0	1.5396E 02	1.5580E 02	1.5908E 02	1.6196E 02	1.6455E 02	1.6691E 02	1.6907E 02	1.7108E 02	1.7296E 02
890.0	1.5645E 02	1.5831E 02	1.6164E 02	1.6457E 02	1.6720E 02	1.6959E 02	1.7178E 02	1.7382E 02	1.7573E 02
900.0	1.5894E 02	1.6083E 02	1.6421E 02	1.6718E 02	1.6985E 02	1.7227E 02	1.7450E 02	1.7657E 02	1.7851E 02
910.0	1.6144E 02	1.6336E 02	1.6679E 02	1.6981E 02	1.7251E 02	1.7497E 02	1.7723E 02	1.7933E 02	1.8129E 02
920.0	1.6395E 02	1.6590E 02	1.6937E 02	1.7243E 02	1.7517E 02	1.7767E 02	1.7996E 02	1.8209E 02	1.8408E 02
930.0	1.6646E 02	1.6844E 02	1.7196E 02	1.7507E 02	1.7785E 02	1.8038E 02	1.8270E 02	1.8486E 02	1.8688E 02
940.0	1.6898E 02	1.7098E 02	1.7456E 02	1.7770E 02	1.8052E 02	1.8309E 02	1.8545E 02	1.8763E 02	1.8968E 02
950.0	1.7151E 02	1.7354E 02	1.7716E 02	1.8035E 02	1.8321E 02	1.8581E 02	1.8820E 02	1.9042E 02	1.9249E 02
960.0	1.7404E 02	1.7609E 02	1.7977E 02	1.8300E 02	1.8590E 02	1.8853E 02	1.9096E 02	1.9320E 02	1.9530E 02
970.0	1.7657E 02	1.7866E 02	1.8238E 02	1.8566E 02	1.8860E 02	1.9126E 02	1.9372E 02	1.9600E 02	1.9812E 02
980.0	1.7912E 02	1.8123E 02	1.8500E 02	1.8832E 02	1.9130E 02	1.9400E 02	1.9649E 02	1.9880E 02	2.0095E 02
990.0	1.8166E 02	1.8380E 02	1.8763E 02	1.9099E 02	1.9400E 02	1.9674E 02	1.9926E 02	2.0160E 02	2.0378E 02
1000.0	1.8422E 02	1.8638E 02	1.9026E 02	1.9366E 02	1.9672E 02	1.9949E 02	2.0204E 02	2.0441E 02	2.0662E 02
1100.0	2.1001E 02	2.1245E 02	2.1683E 02	2.2067E 02	2.2412E 02	2.2725E 02	2.3012E 02	2.3279E 02	2.3528E 02
1200.0	2.3621E 02	2.3894E 02	2.4382E 02	2.4810E 02	2.5194E 02	2.5542E 02	2.5862E 02	2.6159E 02	2.6437E 02
1300.0	2.6275E 02	2.6576E 02	2.7114E 02	2.7586E 02	2.8009E 02	2.8393E 02	2.8746E 02	2.9073E 02	2.9379E 02
1400.0	2.8955E 02	2.9284E 02	2.9872E 02	3.0389E 02	3.0851E 02	3.1271E 02	3.1656E 02	3.2013E 02	3.2347E 02
1500.0	3.1655E 02	3.2013E 02	3.2651E 02	3.3212E 02	3.3713E 02	3.4169E 02	3.4587E 02	3.4974E 02	3.5335E 02
1600.0	3.4373E 02	3.4758E 02	3.5447E 02	3.6051E 02	3.6592E 02	3.7082E 02	3.7533E 02	3.7950E 02	3.8339E 02
1800.0	3.9842E 02	4.0284E 02	4.1072E 02	4.1764E 02	4.2382E 02	4.2943E 02	4.3458E 02	4.3934E 02	4.4379E 02
2000.0	4.5342E 02	4.5839E 02	4.6726E 02	4.7503E 02	4.8199E 02	4.8829E 02	4.9408E 02	4.9943E 02	5.0443E 02
2200.0	5.0855E 02	5.1407E 02	5.2392E 02	5.3254E 02	5.4026E 02	5.4725E 02	5.5366E 02	5.5960E 02	5.6513E 02
2400.0	5.6371E 02	5.6978E 02	5.8059E 02	5.9006E 02	5.9852E 02	6.0619E 02	6.1323E 02	6.1974E 02	6.2580E 02
2600.0	6.1883E 02	6.2543E 02	6.3720E 02	6.4750E 02	6.5671E 02	6.6505E 02	6.7269E 02	6.7977E 02	6.8636E 02
2800.0	6.7386E 02	6.8099E 02	6.9369E 02	7.0482E 02	7.1476E 02	7.2376E 02	7.3201E 02	7.3964E 02	7.4675E 02
3000.0	7.2874E 02	7.3640E 02	7.5004E 02	7.6197E 02	7.7263E 02	7.8228E 02	7.9113E 02	7.9931E 02	8.0693E 02
3200.0	7.8347E 02	7.9164E 02	8.0620E 02	8.1893E 02	8.3030E 02	8.4060E 02	8.5003E 02	8.5875E 02	8.6688E 02
3400.0	8.3801E 02	8.4669E 02	8.6216E 02	8.7569E 02	8.8776E 02	8.9869E 02	9.0870E 02	9.1796E 02	9.2658E 02
3600.0	8.9236E 02	9.0155E 02	9.1791E 02	9.3222E 02	9.4498E 02	9.5654E 02	9.6713E 02	9.7691E 02	9.8602E 02
3800.0	9.4650E 02	9.5619E 02	9.7344E 02	9.8852E 02	1.0020E 03	1.0141E 03	1.0253E 03	1.0356E 03	1.0452E 03
4000.0	1.0004E 03	1.0106E 03	1.0287E 03	1.0446E 03	1.0587E 03	1.0715E 03	1.0832E 03	1.0940E 03	1.1041E 03
4500.0	1.1344E 03	1.1457E 03	1.1660E 03	1.1837E 03	1.1995E 03	1.2138E 03	1.2269E 03	1.2390E 03	1.2502E 03
5000.0	1.2670E 03	1.2795E 03	1.3019E 03	1.3214E 03	1.3388E 03	1.3546E 03	1.3690E 03	1.3823E 03	1.3947E 03

RANGE

ENERGY MEV	I= 260.0	I= 280.0	I= 300.0	I= 320.0	I= 340.0	I= 380.0	I= 420.0	I= 460.0	I= 500.0
1.0	2.4878E-03	2.5871E-03	2.6841E-03	2.7791E-03	2.8723E-03	3.0538E-03	3.2298E-03	3.4008E-03	3.5677E-03
2.0	6.7640E-03	6.9976E-03	7.2258E-03	7.4492E-03	7.6681E-03	8.0942E-03	8.5065E-03	8.9071E-03	9.2973E-03
3.0	1.2628E-02	1.3026E-02	1.3415E-02	1.3795E-02	1.4167E-02	1.4890E-02	1.5588E-02	1.6265E-02	1.6923E-02
4.0	2.0013E-02	2.0603E-02	2.1179E-02	2.1740E-02	2.2289E-02	2.3354E-02	2.4380E-02	2.5372E-02	2.6335E-02
5.0	2.8892E-02	2.9700E-02	3.0486E-02	3.1252E-02	3.1999E-02	3.3447E-02	3.4838E-02	3.6181E-02	3.7481E-02
6.0	3.9256E-02	4.0305E-02	4.1323E-02	4.2315E-02	4.3281E-02	4.5149E-02	4.6939E-02	4.8664E-02	5.0331E-02
7.0	5.1104E-02	5.2415E-02	5.3688E-02	5.4925E-02	5.6129E-02	5.8451E-02	6.0673E-02	6.2808E-02	6.4869E-02
8.0	6.4413E-02	6.6009E-02	6.7555E-02	6.9056E-02	7.0515E-02	7.3324E-02	7.6007E-02	7.8580E-02	8.1057E-02
9.0	7.8555E-02	8.0433E-02	8.2253E-02	8.4019E-02	8.5738E-02	8.9049E-02	9.2213E-02	9.5250E-02	9.8176E-02
10.0	9.3871E-02	9.6045E-02	9.8151E-02	1.0020E-01	1.0219E-01	1.0603E-01	1.0969E-01	1.1322E-01	1.1662E-01
12.0	1.2802E-01	1.3083E-01	1.3356E-01	1.3620E-01	1.3878E-01	1.4375E-01	1.4851E-01	1.5308E-01	1.5750E-01
14.0	1.6672E-01	1.7022E-01	1.7362E-01	1.7692E-01	1.8014E-01	1.8635E-01	1.9230E-01	1.9803E-01	2.0358E-01
16.0	2.0982E-01	2.1408E-01	2.1820E-01	2.2221E-01	2.2612E-01	2.3366E-01	2.4090E-01	2.4788E-01	2.5465E-01
18.0	2.5721E-01	2.6227E-01	2.6717E-01	2.7193E-01	2.7657E-01	2.8554E-01	2.9416E-01	3.0248E-01	3.1056E-01
20.0	3.0879E-01	3.1470E-01	3.2042E-01	3.2598E-01	3.3140E-01	3.4188E-01	3.5195E-01	3.6169E-01	3.7116E-01
22.0	3.6447E-01	3.7126E-01	3.7785E-01	3.8426E-01	3.9050E-01	4.0256E-01	4.1417E-01	4.2540E-01	4.3632E-01
24.0	4.2416E-01	4.3189E-01	4.3939E-01	4.4668E-01	4.5378E-01	4.6751E-01	4.8071E-01	4.9350E-01	5.0595E-01
26.0	4.8778E-01	4.9650E-01	5.0495E-01	5.1316E-01	5.2116E-01	5.3662E-01	5.5150E-01	5.6591E-01	5.7995E-01
28.0	5.5529E-01	5.6503E-01	5.7447E-01	5.8363E-01	5.9257E-01	6.0984E-01	6.2645E-01	6.4254E-01	6.5822E-01
30.0	6.2660E-01	6.3741E-01	6.4787E-01	6.5804E-01	6.6794E-01	6.8707E-01	7.0548E-01	7.2332E-01	7.4070E-01
32.0	7.0166E-01	7.1357E-01	7.2510E-01	7.3630E-01	7.4720E-01	7.6828E-01	7.8854E-01	8.0817E-01	8.2730E-01
34.0	7.8042E-01	7.9347E-01	8.0610E-01	8.1837E-01	8.3031E-01	8.5338E-01	8.7556E-01	8.9704E-01	9.1797E-01
36.0	8.6282E-01	8.7705E-01	8.9082E-01	9.0418E-01	9.1719E-01	9.4232E-01	9.6647E-01	9.8985E-01	1.0126E 00
38.0	9.4882E-01	9.6426E-01	9.7920E-01	9.9370E-01	1.0078E 00	1.0350E 00	1.0612E 00	1.0866E 00	1.1113E 00
40.0	1.0384E 00	1.0551E 00	1.0712E 00	1.0869E 00	1.1021E 00	1.1315E 00	1.1598E 00	1.1871E 00	1.2138E 00
42.0	1.1314E 00	1.1494E 00	1.1668E 00	1.1836E 00	1.2000E 00	1.2317E 00	1.2621E 00	1.2915E 00	1.3201E 00
44.0	1.2279E 00	1.2472E 00	1.2659E 00	1.2839E 00	1.3015E 00	1.3355E 00	1.3680E 00	1.3995E 00	1.4302E 00
46.0	1.3278E 00	1.3485E 00	1.3684E 00	1.3878E 00	1.4066E 00	1.4429E 00	1.4776E 00	1.5113E 00	1.5440E 00
48.0	1.4311E 00	1.4531E 00	1.4744E 00	1.4951E 00	1.5151E 00	1.5538E 00	1.5909E 00	1.6267E 00	1.6616E 00
50.0	1.5377E 00	1.5612E 00	1.5839E 00	1.6058E 00	1.6271E 00	1.6682E 00	1.7076E 00	1.7457E 00	1.7827E 00
55.0	1.8186E 00	1.8458E 00	1.8720E 00	1.8974E 00	1.9220E 00	1.9695E 00	2.0149E 00	2.0587E 00	2.1014E 00
60.0	2.1196E 00	2.1507E 00	2.1806E 00	2.2096E 00	2.2377E 00	2.2918E 00	2.3435E 00	2.3934E 00	2.4418E 00
65.0	2.4402E 00	2.4753E 00	2.5091E 00	2.5419E 00	2.5736E 00	2.6346E 00	2.6930E 00	2.7491E 00	2.8036E 00
70.0	2.7798E 00	2.8191E 00	2.8571E 00	2.8937E 00	2.9293E 00	2.9975E 00	3.0627E 00	3.1254E 00	3.1862E 00
75.0	3.1380E 00	3.1818E 00	3.2240E 00	3.2647E 00	3.3042E 00	3.3799E 00	3.4522E 00	3.5217E 00	3.5889E 00
80.0	3.5144E 00	3.5628E 00	3.6094E 00	3.6543E 00	3.6979E 00	3.7814E 00	3.8610E 00	3.9375E 00	4.0115E 00
85.0	3.9086E 00	3.9618E 00	4.0129E 00	4.0622E 00	4.1100E 00	4.2016E 00	4.2888E 00	4.3724E 00	4.4533E 00
90.0	4.3202E 00	4.3783E 00	4.4341E 00	4.4880E 00	4.5401E 00	4.6399E 00	4.7349E 00	4.8261E 00	4.9141E 00
95.0	4.7487E 00	4.8119E 00	4.8726E 00	4.9312E 00	4.9878E 00	5.0962E 00	5.1992E 00	5.2979E 00	5.3933E 00
100.0	5.1940E 00	5.2624E 00	5.3281E 00	5.3914E 00	5.4527E 00	5.5698E 00	5.6811E 00	5.7877E 00	5.8905E 00
105.0	5.6556E 00	5.7293E 00	5.8002E 00	5.8684E 00	5.9344E 00	6.0606E 00	6.1803E 00	6.2950E 00	6.4054E 00
110.0	6.1331E 00	6.2124E 00	6.2885E 00	6.3618E 00	6.4327E 00	6.5681E 00	6.6965E 00	6.8194E 00	6.9377E 00
115.0	6.6263E 00	6.7113E 00	6.7928E 00	6.8713E 00	6.9471E 00	7.0920E 00	7.2293E 00	7.3605E 00	7.4869E 00
120.0	7.1349E 00	7.2257E 00	7.3127E 00	7.3965E 00	7.4774E 00	7.6319E 00	7.7783E 00	7.9182E 00	8.0527E 00
125.0	7.6585E 00	7.7552E 00	7.8479E 00	7.9371E 00	8.0233E 00	8.1877E 00	8.3433E 00	8.4920E 00	8.6349E 00
130.0	8.1969E 00	8.2997E 00	8.3982E 00	8.4929E 00	8.5844E 00	8.7589E 00	8.9240E 00	9.0816E 00	9.2330E 00
135.0	8.7499E 00	8.8588E 00	8.9632E 00	9.0636E 00	9.1605E 00	9.3452E 00	9.5200E 00	9.6867E 00	9.8468E 00
140.0	9.3170E 00	9.4323E 00	9.5427E 00	9.6488E 00	9.7512E 00	9.9465E 00	1.0131E 01	1.0307E 01	1.0476E 01
145.0	9.8981E 00	1.0020E 01	1.0136E 01	1.0248E 01	1.0356E 01	1.0562E 01	1.0757E 01	1.0942E 01	1.1120E 01
150.0	1.0493E 01	1.0621E 01	1.0744E 01	1.0862E 01	1.0976E 01	1.1193E 01	1.1397E 01	1.1592E 01	1.1779E 01
155.0	1.1101E 01	1.1236E 01	1.1365E 01	1.1489E 01	1.1609E 01	1.1837E 01	1.2052E 01	1.2257E 01	1.2453E 01
160.0	1.1723E 01	1.1864E 01	1.2000E 01	1.2130E 01	1.2256E 01	1.2495E 01	1.2720E 01	1.2935E 01	1.3141E 01
165.0	1.2357E 01	1.2506E 01	1.2648E 01	1.2784E 01	1.2916E 01	1.3167E 01	1.3403E 01	1.3627E 01	1.3843E 01
170.0	1.3004E 01	1.3160E 01	1.3309E 01	1.3452E 01	1.3590E 01	1.3851E 01	1.4099E 01	1.4333E 01	1.4558E 01
175.0	1.3664E 01	1.3827E 01	1.3983E 01	1.4132E 01	1.4276E 01	1.4550E 01	1.4808E 01	1.5053E 01	1.5288E 01
180.0	1.4336E 01	1.4506E 01	1.4669E 01	1.4825E 01	1.4975E 01	1.5261E 01	1.5530E 01	1.5785E 01	1.6030E 01
185.0	1.5021E 01	1.5198E 01	1.5367E 01	1.5530E 01	1.5686E 01	1.5984E 01	1.6265E 01	1.6531E 01	1.6786E 01
190.0	1.5717E 01	1.5901E 01	1.6078E 01	1.6247E 01	1.6410E 01	1.6720E 01	1.7012E 01	1.7289E 01	1.7554E 01
195.0	1.6425E 01	1.6617E 01	1.6800E 01	1.6977E 01	1.7146E 01	1.7468E 01	1.7772E 01	1.8060E 01	1.8335E 01
200.0	1.7144E 01	1.7344E 01	1.7535E 01	1.7718E 01	1.7894E 01	1.8229E 01	1.8544E 01	1.8843E 01	1.9128E 01
210.0	1.8617E 01	1.8832E 01	1.9037E 01	1.9234E 01	1.9424E 01	1.9784E 01	2.0123E 01	2.0445E 01	2.0751E 01
220.0	2.0133E 01	2.0364E 01	2.0585E 01	2.0796E 01	2.1000E 01	2.1386E 01	2.1749E 01	2.2093E 01	2.2421E 01
230.0	2.1692E 01	2.1939E 01	2.2175E 01	2.2401E 01	2.2619E 01	2.3032E 01	2.3419E 01	2.3787E 01	2.4137E 01
240.0	2.3291E 01	2.3555E 01	2.3807E 01	2.4048E 01	2.4280E 01	2.4720E 01	2.5133E 01	2.5524E 01	2.5897E 01
250.0	2.4931E 01	2.5211E 01	2.5479E 01	2.5736E 01	2.5982E 01	2.6450E 01	2.6889E 01	2.7304E 01	2.7700E 01
260.0	2.6609E 01	2.6906E 01	2.7190E 01	2.7463E 01	2.7724E 01	2.8220E 01	2.8685E 01	2.9125E 01	2.9543E 01
270.0	2.8324E 01	2.8639E 01	2.8940E 01	2.9228E 01	2.9504E 01	3.0028E 01	3.0520E 01	3.0985E 01	3.1427E 01
280.0	3.0075E 01	3.0408E 01	3.0726E 01	3.1030E 01	3.1322E 01	3.1875E 01	3.2393E 01	3.2884E 01	3.3350E 01
290.0	3.1862E 01	3.2213E 01	3.2547E 01	3.2868E 01	3.3175E 01	3.3758E 01	3.4304E 01	3.4820E 01	3.5310E 01
300.0	3.3682E 01	3.4051E 01	3.4403E 01	3.4740E 01	3.5064E 01	3.5676E 01	3.6250E 01	3.6792E 01	3.7307E 01
310.0	3.5536E 01	3.5923E 01	3.6293E 01	3.6646E 01	3.6986E 01	3.7629E 01	3.8230E 01	3.8799E 01	3.9339E 01
320.0	3.7421E 01	3.7828E 01	3.8215E 01	3.8586E 01	3.8941E 01	3.9615E 01	4.0245E 01	4.0840E 01	4.1405E 01
330.0	3.9338E 01	3.9763E 01	4.0168E 01	4.0556E 01	4.0929E 01	4.1633E 01	4.2292E 01	4.2914E 01	4.3504E 01
340.0	4.1284E 01	4.1729E 01	4.2153E 01	4.2558E 01	4.2947E 01	4.3682E 01	4.4370E 01	4.5019E 01	4.5636E 01
350.0	4.3260E 01	4.3724E 01	4.4166E 01	4.4589E 01	4.4995E 01	4.5762E 01	4.6480E 01	4.7156E 01	4.7799E 01
360.0	4.5265E 01	4.5748E 01	4.6209E 01	4.6650E 01	4.7072E 01	4.7872E 01	4.8619E 01	4.9323E 01	4.9992E 01
370.0	4.7297E 01	4.7800E 01	4.8280E 01	4.8738E 01	4.9178E 01	5.0010E 01	5.0787E 01	5.1520E 01	5.2215E 01
380.0	4.9355E 01	4.9879E 01	5.0378E 01	5.0854E 01	5.1312E 01	5.2176E 01	5.2983E 01	5.3744E 01	5.4466E 01
390.0	5.1440E 01	5.1984E 01	5.2502E 01	5.2997E 01	5.3472E 01	5.4369E 01	5.5207E 01	5.5997E 01	5.6745E 01
400.0	5.3551E 01	5.4115E 01	5.4652E 01	5.5165E 01	5.5658E 01	5.6588E 01	5.7457E 01	5.8276E 01	5.9052E 01

RANGE

ENERGY MEV	I= 260.0	I= 280.0	I= 300.0	I= 320.0	I= 340.0	I= 380.0	I= 420.0	I= 460.0	I= 500.0
410.0	5.5686E 01	5.6270E 01	5.6827E 01	5.7359E 01	5.7869E 01	5.8833E 01	5.9733E 01	6.0581E 01	6.1384E 01
420.0	5.7844E 01	5.8450E 01	5.9026E 01	5.9577E 01	6.0105E 01	6.1103E 01	6.2034E 01	6.2911E 01	6.3742E 01
430.0	6.0027E 01	6.0653E 01	6.1249E 01	6.1819E 01	6.2365E 01	6.3397E 01	6.4360E 01	6.5266E 01	6.6129E 01
440.0	6.2231E 01	6.2879E 01	6.3495E 01	6.4084E 01	6.4648E 01	6.5714E 01	6.6709E 01	6.7645E 01	6.8531E 01
450.0	6.4458E 01	6.5127E 01	6.5763E 01	6.6371E 01	6.6954E 01	6.8054E 01	6.9081E 01	7.0047E 01	7.0962E 01
460.0	6.6706E 01	6.7396E 01	6.8053E 01	6.8681E 01	6.9282E 01	7.0417E 01	7.1476E 01	7.2472E 01	7.3415E 01
470.0	6.8976E 01	6.9687E 01	7.0364E 01	7.1011E 01	7.1631E 01	7.2801E 01	7.3892E 01	7.4918E 01	7.5890E 01
480.0	7.1265E 01	7.1998E 01	7.2696E 01	7.3362E 01	7.4001E 01	7.5206E 01	7.6329E 01	7.7386E 01	7.8386E 01
490.0	7.3574E 01	7.4329E 01	7.5047E 01	7.5733E 01	7.6391E 01	7.7631E 01	7.8788E 01	7.9875E 01	8.0904E 01
500.0	7.5902E 01	7.6679E 01	7.7419E 01	7.8124E 01	7.8801E 01	8.0076E 01	8.1266E 01	8.2384E 01	8.3442E 01
510.0	7.8250E 01	7.9049E 01	7.9809E 01	8.0534E 01	8.1230E 01	8.2541E 01	8.3764E 01	8.4913E 01	8.6000E 01
520.0	8.0615E 01	8.1436E 01	8.2217E 01	8.2963E 01	8.3677E 01	8.5025E 01	8.6280E 01	8.7461E 01	8.8577E 01
530.0	8.2998E 01	8.3841E 01	8.4644E 01	8.5409E 01	8.6143E 01	8.7526E 01	8.8816E 01	9.0027E 01	9.1173E 01
540.0	8.5398E 01	8.6264E 01	8.7087E 01	8.7874E 01	8.8626E 01	9.0046E 01	9.1369E 01	9.2612E 01	9.3787E 01
550.0	8.7816E 01	8.8704E 01	8.9548E 01	9.0355E 01	9.1127E 01	9.2583E 01	9.3940E 01	9.5214E 01	9.6419E 01
560.0	9.0249E 01	9.1160E 01	9.2026E 01	9.2853E 01	9.3645E 01	9.5137E 01	9.6528E 01	9.7834E 01	9.9068E 01
570.0	9.2699E 01	9.3632E 01	9.4520E 01	9.5367E 01	9.6178E 01	9.7708E 01	9.9132E 01	1.0047E 02	1.0173E 02
580.0	9.5164E 01	9.6120E 01	9.7029E 01	9.7897E 01	9.8728E 01	1.0029E 02	1.0175E 02	1.0312E 02	1.0442E 02
590.0	9.7644E 01	9.8623E 01	9.9554E 01	1.0044E 02	1.0129E 02	1.0290E 02	1.0439E 02	1.0579E 02	1.0712E 02
600.0	1.0014E 02	1.0114E 02	1.0209E 02	1.0300E 02	1.0387E 02	1.0551E 02	1.0704E 02	1.0847E 02	1.0983E 02
610.0	1.0265E 02	1.0367E 02	1.0465E 02	1.0558E 02	1.0647E 02	1.0815E 02	1.0971E 02	1.1117E 02	1.1256E 02
620.0	1.0517E 02	1.0622E 02	1.0722E 02	1.0817E 02	1.0908E 02	1.1079E 02	1.1239E 02	1.1389E 02	1.1530E 02
630.0	1.0771E 02	1.0878E 02	1.0980E 02	1.1077E 02	1.1170E 02	1.1345E 02	1.1508E 02	1.1662E 02	1.1806E 02
640.0	1.1026E 02	1.1135E 02	1.1240E 02	1.1339E 02	1.1434E 02	1.1613E 02	1.1779E 02	1.1936E 02	1.2083E 02
650.0	1.1282E 02	1.1394E 02	1.1500E 02	1.1602E 02	1.1699E 02	1.1882E 02	1.2052E 02	1.2211E 02	1.2362E 02
660.0	1.1540E 02	1.1654E 02	1.1763E 02	1.1866E 02	1.1965E 02	1.2152E 02	1.2325E 02	1.2488E 02	1.2642E 02
670.0	1.1799E 02	1.1915E 02	1.2026E 02	1.2132E 02	1.2233E 02	1.2423E 02	1.2600E 02	1.2766E 02	1.2923E 02
680.0	1.2059E 02	1.2178E 02	1.2291E 02	1.2398E 02	1.2502E 02	1.2696E 02	1.2876E 02	1.3046E 02	1.3206E 02
690.0	1.2320E 02	1.2441E 02	1.2557E 02	1.2666E 02	1.2772E 02	1.2970E 02	1.3154E 02	1.3326E 02	1.3489E 02
700.0	1.2582E 02	1.2706E 02	1.2824E 02	1.2936E 02	1.3043E 02	1.3244E 02	1.3432E 02	1.3608E 02	1.3774E 02
710.0	1.2846E 02	1.2972E 02	1.3092E 02	1.3206E 02	1.3315E 02	1.3521E 02	1.3712E 02	1.3891E 02	1.4060E 02
720.0	1.3111E 02	1.3239E 02	1.3361E 02	1.3477E 02	1.3588E 02	1.3798E 02	1.3993E 02	1.4175E 02	1.4348E 02
730.0	1.3376E 02	1.3507E 02	1.3631E 02	1.3750E 02	1.3863E 02	1.4076E 02	1.4275E 02	1.4461E 02	1.4636E 02
740.0	1.3643E 02	1.3776E 02	1.3903E 02	1.4023E 02	1.4138E 02	1.4356E 02	1.4558E 02	1.4747E 02	1.4925E 02
750.0	1.3911E 02	1.4046E 02	1.4175E 02	1.4298E 02	1.4415E 02	1.4636E 02	1.4842E 02	1.5034E 02	1.5216E 02
760.0	1.4179E 02	1.4317E 02	1.4448E 02	1.4573E 02	1.4693E 02	1.4918E 02	1.5127E 02	1.5323E 02	1.5507E 02
770.0	1.4449E 02	1.4589E 02	1.4723E 02	1.4850E 02	1.4971E 02	1.5200E 02	1.5413E 02	1.5612E 02	1.5800E 02
780.0	1.4720E 02	1.4862E 02	1.4998E 02	1.5127E 02	1.5251E 02	1.5483E 02	1.5700E 02	1.5902E 02	1.6093E 02
790.0	1.4991E 02	1.5136E 02	1.5274E 02	1.5406E 02	1.5531E 02	1.5768E 02	1.5988E 02	1.6194E 02	1.6388E 02
800.0	1.5264E 02	1.5411E 02	1.5551E 02	1.5685E 02	1.5813E 02	1.6053E 02	1.6277E 02	1.6486E 02	1.6683E 02
810.0	1.5537E 02	1.5687E 02	1.5829E 02	1.5965E 02	1.6095E 02	1.6339E 02	1.6566E 02	1.6779E 02	1.6980E 02
820.0	1.5811E 02	1.5963E 02	1.6108E 02	1.6246E 02	1.6378E 02	1.6626E 02	1.6857E 02	1.7073E 02	1.7277E 02
830.0	1.6086E 02	1.6241E 02	1.6388E 02	1.6528E 02	1.6662E 02	1.6914E 02	1.7148E 02	1.7368E 02	1.7575E 02
840.0	1.6362E 02	1.6519E 02	1.6668E 02	1.6811E 02	1.6947E 02	1.7203E 02	1.7441E 02	1.7664E 02	1.7874E 02
850.0	1.6638E 02	1.6798E 02	1.6950E 02	1.7094E 02	1.7232E 02	1.7492E 02	1.7734E 02	1.7960E 02	1.8173E 02
860.0	1.6916E 02	1.7078E 02	1.7232E 02	1.7378E 02	1.7519E 02	1.7783E 02	1.8028E 02	1.8258E 02	1.8474E 02
870.0	1.7194E 02	1.7358E 02	1.7515E 02	1.7663E 02	1.7806E 02	1.8074E 02	1.8323E 02	1.8556E 02	1.8775E 02
880.0	1.7473E 02	1.7640E 02	1.7798E 02	1.7949E 02	1.8094E 02	1.8366E 02	1.8618E 02	1.8855E 02	1.9077E 02
890.0	1.7752E 02	1.7922E 02	1.8082E 02	1.8236E 02	1.8382E 02	1.8658E 02	1.8914E 02	1.9154E 02	1.9380E 02
900.0	1.8032E 02	1.8204E 02	1.8368E 02	1.8523E 02	1.8672E 02	1.8952E 02	1.9211E 02	1.9454E 02	1.9684E 02
910.0	1.8313E 02	1.8488E 02	1.8653E 02	1.8811E 02	1.8962E 02	1.9246E 02	1.9509E 02	1.9756E 02	1.9988E 02
920.0	1.8595E 02	1.8772E 02	1.8940E 02	1.9100E 02	1.9253E 02	1.9540E 02	1.9807E 02	2.0057E 02	2.0293E 02
930.0	1.8877E 02	1.9057E 02	1.9227E 02	1.9389E 02	1.9544E 02	1.9836E 02	2.0106E 02	2.0360E 02	2.0598E 02
940.0	1.9160E 02	1.9342E 02	1.9514E 02	1.9679E 02	1.9836E 02	2.0132E 02	2.0406E 02	2.0663E 02	2.0905E 02
950.0	1.9444E 02	1.9628E 02	1.9803E 02	1.9969E 02	2.0129E 02	2.0428E 02	2.0706E 02	2.0966E 02	2.1211E 02
960.0	1.9728E 02	1.9915E 02	2.0092E 02	2.0261E 02	2.0422E 02	2.0725E 02	2.1007E 02	2.1271E 02	2.1519E 02
970.0	2.0013E 02	2.0202E 02	2.0381E 02	2.0552E 02	2.0716E 02	2.1023E 02	2.1309E 02	2.1576E 02	2.1827E 02
980.0	2.0298E 02	2.0490E 02	2.0671E 02	2.0845E 02	2.1010E 02	2.1322E 02	2.1611E 02	2.1881E 02	2.2136E 02
990.0	2.0584E 02	2.0778E 02	2.0962E 02	2.1138E 02	2.1305E 02	2.1621E 02	2.1913E 02	2.2187E 02	2.2445E 02
1000.0	2.0870E 02	2.1067E 02	2.1253E 02	2.1431E 02	2.1601E 02	2.1920E 02	2.2217E 02	2.2494E 02	2.2755E 02
1100.0	2.3762E 02	2.3984E 02	2.4194E 02	2.4394E 02	2.4585E 02	2.4944E 02	2.5277E 02	2.5588E 02	2.5882E 02
1200.0	2.6697E 02	2.6943E 02	2.7177E 02	2.7399E 02	2.7611E 02	2.8010E 02	2.8380E 02	2.8726E 02	2.9051E 02
1300.0	2.9666E 02	2.9937E 02	3.0193E 02	3.0438E 02	3.0672E 02	3.1111E 02	3.1517E 02	3.1897E 02	3.2254E 02
1400.0	3.2660E 02	3.2956E 02	3.3236E 02	3.3503E 02	3.3758E 02	3.4236E 02	3.4680E 02	3.5094E 02	3.5483E 02
1500.0	3.5675E 02	3.5995E 02	3.6299E 02	3.6588E 02	3.6864E 02	3.7382E 02	3.7862E 02	3.8310E 02	3.8731E 02
1600.0	3.8705E 02	3.9050E 02	3.9377E 02	3.9688E 02	3.9985E 02	4.0543E 02	4.1059E 02	4.1540E 02	4.1993E 02
1800.0	4.4797E 02	4.5190E 02	4.5564E 02	4.5919E 02	4.6257E 02	4.6893E 02	4.7481E 02	4.8029E 02	4.8544E 02
2000.0	5.0911E 02	5.1353E 02	5.1772E 02	5.2170E 02	5.2550E 02	5.3263E 02	5.3922E 02	5.4536E 02	5.5112E 02
2200.0	5.7032E 02	5.7522E 02	5.7986E 02	5.8427E 02	5.8847E 02	5.9635E 02	6.0364E 02	6.1044E 02	6.1681E 02
2400.0	6.3149E 02	6.3686E 02	6.4194E 02	6.4677E 02	6.5137E 02	6.6000E 02	6.6798E 02	6.7541E 02	6.8238E 02
2600.0	6.9254E 02	6.9837E 02	7.0388E 02	7.0913E 02	7.1413E 02	7.2349E 02	7.3215E 02	7.4021E 02	7.4776E 02
2800.0	7.5341E 02	7.5969E 02	7.6564E 02	7.7129E 02	7.7668E 02	7.8677E 02	7.9609E 02	8.0477E 02	8.1290E 02
3000.0	8.1407E 02	8.2080E 02	8.2717E 02	8.3322E 02	8.3899E 02	8.4980E 02	8.5978E 02	8.6907E 02	8.7777E 02
3200.0	8.7449E 02	8.8167E 02	8.8845E 02	8.9490E 02	9.0105E 02	9.1256E 02	9.2318E 02	9.3307E 02	9.4234E 02
3400.0	9.3466E 02	9.4227E 02	9.4947E 02	9.5631E 02	9.6283E 02	9.7503E 02	9.8629E 02	9.9677E 02	1.0066E 03
3600.0	9.9456E 02	1.0026E 03	1.0102E 03	1.0174E 03	1.0243E 03	1.0372E 03	1.0491E 03	1.0602E 03	1.0705E 03
3800.0	1.0542E 03	1.0627E 03	1.0707E 03	1.0783E 03	1.0855E 03	1.0991E 03	1.1116E 03	1.1232E 03	1.1341E 03
4000.0	1.1135E 03	1.1224E 03	1.1308E 03	1.1388E 03	1.1464E 03	1.1607E 03	1.1738E 03	1.1860E 03	1.1974E 03
4500.0	1.2608E 03	1.2707E 03	1.2800E 03	1.2889E 03	1.2974E 03	1.3133E 03	1.3279E 03	1.3415E 03	1.3542E 03
5000.0	1.4063E 03	1.4172E 03	1.4275E 03	1.4373E 03	1.4466E 03	1.4641E 03	1.4801E 03	1.4951E 03	1.5090E 03

RANGE

ENERGY MEV	I= 550.0	I= 600.0	I= 650.0	I= 700.0	I= 750.0	I= 800.0	I= 850.0	I= 900.0	I= 950.0
1.0	3.7711E-03	3.9694E-03	4.1633E-03	4.3533E-03	4.5397E-03	4.7230E-03	4.9035E-03	5.0813E-03	5.2567E-03
2.0	9.7724E-03	1.0235E-02	1.0687E-02	1.1130E-02	1.1564E-02	1.1990E-02	1.2410E-02	1.2823E-02	1.3230E-02
3.0	1.7722E-02	1.8500E-02	1.9258E-02	1.9998E-02	2.0723E-02	2.1434E-02	2.2133E-02	2.2819E-02	2.3495E-02
4.0	2.7503E-02	2.8636E-02	2.9738E-02	3.0813E-02	3.1863E-02	3.2892E-02	3.3900E-02	3.4890E-02	3.5863E-02
5.0	3.9055E-02	4.0579E-02	4.2057E-02	4.3497E-02	4.4901E-02	4.6273E-02	4.7617E-02	4.8934E-02	5.0227E-02
6.0	5.2345E-02	5.4289E-02	5.6173E-02	5.8003E-02	5.9785E-02	6.1524E-02	6.3224E-02	6.4888E-02	6.6519E-02
7.0	6.7351E-02	6.9744E-02	7.2058E-02	7.4301E-02	7.6483E-02	7.8607E-02	8.0681E-02	8.2708E-02	8.4692E-02
8.0	8.4038E-02	8.6905E-02	8.9672E-02	9.2351E-02	9.4951E-02	9.7479E-02	9.9944E-02	1.0235E-01	1.0470E-01
9.0	1.0170E-01	1.0509E-01	1.0836E-01	1.1152E-01	1.1459E-01	1.1757E-01	1.2047E-01	1.2329E-01	1.2604E-01
10.0	1.2071E-01	1.2464E-01	1.2844E-01	1.3212E-01	1.3569E-01	1.3915E-01	1.4251E-01	1.4578E-01	1.4897E-01
12.0	1.6283E-01	1.6797E-01	1.7295E-01	1.7777E-01	1.8246E-01	1.8701E-01	1.9145E-01	1.9578E-01	1.9999E-01
14.0	2.1028E-01	2.1677E-01	2.2307E-01	2.2920E-01	2.3518E-01	2.4102E-01	2.4674E-01	2.5234E-01	2.5783E-01
16.0	2.6286E-01	2.7082E-01	2.7858E-01	2.8616E-01	2.9358E-01	3.0088E-01	3.0805E-01	3.1512E-01	3.2209E-01
18.0	3.2037E-01	3.2992E-01	3.3925E-01	3.4841E-01	3.5741E-01	3.6629E-01	3.7507E-01	3.8376E-01	3.9240E-01
20.0	3.8267E-01	3.9391E-01	4.0492E-01	4.1575E-01	4.2644E-01	4.3702E-01	4.4752E-01	4.5797E-01	4.6839E-01
22.0	4.4963E-01	4.6264E-01	4.7541E-01	4.8801E-01	5.0047E-01	5.1285E-01	5.2518E-01	5.3749E-01	5.4981E-01
24.0	5.2113E-01	5.3599E-01	5.5061E-01	5.6505E-01	5.7937E-01	5.9363E-01	6.0784E-01	6.2211E-01	6.3643E-01
26.0	5.9708E-01	6.1386E-01	6.3039E-01	6.4674E-01	6.6299E-01	6.7919E-01	6.9540E-01	7.1168E-01	7.2805E-01
28.0	6.7737E-01	6.9614E-01	7.1465E-01	7.3298E-01	7.5122E-01	7.6943E-01	7.8768E-01	8.0603E-01	8.2453E-01
30.0	7.6193E-01	7.8275E-01	8.0330E-01	8.2367E-01	8.4395E-01	8.6423E-01	8.8457E-01	9.0505E-01	9.2573E-01
32.0	8.5068E-01	8.7362E-01	8.9626E-01	9.1872E-01	9.4110E-01	9.6349E-01	9.8598E-01	1.0086E 00	1.0315E 00
34.0	9.4356E-01	9.6866E-01	9.9345E-01	1.0181E 00	1.0426E 00	1.0671E 00	1.0918E 00	1.1167E 00	1.1419E 00
36.0	1.0405E 00	1.0678E 00	1.0948E 00	1.1216E 00	1.1483E 00	1.1751E 00	1.2020E 00	1.2291E 00	1.2566E 00
38.0	1.1414E 00	1.1710E 00	1.2003E 00	1.2293E 00	1.2582E 00	1.2873E 00	1.3164E 00	1.3459E 00	1.3757E 00
40.0	1.2463E 00	1.2782E 00	1.3097E 00	1.3411E 00	1.3723E 00	1.4036E 00	1.4351E 00	1.4668E 00	1.4990E 00
42.0	1.3550E 00	1.3893E 00	1.4232E 00	1.4568E 00	1.4904E 00	1.5240E 00	1.5578E 00	1.5920E 00	1.6266E 00
44.0	1.4676E 00	1.5044E 00	1.5406E 00	1.5766E 00	1.6125E 00	1.6485E 00	1.6847E 00	1.7212E 00	1.7582E 00
46.0	1.5840E 00	1.6232E 00	1.6619E 00	1.7003E 00	1.7386E 00	1.7770E 00	1.8155E 00	1.8545E 00	1.8940E 00
48.0	1.7041E 00	1.7458E 00	1.7870E 00	1.8278E 00	1.8685E 00	1.9093E 00	1.9504E 00	1.9918E 00	2.0338E 00
50.0	1.8279E 00	1.8722E 00	1.9158E 00	1.9592E 00	2.0024E 00	2.0456E 00	2.0891E 00	2.1330E 00	2.1775E 00
55.0	2.1533E 00	2.2041E 00	2.2542E 00	2.3039E 00	2.3534E 00	2.4030E 00	2.4528E 00	2.5030E 00	2.5538E 00
60.0	2.5008E 00	2.5585E 00	2.6153E 00	2.6716E 00	2.7276E 00	2.7836E 00	2.8399E 00	2.8966E 00	2.9539E 00
65.0	2.8699E 00	2.9347E 00	2.9984E 00	3.0615E 00	3.1242E 00	3.1868E 00	3.2497E 00	3.3131E 00	3.3771E 00
70.0	3.2600E 00	3.3321E 00	3.4030E 00	3.4730E 00	3.5426E 00	3.6121E 00	3.6818E 00	3.7519E 00	3.8227E 00
75.0	3.6706E 00	3.7503E 00	3.8285E 00	3.9057E 00	3.9824E 00	4.0589E 00	4.1355E 00	4.2125E 00	4.2902E 00
80.0	4.1012E 00	4.1887E 00	4.2744E 00	4.3590E 00	4.4430E 00	4.5266E 00	4.6103E 00	4.6944E 00	4.7791E 00
85.0	4.5514E 00	4.6468E 00	4.7403E 00	4.8325E 00	4.9238E 00	5.0148E 00	5.1057E 00	5.1969E 00	5.2888E 00
90.0	5.0206E 00	5.1243E 00	5.2257E 00	5.3256E 00	5.4246E 00	5.5230E 00	5.6212E 00	5.7198E 00	5.8189E 00
95.0	5.5086E 00	5.6206E 00	5.7302E 00	5.8380E 00	5.9447E 00	6.0507E 00	6.1565E 00	6.2624E 00	6.3690E 00
100.0	6.0148E 00	6.1354E 00	6.2533E 00	6.3692E 00	6.4838E 00	6.5975E 00	6.7109E 00	6.8245E 00	6.9385E 00
105.0	6.5389E 00	6.6683E 00	6.7947E 00	6.9189E 00	7.0415E 00	7.1631E 00	7.2843E 00	7.4055E 00	7.5271E 00
110.0	7.0805E 00	7.2189E 00	7.3540E 00	7.4865E 00	7.6173E 00	7.7470E 00	7.8760E 00	8.0050E 00	8.1344E 00
115.0	7.6393E 00	7.7869E 00	7.9308E 00	8.0719E 00	8.2110E 00	8.3488E 00	8.4859E 00	8.6228E 00	8.7599E 00
120.0	8.2149E 00	8.3719E 00	8.5247E 00	8.6746E 00	8.8221E 00	8.9682E 00	9.1134E 00	9.2583E 00	9.4034E 00
125.0	8.8070E 00	8.9735E 00	9.1355E 00	9.2942E 00	9.4504E 00	9.6049E 00	9.7583E 00	9.9113E 00	1.0064E 01
130.0	9.4153E 00	9.5914E 00	9.7628E 00	9.9305E 00	1.0095E 01	1.0258E 01	1.0420E 01	1.0581E 01	1.0743E 01
135.0	1.0039E 01	1.0225E 01	1.0406E 01	1.0583E 01	1.0757E 01	1.0929E 01	1.1099E 01	1.1268E 01	1.1438E 01
140.0	1.0679E 01	1.0875E 01	1.1066E 01	1.1252E 01	1.1434E 01	1.1615E 01	1.1794E 01	1.1972E 01	1.2149E 01
145.0	1.1334E 01	1.1540E 01	1.1740E 01	1.1936E 01	1.2128E 01	1.2317E 01	1.2505E 01	1.2691E 01	1.2877E 01
150.0	1.2004E 01	1.2220E 01	1.2431E 01	1.2636E 01	1.2837E 01	1.3035E 01	1.3232E 01	1.3427E 01	1.3621E 01
155.0	1.2689E 01	1.2916E 01	1.3136E 01	1.3350E 01	1.3561E 01	1.3768E 01	1.3974E 01	1.4178E 01	1.4381E 01
160.0	1.3388E 01	1.3625E 01	1.3856E 01	1.4080E 01	1.4300E 01	1.4517E 01	1.4731E 01	1.4944E 01	1.5155E 01
165.0	1.4101E 01	1.4349E 01	1.4590E 01	1.4824E 01	1.5054E 01	1.5280E 01	1.5503E 01	1.5725E 01	1.5945E 01
170.0	1.4828E 01	1.5087E 01	1.5338E 01	1.5583E 01	1.5822E 01	1.6058E 01	1.6290E 01	1.6521E 01	1.6750E 01
175.0	1.5569E 01	1.5839E 01	1.6101E 01	1.6355E 01	1.6605E 01	1.6850E 01	1.7091E 01	1.7331E 01	1.7569E 01
180.0	1.6323E 01	1.6605E 01	1.6877E 01	1.7142E 01	1.7401E 01	1.7656E 01	1.7907E 01	1.8156E 01	1.8403E 01
185.0	1.7090E 01	1.7383E 01	1.7666E 01	1.7942E 01	1.8211E 01	1.8475E 01	1.8736E 01	1.8994E 01	1.9250E 01
190.0	1.7871E 01	1.8175E 01	1.8469E 01	1.8755E 01	1.9034E 01	1.9309E 01	1.9579E 01	1.9846E 01	2.0111E 01
195.0	1.8664E 01	1.8980E 01	1.9285E 01	1.9582E 01	1.9871E 01	2.0155E 01	2.0435E 01	2.0712E 01	2.0986E 01
200.0	1.9470E 01	1.9797E 01	2.0114E 01	2.0421E 01	2.0721E 01	2.1015E 01	2.1304E 01	2.1591E 01	2.1874E 01
210.0	2.1118E 01	2.1469E 01	2.1808E 01	2.2137E 01	2.2458E 01	2.2772E 01	2.3082E 01	2.3387E 01	2.3690E 01
220.0	2.2814E 01	2.3189E 01	2.3551E 01	2.3902E 01	2.4244E 01	2.4579E 01	2.4909E 01	2.5234E 01	2.5555E 01
230.0	2.4555E 01	2.4956E 01	2.5341E 01	2.5715E 01	2.6079E 01	2.6435E 01	2.6784E 01	2.7129E 01	2.7470E 01
240.0	2.6342E 01	2.6767E 01	2.7177E 01	2.7573E 01	2.7959E 01	2.8336E 01	2.8706E 01	2.9071E 01	2.9432E 01
250.0	2.8171E 01	2.8622E 01	2.9056E 01	2.9476E 01	2.9884E 01	3.0283E 01	3.0674E 01	3.1059E 01	3.1439E 01
260.0	3.0043E 01	3.0519E 01	3.0978E 01	3.1421E 01	3.1852E 01	3.2273E 01	3.2685E 01	3.3090E 01	3.3491E 01
270.0	3.1954E 01	3.2457E 01	3.2941E 01	3.3408E 01	3.3862E 01	3.4304E 01	3.4738E 01	3.5165E 01	3.5585E 01
280.0	3.3905E 01	3.4435E 01	3.4944E 01	3.5435E 01	3.5912E 01	3.6377E 01	3.6833E 01	3.7280E 01	3.7721E 01
290.0	3.5894E 01	3.6451E 01	3.6985E 01	3.7501E 01	3.8002E 01	3.8489E 01	3.8967E 01	3.9435E 01	3.9897E 01
300.0	3.7920E 01	3.8504E 01	3.9064E 01	3.9605E 01	4.0129E 01	4.0640E 01	4.1139E 01	4.1629E 01	4.2112E 01
310.0	3.9981E 01	4.0593E 01	4.1179E 01	4.1745E 01	4.2293E 01	4.2827E 01	4.3349E 01	4.3861E 01	4.4365E 01
320.0	4.2077E 01	4.2716E 01	4.3330E 01	4.3921E 01	4.4493E 01	4.5051E 01	4.5595E 01	4.6129E 01	4.6654E 01
330.0	4.4206E 01	4.4874E 01	4.5514E 01	4.6131E 01	4.6728E 01	4.7309E 01	4.7876E 01	4.8432E 01	4.8978E 01
340.0	4.6368E 01	4.7065E 01	4.7732E 01	4.8374E 01	4.8996E 01	4.9601E 01	5.0191E 01	5.0769E 01	5.1337E 01
350.0	4.8562E 01	4.9287E 01	4.9981E 01	5.0650E 01	5.1297E 01	5.1926E 01	5.2539E 01	5.3140E 01	5.3729E 01
360.0	5.0786E 01	5.1540E 01	5.2262E 01	5.2957E 01	5.3629E 01	5.4282E 01	5.4919E 01	5.5542E 01	5.6154E 01
370.0	5.3040E 01	5.3824E 01	5.4574E 01	5.5295E 01	5.5993E 01	5.6670E 01	5.7330E 01	5.7976E 01	5.8610E 01
380.0	5.5322E 01	5.6136E 01	5.6914E 01	5.7662E 01	5.8385E 01	5.9087E 01	5.9771E 01	6.0440E 01	6.1096E 01
390.0	5.7633E 01	5.8477E 01	5.9283E 01	6.0058E 01	6.0807E 01	6.1534E 01	6.2242E 01	6.2933E 01	6.3612E 01
400.0	5.9972E 01	6.0845E 01	6.1680E 01	6.2482E 01	6.3257E 01	6.4009E 01	6.4740E 01	6.5455E 01	6.6156E 01

RANGE

ENERGY MEV	I= 550.0	I= 600.0	I= 650.0	I= 700.0	I= 750.0	I= 800.0	I= 850.0	I= 900.0	I= 950.0
410.0	6.2336E 01	6.3240E 01	6.4103E 01	6.4933E 01	6.5734E 01	6.6511E 01	6.7267E 01	6.8005E 01	6.8729E 01
420.0	6.4727E 01	6.5661E 01	6.6553E 01	6.7410E 01	6.8238E 01	6.9039E 01	6.9820E 01	7.0582E 01	7.1328E 01
430.0	6.7142E 01	6.8107E 01	6.9028E 01	6.9913E 01	7.0767E 01	7.1594E 01	7.2399E 01	7.3184E 01	7.3953E 01
440.0	6.9582E 01	7.0578E 01	7.1528E 01	7.2441E 01	7.3321E 01	7.4174E 01	7.5003E 01	7.5812E 01	7.6605E 01
450.0	7.2045E 01	7.3072E 01	7.4052E 01	7.4993E 01	7.5900E 01	7.6778E 01	7.7632E 01	7.8465E 01	7.9280E 01
460.0	7.4531E 01	7.5590E 01	7.6599E 01	7.7568E 01	7.8502E 01	7.9406E 01	8.0285E 01	8.1142E 01	8.1980E 01
470.0	7.7040E 01	7.8130E 01	7.9169E 01	8.0166E 01	8.1127E 01	8.2057E 01	8.2961E 01	8.3842E 01	8.4704E 01
480.0	7.9570E 01	8.0692E 01	8.1761E 01	8.2787E 01	8.3775E 01	8.4731E 01	8.5660E 01	8.6565E 01	8.7450E 01
490.0	8.2122E 01	8.3275E 01	8.4374E 01	8.5429E 01	8.6444E 01	8.7426E 01	8.8380E 01	8.9310E 01	9.0218E 01
500.0	8.4694E 01	8.5879E 01	8.7009E 01	8.8091E 01	8.9134E 01	9.0143E 01	9.1122E 01	9.2076E 01	9.3008E 01
510.0	8.7286E 01	8.8503E 01	8.9663E 01	9.0775E 01	9.1845E 01	9.2880E 01	9.3884E 01	9.4863E 01	9.5818E 01
520.0	8.9897E 01	9.1147E 01	9.2337E 01	9.3478E 01	9.4576E 01	9.5637E 01	9.6667E 01	9.7670E 01	9.8649E 01
530.0	9.2527E 01	9.3809E 01	9.5031E 01	9.6200E 01	9.7326E 01	9.8414E 01	9.9469E 01	1.0050E 02	1.0150E 02
540.0	9.5176E 01	9.6491E 01	9.7743E 01	9.8941E 01	1.0010E 02	1.0121E 02	1.0229E 02	1.0334E 02	1.0437E 02
550.0	9.7843E 01	9.9190E 01	1.0047E 02	1.0170E 02	1.0288E 02	1.0402E 02	1.0513E 02	1.0621E 02	1.0726E 02
560.0	1.0053E 02	1.0191E 02	1.0322E 02	1.0448E 02	1.0569E 02	1.0686E 02	1.0799E 02	1.0909E 02	1.1017E 02
570.0	1.0323E 02	1.0464E 02	1.0599E 02	1.0727E 02	1.0851E 02	1.0971E 02	1.1086E 02	1.1199E 02	1.1309E 02
580.0	1.0595E 02	1.0739E 02	1.0877E 02	1.1008E 02	1.1135E 02	1.1257E 02	1.1376E 02	1.1491E 02	1.1603E 02
590.0	1.0868E 02	1.1016E 02	1.1157E 02	1.1291E 02	1.1421E 02	1.1546E 02	1.1667E 02	1.1784E 02	1.1899E 02
600.0	1.1143E 02	1.1294E 02	1.1438E 02	1.1576E 02	1.1708E 02	1.1835E 02	1.1959E 02	1.2079E 02	1.2196E 02
610.0	1.1419E 02	1.1574E 02	1.1721E 02	1.1862E 02	1.1997E 02	1.2127E 02	1.2253E 02	1.2376E 02	1.2496E 02
620.0	1.1697E 02	1.1855E 02	1.2005E 02	1.2149E 02	1.2287E 02	1.2420E 02	1.2549E 02	1.2674E 02	1.2796E 02
630.0	1.1977E 02	1.2138E 02	1.2291E 02	1.2438E 02	1.2579E 02	1.2715E 02	1.2846E 02	1.2974E 02	1.3098E 02
640.0	1.2258E 02	1.2422E 02	1.2579E 02	1.2728E 02	1.2872E 02	1.3011E 02	1.3145E 02	1.3275E 02	1.3402E 02
650.0	1.2540E 02	1.2708E 02	1.2867E 02	1.3020E 02	1.3167E 02	1.3308E 02	1.3445E 02	1.3577E 02	1.3707E 02
660.0	1.2823E 02	1.2995E 02	1.3158E 02	1.3313E 02	1.3463E 02	1.3607E 02	1.3746E 02	1.3881E 02	1.4013E 02
670.0	1.3108E 02	1.3283E 02	1.3449E 02	1.3608E 02	1.3760E 02	1.3907E 02	1.4049E 02	1.4187E 02	1.4321E 02
680.0	1.3394E 02	1.3572E 02	1.3742E 02	1.3903E 02	1.4059E 02	1.4208E 02	1.4353E 02	1.4493E 02	1.4630E 02
690.0	1.3682E 02	1.3863E 02	1.4036E 02	1.4200E 02	1.4358E 02	1.4511E 02	1.4658E 02	1.4801E 02	1.4940E 02
700.0	1.3970E 02	1.4155E 02	1.4331E 02	1.4499E 02	1.4660E 02	1.4815E 02	1.4965E 02	1.5110E 02	1.5252E 02
710.0	1.4260E 02	1.4448E 02	1.4627E 02	1.4798E 02	1.4962E 02	1.5120E 02	1.5273E 02	1.5421E 02	1.5565E 02
720.0	1.4551E 02	1.4743E 02	1.4925E 02	1.5099E 02	1.5265E 02	1.5426E 02	1.5581E 02	1.5732E 02	1.5879E 02
730.0	1.4843E 02	1.5038E 02	1.5223E 02	1.5400E 02	1.5570E 02	1.5734E 02	1.5892E 02	1.6045E 02	1.6194E 02
740.0	1.5136E 02	1.5335E 02	1.5523E 02	1.5703E 02	1.5876E 02	1.6042E 02	1.6203E 02	1.6359E 02	1.6510E 02
750.0	1.5430E 02	1.5632E 02	1.5824E 02	1.6007E 02	1.6183E 02	1.6352E 02	1.6515E 02	1.6673E 02	1.6827E 02
760.0	1.5725E 02	1.5931E 02	1.6126E 02	1.6312E 02	1.6491E 02	1.6662E 02	1.6828E 02	1.6989E 02	1.7146E 02
770.0	1.6022E 02	1.6230E 02	1.6429E 02	1.6618E 02	1.6799E 02	1.6974E 02	1.7143E 02	1.7306E 02	1.7465E 02
780.0	1.6319E 02	1.6531E 02	1.6733E 02	1.6925E 02	1.7109E 02	1.7287E 02	1.7458E 02	1.7624E 02	1.7786E 02
790.0	1.6617E 02	1.6833E 02	1.7038E 02	1.7233E 02	1.7420E 02	1.7600E 02	1.7775E 02	1.7943E 02	1.8107E 02
800.0	1.6916E 02	1.7135E 02	1.7343E 02	1.7542E 02	1.7732E 02	1.7915E 02	1.8092E 02	1.8263E 02	1.8430E 02
810.0	1.7216E 02	1.7439E 02	1.7650E 02	1.7852E 02	1.8045E 02	1.8231E 02	1.8410E 02	1.8584E 02	1.8753E 02
820.0	1.7517E 02	1.7743E 02	1.7958E 02	1.8162E 02	1.8358E 02	1.8547E 02	1.8729E 02	1.8906E 02	1.9077E 02
830.0	1.7819E 02	1.8048E 02	1.8266E 02	1.8474E 02	1.8673E 02	1.8864E 02	1.9049E 02	1.9228E 02	1.9402E 02
840.0	1.8121E 02	1.8354E 02	1.8576E 02	1.8786E 02	1.8988E 02	1.9183E 02	1.9370E 02	1.9552E 02	1.9728E 02
850.0	1.8425E 02	1.8661E 02	1.8886E 02	1.9100E 02	1.9305E 02	1.9502E 02	1.9692E 02	1.9876E 02	2.0055E 02
860.0	1.8729E 02	1.8969E 02	1.9197E 02	1.9414E 02	1.9622E 02	1.9822E 02	2.0015E 02	2.0201E 02	2.0383E 02
870.0	1.9034E 02	1.9277E 02	1.9508E 02	1.9729E 02	1.9939E 02	2.0142E 02	2.0338E 02	2.0527E 02	2.0711E 02
880.0	1.9340E 02	1.9587E 02	1.9821E 02	2.0044E 02	2.0258E 02	2.0464E 02	2.0662E 02	2.0854E 02	2.1041E 02
890.0	1.9646E 02	1.9897E 02	2.0134E 02	2.0361E 02	2.0577E 02	2.0786E 02	2.0987E 02	2.1182E 02	2.1370E 02
900.0	1.9953E 02	2.0207E 02	2.0448E 02	2.0678E 02	2.0898E 02	2.1109E 02	2.1313E 02	2.1510E 02	2.1701E 02
910.0	2.0261E 02	2.0519E 02	2.0763E 02	2.0996E 02	2.1218E 02	2.1432E 02	2.1639E 02	2.1839E 02	2.2033E 02
920.0	2.0570E 02	2.0831E 02	2.1078E 02	2.1314E 02	2.1540E 02	2.1757E 02	2.1966E 02	2.2168E 02	2.2365E 02
930.0	2.0879E 02	2.1144E 02	2.1395E 02	2.1633E 02	2.1862E 02	2.2082E 02	2.2294E 02	2.2499E 02	2.2698E 02
940.0	2.1189E 02	2.1457E 02	2.1711E 02	2.1953E 02	2.2185E 02	2.2407E 02	2.2622E 02	2.2830E 02	2.3031E 02
950.0	2.1500E 02	2.1771E 02	2.2029E 02	2.2274E 02	2.2508E 02	2.2734E 02	2.2951E 02	2.3161E 02	2.3365E 02
960.0	2.1811E 02	2.2086E 02	2.2347E 02	2.2595E 02	2.2833E 02	2.3061E 02	2.3281E 02	2.3494E 02	2.3700E 02
970.0	2.2123E 02	2.2402E 02	2.2665E 02	2.2917E 02	2.3157E 02	2.3388E 02	2.3611E 02	2.3826E 02	2.4035E 02
980.0	2.2435E 02	2.2718E 02	2.2985E 02	2.3239E 02	2.3483E 02	2.3716E 02	2.3942E 02	2.4160E 02	2.4371E 02
990.0	2.2748E 02	2.3034E 02	2.3305E 02	2.3562E 02	2.3809E 02	2.4045E 02	2.4273E 02	2.4494E 02	2.4708E 02
1000.0	2.3062E 02	2.3351E 02	2.3625E 02	2.3886E 02	2.4135E 02	2.4375E 02	2.4605E 02	2.4829E 02	2.5045E 02
1100.0	2.6226E 02	2.6550E 02	2.6857E 02	2.7149E 02	2.7428E 02	2.7696E 02	2.7954E 02	2.8203E 02	2.8445E 02
1200.0	2.9434E 02	2.9793E 02	3.0133E 02	3.0456E 02	3.0764E 02	3.1060E 02	3.1345E 02	3.1620E 02	3.1887E 02
1300.0	3.2674E 02	3.3068E 02	3.3441E 02	3.3795E 02	3.4133E 02	3.4457E 02	3.4769E 02	3.5070E 02	3.5361E 02
1400.0	3.5940E 02	3.6369E 02	3.6774E 02	3.7159E 02	3.7527E 02	3.7879E 02	3.8217E 02	3.8544E 02	3.8860E 02
1500.0	3.9225E 02	3.9689E 02	4.0126E 02	4.0542E 02	4.0939E 02	4.1319E 02	4.1684E 02	4.2036E 02	4.2376E 02
1600.0	4.2524E 02	4.3022E 02	4.3492E 02	4.3939E 02	4.4364E 02	4.4772E 02	4.5163E 02	4.5540E 02	4.5904E 02
1800.0	4.9148E 02	4.9714E 02	5.0249E 02	5.0755E 02	5.1238E 02	5.1700E 02	5.2143E 02	5.2570E 02	5.2982E 02
2000.0	5.5788E 02	5.6422E 02	5.7019E 02	5.7585E 02	5.8124E 02	5.8639E 02	5.9134E 02	5.9609E 02	6.0068E 02
2200.0	6.2427E 02	6.3127E 02	6.3786E 02	6.4410E 02	6.5004E 02	6.5572E 02	6.6117E 02	6.6640E 02	6.7146E 02
2400.0	6.9054E 02	6.9818E 02	7.0538E 02	7.1220E 02	7.1868E 02	7.2488E 02	7.3082E 02	7.3652E 02	7.4203E 02
2600.0	7.5661E 02	7.6489E 02	7.7268E 02	7.8007E 02	7.8708E 02	7.9379E 02	8.0021E 02	8.0638E 02	8.1232E 02
2800.0	8.2242E 02	8.3133E 02	8.3971E 02	8.4765E 02	8.5519E 02	8.6239E 02	8.6929E 02	8.7591E 02	8.8229E 02
3000.0	8.8795E 02	8.9748E 02	9.0644E 02	9.1492E 02	9.2298E 02	9.3067E 02	9.3803E 02	9.4510E 02	9.5190E 02
3200.0	9.5317E 02	9.6330E 02	9.7283E 02	9.8185E 02	9.9041E 02	9.9858E 02	1.0064E 03	1.0139E 03	1.0211E 03
3400.0	1.0181E 03	1.0288E 03	1.0389E 03	1.0484E 03	1.0575E 03	1.0661E 03	1.0744E 03	1.0823E 03	1.0900E 03
3600.0	1.0826E 03	1.0939E 03	1.1046E 03	1.1147E 03	1.1242E 03	1.1333E 03	1.1420E 03	1.1504E 03	1.1584E 03
3800.0	1.1469E 03	1.1588E 03	1.1699E 03	1.1805E 03	1.1906E 03	1.2001E 03	1.2093E 03	1.2181E 03	1.2265E 03
4000.0	1.2108E 03	1.2232E 03	1.2349E 03	1.2460E 03	1.2565E 03	1.2666E 03	1.2761E 03	1.2853E 03	1.2942E 03
4500.0	1.3690E 03	1.3829E 03	1.3960E 03	1.4083E 03	1.4199E 03	1.4311E 03	1.4417E 03	1.4519E 03	1.4617E 03
5000.0	1.5254E 03	1.5406E 03	1.5549E 03	1.5684E 03	1.5812E 03	1.5934E 03	1.6050E 03	1.6162E 03	1.6269E 03

PRINTOUT TABLE III

STOPPING-POWER AND RANGE TABLE

Stopping-power (Mev/g cm^{-2}) and range (g cm^{-2}) as functions of the particle energy (Mev), for various substances. The density-effect correction is included. Gases are assumed to be at normal pressure. Powers of ten are indicated by the symbol E; thus 1.2345E 02 means 1.2345×10^2. Because of typographical limitations, the adjusted mean excitation energy, I_{adj}, is indicated by the symbol I in the table headings; its units are ev. More figures are tabulated than are significant in order to facilitate interpolation and differencing. a, Protons (rest mass 938.213 Mev); b, kaons (rest mass 493.88 Mev); c, pions (rest mass 139.59 Mev); and muons (rest mass 105.65 Mev).

Note that for Fe a value of $I_{adj} = 273$ ev has been used as derived from the interpolation formula (17b), instead of the value 285 ev previously used in Tables 2, 4 and 7.

PROTON STOPPING POWER, MEV•CM2/G

ENERGY MEV	BE I= 60.0	C I= 78.0	AL I=163.0	FE I=273.0	CU I=314.0	AG I=487.0	AU I=797.0	PB I=826.0	U I=923.0
2.0	1.3882E 02	1.4606E 02	1.1240E 02	8.9791E 01	8.3224E 01	6.5775E 01	4.7870E 01	4.6397E 01	4.2810E 01
4.0	8.1412E 01	8.6414E 01	6.8576E 01	5.6299E 01	5.2615E 01	4.2787E 01	3.2311E 01	3.1407E 01	2.9246E 01
6.0	5.8079E 01	6,1760E 01	4.9597E 01	4.1306E 01	3.8788E 01	3.2097C 01	2.4831E 01	2.4184E 01	2.2661E 01
8.0	4.5315E 01	4.8377E 01	3.9448E 01	3.3362E 01	3.1420E 01	2.6275E 01	2.0521E 01	2.0001E 01	1.8791E 01
10.0	3.7932E 01	4.0741E 01	3.3796E 01	2.8942E 01	2.7315E 01	2.2980E 01	1.7956E 01	1.7497E 01	1.6422E 01
14.0	2.8859E 01	3.1084E 01	2.6066E 01	2.2518E 01	2.1315E 01	1.8069C 01	1.4095E 01	1.3718E 01	1.2802E 01
18.0	2.3511E 01	2.5371E 01	2.1430E 01	1.8623E 01	1.7666E 01	1.5065C 01	1.1793E 01	1.1475E 01	1.0695E 01
22.0	1.9957E 01	2.1566E 01	1.8312E 01	1.5984E 01	1.5187E 01	1.3018E 01	1.0253E 01	9.9808E 00	9.3125E 00
26.0	1.7414E 01	1.8837E 01	1.6059E 01	1.4066E 01	1.3382E 01	1.1522C 01	9.1343E 00	8.8965E 00	8.3160E 00
30.0	1.5498E 01	1.6779E 01	1.4350E 01	1.2605E 01	1.2004E 01	1.0374C 01	8.2750E 00	8.0642E 00	7.5528E 00
34.0	1.4000E 01	1.5168E 01	1.3006E 01	1.1451E 01	1.0915E 01	9.4618E 00	7.5894E 00	7.4001E 00	6.9438E 00
38.0	1.2794E 01	1.3870E 01	1.1919E 01	1.0515E 01	1.0030E 01	8.7184E 00	7.0273E 00	6.8554E 00	6.4435E 00
42.0	1.1802E 01	1.2801E 01	1.1022E 01	9.7399E 00	9.2965E 00	8.0995E 00	6.5565E 00	6.3989E 00	6.0236E 00
46.0	1.0970E 01	1.1905E 01	1.0267E 01	9.0862E 00	8.6773E 00	7.5755E 00	6.1557E 00	6.0100E 00	5.6651E 00
50.0	1.0263E 01	1.1141E 01	9.6226E 00	8.5273E 00	8.1474E 00	7.1256E 00	5.8096E 00	5.6741E 00	5.3549E 00
60.0	8.8809E 00	9.6496E 00	8.3592E 00	7.4278E 00	7.1039E 00	6.2360E 00	5.1195E 00	5.0036E 00	4.7338E 00
70.0	7.8708E 00	8.5879E 00	7.4312E 00	6.6172E 00	6.3335E 00	5.5756C 00	4.6019E 00	4.5002E 00	4.2657E 00
80.0	7.0988E 00	7.7229E 00	6.7191E 00	5.9936E 00	5.7401E 00	5.0649E 00	4.1982E 00	4.1072E 00	3.8990E 00
90.0	6.4890E 00	7.0628E 00	6.1549E 00	5.4982E 00	5.2683E 00	4.6574E 00	3.8740E 00	3.7913E 00	3.6035E 00
100.0	5.9947E 00	6.5274E 00	5.6963E 00	5.0948E 00	4.8839E 00	4.3245E 00	3.6075E 00	3.5315E 00	3.3600E 00
110.0	5.5856E 00	6.0842E 00	5.3159E 00	4.7597E 00	4.5643E 00	4.0471E 00	3.3844E 00	3.3139E 00	3.1557E 00
120.0	5.2413E 00	5.7111E 00	4.9953E 00	4.4768E 00	4.2944E 00	3.8123E 00	3.1948E 00	3.1290E 00	2.9817E 00
130.0	4.9476E 00	5.3925E 00	4.7211E 00	4.2347E 00	4.0633E 00	3.6110C 00	3.0317E 00	2.9697E 00	2.8317E 00
140.0	4.6939E 00	5.1173E 00	4.4841E 00	4.0251E 00	3.8632E 00	3.4363E 00	2.8897E 00	2.8311E 00	2.7011E 00
150.0	4.4726E 00	4.8772E 00	4.2770E 00	3.8419E 00	3.6881E 00	3.2834C 00	2.7651E 00	2.7094E 00	2.5862E 00
160.0	4.2778E 00	4.6658E 00	4.0946E 00	3.6803E 00	3.5338E 00	3.1483E 00	2.6548E 00	2.6017E 00	2.4844E 00
170.0	4.1051E 00	4.4783E 00	3.9327E 00	3.5367E 00	3.3966E 00	3.0282E 00	2.5565E 00	2.5056E 00	2.3936E 00
180.0	3.9508E 00	4.3109E 00	3.7879E 00	3.4083E 00	3.2738E 00	2.9206E 00	2.4683E 00	2.4194E 00	2.3121E 00
190.0	3.8123E 00	4.1604E 00	3.6578E 00	3.2929E 00	3.1634E 00	2.8238E 00	2.3888E 00	2.3417E 00	2.2385C 00
200.0	3.6872E 00	4.0245E 00	3.5402E 00	3.1885E 00	3.0636E 00	2.7361C 00	2.3167E 00	2.2712E 00	2.1718C 00
220.0	3.4701E 00	3.7887E 00	3.3360E 00	3.0070E 00	2.8900E 00	2.5837E 00	2.1911E 00	2.1484E 00	2.0554E 00
240.0	3.2884E 00	3.5913E 00	3.1649E 00	2.8549E 00	2.7444E 00	2.4556E 00	2.0854E 00	2.0450E 00	1.9573E 00
260.0	3.1341E 00	3.4236E 00	3.0195E 00	2.7255E 00	2.6206E 00	2.3466E 00	1.9952C 00	1.9568E 00	1.8737E 00
280.0	3.0016E 00	3.2796E 00	2.8945E 00	2.6142E 00	2.5141E 00	2.2528E 00	1.9175E 00	1.8808E 00	1.8015E 00
300.0	2.8867E 00	3.1546E 00	2.7860E 00	2.5176E 00	2.4216E 00	2.1712E 00	1.8499E 00	1.8146E 00	1.7386E 00
320.0	2.7860E 00	3.0362E 00	2.6909E 00	2.4330E 00	2.3406E 00	2.0997E 00	1.7905E 00	1.7566E 00	1.6834E 00
340.0	2.6972E 00	2.9397E 00	2.6071E 00	2.3583E 00	2.2690E 00	2.0366E 00	1.7381E 00	1.7052E 00	1.6347E 00
360.0	2.6184E 00	2.8540E 00	2.5327E 00	2.2919E 00	2.2055E 00	1.9794E 00	1.6915C 00	1.6596E 00	1.5913E 00
380.0	2.5480E 00	2.7772E 00	2.4661E 00	2.2315E 00	2.1487E 00	1.9300E 00	1.6498E 00	1.6188E 00	1.5525E 00
400.0	2.4848E 00	2.7083E 00	2.4064E 00	2.1783E 00	2.0973E 00	1.8854C 00	1.6124E 00	1.5822E 00	1.5176E 00
420.0	2.4278E 00	2.6460E 00	2.3525E 00	2.1302E 00	2.0513C 00	1.8448C 00	1.5786E 00	1.5491E 00	1.4861E 00
440.0	2.3761E 00	2.5895E 00	2.3037E 00	2.0866E 00	2.0096E 00	1.8080C 00	1.5479E 00	1.5191E 00	1.4576E 00
460.0	2.3289E 00	2.5378E 00	2.2593E 00	2.0470E 00	1.9717E 00	1.7745E 00	1.5201E 00	1.4918E 00	1.4316E 00
480.0	2.2856E 00	2.4907E 00	2.2112E 00	2.0107E 00	1.9371E 00	1.7440E 00	1.4947L 00	1.4669E 00	1.4080E 00
500.0	2.2460E 00	2.4476E 00	2.1745E 00	1.9775E 00	1.9055E 00	1.7161E 00	1.4714E 00	1.4442E 00	1.3863E 00
520.0	2.2095E 00	2.4079E 00	2.1408E 00	1.9470E 00	1.8764E 00	1.6904E 00	1.4501E 00	1.4233E 00	1.3664E 00
540.0	2.1758E 00	2.3713E 00	2.1096E 00	1.9189E 00	1.8496E 00	1.6669E 00	1.4304E 00	1.4040E 00	1.3481E 00
560.0	2.1447E 00	2.3374E 00	2.0809E 00	1.8929E 00	1.8249L 00	1.6451L 00	1.4123E 00	1.3863E 00	1.3312E 00
580.0	2.1158E 00	2.3061E 00	2.0542E 00	1.8666E 00	1.8021E 00	1.6250E 00	1.3956E 00	1.3700E 00	1.3157E 00
600.0	2.0890E 00	2.2770E 00	2.0295E 00	1.8444E 00	1.7809E 00	1.6064C 00	1.3801E 00	1.3548E 00	1.3012E 00
620.0	2.0640E 00	2.2499E 00	2.0065E 00	1.8237E 00	1.7613E 00	1.5891E 00	1.3657E 00	1.3407E 00	1.2879E 00
640.0	2.0407E 00	2.2247E 00	1.9851E 00	1.8045E 00	1.7430E 00	1.5731C 00	1.3524E 00	1.3277E 00	1.2754E 00
660.0	2.0190E 00	2.2011E 00	1.9651E 00	1.7866E 00	1.7260E 00	1.5581E 00	1.3400E 00	1.3155E 00	1.2639E 00
680.0	1.9986E 00	2.1790E 00	1.9464E 00	1.7698E 00	1.7101E 00	1.5442C 00	1.3284E 00	1.3042E 00	1.2531E 00
700.0	1.9795E 00	2.1584E 00	1.9289E 00	1.7541E 00	1.6953E 00	1.5312F 00	1.3176E 00	1.2937E 00	1.2431E 00
720.0	1.9616E 00	2.1390E 00	1.9125E 00	1.7394E 00	1.6814E 00	1.5190L 00	1.3076E 00	1.2838E 00	1.2337E 00
740.0	1.9447E 00	2.1208E 00	1.8971E 00	1.7256E 00	1.6684E 00	1.5077C 00	1.2981E 00	1.2746E 00	1.2249E 00
760.0	1.9289E 00	2.1037E 00	1.8827E 00	1.7127E 00	1.6562E 00	1.4970C 00	1.2893E 00	1.2659E 00	1.2167C 00
780.0	1.9139E 00	2.0876E 00	1.8690E 00	1.7005E 00	1.6447E 00	1.4870C 00	1.2811E 00	1.2579E 00	1.2091E 00
800.0	1.8999E 00	2.0724E 00	1.8562E 00	1.6890E 00	1.6340E 00	1.4776E 00	1.2733E 00	1.2503E 00	1.2019E 00
820.0	1.8865E 00	2.0581E 00	1.8441E 00	1.6782E 00	1.6239E 00	1.4688E 00	1.2660E 00	1.2432E 00	1.1951E 00
840.0	1.8740E 00	2.0445E 00	1.8327E 00	1.6680E 00	1.6090E 00	1.4595E 00	1.2592E 00	1.2365E 00	1.1876E 00
860.0	1.8621E 00	2.0317E 00	1.8220E 00	1.6584E 00	1.5999E 00	1.4518E 00	1.2528E 00	1.2302E 00	1.1817E 00
880.0	1.8508E 00	2.0196E 00	1.8118E 00	1.6493E 00	1.5913E 00	1.4445E 00	1.2468E 00	1.2243E 00	1.1761E 00
900.0	1.8401E 00	2.0082E 00	1.8022E 00	1.6407E 00	1.5832E 00	1.4377E 00	1.2411E 00	1.2187E 00	1.1708E 00
920.0	1.8300E 00	1.9973E 00	1.7930E 00	1.6326L 00	1.5756E 00	1.4312F 00	1.2357E 00	1.2135E 00	1.1659E 00
940.0	1.8204E 00	1.9870E 00	1.7844E 00	1.6248E 00	1.5683E 00	1.4251C 00	1.2307E 00	1.2086E 00	1.1612E 00
960.0	1.8112E 00	1.9772E 00	1.7762E 00	1.6175E 00	1.5614E 00	1.4194E 00	1.2260E 00	1.2040E 00	1.1568E 00
980.0	1.8025E 00	1.9679E 00	1.7685E 00	1.6106E 00	1.5549E 00	1.4140E 00	1.2204E 00	1.1996E 00	1.1526E 00
1000.0	1.7942E 00	1.9590E 00	1.7611E 00	1.6041E 00	1.5487E 00	1.4087E 00	1.2161E 00	1.1955E 00	1.1487E 00
1200.0	1.7300E 00	1.8907E 00	1.7046E 00	1.5540E 00	1.5017E 00	1.3689E 00	1.1836E 00	1.1652C 00	1.1192E 00
1400.0	1.6888E 00	1.8475E 00	1.6696E 00	1.5232E 00	1.4731E 00	1.3453E 00	1.1653E 00	1.1485E 00	1.1028E 00
1600.0	1.6617E 00	1.8194E 00	1.6477E 00	1.5042E 00	1.4556E 00	1.3315E 00	1.1551E 00	1.1360E 00	1.0940E 00
2000.0	1.6314E 00	1.7893E 00	1.6258E 00	1.4860E 00	1.4394E 00	1.3202E 00	1.1483E 00	1.1315E 00	1.0888E 00
2400.0	1.6183E 00	1.7778E 00	1.6196E 00	1.4818E 00	1.4364E 00	1.3204E 00	1.1508E 00	1.1358C 00	1.0923E 00
2800.0	1.6141E 00	1.7755E 00	1.6211E 00	1.4844E 00	1.4398E 00	1.3260C 00	1.1578E 00	1.1441C 00	1.0998E 00
3200.0	1.6146E 00	1.7783E 00	1.6267E 00	1.4906E 00	1.4466E 00	1.3343E 00	1.1668E 00	1.1542E 00	1.1091E 00
3600.0	1.6178E 00	1.7839E 00	1.6344E 00	1.4987E 00	1.4550C 00	1.3439E 00	1.1767E 00	1.1652E 00	1.1193E 00
4000.0	1.6226E 00	1.7910E 00	1.6432E 00	1.5077E 00	1.4642E 00	1.3541E 00	1.1870E 00	1.1763E 00	1.1297E 00
5000.0	1.6375E 00	1.8114E 00	1.6668E 00	1.5312E 00	1.4882E 00	1.3797C 00	1.2123E 00	1.2034E 00	1.1551E 00

PROTON STOPPING POWER, MEV•CM2/G

ENERGY MEV	H I= 18.7	HE I= 42.0	NE I=131.0	A I=210.0	KR I=381.0	XE I=555.0	AIR I= 86.8	CARB.DIOXIDE I= 85.9	METHANE I= 44.1
2.0	3.8577E 02	1.6943E 02	1.2428E 02	9.6061E 01	7.2252E 01	5.8479E 01	1.4170E 02	1.4235E 02	2.0925E 02
4.0	2.2039E 02	9.8358E 01	7.5063E 01	5.9363E 01	4.6234E 01	3.8395E 01	8.4161E 01	8.4516E 01	1.2163E 02
6.0	1.5837E 02	7.0137E 01	5.4041E 01	4.3210E 01	3.4330E 01	2.8973E 01	6.0216E 01	6.0463E 01	8.6725E 01
8.0	1.2415E 02	5.4551E 01	4.2749E 01	3.4613E 01	2.7947E 01	2.3780E 01	4.7270E 01	4.7461E 01	6.7510E 01
10.0	1.0209E 02	4.5315E 01	3.6431E 01	2.9836E 01	2.4373E 01	2.0815E 01	3.9919E 01	4.0073E 01	5.6158E 01
14.0	7.6876E 01	3.4368E 01	2.8002E 01	2.3110E 01	1.9089E 01	1.6389E 01	3.0491E 01	3.0603E 01	4.2592E 01
18.0	6.2198E 01	2.7939E 01	2.2968E 01	1.9054E 01	1.5863E 01	1.3686E 01	2.4906E 01	2.4994E 01	3.4626E 01
22.0	5.2532E 01	2.3678E 01	1.9593E 01	1.6316E 01	1.3666E 01	1.1847E 01	2.1183E 01	2.1256E 01	2.9348E 01
26.0	4.5658E 01	2.0635E 01	1.7160E 01	1.4332E 01	1.2064E 01	1.0501E 01	1.8511E 01	1.8573E 01	2.5578E 01
30.0	4.0507E 01	1.8346E 01	1.5318E 01	1.2824E 01	1.0838E 01	9.4676E 00	1.6495E 01	1.6549E 01	2.2742E 01
34.0	3.6495E 01	1.6558E 01	1.3871E 01	1.1635E 01	9.8667E 00	8.6458E 00	1.4915E 01	1.4964E 01	2.0528E 01
38.0	3.3278E 01	1.5122E 01	1.2704E 01	1.0673E 01	9.0766E 00	7.9748E 00	1.3643E 01	1.3686E 01	1.8748E 01
42.0	3.0638E 01	1.3940E 01	1.1740E 01	9.8772E 00	8.4204E 00	7.4154E 00	1.2594E 01	1.2634E 01	1.7284E 01
46.0	2.8431E 01	1.2951E 01	1.0930E 01	9.2070E 00	7.8659E 00	6.9412E 00	1.1714E 01	1.1751E 01	1.6058E 01
50.0	2.6557E 01	1.2109E 01	1.0239E 01	8.6346E 00	7.3907E 00	6.5336E 00	1.0965E 01	1.0999E 01	1.5016E 01
60.0	2.2908E 01	1.0468E 01	8.8859E 00	7.5104E 00	6.4535E 00	5.7261E 00	9.5003E 00	9.5296E 00	1.2982E 01
70.0	2.0251E 01	9.2696E 00	7.8932E 00	6.6831E 00	5.7601E 00	5.1255E 00	8.4280E 00	8.4536E 00	1.1497E 01
80.0	1.8227E 01	8.3547E 00	7.1324E 00	6.0476E 00	5.2252E 00	4.6602E 00	7.6075E 00	7.6304E 00	1.0363E 01
90.0	1.6632E 01	7.6325E 00	6.5300E 00	5.5435E 00	4.7993E 00	4.2884E 00	6.9587E 00	6.9795E 00	9.4677E 00
100.0	1.5341E 01	7.0474E 00	6.0407E 00	5.1334E 00	4.4519E 00	3.9843E 00	6.4323E 00	6.4514E 00	8.7425E 00
110.0	1.4275E 01	6.5636E 00	5.6352E 00	4.7930E 00	4.1629E 00	3.7307E 00	5.9965E 00	6.0141E 00	8.1427E 00
120.0	1.3379E 01	6.1566E 00	5.2934E 00	4.5059E 00	3.9186E 00	3.5159E 00	5.6295E 00	5.6460E 00	7.6382E 00
130.0	1.2616E 01	5.8095E 00	5.0014E 00	4.2603E 00	3.7093E 00	3.3315E 00	5.3161E 00	5.3316E 00	7.2079E 00
140.0	1.1957E 01	5.5098E 00	4.7489E 00	4.0478E 00	3.5279E 00	3.1715E 00	5.0454E 00	5.0600E 00	6.8364E 00
150.0	1.1383E 01	5.2485E 00	4.5285E 00	3.8621E 00	3.3692E 00	3.0313E 00	4.8091E 00	4.8230E 00	6.5124E 00
160.0	1.0879E 01	5.0186E 00	4.3344E 00	3.6985E 00	3.2292E 00	2.9074E 00	4.6011E 00	4.6144E 00	6.2273E 00
170.0	1.0432E 01	4.8147E 00	4.1620E 00	3.5531E 00	3.1047E 00	2.7972E 00	4.4166E 00	4.4293E 00	5.9745E 00
180.0	1.0033E 01	4.6328E 00	4.0081E 00	3.4232E 00	2.9933E 00	2.6985E 00	4.2518E 00	4.2639E 00	5.7489E 00
190.0	9.6746E 00	4.4693E 00	3.8697E 00	3.3064E 00	2.8930E 00	2.6096E 00	4.1037E 00	4.1154E 00	5.5462E 00
200.0	9.3514E 00	4.3218E 00	3.7446E 00	3.2007E 00	2.8023E 00	2.5291E 00	3.9699E 00	3.9812E 00	5.3633E 00
220.0	8.7910E 00	4.0659E 00	3.5276E 00	3.0173E 00	2.6446E 00	2.3890E 00	3.7378E 00	3.7484E 00	5.0459E 00
240.0	8.3224E 00	3.8517E 00	3.3457E 00	2.8635E 00	2.5122E 00	2.2713E 00	3.5434E 00	3.5534E 00	4.7803E 00
260.0	7.9248E 00	3.6699E 00	3.1912E 00	2.7328E 00	2.3996E 00	2.1710E 00	3.3783E 00	3.3878E 00	4.5549E 00
280.0	7.5834E 00	3.5138E 00	3.0584E 00	2.6204E 00	2.3028E 00	2.0847E 00	3.2365E 00	3.2456E 00	4.3612E 00
300.0	7.2874E 00	3.3783E 00	2.9431E 00	2.5228E 00	2.2186E 00	2.0097E 00	3.1134E 00	3.1221E 00	4.1932E 00
320.0	7.0283E 00	3.2598E 00	2.8422E 00	2.4373E 00	2.1448E 00	1.9439E 00	3.0057E 00	3.0140E 00	4.0462E 00
340.0	6.7999E 00	3.1552E 00	2.7532E 00	2.3619E 00	2.0797E 00	1.8858E 00	2.9106E 00	2.9187E 00	3.9165E 00
360.0	6.5971E 00	3.0624E 00	2.6741E 00	2.2949E 00	2.0219E 00	1.8342E 00	2.8262E 00	2.8340E 00	3.8014E 00
380.0	6.4160E 00	2.9795E 00	2.6035E 00	2.2351E 00	1.9702E 00	1.7881E 00	2.7508E 00	2.7584E 00	3.6986E 00
400.0	6.2534E 00	2.9050E 00	2.5401E 00	2.1814E 00	1.9238E 00	1.7467E 00	2.6831E 00	2.6905E 00	3.6063E 00
420.0	6.1067E 00	2.8379E 00	2.4828E 00	2.1329E 00	1.8819E 00	1.7093E 00	2.6221E 00	2.6292E 00	3.5230E 00
440.0	5.9738E 00	2.7770E 00	2.4310E 00	2.0890E 00	1.8440E 00	1.6754E 00	2.5667E 00	2.5738E 00	3.4475E 00
460.0	5.8529E 00	2.7217E 00	2.3839E 00	2.0490E 00	1.8095E 00	1.6446E 00	2.5164E 00	2.5233E 00	3.3789E 00
480.0	5.7425E 00	2.6712E 00	2.3408E 00	2.0126E 00	1.7780E 00	1.6165E 00	2.4705E 00	2.4772E 00	3.3162E 00
500.0	5.6414E 00	2.6249E 00	2.3014E 00	1.9792E 00	1.7492E 00	1.5908E 00	2.4284E 00	2.4350E 00	3.2588E 00
520.0	5.5485E 00	2.5824E 00	2.2653E 00	1.9486E 00	1.7228E 00	1.5672E 00	2.3898E 00	2.3963E 00	3.2061E 00
540.0	5.4630E 00	2.5433E 00	2.2320E 00	1.9204E 00	1.6984E 00	1.5454E 00	2.3543E 00	2.3606E 00	3.1576E 00
560.0	5.3840E 00	2.5071E 00	2.2013E 00	1.8944E 00	1.6760E 00	1.5254E 00	2.3215E 00	2.3277E 00	3.1128E 00
580.0	5.3109E 00	2.4737E 00	2.1729E 00	1.8703E 00	1.6553E 00	1.5069E 00	2.2911E 00	2.2973E 00	3.0713E 00
600.0	5.2430E 00	2.4427E 00	2.1465E 00	1.8481E 00	1.6361E 00	1.4898E 00	2.2630E 00	2.2691E 00	3.0329E 00
620.0	5.1800E 00	2.4139E 00	2.1221E 00	1.8274E 00	1.6182E 00	1.4739E 00	2.2368E 00	2.2428E 00	2.9972E 00
640.0	5.1212E 00	2.3871E 00	2.0993E 00	1.8081E 00	1.6017E 00	1.4591E 00	2.2125E 00	2.2184E 00	2.9639E 00
660.0	5.0665E 00	2.3621E 00	2.0781E 00	1.7902E 00	1.5862E 00	1.4454E 00	2.1898E 00	2.1957E 00	2.9329E 00
680.0	5.0153E 00	2.3387E 00	2.0583E 00	1.7735E 00	1.5718E 00	1.4325E 00	2.1687E 00	2.1745E 00	2.9039E 00
700.0	4.9674E 00	2.3168E 00	2.0398E 00	1.7579E 00	1.5584E 00	1.4206E 00	2.1489E 00	2.1546E 00	2.8768E 00
720.0	4.9225E 00	2.2964E 00	2.0225E 00	1.7433E 00	1.5458E 00	1.4094E 00	2.1303E 00	2.1360E 00	2.8515E 00
740.0	4.8804E 00	2.2772E 00	2.0063E 00	1.7296E 00	1.5341E 00	1.3990E 00	2.1130E 00	2.1186E 00	2.8277E 00
760.0	4.8408E 00	2.2592E 00	1.9911E 00	1.7167E 00	1.5231E 00	1.3892E 00	2.0967E 00	2.1022E 00	2.8053E 00
780.0	4.8036E 00	2.2422E 00	1.9768E 00	1.7047E 00	1.5127E 00	1.3800E 00	2.0813E 00	2.0869E 00	2.7843E 00
800.0	4.7685E 00	2.2263E 00	1.9633E 00	1.6934E 00	1.5030E 00	1.3714E 00	2.0669E 00	2.0724E 00	2.7645E 00
820.0	4.7354E 00	2.2112E 00	1.9507E 00	1.6827E 00	1.4939E 00	1.3633E 00	2.0534E 00	2.0588E 00	2.7459E 00
840.0	4.7043E 00	2.1970E 00	1.9388E 00	1.6727E 00	1.4853E 00	1.3557E 00	2.0406E 00	2.0460E 00	2.7283E 00
860.0	4.6748E 00	2.1837E 00	1.9275E 00	1.6632E 00	1.4773E 00	1.3485E 00	2.0285E 00	2.0339E 00	2.7117E 00
880.0	4.6470E 00	2.1710E 00	1.9169E 00	1.6543E 00	1.4697E 00	1.3418E 00	2.0171E 00	2.0225E 00	2.6961E 00
900.0	4.6206E 00	2.1591E 00	1.9069E 00	1.6459E 00	1.4625E 00	1.3354E 00	2.0064E 00	2.0117E 00	2.6813E 00
920.0	4.5957E 00	2.1478E 00	1.8975E 00	1.6380E 00	1.4557E 00	1.3295E 00	1.9962E 00	2.0015E 00	2.6673E 00
940.0	4.5720E 00	2.1371E 00	1.8885E 00	1.6305E 00	1.4494E 00	1.3238E 00	1.9866E 00	1.9918E 00	2.6540E 00
960.0	4.5496E 00	2.1269E 00	1.8801E 00	1.6234E 00	1.4433E 00	1.3185E 00	1.9775E 00	1.9827E 00	2.6414E 00
980.0	4.5284E 00	2.1173E 00	1.8721E 00	1.6167E 00	1.4377E 00	1.3135E 00	1.9689E 00	1.9741E 00	2.6295E 00
1000.0	4.5082E 00	2.1082E 00	1.8645E 00	1.6104E 00	1.4323E 00	1.3088E 00	1.9607E 00	1.9659E 00	2.6182E 00
1200.0	4.3533E 00	2.0386E 00	1.8072E 00	1.5627E 00	1.3922E 00	1.2737E 00	1.8987E 00	1.9037E 00	2.5320E 00
1400.0	4.2571E 00	1.9960E 00	1.7730E 00	1.5346E 00	1.3691E 00	1.2539E 00	1.8613E 00	1.8661E 00	2.4792E 00
1600.0	4.1964E 00	1.9696E 00	1.7526E 00	1.5183E 00	1.3563E 00	1.2432E 00	1.8387E 00	1.8434E 00	2.4466E 00
2000.0	4.1353E 00	1.9443E 00	1.7354E 00	1.5056E 00	1.3477E 00	1.2372E 00	1.8185E 00	1.8231E 00	2.4155E 00
2400.0	4.1174E 00	1.9388E 00	1.7346E 00	1.5067E 00	1.3510E 00	1.2417E 00	1.8160E 00	1.8205E 00	2.4088E 00
2800.0	4.1211E 00	1.9429E 00	1.7420E 00	1.5146E 00	1.3600E 00	1.2512E 00	1.8222E 00	1.8267E 00	2.4142E 00
3200.0	4.1363E 00	1.9522E 00	1.7534E 00	1.5259E 00	1.3718E 00	1.2631E 00	1.8329E 00	1.8375E 00	2.4259E 00
3600.0	4.1578E 00	1.9642E 00	1.7670E 00	1.5388E 00	1.3849E 00	1.2761E 00	1.8460E 00	1.8505E 00	2.4410E 00
4000.0	4.1826E 00	1.9776E 00	1.7815E 00	1.5525E 00	1.3985E 00	1.2895E 00	1.8602E 00	1.8647E 00	2.4577E 00
5000.0	4.2502E 00	2.0131E 00	1.8188E 00	1.5872E 00	1.4325E 00	1.3226E 00	1.8970E 00	1.9015E 00	2.5022E 00

PROTON STOPPING POWER, MEV•CM2/G

ENERGY MEV	WATER I= 65.1	AG-CL I=384.5	AG-BR I=434.1	NA-I I=433.0	LI-I I=472.5	POLYETHYLENE I= 54.6	STILBENE I= 65.2	LUCITE I= 65.6	ANTHRACENE I= 67.0
2.0	1.7011E 02	7.4805E 01	6.9394E 01	6.7926E 01	6.4029E 01	1.8247E 02	1.6316E 02	1.6500E 02	1.6048E 02
4.0	1.0003E 02	4.7895E 01	4.4787E 01	4.3833E 01	4.1564E 01	1.0670E 02	9.5944E 01	9.7047E 01	9.4451E 01
6.0	7.1390E 01	3.5576E 01	3.3432E 01	3.2716E 01	3.1138E 01	7.6096E 01	6.8477E 01	6.9266E 01	6.7422E 01
8.0	5.5780E 01	2.8954E 01	2.7299E 01	2.6695E 01	2.5453E 01	5.9318E 01	5.3488E 01	5.4115E 01	5.2684E 01
10.0	4.6790E 01	2.5239E 01	2.3846E 01	2.3296E 01	2.2231E 01	4.9555E 01	4.4858E 01	4.5394E 01	4.4210E 01
14.0	3.5620E 01	1.9746E 01	1.8713E 01	1.8246E 01	1.7438E 01	3.7663E 01	3.4157E 01	3.4564E 01	3.3673E 01
18.0	2.9032E 01	1.6404E 01	1.5577E 01	1.5178E 01	1.4524E 01	3.0662E 01	2.7842E 01	2.8174E 01	2.7454E 01
22.0	2.4652E 01	1.4134E 01	1.3441E 01	1.3095E 01	1.2545E 01	2.6015E 01	2.3644E 01	2.3926E 01	2.3317E 01
26.0	2.1516E 01	1.2479E 01	1.1881E 01	1.1576E 01	1.1101E 01	2.2691E 01	2.0637E 01	2.0884E 01	2.0354E 01
30.0	1.9153E 01	1.1213E 01	1.0686E 01	1.0414E 01	9.9946E 00	2.0188E 01	1.8372E 01	1.8591E 01	1.8121E 01
34.0	1.7305E 01	1.0211E 01	9.7379E 00	9.4925E 00	9.1164E 00	1.8232E 01	1.6599E 01	1.6797E 01	1.6374E 01
38.0	1.5817E 01	9.3951E 00	8.9657E 00	8.7419E 00	8.4006E 00	1.6659E 01	1.5173E 01	1.5354E 01	1.4968E 01
42.0	1.4593E 01	8.7175E 00	8.3236E 00	8.1176E 00	7.8047E 00	1.5364E 01	1.3998E 01	1.4166E 01	1.3810E 01
46.0	1.3567E 01	8.1449E 00	7.7805E 00	7.5894E 00	7.3002E 00	1.4279E 01	1.3014E 01	1.3169E 01	1.2839E 01
50.0	1.2693E 01	7.6541E 00	7.3147E 00	7.1363E 00	6.8671E 00	1.3356E 01	1.2176E 01	1.2322E 01	1.2013E 01
60.0	1.0987E 01	6.6857E 00	6.3946E 00	6.2410E 00	6.0105E 00	1.1555E 01	1.0539E 01	1.0666E 01	1.0399E 01
70.0	9.7391E 00	5.9689E 00	5.7127E 00	5.5771E 00	5.3745E 00	1.0238E 01	9.3427E 00	9.4547E 00	9.2192E 00
80.0	8.7854E 00	5.4157E 00	5.1860E 00	5.0641E 00	4.8826E 00	9.2322E 00	8.4279E 00	8.5290E 00	8.3169E 00
90.0	8.0318E 00	4.9752E 00	4.7662E 00	4.6550E 00	4.4901E 00	8.4377E 00	7.7050E 00	7.7975E 00	7.6040E 00
100.0	7.4208E 00	4.6157E 00	4.4234E 00	4.3209E 00	4.1693E 00	7.7938E 00	7.1189E 00	7.2045E 00	7.0259E 00
110.0	6.9152E 00	4.3166E 00	4.1381E 00	4.0427E 00	3.9020E 00	7.2611E 00	6.6339E 00	6.7137E 00	6.5474E 00
120.0	6.4896E 00	4.0636E 00	3.8967E 00	3.8073E 00	3.6757E 00	6.8128E 00	6.2257E 00	6.3006E 00	6.1447E 00
130.0	6.1264E 00	3.8469E 00	3.6898E 00	3.6054E 00	3.4816E 00	6.4304E 00	5.8773E 00	5.9480E 00	5.8010E 00
140.0	5.8128E 00	3.6590E 00	3.5104E 00	3.4304E 00	3.3133E 00	6.1001E 00	5.5764E 00	5.6435E 00	5.5041E 00
150.0	5.5391E 00	3.4947E 00	3.3533E 00	3.2771E 00	3.1658E 00	5.8120E 00	5.3138E 00	5.3778E 00	5.2451E 00
160.0	5.2982E 00	3.3496E 00	3.2147E 00	3.1419E 00	3.0356E 00	5.5585E 00	5.0828E 00	5.1440E 00	5.0172E 00
170.0	5.0846E 00	3.2206E 00	3.0914E 00	3.0215E 00	2.9198E 00	5.3337E 00	4.8778E 00	4.9366E 00	4.8150E 00
180.0	4.8938E 00	3.1052E 00	2.9811E 00	2.9138E 00	2.8161E 00	5.1330E 00	4.6949E 00	4.7514E 00	4.6344E 00
190.0	4.7225E 00	3.0013E 00	2.8818E 00	2.8168E 00	2.7227E 00	4.9527E 00	4.5305E 00	4.5851E 00	4.4722E 00
200.0	4.5677E 00	2.9073E 00	2.7919E 00	2.7291E 00	2.6382E 00	4.7899E 00	4.3820E 00	4.4348E 00	4.3257E 00
220.0	4.2992E 00	2.7439E 00	2.6356E 00	2.5765E 00	2.4912E 00	4.5075E 00	4.1244E 00	4.1742E 00	4.0716E 00
240.0	4.0744E 00	2.6067E 00	2.5043E 00	2.4483E 00	2.3677E 00	4.2711E 00	3.9088E 00	3.9560E 00	3.8588E 00
260.0	3.8836E 00	2.4900E 00	2.3927E 00	2.3392E 00	2.2626E 00	4.0704E 00	3.7257E 00	3.7707E 00	3.6782E 00
280.0	3.7196E 00	2.3896E 00	2.2965E 00	2.2453E 00	2.1721E 00	3.8980E 00	3.5684E 00	3.6115E 00	3.5230E 00
300.0	3.5774E 00	2.3023E 00	2.2130E 00	2.1638E 00	2.0924E 00	3.7484E 00	3.4319E 00	3.4734E 00	3.3883E 00
320.0	3.4528E 00	2.2258E 00	2.1398E 00	2.0922E 00	2.0244E 00	3.6175E 00	3.3125E 00	3.3525E 00	3.2704E 00
340.0	3.3430E 00	2.1583E 00	2.0752E 00	2.0291E 00	1.9636E 00	3.5020E 00	3.2071E 00	3.2459E 00	3.1664E 00
360.0	3.2455E 00	2.0984E 00	2.0178E 00	1.9730E 00	1.9095E 00	3.3995E 00	3.1136E 00	3.1512E 00	3.0741E 00
380.0	3.1584E 00	2.0448E 00	1.9665E 00	1.9229E 00	1.8612E 00	3.3079E 00	3.0300E 00	3.0666E 00	2.9917E 00
400.0	3.0801E 00	1.9966E 00	1.9204E 00	1.8779E 00	1.8178E 00	3.2257E 00	2.9550E 00	2.9907E 00	2.9176E 00
420.0	3.0096E 00	1.9532E 00	1.8788E 00	1.8372E 00	1.7786E 00	3.1515E 00	2.8873E 00	2.9222E 00	2.8508E 00
440.0	2.9456E 00	1.9139E 00	1.8412E 00	1.8004E 00	1.7431E 00	3.0843E 00	2.8259E 00	2.8601E 00	2.7903E 00
460.0	2.8875E 00	1.8781E 00	1.8069E 00	1.7670E 00	1.7108E 00	3.0232E 00	2.7701E 00	2.8037E 00	2.7353E 00
480.0	2.8344E 00	1.8455E 00	1.7757E 00	1.7364E 00	1.6814E 00	2.9674E 00	2.7192E 00	2.7522E 00	2.6850E 00
500.0	2.7858E 00	1.8156E 00	1.7471E 00	1.7085E 00	1.6544E 00	2.9163E 00	2.6726E 00	2.7050E 00	2.6390E 00
520.0	2.7412E 00	1.7882E 00	1.7208E 00	1.6828E 00	1.6297E 00	2.8694E 00	2.6298E 00	2.6617E 00	2.5968E 00
540.0	2.6980E 00	1.7629E 00	1.6967E 00	1.6592E 00	1.6066E 00	2.8262E 00	2.5904E 00	2.6218E 00	2.5579E 00
560.0	2.6604E 00	1.7397E 00	1.6744E 00	1.6374E 00	1.5857E 00	2.7863E 00	2.5540E 00	2.5849E 00	2.5219E 00
580.0	2.6256E 00	1.7182E 00	1.6505E 00	1.6173E 00	1.5664E 00	2.7494E 00	2.5203E 00	2.5509E 00	2.4886E 00
600.0	2.5932E 00	1.6982E 00	1.6319E 00	1.5987E 00	1.5485E 00	2.7152E 00	2.4890E 00	2.5193E 00	2.4577E 00
620.0	2.5630E 00	1.6798E 00	1.6145E 00	1.5814E 00	1.5319E 00	2.6812E 00	2.4590E 00	2.4899E 00	2.4291E 00
640.0	2.5348E 00	1.6626E 00	1.5984E 00	1.5653E 00	1.5164E 00	2.6505E 00	2.4313E 00	2.4626E 00	2.4017E 00
660.0	2.5085E 00	1.6466E 00	1.5834E 00	1.5504E 00	1.5020E 00	2.6218E 00	2.4054E 00	2.4371E 00	2.3761E 00
680.0	2.4838E 00	1.6317E 00	1.5694E 00	1.5364E 00	1.4886E 00	2.5949E 00	2.3811E 00	2.4008E 00	2.3521E 00
700.0	2.4607E 00	1.6177E 00	1.5563E 00	1.5234E 00	1.4760E 00	2.5698E 00	2.3584E 00	2.3779E 00	2.3296E 00
720.0	2.4390E 00	1.6047E 00	1.5440E 00	1.5112E 00	1.4643E 00	2.5462E 00	2.3370E 00	2.3564E 00	2.3085E 00
740.0	2.4186E 00	1.5925E 00	1.5326E 00	1.4998E 00	1.4533E 00	2.5240E 00	2.3170E 00	2.3363E 00	2.2887E 00
760.0	2.3993E 00	1.5811E 00	1.5218E 00	1.4892E 00	1.4430E 00	2.5031E 00	2.2982E 00	2.3173E 00	2.2701E 00
780.0	2.3812E 00	1.5703E 00	1.5117E 00	1.4789E 00	1.4334E 00	2.4834E 00	2.2804E 00	2.2994E 00	2.2525E 00
800.0	2.3641E 00	1.5603E 00	1.5022E 00	1.4696E 00	1.4243E 00	2.4649E 00	2.2637E 00	2.2825E 00	2.2360E 00
820.0	2.3479E 00	1.5508E 00	1.4933E 00	1.4608E 00	1.4158E 00	2.4474E 00	2.2479E 00	2.2666E 00	2.2204E 00
840.0	2.3326E 00	1.5420E 00	1.4848E 00	1.4525E 00	1.4078E 00	2.4308E 00	2.2329E 00	2.2516E 00	2.2056E 00
860.0	2.3181E 00	1.5336E 00	1.4769E 00	1.4448E 00	1.4003E 00	2.4152E 00	2.2188E 00	2.2374E 00	2.1917E 00
880.0	2.3044E 00	1.5257E 00	1.4695E 00	1.4374E 00	1.3932E 00	2.4003E 00	2.2055E 00	2.2239E 00	2.1785E 00
900.0	2.2914E 00	1.5183E 00	1.4624E 00	1.4305E 00	1.3866E 00	2.3863E 00	2.1928E 00	2.2112E 00	2.1659E 00
920.0	2.2792E 00	1.5113E 00	1.4558E 00	1.4240E 00	1.3803E 00	2.3730E 00	2.1808E 00	2.1991E 00	2.1541E 00
940.0	2.2678E 00	1.5047E 00	1.4495E 00	1.4178E 00	1.3743E 00	2.3603E 00	2.1694E 00	2.1877E 00	2.1428E 00
960.0	2.2570E 00	1.4984E 00	1.4435E 00	1.4120E 00	1.3687E 00	2.3483E 00	2.1586E 00	2.1768E 00	2.1321E 00
980.0	2.2467E 00	1.4925E 00	1.4379E 00	1.4065E 00	1.3635E 00	2.3369E 00	2.1483E 00	2.1664E 00	2.1219E 00
1000.0	2.2369E 00	1.4869E 00	1.4326E 00	1.4013E 00	1.3585E 00	2.3260E 00	2.1385E 00	2.1566E 00	2.1123E 00
1200.0	2.1613E 00	1.4454E 00	1.3925E 00	1.3627E 00	1.3214E 00	2.2417E 00	2.0628E 00	2.0805E 00	2.0374E 00
1400.0	2.1134E 00	1.4215E 00	1.3694E 00	1.3406E 00	1.2990E 00	2.1879E 00	2.0146E 00	2.0321E 00	1.9898E 00
1600.0	2.0822E 00	1.4072E 00	1.3560E 00	1.3283E 00	1.2859E 00	2.1524E 00	1.9832E 00	2.0006E 00	1.9587E 00
2000.0	2.0485E 00	1.3960E 00	1.3456E 00	1.3183E 00	1.2753E 00	2.1131E 00	1.9488E 00	1.9663E 00	1.9247E 00
2400.0	2.0353E 00	1.3968E 00	1.3464E 00	1.3193E 00	1.2758E 00	2.0965E 00	1.9348E 00	1.9526E 00	1.9109E 00
2800.0	2.0323E 00	1.4027E 00	1.3526E 00	1.3257E 00	1.2816E 00	2.0915E 00	1.9313E 00	1.9493E 00	1.9074E 00
3200.0	2.0349E 00	1.4113E 00	1.3614E 00	1.3347E 00	1.2901E 00	2.0927E 00	1.9333E 00	1.9516E 00	1.9094E 00
3600.0	2.0405E 00	1.4213E 00	1.3714E 00	1.3450E 00	1.2998E 00	2.0974E 00	1.9384E 00	1.9571E 00	1.9144E 00
4000.0	2.0478E 00	1.4319E 00	1.3820E 00	1.3558E 00	1.3101E 00	2.1041E 00	1.9452E 00	1.9642E 00	1.9212E 00
5000.0	2.0690E 00	1.4584E 00	1.4084E 00	1.3828E 00	1.3359E 00	2.1248E 00	1.9657E 00	1.9854E 00	1.9414E 00

PROTON RANGE, G/CM2

ENERGY MEV	BE I= 60.0	C I= 78.0	AL I=163.0	FE I=273.0	CU I=314.0	AG I=487.0	AU I=797.0	PB I=826.0	U I=923.0
2.0	8.6892E-03	8.4058E-03	1.1474E-02	1.4857E-02	1.6176E-02	2.1052E-02	2.9836E-02	3.0852E-02	3.3668E-02
4.0	2.8222E-02	2.6862E-02	3.4996E-02	4.3817E-02	4.7267E-02	5.9737E-02	8.1868E-02	8.4446E-02	9.1449E-02
6.0	5.7732E-02	5.4630E-02	6.9742E-02	8.5798E-02	9.2067E-02	1.1430E-01	1.5316E-01	1.5771E-01	1.6986E-01
8.0	9.7079E-02	9.1629E-02	1.1566E-01	1.4264E-01	1.5036E-01	1.8426E-01	2.4273E-01	2.4961E-01	2.6768E-01
10.0	1.4549E-01	1.3676E-01	1.7029E-01	2.0466E-01	2.1827E-01	2.6524E-01	3.4654E-01	3.5613E-01	3.8111E-01
14.0	2.6768E-01	2.5034E-01	3.0639E-01	3.6281E-01	3.8557E-01	4.6326E-01	6.0023E-01	6.1666E-01	6.5960E-01
18.0	4.2216E-01	3.9362E-01	4.7657E-01	5.5918E-01	5.9278E-01	7.0694E-01	9.1216E-01	9.3723E-01	1.0034E 00
22.0	6.0754E-01	5.6528E-01	6.7922E-01	7.9183E-01	8.3782E-01	9.9349E-01	1.2771E 00	1.3122E 00	1.4056E 00
26.0	8.2268E-01	7.6426E-01	9.1307E-01	1.0592E 00	1.1191E 00	1.3208E 00	1.6914E 00	1.7377E 00	1.8611E 00
30.0	1.0666E 00	9.8969E-01	1.1771E 00	1.3602E 00	1.4352E 00	1.6873E 00	2.1522E 00	2.2107E 00	2.3666E 00
34.0	1.3386E 00	1.2408E 00	1.4703E 00	1.6936E 00	1.7852E 00	2.0916E 00	2.6575E 00	2.7291E 00	2.9196E 00
38.0	1.6379E 00	1.5169E 00	1.7919E 00	2.0585E 00	2.1679E 00	2.5325E 00	3.2058E 00	3.2912E 00	3.5182E 00
42.0	1.9637E 00	1.8174E 00	2.1412E 00	2.4541E 00	2.5825E 00	3.0089E 00	3.7955E 00	3.8956E 00	4.1607E 00
46.0	2.3155E 00	2.1417E 00	2.5175E 00	2.8796E 00	3.0281E 00	3.5199E 00	4.4255E 00	4.5410E 00	4.8459E 00
50.0	2.6928E 00	2.4892E 00	2.9202E 00	3.3343E 00	3.5042E 00	4.0647E 00	5.0948E 00	5.2264E 00	5.5725E 00
60.0	3.7436E 00	3.4567E 00	4.0387E 00	4.5946E 00	4.8225E 00	5.5691E 00	6.9332E 00	7.1080E 00	7.5637E 00
70.0	4.9424E 00	4.5596E 00	5.3102E 00	6.0240E 00	6.3165E 00	7.2684E 00	8.9973E 00	9.2193E 00	9.7931E 00
80.0	6.2825E 00	5.7918E 00	6.7278E 00	7.6145E 00	7.9776E 00	9.1531E 00	1.1276E 01	1.1547E 01	1.2248E 01
90.0	7.7579E 00	7.1476E 00	8.2848E 00	9.3586E 00	9.7984E 00	1.1214L 01	1.3758E 01	1.4086E 01	1.4919E 01
100.0	9.3629E 00	8.6219E 00	9.9753E 00	1.1250E 01	1.1772E 01	1.3445E 01	1.6435E 01	1.6821E 01	1.7796E 01
110.0	1.1093E 01	1.0210E 01	1.1794E 01	1.3282E 01	1.3891E 01	1.5837E 01	1.9299E 01	1.9746E 01	2.0869E 01
120.0	1.2942E 01	1.1908E 01	1.3736E 01	1.5450E 01	1.6152E 01	1.8384E 01	2.2342E 01	2.2854E 01	2.4131E 01
130.0	1.4907E 01	1.3711E 01	1.5796E 01	1.7748E 01	1.8547E 01	2.1081C 01	2.5557E 01	2.6136E 01	2.7574E 01
140.0	1.6983E 01	1.5615E 01	1.7971E 01	2.0171E 01	2.1072E 01	2.3921E 01	2.8937E 01	2.9586E 01	3.1191E 01
150.0	1.9166E 01	1.7618E 01	2.0255E 01	2.2715E 01	2.3722E 01	2.6900H 01	3.2476E 01	3.3198E 01	3.4976E 01
160.0	2.1454E 01	1.9715E 01	2.2646E 01	2.5376E 01	2.6493E 01	3.0011E 01	3.6168E 01	3.6966E 01	3.8923E 01
170.0	2.3841E 01	2.1903E 01	2.5139E 01	2.8148E 01	2.9381E 01	3.3251E 01	4.0008E 01	4.0884E 01	4.3024E 01
180.0	2.6324E 01	2.4180E 01	2.7730E 01	3.1029E 01	3.2380E 01	3.6614E 01	4.3990E 01	4.4946E 01	4.7276E 01
190.0	2.8902E 01	2.6542E 01	3.0417E 01	3.4015E 01	3.5488E 01	4.0097E 01	4.8109E 01	4.9148E 01	5.1673E 01
200.0	3.1570E 01	2.8986E 01	3.3197E 01	3.7102E 01	3.8701E 01	4.3695E 01	5.2361E 01	5.3485E 01	5.6209E 01
220.0	3.7165E 01	3.4112E 01	3.9021E 01	4.3566E 01	4.5428E 01	5.1223E 01	6.1244E 01	6.2546E 01	6.5682E 01
240.0	4.3090E 01	3.9537E 01	4.5180E 01	5.0396E 01	5.2534E 01	5.9168E 01	7.0606E 01	7.2093E 01	7.5659E 01
260.0	4.9323E 01	4.5244E 01	5.1653E 01	5.7570E 01	5.9995E 01	6.7504E 01	8.0415E 01	8.2096E 01	8.6107E 01
280.0	5.5847E 01	5.1216E 01	5.8421E 01	6.5066E 01	6.7790E 01	7.6206E 01	9.0645E 01	9.2525E 01	9.6998E 01
300.0	6.2644E 01	5.7436E 01	6.5467E 01	7.2864E 01	7.5899E 01	8.5253E 01	1.0127E 02	1.0335C 02	1.0830E 02
320.0	6.9698E 01	6.3901E 01	7.2774E 01	8.0948E 01	8.4302E 01	9.4623E 01	1.1226E 02	1.1456E 02	1.2000E 02
340.0	7.6996E 01	7.0598E 01	8.0327E 01	8.9300E 01	9.2983E 01	1.0430E 02	1.2360E 02	1.2612E 02	1.3206E 02
360.0	8.4524E 01	7.7504E 01	8.8112E 01	9.7905E 01	1.0193E 02	1.1426E 02	1.3527E 02	1.3801E 02	1.4446E 02
380.0	9.2269E 01	8.4610E 01	9.6116E 01	1.0675E 02	1.1111E 02	1.2450E 02	1.4724E 02	1.5022E 02	1.5719E 02
400.0	1.0022E 02	9.1904E 01	1.0433E 02	1.1582E 02	1.2054E 02	1.3498E 02	1.5951E 02	1.6271E 02	1.7022C 02
420.0	1.0836E 02	9.9376E 01	1.1273E 02	1.2511E 02	1.3018E 02	1.4571E 02	1.7204C 02	1.7549E 02	1.8354E 02
440.0	1.1669E 02	1.0702E 02	1.2133E 02	1.3460E 02	1.4003E 02	1.5666E 02	1.8484E 02	1.8853E 02	1.9713E 02
460.0	1.2519E 02	1.1482E 02	1.3009E 02	1.4428E 02	1.5008E 02	1.6783E 02	1.9788E 02	2.0182E 02	2.1098E 02
480.0	1.3386E 02	1.2278E 02	1.3904E 02	1.5414E 02	1.6032E 02	1.7920E 02	2.1115E 02	2.1534E 02	2.2507E 02
500.0	1.4269E 02	1.3088E 02	1.4817E 02	1.6417E 02	1.7073E 02	1.9076E 02	2.2464E 02	2.2908E 02	2.3938E 02
520.0	1.5167E 02	1.3912E 02	1.5744E 02	1.7436E 02	1.8131E 02	2.0250E 02	2.3833E 02	2.4303E 02	2.5392E 02
540.0	1.6079E 02	1.4749E 02	1.6685E 02	1.8471E 02	1.9204E 02	2.1442F 02	2.5222E 02	2.5718E 02	2.6865E 02
560.0	1.7005E 02	1.5598E 02	1.7640E 02	1.9520E 02	2.0293E 02	2.2650E 02	2.6629E 02	2.7152E 02	2.8358E 02
580.0	1.7944E 02	1.6460E 02	1.8607E 02	2.0584E 02	2.1396E 02	2.3873E 02	2.8054E 02	2.8603E 02	2.9870E 02
600.0	1.8896E 02	1.7333E 02	1.9587E 02	2.1662E 02	2.2512E 02	2.5111E 02	2.9495E 02	3.0071E 02	3.1398E 02
620.0	1.9859E 02	1.8216E 02	2.0578E 02	2.2753E 02	2.3642E 02	2.6363E 02	3.0952E 02	3.1555E 02	3.2943E 02
640.0	2.0833E 02	1.9110E 02	2.1580E 02	2.3855E 02	2.4783E 02	2.7628E 02	3.2424E 02	3.3055E 02	3.4504E 02
660.0	2.1819E 02	2.0014E 02	2.2593E 02	2.4969E 02	2.5936E 02	2.8905E 02	3.3909E 02	3.4568E 02	3.6079E 02
680.0	2.2815E 02	2.0928E 02	2.3615E 02	2.6094E 02	2.7101E 02	3.0195E 02	3.5409E 02	3.6095E 02	3.7669E 02
700.0	2.3820E 02	2.1850E 02	2.4648E 02	2.7229E 02	2.8275E 02	3.1496E 02	3.6920E 02	3.7635E 02	3.9271E 02
720.0	2.4835E 02	2.2781E 02	2.5689E 02	2.8374E 02	2.9460E 02	3.2807E 02	3.8444E 02	3.9187E 02	4.0886E 02
740.0	2.5859E 02	2.3720E 02	2.6739E 02	2.9529E 02	3.0654E 02	3.4129E 02	3.9979E 02	4.0750E 02	4.2513E 02
760.0	2.6892E 02	2.4667E 02	2.7797E 02	3.0692E 02	3.1857E 02	3.5460E 02	4.1525E 02	4.2325E 02	4.4151E 02
780.0	2.7933E 02	2.5621E 02	2.8863E 02	3.1864E 02	3.3069E 02	3.6801E 02	4.3081E 02	4.3910E 02	4.5800E 02
800.0	2.8982E 02	2.6583E 02	2.9937E 02	3.3044E 02	3.4289E 02	3.8150E 02	4.4647E 02	4.5505E 02	4.7460E 02
820.0	3.0038E 02	2.7551E 02	3.1018E 02	3.4232E 02	3.5517E 02	3.9507E 02	4.6223E 02	4.7109E 02	4.9128E 02
840.0	3.1102E 02	2.8526E 02	3.2106E 02	3.5428E 02	3.6754E 02	4.0873E 02	4.7807E 02	4.8722E 02	5.0807E 02
860.0	3.2172E 02	2.9507E 02	3.3201E 02	3.6630E 02	3.8001E 02	4.2247E 02	4.9399E 02	5.0344E 02	5.2496E 02
880.0	3.3250E 02	3.0495E 02	3.4301E 02	3.7840E 02	3.9254E 02	4.3629E 02	5.1000E 02	5.1974E 02	5.4192E 02
900.0	3.4334E 02	3.1488E 02	3.5408E 02	3.9055E 02	4.0514E 02	4.5016E 02	5.2607E 02	5.3611E 02	5.5897E 02
920.0	3.5424E 02	3.2486E 02	3.6521E 02	4.0278E 02	4.1781E 02	4.6411E 02	5.4222E 02	5.5255E 02	5.7608E 02
940.0	3.6519E 02	3.3490E 02	3.7639E 02	4.1506E 02	4.3053E 02	4.7811E 02	5.5844E 02	5.6907E 02	5.9327E 02
960.0	3.7621E 02	3.4500E 02	3.8763E 02	4.2739E 02	4.4331E 02	4.9217E 02	5.7472E 02	5.8565E 02	6.1053E 02
980.0	3.8728E 02	3.5513E 02	3.9891E 02	4.3978E 02	4.5615E 02	5.0629E 02	5.9108E 02	6.0229E 02	6.2785E 02
1000.0	3.9840E 02	3.6532E 02	4.1024E 02	4.5223E 02	4.6904E 02	5.2046E 02	6.0749E 02	6.1899E 02	6.4523E 02
1200.0	5.1207E 02	4.6938E 02	5.2583E 02	5.7907E 02	6.0035E 02	6.6466E 02	7.7440E 02	7.8866E 02	8.2183E 02
1400.0	6.2918E 02	5.7648E 02	6.4447E 02	7.0916E 02	7.3492E 02	8.1214E 02	9.4482E 02	9.6167E 02	1.0020E 03
1600.0	7.4863E 02	6.8563E 02	7.6512E 02	8.4135E 02	8.7157E 02	9.6164E 02	1.1173E 03	1.1368E 03	1.1841E 03
2000.0	9.9187E 02	9.0758E 02	1.0098E 03	1.1092E 03	1.1482E 03	1.2636E 03	1.4649E 03	1.4901E 03	1.5510E 03
2400.0	1.2382E 03	1.1320E 03	1.2564E 03	1.3789E 03	1.4265E 03	1.5668E 03	1.8130E 03	1.8431E 03	1.9179E 03
2800.0	1.4858E 03	1.3572E 03	1.5034E 03	1.6487E 03	1.7048E 03	1.8691E 03	2.1596E 03	2.1940E 03	2.2830C 03
3200.0	1.7336E 03	1.5823E 03	1.7497E 03	1.9176E 03	1.9820E 03	2.1699E 03	2.5038E 03	2.5421E 03	2.6452E 03
3600.0	1.9811E 03	1.8069E 03	1.9951E 03	2.1852E 03	2.2577E 03	2.4686E 03	2.8452E 03	2.8871E 03	3.0042E 03
4000.0	2.2280E 03	2.0307E 03	2.2391E 03	2.4514E 03	2.5317E 03	2.7651E 03	3.1837E 03	3.2288E 03	3.3599E 03
5000.0	2.8416E 03	2.5860E 03	2.8434E 03	3.1095E 03	3.2092E 03	3.4967E 03	4.0172E 03	4.0691E 03	4.2352E 03

PROTON RANGE, G/CM2

ENERGY MEV	H I= 18.7	HE I= 42.0	NE I=131.0	A I=210.0	KR I=381.0	XE I=555.0	AIR I= 86.8	CARB.DIOXIDE I= 85.9	METHANE I= 44.1
2.0	2.8875E-03	6.9490E-03	1.0228E-02	1.3651E-02	1.8866E-02	2.3875E-02	8.7273E-03	8.6804E-03	5.6448E-03
4.0	1.0056E-02	2.3066E-02	3.1634E-02	4.0959E-02	5.4424E-02	6.7153E-02	2.7703E-02	2.7574E-02	1.8683E-02
6.0	2.0928E-02	4.7507E-02	6.3461E-02	8.0951E-02	1.0520E-01	1.2775E-01	5.6195E-02	5.5948E-02	3.8447E-02
8.0	3.5251E-02	8.0059E-02	1.0566E-01	1.3353E-01	1.7088E-01	2.0508E-01	9.4135E-02	9.3734E-02	6.4778E-02
10.0	5.3163E-02	1.2052E-01	1.5628E-01	1.9552E-01	2.4710E-01	2.9455E-01	1.4022E-01	1.3963E-01	9.7432E-02
14.0	9.8825E-02	2.2298E-01	2.8277E-01	3.4932E-01	4.3421E-01	5.1299E-01	2.5607E-01	2.5505E-01	1.8011E-01
18.0	1.5704E-01	3.5286E-01	4.4140E-01	5.4097E-01	6.6526E-01	7.8143E-01	4.0207E-01	4.0053E-01	2.8490E-01
22.0	2.2730E-01	5.0898E-01	6.3065E-01	7.6863E-01	9.3784E-01	1.0966E 00	5.7688E-01	5.7473E-01	4.1087E-01
26.0	3.0920E-01	6.9044E-01	8.4936E-01	1.0309E 00	1.2501E 00	1.4560E 00	7.7941E-01	7.7658E-01	5.5726E-01
30.0	4.0241E-01	8.9643E-01	1.0965E 00	1.3265E 00	1.6005E 00	1.8579E 00	1.0088E 00	1.0052E 00	7.2344E-01
34.0	5.0661E-01	1.1263E 00	1.3714E 00	1.6544E 00	1.9878E 00	2.3005E 00	1.2642E 00	1.2597E 00	9.0885E-01
38.0	6.2153E-01	1.3794E 00	1.6730E 00	2.0137E 00	2.4110E 00	2.7827E 00	1.5449E 00	1.5396E 00	1.1130E 00
42.0	7.4693E-01	1.6551E 00	2.0009E 00	2.4037E 00	2.8689E 00	3.3033E 00	1.8504E 00	1.8441E 00	1.3354E 00
46.0	8.8257E-01	1.9531E 00	2.3543E 00	2.8234E 00	3.3608E 00	3.8613E 00	2.1799E 00	2.1726E 00	1.5757E 00
50.0	1.0282E 00	2.2727E 00	2.7327E 00	3.2723E 00	3.8857E 00	4.4556E 00	2.5331E 00	2.5247E 00	1.8335E 00
60.0	1.4350E 00	3.1638E 00	3.7843E 00	4.5179E 00	5.3379E 00	6.0950E 00	3.5160E 00	3.5045E 00	2.5521E 00
70.0	1.9004E 00	4.1813E 00	4.9810E 00	5.9325E 00	6.9815E 00	7.9446E 00	4.6361E 00	4.6212E 00	3.3725E 00
80.0	2.4218E 00	5.3196E 00	6.3160E 00	7.5080E 00	8.8071E 00	9.9938E 00	5.8871E 00	5.8684E 00	4.2902E 00
90.0	2.9969E 00	6.5736E 00	7.7832E 00	9.2373E 00	1.0806E 01	1.2233E 01	7.2633E 00	7.2405E 00	5.3012E 00
100.0	3.6236E 00	7.9385E 00	9.3770E 00	1.1114E 01	1.2972E 01	1.4655E 01	8.7595E 00	8.7323E 00	6.4015E 00
110.0	4.3000E 00	9.4101E 00	1.1092E 01	1.3131E 01	1.5297E 01	1.7251E 01	1.0371E 01	1.0339E 01	7.5877E 00
120.0	5.0241E 00	1.0984E 01	1.2925E 01	1.5285E 01	1.7774E 01	2.0013E 01	1.2093E 01	1.2056E 01	8.8566E 00
130.0	5.7943E 00	1.2657E 01	1.4869E 01	1.7568E 01	2.0399E 01	2.2937E 01	1.3922E 01	1.3880E 01	1.0205E 01
140.0	6.6089E 00	1.4426E 01	1.6922E 01	1.9978E 01	2.3164E 01	2.6015E 01	1.5854E 01	1.5806E 01	1.1630E 01
150.0	7.4664E 00	1.6286E 01	1.9080E 01	2.2508E 01	2.6066E 01	2.9241E 01	1.7885E 01	1.7831E 01	1.3130E 01
160.0	8.3653E 00	1.8235E 01	2.1337E 01	2.5155E 01	2.9099E 01	3.2611E 01	2.0012E 01	1.9952E 01	1.4701E 01
170.0	9.3043E 00	2.0270E 01	2.3693E 01	2.7914E 01	3.2258E 01	3.6118E 01	2.2231E 01	2.2165E 01	1.6341E 01
180.0	1.0282E 01	2.2388E 01	2.6142E 01	3.0782E 01	3.5539E 01	3.9759E 01	2.4539E 01	2.4466E 01	1.8047E 01
190.0	1.1297E 01	2.4587E 01	2.8682E 01	3.3755E 01	3.8938E 01	4.3529E 01	2.6934E 01	2.6854E 01	1.9819E 01
200.0	1.2349E 01	2.6862E 01	3.1309E 01	3.6830E 01	4.2451E 01	4.7422E 01	2.9412E 01	2.9325E 01	2.1653E 01
220.0	1.4557E 01	3.1637E 01	3.6816E 01	4.3271E 01	4.9803E 01	5.5564E 01	3.4608E 01	3.4507E 01	2.5500E 01
240.0	1.6896E 01	3.6695E 01	4.2642E 01	5.0079E 01	5.7567E 01	6.4156E 01	4.0107E 01	3.9990E 01	2.9575E 01
260.0	1.9360E 01	4.2017E 01	4.8766E 01	5.7232E 01	6.5717E 01	7.3167E 01	4.5891E 01	4.5757E 01	3.3864E 01
280.0	2.1941E 01	4.7589E 01	5.5170E 01	6.4709E 01	7.4229E 01	8.2572E 01	5.1942E 01	5.1792E 01	3.8353E 01
300.0	2.4633E 01	5.3396E 01	6.1839E 01	7.2491E 01	8.3080E 01	9.2346E 01	5.8244E 01	5.8077E 01	4.3032E 01
320.0	2.7428E 01	5.9425E 01	6.8756E 01	8.0559E 01	9.2252E 01	1.0247E 02	6.4785E 01	6.4599E 01	4.7889E 01
340.0	3.0322E 01	6.5663E 01	7.5908E 01	8.8897E 01	1.0172E 02	1.1292E 02	7.1548E 01	7.1344E 01	5.2914E 01
360.0	3.3309E 01	7.2099E 01	8.3281E 01	9.7489E 01	1.1148E 02	1.2367E 02	7.8523E 01	7.8300E 01	5.8099E 01
380.0	3.6384E 01	7.8721E 01	9.0862E 01	1.0632E 02	1.2150E 02	1.3472E 02	8.5698E 01	8.5459E 01	6.3434E 01
400.0	3.9542E 01	8.5521E 01	9.8641E 01	1.1538E 02	1.3178E 02	1.4604E 02	9.3061E 01	9.2797E 01	6.8911E 01
420.0	4.2779E 01	9.2487E 01	1.0661E 02	1.2466E 02	1.4229E 02	1.5761E 02	1.0060E 02	1.0032E 02	7.4523E 01
440.0	4.6091E 01	9.9613E 01	1.1475E 02	1.3413E 02	1.5303E 02	1.6943E 02	1.0831E 02	1.0801E 02	8.0263E 01
460.0	4.9474E 01	1.0689E 02	1.2306E 02	1.4380E 02	1.6398E 02	1.8149E 02	1.1618E 02	1.1586E 02	8.6124E 01
480.0	5.2924E 01	1.1431E 02	1.3153E 02	1.5365E 02	1.7513E 02	1.9375E 02	1.2421E 02	1.2386E 02	9.2099E 01
500.0	5.6438E 01	1.2186E 02	1.4014E 02	1.6367E 02	1.8647E 02	2.0623E 02	1.3237E 02	1.3200E 02	9.8184E 01
520.0	6.0013E 01	1.2954E 02	1.4890E 02	1.7386E 02	1.9799E 02	2.1889E 02	1.4067E 02	1.4028E 02	1.0437E 02
540.0	6.3646E 01	1.3735E 02	1.5780E 02	1.8420E 02	2.0969E 02	2.3175E 02	1.4911E 02	1.4869E 02	1.1066E 02
560.0	6.7334E 01	1.4527E 02	1.6682E 02	1.9468E 02	2.2154E 02	2.4477E 02	1.5766E 02	1.5722E 02	1.1704E 02
580.0	7.1075E 01	1.5330E 02	1.7597E 02	2.0531E 02	2.3355E 02	2.5797E 02	1.6634E 02	1.6587E 02	1.2351E 02
600.0	7.4865E 01	1.6144E 02	1.8523E 02	2.1607E 02	2.4570E 02	2.7132E 02	1.7512E 02	1.7463E 02	1.3006E 02
620.0	7.8703E 01	1.6967E 02	1.9460E 02	2.2695E 02	2.5800E 02	2.8481E 02	1.8401E 02	1.8350E 02	1.3669E 02
640.0	8.2587E 01	1.7801E 02	2.0408E 02	2.3795E 02	2.7042E 02	2.9845E 02	1.9300E 02	1.9247E 02	1.4340E 02
660.0	8.6513E 01	1.8643E 02	2.1365E 02	2.4907E 02	2.8297E 02	3.1222E 02	2.0209E 02	2.0153E 02	1.5019E 02
680.0	9.0481E 01	1.9494E 02	2.2332E 02	2.6030E 02	2.9564E 02	3.2612E 02	2.1127E 02	2.1068E 02	1.5704E 02
700.0	9.4488E 01	2.0353E 02	2.3308E 02	2.7162E 02	3.0842E 02	3.4015E 02	2.2053E 02	2.1992E 02	1.6396E 02
720.0	9.8533E 01	2.1220E 02	2.4293E 02	2.8305E 02	3.2130E 02	3.5428E 02	2.2988E 02	2.2925E 02	1.7095E 02
740.0	1.0261E 02	2.2095E 02	2.5286E 02	2.9457E 02	3.3429E 02	3.6852E 02	2.3931E 02	2.3865E 02	1.7799E 02
760.0	1.0673E 02	2.2977E 02	2.6287E 02	3.0618E 02	3.4737E 02	3.8287E 02	2.4881E 02	2.4813E 02	1.8509E 02
780.0	1.1088E 02	2.3865E 02	2.7295E 02	3.1787E 02	3.6055E 02	3.9732E 02	2.5838E 02	2.5768E 02	1.9225E 02
800.0	1.1506E 02	2.4761E 02	2.8310E 02	3.2964E 02	3.7381E 02	4.1186E 02	2.6803E 02	2.6729E 02	1.9946E 02
820.0	1.1926E 02	2.5662E 02	2.9332E 02	3.4149E 02	3.8716E 02	4.2648E 02	2.7773E 02	2.7698E 02	2.0671E 02
840.0	1.2350E 02	2.6570E 02	3.0361E 02	3.5341E 02	4.0059E 02	4.4120E 02	2.8750E 02	2.8672E 02	2.1402E 02
860.0	1.2777E 02	2.7483E 02	3.1395E 02	3.6540E 02	4.1409E 02	4.5599E 02	2.9734E 02	2.9652E 02	2.2138E 02
880.0	1.3206E 02	2.8401E 02	3.2436E 02	3.7746E 02	4.2766E 02	4.7086E 02	3.0722E 02	3.0639E 02	2.2877E 02
900.0	1.3637E 02	2.9325E 02	3.3482E 02	3.8958E 02	4.4131E 02	4.8580E 02	3.1716E 02	3.1630E 02	2.3621E 02
920.0	1.4071E 02	3.0254E 02	3.4533E 02	4.0176E 02	4.5501E 02	5.0081E 02	3.2716E 02	3.2627E 02	2.4369E 02
940.0	1.4508E 02	3.1187E 02	3.5590E 02	4.1400E 02	4.6878E 02	5.1588E 02	3.3720E 02	3.3629E 02	2.5121E 02
960.0	1.4946E 02	3.2125E 02	3.6651E 02	4.2629E 02	4.8261E 02	5.3102E 02	3.4729E 02	3.4635E 02	2.5876E 02
980.0	1.5387E 02	3.3068E 02	3.7717E 02	4.3864E 02	4.9649E 02	5.4622E 02	3.5743E 02	3.5646E 02	2.6635E 02
1000.0	1.5830E 02	3.4015E 02	3.8788E 02	4.5103E 02	5.1043E 02	5.6147E 02	3.6761E 02	3.6661E 02	2.7397E 02
1200.0	2.0350E 02	4.3675E 02	4.9698E 02	5.7727E 02	6.5224E 02	7.1657E 02	4.7140E 02	4.7014E 02	3.5176E 02
1400.0	2.5000E 02	5.3598E 02	6.0880E 02	7.0652E 02	7.9722E 02	8.7494E 02	5.7787E 02	5.7633E 02	4.3165E 02
1600.0	2.9735E 02	6.3690E 02	7.2232E 02	8.3761E 02	9.4406E 02	1.0352E 03	6.8604E 02	6.8422E 02	5.1290E 02
2000.0	3.9348E 02	8.4155E 02	9.5193E 02	1.1025E 03	1.2402E 03	1.3581E 03	9.0504E 02	9.0267E 02	6.7763E 02
2400.0	4.9048E 02	1.0477E 03	1.1826E 03	1.3682E 03	1.5368E 03	1.6809E 03	1.1253E 03	1.1224E 03	8.4355E 02
2800.0	5.8761E 02	1.2538E 03	1.4128E 03	1.6330E 03	1.8320E 03	2.0019E 03	1.3452E 03	1.3418E 03	1.0095E 03
3200.0	6.8451E 02	1.4593E 03	1.6417E 03	1.8962E 03	2.1249E 03	2.3202E 03	1.5641E 03	1.5601E 03	1.1748E 03
3600.0	7.8097E 02	1.6635E 03	1.8689E 03	2.1572E 03	2.4151E 03	2.6352E 03	1.7816E 03	1.7771E 03	1.3392E 03
4000.0	8.7690E 02	1.8665E 03	2.0944E 03	2.4160E 03	2.7025E 03	2.9470E 03	1.9975E 03	1.9924E 03	1.5025E 03
5000.0	1.1141E 03	2.3677E 03	2.6499E 03	3.0530E 03	3.4090E 03	3.7127E 03	2.5298E 03	2.5235E 03	1.9057E 03

PROTON RANGE, G/CM2

ENERGY MEV	WATER I= 65.1	AG-CL I=384.5	AG-BR I=434.1	NA-I I=433.0	LI-I I=472.5	POLYETHYLENE I= 54.6	STILBENE I= 65.2	LUCITE I= 65.6	ANTHRACENE I= 67.0
2.0	7.1304E-03	1.8233E-02	1.9808E-02	2.0233E-02	2.1584E-02	6.5685E-03	7.4349E-03	7.3544E-03	7.5726E-03
4.0	2.3042E-02	5.2566E-02	5.6645E-02	5.7869E-02	6.1373E-02	2.1458E-02	2.4024E-02	2.3755E-02	2.4429E-02
6.0	4.7053E-02	1.0157E-01	1.0891E-01	1.1127E-01	1.1758E-01	4.3980E-02	4.9056E-02	4.8503E-02	4.9854E-02
8.0	7.9065E-02	1.6494E-01	1.7621E-01	1.8005E-01	1.8974E-01	7.4007E-02	8.2430E-02	8.1496E-02	8.3750E-02
10.0	1.1832E-01	2.3853E-01	2.5418E-01	2.5984E-01	2.7339E-01	1.1105E-01	1.2338E-01	1.2196E-01	1.2530E-01
14.0	2.1735E-01	4.1933E-01	4.4522E-01	4.5559E-01	4.7836E-01	2.0463E-01	2.2665E-01	2.2402E-01	2.3008E-01
18.0	3.4248E-01	6.4273E-01	6.8070E-01	6.9721E-01	7.3100E-01	3.2305E-01	3.5714E-01	3.5297E-01	3.6242E-01
22.0	4.9257E-01	9.0631E-01	9.5805E-01	9.8189E-01	1.0283E 00	4.6523E-01	5.1364E-01	5.0762E-01	5.2112E-01
26.0	6.6672E-01	1.2082E 00	1.2753E 00	1.3075E 00	1.3681E 00	6.3031E-01	6.9520E-01	6.8705E-01	7.0522E-01
30.0	8.6415E-01	1.5470E 00	1.6309E 00	1.6724E 00	1.7485E 00	8.1757E-01	9.0104E-01	8.9045E-01	9.1391E-01
34.0	1.0842E 00	1.9213E 00	2.0236E 00	2.0753E 00	2.1680E 00	1.0264E 00	1.1304E 00	1.1171E 00	1.1465E 00
38.0	1.3263E 00	2.3301E 00	2.4521E 00	2.5149E 00	2.6256E 00	1.2562E 00	1.3828E 00	1.3665E 00	1.4023E 00
42.0	1.5898E 00	2.7725E 00	2.9155E 00	2.9901E 00	3.1200E 00	1.5064E 00	1.6575E 00	1.6380E 00	1.6808E 00
46.0	1.8743E 00	3.2475E 00	3.4129E 00	3.5001E 00	3.6503E 00	1.7767E 00	1.9541E 00	1.9311E 00	1.9814E 00
50.0	2.1793E 00	3.7544E 00	3.9435E 00	4.0439E 00	4.2156E 00	2.0666E 00	2.2721E 00	2.2453E 00	2.3037E 00
60.0	3.0289E 00	5.1564E 00	5.4098E 00	5.5466E 00	5.7765E 00	2.8741E 00	3.1577E 00	3.1204E 00	3.2013E 00
70.0	3.9978E 00	6.7427E 00	7.0678E 00	7.2451E 00	7.5395E 00	3.7957E 00	4.1677E 00	4.1185E 00	4.2249E 00
80.0	5.0807E 00	8.5043E 00	8.9078E 00	9.1297E 00	9.4946E 00	4.8260E 00	5.2966E 00	5.2340E 00	5.3688E 00
90.0	6.2728E 00	1.0433E 01	1.0922E 01	1.1192E 01	1.1633E 01	5.9605E 00	6.5392E 00	6.4619E 00	6.6280E 00
100.0	7.5694E 00	1.2522E 01	1.3102E 01	1.3424E 01	1.3946E 01	7.1950E 00	7.8908E 00	7.7975E 00	7.9975E 00
110.0	8.9666E 00	1.4764E 01	1.5441E 01	1.5818E 01	1.6428E 01	8.5254E 00	9.3472E 00	9.2366E 00	9.4732E 00
120.0	1.0460E 01	1.7153E 01	1.7933E 01	1.8369E 01	1.9070E 01	9.9482E 00	1.0904E 01	1.0775E 01	1.1051E 01
130.0	1.2047E 01	1.9684E 01	2.0571E 01	2.1069E 01	2.1867E 01	1.1460E 01	1.2559E 01	1.2410E 01	1.2727E 01
140.0	1.3724E 01	2.2351E 01	2.3351E 01	2.3914E 01	2.4812E 01	1.3057E 01	1.4306E 01	1.4137E 01	1.4497E 01
150.0	1.5487E 01	2.5148E 01	2.6267E 01	2.6898E 01	2.7901E 01	1.4738E 01	1.6144E 01	1.5953E 01	1.6359E 01
160.0	1.7334E 01	2.8072E 01	2.9314E 01	3.0015E 01	3.1128E 01	1.6498E 01	1.8069E 01	1.7855E 01	1.8309E 01
170.0	1.9261E 01	3.1118E 01	3.2487E 01	3.3262E 01	3.4488E 01	1.8335E 01	2.0078E 01	1.9840E 01	2.0345E 01
180.0	2.1266E 01	3.4281E 01	3.5782E 01	3.6633E 01	3.7976E 01	2.0247E 01	2.2168E 01	2.1905E 01	2.2462E 01
190.0	2.3347E 01	3.7557E 01	3.9195E 01	4.0124E 01	4.1589E 01	2.2230E 01	2.4337E 01	2.4048E 01	2.4659E 01
200.0	2.5500E 01	4.0943E 01	4.2721E 01	4.3732E 01	4.5321E 01	2.4284E 01	2.6582E 01	2.6266E 01	2.6933E 01
220.0	3.0017E 01	4.8030E 01	5.0099E 01	5.1280E 01	5.3128E 01	2.8592E 01	3.1290E 01	3.0918E 01	3.1703E 01
240.0	3.4799E 01	5.5512E 01	5.7889E 01	5.9248E 01	6.1367E 01	3.3153E 01	3.6274E 01	3.5843E 01	3.6752E 01
260.0	3.9829E 01	6.3367E 01	6.6063E 01	6.7609E 01	7.0013E 01	3.7952E 01	4.1518E 01	4.1024E 01	4.2063E 01
280.0	4.5094E 01	7.1569E 01	7.4599E 01	7.6340E 01	7.9038E 01	4.2975E 01	4.7006E 01	4.6446E 01	4.7622E 01
300.0	5.0579E 01	8.0099E 01	8.3474E 01	8.5417E 01	8.8423E 01	4.8210E 01	5.2723E 01	5.2095E 01	5.3413E 01
320.0	5.6271E 01	8.8937E 01	9.2667E 01	9.4819E 01	9.8144E 01	5.3643E 01	5.8657E 01	5.7958E 01	5.9423E 01
340.0	6.2160E 01	9.8064E 01	1.0216E 02	1.0453E 02	1.0818E 02	5.9263E 01	6.4795E 01	6.4023E 01	6.5639E 01
360.0	6.8233E 01	1.0746E 02	1.1194E 02	1.1453E 02	1.1851E 02	6.5061E 01	7.1125E 01	7.0278E 01	7.2051E 01
380.0	7.4481E 01	1.1712E 02	1.2198E 02	1.2480E 02	1.2912E 02	7.1027E 01	7.7638E 01	7.6713E 01	7.8648E 01
400.0	8.0895E 01	1.2702E 02	1.3227E 02	1.3532E 02	1.4000E 02	7.7151E 01	8.4323E 01	8.3318E 01	8.5419E 01
420.0	8.7465E 01	1.3715E 02	1.4280E 02	1.4609E 02	1.5112E 02	8.3424E 01	9.1172E 01	9.0085E 01	9.2355E 01
440.0	9.4183E 01	1.4750E 02	1.5356E 02	1.5709E 02	1.6248E 02	8.9840E 01	9.8175E 01	9.7004E 01	9.9447E 01
460.0	1.0104E 02	1.5805E 02	1.6452E 02	1.6831E 02	1.7406E 02	9.6391E 01	1.0532E 02	1.0407E 02	1.0669E 02
480.0	1.0803E 02	1.6879E 02	1.7569E 02	1.7973E 02	1.8586E 02	1.0307E 02	1.1261E 02	1.1127E 02	1.1407E 02
500.0	1.1515E 02	1.7972E 02	1.8705E 02	1.9134E 02	1.9785E 02	1.0987E 02	1.2003E 02	1.1860E 02	1.2158E 02
520.0	1.2239E 02	1.9082E 02	1.9858E 02	2.0313E 02	2.1003E 02	1.1678E 02	1.2758E 02	1.2605E 02	1.2922E 02
540.0	1.2975E 02	2.0208E 02	2.1029E 02	2.1510E 02	2.2239E 02	1.2381E 02	1.3524E 02	1.3363E 02	1.3698E 02
560.0	1.3721E 02	2.1351E 02	2.2216E 02	2.2724E 02	2.3492E 02	1.3093E 02	1.4302E 02	1.4131E 02	1.4486E 02
580.0	1.4478E 02	2.2507E 02	2.3419E 02	2.3953E 02	2.4761E 02	1.3816E 02	1.5090E 02	1.4910E 02	1.5284E 02
600.0	1.5244E 02	2.3678E 02	2.4638E 02	2.5197E 02	2.6046E 02	1.4548E 02	1.5889E 02	1.5699E 02	1.6093E 02
620.0	1.6020E 02	2.4863E 02	2.5870E 02	2.6455E 02	2.7344E 02	1.5289E 02	1.6697E 02	1.6497E 02	1.6912E 02
640.0	1.6805E 02	2.6059E 02	2.7115E 02	2.7726E 02	2.8657E 02	1.6040E 02	1.7515E 02	1.7305E 02	1.7740E 02
660.0	1.7598E 02	2.7268E 02	2.8372E 02	2.9010E 02	2.9982E 02	1.6799E 02	1.8342E 02	1.8122E 02	1.8577E 02
680.0	1.8399E 02	2.8489E 02	2.9641E 02	3.0306E 02	3.1320E 02	1.7565E 02	1.9178E 02	1.8948E 02	1.9423E 02
700.0	1.9208E 02	2.9720E 02	3.0921E 02	3.1613E 02	3.2669E 02	1.8340E 02	2.0022E 02	1.9786E 02	2.0278E 02
720.0	2.0025E 02	3.0961E 02	3.2211E 02	3.2931E 02	3.4029E 02	1.9122E 02	2.0874E 02	2.0631E 02	2.1140E 02
740.0	2.0848E 02	3.2212E 02	3.3511E 02	3.4260E 02	3.5400E 02	1.9911E 02	2.1733E 02	2.1483E 02	2.2010E 02
760.0	2.1679E 02	3.3473E 02	3.4821E 02	3.5598E 02	3.6782E 02	2.0706E 02	2.2600E 02	2.2343E 02	2.2888E 02
780.0	2.2515E 02	3.4742E 02	3.6139E 02	3.6946E 02	3.8172E 02	2.1509E 02	2.3474E 02	2.3209E 02	2.3772E 02
800.0	2.3358E 02	3.6020E 02	3.7467E 02	3.8303E 02	3.9572E 02	2.2317E 02	2.4354E 02	2.4082E 02	2.4663E 02
820.0	2.4207E 02	3.7305E 02	3.8802E 02	3.9668E 02	4.0980E 02	2.3131E 02	2.5241E 02	2.4961E 02	2.5561E 02
840.0	2.5062E 02	3.8599E 02	4.0145E 02	4.1041E 02	4.2397E 02	2.3951E 02	2.6133E 02	2.5847E 02	2.6465E 02
860.0	2.5922E 02	3.9899E 02	4.1496E 02	4.2421E 02	4.3822E 02	2.4777E 02	2.7032E 02	2.6738E 02	2.7374E 02
880.0	2.6787E 02	4.1207E 02	4.2853E 02	4.3809E 02	4.5253E 02	2.5608E 02	2.7936E 02	2.7634E 02	2.8290E 02
900.0	2.7658E 02	4.2521E 02	4.4218E 02	4.5704E 02	4.6692E 02	2.6443E 02	2.8846E 02	2.8536E 02	2.9210E 02
920.0	2.8533E 02	4.3841E 02	4.5589E 02	4.6605E 02	4.8138E 02	2.7284E 02	2.9760E 02	2.9443E 02	3.0136E 02
940.0	2.9413E 02	4.5168E 02	4.6965E 02	4.8013E 02	4.9590E 02	2.8129E 02	3.0680E 02	3.0355E 02	3.1067E 02
960.0	3.0297E 02	4.6500E 02	4.8348E 02	4.9426E 02	5.1049E 02	2.8978E 02	3.1604E 02	3.1272E 02	3.2003E 02
980.0	3.1185E 02	4.7837E 02	4.9736E 02	5.0846E 02	5.2513E 02	2.9832E 02	3.2533E 02	3.2193E 02	3.2943E 02
1000.0	3.2077E 02	4.9180E 02	5.1130E 02	5.2270E 02	5.3982E 02	3.0690E 02	3.3466E 02	3.3118E 02	3.3888E 02
1200.0	4.1185E 02	6.2839E 02	6.5307E 02	6.6762F 02	6.8929E 02	3.9461E 02	4.3001E 02	4.2573E 02	4.3542E 02
1400.0	5.0550E 02	7.6803E 02	7.9801E 02	8.1571E 02	8.4205E 02	4.8499E 02	5.2820E 02	5.2308E 02	5.3483E 02
1600.0	6.0089E 02	9.0950E 02	9.4485E 02	9.6565E 02	9.9686E 02	5.7720E 02	6.2831E 02	6.2232E 02	6.3620E 02
2000.0	7.9479E 02	1.1952E 03	1.2413E 03	1.2682E 03	1.3095E 03	7.6499E 02	8.3203E 02	8.2424E 02	8.4246E 02
2400.0	9.9080E 02	1.4818E 03	1.5386E 03	1.5717E 03	1.6233E 03	9.5515E 02	1.0381E 03	1.0285E 03	1.0512E 03
2800.0	1.1875E 03	1.7676E 03	1.8351E 03	1.8742E 03	1.9361E 03	1.1442E 03	1.2451E 03	1.2336E 03	1.2607E 03
3200.0	1.3843E 03	2.0519E 03	2.1299E 03	2.1749E 03	2.2473E 03	1.3375E 03	1.4522E 03	1.4387E 03	1.4704E 03
3600.0	1.5806E 03	2.3344E 03	2.4226E 03	2.4735E 03	2.5562E 03	1.5284E 03	1.6588E 03	1.6434E 03	1.6796E 03
4000.0	1.7763E 03	2.6147E 03	2.7132E 03	2.7697E 03	2.8627E 03	1.7188E 03	1.8648E 03	1.8474E 03	1.8882E 03
5000.0	2.2621E 03	3.3067E 03	3.4299E 03	3.5000E 03	3.6186E 03	2.1918E 03	2.3763E 03	2.3539E 03	2.4060E 03

KAON STOPPING POWER, MEV•CM2/G

ENERGY MEV	BE I= 60.0	C I= 78.0	AL I=163.0	FE I=273.0	CU I=314.0	AG I=487.0	AU I=797.0	PB I=826.0	U I=923.0
2.0	8.4865E 01	9.0043E 01	7.1324E 01	5.8444E 01	5.4586E 01	4.4293E 01	3.3350E 01	3.2410E 01	3.0158E 01
4.0	4.7294E 01	5.0287E 01	4.0578E 01	3.4059E 01	3.2071E 01	2.6816E 01	2.1058E 01	2.0535E 01	1.9317E 01
6.0	3.4112E 01	3.6681E 01	3.0561E 01	2.6264E 01	2.4817E 01	2.0942E 01	1.6352E 01	1.5925E 01	1.4912E 01
8.0	2.6993E 01	2.9092E 01	2.4456E 01	2.1169E 01	2.0053E 01	1.7030E 01	1.3292E 01	1.2934E 01	1.2061E 01
10.0	2.2499E 01	2.4289E 01	2.0546E 01	1.7876E 01	1.6965E 01	1.4487E 01	1.1356E 01	1.1051E 01	1.0301E 01
14.0	1.7096E 01	1.8496E 01	1.5776E 01	1.3825E 01	1.3155E 01	1.1332E 01	8.9929E 00	8.7595E 00	8.1903E 00
18.0	1.3936E 01	1.5099E 01	1.2948E 01	1.1401E 01	1.0868E 01	9.4226E 00	7.5598E 00	7.3714E 00	6.9174E 00
22.0	1.1849E 01	1.2852E 01	1.1065E 01	9.7770E 00	9.3317E 00	8.1292E 00	6.5792E 00	6.4209E 00	6.0438E 00
26.0	1.0364E 01	1.1251E 01	9.7147E 00	8.6073E 00	8.2233E 00	7.1901E 00	5.8593E 00	5.7223E 00	5.3995E 00
30.0	9.2495E 00	1.0048E 01	8.6970E 00	7.7222E 00	7.3835E 00	6.4748E 00	5.3056E 00	5.1844E 00	4.9016E 00
34.0	8.3814E 00	9.1099E 00	7.9008E 00	7.0277E 00	6.7238E 00	5.9105E 00	4.8650E 00	4.7561E 00	4.5039E 00
38.0	7.6851E 00	8.3571E 00	7.2601E 00	6.4675E 00	6.1911E 00	5.4532E 00	4.5055E 00	4.4063E 00	4.1782E 00
42.0	7.1136E 00	7.7389E 00	6.7328E 00	6.0056E 00	5.7515E 00	5.0747E 00	4.2060E 00	4.1148E 00	3.9061E 00
46.0	6.6360E 00	7.2220E 00	6.2910E 00	5.6178E 00	5.3823E 00	4.7560E 00	3.9526E 00	3.8679E 00	3.6752E 00
50.0	6.2306E 00	6.7830E 00	5.9152E 00	5.2875E 00	5.0676E 00	4.4837E 00	3.7351E 00	3.6559E 00	3.4767E 00
60.0	5.4419E 00	5.9284E 00	5.1821E 00	4.6417E 00	4.4518E 00	3.9492E 00	3.3054E 00	3.2369E 00	3.0833E 00
70.0	4.8684E 00	5.3066E 00	4.6472E 00	4.1693E 00	4.0009E 00	3.5565E 00	2.9875E 00	2.9265E 00	2.7911E 00
80.0	4.4323E 00	4.8335E 00	4.2393E 00	3.8085E 00	3.6563E 00	3.2555E 00	2.7424E 00	2.6872E 00	2.5652E 00
90.0	4.0894E 00	4.4614E 00	3.9180E 00	3.5237E 00	3.3841E 00	3.0173E 00	2.5476E 00	2.4969E 00	2.3854E 00
100.0	3.8128E 00	4.1610E 00	3.6583E 00	3.2933E 00	3.1639E 00	2.8242E 00	2.3891E 00	2.3420E 00	2.2388E 00
110.0	3.5850E 00	3.9135E 00	3.4441E 00	3.1031E 00	2.9819E 00	2.6644E 00	2.2577E 00	2.2135E 00	2.1171E 00
120.0	3.3941E 00	3.7062E 00	3.2645E 00	2.9434E 00	2.8292E 00	2.5302E 00	2.1470E 00	2.1052E 00	2.0145E 00
130.0	3.2320E 00	3.5300E 00	3.1118E 00	2.8076E 00	2.6992E 00	2.4158E 00	2.0525E 00	2.0128E 00	1.9268E 00
140.0	3.0927E 00	3.3786E 00	2.9804E 00	2.6907E 00	2.5873E 00	2.3173E 00	1.9709E 00	1.9331E 00	1.8511E 00
150.0	2.9717E 00	3.2471E 00	2.8663E 00	2.5891E 00	2.4901E 00	2.2316E 00	1.8999E 00	1.8636E 00	1.7851E 00
160.0	2.8658E 00	3.1319E 00	2.7663E 00	2.5001E 00	2.4048E 00	2.1564E 00	1.8376E 00	1.8026E 00	1.7272E 00
170.0	2.7723E 00	3.0213E 00	2.6780E 00	2.4214E 00	2.3295E 00	2.0900E 00	1.7825E 00	1.7486E 00	1.6759E 00
180.0	2.6892E 00	2.9310E 00	2.5995E 00	2.3515E 00	2.2626E 00	2.0309E 00	1.7334E 00	1.7006E 00	1.6302E 00
190.0	2.6150E 00	2.8502E 00	2.5294E 00	2.2890E 00	2.2027E 00	1.9770E 00	1.6895E 00	1.6576E 00	1.5894E 00
200.0	2.5483E 00	2.7775E 00	2.4664E 00	2.2317E 00	2.1489E 00	1.9302E 00	1.6500E 00	1.6190E 00	1.5526E 00
220.0	2.4335E 00	2.6522E 00	2.3579E 00	2.1350E 00	2.0559E 00	1.8488E 00	1.5819E 00	1.5524E 00	1.4893E 00
240.0	2.3382E 00	2.5480E 00	2.2681E 00	2.0548E 00	1.9792E 00	1.7811E 00	1.5256E 00	1.4972E 00	1.4368E 00
260.0	2.2577E 00	2.4604E 00	2.1854E 00	1.9874E 00	1.9149E 00	1.7244E 00	1.4783E 00	1.4509E 00	1.3927E 00
280.0	2.1892E 00	2.3858E 00	2.1220E 00	1.9300E 00	1.8602E 00	1.6762E 00	1.4382E 00	1.4117E 00	1.3553E 00
300.0	2.1301E 00	2.3217E 00	2.0675E 00	1.8808E 00	1.8134E 00	1.6350E 00	1.4039E 00	1.3781E 00	1.3234E 00
320.0	2.0789E 00	2.2661E 00	2.0203E 00	1.8361E 00	1.7730E 00	1.5994E 00	1.3743E 00	1.3491E 00	1.2959E 00
340.0	2.0342E 00	2.2176E 00	1.9791E 00	1.7991E 00	1.7379E 00	1.5686E 00	1.3487E 00	1.3240E 00	1.2720E 00
360.0	1.9948E 00	2.1750E 00	1.9429E 00	1.7667E 00	1.7072E 00	1.5416E 00	1.3263E 00	1.3021E 00	1.2511E 00
380.0	1.9600E 00	2.1373E 00	1.9110E 00	1.7381E 00	1.6801E 00	1.5179E 00	1.3067E 00	1.2829E 00	1.2329E 00
400.0	1.9290E 00	2.1038E 00	1.8828E 00	1.7128E 00	1.6563E 00	1.4971E 00	1.2894E 00	1.2660E 00	1.2168E 00
420.0	1.9013E 00	2.0740E 00	1.8576E 00	1.6902E 00	1.6351E 00	1.4786E 00	1.2741E 00	1.2511E 00	1.2026E 00
440.0	1.8765E 00	2.0473E 00	1.8351E 00	1.6701E 00	1.6110E 00	1.4612E 00	1.2606E 00	1.2378E 00	1.1889E 00
460.0	1.8542E 00	2.0233E 00	1.8149E 00	1.6520E 00	1.5939E 00	1.4467E 00	1.2486E 00	1.2261E 00	1.1778E 00
480.0	1.8341E 00	2.0017E 00	1.7967E 00	1.6358E 00	1.5786E 00	1.4338E 00	1.2379E 00	1.2156E 00	1.1679E 00
500.0	1.8158E 00	1.9821E 00	1.7803E 00	1.6212E 00	1.5649E 00	1.4223E 00	1.2283E 00	1.2063E 00	1.1590E 00
520.0	1.7992E 00	1.9644E 00	1.7655E 00	1.6080E 00	1.5524E 00	1.4119E 00	1.2187E 00	1.1980E 00	1.1511E 00
540.0	1.7842E 00	1.9483E 00	1.7521E 00	1.5961E 00	1.5412E 00	1.4023E 00	1.2109E 00	1.1905E 00	1.1440E 00
560.0	1.7704E 00	1.9336E 00	1.7399E 00	1.5853E 00	1.5310E 00	1.3937E 00	1.2039E 00	1.1838E 00	1.1376E 00
580.0	1.7578E 00	1.9202E 00	1.7289E 00	1.5754E 00	1.5218E 00	1.3859E 00	1.1976E 00	1.1779E 00	1.1319E 00
600.0	1.7463E 00	1.9080E 00	1.7188E 00	1.5665E 00	1.5134E 00	1.3788E 00	1.1919E 00	1.1725E 00	1.1267E 00
620.0	1.7358E 00	1.8968E 00	1.7096E 00	1.5584E 00	1.5058E 00	1.3724E 00	1.1863E 00	1.1677E 00	1.1217E 00
640.0	1.7261E 00	1.8865E 00	1.7012E 00	1.5510E 00	1.4989E 00	1.3666E 00	1.1817E 00	1.1635E 00	1.1176E 00
660.0	1.7171E 00	1.8771E 00	1.6935E 00	1.5442E 00	1.4926E 00	1.3613E 00	1.1776E 00	1.1597E 00	1.1138E 00
680.0	1.7089E 00	1.8685E 00	1.6865E 00	1.5380E 00	1.4868E 00	1.3566E 00	1.1739E 00	1.1563E 00	1.1105E 00
700.0	1.7013E 00	1.8605E 00	1.6801E 00	1.5324E 00	1.4816E 00	1.3523E 00	1.1706E 00	1.1532E 00	1.1075E 00
720.0	1.6943E 00	1.8532E 00	1.6742E 00	1.5273E 00	1.4768E 00	1.3484E 00	1.1676E 00	1.1505E 00	1.1049E 00
740.0	1.6879E 00	1.8465E 00	1.6688E 00	1.5226E 00	1.4725E 00	1.3448E 00	1.1649E 00	1.1482E 00	1.1025E 00
760.0	1.6819E 00	1.8403E 00	1.6639E 00	1.5183E 00	1.4685E 00	1.3416E 00	1.1625E 00	1.1461E 00	1.1004E 00
780.0	1.6764E 00	1.8346E 00	1.6594E 00	1.5144E 00	1.4649E 00	1.3388E 00	1.1604E 00	1.1442E 00	1.0985E 00
800.0	1.6713E 00	1.8293E 00	1.6553E 00	1.5108E 00	1.4616E 00	1.3362E 00	1.1585E 00	1.1426E 00	1.0968E 00
820.0	1.6665E 00	1.8244E 00	1.6515E 00	1.5075E 00	1.4586E 00	1.3338E 00	1.1568E 00	1.1412E 00	1.0954E 00
840.0	1.6622E 00	1.8199E 00	1.6480E 00	1.5045E 00	1.4559E 00	1.3317E 00	1.1553E 00	1.1400E 00	1.0941E 00
860.0	1.6581E 00	1.8158E 00	1.6449E 00	1.5018E 00	1.4534E 00	1.3299E 00	1.1540E 00	1.1351E 00	1.0930E 00
880.0	1.6543E 00	1.8120E 00	1.6420E 00	1.4994E 00	1.4512E 00	1.3282E 00	1.1528E 00	1.1342E 00	1.0921E 00
900.0	1.6508E 00	1.8084E 00	1.6393E 00	1.4971E 00	1.4492E 00	1.3267E 00	1.1518E 00	1.1335E 00	1.0913E 00
920.0	1.6476E 00	1.8052E 00	1.6369E 00	1.4951E 00	1.4474E 00	1.3254E 00	1.1510E 00	1.1328E 00	1.0906E 00
940.0	1.6446E 00	1.8022E 00	1.6347E 00	1.4933E 00	1.4457E 00	1.3242E 00	1.1503E 00	1.1324E 00	1.0900E 00
960.0	1.6418E 00	1.7994E 00	1.6328E 00	1.4916E 00	1.4443E 00	1.3232E 00	1.1497E 00	1.1320E 00	1.0896E 00
980.0	1.6392E 00	1.7969E 00	1.6310E 00	1.4902E 00	1.4430E 00	1.3224E 00	1.1492E 00	1.1317E 00	1.0893E 00
1000.0	1.6368E 00	1.7946E 00	1.6293E 00	1.4888E 00	1.4418E 00	1.3216E 00	1.1488E 00	1.1316E 00	1.0890E 00
1200.0	1.6211E 00	1.7800E 00	1.6204E 00	1.4821E 00	1.4364E 00	1.3196E 00	1.1495E 00	1.1340E 00	1.0907E 00
1400.0	1.6149E 00	1.7756E 00	1.6200E 00	1.4830E 00	1.4381E 00	1.3236E 00	1.1550E 00	1.1409E 00	1.0968E 00
1600.0	1.6140E 00	1.7768E 00	1.6241E 00	1.4879E 00	1.4436E 00	1.3307E 00	1.1630E 00	1.1500E 00	1.1052E 00
2000.0	1.6200E 00	1.7873E 00	1.6387E 00	1.5031E 00	1.4595E 00	1.3489E 00	1.1818E 00	1.1707E 00	1.1244E 00
2400.0	1.6306E 00	1.8022E 00	1.6563E 00	1.5208E 00	1.4776E 00	1.3685E 00	1.2013E 00	1.1917E 00	1.1441E 00
2800.0	1.6425E 00	1.8182E 00	1.6743E 00	1.5386E 00	1.4957E 00	1.3876E 00	1.2201E 00	1.2116E 00	1.1629E 00
3200.0	1.6547E 00	1.8341E 00	1.6918E 00	1.5558E 00	1.5130E 00	1.4057E 00	1.2377E 00	1.2302E 00	1.1805E 00
3600.0	1.6665E 00	1.8493E 00	1.7083E 00	1.5720E 00	1.5293E 00	1.4226E 00	1.2541E 00	1.2475E 00	1.1968E 00
4000.0	1.6778E 00	1.8638E 00	1.7238E 00	1.5872E 00	1.5445E 00	1.4383E 00	1.2693E 00	1.2635E 00	1.2119E 00
5000.0	1.7036E 00	1.8963E 00	1.7585E 00	1.6210E 00	1.5783E 00	1.4731E 00	1.3027E 00	1.2985E 00	1.2452E 00

KAON STOPPING POWER, MEV•CM2/G

ENERGY MEV	H I= 18.7	HE I= 42.0	NE I=131.0	A I=210.0	KR I=381.0	XE I=555.0	AIR I= 86.8	CARB.DIOXIDE I= 85.9	METHANE I= 44.1
2.0	2.2980E 02	1.0257E 02	7.8123E 01	6.1688E 01	4.7923E 01	3.9718E 01	8.7678E 01	8.8049E 01	1.2683E 02
4.0	1.3051E 02	5.7205E 01	4.4117E 01	3.5472E 01	2.8506E 01	2.4294E 01	4.9042E 01	4.9241E 01	7.0712E 01
6.0	9.1431E 01	4.0701E 01	3.2898E 01	2.7026E 01	2.2176E 01	1.8980E 01	3.5957E 01	3.6093E 01	5.0440E 01
8.0	7.1739E 01	3.2122E 01	2.6252E 01	2.1704E 01	1.7973E 01	1.5454E 01	2.8545E 01	2.8648E 01	3.9810E 01
10.0	5.9440E 01	2.6725E 01	2.2010E 01	1.8279E 01	1.5242E 01	1.3167E 01	2.3848E 01	2.3931E 01	3.3123E 01
14.0	4.4801E 01	2.0255E 01	1.6855E 01	1.4083E 01	1.1862E 01	1.0331E 01	1.8177E 01	1.8238E 01	2.5107E 01
18.0	3.6324E 01	1.6482E 01	1.3810E 01	1.1584E 01	9.8249E 00	8.6104E 00	1.4848E 01	1.4896E 01	2.0433E 01
22.0	3.0764E 01	1.3997E 01	1.1786E 01	9.9154E 00	8.4519E 00	7.4423E 00	1.2644E 01	1.2684E 01	1.7354E 01
26.0	2.6824E 01	1.2229E 01	1.0338E 01	8.7165E 00	7.4588E 00	6.5921E 00	1.1072E 01	1.1107E 01	1.5164E 01
30.0	2.3880E 01	1.0906E 01	9.2474E 00	7.8111E 00	6.7048E 00	5.9431E 00	9.8914E 00	9.9220E 00	1.3524E 01
34.0	2.1593E 01	9.8752E 00	8.3954E 00	7.1019E 00	6.1115E 00	5.4303E 00	8.9702E 00	8.9977E 00	1.2247E 01
38.0	1.9764E 01	9.0494E 00	7.7103E 00	6.5305E 00	5.6318E 00	5.0141E 00	8.2307E 00	8.2556E 00	1.1224E 01
42.0	1.8266E 01	8.3722E 00	7.1470E 00	6.0599E 00	5.2355E 00	4.6691E 00	7.6232E 00	7.6462E 00	1.0385E 01
46.0	1.7016E 01	7.8065E 00	6.6753E 00	5.6652E 00	4.9022E 00	4.3784E 00	7.1151E 00	7.1364E 00	9.6834E 00
50.0	1.5957E 01	7.3266E 00	6.2743E 00	5.3292E 00	4.6180E 00	4.1298E 00	6.6836E 00	6.7034E 00	9.0885E 00
60.0	1.3901E 01	6.3937E 00	5.4925E 00	4.6732E 00	4.0611E 00	3.6412E 00	5.8433E 00	5.8605E 00	7.9321E 00
70.0	1.2410E 01	5.7159E 00	4.9226E 00	4.1940E 00	3.6528E 00	3.2816E 00	5.2316E 00	5.2469E 00	7.0919E 00
80.0	1.1279E 01	5.2010E 00	4.4884E 00	3.8283E 00	3.3403E 00	3.0057E 00	4.7661E 00	4.7799E 00	6.4534E 00
90.0	1.0391E 01	4.7963E 00	4.1464E 00	3.5400E 00	3.0934E 00	2.7872E 00	4.3999E 00	4.4125E 00	5.9517E 00
100.0	9.6760E 00	4.4700E 00	3.8702E 00	3.3068E 00	2.8934E 00	2.6099E 00	4.1043E 00	4.1160E 00	5.5470E 00
110.0	9.0875E 00	4.2013E 00	3.6425E 00	3.1144E 00	2.7281E 00	2.4632E 00	3.8607E 00	3.8716E 00	5.2138E 00
120.0	8.5950E 00	3.9763E 00	3.4515E 00	2.9530E 00	2.5893E 00	2.3398E 00	3.6565E 00	3.6669E 00	4.9348E 00
130.0	8.1770E 00	3.7852E 00	3.2892E 00	2.8157E 00	2.4711E 00	2.2347E 00	3.4831E 00	3.4929E 00	4.6979E 00
140.0	7.8180E 00	3.6211E 00	3.1497E 00	2.6977E 00	2.3694E 00	2.1441E 00	3.3340E 00	3.3433E 00	4.4943E 00
150.0	7.5065E 00	3.4785E 00	3.0284E 00	2.5950E 00	2.2809E 00	2.0652E 00	3.2045E 00	3.2135E 00	4.3176E 00
160.0	7.2337E 00	3.3537E 00	2.9222E 00	2.5051E 00	2.2033E 00	1.9961E 00	3.0911E 00	3.0997E 00	4.1628E 00
170.0	6.9931E 00	3.2436E 00	2.8285E 00	2.4257E 00	2.1348E 00	1.9350E 00	2.9910E 00	2.9993E 00	4.0262E 00
180.0	6.7793E 00	3.1458E 00	2.7451E 00	2.3551E 00	2.0739E 00	1.8806E 00	2.9020E 00	2.9101E 00	3.9049E 00
190.0	6.5883E 00	3.0583E 00	2.6707E 00	2.2920E 00	2.0194E 00	1.8320E 00	2.8225E 00	2.8303E 00	3.7964E 00
200.0	6.4167E 00	2.9798E 00	2.6037E 00	2.2353E 00	1.9704E 00	1.7883E 00	2.7511E 00	2.7587E 00	3.6990E 00
220.0	6.1214E 00	2.8446E 00	2.4885E 00	2.1377E 00	1.8861E 00	1.7130E 00	2.6282E 00	2.6354E 00	3.5313E 00
240.0	5.8768E 00	2.7326E 00	2.3932E 00	2.0569E 00	1.8163E 00	1.6507E 00	2.5263E 00	2.5332E 00	3.3924E 00
260.0	5.6713E 00	2.6386E 00	2.3131E 00	1.9891E 00	1.7577E 00	1.5984E 00	2.4409E 00	2.4475E 00	3.2758E 00
280.0	5.4969E 00	2.5588E 00	2.2452E 00	1.9316E 00	1.7081E 00	1.5540E 00	2.3684E 00	2.3748E 00	3.1768E 00
300.0	5.3472E 00	2.4903E 00	2.1870E 00	1.8823E 00	1.6656E 00	1.5161E 00	2.3062E 00	2.3124E 00	3.0919E 00
320.0	5.2177E 00	2.4311E 00	2.1367E 00	1.8397E 00	1.6289E 00	1.4834E 00	2.2524E 00	2.2585E 00	3.0185E 00
340.0	5.1048E 00	2.3796E 00	2.0929E 00	1.8028E 00	1.5970E 00	1.4550E 00	2.2057E 00	2.2116E 00	2.9546E 00
360.0	5.0058E 00	2.3344E 00	2.0546E 00	1.7704E 00	1.5692E 00	1.4302E 00	2.1647E 00	2.1705E 00	2.8986E 00
380.0	4.9185E 00	2.2946E 00	2.0210E 00	1.7420E 00	1.5447E 00	1.4084E 00	2.1287E 00	2.1344E 00	2.8492E 00
400.0	4.8411E 00	2.2593E 00	1.9912E 00	1.7168E 00	1.5232E 00	1.3892E 00	2.0968E 00	2.1024E 00	2.8055E 00
420.0	4.7722E 00	2.2279E 00	1.9647E 00	1.6946E 00	1.5041E 00	1.3723E 00	2.0685E 00	2.0739E 00	2.7666E 00
440.0	4.7106E 00	2.1999E 00	1.9412E 00	1.6747E 00	1.4871E 00	1.3572E 00	2.0432E 00	2.0486E 00	2.7319E 00
460.0	4.6554E 00	2.1749E 00	1.9201E 00	1.6570E 00	1.4720E 00	1.3438E 00	2.0206E 00	2.0259E 00	2.7008E 00
480.0	4.6057E 00	2.1523E 00	1.9013E 00	1.6412E 00	1.4585E 00	1.3319E 00	2.0003E 00	2.0056E 00	2.6729E 00
500.0	4.5609E 00	2.1320E 00	1.8843E 00	1.6270E 00	1.4464E 00	1.3212E 00	1.9821E 00	1.9873E 00	2.6477E 00
520.0	4.5204E 00	2.1137E 00	1.8691E 00	1.6142E 00	1.4355E 00	1.3116E 00	1.9657E 00	1.9708E 00	2.6250E 00
540.0	4.4836E 00	2.0971E 00	1.8553E 00	1.6027E 00	1.4258E 00	1.3031E 00	1.9508E 00	1.9559E 00	2.6045E 00
560.0	4.4503E 00	2.0821E 00	1.8429E 00	1.5923E 00	1.4170E 00	1.2954E 00	1.9374E 00	1.9424E 00	2.5859E 00
580.0	4.4199E 00	2.0685E 00	1.8316E 00	1.5830E 00	1.4092E 00	1.2885E 00	1.9252E 00	1.9302E 00	2.5690E 00
600.0	4.3923E 00	2.0561E 00	1.8214E 00	1.5745E 00	1.4021E 00	1.2823E 00	1.9142E 00	1.9192E 00	2.5536E 00
620.0	4.3671E 00	2.0448E 00	1.8122E 00	1.5668E 00	1.3957E 00	1.2767E 00	1.9042E 00	1.9091E 00	2.5396E 00
640.0	4.3440E 00	2.0345E 00	1.8038E 00	1.5599E 00	1.3899E 00	1.2717E 00	1.8951E 00	1.9000E 00	2.5269E 00
660.0	4.3229E 00	2.0251E 00	1.7962E 00	1.5536E 00	1.3847E 00	1.2672E 00	1.8868E 00	1.8917E 00	2.5152E 00
680.0	4.3037E 00	2.0165E 00	1.7893E 00	1.5480E 00	1.3800E 00	1.2632E 00	1.8792E 00	1.8841E 00	2.5046E 00
700.0	4.2860E 00	2.0087E 00	1.7831E 00	1.5428E 00	1.3758E 00	1.2596E 00	1.8724E 00	1.8772E 00	2.4950E 00
720.0	4.2698E 00	2.0015E 00	1.7774E 00	1.5382E 00	1.3720E 00	1.2564E 00	1.8661E 00	1.8710E 00	2.4861E 00
740.0	4.2550E 00	1.9950E 00	1.7722E 00	1.5340E 00	1.3687E 00	1.2535E 00	1.8605E 00	1.8653E 00	2.4781E 00
760.0	4.2414E 00	1.9891E 00	1.7675E 00	1.5302E 00	1.3656E 00	1.2509E 00	1.8553E 00	1.8601E 00	2.4707E 00
780.0	4.2289E 00	1.9836E 00	1.7633E 00	1.5268E 00	1.3629E 00	1.2487E 00	1.8506E 00	1.8554E 00	2.4640E 00
800.0	4.2175E 00	1.9787E 00	1.7595E 00	1.5238E 00	1.3605E 00	1.2467E 00	1.8464E 00	1.8511E 00	2.4578E 00
820.0	4.2070E 00	1.9741E 00	1.7560E 00	1.5210E 00	1.3584E 00	1.2449E 00	1.8425E 00	1.8473E 00	2.4522E 00
840.0	4.1974E 00	1.9700E 00	1.7529E 00	1.5186E 00	1.3565E 00	1.2434E 00	1.8390E 00	1.8438E 00	2.4471E 00
860.0	4.1887E 00	1.9662E 00	1.7501E 00	1.5164E 00	1.3548E 00	1.2421E 00	1.8359E 00	1.8406E 00	2.4425E 00
880.0	4.1806E 00	1.9628E 00	1.7476E 00	1.5144E 00	1.3534E 00	1.2409E 00	1.8330E 00	1.8377E 00	2.4383E 00
900.0	4.1733E 00	1.9597E 00	1.7454E 00	1.5127E 00	1.3521E 00	1.2400E 00	1.8305E 00	1.8352E 00	2.4345E 00
920.0	4.1666E 00	1.9569E 00	1.7434E 00	1.5112E 00	1.3510E 00	1.2392E 00	1.8282E 00	1.8329E 00	2.4310E 00
940.0	4.1605E 00	1.9544E 00	1.7417E 00	1.5099E 00	1.3501E 00	1.2385E 00	1.8262E 00	1.8308E 00	2.4279E 00
960.0	4.1549E 00	1.9521E 00	1.7401E 00	1.5088E 00	1.3494E 00	1.2380E 00	1.8243E 00	1.8290E 00	2.4251E 00
980.0	4.1499E 00	1.9501E 00	1.7388E 00	1.5078E 00	1.3488E 00	1.2376E 00	1.8227E 00	1.8274E 00	2.4226E 00
1000.0	4.1453E 00	1.9482E 00	1.7376E 00	1.5070E 00	1.3483E 00	1.2373E 00	1.8213E 00	1.8260E 00	2.4203E 00
1200.0	4.1199E 00	1.9391E 00	1.7337E 00	1.5054E 00	1.3492E 00	1.2396E 00	1.8155E 00	1.8201E 00	2.4092E 00
1400.0	4.1181E 00	1.9407E 00	1.7388E 00	1.5113E 00	1.3564E 00	1.2475E 00	1.8194E 00	1.8239E 00	2.4114E 00
1600.0	4.1292E 00	1.9481E 00	1.7485E 00	1.5211E 00	1.3668E 00	1.2581E 00	1.8283E 00	1.8328E 00	2.4207E 00
2000.0	4.1698E 00	1.9708E 00	1.7742E 00	1.5456E 00	1.3916E 00	1.2828E 00	1.8530E 00	1.8575E 00	2.4492E 00
2400.0	4.2200E 00	1.9974E 00	1.8024E 00	1.5720E 00	1.4176E 00	1.3082E 00	1.8807E 00	1.8853E 00	2.4825E 00
2800.0	4.2721E 00	2.0245E 00	1.8305E 00	1.5980E 00	1.4430E 00	1.3328E 00	1.9086E 00	1.9132E 00	2.5163E 00
3200.0	4.3232E 00	2.0508E 00	1.8575E 00	1.6229E 00	1.4670E 00	1.3561E 00	1.9354E 00	1.9400E 00	2.5492E 00
3600.0	4.3722E 00	2.0759E 00	1.8830E 00	1.6463E 00	1.4896E 00	1.3779E 00	1.9609E 00	1.9656E 00	2.5806E 00
4000.0	4.4188E 00	2.0997E 00	1.9070E 00	1.6683E 00	1.5108E 00	1.3983E 00	1.9849E 00	1.9896E 00	2.6103E 00
5000.0	4.5245E 00	2.1534E 00	1.9610E 00	1.7176E 00	1.5582E 00	1.4438E 00	2.0391E 00	2.0438E 00	2.6773E 00

KAON STOPPING POWER, MEV•CM2/G

ENERGY MEV	WATER I= 65.1	AG-CL I=384.5	AG-BR I=434.1	NA-I I=433.0	LI-I I=472.5	POLYETHYLENE I= 54.6	STILBENE I= 65.2	LUCITE I= 65.6	ANTHRACENE I= 67.0
2.0	1.0426E 02	4.9642E 01	4.6393E 01	4.5405E 01	4.3035E 01	1.1124E 02	1.0000E 02	1.0115E 02	9.8442E 01
4.0	5.8125E 01	2.9547E 01	2.7848E 01	2.7250E 01	2.5994E 01	6.1980E 01	5.5754E 01	5.6396E 01	5.4894E 01
6.0	4.2089E 01	2.2955E 01	2.1714E 01	2.1197E 01	2.0240E 01	4.4546E 01	4.0355E 01	4.0837E 01	3.9777E 01
8.0	3.3322E 01	1.8590E 01	1.7629E 01	1.7184E 01	1.6429E 01	3.5219E 01	3.1954E 01	3.2336E 01	3.1504E 01
10.0	2.7785E 01	1.5762E 01	1.4974E 01	1.4589E 01	1.3964E 01	2.9339E 01	2.6648E 01	2.6965E 01	2.6277E 01
14.0	2.1124E 01	1.2270E 01	1.1684E 01	1.1385E 01	1.0918E 01	2.2275E 01	2.0261E 01	2.0503E 01	1.9984E 01
18.0	1.7226E 01	1.0167E 01	9.6970E 00	9.4528E 00	9.0786E 00	1.8148E 01	1.6523E 01	1.6721E 01	1.6299E 01
22.0	1.4652E 01	8.7500E 00	8.3545E 00	8.1476E 00	7.8333E 00	1.5426E 01	1.4054E 01	1.4222E 01	1.3865E 01
26.0	1.2818E 01	7.7244E 00	7.3815E 00	7.2013E 00	6.9292E 00	1.3488E 01	1.2296E 01	1.2443E 01	1.2131E 01
30.0	1.1442E 01	6.9454E 00	6.6415E 00	6.4813E 00	6.2405E 00	1.2035E 01	1.0976E 01	1.1108E 01	1.0830E 01
34.0	1.0370E 01	6.3322E 00	6.0584E 00	5.9137E 00	5.6971E 00	1.0903E 01	9.9476E 00	1.0067E 01	9.8158E 00
38.0	9.5096E 00	5.8363E 00	5.5864E 00	5.4541E 00	5.2567E 00	9.9960E 00	9.1226E 00	9.2320E 00	9.0021E 00
42.0	8.8037E 00	5.4264E 00	5.1961E 00	5.0739E 00	4.8921E 00	9.2514E 00	8.4454E 00	8.5467E 00	8.3342E 00
46.0	8.2134E 00	5.0816E 00	4.8677E 00	4.7539E 00	4.5850E 00	8.6292E 00	7.8792E 00	7.9738E 00	7.7758E 00
50.0	7.7124E 00	4.7875E 00	4.5873E 00	4.4806E 00	4.3226E 00	8.1010E 00	7.3986E 00	7.4875E 00	7.3017E 00
60.0	6.7375E 00	4.2111E 00	4.0374E 00	3.9445E 00	3.8076E 00	7.0739E 00	6.4635E 00	6.5412E 00	6.3793E 00
70.0	6.0285E 00	3.7883E 00	3.6338E 00	3.5508E 00	3.4291E 00	6.3273E 00	5.7833E 00	5.8529E 00	5.7083E 00
80.0	5.4893E 00	3.4647E 00	3.3247E 00	3.2492E 00	3.1390E 00	5.7596E 00	5.2661E 00	5.3295E 00	5.1980E 00
90.0	5.0653E 00	3.2089E 00	3.0803E 00	3.0106E 00	2.9093E 00	5.3134E 00	4.8593E 00	4.9179E 00	4.7967E 00
100.0	4.7231E 00	3.0017E 00	2.8821E 00	2.8172E 00	2.7231E 00	4.9534E 00	4.5311E 00	4.5857E 00	4.4729E 00
110.0	4.4413E 00	2.8304E 00	2.7183E 00	2.6573E 00	2.5691E 00	4.6569E 00	4.2607E 00	4.3121E 00	4.2061E 00
120.0	4.2052E 00	2.6866E 00	2.5807E 00	2.5229E 00	2.4396E 00	4.4086E 00	4.0343E 00	4.0829E 00	3.9826E 00
130.0	4.0047E 00	2.5641E 00	2.4635E 00	2.4085E 00	2.3293E 00	4.1977E 00	3.8419E 00	3.8883E 00	3.7928E 00
140.0	3.8323E 00	2.4586E 00	2.3626E 00	2.3099E 00	2.2343E 00	4.0165E 00	3.6765E 00	3.7209E 00	3.6296E 00
150.0	3.6826E 00	2.3669E 00	2.2748E 00	2.2241E 00	2.1517E 00	3.8591E 00	3.5329E 00	3.5756E 00	3.4880E 00
160.0	3.5515E 00	2.2865E 00	2.1979E 00	2.1489E 00	2.0783E 00	3.7213E 00	3.4072E 00	3.4484E 00	3.3639E 00
170.0	3.4359E 00	2.2154E 00	2.1299E 00	2.0825E 00	2.0151E 00	3.5997E 00	3.2962E 00	3.3361E 00	3.2544E 00
180.0	3.3331E 00	2.1522E 00	2.0694E 00	2.0234E 00	1.9581E 00	3.4916E 00	3.1976E 00	3.2363E 00	3.1571E 00
190.0	3.2412E 00	2.0958E 00	2.0153E 00	1.9706E 00	1.9072E 00	3.3950E 00	3.1095E 00	3.1471E 00	3.0701E 00
200.0	3.1587E 00	2.0450E 00	1.9667E 00	1.9231E 00	1.8614E 00	3.3083E 00	3.0303E 00	3.0670E 00	2.9920E 00
220.0	3.0166E 00	1.9576E 00	1.8830E 00	1.8413E 00	1.7825E 00	3.1589E 00	2.8940E 00	2.9290E 00	2.8575E 00
240.0	2.8990E 00	1.8852E 00	1.8137E 00	1.7736E 00	1.7172E 00	3.0353E 00	2.7812E 00	2.8148E 00	2.7461E 00
260.0	2.8002E 00	1.8244E 00	1.7555E 00	1.7167E 00	1.6624E 00	2.9314E 00	2.6864E 00	2.7190E 00	2.6526E 00
280.0	2.7140E 00	1.7729E 00	1.7062E 00	1.6686E 00	1.6156E 00	2.8433E 00	2.6060E 00	2.6376E 00	2.5733E 00
300.0	2.6429E 00	1.7288E 00	1.6640E 00	1.6273E 00	1.5760E 00	2.7677E 00	2.5370E 00	2.5678E 00	2.5051E 00
320.0	2.5810E 00	1.6908E 00	1.6249E 00	1.5917E 00	1.5418E 00	2.7024E 00	2.4773E 00	2.5075E 00	2.4462E 00
340.0	2.5269E 00	1.6578E 00	1.5939E 00	1.5608E 00	1.5121E 00	2.6419E 00	2.4235E 00	2.4550E 00	2.3940E 00
360.0	2.4793E 00	1.6289E 00	1.5668E 00	1.5338E 00	1.4861E 00	2.5900E 00	2.3766E 00	2.3963E 00	2.3476E 00
380.0	2.4371E 00	1.6035E 00	1.5429E 00	1.5101E 00	1.4632E 00	2.5441E 00	2.3351E 00	2.3545E 00	2.3067E 00
400.0	2.3995E 00	1.5812E 00	1.5219E 00	1.4892E 00	1.4431E 00	2.5033E 00	2.2983E 00	2.3174E 00	2.2702E 00
420.0	2.3659E 00	1.5614E 00	1.5032E 00	1.4706E 00	1.4253E 00	2.4668E 00	2.2654E 00	2.2843E 00	2.2377E 00
440.0	2.3357E 00	1.5438E 00	1.4866E 00	1.4542E 00	1.4095E 00	2.4342E 00	2.2360E 00	2.2547E 00	2.2086E 00
460.0	2.3086E 00	1.5281E 00	1.4717E 00	1.4396E 00	1.3954E 00	2.4048E 00	2.2095E 00	2.2280E 00	2.1825E 00
480.0	2.2840E 00	1.5141E 00	1.4584E 00	1.4266E 00	1.3828E 00	2.3783E 00	2.1856E 00	2.2040E 00	2.1589E 00
500.0	2.2624E 00	1.5015E 00	1.4465E 00	1.4149E 00	1.3716E 00	2.3544E 00	2.1640E 00	2.1822E 00	2.1375E 00
520.0	2.2428E 00	1.4903E 00	1.4358E 00	1.4044E 00	1.3615E 00	2.3326E 00	2.1444E 00	2.1625E 00	2.1181E 00
540.0	2.2250E 00	1.4802E 00	1.4262E 00	1.3950E 00	1.3524E 00	2.3128E 00	2.1266E 00	2.1446E 00	2.1005E 00
560.0	2.2088E 00	1.4711E 00	1.4175E 00	1.3866E 00	1.3443E 00	2.2947E 00	2.1104E 00	2.1283E 00	2.0844E 00
580.0	2.1940E 00	1.4630E 00	1.4097E 00	1.3790E 00	1.3370E 00	2.2782E 00	2.0955E 00	2.1134E 00	2.0698E 00
600.0	2.1805E 00	1.4556E 00	1.4026E 00	1.3721E 00	1.3305E 00	2.2631E 00	2.0820E 00	2.0998E 00	2.0564E 00
620.0	2.1681E 00	1.4490E 00	1.3959E 00	1.3660E 00	1.3246E 00	2.2493E 00	2.0696E 00	2.0873E 00	2.0441E 00
640.0	2.1567E 00	1.4430E 00	1.3903E 00	1.3604E 00	1.3192E 00	2.2366E 00	2.0582E 00	2.0758E 00	2.0329E 00
660.0	2.1463E 00	1.4376E 00	1.3851E 00	1.3555E 00	1.3144E 00	2.2249E 00	2.0477E 00	2.0653E 00	2.0225E 00
680.0	2.1367E 00	1.4328E 00	1.3805E 00	1.3510E 00	1.3098E 00	2.2141E 00	2.0381E 00	2.0557E 00	2.0130E 00
700.0	2.1279E 00	1.4284E 00	1.3762E 00	1.3469E 00	1.3057E 00	2.2042E 00	2.0292E 00	2.0468E 00	2.0042E 00
720.0	2.1198E 00	1.4245E 00	1.3724E 00	1.3433E 00	1.3019E 00	2.1951E 00	2.0211E 00	2.0386E 00	1.9962E 00
740.0	2.1123E 00	1.4210E 00	1.3689E 00	1.3401E 00	1.2986E 00	2.1866E 00	2.0135E 00	2.0310E 00	1.9887E 00
760.0	2.1054E 00	1.4177E 00	1.3658E 00	1.3372E 00	1.2955E 00	2.1788E 00	2.0066E 00	2.0241E 00	1.9819E 00
780.0	2.0991E 00	1.4147E 00	1.3630E 00	1.3346E 00	1.2928E 00	2.1716E 00	2.0002E 00	2.0176E 00	1.9755E 00
800.0	2.0932E 00	1.4120E 00	1.3604E 00	1.3323E 00	1.2903E 00	2.1649E 00	1.9943E 00	2.0117E 00	1.9697E 00
820.0	2.0878E 00	1.4096E 00	1.3582E 00	1.3303E 00	1.2881E 00	2.1588E 00	1.9888E 00	2.0062E 00	1.9642E 00
840.0	2.0828E 00	1.4075E 00	1.3562E 00	1.3285E 00	1.2862E 00	2.1530E 00	1.9837E 00	2.0012E 00	1.9592E 00
860.0	2.0782E 00	1.4056E 00	1.3544E 00	1.3269E 00	1.2844E 00	2.1478E 00	1.9790E 00	1.9965E 00	1.9546E 00
880.0	2.0739E 00	1.4039E 00	1.3528E 00	1.3255E 00	1.2828E 00	2.1429E 00	1.9747E 00	1.9922E 00	1.9503E 00
900.0	2.0700E 00	1.4024E 00	1.3514E 00	1.3241E 00	1.2814E 00	2.1383E 00	1.9707E 00	1.9882E 00	1.9464E 00
920.0	2.0663E 00	1.4010E 00	1.3502E 00	1.3229E 00	1.2801E 00	2.1341E 00	1.9670E 00	1.9845E 00	1.9427E 00
940.0	2.0630E 00	1.3999E 00	1.3491E 00	1.3218E 00	1.2790E 00	2.1302E 00	1.9636E 00	1.9811E 00	1.9394E 00
960.0	2.0599E 00	1.3989E 00	1.3482E 00	1.3209E 00	1.2781E 00	2.1266E 00	1.9605E 00	1.9779E 00	1.9363E 00
980.0	2.0571E 00	1.3980E 00	1.3475E 00	1.3201E 00	1.2773E 00	2.1233E 00	1.9576E 00	1.9750E 00	1.9334E 00
1000.0	2.0545E 00	1.3973E 00	1.3468E 00	1.3195E 00	1.2766E 00	2.1202E 00	1.9549E 00	1.9724E 00	1.9307E 00
1200.0	2.0379E 00	1.3958E 00	1.3454E 00	1.3183E 00	1.2749E 00	2.1000E 00	1.9376E 00	1.9553E 00	1.9137E 00
1400.0	2.0326E 00	1.4002E 00	1.3500E 00	1.3231E 00	1.2792E 00	2.0923E 00	1.9317E 00	1.9497E 00	1.9078E 00
1600.0	2.0334E 00	1.4076E 00	1.3576E 00	1.3309E 00	1.2865E 00	2.0916E 00	1.9320E 00	1.9502E 00	1.9081E 00
2000.0	2.0440E 00	1.4265E 00	1.3766E 00	1.3503E 00	1.3049E 00	2.1005E 00	1.9416E 00	1.9605E 00	1.9177E 00
2400.0	2.0594E 00	1.4468E 00	1.3969E 00	1.3710E 00	1.3246E 00	2.1153E 00	1.9563E 00	1.9757E 00	1.9322E 00
2800.0	2.0761E 00	1.4665E 00	1.4165E 00	1.3911E 00	1.3438E 00	2.1318E 00	1.9725E 00	1.9924E 00	1.9482E 00
3200.0	2.0926E 00	1.4852E 00	1.4350E 00	1.4101E 00	1.3621E 00	2.1485E 00	1.9886E 00	2.0090E 00	1.9641E 00
3600.0	2.1085E 00	1.5026E 00	1.4523E 00	1.4278E 00	1.3791E 00	2.1647E 00	2.0042E 00	2.0251E 00	1.9796E 00
4000.0	2.1236E 00	1.5187E 00	1.4683E 00	1.4443E 00	1.3949E 00	2.1802E 00	2.0190E 00	2.0403E 00	1.9942E 00
5000.0	2.1574E 00	1.5544E 00	1.5037E 00	1.4806E 00	1.4300E 00	2.2153E 00	2.0525E 00	2.0746E 00	2.0273E 00

KAON RANGE, G/CM2

ENERGY MEV	BE I= 60.0	C I= 78.0	AL I=163.0	FE I=273.0	CU I=314.0	AG I=487.0	AU I=797.0	PB I=826.0	U I=923.0
2.0	1.3585E-02	1.2942E-02	1.6911E-02	2.1224E-02	2.2910E-02	2.9018E-02	3.9877E-02	4.1141E-02	4.4581E-02
4.0	4.6532E-02	4.3936E-02	5.5562E-02	6.7702E-02	7.2431E-02	8.8968E-02	1.1756E-01	1.2092E-01	1.2978E-01
6.0	9.7069E-02	9.1040E-02	1.1253E-01	1.3440E-01	1.4314E-01	1.7314E-01	2.2536E-01	2.3155E-01	2.4765E-01
8.0	1.6349E-01	1.5274E-01	1.8622E-01	2.1980E-01	2.3340E-01	2.7974E-01	3.6198E-01	3.7190E-01	3.9792E-01
10.0	2.4503E-01	2.2833E-01	2.7983E-01	3.2305E-01	3.4228E-01	4.0758E-01	5.2545E-01	5.3990E-01	5.7815E-01
14.0	4.5121E-01	4.1908E-01	5.0029E-01	5.7999E-01	6.1263E-01	7.2264E-01	9.2485E-01	9.5015E-01	1.0176E 00
18.0	7.1195E-01	6.5988E-01	7.8178E-01	9.0037E-01	9.4901E-01	1.1118E 00	1.4123E 00	1.4503E 00	1.5516E 00
22.0	1.0244E 00	9.4813E-01	1.1172E 00	1.2806E 00	1.3476E 00	1.5703E 00	1.9813E 00	2.0335E 00	2.1721E 00
26.0	1.3864E 00	1.2817E 00	1.5040E 00	1.7177E 00	1.8054E 00	2.0948E 00	2.6269E 00	2.6949E 00	2.8737E 00
30.0	1.7957E 00	1.6586E 00	1.9400E 00	2.2093E 00	2.3196E 00	2.6820E 00	3.3455E 00	3.4304E 00	3.6524E 00
34.0	2.2507E 00	2.0773E 00	2.4233E 00	2.7530E 00	2.8881E 00	3.3295E 00	4.1338E 00	4.2369E 00	4.5048E 00
38.0	2.7497E 00	2.5363E 00	2.9520E 00	3.3470E 00	3.5088E 00	4.0348E 00	4.9890E 00	5.1115E 00	5.4277E 00
42.0	3.2912E 00	3.0342E 00	3.5247E 00	3.9894E 00	4.1797E 00	4.7958E 00	5.9086E 00	6.0517E 00	6.4186E 00
46.0	3.8739E 00	3.5696E 00	4.1397E 00	4.6785E 00	4.8992E 00	5.6106E 00	6.8903E 00	7.0550E 00	7.4750E 00
50.0	4.4964E 00	4.1415E 00	4.7959E 00	5.4129E 00	5.6656E 00	6.4774E 00	7.9319E 00	8.1193E 00	8.5946E 00
60.0	6.2191E 00	5.7234E 00	6.6075E 00	7.4374E 00	7.7771E 00	8.8606E 00	1.0786E 01	1.1034E 01	1.1657E 01
70.0	8.1662E 00	7.5101E 00	8.6496E 00	9.7153E 00	1.0152E 01	1.1534E 01	1.3974E 01	1.4289E 01	1.5072E 01
80.0	1.0322E 01	9.4879E 00	1.0906E 01	1.2229E 01	1.2770E 01	1.4477E 01	1.7473E 01	1.7860E 01	1.8815E 01
90.0	1.2674E 01	1.1644E 01	1.3363E 01	1.4962E 01	1.5616E 01	1.7672E 01	2.1260E 01	2.1725E 01	2.2862E 01
100.0	1.5209E 01	1.3967E 01	1.6007E 01	1.7900E 01	1.8675E 01	2.1101E 01	2.5317E 01	2.5864E 01	2.7193E 01
110.0	1.7916E 01	1.6447E 01	1.8826E 01	2.1031E 01	2.1934E 01	2.4749E 01	2.9626E 01	3.0259E 01	3.1789E 01
120.0	2.0785E 01	1.9075E 01	2.1810E 01	2.4341E 01	2.5379E 01	2.8603E 01	3.4171E 01	3.4894E 01	3.6634E 01
130.0	2.3806E 01	2.1841E 01	2.4950E 01	2.7822E 01	2.8999E 01	3.2649E 01	3.8937E 01	3.9755E 01	4.1712E 01
140.0	2.6970E 01	2.4738E 01	2.8235E 01	3.1462E 01	3.2785E 01	3.6878E 01	4.3911E 01	4.4826E 01	4.7009E 01
150.0	3.0270E 01	2.7758E 01	3.1657E 01	3.5252E 01	3.6726E 01	4.1277E 01	4.9080E 01	5.0097E 01	5.2512E 01
160.0	3.3698E 01	3.0895E 01	3.5210E 01	3.9184E 01	4.0814E 01	4.5837E 01	5.4434E 01	5.5554E 01	5.8209E 01
170.0	3.7246E 01	3.4147E 01	3.8885E 01	4.3249E 01	4.5040E 01	5.0549E 01	5.9961E 01	6.1188E 01	6.4088E 01
180.0	4.0910E 01	3.7508E 01	4.2676E 01	4.7441E 01	4.9397E 01	5.5404E 01	6.5651E 01	6.6989E 01	7.0140E 01
190.0	4.4682E 01	4.0969E 01	4.6577E 01	5.1752E 01	5.3877E 01	6.0395E 01	7.1496E 01	7.2946E 01	7.6353E 01
200.0	4.8556E 01	4.4524E 01	5.0581E 01	5.6177E 01	5.8474E 01	6.5515E 01	7.7486E 01	7.9051E 01	8.2720E 01
220.0	5.6593E 01	5.1898E 01	5.8880E 01	6.5346E 01	6.7996E 01	7.6109E 01	8.9873E 01	9.1675E 01	9.5881E 01
240.0	6.4982E 01	5.9595E 01	6.7533E 01	7.4900E 01	7.7916E 01	8.7136E 01	1.0275E 02	1.0480E 02	1.0956E 02
260.0	7.3690E 01	6.7587E 01	7.6520E 01	8.4801E 01	8.8193E 01	9.8553E 01	1.1608E 02	1.1838E 02	1.2370E 02
280.0	8.2690E 01	7.5845E 01	8.5812E 01	9.5016E 01	9.8794E 01	1.1032E 02	1.2980E 02	1.3235E 02	1.3827E 02
300.0	9.1954E 01	8.4345E 01	9.5364E 01	1.0552E 02	1.0969E 02	1.2241E 02	1.4388E 02	1.4670E 02	1.5320E 02
320.0	1.0146E 02	9.3067E 01	1.0515E 02	1.1628E 02	1.2084E 02	1.3478E 02	1.5828E 02	1.6137E 02	1.6848E 02
340.0	1.1119E 02	1.0199E 02	1.1516E 02	1.2729E 02	1.3224E 02	1.4741E 02	1.7297E 02	1.7634E 02	1.8406E 02
360.0	1.2112E 02	1.1110E 02	1.2536E 02	1.3851E 02	1.4385E 02	1.6027E 02	1.8793E 02	1.9157E 02	1.9992E 02
380.0	1.3123E 02	1.2038E 02	1.3574E 02	1.4992E 02	1.5566E 02	1.7335E 02	2.0312E 02	2.0705E 02	2.1602E 02
400.0	1.4152E 02	1.2981E 02	1.4628E 02	1.6152E 02	1.6765E 02	1.8661E 02	2.1853E 02	2.2274E 02	2.3236E 02
420.0	1.5197E 02	1.3939E 02	1.5698E 02	1.7327E 02	1.7981E 02	2.0006E 02	2.3414E 02	2.3864E 02	2.4889E 02
440.0	1.6256E 02	1.4909E 02	1.6781E 02	1.8518E 02	1.9213E 02	2.1367E 02	2.4992E 02	2.5471E 02	2.6562E 02
460.0	1.7328E 02	1.5892E 02	1.7877E 02	1.9722E 02	2.0461E 02	2.2742E 02	2.6587E 02	2.7095E 02	2.8252E 02
480.0	1.8413E 02	1.6886E 02	1.8985E 02	2.0939E 02	2.1722E 02	2.4131E 02	2.8195E 02	2.8733E 02	2.9958E 02
500.0	1.9509E 02	1.7890E 02	2.0103E 02	2.2167E 02	2.2995E 02	2.5532E 02	2.9817E 02	3.0385E 02	3.1677E 02
520.0	2.0615E 02	1.8904E 02	2.1231E 02	2.3406E 02	2.4278E 02	2.6943E 02	3.1452E 02	3.2048E 02	3.3408E 02
540.0	2.1731E 02	1.9926E 02	2.2369E 02	2.4654E 02	2.5571E 02	2.8365E 02	3.3099E 02	3.3723E 02	3.5151E 02
560.0	2.2857E 02	2.0957E 02	2.3514E 02	2.5912E 02	2.6873E 02	2.9795E 02	3.4755E 02	3.5408E 02	3.6905E 02
580.0	2.3991E 02	2.1995E 02	2.4667E 02	2.7177E 02	2.8184E 02	3.1235E 02	3.6421E 02	3.7102E 02	3.8667E 02
600.0	2.5132E 02	2.3040E 02	2.5828E 02	2.8450E 02	2.9502E 02	3.2681E 02	3.8095E 02	3.8804E 02	4.0438E 02
620.0	2.6281E 02	2.4091E 02	2.6994E 02	2.9730E 02	3.0826E 02	3.4135E 02	3.9777E 02	4.0513E 02	4.2218E 02
640.0	2.7436E 02	2.5148E 02	2.8167E 02	3.1017E 02	3.2158E 02	3.5596E 02	4.1466E 02	4.2229E 02	4.4004E 02
660.0	2.8598E 02	2.6211E 02	2.9346E 02	3.2309E 02	3.3495E 02	3.7062E 02	4.3162E 02	4.3951E 02	4.5797E 02
680.0	2.9766E 02	2.7279E 02	3.0529E 02	3.3607E 02	3.4837E 02	3.8534E 02	4.4863E 02	4.5678E 02	4.7595E 02
700.0	3.0939E 02	2.8352E 02	3.1717E 02	3.4910E 02	3.6185E 02	4.0011E 02	4.6569E 02	4.7410E 02	4.9398E 02
720.0	3.2117E 02	2.9429E 02	3.2910E 02	3.6217E 02	3.7537E 02	4.1492E 02	4.8280E 02	4.9146E 02	5.1206E 02
740.0	3.3299E 02	3.0510E 02	3.4106E 02	3.7529E 02	3.8893E 02	4.2977E 02	4.9995E 02	5.0887E 02	5.3018E 02
760.0	3.4487E 02	3.1595E 02	3.5307E 02	3.8844E 02	4.0254E 02	4.4466E 02	5.1713E 02	5.2630E 02	5.4834E 02
780.0	3.5678E 02	3.2684E 02	3.6510E 02	4.0163E 02	4.1617E 02	4.5958E 02	5.3435E 02	5.4377E 02	5.6653E 02
800.0	3.6872E 02	3.3779E 02	3.7717E 02	4.1486E 02	4.2984E 02	4.7454E 02	5.5160E 02	5.6126E 02	5.8476E 02
820.0	3.8071E 02	3.4870E 02	3.8927E 02	4.2811E 02	4.4354E 02	4.8952E 02	5.6888E 02	5.7877E 02	6.0300E 02
840.0	3.9273E 02	3.5968E 02	4.0139E 02	4.4139E 02	4.5726E 02	5.0453E 02	5.8618E 02	5.9631E 02	6.2127E 02
860.0	4.0477E 02	3.7068E 02	4.1354E 02	4.5469E 02	4.7101E 02	5.1955E 02	6.0350E 02	6.1389E 02	6.3956E 02
880.0	4.1685E 02	3.8171E 02	4.2571E 02	4.6802E 02	4.8478E 02	5.3460E 02	6.2084E 02	6.3152E 02	6.5787E 02
900.0	4.2895E 02	3.9275E 02	4.3790E 02	4.8137E 02	4.9857E 02	5.4967E 02	6.3820E 02	6.4916E 02	6.7619E 02
920.0	4.4108E 02	4.0382E 02	4.5011E 02	4.9474E 02	5.1238E 02	5.6475E 02	6.5557E 02	6.6681E 02	6.9452E 02
940.0	4.5323E 02	4.1491E 02	4.6233E 02	5.0812E 02	5.2621E 02	5.7985E 02	6.7295E 02	6.8447E 02	7.1286E 02
960.0	4.6540E 02	4.2602E 02	4.7457E 02	5.2152E 02	5.4005E 02	5.9496E 02	6.9034E 02	7.0213E 02	7.3122E 02
980.0	4.7759E 02	4.3714E 02	4.8683E 02	5.3494E 02	5.5391E 02	6.1008E 02	7.0774E 02	7.1980E 02	7.4957E 02
1000.0	4.8980E 02	4.4828E 02	4.9910E 02	5.4837E 02	5.6777E 02	6.2521E 02	7.2515E 02	7.3747E 02	7.6794E 02
1200.0	6.1266E 02	5.6025E 02	6.2226E 02	6.8308E 02	7.0683E 02	7.7673E 02	8.9928E 02	9.1412E 02	9.5154E 02
1400.0	7.3632E 02	6.7279E 02	7.4574E 02	8.1802E 02	8.4602E 02	9.2811E 02	1.0729E 03	1.0900E 03	1.1344E 03
1600.0	8.6023E 02	7.8541E 02	8.6907E 02	9.5269E 02	9.8485E 02	1.0788E 03	1.2455E 03	1.2646E 03	1.3161E 03
2000.0	1.1077E 03	1.0100E 03	1.1143E 03	1.2202E 03	1.2605E 03	1.3774E 03	1.5867E 03	1.6094E 03	1.6750E 03
2400.0	1.3538E 03	1.2329E 03	1.3571E 03	1.4848E 03	1.5329E 03	1.6718E 03	1.9224E 03	1.9480E 03	2.0276E 03
2800.0	1.5983E 03	1.4538E 03	1.5973E 03	1.7463E 03	1.8019E 03	1.9621E 03	2.2528E 03	2.2809E 03	2.3744E 03
3200.0	1.8409E 03	1.6729E 03	1.8350E 03	2.0048E 03	2.0678E 03	2.2485E 03	2.5783E 03	2.6085E 03	2.7157E 03
3600.0	2.0818E 03	1.8901E 03	2.0703E 03	2.2606E 03	2.3307E 03	2.5313E 03	2.8993E 03	2.9313E 03	3.0522E 03
4000.0	2.3210E 03	2.1055E 03	2.3034E 03	2.5138E 03	2.5910E 03	2.8109E 03	3.2163E 03	3.2499E 03	3.3843E 03
5000.0	2.9123E 03	2.6373E 03	2.8776E 03	3.1370E 03	3.2313E 03	3.4977E 03	3.9937E 03	4.0303E 03	4.1980E 03

KAON RANGE, G/CM2

ENERGY MEV	H I= 18.7	HE I= 42.0	NE I=131.0	A I=210.0	KR I=381.0	XE I=555.0	AIR I= 86.8	CARB.DIOXIDE I= 85.9	METHANE I= 44.1
2.0	4.8239E-03	1.1090E-02	1.5272E-02	1.9815E-02	2.6404E-02	3.2644E-02	1.3353E-02	1.3290E-02	8.9840E-03
4.0	1.6901E-02	3.8364E-02	5.0727E-02	6.4209E-02	8.2396E-02	9.9096E-02	4.5147E-02	4.4954E-02	3.1042E-02
6.0	3.5621E-02	8.0609E-02	1.0352E-01	1.2882E-01	1.6169E-01	1.9205E-01	9.3246E-02	9.2865E-02	6.5138E-02
8.0	6.0520E-02	1.3636E-01	1.7208E-01	2.1198E-01	2.6254E-01	3.0959E-01	1.5615E-01	1.5554E-01	1.1013E-01
10.0	9.1300E-02	2.0495E-01	2.5566E-01	3.1283E-01	3.8387E-01	4.5036E-01	2.3316E-01	2.3228E-01	1.6547E-01
14.0	1.6970E-01	3.7877E-01	4.6549E-01	5.6464E-01	6.8416E-01	7.9646E-01	4.2734E-01	4.2580E-01	3.0571E-01
18.0	2.6948E-01	5.9905E-01	7.2922E-01	8.7960E-01	1.0567E 00	1.2228E 00	6.7229E-01	6.6994E-01	4.8340E-01
22.0	3.8963E-01	8.6345E-01	1.0439E 00	1.2542E 00	1.4972E 00	1.7241E 00	9.6535E-01	9.6207E-01	6.9666E-01
26.0	5.2926E-01	1.1700E 00	1.4073E 00	1.6855E 00	2.0022E 00	2.2965E 00	1.3043E 00	1.3000E 00	9.4391E-01
30.0	6.8763E-01	1.5171E 00	1.8172E 00	2.1712E 00	2.5688E 00	2.9367E 00	1.6873E 00	1.6817E 00	1.2238E 00
34.0	8.6405E-01	1.9031E 00	2.2718E 00	2.7090E 00	3.1946E 00	3.6417E 00	2.1126E 00	2.1057E 00	1.5351E 00
38.0	1.0579E 00	2.3268E 00	2.7696E 00	3.2971E 00	3.8771E 00	4.4091E 00	2.5786E 00	2.5704E 00	1.8766E 00
42.0	1.2686E 00	2.7867E 00	3.3089E 00	3.9335E 00	4.6144E 00	5.2365E 00	3.0841E 00	3.0743E 00	2.2475E 00
46.0	1.4957E 00	3.2819E 00	3.8885E 00	4.6167E 00	5.4045E 00	6.1218E 00	3.6276E 00	3.6162E 00	2.6467E 00
50.0	1.7386E 00	3.8112E 00	4.5069E 00	5.3451E 00	6.2457E 00	7.0630E 00	4.2081E 00	4.1949E 00	3.0734E 00
60.0	2.4122E 00	5.2769E 00	6.2156E 00	7.3550E 00	8.5616E 00	9.6490E 00	5.8132E 00	5.7953E 00	4.2548E 00
70.0	3.1753E 00	6.9347E 00	8.1429E 00	9.6186E 00	1.1163E 01	1.2548E 01	7.6258E 00	7.6026E 00	5.5911E 00
80.0	4.0219E 00	8.7718E 00	1.0274E 01	1.2118E 01	1.4031E 01	1.5737E 01	9.6316E 00	9.6027E 00	7.0717E 00
90.0	4.9468E 00	1.0776E 01	1.2595E 01	1.4838E 01	1.7145E 01	1.9195E 01	1.1818E 01	1.1783E 01	8.6873E 00
100.0	5.9451E 00	1.2938E 01	1.5093E 01	1.7763E 01	2.0491E 01	2.2906E 01	1.4174E 01	1.4132E 01	1.0429E 01
110.0	7.0124E 00	1.5248E 01	1.7759E 01	2.0882E 01	2.4053E 01	2.6853E 01	1.6688E 01	1.6639E 01	1.2290E 01
120.0	8.1446E 00	1.7696E 01	2.0581E 01	2.4181E 01	2.7818E 01	3.1021E 01	1.9351E 01	1.9294E 01	1.4263E 01
130.0	9.3381E 00	2.0275E 01	2.3550E 01	2.7651E 01	3.1773E 01	3.5397E 01	2.2155E 01	2.2090E 01	1.6341E 01
140.0	1.0589E 01	2.2977E 01	2.6659E 01	3.1281E 01	3.5907E 01	3.9967E 01	2.5090E 01	2.5018E 01	1.8518E 01
150.0	1.1895E 01	2.5796E 01	2.9898E 01	3.5062E 01	4.0211E 01	4.4721E 01	2.8151E 01	2.8070E 01	2.0789E 01
160.0	1.3253E 01	2.8725E 01	3.3260E 01	3.8985E 01	4.4673E 01	4.9648E 01	3.1329E 01	3.1239E 01	2.3149E 01
170.0	1.4659E 01	3.1758E 01	3.6739E 01	4.3043E 01	4.9285E 01	5.4738E 01	3.4619E 01	3.4520E 01	2.5592E 01
180.0	1.6112E 01	3.4889E 01	4.0329E 01	4.7228E 01	5.4039E 01	5.9981E 01	3.8014E 01	3.7906E 01	2.8115E 01
190.0	1.7609E 01	3.8114E 01	4.4023E 01	5.1533E 01	5.8926E 01	6.5370E 01	4.1509E 01	4.1391E 01	3.0713E 01
200.0	1.9147E 01	4.1427E 01	4.7816E 01	5.5952E 01	6.3940E 01	7.0896E 01	4.5098E 01	4.4970E 01	3.3382E 01
220.0	2.2340E 01	4.8301E 01	5.5678E 01	6.5107E 01	7.4322E 01	8.2330E 01	5.2541E 01	5.2393E 01	3.8919E 01
240.0	2.5677E 01	5.5478E 01	6.3878E 01	7.4650E 01	8.5133E 01	9.4230E 01	6.0307E 01	6.0137E 01	4.4701E 01
260.0	2.9142E 01	6.2930E 01	7.2382E 01	8.4542E 01	9.6331E 01	1.0655E 02	6.8364E 01	6.8173E 01	5.0703E 01
280.0	3.2726E 01	7.0630E 01	8.1162E 01	9.4749E 01	1.0788E 02	1.1924E 02	7.6686E 01	7.6472E 01	5.6905E 01
300.0	3.6416E 01	7.8555E 01	9.0190E 01	1.0524E 02	1.1974E 02	1.3228E 02	8.5246E 01	8.5009E 01	6.3288E 01
320.0	4.0203E 01	8.6686E 01	9.9445E 01	1.1599E 02	1.3188E 02	1.4562E 02	9.4023E 01	9.3763E 01	6.9837E 01
340.0	4.4080E 01	9.5003E 01	1.0890E 02	1.2698E 02	1.4429E 02	1.5923E 02	1.0300E 02	1.0271E 02	7.6535E 01
360.0	4.8037E 01	1.0349E 02	1.1855E 02	1.3817E 02	1.5692E 02	1.7310E 02	1.1215E 02	1.1184E 02	8.3371E 01
380.0	5.2068E 01	1.1213E 02	1.2837E 02	1.4956E 02	1.6977E 02	1.8719E 02	1.2147E 02	1.2114E 02	9.0331E 01
400.0	5.6167E 01	1.2092E 02	1.3834E 02	1.6113E 02	1.8281E 02	2.0149E 02	1.3094E 02	1.3058E 02	9.7406E 01
420.0	6.0329E 01	1.2983E 02	1.4845E 02	1.7286E 02	1.9603E 02	2.1598E 02	1.4054E 02	1.4016E 02	1.0459E 02
440.0	6.4548E 01	1.3887E 02	1.5869E 02	1.8473E 02	2.0940E 02	2.3064E 02	1.5027E 02	1.4986E 02	1.1186E 02
460.0	6.8819E 01	1.4801E 02	1.6905E 02	1.9674E 02	2.2292E 02	2.4545E 02	1.6012E 02	1.5968E 02	1.1923E 02
480.0	7.3139E 01	1.5726E 02	1.7952E 02	2.0887E 02	2.3657E 02	2.6040E 02	1.7007E 02	1.6960E 02	1.2667E 02
500.0	7.7503E 01	1.6660E 02	1.9009E 02	2.2111E 02	2.5034E 02	2.7548E 02	1.8011E 02	1.7962E 02	1.3419E 02
520.0	8.1908E 01	1.7602E 02	2.0075E 02	2.3345E 02	2.6422E 02	2.9067E 02	1.9024E 02	1.8973E 02	1.4178E 02
540.0	8.6350E 01	1.8552E 02	2.1149E 02	2.4588E 02	2.7820E 02	3.0597E 02	2.0046E 02	1.9992E 02	1.4942E 02
560.0	9.0828E 01	1.9509E 02	2.2230E 02	2.5840E 02	2.9228E 02	3.2136E 02	2.1075E 02	2.1018E 02	1.5713E 02
580.0	9.5338E 01	2.0473E 02	2.3319E 02	2.7100E 02	3.0643E 02	3.3684E 02	2.2110E 02	2.2051E 02	1.6489E 02
600.0	9.9877E 01	2.1443E 02	2.4414E 02	2.8367E 02	3.2066E 02	3.5240E 02	2.3152E 02	2.3090E 02	1.7270E 02
620.0	1.0444E 02	2.2418E 02	2.5515E 02	2.9641E 02	3.3496E 02	3.6804E 02	2.4200E 02	2.4135E 02	1.8055E 02
640.0	1.0904E 02	2.3399E 02	2.6621E 02	3.0920E 02	3.4932E 02	3.8373E 02	2.5253E 02	2.5185E 02	1.8845E 02
660.0	1.1365E 02	2.4384E 02	2.7732E 02	3.2205E 02	3.6373E 02	3.9949E 02	2.6310E 02	2.6240E 02	1.9638E 02
680.0	1.1829E 02	2.5374E 02	2.8848E 02	3.3494E 02	3.7820E 02	4.1530E 02	2.7373E 02	2.7299E 02	2.0435E 02
700.0	1.2295E 02	2.6367E 02	2.9968E 02	3.4788E 02	3.9272E 02	4.3115E 02	2.8439E 02	2.8363E 02	2.1235E 02
720.0	1.2762E 02	2.7365E 02	3.1091E 02	3.6087E 02	4.0727E 02	4.4705E 02	2.9509E 02	2.9430E 02	2.2038E 02
740.0	1.3231E 02	2.8366E 02	3.2218E 02	3.7389E 02	4.2187E 02	4.6299E 02	3.0582E 02	3.0501E 02	2.2844E 02
760.0	1.3702E 02	2.9370E 02	3.3348E 02	3.8694E 02	4.3650E 02	4.7896E 02	3.1659E 02	3.1574E 02	2.3652E 02
780.0	1.4174E 02	3.0377E 02	3.4481E 02	4.0003E 02	4.5116E 02	4.9496E 02	3.2738E 02	3.2651E 02	2.4463E 02
800.0	1.4648E 02	3.1386E 02	3.5617E 02	4.1314E 02	4.6585E 02	5.1099E 02	3.3820E 02	3.3730E 02	2.5276E 02
820.0	1.5123E 02	3.2398E 02	3.6754E 02	4.2628E 02	4.8056E 02	5.2705E 02	3.4904E 02	3.4812E 02	2.6090E 02
840.0	1.5599E 02	3.3412E 02	3.7894E 02	4.3944E 02	4.9529E 02	5.4312E 02	3.5991E 02	3.5896E 02	2.6907E 02
860.0	1.6076E 02	3.4429E 02	3.9036E 02	4.5262E 02	5.1005E 02	5.5922E 02	3.7079E 02	3.6981E 02	2.7725E 02
880.0	1.6554E 02	3.5447E 02	4.0180E 02	4.6581E 02	5.2482E 02	5.7533E 02	3.8170E 02	3.8069E 02	2.8545E 02
900.0	1.7032E 02	3.6466E 02	4.1325E 02	4.7903E 02	5.3960E 02	5.9145E 02	3.9261E 02	3.9158E 02	2.9365E 02
920.0	1.7512E 02	3.7488E 02	4.2472E 02	4.9226E 02	5.5440E 02	6.0759E 02	4.0355E 02	4.0248E 02	3.0188E 02
940.0	1.7992E 02	3.8510E 02	4.3619E 02	5.0550E 02	5.6921E 02	6.2373E 02	4.1449E 02	4.1340E 02	3.1011E 02
960.0	1.8473E 02	3.9534E 02	4.4768E 02	5.1875E 02	5.8403E 02	6.3988E 02	4.2545E 02	4.2433E 02	3.1835E 02
980.0	1.8955E 02	4.0559E 02	4.5918E 02	5.3201E 02	5.9885E 02	6.5604E 02	4.3642E 02	4.3527E 02	3.2660E 02
1000.0	1.9437E 02	4.1586E 02	4.7069E 02	5.4527E 02	6.1368E 02	6.7220E 02	4.4740E 02	4.4622E 02	3.3486E 02
1200.0	2.4280E 02	5.1882E 02	5.8598E 02	6.7813E 02	7.6204E 02	8.3377E 02	5.5745E 02	5.5599E 02	4.1774E 02
1400.0	2.9137E 02	6.2195E 02	7.0120E 02	8.1076E 02	9.0993E 02	9.9464E 02	6.6753E 02	6.6580E 02	5.0074E 02
1600.0	3.3988E 02	7.2483E 02	8.1592E 02	9.4269E 02	1.0568E 03	1.1543E 03	7.7720E 02	7.7520E 02	5.8354E 02
2000.0	4.3631E 02	9.2903E 02	1.0431E 03	1.2036E 03	1.3469E 03	1.4692E 03	9.9458E 02	9.9205E 02	7.4786E 02
2400.0	5.3167E 02	1.1307E 03	1.2668E 03	1.4602E 03	1.6317E 03	1.7780E 03	1.2089E 03	1.2058E 03	9.1009E 02
2800.0	6.2588E 02	1.3296E 03	1.4870E 03	1.7126E 03	1.9113E 03	2.0809E 03	1.4200E 03	1.4164E 03	1.0701E 03
3200.0	7.1895E 02	1.5259E 03	1.7039E 03	1.9610E 03	2.1862E 03	2.3784E 03	1.6281E 03	1.6240E 03	1.2281E 03
3600.0	8.1095E 02	1.7197E 03	1.9178E 03	2.2057E 03	2.4568E 03	2.6710E 03	1.8334E 03	1.8289E 03	1.3840E 03
4000.0	9.0195E 02	1.9113E 03	2.1288E 03	2.4470E 03	2.7234E 03	2.9591E 03	2.0361E 03	2.0311E 03	1.5381E 03
5000.0	1.1255E 03	2.3814E 03	2.6458E 03	3.0375E 03	3.3749E 03	3.6626E 03	2.5330E 03	2.5268E 03	1.9163E 03

KAON RANGE, G/CM2

ENERGY MEV	WATER I= 65.1	AG-CL I=384.5	AG-BR I=434.1	NA-I I=433.0	LI-I I=472.5	POLYETHYLENE I= 54.6	STILBENE I= 65.2	LUCITE I= 65.6	ANTHRACENE I= 67.0
2.0	1.1094E-02	2.5504E-02	2.7500E-02	2.8094E-02	2.9809E-02	1.0325E-02	1.1567E-02	1.1438E-02	1.1763E-02
4.0	3.7901E-02	7.9536E-02	8.5026E-02	8.6878E-02	9.1596E-02	3.5469E-02	3.9514E-02	3.9067E-02	4.0148E-02
6.0	7.8886E-02	1.5611E-01	1.6611E-01	1.6986E-01	1.7858E-01	7.4139E-02	8.2262E-02	8.1312E-02	8.3528E-02
8.0	1.3271E-01	2.5358E-01	2.6901E-01	2.7536E-01	2.8899E-01	1.2503E-01	1.3839E-01	1.3678E-01	1.4046E-01
10.0	1.9875E-01	3.7090E-01	3.9260E-01	4.0220E-01	4.2157E-01	1.8754E-01	2.0725E-01	2.0483E-01	2.1031E-01
14.0	3.6565E-01	6.6126E-01	6.9784E-01	7.1550E-01	7.4853E-01	3.4573E-01	3.8127E-01	3.7679E-01	3.8676E-01
18.0	5.7662E-01	1.0213E 00	1.0756E 00	1.1031E 00	1.1524E 00	5.4589E-01	6.0121E-01	5.9415E-01	6.0974E-01
22.0	8.2938E-01	1.4469E 00	1.5216E 00	1.5605E 00	1.6283E 00	7.8589E-01	8.6472E-01	8.5454E-01	8.7686E-01
26.0	1.1221E 00	1.9346E 00	2.0321E 00	2.0839E 00	2.1725E 00	1.0640E 00	1.1698E 00	1.1560E 00	1.1861E 00
30.0	1.4530E 00	2.4817E 00	2.6044E 00	2.6705E 00	2.7819E 00	1.3785E 00	1.5148E 00	1.4970E 00	1.5358E 00
34.0	1.8208E 00	3.0856E 00	3.2359E 00	3.3174E 00	3.4536E 00	1.7282E 00	1.8982E 00	1.8758E 00	1.9243E 00
38.0	2.2241E 00	3.7443E 00	3.9242E 00	4.0225E 00	4.1853E 00	2.1118E 00	2.3186E 00	2.2912E 00	2.3503E 00
42.0	2.6616E 00	4.4558E 00	4.6673E 00	4.7835E 00	4.9748E 00	2.5282E 00	2.7747E 00	2.7420E 00	2.8126E 00
46.0	3.1324E 00	5.2180E 00	5.4632E 00	5.5986E 00	5.8200E 00	2.9762E 00	3.2655E 00	3.2269E 00	3.3099E 00
50.0	3.6353E 00	6.0295E 00	6.3102E 00	6.4658E 00	6.7190E 00	3.4550E 00	3.7897E 00	3.7449E 00	3.8411E 00
60.0	5.0269E 00	8.2631E 00	8.6405E 00	8.8513E 00	9.1909E 00	4.7801E 00	5.2403E 00	5.1782E 00	5.3108E 00
70.0	6.5994E 00	1.0772E 01	1.1257E 01	1.1529E 01	1.1964E 01	6.2781E 00	6.8795E 00	6.7980E 00	6.9716E 00
80.0	8.3406E 00	1.3536E 01	1.4138E 01	1.4477E 01	1.5017E 01	7.9373E 00	8.6945E 00	8.5914E 00	8.8104E 00
90.0	1.0239E 01	1.6539E 01	1.7266E 01	1.7678E 01	1.8329E 01	9.7472E 00	1.0674E 01	1.0547E 01	1.0816E 01
100.0	1.2286E 01	1.9764E 01	2.0626E 01	2.1115E 01	2.1886E 01	1.1698E 01	1.2807E 01	1.2655E 01	1.2977E 01
110.0	1.4471E 01	2.3197E 01	2.4201E 01	2.4773E 01	2.5669E 01	1.3782E 01	1.5085E 01	1.4905E 01	1.5284E 01
120.0	1.6786E 01	2.6826E 01	2.7979E 01	2.8637E 01	2.9666E 01	1.5991E 01	1.7498E 01	1.7290E 01	1.7729E 01
130.0	1.9225E 01	3.0638E 01	3.1947E 01	3.2696E 01	3.3863E 01	1.8316E 01	2.0040E 01	1.9801E 01	2.0303E 01
140.0	2.1778E 01	3.4623E 01	3.6094E 01	3.6937E 01	3.8248E 01	2.0753E 01	2.2702E 01	2.2432E 01	2.3000E 01
150.0	2.4441E 01	3.8769E 01	4.0409E 01	4.1351E 01	4.2811E 01	2.3294E 01	2.5477E 01	2.5174E 01	2.5811E 01
160.0	2.7207E 01	4.3069E 01	4.4882E 01	4.5926E 01	4.7541E 01	2.5934E 01	2.8361E 01	2.8023E 01	2.8732E 01
170.0	3.0071E 01	4.7514E 01	4.9505E 01	5.0655E 01	5.2429E 01	2.8667E 01	3.1346E 01	3.0972E 01	3.1755E 01
180.0	3.3027E 01	5.2095E 01	5.4270E 01	5.5528E 01	5.7464E 01	3.1488E 01	3.4427E 01	3.4016E 01	3.4875E 01
190.0	3.6070E 01	5.6804E 01	5.9168E 01	6.0537E 01	6.2640E 01	3.4393E 01	3.7599E 01	3.7151E 01	3.8088E 01
200.0	3.9196E 01	6.1635E 01	6.4192E 01	6.5675E 01	6.7949E 01	3.7378E 01	4.0857E 01	4.0370E 01	4.1388E 01
220.0	4.5679E 01	7.1638E 01	7.4591E 01	7.6310E 01	7.8935E 01	4.3568E 01	4.7615E 01	4.7047E 01	4.8233E 01
240.0	5.2446E 01	8.2054E 01	8.5419E 01	8.7383E 01	9.0373E 01	5.0031E 01	5.4668E 01	5.4016E 01	5.5376E 01
260.0	5.9469E 01	9.2843E 01	9.6632E 01	9.8849E 01	1.0221E 02	5.6739E 01	6.1989E 01	6.1249E 01	6.2790E 01
280.0	6.6726E 01	1.0397E 02	1.0819E 02	1.1067E 02	1.1442E 02	6.3669E 01	6.9550E 01	6.8720E 01	7.0448E 01
300.0	7.4196E 01	1.1539E 02	1.2006E 02	1.2281E 02	1.2696E 02	7.0801E 01	7.7331E 01	7.6408E 01	7.8327E 01
320.0	8.1856E 01	1.2709E 02	1.3223E 02	1.3524E 02	1.3979E 02	7.8115E 01	8.5310E 01	8.4291E 01	8.6408E 01
340.0	8.9689E 01	1.3904E 02	1.4466E 02	1.4793E 02	1.5290E 02	8.5602E 01	9.3475E 01	9.2354E 01	9.4675E 01
360.0	9.7681E 01	1.5122E 02	1.5732E 02	1.6086E 02	1.6624E 02	9.3250E 01	1.0181E 02	1.0060E 02	1.0311E 02
380.0	1.0582E 02	1.6359E 02	1.7019E 02	1.7400E 02	1.7980E 02	1.0104E 02	1.1030E 02	1.0902E 02	1.1171E 02
400.0	1.1409E 02	1.7616E 02	1.8324E 02	1.8734E 02	1.9357E 02	1.0897E 02	1.1894E 02	1.1759E 02	1.2045E 02
420.0	1.2249E 02	1.8889E 02	1.9646E 02	2.0086E 02	2.0752E 02	1.1702E 02	1.2770E 02	1.2628E 02	1.2932E 02
440.0	1.3099E 02	2.0177E 02	2.0984E 02	2.1454E 02	2.2163E 02	1.2518E 02	1.3659E 02	1.3510E 02	1.3832E 02
460.0	1.3961E 02	2.1479E 02	2.2337E 02	2.2836E 02	2.3589E 02	1.3345E 02	1.4559E 02	1.4402E 02	1.4743E 02
480.0	1.4832E 02	2.2794E 02	2.3702E 02	2.4232E 02	2.5029E 02	1.4181E 02	1.5469E 02	1.5305E 02	1.5665E 02
500.0	1.5712E 02	2.4121E 02	2.5079E 02	2.5639E 02	2.6482E 02	1.5026E 02	1.6389E 02	1.6217E 02	1.6596E 02
520.0	1.6600E 02	2.5458E 02	2.6467E 02	2.7058E 02	2.7945E 02	1.5880E 02	1.7317E 02	1.7137E 02	1.7536E 02
540.0	1.7495E 02	2.6804E 02	2.7865E 02	2.8487E 02	2.9419E 02	1.6741E 02	1.8254E 02	1.8066E 02	1.8484E 02
560.0	1.8397E 02	2.8160E 02	2.9271E 02	2.9925E 02	3.0903E 02	1.7609E 02	1.9198E 02	1.9002E 02	1.9440E 02
580.0	1.9306E 02	2.9523E 02	3.0686E 02	3.1372E 02	3.2394E 02	1.8484E 02	2.0149E 02	1.9945E 02	2.0403E 02
600.0	2.0220E 02	3.0894E 02	3.2109E 02	3.2826E 02	3.3894E 02	1.9365E 02	2.1107E 02	2.0895E 02	2.1372E 02
620.0	2.1140E 02	3.2271E 02	3.3538E 02	3.4287E 02	3.5401E 02	2.0251E 02	2.2070E 02	2.1850E 02	2.2348E 02
640.0	2.2065E 02	3.3654E 02	3.4974E 02	3.5754E 02	3.6914E 02	2.1143E 02	2.3039E 02	2.2811E 02	2.3329E 02
660.0	2.2995E 02	3.5043E 02	3.6415E 02	3.7227E 02	3.8433E 02	2.2040E 02	2.4013E 02	2.3777E 02	2.4315E 02
680.0	2.3929E 02	3.6436E 02	3.7861E 02	3.8705E 02	3.9957E 02	2.2941E 02	2.4992E 02	2.4748E 02	2.5307E 02
700.0	2.4867E 02	3.7834E 02	3.9312E 02	4.0187E 02	4.1486E 02	2.3846E 02	2.5976E 02	2.5723E 02	2.6302E 02
720.0	2.5808E 02	3.9237E 02	4.0768E 02	4.1674E 02	4.3020E 02	2.4755E 02	2.6964E 02	2.6702E 02	2.7302E 02
740.0	2.6753E 02	4.0642E 02	4.2227E 02	4.3165E 02	4.4559E 02	2.5668E 02	2.7955E 02	2.7685E 02	2.8306E 02
760.0	2.7702E 02	4.2052E 02	4.3690E 02	4.4659E 02	4.6101E 02	2.6585E 02	2.8950E 02	2.8671E 02	2.9313E 02
780.0	2.8653E 02	4.3464E 02	4.5155E 02	4.6156E 02	4.7646E 02	2.7504E 02	2.9948E 02	2.9661E 02	3.0324E 02
800.0	2.9607E 02	4.4879E 02	4.6624E 02	4.7656E 02	4.9195E 02	2.8426E 02	3.0950E 02	3.0654E 02	3.1338E 02
820.0	3.0564E 02	4.6296E 02	4.8096E 02	4.9158E 02	5.0746E 02	2.9352E 02	3.1954E 02	3.1649E 02	3.2355E 02
840.0	3.1523E 02	4.7716E 02	4.9569E 02	5.0663E 02	5.2300E 02	3.0279E 02	3.2961E 02	3.2647E 02	3.3375E 02
860.0	3.2485E 02	4.9138E 02	5.1045E 02	5.2169E 02	5.3856E 02	3.1209E 02	3.3970E 02	3.3648E 02	3.4397E 02
880.0	3.3448E 02	5.0562E 02	5.2523E 02	5.3677E 02	5.5414E 02	3.2142E 02	3.4982E 02	3.4651E 02	3.5421E 02
900.0	3.4413E 02	5.1988E 02	5.4002E 02	5.5187E 02	5.6974E 02	3.3076E 02	3.5996E 02	3.5656E 02	3.6447E 02
920.0	3.5380E 02	5.3414E 02	5.5482E 02	5.6698E 02	5.8536E 02	3.4012E 02	3.7012E 02	3.6663E 02	3.7476E 02
940.0	3.6349E 02	5.4843E 02	5.6964E 02	5.8211E 02	6.0099E 02	3.4950E 02	3.8029E 02	3.7671E 02	3.8506E 02
960.0	3.7319E 02	5.6272E 02	5.8447E 02	5.9724E 02	6.1663E 02	3.5890E 02	3.9049E 02	3.8682E 02	3.9538E 02
980.0	3.8291E 02	5.7702E 02	5.9931E 02	6.1239E 02	6.3228E 02	3.6831E 02	4.0070E 02	3.9694E 02	4.0572E 02
1000.0	3.9264E 02	5.9133E 02	6.1416E 02	6.2754E 02	6.4795E 02	3.7774E 02	4.1092E 02	4.0707E 02	4.1607E 02
1200.0	4.9044E 02	7.3461E 02	7.6281E 02	7.7927E 02	8.0480E 02	4.7259E 02	5.1375E 02	5.0898E 02	5.2019E 02
1400.0	5.8874E 02	8.7771E 02	9.1124E 02	9.3075E 02	9.6145E 02	5.6803E 02	6.1716E 02	6.1145E 02	6.2490E 02
1600.0	6.8714E 02	1.0202E 03	1.0590E 03	1.0815E 03	1.1174E 03	6.6366E 02	7.2071E 02	7.1404E 02	7.2974E 02
2000.0	8.8341E 02	1.3025E 03	1.3516E 03	1.3799E 03	1.4262E 03	8.5456E 02	9.2731E 02	9.1868E 02	9.3892E 02
2400.0	1.0784E 03	1.5809E 03	1.6401E 03	1.6739E 03	1.7304E 03	1.0443E 03	1.1326E 03	1.1219E 03	1.1467E 03
2800.0	1.2718E 03	1.8555E 03	1.9244E 03	1.9635E 03	2.0302E 03	1.2327E 03	1.3362E 03	1.3236E 03	1.3529E 03
3200.0	1.4637E 03	2.1265E 03	2.2050E 03	2.2491E 03	2.3258E 03	1.4196E 03	1.5382E 03	1.5235E 03	1.5574E 03
3600.0	1.6542E 03	2.3943E 03	2.4820E 03	2.5310E 03	2.6177E 03	1.6051E 03	1.7385E 03	1.7218E 03	1.7602E 03
4000.0	1.8432E 03	2.6591E 03	2.7559E 03	2.8095E 03	2.9060E 03	1.7892E 03	1.9374E 03	1.9186E 03	1.9616E 03
5000.0	2.3103E 03	3.3097E 03	3.4286E 03	3.4931E 03	3.6138E 03	2.2441E 03	2.4285E 03	2.4045E 03	2.4588E 03

PION STOPPING POWER, MEV•CM2/G

ENERGY MEV	BE I= 60.0	C I= 78.0	AL I=163.0	FE I=273.0	CU I=314.0	AG I=487.0	AU I=797.0	PB I=826.0	U I=923.0
2.0	2.9830E 01	3.2119E 01	2.6901E 01	2.3216E 01	2.1969E 01	1.8605E 01	1.4513E 01	1.4126E 01	1.3190E 01
4.0	1.6945E 01	1.8334E 01	1.5642E 01	1.3710E 01	1.3047E 01	1.1242E 01	8.9257E 00	8.6944E 00	8.1306E 00
6.0	1.2195E 01	1.3225E 01	1.1378E 01	1.0047E 01	9.5876E 00	8.3453E 00	6.7439E 00	6.5805E 00	6.1908E 00
8.0	9.6857E 00	1.0519E 01	9.0959E 00	8.0695E 00	7.7131E 00	6.7560E 00	5.5239E 00	5.3965E 00	5.0981E 00
10.0	8.1241E 00	8.8318E 00	7.6443E 00	6.8211E 00	6.5274E 00	5.7421E 00	4.7329E 00	4.6276E 00	4.3843E 00
14.0	6.2745E 00	6.8306E 00	5.9560E 00	5.3234E 00	5.1017E 00	4.5133E 00	3.7587E 00	3.6790E 00	3.4983E 00
18.0	5.2105E 00	5.6776E 00	4.9665E 00	4.4514E 00	4.2702E 00	3.7912E 00	3.1777E 00	3.1123E 00	2.9660E 00
22.0	4.5174E 00	4.9258E 00	4.3190E 00	3.8790E 00	3.7236E 00	3.3144E 00	2.7904E 00	2.7341E 00	2.6095E 00
26.0	4.0297E 00	4.3965E 00	3.8619E 00	3.4740E 00	3.3366E 00	2.9757E 00	2.5134E 00	2.4635E 00	2.3538E 00
30.0	3.6678E 00	4.0035E 00	3.5220E 00	3.1723E 00	3.0481E 00	2.7226E 00	2.3056E 00	2.2603E 00	2.1615E 00
34.0	3.3889E 00	3.7005E 00	3.2595E 00	2.9391E 00	2.8250E 00	2.5265E 00	2.1439E 00	2.1023E 00	2.0116E 00
38.0	3.1675E 00	3.4599E 00	3.0509E 00	2.7535E 00	2.6474E 00	2.3702E 00	2.0147E 00	1.9759E 00	1.8918E 00
42.0	2.9876E 00	3.2644E 00	2.8813E 00	2.6025E 00	2.5029E 00	2.2429E 00	1.9093E 00	1.8728E 00	1.7938E 00
46.0	2.8389E 00	3.1026E 00	2.7409E 00	2.4774E 00	2.3831E 00	2.1373E 00	1.8217E 00	1.7871E 00	1.7124E 00
50.0	2.7139E 00	2.9578E 00	2.6228E 00	2.3723E 00	2.2824E 00	2.0485E 00	1.7480E 00	1.7149E 00	1.6438E 00
60.0	2.4751E 00	2.6976E 00	2.3972E 00	2.1701E 00	2.0894E 00	1.8785E 00	1.6066E 00	1.5765E 00	1.5122E 00
70.0	2.3057E 00	2.5126E 00	2.2376E 00	2.0276E 00	1.9532E 00	1.7582E 00	1.5065E 00	1.4785E 00	1.4190E 00
80.0	2.1796E 00	2.3753E 00	2.1131E 00	1.9220E 00	1.8526E 00	1.6695E 00	1.4326E 00	1.4062E 00	1.3501E 00
90.0	2.0827E 00	2.2702E 00	2.0237E 00	1.8392E 00	1.7760E 00	1.6020E 00	1.3765E 00	1.3512E 00	1.2979E 00
100.0	2.0065E 00	2.1876E 00	1.9536E 00	1.7763E 00	1.7162E 00	1.5496E 00	1.3329E 00	1.3086E 00	1.2573E 00
110.0	1.9453E 00	2.1214E 00	1.8976E 00	1.7261E 00	1.6688E 00	1.5080E 00	1.2984E 00	1.2749E 00	1.2252E 00
120.0	1.8954E 00	2.0676E 00	1.8522E 00	1.6854E 00	1.6308E 00	1.4747E 00	1.2709E 00	1.2479E 00	1.1996E 00
130.0	1.8542E 00	2.0233E 00	1.8149E 00	1.6521E 00	1.5940E 00	1.4468E 00	1.2486E 00	1.2261E 00	1.1778E 00
140.0	1.8199E 00	1.9865E 00	1.7840E 00	1.6245E 00	1.5679E 00	1.4249E 00	1.2305E 00	1.2084E 00	1.1610E 00
150.0	1.7910E 00	1.9555E 00	1.7582E 00	1.6015E 00	1.5463E 00	1.4066E 00	1.2144E 00	1.1939E 00	1.1472E 00
160.0	1.7664E 00	1.9294E 00	1.7364E 00	1.5822E 00	1.5281E 00	1.3912E 00	1.2019E 00	1.1819E 00	1.1358E 00
170.0	1.7455E 00	1.9071E 00	1.7181E 00	1.5659E 00	1.5128E 00	1.3783E 00	1.1915E 00	1.1722E 00	1.1263E 00
180.0	1.7275E 00	1.8881E 00	1.7025E 00	1.5521E 00	1.4999E 00	1.3675E 00	1.1824E 00	1.1641E 00	1.1182E 00
190.0	1.7120E 00	1.8717E 00	1.6891E 00	1.5404E 00	1.4890E 00	1.3584E 00	1.1753E 00	1.1575E 00	1.1118E 00
200.0	1.6986E 00	1.8577E 00	1.6778E 00	1.5304E 00	1.4797E 00	1.3507E 00	1.1694E 00	1.1522E 00	1.1065E 00
220.0	1.6768E 00	1.8350E 00	1.6597E 00	1.5147E 00	1.4652E 00	1.3390E 00	1.1605E 00	1.1444E 00	1.0986E 00
240.0	1.6603E 00	1.8180E 00	1.6465E 00	1.5033E 00	1.4547E 00	1.3309E 00	1.1547E 00	1.1356E 00	1.0936E 00
260.0	1.6476E 00	1.8052E 00	1.6369E 00	1.4951E 00	1.4474E 00	1.3254E 00	1.1510E 00	1.1329E 00	1.0906E 00
280.0	1.6379E 00	1.7956E 00	1.6301E 00	1.4894E 00	1.4423E 00	1.3220E 00	1.1490E 00	1.1316E 00	1.0891E 00
300.0	1.6306E 00	1.7886E 00	1.6253E 00	1.4856E 00	1.4391E 00	1.3201E 00	1.1483E 00	1.1316E 00	1.0888E 00
320.0	1.6250E 00	1.7834E 00	1.6222E 00	1.4833E 00	1.4372E 00	1.3194E 00	1.1485E 00	1.1325E 00	1.0894E 00
340.0	1.6209E 00	1.7798E 00	1.6203E 00	1.4821E 00	1.4364E 00	1.3196E 00	1.1495E 00	1.1340E 00	1.0907E 00
360.0	1.6180E 00	1.7775E 00	1.6195E 00	1.4818E 00	1.4364E 00	1.3205E 00	1.1511E 00	1.1361E 00	1.0926E 00
380.0	1.6159E 00	1.7761E 00	1.6195E 00	1.4822E 00	1.4372E 00	1.3221E 00	1.1531E 00	1.1387E 00	1.0948E 00
400.0	1.6147E 00	1.7759E 00	1.6202E 00	1.4832E 00	1.4384E 00	1.3241E 00	1.1555E 00	1.1415E 00	1.0974E 00
420.0	1.6140E 00	1.7756E 00	1.6213E 00	1.4847E 00	1.4402E 00	1.3264E 00	1.1582E 00	1.1446E 00	1.1003E 00
440.0	1.6139E 00	1.7762E 00	1.6229E 00	1.4866E 00	1.4422E 00	1.3290E 00	1.1611E 00	1.1479E 00	1.1033E 00
460.0	1.6141E 00	1.7772E 00	1.6249E 00	1.4887E 00	1.4445E 00	1.3319E 00	1.1642E 00	1.1514E 00	1.1065E 00
480.0	1.6147E 00	1.7786E 00	1.6271E 00	1.4911E 00	1.4471E 00	1.3349E 00	1.1674E 00	1.1549E 00	1.1097E 00
500.0	1.6156E 00	1.7803E 00	1.6296E 00	1.4937E 00	1.4498E 00	1.3380E 00	1.1707E 00	1.1586E 00	1.1131E 00
520.0	1.6168E 00	1.7822E 00	1.6322E 00	1.4965E 00	1.4527E 00	1.3413E 00	1.1740E 00	1.1623E 00	1.1165E 00
540.0	1.6181E 00	1.7844E 00	1.6350E 00	1.4993E 00	1.4557E 00	1.3446E 00	1.1775E 00	1.1660E 00	1.1200E 00
560.0	1.6196E 00	1.7867E 00	1.6379E 00	1.5023E 00	1.4587E 00	1.3480E 00	1.1809E 00	1.1697E 00	1.1235E 00
580.0	1.6212E 00	1.7891E 00	1.6409E 00	1.5053E 00	1.4618E 00	1.3515E 00	1.1844E 00	1.1735E 00	1.1270E 00
600.0	1.6230E 00	1.7916E 00	1.6439E 00	1.5084E 00	1.4650E 00	1.3549E 00	1.1878E 00	1.1772E 00	1.1305E 00
620.0	1.6248E 00	1.7942E 00	1.6470E 00	1.5115E 00	1.4682E 00	1.3584E 00	1.1913E 00	1.1809E 00	1.1340E 00
640.0	1.6267E 00	1.7969E 00	1.6502E 00	1.5147E 00	1.4714E 00	1.3619E 00	1.1948E 00	1.1846E 00	1.1375E 00
660.0	1.6287E 00	1.7996E 00	1.6534E 00	1.5179E 00	1.4747E 00	1.3653E 00	1.1982E 00	1.1883E 00	1.1409E 00
680.0	1.6307E 00	1.8024E 00	1.6566E 00	1.5211E 00	1.4779E 00	1.3688E 00	1.2016E 00	1.1920E 00	1.1444E 00
700.0	1.6328E 00	1.8052E 00	1.6598E 00	1.5242E 00	1.4811E 00	1.3722E 00	1.2050E 00	1.1956E 00	1.1478E 00
720.0	1.6349E 00	1.8080E 00	1.6630E 00	1.5274E 00	1.4844E 00	1.3756E 00	1.2084E 00	1.1992E 00	1.1512E 00
740.0	1.6370E 00	1.8109E 00	1.6662E 00	1.5306E 00	1.4876E 00	1.3790E 00	1.2117E 00	1.2027E 00	1.1545E 00
760.0	1.6392E 00	1.8137E 00	1.6693E 00	1.5337E 00	1.4908E 00	1.3824E 00	1.2150E 00	1.2062E 00	1.1578E 00
780.0	1.6413E 00	1.8166E 00	1.6725E 00	1.5369E 00	1.4939E 00	1.3857E 00	1.2183E 00	1.2097E 00	1.1611E 00
800.0	1.6435E 00	1.8194E 00	1.6757E 00	1.5400E 00	1.4971E 00	1.3890E 00	1.2215E 00	1.2131E 00	1.1643E 00
820.0	1.6456E 00	1.8222E 00	1.6788E 00	1.5431E 00	1.5002E 00	1.3923E 00	1.2247E 00	1.2165E 00	1.1675E 00
840.0	1.6478E 00	1.8251E 00	1.6819E 00	1.5461E 00	1.5033E 00	1.3955E 00	1.2278E 00	1.2198E 00	1.1706E 00
860.0	1.6499E 00	1.8279E 00	1.6850E 00	1.5492E 00	1.5063E 00	1.3987E 00	1.2309E 00	1.2231E 00	1.1737E 00
880.0	1.6521E 00	1.8307E 00	1.6881E 00	1.5522E 00	1.5094E 00	1.4019E 00	1.2340E 00	1.2263E 00	1.1768E 00
900.0	1.6542E 00	1.8335E 00	1.6911E 00	1.5552E 00	1.5124E 00	1.4050E 00	1.2370E 00	1.2295E 00	1.1798E 00
920.0	1.6564E 00	1.8362E 00	1.6941E 00	1.5581E 00	1.5153E 00	1.4081E 00	1.2400E 00	1.2327E 00	1.1828E 00
940.0	1.6585E 00	1.8389E 00	1.6971E 00	1.5610E 00	1.5182E 00	1.4112E 00	1.2430E 00	1.2358E 00	1.1858E 00
960.0	1.6606E 00	1.8417E 00	1.7000E 00	1.5639E 00	1.5211E 00	1.4142E 00	1.2459E 00	1.2389E 00	1.1887E 00
980.0	1.6627E 00	1.8444E 00	1.7029E 00	1.5668E 00	1.5240E 00	1.4171E 00	1.2488E 00	1.2419E 00	1.1915E 00
1000.0	1.6647E 00	1.8470E 00	1.7058E 00	1.5696E 00	1.5268E 00	1.4201E 00	1.2516E 00	1.2449E 00	1.1944E 00
1200.0	1.6845E 00	1.8722E 00	1.7329E 00	1.5961E 00	1.5533E 00	1.4474E 00	1.2781E 00	1.2727E 00	1.2207E 00
1400.0	1.7024E 00	1.8949E 00	1.7570E 00	1.6196E 00	1.5768E 00	1.4716E 00	1.3013E 00	1.2970E 00	1.2438E 00
1600.0	1.7184E 00	1.9152E 00	1.7785E 00	1.6406E 00	1.5977E 00	1.4930E 00	1.3219E 00	1.3186E 00	1.2643E 00
2000.0	1.7467E 00	1.9501E 00	1.8154E 00	1.6764E 00	1.6334E 00	1.5295E 00	1.3569E 00	1.3552E 00	1.2991E 00
2400.0	1.7702E 00	1.9791E 00	1.8460E 00	1.7062E 00	1.6630E 00	1.5596E 00	1.3858E 00	1.3853E 00	1.3278E 00
2800.0	1.7904E 00	2.0038E 00	1.8719E 00	1.7315E 00	1.6880E 00	1.5851E 00	1.4103E 00	1.4107E 00	1.3522E 00
3200.0	1.8079E 00	2.0251E 00	1.8945E 00	1.7534E 00	1.7097E 00	1.6072E 00	1.4314E 00	1.4327E 00	1.3732E 00
3600.0	1.8235E 00	2.0440E 00	1.9143E 00	1.7726E 00	1.7288E 00	1.6266E 00	1.4500E 00	1.4520E 00	1.3916E 00
4000.0	1.8375E 00	2.0607E 00	1.9320E 00	1.7898E 00	1.7459E 00	1.6438E 00	1.4665E 00	1.4692E 00	1.4081E 00
5000.0	1.8671E 00	2.0960E 00	1.9692E 00	1.8260E 00	1.7816E 00	1.6800E 00	1.5012E 00	1.5051E 00	1.4425E 00

PION STOPPING POWER, MEV•CM2/G

ENERGY MEV	H I= 18.7	HE I= 42.0	NE I=131.0	A I=210.0	KR I=381.0	XE I=555.0	AIR I= 86.8	CARB.DIOXIDE I= 85.9	METHANE I= 44.1
2.0	7.9557E 01	3.5537E 01	2.8910E 01	2.3839E 01	1.9665E 01	1.6873E 01	3.1503E 01	3.1619E 01	4.4041E 01
4.0	4.4396E 01	2.0075E 01	1.6710E 01	1.3964E 01	1.1766E 01	1.0250E 01	1.8018E 01	1.8079E 01	2.4884E 01
6.0	3.1682E 01	1.4408E 01	1.2121E 01	1.0193E 01	8.6809E 00	7.6377E 00	1.3009E 01	1.3051E 01	1.7863E 01
8.0	2.5031E 01	1.1424E 01	9.6746E 00	8.1662E 00	7.0009E 00	6.1984E 00	1.0354E 01	1.0386E 01	1.4166E 01
10.0	2.0917E 01	9.5701E 00	8.1425E 00	6.8911E 00	5.9347E 00	5.2770E 00	8.6971E 00	8.7236E 00	1.1869E 01
14.0	1.6071E 01	7.3786E 00	6.3178E 00	5.3657E 00	4.6488E 00	4.1568E 00	6.7304E 00	6.7504E 00	9.1530E 00
18.0	1.3299E 01	6.1202E 00	5.2627E 00	4.4801E 00	3.8967E 00	3.4966E 00	5.5966E 00	5.6129E 00	7.5930E 00
22.0	1.1500E 01	5.3014E 00	4.5732E 00	3.8997E 00	3.4014E 00	3.0597E 00	4.8570E 00	4.8710E 00	6.5780E 00
26.0	1.0237E 01	4.7258E 00	4.0868E 00	3.4896E 00	3.0502E 00	2.7490E 00	4.3360E 00	4.3485E 00	5.8642E 00
30.0	9.3015E 00	4.2990E 00	3.7253E 00	3.1844E 00	2.7883E 00	2.5166E 00	3.9493E 00	3.9605E 00	5.3350E 00
34.0	8.5815E 00	3.9701E 00	3.4463E 00	2.9486E 00	2.5855E 00	2.3364E 00	3.6509E 00	3.6612E 00	4.9272E 00
38.0	8.0107E 00	3.7092E 00	3.2246E 00	2.7610E 00	2.4240E 00	2.1927E 00	3.4140E 00	3.4236E 00	4.6036E 00
42.0	7.5474E 00	3.4973E 00	3.0444E 00	2.6085E 00	2.2925E 00	2.0756E 00	3.2215E 00	3.2305E 00	4.3408E 00
46.0	7.1644E 00	3.3220E 00	2.8952E 00	2.4822E 00	2.1836E 00	1.9785E 00	3.0623E 00	3.0708E 00	4.1234E 00
50.0	6.8427E 00	3.1748E 00	2.7699E 00	2.3761E 00	2.0919E 00	1.8967E 00	2.9284E 00	2.9365E 00	3.9409E 00
60.0	6.2284E 00	2.8936E 00	2.5303E 00	2.1731E 00	1.9167E 00	1.7403E 00	2.6727E 00	2.6800E 00	3.5921E 00
70.0	5.7938E 00	2.6946E 00	2.3608E 00	2.0295E 00	1.7926E 00	1.6295E 00	2.4918E 00	2.4986E 00	3.3453E 00
80.0	5.4725E 00	2.5476E 00	2.2357E 00	1.9235E 00	1.7011E 00	1.5479E 00	2.3582E 00	2.3646E 00	3.1630E 00
90.0	5.2271E 00	2.4354E 00	2.1403E 00	1.8428E 00	1.6316E 00	1.4858E 00	2.2564E 00	2.2624E 00	3.0239E 00
100.0	5.0350E 00	2.3477E 00	2.0659E 00	1.7800E 00	1.5774E 00	1.4375E 00	2.1768E 00	2.1827E 00	2.9151E 00
110.0	4.8817E 00	2.2778E 00	2.0068E 00	1.7300E 00	1.5345E 00	1.3993E 00	2.1135E 00	2.1192E 00	2.8284E 00
120.0	4.7575E 00	2.2212E 00	1.9591E 00	1.6898E 00	1.5000E 00	1.3687E 00	2.0624E 00	2.0679E 00	2.7583E 00
130.0	4.6555E 00	2.1749E 00	1.9202E 00	1.6571E 00	1.4720E 00	1.3438E 00	2.0206E 00	2.0260E 00	2.7009E 00
140.0	4.5709E 00	2.1366E 00	1.8881E 00	1.6301E 00	1.4491E 00	1.3236E 00	1.9862E 00	1.9914E 00	2.6534E 00
150.0	4.5002E 00	2.1046E 00	1.8615E 00	1.6079E 00	1.4302E 00	1.3069E 00	1.9575E 00	1.9626E 00	2.6138E 00
160.0	4.4407E 00	2.0778E 00	1.8393E 00	1.5894E 00	1.4145E 00	1.2932E 00	1.9335E 00	1.9386E 00	2.5805E 00
170.0	4.3903E 00	2.0552E 00	1.8207E 00	1.5739E 00	1.4016E 00	1.2818E 00	1.9134E 00	1.9184E 00	2.5525E 00
180.0	4.3475E 00	2.0360E 00	1.8051E 00	1.5609E 00	1.3908E 00	1.2725E 00	1.8964E 00	1.9013E 00	2.5288E 00
190.0	4.3109E 00	2.0197E 00	1.7919E 00	1.5501E 00	1.3818E 00	1.2647E 00	1.8821E 00	1.8869E 00	2.5086E 00
200.0	4.2796E 00	2.0059E 00	1.7808E 00	1.5410E 00	1.3743E 00	1.2583E 00	1.8699E 00	1.8748E 00	2.4915E 00
220.0	4.2299E 00	1.9840E 00	1.7636E 00	1.5271E 00	1.3631E 00	1.2488E 00	1.8510E 00	1.8558E 00	2.4645E 00
240.0	4.1933E 00	1.9682E 00	1.7516E 00	1.5175E 00	1.3557E 00	1.2427E 00	1.8376E 00	1.8423E 00	2.4450E 00
260.0	4.1666E 00	1.9569E 00	1.7434E 00	1.5112E 00	1.3511E 00	1.2392E 00	1.8282E 00	1.8329E 00	2.4310E 00
280.0	4.1474E 00	1.9491E 00	1.7381E 00	1.5074E 00	1.3485E 00	1.2375E 00	1.8220E 00	1.8266E 00	2.4213E 00
300.0	4.1339E 00	1.9438E 00	1.7351E 00	1.5054E 00	1.3476E 00	1.2372E 00	1.8181E 00	1.8227E 00	2.4149E 00
320.0	4.1250E 00	1.9406E 00	1.7338E 00	1.5049E 00	1.3480E 00	1.2380E 00	1.8161E 00	1.8207E 00	2.4110E 00
340.0	4.1197E 00	1.9391E 00	1.7338E 00	1.5055E 00	1.3493E 00	1.2397E 00	1.8155E 00	1.8201E 00	2.4092E 00
360.0	4.1172E 00	1.9388E 00	1.7349E 00	1.5070E 00	1.3513E 00	1.2421E 00	1.8161E 00	1.8207E 00	2.4089E 00
380.0	4.1170E 00	1.9396E 00	1.7368E 00	1.5092E 00	1.3540E 00	1.2449E 00	1.8177E 00	1.8222E 00	2.4099E 00
400.0	4.1186E 00	1.9411E 00	1.7394E 00	1.5120E 00	1.3571E 00	1.2482E 00	1.8199E 00	1.8244E 00	2.4119E 00
420.0	4.1217E 00	1.9434E 00	1.7426E 00	1.5152E 00	1.3606E 00	1.2518E 00	1.8227E 00	1.8273E 00	2.4148E 00
440.0	4.1261E 00	1.9461E 00	1.7461E 00	1.5188E 00	1.3644E 00	1.2557E 00	1.8260E 00	1.8306E 00	2.4183E 00
460.0	4.1314E 00	1.9494E 00	1.7501E 00	1.5226E 00	1.3684E 00	1.2597E 00	1.8297E 00	1.8343E 00	2.4223E 00
480.0	4.1376E 00	1.9529E 00	1.7543E 00	1.5267E 00	1.3726E 00	1.2639E 00	1.8337E 00	1.8383E 00	2.4268E 00
500.0	4.1444E 00	1.9568E 00	1.7587E 00	1.5310E 00	1.3769E 00	1.2682E 00	1.8380E 00	1.8425E 00	2.4317E 00
520.0	4.1517E 00	1.9609E 00	1.7633E 00	1.5353E 00	1.3813E 00	1.2726E 00	1.8424E 00	1.8469E 00	2.4368E 00
540.0	4.1595E 00	1.9652E 00	1.7680E 00	1.5398E 00	1.3859E 00	1.2771E 00	1.8470E 00	1.8515E 00	2.4421E 00
560.0	4.1676E 00	1.9696E 00	1.7729E 00	1.5444E 00	1.3904E 00	1.2816E 00	1.8517E 00	1.8562E 00	2.4477E 00
580.0	4.1761E 00	1.9741E 00	1.7778E 00	1.5490E 00	1.3950E 00	1.2861E 00	1.8565E 00	1.8610E 00	2.4534E 00
600.0	4.1847E 00	1.9787E 00	1.7827E 00	1.5537E 00	1.3996E 00	1.2906E 00	1.8614E 00	1.8659E 00	2.4592E 00
620.0	4.1936E 00	1.9834E 00	1.7877E 00	1.5584E 00	1.4042E 00	1.2951E 00	1.8663E 00	1.8708E 00	2.4650E 00
640.0	4.2025E 00	1.9882E 00	1.7928E 00	1.5630E 00	1.4088E 00	1.2996E 00	1.8712E 00	1.8758E 00	2.4710E 00
660.0	4.2116E 00	1.9930E 00	1.7978E 00	1.5677E 00	1.4134E 00	1.3041E 00	1.8762E 00	1.8807E 00	2.4770E 00
680.0	4.2208E 00	1.9978E 00	1.8028E 00	1.5724E 00	1.4180E 00	1.3086E 00	1.8812E 00	1.8857E 00	2.4830E 00
700.0	4.2300E 00	2.0026E 00	1.8079E 00	1.5771E 00	1.4226E 00	1.3130E 00	1.8861E 00	1.8907E 00	2.4890E 00
720.0	4.2392E 00	2.0074E 00	1.8129E 00	1.5817E 00	1.4271E 00	1.3174E 00	1.8911E 00	1.8956E 00	2.4950E 00
740.0	4.2484E 00	2.0122E 00	1.8178E 00	1.5863E 00	1.4316E 00	1.3218E 00	1.8960E 00	1.9006E 00	2.5010E 00
760.0	4.2576E 00	2.0170E 00	1.8228E 00	1.5909E 00	1.4361E 00	1.3261E 00	1.9009E 00	1.9055E 00	2.5070E 00
780.0	4.2669E 00	2.0218E 00	1.8277E 00	1.5955E 00	1.4405E 00	1.3304E 00	1.9058E 00	1.9104E 00	2.5130E 00
800.0	4.2760E 00	2.0265E 00	1.8326E 00	1.6000E 00	1.4449E 00	1.3346E 00	1.9107E 00	1.9153E 00	2.5189E 00
820.0	4.2852E 00	2.0312E 00	1.8375E 00	1.6044E 00	1.4492E 00	1.3388E 00	1.9155E 00	1.9201E 00	2.5248E 00
840.0	4.2943E 00	2.0359E 00	1.8423E 00	1.6089E 00	1.4535E 00	1.3430E 00	1.9203E 00	1.9249E 00	2.5307E 00
860.0	4.3033E 00	2.0406E 00	1.8470E 00	1.6133E 00	1.4578E 00	1.3471E 00	1.9250E 00	1.9296E 00	2.5365E 00
880.0	4.3123E 00	2.0452E 00	1.8518E 00	1.6176E 00	1.4620E 00	1.3512E 00	1.9298E 00	1.9344E 00	2.5423E 00
900.0	4.3212E 00	2.0498E 00	1.8564E 00	1.6219E 00	1.4661E 00	1.3552E 00	1.9344E 00	1.9390E 00	2.5480E 00
920.0	4.3301E 00	2.0544E 00	1.8611E 00	1.6262E 00	1.4702E 00	1.3592E 00	1.9390E 00	1.9437E 00	2.5537E 00
940.0	4.3389E 00	2.0589E 00	1.8656E 00	1.6304E 00	1.4743E 00	1.3631E 00	1.9436E 00	1.9482E 00	2.5593E 00
960.0	4.3476E 00	2.0633E 00	1.8702E 00	1.6346E 00	1.4783E 00	1.3670E 00	1.9482E 00	1.9528E 00	2.5649E 00
980.0	4.3562E 00	2.0678E 00	1.8747E 00	1.6387E 00	1.4823E 00	1.3708E 00	1.9526E 00	1.9573E 00	2.5704E 00
1000.0	4.3648E 00	2.0721E 00	1.8791E 00	1.6428E 00	1.4862E 00	1.3746E 00	1.9571E 00	1.9617E 00	2.5759E 00
1200.0	4.4462E 00	2.1136E 00	1.9210E 00	1.6811E 00	1.5232E 00	1.4102E 00	1.9990E 00	2.0037E 00	2.6277E 00
1400.0	4.5199E 00	2.1511E 00	1.9586E 00	1.7155E 00	1.5562E 00	1.4419E 00	2.0367E 00	2.0415E 00	2.6744E 00
1600.0	4.5867E 00	2.1850E 00	1.9925E 00	1.7465E 00	1.5858E 00	1.4703E 00	2.0708E 00	2.0756E 00	2.7167E 00
2000.0	4.7033E 00	2.2440E 00	2.0514E 00	1.8002E 00	1.6372E 00	1.5196E 00	2.1300E 00	2.1348E 00	2.7904E 00
2400.0	4.8023E 00	2.2940E 00	2.1012E 00	1.8456E 00	1.6805E 00	1.5612E 00	2.1801E 00	2.1850E 00	2.8527E 00
2800.0	4.8879E 00	2.3372E 00	2.1442E 00	1.8847E 00	1.7179E 00	1.5970E 00	2.2233E 00	2.2283E 00	2.9067E 00
3200.0	4.9633E 00	2.3752E 00	2.1820E 00	1.9191E 00	1.7508E 00	1.6285E 00	2.2614E 00	2.2664E 00	2.9541E 00
3600.0	5.0306E 00	2.4092E 00	2.2157E 00	1.9498E 00	1.7801E 00	1.6566E 00	2.2953E 00	2.3004E 00	2.9965E 00
4000.0	5.0913E 00	2.4398E 00	2.2461E 00	1.9775E 00	1.8065E 00	1.6819E 00	2.3259E 00	2.3311E 00	3.0347E 00
5000.0	5.2213E 00	2.5053E 00	2.3112E 00	2.0367E 00	1.8629E 00	1.7359E 00	2.3914E 00	2.3967E 00	3.1155E 00

PION STOPPING POWER, MEV•CM2/G

ENERGY MEV	WATER I= 65.1	AG-CL I=384.5	AG-BR I=434.1	NA-I I=433.0	LI-I I=472.5	POLYETHYLENE I= 54.6	STILBENE I= 65.2	LUCITE I= 65.6	ANTHRACENE I= 67.0
2.0	3.6816E 01	2.0345E 01	1.9274E 01	1.8796E 01	1.7961E 01	3.8934E 01	3.5303E 01	3.5724E 01	3.4802E 01
4.0	2.0938E 01	1.2171E 01	1.1590E 01	1.1294E 01	1.0832E 01	2.2079E 01	2.0083E 01	2.0323E 01	1.9808E 01
6.0	1.5078E 01	8.9865E 00	8.5786E 00	8.3655E 00	8.0414E 00	1.5876E 01	1.4463E 01	1.4636E 01	1.4268E 01
8.0	1.1981E 01	7.2514E 00	6.9322E 00	6.7642E 00	6.5112E 00	1.2604E 01	1.1493E 01	1.1630E 01	1.1339E 01
10.0	1.0052E 01	6.1494E 00	5.8845E 00	5.7444E 00	5.5349E 00	1.0568E 01	9.6429E 00	9.7584E 00	9.5152E 00
14.0	7.7667E 00	4.8194E 00	4.6177E 00	4.5103E 00	4.3512E 00	8.1583E 00	7.4507E 00	7.5402E 00	7.3531E 00
18.0	6.4515E 00	4.0409E 00	3.8750E 00	3.7861E 00	3.6553E 00	6.7726E 00	6.1891E 00	6.2635E 00	6.1086E 00
22.0	5.5945E 00	3.5280E 00	3.3852E 00	3.3082E 00	3.1957E 00	5.8704E 00	5.3670E 00	5.4316E 00	5.2976E 00
26.0	4.9913E 00	3.1642E 00	3.0375E 00	2.9689E 00	2.8692E 00	5.2356E 00	4.7884E 00	4.8461E 00	4.7267E 00
30.0	4.5438E 00	2.8928E 00	2.7780E 00	2.7155E 00	2.6252E 00	4.7647E 00	4.3591E 00	4.4116E 00	4.3031E 00
34.0	4.1987E 00	2.6826E 00	2.5770E 00	2.5192E 00	2.4360E 00	4.4018E 00	4.0280E 00	4.0766E 00	3.9765E 00
38.0	3.9248E 00	2.5152E 00	2.4168E 00	2.3628E 00	2.2853E 00	4.1137E 00	3.7653E 00	3.8107E 00	3.7172E 00
42.0	3.7023E 00	2.3790E 00	2.2864E 00	2.2354E 00	2.1625E 00	3.8798E 00	3.5518E 00	3.5947E 00	3.5066E 00
46.0	3.5182E 00	2.2660E 00	2.1783E 00	2.1298E 00	2.0601E 00	3.6862E 00	3.3752E 00	3.4160E 00	3.3323E 00
50.0	3.3636E 00	2.1710E 00	2.0873E 00	2.0410E 00	1.9751E 00	3.5237E 00	3.2269E 00	3.2659E 00	3.1859E 00
60.0	3.0681E 00	1.9892E 00	1.9133E 00	1.8709E 00	1.8111E 00	3.2130E 00	2.9434E 00	2.9790E 00	2.9062E 00
70.0	2.8591E 00	1.8606E 00	1.7902E 00	1.7506E 00	1.6951E 00	2.9933E 00	2.7429E 00	2.7761E 00	2.7084E 00
80.0	2.7025E 00	1.7658E 00	1.6994E 00	1.6618E 00	1.6091E 00	2.8310E 00	2.5948E 00	2.6262E 00	2.5622E 00
90.0	2.5856E 00	1.6936E 00	1.6275E 00	1.5943E 00	1.5443E 00	2.7071E 00	2.4817E 00	2.5119E 00	2.4505E 00
100.0	2.4934E 00	1.6374E 00	1.5748E 00	1.5418E 00	1.4937E 00	2.6053E 00	2.3905E 00	2.4102E 00	2.3613E 00
110.0	2.4192E 00	1.5929E 00	1.5329E 00	1.5002E 00	1.4537E 00	2.5247E 00	2.3177E 00	2.3369E 00	2.2894E 00
120.0	2.3587E 00	1.5571E 00	1.4992E 00	1.4666E 00	1.4215E 00	2.4590E 00	2.2584E 00	2.2772E 00	2.2308E 00
130.0	2.3086E 00	1.5281E 00	1.4717E 00	1.4397E 00	1.3954E 00	2.4049E 00	2.2096E 00	2.2281E 00	2.1825E 00
140.0	2.2673E 00	1.5043E 00	1.4492E 00	1.4175E 00	1.3741E 00	2.3597E 00	2.1689E 00	2.1871E 00	2.1423E 00
150.0	2.2331E 00	1.4848E 00	1.4305E 00	1.3993E 00	1.3565E 00	2.3217E 00	2.1347E 00	2.1527E 00	2.1085E 00
160.0	2.2041E 00	1.4685E 00	1.4150E 00	1.3842E 00	1.3420E 00	2.2895E 00	2.1057E 00	2.1236E 00	2.0798E 00
170.0	2.1795E 00	1.4551E 00	1.4021E 00	1.3717E 00	1.3300E 00	2.2621E 00	2.0810E 00	2.0988E 00	2.0554E 00
180.0	2.1584E 00	1.4439E 00	1.3911E 00	1.3613E 00	1.3200E 00	2.2385E 00	2.0599E 00	2.0775E 00	2.0345E 00
190.0	2.1403E 00	1.4346E 00	1.3822E 00	1.3527E 00	1.3115E 00	2.2182E 00	2.0417E 00	2.0593E 00	2.0166E 00
200.0	2.1247E 00	1.4269E 00	1.3747E 00	1.3455E 00	1.3042E 00	2.2006E 00	2.0260E 00	2.0436E 00	2.0011E 00
220.0	2.0996E 00	1.4149E 00	1.3632E 00	1.3348E 00	1.2930E 00	2.1722E 00	2.0007E 00	2.0181E 00	1.9760E 00
240.0	2.0806E 00	1.4066E 00	1.3553E 00	1.3277E 00	1.2853E 00	2.1506E 00	1.9815E 00	1.9990E 00	1.9571E 00
260.0	2.0664E 00	1.4010E 00	1.3502E 00	1.3229E 00	1.2801E 00	2.1341E 00	1.9670E 00	1.9845E 00	1.9428E 00
280.0	2.0556E 00	1.3976E 00	1.3471E 00	1.3198E 00	1.2769E 00	2.1216E 00	1.9561E 00	1.9736E 00	1.9319E 00
300.0	2.0477E 00	1.3959E 00	1.3455E 00	1.3182E 00	1.2752E 00	2.1121E 00	1.9479E 00	1.9654E 00	1.9238E 00
320.0	2.0419E 00	1.3954E 00	1.3450E 00	1.3178E 00	1.2746E 00	2.1050E 00	1.9418E 00	1.9594E 00	1.9178E 00
340.0	2.0377E 00	1.3959E 00	1.3454E 00	1.3183E 00	1.2750E 00	2.0998E 00	1.9375E 00	1.9552E 00	1.9135E 00
360.0	2.0350E 00	1.3970E 00	1.3466E 00	1.3195E 00	1.2760E 00	2.0961E 00	1.9345E 00	1.9523E 00	1.9106E 00
380.0	2.0333E 00	1.3986E 00	1.3483E 00	1.3213E 00	1.2776E 00	2.0936E 00	1.9326E 00	1.9504E 00	1.9087E 00
400.0	2.0325E 00	1.4007E 00	1.3505E 00	1.3236E 00	1.2797E 00	2.0921E 00	1.9316E 00	1.9495E 00	1.9077E 00
420.0	2.0324E 00	1.4031E 00	1.3530E 00	1.3262E 00	1.2821E 00	2.0914E 00	1.9313E 00	1.9493E 00	1.9074E 00
440.0	2.0329E 00	1.4058E 00	1.3558E 00	1.3290E 00	1.2848E 00	2.0914E 00	1.9316E 00	1.9497E 00	1.9077E 00
460.0	2.0338E 00	1.4088E 00	1.3588E 00	1.3321E 00	1.2876E 00	2.0919E 00	1.9323E 00	1.9506E 00	1.9085E 00
480.0	2.0352E 00	1.4119E 00	1.3620E 00	1.3354E 00	1.2907E 00	2.0929E 00	1.9335E 00	1.9519E 00	1.9096E 00
500.0	2.0369E 00	1.4152E 00	1.3653E 00	1.3388E 00	1.2939E 00	2.0942E 00	1.9350E 00	1.9535E 00	1.9111E 00
520.0	2.0388E 00	1.4186E 00	1.3687E 00	1.3422E 00	1.2972E 00	2.0959E 00	1.9368E 00	1.9554E 00	1.9129E 00
540.0	2.0410E 00	1.4221E 00	1.3722E 00	1.3458E 00	1.3006E 00	2.0978E 00	1.9388E 00	1.9575E 00	1.9149E 00
560.0	2.0433E 00	1.4256E 00	1.3757E 00	1.3494E 00	1.3040E 00	2.0999E 00	1.9410E 00	1.9598E 00	1.9171E 00
580.0	2.0458E 00	1.4292E 00	1.3793E 00	1.3530E 00	1.3074E 00	2.1022E 00	1.9434E 00	1.9623E 00	1.9194E 00
600.0	2.0484E 00	1.4327E 00	1.3829E 00	1.3567E 00	1.3109E 00	2.1047E 00	1.9459E 00	1.9649E 00	1.9218E 00
620.0	2.0511E 00	1.4363E 00	1.3864E 00	1.3604E 00	1.3144E 00	2.1073E 00	1.9484E 00	1.9675E 00	1.9244E 00
640.0	2.0539E 00	1.4399E 00	1.3900E 00	1.3640E 00	1.3179E 00	2.1099E 00	1.9511E 00	1.9703E 00	1.9270E 00
660.0	2.0568E 00	1.4435E 00	1.3936E 00	1.3677E 00	1.3214E 00	2.1127E 00	1.9538E 00	1.9731E 00	1.9297E 00
680.0	2.0596E 00	1.4471E 00	1.3972E 00	1.3713E 00	1.3249E 00	2.1155E 00	1.9566E 00	1.9760E 00	1.9324E 00
700.0	2.0626E 00	1.4506E 00	1.4007E 00	1.3749E 00	1.3284E 00	2.1184E 00	1.9594E 00	1.9789E 00	1.9352E 00
720.0	2.0655E 00	1.4542E 00	1.4042E 00	1.3785E 00	1.3318E 00	2.1213E 00	1.9622E 00	1.9818E 00	1.9380E 00
740.0	2.0685E 00	1.4577E 00	1.4077E 00	1.3821E 00	1.3352E 00	2.1242E 00	1.9651E 00	1.9848E 00	1.9409E 00
760.0	2.0714E 00	1.4612E 00	1.4112E 00	1.3856E 00	1.3386E 00	2.1272E 00	1.9680E 00	1.9878E 00	1.9437E 00
780.0	2.0744E 00	1.4646E 00	1.4146E 00	1.3891E 00	1.3420E 00	2.1301E 00	1.9708E 00	1.9907E 00	1.9466E 00
800.0	2.0773E 00	1.4680E 00	1.4180E 00	1.3926E 00	1.3453E 00	2.1331E 00	1.9737E 00	1.9937E 00	1.9494E 00
820.0	2.0803E 00	1.4714E 00	1.4213E 00	1.3960E 00	1.3486E 00	2.1361E 00	1.9766E 00	1.9967E 00	1.9522E 00
840.0	2.0833E 00	1.4747E 00	1.4246E 00	1.3994E 00	1.3518E 00	2.1390E 00	1.9795E 00	1.9996E 00	1.9551E 00
860.0	2.0862E 00	1.4780E 00	1.4279E 00	1.4028E 00	1.3550E 00	2.1420E 00	1.9823E 00	2.0026E 00	1.9579E 00
880.0	2.0891E 00	1.4813E 00	1.4311E 00	1.4061E 00	1.3582E 00	2.1449E 00	1.9852E 00	2.0055E 00	1.9607E 00
900.0	2.0920E 00	1.4845E 00	1.4343E 00	1.4094E 00	1.3614E 00	2.1479E 00	1.9880E 00	2.0084E 00	1.9635E 00
920.0	2.0949E 00	1.4876E 00	1.4375E 00	1.4126E 00	1.3645E 00	2.1508E 00	1.9908E 00	2.0113E 00	1.9663E 00
940.0	2.0977E 00	1.4908E 00	1.4406E 00	1.4158E 00	1.3675E 00	2.1537E 00	1.9936E 00	2.0142E 00	1.9691E 00
960.0	2.1005E 00	1.4939E 00	1.4437E 00	1.4189E 00	1.3706E 00	2.1566E 00	1.9964E 00	2.0170E 00	1.9718E 00
980.0	2.1033E 00	1.4969E 00	1.4467E 00	1.4221E 00	1.3736E 00	2.1594E 00	1.9991E 00	2.0199E 00	1.9745E 00
1000.0	2.1061E 00	1.5000E 00	1.4497E 00	1.4251E 00	1.3765E 00	2.1623E 00	2.0019E 00	2.0227E 00	1.9772E 00
1200.0	2.1324E 00	1.5281E 00	1.4776E 00	1.4538E 00	1.4041E 00	2.1893E 00	2.0277E 00	2.0492E 00	2.0028E 00
1400.0	2.1560E 00	1.5528E 00	1.5022E 00	1.4791E 00	1.4285E 00	2.2138E 00	2.0510E 00	2.0732E 00	2.0259E 00
1600.0	2.1771E 00	1.5748E 00	1.5240E 00	1.5015E 00	1.4502E 00	2.2359E 00	2.0720E 00	2.0947E 00	2.0466E 00
2000.0	2.2133E 00	1.6121E 00	1.5609E 00	1.5397E 00	1.4872E 00	2.2739E 00	2.1080E 00	2.1316E 00	2.0823E 00
2400.0	2.2435E 00	1.6428E 00	1.5914E 00	1.5713E 00	1.5178E 00	2.3058E 00	2.1381E 00	2.1624E 00	2.1121E 00
2800.0	2.2692E 00	1.6688E 00	1.6172E 00	1.5981E 00	1.5437E 00	2.3329E 00	2.1637E 00	2.1886E 00	2.1374E 00
3200.0	2.2916E 00	1.6913E 00	1.6395E 00	1.6212E 00	1.5662E 00	2.3565E 00	2.1859E 00	2.2113E 00	2.1594E 00
3600.0	2.3113E 00	1.7110E 00	1.6591E 00	1.6415E 00	1.5859E 00	2.3774E 00	2.2055E 00	2.2313E 00	2.1788E 00
4000.0	2.3289E 00	1.7285E 00	1.6765E 00	1.6596E 00	1.6035E 00	2.3960E 00	2.2230E 00	2.2492E 00	2.1962E 00
5000.0	2.3662E 00	1.7653E 00	1.7130E 00	1.6975E 00	1.6404E 00	2.4353E 00	2.2599E 00	2.2868E 00	2.2327E 00

PION RANGE, G/CM2

ENERGY MEV	BE I= 60.0	C I= 78.0	AL I=163.0	FE I=273.0	CU I=314.0	AG I=487.0	AU I=797.0	PB I=826.0	U I=923.0
2.0	3.6998E-02	3.4620E-02	4.2452E-02	5.0351E-02	5.3531E-02	6.4399E-02	8.3502E-02	8.5787E-02	9.1751E-02
4.0	1.3006E-01	1.2079E-01	1.4416E-01	1.6708E-01	1.7646E-01	2.0809E-01	2.6623E-01	2.7350E-01	2.9292E-01
6.0	2.7142E-01	2.5126E-01	2.9635E-01	3.3997E-01	3.5786E-01	4.1739E-01	5.2727E-01	5.4124E-01	5.7828E-01
8.0	4.5692E-01	4.2219E-01	4.9446E-01	5.6374E-01	5.9214E-01	6.8562E-01	8.5706E-01	8.7899E-01	9.3648E-01
10.0	6.8347E-01	6.3068E-01	7.3510E-01	8.3452E-01	8.7526E-01	1.0081E 00	1.2498E 00	1.2808E 00	1.3611E 00
14.0	1.2498E 00	1.1512E 00	1.3333E 00	1.5051E 00	1.5754E 00	1.8015E 00	2.2067E 00	2.2589E 00	2.3914E 00
18.0	1.9535E 00	1.7973E 00	2.0730E 00	2.3314E 00	2.4372E 00	2.7737E 00	3.3700E 00	3.4470E 00	3.6393E 00
22.0	2.7810E 00	2.5565E 00	2.9398E 00	3.2974E 00	3.4438E 00	3.9060E 00	4.7176E 00	4.8227E 00	5.0817E 00
26.0	3.7209E 00	3.4182E 00	3.9216E 00	4.3897E 00	4.5813E 00	5.1826E 00	6.2314E 00	6.3673E 00	6.6991E 00
30.0	4.7632E 00	4.3733E 00	5.0081E 00	5.5967E 00	5.8378E 00	6.5903E 00	7.8957E 00	8.0651E 00	8.4753E 00
34.0	5.8993E 00	5.4139E 00	6.1902E 00	6.9084E 00	7.2026E 00	8.1174E 00	9.6970E 00	9.9023E 00	1.0396E 01
38.0	7.1215E 00	6.5330E 00	7.4599E 00	8.3159E 00	8.6667E 00	9.7536E 00	1.1623E 01	1.1867E 01	1.2448E 01
42.0	8.4228E 00	7.7242E 00	8.8101E 00	9.8113E 00	1.0222E 01	1.1490E 01	1.3664E 01	1.3948E 01	1.4621E 01
46.0	9.7972E 00	8.9819E 00	1.0234E 01	1.1388E 01	1.1861E 01	1.3318E 01	1.5811E 01	1.6136E 01	1.6905E 01
50.0	1.1239E 01	1.0303E 01	1.1727E 01	1.3038E 01	1.3577E 01	1.5231E 01	1.8053E 01	1.8422E 01	1.9290E 01
60.0	1.5107E 01	1.3853E 01	1.5725E 01	1.7456E 01	1.8167E 01	2.0340E 01	2.4034E 01	2.4517E 01	2.5647E 01
70.0	1.9300E 01	1.7701E 01	2.0050E 01	2.2232E 01	2.3125E 01	2.5852E 01	3.0472E 01	3.1077E 01	3.2484E 01
80.0	2.3766E 01	2.1799E 01	2.4654E 01	2.7303E 01	2.8388E 01	3.1695E 01	3.7287E 01	3.8020E 01	3.9717E 01
90.0	2.8464E 01	2.6109E 01	2.9494E 01	3.2626E 01	3.3906E 01	3.7815E 01	4.4414E 01	4.5281E 01	4.7277E 01
100.0	3.3359E 01	3.0599E 01	3.4527E 01	3.8162E 01	3.9637E 01	4.4166E 01	5.1801E 01	5.2806E 01	5.5110E 01
110.0	3.8423E 01	3.5243E 01	3.9723E 01	4.3876E 01	4.5549E 01	5.0711E 01	5.9406E 01	6.0552E 01	6.3171E 01
120.0	4.3633E 01	4.0020E 01	4.5059E 01	4.9741E 01	5.1612E 01	5.7419E 01	6.7193E 01	6.8483E 01	7.1423E 01
130.0	4.8969E 01	4.4911E 01	5.0515E 01	5.5736E 01	5.7817E 01	6.4267E 01	7.5134E 01	7.6570E 01	7.9838E 01
140.0	5.4414E 01	4.9900E 01	5.6074E 01	6.1842E 01	6.4145E 01	7.1234E 01	8.3204E 01	8.4787E 01	8.8392E 01
150.0	5.9954E 01	5.4975E 01	6.1721E 01	6.8043E 01	7.0568E 01	7.8299E 01	9.1386E 01	9.3114E 01	9.7059E 01
160.0	6.5577E 01	6.0124E 01	6.7446E 01	7.4326E 01	7.7075E 01	8.5448E 01	9.9665E 01	1.0153E 02	1.0582E 02
170.0	7.1273E 01	6.5338E 01	7.3236E 01	8.0680E 01	8.3653E 01	9.2671E 01	1.0802E 02	1.1003E 02	1.1466E 02
180.0	7.7032E 01	7.0609E 01	7.9084E 01	8.7096E 01	9.0292E 01	9.9956E 01	1.1645E 02	1.1859E 02	1.2357E 02
190.0	8.2848E 01	7.5929E 01	8.4981E 01	9.3564E 01	9.6984E 01	1.0729E 02	1.2493E 02	1.2721E 02	1.3254E 02
200.0	8.8713E 01	8.1292E 01	9.0922E 01	1.0008E 02	1.0372E 02	1.1468E 02	1.3346E 02	1.3587E 02	1.4156E 02
220.0	1.0057E 02	9.2128E 01	1.0291E 02	1.1322E 02	1.1731E 02	1.2955E 02	1.5063E 02	1.5329E 02	1.5971E 02
240.0	1.1256E 02	1.0308E 02	1.1501E 02	1.2647E 02	1.3101E 02	1.4454E 02	1.6791E 02	1.7084E 02	1.7796E 02
260.0	1.2465E 02	1.1412E 02	1.2720E 02	1.3982E 02	1.4480E 02	1.5960E 02	1.8527E 02	1.8848E 02	1.9627E 02
280.0	1.3683E 02	1.2523E 02	1.3944E 02	1.5322E 02	1.5864E 02	1.7471E 02	2.0266E 02	2.0614E 02	2.1462E 02
300.0	1.4907E 02	1.3639E 02	1.5173E 02	1.6667E 02	1.7252E 02	1.8985E 02	2.2007E 02	2.2382E 02	2.3299E 02
320.0	1.6135E 02	1.4759E 02	1.6405E 02	1.8014E 02	1.8643E 02	2.0501E 02	2.3749E 02	2.4149E 02	2.5136E 02
340.0	1.7368E 02	1.5882E 02	1.7638E 02	1.9363E 02	2.0035E 02	2.2017E 02	2.5490E 02	2.5913E 02	2.6970E 02
360.0	1.8603E 02	1.7006E 02	1.8873E 02	2.0713E 02	2.1428E 02	2.3532E 02	2.7228E 02	2.7675E 02	2.8802E 02
380.0	1.9840E 02	1.8132E 02	2.0108E 02	2.2062E 02	2.2820E 02	2.5045E 02	2.8964E 02	2.9434E 02	3.0631E 02
400.0	2.1078E 02	1.9258E 02	2.1343E 02	2.3411E 02	2.4211E 02	2.6557E 02	3.0697E 02	3.1188E 02	3.2456E 02
420.0	2.2317E 02	2.0385E 02	2.2577E 02	2.4759E 02	2.5600E 02	2.8066E 02	3.2426E 02	3.2938E 02	3.4276E 02
440.0	2.3556E 02	2.1511E 02	2.3810E 02	2.6105E 02	2.6988E 02	2.9573E 02	3.4150E 02	3.4683E 02	3.6091E 02
460.0	2.4795E 02	2.2637E 02	2.5041E 02	2.7450E 02	2.8374E 02	3.1076E 02	3.5871E 02	3.6422E 02	3.7901E 02
480.0	2.6034E 02	2.3762E 02	2.6271E 02	2.8792E 02	2.9757E 02	3.2576E 02	3.7586E 02	3.8157E 02	3.9706E 02
500.0	2.7272E 02	2.4886E 02	2.7500E 02	3.0132E 02	3.1138E 02	3.4072E 02	3.9297E 02	3.9886E 02	4.1506E 02
520.0	2.8510E 02	2.6008E 02	2.8726E 02	3.1470E 02	3.2516E 02	3.5565E 02	4.1003E 02	4.1609E 02	4.3300E 02
540.0	2.9746E 02	2.7130E 02	2.9950E 02	3.2805E 02	3.3891E 02	3.7055E 02	4.2704E 02	4.3327E 02	4.5088E 02
560.0	3.0982E 02	2.8250E 02	3.1172E 02	3.4138E 02	3.5264E 02	3.8540E 02	4.4400E 02	4.5040E 02	4.6871E 02
580.0	3.2216E 02	2.9369E 02	3.2392E 02	3.5468E 02	3.6633E 02	4.0022E 02	4.6091E 02	4.6747E 02	4.8649E 02
600.0	3.3449E 02	3.0486E 02	3.3610E 02	3.6795E 02	3.8000E 02	4.1500E 02	4.7777E 02	4.8449E 02	5.0420E 02
620.0	3.4681E 02	3.1601E 02	3.4826E 02	3.8119E 02	3.9364E 02	4.2974E 02	4.9459E 02	5.0145E 02	5.2187E 02
640.0	3.5911E 02	3.2715E 02	3.6039E 02	3.9441E 02	4.0724E 02	4.4445E 02	5.1135E 02	5.1836E 02	5.3948E 02
660.0	3.7140E 02	3.3827E 02	3.7250E 02	4.0760E 02	4.2082E 02	4.5911E 02	5.2807E 02	5.3521E 02	5.5703E 02
680.0	3.8367E 02	3.4938E 02	3.8458E 02	4.2076E 02	4.3437E 02	4.7374E 02	5.4473E 02	5.5202E 02	5.7454E 02
700.0	3.9592E 02	3.6047E 02	3.9664E 02	4.3390E 02	4.4789E 02	4.8834E 02	5.6136E 02	5.6877E 02	5.9199E 02
720.0	4.0817E 02	3.7154E 02	4.0868E 02	4.4701E 02	4.6138E 02	5.0289E 02	5.7793E 02	5.8548E 02	6.0939E 02
740.0	4.2039E 02	3.8259E 02	4.2070E 02	4.6009E 02	4.7483E 02	5.1741E 02	5.9446E 02	6.0213E 02	6.2673E 02
760.0	4.3260E 02	3.9363E 02	4.3269E 02	4.7314E 02	4.8826E 02	5.3190E 02	6.1094E 02	6.1873E 02	6.4403E 02
780.0	4.4479E 02	4.0464E 02	4.4466E 02	4.8617E 02	5.0167E 02	5.4635F 02	6.2738E 02	6.3529E 02	6.6128E 02
800.0	4.5697E 02	4.1564E 02	4.5660E 02	4.9917E 02	5.1504E 02	5.6076E 02	6.4378E 02	6.5180E 02	6.7849E 02
820.0	4.6913E 02	4.2663E 02	4.6853E 02	5.1214E 02	5.2839E 02	5.7515F 02	6.6013E 02	6.6827E 02	6.9564E 02
840.0	4.8128E 02	4.3760E 02	4.8043E 02	5.2509E 02	5.4170E 02	5.8949E 02	6.7644E 02	6.8468E 02	7.1275E 02
860.0	4.9341E 02	4.4855E 02	4.9231E 02	5.3801E 02	5.5499E 02	6.0381F 02	6.9271E 02	7.0106E 02	7.2981E 02
880.0	5.0552E 02	4.5948E 02	5.0417E 02	5.5091E 02	5.6826E 02	6.1809E 02	7.0893E 02	7.1739E 02	7.4683E 02
900.0	5.1762E 02	4.7040E 02	5.1601E 02	5.6378E 02	5.8150E 02	6.3234E 02	7.2512E 02	7.3368E 02	7.6380E 02
920.0	5.2970E 02	4.8130E 02	5.2782E 02	5.7663E 02	5.9471E 02	6.4656E 02	7.4127E 02	7.4992E 02	7.8073E 02
940.0	5.4177E 02	4.9218E 02	5.3962E 02	5.8945E 02	6.0789E 02	6.6075E 02	7.5738E 02	7.6612E 02	7.9762E 02
960.0	5.5382E 02	5.0305E 02	5.5139E 02	6.0225E 02	6.2105E 02	6.7491E 02	7.7345E 02	7.8229E 02	8.1446E 02
980.0	5.6586E 02	5.1390E 02	5.6315E 02	6.1503E 02	6.3419E 02	6.8903E 02	7.8948E 02	7.9841E 02	8.3127E 02
1000.0	5.7788E 02	5.2474E 02	5.7488E 02	6.2778E 02	6.4730E 02	7.0313E 02	8.0548E 02	8.1450E 02	8.4803E 02
1200.0	6.9730E 02	6.3227E 02	6.9119E 02	7.5412E 02	7.7714E 02	8.4260E 02	9.6357E 02	9.7334E 02	1.0136E 03
1400.0	8.1539E 02	7.3844E 02	8.0579E 02	8.7850E 02	9.0492E 02	9.7961E 02	1.1186E 03	1.1290E 03	1.1759E 03
1600.0	9.3230E 02	8.4342E 02	9.1892E 02	1.0012E 03	1.0309E 03	1.1145E 03	1.2711E 03	1.2819E 03	1.3354E 03
2000.0	1.1631E 03	1.0503E 03	1.1415E 03	1.2423E 03	1.2784E 03	1.3791E 03	1.5696E 03	1.5810E 03	1.6473E 03
2400.0	1.3905E 03	1.2539E 03	1.3599E 03	1.4787E 03	1.5211E 03	1.6380E 03	1.8612E 03	1.8728E 03	1.9518E 03
2800.0	1.6152E 03	1.4547E 03	1.5750E 03	1.7114E 03	1.7597E 03	1.8924E 03	2.1473E 03	2.1589E 03	2.2502E 03
3200.0	1.8375E 03	1.6533E 03	1.7874E 03	1.9409E 03	1.9952E 03	2.1429E 03	2.4288E 03	2.4402E 03	2.5437E 03
3600.0	2.0578E 03	1.8499E 03	1.9974E 03	2.1678E 03	2.2278E 03	2.3903E 03	2.7064E 03	2.7175E 03	2.8330E 03
4000.0	2.2763E 03	2.0447E 03	2.2054E 03	2.3924E 03	2.4580E 03	2.6349E 03	2.9806E 03	2.9913E 03	3.1187E 03
5000.0	2.8160E 03	2.5258E 03	2.7179E 03	2.9453E 03	3.0248E 03	3.2364E 03	3.6543E 03	3.6634E 03	3.8201E 03

PION RANGE, G/CM2

ENERGY MEV	H I= 18.7	HE I= 42.0	NE I=131.0	A I=210.0	KR I=381.0	XE I=555.0	AIR I= 86.8	CARB.DIOXIDE I= 85.9	METHANE I= 44.1
2.0	1.3643E-02	3.0802E-02	3.9155E-02	4.8437E-02	6.0319E-02	7.1334E-02	3.5421E-02	3.5280E-02	2.4881E-02
4.0	4.8928E-02	1.0919E-01	1.3414E-01	1.6268E-01	1.9704E-01	2.2932E-01	1.2317E-01	1.2273E-01	8.8130E-02
6.0	1.0314E-01	2.2869E-01	2.7683E-01	3.3281E-01	3.9773E-01	4.5840E-01	2.5586E-01	2.5498E-01	1.8452E-01
8.0	1.7475E-01	3.8585E-01	4.6295E-01	5.5369E-01	6.5613E-01	7.5108E-01	4.2955E-01	4.2813E-01	3.1127E-01
10.0	2.6259E-01	5.7806E-01	6.8934E-01	8.2152E-01	9.6777E-01	1.1023E 00	6.4131E-01	6.3924E-01	4.6626E-01
14.0	4.8318E-01	1.0593E 00	1.2529E 00	1.4861E 00	1.7369E 00	1.9645E 00	1.1697E 00	1.1661E 00	8.5421E-01
18.0	7.5845E-01	1.6581E 00	1.9506E 00	2.3066E 00	2.6819E 00	3.0193E 00	1.8253E 00	1.8197E 00	1.3369E 00
22.0	1.0831E 00	2.3629E 00	2.7689E 00	3.2670E 00	3.7844E 00	4.2464E 00	2.5953E 00	2.5875E 00	1.9050E 00
26.0	1.4527E 00	3.1641E 00	3.6965E 00	4.3539E 00	5.0292E 00	5.6288E 00	3.4691E 00	3.4588E 00	2.5507E 00
30.0	1.8634E 00	4.0531E 00	4.7234E 00	5.5559E 00	6.4031E 00	7.1521E 00	4.4375E 00	4.4244E 00	3.2671E 00
34.0	2.3118E 00	5.0227E 00	5.8413E 00	6.8630E 00	7.8948E 00	8.8037E 00	5.4923E 00	5.4762E 00	4.0483E 00
38.0	2.7947E 00	6.0661E 00	7.0424E 00	8.2663E 00	9.4942E 00	1.0573E 01	6.6264E 00	6.6072E 00	4.8891E 00
42.0	3.3096E 00	7.1776E 00	8.3201E 00	9.7580E 00	1.1192E 01	1.2449E 01	7.8336E 00	7.8110E 00	5.7846E 00
46.0	3.8539E 00	8.3520E 00	9.6683E 00	1.1331E 01	1.2981E 01	1.4424E 01	9.1079E 00	9.0818E 00	6.7307E 00
50.0	4.4255E 00	9.5843E 00	1.1082E 01	1.2979E 01	1.4854E 01	1.6490E 01	1.0444E 01	1.0415E 01	7.7235E 00
60.0	5.9612E 00	1.2892E 01	1.4868E 01	1.7390E 01	1.9860E 01	2.2007E 01	1.4028E 01	1.3988E 01	1.0388E 01
70.0	7.6287E 00	1.6479E 01	1.8966E 01	2.2160E 01	2.5263E 01	2.7955E 01	1.7909E 01	1.7859E 01	1.3278E 01
80.0	9.4068E 00	2.0300E 01	2.3324E 01	2.7227E 01	3.0996E 01	3.4258E 01	2.2039E 01	2.1978E 01	1.6356E 01
90.0	1.1278E 01	2.4319E 01	2.7900E 01	3.2543E 01	3.7004E 01	4.0858E 01	2.6378E 01	2.6305E 01	1.9592E 01
100.0	1.3229E 01	2.8503E 01	3.2658E 01	3.8068E 01	4.3241E 01	4.7705E 01	3.0893E 01	3.0808E 01	2.2962E 01
110.0	1.5247E 01	3.2830E 01	3.7572E 01	4.3769E 01	4.9672E 01	5.4759E 01	3.5558E 01	3.5460E 01	2.6447E 01
120.0	1.7323E 01	3.7278E 01	4.2617E 01	4.9620E 01	5.6266E 01	6.1988E 01	4.0349E 01	4.0239E 01	3.0028E 01
130.0	1.9448E 01	4.1829E 01	4.7775E 01	5.5598E 01	6.2998E 01	6.9364E 01	4.5249E 01	4.5126E 01	3.3693E 01
140.0	2.1617E 01	4.6469E 01	5.3028E 01	6.1684E 01	6.9846E 01	7.6863E 01	5.0242E 01	5.0106E 01	3.7430E 01
150.0	2.3822E 01	5.1186E 01	5.8363E 01	6.7862E 01	7.6794E 01	8.4468E 01	5.5315E 01	5.5165E 01	4.1228E 01
160.0	2.6059E 01	5.5969E 01	6.3768E 01	7.4119E 01	8.3826E 01	9.2162E 01	6.0456E 01	6.0293E 01	4.5079E 01
170.0	2.8324E 01	6.0808E 01	6.9234E 01	8.0442E 01	9.0929E 01	9.9930E 01	6.5656E 01	6.5479E 01	4.8976E 01
180.0	3.0614E 01	6.5698E 01	7.4750E 01	8.6823E 01	9.8092E 01	1.0776E 02	7.0906E 01	7.0716E 01	5.2912E 01
190.0	3.2924E 01	7.0630E 01	8.0311E 01	9.3252E 01	1.0531E 02	1.1564E 02	7.6200E 01	7.5996E 01	5.6883E 01
200.0	3.5252E 01	7.5598E 01	8.5910E 01	9.9723E 01	1.1256E 02	1.2357E 02	8.1531E 01	8.1313E 01	6.0883E 01
220.0	3.9954E 01	8.5627E 01	9.7198E 01	1.1276E 02	1.2718E 02	1.3953E 02	9.2284E 01	9.2039E 01	6.8957E 01
240.0	4.4704E 01	9.5750E 01	1.0858E 02	1.2590E 02	1.4190E 02	1.5559E 02	1.0313E 02	1.0286E 02	7.7106E 01
260.0	4.9490E 01	1.0594E 02	1.2003E 02	1.3911E 02	1.5668E 02	1.7171E 02	1.1404E 02	1.1374E 02	8.5311E 01
280.0	5.4301E 01	1.1618E 02	1.3152E 02	1.5237E 02	1.7149E 02	1.8786E 02	1.2500E 02	1.2468E 02	9.3556E 01
300.0	5.9132E 01	1.2646E 02	1.4303E 02	1.6564E 02	1.8633E 02	2.0402E 02	1.3599E 02	1.3564E 02	1.0183E 02
320.0	6.3976E 01	1.3676E 02	1.5457E 02	1.7893E 02	2.0117E 02	2.2019E 02	1.4700E 02	1.4662E 02	1.1012E 02
340.0	6.8828E 01	1.4707E 02	1.6610E 02	1.9222E 02	2.1600E 02	2.3633E 02	1.5802E 02	1.5760E 02	1.1842E 02
360.0	7.3684E 01	1.5738E 02	1.7764E 02	2.0550E 02	2.3081E 02	2.5245E 02	1.6903E 02	1.6859E 02	1.2672E 02
380.0	7.8542E 01	1.6770E 02	1.8916E 02	2.1876E 02	2.4560E 02	2.6853E 02	1.8004E 02	1.7957E 02	1.3502E 02
400.0	8.3399E 01	1.7801E 02	2.0066E 02	2.3200E 02	2.6036E 02	2.8458E 02	1.9104E 02	1.9054E 02	1.4331E 02
420.0	8.8254E 01	1.8830E 02	2.1215E 02	2.4522E 02	2.7507E 02	3.0058E 02	2.0202E 02	2.0150E 02	1.5160E 02
440.0	9.3103E 01	1.9859E 02	2.2362E 02	2.5840E 02	2.8975E 02	3.1653E 02	2.1298E 02	2.1243E 02	1.5988E 02
460.0	9.7948E 01	2.0886E 02	2.3506E 02	2.7155E 02	3.0439E 02	3.3243E 02	2.2392E 02	2.2335E 02	1.6814E 02
480.0	1.0279E 02	2.1911E 02	2.4647E 02	2.8467E 02	3.1898E 02	3.4828E 02	2.3484E 02	2.3424E 02	1.7639E 02
500.0	1.0761E 02	2.2934E 02	2.5786E 02	2.9775E 02	3.3353E 02	3.6408E 02	2.4573E 02	2.4511E 02	1.8462E 02
520.0	1.1244E 02	2.3955E 02	2.6922E 02	3.1080E 02	3.4803E 02	3.7982E 02	2.5660E 02	2.5595E 02	1.9284E 02
540.0	1.1725E 02	2.4974E 02	2.8054E 02	3.2380E 02	3.6249E 02	3.9551E 02	2.6745E 02	2.6676E 02	2.0104E 02
560.0	1.2205E 02	2.5990E 02	2.9184E 02	3.3677E 02	3.7690E 02	4.1114E 02	2.7826E 02	2.7755E 02	2.0922E 02
580.0	1.2685E 02	2.7005E 02	3.0311E 02	3.4970E 02	3.9126E 02	4.2672E 02	2.8905E 02	2.8831E 02	2.1738E 02
600.0	1.3163E 02	2.8016E 02	3.1434E 02	3.6260E 02	4.0557E 02	4.4224E 02	2.9981E 02	2.9904E 02	2.2552E 02
620.0	1.3641E 02	2.9026E 02	3.2554E 02	3.7545E 02	4.1984E 02	4.5771E 02	3.1054E 02	3.0975E 02	2.3365E 02
640.0	1.4117E 02	3.0033E 02	3.3672E 02	3.8826E 02	4.3406E 02	4.7313E 02	3.2124E 02	3.2043E 02	2.4175E 02
660.0	1.4592E 02	3.1038E 02	3.4786E 02	4.0104E 02	4.4823E 02	4.8849E 02	3.3191E 02	3.3107E 02	2.4984E 02
680.0	1.5067E 02	3.2040E 02	3.5897E 02	4.1378E 02	4.6236E 02	5.0380E 02	3.4256E 02	3.4169E 02	2.5790E 02
700.0	1.5540E 02	3.3040E 02	3.7004E 02	4.2648E 02	4.7644E 02	5.1906E 02	3.5318E 02	3.5229E 02	2.6594E 02
720.0	1.6012E 02	3.4038E 02	3.8109E 02	4.3914E 02	4.9047E 02	5.3427E 02	3.6377E 02	3.6285E 02	2.7397E 02
740.0	1.6484E 02	3.5033E 02	3.9211E 02	4.5177E 02	5.0447E 02	5.4942E 02	3.7433E 02	3.7339E 02	2.8198E 02
760.0	1.6954E 02	3.6025E 02	4.0309E 02	4.6436E 02	5.1841E 02	5.6453E 02	3.8486E 02	3.8390E 02	2.8996E 02
780.0	1.7423E 02	3.7016E 02	4.1405E 02	4.7691E 02	5.3232E 02	5.7959E 02	3.9537E 02	3.9438E 02	2.9793E 02
800.0	1.7891E 02	3.8004E 02	4.2498E 02	4.8943E 02	5.4618E 02	5.9459E 02	4.0585E 02	4.0483E 02	3.0588E 02
820.0	1.8359E 02	3.8990E 02	4.3588E 02	5.0191E 02	5.6000E 02	6.0956E 02	4.1631E 02	4.1526E 02	3.1381E 02
840.0	1.8825E 02	3.9973E 02	4.4675E 02	5.1436E 02	5.7378E 02	6.2447E 02	4.2673E 02	4.2567E 02	3.2172E 02
860.0	1.9290E 02	4.0954E 02	4.5759E 02	5.2677E 02	5.8752E 02	6.3934E 02	4.3714E 02	4.3604E 02	3.2962E 02
880.0	1.9754E 02	4.1933E 02	4.6841E 02	5.3916E 02	6.0122E 02	6.5417E 02	4.4751E 02	4.4640E 02	3.3749E 02
900.0	2.0218E 02	4.2910E 02	4.7919E 02	5.5150E 02	6.1488E 02	6.6895E 02	4.5786E 02	4.5672E 02	3.4535E 02
920.0	2.0680E 02	4.3885E 02	4.8995E 02	5.6382E 02	6.2851E 02	6.8368E 02	4.6819E 02	4.6703E 02	3.5319E 02
940.0	2.1141E 02	4.4857E 02	5.0069E 02	5.7610E 02	6.4209E 02	6.9838E 02	4.7849E 02	4.7730E 02	3.6102E 02
960.0	2.1602E 02	4.5828E 02	5.1139E 02	5.8835E 02	6.5564E 02	7.1303E 02	4.8877E 02	4.8756E 02	3.6882E 02
980.0	2.2061E 02	4.6796E 02	5.2207E 02	6.0057E 02	6.6915E 02	7.2764E 02	4.9903E 02	4.9779E 02	3.7661E 02
1000.0	2.2520E 02	4.7762E 02	5.3273E 02	6.1276E 02	6.8262E 02	7.4221E 02	5.0926E 02	5.0799E 02	3.8438E 02
1200.0	2.7059E 02	5.7317E 02	6.3797E 02	7.3308E 02	8.1551E 02	8.8582E 02	6.1035E 02	6.0885E 02	4.6124E 02
1400.0	3.1520E 02	6.6695E 02	7.4106E 02	8.5083E 02	9.4539E 02	1.0260E 03	7.0945E 02	7.0772E 02	5.3668E 02
1600.0	3.5912E 02	7.5919E 02	8.4229E 02	9.6635E 02	1.0727E 03	1.1634E 03	8.0682E 02	8.0487E 02	6.1086E 02
2000.0	4.4521E 02	9.3976E 02	1.0400E 03	1.1918E 03	1.3208E 03	1.4308E 03	9.9720E 02	9.9481E 02	7.5608E 02
2400.0	5.2935E 02	1.1160E 03	1.2326E 03	1.4112E 03	1.5619E 03	1.6904E 03	1.1828E 03	1.1800E 03	8.9782E 02
2800.0	6.1189E 02	1.2887E 03	1.4210E 03	1.6256E 03	1.7972E 03	1.9437E 03	1.3644E 03	1.3612E 03	1.0367E 03
3200.0	6.9309E 02	1.4585E 03	1.6059E 03	1.8359E 03	2.0278E 03	2.1916E 03	1.5428E 03	1.5391E 03	1.1732E 03
3600.0	7.7313E 02	1.6257E 03	1.7878E 03	2.0427E 03	2.2543E 03	2.4351E 03	1.7183E 03	1.7143E 03	1.3076E 03
4000.0	8.5216E 02	1.7906E 03	1.9671E 03	2.2463E 03	2.4774E 03	2.6747E 03	1.8914E 03	1.8870E 03	1.4402E 03
5000.0	1.0460E 03	2.1949E 03	2.4058E 03	2.7443E 03	3.0222E 03	3.2597E 03	2.3152E 03	2.3099E 03	1.7653E 03

PION RANGE, G/CM2

ENERGY MEV	WATER I= 65.1	AG-CL I=384.5	AG-BR I=434.1	NA-I I=433.0	LI-I I=472.5	POLYETHYLENE I= 54.6	STILBENE I= 65.2	LUCITE I= 65.6	ANTHRACENE I= 67.0
2.0	3.0046E-02	5.8248E-02	6.1871E-02	6.3303E-02	6.6482E-02	2.8279E-02	3.1333E-02	3.0969E-02	3.1807E-02
4.0	1.0540E-01	1.9044E-01	2.0096E-01	2.0605E-01	2.1555E-01	9.9661E-02	1.0990E-01	1.0861E-01	1.1148E-01
6.0	2.1975E-01	3.8437E-01	4.0432E-01	4.1467E-01	4.3278E-01	2.0820E-01	2.2912E-01	2.2642E-01	2.3234E-01
8.0	3.6975E-01	6.3391E-01	6.6552E-01	6.8243E-01	7.1112E-01	3.5072E-01	3.8549E-01	3.8094E-01	3.9083E-01
10.0	5.5287E-01	9.3472E-01	9.8001E-01	1.0047E 00	1.0457E 00	5.2485E-01	5.7638E-01	5.6958E-01	5.8429E-01
14.0	1.0105E 00	1.6768E 00	1.7549E 00	1.7982E 00	1.8687E 00	9.6030E-01	1.0534E 00	1.0409E 00	1.0677E 00
18.0	1.5789E 00	2.5882E 00	2.7057E 00	2.7714E 00	2.8771E 00	1.5016E 00	1.6459E 00	1.6264E 00	1.6680E 00
22.0	2.2472E 00	3.6512E 00	3.8139E 00	3.9055E 00	4.0514E 00	2.1384E 00	2.3425E 00	2.3147E 00	2.3738E 00
26.0	3.0060E 00	4.8512E 00	5.0642E 00	5.1849E 00	5.3755E 00	2.8617E 00	3.1335E 00	3.0963E 00	3.1751E 00
30.0	3.8475E 00	6.1756E 00	6.4435E 00	6.5960E 00	6.8354E 00	3.6640E 00	4.0106E 00	3.9630E 00	4.0637E 00
34.0	4.7645E 00	7.6133E 00	7.9404E 00	8.1272E 00	8.4192E 00	4.5386E 00	4.9665E 00	4.9075E 00	5.0319E 00
38.0	5.7508E 00	9.1547E 00	9.5448E 00	9.7683E 00	1.0116E 01	5.4796E 00	5.9947E 00	5.9234E 00	6.0734E 00
42.0	6.8010E 00	1.0791E 01	1.1248E 01	1.1510E 01	1.1917E 01	6.4816E 00	7.0894E 00	7.0050E 00	7.1822E 00
46.0	7.9101E 00	1.2515E 01	1.3041E 01	1.3345E 01	1.3813E 01	7.5400E 00	8.2454E 00	8.1472E 00	8.3532E 00
50.0	9.0735E 00	1.4319E 01	1.4918E 01	1.5264E 01	1.5797E 01	8.6505E 00	9.4581E 00	9.3459E 00	9.5815E 00
60.0	1.2194E 01	1.9143E 01	1.9934E 01	2.0394E 01	2.1097E 01	1.1630E 01	1.2711E 01	1.2559E 01	1.2876E 01
70.0	1.5576E 01	2.4349E 01	2.5346E 01	2.5928E 01	2.6813E 01	1.4860E 01	1.6236E 01	1.6043E 01	1.6446E 01
80.0	1.9178E 01	2.9872E 01	3.1086E 01	3.1798E 01	3.2875E 01	1.8299E 01	1.9989E 01	1.9751E 01	2.0247E 01
90.0	2.2965E 01	3.5660E 01	3.7104E 01	3.7946E 01	3.9224E 01	2.1915E 01	2.3933E 01	2.3647E 01	2.4241E 01
100.0	2.6905E 01	4.1669E 01	4.3355E 01	4.4328E 01	4.5812E 01	2.5682E 01	2.8042E 01	2.7714E 01	2.8401E 01
110.0	3.0979E 01	4.7864E 01	4.9794E 01	5.0907E 01	5.2602E 01	2.9584E 01	3.2292E 01	3.1931E 01	3.2704E 01
120.0	3.5167E 01	5.4216E 01	5.6393E 01	5.7651E 01	5.9561E 01	3.3599E 01	3.6665E 01	3.6267E 01	3.7131E 01
130.0	3.9454E 01	6.0700E 01	6.3127E 01	6.4535E 01	6.6664E 01	3.7712E 01	4.1143E 01	4.0708E 01	4.1664E 01
140.0	4.3826E 01	6.7298E 01	6.9976E 01	7.1537E 01	7.3887E 01	4.1911E 01	4.5712E 01	4.5239E 01	4.6290E 01
150.0	4.8271E 01	7.3990E 01	7.6922E 01	7.8638E 01	8.1213E 01	4.6184E 01	5.0361E 01	4.9849E 01	5.0996E 01
160.0	5.2779E 01	8.0763E 01	8.3952E 01	8.5825E 01	8.8626E 01	5.0522E 01	5.5078E 01	5.4527E 01	5.5773E 01
170.0	5.7342E 01	8.7605E 01	9.1053E 01	9.3083E 01	9.6112E 01	5.4917E 01	5.9856E 01	5.9264E 01	6.0610E 01
180.0	6.1953E 01	9.4505E 01	9.8214E 01	1.0040E 02	1.0366E 02	5.9362E 01	6.4687E 01	6.4054E 01	6.5501E 01
190.0	6.6606E 01	1.0145E 02	1.0543E 02	1.0777E 02	1.1126E 02	6.3850E 01	6.9563E 01	6.8889E 01	7.0438E 01
200.0	7.1296E 01	1.0844E 02	1.1268E 02	1.1519E 02	1.1891E 02	6.8376E 01	7.4480E 01	7.3764E 01	7.5416E 01
220.0	8.0768E 01	1.2252E 02	1.2729E 02	1.3011E 02	1.3431E 02	7.7527E 01	8.4417E 01	8.3615E 01	8.5477E 01
240.0	9.0339E 01	1.3670E 02	1.4201E 02	1.4514E 02	1.4983E 02	8.6782E 01	9.4464E 01	9.3575E 01	9.5650E 01
260.0	9.9986E 01	1.5095E 02	1.5680E 02	1.6023E 02	1.6542E 02	9.6120E 01	1.0460E 02	1.0362E 02	1.0591E 02
280.0	1.0969E 02	1.6525E 02	1.7163E 02	1.7537E 02	1.8107E 02	1.0552E 02	1.1479E 02	1.1373E 02	1.1623E 02
300.0	1.1944E 02	1.7957E 02	1.8649E 02	1.9053E 02	1.9674E 02	1.1497E 02	1.2504E 02	1.2388E 02	1.2661E 02
320.0	1.2922E 02	1.9390E 02	2.0135E 02	2.0571E 02	2.1243E 02	1.2445E 02	1.3532E 02	1.3407E 02	1.3702E 02
340.0	1.3903E 02	2.0823E 02	2.1622E 02	2.2089E 02	2.2812E 02	1.3397E 02	1.4564E 02	1.4429E 02	1.4746E 02
360.0	1.4885E 02	2.2255E 02	2.3108E 02	2.3605E 02	2.4380E 02	1.4350E 02	1.5597E 02	1.5453E 02	1.5792E 02
380.0	1.5868E 02	2.3686E 02	2.4592E 02	2.5120E 02	2.5947E 02	1.5305E 02	1.6631E 02	1.6478E 02	1.6840E 02
400.0	1.6852E 02	2.5115E 02	2.6075E 02	2.6632E 02	2.7511E 02	1.6261E 02	1.7664E 02	1.7504E 02	1.7888E 02
420.0	1.7836E 02	2.6542E 02	2.7554E 02	2.8142E 02	2.9073E 02	1.7217E 02	1.8702E 02	1.8530E 02	1.8936E 02
440.0	1.8820E 02	2.7966E 02	2.9031E 02	2.9648E 02	3.0631E 02	1.8173E 02	1.9737E 02	1.9556E 02	1.9985E 02
460.0	1.9804E 02	2.9387E 02	3.0504E 02	3.1151E 02	3.2186E 02	1.9129E 02	2.0773E 02	2.0581E 02	2.1033E 02
480.0	2.0787E 02	3.0805E 02	3.1975E 02	3.2651E 02	3.3737E 02	2.0085E 02	2.1807E 02	2.1606E 02	2.2081E 02
500.0	2.1769E 02	3.2220E 02	3.3441E 02	3.4147E 02	3.5285E 02	2.1041E 02	2.2841E 02	2.2630E 02	2.3128E 02
520.0	2.2751E 02	3.3631E 02	3.4904E 02	3.5639E 02	3.6829E 02	2.1995E 02	2.3875E 02	2.3654E 02	2.4174E 02
540.0	2.3731E 02	3.5039E 02	3.6364E 02	3.7127E 02	3.8368E 02	2.2949E 02	2.4907E 02	2.4676E 02	2.5219E 02
560.0	2.4710E 02	3.6444E 02	3.7819E 02	3.8611E 02	3.9904E 02	2.3902E 02	2.5938E 02	2.5697E 02	2.6262E 02
580.0	2.5689E 02	3.7845E 02	3.9271E 02	4.0091E 02	4.1436E 02	2.4854E 02	2.6967E 02	2.6717E 02	2.7305E 02
600.0	2.6666E 02	3.9243E 02	4.0719E 02	4.1567E 02	4.2964E 02	2.5805E 02	2.7996E 02	2.7735E 02	2.8346E 02
620.0	2.7641E 02	4.0637E 02	4.2164E 02	4.3039E 02	4.4487E 02	2.6754E 02	2.9023E 02	2.8753E 02	2.9386E 02
640.0	2.8616E 02	4.2028E 02	4.3604E 02	4.4508E 02	4.6007E 02	2.7703E 02	3.0049E 02	2.9768E 02	3.0425E 02
660.0	2.9589E 02	4.3415E 02	4.5041E 02	4.5972E 02	4.7522E 02	2.8650E 02	3.1073E 02	3.0783E 02	3.1462E 02
680.0	3.0561E 02	4.4799E 02	4.6475E 02	4.7432E 02	4.9034E 02	2.9596E 02	3.2096E 02	3.1796E 02	3.2498E 02
700.0	3.1531E 02	4.6179E 02	4.7904E 02	4.8889E 02	5.0541E 02	3.0541E 02	3.3118E 02	3.2807E 02	3.3532E 02
720.0	3.2500E 02	4.7556E 02	4.9330E 02	5.0341E 02	5.2045E 02	3.1484E 02	3.4137E 02	3.3817E 02	3.4565E 02
740.0	3.3467E 02	4.8930E 02	5.0753E 02	5.1790E 02	5.3545E 02	3.2427E 02	3.5156E 02	3.4825E 02	3.5596E 02
760.0	3.4434E 02	5.0300E 02	5.2172E 02	5.3236E 02	5.5041E 02	3.3367E 02	3.6173E 02	3.5832E 02	3.6626E 02
780.0	3.5398E 02	5.1668E 02	5.3587E 02	5.4677E 02	5.6533E 02	3.4307E 02	3.7189E 02	3.6838E 02	3.7654E 02
800.0	3.6362E 02	5.3032E 02	5.5000E 02	5.6115E 02	5.8022E 02	3.5245E 02	3.8203E 02	3.7842E 02	3.8681E 02
820.0	3.7324E 02	5.4392E 02	5.6408E 02	5.7549E 02	5.9506E 02	3.6182E 02	3.9215E 02	3.8844E 02	3.9706E 02
840.0	3.8285E 02	5.5750E 02	5.7814E 02	5.8980E 02	6.0988E 02	3.7118E 02	4.0226E 02	3.9845E 02	4.0730E 02
860.0	3.9244E 02	5.7105E 02	5.9216E 02	6.0408E 02	6.2465E 02	3.8052E 02	4.1236E 02	4.0844E 02	4.1752E 02
880.0	4.0202E 02	5.8456E 02	6.0615E 02	6.1832E 02	6.3940E 02	3.8985E 02	4.2244E 02	4.1842E 02	4.2773E 02
900.0	4.1159E 02	5.9805E 02	6.2011E 02	6.3253E 02	6.5411E 02	3.9917E 02	4.3251E 02	4.2839E 02	4.3792E 02
920.0	4.2114E 02	6.1151E 02	6.3404E 02	6.4670E 02	6.6878E 02	4.0848E 02	4.4256E 02	4.3834E 02	4.4810E 02
940.0	4.3068E 02	6.2494E 02	6.4794E 02	6.6084E 02	6.8342E 02	4.1777E 02	4.5260E 02	4.4828E 02	4.5826E 02
960.0	4.4021E 02	6.3834E 02	6.6181E 02	6.7495E 02	6.9803E 02	4.2705E 02	4.6263E 02	4.5820E 02	4.6841E 02
980.0	4.4973E 02	6.5172E 02	6.7564E 02	6.8903E 02	7.1261E 02	4.3632E 02	4.7264E 02	4.6811E 02	4.7855E 02
1000.0	4.5923E 02	6.6506E 02	6.8945E 02	7.0308E 02	7.2715E 02	4.4557E 02	4.8263E 02	4.7800E 02	4.8867E 02
1200.0	5.5359E 02	7.9714E 02	8.2607E 02	8.4200E 02	8.7097E 02	5.3748E 02	5.8189E 02	5.7623E 02	5.8916E 02
1400.0	6.4686E 02	9.2695E 02	9.6029E 02	9.7836E 02	1.0122E 03	6.2832E 02	6.7995E 02	6.7325E 02	6.8844E 02
1600.0	7.3917E 02	1.0548E 03	1.0925E 03	1.1125E 03	1.1511E 03	7.1821E 02	7.7696E 02	7.6922E 02	7.8665E 02
2000.0	9.2133E 02	1.3058E 03	1.3517E 03	1.3755E 03	1.4233E 03	8.9556E 02	9.6830E 02	9.5846E 02	9.8035E 02
2400.0	1.1008E 03	1.5515E 03	1.6054E 03	1.6326E 03	1.6895E 03	1.0702E 03	1.1567E 03	1.1447E 03	1.1710E 03
2800.0	1.2781E 03	1.7930E 03	1.8547E 03	1.8849E 03	1.9508E 03	1.2427E 03	1.3426E 03	1.3286E 03	1.3593E 03
3200.0	1.4534E 03	2.0311E 03	2.1003E 03	2.1334E 03	2.2080E 03	1.4132E 03	1.5265E 03	1.5104E 03	1.5454E 03
3600.0	1.6272E 03	2.2662E 03	2.3428E 03	2.3786E 03	2.4618E 03	1.5822E 03	1.7087E 03	1.6904E 03	1.7298E 03
4000.0	1.7996E 03	2.4988E 03	2.5826E 03	2.6209E 03	2.7126E 03	1.7498E 03	1.8893E 03	1.8690E 03	1.9127E 03
5000.0	2.2255E 03	3.0710E 03	3.1724E 03	3.2164E 03	3.3289E 03	2.1637E 03	2.3353E 03	2.3098E 03	2.3641E 03

MUON STOPPING POWER, MEV•CM2/G

ENERGY MEV	BE I= 60.0	C I= 78.0	AL I=163.0	FE I=273.0	CU I=314.0	AG I=487.0	AU I=797.0	PB I=826.0	U I=923.0
2.0	2.3770E 01	2.5648E 01	2.1657E 01	1.8814E 01	1.7845E 01	1.5213E 01	1.1904E 01	1.1583E 01	1.0796E 01
4.0	1.3512E 01	1.4643E 01	1.2567E 01	1.1073E 01	1.0558E 01	9.1623E 00	7.3634E 00	7.1811E 00	6.7427E 00
6.0	9.7564E 00	1.0595E 01	9.1605E 00	8.1257E 00	7.7664E 00	6.8014E 00	5.5591E 00	5.4307E 00	5.1298E 00
8.0	7.7811E 00	8.4609E 00	7.3485E 00	6.5449E 00	6.2647E 00	5.5165E 00	4.5554E 00	4.4549E 00	4.2235E 00
10.0	6.5554E 00	7.1347E 00	6.2164E 00	5.5522E 00	5.3198E 00	4.7020E 00	3.9095E 00	3.8259E 00	3.6359E 00
14.0	5.1089E 00	5.5675E 00	4.8718E 00	4.3678E 00	4.1904E 00	3.7217E 00	3.1214E 00	3.0573E 00	2.9143E 00
18.0	4.2807E 00	4.6690E 00	4.0974E 00	3.6827E 00	3.5361E 00	3.1504E 00	2.6565E 00	2.6033E 00	2.4860E 00
22.0	3.7437E 00	4.0859E 00	3.5933E 00	3.2356E 00	3.1087E 00	2.7758E 00	2.3493E 00	2.3031E 00	2.2020E 00
26.0	3.3675E 00	3.6772E 00	3.2393E 00	2.9211E 00	2.8078E 00	2.5114E 00	2.1314E 00	2.0900E 00	2.0001E 00
30.0	3.0896E 00	3.3752E 00	2.9775E 00	2.6881E 00	2.5849E 00	2.3151E 00	1.9691E 00	1.9313E 00	1.8494E 00
34.0	2.8764E 00	3.1435E 00	2.7763E 00	2.5090E 00	2.4134E 00	2.1639E 00	1.8439E 00	1.8087E 00	1.7330E 00
38.0	2.7080E 00	2.9515E 00	2.6173E 00	2.3673E 00	2.2777E 00	2.0443E 00	1.7445E 00	1.7115E 00	1.6406E 00
42.0	2.5719E 00	2.8033E 00	2.4887E 00	2.2528E 00	2.1680E 00	1.9468E 00	1.6640E 00	1.6327E 00	1.5656E 00
46.0	2.4599E 00	2.6811E 00	2.3829E 00	2.1573E 00	2.0772E 00	1.8677E 00	1.5976E 00	1.5677E 00	1.5039E 00
50.0	2.3663E 00	2.5788E 00	2.2945E 00	2.0784E 00	2.0018E 00	1.8011E 00	1.5422E 00	1.5134E 00	1.4522E 00
60.0	2.1876E 00	2.3841E 00	2.1206E 00	1.9288E 00	1.8590E 00	1.6751E 00	1.4373E 00	1.4108E 00	1.3545E 00
70.0	2.0621E 00	2.2478E 00	2.0048E 00	1.8221E 00	1.7598E 00	1.5878E 00	1.3646E 00	1.3397E 00	1.2868E 00
80.0	1.9700E 00	2.1482E 00	1.9203E 00	1.7464E 00	1.6879E 00	1.5248E 00	1.3123E 00	1.2884E 00	1.2381E 00
90.0	1.9004E 00	2.0730E 00	1.8567E 00	1.6895E 00	1.6344E 00	1.4780E 00	1.2736E 00	1.2506E 00	1.2021E 00
100.0	1.8465E 00	2.0150E 00	1.8079E 00	1.6458E 00	1.5880E 00	1.4417E 00	1.2444E 00	1.2220E 00	1.1740E 00
110.0	1.8039E 00	1.9693E 00	1.7697E 00	1.6117E 00	1.5559E 00	1.4148E 00	1.2211E 00	1.2003E 00	1.1533E 00
120.0	1.7698E 00	1.9329E 00	1.7394E 00	1.5848E 00	1.5306E 00	1.3933E 00	1.2036E 00	1.1835E 00	1.1373E 00
130.0	1.7421E 00	1.9036E 00	1.7151E 00	1.5633E 00	1.5104E 00	1.3762E 00	1.1899E 00	1.1706E 00	1.1249E 00
140.0	1.7195E 00	1.8797E 00	1.6956E 00	1.5460E 00	1.4943E 00	1.3627E 00	1.1787E 00	1.1607E 00	1.1148E 00
150.0	1.7009E 00	1.8601E 00	1.6797E 00	1.5321E 00	1.4813E 00	1.3520E 00	1.1704E 00	1.1531E 00	1.1074E 00
160.0	1.6855E 00	1.8440E 00	1.6668E 00	1.5208E 00	1.4708E 00	1.3435E 00	1.1639E 00	1.1473E 00	1.1016E 00
170.0	1.6726E 00	1.8306E 00	1.6563E 00	1.5117E 00	1.4624E 00	1.3368E 00	1.1590E 00	1.1430E 00	1.0973E 00
180.0	1.6619E 00	1.8196E 00	1.6478E 00	1.5043E 00	1.4557E 00	1.3316E 00	1.1552E 00	1.1361E 00	1.0940E 00
190.0	1.6529E 00	1.8105E 00	1.6409E 00	1.4984E 00	1.4503E 00	1.3276E 00	1.1524E 00	1.1339E 00	1.0917E 00
200.0	1.6453E 00	1.8029E 00	1.6353E 00	1.4937E 00	1.4461E 00	1.3245E 00	1.1505E 00	1.1325E 00	1.0902E 00
220.0	1.6338E 00	1.7916E 00	1.6273E 00	1.4872E 00	1.4404E 00	1.3208E 00	1.1485E 00	1.1315E 00	1.0888E 00
240.0	1.6257E 00	1.7841E 00	1.6225E 00	1.4835E 00	1.4374E 00	1.3194E 00	1.1484E 00	1.1323E 00	1.0893E 00
260.0	1.6203E 00	1.7793E 00	1.6201E 00	1.4820E 00	1.4363E 00	1.3197E 00	1.1498E 00	1.1344E 00	1.0910E 00
280.0	1.6168E 00	1.7767E 00	1.6194E 00	1.4819E 00	1.4367E 00	1.3212E 00	1.1521E 00	1.1374E 00	1.0937E 00
300.0	1.6148E 00	1.7756E 00	1.6200E 00	1.4830E 00	1.4382E 00	1.3237E 00	1.1551E 00	1.1410E 00	1.0969E 00
320.0	1.6139E 00	1.7756E 00	1.6215E 00	1.4850E 00	1.4404E 00	1.3267E 00	1.1586E 00	1.1451E 00	1.1007E 00
340.0	1.6139E 00	1.7766E 00	1.6238E 00	1.4875E 00	1.4432E 00	1.3303E 00	1.1625E 00	1.1495E 00	1.1047E 00
360.0	1.6146E 00	1.7783E 00	1.6266E 00	1.4906E 00	1.4465E 00	1.3342E 00	1.1667E 00	1.1542E 00	1.1090E 00
380.0	1.6157E 00	1.7805E 00	1.6298E 00	1.4940E 00	1.4501E 00	1.3384E 00	1.1710E 00	1.1589E 00	1.1135E 00
400.0	1.6173E 00	1.7831E 00	1.6334E 00	1.4977E 00	1.4539E 00	1.3427E 00	1.1755E 00	1.1638E 00	1.1180E 00
420.0	1.6192E 00	1.7861E 00	1.6371E 00	1.5015E 00	1.4579E 00	1.3472E 00	1.1800E 00	1.1688E 00	1.1226E 00
440.0	1.6213E 00	1.7892E 00	1.6411E 00	1.5055E 00	1.4621E 00	1.3517E 00	1.1846E 00	1.1737E 00	1.1272E 00
460.0	1.6237E 00	1.7926E 00	1.6451E 00	1.5096E 00	1.4663E 00	1.3563E 00	1.1892E 00	1.1786E 00	1.1319E 00
480.0	1.6262E 00	1.7961E 00	1.6493E 00	1.5138E 00	1.4705E 00	1.3608E 00	1.1937E 00	1.1835E 00	1.1365E 00
500.0	1.6288E 00	1.7997E 00	1.6535E 00	1.5180E 00	1.4748E 00	1.3654E 00	1.1983E 00	1.1884E 00	1.1410E 00
520.0	1.6315E 00	1.8034E 00	1.6577E 00	1.5222E 00	1.4790E 00	1.3700E 00	1.2028E 00	1.1932E 00	1.1456E 00
540.0	1.6342E 00	1.8071E 00	1.6619E 00	1.5264E 00	1.4833E 00	1.3745E 00	1.2073E 00	1.1980E 00	1.1501E 00
560.0	1.6370E 00	1.8108E 00	1.6661E 00	1.5306E 00	1.4875E 00	1.3790E 00	1.2117E 00	1.2027E 00	1.1545E 00
580.0	1.6398E 00	1.8146E 00	1.6703E 00	1.5347E 00	1.4918E 00	1.3835E 00	1.2160E 00	1.2073E 00	1.1588E 00
600.0	1.6427E 00	1.8184E 00	1.6745E 00	1.5389E 00	1.4959E 00	1.3878E 00	1.2203E 00	1.2119E 00	1.1631E 00
620.0	1.6455E 00	1.8221E 00	1.6787E 00	1.5429E 00	1.5001E 00	1.3922E 00	1.2245E 00	1.2163E 00	1.1673E 00
640.0	1.6484E 00	1.8258E 00	1.6828E 00	1.5470E 00	1.5041E 00	1.3964E 00	1.2287E 00	1.2207E 00	1.1715E 00
660.0	1.6512E 00	1.8296E 00	1.6868E 00	1.5510E 00	1.5081E 00	1.4006E 00	1.2328E 00	1.2250E 00	1.1756E 00
680.0	1.6541E 00	1.8332E 00	1.6909E 00	1.5549E 00	1.5121E 00	1.4048E 00	1.2368E 00	1.2293E 00	1.1796E 00
700.0	1.6569E 00	1.8369E 00	1.6948E 00	1.5588E 00	1.5160E 00	1.4088E 00	1.2408E 00	1.2335E 00	1.1835E 00
720.0	1.6597E 00	1.8405E 00	1.6987E 00	1.5627E 00	1.5199E 00	1.4128E 00	1.2446E 00	1.2376E 00	1.1874E 00
740.0	1.6624E 00	1.8440E 00	1.7026E 00	1.5664E 00	1.5237E 00	1.4168E 00	1.2485E 00	1.2416E 00	1.1912E 00
760.0	1.6652E 00	1.8476E 00	1.7064E 00	1.5702E 00	1.5274E 00	1.4207E 00	1.2522E 00	1.2455E 00	1.1949E 00
780.0	1.6679E 00	1.8510E 00	1.7101E 00	1.5738E 00	1.5311E 00	1.4245E 00	1.2559E 00	1.2494E 00	1.1986E 00
800.0	1.6705E 00	1.8545E 00	1.7138E 00	1.5775E 00	1.5347E 00	1.4282E 00	1.2595E 00	1.2532E 00	1.2022E 00
820.0	1.6732E 00	1.8578E 00	1.7175E 00	1.5810E 00	1.5383E 00	1.4319E 00	1.2631E 00	1.2570E 00	1.2058E 00
840.0	1.6758E 00	1.8612E 00	1.7211E 00	1.5845E 00	1.5418E 00	1.4355E 00	1.2666E 00	1.2606E 00	1.2093E 00
860.0	1.6784E 00	1.8645E 00	1.7246E 00	1.5880E 00	1.5452E 00	1.4391E 00	1.2700E 00	1.2642E 00	1.2127E 00
880.0	1.6810E 00	1.8677E 00	1.7281E 00	1.5914E 00	1.5486E 00	1.4426E 00	1.2734E 00	1.2678E 00	1.2160E 00
900.0	1.6835E 00	1.8709E 00	1.7315E 00	1.5947E 00	1.5520E 00	1.4460E 00	1.2767E 00	1.2713E 00	1.2193E 00
920.0	1.6860E 00	1.8741E 00	1.7348E 00	1.5980E 00	1.5553E 00	1.4494E 00	1.2800E 00	1.2747E 00	1.2226E 00
940.0	1.6884E 00	1.8772E 00	1.7382E 00	1.6012E 00	1.5585E 00	1.4527E 00	1.2832E 00	1.2781E 00	1.2258E 00
960.0	1.6908E 00	1.8803E 00	1.7414E 00	1.6044E 00	1.5617E 00	1.4560E 00	1.2863E 00	1.2814E 00	1.2289E 00
980.0	1.6932E 00	1.8833E 00	1.7446E 00	1.6076E 00	1.5648E 00	1.4592E 00	1.2894E 00	1.2846E 00	1.2320E 00
1000.0	1.6956E 00	1.8863E 00	1.7478E 00	1.6106E 00	1.5679E 00	1.4624E 00	1.2925E 00	1.2878E 00	1.2351E 00
1200.0	1.7175E 00	1.9138E 00	1.7770E 00	1.6391E 00	1.5963E 00	1.4915E 00	1.3205E 00	1.3171E 00	1.2629E 00
1400.0	1.7367E 00	1.9378E 00	1.8024E 00	1.6638E 00	1.6208E 00	1.5166E 00	1.3446E 00	1.3423E 00	1.2869E 00
1600.0	1.7538E 00	1.9589E 00	1.8246E 00	1.6854E 00	1.6424E 00	1.5386E 00	1.3657E 00	1.3643E 00	1.3078E 00
2000.0	1.7827E 00	1.9945E 00	1.8622E 00	1.7220E 00	1.6786E 00	1.5755E 00	1.4011E 00	1.4012E 00	1.3430E 00
2400.0	1.8067E 00	2.0237E 00	1.8929E 00	1.7519E 00	1.7083E 00	1.6057E 00	1.4300E 00	1.4312E 00	1.3717E 00
2800.0	1.8271E 00	2.0483E 00	1.9189E 00	1.7771E 00	1.7332E 00	1.6310E 00	1.4543E 00	1.4565E 00	1.3959E 00
3200.0	1.8448E 00	2.0695E 00	1.9412E 00	1.7988E 00	1.7548E 00	1.6529E 00	1.4752E 00	1.4781E 00	1.4167E 00
3600.0	1.8605E 00	2.0881E 00	1.9609E 00	1.8179E 00	1.7736E 00	1.6720E 00	1.4935E 00	1.4971E 00	1.4349E 00
4000.0	1.8745E 00	2.1047E 00	1.9783E 00	1.8349E 00	1.7904E 00	1.6889E 00	1.5097E 00	1.5139E 00	1.4510E 00
5000.0	1.9042E 00	2.1395E 00	2.0150E 00	1.8706E 00	1.8256E 00	1.7244E 00	1.5437E 00	1.5490E 00	1.4848E 00

MUON STOPPING POWER, MEV•CM2/G

ENERGY MEV	H I= 18.7	ME I= 42.0	NE I=131.0	A I=210.0	KR I=381.0	XE I=555.0	AIR I= 86.8	CARB.DIOXIDE I= 85.9	METHANE I= 44.1
2.0	6.2906E 01	2.8250E 01	2.3213E 01	1.9253E 01	1.6021E 01	1.3819E 01	2.5177E 01	2.5266E 01	3.5012E 01
4.0	3.5193E 01	1.5977E 01	1.3400E 01	1.1247E 01	9.5481E 00	8.3756E 00	1.4401E 01	1.4447E 01	1.9808E 01
6.0	2.5218E 01	1.1508E 01	9.7438E 00	8.2236E 00	7.0488E 00	6.2396E 00	1.0429E 01	1.0461E 01	1.4270E 01
8.0	2.0016E 01	9.1632E 00	7.8049E 00	6.6094E 00	5.6982E 00	5.0717E 00	8.3327E 00	8.3580E 00	1.1365E 01
10.0	1.6805E 01	7.7111E 00	6.5956E 00	5.5985E 00	4.8458E 00	4.3291E 00	7.0293E 00	7.0504E 00	9.5651E 00
14.0	1.3035E 01	6.0002E 00	5.1618E 00	4.3952E 00	3.8244E 00	3.4329E 00	5.4883E 00	5.5043E 00	7.4443E 00
18.0	1.0886E 01	5.0221E 00	4.3373E 00	3.7009E 00	3.2313E 00	2.9093E 00	4.6043E 00	4.6175E 00	6.2316E 00
22.0	9.4974E 00	4.3884E 00	3.8011E 00	3.2485E 00	2.8433E 00	2.5654E 00	4.0304E 00	4.0418E 00	5.4459E 00
26.0	8.5262E 00	3.9448E 00	3.4248E 00	2.9304E 00	2.5699E 00	2.3225E 00	3.6280E 00	3.6382E 00	4.8958E 00
30.0	7.8100E 00	3.6174E 00	3.1466E 00	2.6950E 00	2.3671E 00	2.1420E 00	3.3307E 00	3.3400E 00	4.4898E 00
34.0	7.2610E 00	3.3663E 00	2.9329E 00	2.5141E 00	2.2111E 00	2.0030E 00	3.1025E 00	3.1111E 00	4.1783E 00
38.0	6.8276E 00	3.1679E 00	2.7640E 00	2.3711E 00	2.0876E 00	1.8929E 00	2.9222E 00	2.9302E 00	3.9323E 00
42.0	6.4775E 00	3.0076E 00	2.6275E 00	2.2554E 00	1.9878E 00	1.8038E 00	2.7764E 00	2.7841E 00	3.7335E 00
46.0	6.1894E 00	2.8757E 00	2.5151E 00	2.1602E 00	1.9055E 00	1.7303E 00	2.6565E 00	2.6638E 00	3.5699E 00
50.0	5.9487E 00	2.7655E 00	2.4212E 00	2.0807E 00	1.8368E 00	1.6690E 00	2.5563E 00	2.5633E 00	3.4333E 00
60.0	5.4930E 00	2.5570E 00	2.2437E 00	1.9303E 00	1.7070E 00	1.5531E 00	2.3668E 00	2.3732E 00	3.1746E 00
70.0	5.1751E 00	2.4117E 00	2.1202E 00	1.8258E 00	1.6169E 00	1.4727E 00	2.2348E 00	2.2408E 00	2.9944E 00
80.0	4.9437E 00	2.3060E 00	2.0307E 00	1.7502E 00	1.5518E 00	1.4147E 00	2.1391E 00	2.1448E 00	2.8634E 00
90.0	4.7699E 00	2.2269E 00	1.9638E 00	1.6938E 00	1.5034E 00	1.3717E 00	2.0675E 00	2.0730E 00	2.7653E 00
100.0	4.6362E 00	2.1662E 00	1.9129E 00	1.6509E 00	1.4668E 00	1.3392E 00	2.0128E 00	2.0181E 00	2.6901E 00
110.0	4.5317E 00	2.1188E 00	1.8733E 00	1.6178E 00	1.4386E 00	1.3143E 00	1.9702E 00	1.9754E 00	2.6314E 00
120.0	4.4488E 00	2.0814E 00	1.8423E 00	1.5918E 00	1.4166E 00	1.2950E 00	1.9368E 00	1.9418E 00	2.5850E 00
130.0	4.3823E 00	2.0516E 00	1.8178E 00	1.5714E 00	1.3995E 00	1.2801E 00	1.9102E 00	1.9152E 00	2.5481E 00
140.0	4.3286E 00	2.0276E 00	1.7982E 00	1.5553E 00	1.3861E 00	1.2684E 00	1.8890E 00	1.8939E 00	2.5184E 00
150.0	4.2850E 00	2.0082E 00	1.7827E 00	1.5425E 00	1.3756E 00	1.2594E 00	1.8720E 00	1.8768E 00	2.4944E 00
160.0	4.2495E 00	1.9926E 00	1.7703E 00	1.5325E 00	1.3674E 00	1.2524E 00	1.8584E 00	1.8632E 00	2.4750E 00
170.0	4.2204E 00	1.9799E 00	1.7605E 00	1.5246E 00	1.3611E 00	1.2472E 00	1.8475E 00	1.8522E 00	2.4594E 00
180.0	4.1968E 00	1.9697E 00	1.7527E 00	1.5184E 00	1.3563E 00	1.2433E 00	1.8388E 00	1.8435E 00	2.4468E 00
190.0	4.1775E 00	1.9615E 00	1.7467E 00	1.5137E 00	1.3528E 00	1.2405E 00	1.8320E 00	1.8366E 00	2.4367E 00
200.0	4.1620E 00	1.9550E 00	1.7421E 00	1.5102E 00	1.3504E 00	1.2387E 00	1.8267E 00	1.8313E 00	2.4287E 00
220.0	4.1396E 00	1.9460E 00	1.7363E 00	1.5061E 00	1.3479E 00	1.2372E 00	1.8196E 00	1.8243E 00	2.4176E 00
240.0	4.1261E 00	1.9410E 00	1.7339E 00	1.5049E 00	1.3478E 00	1.2378E 00	1.8163E 00	1.8209E 00	2.4115E 00
260.0	4.1191E 00	1.9390E 00	1.7339E 00	1.5057E 00	1.3496E 00	1.2401E 00	1.8156E 00	1.8201E 00	2.4090E 00
280.0	4.1168E 00	1.9391E 00	1.7357E 00	1.5080E 00	1.3526E 00	1.2434E 00	1.8168E 00	1.8213E 00	2.4092E 00
300.0	4.1182E 00	1.9408E 00	1.7389E 00	1.5114E 00	1.3565E 00	1.2476E 00	1.8194E 00	1.8240E 00	2.4115E 00
320.0	4.1223E 00	1.9437E 00	1.7430E 00	1.5157E 00	1.3611E 00	1.2524E 00	1.8232E 00	1.8277E 00	2.4152E 00
340.0	4.1284E 00	1.9476E 00	1.7479E 00	1.5205E 00	1.3662E 00	1.2575E 00	1.8277E 00	1.8322E 00	2.4201E 00
360.0	4.1362E 00	1.9521E 00	1.7533E 00	1.5258E 00	1.3717E 00	1.2630E 00	1.8328E 00	1.8374E 00	2.4258E 00
380.0	4.1451E 00	1.9572E 00	1.7592E 00	1.5314E 00	1.3774E 00	1.2687E 00	1.8384E 00	1.8429E 00	2.4322E 00
400.0	4.1550E 00	1.9627E 00	1.7653E 00	1.5372E 00	1.3832E 00	1.2745E 00	1.8443E 00	1.8489E 00	2.4390E 00
420.0	4.1655E 00	1.9684E 00	1.7716E 00	1.5432E 00	1.3892E 00	1.2804E 00	1.8505E 00	1.8550E 00	2.4463E 00
440.0	4.1766E 00	1.9744E 00	1.7781E 00	1.5493E 00	1.3953E 00	1.2864E 00	1.8568E 00	1.8613E 00	2.4537E 00
460.0	4.1881E 00	1.9806E 00	1.7847E 00	1.5555E 00	1.4014E 00	1.2924E 00	1.8633E 00	1.8678E 00	2.4614E 00
480.0	4.1999E 00	1.9868E 00	1.7913E 00	1.5617E 00	1.4075E 00	1.2983E 00	1.8698E 00	1.8743E 00	2.4692E 00
500.0	4.2119E 00	1.9931E 00	1.7980E 00	1.5679E 00	1.4136E 00	1.3043E 00	1.8763E 00	1.8809E 00	2.4771E 00
520.0	4.2240E 00	1.9995E 00	1.8046E 00	1.5741E 00	1.4196E 00	1.3101E 00	1.8829E 00	1.8874E 00	2.4851E 00
540.0	4.2362E 00	2.0058E 00	1.8112E 00	1.5802E 00	1.4256E 00	1.3160E 00	1.8895E 00	1.8940E 00	2.4930E 00
560.0	4.2484E 00	2.0122E 00	1.8178E 00	1.5863E 00	1.4316E 00	1.3218E 00	1.8960E 00	1.9005E 00	2.5010E 00
580.0	4.2605E 00	2.0185E 00	1.8244E 00	1.5923E 00	1.4375E 00	1.3275E 00	1.9025E 00	1.9070E 00	2.5089E 00
600.0	4.2727E 00	2.0248E 00	1.8308E 00	1.5983E 00	1.4433E 00	1.3331E 00	1.9089E 00	1.9135E 00	2.5167E 00
620.0	4.2848E 00	2.0310E 00	1.8373E 00	1.6043E 00	1.4490E 00	1.3387E 00	1.9153E 00	1.9199E 00	2.5245E 00
640.0	4.2968E 00	2.0372E 00	1.8436E 00	1.6101E 00	1.4547E 00	1.3441E 00	1.9216E 00	1.9262E 00	2.5323E 00
660.0	4.3087E 00	2.0434E 00	1.8499E 00	1.6159E 00	1.4603E 00	1.3495E 00	1.9279E 00	1.9325E 00	2.5399E 00
680.0	4.3205E 00	2.0494E 00	1.8561E 00	1.6216E 00	1.4658E 00	1.3549E 00	1.9341E 00	1.9387E 00	2.5475E 00
700.0	4.3322E 00	2.0554E 00	1.8622E 00	1.6272E 00	1.4712E 00	1.3601E 00	1.9402E 00	1.9448E 00	2.5550E 00
720.0	4.3438E 00	2.0614E 00	1.8682E 00	1.6327E 00	1.4766E 00	1.3653E 00	1.9462E 00	1.9508E 00	2.5624E 00
740.0	4.3552E 00	2.0672E 00	1.8742E 00	1.6382E 00	1.4819E 00	1.3704E 00	1.9521E 00	1.9567E 00	2.5698E 00
760.0	4.3666E 00	2.0730E 00	1.8800E 00	1.6436E 00	1.4871E 00	1.3754E 00	1.9580E 00	1.9626E 00	2.5770E 00
780.0	4.3777E 00	2.0787E 00	1.8858E 00	1.6489E 00	1.4922E 00	1.3803E 00	1.9638E 00	1.9684E 00	2.5841E 00
800.0	4.3888E 00	2.0844E 00	1.8915E 00	1.6541E 00	1.4972E 00	1.3852E 00	1.9695E 00	1.9741E 00	2.5912E 00
820.0	4.3997E 00	2.0900E 00	1.8971E 00	1.6593E 00	1.5022E 00	1.3899E 00	1.9751E 00	1.9798E 00	2.5981E 00
840.0	4.4104E 00	2.0954E 00	1.9027E 00	1.6644E 00	1.5070E 00	1.3946E 00	1.9807E 00	1.9853E 00	2.6050E 00
860.0	4.4211E 00	2.1009E 00	1.9081E 00	1.6694E 00	1.5119E 00	1.3993E 00	1.9861E 00	1.9908E 00	2.6117E 00
880.0	4.4316E 00	2.1062E 00	1.9135E 00	1.6743E 00	1.5166E 00	1.4038E 00	1.9915E 00	1.9962E 00	2.6184E 00
900.0	4.4419E 00	2.1115E 00	1.9188E 00	1.6791E 00	1.5213E 00	1.4083E 00	1.9968E 00	2.0015E 00	2.6250E 00
920.0	4.4521E 00	2.1167E 00	1.9241E 00	1.6839E 00	1.5259E 00	1.4127E 00	2.0021E 00	2.0068E 00	2.6315E 00
940.0	4.4622E 00	2.1218E 00	1.9292E 00	1.6887E 00	1.5304E 00	1.4171E 00	2.0073E 00	2.0119E 00	2.6379E 00
960.0	4.4722E 00	2.1269E 00	1.9343E 00	1.6933E 00	1.5349E 00	1.4214E 00	2.0124E 00	2.0171E 00	2.6442E 00
980.0	4.4820E 00	2.1319E 00	1.9393E 00	1.6979E 00	1.5393E 00	1.4256E 00	2.0174E 00	2.0221E 00	2.6504E 00
1000.0	4.4917E 00	2.1368E 00	1.9443E 00	1.7024E 00	1.5436E 00	1.4298E 00	2.0223E 00	2.0271E 00	2.6566E 00
1200.0	4.5820E 00	2.1826E 00	1.9902E 00	1.7443E 00	1.5838E 00	1.4684E 00	2.0684E 00	2.0732E 00	2.7138E 00
1400.0	4.6618E 00	2.2230E 00	2.0305E 00	1.7811E 00	1.6190E 00	1.5022E 00	2.1090E 00	2.1138E 00	2.7642E 00
1600.0	4.7331E 00	2.2590E 00	2.0664E 00	1.8138E 00	1.6503E 00	1.5322E 00	2.1450E 00	2.1499E 00	2.8091E 00
2000.0	4.8555E 00	2.3209E 00	2.1280E 00	1.8699E 00	1.7038E 00	1.5835E 00	2.2070E 00	2.2120E 00	2.8863E 00
2400.0	4.9581E 00	2.3726E 00	2.1794E 00	1.9168E 00	1.7485E 00	1.6264E 00	2.2588E 00	2.2638E 00	2.9509E 00
2800.0	5.0463E 00	2.4171E 00	2.2236E 00	1.9570E 00	1.7869E 00	1.6631E 00	2.3032E 00	2.3083E 00	3.0063E 00
3200.0	5.1234E 00	2.4560E 00	2.2622E 00	1.9921E 00	1.8204E 00	1.6952E 00	2.3421E 00	2.3473E 00	3.0549E 00
3600.0	5.1920E 00	2.4905E 00	2.2965E 00	2.0233E 00	1.8502E 00	1.7237E 00	2.3767E 00	2.3819E 00	3.0980E 00
4000.0	5.2538E 00	2.5216E 00	2.3274E 00	2.0514E 00	1.8770E 00	1.7494E 00	2.4078E 00	2.4130E 00	3.1344E 00
5000.0	5.3855E 00	2.5880E 00	2.3933E 00	2.1113E 00	1.9341E 00	1.8041E 00	2.4741E 00	2.4795E 00	3.2087E 00

MUON STOPPING POWER, MEV•CM2/G

ENERGY MEV	WATER I= 65.1	AG-CL I=384.5	AG-BR I=434.1	NA-I I=433.0	LI-I I=472.5	POLYETHYLENE I= 54.6	STILBENE I= 65.2	LUCITE I= 65.6	ANTHRACENE I= 67.0
2.0	2.9351E 01	1.6568E 01	1.5731E 01	1.5328E 01	1.4667E 01	3.1001E 01	2.8149E 01	2.8484E 01	2.7755E 01
4.0	1.6703E 01	9.8818E 00	9.4267E 00	9.1900E 00	8.8280E 00	1.7596E 01	1.6022E 01	1.6214E 01	1.5805E 01
6.0	1.2068E 01	7.3009E 00	6.9792E 00	6.8099E 00	6.5550E 00	1.2696E 01	1.1576E 01	1.1715E 01	1.1422E 01
8.0	9.6282E 00	5.9049E 00	5.6518E 00	5.5178E 00	5.3176E 00	1.0121E 01	9.2363E 00	9.3471E 00	9.1143E 00
10.0	8.1138E 00	5.0233E 00	4.8120E 00	4.6997E 00	4.5329E 00	8.5241E 00	7.7837E 00	7.8771E 00	7.6816E 00
14.0	6.3259E 00	3.9660E 00	3.8035E 00	3.7164E 00	3.5883E 00	6.6405E 00	6.0687E 00	6.1417E 00	5.9898E 00
18.0	5.3019E 00	3.3518E 00	3.2168E 00	3.1439E 00	3.0376E 00	5.5624E 00	5.0863E 00	5.1475E 00	5.0206E 00
22.0	4.6376E 00	2.9498E 00	2.8325E 00	2.7688E 00	2.6764E 00	4.8634E 00	4.4491E 00	4.5027E 00	4.3919E 00
26.0	4.1722E 00	2.6664E 00	2.5615E 00	2.5041E 00	2.4215E 00	4.3739E 00	4.0026E 00	4.0509E 00	3.9514E 00
30.0	3.8285E 00	2.4563E 00	2.3604E 00	2.3077E 00	2.2322E 00	4.0124E 00	3.6728E 00	3.7172E 00	3.6260E 00
34.0	3.5647E 00	2.2945E 00	2.2056E 00	2.1565E 00	2.0855E 00	3.7351E 00	3.4198E 00	3.4611E 00	3.3763E 00
38.0	3.3563E 00	2.1665E 00	2.0831E 00	2.0368E 00	1.9710E 00	3.5160E 00	3.2199E 00	3.2588E 00	3.1791E 00
42.0	3.1879E 00	2.0630E 00	1.9839E 00	1.9399E 00	1.8776E 00	3.3390E 00	3.0584E 00	3.0954E 00	3.0197E 00
46.0	3.0494E 00	1.9777E 00	1.9023E 00	1.8601E 00	1.8007E 00	3.1933E 00	2.9254E 00	2.9608E 00	2.8885E 00
50.0	2.9336E 00	1.9065E 00	1.8341E 00	1.7935E 00	1.7364E 00	3.0716E 00	2.8144E 00	2.8484E 00	2.7789E 00
60.0	2.7122E 00	1.7718E 00	1.7052E 00	1.6675E 00	1.6145E 00	2.8413E 00	2.6042E 00	2.6358E 00	2.5715E 00
70.0	2.5607E 00	1.6783E 00	1.6132E 00	1.5801E 00	1.5306E 00	2.6787E 00	2.4568E 00	2.4877E 00	2.4269E 00
80.0	2.4493E 00	1.6108E 00	1.5498E 00	1.5170E 00	1.4698E 00	2.5573E 00	2.3471E 00	2.3666E 00	2.3185E 00
90.0	2.3647E 00	1.5607E 00	1.5026E 00	1.4699E 00	1.4247E 00	2.4656E 00	2.2643E 00	2.2832E 00	2.2366E 00
100.0	2.2991E 00	1.5227E 00	1.4666E 00	1.4346E 00	1.3905E 00	2.3946E 00	2.2003E 00	2.2188E 00	2.1734E 00
110.0	2.2483E 00	1.4934E 00	1.4388E 00	1.4074E 00	1.3643E 00	2.3387E 00	2.1499E 00	2.1680E 00	2.1235E 00
120.0	2.2081E 00	1.4707E 00	1.4171E 00	1.3862E 00	1.3439E 00	2.2939E 00	2.1096E 00	2.1275E 00	2.0837E 00
130.0	2.1756E 00	1.4530E 00	1.4001E 00	1.3697E 00	1.3281E 00	2.2577E 00	2.0771E 00	2.0948E 00	2.0515E 00
140.0	2.1491E 00	1.4390E 00	1.3865E 00	1.3568E 00	1.3157E 00	2.2280E 00	2.0505E 00	2.0681E 00	2.0253E 00
150.0	2.1274E 00	1.4282E 00	1.3760E 00	1.3467E 00	1.3054E 00	2.2036E 00	2.0287E 00	2.0463E 00	2.0037E 00
160.0	2.1095E 00	1.4196E 00	1.3676E 00	1.3389E 00	1.2973E 00	2.1835E 00	2.0107E 00	2.0282E 00	1.9859E 00
170.0	2.0947E 00	1.4127E 00	1.3611E 00	1.3329E 00	1.2910E 00	2.1667E 00	1.9958E 00	2.0132E 00	1.9712E 00
180.0	2.0824E 00	1.4073E 00	1.3560E 00	1.3283E 00	1.2860E 00	2.1527E 00	1.9834E 00	2.0008E 00	1.9589E 00
190.0	2.0723E 00	1.4032E 00	1.3522E 00	1.3249E 00	1.2822E 00	2.1410E 00	1.9730E 00	1.9905E 00	1.9487E 00
200.0	2.0638E 00	1.4002E 00	1.3494E 00	1.3221E 00	1.2793E 00	2.1312E 00	1.9645E 00	1.9819E 00	1.9402E 00
220.0	2.0511E 00	1.3965E 00	1.3461E 00	1.3188E 00	1.2758E 00	2.1162E 00	1.9514E 00	1.9689E 00	1.9273E 00
240.0	2.0426E 00	1.3954E 00	1.3450E 00	1.3178E 00	1.2746E 00	2.1059E 00	1.9426E 00	1.9602E 00	1.9186E 00
260.0	2.0371E 00	1.3960E 00	1.3456E 00	1.3185E 00	1.2751E 00	2.0990E 00	1.9369E 00	1.9546E 00	1.9129E 00
280.0	2.0340E 00	1.3977E 00	1.3474E 00	1.3204E 00	1.2767E 00	2.0947E 00	1.9334E 00	1.9512E 00	1.9095E 00
300.0	2.0325E 00	1.4003E 00	1.3501E 00	1.3231E 00	1.2793E 00	2.0923E 00	1.9317E 00	1.9496E 00	1.9078E 00
320.0	2.0324E 00	1.4035E 00	1.3534E 00	1.3266E 00	1.2824E 00	2.0914E 00	1.9313E 00	1.9493E 00	1.9074E 00
340.0	2.0333E 00	1.4072E 00	1.3572E 00	1.3304E 00	1.2861E 00	2.0915E 00	1.9319E 00	1.9501E 00	1.9080E 00
360.0	2.0349E 00	1.4112E 00	1.3613E 00	1.3347E 00	1.2900E 00	2.0926E 00	1.9332E 00	1.9516E 00	1.9093E 00
380.0	2.0371E 00	1.4156E 00	1.3657E 00	1.3391E 00	1.2942E 00	2.0944E 00	1.9352E 00	1.9537E 00	1.9113E 00
400.0	2.0397E 00	1.4201E 00	1.3702E 00	1.3437E 00	1.2986E 00	2.0967E 00	1.9376E 00	1.9563E 00	1.9137E 00
420.0	2.0427E 00	1.4247E 00	1.3748E 00	1.3485E 00	1.3031E 00	2.0994E 00	1.9405E 00	1.9592E 00	1.9165E 00
440.0	2.0460E 00	1.4294E 00	1.3795E 00	1.3533E 00	1.3077E 00	2.1024E 00	1.9435E 00	1.9625E 00	1.9195E 00
460.0	2.0495E 00	1.4341E 00	1.3842E 00	1.3581E 00	1.3123E 00	2.1057E 00	1.9468E 00	1.9659E 00	1.9228E 00
480.0	2.0531E 00	1.4389E 00	1.3890E 00	1.3630E 00	1.3169E 00	2.1092E 00	1.9503E 00	1.9695E 00	1.9262E 00
500.0	2.0568E 00	1.4436E 00	1.3937E 00	1.3678E 00	1.3215E 00	2.1128E 00	1.9539E 00	1.9732E 00	1.9298E 00
520.0	2.0607E 00	1.4483E 00	1.3984E 00	1.3726E 00	1.3261E 00	2.1165E 00	1.9576E 00	1.9770E 00	1.9334E 00
540.0	2.0645E 00	1.4530E 00	1.4031E 00	1.3774E 00	1.3307E 00	2.1203E 00	1.9613E 00	1.9809E 00	1.9371E 00
560.0	2.0684E 00	1.4577E 00	1.4077E 00	1.3821E 00	1.3352E 00	2.1242E 00	1.9651E 00	1.9848E 00	1.9408E 00
580.0	2.0723E 00	1.4622E 00	1.4122E 00	1.3867E 00	1.3397E 00	2.1281E 00	1.9689E 00	1.9887E 00	1.9446E 00
600.0	2.0763E 00	1.4668E 00	1.4167E 00	1.3913E 00	1.3441E 00	2.1320E 00	1.9727E 00	1.9926E 00	1.9484E 00
620.0	2.0802E 00	1.4712E 00	1.4212E 00	1.3959E 00	1.3484E 00	2.1359E 00	1.9765E 00	1.9965E 00	1.9521E 00
640.0	2.0841E 00	1.4756E 00	1.4255E 00	1.4004E 00	1.3527E 00	2.1398E 00	1.9803E 00	2.0004E 00	1.9559E 00
660.0	2.0879E 00	1.4800E 00	1.4298E 00	1.4048E 00	1.3570E 00	2.1437E 00	1.9840E 00	2.0043E 00	1.9596E 00
680.0	2.0918E 00	1.4842E 00	1.4341E 00	1.4091E 00	1.3611E 00	2.1476E 00	1.9878E 00	2.0082E 00	1.9633E 00
700.0	2.0955E 00	1.4884E 00	1.4382E 00	1.4134E 00	1.3652E 00	2.1515E 00	1.9915E 00	2.0120E 00	1.9670E 00
720.0	2.0993E 00	1.4925E 00	1.4423E 00	1.4176E 00	1.3693E 00	2.1553E 00	1.9952E 00	2.0158E 00	1.9706E 00
740.0	2.1030E 00	1.4966E 00	1.4464E 00	1.4217E 00	1.3732E 00	2.1591E 00	1.9988E 00	2.0195E 00	1.9742E 00
760.0	2.1067E 00	1.5006E 00	1.4503E 00	1.4258E 00	1.3771E 00	2.1628E 00	2.0024E 00	2.0232E 00	1.9778E 00
780.0	2.1103E 00	1.5045E 00	1.4542E 00	1.4298E 00	1.3810E 00	2.1665E 00	2.0060E 00	2.0269E 00	1.9813E 00
800.0	2.1139E 00	1.5083E 00	1.4580E 00	1.4337E 00	1.3848E 00	2.1702E 00	2.0095E 00	2.0305E 00	1.9848E 00
820.0	2.1174E 00	1.5121E 00	1.4618E 00	1.4375E 00	1.3885E 00	2.1739E 00	2.0129E 00	2.0341E 00	1.9882E 00
840.0	2.1209E 00	1.5159E 00	1.4655E 00	1.4413E 00	1.3921E 00	2.1774E 00	2.0164E 00	2.0376E 00	1.9916E 00
860.0	2.1243E 00	1.5195E 00	1.4691E 00	1.4451E 00	1.3957E 00	2.1810E 00	2.0198E 00	2.0411E 00	1.9949E 00
880.0	2.1277E 00	1.5231E 00	1.4727E 00	1.4487E 00	1.3992E 00	2.1845E 00	2.0231E 00	2.0445E 00	1.9982E 00
900.0	2.1310E 00	1.5266E 00	1.4762E 00	1.4523E 00	1.4027E 00	2.1879E 00	2.0264E 00	2.0479E 00	2.0015E 00
920.0	2.1343E 00	1.5301E 00	1.4796E 00	1.4559E 00	1.4061E 00	2.1913E 00	2.0296E 00	2.0512E 00	2.0047E 00
940.0	2.1375E 00	1.5335E 00	1.4830E 00	1.4594E 00	1.4095E 00	2.1947E 00	2.0328E 00	2.0545E 00	2.0079E 00
960.0	2.1407E 00	1.5369E 00	1.4864E 00	1.4628E 00	1.4128E 00	2.1980E 00	2.0360E 00	2.0577E 00	2.0110E 00
980.0	2.1439E 00	1.5402E 00	1.4896E 00	1.4662E 00	1.4161E 00	2.2012E 00	2.0391E 00	2.0609E 00	2.0141E 00
1000.0	2.1470E 00	1.5435E 00	1.4929E 00	1.4695E 00	1.4193E 00	2.2044E 00	2.0421E 00	2.0640E 00	2.0171E 00
1200.0	2.1756E 00	1.5733E 00	1.5224E 00	1.5000E 00	1.4487E 00	2.2343E 00	2.0705E 00	2.0932E 00	2.0452E 00
1400.0	2.2005E 00	1.5990E 00	1.5479E 00	1.5263E 00	1.4741E 00	2.2605E 00	2.0953E 00	2.1186E 00	2.0697E 00
1600.0	2.2225E 00	1.6214E 00	1.5702E 00	1.5493E 00	1.4964E 00	2.2836E 00	2.1171E 00	2.1409E 00	2.0913E 00
2000.0	2.2595E 00	1.6590E 00	1.6076E 00	1.5880E 00	1.5339E 00	2.3227E 00	2.1540E 00	2.1787E 00	2.1279E 00
2400.0	2.2900E 00	1.6897E 00	1.6380E 00	1.6196E 00	1.5646E 00	2.3549E 00	2.1844E 00	2.2098E 00	2.1579E 00
2800.0	2.3158E 00	1.7155E 00	1.6636E 00	1.6462E 00	1.5905E 00	2.3822E 00	2.2100E 00	2.2360E 00	2.1833E 00
3200.0	2.3381E 00	1.7377E 00	1.6856E 00	1.6690E 00	1.6127E 00	2.4058E 00	2.2322E 00	2.2586E 00	2.2053E 00
3600.0	2.3578E 00	1.7571E 00	1.7049E 00	1.6891E 00	1.6322E 00	2.4265E 00	2.2516E 00	2.2784E 00	2.2245E 00
4000.0	2.3754E 00	1.7743E 00	1.7219E 00	1.7068E 00	1.6495E 00	2.4450E 00	2.2690E 00	2.2961E 00	2.2417E 00
5000.0	2.4126E 00	1.8103E 00	1.7577E 00	1.7440E 00	1.6857E 00	2.4841E 00	2.3055E 00	2.3334E 00	2.2779E 00

MUON RANGE, G/CM2

ENERGY MEV	BE I= 60.0	C I= 78.0	AL I=163.0	FE I=273.0	CU I=314.0	AG I=487.0	AU I=797.0	PB I=826.0	U I=923.0
2.0	4.6420E-02	4.3306E-02	5.2510E-02	6.1675E-02	6.5387E-02	7.7994E-02	1.0058E-01	1.0334E-01	1.1061E-01
4.0	1.6322E-01	1.5126E-01	1.7906E-01	2.0607E-01	2.1713E-01	2.5410E-01	3.2231E-01	3.3095E-01	3.5393E-01
6.0	3.4019E-01	3.1436E-01	3.6831E-01	4.2003E-01	4.4122E-01	5.1098E-01	6.3889E-01	6.5525E-01	6.9816E-01
8.0	5.7157E-01	5.2727E-01	6.1394E-01	6.9633E-01	7.3006E-01	8.3980E-01	1.0389E 00	1.0645E 00	1.1305E 00
10.0	8.5293E-01	7.8591E-01	9.1122E-01	1.0296E 00	1.0780E 00	1.2342E 00	1.5147E 00	1.5509E 00	1.6429E 00
14.0	1.5515E 00	1.4273E 00	1.6456E 00	1.8500E 00	1.9337E 00	2.1997E 00	2.6702E 00	2.7310E 00	2.8826E 00
18.0	2.4117E 00	2.2163E 00	2.5459E 00	2.8529E 00	2.9785E 00	3.3740E 00	4.0664E 00	4.1560E 00	4.3760E 00
22.0	3.4145E 00	3.1354E 00	3.5920E 00	4.0156E 00	4.1891E 00	4.7312E 00	5.6726E 00	5.7948E 00	6.0910E 00
26.0	4.5438E 00	4.1698E 00	4.7671E 00	5.3197E 00	5.5461E 00	6.2496E 00	7.4640E 00	7.6219E 00	8.0011E 00
30.0	5.7860E 00	5.3071E 00	6.0573E 00	6.7495E 00	7.0333E 00	7.9112E 00	9.4195E 00	9.6159E 00	1.0084E 01
34.0	7.1295E 00	6.5367E 00	7.4502E 00	8.2916E 00	8.6367E 00	9.7004E 00	1.1521E 01	1.1759E 01	1.2321E 01
38.0	8.5641E 00	7.8512E 00	8.9355E 00	9.9344E 00	1.0344E 01	1.1604E 01	1.3753E 01	1.4034E 01	1.4695E 01
42.0	1.0081E 01	9.2430E 00	1.0504E 01	1.1668E 01	1.2146E 01	1.3611E 01	1.6103E 01	1.6429E 01	1.7193E 01
46.0	1.1672E 01	1.0703E 01	1.2147E 01	1.3483E 01	1.4032E 01	1.5709E 01	1.8558E 01	1.8930E 01	1.9801E 01
50.0	1.3331E 01	1.2225E 01	1.3859E 01	1.5373E 01	1.5994E 01	1.7891E 01	2.1107E 01	2.1528E 01	2.2509E 01
60.0	1.7736E 01	1.6267E 01	1.8402E 01	2.0378E 01	2.1189E 01	2.3661E 01	2.7838E 01	2.8386E 01	2.9654E 01
70.0	2.2451E 01	2.0593E 01	2.3260E 01	2.5720E 01	2.6726E 01	2.9801E 01	3.4988E 01	3.5670E 01	3.7238E 01
80.0	2.7417E 01	2.5148E 01	2.8362E 01	3.1332E 01	3.2534E 01	3.6234E 01	4.2468E 01	4.3289E 01	4.5168E 01
90.0	3.2589E 01	2.9891E 01	3.3662E 01	3.7158E 01	3.8558E 01	4.2900E 01	5.0208E 01	5.1172E 01	5.3371E 01
100.0	3.7931E 01	3.4786E 01	3.9123E 01	4.3158E 01	4.4768E 01	4.9755E 01	5.8155E 01	5.9265E 01	6.1793E 01
110.0	4.3412E 01	3.9809E 01	4.4716E 01	4.9301E 01	5.1133E 01	5.6759E 01	6.6270E 01	6.7525E 01	7.0390E 01
120.0	4.9011E 01	4.4936E 01	5.0417E 01	5.5560E 01	5.7615E 01	6.3884E 01	7.4522E 01	7.5918E 01	7.9124E 01
130.0	5.4708E 01	5.0150E 01	5.6208E 01	6.1914E 01	6.4194E 01	7.1107E 01	8.2880E 01	8.4416E 01	8.7967E 01
140.0	6.0486E 01	5.5438E 01	6.2073E 01	6.8348E 01	7.0852E 01	7.8410E 01	9.1325E 01	9.2996E 01	9.6899E 01
150.0	6.6335E 01	6.0787E 01	6.8000E 01	7.4847E 01	7.7574E 01	8.5779E 01	9.9841E 01	1.0164E 02	1.0590E 02
160.0	7.2242E 01	6.6187E 01	7.3977E 01	8.1399E 01	8.4350E 01	9.3199E 01	1.0841E 02	1.1034E 02	1.1496E 02
170.0	7.8198E 01	7.1631E 01	7.9996E 01	8.7995E 01	9.1169E 01	1.0066E 02	1.1702E 02	1.1907E 02	1.2405E 02
180.0	8.4197E 01	7.7110E 01	8.6049E 01	9.4628E 01	9.8023E 01	1.0816E 02	1.2566E 02	1.2785E 02	1.3318E 02
190.0	9.0231E 01	8.2620E 01	9.2131E 01	1.0129E 02	1.0491E 02	1.1568E 02	1.3433E 02	1.3666E 02	1.4233E 02
200.0	9.6295E 01	8.8155E 01	9.8237E 01	1.0797E 02	1.1181E 02	1.2322E 02	1.4302E 02	1.4548E 02	1.5150E 02
220.0	1.0850E 02	9.9286E 01	1.1050E 02	1.2139E 02	1.2567E 02	1.3834E 02	1.6042E 02	1.6316E 02	1.6986E 02
240.0	1.2077E 02	1.1047E 02	1.2281E 02	1.3486E 02	1.3957E 02	1.5350E 02	1.7784E 02	1.8083E 02	1.8822E 02
260.0	1.3309E 02	1.2170E 02	1.3515E 02	1.4835E 02	1.5349E 02	1.6865E 02	1.9524E 02	1.9848E 02	2.0657E 02
280.0	1.4545E 02	1.3295E 02	1.4749E 02	1.6185E 02	1.6742E 02	1.8380E 02	2.1262E 02	2.1608E 02	2.2488E 02
300.0	1.5783E 02	1.4421E 02	1.5984E 02	1.7534E 02	1.8133E 02	1.9893E 02	2.2996E 02	2.3364E 02	2.4314E 02
320.0	1.7022E 02	1.5548E 02	1.7218E 02	1.8882E 02	1.9523E 02	2.1402E 02	2.4725E 02	2.5114E 02	2.6134E 02
340.0	1.8261E 02	1.6674E 02	1.8451E 02	2.0227E 02	2.0910E 02	2.2907E 02	2.6448E 02	2.6857E 02	2.7948E 02
360.0	1.9500E 02	1.7799E 02	1.9682E 02	2.1570E 02	2.2294E 02	2.4409E 02	2.8165E 02	2.8594E 02	2.9755E 02
380.0	2.0738E 02	1.8923E 02	2.0910E 02	2.2911E 02	2.3675E 02	2.5905E 02	2.9876E 02	3.0323E 02	3.1555E 02
400.0	2.1976E 02	2.0045E 02	2.2136E 02	2.4248E 02	2.5052E 02	2.7397E 02	3.1581E 02	3.2045E 02	3.3347E 02
420.0	2.3212E 02	2.1166E 02	2.3359E 02	2.5581E 02	2.6426E 02	2.8884E 02	3.3279E 02	3.3760E 02	3.5133E 02
440.0	2.4446E 02	2.2285E 02	2.4579E 02	2.6912E 02	2.7796E 02	3.0366E 02	3.4971E 02	3.5467E 02	3.6911E 02
460.0	2.5679E 02	2.3402E 02	2.5796E 02	2.8238E 02	2.9162E 02	3.1844E 02	3.6656E 02	3.7168E 02	3.8681E 02
480.0	2.6910E 02	2.4516E 02	2.7010E 02	2.9561E 02	3.0524E 02	3.3316E 02	3.8335E 02	3.8861E 02	4.0445E 02
500.0	2.8138E 02	2.5629E 02	2.8222E 02	3.0881E 02	3.1882E 02	3.4783E 02	4.0007E 02	4.0548E 02	4.2201E 02
520.0	2.9365E 02	2.6739E 02	2.9430E 02	3.2196E 02	3.3236E 02	3.6245E 02	4.1673E 02	4.2227E 02	4.3950E 02
540.0	3.0590E 02	2.7847E 02	3.0635E 02	3.3509E 02	3.4587E 02	3.7703E 02	4.3332E 02	4.3900E 02	4.5693E 02
560.0	3.1813E 02	2.8952E 02	3.1836E 02	3.4817E 02	3.5933E 02	3.9155E 02	4.4986E 02	4.5566E 02	4.7428E 02
580.0	3.3034E 02	3.0056E 02	3.3035E 02	3.6122E 02	3.7276E 02	4.0603E 02	4.6634E 02	4.7226E 02	4.9157E 02
600.0	3.4252E 02	3.1157E 02	3.4231E 02	3.7423E 02	3.8614E 02	4.2047E 02	4.8276E 02	4.8879E 02	5.0880E 02
620.0	3.5469E 02	3.2255E 02	3.5424E 02	3.8721E 02	3.9950E 02	4.3486E 02	4.9912E 02	5.0527E 02	5.2597E 02
640.0	3.6683E 02	3.3352E 02	3.6614E 02	4.0016E 02	4.1281E 02	4.4920E 02	5.1542E 02	5.2168E 02	5.4307E 02
660.0	3.7895E 02	3.4446E 02	3.7801E 02	4.1307E 02	4.2609E 02	4.6350E 02	5.3167E 02	5.3803E 02	5.6011E 02
680.0	3.9105E 02	3.5538E 02	3.8985E 02	4.2595E 02	4.3933E 02	4.7776E 02	5.4787E 02	5.5433E 02	5.7709E 02
700.0	4.0314E 02	3.6628E 02	4.0167E 02	4.3879E 02	4.5254E 02	4.9198E 02	5.6401E 02	5.7057E 02	5.9402E 02
720.0	4.1520E 02	3.7716E 02	4.1345E 02	4.5161E 02	4.6572E 02	5.0615E 02	5.8011E 02	5.8676E 02	6.1089E 02
740.0	4.2724E 02	3.8801E 02	4.2522E 02	4.6439E 02	4.7886E 02	5.2029E 02	5.9615E 02	6.0290E 02	6.2771E 02
760.0	4.3926E 02	3.9885E 02	4.3695E 02	4.7714E 02	4.9197E 02	5.3438E 02	6.1215E 02	6.1898E 02	6.4447E 02
780.0	4.5126E 02	4.0967E 02	4.4866E 02	4.8987E 02	5.0505E 02	5.4844E 02	6.2810E 02	6.3501E 02	6.6118E 02
800.0	4.6324E 02	4.2046E 02	4.6034E 02	5.0256E 02	5.1810E 02	5.6247E 02	6.4400E 02	6.5099E 02	6.7784E 02
820.0	4.7520E 02	4.3123E 02	4.7200E 02	5.1522E 02	5.3111E 02	5.7645E 02	6.5985E 02	6.6693E 02	6.9446E 02
840.0	4.8715E 02	4.4199E 02	4.8363E 02	5.2786E 02	5.4410E 02	5.9040E 02	6.7567E 02	6.8282E 02	7.1102E 02
860.0	4.9907E 02	4.5273E 02	4.9524E 02	5.4047E 02	5.5706E 02	6.0432E 02	6.9144E 02	6.9866E 02	7.2753E 02
880.0	5.1098E 02	4.6344E 02	5.0682E 02	5.5305E 02	5.6999E 02	6.1820E 02	7.0716E 02	7.1446E 02	7.4400E 02
900.0	5.2287E 02	4.7414E 02	5.1839E 02	5.6560E 02	5.8289E 02	6.3204E 02	7.2285E 02	7.3021E 02	7.6043E 02
920.0	5.3474E 02	4.8482E 02	5.2993E 02	5.7813E 02	5.9576E 02	6.4586E 02	7.3849E 02	7.4592E 02	7.7681E 02
940.0	5.4659E 02	4.9549E 02	5.4144E 02	5.9064E 02	6.0861E 02	6.5964E 02	7.5410E 02	7.6159E 02	7.9314E 02
960.0	5.5843E 02	5.0613E 02	5.5294E 02	6.0311E 02	6.2143E 02	6.7339E 02	7.6967E 02	7.7722E 02	8.0944E 02
980.0	5.7025E 02	5.1676E 02	5.6441E 02	6.1557E 02	6.3422E 02	6.8711E 02	7.8520E 02	7.9281E 02	8.2569E 02
1000.0	5.8205E 02	5.2737E 02	5.7587E 02	6.2800E 02	6.4699E 02	7.0080E 02	8.0069E 02	8.0836E 02	8.4191E 02
1200.0	6.9923E 02	6.3262E 02	6.8933E 02	7.5106E 02	7.7338E 02	8.3619E 02	9.5374E 02	9.6187E 02	1.0020E 03
1400.0	8.1502E 02	7.3646E 02	8.0106E 02	8.7215E 02	8.9770E 02	9.6914E 02	1.1038E 03	1.1123E 03	1.1588E 03
1600.0	9.2961E 02	8.3910E 02	9.1133E 02	9.9156E 02	1.0203E 03	1.1000E 03	1.2514E 03	1.2600E 03	1.3130E 03
2000.0	1.1558E 03	1.0414E 03	1.1283E 03	1.2263E 03	1.2611E 03	1.3568E 03	1.5404E 03	1.5492E 03	1.6146E 03
2400.0	1.3786E 03	1.2405E 03	1.3412E 03	1.4565E 03	1.4972E 03	1.6082E 03	1.8229E 03	1.8315E 03	1.9092E 03
2800.0	1.5987E 03	1.4369E 03	1.5511E 03	1.6832E 03	1.7296E 03	1.8554E 03	2.1002E 03	2.1085E 03	2.1982E 03
3200.0	1.8166E 03	1.6311E 03	1.7583E 03	1.9069E 03	1.9590E 03	2.0989E 03	2.3733E 03	2.3811E 03	2.4826E 03
3600.0	2.0325E 03	1.8235E 03	1.9633E 03	2.1280E 03	2.1857E 03	2.3395E 03	2.6427E 03	2.6499E 03	2.7632E 03
4000.0	2.2466E 03	2.0143E 03	2.1664E 03	2.3470E 03	2.4101E 03	2.5775E 03	2.9091E 03	2.9156E 03	3.0403E 03
5000.0	2.7758E 03	2.4854E 03	2.6671E 03	2.8866E 03	2.9630E 03	3.1633E 03	3.5638E 03	3.5683E 03	3.7213E 03

MUON RANGE, G/CM2

ENERGY MEV	H I= 18.7	HE I= 42.0	NE I=131.0	A I=210.0	KR I=381.0	XE I=555.0	AIR I= 86.8	CARB.DIOXIDE I= 85.9	METHANE I= 44.1
2.0	1.7239E-02	3.8772E-02	4.8613E-02	5.9636E-02	7.3394E-02	8.6206E-02	4.4247E-02	4.4077E-02	3.1309E-02
4.0	6.1814E-02	1.3736E-01	1.6707E-01	2.0140E-01	2.4167E-01	2.7936E-01	1.5409E-01	1.5355E-01	1.1084E-01
6.0	1.3006E-01	2.8724E-01	3.4480E-01	4.1248E-01	4.8894E-01	5.5980E-01	3.1986E-01	3.1880E-01	2.3172E-01
8.0	2.1981E-01	4.8357E-01	5.7592E-01	6.8582E-01	8.0681E-01	9.1781E-01	5.3610E-01	5.3438E-01	3.9003E-01
10.0	3.2939E-01	7.2265E-01	8.5597E-01	1.0161E 00	1.1891E 00	1.3464E 00	7.9866E-01	7.9615E-01	5.8278E-01
14.0	6.0260E-01	1.3170E 00	1.5486E 00	1.8307E 00	2.1274E 00	2.3940E 00	1.4494E 00	1.4450E 00	1.0619E 00
18.0	9.4037E-01	2.0499E 00	2.3988E 00	2.8280E 00	3.2715E 00	3.6664E 00	2.2497E 00	2.2430E 00	1.6526E 00
22.0	1.3352E 00	2.9050E 00	3.3874E 00	3.9856E 00	4.5956E 00	5.1353E 00	3.1816E 00	3.1722E 00	2.3417E 00
26.0	1.7808E 00	3.8687E 00	4.4986E 00	5.2851E 00	6.0787E 00	6.7777E 00	4.2301E 00	4.2178E 00	3.1182E 00
30.0	2.2718E 00	4.9294E 00	5.7191E 00	6.7108E 00	7.7031E 00	8.5739E 00	5.3828E 00	5.3672E 00	3.9729E 00
34.0	2.8037E 00	6.0772E 00	7.0375E 00	8.2494E 00	9.4537E 00	1.0507E 01	6.6287E 00	6.6096E 00	4.8976E 00
38.0	3.3723E 00	7.3033E 00	8.4437E 00	9.8892E 00	1.1317E 01	1.2563E 01	7.9584E 00	7.9357E 00	5.8853E 00
42.0	3.9743E 00	8.6001E 00	9.9292E 00	1.1620E 01	1.3282E 01	1.4730E 01	9.3638E 00	9.3372E 00	6.9301E 00
46.0	4.6064E 00	9.9611E 00	1.1486E 01	1.3433E 01	1.5339E 01	1.6995E 01	1.0838E 01	1.0807E 01	8.0264E 00
50.0	5.2659E 00	1.1380E 01	1.3108E 01	1.5321E 01	1.7478E 01	1.9350E 01	1.2373E 01	1.2338E 01	9.1695E 00
60.0	7.0193E 00	1.5149E 01	1.7408E 01	2.0322E 01	2.3137E 01	2.5574E 01	1.6448E 01	1.6402E 01	1.2205E 01
70.0	8.8978E 00	1.9182E 01	2.1999E 01	2.5656E 01	2.9165E 01	3.2196E 01	2.0802E 01	2.0745E 01	1.5454E 01
80.0	1.0877E 01	2.3427E 01	2.6824E 01	3.1256E 01	3.5485E 01	3.9131E 01	2.5381E 01	2.5311E 01	1.8872E 01
90.0	1.2938E 01	2.7843E 01	3.1835E 01	3.7068E 01	4.2036E 01	4.6315E 01	3.0139E 01	3.0057E 01	2.2429E 01
100.0	1.5065E 01	3.2399E 01	3.6997E 01	4.3052E 01	4.8774E 01	5.3696E 01	3.5044E 01	3.4949E 01	2.6097E 01
110.0	1.7248E 01	3.7068E 01	4.2282E 01	4.9173E 01	5.5661E 01	6.1237E 01	4.0068E 01	3.9959E 01	2.9857E 01
120.0	1.9476E 01	4.1832E 01	4.7667E 01	5.5407E 01	6.2668E 01	6.8904E 01	4.5189E 01	4.5067E 01	3.3693E 01
130.0	2.1741E 01	4.6672E 01	5.3133E 01	6.1731E 01	6.9772E 01	7.6673E 01	5.0389E 01	5.0254E 01	3.7590E 01
140.0	2.4038E 01	5.1576E 01	5.8665E 01	6.8129E 01	7.6953E 01	8.4522E 01	5.5655E 01	5.5505E 01	4.1539E 01
150.0	2.6360E 01	5.6533E 01	6.4251E 01	7.4586E 01	8.4196E 01	9.2436E 01	6.0973E 01	6.0810E 01	4.5529E 01
160.0	2.8704E 01	6.1533E 01	6.9881E 01	8.1091E 01	9.1489E 01	1.0040E 02	6.6335E 01	6.6159E 01	4.9554E 01
170.0	3.1066E 01	6.6568E 01	7.5546E 01	8.7634E 01	9.8819E 01	1.0840E 02	7.1733E 01	7.1542E 01	5.3608E 01
180.0	3.3442E 01	7.1632E 01	8.1239E 01	9.4207E 01	1.0618E 02	1.1643E 02	7.7159E 01	7.6954E 01	5.7685E 01
190.0	3.5830E 01	7.6720E 01	8.6955E 01	1.0080E 02	1.1356E 02	1.2448E 02	8.2608E 01	8.2389E 01	6.1781E 01
200.0	3.8229E 01	8.1827E 01	9.2688E 01	1.0742E 02	1.2096E 02	1.3255E 02	8.8075E 01	8.7842E 01	6.5892E 01
220.0	4.3048E 01	9.2082E 01	1.0419E 02	1.2068E 02	1.3579E 02	1.4871E 02	9.9047E 01	9.8787E 01	7.4147E 01
240.0	4.7888E 01	1.0237E 02	1.1572E 02	1.3397E 02	1.5063E 02	1.6488E 02	1.1005E 02	1.0976E 02	8.2432E 01
260.0	5.2740E 01	1.1269E 02	1.2725E 02	1.4726E 02	1.6546E 02	1.8102E 02	1.2106E 02	1.2075E 02	9.0730E 01
280.0	5.7597E 01	1.2300E 02	1.3878E 02	1.6053E 02	1.8026E 02	1.9713E 02	1.3208E 02	1.3173E 02	9.9033E 01
300.0	6.2455E 01	1.3331E 02	1.5030E 02	1.7378E 02	1.9503E 02	2.1319E 02	1.4308E 02	1.4271E 02	1.0733E 02
320.0	6.7309E 01	1.4361E 02	1.6178E 02	1.8699E 02	2.0975E 02	2.2919E 02	1.5406E 02	1.5366E 02	1.1562E 02
340.0	7.2157E 01	1.5389E 02	1.7324E 02	2.0017E 02	2.2442E 02	2.4512E 02	1.6502E 02	1.6459E 02	1.2389E 02
360.0	7.6997E 01	1.6415E 02	1.8467E 02	2.1330E 02	2.3903E 02	2.6099E 02	1.7594E 02	1.7549E 02	1.3215E 02
380.0	8.1828E 01	1.7438E 02	1.9606E 02	2.2638E 02	2.5358E 02	2.7679E 02	1.8684E 02	1.8636E 02	1.4038E 02
400.0	8.6647E 01	1.8458E 02	2.0741E 02	2.3942E 02	2.6807E 02	2.9252E 02	1.9770E 02	1.9720E 02	1.4859E 02
420.0	9.1455E 01	1.9476E 02	2.1871E 02	2.5240E 02	2.8249E 02	3.0818E 02	2.0853E 02	2.0800E 02	1.5678E 02
440.0	9.6249E 01	2.0490E 02	2.2998E 02	2.6534E 02	2.9686E 02	3.2376E 02	2.1932E 02	2.1876E 02	1.6494E 02
460.0	1.0103E 02	2.1502E 02	2.4121E 02	2.7822E 02	3.1116E 02	3.3927E 02	2.3007E 02	2.2949E 02	1.7308E 02
480.0	1.0580E 02	2.2510E 02	2.5240E 02	2.9105E 02	3.2540E 02	3.5471E 02	2.4078E 02	2.4018E 02	1.8119E 02
500.0	1.1056E 02	2.3515E 02	2.6354E 02	3.0383E 02	3.3958E 02	3.7008E 02	2.5146E 02	2.5083E 02	1.8928E 02
520.0	1.1530E 02	2.4517E 02	2.7464E 02	3.1656E 02	3.5370E 02	3.8538E 02	2.6210E 02	2.6144E 02	1.9734E 02
540.0	1.2003E 02	2.5515E 02	2.8571E 02	3.2924E 02	3.6776E 02	4.0061E 02	2.7271E 02	2.7202E 02	2.0538E 02
560.0	1.2474E 02	2.6511E 02	2.9673E 02	3.4188E 02	3.8176E 02	4.1578E 02	2.8327E 02	2.8256E 02	2.1339E 02
580.0	1.2944E 02	2.7503E 02	3.0771E 02	3.5446E 02	3.9570E 02	4.3088E 02	2.9380E 02	2.9307E 02	2.2137E 02
600.0	1.3413E 02	2.8493E 02	3.1865E 02	3.6700E 02	4.0958E 02	4.4591E 02	3.0430E 02	3.0354E 02	2.2933E 02
620.0	1.3880E 02	2.9479E 02	3.2956E 02	3.7949E 02	4.2341E 02	4.6088E 02	3.1476E 02	3.1397E 02	2.3726E 02
640.0	1.4346E 02	3.0462E 02	3.4043E 02	3.9193E 02	4.3719E 02	4.7579E 02	3.2518E 02	3.2437E 02	2.4517E 02
660.0	1.4811E 02	3.1442E 02	3.5126E 02	4.0433E 02	4.5091E 02	4.9064E 02	3.3557E 02	3.3474E 02	2.5306E 02
680.0	1.5275E 02	3.2420E 02	3.6205E 02	4.1669E 02	4.6458E 02	5.0543E 02	3.4593E 02	3.4507E 02	2.6092E 02
700.0	1.5737E 02	3.3394E 02	3.7281E 02	4.2900E 02	4.7820E 02	5.2016E 02	3.5626E 02	3.5537E 02	2.6876E 02
720.0	1.6198E 02	3.4366E 02	3.8353E 02	4.4127E 02	4.9177E 02	5.3484E 02	3.6655E 02	3.6564E 02	2.7658E 02
740.0	1.6658E 02	3.5335E 02	3.9422E 02	4.5350E 02	5.0529E 02	5.4946E 02	3.7681E 02	3.7587E 02	2.8437E 02
760.0	1.7116E 02	3.6301E 02	4.0487E 02	4.6569E 02	5.1876E 02	5.6403E 02	3.8704E 02	3.8608E 02	2.9214E 02
780.0	1.7574E 02	3.7264E 02	4.1549E 02	4.7783E 02	5.3219E 02	5.7855E 02	3.9724E 02	3.9626E 02	2.9989E 02
800.0	1.8030E 02	3.8225E 02	4.2608E 02	4.8995E 02	5.4557E 02	5.9301E 02	4.0741E 02	4.0640E 02	3.0762E 02
820.0	1.8485E 02	3.9183E 02	4.3664E 02	5.0202E 02	5.5891E 02	6.0742E 02	4.1755E 02	4.1652E 02	3.1533E 02
840.0	1.8939E 02	4.0139E 02	4.4717E 02	5.1405E 02	5.7220E 02	6.2179E 02	4.2766E 02	4.2661E 02	3.2302E 02
860.0	1.9392E 02	4.1092E 02	4.5767E 02	5.2605E 02	5.8545E 02	6.3611E 02	4.3774E 02	4.3667E 02	3.3069E 02
880.0	1.9844E 02	4.2043E 02	4.6813E 02	5.3801E 02	5.9866E 02	6.5038E 02	4.4780E 02	4.4670E 02	3.3833E 02
900.0	2.0295E 02	4.2991E 02	4.7857E 02	5.4994E 02	6.1182E 02	6.6460E 02	4.5783E 02	4.5670E 02	3.4596E 02
920.0	2.0745E 02	4.3937E 02	4.8898E 02	5.6184E 02	6.2495E 02	6.7878E 02	4.6783E 02	4.6668E 02	3.5357E 02
940.0	2.1193E 02	4.4881E 02	4.9936E 02	5.7370E 02	6.3804E 02	6.9291E 02	4.7781E 02	4.7664E 02	3.6116E 02
960.0	2.1641E 02	4.5823E 02	5.0971E 02	5.8552E 02	6.5109E 02	7.0701E 02	4.8776E 02	4.8657E 02	3.6874E 02
980.0	2.2088E 02	4.6762E 02	5.2004E 02	5.9732E 02	6.6410E 02	7.2106E 02	4.9769E 02	4.9647E 02	3.7629E 02
1000.0	2.2534E 02	4.7699E 02	5.3034E 02	6.0908E 02	6.7707E 02	7.3506E 02	5.0759E 02	5.0635E 02	3.8383E 02
1200.0	2.6941E 02	5.6958E 02	6.3198E 02	7.2511E 02	8.0495E 02	8.7305E 02	6.0535E 02	6.0388E 02	4.5830E 02
1400.0	3.1268E 02	6.6036E 02	7.3145E 02	8.3855E 02	9.2982E 02	1.0077E 03	7.0109E 02	6.9940E 02	5.3131E 02
1600.0	3.5525E 02	7.4959E 02	8.2907E 02	9.4980E 02	1.0522E 03	1.1395E 03	7.9511E 02	7.9320E 02	6.0307E 02
2000.0	4.3865E 02	9.2420E 02	1.0197E 03	1.1669E 03	1.2906E 03	1.3961E 03	9.7886E 02	9.7654E 02	7.4348E 02
2400.0	5.2015E 02	1.0946E 03	1.2054E 03	1.3781E 03	1.5222E 03	1.6453E 03	1.1579E 03	1.1552E 03	8.8050E 02
2800.0	6.0010E 02	1.2616E 03	1.3871E 03	1.5846E 03	1.7485E 03	1.8884E 03	1.3333E 03	1.3302E 03	1.0148E 03
3200.0	6.7875E 02	1.4257E 03	1.5654E 03	1.7871E 03	1.9702E 03	2.1266E 03	1.5055E 03	1.5020E 03	1.1467E 03
3600.0	7.5630E 02	1.5875E 03	1.7408E 03	1.9863E 03	2.1881E 03	2.3606E 03	1.6750E 03	1.6711E 03	1.2767E 03
4000.0	8.3288E 02	1.7471E 03	1.9138E 03	2.1826E 03	2.4027E 03	2.5909E 03	1.8422E 03	1.8379E 03	1.4051E 03
5000.0	1.0208E 03	2.1383E 03	2.3373E 03	2.6629E 03	2.9273E 03	3.1534E 03	2.2517E 03	2.2466E 03	1.7202E 03

MUON RANGE, G/CM2

ENERGY MEV	WATER I= 65.1	AG-CL I=384.5	AG-BR I=434.1	NA-I I=433.0	LI-I I=472.5	POLYETHYLENE I= 54.6	STILBENE I= 65.2	LUCITE I= 65.6	ANTHRACENE I= 67.0
2.0	3.7665E-02	7.0904E-02	7.5099E-02	7.6913E-02	8.0640E-02	3.5515E-02	3.9277E-02	3.8819E-02	3.9860E-02
4.0	1.3219E-01	2.3357E-01	2.4592E-01	2.5220E-01	2.6340E-01	1.2515E-01	1.3782E-01	1.3620E-01	1.3978E-01
6.0	2.7530E-01	4.7239E-01	4.9597E-01	5.0857E-01	5.2997E-01	2.6111E-01	2.8701E-01	2.8363E-01	2.9100E-01
8.0	4.6232E-01	7.7920E-01	8.1670E-01	8.3717E-01	8.7113E-01	4.3896E-01	4.8197E-01	4.7628E-01	4.8858E-01
10.0	6.8967E-01	1.1480E 00	1.2019E 00	1.2316E 00	1.2802E 00	6.5531E-01	7.1897E-01	7.1047E-01	7.2873E-01
14.0	1.2539E 00	2.0530E 00	2.1460E 00	2.1981E 00	2.2816E 00	1.1926E 00	1.3071E 00	1.2917E 00	1.3247E 00
18.0	1.9486E 00	3.1560E 00	3.2957E 00	3.3745E 00	3.4996E 00	1.8546E 00	2.0313E 00	2.0072E 00	2.0583E 00
22.0	2.7581E 00	4.4324E 00	4.6252E 00	4.7348E 00	4.9072E 00	2.6264E 00	2.8751E 00	2.8410E 00	2.9132E 00
26.0	3.6697E 00	5.8619E 00	6.1136E 00	6.2574E 00	6.4819E 00	3.4958E 00	3.8253E 00	3.7798E 00	3.8757E 00
30.0	4.6722E 00	7.4275E 00	7.7430E 00	7.9240E 00	8.2052E 00	4.4522E 00	4.8703E 00	4.8124E 00	4.9342E 00
34.0	5.7564E 00	9.1144E 00	9.4982E 00	9.7192E 00	1.0061E 01	5.4868E 00	6.0004E 00	5.9290E 00	6.0789E 00
38.0	6.9139E 00	1.0910E 01	1.1366E 01	1.1630E 01	1.2036E 01	6.5916E 00	7.2070E 00	7.1211E 00	7.3010E 00
42.0	8.1377E 00	1.2804E 01	1.3335E 01	1.3643E 01	1.4117E 01	7.7600E 00	8.4826E 00	8.3815E 00	8.5930E 00
46.0	9.4214E 00	1.4785E 01	1.5395E 01	1.5750E 01	1.6294E 01	8.9857E 00	9.8207E 00	9.7036E 00	9.9482E 00
50.0	1.0759E 01	1.6846E 01	1.7538E 01	1.7941E 01	1.8557E 01	1.0263E 01	1.1215E 01	1.1082E 01	1.1361E 01
60.0	1.4313E 01	2.2299E 01	2.3205E 01	2.3736E 01	2.4542E 01	1.3656E 01	1.4918E 01	1.4739E 01	1.5110E 01
70.0	1.8113E 01	2.8106E 01	2.9243E 01	2.9906E 01	3.0912E 01	1.7286E 01	1.8877E 01	1.8651E 01	1.9119E 01
80.0	2.2110E 01	3.4194E 01	3.5574E 01	3.6371E 01	3.7586E 01	2.1111E 01	2.3045E 01	2.2776E 01	2.3339E 01
90.0	2.6268E 01	4.0505E 01	4.2131E 01	4.3072E 01	4.4501E 01	2.5096E 01	2.7386E 01	2.7082E 01	2.7733E 01
100.0	3.0559E 01	4.6995E 01	4.8871E 01	4.9962E 01	5.1610E 01	2.9214E 01	3.1869E 01	3.1527E 01	3.2271E 01
110.0	3.4959E 01	5.3629E 01	5.5758E 01	5.7003E 01	5.8873E 01	3.3441E 01	3.6469E 01	3.6089E 01	3.6928E 01
120.0	3.9449E 01	6.0379E 01	6.2763E 01	6.4165E 01	6.6260E 01	3.7760E 01	4.1166E 01	4.0747E 01	4.1684E 01
130.0	4.4013E 01	6.7221E 01	6.9864E 01	7.1424E 01	7.3747E 01	4.2155E 01	4.5944E 01	4.5485E 01	4.6522E 01
140.0	4.8638E 01	7.4138E 01	7.7043E 01	7.8761E 01	8.1313E 01	4.6615E 01	5.0791E 01	5.0290E 01	5.1428E 01
150.0	5.3316E 01	8.1115E 01	8.4284E 01	8.6159E 01	8.8945E 01	5.1129E 01	5.5694E 01	5.5152E 01	5.6393E 01
160.0	5.8037E 01	8.8139E 01	9.1575E 01	9.3607E 01	9.6630E 01	5.5688E 01	6.0646E 01	6.0061E 01	6.1407E 01
170.0	6.2795E 01	9.5201E 01	9.8905E 01	1.0109E 02	1.0436E 02	6.0287E 01	6.5639E 01	6.5011E 01	6.6462E 01
180.0	6.7583E 01	1.0229E 02	1.0627E 02	1.0861E 02	1.1212E 02	6.4917E 01	7.0665E 01	6.9994E 01	7.1551E 01
190.0	7.2397E 01	1.0941E 02	1.1365E 02	1.1615E 02	1.1991E 02	6.9576E 01	7.5721E 01	7.5005E 01	7.6670E 01
200.0	7.7233E 01	1.1654E 02	1.2106E 02	1.2370E 02	1.2772E 02	7.4258E 01	8.0801E 01	8.0040E 01	8.1813E 01
220.0	8.6956E 01	1.3085E 02	1.3590E 02	1.3885E 02	1.4337E 02	8.3677E 01	9.1018E 01	9.0167E 01	9.2158E 01
240.0	9.6728E 01	1.4518E 02	1.5076E 02	1.5403E 02	1.5906E 02	9.3153E 01	1.0129E 02	1.0035E 02	1.0256E 02
260.0	1.0653E 02	1.5951E 02	1.6563E 02	1.6920E 02	1.7475E 02	1.0267E 02	1.1160E 02	1.1057E 02	1.1300E 02
280.0	1.1636E 02	1.7383E 02	1.8048E 02	1.8436E 02	1.9042E 02	1.1221E 02	1.2194E 02	1.2081E 02	1.2347E 02
300.0	1.2620E 02	1.8812E 02	1.9531E 02	1.9949E 02	2.0607E 02	1.2176E 02	1.3229E 02	1.3106E 02	1.3395E 02
320.0	1.3604E 02	2.0239E 02	2.1011E 02	2.1459E 02	2.2169E 02	1.3132E 02	1.4264E 02	1.4132E 02	1.4443E 02
340.0	1.4588E 02	2.1662E 02	2.2487E 02	2.2964E 02	2.3726E 02	1.4088E 02	1.5300E 02	1.5158E 02	1.5491E 02
360.0	1.5571E 02	2.3082E 02	2.3958E 02	2.4465E 02	2.5279E 02	1.5044E 02	1.6335E 02	1.6183E 02	1.6539E 02
380.0	1.6553E 02	2.4497E 02	2.5425E 02	2.5961E 02	2.6827E 02	1.6000E 02	1.7369E 02	1.7208E 02	1.7586E 02
400.0	1.7534E 02	2.5907E 02	2.6887E 02	2.7452E 02	2.8370E 02	1.6954E 02	1.8402E 02	1.8231E 02	1.8632E 02
420.0	1.8514E 02	2.7313E 02	2.8344E 02	2.8938E 02	2.9907E 02	1.7908E 02	1.9433E 02	1.9252E 02	1.9676E 02
440.0	1.9493E 02	2.8715E 02	2.9797E 02	3.0419E 02	3.1439E 02	1.8860E 02	2.0463E 02	2.0272E 02	2.0719E 02
460.0	2.0469E 02	3.0112E 02	3.1244E 02	3.1894E 02	3.2966E 02	1.9810E 02	2.1491E 02	2.1291E 02	2.1760E 02
480.0	2.1444E 02	3.1504E 02	3.2686E 02	3.3364E 02	3.4487E 02	2.0759E 02	2.2518E 02	2.2307E 02	2.2799E 02
500.0	2.2418E 02	3.2892E 02	3.4124E 02	3.4829E 02	3.6004E 02	2.1707E 02	2.3542E 02	2.3322E 02	2.3837E 02
520.0	2.3389E 02	3.4275E 02	3.5556E 02	3.6288E 02	3.7514E 02	2.2652E 02	2.4565E 02	2.4334E 02	2.4872E 02
540.0	2.4359E 02	3.5654E 02	3.6984E 02	3.7743E 02	3.9020E 02	2.3596E 02	2.5586E 02	2.5345E 02	2.5906E 02
560.0	2.5326E 02	3.7028E 02	3.8407E 02	3.9193E 02	4.0520E 02	2.4539E 02	2.6604E 02	2.6353E 02	2.6937E 02
580.0	2.6292E 02	3.8398E 02	3.9826E 02	4.0637E 02	4.2016E 02	2.5480E 02	2.7621E 02	2.7360E 02	2.7967E 02
600.0	2.7257E 02	3.9763E 02	4.1240E 02	4.2077E 02	4.3506E 02	2.6418E 02	2.8636E 02	2.8365E 02	2.8994E 02
620.0	2.8219E 02	4.1125E 02	4.2649E 02	4.3512E 02	4.4992E 02	2.7356E 02	2.9649E 02	2.9368E 02	3.0020E 02
640.0	2.9180E 02	4.2482E 02	4.4054E 02	4.4943E 02	4.6473E 02	2.8291E 02	3.0660E 02	3.0368E 02	3.1043E 02
660.0	3.0138E 02	4.3836E 02	4.5455E 02	4.6369E 02	4.7949E 02	2.9225E 02	3.1669E 02	3.1367E 02	3.2065E 02
680.0	3.1095E 02	4.5185E 02	4.6852E 02	4.7790E 02	4.9420E 02	3.0157E 02	3.2676E 02	3.2364E 02	3.3084E 02
700.0	3.2051E 02	4.6531E 02	4.8244E 02	4.9207E 02	5.0888E 02	3.1088E 02	3.3681E 02	3.3359E 02	3.4102E 02
720.0	3.3004E 02	4.7873E 02	4.9633E 02	5.0620E 02	5.2350E 02	3.2016E 02	3.4684E 02	3.4352E 02	3.5118E 02
740.0	3.3956E 02	4.9211E 02	5.1018E 02	5.2029E 02	5.3809E 02	3.2943E 02	3.5686E 02	3.5343E 02	3.6132E 02
760.0	3.4906E 02	5.0545E 02	5.2399E 02	5.3434E 02	5.5263E 02	3.3869E 02	3.6686E 02	3.6333E 02	3.7144E 02
780.0	3.5855E 02	5.1876E 02	5.3776E 02	5.4835E 02	5.6714E 02	3.4793E 02	3.7684E 02	3.7320E 02	3.8155E 02
800.0	3.6802E 02	5.3204E 02	5.5149E 02	5.6232E 02	5.8160E 02	3.5715E 02	3.8680E 02	3.8306E 02	3.9163E 02
820.0	3.7747E 02	5.4528E 02	5.6519E 02	5.7625E 02	5.9602E 02	3.6636E 02	3.9674E 02	3.9290E 02	4.0170E 02
840.0	3.8691E 02	5.5849E 02	5.7886E 02	5.9014E 02	6.1041E 02	3.7555E 02	4.0667E 02	4.0273E 02	4.1175E 02
860.0	3.9633E 02	5.7167E 02	5.9249E 02	6.0400E 02	6.2476E 02	3.8473E 02	4.1658E 02	4.1254E 02	4.2178E 02
880.0	4.0574E 02	5.8482E 02	6.0608E 02	6.1782E 02	6.3907E 02	3.9389E 02	4.2647E 02	4.2233E 02	4.3180E 02
900.0	4.1513E 02	5.9793E 02	6.1965E 02	6.3161E 02	6.5334E 02	4.0304E 02	4.3635E 02	4.3210E 02	4.4180E 02
920.0	4.2451E 02	6.1102E 02	6.3318E 02	6.4536E 02	6.6758E 02	4.1218E 02	4.4621E 02	4.4186E 02	4.5179E 02
940.0	4.3387E 02	6.2408E 02	6.4668E 02	6.5908E 02	6.8179E 02	4.2130E 02	4.5606E 02	4.5160E 02	4.6175E 02
960.0	4.4322E 02	6.3710E 02	6.6015E 02	6.7277E 02	6.9596E 02	4.3040E 02	4.6589E 02	4.6133E 02	4.7171E 02
980.0	4.5256E 02	6.5010E 02	6.7359E 02	6.8643E 02	7.1010E 02	4.3949E 02	4.7571E 02	4.7104E 02	4.8164E 02
1000.0	4.6188E 02	6.6307E 02	6.8701E 02	7.0006E 02	7.2421E 02	4.4857E 02	4.8551E 02	4.8074E 02	4.9157E 02
1200.0	5.5440E 02	7.9139E 02	8.1963E 02	8.3473E 02	8.6365E 02	5.3868E 02	5.8275E 02	5.7694E 02	5.9002E 02
1400.0	6.4580E 02	9.1746E 02	9.4989E 02	9.6688E 02	1.0005E 03	6.2766E 02	6.7876E 02	6.7190E 02	6.8722E 02
1600.0	7.3623E 02	1.0417E 03	1.0782E 03	1.0969E 03	1.1351E 03	7.1568E 02	7.7371E 02	7.6580E 02	7.8334E 02
2000.0	9.1467E 02	1.2854E 03	1.3298E 03	1.3518E 03	1.3990E 03	8.8931E 02	9.6096E 02	9.5095E 02	9.7289E 02
2400.0	1.0905E 03	1.5243E 03	1.5762E 03	1.6012E 03	1.6571E 03	1.0603E 03	1.1453E 03	1.1332E 03	1.1595E 03
2800.0	1.2641E 03	1.7591E 03	1.8185E 03	1.8461E 03	1.9106E 03	1.2292E 03	1.3273E 03	1.3131E 03	1.3438E 03
3200.0	1.4360E 03	1.9908E 03	2.0573E 03	2.0873E 03	2.1603E 03	1.3962E 03	1.5074E 03	1.4911E 03	1.5260E 03
3600.0	1.6064E 03	2.2197E 03	2.2933E 03	2.3255E 03	2.4069E 03	1.5618E 03	1.6858E 03	1.6674E 03	1.7066E 03
4000.0	1.7754E 03	2.4462E 03	2.5267E 03	2.5611E 03	2.6506E 03	1.7260E 03	1.8628E 03	1.8423E 03	1.8857E 03
5000.0	2.1930E 03	3.0039E 03	3.1013E 03	3.1405E 03	3.2500E 03	2.1316E 03	2.2999E 03	2.2742E 03	2.3281E 03

PRINTOUT TABLE IV

STOPPING-POWER AND RANGE TABLE FOR PROTONS

Stopping powers (Mev/g cm^{-2}) and ranges (g cm^{-2}) for protons in various substances. The density effect correction is not included. Powers of ten are indicated by the symbol E; thus 1.2345E 02 means 1.2345×10^2. Because of typographical limitations, the adjusted mean excitation energy, I_{adj}, is indicated by the symbol I in the table headings; its units are ev. More figures are tabulated than are significant in order to facilitate interpolation and differencing. Freon 1, C_3F_8; Freon 2, C_2F_5Cl; Freon 3, CF_3BR. Assumed composition by weight: Bone, 0.064 H, 0.278 C, 0.027 N, 0.410 O, 0.002 Mg, 0.070 P, 0.002 S, 0.147 Ca; muscle, 0.1020 H, 0.1230 C, 0.0350 N, 0.7290 O, 0.0008 Na, 0.0002 Mg, 0.0020 P, 0.0050 S, 0.0030 K; concrete, 0.0056 H, 0.4983 O, 0.0171 Na, 0.0024 Mg, 0.0456 Al, 0.3158 Si, 0.0012 S, 0.0192 K, 0.0826 Ca, 0.0122 Fe.

PROTON STOPPING POWER, MEV•CM2/G

ENERGY MEV	PROPANE I= 50.3	FREON 1 I=111.9	FREON 2 I=127.1	FREON 3 I=208.2	MYLAR I= 72.6	QUARTZ I=121.0	CONCRETE I=124.2	MUSCLE I= 66.2	BONE I= 85.2
2.0	1.9227E 02	1.2611E 02	1.2132E 02	9.7646E 01	1.5510E 02	1.2841E 02	1.2762E 02	1.6787E 02	1.5131E 02
4.0	1.1217E 02	7.5655E 01	7.3179E 01	6.0314E 01	9.1529E 01	7.7292E 01	7.6902E 01	9.8762E 01	8.9804E 01
6.0	7.9978E 01	5.4318E 01	5.2655E 01	4.3893E 01	6.5375E 01	5.5566E 01	5.5311E 01	7.0495E 01	6.4240E 01
8.0	6.2302E 01	4.2810E 01	4.1619E 01	3.5116E 01	5.1153E 01	4.3900E 01	4.3719E 01	5.5089E 01	5.0370E 01
10.0	5.1959E 01	3.6343E 01	3.5439E 01	3.0235E 01	4.3009E 01	3.7356E 01	3.7222E 01	4.6224E 01	4.2490E 01
14.0	3.9458E 01	2.7869E 01	2.7226E 01	2.3402E 01	3.2785E 01	2.8667E 01	2.8575E 01	3.5197E 01	3.2455E 01
18.0	3.2106E 01	2.2824E 01	2.2325E 01	1.9290E 01	2.6744E 01	2.3490E 01	2.3421E 01	2.8691E 01	2.6511E 01
22.0	2.7229E 01	1.9448E 01	1.9040E 01	1.6517E 01	2.2723E 01	2.0024E 01	1.9969E 01	2.4365E 01	2.2548E 01
26.0	2.3742E 01	1.7019E 01	1.6673E 01	1.4510E 01	1.9842E 01	1.7528E 01	1.7483E 01	2.1267E 01	1.9705E 01
30.0	2.1118E 01	1.5182E 01	1.4882E 01	1.2985E 01	1.7669E 01	1.5641E 01	1.5603E 01	1.8933E 01	1.7558E 01
34.0	1.9068E 01	1.3741E 01	1.3475E 01	1.1783E 01	1.5969E 01	1.4159E 01	1.4126E 01	1.7107E 01	1.5877E 01
38.0	1.7419E 01	1.2578E 01	1.2339E 01	1.0810E 01	1.4600E 01	1.2963E 01	1.2934E 01	1.5637E 01	1.4523E 01
42.0	1.6063E 01	1.1618E 01	1.1402E 01	1.0005E 01	1.3473E 01	1.1977E 01	1.1951E 01	1.4427E 01	1.3407E 01
46.0	1.4927E 01	1.0813E 01	1.0615E 01	9.3271E 00	1.2528E 01	1.1149E 01	1.1125E 01	1.3413E 01	1.2470E 01
50.0	1.3960E 01	1.0127E 01	9.9436E 00	8.7479E 00	1.1723E 01	1.0442E 01	1.0421E 01	1.2549E 01	1.1673E 01
60.0	1.2074E 01	8.7827E 00	8.6287E 00	7.6104E 00	1.0151E 01	9.0592E 00	9.0420E 00	1.0863E 01	1.0113E 01
70.0	1.0696E 01	7.7976E 00	7.6641E 00	6.7731E 00	9.0008E 00	8.0451E 00	8.0305E 00	9.6299E 00	8.9717E 00
80.0	9.6438E 00	7.0431E 00	6.9249E 00	6.1297E 00	8.1213E 00	7.2681E 00	7.2555E 00	8.6872E 00	8.0983E 00
90.0	8.8127E 00	6.4459E 00	6.3396E 00	5.6192E 00	7.4262E 00	6.6530E 00	6.6419E 00	7.9423E 00	7.4076E 00
100.0	8.1392E 00	5.9611E 00	5.8643E 00	5.2039E 00	6.8624E 00	6.1535E 00	6.1436E 00	7.3383E 00	6.8472E 00
110.0	7.5821E 00	5.5595E 00	5.4704E 00	4.8591E 00	6.3958E 00	5.7396E 00	5.7307E 00	6.8385E 00	6.3832E 00
120.0	7.1134E 00	5.2211E 00	5.1384E 00	4.5683E 00	6.0030E 00	5.3909E 00	5.3827E 00	6.4178E 00	5.9925E 00
130.0	6.7134E 00	4.9321E 00	4.8547E 00	4.3194E 00	5.6677E 00	5.0930E 00	5.0854E 00	6.0587E 00	5.6588E 00
140.0	6.3682E 00	4.6822E 00	4.6096E 00	4.1042E 00	5.3781E 00	4.8354E 00	4.8284E 00	5.7486E 00	5.3706E 00
150.0	6.0670E 00	4.4642E 00	4.3955E 00	3.9160E 00	5.1254E 00	4.6106E 00	4.6041E 00	5.4780E 00	5.1191E 00
160.0	5.8020E 00	4.2721E 00	4.2069E 00	3.7502E 00	4.9030E 00	4.4126E 00	4.4065E 00	5.2399E 00	4.8976E 00
170.0	5.5670E 00	4.1017E 00	4.0395E 00	3.6029E 00	4.7057E 00	4.2368E 00	4.2311E 00	5.0287E 00	4.7012E 00
180.0	5.3572E 00	3.9494E 00	3.8900E 00	3.4712E 00	4.5295E 00	4.0798E 00	4.0744E 00	4.8401E 00	4.5257E 00
190.0	5.1688E 00	3.8126E 00	3.7556E 00	3.3528E 00	4.3712E 00	3.9387E 00	3.9335E 00	4.6707E 00	4.3681E 00
200.0	4.9986E 00	3.6890E 00	3.6342E 00	3.2457E 00	4.2282E 00	3.8112E 00	3.8063E 00	4.5176E 00	4.2256E 00
220.0	4.7035E 00	3.4744E 00	3.4234E 00	3.0598E 00	3.9801E 00	3.5899E 00	3.5854E 00	4.2522E 00	3.9785E 00
240.0	4.4565E 00	3.2946E 00	3.2468E 00	2.9039E 00	3.7724E 00	3.4045E 00	3.4003E 00	4.0299E 00	3.7716E 00
260.0	4.2468E 00	3.1420E 00	3.0968E 00	2.7714E 00	3.5961E 00	3.2470E 00	3.2431E 00	3.8412E 00	3.5958E 00
280.0	4.0666E 00	3.0108E 00	2.9678E 00	2.6574E 00	3.4446E 00	3.1117E 00	3.1080E 00	3.6791E 00	3.4448E 00
300.0	3.9104E 00	2.8969E 00	2.8559E 00	2.5585E 00	3.3131E 00	2.9942E 00	2.9907E 00	3.5384E 00	3.3138E 00
320.0	3.7736E 00	2.7972E 00	2.7579E 00	2.4718E 00	3.1980E 00	2.8913E 00	2.8881E 00	3.4153E 00	3.1990E 00
340.0	3.6529E 00	2.7092E 00	2.6714E 00	2.3954E 00	3.0965E 00	2.8005E 00	2.7975E 00	3.3067E 00	3.0978E 00
360.0	3.5458E 00	2.6311E 00	2.5947E 00	2.3275E 00	3.0064E 00	2.7200E 00	2.7170E 00	3.2102E 00	3.0080E 00
380.0	3.4502E 00	2.5614E 00	2.5261E 00	2.2668E 00	2.9259E 00	2.6480E 00	2.6452E 00	3.1241E 00	2.9277E 00
400.0	3.3643E 00	2.4987E 00	2.4645E 00	2.2123E 00	2.8536E 00	2.5833E 00	2.5806E 00	3.0468E 00	2.8557E 00
420.0	3.2868E 00	2.4422E 00	2.4089E 00	2.1631E 00	2.7884E 00	2.5250E 00	2.5224E 00	2.9770E 00	2.7906E 00
440.0	3.2165E 00	2.3910E 00	2.3586E 00	2.1186E 00	2.7293E 00	2.4722E 00	2.4697E 00	2.9130E 00	2.7317E 00
460.0	3.1527E 00	2.3444E 00	2.3128E 00	2.0781E 00	2.6755E 00	2.4242E 00	2.4217E 00	2.8563E 00	2.6781E 00
480.0	3.0944E 00	2.3019E 00	2.2711E 00	2.0411E 00	2.6265E 00	2.3803E 00	2.3780E 00	2.8038E 00	2.6293E 00
500.0	3.0410E 00	2.2630E 00	2.2328E 00	2.0073E 00	2.5816E 00	2.3402E 00	2.3379E 00	2.7557E 00	2.5845E 00
520.0	2.9920E 00	2.2273E 00	2.1977E 00	1.9763E 00	2.5403E 00	2.3033E 00	2.3011E 00	2.7116E 00	2.5434E 00
540.0	2.9468E 00	2.1944E 00	2.1654E 00	1.9477E 00	2.5024E 00	2.2694E 00	2.2672E 00	2.6710E 00	2.5055E 00
560.0	2.9052E 00	2.1641E 00	2.1355E 00	1.9213E 00	2.4673E 00	2.2381E 00	2.2360E 00	2.6335E 00	2.4706E 00
580.0	2.8666E 00	2.1360E 00	2.1079E 00	1.8969E 00	2.4349E 00	2.2091E 00	2.2071E 00	2.5988E 00	2.4383E 00
600.0	2.8308E 00	2.1099E 00	2.0824E 00	1.8743E 00	2.4048E 00	2.1822E 00	2.1803E 00	2.5666E 00	2.4083E 00
620.0	2.7976E 00	2.0858E 00	2.0586E 00	1.8533E 00	2.3769E 00	2.1573E 00	2.1554E 00	2.5367E 00	2.3805E 00
640.0	2.7667E 00	2.0633E 00	2.0365E 00	1.8338E 00	2.3509E 00	2.1341E 00	2.1322E 00	2.5089E 00	2.3546E 00
660.0	2.7378E 00	2.0423E 00	2.0159E 00	1.8156E 00	2.3267E 00	2.1125E 00	2.1106E 00	2.4829E 00	2.3304E 00
680.0	2.7109E 00	2.0228E 00	1.9967E 00	1.7987E 00	2.3040E 00	2.0923E 00	2.0905E 00	2.4587E 00	2.3079E 00
700.0	2.6857E 00	2.0045E 00	1.9787E 00	1.7828E 00	2.2829E 00	2.0735E 00	2.0717E 00	2.4361E 00	2.2868E 00
720.0	2.6621E 00	1.9874E 00	1.9619E 00	1.7680E 00	2.2631E 00	2.0558E 00	2.0541E 00	2.4149E 00	2.2671E 00
740.0	2.6400E 00	1.9713E 00	1.9462E 00	1.7541E 00	2.2445E 00	2.0393E 00	2.0375E 00	2.3950E 00	2.2486E 00
760.0	2.6192E 00	1.9563E 00	1.9314E 00	1.7411E 00	2.2270E 00	2.0237E 00	2.0221E 00	2.3763E 00	2.2312E 00
780.0	2.5997E 00	1.9421E 00	1.9175E 00	1.7289E 00	2.2107E 00	2.0092E 00	2.0075E 00	2.3588E 00	2.2149E 00
800.0	2.5813E 00	1.9288E 00	1.9044E 00	1.7174E 00	2.1952E 00	1.9954E 00	1.9938E 00	2.3423E 00	2.1996E 00
820.0	2.5640E 00	1.9163E 00	1.8922E 00	1.7066E 00	2.1807E 00	1.9825E 00	1.9809E 00	2.3267E 00	2.1851E 00
840.0	2.5477E 00	1.9045E 00	1.8806E 00	1.6964E 00	2.1671E 00	1.9704E 00	1.9688E 00	2.3121E 00	2.1715E 00
860.0	2.5323E 00	1.8934E 00	1.8697E 00	1.6869E 00	2.1541E 00	1.9589E 00	1.9574E 00	2.2982E 00	2.1586E 00
880.0	2.5177E 00	1.8829E 00	1.8594E 00	1.6778E 00	2.1420E 00	1.9481E 00	1.9466E 00	2.2852E 00	2.1465E 00
900.0	2.5040E 00	1.8730E 00	1.8497E 00	1.6693E 00	2.1304E 00	1.9379E 00	1.9364E 00	2.2729E 00	2.1351E 00
920.0	2.4909E 00	1.8636E 00	1.8405E 00	1.6612E 00	2.1196E 00	1.9282E 00	1.9268E 00	2.2612E 00	2.1242E 00
940.0	2.4786E 00	1.8547E 00	1.8318E 00	1.6536E 00	2.1093E 00	1.9191E 00	1.9177E 00	2.2502E 00	2.1140E 00
960.0	2.4670E 00	1.8464E 00	1.8236E 00	1.6465E 00	2.0995E 00	1.9105E 00	1.9090E 00	2.2397E 00	2.1043E 00
980.0	2.4559E 00	1.8384E 00	1.8158E 00	1.6397E 00	2.0903E 00	1.9023E 00	1.9009E 00	2.2298E 00	2.0951E 00
1000.0	2.4454E 00	1.8309E 00	1.8084E 00	1.6332E 00	2.0815E 00	1.8946E 00	1.8932E 00	2.2204E 00	2.0864E 00

PROTON RANGE, G/CM2

ENERGY MEV	PROPANE I= 50.3	FREON 1 I=111.9	FREON 2 I=127.1	FREON 3 I=208.2	MYLAR I= 72.6	QUARTZ I=121.0	CONCRETE I=124.2	MUSCLE I= 66.2	BONE I= 85.2
2.0	6.1986E-03	9.9738E-03	1.0456E-02	1.3422E-02	7.8778E-03	9.8467E-03	9.9251E-03	7.2334E-03	8.1624E-03
4.0	2.0352E-02	3.1159E-02	3.2403E-02	4.0294E-02	2.5287E-02	3.0609E-02	3.0801E-02	2.3351E-02	2.5942E-02
6.0	4.1781E-02	6.2788E-02	6.5060E-02	7.9660E-02	5.1514E-02	6.1544E-02	6.1885E-02	4.7668E-02	5.2647E-02
8.0	7.0345E-02	1.0481E-01	1.0838E-01	1.3143E-01	8.6470E-02	1.0261E-01	1.0313E-01	8.0086E-02	8.8212E-02
10.0	1.0566E-01	1.5550E-01	1.6040E-01	1.9259E-01	1.2920E-01	1.5194E-01	1.5265E-01	1.1983E-01	1.3150E-01
14.0	1.9495E-01	2.8247E-01	2.9048E-01	3.4442E-01	2.3685E-01	2.7542E-01	2.7655E-01	2.2005E-01	2.4034E-01
18.0	3.0802E-01	4.4198E-01	4.5365E-01	5.3372E-01	3.7274E-01	4.3045E-01	4.3205E-01	3.4668E-01	3.7751E-01
22.0	4.4383E-01	6.3254E-01	6.4838E-01	7.5861E-01	5.3562E-01	6.1556E-01	6.1769E-01	4.9854E-01	5.4173E-01
26.0	6.0158E-01	8.5297E-01	8.7346E-01	1.0176E 00	7.2450E-01	8.2963E-01	8.3232E-01	6.7473E-01	7.3200E-01
30.0	7.8057E-01	1.1023E 00	1.1279E 00	1.3096E 00	9.3855E-01	1.0717E 00	1.0750E 00	8.7447E-01	9.4747E-01
34.0	9.8021E-01	1.3796E 00	1.4108E 00	1.6334E 00	1.1770E 00	1.3409E 00	1.3448E 00	1.0971E 00	1.1874E 00
38.0	1.2000E 00	1.6843E 00	1.7213E 00	1.9882E 00	1.4393E 00	1.6364E 00	1.6411E 00	1.3419E 00	1.4511E 00
42.0	1.4393E 00	2.0155E 00	2.0589E 00	2.3732E 00	1.7248E 00	1.9578E 00	1.9631E 00	1.6085E 00	1.7381E 00
46.0	1.6978E 00	2.3726E 00	2.4227E 00	2.7876E 00	2.0329E 00	2.3042E 00	2.3103E 00	1.8963E 00	2.0477E 00
50.0	1.9751E 00	2.7551E 00	2.8123E 00	3.2307E 00	2.3632E 00	2.6752E 00	2.6820E 00	2.2048E 00	2.3794E 00
60.0	2.7478E 00	3.8188E 00	3.8953E 00	4.4600E 00	3.2828E 00	3.7065E 00	3.7154E 00	3.0640E 00	3.3027E 00
70.0	3.6298E 00	5.0299E 00	5.1277E 00	5.8559E 00	4.3314E 00	4.8805E 00	4.8915E 00	4.0440E 00	4.3549E 00
80.0	4.6161E 00	6.3816E 00	6.5027E 00	7.4104E 00	5.5030E 00	6.1904E 00	6.2038E 00	5.1391E 00	5.5301E 00
90.0	5.7023E 00	7.8676E 00	8.0139E 00	9.1164E 00	6.7923E 00	7.6304E 00	7.6462E 00	6.3446E 00	6.8229E 00
100.0	6.8843E 00	9.4825E 00	9.6556E 00	1.0968E 01	8.1946E 00	9.1949E 00	9.2133E 00	7.6559E 00	8.2285E 00
110.0	8.1583E 00	1.1221E 01	1.1423E 01	1.2958E 01	9.7053E 00	1.0879E 01	1.0900E 01	9.0687E 00	9.7424E 00
120.0	9.5209E 00	1.3078E 01	1.3310E 01	1.5082E 01	1.1320E 01	1.2678E 01	1.2702E 01	1.0579E 01	1.1360E 01
130.0	1.0969E 01	1.5050E 01	1.5313E 01	1.7334E 01	1.3036E 01	1.4588E 01	1.4614E 01	1.2184E 01	1.3079E 01
140.0	1.2499E 01	1.7132E 01	1.7428E 01	1.9710E 01	1.4848E 01	1.6604E 01	1.6633E 01	1.3879E 01	1.4894E 01
150.0	1.4109E 01	1.9320E 01	1.9651E 01	2.2206E 01	1.6753E 01	1.8722E 01	1.8755E 01	1.5662E 01	1.6802E 01
160.0	1.5795E 01	2.1611E 01	2.1977E 01	2.4816E 01	1.8749E 01	2.0940E 01	2.0976E 01	1.7529E 01	1.8799E 01
170.0	1.7555E 01	2.4001E 01	2.4404E 01	2.7538E 01	2.0832E 01	2.3254E 01	2.3293E 01	1.9478E 01	2.0884E 01
180.0	1.9386E 01	2.6486E 01	2.6927E 01	3.0366E 01	2.2998E 01	2.5660E 01	2.5702E 01	2.1505E 01	2.3053E 01
190.0	2.1287E 01	2.9064E 01	2.9544E 01	3.3298E 01	2.5246E 01	2.8155E 01	2.8200E 01	2.3609E 01	2.5302E 01
200.0	2.3255E 01	3.1731E 01	3.2252E 01	3.6330E 01	2.7573E 01	3.0737E 01	3.0785E 01	2.5787E 01	2.7631E 01
220.0	2.7383E 01	3.7322E 01	3.7926E 01	4.2681E 01	3.2452E 01	3.6148E 01	3.6204E 01	3.0353E 01	3.2512E 01
240.0	3.1754E 01	4.3237E 01	4.3929E 01	4.9395E 01	3.7617E 01	4.1872E 01	4.1935E 01	3.5188E 01	3.7679E 01
260.0	3.6354E 01	4.9456E 01	5.0240E 01	5.6449E 01	4.3050E 01	4.7891E 01	4.7961E 01	4.0274E 01	4.3112E 01
280.0	4.1169E 01	5.5962E 01	5.6840E 01	6.3822E 01	4.8735E 01	5.4186E 01	5.4263E 01	4.5597E 01	4.8797E 01
300.0	4.6186E 01	6.2736E 01	6.3712E 01	7.1495E 01	5.4657E 01	6.0740E 01	6.0826E 01	5.1142E 01	5.4719E 01
320.0	5.1394E 01	6.9765E 01	7.0841E 01	7.9450E 01	6.0804E 01	6.7540E 01	6.7633E 01	5.6897E 01	6.0864E 01
340.0	5.6783E 01	7.7032E 01	7.8211E 01	8.7672E 01	6.7161E 01	7.4571E 01	7.4671E 01	6.2850E 01	6.7219E 01
360.0	6.2341E 01	8.4525E 01	8.5810E 01	9.6144E 01	7.3718E 01	8.1819E 01	8.1927E 01	6.8990E 01	7.3772E 01
380.0	6.8061E 01	9.2230E 01	9.3623E 01	1.0485E 02	8.0462E 01	8.9273E 01	8.9389E 01	7.5307E 01	8.0513E 01
400.0	7.3932E 01	1.0014E 02	1.0164E 02	1.1379E 02	8.7385E 01	9.6921E 01	9.7046E 01	8.1791E 01	8.7432E 01
420.0	7.9948E 01	1.0824E 02	1.0985E 02	1.2293E 02	9.4477E 01	1.0475E 02	1.0489E 02	8.8433E 01	9.4518E 01
440.0	8.6100E 01	1.1651E 02	1.1824E 02	1.3227E 02	1.0173E 02	1.1276E 02	1.1290E 02	9.5225E 01	1.0176E 02
460.0	9.2381E 01	1.2496E 02	1.2681E 02	1.4181E 02	1.0913E 02	1.2093E 02	1.2108E 02	1.0216E 02	1.0916E 02
480.0	9.8785E 01	1.3357E 02	1.3553E 02	1.5152E 02	1.1668E 02	1.2926E 02	1.2941E 02	1.0923E 02	1.1670E 02
500.0	1.0531E 02	1.4234E 02	1.4442E 02	1.6140E 02	1.2436E 02	1.3773E 02	1.3790E 02	1.1642E 02	1.2437E 02
520.0	1.1194E 02	1.5124E 02	1.5345E 02	1.7144E 02	1.3217E 02	1.4635E 02	1.4652E 02	1.2374E 02	1.3217E 02
540.0	1.1867E 02	1.6029E 02	1.6262E 02	1.8164E 02	1.4010E 02	1.5510E 02	1.5528E 02	1.3117E 02	1.4009E 02
560.0	1.2551E 02	1.6947E 02	1.7192E 02	1.9198E 02	1.4815E 02	1.6397E 02	1.6416E 02	1.3871E 02	1.4813E 02
580.0	1.3244E 02	1.7877E 02	1.8134E 02	2.0246E 02	1.5631E 02	1.7297E 02	1.7317E 02	1.4636E 02	1.5628E 02
600.0	1.3946E 02	1.8820E 02	1.9089E 02	2.1306E 02	1.6458E 02	1.8208E 02	1.8228E 02	1.5410E 02	1.6454E 02
620.0	1.4657E 02	1.9773E 02	2.0055E 02	2.2379E 02	1.7294E 02	1.9129E 02	1.9151E 02	1.6194E 02	1.7289E 02
640.0	1.5376E 02	2.0737E 02	2.1032E 02	2.3464E 02	1.8140E 02	2.0062E 02	2.0084E 02	1.6987E 02	1.8134E 02
660.0	1.6103E 02	2.1711E 02	2.2019E 02	2.4561E 02	1.8996E 02	2.1004E 02	2.1027E 02	1.7788E 02	1.8988E 02
680.0	1.6837E 02	2.2696E 02	2.3016E 02	2.5667E 02	1.9859E 02	2.1955E 02	2.1979E 02	1.8598E 02	1.9850E 02
700.0	1.7578E 02	2.3689E 02	2.4022E 02	2.6784E 02	2.0732E 02	2.2915E 02	2.2940E 02	1.9415E 02	2.0721E 02
720.0	1.8326E 02	2.4691E 02	2.5037E 02	2.7911E 02	2.1612E 02	2.3884E 02	2.3910E 02	2.0240E 02	2.1599E 02
740.0	1.9080E 02	2.5701E 02	2.6061E 02	2.9046E 02	2.2499E 02	2.4861E 02	2.4887E 02	2.1071E 02	2.2485E 02
760.0	1.9841E 02	2.6720E 02	2.7092E 02	3.0191E 02	2.3394E 02	2.5845E 02	2.5873E 02	2.1910E 02	2.3378E 02
780.0	2.0607E 02	2.7746E 02	2.8132E 02	3.1344E 02	2.4295E 02	2.6837E 02	2.6865E 02	2.2755E 02	2.4278E 02
800.0	2.1380E 02	2.8779E 02	2.9178E 02	3.2504E 02	2.5203E 02	2.7836E 02	2.7865E 02	2.3606E 02	2.5184E 02
820.0	2.2157E 02	2.9820E 02	3.0232E 02	3.3673E 02	2.6117E 02	2.8842E 02	2.8871E 02	2.4462E 02	2.6096E 02
840.0	2.2940E 02	3.0867E 02	3.1292E 02	3.4848E 02	2.7037E 02	2.9854E 02	2.9884E 02	2.5325E 02	2.7014E 02
860.0	2.3727E 02	3.1920E 02	3.2359E 02	3.6030E 02	2.7963E 02	3.0872E 02	3.0903E 02	2.6192E 02	2.7938E 02
880.0	2.4519E 02	3.2979E 02	3.3432E 02	3.7219E 02	2.8894E 02	3.1895E 02	3.1928E 02	2.7065E 02	2.8867E 02
900.0	2.5316E 02	3.4044E 02	3.4510E 02	3.8414E 02	2.9830E 02	3.2925E 02	3.2958E 02	2.7943E 02	2.9801E 02
920.0	2.6117E 02	3.5115E 02	3.5594E 02	3.9615E 02	3.0771E 02	3.3959E 02	3.3993E 02	2.8825E 02	3.0741E 02
940.0	2.6921E 02	3.6191E 02	3.6683E 02	4.0822E 02	3.1717E 02	3.4999E 02	3.5034E 02	2.9712E 02	3.1684E 02
960.0	2.7730E 02	3.7271E 02	3.7778E 02	4.2034E 02	3.2668E 02	3.6044E 02	3.6079E 02	3.0602E 02	3.2633E 02
980.0	2.8543E 02	3.8357E 02	3.8877E 02	4.3252E 02	3.3622E 02	3.7093E 02	3.7129E 02	3.1497E 02	3.3585E 02
1000.0	2.9359E 02	3.9447E 02	3.9981E 02	4.4474E 02	3.4581E 02	3.8146E 02	3.8183E 02	3.2396E 02	3.4542E 02

8. PASSAGE OF HEAVY IONS THROUGH MATTER II. RANGE-ENERGY CURVES[1]

Lee C. Northcliffe[2]

Abstract

Semi-empirical range-energy relationships are presented for heavy ions with energies up to 10 Mev/amu in various solid materials. Range-energy curves for He^4, B^{11}, C^{12}, N^{14}, O^{16}, F^{19}, and Ne^{20} ions in carbon, aluminum, nickel, silver, and gold calculated from smoothed semi-empirical stopping-power curves by numerical integration are compared with available range and energy-loss data and with other calculations. In addition, range-energy relationships in aluminum inferred from experimental energy-loss data for representative heavy ions in aluminum are presented for ions of various isotopes of helium, lithium, beryllium, boron, carbon, nitrogen, oxygen, fluorine, neon, sodium, magnesium, aluminum, and silver.

In the recent review article reprinted as Appendix B of this volume, an attempt was made to summarize and correlate various kinds of experimental information on the penetration of heavy ions through matter. In particular, the numerous data pertaining to the stopping power of certain solids (C, Al, Ni, Ag, Au) for ions of relatively low atomic number ($1 \leq Z \leq 10$) were presented and discussed with relative thoroughness. Range-energy relations also were discussed, but the presentation of range data was representative rather than comprehensive and included only a few of the many curves and numerical data needed by experimental physicists. The present report is prompted by the need for a comprehensive collection of heavy ion range-energy curves.

It seems reasonable to attempt the calculation of range values from the stopping-power curves of Appendix B by numerical integration of Equation 24 (in Appendix B). Such calculations are suggested and discussed in sections II. F. and III. D. 1 of Appendix B. Their validity is demonstrated in Figure 10 of Appendix B, which shows that a set of range-energy curves for C^{12} ions calculated by this method is in good agreement with the available experimental range and energy loss data. While the good agreement is not really surprising, it is welcomed as practical justification for further calculations of this type.

---

[1] This work, supported by the U. S. Atomic Energy Commission, is essentially a supplement to a review article by L. C. Northcliffe that was published in Annual Review of Nuclear Science (vol. 13, p. 69, 1963) and which is reprinted, with permission of Annual Reviews, Inc., as Appendix B of the present volume. The literature references already cited in the earlier article are designated by the same reference numbers in this paper; new references are numbered serially beginning with No. 124; and the figures are assigned numbers beginning with No. 12.

[2] Department of Physics, Yale University, New Haven, Conn.

A set of range-energy relations has been generated from the set of smoothed electronic stopping-power curves given in Figures 5-7 of Appendix B. Range values were obtained by numerical integration of Equation 24 of Appendix B and then corrected for the reduction expected as a consequence of "nuclear" stopping, the correction being that given by the theory of Lindhard, Scharff, and Schiøtt (38). The corrected range values are displayed graphically as solid lines in Figures 12-18 of the present paper. These curves are similar to those in Figure 10 of Appendix B in most respects, but differ in that the present curves have been corrected for nuclear stopping while those of Figure 10 were not. (Actually, this is the only difference between Figures 10 and 14.)

A few range-energy relations calculated elsewhere are available for comparison with these results. In the case of alpha particles, for example, range-energy relations have been calculated by Whaling (2) and by Aron, Hoffman, and Williams (125). Their curves can be seen in Figure 12. In those calculations, the stopping power for alpha particles was taken to be four times that for protons of the same velocity, and the reciprocal of the stopping power was integrated numerically to get the range. Aron, Hoffman, and Williams calculated the proton stopping power using the relativistic form of the Bethe formula (Equations 1, 3, and 6 of Appendix B) and the Bloch relation (Equation 7 of Appendix B), taking 11.5 ev for the value of the Bloch constant $K = I/Z$, while Whaling relied upon empirical proton stopping-power curves. In order to compensate for the range increase caused by partial charge-neutralization of the alpha particle, Whaling adjusted his calculated ranges to match the experimental values of Rosenblum (124) at 7.68 Mev ($\mathcal{E}_m = 1.92$ Mev/amu). Whaling's stopping-power curves are based on more recent and more accurate measurements, and therefore his range values are more reliable.

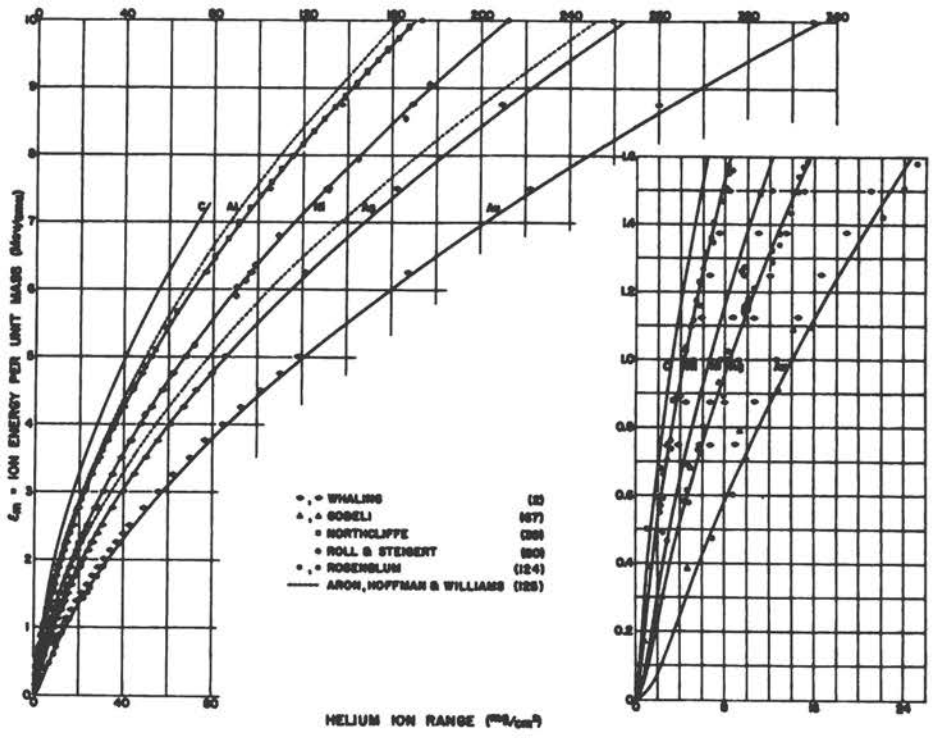

Figure 12. Range energy relations for He^4 ions in carbon, aluminum, nickel, silver, and gold. The solid lines were obtained by numerical integration from the smoothed stopping-power curves of Figure 5 (Appendix B). A correction for the effect of "nuclear" collisions has been applied.

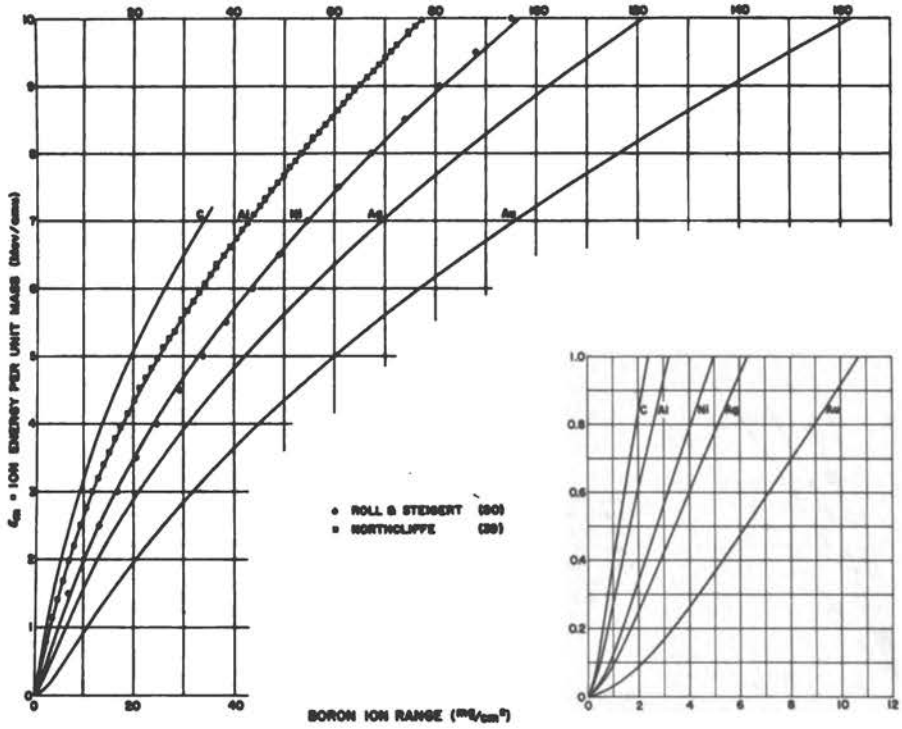

Figure 13. Range energy relations for B^{11} ions in carbon, aluminum, nickel, silver, and gold. The solid lines were obtained by numerical integration from the smoothed stopping-power curves of Figure 6 (Appendix B). A correction for the effect of "nuclear" collisions has been applied.

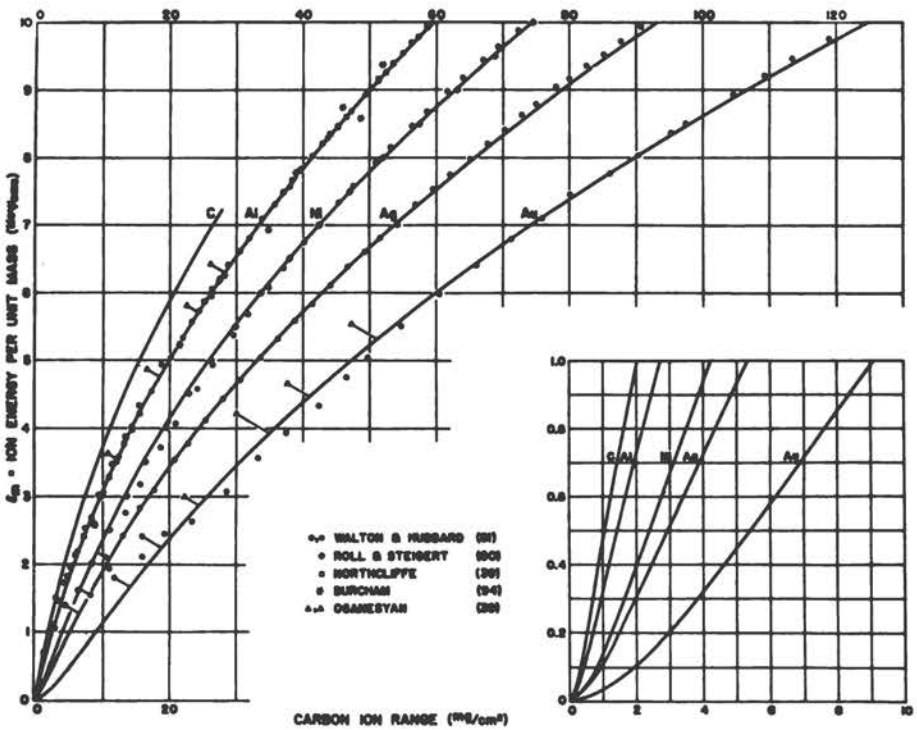

Figure 14. Range energy relations for C^{12} ions in carbon, aluminum, nickel, silver, and gold. The solid lines were obtained by numerical integration from the smoothed stopping-power curves of Figure 6 (Appendix B). A correction for the effect of "nuclear" collisions has been applied.

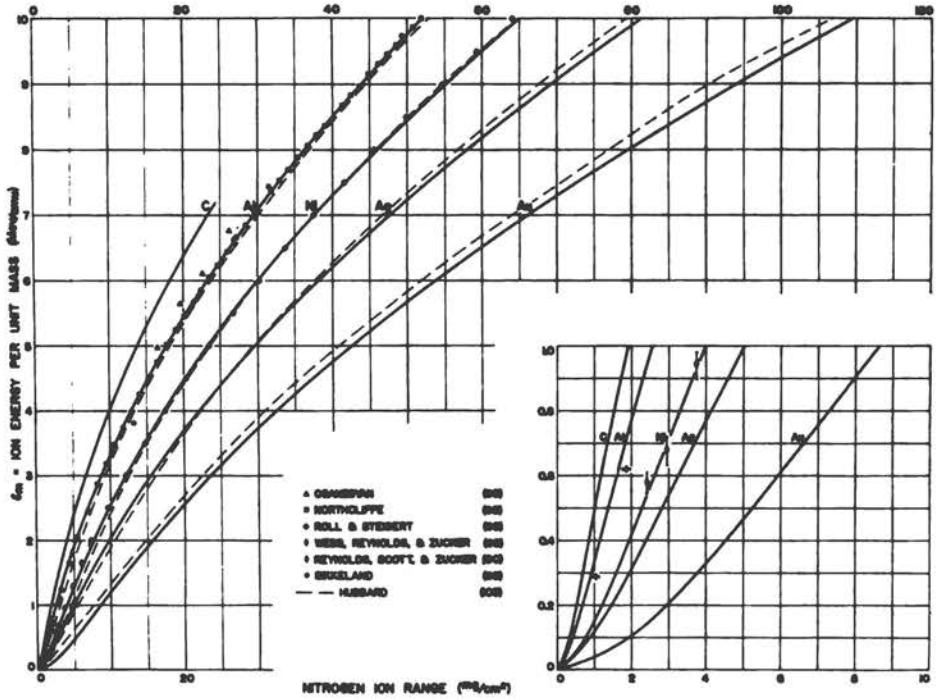

Figure 15. Range energy relations for N^{14} ions in carbon, aluminum, nickel, silver, and gold. The solid lines were obtained by numerical integration from the smoothed stopping-power curves of Figure 6 (Appendix B). A correction for the effect of "nuclear" collisions has been applied.

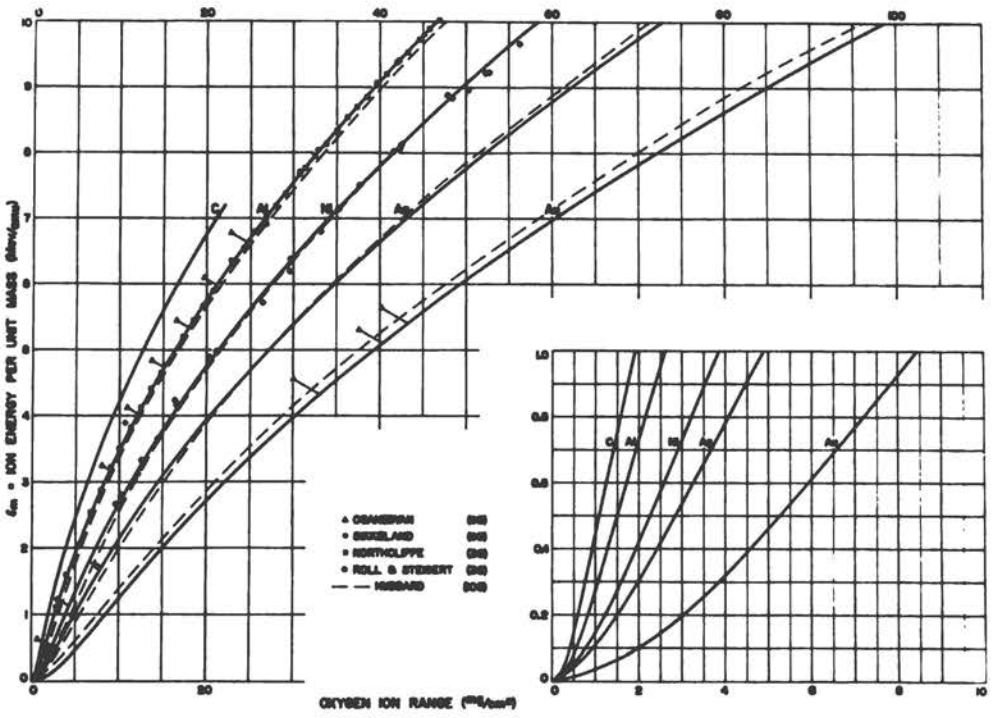

Figure 16. Range energy relations for O^{16} ions in carbon, aluminum, nickel, silver, and gold. The solid lines were obtained by numerical integration from the smoothed stopping-power curves of Figure 7 (Appendix B). A correction for the effect of "nuclear" collisions has been applied.

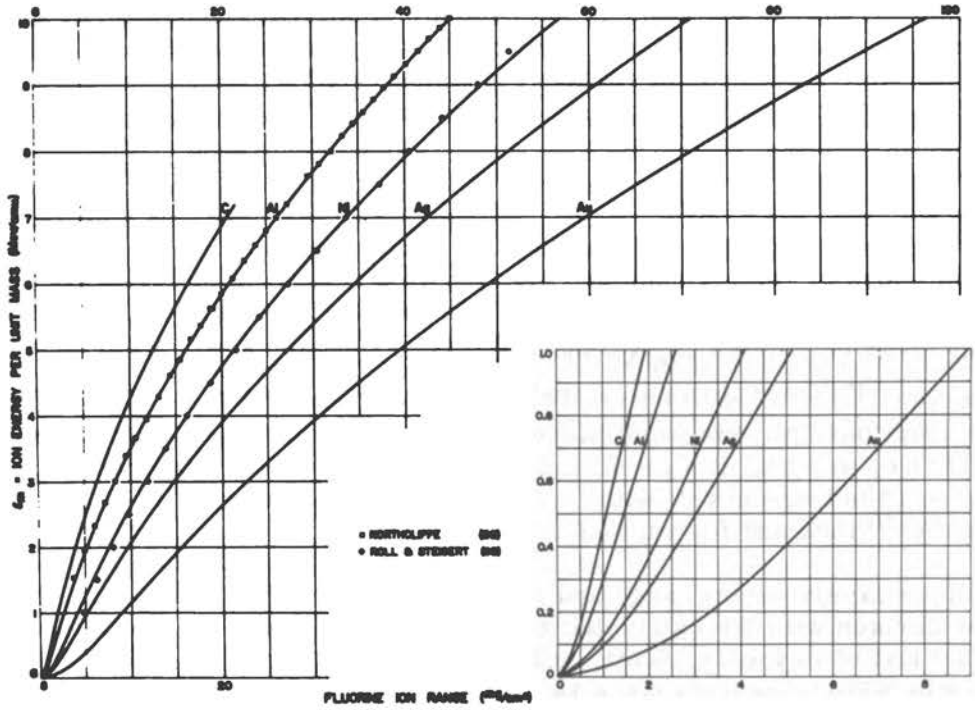

Figure 17. Range energy relations for F^{19} ions in carbon, aluminum, nickel, silver, and gold. The solid lines were obtained by numerical integration from the smoothed stopping-power curves of Figure 7 (Appendix B). A correction for the effect of "nuclear" collisions has been applied.

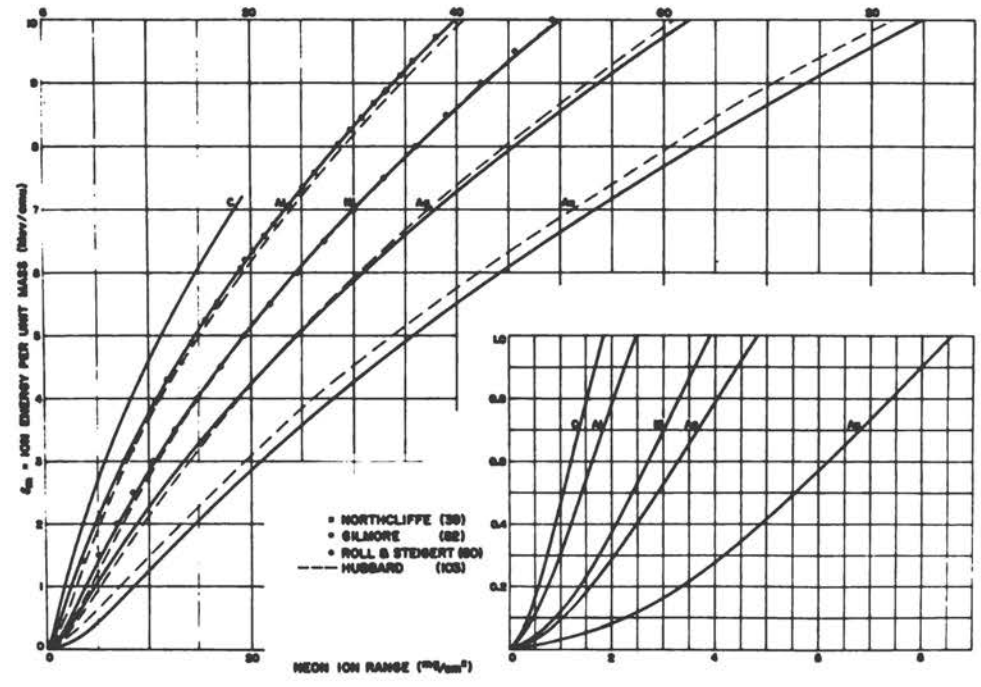

Figure 18. Range energy relations for Ne^{20} ions in carbon, aluminum, nickel, silver, and gold. The solid lines were obtained by numerical integration from the smoothed stopping-power curves of Figure 7 (Appendix B). A correction for the effect of "nuclear" collisions has been applied.

Hubbard (103) has generated a set of semi-empirical range-energy curves for heavier ions by a somewhat different method based on a simple assumption concerning relative range values for heavy ions. If the symbol $R_{x,A}$ denotes the range of ion x in material A, the assumption may be represented symbolically by the relationship

$$R_{x,A}/R_{x,B} = R_{y,A}/R_{y,B}$$

between range values for ions having the same initial velocity. Taking alpha particles as reference ions ($y \rightarrow \alpha$) and nuclear emulsion as a reference material (B → emulsion), Hubbard used the data of Heckman, et al. (86) to determine $R_{x,\ \text{emulsion}}$, the data of Whaling (2) to determine $R_{\alpha,A}$, and the data of Barkas, et al. (126) to determine $R_{\alpha,\ \text{emulsion}}$. Hubbard then calculated the Range $R_{x,A}$ of ion x in material A from the above relationship. His predictions for N^{14}, O^{16}, and Ne^{20} ions are seen in Figures 15, 16, and 18. His predictions for C^{12} ions were inadvertently omitted from Figure 14 but agree well with the solid line curves there. He also has calculated curves for Ar^{40} ions and for various ions in beryllium, copper, and lead.

Various experimental range and energy-loss data are displayed in Figures 12-18 for comparison with the calculated curves. The data of Webb, Reynolds, and Zucker (89) and of Reynolds, Scott, and Zucker (90) shown in Figure 15 and the data of Oganesyan (95) shown in Figures 14-16 are range measurements and are presented as published. All other experimental values shown are based on energy-loss measurements. The alpha particle range values attributed to Gobeli (67) are those he derived from his energy-loss measurements. The energy-loss measurements of other authors have been interpreted as range measurements by regarding absorber thicknesses as range differences and subtracting them from a constant (the estimated range of the ion at its initial energy) which is chosen to give a good fit of the data to the calculated (solid line) curve. Among the data treated in this way, the most comprehensive are the measurements of Northcliffe (39) and of Roll and Steigert (80), which are shown for all of the ions in Figures 12-18, and the data of Walton and Hubbard (81), which show the behavior of C^{12} ions in several materials (Fig. 14). Similar measurements by Sikkeland (83) for N^{14} and O^{16} ions and by Gilmore (82) for Ne^{20} ions are shown in Figures 15, 16, and 18. Some older measurements by Burcham (94) for C^{12} ions are shown in Figure 14, and some very old measurements by Rosenblum (124) made with natural alpha particles are shown in Figure 12.

Another set of calculated range-energy curves is presented for the convenience of the experimentalist in Figures 19-31.[3] In a few cases one of these curves duplicates one of the solid-line curves of Figures 12-18. In such cases the agreement is excellent, even though the two sets of curves are derived by somewhat different methods. The point of departure for the set of curves in Figures 19-31 is the experimental measurements of the energy loss of heavy ions in aluminum (Ref. 39). In particular, the curves for He^4, B^{10}, B^{11}, C^{12}, N^{14}, O^{16}, F^{19}, and Ne^{20} ions are the smoothed experimental energy-loss curves converted to range-energy curves by the process described in the preceding paragraph. The curves for other isotopes of helium, beryllium, carbon, nitrogen, oxygen, fluorine, and neon have been calculated

[3] An earlier version of these curves has been circulated privately and was included in a preliminary report entitled "The Penetration of Matter by Heavy Ions with Energies above 1/2 Mev per AMU" prepared for the Subcommittee on the Penetration of Charged Particles in Matter (NAS-NRC) by L. C. Northcliffe and R. L. Gluckstern, March 1961, and revised by L. C. Northcliffe, March 1962.

from these experimental curves on the assumption that for two isotopic ions with the same velocity (i.e., same energy per unit mass) the ranges are in the same ratio as the masses.[4] In this way all of the curves shown in Figures 19, 22-27 were obtained. The curves of Figures 20 and 21 for lithium and beryllium ions were obtained from Figure 11 of Appendix B by interpolation between the curves for helium and boron. The curves of Figures 28-31 for sodium, magnesium, aluminum, and silver ions were obtained by an extrapolation process and therefore are less reliable than the other curves.

The author is grateful to several members of the Subcommittee, particularly Dr. R. L. Gluckstern, Dr. Jens Lindhard, and Dr. R. L. Platzman, for aid, information, and critical comments offered at various stages in the preparation of this paper, and to the many other persons who provided substantial assistance in its preparation, notably Mr. C. A. Whitten, Mrs. Jane Hilberg, and Mr. William Poe.

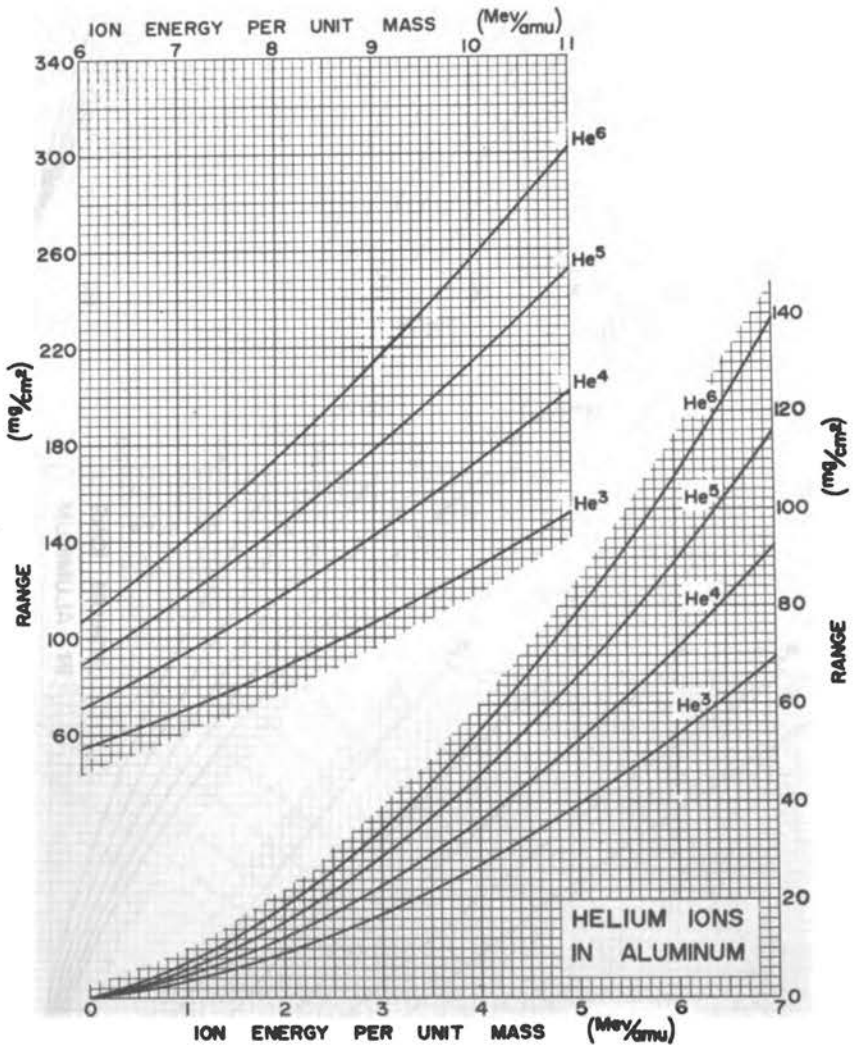

Figure 19. Range energy relations for helium isotopes in aluminum.

[4] Experimental confirmation of this assumption has been found in the case of B^{10} and B^{11} ions by Roll and Steigert (80) and by Northcliffe (39).

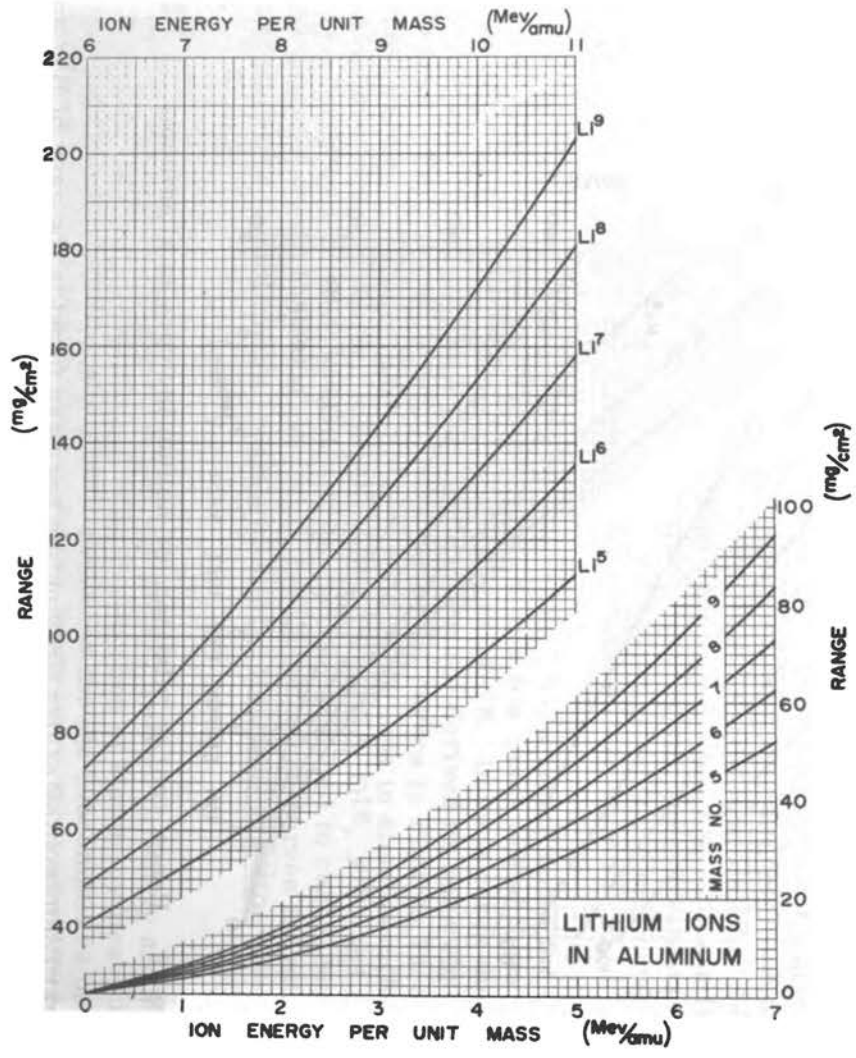

Figure 20. Range energy relations for lithium isotopes in aluminum.

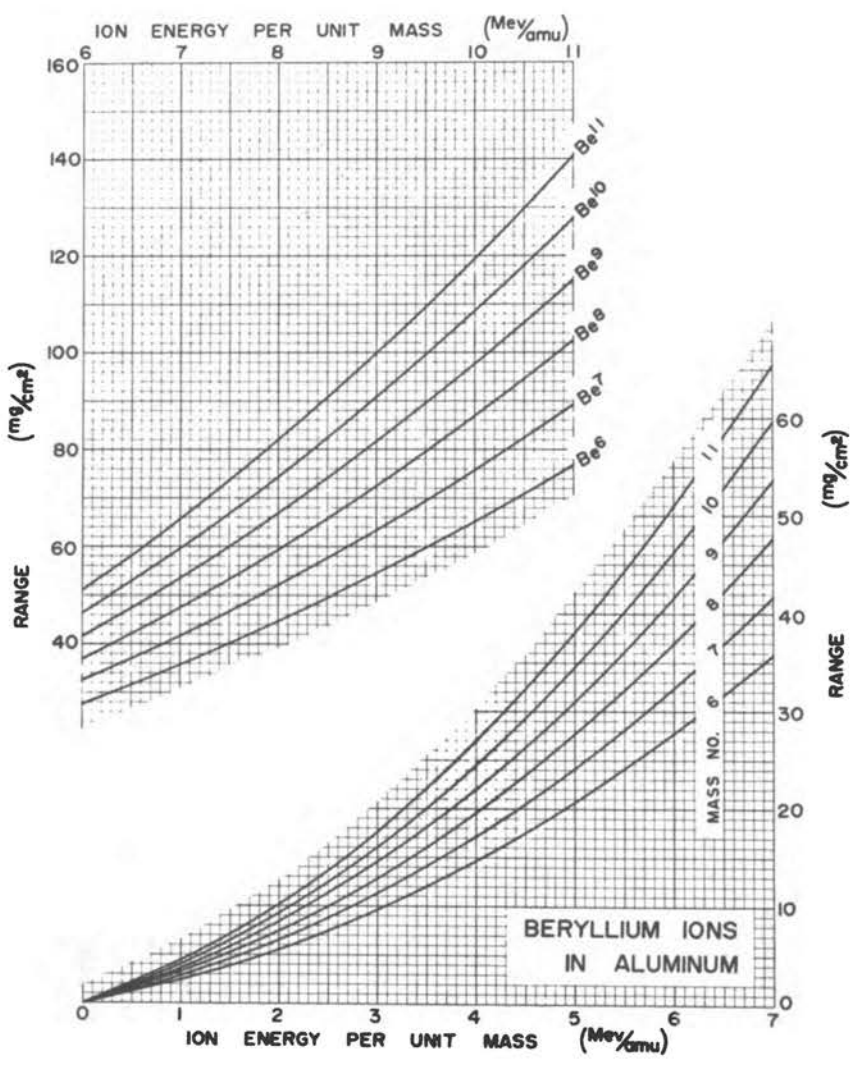

Figure 21. Range energy relations for beryllium isotopes in aluminum.

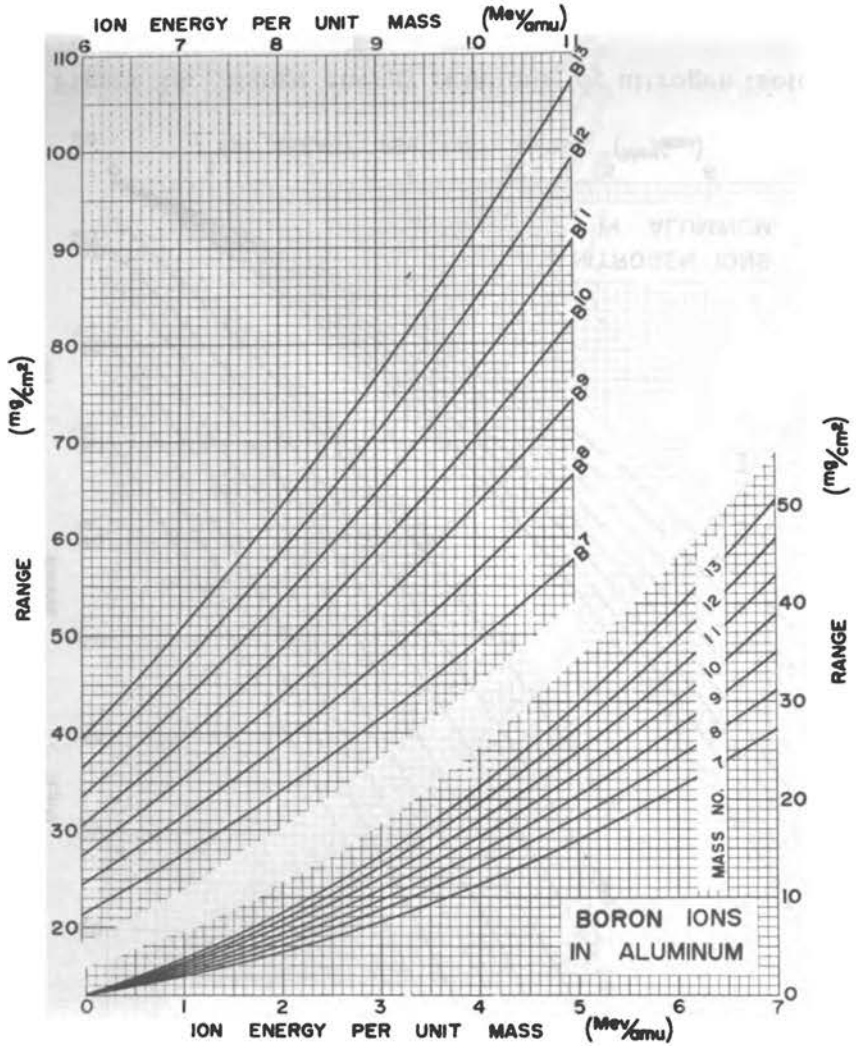

Figure 22. Range energy relations for boron isotopes in aluminum.

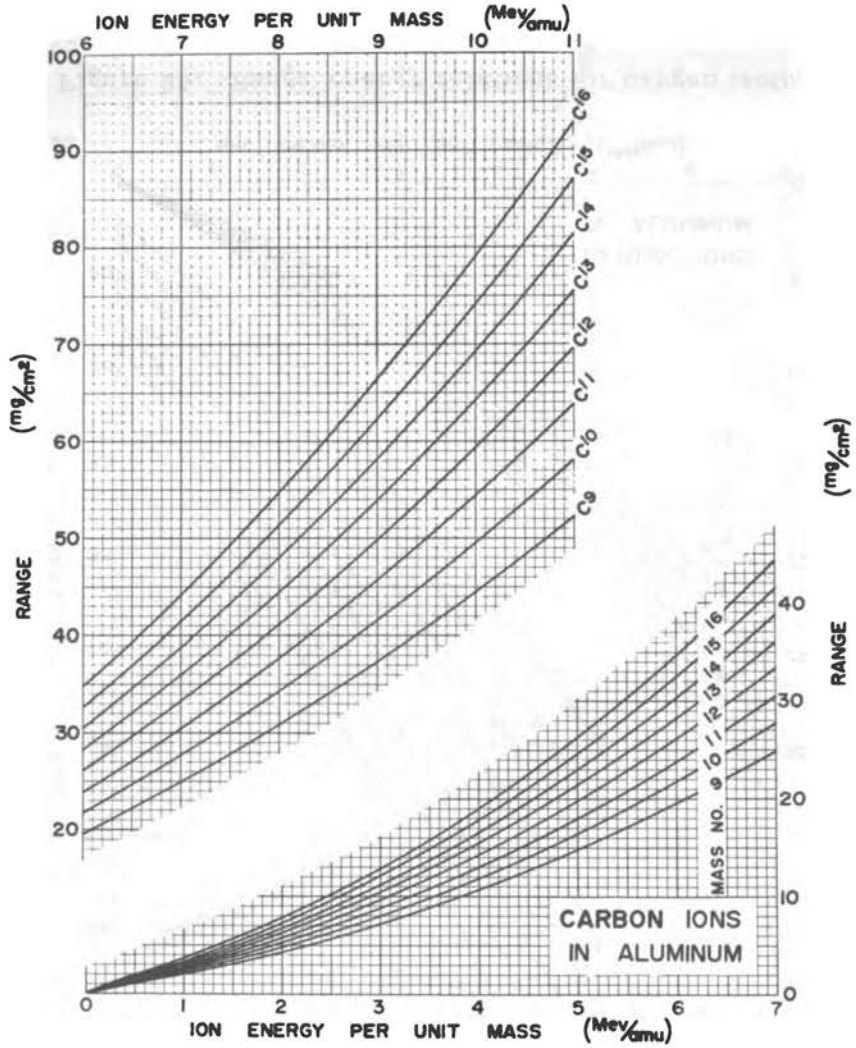

Figure 23. Range energy relations for carbon isotopes in aluminum.

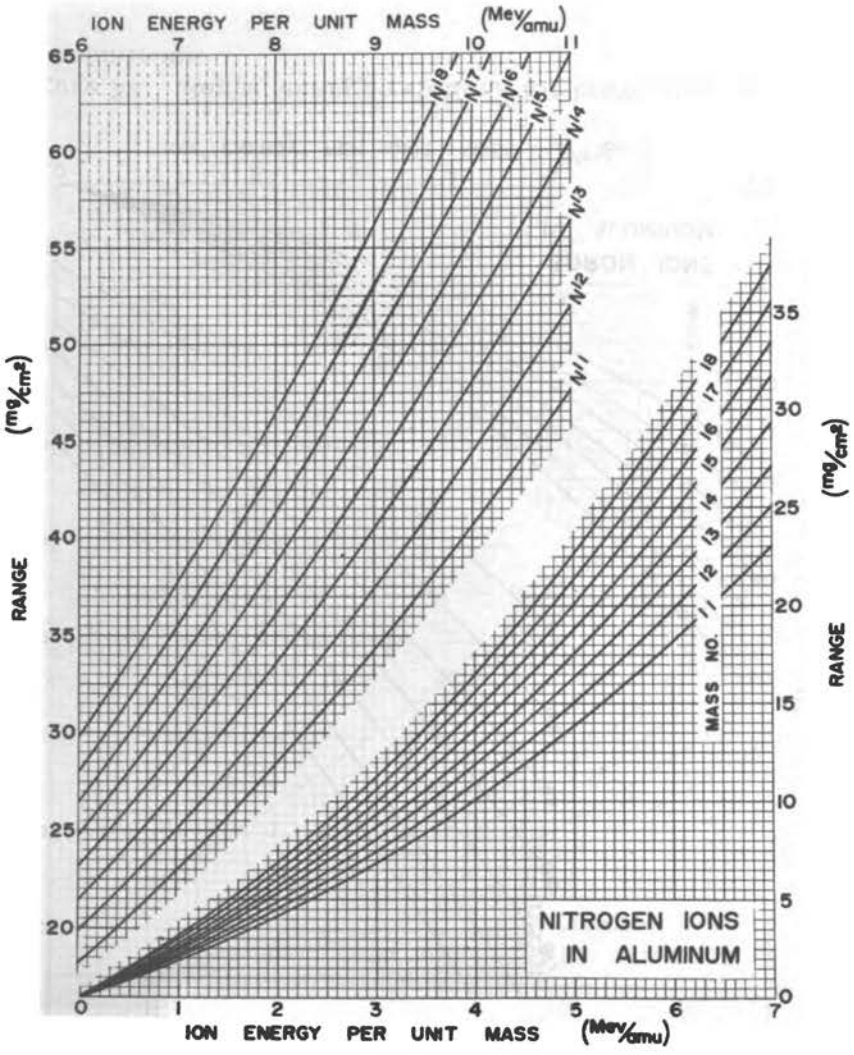

Figure 24. Range energy relations for nitrogen isotopes in aluminum.

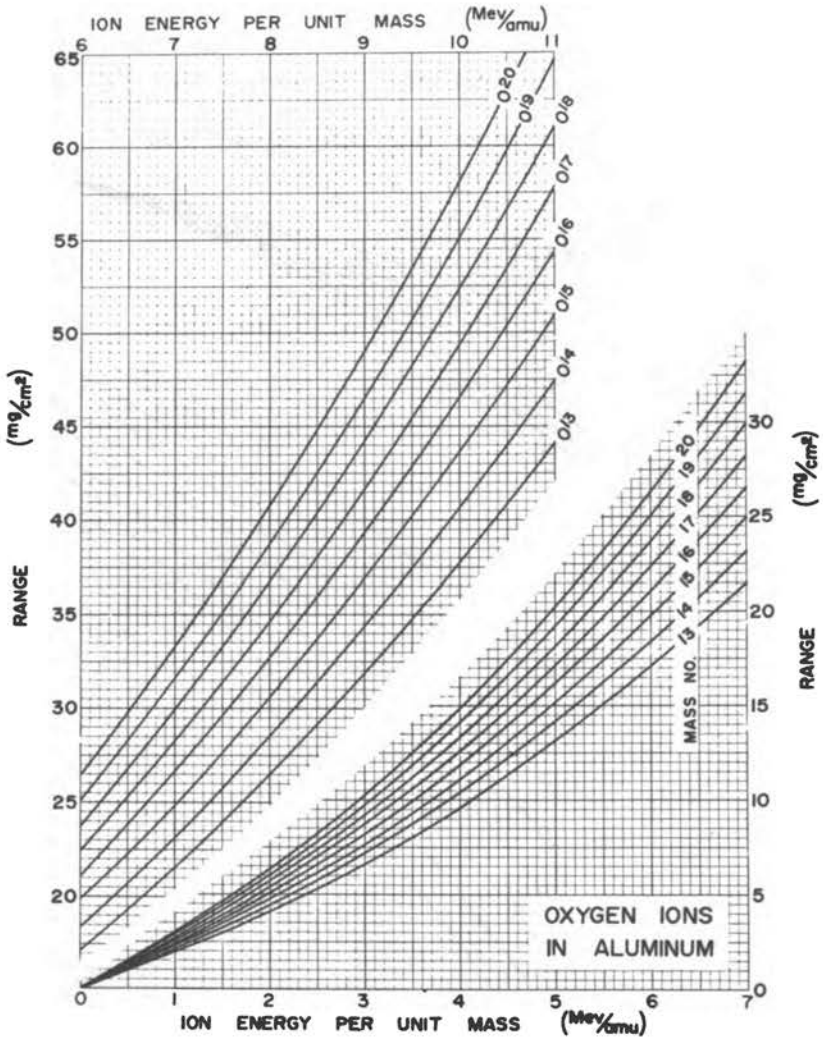

Figure 25. Range energy relations for oxygen isotopes in aluminum.

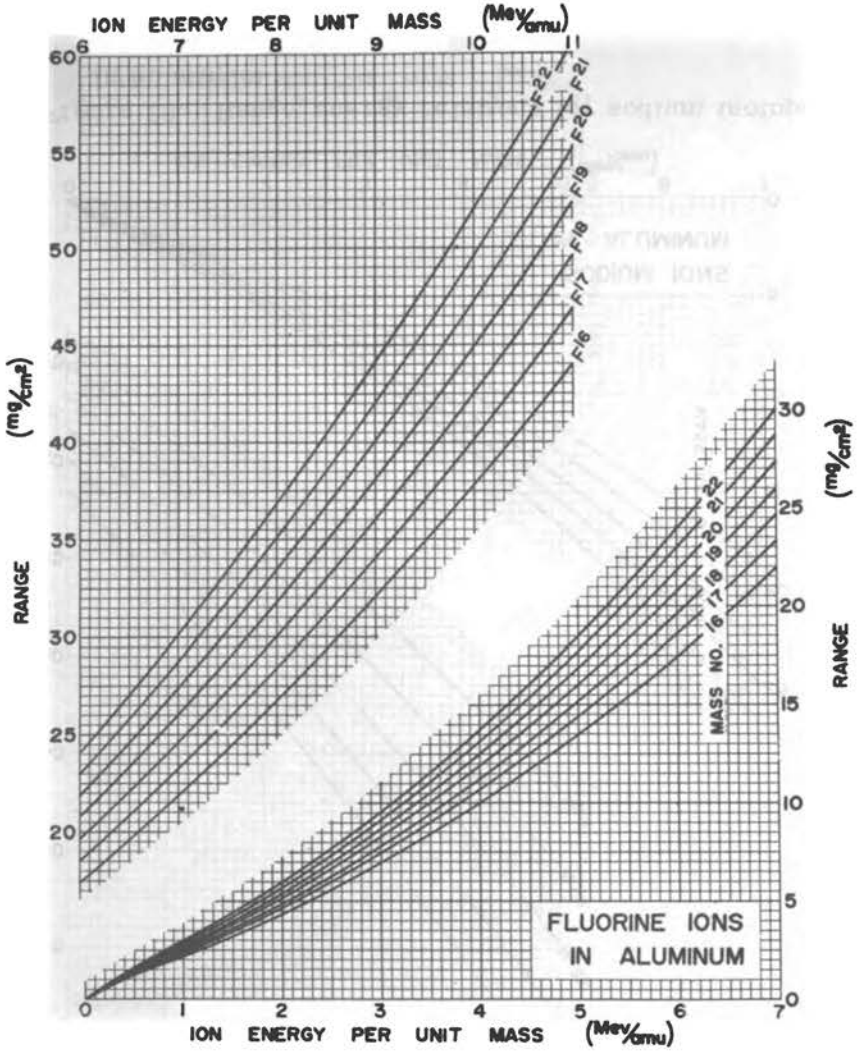

Figure 26. Range energy relations for fluorine isotopes in aluminum.

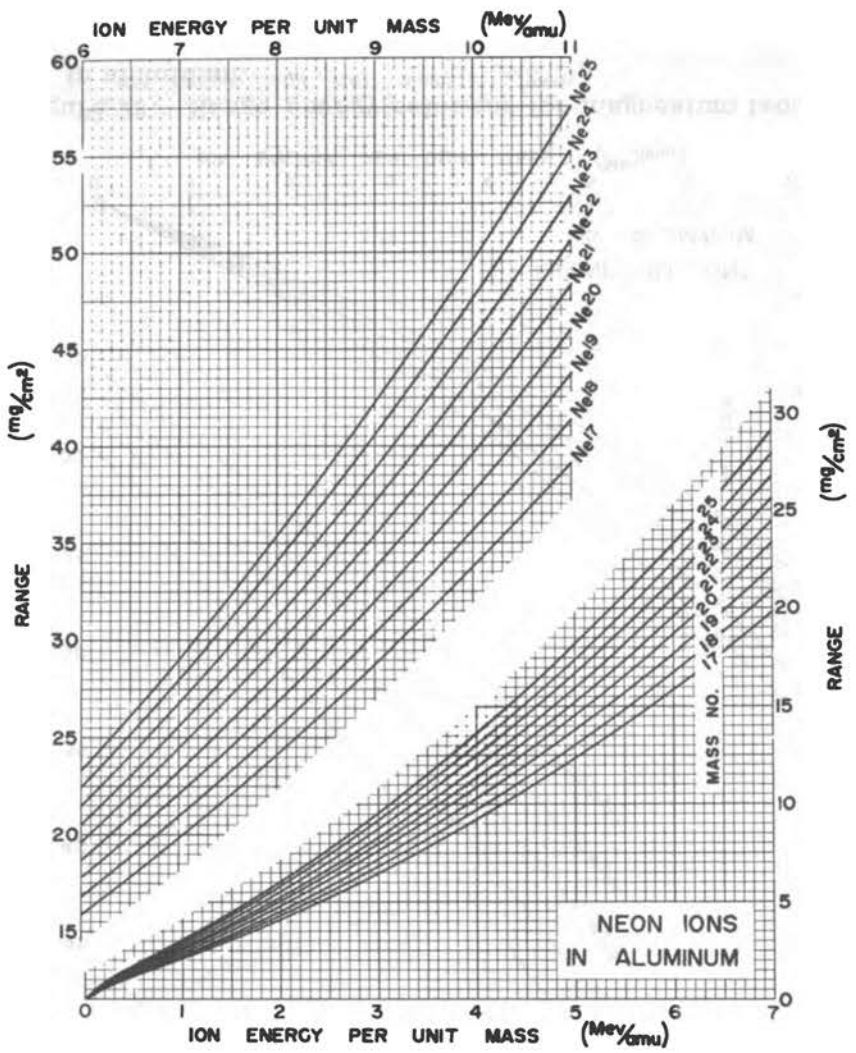

Figure 27. Range energy relations for neon isotopes in aluminum.

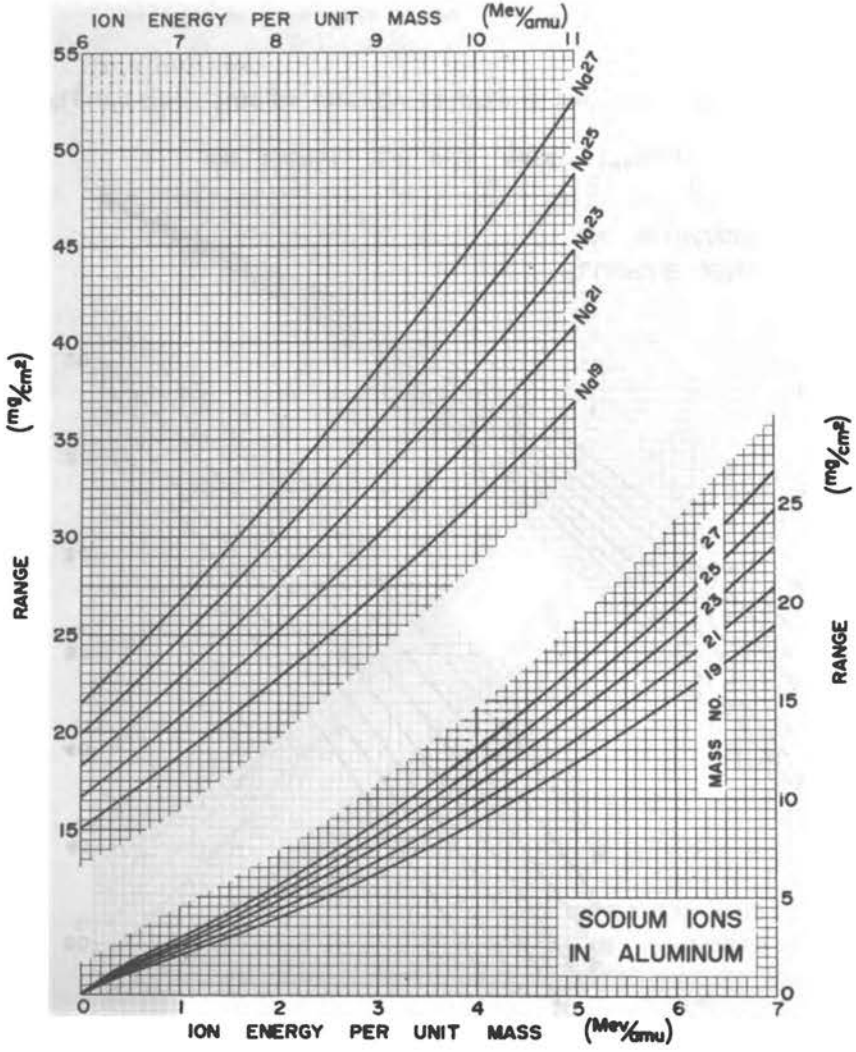

Figure 28. Range energy relations for sodium isotopes in aluminum.

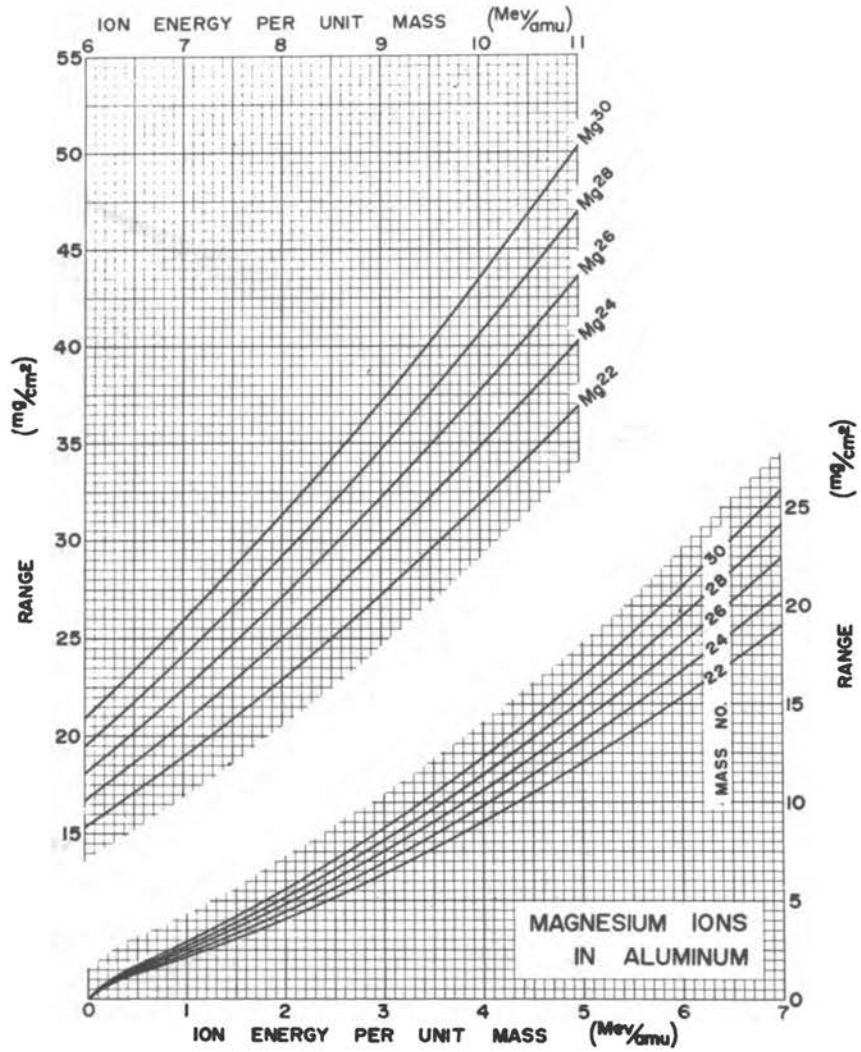

Figure 29. Range energy relations for magnesium isotopes in aluminum.

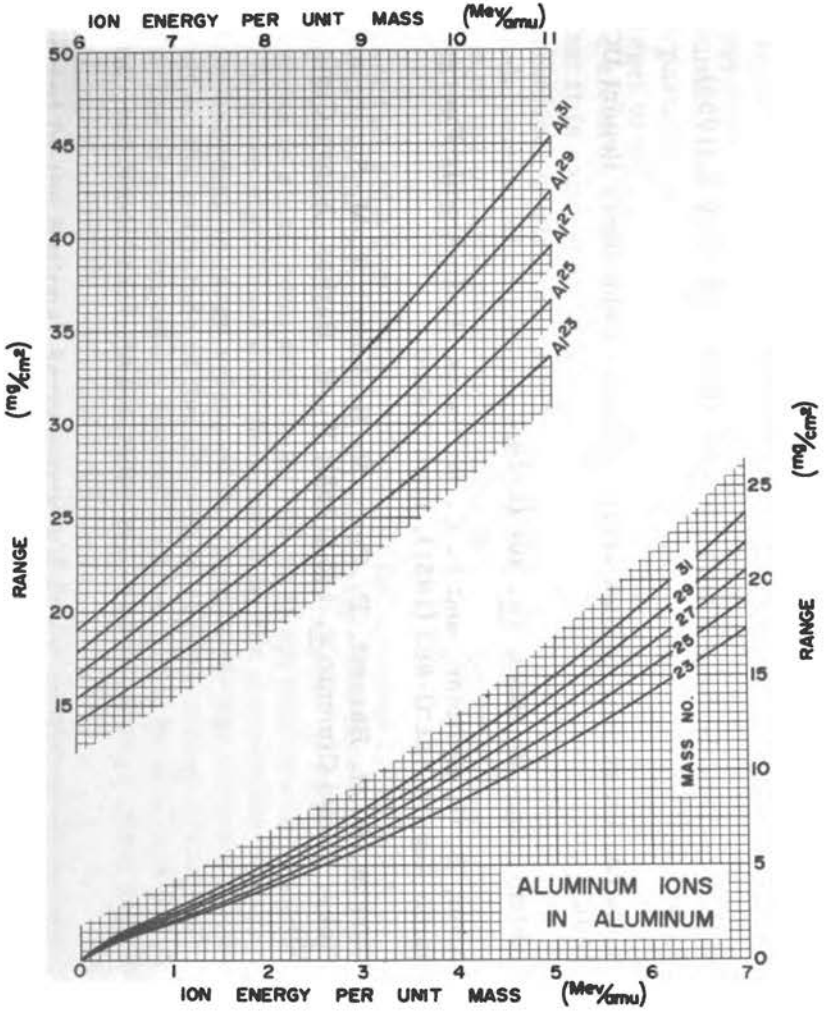

Figure 30. Range energy relations for aluminum isotopes in aluminum.

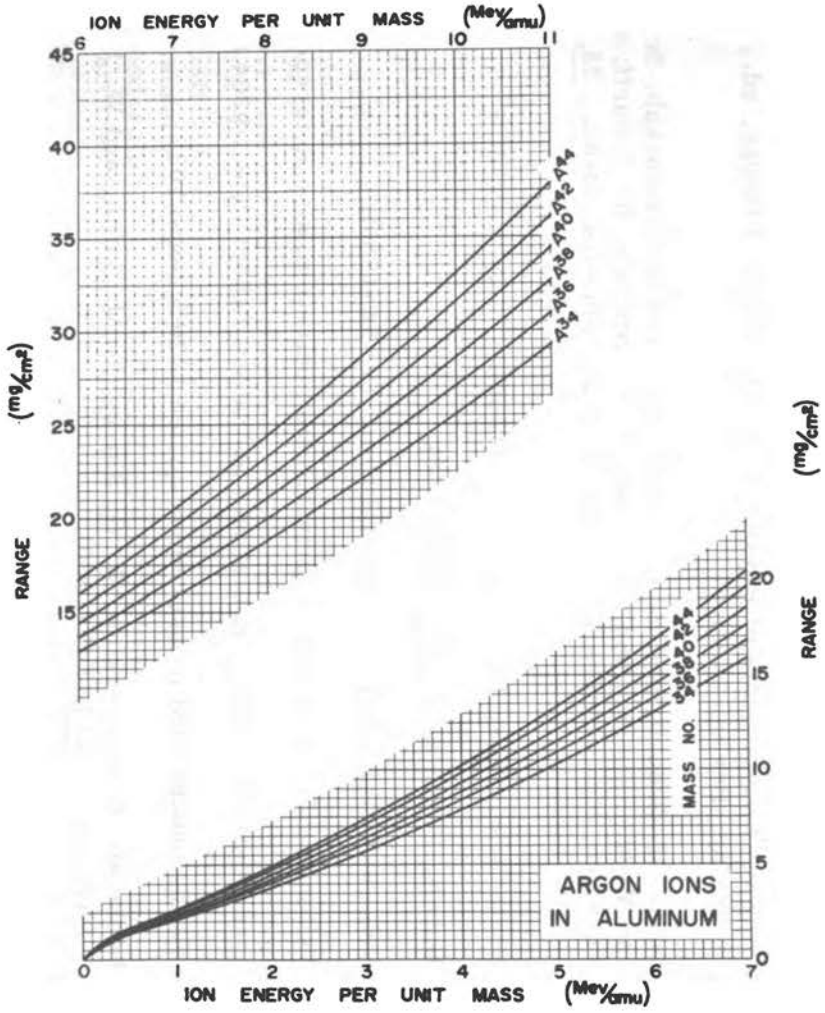

Figure 31. Range energy relations for argon isotopes in aluminum.

References

2. W. Whaling in "Encyclopedia of Physics," 34 (1), 193 (S. Fluegge, ed., Springer-Verlag, Berlin, 1958).

38. J. Lindhard, M. Scharff, and H. E. Schiøtt, Kgl. Danske Videnskab. Selskab, Mat.-fys. Medd., 33, 14 (1963); J. Lindhard, V. Nielsen, M. Scharff; and P. V. Thomsen, Kgl. Danske Videnskab. Selskab, Mat-fys. Medd., 33, 10 (1963).

39. L. C. Northcliffe, Phys. Rev., 120, 1744 (1960).

67. G. W. Gobeli, Phys. Rev., 103, 275 (1956).

80. P. G. Roll, and F. E. Steigert, Nucl. Phys., 17, 54 (1960).

81. J. R. Walton and E. L. Hubbard, private communication; also Reference 103.

82. J. Gilmore, Univ. California Radiation Laboratory Report UCRL-9304 (1960).

83. T. Sikkeland, unpublished measurement quoted in Reference 103.

86. H. H. Heckman, B. L. Perkins, W. G. Simon, F. M. Smith, and W. H. Barkas, Phys. Rev., 117, 544 (1960).

89. W. H. Webb, H. L. Reynolds, and A. Zucker, Phys. Rev., 102, 749 (1956).

90. H. L. Reynolds, D. W. Scott, and A. Zucker, Phys. Rev., 95, 671 (1954).

94. W. E. Burcham, Proc. Phys. Soc. (London), A70, 309 (1957).

95. Oganesyan, Yu, Ts., J. Exp. Theor. Phys. (USSR), 36, 936 L (1959). Transl. JETP, 9, 661 L (1959).

103. E. L. Hubbard, University of California Radiation Laboratory Report UCRL-9053 (1960).

124. S. Rosenblum, Ann. de Phys. 10, 408 (1928).

125. W. A. Aron, B. G. Hoffman, and F. C. Williams, U.S. Atomic Energy Commission Report AECU-663 (1951), unpublished.

126. W. H. Barkas, P. H. Barrett, P. Cuer, H. Heckman, F. M. Smith, and H. K. Ticho, Nuovo Cimento 8, 185 (1958); W. H. Barkas, Nuovo Cimento 8, 201 (1958).

9. ENERGY-LOSS STRAGGLING OF PROTONS AND MESONS: TABULATION OF THE VAVILOV DISTRIBUTION[1]

Stephen M. Seltzer[2] and Martin J. Berger[2]

Abstract

This paper contains a tabulation of the Vavilov distribution which describes the energy-loss straggling of charged particles traversing a thin layer of matter. The distribution depends on the particle velocity and on a parameter, κ, indicative of the ratio of the mean energy-loss over the pathlength considered to the largest energy-transfer possible in a single collision with an atomic electron. As $\kappa \to 0$, the Vavilov distribution goes over into the Landau distribution; for $\kappa \gtrsim 10$ it becomes Gaussian. Intermediate values of κ occur for protons and mesons of moderate velocity traversing very thin targets or for extremely fast particles in targets of moderate thickness.

1. Introduction

The transport equation describing the energy-loss of heavy charged particles in thin targets has been solved rigorously by Vavilov (1), whose distribution is a generalization of the well-known Landau distribution. Whereas the Landau distribution, applicable primarily to electrons, has a universal character and depends only on a suitably scaled energy-loss variable, the Vavilov distribution depends in addition on the particle velocity and on a parameter indicative of the ratio of the mean loss in the target to the maximum-allowed energy-transfer in a single collision with an atomic electron. The evaluation of the Vavilov distribution is made difficult by the fact that it is expressed as an integral over some rather complicated functions, so that numerical quadrature is required except in some limiting cases. Vavilov himself made numerical calculations for some representative parameter choices. The purpose of the present paper is to make a more systematic and comprehensive tabulation of the Vavilov distribution.

Let $f(\Delta, s)d\Delta$ denote the probability that a proton (or meson), in traversing a pathlength s in the target, will suffer an energy-loss between Δ and $\Delta+d\Delta$ as the result of many successive collisions with atomic electrons. If each of the energy-transfers to electrons is small compared to Δ, $f(\Delta, s)$ is approximately Gaussian. If individual transfers make significant contributions to Δ, the distribution is asymmetric, with a tail corresponding to large values of Δ. Landau (2) has derived $f(\Delta, s)$ without placing any limit on the magnitude of the allowed individual energy-transfers. Symon (3), with the use of some ingenious approximations which have turned out to be surprisingly accurate, and Vavilov (1), in his more rigorous treatment, have explicitly taken into

[1]Supported by the National Aeronautics and Space Administration under Contract R-80 with National Bureau of Standards.

[2]National Bureau of Standards, Washington, D. C.

account the allowed maximum-energy transfer per collision and have derived distributions which bridge the gap between a Gaussian and a Landau distribution. In neither theory is a distinction made between the depth of penetration (thickness of the target) and the pathlength. Moreover, the collision cross section is assumed to be independent of the particle velocity and, therefore, of the position of the particle within the target. This implies that the results are valid only when the energy-loss in the target is small compared to the initial particle energy. Symon has indicated that his results can be extended, in an approximate manner, to the case of large energy-loss.

2. Significant Parameters

Because of the conservation of energy and momentum, the largest energy-transfer possible in a collision between a particle of mass M and a free electron is

$$\epsilon_{max} = \frac{2mc^2\beta^2}{1-\beta^2}\left[1 + \frac{2m}{M}\frac{1}{\sqrt{1-\beta^2}} + \left(\frac{m}{M}\right)^2\right]^{-1}, \qquad (1)$$

where mc^2 is the electron rest energy and βc the velocity of the particle. For small β, ϵ_{max} is also very small. Because of the small value of m/M for protons or mesons, the factor in square brackets is practically unity, except when $\beta \to 1$. For $\beta \to 1$, $\epsilon_{max} \to \frac{Mc^2\beta^2}{1-\beta^2}$, which means that almost the entire energy of the particle can then be transferred in a single collision.

The mean energy-loss in a short pathlength s(g cm^{-2}) is given by

$$\bar{\Delta} = 0.30058\ \frac{mc^2}{\beta^2}\frac{Z}{A}s\left[\log\frac{2mc^2\beta^2\epsilon_{max}}{I^2(1-\beta^2)} - 2\beta^2 - 2\frac{C}{Z} - \delta\right], \qquad (2)$$

where Z, A, and I are, respectively, the atomic number, atomic weight, and mean excitation energy of the medium, $2\frac{C}{Z}$ is the shell correction, and δ is the density effect correction. (See, e.g., p. 14 of Appendix A of this volume.)

The shape of the energy-loss distribution depends on the ratio of $\bar{\Delta}$ to ϵ_{max}. Inasmuch as the factor in square brackets in Equation 2 is independent of s and a very slowly varying function of the particle energy, both Symon and Vavilov disregard it in forming their significant parameter, which they take to be

$$\varkappa = 0.30058\frac{mc^2}{\beta^2}\frac{Z}{A}s/\epsilon_{max} = \frac{\xi}{\epsilon_{max}}. \qquad (3)$$

The value $\varkappa = 0$ corresponds to a Landau distribution, and $\varkappa \gg 1$ to a Gaussian. Tables 1a-1d* give the quantities ϵ_{max}, $\frac{A}{Z}\frac{\xi}{s}$, and $\frac{A}{Z}\frac{\varkappa}{s}$ as functions of the particle energy for protons, kaons, pions, and muons. Upon substitution of the desired values of Z, A, and s, these tables can be applied to a target of any desired composition and thickness.

*Powers of ten are indicated by the symbol E; thus 1.2345E 02 means 1.2345×10^2.

Table 1a. Parameters characterizing the energy loss distribution for protons (rest mass = 938.213 Mev).

Energy (Mev)	β^2	ϵ_{max} (Mev)	$(A/Z)\cdot(\xi/s)$ (Mev/g cm^{-2})	$(A/Z)\cdot(\kappa/s)$ (cm^2/g)
1.0	2.1283E-03	2.1773E-03	7.2166E 01	3.3146E 04
1.5	3.1898E-03	3.2667E-03	4.8149E 01	1.4739E 04
2.0	4.2497E-03	4.3568E-03	3.6141E 01	8.2952E 03
3.0	6.3645E-03	6.5387E-03	2.4132E 01	3.6907E 03
4.0	8.4725E-03	8.7229E-03	1.8128E 01	2.0782E 03
5.0	1.0574E-02	1.0909E-02	1.4525E 01	1.3315E 03
6.0	1.2668E-02	1.3098E-02	1.2124E 01	9.2561E 02
8.0	1.6838E-02	1.7483E-02	9.1217E 00	5.2175E 02
10.0	2.0981E-02	2.1877E-02	7.3205E 00	3.3463E 02
15.0	3.1224E-02	3.2902E-02	4.9189E 00	1.4950E 02
20.0	4.1308E-02	4.3985E-02	3.7181E 00	8.4533E 01
30.0	6.1009E-02	6.6324E-02	2.5175E 00	3.7957E 01
40.0	8.0108E-02	8.8895E-02	1.9173E 00	2.1568E 01
50.0	9.8631E-02	1.1170E-01	1.5572E 00	1.3941E 01
60.0	1.1660E-01	1.3473E-01	1.3172E 00	9.7767E 00
80.0	1.5096E-01	1.8149E-01	1.0174E 00	5.6057E 00
100.0	1.8336E-01	2.2918E-01	8.3764E-01	3.6550E 00
150.0	2.5668E-01	3.5245E-01	5.9837E-01	1.6978E 00
200.0	3.2055E-01	4.8149E-01	4.7915E-01	9.9512E-01
300.0	4.2586E-01	7.5694E-01	3.6065E-01	4.7647E-01
400.0	5.0846E-01	1.0555E 00	3.0207E-01	2.8618E-01
500.0	5.7444E-01	1.3772E 00	2.6737E-01	1.9415E-01
600.0	6.2797E-01	1.7219E 00	2.4458E-01	1.4204E-01
800.0	7.0866E-01	2.4808E 00	2.1673E-01	8.7365E-02
1000.0	7.6568E-01	3.3319E 00	2.0059E-01	6.0209E-02
1500.0	8.5193E-01	5.8632E 00	1.8028E-01	3.0748E-02
2000.0	8.9804E-01	8.9701E 00	1.7103E-01	1.9066E-02
3000.0	9.4324E-01	1.6907E 01	1.6283E-01	9.6312E-03
4000.0	9.6390E-01	2.7133E 01	1.5934E-01	5.8725E-03
5000.0	9.7504E-01	3.9643E 01	1.5752E-01	3.9735E-03
6000.0	9.8171E-01	5.4426E 01	1.5645E-01	2.8745E-03
8000.0	9.8898E-01	9.0786E 01	1.5530E-01	1.7106E-03
10000.0	9.9264E-01	1.3615E 02	1.5473E-01	1.1364E-03

Table 1b. Parameters characterizing the energy loss distribution for kaons (rest mass = 493.9 Mev).

Energy (Mev)	β^2	ϵ_{max} (Mev)	$(A/Z)\cdot(\xi/s)$ (Mev/g cm^{-2})	$(A/Z)\cdot(\kappa/s)$ (cm^2/g)
1.0	4.0371E-03	4.1339E-03	3.8044E 01	9.2029E 03
1.5	6.0465E-03	6.2040E-03	2.5401E 01	4.0943E 03
2.0	8.0499E-03	8.2761E-03	1.9080E 01	2.3054E 03
3.0	1.2038E-02	1.2427E-02	1.2758E 01	1.0267E 03
4.0	1.6003E-02	1.6586E-02	9.5975E 00	5.7867E 02
5.0	1.9944E-02	2.0753E-02	7.7011E 00	3.7109E 02
6.0	2.3861E-02	2.4928E-02	6.4369E 00	2.5822E 02
8.0	3.1625E-02	3.3304E-02	4.8566E 00	1.4582E 02
10.0	3.9297E-02	4.1714E-02	3.9085E 00	9.3697E 01
15.0	5.8082E-02	6.2883E-02	2.6444E 00	4.2052E 01
20.0	7.6322E-02	8.4260E-02	2.0124E 00	2.3883E 01
30.0	1.1125E-01	1.2764E-01	1.3806E 00	1.0817E 01
40.0	1.4423E-01	1.7185E-01	1.0649E 00	6.1967E 00
50.0	1.7541E-01	2.1689E-01	8.7562E-01	4.0371E 00
60.0	2.0491E-01	2.6277E-01	7.4954E-01	2.8525E 00
80.0	2.5936E-01	3.5702E-01	5.9218E-01	1.6587E 00
100.0	3.0841E-01	4.5459E-01	4.9801E-01	1.0955E 00
150.0	4.1164E-01	7.1308E-01	3.7311E-01	5.2324E-01
200.0	4.9338E-01	9.9235E-01	3.1130E-01	3.1370E-01
300.0	6.1297E-01	1.6132E 00	2.5057E-01	1.5533E-01
400.0	6.9472E-01	2.3169E 00	2.2108E-01	9.5419E-02
500.0	7.5306E-01	3.1036E 00	2.0395E-01	6.5716E-02
600.0	7.9614E-01	3.9730E 00	1.9292E-01	4.8557E-02
800.0	8.5429E-01	5.9595E 00	1.7978E-01	3.0168E-02
1000.0	8.9070E-01	8.2759E 00	1.7244E-01	2.0836E-02
1500.0	9.3864E-01	1.5504E 01	1.6363E-01	1.0554E-02
2000.0	9.6078E-01	2.4775E 01	1.5986E-01	6.4523E-03
3000.0	9.8002E-01	4.9396E 01	1.5672E-01	3.1727E-03
4000.0	9.8792E-01	8.2039E 01	1.5547E-01	1.8950E-03
5000.0	9.9192E-01	1.2260E 02	1.5484E-01	1.2629E-03
6000.0	9.9422E-01	1.7100E 02	1.5448E-01	9.0343E-04
8000.0	9.9662E-01	2.9088E 02	1.5411E-01	5.2981E-04
10000.0	9.9778E-01	4.4094E 02	1.5393E-01	3.4910E-04

Table 1c. Parameters characterizing the energy loss distribution for pions (rest mass = 139.59 Mev).

Energy (Mev)	β^2	ϵ_{max} (Mev)	$(A/Z)\cdot(\xi/s)$ (Mev/g cm^{-2})	$(A/Z)\cdot(\kappa/s)$ (cm^2/g)
1.0	1.4175E-02	1.4587E-02	1.0835E 01	7.4280E 02
1.5	2.1150E-02	2.1919E-02	7.2619E 00	3.3131E 02
2.0	2.8051E-02	2.9276E-02	5.4753E 00	1.8702E 02
3.0	4.1636E-02	4.4068E-02	3.6888E 00	8.3707E 01
4.0	5.4938E-02	5.8963E-02	2.7957E 00	4.7414E 01
5.0	6.7965E-02	7.3960E-02	2.2598E 00	3.0554E 01
6.0	8.0725E-02	8.9060E-02	1.9026E 00	2.1363E 01
8.0	1.0547E-01	1.1957E-01	1.4562E 00	1.2179E 01
10.0	1.2923E-01	1.5048E-01	1.1885E 00	7.8978E 00
15.0	1.8465E-01	2.2957E-01	8.3180E-01	3.6233E 00
20.0	2.3494E-01	3.1121E-01	6.5375E-01	2.1006E 00
30.0	3.2250E-01	4.8217E-01	4.7624E-01	9.8770E-01
40.0	3.9585E-01	6.6335E-01	3.8800E-01	5.8491E-01
50.0	4.5790E-01	8.5472E-01	3.3542E-01	3.9243E-01
60.0	5.1086E-01	1.0563E 00	3.0065E-01	2.8463E-01
80.0	5.9590E-01	1.4899E 00	2.5774E-01	1.7300E-01
100.0	6.6055E-01	1.9640E 00	2.3252E-01	1.1839E-01
150.0	7.6765E-01	3.3258E 00	2.0008E-01	6.0158E-02
200.0	8.3103E-01	4.9383E 00	1.8482E-01	3.7425E-02
300.0	8.9916E-01	8.9074E 00	1.7081E-01	1.9176E-02
400.0	9.3308E-01	1.3856E 01	1.6460E-01	1.1880E-02
500.0	9.5237E-01	1.9769E 01	1.6127E-01	8.1576E-03
600.0	9.6438E-01	2.6633E 01	1.5926E-01	5.9799E-03
800.0	9.7793E-01	4.3153E 01	1.5706E-01	3.6395E-03
1000.0	9.8500E-01	6.3305E 01	1.5593E-01	2.4631E-03
1500.0	9.9275E-01	1.2888E 02	1.5471E-01	1.2004E-03
2000.0	9.9574E-01	2.1495E 02	1.5425E-01	7.1759E-04
3000.0	9.9802E-01	4.4300E 02	1.5389E-01	3.4739E-04
4000.0	9.9886E-01	7.3758E 02	1.5376E-01	2.0847E-04
5000.0	9.9926E-01	1.0904E 03	1.5370E-01	1.4095E-04
6000.0	9.9948E-01	1.4946E 03	1.5367E-01	1.0281E-04
8000.0	9.9971E-01	2.4345E 03	1.5363E-01	6.3108E-05
10000.0	9.9981E-01	3.5195E 03	1.5362E-01	4.3648E-05

Table 1d. Parameters characterizing the energy loss distribution for muons (rest mass = 105.65 Mev).

Energy (Mev)	β^2	ϵ_{max} (Mev)	$(A/Z)\cdot(\xi/s)$ (Mev/g cm^{-2})	$(A/Z)\cdot(\kappa/s)$ (cm^2/g)
1.0	1.8664E-02	1.9248E-02	8.2291E 00	4.2752E 02
1.5	2.7801E-02	2.8939E-02	5.5246E 00	1.9091E 02
2.0	3.6811E-02	3.8674E-02	4.1724E 00	1.0789E 02
3.0	5.4458E-02	5.8278E-02	2.8203E 00	4.8394E 01
4.0	7.1625E-02	7.8060E-02	2.1443E 00	2.7470E 01
5.0	8.8329E-02	9.8019E-02	1.7388E 00	1.7740E 01
6.0	1.0459E-01	1.1816E-01	1.4685E 00	1.2429E 01
8.0	1.3582E-01	1.5896E-01	1.1308E 00	7.1137E 00
10.0	1.6545E-01	2.0048E-01	9.2830E-01	4.6304E 00
15.0	2.3319E-01	3.0737E-01	6.5865E-01	2.1428E 00
20.0	2.9300E-01	4.1869E-01	5.2420E-01	1.2520E 00
30.0	3.9339E-01	6.5460E-01	3.9042E-01	5.9643E-01
40.0	4.7383E-01	9.0815E-01	3.2415E-01	3.5693E-01
50.0	5.3926E-01	1.1793E 00	2.8481E-01	2.4151E-01
60.0	5.9321E-01	1.4680E 00	2.5891E-01	1.7637E-01
80.0	6.7613E-01	2.0978E 00	2.2716E-01	1.0828E-01
100.0	7.3606E-01	2.7973E 00	2.0866E-01	7.4596E-02
150.0	8.2921E-01	4.8480E 00	1.8522E-01	3.8206E-02
200.0	8.8051E-01	7.3258E 00	1.7443E-01	2.3811E-02
300.0	9.3216E-01	1.3540E 01	1.6477E-01	1.2169E-02
400.0	9.5634E-01	2.1395E 01	1.6060E-01	7.5065E-03
500.0	9.6957E-01	3.0848E 01	1.5841E-01	5.1351E-03
600.0	9.7758E-01	4.1859E 01	1.5711E-01	3.7533E-03
800.0	9.8639E-01	6.8395E 01	1.5571E-01	2.2766E-03
1000.0	9.9087E-01	1.0070E 02	1.5500E-01	1.5393E-03
1500.0	9.9567E-01	2.0488E 02	1.5426E-01	7.5291E-04
2000.0	9.9748E-01	3.3944E 02	1.5398E-01	4.5362E-04
3000.0	9.9884E-01	6.8671E 02	1.5377E-01	2.2392E-04
4000.0	9.9934E-01	1.1208E 03	1.5369E-01	1.3712E-04
5000.0	9.9957E-01	1.6256E 03	1.5365E-01	9.4523E-05
6000.0	9.9970E-01	2.1885E 03	1.5364E-01	7.0202E-05
8000.0	9.9983E-01	3.4521E 03	1.5362E-01	4.4499E-05
10000.0	9.9989E-01	4.8558E 03	1.5361E-01	3.1633E-05

3. Results of Symon

Symon used a variety of mathematical techniques for solving the energy-loss transport equation. He made some use of Laplace transforms, but his principal results were obtained through establishing general relations by means of which the moments of the multiple-scattering distributions $\int_0^\infty \Delta^n f(\Delta, s)d\Delta$ can be obtained from the moments of the single-scattering distribution $\int_0^\infty \epsilon^n w(\epsilon)d\epsilon$, with $w(\epsilon)$ being the distribution law for energy-transfers to atomic electrons in single collisions. Symon then determined the distribution $f(\Delta, s)$ by using a knowledge of its Laplace transform and of its moments, and by a combination of different, approximate procedures. He was guided by the condition that for $\varkappa = 0$ his family of distributions must go over into the Landau distribution, and for $\varkappa \gg 1$ into a Gaussian. The results are summarized in a series of graphs, which have also been reproduced—in a more accessible location—in a book by Rossi (5). From these graphs one determines the most probable loss, Δ_p, the width of the distribution, Δ_0, and a skewness parameter, λ_{sk}, all as functions of $\varkappa$. Having determined these quantities, one selects a scaled energy-loss distribution (a function of $(\Delta-\Delta_p)/\Delta_0$) from a family of curves each of which corresponds to a different skewness. Yet another graph provides the absolute normalization. To apply Symon's results to a particular situation requires a good deal of interpolation. The error incurred thereby could be reduced by producing additional intermediate graphs in the manner of Symon; this would not be a straightforward task, however, but would require considerable judgment and skill.

4. Theory of Vavilov

The transport equation to be solved is

$$\frac{\partial f(\Delta, s)}{\partial s} = \int_0^b w(\epsilon)\, f(\Delta - \epsilon, s)\, d\epsilon - f(\Delta, s) \int_0^{\epsilon_{max}} w(\epsilon)\, d\epsilon \qquad (4)$$

($b = \Delta$ for $\Delta < \epsilon_{max}$; $b = \epsilon_{max}$ for $\Delta > \epsilon_{max}$). Landau has shown that the solution of Equation 4, for an arbitrary single-scattering collision-loss law $w(\epsilon)$, can be expressed as the following inverse Laplace transform:

$$f(\Delta, s) = \frac{1}{2\pi i} \int_{c-i\infty}^{c+i\infty} \exp\left\{p\Delta - s \int_0^{\epsilon_{max}} w(\epsilon)\,(1-e^{-\epsilon p})\, d\epsilon\right\} dp \qquad (5)$$

For protons or mesons, the collision-loss law is

$$w(\epsilon) = \begin{cases} \frac{\xi}{s} \frac{1-\beta^2 \epsilon/\epsilon_{max}}{\epsilon^2}, & \epsilon \le \epsilon_{max} \\ 0, & \epsilon > \epsilon_{max} \end{cases} \qquad (6)$$

This expression does not hold for distant collisions in which the energy-transfer is very small; in fact, the distribution for small ϵ has not been studied in detail. In order to be able to evaluate the exponent in Equation 5, Vavilov, following Landau's

procedure, adds and subtracts the mean energy-loss. In the resultant exponent,

$$p(\Delta-\bar{\Delta}) - s\int_0^{\epsilon_{max}} w(\epsilon)(1-e^{-\epsilon p}-\epsilon p)\,d\epsilon\ , \tag{7}$$

the term $p\bar{\Delta}$ now takes into account distant collisions evaluated according to Bethe's stopping-power theory. For small ϵ, the factor accompanying $w(\epsilon)$ is practically zero, so that the form of $w(\epsilon)$ does not matter. From another point of view, Vavilov' procedure is, in effect, equivalent to the assumption that $w(\epsilon)$ vanishes below a cut-off energy

$$\epsilon_{min} = \frac{(1-\beta^2)I^2}{2mc^2\beta^2}\exp\left\{\beta^2 + 2\frac{C}{Z} + \delta\right\}\ . \tag{8}$$

Performing the integration in Equation 5 along the imaginary axis, Vavilov arrives, after some further manipulations, at the following result:

$$f(\Delta, s)\,d\Delta = \frac{1}{\xi}\,\varphi_v(\lambda_v, \kappa, \beta^2)\,d\lambda_v\ ,$$

where

$$\varphi_v(\lambda_v, \kappa, \beta^2) = \frac{1}{\pi}\,e^{\kappa(1+\beta^2\gamma)}\int_0^{\infty} e^{\kappa f_1}\cos(y\lambda_v + \kappa f_2)\,dy$$

$$\lambda_v = \frac{\Delta-\bar{\Delta}}{\epsilon_{max}} - \kappa(1+\beta^2-\gamma)$$

$$\gamma = 0.577216\ -\ -\ -\ \text{(Euler's constant)}$$

$$f_1(y) = \beta^2[\log y + \mathrm{Ci}(y)\,] - \cos y - y\,\mathrm{Si}(y) \tag{9}$$

$$f_2(y) = y\,[\log y + \mathrm{Ci}(y)\,] + \sin y + \beta^2\mathrm{Si}(y)$$

$$\mathrm{Si}(y) = \int_0^y \frac{\sin u}{u}\,du\ \text{(sine integral)}$$

$$\mathrm{Ci}(y) = \int_{-\infty}^y \frac{\cos u}{u}\,du\ \text{(cosine integral)}\ .$$

5. Limiting Cases of Vavilov's Distribution

In the limit $\kappa \to 0$, the Vavilov distribution (Eq. 9) goes over into the Landau distribution. Introducing the Landau parameter

$$\lambda = \lambda_v/\kappa - \log\kappa = \frac{\Delta-\bar{\Delta}}{\xi} - 1 - \beta^2 + \gamma - \log\kappa\ , \tag{10}$$

setting $y = x/\kappa$, and noting that $\mathrm{Ci}(y) \sim \frac{\sin y}{y}$ and $\mathrm{Si}(y) \sim \frac{\pi}{2}$ for large y, one obtains the result that

$$\lim_{\varkappa \to 0} f(\Delta, s) = \frac{1}{\pi\xi} \int_0^\infty e^{-\frac{\pi x}{2}} \cos\left[x(\log \varkappa + \lambda)\right] dx \quad . \tag{11}$$

(Landau distribution)

The difference between the Landau and Vavilov distributions already becomes insignificant when $\varkappa \sim 0.01$ (see, e.g., Fig. 1).

Vavilov has shown that for $\varkappa \gtrsim 1$ his distribution can be approximated with the use of Airey's function:

$$f(\Delta, s) \sim \frac{1}{\eta\sqrt{\pi}} e^{at - a^3/3} \upsilon(t)$$

$$\upsilon(t) = \frac{1}{\sqrt{\pi}} \int_0^\infty \cos(ut + u^3/3)\, du \quad \text{(Airey's function)}$$

$$\eta = \xi \left[(2\varkappa)^2 / \left(1 - \frac{2}{3}\beta^2\right)\right]^{-1/3} \tag{12}$$

$$a = \left(1 - \frac{\beta^2}{2}\right)\left[(2\varkappa)/\left(1 - \frac{2}{3}\beta^2\right)^2\right]^{1/3}$$

$$t = \frac{\Delta - \bar{\Delta}}{\eta} + a^2 \quad .$$

In this approximation, the most probable energy-loss is

$$\Delta_p = \bar{\Delta} + (t_p - a^2)\,\eta \quad , \tag{13}$$

where t_p is the value of t for which

$$\frac{\upsilon'(t)}{\upsilon(t)} = -a \quad . \tag{14}$$

Airey's function and its derivative have been tabulated by Fock (6) in the range -9(0.02)+9 and by Miller (7) in the range -20(0.01)+2. In order to achieve a coverage equal to that in Table 3, page 197, one would need the Airey function for the following range of arguments: for $\varkappa = 1$, $\beta^2 = 0$: -4.9 to 9.4; for $\varkappa = 1$, $\beta^2 = 1$: -3.0 to 10.7; for $\varkappa = 10$, $\beta^2 = 0$: -9.4 to 11.3; for $\varkappa = 10$, $\beta^2 = 1$: -1.3 to 20.0. Thus, for the present application, the Fock tables would cover most of the region of interest, whereas the Miller tables do not. Unfortunately, the Fock tables appear to be very difficult to obtain in the United States.

For $\varkappa \gg 1$, the distribution becomes approximately Gaussian:

$$f(\Delta, s) \sim \frac{1}{\xi\sqrt{\frac{2\pi}{\varkappa}(1 - \beta^2/2)}} \exp\left\{-(\Delta - \bar{\Delta})^2 \varkappa / 2\xi^2(1 - \beta^2/2)\right\} \quad . \tag{15}$$

Table 2* compares the exact and Gaussian distributions for $\varkappa = 10$ and $\beta^2 = 0$ and 1.

*Powers of ten are indicated by the numbers in parentheses; thus 1.23 (-2) means 1.23×10^{-2}.

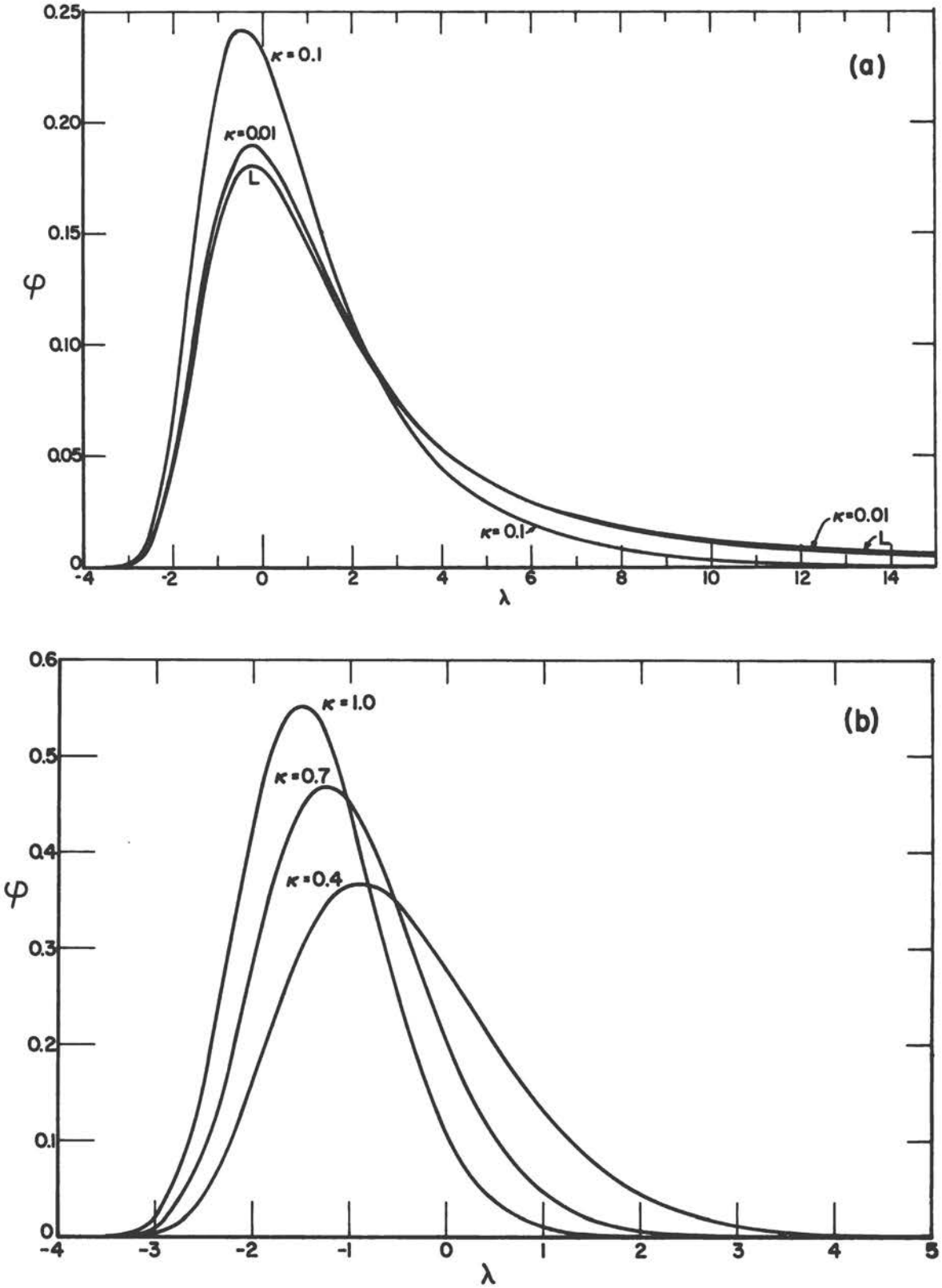

Figure 1. Vavilov distribution for $\beta^2 = 0.9$. (a) $\varkappa = 0$ (Landau), 0.01, and 0.1; (b) $\varkappa = 0.4$, 0.7, and 1.0.

TABLE 2

Comparison of the Gaussian Approximation (Eq. 15) with Exact Vavilov Distribution (Eq. 9) for $\kappa = 10$

$\beta^2 = 0.0$			$\beta^2 = 1.0$		
λ	Exact	Gaussian approx.	λ	Exact	Gaussian approx.
-4.0	5.27(-5)	3.74(-4)	-4.6	1.79(-4)	8.50(-4)
-3.8	1.43(-3)	3.92(-3)	-4.4	1.07(-2)	1.88(-2)
-3.6	1.79(-2)	2.75(-2)	-4.2	1.70(-1)	1.88(-1)
-3.4	1.16(-1)	1.30(-1)	-4.0	8.79(-1)	8.39(-1)
-3.2	4.21(-1)	4.09(-1)	-3.8	1.73	1.69
-3.0	9.12(-1)	8.65(-1)	-3.6	1.47	1.52
-2.8	1.25	1.23	-3.4	5.99(-1)	6.19(-1)
-2.6	1.13	1.17	-3.2	1.28(-1)	1.13(-1)
-2.4	7.06(-1)	7.43(-1)	-3.0	1.53(-2)	9.25(-3)
-2.2	3.13(-1)	3.17(-1)	-2.8	1.09(-3)	3.41(-4)
-2.0	1.02(-1)	9.09(-2)	-2.6	4.87(-5)	5.64(-6)
-1.8	2.48(-2)	1.74(-2)			
-1.6	4.64(-3)	2.24(-3)			
-1.4	6.77(-4)	1.93(-4)			
-1.2	7.84(-5)	1.12(-5)			

6. Numerical Evaluation of Vavilov's Distribution

We have written a program in FORTRAN language to evaluate the Vavilov distribution. The program has been run on an IBM 7094 computer to obtain distribution for $\kappa = 0.01$, 0.04, 0.07, 0.1, 0.4, 0.7, 1.0, 4.0, 7.0, and 10.0, and for β^2 in the range 0.0 (0.1) 1.0. These distributions are given in Table 3* as functions of the Landau parameter λ defined by Equation 10. Note that the change from the Vavilov parameter λ_v to λ involves a renormalization, so that the quantity given is, in fact, $\varphi(\lambda) = \kappa\varphi_v[\lambda_v(\lambda)]$. For $\kappa < 0.01$, one can use the Landau distribution, which has been very thoroughly tabulated by Börsch-Supan (8). For $\kappa > 10$, one can use either the Airey-function approximation (Eq. 12) or the Gaussian approximation (Eq. 15).

The sine and cosine integrals occurring in the integrand of Equation 9 have been computed with the use of the following expansions:

(i) $y < 10$:

$$\mathrm{Si}(y) = T_1(y) - T_3(y) + T_5(y) - \ldots$$

$$\mathrm{Ci}(y) = \gamma + \log y - T_2(y) + T_4(y) - T_6(y) + \ldots \qquad (16)$$

$$T_n(y) = y^n/(n!\,n)$$

*Powers of ten are indicated by the numbers in parentheses; thus 1.23 (-2) means 1.23×10^{-2}.

(ii) $y > 10$:

$$\begin{aligned} \mathrm{Si}(y) &= \tfrac{1}{2}\pi - P(y)\cos y - Q(y)\sin(y) \\ \mathrm{Ci}(y) &= P(y)\sin y - Q(y)\cos y \\ P(y) &= [1 - B_2(y) + B_4(y) - B_6(y) + \ldots]/y \\ Q(y) &= [B_1(y) - B_3(y) + B_5(y) - \ldots]/y \\ B_n(y) &= n!/y^n \ . \end{aligned} \tag{16}$$

With these expansions, the integrand in Equation 9 was computed to at least five-place accuracy. The numerical integration was done by Simpson's rule. Experimentation with various integration-interval sizes indicates that the majority of the entries in Table 3 may be presumed to be accurate to the three figures shown. It is expected that only in a few instances there is an error of one unit, or at most two units, in the third figure.

Figure 1 shows plots of the Vavilov distribution for $\beta^2 = 0.9$, for various values of κ, in order to illustrate the transition from a Landau to a Gaussian distribution. Figure 2 shows, for $\beta^2 = 0.5$, the most probable energy-loss and the width of the energy-loss distribution, both as functions of the parameter κ.

7. Comparison with an Experiment

Energy-loss distributions for 37-Mev protons, in plastic scintillators and in argon-filled proportional counters, have been measured by Gooding and Eisberg (9). Figures 3a and 3b of this paper are reproductions of Figures 4 and 5 of Gooding and Eisberg's paper containing the experimental and Symon distributions, to which we have added the corresponding Vavilov distributions. The experimental points apparently were normalized to the peak of the Symon distribution, but this is not explicitly stated. It can be seen that there is good agreement between the Symon and Vavilov distributions, which predict the experimental results quite well.

TABLE 3

Vavilov Distribution ($\kappa = 0.01$)

λ	β^2=0.0	0.1	0.2	0.3	0.4	0.5	0.6	0.7	0.8	0.9	1.0
-3.0	6.80(-4)	6.85(-4)	6.90(-4)	6.95(-4)	7.00(-4)	7.05(-4)	7.10(-4)	7.15(-4)	7.21(-4)	7.26(-4)	7.31(-4)
-2.5	9.73(-3)	9.80(-3)	9.87(-3)	9.93(-3)	1.00(-2)	1.01(-2)	1.01(-2)	1.02(-2)	1.03(-2)	1.03(-2)	1.04(-2)
-2.0	4.44(-2)	4.47(-2)	4.50(-2)	4.52(-2)	4.55(-2)	4.58(-2)	4.61(-2)	4.64(-2)	4.67(-2)	4.70(-2)	4.72(-2)
-1.5	1.02(-1)	1.02(-1)	1.03(-1)	1.03(-1)	1.04(-1)	1.05(-1)	1.05(-1)	1.06(-1)	1.06(-1)	1.07(-1)	1.08(-1)
-1.0	1.53(-1)	1.54(-1)	1.55(-1)	1.55(-1)	1.56(-1)	1.57(-1)	1.58(-1)	1.59(-1)	1.59(-1)	1.60(-1)	1.61(-1)
-0.5	1.79(-1)	1.80(-1)	1.81(-1)	1.82(-1)	1.83(-1)	1.83(-1)	1.84(-1)	1.85(-1)	1.86(-1)	1.87(-1)	1.88(-1)
0.0	1.81(-1)	1.81(-1)	1.82(-1)	1.83(-1)	1.84(-1)	1.84(-1)	1.85(-1)	1.86(-1)	1.87(-1)	1.88(-1)	1.88(-1)
0.5	1.67(-1)	1.68(-1)	1.68(-1)	1.69(-1)	1.69(-1)	1.70(-1)	1.71(-1)	1.71(-1)	1.72(-1)	1.73(-1)	1.73(-1)
1.0	1.47(-1)	1.47(-1)	1.48(-1)	1.48(-1)	1.49(-1)	1.49(-1)	1.49(-1)	1.50(-1)	1.50(-1)	1.51(-1)	1.51(-1)
1.5	1.25(-1)	1.26(-1)	1.26(-1)	1.26(-1)	1.27(-1)	1.27(-1)	1.28(-1)	1.28(-1)	1.28(-1)	1.29(-1)	1.29(-1)
2.0	1.06(-1)	1.06(-1)	1.06(-1)	1.07(-1)	1.07(-1)	1.07(-1)	1.07(-1)	1.08(-1)	1.08(-1)	1.08(-1)	1.08(-1)
2.5	8.91(-2)	8.93(-2)	8.94(-2)	8.96(-2)	8.97(-2)	8.99(-2)	9.00(-2)	9.02(-2)	9.03(-2)	9.04(-2)	9.06(-2)
3.0	7.50(-2)	7.51(-2)	7.52(-2)	7.53(-2)	7.53(-2)	7.54(-2)	7.55(-2)	7.56(-2)	7.57(-2)	7.58(-2)	7.59(-2)
3.5	6.34(-2)	6.34(-2)	6.34(-2)	6.35(-2)	6.35(-2)	6.36(-2)	6.36(-2)	6.36(-2)	6.37(-2)	6.37(-2)	6.37(-2)
4.0	5.38(-2)	5.38(-2)	5.38(-2)	5.38(-2)	5.38(-2)	5.38(-2)	5.39(-2)	5.39(-2)	5.39(-2)	5.39(-2)	5.39(-2)
4.5	4.60(-2)	4.60(-2)	4.60(-2)	4.59(-2)	4.59(-2)	4.59(-2)	4.59(-2)	4.59(-2)	4.58(-2)	4.58(-2)	4.58(-2)
5.0	3.96(-2)	3.95(-2)	3.95(-2)	3.95(-2)	3.94(-2)	3.94(-2)	3.93(-2)	3.93(-2)	3.93(-2)	3.92(-2)	3.92(-2)
5.5	3.43(-2)	3.42(-2)	3.42(-2)	3.41(-2)	3.41(-2)	3.40(-2)	3.40(-2)	3.39(-2)	3.39(-2)	3.38(-2)	3.38(-2)
6.0	2.99(-2)	2.98(-2)	2.97(-2)	2.97(-2)	2.96(-2)	2.96(-2)	2.95(-2)	2.95(-2)	2.94(-2)	2.93(-2)	2.93(-2)
6.5	2.62(-2)	2.61(-2)	2.61(-2)	2.60(-2)	2.59(-2)	2.59(-2)	2.58(-2)	2.57(-2)	2.57(-2)	2.56(-2)	2.55(-2)
7.0	2.31(-2)	2.30(-2)	2.30(-2)	2.29(-2)	2.28(-2)	2.28(-2)	2.27(-2)	2.26(-2)	2.26(-2)	2.25(-2)	2.24(-2)
7.5	2.05(-2)	2.04(-2)	2.04(-2)	2.03(-2)	2.02(-2)	2.01(-2)	2.01(-2)	2.00(-2)	1.99(-2)	1.99(-2)	1.98(-2)
8.0	1.83(-2)	1.82(-2)	1.81(-2)	1.81(-2)	1.80(-2)	1.79(-2)	1.78(-2)	1.78(-2)	1.77(-2)	1.76(-2)	1.75(-2)
8.5	1.64(-2)	1.63(-2)	1.62(-2)	1.62(-2)	1.61(-2)	1.60(-2)	1.59(-2)	1.59(-2)	1.58(-2)	1.57(-2)	1.56(-2)
9.0	1.47(-2)	1.47(-2)	1.46(-2)	1.45(-2)	1.45(-2)	1.44(-2)	1.43(-2)	1.42(-2)	1.42(-2)	1.41(-2)	1.40(-2)
9.5	1.33(-2)	1.33(-2)	1.32(-2)	1.31(-2)	1.30(-2)	1.30(-2)	1.29(-2)	1.28(-2)	1.27(-2)	1.27(-2)	1.26(-2)
10.0	1.21(-2)	1.20(-2)	1.20(-2)	1.19(-2)	1.18(-2)	1.17(-2)	1.17(-2)	1.16(-2)	1.15(-2)	1.14(-2)	1.14(-2)
11.0	1.01(-2)	1.00(-2)	9.94(-3)	9.87(-3)	9.80(-3)	9.73(-3)	9.66(-3)	9.59(-3)	9.51(-3)	9.44(-3)	9.37(-3)
12.0	8.51(-3)	8.44(-3)	8.37(-3)	8.31(-3)	8.24(-3)	8.17(-3)	8.10(-3)	8.03(-3)	7.96(-3)	7.89(-3)	7.82(-3)
13.0	7.26(-3)	7.20(-3)	7.14(-3)	7.07(-3)	7.00(-3)	6.94(-3)	6.87(-3)	6.81(-3)	6.74(-3)	6.67(-3)	6.61(-3)
14.0	6.27(-3)	6.20(-3)	6.14(-3)	6.08(-3)	6.02(-3)	5.95(-3)	5.89(-3)	5.83(-3)	5.76(-3)	5.70(-3)	5.64(-3)
15.0	5.46(-3)	5.40(-3)	5.34(-3)	5.28(-3)	5.22(-3)	5.16(-3)	5.10(-3)	5.04(-3)	4.97(-3)	4.91(-3)	4.85(-3)
16.0	4.79(-3)	4.73(-3)	4.67(-3)	4.62(-3)	4.56(-3)	4.50(-3)	4.44(-3)	4.39(-3)	4.33(-3)	4.27(-3)	4.21(-3)
17.0	4.23(-3)	4.18(-3)	4.12(-3)	4.07(-3)	4.01(-3)	3.96(-3)	3.90(-3)	3.85(-3)	3.79(-3)	3.73(-3)	3.68(-3)
18.0	3.77(-3)	3.71(-3)	3.66(-3)	3.61(-3)	3.56(-3)	3.50(-3)	3.45(-3)	3.40(-3)	3.34(-3)	3.29(-3)	3.24(-3)
19.0	3.37(-3)	3.32(-3)	3.27(-3)	3.22(-3)	3.17(-3)	3.12(-3)	3.07(-3)	3.02(-3)	2.97(-3)	2.91(-3)	2.86(-3)
20.0	3.04(-3)	2.99(-3)	2.94(-3)	2.89(-3)	2.84(-3)	2.79(-3)	2.74(-3)	2.69(-3)	2.64(-3)	2.60(-3)	2.55(-3)
22.0	2.49(-3)	2.45(-3)	2.40(-3)	2.36(-3)	2.31(-3)	2.27(-3)	2.22(-3)	2.18(-3)	2.13(-3)	2.09(-3)	2.04(-3)
24.0	2.08(-3)	2.04(-3)	2.00(-3)	1.96(-3)	1.92(-3)	1.88(-3)	1.83(-3)	1.79(-3)	1.75(-3)	1.71(-3)	1.66(-3)
26.0	1.77(-3)	1.73(-3)	1.69(-3)	1.65(-3)	1.61(-3)	1.57(-3)	1.53(-3)	1.49(-3)	1.45(-3)	1.41(-3)	1.37(-3)
28.0	1.51(-3)	1.48(-3)	1.44(-3)	1.41(-3)	1.37(-3)	1.33(-3)	1.30(-3)	1.26(-3)	1.22(-3)	1.18(-3)	1.15(-3)
30.0	1.31(-3)	1.28(-3)	1.24(-3)	1.21(-3)	1.18(-3)	1.14(-3)	1.11(-3)	1.07(-3)	1.04(-3)	1.00(-3)	9.68(-4)
32.0	1.15(-3)	1.12(-3)	1.08(-3)	1.05(-3)	1.02(-3)	9.87(-4)	9.56(-4)	9.22(-4)	8.89(-4)	8.56(-4)	8.24(-4)
34.0	1.01(-3)	9.81(-4)	9.51(-4)	9.21(-4)	8.90(-4)	8.60(-4)	8.29(-4)	7.98(-4)	7.68(-4)	7.37(-4)	7.06(-4)
36.0	8.98(-4)	8.70(-4)	8.41(-4)	8.12(-4)	7.83(-4)	7.54(-4)	7.25(-4)	6.96(-4)	6.67(-4)	6.38(-4)	6.09(-4)

Vavilov Distribution ($\kappa = 0.04$)

λ	β^2=0.0	0.1	0.2	0.3	0.4	0.5	0.6	0.7	0.8	0.9	1.0
-3.0	7.01(-4)	7.18(-4)	7.34(-4)	7.52(-4)	7.69(-4)	7.87(-4)	8.06(-4)	8.25(-4)	8.44(-4)	8.64(-4)	8.84(-4)
-2.5	1.00(-2)	1.02(-2)	1.05(-2)	1.07(-2)	1.09(-2)	1.12(-2)	1.14(-2)	1.16(-2)	1.19(-2)	1.21(-2)	1.24(-2)
-2.0	4.58(-2)	4.67(-2)	4.76(-2)	4.85(-2)	4.94(-2)	5.04(-2)	5.13(-2)	5.23(-2)	5.33(-2)	5.44(-2)	5.54(-2)
-1.5	1.05(-1)	1.06(-1)	1.08(-1)	1.10(-1)	1.12(-1)	1.14(-1)	1.16(-1)	1.18(-1)	1.20(-1)	1.22(-1)	1.24(-1)
-1.0	1.58(-1)	1.60(-1)	1.62(-1)	1.65(-1)	1.67(-1)	1.70(-1)	1.73(-1)	1.75(-1)	1.78(-1)	1.81(-1)	1.83(-1)
-0.5	1.85(-1)	1.87(-1)	1.90(-1)	1.92(-1)	1.95(-1)	1.97(-1)	2.00(-1)	2.02(-1)	2.05(-1)	2.08(-1)	2.10(-1)
0.0	1.86(-1)	1.88(-1)	1.90(-1)	1.92(-1)	1.95(-1)	1.97(-1)	1.99(-1)	2.01(-1)	2.03(-1)	2.06(-1)	2.08(-1)
0.5	1.72(-1)	1.74(-1)	1.75(-1)	1.77(-1)	1.78(-1)	1.80(-1)	1.82(-1)	1.83(-1)	1.85(-1)	1.87(-1)	1.88(-1)
1.0	1.51(-1)	1.52(-1)	1.53(-1)	1.54(-1)	1.55(-1)	1.57(-1)	1.58(-1)	1.59(-1)	1.60(-1)	1.61(-1)	1.62(-1)
1.5	1.29(-1)	1.30(-1)	1.31(-1)	1.31(-1)	1.32(-1)	1.33(-1)	1.33(-1)	1.34(-1)	1.34(-1)	1.35(-1)	1.36(-1)
2.0	1.09(-1)	1.10(-1)	1.10(-1)	1.10(-1)	1.11(-1)	1.11(-1)	1.11(-1)	1.11(-1)	1.12(-1)	1.12(-1)	1.12(-1)
2.5	9.18(-2)	9.19(-2)	9.20(-2)	9.21(-2)	9.22(-2)	9.22(-2)	9.23(-2)	9.23(-2)	9.23(-2)	9.24(-2)	9.24(-2)
3.0	7.73(-2)	7.72(-2)	7.71(-2)	7.70(-2)	7.69(-2)	7.68(-2)	7.67(-2)	7.66(-2)	7.64(-2)	7.62(-2)	7.61(-2)
3.5	6.53(-2)	6.51(-2)	6.49(-2)	6.47(-2)	6.45(-2)	6.42(-2)	6.40(-2)	6.37(-2)	6.34(-2)	6.32(-2)	6.29(-2)
4.0	5.54(-2)	5.52(-2)	5.49(-2)	5.46(-2)	5.43(-2)	5.40(-2)	5.36(-2)	5.33(-2)	5.29(-2)	5.26(-2)	5.22(-2)
4.5	4.74(-2)	4.71(-2)	4.67(-2)	4.64(-2)	4.60(-2)	4.56(-2)	4.53(-2)	4.49(-2)	4.45(-2)	4.40(-2)	4.36(-2)
5.0	4.08(-2)	4.04(-2)	4.00(-2)	3.96(-2)	3.92(-2)	3.88(-2)	3.84(-2)	3.80(-2)	3.76(-2)	3.71(-2)	3.67(-2)
5.5	3.53(-2)	3.49(-2)	3.45(-2)	3.41(-2)	3.37(-2)	3.33(-2)	3.28(-2)	3.24(-2)	3.19(-2)	3.15(-2)	3.10(-2)
6.0	3.08(-2)	3.04(-2)	3.00(-2)	2.95(-2)	2.91(-2)	2.87(-2)	2.82(-2)	2.78(-2)	2.73(-2)	2.69(-2)	2.64(-2)
6.5	2.70(-2)	2.66(-2)	2.62(-2)	2.57(-2)	2.53(-2)	2.49(-2)	2.44(-2)	2.40(-2)	2.35(-2)	2.31(-2)	2.26(-2)
7.0	2.38(-2)	2.34(-2)	2.30(-2)	2.26(-2)	2.21(-2)	2.17(-2)	2.13(-2)	2.08(-2)	2.04(-2)	1.99(-2)	1.94(-2)
7.5	2.11(-2)	2.07(-2)	2.03(-2)	1.99(-2)	1.95(-2)	1.90(-2)	1.86(-2)	1.82(-2)	1.77(-2)	1.73(-2)	1.68(-2)
8.0	1.88(-2)	1.84(-2)	1.80(-2)	1.76(-2)	1.72(-2)	1.68(-2)	1.64(-2)	1.59(-2)	1.55(-2)	1.51(-2)	1.46(-2)
8.5	1.69(-2)	1.65(-2)	1.61(-2)	1.57(-2)	1.53(-2)	1.49(-2)	1.45(-2)	1.40(-2)	1.36(-2)	1.32(-2)	1.27(-2)
9.0	1.52(-2)	1.48(-2)	1.44(-2)	1.40(-2)	1.36(-2)	1.32(-2)	1.28(-2)	1.24(-2)	1.20(-2)	1.16(-2)	1.12(-2)
9.5	1.37(-2)	1.34(-2)	1.30(-2)	1.26(-2)	1.22(-2)	1.18(-2)	1.14(-2)	1.10(-2)	1.06(-2)	1.02(-2)	9.81(-3)
10.0	1.25(-2)	1.21(-2)	1.17(-2)	1.14(-2)	1.10(-2)	1.06(-2)	1.02(-2)	9.84(-3)	9.45(-3)	9.05(-3)	8.65(-3)
11.0	1.04(-2)	1.00(-2)	9.40(-3)	9.35(-3)	8.89(-3)	8.63(-3)	8.27(-3)	7.91(-3)	7.54(-3)	7.17(-3)	6.79(-3)
12.0	8.77(-3)	8.44(-3)	8.11(-3)	7.78(-3)	7.45(-3)	7.11(-3)	6.77(-3)	6.43(-3)	6.08(-3)	5.73(-3)	5.38(-3)
13.0	7.49(-3)	7.18(-3)	6.87(-3)	6.56(-3)	6.24(-3)	5.92(-3)	5.60(-3)	5.28(-3)	4.95(-3)	4.63(-3)	4.30(-3)
14.0	6.46(-3)	6.17(-3)	5.87(-3)	5.58(-3)	5.28(-3)	4.98(-3)	4.68(-3)	4.38(-3)	4.07(-3)	3.76(-3)	3.45(-3)
15.0	5.62(-3)	5.35(-3)	5.07(-3)	4.79(-3)	4.51(-3)	4.22(-3)	3.94(-3)	3.65(-3)	3.36(-3)	3.07(-3)	2.78(-3)
16.0	4.93(-3)	4.67(-3)	4.41(-3)	4.14(-3)	3.88(-3)	3.61(-3)	3.34(-3)	3.07(-3)	2.80(-3)	2.52(-3)	2.24(-3)
17.0	4.36(-3)	4.11(-3)	3.86(-3)	3.61(-3)	3.36(-3)	3.10(-3)	2.85(-3)	2.59(-3)	2.33(-3)	2.07(-3)	1.81(-3)
18.0	3.88(-3)	3.65(-3)	3.41(-3)	3.17(-3)	2.93(-3)	2.69(-3)	2.44(-3)	2.20(-3)	1.95(-3)	1.71(-3)	1.46(-3)
19.0	3.48(-3)	3.25(-3)	3.02(-3)	2.79(-3)	2.57(-3)	2.34(-3)	2.10(-3)	1.87(-3)	1.64(-3)	1.41(-3)	1.17(-3)
20.0	3.13(-3)	2.91(-3)	2.70(-3)	2.48(-3)	2.26(-3)	2.04(-3)	1.82(-3)	1.60(-3)	1.38(-3)	1.16(-3)	9.32(-4)
22.0	2.57(-3)	2.37(-3)	2.17(-3)	1.98(-3)	1.78(-3)	1.58(-3)	1.37(-3)	1.17(-3)	9.71(-4)	7.69(-4)	5.66(-4)
24.0	1.97(-3)	1.80(-3)	1.63(-3)	1.47(-3)	1.30(-3)	1.13(-3)	9.69(-4)	8.04(-4)	6.39(-4)	4.75(-4)	3.11(-4)
26.0	1.14(-3)	1.04(-3)	9.34(-4)	8.32(-4)	7.31(-4)	6.31(-4)	5.34(-4)	4.38(-4)	3.44(-4)	2.52(-4)	1.61(-4)
28.0	6.50(-4)	5.85(-4)	5.22(-4)	4.61(-4)	4.02(-4)	3.45(-4)	2.89(-4)	2.35(-4)	1.84(-4)	1.34(-4)	8.60(-5)
30.0	3.95(-4)	3.53(-4)	3.12(-4)	2.73(-4)	2.36(-4)	2.00(-4)	1.66(-4)	1.34(-4)	1.03(-4)	7.46(-5)	4.76(-5)

TABLE 3 (Cont'd)

Vavilov Distribution (κ = 0.07)

λ	β^2=0.0	0.1	0.2	0.3	0.4	0.5	0.6	0.7	0.8	0.9	1.0
-3.5	-	-	-	-	-	-	1.01(-5)	1.06(-5)	1.10(-5)	1.14(-5)	1.19(-5)
-3.0	7.23(-4)	7.50(-4)	7.78(-4)	8.07(-4)	8.37(-4)	8.68(-4)	9.00(-4)	9.34(-4)	9.69(-4)	1.01(-3)	1.04(-3)
-2.5	1.03(-2)	1.07(-2)	1.10(-2)	1.14(-2)	1.18(-2)	1.22(-2)	1.26(-2)	1.30(-2)	1.35(-2)	1.39(-2)	1.44(-2)
-2.0	4.72(-2)	4.86(-2)	5.00(-2)	5.15(-2)	5.31(-2)	5.47(-2)	5.63(-2)	5.80(-2)	5.98(-2)	6.15(-2)	6.34(-2)
-1.5	1.08(-1)	1.11(-1)	1.14(-1)	1.17(-1)	1.20(-1)	1.23(-1)	1.26(-1)	1.29(-1)	1.33(-1)	1.36(-1)	1.40(-1)
-1.0	1.62(-1)	1.66(-1)	1.70(-1)	1.74(-1)	1.78(-1)	1.82(-1)	1.86(-1)	1.90(-1)	1.94(-1)	1.99(-1)	2.03(-1)
-0.5	1.90(-1)	1.94(-1)	1.98(-1)	2.01(-1)	2.05(-1)	2.09(-1)	2.13(-1)	2.17(-1)	2.21(-1)	2.25(-1)	2.30(-1)
0.0	1.92(-1)	1.95(-1)	1.98(-1)	2.01(-1)	2.04(-1)	2.07(-1)	2.10(-1)	2.14(-1)	2.17(-1)	2.20(-1)	2.23(-1)
0.5	1.77(-1)	1.79(-1)	1.82(-1)	1.84(-1)	1.86(-1)	1.88(-1)	1.90(-1)	1.92(-1)	1.95(-1)	1.97(-1)	1.99(-1)
1.0	1.56(-1)	1.57(-1)	1.58(-1)	1.60(-1)	1.61(-1)	1.62(-1)	1.64(-1)	1.65(-1)	1.66(-1)	1.67(-1)	1.68(-1)
1.5	1.33(-1)	1.34(-1)	1.35(-1)	1.35(-1)	1.36(-1)	1.36(-1)	1.37(-1)	1.37(-1)	1.38(-1)	1.38(-1)	1.39(-1)
2.0	1.13(-1)	1.13(-1)	1.13(-1)	1.13(-1)	1.13(-1)	1.13(-1)	1.13(-1)	1.13(-1)	1.13(-1)	1.13(-1)	1.13(-1)
2.5	9.46(-2)	9.44(-2)	9.42(-2)	9.40(-2)	9.37(-2)	9.33(-2)	9.30(-2)	9.26(-2)	9.21(-2)	9.16(-2)	9.11(-2)
3.0	7.96(-2)	7.92(-2)	7.87(-2)	7.82(-2)	7.77(-2)	7.71(-2)	7.65(-2)	7.58(-2)	7.51(-2)	7.44(-2)	7.36(-2)
3.5	6.73(-2)	6.67(-2)	6.60(-2)	6.53(-2)	6.46(-2)	6.39(-2)	6.31(-2)	6.23(-2)	6.14(-2)	6.06(-2)	5.96(-2)
4.0	5.71(-2)	5.64(-2)	5.57(-2)	5.49(-2)	5.41(-2)	5.32(-2)	5.24(-2)	5.14(-2)	5.05(-2)	4.95(-2)	4.85(-2)
4.5	4.88(-2)	4.80(-2)	4.72(-2)	4.64(-2)	4.55(-2)	4.46(-2)	4.37(-2)	4.27(-2)	4.17(-2)	4.07(-2)	3.97(-2)
5.0	4.20(-2)	4.12(-2)	4.03(-2)	3.95(-2)	3.86(-2)	3.76(-2)	3.67(-2)	3.57(-2)	3.47(-2)	3.36(-2)	3.26(-2)
5.5	3.64(-2)	3.55(-2)	3.47(-2)	3.38(-2)	3.29(-2)	3.19(-2)	3.10(-2)	3.00(-2)	2.90(-2)	2.80(-2)	2.69(-2)
6.0	3.17(-2)	3.09(-2)	3.00(-2)	2.91(-2)	2.82(-2)	2.73(-2)	2.63(-2)	2.53(-2)	2.44(-2)	2.33(-2)	2.23(-2)
6.5	2.78(-2)	2.70(-2)	2.61(-2)	2.52(-2)	2.43(-2)	2.34(-2)	2.25(-2)	2.15(-2)	2.06(-2)	1.96(-2)	1.86(-2)
7.0	2.45(-2)	2.37(-2)	2.29(-2)	2.20(-2)	2.11(-2)	2.02(-2)	1.93(-2)	1.84(-2)	1.74(-2)	1.65(-2)	1.55(-2)
7.5	2.18(-2)	2.09(-2)	2.01(-2)	1.93(-2)	1.84(-2)	1.76(-2)	1.67(-2)	1.58(-2)	1.49(-2)	1.39(-2)	1.30(-2)
8.0	1.94(-2)	1.86(-2)	1.78(-2)	1.70(-2)	1.62(-2)	1.53(-2)	1.45(-2)	1.36(-2)	1.27(-2)	1.18(-2)	1.09(-2)
8.5	1.74(-2)	1.66(-2)	1.58(-2)	1.50(-2)	1.42(-2)	1.34(-2)	1.26(-2)	1.18(-2)	1.09(-2)	1.00(-2)	9.17(-3)
9.0	1.57(-2)	1.49(-2)	1.41(-2)	1.34(-2)	1.26(-2)	1.18(-2)	1.10(-2)	1.02(-2)	9.39(-3)	8.56(-3)	7.72(-3)
8.5	1.42(-2)	1.34(-2)	1.27(-2)	1.20(-2)	1.12(-2)	1.04(-2)	9.66(-3)	8.88(-3)	8.09(-3)	7.30(-3)	6.49(-3)
10.0	1.28(-2)	1.21(-2)	1.14(-2)	1.07(-2)	9.99(-3)	9.25(-3)	8.51(-3)	7.75(-3)	6.99(-3)	6.23(-3)	5.45(-3)
11.0	1.07(-2)	1.00(-2)	9.37(-3)	8.70(-3)	8.02(-3)	7.34(-3)	6.64(-3)	5.95(-3)	5.24(-3)	4.53(-3)	3.81(-3)
12.0	9.01(-3)	8.39(-3)	7.77(-3)	7.14(-3)	6.50(-3)	5.87(-3)	5.22(-3)	4.58(-3)	3.83(-3)	3.27(-3)	2.61(-3)
13.0	7.35(-3)	6.79(-3)	6.23(-3)	5.68(-3)	5.12(-3)	4.55(-3)	3.99(-3)	3.43(-3)	2.86(-3)	2.29(-3)	1.73(-3)
14.0	5.54(-3)	5.08(-3)	4.63(-3)	4.18(-3)	3.73(-3)	3.28(-3)	2.84(-3)	2.40(-3)	1.97(-3)	1.54(-3)	1.11(-3)
15.0	3.97(-3)	3.61(-3)	3.27(-3)	2.92(-3)	2.59(-3)	2.26(-3)	1.93(-3)	1.62(-3)	1.31(-3)	1.00(-3)	7.05(-4)
16.0	2.81(-3)	2.54(-3)	2.28(-3)	2.02(-3)	1.78(-3)	1.54(-3)	1.30(-3)	1.08(-3)	8.59(-4)	6.49(-4)	4.48(-4)
17.0	2.00(-3)	1.80(-3)	1.60(-3)	1.41(-3)	1.23(-3)	1.05(-3)	8.82(-4)	7.21(-4)	5.68(-4)	4.23(-4)	2.86(-4)
18.0	1.44(-3)	1.29(-3)	1.14(-3)	9.93(-4)	8.56(-4)	7.26(-4)	6.03(-4)	4.87(-4)	3.79(-4)	2.77(-4)	1.83(-4)
19.0	1.05(-3)	9.32(-4)	8.17(-4)	7.08(-4)	6.05(-4)	5.08(-4)	4.17(-4)	3.33(-4)	2.55(-4)	1.83(-4)	1.18(-4)
20.0	7.77(-4)	6.83(-4)	5.94(-4)	5.10(-4)	4.32(-4)	3.59(-4)	2.91(-4)	2.29(-4)	1.72(-4)	1.21(-4)	2.58(-5)
22.0	4.31(-4)	3.73(-4)	3.20(-4)	2.70(-4)	2.24(-4)	1.82(-4)	1.44(-4)	1.10(-4)	7.96(-5)	5.34(-5)	3.11(-5)
24.0	2.40(-4)	2.05(-4)	1.73(-4)	1.43(-4)	1.16(-4)	9.22(-5)	7.08(-5)	5.32(-5)	3.63(-5)	2.30(-5)	1.23(-5)
26.0	1.30(-4)	1.09(-4)	9.02(-5)	7.34(-5)	5.84(-5)	4.51(-5)	3.37(-5)	2.39(-5)	1.58(-5)		

Vavilov Distribution (κ = 0.1)

λ	β^2=0.0	0.1	0.2	0.3	0.4	0.5	0.6	0.7	0.8	0.9	1.0
-3.5	-	-	-	-	1.00(-5)	1.06(-5)	1.11(-5)	1.18(-5)	1.24(-5)	1.31(-5)	1.38(-5)
-3.0	7.45(-4)	7.82(-4)	8.21(-4)	8.62(-4)	9.05(-4)	9.50(-4)	9.98(-4)	1.05(-3)	1.10(-3)	1.15(-3)	1.21(-3)
-2.5	1.07(-2)	1.11(-2)	1.16(-2)	1.21(-2)	1.27(-2)	1.33(-2)	1.38(-2)	1.45(-2)	1.51(-2)	1.58(-2)	1.65(-2)
-2.0	4.86(-2)	5.05(-2)	5.25(-2)	5.46(-2)	5.67(-2)	5.90(-2)	6.13(-2)	6.37(-2)	6.62(-2)	6.88(-2)	7.15(-2)
-1.5	1.11(-1)	1.15(-1)	1.19(-1)	1.23(-1)	1.27(-1)	1.32(-1)	1.36(-1)	1.41(-1)	1.45(-1)	1.50(-1)	1.55(-1)
-1.0	1.67(-1)	1.72(-1)	1.77(-1)	1.82(-1)	1.88(-1)	1.93(-1)	1.99(-1)	2.04(-1)	2.10(-1)	2.16(-1)	2.22(-1)
-0.5	1.96(-1)	2.01(-1)	2.06(-1)	2.10(-1)	2.15(-1)	2.20(-1)	2.26(-1)	2.31(-1)	2.36(-1)	2.42(-1)	2.47(-1)
0.0	1.98(-1)	2.01(-1)	2.05(-1)	2.09(-1)	2.13(-1)	2.17(-1)	2.21(-1)	2.25(-1)	2.28(-1)	2.32(-1)	2.37(-1)
0.5	1.83(-1)	1.85(-1)	1.88(-1)	1.90(-1)	1.93(-1)	1.95(-1)	1.98(-1)	2.00(-1)	2.02(-1)	2.05(-1)	2.07(-1)
1.0	1.60(-1)	1.62(-1)	1.63(-1)	1.65(-1)	1.66(-1)	1.67(-1)	1.68(-1)	1.69(-1)	1.70(-1)	1.71(-1)	1.72(-1)
1.5	1.37(-1)	1.38(-1)	1.38(-1)	1.39(-1)	1.39(-1)	1.39(-1)	1.39(-1)	1.39(-1)	1.39(-1)	1.39(-1)	1.39(-1)
2.0	1.16(-1)	1.16(-1)	1.16(-1)	1.15(-1)	1.15(-1)	1.14(-1)	1.14(-1)	1.13(-1)	1.13(-1)	1.12(-1)	1.11(-1)
2.5	9.75(-2)	9.69(-2)	9.62(-2)	9.54(-2)	9.45(-2)	9.36(-2)	9.26(-2)	9.16(-2)	9.04(-2)	8.92(-2)	8.79(-2)
3.0	8.21(-2)	8.11(-2)	8.01(-2)	7.90(-2)	7.79(-2)	7.66(-2)	7.54(-2)	7.40(-2)	7.26(-2)	7.10(-2)	6.94(-2)
3.5	6.93(-2)	6.82(-2)	6.70(-2)	6.57(-2)	6.43(-2)	6.29(-2)	6.15(-2)	5.99(-2)	5.83(-2)	5.67(-2)	5.49(-2)
4.0	5.89(-2)	5.76(-2)	5.63(-2)	5.49(-2)	5.34(-2)	5.19(-2)	5.04(-2)	4.88(-2)	4.71(-2)	4.53(-2)	4.35(-2)
4.5	5.03(-2)	4.90(-2)	4.76(-2)	4.61(-2)	4.46(-2)	4.31(-2)	4.15(-2)	3.99(-2)	3.82(-2)	3.64(-2)	3.46(-2)
5.0	4.33(-2)	4.19(-2)	4.05(-2)	3.90(-2)	3.75(-2)	3.60(-2)	3.44(-2)	3.27(-2)	3.11(-2)	2.93(-2)	2.75(-2)
5.5	3.75(-2)	3.61(-2)	3.47(-2)	3.32(-2)	3.17(-2)	3.02(-2)	2.86(-2)	2.70(-2)	2.54(-2)	2.37(-2)	2.20(-2)
6.0	3.27(-2)	3.13(-2)	2.99(-2)	2.85(-2)	2.70(-2)	2.55(-2)	2.40(-2)	2.24(-2)	2.08(-2)	1.92(-2)	1.75(-2)
6.5	2.86(-2)	2.73(-2)	2.59(-2)	2.45(-2)	2.31(-2)	2.17(-2)	2.02(-2)	1.87(-2)	1.71(-2)	1.55(-2)	1.39(-2)
7.0	2.53(-2)	2.40(-2)	2.26(-2)	2.13(-2)	1.99(-2)	1.85(-2)	1.70(-2)	1.56(-2)	1.41(-2)	1.26(-2)	1.11(-2)
7.5	2.24(-2)	2.11(-2)	1.98(-2)	1.85(-2)	1.72(-2)	1.58(-2)	1.45(-2)	1.31(-2)	1.16(-2)	1.02(-2)	8.73(-3)
8.0	1.98(-2)	1.86(-2)	1.74(-2)	1.61(-2)	1.48(-2)	1.35(-2)	1.22(-2)	1.09(-2)	9.57(-3)	8.21(-3)	6.83(-3)
8.5	1.74(-2)	1.62(-2)	1.51(-2)	1.39(-2)	1.27(-2)	1.15(-2)	1.03(-2)	9.04(-3)	7.80(-3)	6.55(-3)	5.29(-3)
9.0	1.50(-2)	1.39(-2)	1.28(-2)	1.18(-2)	1.07(-2)	9.57(-3)	8.47(-3)	7.37(-3)	6.27(-3)	5.16(-3)	4.06(-3)
9.5	1.27(-2)	1.17(-2)	1.07(-2)	9.77(-3)	8.80(-3)	7.84(-3)	6.88(-3)	5.92(-3)	4.97(-3)	4.03(-3)	3.09(-3)
10.0	1.05(-2)	9.69(-3)	8.84(-3)	7.99(-3)	7.16(-3)	6.33(-3)	5.51(-3)	4.70(-3)	3.90(-3)	3.11(-3)	2.33(-3)
11.0	7.12(-3)	6.48(-3)	5.85(-3)	5.23(-3)	4.62(-3)	4.03(-3)	3.45(-3)	2.89(-3)	2.35(-3)	1.83(-3)	1.32(-3)
12.0	4.77(-3)	4.30(-3)	3.84(-3)	3.39(-3)	2.96(-3)	2.54(-3)	2.15(-3)	1.77(-3)	1.41(-3)	1.07(-3)	7.45(-4)
13.0	3.21(-3)	2.86(-3)	2.53(-3)	2.21(-3)	1.90(-3)	1.61(-3)	1.34(-3)	1.08(-3)	8.42(-4)	6.21(-4)	4.18(-4)
14.0	2.18(-3)	1.92(-3)	1.68(-3)	1.45(-3)	1.23(-3)	1.03(-3)	8.38(-4)	6.65(-4)	5.06(-4)	3.62(-4)	2.34(-4)
15.0	1.49(-3)	1.30(-3)	1.12(-3)	9.53(-4)	7.99(-4)	6.57(-4)	5.27(-4)	4.09(-4)	3.04(-4)	2.11(-4)	1.30(-4)
16.0	1.01(-3)	8.76(-4)	7.47(-4)	6.28(-4)	5.19(-4)	4.20(-4)	3.31(-4)	2.51(-4)	1.81(-4)	1.21(-4)	7.12(-5)
17.0	6.88(-4)	5.88(-4)	4.96(-4)	4.12(-4)	3.35(-4)	2.67(-4)	2.06(-4)	1.53(-4)	1.07(-4)	6.91(-5)	3.84(-5)
18.0	4.60(-4)	3.89(-4)	3.24(-4)	2.66(-4)	2.13(-4)	1.67(-4)	1.26(-4)	9.16(-5)	6.25(-5)	3.87(-5)	2.03(-5)
19.0	3.01(-4)	2.52(-4)	2.07(-4)	1.68(-4)	1.33(-4)	1.02(-4)	7.62(-5)	5.41(-5)	3.59(-5)	2.15(-5)	1.07(-5)
20.0	1.94(-4)	1.61(-4)	1.31(-4)	1.05(-4)	8.18(-5)	6.21(-5)	4.55(-5)	3.17(-5)	2.06(-5)	1.20(-5)	
22.0	7.97(-5)	6.47(-5)	5.16(-5)	4.03(-5)	3.07(-5)	2.27(-5)	1.61(-5)	1.08(-5)			
24.0	3.26(-5)	2.59(-5)	2.01(-5)	1.53(-5)	1.12(-5)						
26.0	1.33(-5)	1.04(-5)									

TABLE 3 (Cont'd)

Vavilov Distribution (κ = 0.4)

λ	β^2=0.0	0.1	0.2	0.3	0.4	0.5	0.6	0.7	0.8	0.9	1.0
-3.5	1.07(-5)	1.26(-5)	1.47(-5)	1.73(-5)	2.03(-5)	2.37(-5)	2.78(-5)	3.26(-5)	3.82(-5)	4.48(-5)	5.24(-5)
-3.0	1.00(-3)	1.16(-3)	1.33(-3)	1.53(-3)	1.75(-3)	2.02(-3)	2.32(-3)	2.66(-3)	3.05(-3)	3.50(-3)	4.02(-3)
-2.5	1.44(-2)	1.62(-2)	1.83(-2)	2.06(-2)	2.32(-2)	2.61(-2)	2.93(-2)	3.30(-2)	3.71(-2)	4.17(-2)	4.68(-2)
-2.0	6.56(-2)	7.25(-2)	8.00(-2)	8.83(-2)	9.74(-2)	1.07(-1)	1.18(-1)	1.30(-1)	1.43(-1)	1.57(-1)	1.73(-1)
-1.5	1.50(-1)	1.62(-1)	1.76(-1)	1.90(-1)	2.05(-1)	2.21(-1)	2.38(-1)	2.57(-1)	2.76(-1)	2.97(-1)	3.19(-1)
-1.0	2.26(-1)	2.40(-1)	2.54(-1)	2.69(-1)	2.84(-1)	3.00(-1)	3.16(-1)	3.32(-1)	3.49(-1)	3.66(-1)	3.83(-1)
-0.5	2.65(-1)	2.75(-1)	2.85(-1)	2.96(-1)	3.05(-1)	3.15(-1)	3.24(-1)	3.32(-1)	3.40(-1)	3.47(-1)	3.52(-1)
0.0	2.66(-1)	2.71(-1)	2.76(-1)	2.79(-1)	2.82(-1)	2.84(-1)	2.84(-1)	2.84(-1)	2.82(-1)	2.78(-1)	2.73(-1)
0.5	2.44(-1)	2.43(-1)	2.42(-1)	2.39(-1)	2.36(-1)	2.31(-1)	2.25(-1)	2.18(-1)	2.09(-1)	1.99(-1)	1.88(-1)
1.0	2.07(-1)	2.03(-1)	1.97(-1)	1.91(-1)	1.83(-1)	1.75(-1)	1.65(-1)	1.55(-1)	1.44(-1)	1.31(-1)	1.18(-1)
1.5	1.66(-1)	1.59(-1)	1.51(-1)	1.43(-1)	1.34(-1)	1.24(-1)	1.14(-1)	1.03(-1)	9.21(-2)	8.05(-2)	6.86(-2)
2.0	1.26(-1)	1.18(-1)	1.10(-1)	1.01(-1)	9.25(-2)	8.35(-2)	7.43(-2)	6.51(-2)	5.58(-2)	4.66(-2)	3.75(-2)
2.5	9.11(-2)	8.37(-2)	7.62(-2)	6.87(-2)	6.11(-2)	5.36(-2)	4.63(-2)	3.91(-2)	3.22(-2)	2.56(-2)	1.94(-2)
3.0	6.35(-2)	5.71(-2)	5.09(-2)	4.48(-2)	3.88(-2)	3.31(-2)	2.77(-2)	2.26(-2)	1.78(-2)	1.35(-2)	9.60(-3)
3.5	4.28(-2)	3.77(-2)	3.29(-2)	2.82(-2)	2.39(-2)	1.98(-2)	1.60(-2)	1.26(-2)	9.52(-3)	6.84(-3)	4.55(-3)
4.0	2.79(-2)	2.41(-2)	2.06(-2)	1.72(-2)	1.42(-2)	1.14(-2)	8.95(-3)	6.78(-3)	4.91(-3)	3.35(-3)	2.08(-3)
4.5	1.77(-2)	1.50(-2)	1.25(-2)	1.02(-2)	8.21(-3)	6.42(-3)	4.87(-3)	3.55(-3)	2.46(-3)	1.59(-3)	9.22(-4)
5.0	1.10(-2)	9.10(-3)	7.42(-3)	5.93(-3)	4.63(-3)	3.51(-3)	2.58(-3)	1.81(-3)	1.20(-3)	7.34(-4)	3.96(-4)
5.5	6.65(-3)	5.39(-3)	4.30(-3)	3.39(-3)	2.55(-3)	1.88(-3)	1.33(-3)	9.02(-4)	5.72(-4)	3.30(-4)	1.66(-4)
6.0	3.93(-3)	3.13(-3)	2.44(-3)	1.85(-3)	1.37(-3)	9.83(-4)	6.75(-4)	4.39(-4)	2.66(-4)	1.45(-4)	6.73(-5)
6.5	2.28(-3)	1.78(-3)	1.35(-3)	1.01(-3)	7.25(-4)	5.04(-4)	3.34(-4)	2.09(-4)	1.21(-4)	6.24(-5)	2.68(-5)
7.0	1.30(-3)	9.91(-4)	7.38(-4)	5.35(-4)	3.76(-4)	2.53(-4)	1.63(-4)	9.79(-5)	5.41(-5)	2.64(-5)	1.05(-5)
7.5	7.27(-4)	5.43(-4)	3.96(-4)	2.80(-4)	1.91(-4)	1.25(-4)	7.76(-5)	4.49(-5)	2.36(-5)	1.08(-5)	
8.0	4.00(-4)	2.92(-4)	2.08(-4)	1.44(-4)	9.57(-5)	6.08(-5)	3.64(-5)	2.02(-5)	1.02(-5)		
8.5	2.17(-4)	1.55(-4)	1.08(-4)	7.29(-5)	4.72(-5)	2.91(-5)	1.69(-5)				
9.0	1.16(-4)	8.12(-5)	5.53(-5)	3.63(-5)	2.29(-5)	1.37(-5)					
9.5	6.08(-5)	4.19(-5)	2.79(-5)	1.79(-5)	1.09(-5)						
10.0	3.17(-5)	2.13(-5)	1.39(-5)								

Vavilov Distribution (κ = 0.7)

λ	β^2=0.0	0.1	0.2	0.3	0.4	0.5	0.6	0.7	0.8	0.9	1.0
-3.5	1.44(-5)	1.83(-5)	2.32(-5)	2.95(-5)	3.75(-5)	4.76(-5)	6.04(-5)	7.69(-5)	9.72(-5)	1.23(-4)	1.56(-4)
-3.0	1.36(-3)	1.67(-3)	2.04(-3)	2.50(-3)	3.07(-3)	3.76(-3)	4.60(-3)	5.62(-3)	6.87(-3)	8.39(-3)	1.02(-2)
-2.5	1.94(-2)	2.30(-2)	2.72(-2)	3.22(-2)	3.81(-2)	4.49(-2)	5.29(-2)	6.23(-2)	7.33(-2)	8.61(-2)	1.01(-1)
-2.0	8.86(-2)	1.01(-1)	1.16(-1)	1.32(-1)	1.50(-1)	1.71(-1)	1.94(-1)	2.19(-1)	2.47(-1)	2.79(-1)	3.13(-1)
-1.5	2.02(-1)	2.23(-1)	2.46(-1)	2.70(-1)	2.96(-1)	3.23(-1)	3.52(-1)	3.82(-1)	4.13(-1)	4.44(-1)	4.76(-1)
-1.0	3.03(-1)	3.23(-1)	3.42(-1)	3.62(-1)	3.81(-1)	3.99(-1)	4.15(-1)	4.30(-1)	4.42(-1)	4.52(-1)	4.57(-1)
-0.5	3.44(-1)	3.54(-1)	3.62(-1)	3.68(-1)	3.71(-1)	3.72(-1)	3.70(-1)	3.64(-1)	3.54(-1)	3.40(-1)	3.22(-1)
0.0	3.23(-1)	3.20(-1)	3.15(-1)	3.09(-1)	2.97(-1)	2.85(-1)	2.69(-1)	2.51(-1)	2.30(-1)	2.07(-1)	1.81(-1)
0.5	2.60(-1)	2.49(-1)	2.36(-1)	2.21(-1)	2.05(-1)	1.87(-1)	1.61(-1)	1.48(-1)	1.27(-1)	1.06(-1)	8.54(-2)
1.0	1.86(-1)	1.72(-1)	1.57(-1)	1.41(-1)	1.25(-1)	1.09(-1)	9.28(-2)	7.71(-2)	6.20(-2)	4.79(-2)	3.50(-2)
1.5	1.21(-1)	1.08(-1)	9.44(-2)	8.15(-2)	6.91(-2)	5.73(-2)	4.69(-2)	3.82(-2)	2.72(-2)	1.93(-2)	1.28(-2)
2.0	7.20(-2)	6.19(-2)	5.22(-2)	4.33(-2)	3.51(-2)	2.79(-2)	2.11(-2)	1.55(-2)	1.09(-2)	7.11(-3)	4.22(-3)
2.5	3.99(-2)	3.31(-2)	2.69(-2)	2.13(-2)	1.65(-2)	1.24(-2)	8.97(-3)	6.19(-3)	4.02(-3)	2.41(-3)	1.28(-3)
3.0	2.07(-2)	1.66(-2)	1.30(-2)	9.87(-3)	7.30(-3)	5.21(-3)	3.56(-3)	2.31(-3)	1.39(-3)	7.61(-4)	3.60(-4)
3.5	1.02(-2)	7.84(-3)	5.89(-3)	4.31(-3)	3.04(-3)	2.06(-3)	1.33(-3)	8.09(-4)	4.52(-4)	2.26(-4)	9.47(-5)
4.0	4.74(-3)	3.52(-3)	2.55(-3)	1.78(-3)	1.20(-3)	7.76(-4)	4.73(-4)	2.69(-4)	1.39(-4)	6.32(-5)	2.34(-5)
4.5	2.10(-3)	1.51(-3)	1.05(-3)	7.05(-4)	4.54(-4)	2.78(-4)	1.60(-4)	8.52(-5)	4.08(-5)	1.68(-5)	
5.0	8.98(-4)	6.21(-4)	4.15(-4)	2.67(-4)	1.64(-4)	9.55(-5)	5.19(-5)	2.58(-5)	1.14(-5)		
5.5	3.68(-4)	2.45(-4)	1.58(-4)	9.71(-5)	5.70(-5)	3.15(-5)	1.61(-5)				
6.0	1.45(-4)	9.32(-5)	5.96(-5)	3.41(-5)	1.91(-5)	1.00(-5)					
6.5	5.53(-5)	3.43(-5)	2.04(-5)	1.15(-5)							
7.0	2.04(-5)	1.22(-5)									

Vavilov Distribution (κ = 1.0)

λ	β^2=0.0	0.1	0.2	0.3	0.4	0.5	0.6	0.7	0.8	0.9	1.0
-3.5	1.94(-5)	2.64(-5)	3.59(-5)	4.87(-5)	6.61(-5)	8.96(-5)	1.21(-4)	1.64(-4)	2.22(-4)	3.00(-4)	4.05(-4)
-3.0	1.83(-3)	2.37(-3)	3.06(-3)	3.94(-3)	5.08(-3)	6.53(-3)	8.39(-3)	1.08(-2)	1.38(-2)	1.76(-2)	2.29(-2)
-2.5	2.62(-2)	3.22(-2)	3.95(-2)	4.84(-2)	5.91(-2)	7.20(-2)	8.76(-2)	1.06(-1)	1.28(-1)	1.55(-1)	1.86(-1)
-2.0	1.19(-1)	1.39(-1)	1.63(-1)	1.89(-1)	2.18(-1)	2.51(-1)	2.88(-1)	3.29(-1)	3.74(-1)	4.23(-1)	4.75(-1)
-1.5	2.69(-1)	2.99(-1)	3.31(-1)	3.64(-1)	3.97(-1)	4.31(-1)	4.65(-1)	4.97(-1)	5.26(-1)	5.52(-1)	5.73(-1)
-1.0	3.85(-1)	4.07(-1)	4.26(-1)	4.43(-1)	4.56(-1)	4.66(-1)	4.69(-1)	4.67(-1)	4.58(-1)	4.42(-1)	4.17(-1)
-0.5	4.01(-1)	4.02(-1)	4.00(-1)	3.92(-1)	3.80(-1)	3.63(-1)	3.42(-1)	3.15(-1)	2.84(-1)	2.49(-1)	2.11(-1)
0.0	3.29(-1)	3.13(-1)	2.94(-1)	2.73(-1)	2.49(-1)	2.22(-1)	1.94(-1)	1.65(-1)	1.36(-1)	1.08(-1)	8.10(-2)
0.5	2.23(-1)	2.02(-1)	1.80(-1)	1.57(-1)	1.34(-1)	1.12(-1)	9.10(-2)	7.13(-2)	5.35(-2)	3.40(-2)	2.50(-2)
1.0	1.29(-1)	1.11(-1)	9.38(-2)	7.73(-2)	6.21(-2)	4.84(-2)	3.64(-2)	2.61(-2)	1.78(-2)	1.12(-2)	6.42(-3)
1.5	6.60(-2)	5.39(-2)	4.30(-2)	3.34(-2)	2.51(-2)	1.83(-2)	1.27(-2)	8.37(-3)	5.15(-3)	2.88(-3)	1.42(-3)
2.0	3.01(-2)	2.33(-2)	1.76(-2)	1.29(-2)	9.10(-3)	6.15(-3)	3.95(-3)	2.38(-3)	1.32(-3)	6.54(-4)	2.74(-4)
2.5	1.24(-2)	9.15(-3)	6.53(-3)	4.50(-3)	2.98(-3)	1.88(-3)	1.11(-3)	6.12(-4)	3.05(-4)	1.33(-4)	4.73(-5)
3.0	4.71(-3)	3.29(-3)	2.22(-3)	1.44(-3)	8.94(-4)	5.24(-4)	2.87(-4)	1.44(-4)	6.44(-5)	2.46(-5)	
3.5	1.65(-3)	1.09(-3)	6.99(-4)	4.28(-4)	2.48(-4)	1.35(-4)	6.81(-5)	3.11(-5)	1.25(-5)		
4.0	5.38(-4)	3.39(-4)	2.05(-4)	1.18(-4)	6.41(-5)	3.24(-5)	1.51(-5)				
4.5	1.65(-4)	9.86(-5)	5.64(-5)	3.05(-5)	1.55(-5)						
5.0	4.75(-5)	2.70(-5)	1.46(-5)								
5.5	1.30(-5)										

TABLE 3 (Cont'd)

Vavilov Distribution ($\kappa = 4.0$)

λ	β^2=0.0	0.1	0.2	0.3	0.4	0.5	0.6	0.7	0.8	0.9	1.0
-4.00	-	-	-	-	-	1.32(-5)	3.04(-5)	6.90(-5)	1.55(-4)	3.44(-4)	7.55(-4)
-3.75	1.38(-5)	2.98(-5)	6.38(-5)	1.35(-4)	2.83(-4)	5.85(-4)	1.20(-3)	2.41(-3)	4.78(-3)	9.35(-3)	1.80(-2)
-3.50	3.81(-4)	7.44(-4)	1.44(-3)	2.73(-3)	5.12(-3)	9.45(-3)	1.71(-2)	3.05(-2)	5.33(-2)	9.11(-2)	1.52(-1)
-3.25	4.78(-3)	8.44(-3)	1.47(-2)	2.50(-2)	4.19(-2)	6.88(-2)	1.10(-1)	1.73(-1)	2.64(-1)	3.90(-1)	5.57(-1)
-3.00	3.19(-2)	5.08(-2)	7.95(-2)	1.22(-1)	1.82(-1)	2.64(-1)	3.73(-1)	5.11(-1)	6.75(-1)	8.56(-1)	1.03
-2.75	1.27(-1)	1.83(-1)	2.56(-1)	3.51(-1)	4.66(-1)	6.00(-1)	7.44(-1)	8.86(-1)	1.01	1.08	1.09
-2.50	3.28(-1)	4.26(-1)	5.38(-1)	6.58(-1)	7.77(-1)	8.81(-1)	9.56(-1)	9.85(-1)	9.56(-1)	8.63(-1)	7.14(-1)
-2.25	5.89(-1)	6.91(-1)	7.84(-1)	8.57(-1)	8.97(-1)	8.95(-1)	8.46(-1)	7.51(-1)	6.18(-1)	4.65(-1)	3.12(-1)
-2.00	7.75(-1)	8.22(-1)	8.37(-1)	8.15(-1)	7.56(-1)	6.63(-1)	5.44(-1)	4.14(-1)	2.88(-1)	1.78(-1)	9.59(-2)
-1.75	7.79(-1)	7.45(-1)	6.81(-1)	5.91(-1)	4.85(-1)	3.73(-1)	2.65(-1)	1.72(-1)	1.01(-1)	5.10(-2)	2.17(-2)
-1.50	6.16(-1)	5.32(-1)	4.36(-1)	3.38(-1)	2.45(-1)	1.64(-1)	1.01(-1)	5.60(-2)	2.73(-2)	1.13(-2)	3.74(-3)
-1.25	3.95(-1)	3.07(-1)	2.26(-1)	1.56(-1)	9.96(-2)	5.85(-2)	3.11(-2)	1.46(-2)	5.90(-3)	1.97(-3)	5.05(-4)
-1.00	2.09(-1)	1.47(-1)	9.68(-2)	5.94(-2)	3.35(-2)	1.72(-2)	7.85(-3)	3.12(-3)	1.05(-3)	2.80(-4)	5.49(-5)
-0.75	9.33(-2)	5.91(-2)	3.49(-2)	1.91(-2)	9.47(-3)	4.23(-3)	1.66(-3)	5.59(-4)	1.54(-4)	3.29(-5)	
-0.50	3.56(-2)	2.04(-2)	1.08(-2)	5.22(-3)	2.29(-3)	8.90(-4)	3.00(-4)	8.49(-5)	1.93(-5)		
-0.25	1.18(-2)	6.07(-3)	2.88(-3)	1.24(-3)	4.78(-4)	1.62(-4)	4.67(-5)	1.12(-5)			
0.00	3.41(-3)	1.59(-3)	6.74(-4)	2.58(-4)	8.75(-5)	2.57(-5)					
0.25	8.74(-4)	3.67(-4)	1.40(-4)	4.74(-5)	1.42(-5)						
0.50	2.00(-4)	7.57(-5)	2.58(-5)								
0.75	4.11(-5)	1.41(-5)									

Vavilov Distribution ($\kappa = 7.0$)

λ	β^2=0.0	0.1	0.2	0.3	0.4	0.5	0.6	0.7	0.8	0.9	1.0
-4.4	-	-	-	-	-	-	-	-	1.11(-5)	3.90(-5)	1.33(-4)
-4.2	-	-	-	-	-	2.17(-5)	6.93(-5)	2.15(-4)	6.46(-4)	1.88(-3)	5.28(-3)
-4.0	-	1.07(-5)	3.24(-5)	9.54(-5)	2.73(-4)	7.60(-4)	2.04(-3)	5.31(-3)	1.33(-2)	3.18(-2)	7.28(-2)
-3.8	1.11(-4)	2.99(-4)	7.80(-4)	1.97(-3)	4.82(-3)	1.14(-2)	2.57(-2)	5.57(-2)	1.15(-1)	2.24(-1)	4.12(-1)
-3.6	1.77(-3)	4.11(-3)	9.26(-3)	2.01(-2)	4.18(-2)	8.32(-2)	1.58(-1)	2.83(-1)	4.78(-1)	7.51(-1)	1.09
-3.4	1.54(-2)	3.10(-2)	6.01(-2)	1.12(-1)	1.97(-1)	3.31(-1)	5.23(-1)	7.74(-1)	1.06	1.33	1.50
-3.2	7.96(-2)	1.39(-1)	2.33(-1)	3.69(-1)	5.54(-1)	7.81(-1)	1.02	1.24	1.37	1.35	1.17
-3.0	2.63(-1)	3.99(-1)	5.74(-1)	7.78(-1)	9.89(-1)	1.17	1.27	1.25	1.10	8.46(-1)	5.51(-1)
-2.8	5.86(-1)	7.71(-1)	9.54(-1)	1.10	1.18	1.17	1.04	8.35(-1)	5.83(-1)	3.46(-1)	1.68(-1)
-2.6	9.21(-1)	1.05	1.12	1.10	9.97(-1)	8.19(-1)	6.02(-1)	3.88(-1)	2.14(-1)	9.71(-2)	3.44(-2)
-2.4	1.06	1.04	9.55(-1)	8.02(-1)	6.12(-1)	4.18	2.52(-1)	1.30(-1)	5.63(-2)	1.94(-2)	4.95(-3)
-2.2	9.18(-1)	7.85(-1)	6.16(-1)	4.40(-1)	2.83(-1)	1.61(-1)	7.89(-2)	3.27(-2)	1.10(-2)	2.84(-3)	5.18(-4)
-2.0	6.17(-1)	4.57(-1)	3.08(-1)	1.87(-1)	1.01(-1)	4.75(-2)	1.90(-2)	6.29(-3)	1.64(-3)	3.16(-4)	4.05(-5)
-1.8	3.28(-1)	2.10(-1)	1.22(-1)	6.30(-2)	2.85(-2)	1.11(-2)	3.62(-3)	9.50(-4)	1.91(-4)	2.72(-5)	
-1.6	1.41(-1)	7.84(-2)	3.89(-2)	1.71(-2)	6.49(-3)	2.09(-3)	5.52(-4)	1.15(-4)	1.77(-5)		
-1.4	4.99(-2)	2.40(-2)	1.02(-2)	3.80(-3)	1.21(-3)	3.22(-4)	6.88(-5)	1.13(-5)			
-1.2	1.47(-2)	6.10(-3)	2.23(-3)	7.05(-4)	1.88(-4)	4.12(-5)					
-1.0	3.64(-3)	1.31(-3)	4.11(-4)	1.10(-4)	2.46(-5)						
-0.8	7.71(-4)	2.40(-4)	6.46(-5)	1.47(-5)							
-0.6	1.41(-4)	3.80(-5)									
-0.4	2.24(-5)										

Vavilov Distribution ($\kappa = 10.0$)

λ	β^2=0.0	0.1	0.2	0.3	0.4	0.5	0.6	0.7	0.8	0.9	1.0
-4.6	-	-	-	-	-	-	-	-	-	3.85(-5)	1.79(-4)
-4.4	-	-	-	-	-	1.18(-5)	5.14(-5)	2.12(-4)	8.32(-4)	3.08(-3)	1.07(-2)
-4.2	-	-	1.41(-5)	5.57(-5)	2.10(-4)	7.50(-4)	2.54(-3)	8.11(-3)	2.42(-2)	6.69(-2)	1.70(-1)
-4.0	5.27(-5)	1.84(-4)	6.15(-4)	1.95(-3)	5.83(-3)	1.64(-2)	4.32(-2)	1.06(-1)	2.37(-1)	4.82(-1)	8.79(-1)
-3.8	1.43(-3)	4.07(-3)	1.10(-2)	2.78(-2)	6.61(-2)	1.46(-1)	2.96(-1)	5.49(-1)	9.16(-1)	1.35	1.73
-3.6	1.79(-2)	4.17(-2)	9.09(-2)	1.85(-1)	3.46(-1)	5.96(-1)	9.30(-1)	1.30	1.59	1.68	1.47
-3.4	1.16(-1)	2.20(-1)	3.88(-1)	6.29(-1)	9.31(-1)	1.24	1.48	1.54	1.38	1.02	9.99(-1)
-3.2	4.21(-1)	6.50(-1)	9.23(-1)	1.19	1.39	1.44	1.30	1.01	6.46(-1)	3.31(-1)	1.28(-1)
-3.0	9.12(-1)	1.15	1.31	1.35	1.24	9.87(-1)	6.74(-1)	3.84(-1)	1.76(-1)	6.16(-2)	1.53(-2)
-2.8	1.25	1.28	1.18	9.66(-1)	6.92(-1)	4.25(-1)	2.18(-1)	9.11(-2)	2.95(-2)	6.96(-3)	1.09(-3)
-2.6	1.13	9.45(-1)	7.01(-1)	4.56(-1)	2.55(-1)	1.20(-1)	4.64(-2)	1.41(-2)	3.19(-3)	5.02(-4)	4.87(-5)
-2.4	7.06(-1)	4.80(-1)	2.87(-1)	1.48(-1)	6.46(-2)	2.33(-2)	6.71(-3)	1.47(-3)	2.33(-4)	2.41(-5)	
-2.2	3.13(-1)	1.73(-1)	8.33(-2)	3.41(-2)	1.16(-2)	3.19(-3)	6.84(-4)	1.08(-4)	1.18(-5)		
-2.0	1.02(-1)	4.59(-2)	1.77(-2)	5.74(-3)	1.52(-3)	3.19(-4)	5.06(-5)				
-1.8	2.48(-2)	9.10(-3)	2.82(-3)	7.24(-4)	1.49(-4)	2.37(-5)					
-1.6	4.64(-3)	1.38(-3)	3.45(-4)	6.99(-5)	1.11(-5)						
-1.4	6.77(-4)	1.64(-4)	3.29(-5)								
-1.2	7.84(-5)	1.55(-5)									

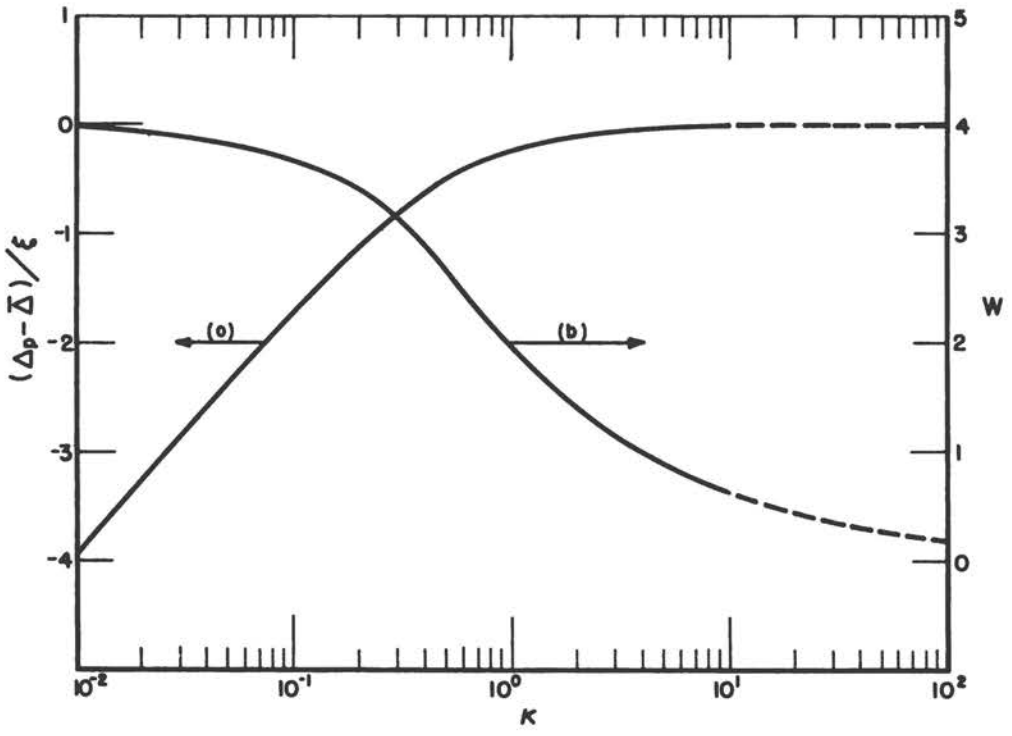

Figure 2. Most probable energy-loss and width of Vavilov distribution, as function of κ, for $\beta^2 = 0.5$. To obtain the most probable energy-loss Δ_p, the value of $(\Delta_p-\bar{\Delta})/\xi$ is read from curve (a), and $\bar{\Delta}$ and ξ are calculated according to Equations 1-3. Curve (b) is a plot of the quantity $w = (\Delta_1-\Delta_2)/\xi$, with Δ_1 and Δ_2 being the two values of the energy-loss at which the Vavilov distribution has fallen to 50 percent of its peak value.

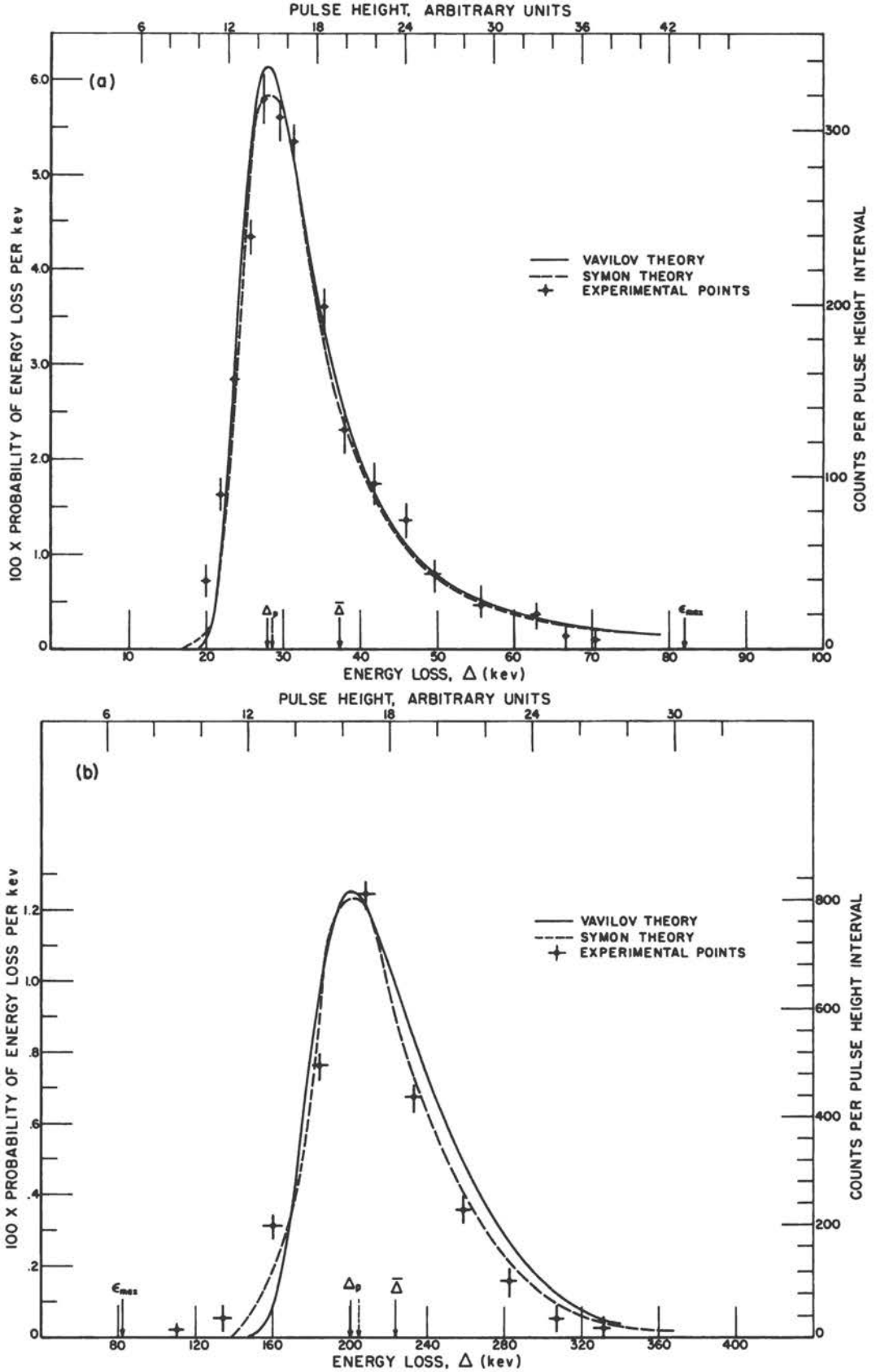

Figure 3. Comparison of the Vavilov and Symon distributions with the experimental results of Gooding and Eisberg, for 37-Mev protons. (a) 10-cm pathlength in argon at a pressure of 0.2 atmospheres; (b) 10-cm pathlength in argon at a pressure of 1.2 atmospheres.

References

1. P. V. Vavilov, Zh. Exper. Teor. Fiz. 32, 320 (1957). Transl., JETP. 5, 749 (1957).

2. L. Landau, J. Exp. Phys. (USSR), 8, 201 (1944).

3. K. R. Symon, "Fluctuations in Energy Loss by High Energy Charged Particles in Passing through Matter." Thesis, Harvard Univ. (1948).

4. U. Fano, Ann. Rev. Nucl. Sci., 13 (1963). Reprinted as Appendix A of the present volume.

5. B. Rossi, "High Energy Particles" (Prentice-Hall, New York, 1952).

6. V. A. Fock, "Tables of Airey Functions" (Moscow, 1946).

7. J. C. P. Miller, "The Airey Integral," British Assoc. Adv. Sci., Mathematical Tables, Part Volume B (Cambridge University Press, 1946).

8. W. Börsch-Supan, J. Research Natl. Bur. Standards 65B, 245 (1961).

9. T. J. Gooding and R. M. Eisberg, Phys. Rev. 105, 357 (1957).

10. TABLES OF ENERGY-LOSSES AND RANGES OF ELECTRONS AND POSITRONS[1]

Martin J. Berger[2] and Stephen M. Seltzer[2]

Abstract

Tables are presented for approximately 40 materials and 80 energies between 10 kev and 1000 Mev. The tables contain the following information: mean energy-loss of electrons by collisions with atomic electrons and by bremsstrahlung, the mean range, and the radiation yield (conversion of electron kinetic energy into bremsstrahlung energy). Auxiliary tables contain information about restricted collision losses in water, critical energies (at which the collision and bremsstrahlung losses are equal), and electron-positron differences in regard to energy-loss and range. Some comparisons are made between calculated and experimental values of the mean energy-loss.

1. Introduction

The most recent extensive tables of electron and positron stopping power and range were made by Nelms (1). These tables include only energy-loss by collision with atomic electrons and are therefore limited to energies of a few Mev, or smaller, at which the neglected bremsstrahlung loss is only a few percent of the total energy-loss. Hansen and Fultz (2), in the course of evaluating thin-target bremsstrahlung spectra and the conversion of electron kinetic energy into bremsstrahlung, calculated the mean energy-loss by collision and bremsstrahlung for five materials at energies up to 35 Mev. Some data on collision and radiative losses at very high energies in air, water, and lead also have been given by Heitler (3).

The present tables are characterized as follows:

Approximately forty elements, mixtures and compounds are included.

The best current values of the mean excitation energy are used for the computation of the collision loss.

Bremsstrahlung losses are included.

The energy region covered extends from 10 kev to 1000 Mev.

[1] Supported by the National Aeronautics and Space Administration under Contract R-80 with National Bureau of Standards.

[2] National Bureau of Standards, Washington, D. C.

An estimate is given of the radiation yield, i.e., the fraction of electron kinetic energy converted into bremsstrahlung energy.

Positron-electron energy-loss ratios and range ratios are tabulated for a set of representative substances. (Detailed tables for positrons, similar to those for electrons, have been prepared for all substances considered, but these additional tables are too lengthy for inclusion in the present paper.)

The energy-loss per unit pathlength and the range[3] are both subject to strong statistical fluctuations. The mean values of these quantities are therefore not sufficient to characterize the penetration and diffusion of electrons, particularly at high energies where radiative energy-losses predominate. To obtain a realistic description, one must include not only energy-loss straggling but also the detours (wiggliness of the track) caused by multiple elastic Coulomb scattering by atoms. At high energies, one cannot treat the electrons or positrons by themselves, but must simultaneously take into account the transport of associated bremsstrahlung and annihilation radiation and consider, in turn, the pair electrons and Compton electrons produced by photons. All these processes can be described only by rather complicated transport theory.

Nevertheless, there are justifications for tabulating such relatively crude parameters as the mean energy loss and range:

1. They are among the few quantities, in the present state of the art, that can be tabulated systematically, for all kinds of media and electron energies, with a modest amount of computing effort.

2. They provide useful typical values and orders of magnitude characterizing penetration and diffusion. Even in the presence of strong fluctuations, mean values are informative.

3. The mean energy-loss and range are required as input data for more elaborate and realistic transport calculations. In fact, it was as part of the preparatory work for such calculations that the present tabulations were undertaken.

The theory of collision losses has recently been the subject of thorough review by Fano (4), and bremsstrahlung cross sections have been reviewed by Koch and Motz (5); therefore, in this paper we limit ourselves to a brief statement of the method of computation.

2. Method of Calculation

Collision-Loss

The mean collision-loss was calculated according to Bethe's stopping-power theory, using the formulation of Rohrlich and Carlson (6):

[3] A definition of the range is given in Section 2 (p. 212).

$$-\frac{1}{\rho}\left(\frac{dE}{dx}\right)^{\pm}_{col} = \frac{2\pi N_a r_0^2 mc^2}{\beta^2}\frac{Z}{A}\left\{\log\left[\frac{\tau^2(\tau+2)}{2(I/mc^2)^2}\right] + F^{\pm}(\tau) - \delta\right\} \quad (1)$$

$$F^{-}(\tau) = 1 - \beta^2 + [\tau^2/8 - (2\tau+1)\log 2]/(\tau+1)^2 \quad \text{, for electrons} \quad (2)$$

$$F^{+}(\tau) = 2\log 2 - \frac{\beta^2}{12}\left[23 + \frac{14}{\tau+2} + \frac{10}{(\tau+2)^2} + \frac{4}{(\tau+2)^3}\right] \quad \text{, for positrons .} \quad (3)$$

The various symbols have the following meanings:

Properties of the Electron or Positron:

mc^2 = rest energy = 0.510976 Mev

τ = kinetic energy in units of mc^2

$\beta = [\tau(\tau+2)]^{1/2}/(\tau+1)$ = velocity/c

Properties of the Medium:

Z = atomic number

A = atomic weight

ρ = density

I = mean excitation energy

δ = density effect correction

Other Parameters:

N_a = Avogadro's number = 6.02486×10^{23} electron/mole[4]

$r_0^2 = (e^2/mc^2)^2 = 7.94030 \times 10^{26}$ cm^2 .

Corresponding equations are given in Section 3 (under "Restricted Stopping Power") for the restricted mean energy-loss resulting from collision against atomic electrons with energy transfers less than some arbitrary value Δ.

Mean Excitation Energy

The mean excitation energy, I, is an atomic parameter which—in principle, if not yet in practice—can be calculated from a knowledge of the absorption frequencies and oscillator strengths of the medium. The scarcity of information about oscillator strengths requires one to obtain the mean excitation energy empirically through the

[4]This value of Avogadro's number corresponds to the old mass scale in which the atomic weight of O^{16} is exactly 16.

analysis of stopping power or range experiments. Experimental data for protons or other heavy particles are commonly used rather than electron data because the required energy-loss straggling and multiple-scattering corrections are smaller and easier to make. Even so, the experimental data for heavy particles are subject to considerable uncertainties. Moreover, the percent error of the mean excitation energy is several times larger than the corresponding percent error of the stopping power or range because it enters logarithmically into the stopping-power formula. As new information is developed, the value of the mean excitation energy must therefore be revised, and there is no reason for assuming that this process has come to an end.

The values of the mean excitation energy used in the present work are based on the analysis of proton stopping data in which the assumption was made that shell corrections (decrease of stopping power due to the binding of atomic electrons) vanish in the high-energy limit. Fano (4) has stressed that the proton shell corrections in the high-energy limit are small but nonvanishing. If the limiting value of these corrections is disregarded in the analysis of stopping-power data, one obtains a quantity denoted as the adjusted mean excitation energy (I_{adj}) that is slightly larger than the theoretical mean excitation energy, I, defined in terms of oscillator strengths (see Paper No. 6 of this volume).

We have used the adjusted mean excitation energies, I_{adj}, for the evaluation of electron and positron collision-losses. This involves the assumption that shell corrections in the high-energy limit can be defined equally for electrons and positrons as for protons. There is no evidence for or against this assumption, which we have used for lack of a more justifiable procedure.

The values of I_{adj} were chosen to conform with the recommendations of the Subcommittee (see Report No. 6 of this volume). For low-Z materials, the values of I_{adj} are 18.7 ev for hydrogen, 42 ev for helium, 38 ev for lithium, 60 ev for beryllium, 78 ev for carbon; 85 ev for nitrogen, 89 ev for oxygen, and 131 ev for neon. For $Z \geq 13$, there is recommended an empirical relation between I_{adj} and Z that has been proposed by Sternheimer (private communication). This relation yields 163 ev for aluminum, 314 ev for copper, and 826 ev for lead:

$$\frac{I_{adj}}{Z} = 9.76 + 58.8\, Z^{-1.19} \text{ ev} \quad . \tag{4}$$

For mixtures and compounds, we have assumed the mean energy-loss to be the sum of the losses in the constituent elements (Bragg's rule). This implies the use of an average

$$\log \langle I_{adj} \rangle = \left\langle \frac{Z}{A} \right\rangle^{-1} \frac{1}{\rho} \sum_j \frac{Z_j}{A_j} \rho_j \log I_{adj,j} \tag{5}$$

with

$$\left\langle \frac{Z}{A} \right\rangle = \frac{1}{\rho} \sum_j \frac{Z_j}{A_j} \rho_j \quad , \tag{6}$$

where Z_j, A_j and ρ_j pertain to the j'th constituent ($\sum_j \rho_j = \rho$).

For compounds, particularly those of low average atomic number, departures from additivity occur due to chemical binding effects (7). It would then be better to

use I_{adj}-values obtained directly from an expériment with the substance under consideration.

Density-Effect Correction

The density-effect correction, δ, takes into account the reduction of the collision-loss due to the polarization of the medium. We have relied upon the systematic evaluation by Sternheimer (8), who expressed δ as function of the particle velocity by means of an empirical formula with parameters that depend on the characteristics of the medium:

$$\delta[\beta^2/(1-\beta^2)] = \begin{cases} 0 & , \ X<X_0 \\ \log[\beta^2/(1-\beta^2)] + C + a(X_1 - X)^m & , \ X_0 \le X < X_1 , \\ \log[\beta^2/(1-\beta^2)] + C & , \ X \ge X_1 , \end{cases} \tag{7}$$

where

$$X = (\log_{10} e)\,\frac{1}{2}\log[\beta^2/(1-\beta^2)] = 0.21715 \log[\beta^2/(1-\beta^2)] . \tag{8}$$

The values of the quantities X_0, X_1, C, a, and m depend, among other things, on the value of the mean excitation energy. Two sets of these parameters have been given by Sternheimer—in his 1952 paper with the use of one set of I-values, and in his 1956 paper with the use of another set. Following his recommendation, we have adjusted the density-effect correction to the I_{adj}-values adopted in the present work through the following interpolation procedure: Let δ_1 and δ_2 denote the corrections for a given medium and energy, evaluated with mean excitation energies I_1 and I_2. The desired value, corresponding to mean excitation energy I_{adj}, is calculated as

$$\delta = [\delta_1 \log(I_2/I_{adj}) + \delta_2 \log(I_{adj}/I_1)]/\log(I_2/I_1) . \tag{9}$$

For lead and copper we have also used additional parameter values (Sternheimer, private communication) as follows:

	I	C	a	m	X_0	X_1
Cu	323 ev	-4.43	0.109	3.39	0.2	3.0
Pb	826 ev	-6.21	0.355	2.64	0.4	3.0

Sternheimer's density-effect parameters apply to gases at normal pressure. The correction δ_P for a gas at a pressure of P atmospheres is

$$\delta_P[\beta^2/(1-\beta^2)] = \delta[P\beta^2/(1-\beta^2)] . \tag{10}$$

Bremsstrahlung Loss

The mean energy loss by bremsstrahlung was calculated according to the Bethe-Heitler theory modified by empirical corrections. These modifications are required because the Born approximation underlying the Bethe-Heitler theory becomes less reliable as the kinetic energy of the electron decreases, particularly for media of large atomic number, and as the photon energy approaches the initial electron energy (high-frequency limit). Exact theoretical results are available only

in the high-frequency limit. Otherwise the required modifications must be based on the analysis of the rather scarce experimental data. We have relied for this purpose on the detailed and comprehensive review of Koch and Motz (5). In the notation of these authors, the forms of the bremsstrahlung cross sections used by us are designated as 3BN, 3BS and 3CS:

3BN: screening disregarded [Bethe and Heitler (9), Sauter (10), Racah (11)].

3BS: screening included; extreme relativistic approximation [Bethe and Heitler (9)].

3CS: screening and Coulomb correction included; extreme relativistic approximation [Olsen (12)].

In addition, three other modifications were made:

a) For low electron energies, the Elwert (13) factor f_E was applied which is a multiplicative Coulomb correction derived on the basis of a comparison between the non-relativistic Born approximation and the non-relativistic calculations of Sommerfeld (14).

The expression for this factor is

$$f_E = \frac{\beta\{1-\exp[-(2\pi Z/137\beta)]\}}{\beta_F\{1-\exp[-(2\pi Z/137\beta_F)]\}} \quad , \tag{11}$$

where β and β_F are the ratios of the initial and final electron velocities to the velocity of light.

b) At low and intermediate electron energies an empirical correction factor b was applied to the bremsstrahlung cross section. For aluminum and gold, correction factors have been estimated by Koch and Motz from experimental data for electron energies between 50 kev and 5 Mev. We have extrapolated these to energies somewhat below 50 kev until they reach the value unity which they were assumed to retain for all lower energies. Furthermore, we have by interpolation estimated similar correction factors for materials of different atomic number, assuming that no correction is required for hydrogen. Figure 1 gives some typical correction factors.

c) The bremsstrahlung cross section in the high-frequency limit has been obtained from experimental data presented by Fano, Koch and Motz (15) for aluminum and gold (see also Fig. 12 of Ref. 5), and by interpolation for other materials. In this interpolation it was assumed that the cross section can be represented in the form $aZ^3+bZ^4+cZ^5$. This form of Z-dependence is consistent with the theory of Jabbur and Pratt (16) which treats bremsstrahlung as the approximate inverse of the photoelectric process and which gives results for high-energy electrons in close agreement with experiment.

Following essentially the recommendations of Koch and Motz, we have adopted, for the purpose of calculating the mean energy loss, the following cross section package:

Kinetic energy range for incident electron	Cross section
$\tau < 4mc^2$	$d\sigma = bf_E\ (3BN)$
$4mc^2 < \tau < 30mc^2$	$d\sigma = bf_E\ (3BN)$ if $Y > 15$
	$= bf_E\ (3BS)$ if $Y < 15$ (12)
$30mc^2 < \tau$	$d\sigma = (3BN)$ if $Y > 15$
	$= (3CS)$ if $Y < 15$

(3BN), (3BS) and (3CS) indicate the Born-approximation cross sections discussed above, f_E is the Elwert factor, b the empirical Koch-Motz correction factor, and

$$Y = 100\, Z^{-1/3}\, \Delta/(\tau+1)\,(\tau+1-\Delta)\ , \tag{13}$$

with Δ the energy of the bremsstrahlung photon. The spectral shape for $\Delta > 0.95\,\tau$ has been adjusted so that the cross sections go into the appropriate high-frequency limit. The mean radiative energy loss as function of the electron energy was smoothed slightly to overcome the effect of using a patchwork of cross sections. The necessary corrections were negligible for low-Z materials, were confined to the region 4 mc^2 to 30 mc^2, and even fpr Z=82 amounted to no more than 5-10 percent, well within the accuracy of the cross sections used.

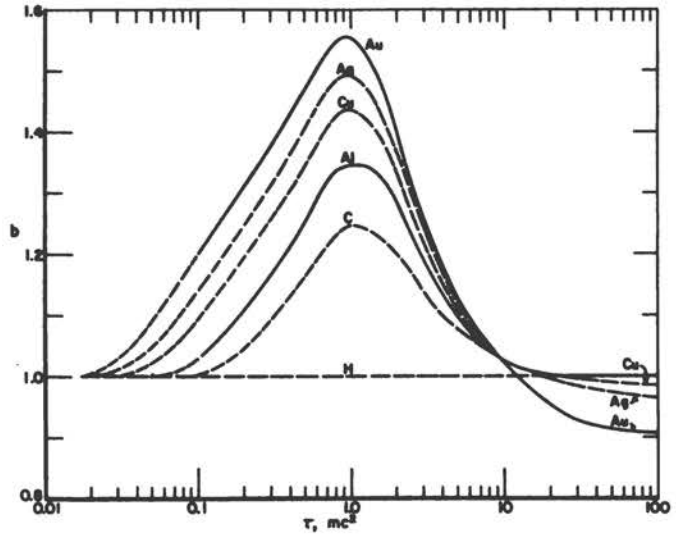

Figure 1. Correction factor $b(Z, \tau/mc^2)$ used in the computation of the mean energy-loss of electrons by radiation. The correction represents an estimate of the deviation of the true energy-loss from the Born-approximation result of Bethe and Heitler. The solid curves are derived from the analysis of experimental data by Koch and Motz. The dotted curves represent interpolations or extrapolations.

In order to take into account bremsstrahlung in the field of atomic electrons, the factor Z^2 in the bremsstrahlung cross section was replaced by $Z(Z+1)$. It would have been more correct to use a factor $Z(Z+\eta)$, with a parameter η that depends on

the energy as well as on Z. However, the precise value of η is not well known except that it is expected to be quite close to unity. Heitler (3) recommends $\eta \sim 0.8$. Koch and Motz state that at extremely relativistic energies and for complete screening

$$\eta = \log \frac{530}{Z^{2/3}} \Big/ \left(\log \frac{183}{Z^{1/3}} + \frac{1}{18}\right) , \tag{14}$$

which varies from 1.04 for magnesium to 0.88 for lead. In view of the uncertainty of the proper value of η, we have set $\eta = 1.0$ throughout, which is correct to first order and which makes it easy for the user of the tables to apply his own correction by using the value of η which he prefers.

For compounds and mixtures, the mean bremsstrahlung loss was calculated for each element, and the results were averaged in proportion by weight.

Range

The c.s.d.a. range, as defined in the preface to this volume, was calculated by integrating the reciprocal of the total stopping power:

$$r^{\pm}(\tau) = \int_0^{\tau} \left[-\frac{1}{\rho} \left(\frac{dE}{dx}\right)^{\pm}_{tot} \right]^{-1} d\tau' , \tag{15}$$

where

$$-\frac{1}{\rho}\left(\frac{dE}{dx}\right)^{\pm}_{tot} = -\frac{1}{\rho}\left(\frac{dE}{dx}\right)^{\pm}_{col} - \frac{1}{\rho}\left(\frac{dE}{dx}\right)^{\pm}_{rad} . \tag{16}$$

The abbreviation c.s.d.a. stands for "continuous-slowing-down approximation." The c.s.d.a. range is the pathlength which a particle would travel in the course of slowing down, in an unbounded homogeneous medium, from energy τ to zero energy if its rate of energy-loss along the entire track were always equal to the mean rate of energy-loss. Actually the rate of energy-loss fluctuates, but this is neglected in the continuous-slowing-down approximation, so that the residual range of a particle becomes a deterministic function of its energy, and vice versa. It should also be noted that the definition of the c.s.d.a. range involves the pathlength and not the depth of penetration in any special direction. The c.s.d.a. range thus differs from other types of range such as the "projected range" (see Preface) and "extrapolated range," which are usually defined with reference to transmission through a plane-parallel absorber. The c.s.d.a. range pertains to a particle track that is typical but not experimentally realizable. If the pathlength distribution were to be measured in a track visualization device such as a photographic emulsion, the arithmetic average of this distribution would be somewhat greater than the c.s.d.a. range.[5]

When the velocity of the particle being stopped falls to a value comparable with the velocity of the atomic electrons, the stopping-power formula (Eq. 1) ceases to be valid, and the exact form of the stopping law is not known. This forces one to use an arbitrary approximate procedure for the evaluation of the range integral (Eq. 15) at very low energies. We have followed the procedure of Nelms, assuming the function

---

[5] This has been shown by Lewis (17) for heavy charged particles for which the difference is quite small. For electrons, the difference is expected to be greater (see also pp. 45-46 of Appendix A of this volume.

$\left[-\frac{1}{\rho}\left(\frac{dE}{dx}\right)^{\pm}_{tot}\right]^{-1}$ to be zero at $\tau = 0$ and interpolating linearly between zero and a value at energy $\tau = \tau_0$. However, we have used $mc^2\tau_0 = 1$ kev, whereas Nelms used 5 kev. The result is that our ranges at 10 kev are somewhat higher than those of Nelms (12 percent for Pb, 6 percent for Ag, 2 percent for Al and 1 percent for H_2). At 50 kev, the differences are at most 0.5 percent, and at higher energies they are completely negligible. The ranges of Nelms are on the low side, ours on the high side, and the discrepancies give an indication of the error likely to result from lack of knowledge of low-energy stopping behavior.

Radiation Yield

The radiation yield $Y(\tau)$ is defined to be the fraction of its energy that an electron, with initial kinetic energy τ, will radiate in the form of bremsstrahlung in the course of slowing down. In the continuous-slowing-down approximation

$$Y^{\pm}(\tau) = \frac{1}{\tau}\int_0^{\tau} \frac{\left(\frac{dE}{dx}\right)^{\pm}_{rad}}{\left(\frac{dE}{dx}\right)^{\pm}_{tot}}\, d\tau' . \qquad (17)$$

3. Miscellaneous Information

Influence of the Density-Effect Correction

Table 1 shows the percent reduction of the collision energy-loss due to the density effect correction for a selected set of materials. Table 2 gives the actual

TABLE 1

Percent Reduction of Collision Energy-loss Due to Density-effect Correction, for Selected Materials

T (Mev)	H_2 (normal pressure)	C	Al	Cu	Ag	Au
0.1	0.0	0.0	0.0	0.0	0.0	0.0
0.2	0.0	0.4	0.0	0.0	0.0	0.0
0.5	0.0	1.2	0.5	0.5	0.1	0.0
1.0	0.0	2.7	1.5	1.5	0.7	0.7
2.0	0.0	4.8	3.4	3.4	2.2	2.0
5.0	0.0	8.5	6.8	6.8	5.3	4.9
10	0.0	11.8	9.8	9.9	8.2	7.6
20	0.0	15.2	13.1	13.3	11.3	10.7
50	0.7	19.5	17.3	17.6	15.7	14.9
100	3.3	22.5	20.3	20.7	18.8	18.1
200	6.6	25.1	23.1	23.6	21.8	21.1
500	10.6	28.1	26.4	27.0	25.4	24.8
1000	13.4	30.1	28.6	29.2	27.8	27.3

TABLE 2

Reduction of Collision Energy-Loss Due to Density-Effect Correction for Various Gases at Normal Pressure, Mev/g cm^{-2}

T (Mev)	Momentum pc (Mev)	H_2	He	N	O	Ne	A	Kr	Xe	CO_2	Air	Methane	Acetylene
10	10.499	0.0	0.0	0.0	0.0	0.0	0.0	0.0	0.0	0.0	0.0	0.0	0.0
20	20.505	0.0	0.0	0.0	0.0	0.0	0.0	0.0	0.0	0.0	0.0	0.003	0.0
30	30.507	0.0	0.0	0.0	0.0	0.0	0.0	0.0	0.0	0.011	0.0	0.023	0.012
40	40.508	0.008	0.0	0.009	0.003	0.0	0.0	0.0	0.001	0.029	0.008	0.045	0.027
50	50.508	0.034	0.0	0.018	0.018	0.0	0.0	0.0	0.003	0.046	0.018	0.065	0.043
60	60.509	0.065	0.001	0.028	0.032	0.0	0.003	0.003	0.006	0.060	0.029	0.084	0.057
80	80.509	0.126	0.002	0.048	0.056	0.006	0.012	0.009	0.013	0.084	0.050	0.118	0.084
100	100.51	0.182	0.010	0.067	0.076	0.019	0.022	0.017	0.020	0.105	0.068	0.147	0.107
200	200.51	0.379	0.074	0.139	0.149	0.074	0.065	0.051	0.050	0.178	0.140	0.251	0.191
300	300.51	0.501	0.130	0.188	0.197	0.116	0.099	0.079	0.074	0.226	0.189	0.319	0.247
400	400.51	0.589	0.173	0.226	0.234	0.148	0.126	0.102	0.093	0.262	0.227	0.370	0.289
500	500.51	0.656	0.207	0.257	0.263	0.175	0.148	0.122	0.110	0.292	0.257	0.410	0.323
600	600.51	0.712	0.235	0.283	0.288	0.198	0.168	0.138	0.124	0.316	0.283	0.444	0.351
800	800.51	0.800	0.279	0.325	0.328	0.236	0.200	0.166	0.149	0.356	0.324	0.497	0.397
1000	1000.5	0.868	0.313	0.357	0.360	0.267	0.226	0.190	0.169	0.388	0.356	0.539	0.433

reduction (in Mev/g cm^{-2}) for various gases at normal pressure. The corresponding reduction for an electron of momentum pc, in a gas at a pressure of P atmospheres, is found by interpolating in Table 2 to a momentum pc $\sqrt{P}$.

Critical Energies

The critical energy is a parameter used frequently in the theory of electron-photon cascades. It is defined as the electron energy at which the collision loss is equal to the radiation loss, and thus provides the dividing line below which the development of a cascade is dominated by collision phenomena, and above which it is governed by radiative effects. Table 3 gives a list of critical energies for various substances. In the literature on cascade theory, the critical energy is often approximated by the expression

$$T_{crit} = \frac{800}{Z + 1.2} \text{ Mev} . \qquad (18)$$

As can be seen in Figure 2, this approximation is quite satisfactory.

TABLE 3

Critical Energies for Electrons
(Gases at Normal Pressure)

Medium	T_{crit} (Mev)	Medium	T_{crit} (Mev)
H_2	403	H_2O	92.0
He	280	CO_2	100
Li	169	AgCl	19.8
Be	132	AgBr	18.3
C	97.1	NaI	17.4
N	107	LiI	15.6
O	95.2	Methane	169
Ne	78.8	Ethylene	146
Mg	55.4	Polyethylene	119
Al	51.0	Xylene	112
A	45.6	Toluene	111
Fe	27.4	Acetylene	132
Cu	24.8	Polystyrene	109
Kr	23.6	Stilbene	108
Ag	16.2	Lucite	100
Sn	15.5	Anthracene	105
Xe	15.8	Muscle	112
W	10.2	Bone	81.9
Au	9.66	Air	102
Pb	9.51	Standard Emulsion	22.3
U	8.36		

Radiation Yield

The correct evaluation of the radiation yield must be based on the electron slowing-down spectrum $y(\tau, \tau')d\tau'$. This quantity is the differential tracklength equal to the average distance traveled by an electron of initial energy τ in the course of slowing down, while its energy is between τ' and $\tau' + d\tau'$. The average fractional

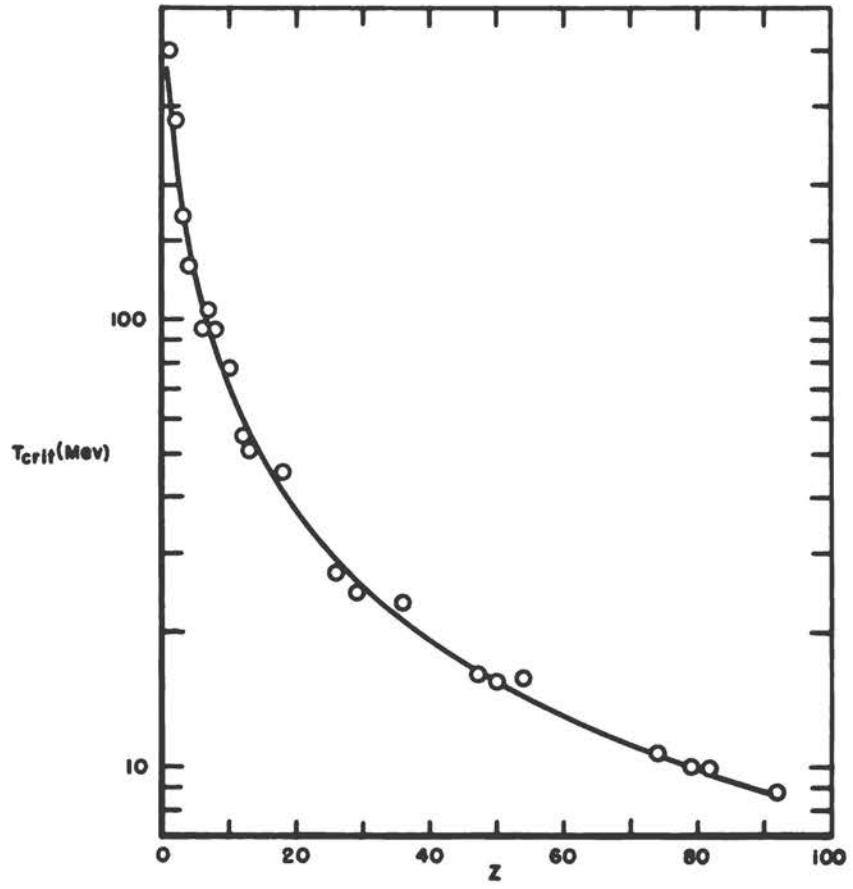

Figure 2. Critical energy for electrons (at which the mean values of the collision and radiative losses are equal). The points are derived from Printout Table I; the curve represents the approximation formula (Eq. 18).

energy conversion from electron kinetic energy to bremsstrahlung is then equal to

$$Y(\tau) = \int_0^{\tau} y(\tau, \tau') \left[-\frac{1}{\rho} \left(\frac{dE}{dx} \right)_{rad} \right] d\tau' \ . \qquad (19)$$

An accurate method of computing the slowing-down spectrum, taking into account the discontinuous nature of collision losses and bremsstrahlung losses as well as the production of secondary knock-on electrons, has been developed by Spencer and Fano (18). Their method is numerical, and it is difficult computationally when bremsstrahlung losses are included, so that only a few selected cases were treated. A first-approximation to the slowing-down spectrum is obtained in the form of the reciprocal of the total stopping power at energy τ':

$$y(\tau, \tau') \approx \left[-\frac{1}{\rho} \left(\frac{dE}{dx} \right)_{tot} \right]^{-1} \ . \qquad (20)$$

With this substitution, one obtains the radiation yield in the continuous-slowing-down approximation (Eq. 17). Actually, the true slowing-down spectrum exceeds the reciprocal stopping power at energies close to the source energy, then it is smaller,

and at very low energies it again becomes the larger of the two because it includes secondary knock-on electrons.

In Table 4 we compare radiation yields based on Spencer-Fano slowing-down spectra with yields computed in the continuous-slowing-down approximation. The approximation does not include radiation from secondary electrons, but their contribution would in any case be quite small except under cascade conditions. It can be seen that the continuous-slowing-down approximation is quite serviceable for the cases where a comparison can be made, giving rise to errors of no more than a few percent.

TABLE 4

Comparison of Radiation Yields Obtained from Spencer-Fano Slowing-down Spectra and from the Continuous-slowing-down Approximation

Medium	Electron source energy τ_0 (mc^2)	Radiation Yield, Percent		
		Spencer-Fano	Continuous-slowing-down	
		No density effect	No density effect	Density effect
Al	4	1.95	1.90	1.91
	80	24.8	23.1	25.6
Pb	4	14.2	13.4	13.5
	80	56.4	59.3	61.0

An approximation for the radiation yield has been developed by Koch and Motz (5):

$$Y(\tau) = \frac{3\times10^{-4} Z\tau}{1+3\times10^{-4} Z\tau} \quad . \tag{21}$$

As shown in Figures 3a and 3b, this formula is quite adequate for all materials except for those with very low Z.

Experimental and Calculated Stopping Powers

Tables 5 and 6 contain comparisons with the measurements of Paul and Reich (19) at 2.8 and 4.7 Mev and of Ziegler (20) at 32 Mev. The results are somewhat inconsistent. At 2.8 Mev, the experimental stopping powers are slightly lower than the calculated values by an amount roughly equal to the experimental error; at 4.7 Mev they are higher by amounts equal to or larger than the experimental errors; at 32 Mev there is close agreement.

Tables 7 and 8 contain comparisons with relative stopping-power measurements of Hereford (21) at energies between 1.4 and 9.0 Mev and of Westermark (22) at energies in the neighborhood of 1 Mev. In both cases the agreement with calculated values is very good.

We have found no data that could be used to test the validity of the formulas for radiative energy-loss at very high energies.

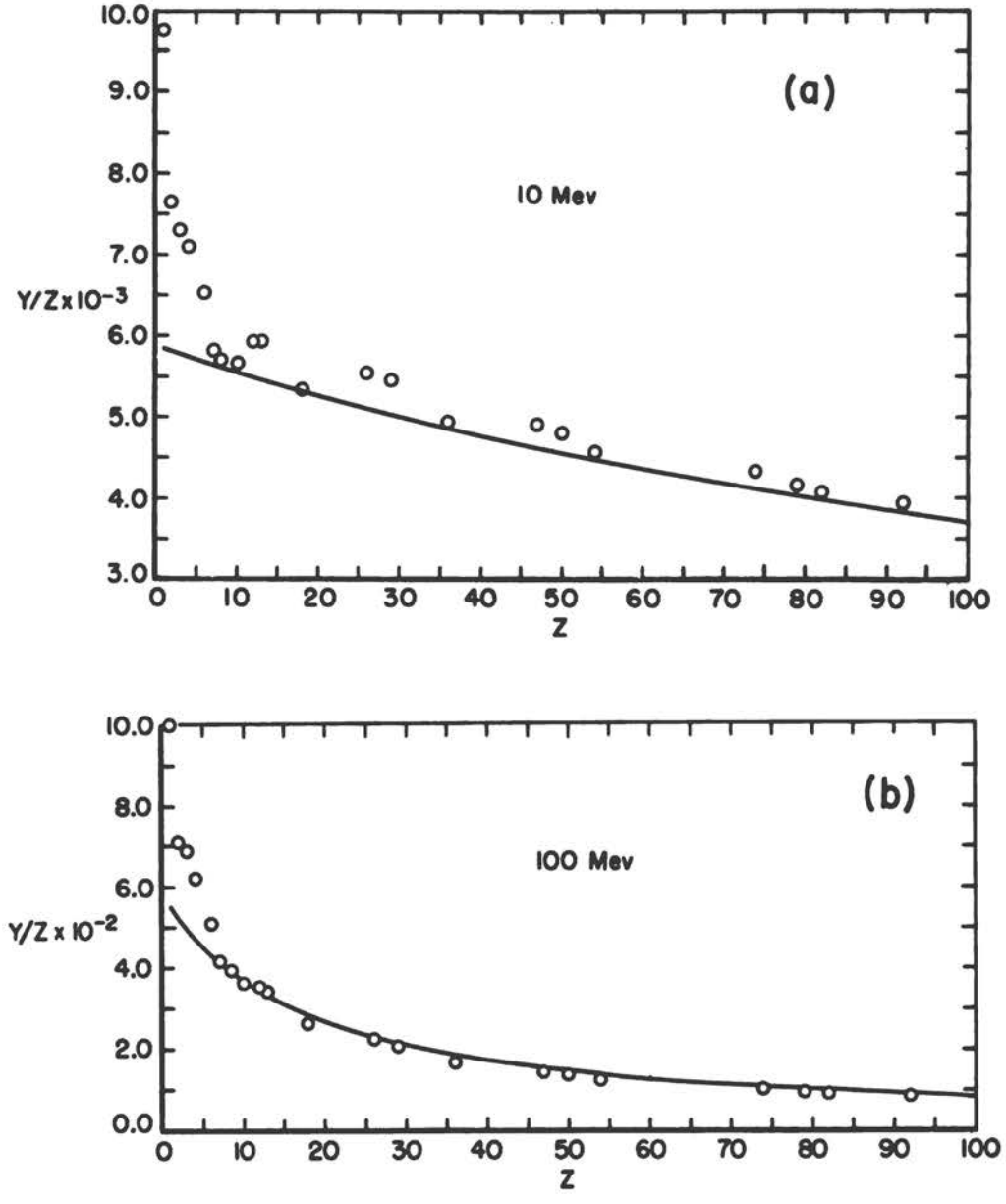

Figure 3. Radiation yield Y (fraction of initial electron kinetic energy converted into bremsstrahlung energy in the course of slowing down). Y/Z is plotted against the atomic number Z. The curve represents the Koch-Motz approximation formula (Eq. 21); the points, from Printout Table I, are calculated in the continuous-slowing-down approximation.

TABLE 5

Comparison with Energy-loss Measurements of Paul and Reich (1950)

Electron energy T (Mev)	Medium	$-\frac{1}{\rho}\left(\frac{dE}{dx}\right)^{-}_{tot}$, Mev/g cm^{-2}	
		Experimental	Calculated
2.8 ± 3%	Be	1.45 ± 0.06	1.51
	C	1.53 ± 0.08	1.68
	Fe	1.43 ± 0.10	1.51
	Pb	1.32 ± 0.10	1.44
	H_2O	1.83 ± 0.10	1.92
4.7 ± 3%	Be	1.73 ± 0.12	1.56
	C	1.89 ± 0.16	1.75
	Fe	1.94 ± 0.19	1.66
	Pb	2.04 ± 0.22	1.73
	H_2O	2.43 ± 0.20	2.00

TABLE 6

Comparison with Stopping-power Measurements for 32-Mev Electrons by Ziegler (1958)

Medium	$-\frac{1}{\rho}\left(\frac{dE}{dx}\right)^{-}_{tot}$, Mev/g cm^{-2}	
	Experimental	Calculated
Be	2.0 ± 0.1	2.03
C	2.4 ± 0.1	2.44

TABLE 7

Comparison with Relative Stopping-power Measurements by Hereford (1948)

Electron energy T (Mev)	$\frac{1}{\rho}\left(\frac{dE}{dx}\right)^{-}_{water} \Big/ \frac{1}{\rho}\left(\frac{dE}{dx}\right)^{-}_{carbon}$	
	Experimental	Calculated
1.4	1.17 ± 0.02	1.15
1.6	1.16 ± 0.02	1.15
7.4	1.16 ± 0.02	1.14
9.0	1.14 ± 0.02	1.14

TABLE 8a

Total Energy-loss Relative to that in Beryllium for 2.8-Mev Electrons. Comparison with the Experiment of Westermark (1960)

Medium	$\frac{1}{\rho}\left(\frac{dE}{dx}\right)^{-}_{medium} \Big/ \frac{1}{\rho}\left(\frac{dE}{dx}\right)^{-}_{beryllium}$	
	Experimental	Calculated
Li	1.051 ± 0.021	1.017
C	1.09 ± 0.02	1.111
Mg	1.092 ± 0.016	1.079
Al	1.050 ± 0.016	1.042

TABLE 8b

Total Energy-loss Relative to that in Aluminum for 2.8-Mev Electrons. Comparison with the Experiment of Westermark (1960)

Medium	$\frac{1}{\rho}\left(\frac{dE}{dx}\right)^{-}_{medium} \Big/ \frac{1}{\rho}\left(\frac{dE}{dx}\right)^{-}_{aluminum}$	
	Experimental	Calculated
H_2O	1.224 ± 0.013	1.222
Toluene	1.187 ± 0.018	1.189

Restricted Stopping Power

In some applications, one is interested in the energy deposited by an electron along its track or, rather, in a region of specified dimensions surrounding the track. One must then exclude from the calculated stopping power the energy that escapes from the region of interest in the form of fast knock-on electrons (delta rays). One simple device for achieving this exclusion is to introduce the restricted collision law, i.e., the mean energy-loss due to collisions against atomic electrons with energy-transfers less than some specified value Δ (see also pp. 49-50 of Appendix A of this volume).

The expressions for the restricted mean collision-loss, $L^{\pm}(\tau, \Delta)$, for positrons and electrons can readily be derived from the formulation of stopping-power theory of Rohrlich and Carlson (6):

$$L^{\pm}(\tau,\Delta) \quad \frac{2\pi N_a r_0^2 mc^2}{\beta^2} \frac{Z}{A} \left\{ \log\left[\frac{2(\tau+2)}{(I/mc^2)^2}\right] + F^{\pm}(\tau,\Delta) - \delta \right\} \qquad (22)$$

$$F^-(\tau, \Delta) = -1 - \beta^2 + \log\left[(\tau - \Delta)\Delta\right] + \tau/(\tau - \Delta) + \left[\Delta^2/2 + (2\tau+1)\log(1-\Delta/\tau)\right]/(\tau+1)^2 \quad (23)$$

$$F^+(\tau, \Delta) = \log(\tau\Delta) - \frac{\beta}{\tau}\left[\tau + \Delta - \frac{5\Delta^2/4}{\tau+2} + \frac{(\tau+1)(\tau+3)\Delta - \Delta^3/3}{(\tau+2)^2} - \frac{(\tau+1)(\tau+3)\Delta^4/4 - \tau\Delta^3/3 + \Delta^4/4}{(\tau+2)^3}\right]. \quad (24)$$

For electrons, Δ cannot exceed $\tau/2$, because the faster of the particles emerging from an electron-electron collision is, by definition, considered to be the primary electron. Thus, $L^-(\tau, \tau/2) = -\frac{1}{\rho}\left(\frac{dE}{dx}\right)^-_{col}$. For positrons, the upper limit of Δ is equal to τ, and $L^+(\tau, \tau) = -\frac{1}{\rho}\left(\frac{dE}{dx}\right)^+_{col}$.

Figure 4a shows the ratio of the restricted to the unrestricted collision-loss for electrons in water, for different electron energies T (in Mev), and as function of the parameter $g = \Delta/\tau = mc^2\,\Delta/T$. Figure 4b gives similar data for positrons.

Figures 5a and 5b compare specific-ionization measurements by Barber (23) with restricted-collision-loss calculations. Barber's experiments were done with electrons having energies up to 35 Mev, and the detection device was an ionization chamber filled with hydrogen or helium at a pressure of 10 atmospheres. The size and content of the ionization chamber were such that a cut-off was imposed on the energy of secondary electrons, which were fully detected. In the calculation, we used Barber's estimates of $mc^2\Delta = 56$ kev for hydrogen and 51 kev for helium.

Electron-Positron Differences

In the calculation of the positron energy loss by collision, Equations 1 and 3 have been used. For the radiative loss, the Born-approximation cross sections (3BN) and (3CS) can be expected to hold for positrons as well as electrons, but the Elwert factor f_E and the Koch-Motz correction factor b no longer apply to positrons, and the appropriate corrections are not known. We have therefore, in Table 9, given the positron-electron ratio for the collision stopping power for all energies, but the corresponding ratios for the total stopping power and range only for energies above 30 mc^2.

4. Main Tables: Electron Mean Energy Loss, Range, and Radiation Yield

Table 10 gives the assumed values of the mean excitation energy I_{adj} (in ev), as well as the composition by weight where required, for all of the substances considered. Printout Table I, the main table, contains the following information for electrons: $-\frac{1}{\rho}\left(\frac{dE}{dx}\right)^-_{col}$, $-\frac{1}{\rho}\left(\frac{dE}{dx}\right)^-_{rad}$, and $-\frac{1}{\rho}\left(\frac{dE}{dx}\right)^-_{tot}$ in units of Mev/g cm^{-2}, the

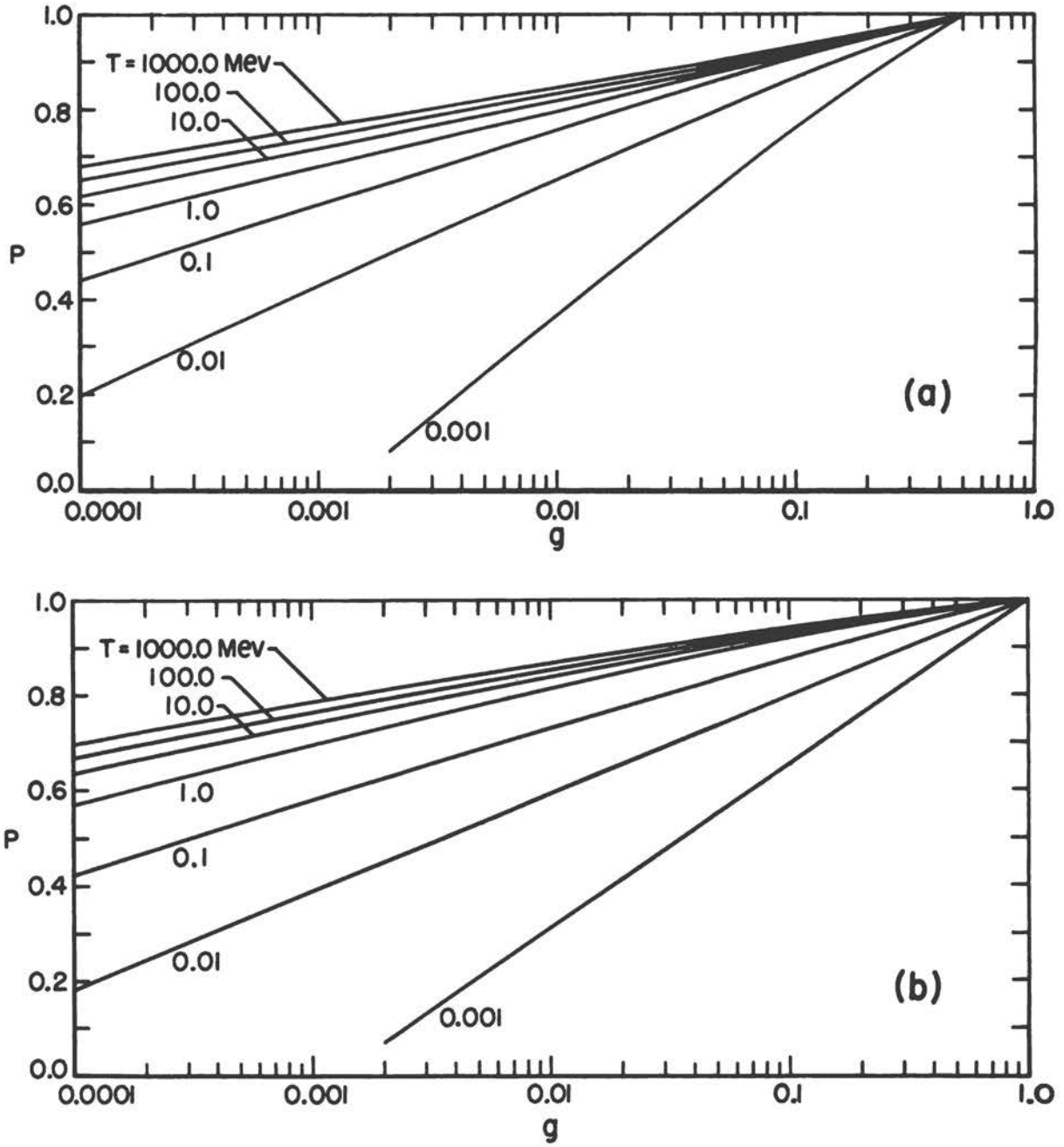

Figure 4. Ratio P of restricted to unrestricted mean collision-loss, as function of the parameter $g = \frac{mc^2\Delta}{T}$; g is the largest fraction of its energy which an electron or positron is allowed to lose in a single collision with an atomic electron. a, Electrons, $g \leq 0.5$; b, positrons, $g \leq 1.0$.

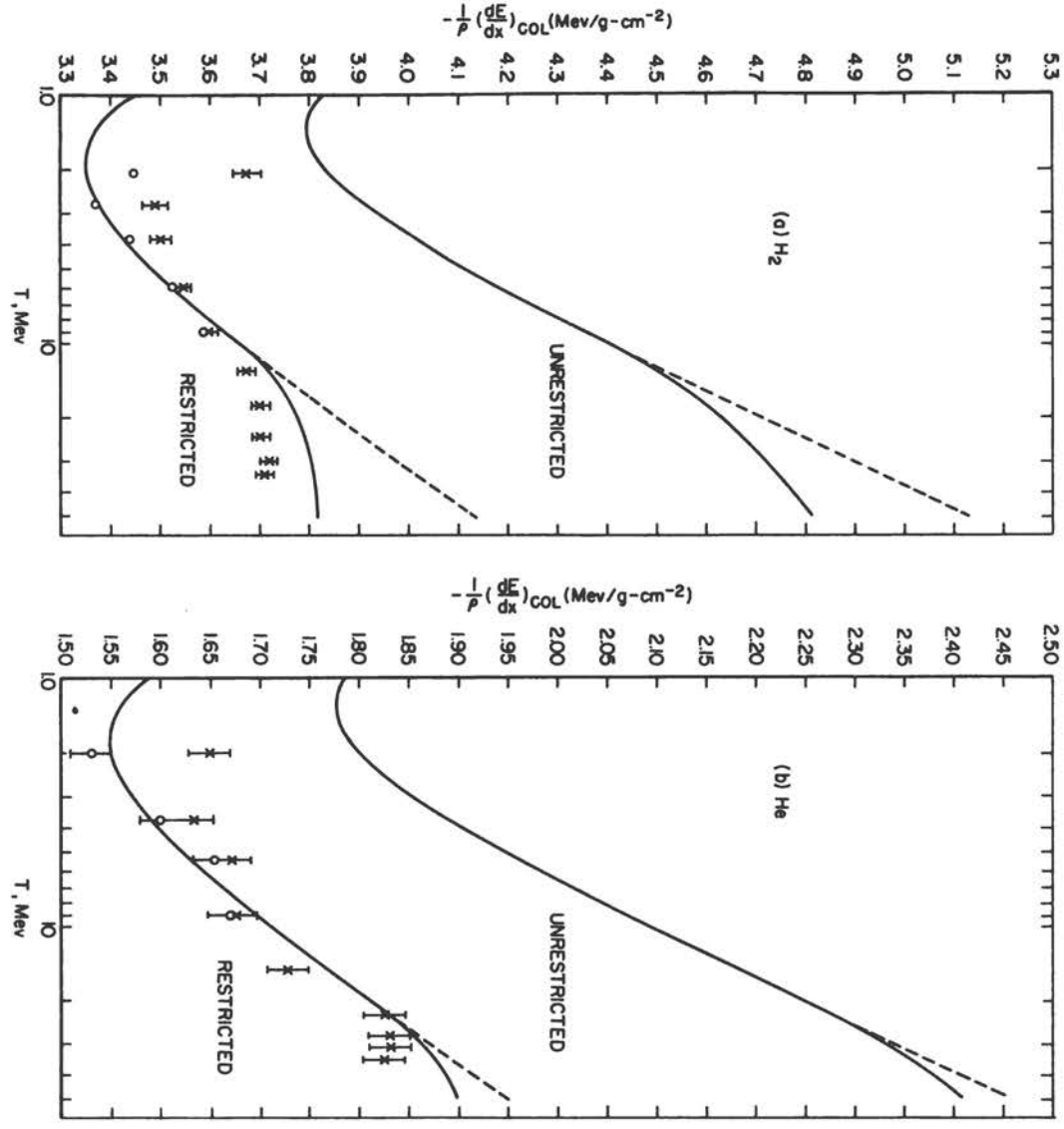

Figure 5. Comparison of restricted and unrestricted mean collision-loss for electrons (solid curves with, dotted curves without, density-effect correction). The experimental points for the restricted loss are from Barber, whose normalization relative to the calculated loss has been used. a, Hydrogen at 10 atmospheres, largest allowed energy transfer per collision 56 kev; b, helium at 10 atmospheres; largest allowed energy transfer per collision 51 kev.

TABLE 9

Comparison of Positron and Electron Energy-loss and Range for Representative Substances

Energy (Mev)	H_2 $\frac{(dE/dx)^+_{col}}{(dE/dx)^-_{col}}$	H_2 $\frac{(dE/dx)^+_{tot}}{(dE/dx)^-_{tot}}$	H_2 $\frac{r^+}{r^-}$	C $\frac{(dE/dx)^+_{tot}}{(dE/dx)^-_{col}}$	C $\frac{(dE/dx)^+_{tot}}{(dE/dx)^-_{tot}}$	C $\frac{r^+}{r^-}$	Al $\frac{(dE/dx)^+_{col}}{(dE/dx)^-_{col}}$	Al $\frac{(dE/dx)^+_{tot}}{(dE/dx)^-_{tot}}$	Al $\frac{r^+}{r^-}$
0.01	1.08			1.10			1.12		
0.02	1.07			1.08			1.10		
0.05	1.05			1.06			1.07		
0.1	1.03			1.04			1.04		
0.2	1.01			1.02			1.02		
0.5	0.992			0.990			0.989		
1.0	0.982			0.979			0.977		
2.0	0.978			0.974			0.972		
5.0	0.977			0.972			0.971		
10.0	0.978			0.972			0.971		
20.0	0.979	0.980	1.02	0.973	0.977	1.03	0.972	0.980	1.03
50.0	0.981	0.983	1.02	0.974	0.982	1.02	0.973	0.986	1.02
100.0	0.981	0.985	1.02	0.974	0.987	1.02	0.974	0.991	1.02
200.0	0.981	0.988	1.02	0.975	0.992	1.02	0.975	0.995	1.01
500.0	0.982	0.992	1.01	0.976	0.996	1.01	0.975	0.998	1.01
1000.0	0.982	0.995	1.01	0.976	0.998	1.01	0.976	0.999	1.01

Energy (Mev)	Cu $\frac{(dE/dx)^+_{col}}{(dE/dx)^-_{col}}$	Cu $\frac{(dE/dx)^+_{tot}}{(dE/dx)^-_{tot}}$	Cu $\frac{r^+}{r^-}$	Ag $\frac{(dE/dx)^+_{col}}{(dE/dx)^-_{col}}$	Ag $\frac{(dE/dx)^+_{tot}}{(dE/dx)^-_{tot}}$	Ag $\frac{r^+}{r^-}$	Au $\frac{(dE/dx)^+_{col}}{(dE/dx)^-_{col}}$	Au $\frac{(dE/dx)^+_{tot}}{(dE/dx)^-_{tot}}$	Au $\frac{r^+}{r^-}$
0.01	1.14	1.14	0.847	1.16	1.16	0.820	1.19	1.19	0.762
0.02	1.11	1.11	0.877	1.12	1.12	0.860	1.14	1.14	0.827
0.05	1.08	1.08	0.910	1.08	1.08	0.900	1.09	1.09	0.884
0.1	1.05	1.05	0.933	1.05	1.05	0.927	1.06	1.05	0.919
0.2	1.02	1.02	0.959	1.02	1.02	0.956	1.02	1.01	0.953
0.5	0.988	0.980	0.993	0.988	0.972	0.996	0.987	0.957	1.00
1.0	0.975	0.963	1.02	0.974	0.950	1.02	0.972	0.929	1.04
2.0	0.970	0.958	1.03	0.969	0.945	1.04	0.967	0.923	1.06
5.0	0.969	0.962	1.04	0.968	0.950	1.05	0.967	0.928	1.07
10.0	0.970	0.969	1.04	0.969	0.960	1.05	0.968	0.944	1.07
20.0	0.971	0.978	1.03	0.970	0.973	1.04	0.969	0.963	1.06
50.0	0.972	0.991	1.03	0.972	0.993	1.03	0.971	0.995	1.05
100.0	0.973	0.995	1.02	0.972	0.996	1.03	0.972	0.997	1.04
200.0	0.973	0.997	1.02	0.973	0.998	1.02	0.973	0.999	1.03
500.0	0.974	0.999	1.01	0.974	0.999	1.02	0.974	0.999	1.02
1000.0	0.975	0.999	1.01	0.975	1.00	1.01	0.974	1.00	1.02

TABLE 10a

Values of Mean Excitation Energies Used in the Calculation of Printout Table I

Medium	I_{adj} (ev)	Medium	I_{adj} (ev)
H_2	18.7	Pb	826
He	42.0	U	923
Li	38.0	H_2O	65.1
Be	60.0	CO_2	85.9
C	78.0	AgCl	384
N	85.0	AgBr	434
O	89.0	NaI	433
Ne	131	LiI	473
Mg	156	Methane	44.6
Al	163	Ethylene	54.6
A	210	Polyethylene	54.6
Fe	273	Xylene	61.0
Cu	314	Toluene	62.1
Kr	381	Acetylene	63.6
Ag	487	Polystyrene	63.6
Sn	516	Stilbene	65.2
Xe	555	Lucite	65.6
W	748	Anthracene	67.0
Au	797		

TABLE 10b

Values of Mean Excitation Energies and Composition, by Weight, Used in Calculation of Printout Table I

Medium	I_{adj} (ev)	Composition (fraction by weight)
Muscle	66.2	0.1020 H, 0.1230 C, 0.0350 N, 0.7290 O, 0.0008 Na, 0.0002 Mg, 0.0020 P, 0.0050 S, 0.0030 K
Bone	85.2	0.064 H, 0.278 C, 0.027 N, 0.410 O, 0.002 Mg, 0.070 P, 0.002 S, 0.147 Ca
Air	86.8	0.755 N, 0.232 O, 0.013 A
Standard Emulsion	320	0.01410 H, 0.07226 C, 0.01932 N, 0.06611 O, 0.00189 S, 0.34910 Br, 0.47410 Ag, 0.00312 I

range r^- in units of g cm^{-2}, and the radiation yield Y^-. All quantities are shown as functions of the electron energy T in Mev. The various substances make their appearance in Printout Table I[10] in the same order in which they are listed in Table 10.

It is difficult to estimate very closely the error of the data in Printout Table I. The available experimental data on stopping power have uncertainties ranging from 4 to 10 percent and are presumably less accurate than the calculated values. The principal source of error in the evaluation of $-\frac{1}{\rho}\left(\frac{dE}{dx}\right)^-_{col}$ is the uncertainty of I_{adj}, which may be as high as 10 percent for materials with very small Z but considerably smaller for high Z. A secondary source of error is the uncertainty in the density-effect correction δ, which is stated by Sternheimer to be of the order of 0.1. Taking into account that the percent error of the mean collision-loss is several times smaller than the corresponding error of I_{adj} and that the density effect introduces only a relatively minor correction except at the highest energies, one might expect that the error of $-\frac{1}{\rho}\left(\frac{dE}{dx}\right)^-_{col}$ will not exceed 1 to 2 percent.

The bremsstrahlung cross section on which the radiative energy loss $-\frac{1}{\rho}\left(\frac{dE}{dx}\right)^-_{rad}$ is based have been estimated by Koch and Motz to be accurate to within 20 percent up to 2 Mev, to within 5 percent between 2 and 15 Mev, and to within 3 percent above 15 Mev. The error of $-\frac{1}{\rho}\left(\frac{dE}{dx}\right)^-_{tot}$ as well as of r^- and Y^- will vary depending on the relative magnitudes of collision and radiation losses.

References

1. A. Nelms, Energy Loss and Range of Electrons and Positrons, NBS Circular 577 (1956), and Supplement to NBS Circular 577 (1958).

2. N. E. Hansen and S. C. Fultz, Cross Sections and Spectra for Negative Electron Bremsstrahlung, UCRL-6099 (1960).

3. W. Heitler, The Quantum Theory of Radiation, Oxford University Press, London (1954).

4. U. Fano, Penetration of Protons, α Particles and Mesons, Annual Reviews of Nuclear Science (1963), Appendix A of this volume.

5. H. W. Koch and J. W. Motz, Rev. Mod. Phys. 31, 29 (1959).

6. F. Rohrlich and B. C. Carlson, Phys. Rev. 93, 38 (1954).

7. T. J. Thompson, Effect of Chemical Structure on Stopping Powers for High-energy Protons, Thesis, Univ. of California, Berkeley. Also in UCRL-1910 (1952).

[10]Powers of ten are indicated by the symbol E; thus 1.2345E 02 means 1.2345×10^2.

8. R. M. Sternheimer, Phys. Rev. 88, 851 (1952); 91, 256 (1953); 103, 511 (1956).

9. H. Bethe and W. Heitler, Proc. Roy. Soc. A146, 83 (1934).

10. F. Sauter, Ann. Physik 20, 404 (1934).

11. G. Racah, Nuovo Cimento 11, 469 (1934).

12. H. Olsen, Phys. Rev. 99, 1335 (1955).

13. G. Elwert, Ann. Physik 34, 178 (1939).

14. A. Sommerfeld, Wellenmechanik (Frederick Ungar, New York (1950)), Chap. 7.

15. U. Fano, H. W. Koch and J. W. Motz, Phys. Rev. 112, 1679 (1958).

16. R. J. Jabbur and R. H. Pratt, Phys. Rev. 129, 184 (1962); 133, B1090 (1964).

17. H. W. Lewis, Phys. Rev. 85, 20 (1952).

18. L. V. Spencer and U. Fano, Phys. Rev. 93, 1172 (1954).

19. W. Paul and H. Reich, Z. Phys. 127, 429 (1950).

20. B. Ziegler, Z. Physik 151, 556 (1958).

21. F. L. Hereford, Phys. Rev. 74 , 574 (1948).

22. T. Westermark, Arkiv for Kemi 17, 101 (1961).

23. W. C. Barber, Phys. Rev. 103, 1281 (1956).

PRINTOUT TABLE I. Energy-loss, range, and radiation yield for electrons in various materials. The order in which each material appears and the values of the mean excitation energy used are given in Tables 10a and 10b.

ELECTRONS IN HYDROGEN

ENERGY	STOPPING POWER			RANGE	RADIATION YIELD
	COLLISION	RADIATION	TOTAL		
MEV	MEV CM2/G	MEV CM2/G	MEV CM2/G	G/CM2	
0.010	5.147E 01	1.970E-03	5.147E 01	1.071E-04	2.098E-05
0.015	3.697E 01	1.965E-03	3.697E 01	2.235E-04	2.926E-05
0.020	2.928E 01	1.969E-03	2.928E 01	3.767E-04	3.701E-05
0.025	2.448E 01	1.975E-03	2.448E 01	5.643E-04	4.441E-05
0.030	2.118E 01	1.983E-03	2.118E 01	7.846E-04	5.154E-05
0.035	1.877E 01	1.993E-03	1.877E 01	1.036E-03	5.845E-05
0.040	1.693E 01	2.003E-03	1.693E 01	1.317E-03	6.518E-05
0.045	1.547E 01	2.014E-03	1.547E 01	1.626E-03	7.174E-05
0.050	1.429E 01	2.026E-03	1.429E 01	1.963E-03	7.817E-05
0.055	1.331E 01	2.038E-03	1.331E 01	2.325E-03	8.446E-05
0.060	1.249E 01	2.050E-03	1.249E 01	2.713E-03	9.064E-05
0.065	1.179E 01	2.063E-03	1.179E 01	3.126E-03	9.671E-05
0.070	1.118E 01	2.076E-03	1.118E 01	3.562E-03	1.027E-04
0.075	1.065E 01	2.090E-03	1.065E 01	4.020E-03	1.086E-04
0.080	1.018E 01	2.103E-03	1.018E 01	4.500E-03	1.144E-04
0.085	9.768E 00	2.108E-03	9.770E 00	5.002E-03	1.200E-04
0.090	9.398E 00	2.122E-03	9.400E 00	5.523E-03	1.256E-04
0.095	9.066E 00	2.137E-03	9.068E 00	6.065E-03	1.312E-04
0.100	8.766E 00	2.152E-03	8.768E 00	6.626E-03	1.366E-04
0.150	6.840E 00	2.315E-03	6.842E 00	1.317E-02	1.886E-04
0.200	5.869E 00	2.480E-03	5.871E 00	2.111E-02	2.367E-04
0.250	5.290E 00	2.671E-03	5.293E 00	3.011E-02	2.821E-04
0.300	4.912E 00	2.874E-03	4.915E 00	3.993E-02	3.259E-04
0.350	4.649E 00	3.082E-03	4.652E 00	5.041E-02	3.685E-04
0.400	4.458E 00	3.305E-03	4.461E 00	6.139E-02	4.101E-04
0.450	4.315E 00	3.536E-03	4.318E 00	7.279E-02	4.512E-04
0.500	4.205E 00	3.779E-03	4.209E 00	8.453E-02	4.919E-04
0.550	4.120E 00	4.031E-03	4.124E 00	9.653E-02	5.324E-04
0.600	4.053E 00	4.291E-03	4.057E 00	1.088E-01	5.729E-04
0.650	3.999E 00	4.560E-03	4.004E 00	1.212E-01	6.133E-04
0.700	3.956E 00	4.836E-03	3.961E 00	1.337E-01	6.537E-04
0.750	3.921E 00	5.118E-03	3.926E 00	1.464E-01	6.943E-04
0.800	3.893E 00	5.407E-03	3.899E 00	1.592E-01	7.350E-04
0.850	3.870E 00	5.732E-03	3.876E 00	1.721E-01	7.762E-04
0.900	3.852E 00	6.033E-03	3.858E 00	1.850E-01	8.176E-04
0.950	3.837E 00	6.338E-03	3.844E 00	1.980E-01	8.591E-04
1.000	3.826E 00	6.647E-03	3.832E 00	2.110E-01	9.007E-04
1.100	3.809E 00	7.278E-03	3.816E 00	2.372E-01	9.844E-04
1.200	3.800E 00	7.926E-03	3.808E 00	2.634E-01	1.069E-03
1.300	3.796E 00	8.588E-03	3.804E 00	2.897E-01	1.153E-03

ELECTRONS IN HYDROGEN

ENERGY	STOPPING POWER			RANGE	RADIATION YIELD
	COLLISION	RADIATION	TOTAL		
MEV	MEV CM2/G	MEV CM2/G	MEV CM2/G	G/CM2	
1.400	3.795E 00	9.265E-03	3.805E 00	3.160E-01	1.238E-03
1.500	3.798E 00	9.956E-03	3.808E 00	3.422E-01	1.324E-03
1.600	3.802E 00	1.066E-02	3.813E 00	3.685E-01	1.410E-03
1.700	3.808E 00	1.139E-02	3.820E 00	3.947E-01	1.497E-03
1.800	3.816E 00	1.211E-02	3.828E 00	4.208E-01	1.585E-03
1.900	3.824E 00	1.285E-02	3.837E 00	4.469E-01	1.673E-03
2.000	3.833E 00	1.360E-02	3.846E 00	4.730E-01	1.762E-03
2.200	3.852E 00	1.512E-02	3.867E 00	5.248E-01	1.940E-03
2.400	3.872E 00	1.668E-02	3.888E 00	5.764E-01	2.120E-03
2.600	3.892E 00	1.828E-02	3.911E 00	6.277E-01	2.302E-03
2.800	3.913E 00	1.991E-02	3.933E 00	6.787E-01	2.485E-03
3.000	3.933E 00	2.157E-02	3.955E 00	7.294E-01	2.670E-03
3.500	3.982E 00	2.583E-02	4.008E 00	8.550E-01	3.138E-03
4.000	4.029E 00	3.026E-02	4.059E 00	9.789E-01	3.614E-03
4.500	4.072E 00	3.486E-02	4.107E 00	1.101E 00	4.098E-03
5.000	4.112E 00	3.954E-02	4.152E 00	1.222E 00	4.589E-03
5.500	4.149E 00	4.432E-02	4.194E 00	1.342E 00	5.085E-03
6.000	4.184E 00	4.918E-02	4.234E 00	1.461E 00	5.585E-03
6.500	4.217E 00	5.411E-02	4.271E 00	1.579E 00	6.090E-03
7.000	4.248E 00	5.911E-02	4.307E 00	1.695E 00	6.597E-03
7.500	4.277E 00	6.418E-02	4.341E 00	1.811E 00	7.108E-03
8.000	4.304E 00	6.931E-02	4.373E 00	1.925E 00	7.621E-03
8.500	4.330E 00	7.449E-02	4.404E 00	2.039E 00	8.136E-03
9.000	4.354E 00	7.999E-02	4.434E 00	2.153E 00	8.655E-03
9.500	4.377E 00	8.529E-02	4.463E 00	2.265E 00	9.177E-03
10.000	4.400E 00	9.064E-02	4.490E 00	2.377E 00	9.700E-03
20.000	4.707E 00	2.042E-01	4.912E 00	4.498E 00	2.030E-02
30.000	4.890E 00	3.255E-01	5.216E 00	6.471E 00	3.089E-02
40.000	5.013E 00	4.512E-01	5.464E 00	8.343E 00	4.130E-02
50.000	5.089E 00	5.797E-01	5.669E 00	1.014E 01	5.153E-02
60.000	5.141E 00	7.102E-01	5.852E 00	1.187E 01	6.159E-02
80.000	5.211E 00	9.756E-01	6.187E 00	1.520E 01	8.112E-02
100.000	5.258E 00	1.245E 00	6.503E 00	1.835E 01	9.985E-02
200.000	5.377E 00	2.623E 00	8.000E 00	3.218E 01	1.818E-01
300.000	5.440E 00	4.026E 00	9.466E 00	4.365E 01	2.476E-01
400.000	5.484E 00	5.439E 00	1.092E 01	5.348E 01	3.015E-01
500.000	5.518E 00	6.857E 00	1.238E 01	6.207E 01	3.466E-01
600.000	5.546E 00	8.281E 00	1.383E 01	6.972E 01	3.851E-01
800.000	5.590E 00	1.114E 01	1.673E 01	8.285E 01	4.474E-01
1000.000	5.624E 00	1.400E 01	1.962E 01	9.388E 01	4.961E-01

ELECTRONS IN HELIUM

ENERGY	STOPPING POWER			RANGE	RADIATION YIELD
	COLLISION	RADIATION	TOTAL		
MEV	MEV CM2/G	MEV CM2/G	MEV CM2/G	G/CM2	
0.010	2.265E 01	1.551E-03	2.266E 01	2.469E-04	3.849E-05
0.015	1.641E 01	1.536E-03	1.641E 01	5.102E-04	5.273E-05
0.020	1.307E 01	1.532E-03	1.307E 01	8.543E-04	6.593E-05
0.025	1.097E 01	1.532E-03	1.097E 01	1.274E-03	7.846E-05
0.030	9.516E 00	1.535E-03	9.518E 00	1.765E-03	9.047E-05
0.035	8.453E 00	1.539E-03	8.455E 00	2.323E-03	1.021E-04
0.040	7.638E 00	1.545E-03	7.640E 00	2.947E-03	1.133E-04
0.045	6.992E 00	1.551E-03	6.994E 00	3.632E-03	1.243E-04
0.050	6.468E 00	1.558E-03	6.469E 00	4.376E-03	1.350E-04
0.055	6.033E 00	1.566E-03	6.034E 00	5.177E-03	1.455E-04
0.060	5.666E 00	1.575E-03	5.668E 00	6.032E-03	1.558E-04
0.065	5.353E 00	1.584E-03	5.354E 00	6.940E-03	1.658E-04
0.070	5.081E 00	1.593E-03	5.083E 00	7.899E-03	1.758E-04
0.075	4.845E 00	1.602E-03	4.846E 00	8.907E-03	1.855E-04
0.080	4.636E 00	1.612E-03	4.638E 00	9.962E-03	1.951E-04
0.085	4.451E 00	1.602E-03	4.452E 00	1.106E-02	2.043E-04
0.090	4.285E 00	1.613E-03	4.287E 00	1.221E-02	2.134E-04
0.095	4.136E 00	1.624E-03	4.138E 00	1.340E-02	2.224E-04
0.100	4.001E 00	1.637E-03	4.003E 00	1.462E-02	2.313E-04
0.150	3.136E 00	1.785E-03	3.138E 00	2.892E-02	3.173E-04
0.200	2.699E 00	1.954E-03	2.701E 00	4.621E-02	3.996E-04
0.250	2.438E 00	2.139E-03	2.440E 00	6.575E-02	4.797E-04
0.300	2.268E 00	2.332E-03	2.270E 00	8.704E-02	5.585E-04
0.350	2.149E 00	2.534E-03	2.152E 00	1.097E-01	6.362E-04
0.400	2.064E 00	2.737E-03	2.067E 00	1.334E-01	7.131E-04
0.450	2.000E 00	2.944E-03	2.003E 00	1.580E-01	7.891E-04
0.500	1.951E 00	3.155E-03	1.954E 00	1.833E-01	8.644E-04
0.550	1.913E 00	3.371E-03	1.917E 00	2.091E-01	9.392E-04
0.600	1.884E 00	3.590E-03	1.887E 00	2.354E-01	1.013E-03
0.650	1.860E 00	3.813E-03	1.864E 00	2.621E-01	1.087E-03
0.700	1.841E 00	4.040E-03	1.845E 00	2.891E-01	1.161E-03
0.750	1.826E 00	4.270E-03	1.831E 00	3.163E-01	1.234E-03
0.800	1.814E 00	4.502E-03	1.819E 00	3.437E-01	1.307E-03
0.850	1.805E 00	4.743E-03	1.809E 00	3.713E-01	1.380E-03
0.900	1.797E 00	4.982E-03	1.802E 00	3.990E-01	1.453E-03
0.950	1.791E 00	5.223E-03	1.796E 00	4.267E-01	1.526E-03
1.000	1.786E 00	5.467E-03	1.792E 00	4.546E-01	1.599E-03
1.100	1.780E 00	5.962E-03	1.786E 00	5.105E-01	1.744E-03
1.200	1.777E 00	6.467E-03	1.784E 00	5.665E-01	1.889E-03
1.300	1.777E 00	6.980E-03	1.784E 00	6.226E-01	2.033E-03

ELECTRONS IN HELIUM

ENERGY	STOPPING POWER			RANGE	RADIATION YIELD
	COLLISION	RADIATION	TOTAL		
MEV	MEV CM2/G	MEV CM2/G	MEV CM2/G	G/CM2	
1.400	1.778E 00	7.502E-03	1.785E 00	6.787E-01	2.178E-03
1.500	1.780E 00	8.033E-03	1.788E 00	7.346E-01	2.323E-03
1.600	1.783E 00	8.571E-03	1.792E 00	7.905E-01	2.467E-03
1.700	1.787E 00	9.125E-03	1.796E 00	8.463E-01	2.612E-03
1.800	1.791E 00	9.677E-03	1.801E 00	9.019E-01	2.758E-03
1.900	1.796E 00	1.023E-02	1.806E 00	9.573E-01	2.903E-03
2.000	1.801E 00	1.080E-02	1.811E 00	1.013E 00	3.049E-03
2.200	1.811E 00	1.194E-02	1.823E 00	1.123E 00	3.340E-03
2.400	1.822E 00	1.310E-02	1.835E 00	1.232E 00	3.632E-03
2.600	1.833E 00	1.429E-02	1.847E 00	1.341E 00	3.925E-03
2.800	1.843E 00	1.546E-02	1.859E 00	1.449E 00	4.219E-03
3.000	1.854E 00	1.668E-02	1.871E 00	1.556E 00	4.512E-03
3.500	1.879E 00	1.981E-02	1.899E 00	1.821E 00	5.249E-03
4.000	1.903E 00	2.305E-02	1.926E 00	2.083E 00	5.992E-03
4.500	1.925E 00	2.641E-02	1.952E 00	2.340E 00	6.743E-03
5.000	1.946E 00	2.983E-02	1.976E 00	2.595E 00	7.500E-03
5.500	1.965E 00	3.333E-02	1.998E 00	2.847E 00	8.263E-03
6.000	1.982E 00	3.688E-02	2.019E 00	3.096E 00	9.030E-03
6.500	1.999E 00	4.049E-02	2.039E 00	3.342E 00	9.801E-03
7.000	2.014E 00	4.415E-02	2.059E 00	3.586E 00	1.058E-02
7.500	2.029E 00	4.786E-02	2.077E 00	3.828E 00	1.135E-02
8.000	2.043E 00	5.162E-02	2.094E 00	4.067E 00	1.213E-02
8.500	2.056E 00	5.543E-02	2.111E 00	4.305E 00	1.292E-02
9.000	2.068E 00	5.958E-02	2.128E 00	4.541E 00	1.371E-02
9.500	2.080E 00	6.347E-02	2.144E 00	4.775E 00	1.450E-02
10.000	2.091E 00	6.740E-02	2.159E 00	5.008E 00	1.530E-02
20.000	2.246E 00	1.511E-01	2.398E 00	9.386E 00	3.124E-02
30.000	2.339E 00	2.403E-01	2.579E 00	1.340E 01	4.691E-02
40.000	2.405E 00	3.324E-01	2.737E 00	1.716E 01	6.205E-02
50.000	2.456E 00	4.264E-01	2.882E 00	2.072E 01	7.660E-02
60.000	2.497E 00	5.219E-01	3.019E 00	2.411E 01	9.059E-02
80.000	2.561E 00	7.156E-01	3.277E 00	3.047E 01	1.170E-01
100.000	2.605E 00	9.119E-01	3.517E 00	3.635E 01	1.414E-01
200.000	2.700E 00	1.914E 00	4.614E 00	6.106E 01	2.422E-01
300.000	2.738E 00	2.932E 00	5.670E 00	8.057E 01	3.179E-01
400.000	2.761E 00	3.956E 00	6.717E 00	9.675E 01	3.771E-01
500.000	2.779E 00	4.983E 00	7.762E 00	1.106E 02	4.250E-01
600.000	2.793E 00	6.014E 00	8.807E 00	1.227E 02	4.647E-01
800.000	2.815E 00	8.080E 00	1.089E 01	1.431E 02	5.271E-01
1000.000	2.832E 00	1.015E 01	1.298E 01	1.599E 02	5.743E-01

ELECTRONS IN LITHIUM

ENERGY	STOPPING POWER			RANGE	RADIATION YIELD
	COLLISION	RADIATION	TOTAL		
MEV	MEV CM2/G	MEV CM2/G	MEV CM2/G	G/CM2	
0.010	1.995E 01	1.857E-03	1.995E 01	2.797E-04	5.260E-05
0.015	1.443E 01	1.830E-03	1.443E 01	5.789E-04	7.178E-05
0.020	1.148E 01	1.818E-03	1.149E 01	9.702E-04	8.950E-05
0.025	9.633E 00	1.813E-03	9.635E 00	1.448E-03	1.063E-04
0.030	8.357E 00	1.811E-03	8.359E 00	2.007E-03	1.223E-04
0.035	7.421E 00	1.812E-03	7.423E 00	2.643E-03	1.378E-04
0.040	6.703E 00	1.816E-03	6.705E 00	3.353E-03	1.527E-04
0.045	6.135E 00	1.822E-03	6.137E 00	4.133E-03	1.673E-04
0.050	5.674E 00	1.830E-03	5.676E 00	4.981E-03	1.815E-04
0.055	5.291E 00	1.839E-03	5.293E 00	5.894E-03	1.955E-04
0.060	4.969E 00	1.849E-03	4.971E 00	6.870E-03	2.092E-04
0.065	4.693E 00	1.859E-03	4.695E 00	7.905E-03	2.226E-04
0.070	4.455E 00	1.871E-03	4.457E 00	8.999E-03	2.358E-04
0.075	4.247E 00	1.883E-03	4.249E 00	1.015E-02	2.489E-04
0.080	4.064E 00	1.896E-03	4.066E 00	1.135E-02	2.618E-04
0.085	3.901E 00	1.887E-03	3.903E 00	1.261E-02	2.742E-04
0.090	3.755E 00	1.901E-03	3.757E 00	1.391E-02	2.864E-04
0.095	3.624E 00	1.916E-03	3.626E 00	1.527E-02	2.986E-04
0.100	3.506E 00	1.932E-03	3.508E 00	1.667E-02	3.106E-04
0.150	2.746E 00	2.120E-03	2.749E 00	3.299E-02	4.275E-04
0.200	2.359E 00	2.335E-03	2.361E 00	5.275E-02	5.408E-04
0.250	2.130E 00	2.569E-03	2.133E 00	7.510E-02	6.520E-04
0.300	1.979E 00	2.813E-03	1.982E 00	9.947E-02	7.619E-04
0.350	1.874E 00	3.068E-03	1.877E 00	1.254E-01	8.712E-04
0.400	1.797E 00	3.323E-03	1.800E 00	1.527E-01	9.799E-04
0.450	1.738E 00	3.581E-03	1.742E 00	1.809E-01	1.088E-03
0.500	1.693E 00	3.841E-03	1.697E 00	2.100E-01	1.195E-03
0.550	1.658E 00	4.104E-03	1.662E 00	2.398E-01	1.301E-03
0.600	1.629E 00	4.370E-03	1.634E 00	2.702E-01	1.407E-03
0.650	1.607E 00	4.639E-03	1.611E 00	3.010E-01	1.513E-03
0.700	1.588E 00	4.910E-03	1.593E 00	3.322E-01	1.618E-03
0.750	1.573E 00	5.183E-03	1.578E 00	3.637E-01	1.722E-03
0.800	1.560E 00	5.459E-03	1.565E 00	3.956E-01	1.826E-03
0.850	1.549E 00	5.734E-03	1.555E 00	4.276E-01	1.930E-03
0.900	1.541E 00	6.015E-03	1.547E 00	4.598E-01	2.033E-03
0.950	1.533E 00	6.298E-03	1.540E 00	4.922E-01	2.136E-03
1.000	1.527E 00	6.583E-03	1.534E 00	5.248E-01	2.239E-03
1.100	1.518E 00	7.161E-03	1.525E 00	5.902E-01	2.444E-03
1.200	1.511E 00	7.747E-03	1.519E 00	6.559E-01	2.648E-03
1.300	1.507E 00	8.341E-03	1.515E 00	7.218E-01	2.852E-03

ELECTRONS IN LITHIUM

ENERGY	STOPPING POWER			RANGE	RADIATION YIELD
	COLLISION	RADIATION	TOTAL		
MEV	MEV CM2/G	MEV CM2/G	MEV CM2/G	G/CM2	
1.400	1.504E 00	8.943E-03	1.513E 00	7.878E-01	3.056E-03
1.500	1.503E 00	9.553E-03	1.512E 00	8.540E-01	3.260E-03
1.600	1.502E 00	1.017E-02	1.512E 00	9.201E-01	3.464E-03
1.700	1.502E 00	1.080E-02	1.512E 00	9.862E-01	3.668E-03
1.800	1.502E 00	1.143E-02	1.513E 00	1.052E 00	3.872E-03
1.900	1.503E 00	1.206E-02	1.515E 00	1.118E 00	4.077E-03
2.000	1.504E 00	1.271E-02	1.517E 00	1.184E 00	4.281E-03
2.200	1.507E 00	1.401E-02	1.521E 00	1.316E 00	4.691E-03
2.400	1.510E 00	1.533E-02	1.526E 00	1.447E 00	5.103E-03
2.600	1.514E 00	1.668E-02	1.531E 00	1.578E 00	5.516E-03
2.800	1.518E 00	1.798E-02	1.536E 00	1.709E 00	5.930E-03
3.000	1.522E 00	1.937E-02	1.542E 00	1.839E 00	6.343E-03
3.500	1.532E 00	2.292E-02	1.555E 00	2.161E 00	7.387E-03
4.000	1.542E 00	2.661E-02	1.568E 00	2.482E 00	8.444E-03
4.500	1.550E 00	3.044E-02	1.581E 00	2.799E 00	9.517E-03
5.000	1.559E 00	3.434E-02	1.593E 00	3.114E 00	1.061E-02
5.500	1.566E 00	3.831E-02	1.604E 00	3.427E 00	1.171E-02
6.000	1.573E 00	4.235E-02	1.615E 00	3.738E 00	1.282E-02
6.500	1.579E 00	4.645E-02	1.626E 00	4.046E 00	1.394E-02
7.000	1.585E 00	5.062E-02	1.636E 00	4.353E 00	1.507E-02
7.500	1.591E 00	5.483E-02	1.646E 00	4.657E 00	1.621E-02
8.000	1.596E 00	5.910E-02	1.655E 00	4.960E 00	1.735E-02
8.500	1.601E 00	6.342E-02	1.664E 00	5.262E 00	1.850E-02
9.000	1.605E 00	6.808E-02	1.673E 00	5.561E 00	1.966E-02
9.500	1.610E 00	7.250E-02	1.682E 00	5.859E 00	2.083E-02
10.000	1.614E 00	7.696E-02	1.691E 00	6.156E 00	2.201E-02
20.000	1.666E 00	1.719E-01	1.837E 00	1.182E 01	4.581E-02
30.000	1.694E 00	2.730E-01	1.967E 00	1.708E 01	6.937E-02
40.000	1.714E 00	3.773E-01	2.091E 00	2.201E 01	9.200E-02
50.000	1.729E 00	4.837E-01	2.212E 00	2.666E 01	1.136E-01
60.000	1.741E 00	5.915E-01	2.332E 00	3.106E 01	1.340E-01
80.000	1.760E 00	8.104E-01	2.570E 00	3.922E 01	1.719E-01
100.000	1.775E 00	1.032E 00	2.807E 00	4.667E 01	2.059E-01
200.000	1.821E 00	2.161E 00	3.982E 00	7.642E 01	3.353E-01
300.000	1.848E 00	3.306E 00	5.155E 00	9.843E 01	4.222E-01
400.000	1.867E 00	4.458E 00	6.325E 00	1.159E 02	4.854E-01
500.000	1.882E 00	5.613E 00	7.495E 00	1.304E 02	5.340E-01
600.000	1.894E 00	6.771E 00	8.665E 00	1.428E 02	5.726E-01
800.000	1.913E 00	9.092E 00	1.101E 01	1.632E 02	6.308E-01
1000.000	1.928E 00	1.142E 01	1.334E 01	1.797E 02	6.730E-01

ELECTRONS IN BERYLLIUM

ENERGY	STOPPING POWER			RANGE	RADIATION YIELD
	COLLISION	RADIATION	TOTAL		
MEV	MEV CM2/G	MEV CM2/G	MEV CM2/G	G/CM2	
0.010	1.884E 01	2.463E-03	1.885E 01	2.993E-04	7.482E-05
0.015	1.371E 01	2.418E-03	1.371E 01	6.150E-04	1.012E-04
0.020	1.095E 01	2.396E-03	1.095E 01	1.026E-03	1.253E-04
0.025	9.207E 00	2.382E-03	9.209E 00	1.526E-03	1.480E-04
0.030	8.002E 00	2.375E-03	8.005E 00	2.110E-03	1.697E-04
0.035	7.117E 00	2.370E-03	7.119E 00	2.774E-03	1.904E-04
0.040	6.437E 00	2.373E-03	6.440E 00	3.514E-03	2.105E-04
0.045	5.898E 00	2.379E-03	5.900E 00	4.326E-03	2.299E-04
0.050	5.460E 00	2.388E-03	5.462E 00	5.208E-03	2.490E-04
0.055	5.096E 00	2.400E-03	5.098E 00	6.156E-03	2.676E-04
0.060	4.789E 00	2.413E-03	4.791E 00	7.168E-03	2.859E-04
0.065	4.526E 00	2.428E-03	4.529E 00	8.242E-03	3.039E-04
0.070	4.299E 00	2.445E-03	4.301E 00	9.376E-03	3.217E-04
0.075	4.100E 00	2.462E-03	4.103E 00	1.057E-02	3.392E-04
0.080	3.925E 00	2.480E-03	3.928E 00	1.181E-02	3.565E-04
0.085	3.770E 00	2.479E-03	3.772E 00	1.311E-02	3.733E-04
0.090	3.631E 00	2.499E-03	3.633E 00	1.446E-02	3.899E-04
0.095	3.506E 00	2.521E-03	3.508E 00	1.586E-02	4.064E-04
0.100	3.393E 00	2.543E-03	3.395E 00	1.731E-02	4.228E-04
0.150	2.666E 00	2.802E-03	2.669E 00	3.415E-02	5.819E-04
0.200	2.298E 00	3.095E-03	2.301E 00	5.445E-02	7.360E-04
0.250	2.077E 00	3.407E-03	2.080E 00	7.738E-02	8.871E-04
0.300	1.932E 00	3.732E-03	1.935E 00	1.024E-01	1.036E-03
0.350	1.830E 00	4.068E-03	1.834E 00	1.289E-01	1.185E-03
0.400	1.755E 00	4.408E-03	1.760E 00	1.568E-01	1.332E-03
0.450	1.699E 00	4.756E-03	1.704E 00	1.857E-01	1.478E-03
0.500	1.655E 00	5.104E-03	1.660E 00	2.154E-01	1.624E-03
0.550	1.621E 00	5.453E-03	1.626E 00	2.459E-01	1.768E-03
0.600	1.594E 00	5.803E-03	1.599E 00	2.769E-01	1.912E-03
0.650	1.571E 00	6.155E-03	1.578E 00	3.084E-01	2.054E-03
0.700	1.553E 00	6.508E-03	1.560E 00	3.402E-01	2.196E-03
0.750	1.539E 00	6.863E-03	1.545E 00	3.725E-01	2.337E-03
0.800	1.526E 00	7.220E-03	1.533E 00	4.049E-01	2.476E-03
0.850	1.516E 00	6.600E-03	1.523E 00	4.377E-01	2.581E-03
0.900	1.507E 00	6.969E-03	1.514E 00	4.706E-01	2.686E-03
0.950	1.500E 00	7.370E-03	1.508E 00	5.037E-01	2.794E-03
1.000	1.494E 00	7.803E-03	1.502E 00	5.369E-01	2.907E-03
1.100	1.485E 00	8.757E-03	1.494E 00	6.037E-01	3.144E-03
1.200	1.479E 00	9.821E-03	1.489E 00	6.707E-01	3.401E-03
1.300	1.475E 00	1.099E-02	1.486E 00	7.380E-01	3.677E-03

ELECTRONS IN BERYLLIUM

ENERGY	STOPPING POWER			RANGE	RADIATION YIELD
	COLLISION	RADIATION	TOTAL		
MEV	MEV CM2/G	MEV CM2/G	MEV CM2/G	G/CM2	
1.400	1.472E 00	1.225E-02	1.484E 00	8.054E-01	3.973E-03
1.500	1.470E 00	1.360E-02	1.484E 00	8.728E-01	4.289E-03
1.600	1.469E 00	1.504E-02	1.484E 00	9.401E-01	4.624E-03
1.700	1.469E 00	1.781E-02	1.487E 00	1.007E 00	5.023E-03
1.800	1.469E 00	1.925E-02	1.489E 00	1.075E 00	5.436E-03
1.900	1.470E 00	2.060E-02	1.491E 00	1.142E 00	5.854E-03
2.000	1.471E 00	2.186E-02	1.493E 00	1.209E 00	6.273E-03
2.200	1.474E 00	2.416E-02	1.498E 00	1.343E 00	7.103E-03
2.400	1.477E 00	2.615E-02	1.503E 00	1.476E 00	7.909E-03
2.600	1.481E 00	2.786E-02	1.509E 00	1.609E 00	8.682E-03
2.800	1.484E 00	2.560E-02	1.510E 00	1.741E 00	9.399E-03
3.000	1.488E 00	2.673E-02	1.515E 00	1.873E 00	9.925E-03
3.500	1.498E 00	3.004E-02	1.528E 00	2.202E 00	1.117E-02
4.000	1.507E 00	3.401E-02	1.541E 00	2.528E 00	1.238E-02
4.500	1.515E 00	3.901E-02	1.554E 00	2.851E 00	1.361E-02
5.000	1.522E 00	4.393E-02	1.566E 00	3.172E 00	1.490E-02
5.500	1.530E 00	4.894E-02	1.579E 00	3.489E 00	1.623E-02
6.000	1.536E 00	5.404E-02	1.590E 00	3.805E 00	1.759E-02
6.500	1.542E 00	5.923E-02	1.601E 00	4.118E 00	1.896E-02
7.000	1.548E 00	6.449E-02	1.612E 00	4.430E 00	2.036E-02
7.500	1.553E 00	6.982E-02	1.623E 00	4.739E 00	2.177E-02
8.000	1.558E 00	7.522E-02	1.633E 00	5.046E 00	2.319E-02
8.500	1.563E 00	8.069E-02	1.643E 00	5.351E 00	2.463E-02
9.000	1.567E 00	8.675E-02	1.654E 00	5.654E 00	2.608E-02
9.500	1.571E 00	9.235E-02	1.663E 00	5.956E 00	2.755E-02
10.000	1.575E 00	9.800E-02	1.673E 00	6.255E 00	2.902E-02
20.000	1.626E 00	2.184E-01	1.844E 00	1.194E 01	5.888E-02
30.000	1.654E 00	3.464E-01	2.001E 00	1.714E 01	8.801E-02
40.000	1.674E 00	4.783E-01	2.152E 00	2.196E 01	1.155E-01
50.000	1.690E 00	6.129E-01	2.302E 00	2.645E 01	1.414E-01
60.000	1.702E 00	7.492E-01	2.451E 00	3.066E 01	1.655E-01
80.000	1.722E 00	1.026E 00	2.748E 00	3.836E 01	2.093E-01
100.000	1.737E 00	1.305E 00	3.042E 00	4.528E 01	2.478E-01
200.000	1.785E 00	2.729E 00	4.513E 00	7.208E 01	3.877E-01
300.000	1.812E 00	4.172E 00	5.984E 00	9.126E 01	4.768E-01
400.000	1.832E 00	5.623E 00	7.455E 00	1.062E 02	5.395E-01
500.000	1.847E 00	7.078E 00	8.925E 00	1.184E 02	5.866E-01
600.000	1.860E 00	8.536E 00	1.040E 01	1.288E 02	6.234E-01
800.000	1.879E 00	1.146E 01	1.334E 01	1.458E 02	6.780E-01
1000.000	1.895E 00	1.438E 01	1.628E 01	1.593E 02	7.168E-01

ELECTRONS IN CARBON

ENERGY	STOPPING POWER			RANGE	RADIATION YIELD
	COLLISION	RADIATION	TOTAL		
MEV	MEV CM2/G	MEV CM2/G	MEV CM2/G	G/CM2	
0.010	2.015E 01	4.089E-03	2.016E 01	2.819E-04	1.168E-04
0.015	1.472E 01	4.002E-03	1.472E 01	5.764E-04	1.572E-04
0.020	1.178E 01	3.952E-03	1.178E 01	9.589E-04	1.939E-04
0.025	9.921E 00	3.917E-03	9.925E 00	1.423E-03	2.282E-04
0.030	8.634E 00	3.893E-03	8.638E 00	1.965E-03	2.606E-04
0.035	7.686E 00	3.872E-03	7.690E 00	2.580E-03	2.916E-04
0.040	6.958E 00	3.869E-03	6.962E 00	3.264E-03	3.214E-04
0.045	6.380E 00	3.873E-03	6.383E 00	4.015E-03	3.502E-04
0.050	5.909E 00	3.885E-03	5.913E 00	4.830E-03	3.784E-04
0.055	5.518E 00	3.901E-03	5.522E 00	5.706E-03	4.060E-04
0.060	5.188E 00	3.921E-03	5.192E 00	6.640E-03	4.331E-04
0.065	4.906E 00	3.945E-03	4.910E 00	7.631E-03	4.597E-04
0.070	4.661E 00	3.971E-03	4.665E 00	8.676E-03	4.860E-04
0.075	4.447E 00	3.999E-03	4.451E 00	9.774E-03	5.119E-04
0.080	4.259E 00	4.029E-03	4.263E 00	1.092E-02	5.375E-04
0.085	4.091E 00	4.039E-03	4.095E 00	1.212E-02	5.626E-04
0.090	3.941E 00	4.073E-03	3.945E 00	1.336E-02	5.874E-04
0.095	3.807E 00	4.109E-03	3.811E 00	1.465E-02	6.121E-04
0.100	3.685E 00	4.145E-03	3.689E 00	1.599E-02	6.365E-04
0.150	2.900E 00	4.568E-03	2.904E 00	3.147E-02	8.741E-04
0.200	2.493E 00	5.042E-03	2.498E 00	5.015E-02	1.105E-03
0.250	2.254E 00	5.549E-03	2.260E 00	7.126E-02	1.331E-03
0.300	2.097E 00	6.078E-03	2.103E 00	9.425E-02	1.555E-03
0.350	1.987E 00	6.627E-03	1.994E 00	1.187E-01	1.777E-03
0.400	1.907E 00	7.177E-03	1.914E 00	1.443E-01	1.997E-03
0.450	1.847E 00	7.736E-03	1.855E 00	1.709E-01	2.215E-03
0.500	1.801E 00	8.295E-03	1.809E 00	1.982E-01	2.431E-03
0.550	1.764E 00	8.855E-03	1.773E 00	2.261E-01	2.646E-03
0.600	1.735E 00	9.418E-03	1.745E 00	2.545E-01	2.858E-03
0.650	1.712E 00	9.983E-03	1.722E 00	2.834E-01	3.069E-03
0.700	1.693E 00	1.055E-02	1.704E 00	3.126E-01	3.278E-03
0.750	1.678E 00	1.112E-02	1.689E 00	3.421E-01	3.485E-03
0.800	1.665E 00	1.169E-02	1.677E 00	3.718E-01	3.691E-03
0.850	1.655E 00	1.227E-02	1.667E 00	4.017E-01	3.896E-03
0.900	1.646E 00	1.285E-02	1.659E 00	4.317E-01	4.099E-03
0.950	1.639E 00	1.343E-02	1.653E 00	4.619E-01	4.301E-03
1.000	1.634E 00	1.402E-02	1.648E 00	4.922E-01	4.502E-03
1.100	1.625E 00	1.519E-02	1.640E 00	5.531E-01	4.900E-03
1.200	1.619E 00	1.638E-02	1.636E 00	6.141E-01	5.295E-03
1.300	1.616E 00	1.757E-02	1.633E 00	6.753E-01	5.686E-03

ELECTRONS IN CARBON

ENERGY	STOPPING POWER			RANGE	RADIATION YIELD
	COLLISION	RADIATION	TOTAL		
MEV	MEV CM2/G	MEV CM2/G	MEV CM2/G	G/CM2	
1.400	1.614E 00	1.877E-02	1.633E 00	7.366E-01	6.075E-03
1.500	1.613E 00	1.999E-02	1.633E 00	7.978E-01	6.461E-03
1.600	1.613E 00	2.121E-02	1.635E 00	8.590E-01	6.845E-03
1.700	1.614E 00	2.241E-02	1.637E 00	9.202E-01	7.227E-03
1.800	1.615E 00	2.365E-02	1.639E 00	9.812E-01	7.606E-03
1.900	1.617E 00	2.491E-02	1.642E 00	1.042E 00	7.985E-03
2.000	1.619E 00	2.617E-02	1.645E 00	1.103E 00	8.362E-03
2.200	1.624E 00	2.874E-02	1.653E 00	1.224E 00	9.116E-03
2.400	1.629E 00	3.135E-02	1.660E 00	1.345E 00	9.868E-03
2.600	1.634E 00	3.400E-02	1.668E 00	1.465E 00	1.062E-02
2.800	1.640E 00	3.659E-02	1.676E 00	1.585E 00	1.137E-02
3.000	1.645E 00	3.931E-02	1.684E 00	1.704E 00	1.212E-02
3.500	1.658E 00	4.631E-02	1.704E 00	1.999E 00	1.399E-02
4.000	1.670E 00	5.357E-02	1.724E 00	2.291E 00	1.588E-02
4.500	1.682E 00	6.111E-02	1.743E 00	2.579E 00	1.779E-02
5.000	1.692E 00	6.878E-02	1.761E 00	2.864E 00	1.972E-02
5.500	1.701E 00	7.659E-02	1.778E 00	3.147E 00	2.166E-02
6.000	1.710E 00	8.454E-02	1.795E 00	3.427E 00	2.361E-02
6.500	1.718E 00	9.260E-02	1.811E 00	3.704E 00	2.557E-02
7.000	1.726E 00	1.008E-01	1.826E 00	3.979E 00	2.754E-02
7.500	1.733E 00	1.091E-01	1.842E 00	4.252E 00	2.952E-02
8.000	1.739E 00	1.174E-01	1.856E 00	4.522E 00	3.150E-02
8.500	1.745E 00	1.259E-01	1.871E 00	4.791E 00	3.349E-02
9.000	1.751E 00	1.351E-01	1.886E 00	5.057E 00	3.549E-02
9.500	1.756E 00	1.438E-01	1.900E 00	5.321E 00	3.750E-02
10.000	1.761E 00	1.526E-01	1.914E 00	5.583E 00	3.951E-02
20.000	1.825E 00	3.388E-01	2.164E 00	1.049E 01	7.913E-02
30.000	1.859E 00	5.367E-01	2.396E 00	1.488E 01	1.165E-01
40.000	1.882E 00	7.402E-01	2.622E 00	1.887E 01	1.508E-01
50.000	1.899E 00	9.475E-01	2.847E 00	2.252E 01	1.823E-01
60.000	1.914E 00	1.158E 00	3.071E 00	2.591E 01	2.111E-01
80.000	1.936E 00	1.583E 00	3.519E 00	3.198E 01	2.621E-01
100.000	1.953E 00	2.013E 00	3.966E 00	3.734E 01	3.056E-01
200.000	2.007E 00	4.200E 00	6.206E 00	5.732E 01	4.548E-01
300.000	2.038E 00	6.414E 00	8.452E 00	7.108E 01	5.438E-01
400.000	2.060E 00	8.639E 00	1.070E 01	8.157E 01	6.041E-01
500.000	2.077E 00	1.087E 01	1.295E 01	9.005E 01	6.482E-01
600.000	2.091E 00	1.311E 01	1.520E 01	9.718E 01	6.821E-01
800.000	2.113E 00	1.758E 01	1.970E 01	1.087E 02	7.313E-01
1000.000	2.130E 00	2.206E 01	2.419E 01	1.178E 02	7.656E-01

ELECTRONS IN NITROGEN

ENERGY	STOPPING POWER			RANGE	RADIATION YIELD
	COLLISION	RADIATION	TOTAL		
MEV	MEV CM2/G	MEV CM2/G	MEV CM2/G	G/CM2	
0.010	1.981E 01	4.769E-03	1.982E 01	2.874E-04	1.386E-04
0.015	1.449E 01	4.669E-03	1.449E 01	5.868E-04	1.864E-04
0.020	1.160E 01	4.606E-03	1.161E 01	9.752E-04	2.298E-04
0.025	9.780E 00	4.562E-03	9.784E 00	1.446E-03	2.702E-04
0.030	8.515E 00	4.530E-03	8.519E 00	1.996E-03	3.084E-04
0.035	7.583E 00	4.502E-03	7.587E 00	2.619E-03	3.447E-04
0.040	6.866E 00	4.497E-03	6.870E 00	3.313E-03	3.796E-04
0.045	6.297E 00	4.502E-03	6.301E 00	4.073E-03	4.135E-04
0.050	5.834E 00	4.516E-03	5.838E 00	4.899E-03	4.466E-04
0.055	5.449E 00	4.535E-03	5.453E 00	5.786E-03	4.789E-04
0.060	5.124E 00	4.560E-03	5.128E 00	6.732E-03	5.107E-04
0.065	4.845E 00	4.589E-03	4.850E 00	7.735E-03	5.421E-04
0.070	4.604E 00	4.621E-03	4.609E 00	8.793E-03	5.729E-04
0.075	4.394E 00	4.656E-03	4.398E 00	9.904E-03	6.035E-04
0.080	4.208E 00	4.693E-03	4.213E 00	1.107E-02	6.336E-04
0.085	4.043E 00	4.716E-03	4.048E 00	1.228E-02	6.633E-04
0.090	3.895E 00	4.757E-03	3.900E 00	1.354E-02	6.927E-04
0.095	3.762E 00	4.800E-03	3.767E 00	1.484E-02	7.219E-04
0.100	3.642E 00	4.844E-03	3.647E 00	1.619E-02	7.508E-04
0.150	2.868E 00	5.344E-03	2.873E 00	3.184E-02	1.032E-03
0.200	2.475E 00	5.894E-03	2.481E 00	5.068E-02	1.304E-03
0.250	2.242E 00	6.486E-03	2.248E 00	7.192E-02	1.569E-03
0.300	2.089E 00	7.104E-03	2.096E 00	9.501E-02	1.831E-03
0.350	1.983E 00	7.747E-03	1.991E 00	1.195E-01	2.089E-03
0.400	1.906E 00	8.390E-03	1.915E 00	1.452E-01	2.345E-03
0.450	1.849E 00	9.048E-03	1.858E 00	1.717E-01	2.599E-03
0.500	1.806E 00	9.701E-03	1.816E 00	1.989E-01	2.849E-03
0.550	1.773E 00	1.035E-02	1.783E 00	2.267E-01	3.097E-03
0.600	1.747E 00	1.101E-02	1.758E 00	2.550E-01	3.342E-03
0.650	1.726E 00	1.166E-02	1.738E 00	2.836E-01	3.584E-03
0.700	1.710E 00	1.232E-02	1.722E 00	3.125E-01	3.823E-03
0.750	1.697E 00	1.297E-02	1.710E 00	3.416E-01	4.059E-03
0.800	1.687E 00	1.363E-02	1.701E 00	3.709E-01	4.293E-03
0.850	1.679E 00	1.424E-02	1.693E 00	4.004E-01	4.523E-03
0.900	1.673E 00	1.490E-02	1.688E 00	4.300E-01	4.751E-03
0.950	1.668E 00	1.557E-02	1.684E 00	4.597E-01	4.976E-03
1.000	1.665E 00	1.624E-02	1.681E 00	4.894E-01	5.200E-03
1.100	1.660E 00	1.759E-02	1.678E 00	5.489E-01	5.643E-03
1.200	1.659E 00	1.895E-02	1.678E 00	6.085E-01	6.080E-03
1.300	1.659E 00	2.033E-02	1.680E 00	6.681E-01	6.513E-03

ELECTRONS IN NITROGEN

ENERGY	STOPPING POWER			RANGE	RADIATION YIELD
	COLLISION	RADIATION	TOTAL		
MEV	MEV CM2/G	MEV CM2/G	MEV CM2/G	G/CM2	
1.400	1.661E 00	2.172E-02	1.683E 00	7.276E-01	6.941E-03
1.500	1.664E 00	2.312E-02	1.688E 00	7.869E-01	7.365E-03
1.600	1.668E 00	2.454E-02	1.693E 00	8.461E-01	7.786E-03
1.700	1.673E 00	2.596E-02	1.699E 00	9.051E-01	8.204E-03
1.800	1.678E 00	2.740E-02	1.705E 00	9.638E-01	8.619E-03
1.900	1.683E 00	2.885E-02	1.712E 00	1.022E 00	9.032E-03
2.000	1.688E 00	3.030E-02	1.718E 00	1.081E 00	9.442E-03
2.200	1.699E 00	3.325E-02	1.732E 00	1.197E 00	1.026E-02
2.400	1.710E 00	3.623E-02	1.747E 00	1.312E 00	1.107E-02
2.600	1.722E 00	3.924E-02	1.761E 00	1.426E 00	1.187E-02
2.800	1.733E 00	4.207E-02	1.775E 00	1.539E 00	1.267E-02
3.000	1.744E 00	4.515E-02	1.789E 00	1.651E 00	1.346E-02
3.500	1.770E 00	5.306E-02	1.823E 00	1.928E 00	1.541E-02
4.000	1.794E 00	6.127E-02	1.855E 00	2.200E 00	1.737E-02
4.500	1.816E 00	6.982E-02	1.886E 00	2.467E 00	1.933E-02
5.000	1.837E 00	7.851E-02	1.915E 00	2.730E 00	2.130E-02
5.500	1.856E 00	8.735E-02	1.943E 00	2.989E 00	2.327E-02
6.000	1.874E 00	9.635E-02	1.970E 00	3.245E 00	2.524E-02
6.500	1.890E 00	1.055E-01	1.996E 00	3.497E 00	2.721E-02
7.000	1.906E 00	1.148E-01	2.021E 00	3.746E 00	2.918E-02
7.500	1.921E 00	1.241E-01	2.045E 00	3.992E 00	3.115E-02
8.000	1.935E 00	1.336E-01	2.068E 00	4.235E 00	3.312E-02
8.500	1.948E 00	1.433E-01	2.091E 00	4.475E 00	3.509E-02
9.000	1.960E 00	1.538E-01	2.114E 00	4.713E 00	3.706E-02
9.500	1.972E 00	1.636E-01	2.136E 00	4.948E 00	3.904E-02
10.000	1.983E 00	1.736E-01	2.157E 00	5.181E 00	4.102E-02
20.000	2.139E 00	3.849E-01	2.523E 00	9.451E 00	7.913E-02
30.000	2.231E 00	6.094E-01	2.840E 00	1.318E 01	1.142E-01
40.000	2.288E 00	8.401E-01	3.128E 00	1.653E 01	1.462E-01
50.000	2.330E 00	1.075E 00	3.405E 00	1.960E 01	1.755E-01
60.000	2.361E 00	1.313E 00	3.674E 00	2.242E 01	2.024E-01
80.000	2.408E 00	1.795E 00	4.203E 00	2.751E 01	2.502E-01
100.000	2.440E 00	2.282E 00	4.722E 00	3.199E 01	2.914E-01
200.000	2.528E 00	4.757E 00	7.285E 00	4.890E 01	4.354E-01
300.000	2.572E 00	7.262E 00	9.834E 00	6.067E 01	5.235E-01
400.000	2.600E 00	9.778E 00	1.238E 01	6.971E 01	5.842E-01
500.000	2.620E 00	1.230E 01	1.492E 01	7.706E 01	6.290E-01
600.000	2.637E 00	1.483E 01	1.747E 01	8.325E 01	6.637E-01
800.000	2.661E 00	1.989E 01	2.256E 01	9.330E 01	7.145E-01
1000.000	2.680E 00	2.496E 01	2.764E 01	1.013E 02	7.502E-01

ELECTRONS IN OXYGEN

ENERGY	STOPPING POWER			RANGE	RADIATION YIELD
	COLLISION	RADIATION	TOTAL		
MEV	MEV CM2/G	MEV CM2/G	MEV CM2/G	G/CM2	
0.010	1.964E 01	5.460E-03	1.964E 01	2.904E-04	1.598E-04
0.015	1.437E 01	5.348E-03	1.437E 01	5.923E-04	2.152E-04
0.020	1.152E 01	5.274E-03	1.152E 01	9.837E-04	2.652E-04
0.025	9.708E 00	5.221E-03	9.713E 00	1.458E-03	3.118E-04
0.030	8.454E 00	5.183E-03	8.459E 00	2.012E-03	3.558E-04
0.035	7.530E 00	5.145E-03	7.535E 00	2.639E-03	3.975E-04
0.040	6.819E 00	5.139E-03	6.825E 00	3.338E-03	4.375E-04
0.045	6.255E 00	5.146E-03	6.260E 00	4.104E-03	4.764E-04
0.050	5.795E 00	5.163E-03	5.801E 00	4.934E-03	5.144E-04
0.055	5.414E 00	5.188E-03	5.419E 00	5.827E-03	5.516E-04
0.060	5.091E 00	5.218E-03	5.096E 00	6.779E-03	5.882E-04
0.065	4.815E 00	5.253E-03	4.820E 00	7.788E-03	6.243E-04
0.070	4.576E 00	5.291E-03	4.581E 00	8.853E-03	6.598E-04
0.075	4.367E 00	5.333E-03	4.372E 00	9.970E-03	6.950E-04
0.080	4.182E 00	5.377E-03	4.188E 00	1.114E-02	7.298E-04
0.085	4.019E 00	5.414E-03	4.024E 00	1.236E-02	7.642E-04
0.090	3.872E 00	5.463E-03	3.877E 00	1.362E-02	7.982E-04
0.095	3.740E 00	5.514E-03	3.745E 00	1.494E-02	8.320E-04
0.100	3.621E 00	5.566E-03	3.626E 00	1.629E-02	8.656E-04
0.150	2.852E 00	6.144E-03	2.858E 00	3.203E-02	1.192E-03
0.200	2.462E 00	6.765E-03	2.469E 00	5.097E-02	1.505E-03
0.250	2.230E 00	7.443E-03	2.237E 00	7.231E-02	1.811E-03
0.300	2.078E 00	8.152E-03	2.086E 00	9.550E-02	2.112E-03
0.350	1.973E 00	8.893E-03	1.982E 00	1.201E-01	2.410E-03
0.400	1.897E 00	9.629E-03	1.907E 00	1.459E-01	2.705E-03
0.450	1.841E 00	1.038E-02	1.851E 00	1.725E-01	2.997E-03
0.500	1.798E 00	1.112E-02	1.809E 00	1.998E-01	3.285E-03
0.550	1.764E 00	1.187E-02	1.776E 00	2.277E-01	3.569E-03
0.600	1.739E 00	1.261E-02	1.751E 00	2.561E-01	3.850E-03
0.650	1.718E 00	1.335E-02	1.732E 00	2.848E-01	4.128E-03
0.700	1.702E 00	1.410E-02	1.716E 00	3.138E-01	4.402E-03
0.750	1.690E 00	1.485E-02	1.704E 00	3.431E-01	4.672E-03
0.800	1.680E 00	1.559E-02	1.695E 00	3.725E-01	4.940E-03
0.850	1.672E 00	1.634E-02	1.688E 00	4.020E-01	5.205E-03
0.900	1.666E 00	1.709E-02	1.683E 00	4.317E-01	5.467E-03
0.950	1.661E 00	1.785E-02	1.679E 00	4.615E-01	5.726E-03
1.000	1.658E 00	1.860E-02	1.676E 00	4.913E-01	5.983E-03
1.100	1.653E 00	2.012E-02	1.674E 00	5.510E-01	6.490E-03
1.200	1.652E 00	2.165E-02	1.674E 00	6.107E-01	6.990E-03
1.300	1.653E 00	2.319E-02	1.676E 00	6.705E-01	7.482E-03

ELECTRONS IN OXYGEN

ENERGY	STOPPING POWER			RANGE	RADIATION YIELD
	COLLISION	RADIATION	TOTAL		
MEV	MEV CM2/G	MEV CM2/G	MEV CM2/G	G/CM2	
1.400	1.655E 00	2.474E-02	1.679E 00	7.301E-01	7.968E-03
1.500	1.658E 00	2.629E-02	1.684E 00	7.895E-01	8.448E-03
1.600	1.662E 00	2.786E-02	1.690E 00	8.488E-01	8.923E-03
1.700	1.666E 00	2.937E-02	1.696E 00	9.079E-01	9.392E-03
1.800	1.671E 00	3.096E-02	1.702E 00	9.668E-01	9.857E-03
1.900	1.676E 00	3.256E-02	1.709E 00	1.025E 00	1.032E-02
2.000	1.682E 00	3.417E-02	1.716E 00	1.084E 00	1.078E-02
2.200	1.693E 00	3.744E-02	1.730E 00	1.200E 00	1.169E-02
2.400	1.704E 00	4.076E-02	1.745E 00	1.315E 00	1.259E-02
2.600	1.715E 00	4.412E-02	1.760E 00	1.429E 00	1.348E-02
2.800	1.727E 00	4.739E-02	1.774E 00	1.542E 00	1.437E-02
3.000	1.738E 00	5.085E-02	1.788E 00	1.655E 00	1.525E-02
3.500	1.764E 00	5.972E-02	1.823E 00	1.931E 00	1.744E-02
4.000	1.788E 00	6.890E-02	1.857E 00	2.203E 00	1.963E-02
4.500	1.810E 00	7.844E-02	1.889E 00	2.470E 00	2.181E-02
5.000	1.831E 00	8.814E-02	1.919E 00	2.733E 00	2.401E-02
5.500	1.850E 00	9.803E-02	1.948E 00	2.991E 00	2.620E-02
6.000	1.868E 00	1.081E-01	1.976E 00	3.246E 00	2.839E-02
6.500	1.884E 00	1.183E-01	2.003E 00	3.498E 00	3.058E-02
7.000	1.900E 00	1.286E-01	2.029E 00	3.746E 00	3.277E-02
7.500	1.915E 00	1.391E-01	2.054E 00	3.991E 00	3.496E-02
8.000	1.929E 00	1.498E-01	2.078E 00	4.233E 00	3.714E-02
8.500	1.942E 00	1.605E-01	2.102E 00	4.472E 00	3.932E-02
9.000	1.954E 00	1.724E-01	2.127E 00	4.708E 00	4.151E-02
9.500	1.966E 00	1.834E-01	2.149E 00	4.942E 00	4.370E-02
10.000	1.977E 00	1.945E-01	2.172E 00	5.174E 00	4.589E-02
20.000	2.133E 00	4.308E-01	2.564E 00	9.395E 00	8.781E-02
30.000	2.225E 00	6.817E-01	2.907E 00	1.305E 01	1.260E-01
40.000	2.288E 00	9.395E-01	3.227E 00	1.631E 01	1.603E-01
50.000	2.324E 00	1.202E 00	3.526E 00	1.928E 01	1.916E-01
60.000	2.352E 00	1.468E 00	3.820E 00	2.200E 01	2.201E-01
80.000	2.394E 00	2.005E 00	4.400E 00	2.687E 01	2.705E-01
100.000	2.425E 00	2.549E 00	4.974E 00	3.115E 01	3.134E-01
200.000	2.512E 00	5.311E 00	7.823E 00	4.703E 01	4.604E-01
300.000	2.557E 00	8.105E 00	1.066E 01	5.794E 01	5.481E-01
400.000	2.587E 00	1.091E 01	1.350E 01	6.626E 01	6.076E-01
500.000	2.609E 00	1.372E 01	1.633E 01	7.298E 01	6.511E-01
600.000	2.626E 00	1.654E 01	1.917E 01	7.863E 01	6.846E-01
800.000	2.652E 00	2.219E 01	2.484E 01	8.777E 01	7.333E-01
1000.000	2.672E 00	2.784E 01	3.051E 01	9.502E 01	7.673E-01

ELECTRONS IN NEON

ENERGY	STOPPING POWER			RANGE	RADIATION YIELD
	COLLISION	RADIATION	TOTAL		
MEV	MEV CM2/G	MEV CM2/G	MEV CM2/G	G/CM2	
0.010	1.791E 01	6.784E-03	1.792E 01	3.226E-04	2.190E-04
0.015	1.319E 01	6.661E-03	1.320E 01	6.523E-04	2.936E-04
0.020	1.061E 01	6.571E-03	1.062E 01	1.078E-03	3.608E-04
0.025	8.974E 00	6.506E-03	8.981E 00	1.592E-03	4.231E-04
0.030	7.832E 00	6.457E-03	7.838E 00	2.190E-03	4.817E-04
0.035	6.988E 00	6.408E-03	6.994E 00	2.866E-03	5.372E-04
0.040	6.337E 00	6.400E-03	6.344E 00	3.618E-03	5.904E-04
0.045	5.820E 00	6.409E-03	5.826E 00	4.442E-03	6.419E-04
0.050	5.397E 00	6.430E-03	5.404E 00	5.334E-03	6.923E-04
0.055	5.046E 00	6.461E-03	5.053E 00	6.291E-03	7.415E-04
0.060	4.749E 00	6.499E-03	4.756E 00	7.312E-03	7.900E-04
0.065	4.495E 00	6.542E-03	4.502E 00	8.393E-03	8.377E-04
0.070	4.275E 00	6.590E-03	4.281E 00	9.533E-03	8.847E-04
0.075	4.082E 00	6.643E-03	4.088E 00	1.073E-02	9.312E-04
0.080	3.911E 00	6.698E-03	3.918E 00	1.198E-02	9.772E-04
0.085	3.760E 00	6.753E-03	3.767E 00	1.328E-02	1.023E-03
0.090	3.624E 00	6.814E-03	3.631E 00	1.463E-02	1.068E-03
0.095	3.502E 00	6.876E-03	3.509E 00	1.603E-02	1.113E-03
0.100	3.392E 00	6.941E-03	3.399E 00	1.748E-02	1.157E-03
0.150	2.680E 00	7.653E-03	2.688E 00	3.424E-02	1.587E-03
0.200	2.318E 00	8.409E-03	2.327E 00	5.436E-02	1.999E-03
0.250	2.103E 00	9.238E-03	2.112E 00	7.699E-02	2.398E-03
0.300	1.962E 00	1.010E-02	1.972E 00	1.015E-01	2.790E-03
0.350	1.864E 00	1.102E-02	1.875E 00	1.276E-01	3.177E-03
0.400	1.794E 00	1.191E-02	1.806E 00	1.548E-01	3.560E-03
0.450	1.742E 00	1.281E-02	1.755E 00	1.829E-01	3.936E-03
0.500	1.702E 00	1.371E-02	1.716E 00	2.117E-01	4.307E-03
0.550	1.672E 00	1.461E-02	1.686E 00	2.411E-01	4.673E-03
0.600	1.648E 00	1.551E-02	1.664E 00	2.710E-01	5.033E-03
0.650	1.630E 00	1.641E-02	1.646E 00	3.012E-01	5.387E-03
0.700	1.615E 00	1.732E-02	1.633E 00	3.317E-01	5.738E-03
0.750	1.604E 00	1.822E-02	1.622E 00	3.624E-01	6.083E-03
0.800	1.595E 00	1.914E-02	1.614E 00	3.933E-01	6.425E-03
0.850	1.588E 00	2.011E-02	1.608E 00	4.244E-01	6.764E-03
0.900	1.583E 00	2.102E-02	1.604E 00	4.555E-01	7.100E-03
0.950	1.579E 00	2.194E-02	1.601E 00	4.867E-01	7.432E-03
1.000	1.576E 00	2.286E-02	1.599E 00	5.179E-01	7.760E-03
1.100	1.573E 00	2.470E-02	1.598E 00	5.805E-01	8.408E-03
1.200	1.572E 00	2.655E-02	1.599E 00	6.431E-01	9.043E-03
1.300	1.574E 00	2.840E-02	1.602E 00	7.056E-01	9.668E-03

ELECTRONS IN NEON

ENERGY	STOPPING POWER			RANGE	RADIATION YIELD
	COLLISION	RADIATION	TOTAL		
MEV	MEV CM2/G	MEV CM2/G	MEV CM2/G	G/CM2	
1.400	1.576E 00	3.026E-02	1.607E 00	7.679E-01	1.028E-02
1.500	1.580E 00	3.213E-02	1.612E 00	8.301E-01	1.089E-02
1.600	1.584E 00	3.400E-02	1.618E 00	8.920E-01	1.149E-02
1.700	1.589E 00	3.579E-02	1.625E 00	9.536E-01	1.208E-02
1.800	1.594E 00	3.769E-02	1.632E 00	1.015E 00	1.266E-02
1.900	1.599E 00	3.960E-02	1.639E 00	1.076E 00	1.324E-02
2.000	1.605E 00	4.153E-02	1.647E 00	1.137E 00	1.381E-02
2.200	1.616E 00	4.544E-02	1.662E 00	1.258E 00	1.494E-02
2.400	1.628E 00	4.940E-02	1.677E 00	1.378E 00	1.607E-02
2.600	1.639E 00	5.343E-02	1.693E 00	1.496E 00	1.718E-02
2.800	1.651E 00	5.726E-02	1.708E 00	1.614E 00	1.828E-02
3.000	1.662E 00	6.139E-02	1.723E 00	1.731E 00	1.936E-02
3.500	1.688E 00	7.203E-02	1.760E 00	2.018E 00	2.207E-02
4.000	1.712E 00	8.308E-02	1.795E 00	2.299E 00	2.476E-02
4.500	1.734E 00	9.464E-02	1.829E 00	2.575E 00	2.745E-02
5.000	1.755E 00	1.064E-01	1.861E 00	2.846E 00	3.015E-02
5.500	1.774E 00	1.183E-01	1.892E 00	3.112E 00	3.285E-02
6.000	1.792E 00	1.304E-01	1.922E 00	3.375E 00	3.554E-02
6.500	1.808E 00	1.427E-01	1.951E 00	3.633E 00	3.823E-02
7.000	1.824E 00	1.552E-01	1.979E 00	3.887E 00	4.092E-02
7.500	1.838E 00	1.678E-01	2.006E 00	4.138E 00	4.359E-02
8.000	1.852E 00	1.806E-01	2.033E 00	4.386E 00	4.626E-02
8.500	1.865E 00	1.935E-01	2.059E 00	4.630E 00	4.892E-02
9.000	1.877E 00	2.074E-01	2.085E 00	4.871E 00	5.157E-02
9.500	1.889E 00	2.206E-01	2.110E 00	5.110E 00	5.423E-02
10.000	1.900E 00	2.339E-01	2.134E 00	5.345E 00	5.687E-02
20.000	2.055E 00	5.167E-01	2.571E 00	9.597E 00	1.068E-01
30.000	2.146E 00	8.167E-01	2.963E 00	1.321E 01	1.510E-01
40.000	2.211E 00	1.125E 00	3.336E 00	1.639E 01	1.901E-01
50.000	2.262E 00	1.439E 00	3.701E 00	1.924E 01	2.248E-01
60.000	2.304E 00	1.756E 00	4.060E 00	2.182E 01	2.559E-01
80.000	2.364E 00	2.399E 00	4.762E 00	2.636E 01	3.093E-01
100.000	2.401E 00	3.047E 00	5.448E 00	3.028E 01	3.540E-01
200.000	2.504E 00	6.341E 00	8.845E 00	4.454E 01	5.019E-01
300.000	2.555E 00	9.672E 00	1.223E 01	5.411E 01	5.872E-01
400.000	2.588E 00	1.302E 01	1.560E 01	6.133E 01	6.439E-01
500.000	2.612E 00	1.637E 01	1.898E 01	6.714E 01	6.850E-01
600.000	2.631E 00	1.973E 01	2.236E 01	7.198E 01	7.163E-01
800.000	2.658E 00	2.645E 01	2.911E 01	7.980E 01	7.614E-01
1000.000	2.679E 00	3.318E 01	3.586E 01	8.598E 01	7.926E-01

ELECTRONS IN MAGNESIUM

ENERGY	STOPPING POWER			RANGE	RADIATION YIELD
	COLLISION	RADIATION	TOTAL		
MEV	MEV CM2/G	MEV CM2/G	MEV CM2/G	G/CM2	
0.010	1.714E 01	8.125E-03	1.715E 01	3.395E-04	2.744E-04
0.015	1.267E 01	8.001E-03	1.268E 01	6.833E-04	3.676E-04
0.020	1.021E 01	7.895E-03	1.022E 01	1.126E-03	4.514E-04
0.025	8.646E 00	7.831E-03	8.654E 00	1.660E-03	5.290E-04
0.030	7.554E 00	7.788E-03	7.562E 00	2.280E-03	6.022E-04
0.035	6.746E 00	7.747E-03	6.753E 00	2.981E-03	6.717E-04
0.040	6.122E 00	7.752E-03	6.130E 00	3.759E-03	7.385E-04
0.045	5.625E 00	7.777E-03	5.633E 00	4.611E-03	8.034E-04
0.050	5.220E 00	7.815E-03	5.227E 00	5.533E-03	8.668E-04
0.055	4.882E 00	7.863E-03	4.890E 00	6.523E-03	9.291E-04
0.060	4.597E 00	7.918E-03	4.605E 00	7.577E-03	9.903E-04
0.065	4.352E 00	7.980E-03	4.360E 00	8.694E-03	1.051E-03
0.070	4.140E 00	8.047E-03	4.148E 00	9.870E-03	1.110E-03
0.075	3.954E 00	8.117E-03	3.962E 00	1.110E-02	1.169E-03
0.080	3.790E 00	8.192E-03	3.799E 00	1.239E-02	1.228E-03
0.085	3.645E 00	8.277E-03	3.653E 00	1.374E-02	1.285E-03
0.090	3.514E 00	8.356E-03	3.522E 00	1.513E-02	1.343E-03
0.095	3.396E 00	8.437E-03	3.405E 00	1.657E-02	1.400E-03
0.100	3.290E 00	8.520E-03	3.298E 00	1.807E-02	1.456E-03
0.150	2.603E 00	9.405E-03	2.612E 00	3.532E-02	2.003E-03
0.200	2.254E 00	1.031E-02	2.264E 00	5.600E-02	2.523E-03
0.250	2.046E 00	1.132E-02	2.057E 00	7.925E-02	3.024E-03
0.300	1.910E 00	1.237E-02	1.922E 00	1.044E-01	3.515E-03
0.350	1.809E 00	1.348E-02	1.822E 00	1.312E-01	4.003E-03
0.400	1.742E 00	1.457E-02	1.757E 00	1.592E-01	4.484E-03
0.450	1.693E 00	1.567E-02	1.709E 00	1.881E-01	4.955E-03
0.500	1.655E 00	1.675E-02	1.672E 00	2.177E-01	5.420E-03
0.550	1.626E 00	1.784E-02	1.643E 00	2.479E-01	5.876E-03
0.600	1.602E 00	1.892E-02	1.621E 00	2.785E-01	6.325E-03
0.650	1.584E 00	2.000E-02	1.604E 00	3.095E-01	6.767E-03
0.700	1.569E 00	2.108E-02	1.591E 00	3.408E-01	7.202E-03
0.750	1.558E 00	2.217E-02	1.580E 00	3.724E-01	7.632E-03
0.800	1.548E 00	2.325E-02	1.572E 00	4.041E-01	8.055E-03
0.850	1.541E 00	2.440E-02	1.565E 00	4.360E-01	8.476E-03
0.900	1.535E 00	2.549E-02	1.560E 00	4.680E-01	8.892E-03
0.950	1.530E 00	2.657E-02	1.557E 00	5.001E-01	9.303E-03
1.000	1.526E 00	2.766E-02	1.554E 00	5.322E-01	9.710E-03
1.100	1.521E 00	2.982E-02	1.551E 00	5.966E-01	1.051E-02
1.200	1.519E 00	3.199E-02	1.551E 00	6.611E-01	1.129E-02
1.300	1.518E 00	3.416E-02	1.552E 00	7.256E-01	1.207E-02

ELECTRONS IN MAGNESIUM

ENERGY	STOPPING POWER			RANGE	RADIATION YIELD
	COLLISION	RADIATION	TOTAL		
MEV	MEV CM2/G	MEV CM2/G	MEV CM2/G	G/CM2	
1.400	1.518E 00	3.634E-02	1.555E 00	7.899E-01	1.282E-02
1.500	1.520E 00	3.851E-02	1.558E 00	8.542E-01	1.357E-02
1.600	1.522E 00	4.068E-02	1.562E 00	9.183E-01	1.431E-02
1.700	1.524E 00	4.272E-02	1.567E 00	9.822E-01	1.503E-02
1.800	1.527E 00	4.491E-02	1.572E 00	1.046E 00	1.575E-02
1.900	1.530E 00	4.713E-02	1.577E 00	1.109E 00	1.646E-02
2.000	1.534E 00	4.937E-02	1.583E 00	1.173E 00	1.716E-02
2.200	1.540E 00	5.390E-02	1.594E 00	1.299E 00	1.856E-02
2.400	1.547E 00	5.851E-02	1.606E 00	1.424E 00	1.994E-02
2.600	1.555E 00	6.318E-02	1.618E 00	1.548E 00	2.131E-02
2.800	1.562E 00	6.764E-02	1.629E 00	1.671E 00	2.267E-02
3.000	1.568E 00	7.243E-02	1.641E 00	1.793E 00	2.401E-02
3.500	1.585E 00	8.481E-02	1.669E 00	2.095E 00	2.736E-02
4.000	1.599E 00	9.769E-02	1.697E 00	2.392E 00	3.071E-02
4.500	1.613E 00	1.112E-01	1.724E 00	2.685E 00	3.408E-02
5.000	1.625E 00	1.249E-01	1.750E 00	2.972E 00	3.746E-02
5.500	1.636E 00	1.388E-01	1.775E 00	3.256E 00	4.085E-02
6.000	1.646E 00	1.529E-01	1.799E 00	3.536E 00	4.425E-02
6.500	1.656E 00	1.672E-01	1.823E 00	3.812E 00	4.764E-02
7.000	1.665E 00	1.818E-01	1.846E 00	4.084E 00	5.103E-02
7.500	1.673E 00	1.965E-01	1.869E 00	4.354E 00	5.442E-02
8.000	1.680E 00	2.114E-01	1.891E 00	4.620E 00	5.779E-02
8.500	1.687E 00	2.264E-01	1.914E 00	4.882E 00	6.116E-02
9.000	1.694E 00	2.426E-01	1.936E 00	5.142E 00	6.453E-02
9.500	1.700E 00	2.580E-01	1.958E 00	5.399E 00	6.789E-02
10.000	1.706E 00	2.734E-01	1.979E 00	5.653E 00	7.125E-02
20.000	1.781E 00	6.029E-01	2.383E 00	1.025E 01	1.344E-01
30.000	1.820E 00	9.524E-01	2.773E 00	1.413E 01	1.896E-01
40.000	1.847E 00	1.311E 00	3.158E 00	1.751E 01	2.374E-01
50.000	1.867E 00	1.676E 00	3.543E 00	2.050E 01	2.789E-01
60.000	1.883E 00	2.046E 00	3.928E 00	2.318E 01	3.154E-01
80.000	1.907E 00	2.793E 00	4.700E 00	2.782E 01	3.764E-01
100.000	1.925E 00	3.546E 00	5.471E 00	3.177E 01	4.256E-01
200.000	1.980E 00	7.374E 00	9.353E 00	4.558E 01	5.779E-01
300.000	2.011E 00	1.124E 01	1.325E 01	5.452E 01	6.591E-01
400.000	2.033E 00	1.512E 01	1.716E 01	6.113E 01	7.109E-01
500.000	2.050E 00	1.902E 01	2.107E 01	6.638E 01	7.473E-01
600.000	2.063E 00	2.292E 01	2.498E 01	7.074E 01	7.745E-01
800.000	2.085E 00	3.072E 01	3.281E 01	7.770E 01	8.128E-01
1000.000	2.102E 00	3.853E 01	4.063E 01	8.317E 01	8.388E-01

ELECTRONS IN ALUMINUM

ENERGY	STOPPING POWER			RANGE	RADIATION YIELD
	COLLISION	RADIATION	TOTAL		
MEV	MEV CM2/G	MEV CM2/G	MEV CM2/G	G/CM2	
0.010	1.657E 01	8.600E-03	1.658E 01	3.519E-04	3.002E-04
0.015	1.225E 01	8.482E-03	1.226E 01	7.074E-04	4.025E-04
0.020	9.885E 00	8.373E-03	9.893E 00	1.165E-03	4.944E-04
0.025	8.372E 00	8.313E-03	8.380E 00	1.716E-03	5.795E-04
0.030	7.316E 00	8.276E-03	7.325E 00	2.356E-03	6.598E-04
0.035	6.535E 00	8.241E-03	6.543E 00	3.080E-03	7.362E-04
0.040	5.932E 00	8.252E-03	5.940E 00	3.883E-03	8.098E-04
0.045	5.451E 00	8.285E-03	5.459E 00	4.762E-03	8.813E-04
0.050	5.059E 00	8.329E-03	5.067E 00	5.714E-03	9.512E-04
0.055	4.733E 00	8.384E-03	4.741E 00	6.735E-03	1.020E-03
0.060	4.456E 00	8.446E-03	4.465E 00	7.822E-03	1.087E-03
0.065	4.220E 00	8.515E-03	4.228E 00	8.974E-03	1.154E-03
0.070	4.014E 00	8.588E-03	4.023E 00	1.019E-02	1.220E-03
0.075	3.834E 00	8.666E-03	3.843E 00	1.146E-02	1.285E-03
0.080	3.676E 00	8.746E-03	3.684E 00	1.279E-02	1.349E-03
0.085	3.534E 00	8.843E-03	3.543E 00	1.417E-02	1.413E-03
0.090	3.408E 00	8.928E-03	3.417E 00	1.561E-02	1.476E-03
0.095	3.294E 00	9.016E-03	3.303E 00	1.710E-02	1.539E-03
0.100	3.191E 00	9.105E-03	3.200E 00	1.864E-02	1.602E-03
0.150	2.526E 00	1.005E-02	2.536E 00	3.641E-02	2.204E-03
0.200	2.188E 00	1.100E-02	2.199E 00	5.772E-02	2.775E-03
0.250	1.986E 00	1.206E-02	1.998E 00	8.165E-02	3.324E-03
0.300	1.848E 00	1.317E-02	1.861E 00	1.077E-01	3.864E-03
0.350	1.757E 00	1.434E-02	1.771E 00	1.353E-01	4.397E-03
0.400	1.691E 00	1.549E-02	1.706E 00	1.640E-01	4.921E-03
0.450	1.641E 00	1.666E-02	1.658E 00	1.938E-01	5.437E-03
0.500	1.603E 00	1.782E-02	1.621E 00	2.243E-01	5.946E-03
0.550	1.574E 00	1.897E-02	1.593E 00	2.554E-01	6.446E-03
0.600	1.551E 00	2.011E-02	1.571E 00	2.871E-01	6.939E-03
0.650	1.532E 00	2.126E-02	1.553E 00	3.191E-01	7.424E-03
0.700	1.517E 00	2.240E-02	1.540E 00	3.514E-01	7.902E-03
0.750	1.505E 00	2.354E-02	1.529E 00	3.840E-01	8.374E-03
0.800	1.496E 00	2.469E-02	1.521E 00	4.168E-01	8.839E-03
0.850	1.488E 00	2.590E-02	1.514E 00	4.498E-01	9.301E-03
0.900	1.482E 00	2.704E-02	1.509E 00	4.828E-01	9.757E-03
0.950	1.477E 00	2.819E-02	1.505E 00	5.160E-01	1.021E-02
1.000	1.473E 00	2.933E-02	1.502E 00	5.493E-01	1.065E-02
1.100	1.468E 00	3.161E-02	1.499E 00	6.159E-01	1.153E-02
1.200	1.465E 00	3.388E-02	1.498E 00	6.826E-01	1.239E-02
1.300	1.463E 00	3.616E-02	1.499E 00	7.493E-01	1.324E-02

ELECTRONS IN ALUMINUM

ENERGY	STOPPING POWER			RANGE	RADIATION YIELD
	COLLISION	RADIATION	TOTAL		
MEV	MEV CM2/G	MEV CM2/G	MEV CM2/G	G/CM2	
1.400	1.463E 00	3.843E-02	1.502E 00	8.160E-01	1.407E-02
1.500	1.464E 00	4.071E-02	1.505E 00	8.825E-01	1.488E-02
1.600	1.466E 00	4.298E-02	1.509E 00	9.489E-01	1.569E-02
1.700	1.468E 00	4.509E-02	1.513E 00	1.015E 00	1.648E-02
1.800	1.470E 00	4.738E-02	1.518E 00	1.081E 00	1.726E-02
1.900	1.473E 00	4.970E-02	1.523E 00	1.147E 00	1.803E-02
2.000	1.476E 00	5.204E-02	1.528E 00	1.212E 00	1.879E-02
2.200	1.482E 00	5.677E-02	1.539E 00	1.343E 00	2.031E-02
2.400	1.489E 00	6.158E-02	1.550E 00	1.472E 00	2.181E-02
2.600	1.495E 00	6.647E-02	1.562E 00	1.601E 00	2.330E-02
2.800	1.502E 00	7.111E-02	1.573E 00	1.728E 00	2.477E-02
3.000	1.508E 00	7.612E-02	1.584E 00	1.855E 00	2.623E-02
3.500	1.523E 00	8.907E-02	1.612E 00	2.168E 00	2.986E-02
4.000	1.537E 00	1.025E-01	1.639E 00	2.476E 00	3.349E-02
4.500	1.549E 00	1.167E-01	1.666E 00	2.778E 00	3.713E-02
5.000	1.561E 00	1.310E-01	1.692E 00	3.076E 00	4.079E-02
5.500	1.571E 00	1.456E-01	1.717E 00	3.369E 00	4.446E-02
6.000	1.581E 00	1.604E-01	1.741E 00	3.658E 00	4.813E-02
6.500	1.590E 00	1.755E-01	1.765E 00	3.944E 00	5.179E-02
7.000	1.598E 00	1.907E-01	1.789E 00	4.225E 00	5.545E-02
7.500	1.606E 00	2.061E-01	1.812E 00	4.503E 00	5.910E-02
8.000	1.613E 00	2.217E-01	1.835E 00	4.777E 00	6.273E-02
8.500	1.620E 00	2.375E-01	1.857E 00	5.048E 00	6.636E-02
9.000	1.626E 00	2.545E-01	1.880E 00	5.315E 00	6.998E-02
9.500	1.632E 00	2.706E-01	1.902E 00	5.580E 00	7.360E-02
10.000	1.637E 00	2.869E-01	1.924E 00	5.841E 00	7.721E-02
20.000	1.709E 00	6.317E-01	2.341E 00	1.054E 01	1.445E-01
30.000	1.747E 00	9.973E-01	2.745E 00	1.448E 01	2.026E-01
40.000	1.773E 00	1.373E 00	3.146E 00	1.788E 01	2.522E-01
50.000	1.792E 00	1.755E 00	3.547E 00	2.087E 01	2.951E-01
60.000	1.808E 00	2.141E 00	3.949E 00	2.355E 01	3.325E-01
80.000	1.831E 00	2.923E 00	4.754E 00	2.816E 01	3.945E-01
100.000	1.849E 00	3.710E 00	5.559E 00	3.204E 01	4.441E-01
200.000	1.902E 00	7.712E 00	9.614E 00	4.555E 01	5.953E-01
300.000	1.933E 00	1.176E 01	1.369E 01	5.423E 01	6.747E-01
400.000	1.954E 00	1.581E 01	1.777E 01	6.062E 01	7.250E-01
500.000	1.971E 00	1.988E 01	2.185E 01	6.569E 01	7.601E-01
600.000	1.984E 00	2.396E 01	2.594E 01	6.988E 01	7.863E-01
800.000	2.005E 00	3.212E 01	3.412E 01	7.658E 01	8.230E-01
1000.000	2.022E 00	4.028E 01	4.230E 01	8.184E 01	8.478E-01

ELECTRONS IN ARGON

ENERGY	STOPPING POWER			RANGE	RADIATION YIELD
	COLLISION	RADIATION	TOTAL		
MEV	MEV CM2/G	MEV CM2/G	MEV CM2/G	G/CM2	
0.010	1.457E 01	1.112E-02	1.458E 01	4.050E-04	4.425E-04
0.015	1.084E 01	1.104E-02	1.085E 01	8.078E-04	5.924E-04
0.020	8.770E 00	1.091E-02	8.781E 00	1.324E-03	7.273E-04
0.025	7.445E 00	1.090E-02	7.456E 00	1.944E-03	8.524E-04
0.030	6.517E 00	1.093E-02	6.528E 00	2.663E-03	9.718E-04
0.035	5.829E 00	1.100E-02	5.840E 00	3.474E-03	1.087E-03
0.040	5.297E 00	1.107E-02	5.308E 00	4.374E-03	1.199E-03
0.045	4.872E 00	1.116E-02	4.884E 00	5.357E-03	1.309E-03
0.050	4.525E 00	1.125E-02	4.537E 00	6.420E-03	1.416E-03
0.055	4.236E 00	1.135E-02	4.248E 00	7.560E-03	1.522E-03
0.060	3.992E 00	1.145E-02	4.003E 00	8.773E-03	1.626E-03
0.065	3.782E 00	1.156E-02	3.793E 00	1.006E-02	1.728E-03
0.070	3.599E 00	1.167E-02	3.611E 00	1.141E-02	1.829E-03
0.075	3.440E 00	1.178E-02	3.451E 00	1.283E-02	1.928E-03
0.080	3.299E 00	1.189E-02	3.311E 00	1.431E-02	2.027E-03
0.085	3.173E 00	1.199E-02	3.185E 00	1.585E-02	2.124E-03
0.090	3.061E 00	1.211E-02	3.073E 00	1.744E-02	2.220E-03
0.095	2.959E 00	1.222E-02	2.972E 00	1.910E-02	2.315E-03
0.100	2.868E 00	1.234E-02	2.880E 00	2.081E-02	2.409E-03
0.150	2.275E 00	1.357E-02	2.289E 00	4.053E-02	3.312E-03
0.200	1.973E 00	1.477E-02	1.988E 00	6.411E-02	4.157E-03
0.250	1.793E 00	1.615E-02	1.810E 00	9.056E-02	4.962E-03
0.300	1.676E 00	1.759E-02	1.694E 00	1.192E-01	5.744E-03
0.350	1.595E 00	1.913E-02	1.614E 00	1.495E-01	6.513E-03
0.400	1.536E 00	2.062E-02	1.557E 00	1.810E-01	7.268E-03
0.450	1.493E 00	2.212E-02	1.515E 00	2.136E-01	8.007E-03
0.500	1.461E 00	2.361E-02	1.484E 00	2.470E-01	8.732E-03
0.550	1.436E 00	2.509E-02	1.461E 00	2.809E-01	9.442E-03
0.600	1.416E 00	2.656E-02	1.443E 00	3.154E-01	1.014E-02
0.650	1.401E 00	2.802E-02	1.429E 00	3.502E-01	1.082E-02
0.700	1.390E 00	2.948E-02	1.419E 00	3.853E-01	1.149E-02
0.750	1.381E 00	3.094E-02	1.412E 00	4.207E-01	1.215E-02
0.800	1.374E 00	3.240E-02	1.406E 00	4.562E-01	1.279E-02
0.850	1.368E 00	3.394E-02	1.402E 00	4.918E-01	1.343E-02
0.900	1.364E 00	3.539E-02	1.400E 00	5.275E-01	1.406E-02
0.950	1.362E 00	3.684E-02	1.398E 00	5.632E-01	1.468E-02
1.000	1.360E 00	3.829E-02	1.398E 00	5.990E-01	1.529E-02
1.100	1.358E 00	4.117E-02	1.399E 00	6.705E-01	1.648E-02
1.200	1.358E 00	4.404E-02	1.402E 00	7.419E-01	1.764E-02
1.300	1.360E 00	4.691E-02	1.407E 00	8.130E-01	1.878E-02

ELECTRONS IN ARGON

ENERGY	STOPPING POWER			RANGE	RADIATION YIELD
	COLLISION	RADIATION	TOTAL		
MEV	MEV CM2/G	MEV CM2/G	MEV CM2/G	G/CM2	
1.400	1.363E 00	4.977E-02	1.413E 00	8.840E-01	1.988E-02
1.500	1.367E 00	5.262E-02	1.420E 00	9.546E-01	2.097E-02
1.600	1.371E 00	5.547E-02	1.427E 00	1.025E 00	2.203E-02
1.700	1.376E 00	5.808E-02	1.434E 00	1.095E 00	2.306E-02
1.800	1.381E 00	6.094E-02	1.442E 00	1.164E 00	2.408E-02
1.900	1.386E 00	6.384E-02	1.450E 00	1.233E 00	2.508E-02
2.000	1.392E 00	6.676E-02	1.458E 00	1.302E 00	2.608E-02
2.200	1.402E 00	7.267E-02	1.475E 00	1.439E 00	2.803E-02
2.400	1.413E 00	7.867E-02	1.492E 00	1.573E 00	2.994E-02
2.600	1.424E 00	8.476E-02	1.509E 00	1.707E 00	3.183E-02
2.800	1.434E 00	9.054E-02	1.525E 00	1.838E 00	3.369E-02
3.000	1.445E 00	9.679E-02	1.541E 00	1.969E 00	3.551E-02
3.500	1.469E 00	1.129E-01	1.582E 00	2.289E 00	4.002E-02
4.000	1.491E 00	1.297E-01	1.621E 00	2.601E 00	4.448E-02
4.500	1.511E 00	1.472E-01	1.659E 00	2.906E 00	4.891E-02
5.000	1.530E 00	1.650E-01	1.695E 00	3.205E 00	5.332E-02
5.500	1.548E 00	1.831E-01	1.731E 00	3.496E 00	5.771E-02
6.000	1.564E 00	2.016E-01	1.765E 00	3.783E 00	6.207E-02
6.500	1.579E 00	2.203E-01	1.799E 00	4.063E 00	6.640E-02
7.000	1.593E 00	2.393E-01	1.832E 00	4.338E 00	7.069E-02
7.500	1.606E 00	2.585E-01	1.865E 00	4.609E 00	7.495E-02
8.000	1.619E 00	2.779E-01	1.897E 00	4.875E 00	7.918E-02
8.500	1.631E 00	2.976E-01	1.928E 00	5.136E 00	8.337E-02
9.000	1.642E 00	3.204E-01	1.962E 00	5.393E 00	8.755E-02
9.500	1.653E 00	3.405E-01	1.993E 00	5.646E 00	9.174E-02
10.000	1.663E 00	3.609E-01	2.024E 00	5.895E 00	9.588E-02
20.000	1.803E 00	7.888E-01	2.592E 00	1.024E 01	1.703E-01
30.000	1.887E 00	1.242E 00	3.128E 00	1.375E 01	2.311E-01
40.000	1.946E 00	1.708E 00	3.654E 00	1.670E 01	2.818E-01
50.000	1.992E 00	2.182E 00	4.174E 00	1.926E 01	3.247E-01
60.000	2.026E 00	2.661E 00	4.687E 00	2.152E 01	3.615E-01
80.000	2.077E 00	3.630E 00	5.707E 00	2.538E 01	4.221E-01
100.000	2.114E 00	4.606E 00	6.720E 00	2.860E 01	4.701E-01
200.000	2.215E 00	9.559E 00	1.177E 01	3.970E 01	6.148E-01
300.000	2.265E 00	1.456E 01	1.683E 01	4.677E 01	6.904E-01
400.000	2.298E 00	1.958E 01	2.188E 01	5.196E 01	7.382E-01
500.000	2.321E 00	2.460E 01	2.692E 01	5.608E 01	7.715E-01
600.000	2.340E 00	2.964E 01	3.198E 01	5.948E 01	7.964E-01
800.000	2.367E 00	3.972E 01	4.208E 01	6.491E 01	8.313E-01
1000.000	2.388E 00	4.980E 01	5.219E 01	6.917E 01	8.549E-01

ELECTRONS IN IRON

ENERGY	STOPPING POWER			RANGE	RADIATION YIELD
	COLLISION	RADIATION	TOTAL		
MEV	MEV CM2/G	MEV CM2/G	MEV CM2/G	G/CM2	
0.010	1.407E 01	1.645E-02	1.408E 01	4.259E-04	6.843E-04
0.015	1.053E 01	1.642E-02	1.054E 01	8.415E-04	9.116E-04
0.020	8.553E 00	1.630E-02	8.569E 00	1.371E-03	1.117E-03
0.025	7.279E 00	1.638E-02	7.296E 00	2.006E-03	1.308E-03
0.030	6.385E 00	1.652E-02	6.401E 00	2.740E-03	1.493E-03
0.035	5.719E 00	1.673E-02	5.736E 00	3.566E-03	1.672E-03
0.040	5.204E 00	1.691E-02	5.221E 00	4.481E-03	1.848E-03
0.045	4.792E 00	1.710E-02	4.809E 00	5.480E-03	2.020E-03
0.050	4.455E 00	1.729E-02	4.472E 00	6.560E-03	2.189E-03
0.055	4.174E 00	1.747E-02	4.191E 00	7.715E-03	2.355E-03
0.060	3.935E 00	1.766E-02	3.953E 00	8.945E-03	2.519E-03
0.065	3.730E 00	1.784E-02	3.748E 00	1.024E-02	2.680E-03
0.070	3.553E 00	1.802E-02	3.571E 00	1.161E-02	2.839E-03
0.075	3.397E 00	1.820E-02	3.415E 00	1.304E-02	2.996E-03
0.080	3.259E 00	1.839E-02	3.278E 00	1.454E-02	3.150E-03
0.085	3.136E 00	1.852E-02	3.155E 00	1.609E-02	3.302E-03
0.090	3.027E 00	1.870E-02	3.045E 00	1.771E-02	3.452E-03
0.095	2.927E 00	1.888E-02	2.946E 00	1.938E-02	3.601E-03
0.100	2.838E 00	1.907E-02	2.857E 00	2.110E-02	3.748E-03
0.150	2.257E 00	2.094E-02	2.278E 00	4.095E-02	5.149E-03
0.200	1.961E 00	2.270E-02	1.984E 00	6.461E-02	6.446E-03
0.250	1.783E 00	2.474E-02	1.808E 00	9.110E-02	7.670E-03
0.300	1.667E 00	2.689E-02	1.694E 00	1.197E-01	8.855E-03
0.350	1.584E 00	2.918E-02	1.613E 00	1.500E-01	1.002E-02
0.400	1.526E 00	3.139E-02	1.557E 00	1.816E-01	1.116E-02
0.450	1.482E 00	3.360E-02	1.516E 00	2.142E-01	1.227E-02
0.500	1.449E 00	3.578E-02	1.485E 00	2.475E-01	1.336E-02
0.550	1.424E 00	3.795E-02	1.461E 00	2.814E-01	1.442E-02
0.600	1.403E 00	4.011E-02	1.443E 00	3.159E-01	1.546E-02
0.650	1.387E 00	4.226E-02	1.430E 00	3.507E-01	1.647E-02
0.700	1.375E 00	4.441E-02	1.419E 00	3.858E-01	1.747E-02
0.750	1.364E 00	4.655E-02	1.411E 00	4.211E-01	1.845E-02
0.800	1.356E 00	4.868E-02	1.405E 00	4.567E-01	1.941E-02
0.850	1.350E 00	5.055E-02	1.400E 00	4.923E-01	2.034E-02
0.900	1.345E 00	5.268E-02	1.397E 00	5.281E-01	2.126E-02
0.950	1.341E 00	5.482E-02	1.395E 00	5.639E-01	2.217E-02
1.000	1.337E 00	5.696E-02	1.394E 00	5.997E-01	2.307E-02
1.100	1.333E 00	6.127E-02	1.395E 00	6.714E-01	2.482E-02
1.200	1.331E 00	6.561E-02	1.397E 00	7.431E-01	2.654E-02
1.300	1.331E 00	6.997E-02	1.401E 00	8.146E-01	2.823E-02

ELECTRONS IN IRON

ENERGY	STOPPING POWER			RANGE	RADIATION YIELD
	COLLISION	RADIATION	TOTAL		
MEV	MEV CM2/G	MEV CM2/G	MEV CM2/G	G/CM2	
1.400	1.331E 00	7.436E-02	1.406E 00	8.858E-01	2.989E-02
1.500	1.333E 00	7.876E-02	1.411E 00	9.568E-01	3.152E-02
1.600	1.335E 00	8.319E-02	1.418E 00	1.028E 00	3.312E-02
1.700	1.337E 00	8.748E-02	1.425E 00	1.098E 00	3.471E-02
1.800	1.340E 00	9.197E-02	1.432E 00	1.168E 00	3.627E-02
1.900	1.343E 00	9.650E-02	1.439E 00	1.238E 00	3.781E-02
2.000	1.346E 00	1.011E-01	1.447E 00	1.307E 00	3.935E-02
2.200	1.352E 00	1.103E-01	1.462E 00	1.444E 00	4.237E-02
2.400	1.359E 00	1.197E-01	1.478E 00	1.580E 00	4.536E-02
2.600	1.365E 00	1.292E-01	1.494E 00	1.715E 00	4.831E-02
2.800	1.372E 00	1.394E-01	1.511E 00	1.848E 00	5.123E-02
3.000	1.378E 00	1.492E-01	1.527E 00	1.980E 00	5.415E-02
3.500	1.393E 00	1.739E-01	1.567E 00	2.303E 00	6.132E-02
4.000	1.406E 00	1.990E-01	1.605E 00	2.618E 00	6.835E-02
4.500	1.419E 00	2.243E-01	1.643E 00	2.926E 00	7.523E-02
5.000	1.430E 00	2.500E-01	1.680E 00	3.227E 00	8.197E-02
5.500	1.440E 00	2.762E-01	1.717E 00	3.521E 00	8.860E-02
6.000	1.450E 00	3.027E-01	1.752E 00	3.810E 00	9.512E-02
6.500	1.459E 00	3.295E-01	1.788E 00	4.092E 00	1.015E-01
7.000	1.467E 00	3.566E-01	1.823E 00	4.369E 00	1.078E-01
7.500	1.474E 00	3.841E-01	1.858E 00	4.641E 00	1.141E-01
8.000	1.481E 00	4.118E-01	1.893E 00	4.907E 00	1.202E-01
8.500	1.488E 00	4.398E-01	1.927E 00	5.169E 00	1.262E-01
9.000	1.494E 00	4.706E-01	1.964E 00	5.426E 00	1.322E-01
9.500	1.499E 00	4.992E-01	1.999E 00	5.678E 00	1.381E-01
10.000	1.505E 00	5.279E-01	2.033E 00	5.926E 00	1.440E-01
20.000	1.575E 00	1.133E 00	2.708E 00	1.017E 01	2.444E-01
30.000	1.612E 00	1.776E 00	3.388E 00	1.347E 01	3.211E-01
40.000	1.637E 00	2.443E 00	4.080E 00	1.615E 01	3.817E-01
50.000	1.656E 00	3.118E 00	4.774E 00	1.842E 01	4.308E-01
60.000	1.671E 00	3.801E 00	5.472E 00	2.037E 01	4.715E-01
80.000	1.694E 00	5.180E 00	6.874E 00	2.363E 01	5.352E-01
100.000	1.711E 00	6.570F 00	8.281E 00	2.628E 01	5.830E-01
200.000	1.763E 00	1.361E 01	1.537E 01	3.500E 01	7.157E-01
300.000	1.792E 00	2.072E 01	2.251E 01	4.034E 01	7.788E-01
400.000	1.813E 00	2.785E 01	2.966E 01	4.420E 01	8.167E-01
500.000	1.829E 00	3.498E 01	3.681E 01	4.722E 01	8.424E-01
600.000	1.842E 00	4.212E 01	4.397E 01	4.970E 01	8.610E-01
800.000	1.863E 00	5.643E 01	5.829E 01	5.364E 01	8.867E-01
1000.000	1.879E 00	7.074E 01	7.262E 01	5.671E 01	9.036E-01

ELECTRONS IN COPPER

ENERGY	STOPPING POWER COLLISION	STOPPING POWER RADIATION	STOPPING POWER TOTAL	RANGE	RADIATION YIELD
MEV	MEV CM2/G	MEV CM2/G	MEV CM2/G	G/CM2	
0.010	1.328E 01	1.793E-02	1.329E 01	4.556E-04	7.967E-04
0.015	9.973E 00	1.792E-02	9.991E 00	8.949E-04	1.056E-03
0.020	8.120E 00	1.773E-02	8.137E 00	1.453E-03	1.290E-03
0.025	6.921E 00	1.790E-02	6.939E 00	2.121E-03	1.508E-03
0.030	6.078E 00	1.818E-02	6.096E 00	2.892E-03	1.720E-03
0.035	5.449E 00	1.857E-02	5.468E 00	3.760E-03	1.930E-03
0.040	4.962E 00	1.886E-02	4.981E 00	4.719E-03	2.138E-03
0.045	4.572E 00	1.914E-02	4.591E 00	5.766E-03	2.342E-03
0.050	4.252E 00	1.940E-02	4.272E 00	6.896E-03	2.544E-03
0.055	3.986E 00	1.964E-02	4.005E 00	8.106E-03	2.742E-03
0.060	3.759E 00	1.988E-02	3.779E 00	9.392E-03	2.937E-03
0.065	3.565E 00	2.011E-02	3.585E 00	1.075E-02	3.129E-03
0.070	3.396E 00	2.033E-02	3.417E 00	1.218E-02	3.318E-03
0.075	3.248E 00	2.054E-02	3.269E 00	1.368E-02	3.505E-03
0.080	3.118E 00	2.076E-02	3.138E 00	1.524E-02	3.689E-03
0.085	3.001E 00	2.084E-02	3.022E 00	1.686E-02	3.868E-03
0.090	2.896E 00	2.105E-02	2.917E 00	1.855E-02	4.046E-03
0.095	2.802E 00	2.126E-02	2.823E 00	2.029E-02	4.221E-03
0.100	2.717E 00	2.147E-02	2.738E 00	2.209E-02	4.394E-03
0.150	2.164E 00	2.359E-02	2.188E 00	4.277E-02	6.041E-03
0.200	1.882E 00	2.557E-02	1.908E 00	6.739E-02	7.560E-03
0.250	1.713E 00	2.784E-02	1.741E 00	9.492E-02	8.989E-03
0.300	1.603E 00	3.022E-02	1.634E 00	1.246E-01	1.037E-02
0.350	1.527E 00	3.275E-02	1.560E 00	1.560E-01	1.171E-02
0.400	1.473E 00	3.519E-02	1.508E 00	1.886E-01	1.302E-02
0.450	1.427E 00	3.767E-02	1.465E 00	2.222E-01	1.429E-02
0.500	1.396E 00	4.010E-02	1.436E 00	2.567E-01	1.554E-02
0.550	1.372E 00	4.251E-02	1.414E 00	2.918E-01	1.677E-02
0.600	1.353E 00	4.489E-02	1.398E 00	3.274E-01	1.796E-02
0.650	1.338E 00	4.726E-02	1.386E 00	3.633E-01	1.913E-02
0.700	1.327E 00	4.961E-02	1.376E 00	3.995E-01	2.027E-02
0.750	1.317E 00	5.195E-02	1.369E 00	4.360E-01	2.138E-02
0.800	1.310E 00	5.428E-02	1.364E 00	4.725E-01	2.247E-02
0.850	1.304E 00	5.605E-02	1.360E 00	5.093E-01	2.353E-02
0.900	1.299E 00	5.837E-02	1.358E 00	5.461E-01	2.456E-02
0.950	1.296E 00	6.070E-02	1.357E 00	5.829E-01	2.557E-02
1.000	1.293E 00	6.304E-02	1.356E 00	6.198E-01	2.658E-02
1.100	1.290E 00	6.774E-02	1.358E 00	6.935E-01	2.854E-02
1.200	1.288E 00	7.248E-02	1.361E 00	7.670E-01	3.046E-02
1.300	1.288E 00	7.725E-02	1.366E 00	8.404E-01	3.234E-02

ELECTRONS IN COPPER

ENERGY	STOPPING POWER COLLISION	STOPPING POWER RADIATION	STOPPING POWER TOTAL	RANGE	RADIATION YIELD
MEV	MEV CM2/G	MEV CM2/G	MEV CM2/G	G/CM2	
1.400	1.289E 00	8.206E-02	1.371E 00	9.135E-01	3.419E-02
1.500	1.291E 00	8.689E-02	1.378E 00	9.862E-01	3.601E-02
1.600	1.293E 00	9.176E-02	1.385E 00	1.059E 00	3.780E-02
1.700	1.296E 00	9.659E-02	1.392E 00	1.131E 00	3.956E-02
1.800	1.299E 00	1.015E-01	1.400E 00	1.202E 00	4.131E-02
1.900	1.302E 00	1.065E-01	1.408E 00	1.273E 00	4.303E-02
2.000	1.305E 00	1.115E-01	1.417E 00	1.344E 00	4.474E-02
2.200	1.312E 00	1.216E-01	1.433E 00	1.485E 00	4.810E-02
2.400	1.319E 00	1.318E-01	1.450E 00	1.623E 00	5.141E-02
2.600	1.325E 00	1.421E-01	1.467E 00	1.760E 00	5.468E-02
2.800	1.332E 00	1.529E-01	1.485E 00	1.896E 00	5.791E-02
3.000	1.338E 00	1.635E-01	1.502E 00	2.030E 00	6.111E-02
3.500	1.353E 00	1.902E-01	1.544E 00	2.358E 00	6.896E-02
4.000	1.367E 00	2.173E-01	1.584E 00	2.678E 00	7.662E-02
4.500	1.380E 00	2.446E-01	1.624E 00	2.990E 00	8.409E-02
5.000	1.391E 00	2.724E-01	1.663E 00	3.294E 00	9.141E-02
5.500	1.401E 00	3.007E-01	1.702E 00	3.591E 00	9.857E-02
6.000	1.411E 00	3.292E-01	1.740E 00	3.881E 00	1.056E-01
6.500	1.419E 00	3.582E-01	1.778E 00	4.166E 00	1.125E-01
7.000	1.428E 00	3.875E-01	1.815E 00	4.444E 00	1.193E-01
7.500	1.435E 00	4.171E-01	1.852E 00	4.717E 00	1.260E-01
8.000	1.442E 00	4.470E-01	1.889E 00	4.984E 00	1.325E-01
8.500	1.449E 00	4.771E-01	1.926E 00	5.246E 00	1.390E-01
9.000	1.455E 00	5.104E-01	1.965E 00	5.503E 00	1.454E-01
9.500	1.460E 00	5.412E-01	2.002E 00	5.755E 00	1.517E-01
10.000	1.466E 00	5.722E-01	2.038E 00	6.003E 00	1.579E-01
20.000	1.535E 00	1.224E 00	2.759E 00	1.020E 01	2.632E-01
30.000	1.573E 00	1.917E 00	3.490E 00	1.342E 01	3.421E-01
40.000	1.597E 00	2.637E 00	4.234E 00	1.602E 01	4.037E-01
50.000	1.616E 00	3.365E 00	4.981E 00	1.819E 01	4.530E-01
60.000	1.631E 00	4.101E 00	5.732E 00	2.006E 01	4.936E-01
80.000	1.653E 00	5.588E 00	7.242E 00	2.316E 01	5.566E-01
100.000	1.670E 00	7.086E 00	8.756E 00	2.567E 01	6.036E-01
200.000	1.721E 00	1.468E 01	1.640E 01	3.388E 01	7.321E-01
300.000	1.750E 00	2.234E 01	2.409E 01	3.888E 01	7.925E-01
400.000	1.770E 00	3.002E 01	3.179E 01	4.249E 01	8.285E-01
500.000	1.786E 00	3.770E 01	3.949E 01	4.530E 01	8.528E-01
600.000	1.799E 00	4.540E 01	4.720E 01	4.762E 01	8.704E-01
800.000	1.819E 00	6.081E 01	6.263E 01	5.128E 01	8.945E-01
1000.000	1.835E 00	7.623E 01	7.807E 01	5.414E 01	9.104E-01

ELECTRONS IN KRYPTON

ENERGY	STOPPING POWER			RANGE	RADIATION YIELD
	COLLISION	RADIATION	TOTAL		
MEV	MEV CM2/G	MEV CM2/G	MEV CM2/G	G/CM2	
0.010	1.182E 01	2.083E-02	1.185E 01	5.194E-04	1.052E-03
0.015	8.933E 00	2.085E-02	8.954E 00	1.011E-03	1.384E-03
0.020	7.297E 00	2.057E-02	7.318E 00	1.632E-03	1.682E-03
0.025	6.235E 00	2.087E-02	6.256E 00	2.374E-03	1.960E-03
0.030	5.484E 00	2.135E-02	5.505E 00	3.229E-03	2.234E-03
0.035	4.923E 00	2.202E-02	4.946E 00	4.189E-03	2.510E-03
0.040	4.488E 00	2.249E-02	4.510E 00	5.249E-03	2.787E-03
0.045	4.139E 00	2.291E-02	4.162E 00	6.404E-03	3.060E-03
0.050	3.853E 00	2.330E-02	3.876E 00	7.650E-03	3.330E-03
0.055	3.613E 00	2.366E-02	3.637E 00	8.983E-03	3.596E-03
0.060	3.410E 00	2.399E-02	3.434E 00	1.040E-02	3.859E-03
0.065	3.236E 00	2.431E-02	3.260E 00	1.189E-02	4.118E-03
0.070	3.084E 00	2.461E-02	3.109E 00	1.346E-02	4.373E-03
0.075	2.951E 00	2.490E-02	2.976E 00	1.511E-02	4.624E-03
0.080	2.833E 00	2.517E-02	2.858E 00	1.682E-02	4.871E-03
0.085	2.728E 00	2.524E-02	2.754E 00	1.861E-02	5.112E-03
0.090	2.634E 00	2.551E-02	2.660E 00	2.046E-02	5.349E-03
0.095	2.549E 00	2.577E-02	2.575E 00	2.237E-02	5.583E-03
0.100	2.472E 00	2.604E-02	2.498E 00	2.434E-02	5.815E-03
0.150	1.973E 00	2.864E-02	2.002E 00	4.697E-02	8.010E-03
0.200	1.719E 00	3.101E-02	1.750E 00	7.384E-02	1.002E-02
0.250	1.567E 00	3.372E-02	1.600E 00	1.038E-01	1.190E-02
0.300	1.467E 00	3.656E-02	1.504E 00	1.361E-01	1.370E-02
0.350	1.399E 00	3.957E-02	1.439E 00	1.701E-01	1.544E-02
0.400	1.350E 00	4.247E-02	1.392E 00	2.055E-01	1.714E-02
0.450	1.314E 00	4.537E-02	1.359E 00	2.419E-01	1.879E-02
0.500	1.287E 00	4.822E-02	1.335E 00	2.790E-01	2.038E-02
0.550	1.266E 00	5.103E-02	1.317E 00	3.167E-01	2.193E-02
0.600	1.250E 00	5.381E-02	1.304E 00	3.549E-01	2.344E-02
0.650	1.238E 00	5.657E-02	1.295E 00	3.934E-01	2.490E-02
0.700	1.229E 00	5.930E-02	1.288E 00	4.321E-01	2.633E-02
0.750	1.222E 00	6.202E-02	1.284E 00	4.710E-01	2.772E-02
0.800	1.217E 00	6.472E-02	1.282E 00	5.099E-01	2.907E-02
0.850	1.213E 00	6.654E-02	1.280E 00	5.490E-01	3.036E-02
0.900	1.210E 00	6.922E-02	1.279E 00	5.881E-01	3.162E-02
0.950	1.208E 00	7.192E-02	1.280E 00	6.271E-01	3.286E-02
1.000	1.207E 00	7.463E-02	1.282E 00	6.662E-01	3.408E-02
1.100	1.207E 00	8.010E-02	1.287E 00	7.440E-01	3.645E-02
1.200	1.209E 00	8.562E-02	1.294E 00	8.215E-01	3.877E-02
1.300	1.211E 00	9.119E-02	1.303E 00	8.985E-01	4.102E-02

ELECTRONS IN KRYPTON

ENERGY	STOPPING POWER			RANGE	RADIATION YIELD
	COLLISION	RADIATION	TOTAL		
MEV	MEV CM2/G	MEV CM2/G	MEV CM2/G	G/CM2	
1.400	1.215E 00	9.681E-02	1.312E 00	9.750E-01	4.323E-02
1.500	1.219E 00	1.025E-01	1.322E 00	1.051E 00	4.539E-02
1.600	1.224E 00	1.082E-01	1.332E 00	1.126E 00	4.751E-02
1.700	1.229E 00	1.140E-01	1.343E 00	1.201E 00	4.960E-02
1.800	1.234E 00	1.198E-01	1.354E 00	1.275E 00	5.166E-02
1.900	1.239E 00	1.256E-01	1.365E 00	1.349E 00	5.369E-02
2.000	1.245E 00	1.314E-01	1.376E 00	1.422E 00	5.570E-02
2.200	1.255E 00	1.432E-01	1.399E 00	1.566E 00	5.963E-02
2.400	1.266E 00	1.552E-01	1.421E 00	1.708E 00	6.348E-02
2.600	1.277E 00	1.672E-01	1.444E 00	1.847E 00	6.725E-02
2.800	1.287E 00	1.798E-01	1.467E 00	1.985E 00	7.095E-02
3.000	1.297E 00	1.921E-01	1.489E 00	2.120E 00	7.461E-02
3.500	1.320E 00	2.230E-01	1.543E 00	2.450E 00	8.350E-02
4.000	1.342E 00	2.542E-01	1.596E 00	2.769E 00	9.206E-02
4.500	1.361E 00	2.855E-01	1.647E 00	3.077E 00	1.003E-01
5.000	1.379E 00	3.173E-01	1.697E 00	3.376E 00	1.083E-01
5.500	1.396E 00	3.495E-01	1.746E 00	3.667E 00	1.161E-01
6.000	1.412E 00	3.821E-01	1.794E 00	3.949E 00	1.236E-01
6.500	1.426E 00	4.151E-01	1.841E 00	4.224E 00	1.310E-01
7.000	1.440E 00	4.485E-01	1.888E 00	4.492E 00	1.381E-01
7.500	1.452E 00	4.821E-01	1.935E 00	4.754E 00	1.452E-01
8.000	1.464E 00	5.161E-01	1.981E 00	5.009E 00	1.520E-01
8.500	1.476E 00	5.505E-01	2.026E 00	5.259E 00	1.587E-01
9.000	1.487E 00	5.881E-01	2.075E 00	5.503E 00	1.653E-01
9.500	1.497E 00	6.231E-01	2.120E 00	5.741E 00	1.718E-01
10.000	1.507E 00	6.583E-01	2.165E 00	5.975E 00	1.782E-01
20.000	1.640E 00	1.395E 00	3.036E 00	9.852E 00	2.833E-01
30.000	1.720E 00	2.180E 00	3.900E 00	1.275E 01	3.597E-01
40.000	1.777E 00	2.999E 00	4.775E 00	1.506E 01	4.187E-01
50.000	1.821E 00	3.827E 00	5.647E 00	1.699E 01	4.658E-01
60.000	1.854E 00	4.663E 00	6.517E 00	1.863E 01	5.044E-01
80.000	1.904E 00	6.352E 00	8.256E 00	2.135E 01	5.644E-01
100.000	1.941E 00	8.050E 00	9.991E 00	2.355E 01	6.092E-01
200.000	2.043E 00	1.666E 01	1.870E 01	3.075E 01	7.329E-01
300.000	2.095E 00	2.535E 01	2.744E 01	3.514E 01	7.916E-01
400.000	2.130E 00	3.406E 01	3.619E 01	3.830E 01	8.270E-01
500.000	2.154E 00	4.276E 01	4.492E 01	4.078E 01	8.510E-01
600.000	2.174E 00	5.149E 01	5.366E 01	4.281E 01	8.685E-01
800.000	2.202E 00	6.896E 01	7.116E 01	4.604E 01	8.926E-01
1000.000	2.223E 00	8.643E 01	8.866E 01	4.855E 01	9.085E-01

ELECTRONS IN SILVER

ENERGY	STOPPING POWER			RANGE	RADIATION YIELD
	COLLISION	RADIATION	TOTAL		
MEV	MEV CM2/G	MEV CM2/G	MEV CM2/G	G/CM2	
0.010	1.113E 01	2.740E-02	1.116E 01	5.656E-04	1.501E-03
0.015	8.475E 00	2.744E-02	8.502E 00	1.085E-03	1.950E-03
0.020	6.956E 00	2.708E-02	6.983E 00	1.738E-03	2.353E-03
0.025	5.962E 00	2.752E-02	5.990E 00	2.514E-03	2.729E-03
0.030	5.257E 00	2.820E-02	5.285E 00	3.405E-03	3.101E-03
0.035	4.728E 00	2.914E-02	4.758E 00	4.404E-03	3.477E-03
0.040	4.316E 00	2.981E-02	4.346E 00	5.505E-03	3.855E-03
0.045	3.986E 00	3.041E-02	4.016E 00	6.703E-03	4.228E-03
0.050	3.714E 00	3.096E-02	3.745E 00	7.993E-03	4.597E-03
0.055	3.487E 00	3.147E-02	3.518E 00	9.372E-03	4.962E-03
0.060	3.294E 00	3.196E-02	3.326E 00	1.083E-02	5.322E-03
0.065	3.127E 00	3.241E-02	3.160E 00	1.238E-02	5.676E-03
0.070	2.983E 00	3.285E-02	3.016E 00	1.400E-02	6.027E-03
0.075	2.856E 00	3.327E-02	2.889E 00	1.569E-02	6.372E-03
0.080	2.743E 00	3.368E-02	2.777E 00	1.746E-02	6.713E-03
0.085	2.643E 00	3.396E-02	2.677E 00	1.929E-02	7.047E-03
0.090	2.553E 00	3.435E-02	2.587E 00	2.119E-02	7.377E-03
0.095	2.472E 00	3.474E-02	2.506E 00	2.316E-02	7.703E-03
0.100	2.398E 00	3.511E-02	2.433E 00	2.518E-02	8.025E-03
0.150	1.920E 00	3.870E-02	1.958E 00	4.836E-02	1.107E-02
0.200	1.674E 00	4.178E-02	1.716E 00	7.579E-02	1.383E-02
0.250	1.529E 00	4.535E-02	1.574E 00	1.063E-01	1.638E-02
0.300	1.434E 00	4.908E-02	1.483E 00	1.391E-01	1.881E-02
0.350	1.368E 00	5.304E-02	1.421E 00	1.736E-01	2.116E-02
0.400	1.321E 00	5.684E-02	1.378E 00	2.093E-01	2.342E-02
0.450	1.286E 00	6.067E-02	1.346E 00	2.461E-01	2.562E-02
0.500	1.260E 00	6.441E-02	1.324E 00	2.835E-01	2.774E-02
0.550	1.241E 00	6.811E-02	1.309E 00	3.215E-01	2.980E-02
0.600	1.225E 00	7.177E-02	1.297E 00	3.599E-01	3.179E-02
0.650	1.213E 00	7.540E-02	1.288E 00	3.986E-01	3.372E-02
0.700	1.204E 00	7.900E-02	1.283E 00	4.375E-01	3.560E-02
0.750	1.196E 00	8.258E-02	1.279E 00	4.765E-01	3.744E-02
0.800	1.191E 00	8.613E-02	1.277E 00	5.157E-01	3.922E-02
0.850	1.187E 00	8.830E-02	1.275E 00	5.549E-01	4.091E-02
0.900	1.183E 00	9.183E-02	1.275E 00	5.941E-01	4.256E-02
0.950	1.181E 00	9.538E-02	1.276E 00	6.333E-01	4.419E-02
1.000	1.179E 00	9.897E-02	1.278E 00	6.724E-01	4.578E-02
1.100	1.178E 00	1.062E-01	1.284E 00	7.505E-01	4.890E-02
1.200	1.178E 00	1.135E-01	1.291E 00	8.282E-01	5.193E-02
1.300	1.179E 00	1.209E-01	1.300E 00	9.054E-01	5.490E-02

ELECTRONS IN SILVER

ENERGY	STOPPING POWER			RANGE	RADIATION YIELD
	COLLISION	RADIATION	TOTAL		
MEV	MEV CM2/G	MEV CM2/G	MEV CM2/G	G/CM2	
1.400	1.181E 00	1.284E-01	1.310E 00	9.820E-01	5.781E-02
1.500	1.184E 00	1.360E-01	1.320E 00	1.058E 00	6.066E-02
1.600	1.187E 00	1.437E-01	1.330E 00	1.134E 00	6.346E-02
1.700	1.190E 00	1.517E-01	1.342E 00	1.208E 00	6.624E-02
1.800	1.194E 00	1.595E-01	1.353E 00	1.283E 00	6.897E-02
1.900	1.197E 00	1.672E-01	1.365E 00	1.356E 00	7.167E-02
2.000	1.201E 00	1.750E-01	1.376E 00	1.429E 00	7.433E-02
2.200	1.209E 00	1.907E-01	1.399E 00	1.573E 00	7.955E-02
2.400	1.216E 00	2.064E-01	1.423E 00	1.715E 00	8.464E-02
2.600	1.224E 00	2.221E-01	1.446E 00	1.854E 00	8.962E-02
2.800	1.231E 00	2.378E-01	1.469E 00	1.992E 00	9.449E-02
3.000	1.238E 00	2.537E-01	1.491E 00	2.127E 00	9.926E-02
3.500	1.254E 00	2.937E-01	1.548E 00	2.456E 00	1.108E-01
4.000	1.269E 00	3.343E-01	1.603E 00	2.773E 00	1.219E-01
4.500	1.282E 00	3.750E-01	1.657E 00	3.080E 00	1.325E-01
5.000	1.294E 00	4.164E-01	1.710E 00	3.377E 00	1.427E-01
5.500	1.305E 00	4.581E-01	1.763E 00	3.665E 00	1.526E-01
6.000	1.315E 00	5.003E-01	1.815E 00	3.944E 00	1.622E-01
6.500	1.324E 00	5.429E-01	1.867E 00	4.216E 00	1.715E-01
7.000	1.333E 00	5.859E-01	1.918E 00	4.480E 00	1.806E-01
7.500	1.340E 00	6.292E-01	1.970E 00	4.737E 00	1.894E-01
8.000	1.348E 00	6.729E-01	2.021E 00	4.988E 00	1.979E-01
8.500	1.355E 00	7.168E-01	2.071E 00	5.233E 00	2.063E-01
9.000	1.361E 00	7.637E-01	2.125E 00	5.471E 00	2.144E-01
9.500	1.367E 00	8.084E-01	2.175E 00	5.703E 00	2.224E-01
10.000	1.373E 00	8.533E-01	2.226E 00	5.931E 00	2.301E-01
20.000	1.446E 00	1.785E 00	3.231E 00	9.637E 00	3.534E-01
30.000	1.485E 00	2.780E 00	4.264E 00	1.232E 01	4.376E-01
40.000	1.510E 00	3.824E 00	5.335E 00	1.442E 01	4.999E-01
50.000	1.530E 00	4.879E 00	6.408E 00	1.612E 01	5.480E-01
60.000	1.545E 00	5.944E 00	7.488E 00	1.757E 01	5.864E-01
80.000	1.568E 00	8.094E 00	9.661E 00	1.991E 01	6.442E-01
100.000	1.585E 00	1.025E 01	1.184E 01	2.178E 01	6.859E-01
200.000	1.635E 00	2.121E 01	2.284E 01	2.775E 01	7.948E-01
300.000	1.663E 00	3.225E 01	3.391E 01	3.133E 01	8.436E-01
400.000	1.682E 00	4.330E 01	4.499E 01	3.388E 01	8.720E-01
500.000	1.697E 00	5.438E 01	5.608E 01	3.586E 01	8.909E-01
600.000	1.709E 00	6.548E 01	6.719E 01	3.749E 01	9.045E-01
800.000	1.729E 00	8.768E 01	8.941E 01	4.006E 01	9.228E-01
1000.000	1.744E 00	1.099E 02	1.116E 02	4.206E 01	9.348E-01

ELECTRONS IN TIN

ENERGY	STOPPING POWER			RANGE	RADIATION YIELD
	COLLISION	RADIATION	TOTAL		
MEV	MEV CM2/G	MEV CM2/G	MEV CM2/G	G/CM2	
0.010	1.056E 01	2.815E-02	1.059E 01	6.000E-04	1.633E-03
0.015	8.061E 00	2.819E-02	8.089E 00	1.146E-03	2.115E-03
0.020	6.624E 00	2.769E-02	6.652E 00	1.832E-03	2.545E-03
0.025	5.683E 00	2.826E-02	5.711E 00	2.646E-03	2.946E-03
0.030	5.013E 00	2.914E-02	5.042E 00	3.581E-03	3.348E-03
0.035	4.511E 00	3.039E-02	4.542E 00	4.627E-03	3.762E-03
0.040	4.120E 00	3.122E-02	4.151E 00	5.780E-03	4.180E-03
0.045	3.806E 00	3.195E-02	3.838E 00	7.035E-03	4.596E-03
0.050	3.547E 00	3.260E-02	3.580E 00	8.385E-03	5.008E-03
0.055	3.331E 00	3.318E-02	3.364E 00	9.827E-03	5.415E-03
0.060	3.147E 00	3.372E-02	3.181E 00	1.136E-02	5.817E-03
0.065	2.989E 00	3.422E-02	3.023E 00	1.297E-02	6.213E-03
0.070	2.851E 00	3.469E-02	2.886E 00	1.466E-02	6.603E-03
0.075	2.730E 00	3.513E-02	2.765E 00	1.643E-02	6.987E-03
0.080	2.623E 00	3.555E-02	2.658E 00	1.828E-02	7.365E-03
0.085	2.527E 00	3.559E-02	2.563E 00	2.020E-02	7.731E-03
0.090	2.441E 00	3.598E-02	2.477E 00	2.218E-02	8.090E-03
0.095	2.364E 00	3.638E-02	2.400E 00	2.423E-02	8.446E-03
0.100	2.294E 00	3.677E-02	2.330E 00	2.635E-02	8.797E-03
0.150	1.837E 00	4.054E-02	1.878E 00	5.053E-02	1.211E-02
0.200	1.604E 00	4.391E-02	1.648E 00	7.911E-02	1.513E-02
0.250	1.465E 00	4.774E-02	1.512E 00	1.109E-01	1.793E-02
0.300	1.374E 00	5.173E-02	1.425E 00	1.450E-01	2.060E-02
0.350	1.311E 00	5.599E-02	1.367E 00	1.809E-01	2.318E-02
0.400	1.266E 00	5.996E-02	1.326E 00	2.180E-01	2.567E-02
0.450	1.233E 00	6.388E-02	1.296E 00	2.562E-01	2.806E-02
0.500	1.208E 00	6.773E-02	1.276E 00	2.951E-01	3.038E-02
0.550	1.189E 00	7.152E-02	1.261E 00	3.345E-01	3.261E-02
0.600	1.175E 00	7.528E-02	1.250E 00	3.743E-01	3.476E-02
0.650	1.164E 00	7.900E-02	1.243E 00	4.144E-01	3.685E-02
0.700	1.155E 00	8.269E-02	1.238E 00	4.547E-01	3.887E-02
0.750	1.149E 00	8.636E-02	1.235E 00	4.952E-01	4.084E-02
0.800	1.144E 00	8.999E-02	1.234E 00	5.357E-01	4.275E-02
0.850	1.140E 00	9.230E-02	1.232E 00	5.763E-01	4.456E-02
0.900	1.137E 00	9.591E-02	1.233E 00	6.168E-01	4.633E-02
0.950	1.135E 00	9.954E-02	1.235E 00	6.573E-01	4.806E-02
1.000	1.134E 00	1.032E-01	1.237E 00	6.978E-01	4.975E-02
1.100	1.133E 00	1.106E-01	1.244E 00	7.784E-01	5.306E-02
1.200	1.134E 00	1.180E-01	1.252E 00	8.586E-01	5.628E-02
1.300	1.135E 00	1.255E-01	1.261E 00	9.382E-01	5.940E-02

ELECTRONS IN TIN

ENERGY	STOPPING POWER			RANGE	RADIATION YIELD
	COLLISION	RADIATION	TOTAL		
MEV	MEV CM2/G	MEV CM2/G	MEV CM2/G	G/CM2	
1.400	1.138E 00	1.331E-01	1.271E 00	1.017E 00	6.245E-02
1.500	1.141E 00	1.407E-01	1.281E 00	1.096E 00	6.544E-02
1.600	1.144E 00	1.484E-01	1.292E 00	1.173E 00	6.837E-02
1.700	1.148E 00	1.563E-01	1.304E 00	1.250E 00	7.126E-02
1.800	1.151E 00	1.641E-01	1.316E 00	1.327E 00	7.410E-02
1.900	1.155E 00	1.720E-01	1.327E 00	1.402E 00	7.689E-02
2.000	1.159E 00	1.799E-01	1.339E 00	1.477E 00	7.964E-02
2.200	1.167E 00	1.957E-01	1.363E 00	1.625E 00	8.504E-02
2.400	1.175E 00	2.117E-01	1.387E 00	1.771E 00	9.029E-02
2.600	1.183E 00	2.278E-01	1.410E 00	1.914E 00	9.543E-02
2.800	1.190E 00	2.443E-01	1.434E 00	2.054E 00	1.005E-01
3.000	1.197E 00	2.606E-01	1.458E 00	2.193E 00	1.054E-01
3.500	1.214E 00	3.018E-01	1.516E 00	2.529E 00	1.173E-01
4.000	1.229E 00	3.434E-01	1.572E 00	2.853E 00	1.288E-01
4.500	1.243E 00	3.853E-01	1.628E 00	3.165E 00	1.398E-01
5.000	1.255E 00	4.277E-01	1.683E 00	3.467E 00	1.503E-01
5.500	1.266E 00	4.706E-01	1.737E 00	3.760E 00	1.605E-01
6.000	1.277E 00	5.139E-01	1.790E 00	4.043E 00	1.704E-01
6.500	1.286E 00	5.575E-01	1.844E 00	4.319E 00	1.800E-01
7.000	1.295E 00	6.015E-01	1.896E 00	4.586E 00	1.893E-01
7.500	1.303E 00	6.459E-01	1.949E 00	4.846E 00	1.983E-01
8.000	1.310E 00	6.905E-01	2.001E 00	5.099E 00	2.070E-01
8.500	1.318E 00	7.355E-01	2.053E 00	5.346E 00	2.155E-01
9.000	1.324E 00	7.836E-01	2.108E 00	5.586E 00	2.238E-01
9.500	1.330E 00	8.292E-01	2.160E 00	5.821E 00	2.319E-01
10.000	1.336E 00	8.751E-01	2.211E 00	6.050E 00	2.398E-01
20.000	1.412E 00	1.821E 00	3.233E 00	9.764E 00	3.642E-01
30.000	1.452E 00	2.830E 00	4.282E 00	1.245E 01	4.481E-01
40.000	1.479E 00	3.895E 00	5.374E 00	1.453E 01	5.099E-01
50.000	1.498E 00	4.969E 00	6.468E 00	1.622E 01	5.575E-01
60.000	1.514E 00	6.054E 00	7.568E 00	1.765E 01	5.954E-01
80.000	1.537E 00	8.243E 00	9.780E 00	1.997E 01	6.523E-01
100.000	1.555E 00	1.044E 01	1.200E 01	2.181E 01	6.934E-01
200.000	1.605E 00	2.160E 01	2.320E 01	2.770E 01	8.001E-01
300.000	1.633E 00	3.283E 01	3.447E 01	3.121E 01	8.478E-01
400.000	1.652E 00	4.409E 01	4.574E 01	3.372E 01	8.755E-01
500.000	1.666E 00	5.537E 01	5.703E 01	3.568E 01	8.940E-01
600.000	1.678E 00	6.666E 01	6.834E 01	3.728E 01	9.072E-01
800.000	1.697E 00	8.926E 01	9.096E 01	3.980E 01	9.250E-01
1000.000	1.711E 00	1.119E 02	1.136E 02	4.177E 01	9.367E-01

ELECTRONS IN XENON

ENERGY	STOPPING POWER			RANGE	RADIATION YIELD
	COLLISION	RADIATION	TOTAL		
MEV	MEV CM2/G	MEV CM2/G	MEV CM2/G	G/CM2	
0.010	1.007E 01	3.012E-02	1.010E 01	6.353E-04	1.824E-03
0.015	7.707E 00	3.064E-02	7.737E 00	1.207E-03	2.375E-03
0.020	6.343E 00	3.097E-02	6.374E 00	1.923E-03	2.885E-03
0.025	5.447E 00	3.157E-02	5.479E 00	2.773E-03	3.370E-03
0.030	4.809E 00	3.223E-02	4.842E 00	3.746E-03	3.843E-03
0.035	4.331E 00	3.297E-02	4.364E 00	4.836E-03	4.310E-03
0.040	3.957E 00	3.359E-02	3.990E 00	6.036E-03	4.770E-03
0.045	3.656E 00	3.419E-02	3.691E 00	7.340E-03	5.222E-03
0.050	3.409E 00	3.474E-02	3.444E 00	8.744E-03	5.668E-03
0.055	3.202E 00	3.526E-02	3.238E 00	1.024E-02	6.106E-03
0.060	3.026E 00	3.576E-02	3.062E 00	1.183E-02	6.538E-03
0.065	2.875E 00	3.625E-02	2.911E 00	1.351E-02	6.963E-03
0.070	2.743E 00	3.671E-02	2.780E 00	1.527E-02	7.382E-03
0.075	2.627E 00	3.717E-02	2.664E 00	1.710E-02	7.795E-03
0.080	2.524E 00	3.761E-02	2.562E 00	1.902E-02	8.203E-03
0.085	2.433E 00	3.794E-02	2.470E 00	2.101E-02	8.603E-03
0.090	2.350E 00	3.837E-02	2.389E 00	2.306E-02	8.998E-03
0.095	2.276E 00	3.880E-02	2.315E 00	2.519E-02	9.388E-03
0.100	2.209E 00	3.922E-02	2.248E 00	2.738E-02	9.774E-03
0.150	1.771E 00	4.328E-02	1.814E 00	5.244E-02	1.342E-02
0.200	1.547E 00	4.693E-02	1.594E 00	8.200E-02	1.674E-02
0.250	1.413E 00	5.099E-02	1.464E 00	1.148E-01	1.982E-02
0.300	1.326E 00	5.520E-02	1.381E 00	1.501E-01	2.276E-02
0.350	1.266E 00	5.961E-02	1.326E 00	1.871E-01	2.558E-02
0.400	1.223E 00	6.383E-02	1.287E 00	2.254E-01	2.829E-02
0.450	1.192E 00	6.804E-02	1.260E 00	2.647E-01	3.091E-02
0.500	1.168E 00	7.216E-02	1.240E 00	3.047E-01	3.343E-02
0.550	1.150E 00	7.621E-02	1.227E 00	3.452E-01	3.586E-02
0.600	1.137E 00	8.020E-02	1.217E 00	3.862E-01	3.821E-02
0.650	1.127E 00	8.415E-02	1.211E 00	4.274E-01	4.048E-02
0.700	1.119E 00	8.806E-02	1.207E 00	4.687E-01	4.267E-02
0.750	1.113E 00	9.193E-02	1.205E 00	5.102E-01	4.480E-02
0.800	1.109E 00	9.577E-02	1.205E 00	5.517E-01	4.687E-02
0.850	1.106E 00	9.802E-02	1.204E 00	5.932E-01	4.882E-02
0.900	1.104E 00	1.018E-01	1.206E 00	6.347E-01	5.072E-02
0.950	1.103E 00	1.056E-01	1.208E 00	6.762E-01	5.257E-02
1.000	1.102E 00	1.095E-01	1.212E 00	7.175E-01	5.438E-02
1.100	1.103E 00	1.172E-01	1.220E 00	7.997E-01	5.791E-02
1.200	1.105E 00	1.250E-01	1.230E 00	8.814E-01	6.133E-02
1.300	1.108E 00	1.329E-01	1.241E 00	9.623E-01	6.464E-02

ELECTRONS IN XENON

ENERGY	STOPPING POWER			RANGE	RADIATION YIELD
	COLLISION	RADIATION	TOTAL		
MEV	MEV CM2/G	MEV CM2/G	MEV CM2/G	G/CM2	
1.400	1.112E 00	1.409E-01	1.253E 00	1.043E 00	6.786E-02
1.500	1.116E 00	1.489E-01	1.265E 00	1.122E 00	7.101E-02
1.600	1.121E 00	1.570E-01	1.278E 00	1.201E 00	7.409E-02
1.700	1.126E 00	1.652E-01	1.292E 00	1.278E 00	7.711E-02
1.800	1.131E 00	1.734E-01	1.305E 00	1.355E 00	8.007E-02
1.900	1.137E 00	1.817E-01	1.318E 00	1.432E 00	8.298E-02
2.000	1.142E 00	1.900E-01	1.332E 00	1.507E 00	8.584E-02
2.200	1.153E 00	2.066E-01	1.359E 00	1.656E 00	9.143E-02
2.400	1.163E 00	2.235E-01	1.387E 00	1.801E 00	9.686E-02
2.600	1.173E 00	2.404E-01	1.414E 00	1.944E 00	1.022E-01
2.800	1.183E 00	2.582E-01	1.442E 00	2.084E 00	1.073E-01
3.000	1.193E 00	2.755E-01	1.468E 00	2.222E 00	1.124E-01
3.500	1.216E 00	3.188E-01	1.534E 00	2.555E 00	1.246E-01
4.000	1.236E 00	3.625E-01	1.599E 00	2.874E 00	1.362E-01
4.500	1.255E 00	4.062E-01	1.661E 00	3.181E 00	1.472E-01
5.000	1.273E 00	4.505E-01	1.723E 00	3.476E 00	1.578E-01
5.500	1.289E 00	4.952E-01	1.784E 00	3.761E 00	1.680E-01
6.000	1.304E 00	5.404E-01	1.844E 00	4.037E 00	1.778E-01
6.500	1.318E 00	5.860E-01	1.904E 00	4.304E 00	1.872E-01
7.000	1.331E 00	6.319E-01	1.963E 00	4.563E 00	1.963E-01
7.500	1.343E 00	6.782E-01	2.021E 00	4.814E 00	2.052E-01
8.000	1.354E 00	7.249E-01	2.079E 00	5.058E 00	2.137E-01
8.500	1.365E 00	7.718E-01	2.137E 00	5.295E 00	2.220E-01
9.000	1.376E 00	8.243E-01	2.200E 00	5.525E 00	2.301E-01
9.500	1.385E 00	8.721E-01	2.257E 00	5.750E 00	2.380E-01
10.000	1.395E 00	9.201E-01	2.315E 00	5.969E 00	2.457E-01
20.000	1.523E 00	1.900E 00	3.423E 00	9.491E 00	3.654E-01
30.000	1.599E 00	2.945E 00	4.544E 00	1.202E 01	4.453E-01
40.000	1.653E 00	4.055E 00	5.708E 00	1.398E 01	5.043E-01
50.000	1.692E 00	5.173E 00	6.865E 00	1.557E 01	5.501E-01
60.000	1.724E 00	6.302E 00	8.025E 00	1.692E 01	5.868E-01
80.000	1.771E 00	8.580E 00	1.035E 01	1.911E 01	6.423E-01
100.000	1.807E 00	1.087E 01	1.268E 01	2.085E 01	6.826E-01
200.000	1.907E 00	2.247E 01	2.438E 01	2.644E 01	7.894E-01
300.000	1.961E 00	3.416E 01	3.613E 01	2.979E 01	8.380E-01
400.000	1.996E 00	4.587E 01	4.787E 01	3.219E 01	8.666E-01
500.000	2.021E 00	5.761E 01	5.963E 01	3.405E 01	8.858E-01
600.000	2.041E 00	6.935E 01	7.140E 01	3.559E 01	8.997E-01
800.000	2.072E 00	9.287E 01	9.494E 01	3.801E 01	9.185E-01
1000.000	2.094E 00	1.164E 02	1.185E 02	3.989E 01	9.309E-01

ELECTRONS IN TUNGSTEN

ENERGY	STOPPING POWER			RANGE	RADIATION YIELD
	COLLISION	RADIATION	TOTAL		
MEV	MEV CM2/G	MEV CM2/G	MEV CM2/G	G/CM2	
0.010	8.882E 00	4.022E-02	8.922E 00	7.603E-04	2.869E-03
0.015	6.883E 00	4.097E-02	6.924E 00	1.403E-03	3.652E-03
0.020	5.707E 00	4.150E-02	5.748E 00	2.200E-03	4.383E-03
0.025	4.924E 00	4.232E-02	4.966E 00	3.139E-03	5.081E-03
0.030	4.363E 00	4.320E-02	4.406E 00	4.210E-03	5.762E-03
0.035	3.939E 00	4.416E-02	3.984E 00	5.406E-03	6.431E-03
0.040	3.607E 00	4.499E-02	3.652E 00	6.719E-03	7.090E-03
0.045	3.340E 00	4.579E-02	3.385E 00	8.142E-03	7.738E-03
0.050	3.119E 00	4.653E-02	3.165E 00	9.671E-03	8.376E-03
0.055	2.933E 00	4.724E-02	2.981E 00	1.130E-02	9.003E-03
0.060	2.775E 00	4.793E-02	2.823E 00	1.302E-02	9.621E-03
0.065	2.639E 00	4.859E-02	2.688E 00	1.484E-02	1.023E-02
0.070	2.520E 00	4.923E-02	2.570E 00	1.674E-02	1.083E-02
0.075	2.416E 00	4.985E-02	2.466E 00	1.873E-02	1.142E-02
0.080	2.323E 00	5.046E-02	2.374E 00	2.080E-02	1.200E-02
0.085	2.241E 00	5.089E-02	2.291E 00	2.294E-02	1.257E-02
0.090	2.166E 00	5.149E-02	2.218E 00	2.516E-02	1.314E-02
0.095	2.099E 00	5.208E-02	2.151E 00	2.745E-02	1.369E-02
0.100	2.038E 00	5.266E-02	2.091E 00	2.981E-02	1.424E-02
0.150	1.641E 00	5.837E-02	1.699E 00	5.664E-02	1.945E-02
0.200	1.437E 00	6.384E-02	1.501E 00	8.812E-02	2.421E-02
0.250	1.315E 00	6.940E-02	1.385E 00	1.229E-01	2.864E-02
0.300	1.236E 00	7.499E-02	1.311E 00	1.601E-01	3.282E-02
0.350	1.182E 00	8.063E-02	1.262E 00	1.990E-01	3.678E-02
0.400	1.143E 00	8.624E-02	1.229E 00	2.392E-01	4.057E-02
0.450	1.114E 00	9.197E-02	1.206E 00	2.803E-01	4.419E-02
0.500	1.093E 00	9.752E-02	1.191E 00	3.220E-01	4.769E-02
0.550	1.077E 00	1.030E-01	1.180E 00	3.642E-01	5.104E-02
0.600	1.065E 00	1.084E-01	1.174E 00	4.067E-01	5.427E-02
0.650	1.055E 00	1.137E-01	1.169E 00	4.494E-01	5.739E-02
0.700	1.049E 00	1.189E-01	1.168E 00	4.922E-01	6.040E-02
0.750	1.044E 00	1.241E-01	1.168E 00	5.350E-01	6.331E-02
0.800	1.040E 00	1.292E-01	1.169E 00	5.778E-01	6.612E-02
0.850	1.037E 00	1.318E-01	1.169E 00	6.206E-01	6.876E-02
0.900	1.035E 00	1.368E-01	1.172E 00	6.633E-01	7.131E-02
0.950	1.033E 00	1.419E-01	1.175E 00	7.059E-01	7.381E-02
1.000	1.033E 00	1.471E-01	1.180E 00	7.484E-01	7.626E-02
1.100	1.032E 00	1.575E-01	1.190E 00	8.328E-01	8.101E-02
1.200	1.033E 00	1.680E-01	1.201E 00	9.165E-01	8.560E-02
1.300	1.035E 00	1.787E-01	1.214E 00	9.993E-01	9.006E-02

ELECTRONS IN TUNGSTEN

ENERGY	STOPPING POWER			RANGE	RADIATION YIELD
	COLLISION	RADIATION	TOTAL		
MEV	MEV CM2/G	MEV CM2/G	MEV CM2/G	G/CM2	
1.400	1.038E 00	1.895E-01	1.228E 00	1.081E 00	9.439E-02
1.500	1.041E 00	2.003E-01	1.242E 00	1.162E 00	9.862E-02
1.600	1.045E 00	2.113E-01	1.256E 00	1.242E 00	1.028E-01
1.700	1.048E 00	2.231E-01	1.271E 00	1.321E 00	1.068E-01
1.800	1.052E 00	2.342E-01	1.286E 00	1.400E 00	1.108E-01
1.900	1.056E 00	2.453E-01	1.301E 00	1.477E 00	1.148E-01
2.000	1.060E 00	2.565E-01	1.316E 00	1.553E 00	1.186E-01
2.200	1.067E 00	2.788E-01	1.346E 00	1.704E 00	1.261E-01
2.400	1.075E 00	3.012E-01	1.376E 00	1.851E 00	1.333E-01
2.600	1.082E 00	3.236E-01	1.406E 00	1.994E 00	1.404E-01
2.800	1.089E 00	3.459E-01	1.435E 00	2.135E 00	1.472E-01
3.000	1.096E 00	3.684E-01	1.464E 00	2.273E 00	1.538E-01
3.500	1.112E 00	4.249E-01	1.537E 00	2.606E 00	1.696E-01
4.000	1.126E 00	4.818E-01	1.608E 00	2.924E 00	1.844E-01
4.500	1.139E 00	5.387E-01	1.677E 00	3.229E 00	1.984E-01
5.000	1.150E 00	5.962E-01	1.747E 00	3.521E 00	2.117E-01
5.500	1.161E 00	6.541E-01	1.815E 00	3.802E 00	2.244E-01
6.000	1.170E 00	7.124E-01	1.883E 00	4.072E 00	2.365E-01
6.500	1.179E 00	7.710E-01	1.950E 00	4.333E 00	2.480E-01
7.000	1.187E 00	8.300E-01	2.017E 00	4.585E 00	2.591E-01
7.500	1.195E 00	8.893E-01	2.084E 00	4.829E 00	2.698E-01
8.000	1.202E 00	9.489E-01	2.151E 00	5.065E 00	2.801E-01
8.500	1.208E 00	1.009E 00	2.217E 00	5.294E 00	2.900E-01
9.000	1.215E 00	1.077E 00	2.291E 00	5.516E 00	2.995E-01
9.500	1.220E 00	1.137E 00	2.358E 00	5.731E 00	3.088E-01
10.000	1.226E 00	1.198E 00	2.424E 00	5.940E 00	3.178E-01
20.000	1.296E 00	2.407E 00	3.703E 00	9.242E 00	4.504E-01
30.000	1.333E 00	3.700E 00	5.033E 00	1.155E 01	5.323E-01
40.000	1.357E 00	5.105E 00	6.462E 00	1.330E 01	5.904E-01
50.000	1.376E 00	6.511E 00	7.887E 00	1.470E 01	6.341E-01
60.000	1.390E 00	7.932E 00	9.322E 00	1.587E 01	6.682E-01
80.000	1.412E 00	1.080E 01	1.221E 01	1.773E 01	7.184E-01
100.000	1.428E 00	1.368E 01	1.511E 01	1.920E 01	7.539E-01
200.000	1.476E 00	2.828E 01	2.976E 01	2.383E 01	8.433E-01
300.000	1.502E 00	4.298E 01	4.449E 01	2.656E 01	8.820E-01
400.000	1.521E 00	5.771E 01	5.923E 01	2.851E 01	9.042E-01
500.000	1.535E 00	7.245E 01	7.399E 01	3.001E 01	9.187E-01
600.000	1.546E 00	8.722E 01	8.877E 01	3.124E 01	9.291E-01
800.000	1.564E 00	1.168E 02	1.183E 02	3.319E 01	9.430E-01
1000.000	1.578E 00	1.463E 02	1.479E 02	3.470E 01	9.521E-01

ELECTRONS IN GOLD

ENERGY	STOPPING POWER			RANGE	RADIATION YIELD
	COLLISION	RADIATION	TOTAL		
MEV	MEV CM2/G	MEV CM2/G	MEV CM2/G	G/CM2	
0.010	8.647E 00	4.383E-02	8.691E 00	7.944E-04	3.182E-03
0.015	6.722E 00	4.477E-02	6.766E 00	1.453E-03	4.069E-03
0.020	5.582E 00	4.490E-02	5.627E 00	2.268E-03	4.880E-03
0.025	4.822E 00	4.578E-02	4.868E 00	3.226E-03	5.642E-03
0.030	4.276E 00	4.686E-02	4.323E 00	4.319E-03	6.389E-03
0.035	3.863E 00	4.815E-02	3.911E 00	5.537E-03	7.130E-03
0.040	3.540E 00	4.916E-02	3.589E 00	6.873E-03	7.865E-03
0.045	3.278E 00	5.010E-02	3.328E 00	8.322E-03	8.589E-03
0.050	3.063E 00	5.096E-02	3.113E 00	9.876E-03	9.301E-03
0.055	2.881E 00	5.178E-02	2.933E 00	1.153E-02	1.000E-02
0.060	2.727E 00	5.256E-02	2.780E 00	1.328E-02	1.069E-02
0.065	2.594E 00	5.330E-02	2.647E 00	1.513E-02	1.137E-02
0.070	2.478E 00	5.402E-02	2.532E 00	1.706E-02	1.204E-02
0.075	2.375E 00	5.471E-02	2.430E 00	1.908E-02	1.270E-02
0.080	2.285E 00	5.538E-02	2.340E 00	2.117E-02	1.335E-02
0.085	2.204E 00	5.586E-02	2.259E 00	2.335E-02	1.399E-02
0.090	2.131E 00	5.651E-02	2.187E 00	2.560E-02	1.461E-02
0.095	2.065E 00	5.715E-02	2.122E 00	2.792E-02	1.523E-02
0.100	2.005E 00	5.778E-02	2.063E 00	3.031E-02	1.584E-02
0.150	1.616E 00	6.388E-02	1.680E 00	5.748E-02	2.160E-02
0.200	1.416E 00	6.944E-02	1.486E 00	8.929E-02	2.682E-02
0.250	1.297E 00	7.543E-02	1.372E 00	1.244E-01	3.164E-02
0.300	1.219E 00	8.155E-02	1.301E 00	1.619E-01	3.618E-02
0.350	1.166E 00	8.790E-02	1.253E 00	2.011E-01	4.050E-02
0.400	1.127E 00	9.403E-02	1.221E 00	2.416E-01	4.464E-02
0.450	1.100E 00	1.002E-01	1.200E 00	2.829E-01	4.859E-02
0.500	1.079E 00	1.062E-01	1.185E 00	3.248E-01	5.239E-02
0.550	1.062E 00	1.120E-01	1.174E 00	3.672E-01	5.604E-02
0.600	1.050E 00	1.178E-01	1.168E 00	4.099E-01	5.955E-02
0.650	1.041E 00	1.235E-01	1.164E 00	4.528E-01	6.293E-02
0.700	1.034E 00	1.291E-01	1.163E 00	4.958E-01	6.619E-02
0.750	1.028E 00	1.346E-01	1.163E 00	5.388E-01	6.934E-02
0.800	1.024E 00	1.401E-01	1.165E 00	5.818E-01	7.238E-02
0.850	1.022E 00	1.427E-01	1.164E 00	6.247E-01	7.522E-02
0.900	1.020E 00	1.481E-01	1.168E 00	6.676E-01	7.797E-02
0.950	1.018E 00	1.535E-01	1.172E 00	7.104E-01	8.065E-02
1.000	1.018E 00	1.590E-01	1.177E 00	7.529E-01	8.327E-02
1.100	1.018E 00	1.700E-01	1.187E 00	8.376E-01	8.835E-02
1.200	1.019E 00	1.811E-01	1.200E 00	9.213E-01	9.324E-02
1.300	1.021E 00	1.923E-01	1.213E 00	1.004E 00	9.797E-02

ELECTRONS IN GOLD

ENERGY	STOPPING POWER			RANGE	RADIATION YIELD
	COLLISION	RADIATION	TOTAL		
MEV	MEV CM2/G	MEV CM2/G	MEV CM2/G	G/CM2	
1.400	1.024E 00	2.036E-01	1.227E 00	1.086E 00	1.026E-01
1.500	1.027E 00	2.150E-01	1.242E 00	1.167E 00	1.070E-01
1.600	1.030E 00	2.265E-01	1.257E 00	1.247E 00	1.114E-01
1.700	1.034E 00	2.385E-01	1.273E 00	1.326E 00	1.156E-01
1.800	1.038E 00	2.502E-01	1.288E 00	1.404E 00	1.198E-01
1.900	1.042E 00	2.618E-01	1.303E 00	1.482E 00	1.239E-01
2.000	1.046E 00	2.735E-01	1.319E 00	1.558E 00	1.279E-01
2.200	1.053E 00	2.970E-01	1.350E 00	1.708E 00	1.357E-01
2.400	1.061E 00	3.206E-01	1.382E 00	1.854E 00	1.433E-01
2.600	1.068E 00	3.442E-01	1.413E 00	1.997E 00	1.505E-01
2.800	1.076E 00	3.684E-01	1.444E 00	2.137E 00	1.576E-01
3.000	1.082E 00	3.923E-01	1.475E 00	2.274E 00	1.645E-01
3.500	1.099E 00	4.520E-01	1.551E 00	2.605E 00	1.808E-01
4.000	1.113E 00	5.120E-01	1.625E 00	2.920E 00	1.961E-01
4.500	1.126E 00	5.719E-01	1.698E 00	3.221E 00	2.106E-01
5.000	1.138E 00	6.322E-01	1.770E 00	3.509E 00	2.242E-01
5.500	1.148E 00	6.930E-01	1.841E 00	3.786E 00	2.372E-01
6.000	1.158E 00	7.541E-01	1.912E 00	4.053E 00	2.496E-01
6.500	1.167E 00	8.155E-01	1.983E 00	4.310E 00	2.614E-01
7.000	1.175E 00	8.773E-01	2.053E 00	4.557E 00	2.727E-01
7.500	1.183E 00	9.393E-01	2.122E 00	4.797E 00	2.835E-01
8.000	1.190E 00	1.002E 00	2.192E 00	5.029E 00	2.939E-01
8.500	1.197E 00	1.064E 00	2.261E 00	5.253E 00	3.039E-01
9.000	1.203E 00	1.128E 00	2.331E 00	5.471E 00	3.135E-01
9.500	1.209E 00	1.191E 00	2.400E 00	5.682E 00	3.228E-01
10.000	1.215E 00	1.254E 00	2.469E 00	5.888E 00	3.318E-01
20.000	1.286E 00	2.553E 00	3.839E 00	9.108E 00	4.642E-01
30.000	1.324E 00	3.918E 00	5.242E 00	1.133E 01	5.461E-01
40.000	1.350E 00	5.345E 00	6.694E 00	1.302E 01	6.033E-01
50.000	1.368E 00	6.822E 00	8.190E 00	1.436E 01	6.460E-01
60.000	1.383E 00	8.310E 00	9.693E 00	1.548E 01	6.793E-01
80.000	1.405E 00	1.132E 01	1.272E 01	1.728E 01	7.281E-01
100.000	1.422E 00	1.434E 01	1.576E 01	1.869E 01	7.626E-01
200.000	1.470E 00	2.963E 01	3.111E 01	2.312E 01	8.492E-01
300.000	1.497E 00	4.504E 01	4.653E 01	2.574E 01	8.866E-01
400.000	1.515E 00	6.046E 01	6.197E 01	2.759E 01	9.079E-01
500.000	1.529E 00	7.591E 01	7.744E 01	2.903E 01	9.220E-01
600.000	1.541E 00	9.138E 01	9.292E 01	3.021E 01	9.320E-01
800.000	1.558E 00	1.223E 02	1.239E 02	3.207E 01	9.454E-01
1000.000	1.572E 00	1.533E 02	1.549E 02	3.351E 01	9.540E-01

ELECTRONS IN LEAD

ENERGY	STOPPING POWER COLLISION	STOPPING POWER RADIATION	STOPPING POWER TOTAL	RANGE	RADIATION YIELD
MEV	MEV CM2/G	MEV CM2/G	MEV CM2/G	G/CM2	
0.010	8.419E 00	4.513E-02	8.464E 00	8.251E-04	3.372E-03
0.015	6.556E 00	4.614E-02	6.602E 00	1.501E-03	4.306E-03
0.020	5.450E 00	4.620E-02	5.496E 00	2.335E-03	5.158E-03
0.025	4.711E 00	4.713E-02	4.758E 00	3.316E-03	5.958E-03
0.030	4.179E 00	4.827E-02	4.228E 00	4.434E-03	6.742E-03
0.035	3.777E 00	4.967E-02	3.827E 00	5.679E-03	7.522E-03
0.040	3.462E 00	5.074E-02	3.513E 00	7.044E-03	8.296E-03
0.045	3.207E 00	5.172E-02	3.259E 00	8.524E-03	9.059E-03
0.050	2.997E 00	5.262E-02	3.049E 00	1.011E-02	9.810E-03
0.055	2.820E 00	5.346E-02	2.873E 00	1.180E-02	1.055E-02
0.060	2.669E 00	5.426E-02	2.724E 00	1.359E-02	1.127E-02
0.065	2.539E 00	5.503E-02	2.594E 00	1.547E-02	1.199E-02
0.070	2.426E 00	5.576E-02	2.481E 00	1.744E-02	1.269E-02
0.075	2.326E 00	5.647E-02	2.382E 00	1.950E-02	1.339E-02
0.080	2.237E 00	5.716E-02	2.294E 00	2.164E-02	1.407E-02
0.085	2.158E 00	5.745E-02	2.216E 00	2.386E-02	1.473E-02
0.090	2.087E 00	5.812E-02	2.145E 00	2.615E-02	1.539E-02
0.095	2.023E 00	5.878E-02	2.082E 00	2.852E-02	1.603E-02
0.100	1.964E 00	5.944E-02	2.024E 00	3.096E-02	1.667E-02
0.150	1.584E 00	6.593E-02	1.650E 00	5.863E-02	2.270E-02
0.200	1.389E 00	7.251E-02	1.461E 00	9.100E-02	2.824E-02
0.250	1.272E 00	7.864E-02	1.350E 00	1.267E-01	3.339E-02
0.300	1.196E 00	8.460E-02	1.280E 00	1.648E-01	3.820E-02
0.350	1.143E 00	9.041E-02	1.234E 00	2.046E-01	4.270E-02
0.400	1.106E 00	9.623E-02	1.203E 00	2.457E-01	4.695E-02
0.450	1.079E 00	1.020E-01	1.181E 00	2.877E-01	5.098E-02
0.500	1.059E 00	1.078E-01	1.167E 00	3.303E-01	5.482E-02
0.550	1.044E 00	1.136E-01	1.158E 00	3.733E-01	5.850E-02
0.600	1.033E 00	1.194E-01	1.152E 00	4.166E-01	6.204E-02
0.650	1.024E 00	1.252E-01	1.149E 00	4.601E-01	6.544E-02
0.700	1.018E 00	1.310E-01	1.149E 00	5.036E-01	6.873E-02
0.750	1.013E 00	1.367E-01	1.150E 00	5.471E-01	7.191E-02
0.800	1.010E 00	1.425E-01	1.153E 00	5.906E-01	7.500E-02
0.850	1.008E 00	1.487E-01	1.157E 00	6.339E-01	7.801E-02
0.900	1.003E 00	1.545E-01	1.157E 00	6.771E-01	8.096E-02
0.950	1.002E 00	1.603E-01	1.162E 00	7.202E-01	8.384E-02
1.000	1.002E 00	1.661E-01	1.168E 00	7.631E-01	8.666E-02
1.100	1.003E 00	1.776E-01	1.180E 00	8.483E-01	9.208E-02
1.200	1.005E 00	1.891E-01	1.194E 00	9.326E-01	9.728E-02
1.300	1.008E 00	2.005E-01	1.208E 00	1.016E 00	1.023E-01

ELECTRONS IN LEAD

ENERGY	STOPPING POWER COLLISION	STOPPING POWER RADIATION	STOPPING POWER TOTAL	RANGE	RADIATION YIELD
MEV	MEV CM2/G	MEV CM2/G	MEV CM2/G	G/CM2	
1.400	1.011E 00	2.120E-01	1.223E 00	1.098E 00	1.071E-01
1.500	1.015E 00	2.234E-01	1.238E 00	1.179E 00	1.117E-01
1.600	1.019E 00	2.348E-01	1.254E 00	1.260E 00	1.163E-01
1.700	1.023E 00	2.457E-01	1.269E 00	1.339E 00	1.206E-01
1.800	1.027E 00	2.571E-01	1.284E 00	1.417E 00	1.249E-01
1.900	1.032E 00	2.686E-01	1.300E 00	1.495E 00	1.290E-01
2.000	1.036E 00	2.802E-01	1.316E 00	1.571E 00	1.330E-01
2.200	1.044E 00	3.035E-01	1.348E 00	1.721E 00	1.409E-01
2.400	1.053E 00	3.270E-01	1.380E 00	1.868E 00	1.484E-01
2.600	1.061E 00	3.508E-01	1.412E 00	2.011E 00	1.556E-01
2.800	1.069E 00	3.758E-01	1.444E 00	2.151E 00	1.627E-01
3.000	1.076E 00	3.999E-01	1.476E 00	2.288E 00	1.695E-01
3.500	1.093E 00	4.603E-01	1.554E 00	2.618E 00	1.858E-01
4.000	1.109E 00	5.212E-01	1.630E 00	2.933E 00	2.011E-01
4.500	1.123E 00	5.822E-01	1.705E 00	3.232E 00	2.155E-01
5.000	1.135E 00	6.437E-01	1.779E 00	3.519E 00	2.292E-01
5.500	1.147E 00	7.056E-01	1.852E 00	3.795E 00	2.421E-01
6.000	1.157E 00	7.678E-01	1.925E 00	4.060E 00	2.544E-01
6.500	1.167E 00	8.304E-01	1.997E 00	4.315E 00	2.662E-01
7.000	1.176E 00	8.933E-01	2.069E 00	4.561E 00	2.775E-01
7.500	1.184E 00	9.565E-01	2.140E 00	4.798E 00	2.882E-01
8.000	1.191E 00	1.020E 00	2.211E 00	5.028E 00	2.986E-01
8.500	1.199E 00	1.084E 00	2.282E 00	5.251E 00	3.086E-01
9.000	1.205E 00	1.146E 00	2.352E 00	5.466E 00	3.182E-01
9.500	1.212E 00	1.211E 00	2.422E 00	5.676E 00	3.274E-01
10.000	1.217E 00	1.275E 00	2.493E 00	5.879E 00	3.363E-01
20.000	1.293E 00	2.614E 00	3.907E 00	9.060E 00	4.682E-01
30.000	1.334E 00	4.003E 00	5.337E 00	1.124E 01	5.499E-01
40.000	1.360E 00	5.422E 00	6.783E 00	1.290E 01	6.065E-01
50.000	1.380E 00	6.923E 00	8.303E 00	1.423E 01	6.487E-01
60.000	1.396E 00	8.434E 00	9.829E 00	1.534E 01	6.817E-01
80.000	1.419E 00	1.148E 01	1.290E 01	1.711E 01	7.301E-01
100.000	1.436E 00	1.455E 01	1.599E 01	1.850E 01	7.642E-01
200.000	1.485E 00	3.008E 01	3.156E 01	2.287E 01	8.502E-01
300.000	1.511E 00	4.571E 01	4.722E 01	2.544E 01	8.873E-01
400.000	1.529E 00	6.136E 01	6.289E 01	2.727E 01	9.085E-01
500.000	1.543E 00	7.704E 01	7.858E 01	2.869E 01	9.225E-01
600.000	1.554E 00	9.274E 01	9.430E 01	2.985E 01	9.324E-01
800.000	1.571E 00	1.242E 02	1.257E 02	3.168E 01	9.457E-01
1000.000	1.585E 00	1.556E 02	1.572E 02	3.310E 01	9.543E-01

ELECTRONS IN URANIUM

ENERGY	STOPPING POWER			RANGE	RADIATION YIELD
	COLLISION	RADIATION	TOTAL		
MEV	MEV CM2/G	MEV CM2/G	MEV CM2/G	G/CM2	
0.010	7.874E 00	4.947E-02	7.924E 00	9.243E-04	4.044E-03
0.015	6.167E 00	5.061E-02	6.218E 00	1.643E-03	5.099E-03
0.020	5.143E 00	5.070E-02	5.194E 00	2.528E-03	6.067E-03
0.025	4.456E 00	5.171E-02	4.507E 00	3.565E-03	6.977E-03
0.030	3.959E 00	5.295E-02	4.012E 00	4.743E-03	7.870E-03
0.035	3.583E 00	5.444E-02	3.637E 00	6.054E-03	8.758E-03
0.040	3.286E 00	5.560E-02	3.342E 00	7.490E-03	9.639E-03
0.045	3.047E 00	5.667E-02	3.104E 00	9.044E-03	1.051E-02
0.050	2.849E 00	5.767E-02	2.907E 00	1.071E-02	1.136E-02
0.055	2.682E 00	5.861E-02	2.741E 00	1.248E-02	1.220E-02
0.060	2.540E 00	5.950E-02	2.600E 00	1.436E-02	1.303E-02
0.065	2.418E 00	6.035E-02	2.478E 00	1.633E-02	1.385E-02
0.070	2.311E 00	6.117E-02	2.372E 00	1.839E-02	1.465E-02
0.075	2.216E 00	6.197E-02	2.278E 00	2.054E-02	1.544E-02
0.080	2.133E 00	6.274E-02	2.195E 00	2.278E-02	1.622E-02
0.085	2.058E 00	6.325E-02	2.121E 00	2.510E-02	1.698E-02
0.090	1.990E 00	6.400E-02	2.054E 00	2.749E-02	1.773E-02
0.095	1.930E 00	6.474E-02	1.994E 00	2.996E-02	1.847E-02
0.100	1.874E 00	6.547E-02	1.940E 00	3.251E-02	1.920E-02
0.150	1.514E 00	7.253E-02	1.587E 00	6.133E-02	2.609E-02
0.200	1.329E 00	7.944E-02	1.408E 00	9.495E-02	3.235E-02
0.250	1.218E 00	8.605E-02	1.304E 00	1.320E-01	3.814E-02
0.300	1.146E 00	9.254E-02	1.238E 00	1.714E-01	4.352E-02
0.350	1.096E 00	9.892E-02	1.195E 00	2.125E-01	4.856E-02
0.400	1.061E 00	1.053E-01	1.166E 00	2.549E-01	5.331E-02
0.450	1.034E 00	1.116E-01	1.146E 00	2.982E-01	5.781E-02
0.500	1.015E 00	1.180E-01	1.133E 00	3.420E-01	6.211E-02
0.550	1.001E 00	1.243E-01	1.125E 00	3.863E-01	6.622E-02
0.600	9.903E-01	1.306E-01	1.121E 00	4.309E-01	7.016E-02
0.650	9.817E-01	1.370E-01	1.119E 00	4.755E-01	7.396E-02
0.700	9.756E-01	1.433E-01	1.119E 00	5.202E-01	7.762E-02
0.750	9.710E-01	1.496E-01	1.121E 00	5.649E-01	8.117E-02
0.800	9.677E-01	1.560E-01	1.124E 00	6.094E-01	8.461E-02
0.850	9.653E-01	1.626E-01	1.128E 00	6.539E-01	8.796E-02
0.900	9.638E-01	1.689E-01	1.133E 00	6.981E-01	9.122E-02
0.950	9.629E-01	1.752E-01	1.138E 00	7.421E-01	9.439E-02
1.000	9.625E-01	1.816E-01	1.144E 00	7.860E-01	9.749E-02
1.100	9.630E-01	1.942E-01	1.157E 00	8.729E-01	1.035E-01
1.200	9.646E-01	2.068E-01	1.171E 00	9.588E-01	1.092E-01
1.300	9.671E-01	2.194E-01	1.187E 00	1.044E 00	1.147E-01

ELECTRONS IN URANIUM

ENERGY	STOPPING POWER			RANGE	RADIATION YIELD
	COLLISION	RADIATION	TOTAL		
MEV	MEV CM2/G	MEV CM2/G	MEV CM2/G	G/CM2	
1.400	9.701E-01	2.321E-01	1.202E 00	1.127E 00	1.200E-01
1.500	9.736E-01	2.447E-01	1.218E 00	1.210E 00	1.251E-01
1.600	9.772E-01	2.573E-01	1.234E 00	1.291E 00	1.301E-01
1.700	9.811E-01	2.696E-01	1.251E 00	1.372E 00	1.349E-01
1.800	9.850E-01	2.822E-01	1.267E 00	1.451E 00	1.396E-01
1.900	9.890E-01	2.948E-01	1.284E 00	1.530E 00	1.442E-01
2.000	9.930E-01	3.075E-01	1.301E 00	1.607E 00	1.486E-01
2.200	1.001E 00	3.330E-01	1.334E 00	1.759E 00	1.572E-01
2.400	1.009E 00	3.586E-01	1.367E 00	1.907E 00	1.654E-01
2.600	1.016E 00	3.843E-01	1.401E 00	2.052E 00	1.733E-01
2.800	1.024E 00	4.108E-01	1.434E 00	2.193E 00	1.810E-01
3.000	1.030E 00	4.367E-01	1.467E 00	2.331E 00	1.884E-01
3.500	1.047E 00	5.016E-01	1.548E 00	2.662E 00	2.059E-01
4.000	1.061E 00	5.666E-01	1.628E 00	2.977E 00	2.222E-01
4.500	1.074E 00	6.314E-01	1.706E 00	3.277E 00	2.374E-01
5.000	1.086E 00	6.967E-01	1.783E 00	3.564E 00	2.517E-01
5.500	1.097E 00	7.623E-01	1.859E 00	3.839E 00	2.653E-01
6.000	1.107E 00	8.283E-01	1.935E 00	4.102E 00	2.781E-01
6.500	1.116E 00	8.946E-01	2.010E 00	4.356E 00	2.903E-01
7.000	1.124E 00	9.612E-01	2.085E 00	4.600E 00	3.019E-01
7.500	1.132E 00	1.028E 00	2.160E 00	4.836E 00	3.130E-01
8.000	1.139E 00	1.095E 00	2.234E 00	5.063E 00	3.237E-01
8.500	1.146E 00	1.163E 00	2.308E 00	5.283E 00	3.339E-01
9.000	1.152E 00	1.230E 00	2.382E 00	5.497E 00	3.437E-01
9.500	1.158E 00	1.298E 00	2.456E 00	5.703E 00	3.531E-01
10.000	1.164E 00	1.366E 00	2.530E 00	5.904E 00	3.621E-01
20.000	1.236E 00	2.770E 00	4.006E 00	9.018E 00	4.940E-01
30.000	1.274E 00	4.238E 00	5.512E 00	1.114E 01	5.739E-01
40.000	1.300E 00	5.760E 00	7.059E 00	1.274E 01	6.289E-01
50.000	1.319E 00	7.354E 00	8.673E 00	1.402E 01	6.697E-01
60.000	1.334E 00	8.961E 00	1.029E 01	1.507E 01	7.014E-01
80.000	1.356E 00	1.220E 01	1.356E 01	1.676E 01	7.477E-01
100.000	1.373E 00	1.546E 01	1.684E 01	1.808E 01	7.801E-01
200.000	1.421E 00	3.197E 01	3.339E 01	2.222E 01	8.611E-01
300.000	1.446E 00	4.858E 01	5.003E 01	2.465E 01	8.958E-01
400.000	1.464E 00	6.521E 01	6.668E 01	2.638E 01	9.156E-01
500.000	1.478E 00	8.188E 01	8.335E 01	2.772E 01	9.285E-01
600.000	1.489E 00	9.856E 01	1.001E 02	2.881E 01	9.377E-01
800.000	1.506E 00	1.320E 02	1.335E 02	3.053E 01	9.501E-01
1000.000	1.519E 00	1.653E 02	1.669E 02	3.187E 01	9.580E-01

ELECTRONS IN WATER

ENERGY	STOPPING POWER			RANGE	RADIATION YIELD
	COLLISION	RADIATION	TOTAL		
MEV	MEV CM2/G	MEV CM2/G	MEV CM2/G	G/CM2	
0.010	2.320E 01	5.069E-03	2.321E 01	2.436E-04	1.245E-04
0.015	1.690E 01	4.969E-03	1.691E 01	4.998E-04	1.686E-04
0.020	1.350E 01	4.904E-03	1.351E 01	8.331E-04	2.087E-04
0.025	1.136E 01	4.858E-03	1.137E 01	1.238E-03	2.460E-04
0.030	9.879E 00	4.825E-03	9.884E 00	1.712E-03	2.814E-04
0.035	8.789E 00	4.792E-03	8.794E 00	2.249E-03	3.150E-04
0.040	7.951E 00	4.788E-03	7.956E 00	2.848E-03	3.473E-04
0.045	7.287E 00	4.796E-03	7.292E 00	3.505E-03	3.787E-04
0.050	6.747E 00	4.812E-03	6.751E 00	4.218E-03	4.093E-04
0.055	6.298E 00	4.835E-03	6.303E 00	4.986E-03	4.394E-04
0.060	5.919E 00	4.863E-03	5.924E 00	5.804E-03	4.689E-04
0.065	5.596E 00	4.896E-03	5.600E 00	6.673E-03	4.981E-04
0.070	5.315E 00	4.932E-03	5.320E 00	7.589E-03	5.268E-04
0.075	5.070E 00	4.970E-03	5.075E 00	8.552E-03	5.552E-04
0.080	4.854E 00	5.011E-03	4.859E 00	9.559E-03	5.834E-04
0.085	4.662E 00	5.044E-03	4.667E 00	1.061E-02	6.111E-04
0.090	4.491E 00	5.089E-03	4.496E 00	1.170E-02	6.386E-04
0.095	4.336E 00	5.136E-03	4.341E 00	1.283E-02	6.660E-04
0.100	4.197E 00	5.184E-03	4.202E 00	1.400E-02	6.931E-04
0.150	3.299E 00	5.716E-03	3.304E 00	2.760E-02	9.565E-04
0.200	2.844E 00	6.286E-03	2.850E 00	4.400E-02	1.210E-03
0.250	2.573E 00	6.909E-03	2.580E 00	6.250E-02	1.456E-03
0.300	2.394E 00	7.561E-03	2.401E 00	8.263E-02	1.699E-03
0.350	2.271E 00	8.243E-03	2.280E 00	1.040E-01	1.940E-03
0.400	2.181E 00	8.921E-03	2.190E 00	1.264E-01	2.178E-03
0.450	2.113E 00	9.613E-03	2.123E 00	1.496E-01	2.414E-03
0.500	2.061E 00	1.030E-02	2.071E 00	1.735E-01	2.647E-03
0.550	2.021E 00	1.099E-02	2.032E 00	1.979E-01	2.879E-03
0.600	1.989E 00	1.168E-02	2.000E 00	2.227E-01	3.107E-03
0.650	1.963E 00	1.237E-02	1.975E 00	2.478E-01	3.334E-03
0.700	1.942E 00	1.306E-02	1.955E 00	2.733E-01	3.558E-03
0.750	1.925E 00	1.376E-02	1.939E 00	2.990E-01	3.780E-03
0.800	1.911E 00	1.445E-02	1.926E 00	3.248E-01	4.000E-03
0.850	1.900E 00	1.515E-02	1.915E 00	3.509E-01	4.218E-03
0.900	1.890E 00	1.586E-02	1.906E 00	3.771E-01	4.435E-03
0.950	1.882E 00	1.656E-02	1.899E 00	4.033E-01	4.650E-03
1.000	1.876E 00	1.727E-02	1.893E 00	4.297E-01	4.863E-03
1.100	1.866E 00	1.869E-02	1.885E 00	4.827E-01	5.287E-03
1.200	1.860E 00	2.012E-02	1.880E 00	5.358E-01	5.705E-03
1.300	1.856E 00	2.156E-02	1.877E 00	5.890E-01	6.120E-03

ELECTRONS IN WATER

ENERGY	STOPPING POWER			RANGE	RADIATION YIELD
	COLLISION	RADIATION	TOTAL		
MEV	MEV CM2/G	MEV CM2/G	MEV CM2/G	G/CM2	
1.400	1.853E 00	2.301E-02	1.876E 00	6.423E-01	6.531E-03
1.500	1.852E 00	2.447E-02	1.877E 00	6.956E-01	6.939E-03
1.600	1.852E 00	2.593E-02	1.878E 00	7.489E-01	7.344E-03
1.700	1.853E 00	2.736E-02	1.880E 00	8.021E-01	7.745E-03
1.800	1.854E 00	2.885E-02	1.883E 00	8.553E-01	8.145E-03
1.900	1.856E 00	3.035E-02	1.886E 00	9.083E-01	8.543E-03
2.000	1.858E 00	3.187E-02	1.889E 00	9.613E-01	8.940E-03
2.200	1.862E 00	3.494E-02	1.897E 00	1.067E 00	9.731E-03
2.400	1.867E 00	3.806E-02	1.905E 00	1.172E 00	1.052E-02
2.600	1.873E 00	4.123E-02	1.914E 00	1.277E 00	1.131E-02
2.800	1.878E 00	4.432E-02	1.922E 00	1.381E 00	1.209E-02
3.000	1.884E 00	4.757E-02	1.931E 00	1.485E 00	1.288E-02
3.500	1.897E 00	5.593E-02	1.953E 00	1.742E 00	1.484E-02
4.000	1.909E 00	6.458E-02	1.974E 00	1.997E 00	1.682E-02
4.500	1.920E 00	7.356E-02	1.994E 00	2.249E 00	1.882E-02
5.000	1.931E 00	8.270E-02	2.014E 00	2.499E 00	2.083E-02
5.500	1.940E 00	9.202E-02	2.032E 00	2.746E 00	2.287E-02
6.000	1.949E 00	1.015E-01	2.051E 00	2.991E 00	2.491E-02
6.500	1.957E 00	1.111E-01	2.068E 00	3.234E 00	2.696E-02
7.000	1.964E 00	1.209E-01	2.085E 00	3.474E 00	2.902E-02
7.500	1.971E 00	1.307E-01	2.102E 00	3.713E 00	3.109E-02
8.000	1.978E 00	1.408E-01	2.119E 00	3.950E 00	3.317E-02
8.500	1.984E 00	1.509E-01	2.135E 00	4.185E 00	3.525E-02
9.000	1.989E 00	1.621E-01	2.152E 00	4.418E 00	3.735E-02
9.500	1.995E 00	1.724E-01	2.167E 00	4.650E 00	3.946E-02
10.000	2.000E 00	1.829E-01	2.183E 00	4.880E 00	4.157E-02
20.000	2.064E 00	4.055E-01	2.470E 00	9.180E 00	8.311E-02
30.000	2.100E 00	6.419E-01	2.742E 00	1.302E 01	1.221E-01
40.000	2.125E 00	8.849E-01	3.010E 00	1.650E 01	1.578E-01
50.000	2.144E 00	1.132E 00	3.276E 00	1.968E 01	1.903E-01
60.000	2.160E 00	1.383E 00	3.543E 00	2.262E 01	2.200E-01
80.000	2.185E 00	1.890E 00	4.075E 00	2.788E 01	2.722E-01
100.000	2.204E 00	2.403E 00	4.607E 00	3.249E 01	3.165E-01
200.000	2.263E 00	5.010E 00	7.273E 00	4.962E 01	4.669E-01
300.000	2.298E 00	7.648E 00	9.946E 00	6.133E 01	5.556E-01
400.000	2.322E 00	1.030E 01	1.262E 01	7.023E 01	6.152E-01
500.000	2.341E 00	1.296E 01	1.530E 01	7.742E 01	6.587E-01
600.000	2.357E 00	1.562E 01	1.798E 01	8.344E 01	6.920E-01
800.000	2.382E 00	2.095E 01	2.333E 01	9.318E 01	7.401E-01
1000.000	2.401E 00	2.629E 01	2.869E 01	1.009E 02	7.737E-01

ELECTRONS IN CARBON DIOXIDE

ENERGY	STOPPING POWER			RANGE	RADIATION YIELD
	COLLISION	RADIATION	TOTAL		
MEV	MEV CM2/G	MEV CM2/G	MEV CM2/G	G/CM2	
0.010	1.978E 01	5.086E-03	1.978E 01	2.880E-04	1.478E-04
0.015	1.446E 01	4.981E-03	1.447E 01	5.879E-04	1.990E-04
0.020	1.159E 01	4.913E-03	1.159E 01	9.769E-04	2.454E-04
0.025	9.765E 00	4.865E-03	9.770E 00	1.449E-03	2.886E-04
0.030	8.502E 00	4.831E-03	8.507E 00	1.999E-03	3.294E-04
0.035	7.572E 00	4.798E-03	7.577E 00	2.623E-03	3.681E-04
0.040	6.857E 00	4.792E-03	6.861E 00	3.318E-03	4.053E-04
0.045	6.289E 00	4.799E-03	6.293E 00	4.080E-03	4.415E-04
0.050	5.826E 00	4.814E-03	5.831E 00	4.906E-03	4.767E-04
0.055	5.442E 00	4.837E-03	5.446E 00	5.794E-03	5.113E-04
0.060	5.117E 00	4.864E-03	5.122E 00	6.741E-03	5.453E-04
0.065	4.839E 00	4.896E-03	4.844E 00	7.745E-03	5.787E-04
0.070	4.599E 00	4.931E-03	4.604E 00	8.805E-03	6.117E-04
0.075	4.388E 00	4.969E-03	4.393E 00	9.917E-03	6.444E-04
0.080	4.203E 00	5.009E-03	4.208E 00	1.108E-02	6.766E-04
0.085	4.038E 00	5.039E-03	4.043E 00	1.229E-02	7.084E-04
0.090	3.891E 00	5.084E-03	3.896E 00	1.355E-02	7.400E-04
0.095	3.758E 00	5.130E-03	3.763E 00	1.486E-02	7.712E-04
0.100	3.638E 00	5.178E-03	3.643E 00	1.621E-02	8.023E-04
0.150	2.865E 00	5.714E-03	2.870E 00	3.188E-02	1.104E-03
0.200	2.473E 00	6.295E-03	2.479E 00	5.073E-02	1.395E-03
0.250	2.239E 00	6.926E-03	2.246E 00	7.199E-02	1.678E-03
0.300	2.087E 00	7.586E-03	2.094E 00	9.509E-02	1.957E-03
0.350	1.981E 00	8.275E-03	1.989E 00	1.196E-01	2.234E-03
0.400	1.904E 00	8.960E-03	1.913E 00	1.453E-01	2.507E-03
0.450	1.848E 00	9.657E-03	1.857E 00	1.718E-01	2.778E-03
0.500	1.804E 00	1.035E-02	1.815E 00	1.991E-01	3.045E-03
0.550	1.771E 00	1.104E-02	1.782E 00	2.269E-01	3.309E-03
0.600	1.745E 00	1.174E-02	1.757E 00	2.551E-01	3.570E-03
0.650	1.725E 00	1.243E-02	1.737E 00	2.838E-01	3.828E-03
0.700	1.709E 00	1.313E-02	1.722E 00	3.127E-01	4.082E-03
0.750	1.696E 00	1.383E-02	1.710E 00	3.418E-01	4.334E-03
0.800	1.686E 00	1.453E-02	1.700E 00	3.712E-01	4.583E-03
0.850	1.678E 00	1.523E-02	1.693E 00	4.006E-01	4.830E-03
0.900	1.672E 00	1.594E-02	1.687E 00	4.302E-01	5.073E-03
0.950	1.667E 00	1.664E-02	1.683E 00	4.599E-01	5.315E-03
1.000	1.663E 00	1.735E-02	1.681E 00	4.896E-01	5.555E-03
1.100	1.659E 00	1.878E-02	1.678E 00	5.492E-01	6.028E-03
1.200	1.658E 00	2.021E-02	1.678E 00	6.088E-01	6.494E-03
1.300	1.658E 00	2.166E-02	1.680E 00	6.684E-01	6.954E-03

ELECTRONS IN CARBON DIOXIDE

ENERGY	STOPPING POWER			RANGE	RADIATION YIELD
	COLLISION	RADIATION	TOTAL		
MEV	MEV CM2/G	MEV CM2/G	MEV CM2/G	G/CM2	
1.400	1.660E 00	2.311E-02	1.683E 00	7.278E-01	7.408E-03
1.500	1.663E 00	2.457E-02	1.688E 00	7.872E-01	7.857E-03
1.600	1.667E 00	2.604E-02	1.693E 00	8.463E-01	8.302E-03
1.700	1.672E 00	2.747E-02	1.699E 00	9.053E-01	8.740E-03
1.800	1.676E 00	2.896E-02	1.705E 00	9.640E-01	9.176E-03
1.900	1.682E 00	3.047E-02	1.712E 00	1.023E 00	9.608E-03
2.000	1.687E 00	3.199E-02	1.719E 00	1.081E 00	1.004E-02
2.200	1.698E 00	3.506E-02	1.733E 00	1.197E 00	1.089E-02
2.400	1.709E 00	3.819E-02	1.748E 00	1.312E 00	1.174E-02
2.600	1.721E 00	4.136E-02	1.762E 00	1.426E 00	1.258E-02
2.800	1.732E 00	4.444E-02	1.776E 00	1.539E 00	1.341E-02
3.000	1.743E 00	4.770E-02	1.790E 00	1.651E 00	1.424E-02
3.500	1.769E 00	5.606E-02	1.825E 00	1.927E 00	1.630E-02
4.000	1.793E 00	6.472E-02	1.858E 00	2.199E 00	1.836E-02
4.500	1.815E 00	7.371E-02	1.889E 00	2.466E 00	2.042E-02
5.000	1.836E 00	8.286E-02	1.919E 00	2.729E 00	2.249E-02
5.500	1.855E 00	9.218E-02	1.947E 00	2.987E 00	2.456E-02
6.000	1.873E 00	1.017E-01	1.974E 00	3.242E 00	2.663E-02
6.500	1.889E 00	1.113E-01	2.001E 00	3.494E 00	2.870E-02
7.000	1.905E 00	1.210E-01	2.026E 00	3.742E 00	3.077E-02
7.500	1.920E 00	1.309E-01	2.051E 00	3.987E 00	3.284E-02
8.000	1.934E 00	1.409E-01	2.075E 00	4.230E 00	3.491E-02
8.500	1.947E 00	1.511E-01	2.098E 00	4.469E 00	3.697E-02
9.000	1.959E 00	1.622E-01	2.121E 00	4.706E 00	3.904E-02
9.500	1.971E 00	1.726E-01	2.144E 00	4.941E 00	4.112E-02
10.000	1.982E 00	1.831E-01	2.165E 00	5.173E 00	4.319E-02
20.000	2.138E 00	4.057E-01	2.543E 00	9.418E 00	8.302E-02
30.000	2.219E 00	6.422E-01	2.861E 00	1.312E 01	1.196E-01
40.000	2.266E 00	8.851E-01	3.152E 00	1.644E 01	1.530E-01
50.000	2.301E 00	1.132E 00	3.434E 00	1.948E 01	1.836E-01
60.000	2.329E 00	1.383E 00	3.712E 00	2.228E 01	2.116E-01
80.000	2.371E 00	1.890E 00	4.261E 00	2.731E 01	2.611E-01
100.000	2.401E 00	2.403E 00	4.804E 00	3.172E 01	3.034E-01
200.000	2.488E 00	5.007E 00	7.496E 00	4.824E 01	4.495E-01
300.000	2.534E 00	7.643E 00	1.018E 01	5.965E 01	5.375E-01
400.000	2.563E 00	1.029E 01	1.285E 01	6.837E 01	5.976E-01
500.000	2.585E 00	1.295E 01	1.553E 01	7.544E 01	6.417E-01
600.000	2.603E 00	1.561E 01	1.821E 01	8.138E 01	6.757E-01
800.000	2.629E 00	2.093E 01	2.356E 01	9.101E 01	7.253E-01
1000.000	2.648E 00	2.626E 01	2.891E 01	9.866E 01	7.600E-01

ELECTRONS IN SILVER CHLORIDE

ENERGY	STOPPING POWER COLLISION	STOPPING POWER RADIATION	STOPPING POWER TOTAL	RANGE	RADIATION YIELD
MEV	MEV CM2/G	MEV CM2/G	MEV CM2/G	G/CM2	
0.010	1.226E 01	2.339E-02	1.229E 01	5.012E-04	1.141E-03
0.015	9.265E 00	2.340E-02	9.289E 00	9.749E-04	1.499E-03
0.020	7.570E 00	2.309E-02	7.593E 00	1.574E-03	1.821E-03
0.025	6.468E 00	2.341E-02	6.492E 00	2.289E-03	2.121E-03
0.030	5.690E 00	2.393E-02	5.714E 00	3.112E-03	2.417E-03
0.035	5.109E 00	2.465E-02	5.133E 00	4.037E-03	2.714E-03
0.040	4.657E 00	2.517E-02	4.682E 00	5.059E-03	3.011E-03
0.045	4.295E 00	2.564E-02	4.320E 00	6.172E-03	3.305E-03
0.050	3.998E 00	2.607E-02	4.024E 00	7.372E-03	3.596E-03
0.055	3.750E 00	2.648E-02	3.776E 00	8.655E-03	3.882E-03
0.060	3.539E 00	2.687E-02	3.566E 00	1.002E-02	4.165E-03
0.065	3.358E 00	2.724E-02	3.385E 00	1.146E-02	4.444E-03
0.070	3.201E 00	2.760E-02	3.228E 00	1.297E-02	4.719E-03
0.075	3.063E 00	2.794E-02	3.091E 00	1.456E-02	4.991E-03
0.080	2.940E 00	2.828E-02	2.969E 00	1.621E-02	5.259E-03
0.085	2.832E 00	2.851E-02	2.860E 00	1.792E-02	5.522E-03
0.090	2.734E 00	2.884E-02	2.763E 00	1.970E-02	5.783E-03
0.095	2.646E 00	2.915E-02	2.675E 00	2.154E-02	6.040E-03
0.100	2.566E 00	2.947E-02	2.595E 00	2.344E-02	6.294E-03
0.150	2.048E 00	3.247E-02	2.081E 00	4.522E-02	8.703E-03
0.200	1.784E 00	3.509E-02	1.819E 00	7.106E-02	1.090E-02
0.250	1.626E 00	3.812E-02	1.664E 00	9.989E-02	1.294E-02
0.300	1.523E 00	4.129E-02	1.565E 00	1.309E-01	1.489E-02
0.350	1.452E 00	4.465E-02	1.497E 00	1.636E-01	1.678E-02
0.400	1.401E 00	4.788E-02	1.449E 00	1.976E-01	1.862E-02
0.450	1.364E 00	5.113E-02	1.415E 00	2.326E-01	2.039E-02
0.500	1.336E 00	5.432E-02	1.390E 00	2.682E-01	2.211E-02
0.550	1.315E 00	5.748E-02	1.372E 00	3.044E-01	2.378E-02
0.600	1.298E 00	6.060E-02	1.359E 00	3.411E-01	2.541E-02
0.650	1.286E 00	6.369E-02	1.349E 00	3.780E-01	2.698E-02
0.700	1.276E 00	6.677E-02	1.343E 00	4.151E-01	2.852E-02
0.750	1.269E 00	6.982E-02	1.339E 00	4.524E-01	3.001E-02
0.800	1.263E 00	7.286E-02	1.336E 00	4.898E-01	3.147E-02
0.850	1.259E 00	7.488E-02	1.334E 00	5.273E-01	3.286E-02
0.900	1.255E 00	7.790E-02	1.333E 00	5.648E-01	3.422E-02
0.950	1.253E 00	8.093E-02	1.334E 00	6.023E-01	3.555E-02
1.000	1.252E 00	8.399E-02	1.336E 00	6.397E-01	3.686E-02
1.100	1.250E 00	9.016E-02	1.340E 00	7.145E-01	3.943E-02
1.200	1.251E 00	9.639E-02	1.347E 00	7.889E-01	4.193E-02
1.300	1.252E 00	1.027E-01	1.355E 00	8.630E-01	4.437E-02

ELECTRONS IN SILVER CHLORIDE

ENERGY	STOPPING POWER COLLISION	STOPPING POWER RADIATION	STOPPING POWER TOTAL	RANGE	RADIATION YIELD
MEV	MEV CM2/G	MEV CM2/G	MEV CM2/G	G/CM2	
1.400	1.254E 00	1.090E-01	1.363E 00	9.365E-01	4.676E-02
1.500	1.257E 00	1.155E-01	1.372E 00	1.010E 00	4.912E-02
1.600	1.260E 00	1.219E-01	1.382E 00	1.082E 00	5.143E-02
1.700	1.264E 00	1.287E-01	1.392E 00	1.154E 00	5.372E-02
1.800	1.267E 00	1.352E-01	1.403E 00	1.226E 00	5.598E-02
1.900	1.271E 00	1.418E-01	1.413E 00	1.297E 00	5.821E-02
2.000	1.275E 00	1.484E-01	1.423E 00	1.367E 00	6.042E-02
2.200	1.283E 00	1.616E-01	1.445E 00	1.507E 00	6.475E-02
2.400	1.291E 00	1.749E-01	1.466E 00	1.644E 00	6.899E-02
2.600	1.299E 00	1.883E-01	1.487E 00	1.780E 00	7.314E-02
2.800	1.306E 00	2.015E-01	1.507E 00	1.913E 00	7.722E-02
3.000	1.313E 00	2.151E-01	1.528E 00	2.045E 00	8.122E-02
3.500	1.330E 00	2.493E-01	1.579E 00	2.367E 00	9.095E-02
4.000	1.345E 00	2.839E-01	1.629E 00	2.679E 00	1.003E-01
4.500	1.359E 00	3.190E-01	1.678E 00	2.981E 00	1.095E-01
5.000	1.371E 00	3.546E-01	1.725E 00	3.275E 00	1.183E-01
5.500	1.382E 00	3.906E-01	1.773E 00	3.561E 00	1.269E-01
6.000	1.392E 00	4.269E-01	1.819E 00	3.839E 00	1.353E-01
6.500	1.402E 00	4.636E-01	1.865E 00	4.111E 00	1.435E-01
7.000	1.410E 00	5.007E-01	1.911E 00	4.376E 00	1.515E-01
7.500	1.418E 00	5.381E-01	1.956E 00	4.634E 00	1.593E-01
8.000	1.426E 00	5.758E-01	2.002E 00	4.887E 00	1.669E-01
8.500	1.433E 00	6.139E-01	2.047E 00	5.134E 00	1.744E-01
9.000	1.439E 00	6.548E-01	2.094E 00	5.375E 00	1.817E-01
9.500	1.445E 00	6.935E-01	2.139E 00	5.612E 00	1.889E-01
10.000	1.451E 00	7.323E-01	2.184E 00	5.843E 00	1.959E-01
20.000	1.525E 00	1.541E 00	3.066E 00	9.688E 00	3.113E-01
30.000	1.564E 00	2.403E 00	3.967E 00	1.255E 01	3.935E-01
40.000	1.590E 00	3.306E 00	4.896E 00	1.481E 01	4.558E-01
50.000	1.610E 00	4.218E 00	5.828E 00	1.668E 01	5.048E-01
60.000	1.625E 00	5.139E 00	6.764E 00	1.827E 01	5.445E-01
80.000	1.648E 00	7.000E 00	8.648E 00	2.088E 01	6.050E-01
100.000	1.665E 00	8.871E 00	1.054E 01	2.298E 01	6.493E-01
200.000	1.717E 00	1.836E 01	2.007E 01	2.974E 01	7.675E-01
300.000	1.746E 00	2.792E 01	2.966E 01	3.381E 01	8.215E-01
400.000	1.766E 00	3.750E 01	3.926E 01	3.673E 01	8.533E-01
500.000	1.781E 00	4.709E 01	4.887E 01	3.901E 01	8.745E-01
600.000	1.794E 00	5.670E 01	5.850E 01	4.088E 01	8.899E-01
800.000	1.814E 00	7.594E 01	7.775E 01	4.383E 01	9.108E-01
1000.000	1.829E 00	9.518E 01	9.701E 01	4.613E 01	9.244E-01

ELECTRONS IN SILVER BROMIDE

ENERGY	STOPPING POWER COLLISION	STOPPING POWER RADIATION	STOPPING POWER TOTAL	RANGE	RADIATION YIELD
MEV	MEV CM2/G	MEV CM2/G	MEV CM2/G	G/CM2	
0.010	1.156E 01	2.453E-02	1.158E 01	5.378E-04	1.281E-03
0.015	8.769E 00	2.456E-02	8.793E 00	1.039E-03	1.674E-03
0.020	7.181E 00	2.426E-02	7.205E 00	1.671E-03	2.027E-03
0.025	6.145E 00	2.462E-02	6.170E 00	2.424E-03	2.357E-03
0.030	5.412E 00	2.518E-02	5.437E 00	3.290E-03	2.682E-03
0.035	4.864E 00	2.596E-02	4.889E 00	4.261E-03	3.010E-03
0.040	4.437E 00	2.652E-02	4.463E 00	5.333E-03	3.337E-03
0.045	4.094E 00	2.702E-02	4.121E 00	6.500E-03	3.660E-03
0.050	3.813E 00	2.748E-02	3.841E 00	7.758E-03	3.980E-03
0.055	3.578E 00	2.791E-02	3.606E 00	9.102E-03	4.295E-03
0.060	3.379E 00	2.832E-02	3.407E 00	1.053E-02	4.606E-03
0.065	3.207E 00	2.870E-02	3.236E 00	1.204E-02	4.913E-03
0.070	3.058E 00	2.907E-02	3.087E 00	1.362E-02	5.215E-03
0.075	2.927E 00	2.943E-02	2.956E 00	1.528E-02	5.513E-03
0.080	2.811E 00	2.977E-02	2.840E 00	1.700E-02	5.808E-03
0.085	2.707E 00	2.997E-02	2.737E 00	1.880E-02	6.095E-03
0.090	2.614E 00	3.030E-02	2.645E 00	2.065E-02	6.379E-03
0.095	2.531E 00	3.063E-02	2.561E 00	2.258E-02	6.659E-03
0.100	2.455E 00	3.095E-02	2.486E 00	2.456E-02	6.937E-03
0.150	1.962E 00	3.408E-02	1.997E 00	4.728E-02	9.560E-03
0.200	1.711E 00	3.684E-02	1.748E 00	7.420E-02	1.195E-02
0.250	1.560E 00	4.003E-02	1.600E 00	1.042E-01	1.417E-02
0.300	1.463E 00	4.336E-02	1.506E 00	1.365E-01	1.630E-02
0.350	1.393E 00	4.689E-02	1.440E 00	1.705E-01	1.836E-02
0.400	1.345E 00	5.028E-02	1.396E 00	2.058E-01	2.035E-02
0.450	1.311E 00	5.368E-02	1.364E 00	2.420E-01	2.228E-02
0.500	1.284E 00	5.702E-02	1.341E 00	2.790E-01	2.414E-02
0.550	1.264E 00	6.032E-02	1.324E 00	3.166E-01	2.595E-02
0.600	1.249E 00	6.359E-02	1.312E 00	3.545E-01	2.771E-02
0.650	1.236E 00	6.683E-02	1.303E 00	3.927E-01	2.941E-02
0.700	1.227E 00	7.005E-02	1.297E 00	4.312E-01	3.107E-02
0.750	1.220E 00	7.324E-02	1.293E 00	4.698E-01	3.269E-02
0.800	1.215E 00	7.643E-02	1.291E 00	5.085E-01	3.427E-02
0.850	1.211E 00	7.846E-02	1.289E 00	5.473E-01	3.576E-02
0.900	1.208E 00	8.162E-02	1.289E 00	5.861E-01	3.723E-02
0.950	1.205E 00	8.481E-02	1.290E 00	6.248E-01	3.866E-02
1.000	1.204E 00	8.801E-02	1.292E 00	6.636E-01	4.008E-02
1.100	1.203E 00	9.448E-02	1.297E 00	7.408E-01	4.284E-02
1.200	1.203E 00	1.010E-01	1.304E 00	8.177E-01	4.553E-02
1.300	1.205E 00	1.077E-01	1.312E 00	8.942E-01	4.816E-02

ELECTRONS IN SILVER BROMIDE

ENERGY	STOPPING POWER COLLISION	STOPPING POWER RADIATION	STOPPING POWER TOTAL	RANGE	RADIATION YIELD
MEV	MEV CM2/G	MEV CM2/G	MEV CM2/G	G/CM2	
1.400	1.207E 00	1.143E-01	1.321E 00	9.701E-01	5.075E-02
1.500	1.210E 00	1.211E-01	1.331E 00	1.045E 00	5.328E-02
1.600	1.213E 00	1.279E-01	1.341E 00	1.120E 00	5.577E-02
1.700	1.217E 00	1.351E-01	1.352E 00	1.195E 00	5.824E-02
1.800	1.221E 00	1.420E-01	1.363E 00	1.268E 00	6.067E-02
1.900	1.224E 00	1.489E-01	1.373E 00	1.341E 00	6.308E-02
2.000	1.228E 00	1.558E-01	1.384E 00	1.414E 00	6.545E-02
2.200	1.236E 00	1.698E-01	1.406E 00	1.557E 00	7.011E-02
2.400	1.244E 00	1.839E-01	1.428E 00	1.698E 00	7.466E-02
2.600	1.252E 00	1.980E-01	1.450E 00	1.837E 00	7.913E-02
2.800	1.259E 00	2.122E-01	1.471E 00	1.974E 00	8.351E-02
3.000	1.266E 00	2.265E-01	1.493E 00	2.109E 00	8.780E-02
3.500	1.283E 00	2.626E-01	1.546E 00	2.438E 00	9.824E-02
4.000	1.298E 00	2.990E-01	1.597E 00	2.757E 00	1.083E-01
4.500	1.312E 00	3.358E-01	1.648E 00	3.065E 00	1.180E-01
5.000	1.324E 00	3.731E-01	1.697E 00	3.364E 00	1.274E-01
5.500	1.335E 00	4.108E-01	1.746E 00	3.654E 00	1.365E-01
6.000	1.345E 00	4.489E-01	1.794E 00	3.937E 00	1.453E-01
6.500	1.355E 00	4.874E-01	1.842E 00	4.212E 00	1.540E-01
7.000	1.363E 00	5.262E-01	1.890E 00	4.480E 00	1.624E-01
7.500	1.371E 00	5.654E-01	1.937E 00	4.741E 00	1.706E-01
8.000	1.379E 00	6.049E-01	1.984E 00	4.996E 00	1.785E-01
8.500	1.386E 00	6.448E-01	2.031E 00	5.245E 00	1.864E-01
9.000	1.392E 00	6.874E-01	2.080E 00	5.488E 00	1.940E-01
9.500	1.399E 00	7.278E-01	2.126E 00	5.726E 00	2.015E-01
10.000	1.404E 00	7.685E-01	2.173E 00	5.959E 00	2.088E-01
20.000	1.478E 00	1.616E 00	3.094E 00	9.794E 00	3.275E-01
30.000	1.517E 00	2.520E 00	4.037E 00	1.262E 01	4.106E-01
40.000	1.544E 00	3.466E 00	5.010E 00	1.484E 01	4.731E-01
50.000	1.563E 00	4.423E 00	5.986E 00	1.666E 01	5.218E-01
60.000	1.578E 00	5.388E 00	6.967E 00	1.821E 01	5.610E-01
80.000	1.601E 00	7.338E 00	8.940E 00	2.074E 01	6.205E-01
100.000	1.619E 00	9.299E 00	1.092E 01	2.276E 01	6.639E-01
200.000	1.670E 00	1.924E 01	2.091E 01	2.926E 01	7.784E-01
300.000	1.698E 00	2.926E 01	3.096E 01	3.317E 01	8.304E-01
400.000	1.718E 00	3.930E 01	4.102E 01	3.597E 01	8.608E-01
500.000	1.733E 00	4.935E 01	5.108E 01	3.815E 01	8.811E-01
600.000	1.746E 00	5.942E 01	6.116E 01	3.993E 01	8.958E-01
800.000	1.765E 00	7.957E 01	8.134E 01	4.276E 01	9.156E-01
1000.000	1.780E 00	9.973E 01	1.015E 02	4.496E 01	9.286E-01

ELECTRONS IN SODIUM IODIDE

ENERGY	STOPPING POWER			RANGE	RADIATION YIELD
	COLLISION	RADIATION	TOTAL		
MEV	MEV CM2/G	MEV CM2/G	MEV CM2/G	G/CM2	
0.010	1.131E 01	2.643E-02	1.134E 01	5.494E-04	1.398E-03
0.015	8.579E 00	2.683E-02	8.606E 00	1.062E-03	1.842E-03
0.020	7.025E 00	2.711E-02	7.053E 00	1.707E-03	2.253E-03
0.025	6.012E 00	2.761E-02	6.040E 00	2.476E-03	2.644E-03
0.030	5.295E 00	2.816E-02	5.323E 00	3.361E-03	3.025E-03
0.035	4.758E 00	2.878E-02	4.787E 00	4.353E-03	3.400E-03
0.040	4.340E 00	2.931E-02	4.370E 00	5.448E-03	3.771E-03
0.045	4.005E 00	2.980E-02	4.035E 00	6.640E-03	4.135E-03
0.050	3.730E 00	3.027E-02	3.761E 00	7.925E-03	4.493E-03
0.055	3.500E 00	3.072E-02	3.531E 00	9.298E-03	4.846E-03
0.060	3.305E 00	3.114E-02	3.336E 00	1.076E-02	5.194E-03
0.065	3.137E 00	3.155E-02	3.169E 00	1.229E-02	5.536E-03
0.070	2.991E 00	3.195E-02	3.023E 00	1.391E-02	5.874E-03
0.075	2.863E 00	3.234E-02	2.895E 00	1.560E-02	6.207E-03
0.080	2.749E 00	3.272E-02	2.782E 00	1.736E-02	6.536E-03
0.085	2.648E 00	3.301E-02	2.681E 00	1.919E-02	6.859E-03
0.090	2.557E 00	3.338E-02	2.591E 00	2.109E-02	7.178E-03
0.095	2.475E 00	3.375E-02	2.509E 00	2.305E-02	7.493E-03
0.100	2.401E 00	3.411E-02	2.435E 00	2.508E-02	7.805E-03
0.150	1.920E 00	3.762E-02	1.957E 00	4.826E-02	1.076E-02
0.200	1.673E 00	4.078E-02	1.714E 00	7.571E-02	1.346E-02
0.250	1.526E 00	4.433E-02	1.571E 00	1.063E-01	1.597E-02
0.300	1.430E 00	4.801E-02	1.478E 00	1.391E-01	1.837E-02
0.350	1.364E 00	5.189E-02	1.416E 00	1.737E-01	2.068E-02
0.400	1.317E 00	5.559E-02	1.373E 00	2.096E-01	2.292E-02
0.450	1.282E 00	5.930E-02	1.342E 00	2.465E-01	2.508E-02
0.500	1.256E 00	6.293E-02	1.319E 00	2.841E-01	2.717E-02
0.550	1.237E 00	6.649E-02	1.303E 00	3.223E-01	2.919E-02
0.600	1.221E 00	7.002E-02	1.291E 00	3.608E-01	3.114E-02
0.650	1.210E 00	7.350E-02	1.283E 00	3.997E-01	3.304E-02
0.700	1.201E 00	7.694E-02	1.278E 00	4.387E-01	3.487E-02
0.750	1.195E 00	8.036E-02	1.275E 00	4.779E-01	3.666E-02
0.800	1.190E 00	8.375E-02	1.273E 00	5.171E-01	3.839E-02
0.850	1.186E 00	8.578E-02	1.272E 00	5.564E-01	4.003E-02
0.900	1.183E 00	8.913E-02	1.272E 00	5.957E-01	4.162E-02
0.950	1.181E 00	9.250E-02	1.274E 00	6.350E-01	4.319E-02
1.000	1.180E 00	9.589E-02	1.276E 00	6.742E-01	4.472E-02
1.100	1.179E 00	1.027E-01	1.281E 00	7.525E-01	4.772E-02
1.200	1.179E 00	1.096E-01	1.289E 00	8.303E-01	5.063E-02
1.300	1.181E 00	1.166E-01	1.297E 00	9.076E-01	5.346E-02

ELECTRONS IN SODIUM IODIDE

ENERGY	STOPPING POWER			RANGE	RADIATION YIELD
	COLLISION	RADIATION	TOTAL		
MEV	MEV CM2/G	MEV CM2/G	MEV CM2/G	G/CM2	
1.400	1.183E 00	1.237E-01	1.307E 00	9.844E-01	5.623E-02
1.500	1.186E 00	1.308E-01	1.317E 00	1.061E 00	5.895E-02
1.600	1.190E 00	1.379E-01	1.328E 00	1.136E 00	6.161E-02
1.700	1.193E 00	1.452E-01	1.339E 00	1.211E 00	6.424E-02
1.800	1.197E 00	1.525E-01	1.350E 00	1.286E 00	6.682E-02
1.900	1.201E 00	1.598E-01	1.361E 00	1.359E 00	6.937E-02
2.000	1.205E 00	1.671E-01	1.372E 00	1.433E 00	7.188E-02
2.200	1.213E 00	1.818E-01	1.395E 00	1.577E 00	7.680E-02
2.400	1.222E 00	1.967E-01	1.418E 00	1.719E 00	8.161E-02
2.600	1.229E 00	2.117E-01	1.441E 00	1.859E 00	8.632E-02
2.800	1.237E 00	2.272E-01	1.464E 00	1.997E 00	9.093E-02
3.000	1.245E 00	2.424E-01	1.487E 00	2.132E 00	9.548E-02
3.500	1.262E 00	2.807E-01	1.543E 00	2.463E 00	1.065E-01
4.000	1.278E 00	3.194E-01	1.597E 00	2.781E 00	1.171E-01
4.500	1.292E 00	3.581E-01	1.650E 00	3.089E 00	1.272E-01
5.000	1.305E 00	3.974E-01	1.702E 00	3.387E 00	1.370E-01
5.500	1.316E 00	4.371E-01	1.754E 00	3.677E 00	1.465E-01
6.000	1.327E 00	4.771E-01	1.804E 00	3.958E 00	1.557E-01
6.500	1.337E 00	5.176E-01	1.855E 00	4.231E 00	1.647E-01
7.000	1.346E 00	5.584E-01	1.905E 00	4.497E 00	1.733E-01
7.500	1.355E 00	5.995E-01	1.954E 00	4.756E 00	1.818E-01
8.000	1.363E 00	6.409E-01	2.004E 00	5.009E 00	1.900E-01
8.500	1.370E 00	6.826E-01	2.053E 00	5.256E 00	1.980E-01
9.000	1.377E 00	7.284E-01	2.105E 00	5.496E 00	2.059E-01
9.500	1.383E 00	7.708E-01	2.154E 00	5.731E 00	2.136E-01
10.000	1.390E 00	8.134E-01	2.203E 00	5.960E 00	2.211E-01
20.000	1.469E 00	1.690E 00	3.159E 00	9.726E 00	3.409E-01
30.000	1.511E 00	2.625E 00	4.136E 00	1.249E 01	4.234E-01
40.000	1.539E 00	3.614E 00	5.153E 00	1.465E 01	4.851E-01
50.000	1.560E 00	4.610E 00	6.170E 00	1.642E 01	5.332E-01
60.000	1.576E 00	5.617E 00	7.193E 00	1.792E 01	5.718E-01
80.000	1.601E 00	7.648E 00	9.249E 00	2.037E 01	6.303E-01
100.000	1.619E 00	9.690E 00	1.131E 01	2.232E 01	6.728E-01
200.000	1.671E 00	2.004E 01	2.171E 01	2.859E 01	7.848E-01
300.000	1.699E 00	3.047E 01	3.217E 01	3.235E 01	8.354E-01
400.000	1.719E 00	4.092E 01	4.264E 01	3.504E 01	8.651E-01
500.000	1.733E 00	5.140E 01	5.313E 01	3.714E 01	8.848E-01
600.000	1.745E 00	6.188E 01	6.362E 01	3.886E 01	8.990E-01
800.000	1.764E 00	8.286E 01	8.463E 01	4.157E 01	9.183E-01
1000.000	1.779E 00	1.038E 02	1.056E 02	4.368E 01	9.309E-01

ELECTRONS IN LITHIUM IODIDE

ENERGY	STOPPING POWER COLLISION	STOPPING POWER RADIATION	STOPPING POWER TOTAL	RANGE	RADIATION YIELD
MEV	MEV CM2/G	MEV CM2/G	MEV CM2/G	G/CM2	
0.010	1.078E 01	2.846E-02	1.081E 01	5.815E-04	1.589E-03
0.015	8.205E 00	2.893E-02	8.234E 00	1.118E-03	2.085E-03
0.020	6.731E 00	2.925E-02	6.760E 00	1.792E-03	2.545E-03
0.025	5.767E 00	2.982E-02	5.797E 00	2.594E-03	2.983E-03
0.030	5.083E 00	3.045E-02	5.114E 00	3.514E-03	3.411E-03
0.035	4.571E 00	3.115E-02	4.602E 00	4.547E-03	3.833E-03
0.040	4.172E 00	3.174E-02	4.204E 00	5.685E-03	4.249E-03
0.045	3.852E 00	3.229E-02	3.884E 00	6.924E-03	4.658E-03
0.050	3.589E 00	3.281E-02	3.622E 00	8.259E-03	5.061E-03
0.055	3.369E 00	3.330E-02	3.402E 00	9.684E-03	5.458E-03
0.060	3.182E 00	3.377E-02	3.216E 00	1.120E-02	5.849E-03
0.065	3.021E 00	3.423E-02	3.055E 00	1.279E-02	6.234E-03
0.070	2.881E 00	3.466E-02	2.916E 00	1.447E-02	6.613E-03
0.075	2.758E 00	3.509E-02	2.793E 00	1.622E-02	6.988E-03
0.080	2.649E 00	3.550E-02	2.685E 00	1.805E-02	7.357E-03
0.085	2.552E 00	3.582E-02	2.588E 00	1.995E-02	7.719E-03
0.090	2.465E 00	3.622E-02	2.501E 00	2.191E-02	8.077E-03
0.095	2.387E 00	3.662E-02	2.423E 00	2.394E-02	8.431E-03
0.100	2.315E 00	3.701E-02	2.352E 00	2.604E-02	8.781E-03
0.150	1.853E 00	4.082E-02	1.894E 00	5.001E-02	1.209E-02
0.200	1.616E 00	4.423E-02	1.661E 00	7.837E-02	1.510E-02
0.250	1.475E 00	4.806E-02	1.523E 00	1.099E-01	1.791E-02
0.300	1.383E 00	5.203E-02	1.435E 00	1.438E-01	2.058E-02
0.350	1.320E 00	5.622E-02	1.376E 00	1.794E-01	2.315E-02
0.400	1.274E 00	6.022E-02	1.334E 00	2.164E-01	2.563E-02
0.450	1.241E 00	6.422E-02	1.305E 00	2.543E-01	2.803E-02
0.500	1.216E 00	6.813E-02	1.284E 00	2.929E-01	3.034E-02
0.550	1.197E 00	7.197E-02	1.269E 00	3.321E-01	3.257E-02
0.600	1.183E 00	7.576E-02	1.258E 00	3.717E-01	3.473E-02
0.650	1.172E 00	7.951E-02	1.251E 00	4.115E-01	3.682E-02
0.700	1.163E 00	8.322E-02	1.246E 00	4.516E-01	3.885E-02
0.750	1.156E 00	8.689E-02	1.243E 00	4.918E-01	4.081E-02
0.800	1.151E 00	9.054E-02	1.241E 00	5.320E-01	4.273E-02
0.850	1.147E 00	9.265E-02	1.239E 00	5.724E-01	4.453E-02
0.900	1.143E 00	9.625E-02	1.240E 00	6.127E-01	4.629E-02
0.950	1.141E 00	9.987E-02	1.241E 00	6.530E-01	4.802E-02
1.000	1.140E 00	1.035E-01	1.243E 00	6.933E-01	4.971E-02
1.100	1.138E 00	1.109E-01	1.249E 00	7.735E-01	5.301E-02
1.200	1.139E 00	1.183E-01	1.257E 00	8.533E-01	5.621E-02
1.300	1.140E 00	1.258E-01	1.266E 00	9.326E-01	5.933E-02

ELECTRONS IN LITHIUM IODIDE

ENERGY	STOPPING POWER COLLISION	STOPPING POWER RADIATION	STOPPING POWER TOTAL	RANGE	RADIATION YIELD
MEV	MEV CM2/G	MEV CM2/G	MEV CM2/G	G/CM2	
1.400	1.142E 00	1.334E-01	1.276E 00	1.011E 00	6.238E-02
1.500	1.145E 00	1.410E-01	1.286E 00	1.089E 00	6.536E-02
1.600	1.148E 00	1.488E-01	1.297E 00	1.167E 00	6.829E-02
1.700	1.151E 00	1.567E-01	1.308E 00	1.244E 00	7.117E-02
1.800	1.155E 00	1.645E-01	1.320E 00	1.320E 00	7.401E-02
1.900	1.159E 00	1.723E-01	1.331E 00	1.395E 00	7.680E-02
2.000	1.163E 00	1.802E-01	1.343E 00	1.470E 00	7.955E-02
2.200	1.170E 00	1.961E-01	1.367E 00	1.618E 00	8.494E-02
2.400	1.178E 00	2.121E-01	1.390E 00	1.763E 00	9.020E-02
2.600	1.186E 00	2.282E-01	1.414E 00	1.905E 00	9.534E-02
2.800	1.193E 00	2.450E-01	1.438E 00	2.046E 00	1.004E-01
3.000	1.200E 00	2.614E-01	1.461E 00	2.184E 00	1.053E-01
3.500	1.217E 00	3.025E-01	1.519E 00	2.519E 00	1.173E-01
4.000	1.232E 00	3.440E-01	1.576E 00	2.842E 00	1.287E-01
4.500	1.245E 00	3.855E-01	1.631E 00	3.154E 00	1.397E-01
5.000	1.258E 00	4.276E-01	1.685E 00	3.456E 00	1.502E-01
5.500	1.269E 00	4.701E-01	1.739E 00	3.748E 00	1.604E-01
6.000	1.279E 00	5.130E-01	1.792E 00	4.031E 00	1.702E-01
6.500	1.289E 00	5.563E-01	1.845E 00	4.306E 00	1.798E-01
7.000	1.298E 00	5.999E-01	1.897E 00	4.573E 00	1.890E-01
7.500	1.306E 00	6.439E-01	1.950E 00	4.833E 00	1.979E-01
8.000	1.313E 00	6.883E-01	2.002E 00	5.086E 00	2.066E-01
8.500	1.320E 00	7.329E-01	2.053E 00	5.333E 00	2.151E-01
9.000	1.327E 00	7.819E-01	2.109E 00	5.573E 00	2.233E-01
9.500	1.334E 00	8.272E-01	2.161E 00	5.807E 00	2.314E-01
10.000	1.339E 00	8.728E-01	2.212E 00	6.036E 00	2.393E-01
20.000	1.416E 00	1.808E 00	3.225E 00	9.754E 00	3.630E-01
30.000	1.457E 00	2.807E 00	4.264E 00	1.244E 01	4.464E-01
40.000	1.485E 00	3.864E 00	5.349E 00	1.453E 01	5.080E-01
50.000	1.505E 00	4.929E 00	6.434E 00	1.624E 01	5.555E-01
60.000	1.521E 00	6.005E 00	7.526E 00	1.767E 01	5.934E-01
80.000	1.545E 00	8.176E 00	9.721E 00	2.000E 01	6.503E-01
100.000	1.563E 00	1.036E 01	1.192E 01	2.186E 01	6.914E-01
200.000	1.615E 00	2.142E 01	2.303E 01	2.779E 01	7.986E-01
300.000	1.642E 00	3.256E 01	3.420E 01	3.133E 01	8.469E-01
400.000	1.661E 00	4.372E 01	4.539E 01	3.386E 01	8.744E-01
500.000	1.676E 00	5.491E 01	5.658E 01	3.583E 01	8.930E-01
600.000	1.687E 00	6.611E 01	6.779E 01	3.744E 01	9.063E-01
800.000	1.706E 00	8.852E 01	9.022E 01	3.999E 01	9.243E-01
1000.000	1.720E 00	1.109E 02	1.127E 02	4.197E 01	9.361E-01

ELECTRONS IN METHANE

ENERGY	STOPPING POWER			RANGE	RADIATION YIELD
	COLLISION	RADIATION	TOTAL		
MEV	MEV CM2/G	MEV CM2/G	MEV CM2/G	G/CM2	
0.010	2.803E 01	3.556E-03	2.803E 01	1.997E-04	7.186E-05
0.015	2.031E 01	3.490E-03	2.032E 01	4.125E-04	9.780E-05
0.020	1.618E 01	3.453E-03	1.618E 01	6.903E-04	1.216E-04
0.025	1.358E 01	3.429E-03	1.359E 01	1.029E-03	1.439E-04
0.030	1.179E 01	3.413E-03	1.179E 01	1.425E-03	1.651E-04
0.035	1.047E 01	3.400E-03	1.048E 01	1.876E-03	1.853E-04
0.040	9.465E 00	3.400E-03	9.469E 00	2.379E-03	2.049E-04
0.045	8.666E 00	3.406E-03	8.670E 00	2.932E-03	2.239E-04
0.050	8.017E 00	3.418E-03	8.020E 00	3.532E-03	2.425E-04
0.055	7.478E 00	3.433E-03	7.482E 00	4.178E-03	2.607E-04
0.060	7.024E 00	3.451E-03	7.028E 00	4.868E-03	2.785E-04
0.065	6.636E 00	3.472E-03	6.639E 00	5.600E-03	2.961E-04
0.070	6.300E 00	3.495E-03	6.304E 00	6.373E-03	3.134E-04
0.075	6.007E 00	3.519E-03	6.010E 00	7.186E-03	3.305E-04
0.080	5.748E 00	3.545E-03	5.752E 00	8.037E-03	3.474E-04
0.085	5.519E 00	3.554E-03	5.522E 00	8.924E-03	3.640E-04
0.090	5.314E 00	3.583E-03	5.317E 00	9.847E-03	3.804E-04
0.095	5.129E 00	3.613E-03	5.133E 00	1.080E-02	3.966E-04
0.100	4.962E 00	3.645E-03	4.966E 00	1.180E-02	4.127E-04
0.150	3.891E 00	4.002E-03	3.895E 00	2.332E-02	5.690E-04
0.200	3.349E 00	4.398E-03	3.353E 00	3.724E-02	7.193E-04
0.250	3.026E 00	4.826E-03	3.031E 00	5.298E-02	8.660E-04
0.300	2.815E 00	5.273E-03	2.820E 00	7.012E-02	1.010E-03
0.350	2.668E 00	5.736E-03	2.674E 00	8.836E-02	1.153E-03
0.400	2.562E 00	6.204E-03	2.568E 00	1.075E-01	1.294E-03
0.450	2.483E 00	6.681E-03	2.489E 00	1.272E-01	1.433E-03
0.500	2.422E 00	7.160E-03	2.429E 00	1.476E-01	1.572E-03
0.550	2.375E 00	7.643E-03	2.383E 00	1.684E-01	1.708E-03
0.600	2.339E 00	8.129E-03	2.347E 00	1.895E-01	1.844E-03
0.650	2.309E 00	8.620E-03	2.318E 00	2.110E-01	1.979E-03
0.700	2.286E 00	9.114E-03	2.295E 00	2.327E-01	2.112E-03
0.750	2.268E 00	9.612E-03	2.277E 00	2.545E-01	2.244E-03
0.800	2.253E 00	1.011E-02	2.263E 00	2.766E-01	2.375E-03
0.850	2.241E 00	1.063E-02	2.252E 00	2.987E-01	2.506E-03
0.900	2.232E 00	1.114E-02	2.243E 00	3.210E-01	2.636E-03
0.950	2.224E 00	1.165E-02	2.236E 00	3.433E-01	2.765E-03
1.000	2.219E 00	1.216E-02	2.231E 00	3.657E-01	2.893E-03
1.100	2.211E 00	1.320E-02	2.224E 00	4.106E-01	3.148E-03
1.200	2.208E 00	1.425E-02	2.222E 00	4.556E-01	3.400E-03
1.300	2.207E 00	1.531E-02	2.222E 00	5.006E-01	3.650E-03

ELECTRONS IN METHANE

ENERGY	STOPPING POWER			RANGE	RADIATION YIELD
	COLLISION	RADIATION	TOTAL		
MEV	MEV CM2/G	MEV CM2/G	MEV CM2/G	G/CM2	
1.400	2.208E 00	1.638E-02	2.225E 00	5.455E-01	3.899E-03
1.500	2.211E 00	1.747E-02	2.228E 00	5.905E-01	4.146E-03
1.600	2.215E 00	1.856E-02	2.233E 00	6.353E-01	4.391E-03
1.700	2.220E 00	1.964E-02	2.239E 00	6.800E-01	4.635E-03
1.800	2.225E 00	2.075E-02	2.246E 00	7.246E-01	4.878E-03
1.900	2.231E 00	2.188E-02	2.253E 00	7.691E-01	5.120E-03
2.000	2.237E 00	2.301E-02	2.260E 00	8.134E-01	5.361E-03
2.200	2.250E 00	2.532E-02	2.275E 00	9.016E-01	5.842E-03
2.400	2.264E 00	2.766E-02	2.291E 00	9.892E-01	6.322E-03
2.600	2.277E 00	3.005E-02	2.307E 00	1.076E 00	6.801E-03
2.800	2.291E 00	3.239E-02	2.323E 00	1.163E 00	7.279E-03
3.000	2.304E 00	3.485E-02	2.339E 00	1.248E 00	7.756E-03
3.500	2.336E 00	4.116E-02	2.377E 00	1.460E 00	8.949E-03
4.000	2.365E 00	4.771E-02	2.413E 00	1.669E 00	1.015E-02
4.500	2.393E 00	5.451E-02	2.447E 00	1.875E 00	1.135E-02
5.000	2.418E 00	6.143E-02	2.480E 00	2.078E 00	1.257E-02
5.500	2.442E 00	6.848E-02	2.511E 00	2.278E 00	1.379E-02
6.000	2.464E 00	7.565E-02	2.540E 00	2.476E 00	1.502E-02
6.500	2.485E 00	8.293E-02	2.568E 00	2.672E 00	1.625E-02
7.000	2.504E 00	9.031E-02	2.595E 00	2.866E 00	1.749E-02
7.500	2.522E 00	9.778E-02	2.620E 00	3.057E 00	1.873E-02
8.000	2.540E 00	1.053E-01	2.645E 00	3.247E 00	1.997E-02
8.500	2.556E 00	1.130E-01	2.669E 00	3.436E 00	2.121E-02
9.000	2.571E 00	1.213E-01	2.693E 00	3.622E 00	2.246E-02
9.500	2.586E 00	1.291E-01	2.715E 00	3.807E 00	2.371E-02
10.000	2.600E 00	1.370E-01	2.737E 00	3.990E 00	2.497E-02
20.000	2.790E 00	3.050E-01	3.095E 00	7.411E 00	4.974E-02
30.000	2.886E 00	4.836E-01	3.369E 00	1.050E 01	7.361E-02
40.000	2.946E 00	6.675E-01	3.614E 00	1.337E 01	9.631E-02
50.000	2.990E 00	8.551E-01	3.845E 00	1.605E 01	1.178E-01
60.000	3.023E 00	1.045E 00	4.068E 00	1.858E 01	1.382E-01
80.000	3.071E 00	1.430E 00	4.502E 00	2.325E 01	1.757E-01
100.000	3.106E 00	1.820E 00	4.926E 00	2.749E 01	2.094E-01
200.000	3.201E 00	3.803E 00	7.005E 00	4.442E 01	3.375E-01
300.000	3.250E 00	5.814E 00	9.064E 00	5.693E 01	4.237E-01
400.000	3.282E 00	7.834E 00	1.112E 01	6.688E 01	4.866E-01
500.000	3.305E 00	9.861E 00	1.317E 01	7.513E 01	5.349E-01
600.000	3.324E 00	1.189E 01	1.522E 01	8.219E 01	5.734E-01
800.000	3.353E 00	1.596E 01	1.932E 01	9.383E 01	6.315E-01
1000.000	3.376E 00	2.004E 01	2.341E 01	1.032E 02	6.736E-01

ELECTRONS IN ETHYLENE

ENERGY	STOPPING POWER			RANGE	RADIATION YIELD
	COLLISION	RADIATION	TOTAL		
MEV	MEV CM2/G	MEV CM2/G	MEV CM2/G	G/CM2	
0.010	2.465E 01	3.784E-03	2.465E 01	2.282E-04	8.747E-05
0.015	1.791E 01	3.709E-03	1.792E 01	4.697E-04	1.185E-04
0.020	1.429E 01	3.667E-03	1.430E 01	7.845E-04	1.469E-04
0.025	1.201E 01	3.638E-03	1.202E 01	1.168E-03	1.735E-04
0.030	1.044E 01	3.619E-03	1.044E 01	1.616E-03	1.987E-04
0.035	9.279E 00	3.602E-03	9.283E 00	2.125E-03	2.228E-04
0.040	8.390E 00	3.601E-03	8.394E 00	2.692E-03	2.460E-04
0.045	7.686E 00	3.606E-03	7.690E 00	3.315E-03	2.686E-04
0.050	7.113E 00	3.618E-03	7.117E 00	3.992E-03	2.906E-04
0.055	6.638E 00	3.633E-03	6.641E 00	4.720E-03	3.122E-04
0.060	6.237E 00	3.653E-03	6.241E 00	5.497E-03	3.333E-04
0.065	5.894E 00	3.675E-03	5.898E 00	6.321E-03	3.542E-04
0.070	5.598E 00	3.699E-03	5.601E 00	7.192E-03	3.747E-04
0.075	5.338E 00	3.725E-03	5.342E 00	8.106E-03	3.950E-04
0.080	5.110E 00	3.753E-03	5.114E 00	9.063E-03	4.150E-04
0.085	4.907E 00	3.762E-03	4.911E 00	1.006E-02	4.346E-04
0.090	4.725E 00	3.793E-03	4.729E 00	1.110E-02	4.541E-04
0.095	4.562E 00	3.825E-03	4.566E 00	1.218E-02	4.733E-04
0.100	4.415E 00	3.859E-03	4.419E 00	1.329E-02	4.924E-04
0.150	3.466E 00	4.245E-03	3.470E 00	2.623E-02	6.780E-04
0.200	2.986E 00	4.674E-03	2.990E 00	4.185E-02	8.570E-04
0.250	2.700E 00	5.136E-03	2.705E 00	5.949E-02	1.032E-03
0.300	2.513E 00	5.617E-03	2.518E 00	7.869E-02	1.204E-03
0.350	2.383E 00	6.118E-03	2.389E 00	9.910E-02	1.374E-03
0.400	2.289E 00	6.620E-03	2.295E 00	1.205E-01	1.543E-03
0.450	2.219E 00	7.133E-03	2.226E 00	1.426E-01	1.710E-03
0.500	2.165E 00	7.646E-03	2.173E 00	1.654E-01	1.875E-03
0.550	2.124E 00	8.162E-03	2.132E 00	1.886E-01	2.038E-03
0.600	2.092E 00	8.681E-03	2.100E 00	2.122E-01	2.200E-03
0.650	2.066E 00	9.203E-03	2.075E 00	2.362E-01	2.361E-03
0.700	2.046E 00	9.729E-03	2.056E 00	2.604E-01	2.519E-03
0.750	2.030E 00	1.026E-02	2.040E 00	2.848E-01	2.677E-03
0.800	2.017E 00	1.079E-02	2.028E 00	3.094E-01	2.833E-03
0.850	2.007E 00	1.133E-02	2.018E 00	3.341E-01	2.988E-03
0.900	1.998E 00	1.187E-02	2.010E 00	3.589E-01	3.142E-03
0.950	1.992E 00	1.241E-02	2.005E 00	3.839E-01	3.295E-03
1.000	1.987E 00	1.296E-02	2.000E 00	4.088E-01	3.447E-03
1.100	1.981E 00	1.405E-02	1.995E 00	4.589E-01	3.748E-03
1.200	1.978E 00	1.516E-02	1.994E 00	5.090E-01	4.046E-03
1.300	1.978E 00	1.628E-02	1.994E 00	5.592E-01	4.342E-03

ELECTRONS IN ETHYLENE

ENERGY	STOPPING POWER			RANGE	RADIATION YIELD
	COLLISION	RADIATION	TOTAL		
MEV	MEV CM2/G	MEV CM2/G	MEV CM2/G	G/CM2	
1.400	1.980E 00	1.741E-02	1.997E 00	6.093E-01	4.634E-03
1.500	1.983E 00	1.855E-02	2.001E 00	6.593E-01	4.925E-03
1.600	1.986E 00	1.969E-02	2.006E 00	7.092E-01	5.214E-03
1.700	1.991E 00	2.082E-02	2.012E 00	7.590E-01	5.500E-03
1.800	1.996E 00	2.199E-02	2.018E 00	8.086E-01	5.784E-03
1.900	2.002E 00	2.317E-02	2.025E 00	8.581E-01	6.068E-03
2.000	2.008E 00	2.437E-02	2.032E 00	9.074E-01	6.350E-03
2.200	2.020E 00	2.678E-02	2.046E 00	1.006E 00	6.913E-03
2.400	2.032E 00	2.924E-02	2.061E 00	1.103E 00	7.473E-03
2.600	2.045E 00	3.174E-02	2.076E 00	1.200E 00	8.032E-03
2.800	2.057E 00	3.419E-02	2.091E 00	1.296E 00	8.589E-03
3.000	2.069E 00	3.676E-02	2.106E 00	1.391E 00	9.143E-03
3.500	2.099E 00	4.337E-02	2.142E 00	1.626E 00	1.053E-02
4.000	2.126E 00	5.022E-02	2.176E 00	1.858E 00	1.192E-02
4.500	2.151E 00	5.734E-02	2.209E 00	2.086E 00	1.332E-02
5.000	2.175E 00	6.458E-02	2.239E 00	2.311E 00	1.473E-02
5.500	2.196E 00	7.196E-02	2.268E 00	2.532E 00	1.614E-02
6.000	2.217E 00	7.946E-02	2.296E 00	2.752E 00	1.756E-02
6.500	2.236E 00	8.707E-02	2.323E 00	2.968E 00	1.898E-02
7.000	2.253E 00	9.479E-02	2.348E 00	3.182E 00	2.041E-02
7.500	2.270E 00	1.026E-01	2.373E 00	3.394E 00	2.183E-02
8.000	2.286E 00	1.105E-01	2.396E 00	3.604E 00	2.326E-02
8.500	2.301E 00	1.185E-01	2.419E 00	3.811E 00	2.469E-02
9.000	2.315E 00	1.272E-01	2.442E 00	4.017E 00	2.613E-02
9.500	2.328E 00	1.354E-01	2.464E 00	4.221E 00	2.757E-02
10.000	2.341E 00	1.437E-01	2.485E 00	4.423E 00	2.901E-02
20.000	2.513E 00	3.194E-01	2.832E 00	8.176E 00	5.730E-02
30.000	2.597E 00	5.063E-01	3.104E 00	1.154E 01	8.433E-02
40.000	2.652E 00	6.986E-01	3.350E 00	1.464E 01	1.098E-01
50.000	2.691E 00	8.947E-01	3.585E 00	1.753E 01	1.337E-01
60.000	2.720E 00	1.093E 00	3.814E 00	2.023E 01	1.562E-01
80.000	2.765E 00	1.496E 00	4.260E 00	2.519E 01	1.971E-01
100.000	2.796E 00	1.902E 00	4.699E 00	2.966E 01	2.334E-01
200.000	2.884E 00	3.973E 00	6.857E 00	4.716E 01	3.678E-01
300.000	2.930E 00	6.071E 00	9.000E 00	5.985E 01	4.556E-01
400.000	2.960E 00	8.179E 00	1.114E 01	6.982E 01	5.183E-01
500.000	2.982E 00	1.029E 01	1.327E 01	7.803E 01	5.658E-01
600.000	3.000E 00	1.241E 01	1.541E 01	8.501E 01	6.034E-01
800.000	3.027E 00	1.666E 01	1.968E 01	9.647E 01	6.594E-01
1000.000	3.047E 00	2.090E 01	2.395E 01	1.057E 02	6.996E-01

ELECTRONS IN POLYETHYLENE

ENERGY	STOPPING POWER			RANGE	RADIATION YIELD
	COLLISION	RADIATION	TOTAL		
MEV	MEV CM2/G	MEV CM2/G	MEV CM2/G	G/CM2	
0.010	2.465E 01	3.784E-03	2.465E 01	2.282E-04	8.747E-05
0.015	1.791E 01	3.709E-03	1.792E 01	4.697E-04	1.185E-04
0.020	1.429E 01	3.667E-03	1.430E 01	7.845E-04	1.469E-04
0.025	1.201E 01	3.638E-03	1.202E 01	1.168E-03	1.735E-04
0.030	1.044E 01	3.619E-03	1.044E 01	1.616E-03	1.987E-04
0.035	9.279E 00	3.602E-03	9.283E 00	2.125E-03	2.228E-04
0.040	8.390E 00	3.601E-03	8.394E 00	2.692E-03	2.460E-04
0.045	7.686E 00	3.606E-03	7.690E 00	3.315E-03	2.686E-04
0.050	7.113E 00	3.618E-03	7.117E 00	3.992E-03	2.906E-04
0.055	6.638E 00	3.633E-03	6.641E 00	4.720E-03	3.122E-04
0.060	6.237E 00	3.653E-03	6.241E 00	5.497E-03	3.333E-04
0.065	5.894E 00	3.675E-03	5.898E 00	6.321E-03	3.542E-04
0.070	5.598E 00	3.699E-03	5.601E 00	7.192E-03	3.747E-04
0.075	5.338E 00	3.725E-03	5.342E 00	8.106E-03	3.950E-04
0.080	5.110E 00	3.753E-03	5.114E 00	9.063E-03	4.150E-04
0.085	4.907E 00	3.762E-03	4.911E 00	1.006E-02	4.346E-04
0.090	4.725E 00	3.793E-03	4.729E 00	1.110E-02	4.541E-04
0.095	4.562E 00	3.825E-03	4.566E 00	1.218E-02	4.733E-04
0.100	4.415E 00	3.859E-03	4.419E 00	1.329E-02	4.924E-04
0.150	3.466E 00	4.245E-03	3.470E 00	2.623E-02	6.780E-04
0.200	2.986E 00	4.674E-03	2.990E 00	4.185E-02	8.570E-04
0.250	2.700E 00	5.136E-03	2.705E 00	5.949E-02	1.032E-03
0.300	2.513E 00	5.617E-03	2.518E 00	7.869E-02	1.204E-03
0.350	2.379E 00	6.118E-03	2.385E 00	9.911E-02	1.375E-03
0.400	2.280E 00	6.620E-03	2.287E 00	1.205E-01	1.544E-03
0.450	2.206E 00	7.133E-03	2.213E 00	1.428E-01	1.712E-03
0.500	2.148E 00	7.646E-03	2.156E 00	1.657E-01	1.879E-03
0.550	2.103E 00	8.162E-03	2.111E 00	1.891E-01	2.046E-03
0.600	2.067E 00	8.681E-03	2.076E 00	2.130E-01	2.210E-03
0.650	2.038E 00	9.203E-03	2.047E 00	2.373E-01	2.374E-03
0.700	2.014E 00	9.729E-03	2.024E 00	2.618E-01	2.537E-03
0.750	1.995E 00	1.026E-02	2.005E 00	2.867E-01	2.698E-03
0.800	1.979E 00	1.079E-02	1.989E 00	3.117E-01	2.859E-03
0.850	1.965E 00	1.133E-02	1.977E 00	3.369E-01	3.019E-03
0.900	1.954E 00	1.187E-02	1.966E 00	3.623E-01	3.179E-03
0.950	1.945E 00	1.241E-02	1.957E 00	3.878E-01	3.337E-03
1.000	1.937E 00	1.296E-02	1.950E 00	4.134E-01	3.495E-03
1.100	1.925E 00	1.405E-02	1.939E 00	4.648E-01	3.809E-03
1.200	1.917E 00	1.516E-02	1.932E 00	5.165E-01	4.120E-03
1.300	1.912E 00	1.628E-02	1.928E 00	5.683E-01	4.430E-03

ELECTRONS IN POLYETHYLENE

ENERGY	STOPPING POWER			RANGE	RADIATION YIELD
	COLLISION	RADIATION	TOTAL		
MEV	MEV CM2/G	MEV CM2/G	MEV CM2/G	G/CM2	
1.400	1.908E 00	1.741E-02	1.926E 00	6.202E-01	4.738E-03
1.500	1.906E 00	1.855E-02	1.925E 00	6.721E-01	5.044E-03
1.600	1.906E 00	1.969E-02	1.925E 00	7.241E-01	5.350E-03
1.700	1.906E 00	2.082E-02	1.926E 00	7.760E-01	5.654E-03
1.800	1.906E 00	2.199E-02	1.928E 00	8.279E-01	5.957E-03
1.900	1.907E 00	2.317E-02	1.931E 00	8.797E-01	6.259E-03
2.000	1.909E 00	2.437E-02	1.933E 00	9.315E-01	6.561E-03
2.200	1.913E 00	2.678E-02	1.940E 00	1.035E 00	7.165E-03
2.400	1.918E 00	2.924E-02	1.947E 00	1.138E 00	7.769E-03
2.600	1.923E 00	3.174E-02	1.955E 00	1.240E 00	8.374E-03
2.800	1.928E 00	3.419E-02	1.963E 00	1.342E 00	8.979E-03
3.000	1.934E 00	3.676E-02	1.971E 00	1.444E 00	9.583E-03
3.500	1.947E 00	4.337E-02	1.990E 00	1.696E 00	1.110E-02
4.000	1.960E 00	5.022E-02	2.010E 00	1.946E 00	1.264E-02
4.500	1.971E 00	5.734E-02	2.029E 00	2.194E 00	1.419E-02
5.000	1.982E 00	6.458E-02	2.047E 00	2.439E 00	1.576E-02
5.500	1.992E 00	7.196E-02	2.064E 00	2.683E 00	1.735E-02
6.000	2.002E 00	7.946E-02	2.081E 00	2.924E 00	1.894E-02
6.500	2.010E 00	8.707E-02	2.097E 00	3.163E 00	2.055E-02
7.000	2.018E 00	9.479E-02	2.113E 00	3.401E 00	2.217E-02
7.500	2.025E 00	1.026E-01	2.128E 00	3.637E 00	2.379E-02
8.000	2.032E 00	1.105E-01	2.143E 00	3.871E 00	2.543E-02
8.500	2.039E 00	1.185E-01	2.157E 00	4.103E 00	2.706E-02
9.000	2.045E 00	1.272E-01	2.172E 00	4.334E 00	2.871E-02
9.500	2.050E 00	1.354E-01	2.186E 00	4.564E 00	3.037E-02
10.000	2.056E 00	1.437E-01	2.200E 00	4.792E 00	3.204E-02
20.000	2.125E 00	3.194E-01	2.445E 00	9.096E 00	6.519E-02
30.000	2.163E 00	5.063E-01	2.670E 00	1.301E 01	9.704E-02
40.000	2.189E 00	6.986E-01	2.888E 00	1.661E 01	1.269E-01
50.000	2.209E 00	8.947E-01	3.104E 00	1.995E 01	1.546E-01
60.000	2.225E 00	1.093E 00	3.319E 00	2.306E 01	1.804E-01
80.000	2.251E 00	1.496E 00	3.746E 00	2.873E 01	2.267E-01
100.000	2.270E 00	1.902E 00	4.173E 00	3.379E 01	2.670E-01
200.000	2.331E 00	3.973E 00	6.305E 00	5.314E 01	4.107E-01
300.000	2.367E 00	6.071E 00	8.438E 00	6.681E 01	5.001E-01
400.000	2.392E 00	8.179E 00	1.057E 01	7.737E 01	5.622E-01
500.000	2.412E 00	1.029E 01	1.270E 01	8.599E 01	6.084E-01
600.000	2.428E 00	1.241E 01	1.484E 01	9.327E 01	6.443E-01
800.000	2.453E 00	1.666E 01	1.911E 01	1.051E 02	6.971E-01
1000.000	2.473E 00	2.090E 01	2.338E 01	1.146E 02	7.344E-01

ELECTRONS IN XYLENE

ENERGY	STOPPING POWER			RANGE	RADIATION YIELD
	COLLISION	RADIATION	TOTAL		
MEV	MEV CM2/G	MEV CM2/G	MEV CM2/G	G/CM2	
0.010	2.312E 01	3.887E-03	2.313E 01	2.440E-04	9.610E-05
0.015	1.683E 01	3.809E-03	1.683E 01	5.012E-04	1.300E-04
0.020	1.344E 01	3.764E-03	1.344E 01	8.361E-04	1.608E-04
0.025	1.130E 01	3.733E-03	1.131E 01	1.244E-03	1.897E-04
0.030	9.825E 00	3.712E-03	9.828E 00	1.719E-03	2.171E-04
0.035	8.738E 00	3.694E-03	8.742E 00	2.260E-03	2.433E-04
0.040	7.904E 00	3.692E-03	7.908E 00	2.862E-03	2.685E-04
0.045	7.242E 00	3.697E-03	7.246E 00	3.524E-03	2.929E-04
0.050	6.704E 00	3.708E-03	6.708E 00	4.242E-03	3.168E-04
0.055	6.258E 00	3.724E-03	6.261E 00	5.014E-03	3.402E-04
0.060	5.881E 00	3.744E-03	5.885E 00	5.838E-03	3.631E-04
0.065	5.559E 00	3.766E-03	5.562E 00	6.712E-03	3.857E-04
0.070	5.280E 00	3.791E-03	5.283E 00	7.635E-03	4.080E-04
0.075	5.036E 00	3.818E-03	5.040E 00	8.605E-03	4.299E-04
0.080	4.821E 00	3.847E-03	4.825E 00	9.619E-03	4.517E-04
0.085	4.630E 00	3.856E-03	4.634E 00	1.068E-02	4.729E-04
0.090	4.459E 00	3.888E-03	4.463E 00	1.178E-02	4.940E-04
0.095	4.306E 00	3.921E-03	4.310E 00	1.292E-02	5.148E-04
0.100	4.167E 00	3.956E-03	4.171E 00	1.410E-02	5.355E-04
0.150	3.274E 00	4.355E-03	3.278E 00	2.780E-02	7.368E-04
0.200	2.821E 00	4.799E-03	2.826E 00	4.433E-02	9.311E-04
0.250	2.552E 00	5.276E-03	2.557E 00	6.299E-02	1.121E-03
0.300	2.376E 00	5.773E-03	2.382E 00	8.329E-02	1.308E-03
0.350	2.254E 00	6.291E-03	2.260E 00	1.049E-01	1.493E-03
0.400	2.165E 00	6.809E-03	2.171E 00	1.275E-01	1.677E-03
0.450	2.095E 00	7.337E-03	2.103E 00	1.509E-01	1.858E-03
0.500	2.042E 00	7.866E-03	2.050E 00	1.750E-01	2.039E-03
0.550	2.000E 00	8.397E-03	2.009E 00	1.996E-01	2.218E-03
0.600	1.967E 00	8.931E-03	1.976E 00	2.247E-01	2.396E-03
0.650	1.940E 00	9.468E-03	1.950E 00	2.502E-01	2.572E-03
0.700	1.918E 00	1.001E-02	1.928E 00	2.760E-01	2.747E-03
0.750	1.901E 00	1.055E-02	1.911E 00	3.021E-01	2.921E-03
0.800	1.886E 00	1.110E-02	1.897E 00	3.283E-01	3.094E-03
0.850	1.874E 00	1.165E-02	1.885E 00	3.548E-01	3.266E-03
0.900	1.864E 00	1.220E-02	1.876E 00	3.813E-01	3.437E-03
0.950	1.855E 00	1.276E-02	1.868E 00	4.081E-01	3.607E-03
1.000	1.848E 00	1.332E-02	1.862E 00	4.349E-01	3.776E-03
1.100	1.838E 00	1.444E-02	1.853E 00	4.887E-01	4.112E-03
1.200	1.831E 00	1.557E-02	1.847E 00	5.428E-01	4.446E-03
1.300	1.827E 00	1.672E-02	1.843E 00	5.970E-01	4.777E-03

ELECTRONS IN XYLENE

ENERGY	STOPPING POWER			RANGE	RADIATION YIELD
	COLLISION	RADIATION	TOTAL		
MEV	MEV CM2/G	MEV CM2/G	MEV CM2/G	G/CM2	
1.400	1.824E 00	1.787E-02	1.842E 00	6.513E-01	5.106E-03
1.500	1.823E 00	1.904E-02	1.842E 00	7.056E-01	5.434E-03
1.600	1.822E 00	2.021E-02	1.842E 00	7.599E-01	5.760E-03
1.700	1.823E 00	2.136E-02	1.844E 00	8.141E-01	6.084E-03
1.800	1.824E 00	2.256E-02	1.846E 00	8.683E-01	6.407E-03
1.900	1.825E 00	2.376E-02	1.849E 00	9.224E-01	6.730E-03
2.000	1.827E 00	2.498E-02	1.852E 00	9.765E-01	7.052E-03
2.200	1.832E 00	2.745E-02	1.859E 00	1.084E 00	7.695E-03
2.400	1.837E 00	2.996E-02	1.867E 00	1.192E 00	8.337E-03
2.600	1.842E 00	3.251E-02	1.875E 00	1.299E 00	8.980E-03
2.800	1.848E 00	3.500E-02	1.883E 00	1.405E 00	9.623E-03
3.000	1.853E 00	3.762E-02	1.891E 00	1.511E 00	1.026E-02
3.500	1.867E 00	4.437E-02	1.911E 00	1.774E 00	1.188E-02
4.000	1.880E 00	5.135E-02	1.931E 00	2.034E 00	1.350E-02
4.500	1.892E 00	5.862E-02	1.950E 00	2.292E 00	1.515E-02
5.000	1.902E 00	6.601E-02	1.968E 00	2.547E 00	1.681E-02
5.500	1.912E 00	7.353E-02	1.986E 00	2.800E 00	1.849E-02
6.000	1.922E 00	8.118E-02	2.003E 00	3.051E 00	2.018E-02
6.500	1.930E 00	8.895E-02	2.019E 00	3.299E 00	2.188E-02
7.000	1.938E 00	9.682E-02	2.035E 00	3.546E 00	2.359E-02
7.500	1.945E 00	1.048E-01	2.050E 00	3.791E 00	2.531E-02
8.000	1.952E 00	1.129E-01	2.065E 00	4.034E 00	2.703E-02
8.500	1.958E 00	1.210E-01	2.079E 00	4.275E 00	2.876E-02
9.000	1.964E 00	1.299E-01	2.094E 00	4.515E 00	3.051E-02
9.500	1.970E 00	1.383E-01	2.108E 00	4.753E 00	3.226E-02
10.000	1.975E 00	1.467E-01	2.122E 00	4.989E 00	3.401E-02
20.000	2.043E 00	3.260E-01	2.369E 00	9.441E 00	6.890E-02
30.000	2.080E 00	5.166E-01	2.596E 00	1.347E 01	1.022E-01
40.000	2.105E 00	7.127E-01	2.817E 00	1.717E 01	1.333E-01
50.000	2.124E 00	9.126E-01	3.036E 00	2.058E 01	1.621E-01
60.000	2.139E 00	1.115E 00	3.254E 00	2.377E 01	1.888E-01
80.000	2.163E 00	1.525E 00	3.689E 00	2.953E 01	2.364E-01
100.000	2.182E 00	1.940E 00	4.122E 00	3.466E 01	2.777E-01
200.000	2.241E 00	4.050E 00	6.291E 00	5.415E 01	4.232E-01
300.000	2.275E 00	6.187E 00	8.462E 00	6.781E 01	5.127E-01
400.000	2.299E 00	8.335E 00	1.063E 01	7.833E 01	5.744E-01
500.000	2.318E 00	1.049E 01	1.281E 01	8.688E 01	6.200E-01
600.000	2.333E 00	1.265E 01	1.498E 01	9.410E 01	6.554E-01
800.000	2.357E 00	1.697E 01	1.933E 01	1.058E 02	7.072E-01
1000.000	2.376E 00	2.130E 01	2.367E 01	1.152E 02	7.436E-01

ELECTRONS IN TOLUENE

ENERGY	STOPPING POWER			RANGE	RADIATION YIELD
	COLLISION	RADIATION	TOTAL		
MEV	MEV CM2/G	MEV CM2/G	MEV CM2/G	G/CM2	
0.010	2.289E 01	3.903E-03	2.289E 01	2.466E-04	9.752E-05
0.015	1.666E 01	3.824E-03	1.667E 01	5.064E-04	1.318E-04
0.020	1.331E 01	3.778E-03	1.331E 01	8.446E-04	1.631E-04
0.025	1.119E 01	3.747E-03	1.120E 01	1.256E-03	1.924E-04
0.030	9.731E 00	3.726E-03	9.735E 00	1.736E-03	2.201E-04
0.035	8.656E 00	3.708E-03	8.659E 00	2.282E-03	2.466E-04
0.040	7.830E 00	3.706E-03	7.834E 00	2.890E-03	2.721E-04
0.045	7.175E 00	3.711E-03	7.178E 00	3.558E-03	2.969E-04
0.050	6.642E 00	3.722E-03	6.646E 00	4.282E-03	3.211E-04
0.055	6.200E 00	3.738E-03	6.203E 00	5.062E-03	3.447E-04
0.060	5.827E 00	3.758E-03	5.830E 00	5.894E-03	3.680E-04
0.065	5.507E 00	3.780E-03	5.511E 00	6.776E-03	3.908E-04
0.070	5.231E 00	3.805E-03	5.235E 00	7.708E-03	4.134E-04
0.075	4.990E 00	3.832E-03	4.994E 00	8.686E-03	4.356E-04
0.080	4.777E 00	3.861E-03	4.781E 00	9.710E-03	4.576E-04
0.085	4.588E 00	3.870E-03	4.592E 00	1.078E-02	4.792E-04
0.090	4.419E 00	3.902E-03	4.423E 00	1.189E-02	5.005E-04
0.095	4.267E 00	3.936E-03	4.270E 00	1.304E-02	5.216E-04
0.100	4.129E 00	3.971E-03	4.133E 00	1.423E-02	5.426E-04
0.150	3.244E 00	4.371E-03	3.249E 00	2.806E-02	7.464E-04
0.200	2.796E 00	4.818E-03	2.801E 00	4.473E-02	9.432E-04
0.250	2.530E 00	5.297E-03	2.535E 00	6.356E-02	1.136E-03
0.300	2.355E 00	5.797E-03	2.361E 00	8.404E-02	1.325E-03
0.350	2.234E 00	6.317E-03	2.240E 00	1.058E-01	1.513E-03
0.400	2.146E 00	6.838E-03	2.153E 00	1.286E-01	1.698E-03
0.450	2.079E 00	7.369E-03	2.086E 00	1.522E-01	1.882E-03
0.500	2.026E 00	7.900E-03	2.034E 00	1.765E-01	2.065E-03
0.550	1.985E 00	8.433E-03	1.993E 00	2.013E-01	2.246E-03
0.600	1.952E 00	8.969E-03	1.961E 00	2.266E-01	2.426E-03
0.650	1.925E 00	9.508E-03	1.935E 00	2.523E-01	2.604E-03
0.700	1.904E 00	1.005E-02	1.914E 00	2.783E-01	2.781E-03
0.750	1.886E 00	1.060E-02	1.897E 00	3.046E-01	2.957E-03
0.800	1.872E 00	1.114E-02	1.883E 00	3.310E-01	3.132E-03
0.850	1.860E 00	1.170E-02	1.871E 00	3.577E-01	3.306E-03
0.900	1.850E 00	1.225E-02	1.862E 00	3.844E-01	3.479E-03
0.950	1.842E 00	1.281E-02	1.854E 00	4.114E-01	3.651E-03
1.000	1.835E 00	1.337E-02	1.848E 00	4.384E-01	3.822E-03
1.100	1.825E 00	1.450E-02	1.839E 00	4.926E-01	4.161E-03
1.200	1.818E 00	1.564E-02	1.833E 00	5.471E-01	4.498E-03
1.300	1.813E 00	1.678E-02	1.830E 00	6.017E-01	4.833E-03

ELECTRONS IN TOLUENE

ENERGY	STOPPING POWER			RANGE	RADIATION YIELD
	COLLISION	RADIATION	TOTAL		
MEV	MEV CM2/G	MEV CM2/G	MEV CM2/G	G/CM2	
1.400	1.811E 00	1.794E-02	1.829E 00	6.563E-01	5.166E-03
1.500	1.810E 00	1.911E-02	1.829E 00	7.110E-01	5.497E-03
1.600	1.809E 00	2.029E-02	1.830E 00	7.657E-01	5.826E-03
1.700	1.810E 00	2.144E-02	1.831E 00	8.203E-01	6.154E-03
1.800	1.811E 00	2.264E-02	1.834E 00	8.749E-01	6.480E-03
1.900	1.813E 00	2.385E-02	1.837E 00	9.294E-01	6.806E-03
2.000	1.815E 00	2.507E-02	1.840E 00	9.838E-01	7.131E-03
2.200	1.819E 00	2.755E-02	1.847E 00	1.092E 00	7.780E-03
2.400	1.824E 00	3.007E-02	1.854E 00	1.200E 00	8.429E-03
2.600	1.830E 00	3.262E-02	1.862E 00	1.308E 00	9.078E-03
2.800	1.835E 00	3.513E-02	1.871E 00	1.415E 00	9.727E-03
3.000	1.841E 00	3.776E-02	1.879E 00	1.522E 00	1.037E-02
3.500	1.855E 00	4.452E-02	1.899E 00	1.787E 00	1.200E-02
4.000	1.867E 00	5.153E-02	1.919E 00	2.048E 00	1.364E-02
4.500	1.879E 00	5.881E-02	1.938E 00	2.308E 00	1.530E-02
5.000	1.890E 00	6.622E-02	1.956E 00	2.564E 00	1.698E-02
5.500	1.900E 00	7.377E-02	1.974E 00	2.819E 00	1.868E-02
6.000	1.909E 00	8.144E-02	1.991E 00	3.071E 00	2.038E-02
6.500	1.918E 00	8.923E-02	2.007E 00	3.321E 00	2.210E-02
7.000	1.926E 00	9.713E-02	2.023E 00	3.569E 00	2.382E-02
7.500	1.933E 00	1.051E-01	2.038E 00	3.816E 00	2.555E-02
8.000	1.940E 00	1.132E-01	2.053E 00	4.060E 00	2.729E-02
8.500	1.946E 00	1.214E-01	2.068E 00	4.303E 00	2.904E-02
9.000	1.952E 00	1.303E-01	2.082E 00	4.544E 00	3.079E-02
9.500	1.958E 00	1.387E-01	2.096E 00	4.783E 00	3.256E-02
10.000	1.963E 00	1.472E-01	2.110E 00	5.021E 00	3.433E-02
20.000	2.031E 00	3.270E-01	2.358E 00	9.496E 00	6.949E-02
30.000	2.067E 00	5.182E-01	2.585E 00	1.354E 01	1.031E-01
40.000	2.092E 00	7.149E-01	2.807E 00	1.725E 01	1.343E-01
50.000	2.111E 00	9.153E-01	3.026E 00	2.069E 01	1.633E-01
60.000	2.126E 00	1.118E 00	3.244E 00	2.388E 01	1.901E-01
80.000	2.150E 00	1.530E 00	3.680E 00	2.966E 01	2.379E-01
100.000	2.169E 00	1.946E 00	4.115E 00	3.480E 01	2.794E-01
200.000	2.227E 00	4.062E 00	6.289E 00	5.431E 01	4.251E-01
300.000	2.261E 00	6.205E 00	8.466E 00	6.796E 01	5.146E-01
400.000	2.285E 00	8.358E 00	1.064E 01	7.848E 01	5.762E-01
500.000	2.304E 00	1.052E 01	1.282E 01	8.702E 01	6.218E-01
600.000	2.319E 00	1.268E 01	1.500E 01	9.423E 01	6.571E-01
800.000	2.343E 00	1.702E 01	1.936E 01	1.059E 02	7.087E-01
1000.000	2.361E 00	2.136E 01	2.372E 01	1.152E 02	7.450E-01

ELECTRONS IN ACETYLENE

ENERGY	STOPPING POWER			RANGE	RADIATION YIELD
	COLLISION	RADIATION	TOTAL		
MEV	MEV CM2/G	MEV CM2/G	MEV CM2/G	G/CM2	
0.010	2.258E 01	3.924E-03	2.258E 01	2.502E-04	9.948E-05
0.015	1.644E 01	3.844E-03	1.644E 01	5.135E-04	1.344E-04
0.020	1.313E 01	3.798E-03	1.314E 01	8.563E-04	1.663E-04
0.025	1.105E 01	3.767E-03	1.105E 01	1.273E-03	1.960E-04
0.030	9.606E 00	3.745E-03	9.609E 00	1.760E-03	2.243E-04
0.035	8.545E 00	3.727E-03	8.548E 00	2.313E-03	2.512E-04
0.040	7.730E 00	3.725E-03	7.734E 00	2.929E-03	2.772E-04
0.045	7.084E 00	3.730E-03	7.087E 00	3.605E-03	3.024E-04
0.050	6.558E 00	3.741E-03	6.562E 00	4.339E-03	3.270E-04
0.055	6.122E 00	3.757E-03	6.125E 00	5.128E-03	3.510E-04
0.060	5.753E 00	3.777E-03	5.757E 00	5.971E-03	3.747E-04
0.065	5.438E 00	3.799E-03	5.442E 00	6.864E-03	3.979E-04
0.070	5.166E 00	3.824E-03	5.170E 00	7.808E-03	4.209E-04
0.075	4.928E 00	3.852E-03	4.931E 00	8.798E-03	4.435E-04
0.080	4.717E 00	3.880E-03	4.721E 00	9.835E-03	4.659E-04
0.085	4.531E 00	3.890E-03	4.535E 00	1.092E-02	4.878E-04
0.090	4.364E 00	3.922E-03	4.368E 00	1.204E-02	5.095E-04
0.095	4.214E 00	3.956E-03	4.218E 00	1.320E-02	5.310E-04
0.100	4.078E 00	3.991E-03	4.082E 00	1.441E-02	5.523E-04
0.150	3.205E 00	4.394E-03	3.209E 00	2.841E-02	7.597E-04
0.200	2.763E 00	4.844E-03	2.767E 00	4.529E-02	9.599E-04
0.250	2.499E 00	5.326E-03	2.504E 00	6.435E-02	1.156E-03
0.300	2.327E 00	5.830E-03	2.333E 00	8.508E-02	1.349E-03
0.350	2.207E 00	6.353E-03	2.214E 00	1.071E-01	1.540E-03
0.400	2.121E 00	6.877E-03	2.128E 00	1.302E-01	1.728E-03
0.450	2.057E 00	7.411E-03	2.064E 00	1.540E-01	1.915E-03
0.500	2.008E 00	7.945E-03	2.016E 00	1.786E-01	2.101E-03
0.550	1.970E 00	8.482E-03	1.978E 00	2.036E-01	2.284E-03
0.600	1.940E 00	9.021E-03	1.949E 00	2.291E-01	2.465E-03
0.650	1.917E 00	9.563E-03	1.926E 00	2.549E-01	2.644E-03
0.700	1.898E 00	1.011E-02	1.908E 00	2.810E-01	2.822E-03
0.750	1.883E 00	1.066E-02	1.894E 00	3.073E-01	2.998E-03
0.800	1.872E 00	1.121E-02	1.883E 00	3.338E-01	3.172E-03
0.850	1.862E 00	1.177E-02	1.874E 00	3.604E-01	3.346E-03
0.900	1.855E 00	1.232E-02	1.867E 00	3.871E-01	3.517E-03
0.950	1.849E 00	1.288E-02	1.862E 00	4.139E-01	3.688E-03
1.000	1.845E 00	1.345E-02	1.859E 00	4.408E-01	3.857E-03
1.100	1.840E 00	1.458E-02	1.854E 00	4.947E-01	4.193E-03
1.200	1.837E 00	1.572E-02	1.853E 00	5.486E-01	4.525E-03
1.300	1.837E 00	1.688E-02	1.854E 00	6.026E-01	4.853E-03

ELECTRONS IN ACETYLENE

ENERGY	STOPPING POWER			RANGE	RADIATION YIELD
	COLLISION	RADIATION	TOTAL		
MEV	MEV CM2/G	MEV CM2/G	MEV CM2/G	G/CM2	
1.400	1.839E 00	1.804E-02	1.857E 00	6.565E-01	5.178E-03
1.500	1.842E 00	1.921E-02	1.861E 00	7.103E-01	5.501E-03
1.600	1.846E 00	2.039E-02	1.866E 00	7.639E-01	5.821E-03
1.700	1.850E 00	2.156E-02	1.872E 00	8.174E-01	6.138E-03
1.800	1.855E 00	2.276E-02	1.878E 00	8.708E-01	6.454E-03
1.900	1.861E 00	2.397E-02	1.885E 00	9.239E-01	6.768E-03
2.000	1.866E 00	2.520E-02	1.891E 00	9.769E-01	7.080E-03
2.200	1.878E 00	2.769E-02	1.906E 00	1.082E 00	7.703E-03
2.400	1.890E 00	3.021E-02	1.920E 00	1.187E 00	8.322E-03
2.600	1.902E 00	3.278E-02	1.935E 00	1.291E 00	8.939E-03
2.800	1.914E 00	3.529E-02	1.949E 00	1.394E 00	9.554E-03
3.000	1.925E 00	3.793E-02	1.963E 00	1.496E 00	1.016E-02
3.500	1.953E 00	4.472E-02	1.998E 00	1.748E 00	1.169E-02
4.000	1.979E 00	5.176E-02	2.030E 00	1.997E 00	1.322E-02
4.500	2.003E 00	5.908E-02	2.062E 00	2.241E 00	1.476E-02
5.000	2.025E 00	6.652E-02	2.091E 00	2.482E 00	1.631E-02
5.500	2.045E 00	7.410E-02	2.119E 00	2.719E 00	1.786E-02
6.000	2.064E 00	8.180E-02	2.146E 00	2.954E 00	1.942E-02
6.500	2.082E 00	8.962E-02	2.172E 00	3.185E 00	2.098E-02
7.000	2.099E 00	9.755E-02	2.197E 00	3.414E 00	2.254E-02
7.500	2.115E 00	1.056E-01	2.220E 00	3.640E 00	2.410E-02
8.000	2.130E 00	1.137E-01	2.243E 00	3.864E 00	2.566E-02
8.500	2.144E 00	1.219E-01	2.266E 00	4.086E 00	2.723E-02
9.000	2.157E 00	1.309E-01	2.288E 00	4.306E 00	2.880E-02
9.500	2.170E 00	1.393E-01	2.309E 00	4.523E 00	3.038E-02
10.000	2.182E 00	1.478E-01	2.330E 00	4.739E 00	3.195E-02
20.000	2.349E 00	3.284E-01	2.677E 00	8.728E 00	6.272E-02
30.000	2.436E 00	5.203E-01	2.956E 00	1.228E 01	9.175E-02
40.000	2.492E 00	7.178E-01	3.210E 00	1.552E 01	1.189E-01
50.000	2.531E 00	9.190E-01	3.451E 00	1.852E 01	1.442E-01
60.000	2.562E 00	1.123E 00	3.685E 00	2.133E 01	1.678E-01
80.000	2.607E 00	1.536E 00	4.143E 00	2.644E 01	2.106E-01
100.000	2.639E 00	1.953E 00	4.592E 00	3.103E 01	2.482E-01
200.000	2.726E 00	4.078E 00	6.804E 00	4.879E 01	3.855E-01
300.000	2.771E 00	6.229E 00	9.000E 00	6.153E 01	4.736E-01
400.000	2.800E 00	8.391E 00	1.119E 01	7.147E 01	5.360E-01
500.000	2.821E 00	1.056E 01	1.338E 01	7.963E 01	5.829E-01
600.000	2.838E 00	1.273E 01	1.557E 01	8.655E 01	6.198E-01
800.000	2.864E 00	1.708E 01	1.995E 01	9.787E 01	6.745E-01
1000.000	2.883E 00	2.144E 01	2.432E 01	1.069E 02	7.135E-01

ELECTRONS IN POLYSTYRENE

ENERGY	STOPPING POWER			RANGE	RADIATION YIELD
	COLLISION	RADIATION	TOTAL		
MEV	MEV CM2/G	MEV CM2/G	MEV CM2/G	G/CM2	
0.010	2.260E 01	3.926E-03	2.261E 01	2.499E-04	9.940E-05
0.015	1.646E 01	3.846E-03	1.646E 01	5.129E-04	1.343E-04
0.020	1.315E 01	3.799E-03	1.315E 01	8.553E-04	1.661E-04
0.025	1.106E 01	3.768E-03	1.106E 01	1.272E-03	1.959E-04
0.030	9.617E 00	3.747E-03	9.620E 00	1.758E-03	2.241E-04
0.035	8.554E 00	3.728E-03	8.558E 00	2.310E-03	2.510E-04
0.040	7.739E 00	3.726E-03	7.743E 00	2.925E-03	2.770E-04
0.045	7.092E 00	3.731E-03	7.096E 00	3.601E-03	3.021E-04
0.050	6.565E 00	3.742E-03	6.569E 00	4.334E-03	3.267E-04
0.055	6.129E 00	3.758E-03	6.132E 00	5.122E-03	3.508E-04
0.060	5.760E 00	3.778E-03	5.764E 00	5.964E-03	3.744E-04
0.065	5.445E 00	3.801E-03	5.448E 00	6.857E-03	3.976E-04
0.070	5.172E 00	3.826E-03	5.176E 00	7.799E-03	4.205E-04
0.075	4.933E 00	3.853E-03	4.937E 00	8.788E-03	4.432E-04
0.080	4.723E 00	3.882E-03	4.727E 00	9.824E-03	4.655E-04
0.085	4.536E 00	3.891E-03	4.540E 00	1.090E-02	4.874E-04
0.090	4.369E 00	3.923E-03	4.373E 00	1.203E-02	5.090E-04
0.095	4.219E 00	3.957E-03	4.223E 00	1.319E-02	5.305E-04
0.100	4.083E 00	3.992E-03	4.087E 00	1.439E-02	5.518E-04
0.150	3.208E 00	4.395E-03	3.213E 00	2.838E-02	7.590E-04
0.200	2.766E 00	4.845E-03	2.771E 00	4.524E-02	9.591E-04
0.250	2.502E 00	5.328E-03	2.507E 00	6.427E-02	1.155E-03
0.300	2.330E 00	5.831E-03	2.335E 00	8.498E-02	1.347E-03
0.350	2.209E 00	6.355E-03	2.216E 00	1.070E-01	1.538E-03
0.400	2.119E 00	6.879E-03	2.126E 00	1.301E-01	1.728E-03
0.450	2.051E 00	7.413E-03	2.059E 00	1.540E-01	1.915E-03
0.500	1.999E 00	7.948E-03	2.007E 00	1.786E-01	2.102E-03
0.550	1.958E 00	8.484E-03	1.966E 00	2.038E-01	2.287E-03
0.600	1.925E 00	9.024E-03	1.934E 00	2.294E-01	2.471E-03
0.650	1.899E 00	9.566E-03	1.908E 00	2.554E-01	2.653E-03
0.700	1.878E 00	1.011E-02	1.888E 00	2.818E-01	2.834E-03
0.750	1.860E 00	1.066E-02	1.871E 00	3.084E-01	3.013E-03
0.800	1.846E 00	1.121E-02	1.857E 00	3.352E-01	3.192E-03
0.850	1.834E 00	1.177E-02	1.845E 00	3.622E-01	3.369E-03
0.900	1.824E 00	1.233E-02	1.836E 00	3.894E-01	3.546E-03
0.950	1.816E 00	1.289E-02	1.828E 00	4.167E-01	3.721E-03
1.000	1.809E 00	1.345E-02	1.822E 00	4.441E-01	3.896E-03
1.100	1.798E 00	1.458E-02	1.813E 00	4.991E-01	4.243E-03
1.200	1.792E 00	1.573E-02	1.807E 00	5.544E-01	4.587E-03
1.300	1.787E 00	1.688E-02	1.804E 00	6.098E-01	4.929E-03

ELECTRONS IN POLYSTYRENE

ENERGY	STOPPING POWER			RANGE	RADIATION YIELD
	COLLISION	RADIATION	TOTAL		
MEV	MEV CM2/G	MEV CM2/G	MEV CM2/G	G/CM2	
1.400	1.784E 00	1.804E-02	1.802E 00	6.652E-01	5.268E-03
1.500	1.783E 00	1.922E-02	1.802E 00	7.207E-01	5.606E-03
1.600	1.783E 00	2.040E-02	1.803E 00	7.762E-01	5.943E-03
1.700	1.783E 00	2.156E-02	1.805E 00	8.316E-01	6.277E-03
1.800	1.784E 00	2.277E-02	1.807E 00	8.870E-01	6.610E-03
1.900	1.786E 00	2.398E-02	1.810E 00	9.423E-01	6.942E-03
2.000	1.787E 00	2.521E-02	1.813E 00	9.975E-01	7.274E-03
2.200	1.792E 00	2.770E-02	1.819E 00	1.108E 00	7.937E-03
2.400	1.797E 00	3.023E-02	1.827E 00	1.217E 00	8.599E-03
2.600	1.802E 00	3.279E-02	1.835E 00	1.327E 00	9.261E-03
2.800	1.807E 00	3.531E-02	1.843E 00	1.435E 00	9.924E-03
3.000	1.813E 00	3.795E-02	1.851E 00	1.544E 00	1.058E-02
3.500	1.826E 00	4.474E-02	1.871E 00	1.812E 00	1.224E-02
4.000	1.838E 00	5.178E-02	1.890E 00	2.078E 00	1.392E-02
4.500	1.850E 00	5.910E-02	1.909E 00	2.341E 00	1.561E-02
5.000	1.861E 00	6.654E-02	1.927E 00	2.602E 00	1.733E-02
5.500	1.870E 00	7.412E-02	1.944E 00	2.860E 00	1.905E-02
6.000	1.879E 00	8.183E-02	1.961E 00	3.116E 00	2.079E-02
6.500	1.888E 00	8.965E-02	1.977E 00	3.370E 00	2.254E-02
7.000	1.895E 00	9.759E-02	1.993E 00	3.622E 00	2.430E-02
7.500	1.902E 00	1.056E-01	2.008E 00	3.872E 00	2.607E-02
8.000	1.909E 00	1.138E-01	2.023E 00	4.120E 00	2.784E-02
8.500	1.915E 00	1.220E-01	2.037E 00	4.367E 00	2.962E-02
9.000	1.921E 00	1.309E-01	2.052E 00	4.611E 00	3.141E-02
9.500	1.926E 00	1.393E-01	2.066E 00	4.854E 00	3.321E-02
10.000	1.932E 00	1.478E-01	2.079E 00	5.095E 00	3.501E-02
20.000	1.998E 00	3.285E-01	2.327E 00	9.633E 00	7.080E-02
30.000	2.034E 00	5.205E-01	2.555E 00	1.373E 01	1.049E-01
40.000	2.059E 00	7.181E-01	2.777E 00	1.749E 01	1.366E-01
50.000	2.077E 00	9.194E-01	2.997E 00	2.095E 01	1.659E-01
60.000	2.093E 00	1.123E 00	3.216E 00	2.417E 01	1.930E-01
80.000	2.117E 00	1.537E 00	3.653E 00	3.000E 01	2.414E-01
100.000	2.135E 00	1.954E 00	4.089E 00	3.517E 01	2.831E-01
200.000	2.193E 00	4.079E 00	6.272E 00	5.477E 01	4.294E-01
300.000	2.226E 00	6.232E 00	8.458E 00	6.845E 01	5.188E-01
400.000	2.250E 00	8.394E 00	1.064E 01	7.896E 01	5.803E-01
500.000	2.269E 00	1.056E 01	1.283E 01	8.751E 01	6.256E-01
600.000	2.284E 00	1.274E 01	1.502E 01	9.470E 01	6.607E-01
800.000	2.308E 00	1.709E 01	1.940E 01	1.064E 02	7.120E-01
1000.000	2.326E 00	2.145E 01	2.377E 01	1.157E 02	7.481E-01

ELECTRONS IN STILBENE

ENERGY	STOPPING POWER			RANGE	RADIATION YIELD
	COLLISION	RADIATION	TOTAL		
MEV	MEV CM2/G	MEV CM2/G	MEV CM2/G	G/CM2	
0.010	2.226E 01	3.946E-03	2.226E 01	2.539E-04	1.015E-04
0.015	1.621E 01	3.865E-03	1.622E 01	5.210E-04	1.371E-04
0.020	1.295E 01	3.819E-03	1.296E 01	8.686E-04	1.696E-04
0.025	1.090E 01	3.787E-03	1.090E 01	1.291E-03	1.999E-04
0.030	9.477E 00	3.765E-03	9.481E 00	1.784E-03	2.287E-04
0.035	8.431E 00	3.746E-03	8.435E 00	2.345E-03	2.561E-04
0.040	7.628E 00	3.744E-03	7.632E 00	2.969E-03	2.825E-04
0.045	6.991E 00	3.749E-03	6.994E 00	3.654E-03	3.082E-04
0.050	6.472E 00	3.760E-03	6.476E 00	4.398E-03	3.332E-04
0.055	6.042E 00	3.776E-03	6.046E 00	5.198E-03	3.577E-04
0.060	5.679E 00	3.796E-03	5.682E 00	6.051E-03	3.817E-04
0.065	5.368E 00	3.819E-03	5.372E 00	6.957E-03	4.054E-04
0.070	5.099E 00	3.844E-03	5.103E 00	7.912E-03	4.287E-04
0.075	4.864E 00	3.871E-03	4.868E 00	8.916E-03	4.518E-04
0.080	4.657E 00	3.900E-03	4.661E 00	9.966E-03	4.746E-04
0.085	4.473E 00	3.910E-03	4.477E 00	1.106E-02	4.968E-04
0.090	4.308E 00	3.942E-03	4.312E 00	1.220E-02	5.189E-04
0.095	4.160E 00	3.976E-03	4.164E 00	1.338E-02	5.408E-04
0.100	4.026E 00	4.012E-03	4.030E 00	1.460E-02	5.625E-04
0.150	3.164E 00	4.417E-03	3.169E 00	2.878E-02	7.735E-04
0.200	2.728E 00	4.870E-03	2.733E 00	4.587E-02	9.773E-04
0.250	2.468E 00	5.356E-03	2.473E 00	6.517E-02	1.177E-03
0.300	2.298E 00	5.863E-03	2.304E 00	8.616E-02	1.373E-03
0.350	2.178E 00	6.389E-03	2.185E 00	1.085E-01	1.568E-03
0.400	2.090E 00	6.917E-03	2.096E 00	1.319E-01	1.761E-03
0.450	2.023E 00	7.454E-03	2.030E 00	1.561E-01	1.952E-03
0.500	1.971E 00	7.992E-03	1.979E 00	1.811E-01	2.143E-03
0.550	1.931E 00	8.532E-03	1.939E 00	2.066E-01	2.331E-03
0.600	1.899E 00	9.074E-03	1.908E 00	2.326E-01	2.519E-03
0.650	1.873E 00	9.619E-03	1.882E 00	2.590E-01	2.704E-03
0.700	1.851E 00	1.017E-02	1.862E 00	2.857E-01	2.889E-03
0.750	1.834E 00	1.072E-02	1.845E 00	3.127E-01	3.072E-03
0.800	1.820E 00	1.127E-02	1.831E 00	3.399E-01	3.254E-03
0.850	1.808E 00	1.183E-02	1.820E 00	3.673E-01	3.435E-03
0.900	1.798E 00	1.239E-02	1.811E 00	3.948E-01	3.615E-03
0.950	1.790E 00	1.296E-02	1.803E 00	4.225E-01	3.794E-03
1.000	1.784E 00	1.352E-02	1.797E 00	4.503E-01	3.972E-03
1.100	1.774E 00	1.466E-02	1.788E 00	5.061E-01	4.325E-03
1.200	1.767E 00	1.581E-02	1.783E 00	5.621E-01	4.676E-03
1.300	1.762E 00	1.697E-02	1.779E 00	6.182E-01	5.024E-03

ELECTRONS IN STILBENE

ENERGY	STOPPING POWER			RANGE	RADIATION YIELD
	COLLISION	RADIATION	TOTAL		
MEV	MEV CM2/G	MEV CM2/G	MEV CM2/G	G/CM2	
1.400	1.760E 00	1.814E-02	1.778E 00	6.745E-01	5.370E-03
1.500	1.758E 00	1.931E-02	1.778E 00	7.307E-01	5.714E-03
1.600	1.758E 00	2.050E-02	1.779E 00	7.870E-01	6.057E-03
1.700	1.758E 00	2.167E-02	1.780E 00	8.432E-01	6.397E-03
1.800	1.759E 00	2.288E-02	1.782E 00	8.993E-01	6.737E-03
1.900	1.761E 00	2.410E-02	1.785E 00	9.554E-01	7.075E-03
2.000	1.763E 00	2.533E-02	1.788E 00	1.011E 00	7.413E-03
2.200	1.767E 00	2.783E-02	1.795E 00	1.123E 00	8.088E-03
2.400	1.772E 00	3.037E-02	1.802E 00	1.234E 00	8.762E-03
2.600	1.777E 00	3.295E-02	1.810E 00	1.345E 00	9.436E-03
2.800	1.782E 00	3.547E-02	1.818E 00	1.455E 00	1.011E-02
3.000	1.788E 00	3.812E-02	1.826E 00	1.565E 00	1.078E-02
3.500	1.801E 00	4.494E-02	1.846E 00	1.837E 00	1.247E-02
4.000	1.813E 00	5.200E-02	1.865E 00	2.107E 00	1.418E-02
4.500	1.824E 00	5.935E-02	1.884E 00	2.374E 00	1.590E-02
5.000	1.835E 00	6.682E-02	1.902E 00	2.638E 00	1.764E-02
5.500	1.844E 00	7.443E-02	1.919E 00	2.900E 00	1.940E-02
6.000	1.853E 00	8.216E-02	1.935E 00	3.159E 00	2.117E-02
6.500	1.861E 00	9.002E-02	1.951E 00	3.416E 00	2.294E-02
7.000	1.869E 00	9.798E-02	1.967E 00	3.671E 00	2.473E-02
7.500	1.876E 00	1.061E-01	1.982E 00	3.925E 00	2.653E-02
8.000	1.882E 00	1.142E-01	1.997E 00	4.176E 00	2.833E-02
8.500	1.889E 00	1.225E-01	2.011E 00	4.426E 00	3.014E-02
9.000	1.894E 00	1.314E-01	2.026E 00	4.673E 00	3.195E-02
9.500	1.900E 00	1.399E-01	2.040E 00	4.919E 00	3.379E-02
10.000	1.905E 00	1.484E-01	2.053E 00	5.164E 00	3.562E-02
20.000	1.971E 00	3.298E-01	2.300E 00	9.757E 00	7.195E-02
30.000	2.006E 00	5.225E-01	2.529E 00	1.390E 01	1.065E-01
40.000	2.030E 00	7.208E-01	2.751E 00	1.769E 01	1.386E-01
50.000	2.049E 00	9.228E-01	2.972E 00	2.119E 01	1.683E-01
60.000	2.064E 00	1.127E 00	3.191E 00	2.443E 01	1.956E-01
80.000	2.088E 00	1.542E 00	3.630E 00	3.031E 01	2.443E-01
100.000	2.106E 00	1.961E 00	4.067E 00	3.551E 01	2.864E-01
200.000	2.163E 00	4.094E 00	6.257E 00	5.518E 01	4.331E-01
300.000	2.196E 00	6.254E 00	8.450E 00	6.888E 01	5.225E-01
400.000	2.220E 00	8.424E 00	1.064E 01	7.940E 01	5.838E-01
500.000	2.238E 00	1.060E 01	1.284E 01	8.794E 01	6.290E-01
600.000	2.253E 00	1.278E 01	1.503E 01	9.513E 01	6.639E-01
800.000	2.277E 00	1.715E 01	1.943E 01	1.068E 02	7.149E-01
1000.000	2.295E 00	2.152E 01	2.382E 01	1.161E 02	7.507E-01

ELECTRONS IN LUCITE

ENERGY	STOPPING POWER			RANGE	RADIATION YIELD
	COLLISION	RADIATION	TOTAL		
MEV	MEV CM2/G	MEV CM2/G	MEV CM2/G	G/CM2	
0.010	2.251E 01	4.356E-03	2.252E 01	2.511E-04	1.106E-04
0.015	1.640E 01	4.268E-03	1.640E 01	5.151E-04	1.495E-04
0.020	1.311E 01	4.215E-03	1.311E 01	8.587E-04	1.850E-04
0.025	1.103E 01	4.177E-03	1.103E 01	1.276E-03	2.180E-04
0.030	9.588E 00	4.151E-03	9.592E 00	1.764E-03	2.494E-04
0.035	8.530E 00	4.128E-03	8.534E 00	2.318E-03	2.792E-04
0.040	7.717E 00	4.125E-03	7.722E 00	2.935E-03	3.079E-04
0.045	7.073E 00	4.130E-03	7.077E 00	3.612E-03	3.358E-04
0.050	6.548E 00	4.144E-03	6.552E 00	4.347E-03	3.631E-04
0.055	6.113E 00	4.162E-03	6.117E 00	5.137E-03	3.897E-04
0.060	5.746E 00	4.185E-03	5.750E 00	5.981E-03	4.159E-04
0.065	5.431E 00	4.211E-03	5.436E 00	6.876E-03	4.417E-04
0.070	5.159E 00	4.240E-03	5.164E 00	7.820E-03	4.672E-04
0.075	4.922E 00	4.272E-03	4.926E 00	8.812E-03	4.923E-04
0.080	4.712E 00	4.305E-03	4.716E 00	9.850E-03	5.172E-04
0.085	4.526E 00	4.323E-03	4.530E 00	1.093E-02	5.416E-04
0.090	4.359E 00	4.360E-03	4.363E 00	1.206E-02	5.658E-04
0.095	4.209E 00	4.399E-03	4.214E 00	1.322E-02	5.898E-04
0.100	4.074E 00	4.439E-03	4.078E 00	1.443E-02	6.136E-04
0.150	3.202E 00	4.891E-03	3.207E 00	2.844E-02	8.450E-04
0.200	2.761E 00	5.386E-03	2.766E 00	4.533E-02	1.068E-03
0.250	2.498E 00	5.923E-03	2.504E 00	6.440E-02	1.286E-03
0.300	2.326E 00	6.483E-03	2.332E 00	8.513E-02	1.500E-03
0.350	2.206E 00	7.066E-03	2.213E 00	1.072E-01	1.713E-03
0.400	2.106E 00	7.649E-03	2.113E 00	1.304E-01	1.925E-03
0.450	2.039E 00	8.242E-03	2.047E 00	1.544E-01	2.136E-03
0.500	1.987E 00	8.835E-03	1.996E 00	1.792E-01	2.345E-03
0.550	1.946E 00	9.429E-03	1.956E 00	2.045E-01	2.552E-03
0.600	1.914E 00	1.002E-02	1.924E 00	2.303E-01	2.758E-03
0.650	1.888E 00	1.062E-02	1.898E 00	2.564E-01	2.961E-03
0.700	1.867E 00	1.122E-02	1.878E 00	2.829E-01	3.163E-03
0.750	1.849E 00	1.183E-02	1.861E 00	3.097E-01	3.363E-03
0.800	1.835E 00	1.243E-02	1.847E 00	3.367E-01	3.562E-03
0.850	1.823E 00	1.305E-02	1.836E 00	3.638E-01	3.760E-03
0.900	1.814E 00	1.366E-02	1.827E 00	3.911E-01	3.956E-03
0.950	1.806E 00	1.427E-02	1.820E 00	4.185E-01	4.151E-03
1.000	1.799E 00	1.489E-02	1.814E 00	4.460E-01	4.344E-03
1.100	1.789E 00	1.613E-02	1.805E 00	5.013E-01	4.729E-03
1.200	1.782E 00	1.738E-02	1.800E 00	5.568E-01	5.110E-03
1.300	1.778E 00	1.864E-02	1.796E 00	6.124E-01	5.487E-03

ELECTRONS IN LUCITE

ENERGY	STOPPING POWER			RANGE	RADIATION YIELD
	COLLISION	RADIATION	TOTAL		
MEV	MEV CM2/G	MEV CM2/G	MEV CM2/G	G/CM2	
1.400	1.775E 00	1.991E-02	1.795E 00	6.681E-01	5.862E-03
1.500	1.774E 00	2.120E-02	1.795E 00	7.238E-01	6.235E-03
1.600	1.774E 00	2.248E-02	1.796E 00	7.795E-01	6.605E-03
1.700	1.775E 00	2.375E-02	1.798E 00	8.352E-01	6.973E-03
1.800	1.776E 00	2.506E-02	1.801E 00	8.907E-01	7.339E-03
1.900	1.777E 00	2.638E-02	1.804E 00	9.462E-01	7.703E-03
2.000	1.779E 00	2.772E-02	1.807E 00	1.002E 00	8.067E-03
2.200	1.784E 00	3.042E-02	1.814E 00	1.112E 00	8.794E-03
2.400	1.789E 00	3.318E-02	1.822E 00	1.222E 00	9.518E-03
2.600	1.794E 00	3.597E-02	1.830E 00	1.332E 00	1.024E-02
2.800	1.800E 00	3.870E-02	1.838E 00	1.441E 00	1.097E-02
3.000	1.805E 00	4.157E-02	1.847E 00	1.549E 00	1.169E-02
3.500	1.819E 00	4.895E-02	1.868E 00	1.818E 00	1.350E-02
4.000	1.832E 00	5.659E-02	1.888E 00	2.085E 00	1.532E-02
4.500	1.843E 00	6.453E-02	1.908E 00	2.348E 00	1.716E-02
5.000	1.854E 00	7.262E-02	1.927E 00	2.609E 00	1.902E-02
5.500	1.864E 00	8.085E-02	1.945E 00	2.867E 00	2.089E-02
6.000	1.873E 00	8.921E-02	1.962E 00	3.123E 00	2.278E-02
6.500	1.882E 00	9.771E-02	1.979E 00	3.377E 00	2.467E-02
7.000	1.889E 00	1.063E-01	1.996E 00	3.628E 00	2.658E-02
7.500	1.897E 00	1.151E-01	2.012E 00	3.878E 00	2.849E-02
8.000	1.903E 00	1.239E-01	2.027E 00	4.125E 00	3.040E-02
8.500	1.910E 00	1.328E-01	2.043E 00	4.371E 00	3.233E-02
9.000	1.916E 00	1.426E-01	2.058E 00	4.615E 00	3.426E-02
9.500	1.921E 00	1.518E-01	2.073E 00	4.857E 00	3.621E-02
10.000	1.926E 00	1.610E-01	2.087E 00	5.097E 00	3.815E-02
20.000	1.994E 00	3.574E-01	2.351E 00	9.603E 00	7.663E-02
30.000	2.030E 00	5.660E-01	2.596E 00	1.365E 01	1.130E-01
40.000	2.055E 00	7.806E-01	2.836E 00	1.733E 01	1.466E-01
50.000	2.074E 00	9.992E-01	3.073E 00	2.072E 01	1.774E-01
60.000	2.089E 00	1.221E 00	3.310E 00	2.385E 01	2.058E-01
80.000	2.113E 00	1.669E 00	3.782E 00	2.950E 01	2.560E-01
100.000	2.132E 00	2.122E 00	4.254E 00	3.449E 01	2.990E-01
200.000	2.189E 00	4.428E 00	6.617E 00	5.318E 01	4.474E-01
300.000	2.223E 00	6.762E 00	8.985E 00	6.610E 01	5.366E-01
400.000	2.247E 00	9.107E 00	1.135E 01	7.598E 01	5.973E-01
500.000	2.265E 00	1.146E 01	1.372E 01	8.398E 01	6.417E-01
600.000	2.281E 00	1.382E 01	1.610E 01	9.070E 01	6.760E-01
800.000	2.304E 00	1.854E 01	2.084E 01	1.016E 02	7.258E-01
1000.000	2.323E 00	2.326E 01	2.558E 01	1.102E 02	7.606E-01

ELECTRONS IN ANTHRACENE

ENERGY	STOPPING POWER			RANGE	RADIATION YIELD
	COLLISION	RADIATION	TOTAL		
MEV	MEV CM2/G	MEV CM2/G	MEV CM2/G	G/CM2	
0.010	2.192E 01	3.969E-03	2.193E 01	2.580E-04	1.038E-04
0.015	1.597E 01	3.887E-03	1.598E 01	5.291E-04	1.401E-04
0.020	1.277E 01	3.840E-03	1.277E 01	8.817E-04	1.731E-04
0.025	1.074E 01	3.807E-03	1.075E 01	1.310E-03	2.040E-04
0.030	9.344E 00	3.785E-03	9.348E 00	1.811E-03	2.333E-04
0.035	8.313E 00	3.766E-03	8.317E 00	2.379E-03	2.613E-04
0.040	7.522E 00	3.764E-03	7.526E 00	3.012E-03	2.882E-04
0.045	6.894E 00	3.768E-03	6.898E 00	3.707E-03	3.143E-04
0.050	6.383E 00	3.780E-03	6.387E 00	4.461E-03	3.398E-04
0.055	5.959E 00	3.796E-03	5.963E 00	5.272E-03	3.647E-04
0.060	5.601E 00	3.816E-03	5.605E 00	6.137E-03	3.892E-04
0.065	5.295E 00	3.839E-03	5.299E 00	7.055E-03	4.133E-04
0.070	5.030E 00	3.864E-03	5.034E 00	8.024E-03	4.371E-04
0.075	4.798E 00	3.891E-03	4.802E 00	9.042E-03	4.606E-04
0.080	4.594E 00	3.921E-03	4.598E 00	1.011E-02	4.838E-04
0.085	4.412E 00	3.930E-03	4.416E 00	1.122E-02	5.064E-04
0.090	4.250E 00	3.963E-03	4.254E 00	1.237E-02	5.289E-04
0.095	4.104E 00	3.997E-03	4.108E 00	1.357E-02	5.512E-04
0.100	3.972E 00	4.033E-03	3.976E 00	1.480E-02	5.733E-04
0.150	3.123E 00	4.441E-03	3.127E 00	2.917E-02	7.883E-04
0.200	2.692E 00	4.897E-03	2.697E 00	4.650E-02	9.959E-04
0.250	2.436E 00	5.386E-03	2.441E 00	6.605E-02	1.199E-03
0.300	2.268E 00	5.896E-03	2.274E 00	8.731E-02	1.399E-03
0.350	2.151E 00	6.427E-03	2.157E 00	1.099E-01	1.597E-03
0.400	2.063E 00	6.958E-03	2.070E 00	1.336E-01	1.794E-03
0.450	1.997E 00	7.499E-03	2.005E 00	1.582E-01	1.989E-03
0.500	1.946E 00	8.039E-03	1.954E 00	1.834E-01	2.183E-03
0.550	1.906E 00	8.582E-03	1.915E 00	2.093E-01	2.375E-03
0.600	1.875E 00	9.128E-03	1.884E 00	2.356E-01	2.566E-03
0.650	1.849E 00	9.676E-03	1.859E 00	2.623E-01	2.755E-03
0.700	1.828E 00	1.023E-02	1.838E 00	2.894E-01	2.943E-03
0.750	1.811E 00	1.078E-02	1.822E 00	3.167E-01	3.129E-03
0.800	1.797E 00	1.134E-02	1.808E 00	3.443E-01	3.315E-03
0.850	1.785E 00	1.190E-02	1.797E 00	3.720E-01	3.499E-03
0.900	1.776E 00	1.247E-02	1.788E 00	3.999E-01	3.682E-03
0.950	1.768E 00	1.303E-02	1.781E 00	4.279E-01	3.864E-03
1.000	1.761E 00	1.360E-02	1.775E 00	4.560E-01	4.046E-03
1.100	1.751E 00	1.474E-02	1.766E 00	5.125E-01	4.406E-03
1.200	1.744E 00	1.590E-02	1.760E 00	5.693E-01	4.763E-03
1.300	1.740E 00	1.706E-02	1.757E 00	6.261E-01	5.117E-03

ELECTRONS IN ANTHRACENE

ENERGY	STOPPING POWER			RANGE	RADIATION YIELD
	COLLISION	RADIATION	TOTAL		
MEV	MEV CM2/G	MEV CM2/G	MEV CM2/G	G/CM2	
1.400	1.737E 00	1.824E-02	1.756E 00	6.831E-01	5.470E-03
1.500	1.736E 00	1.942E-02	1.756E 00	7.400E-01	5.820E-03
1.600	1.736E 00	2.061E-02	1.756E 00	7.970E-01	6.169E-03
1.700	1.736E 00	2.179E-02	1.758E 00	8.539E-01	6.515E-03
1.800	1.737E 00	2.300E-02	1.760E 00	9.107E-01	6.860E-03
1.900	1.739E 00	2.423E-02	1.763E 00	9.675E-01	7.205E-03
2.000	1.740E 00	2.546E-02	1.766E 00	1.024E 00	7.548E-03
2.200	1.745E 00	2.797E-02	1.773E 00	1.137E 00	8.235E-03
2.400	1.749E 00	3.052E-02	1.780E 00	1.250E 00	8.920E-03
2.600	1.755E 00	3.311E-02	1.788E 00	1.362E 00	9.606E-03
2.800	1.760E 00	3.564E-02	1.796E 00	1.474E 00	1.029E-02
3.000	1.765E 00	3.831E-02	1.803E 00	1.585E 00	1.098E-02
3.500	1.778E 00	4.515E-02	1.823E 00	1.860E 00	1.269E-02
4.000	1.790E 00	5.225E-02	1.842E 00	2.133E 00	1.443E-02
4.500	1.801E 00	5.963E-02	1.861E 00	2.403E 00	1.618E-02
5.000	1.812E 00	6.713E-02	1.879E 00	2.671E 00	1.795E-02
5.500	1.821E 00	7.477E-02	1.896E 00	2.936E 00	1.973E-02
6.000	1.830E 00	8.254E-02	1.913E 00	3.198E 00	2.153E-02
6.500	1.838E 00	9.042E-02	1.929E 00	3.458E 00	2.334E-02
7.000	1.846E 00	9.842E-02	1.944E 00	3.717E 00	2.515E-02
7.500	1.853E 00	1.065E-01	1.959E 00	3.973E 00	2.697E-02
8.000	1.859E 00	1.147E-01	1.974E 00	4.227E 00	2.880E-02
8.500	1.865E 00	1.230E-01	1.988E 00	4.480E 00	3.064E-02
9.000	1.871E 00	1.320E-01	2.003E 00	4.730E 00	3.249E-02
9.500	1.876E 00	1.405E-01	2.017E 00	4.979E 00	3.434E-02
10.000	1.881E 00	1.491E-01	2.030E 00	5.226E 00	3.621E-02
20.000	1.946E 00	3.312E-01	2.277E 00	9.868E 00	7.306E-02
30.000	1.981E 00	5.247E-01	2.506E 00	1.405E 01	1.081E-01
40.000	2.005E 00	7.238E-01	2.729E 00	1.787E 01	1.405E-01
50.000	2.024E 00	9.267E-01	2.951E 00	2.140E 01	1.705E-01
60.000	2.039E 00	1.132E 00	3.171E 00	2.466E 01	1.981E-01
80.000	2.062E 00	1.549E 00	3.611E 00	3.057E 01	2.471E-01
100.000	2.080E 00	1.969E 00	4.050E 00	3.580E 01	2.894E-01
200.000	2.137E 00	4.111E 00	6.247E 00	5.552E 01	4.366E-01
300.000	2.170E 00	6.279E 00	8.449E 00	6.924E 01	5.260E-01
400.000	2.193E 00	8.458E 00	1.065E 01	7.975E 01	5.871E-01
500.000	2.211E 00	1.064E 01	1.285E 01	8.829E 01	6.321E-01
600.000	2.226E 00	1.283E 01	1.506E 01	9.547E 01	6.669E-01
800.000	2.249E 00	1.722E 01	1.947E 01	1.071E 02	7.176E-01
1000.000	2.267E 00	2.161E 01	2.387E 01	1.164E 02	7.531E-01

ELECTRONS IN MUSCLE

ENERGY	STOPPING POWER			RANGE	RADIATION YIELD
	COLLISION	RADIATION	TOTAL		
MEV	MEV CM2/G	MEV CM2/G	MEV CM2/G	G/CM2	
0.010	2.292E 01	4.971E-03	2.292E 01	2.467E-04	1.236E-04
0.015	1.670E 01	4.874E-03	1.670E 01	5.061E-04	1.674E-04
0.020	1.334E 01	4.810E-03	1.335E 01	8.435E-04	2.072E-04
0.025	1.123E 01	4.766E-03	1.123E 01	1.254E-03	2.443E-04
0.030	9.763E 00	4.735E-03	9.768E 00	1.733E-03	2.794E-04
0.035	8.686E 00	4.705E-03	8.691E 00	2.276E-03	3.128E-04
0.040	7.859E 00	4.702E-03	7.863E 00	2.882E-03	3.449E-04
0.045	7.202E 00	4.710E-03	7.207E 00	3.547E-03	3.761E-04
0.050	6.669E 00	4.726E-03	6.673E 00	4.269E-03	4.066E-04
0.055	6.225E 00	4.749E-03	6.230E 00	5.045E-03	4.365E-04
0.060	5.851E 00	4.777E-03	5.856E 00	5.873E-03	4.659E-04
0.065	5.531E 00	4.808E-03	5.536E 00	6.752E-03	4.948E-04
0.070	5.254E 00	4.843E-03	5.259E 00	7.679E-03	5.234E-04
0.075	5.012E 00	4.881E-03	5.017E 00	8.653E-03	5.516E-04
0.080	4.799E 00	4.921E-03	4.804E 00	9.672E-03	5.795E-04
0.085	4.609E 00	4.952E-03	4.614E 00	1.073E-02	6.071E-04
0.090	4.440E 00	4.995E-03	4.445E 00	1.184E-02	6.344E-04
0.095	4.287E 00	5.041E-03	4.292E 00	1.298E-02	6.615E-04
0.100	4.149E 00	5.087E-03	4.154E 00	1.417E-02	6.884E-04
0.150	3.261E 00	5.609E-03	3.267E 00	2.792E-02	9.497E-04
0.200	2.811E 00	6.169E-03	2.817E 00	4.451E-02	1.201E-03
0.250	2.543E 00	6.781E-03	2.550E 00	6.323E-02	1.446E-03
0.300	2.367E 00	7.420E-03	2.375E 00	8.359E-02	1.687E-03
0.350	2.245E 00	8.088E-03	2.254E 00	1.052E-01	1.926E-03
0.400	2.157E 00	8.754E-03	2.166E 00	1.279E-01	2.162E-03
0.450	2.092E 00	9.432E-03	2.101E 00	1.513E-01	2.396E-03
0.500	2.041E 00	1.011E-02	2.052E 00	1.754E-01	2.627E-03
0.550	2.003E 00	1.078E-02	2.013E 00	2.000E-01	2.855E-03
0.600	1.972E 00	1.146E-02	1.984E 00	2.251E-01	3.081E-03
0.650	1.948E 00	1.214E-02	1.960E 00	2.504E-01	3.305E-03
0.700	1.929E 00	1.282E-02	1.942E 00	2.761E-01	3.525E-03
0.750	1.914E 00	1.350E-02	1.927E 00	3.019E-01	3.744E-03
0.800	1.902E 00	1.418E-02	1.916E 00	3.279E-01	3.960E-03
0.850	1.892E 00	1.487E-02	1.907E 00	3.541E-01	4.174E-03
0.900	1.884E 00	1.556E-02	1.900E 00	3.804E-01	4.387E-03
0.950	1.878E 00	1.625E-02	1.894E 00	4.067E-01	4.597E-03
1.000	1.874E 00	1.694E-02	1.890E 00	4.332E-01	4.806E-03
1.100	1.868E 00	1.834E-02	1.886E 00	4.861E-01	5.218E-03
1.200	1.865E 00	1.975E-02	1.885E 00	5.392E-01	5.625E-03
1.300	1.864E 00	2.116E-02	1.886E 00	5.922E-01	6.027E-03

ELECTRONS IN MUSCLE

ENERGY	STOPPING POWER			RANGE	RADIATION YIELD
	COLLISION	RADIATION	TOTAL		
MEV	MEV CM2/G	MEV CM2/G	MEV CM2/G	G/CM2	
1.400	1.866E 00	2.259E-02	1.888E 00	6.452E-01	6.425E-03
1.500	1.868E 00	2.402E-02	1.892E 00	6.981E-01	6.818E-03
1.600	1.872E 00	2.546E-02	1.897E 00	7.509E-01	7.208E-03
1.700	1.876E 00	2.687E-02	1.903E 00	8.035E-01	7.594E-03
1.800	1.881E 00	2.833E-02	1.909E 00	8.560E-01	7.976E-03
1.900	1.886E 00	2.981E-02	1.916E 00	9.083E-01	8.356E-03
2.000	1.891E 00	3.130E-02	1.922E 00	9.604E-01	8.735E-03
2.200	1.902E 00	3.432E-02	1.936E 00	1.064E 00	9.486E-03
2.400	1.913E 00	3.739E-02	1.951E 00	1.167E 00	1.023E-02
2.600	1.925E 00	4.050E-02	1.965E 00	1.269E 00	1.098E-02
2.800	1.936E 00	4.354E-02	1.980E 00	1.371E 00	1.171E-02
3.000	1.948E 00	4.673E-02	1.994E 00	1.471E 00	1.245E-02
3.500	1.974E 00	5.495E-02	2.029E 00	1.720E 00	1.428E-02
4.000	1.999E 00	6.346E-02	2.063E 00	1.964E 00	1.611E-02
4.500	2.022E 00	7.230E-02	2.094E 00	2.205E 00	1.794E-02
5.000	2.043E 00	8.129E-02	2.125E 00	2.442E 00	1.979E-02
5.500	2.063E 00	9.045E-02	2.154E 00	2.675E 00	2.164E-02
6.000	2.082E 00	9.977E-02	2.181E 00	2.906E 00	2.349E-02
6.500	2.099E 00	1.092E-01	2.208E 00	3.134E 00	2.534E-02
7.000	2.115E 00	1.188E-01	2.234E 00	3.359E 00	2.720E-02
7.500	2.130E 00	1.285E-01	2.259E 00	3.582E 00	2.906E-02
8.000	2.144E 00	1.384E-01	2.283E 00	3.802E 00	3.092E-02
8.500	2.158E 00	1.483E-01	2.306E 00	4.020E 00	3.277E-02
9.000	2.171E 00	1.593E-01	2.330E 00	4.235E 00	3.464E-02
9.500	2.183E 00	1.695E-01	2.352E 00	4.449E 00	3.651E-02
10.000	2.194E 00	1.798E-01	2.374E 00	4.661E 00	3.838E-02
20.000	2.353E 00	3.986E-01	2.752E 00	8.559E 00	7.466E-02
30.000	2.447E 00	6.311E-01	3.078E 00	1.199E 01	1.083E-01
40.000	2.510E 00	8.701E-01	3.381E 00	1.509E 01	1.392E-01
50.000	2.549E 00	1.113E 00	3.662E 00	1.793E 01	1.676E-01
60.000	2.577E 00	1.360E 00	3.937E 00	2.056E 01	1.938E-01
80.000	2.620E 00	1.859E 00	4.479E 00	2.532E 01	2.407E-01
100.000	2.651E 00	2.363E 00	5.014E 00	2.954E 01	2.814E-01
200.000	2.737E 00	4.927E 00	7.663E 00	4.554E 01	4.249E-01
300.000	2.782E 00	7.521E 00	1.030E 01	5.676E 01	5.134E-01
400.000	2.812E 00	1.013E 01	1.294E 01	6.540E 01	5.747E-01
500.000	2.834E 00	1.274E 01	1.558E 01	7.243E 01	6.200E-01
600.000	2.852E 00	1.536E 01	1.821E 01	7.836E 01	6.552E-01
800.000	2.879E 00	2.061E 01	2.348E 01	8.801E 01	7.069E-01
1000.000	2.900E 00	2.585E 01	2.875E 01	9.569E 01	7.433E-01

ELECTRONS IN BONE

ENERGY	STOPPING POWER			RANGE	RADIATION YIELD
	COLLISION	RADIATION	TOTAL		
MEV	MEV CM2/G	MEV CM2/G	MEV CM2/G	G/CM2	
0.010	2.101E 01	6.373E-03	2.101E 01	2.711E-04	1.726E-04
0.015	1.536E 01	6.282E-03	1.537E 01	5.533E-04	2.341E-04
0.020	1.231E 01	6.206E-03	1.231E 01	9.195E-04	2.898E-04
0.025	1.037E 01	6.172E-03	1.038E 01	1.364E-03	3.418E-04
0.030	9.030E 00	6.159E-03	9.036E 00	1.882E-03	3.913E-04
0.035	8.041E 00	6.153E-03	8.047E 00	2.469E-03	4.387E-04
0.040	7.281E 00	6.169E-03	7.287E 00	3.123E-03	4.846E-04
0.045	6.678E 00	6.196E-03	6.684E 00	3.841E-03	5.292E-04
0.050	6.186E 00	6.231E-03	6.193E 00	4.619E-03	5.730E-04
0.055	5.778E 00	6.271E-03	5.785E 00	5.455E-03	6.159E-04
0.060	5.434E 00	6.316E-03	5.440E 00	6.347E-03	6.581E-04
0.065	5.139E 00	6.365E-03	5.145E 00	7.292E-03	6.998E-04
0.070	4.883E 00	6.417E-03	4.890E 00	8.290E-03	7.409E-04
0.075	4.660E 00	6.472E-03	4.666E 00	9.337E-03	7.814E-04
0.080	4.463E 00	6.528E-03	4.469E 00	1.043E-02	8.216E-04
0.085	4.288E 00	6.571E-03	4.294E 00	1.157E-02	8.612E-04
0.090	4.131E 00	6.631E-03	4.138E 00	1.276E-02	9.003E-04
0.095	3.990E 00	6.693E-03	3.997E 00	1.399E-02	9.392E-04
0.100	3.862E 00	6.757E-03	3.869E 00	1.526E-02	9.778E-04
0.150	3.041E 00	7.442E-03	3.049E 00	3.001E-02	1.351E-03
0.200	2.623E 00	8.154E-03	2.631E 00	4.778E-02	1.706E-03
0.250	2.374E 00	8.941E-03	2.383E 00	6.781E-02	2.050E-03
0.300	2.210E 00	9.765E-03	2.220E 00	8.960E-02	2.388E-03
0.350	2.097E 00	1.063E-02	2.107E 00	1.128E-01	2.722E-03
0.400	2.015E 00	1.148E-02	2.026E 00	1.370E-01	3.051E-03
0.450	1.953E 00	1.235E-02	1.965E 00	1.620E-01	3.376E-03
0.500	1.906E 00	1.321E-02	1.919E 00	1.878E-01	3.697E-03
0.550	1.869E 00	1.407E-02	1.883E 00	2.141E-01	4.013E-03
0.600	1.840E 00	1.493E-02	1.855E 00	2.409E-01	4.325E-03
0.650	1.817E 00	1.578E-02	1.833E 00	2.680E-01	4.633E-03
0.700	1.799E 00	1.664E-02	1.816E 00	2.954E-01	4.937E-03
0.750	1.784E 00	1.750E-02	1.802E 00	3.230E-01	5.237E-03
0.800	1.772E 00	1.836E-02	1.791E 00	3.509E-01	5.534E-03
0.850	1.763E 00	1.925E-02	1.782E 00	3.789E-01	5.828E-03
0.900	1.755E 00	2.012E-02	1.775E 00	4.070E-01	6.119E-03
0.950	1.749E 00	2.098E-02	1.770E 00	4.352E-01	6.407E-03
1.000	1.744E 00	2.185E-02	1.766E 00	4.635E-01	6.693E-03
1.100	1.738E 00	2.359E-02	1.761E 00	5.202E-01	7.255E-03
1.200	1.734E 00	2.533E-02	1.760E 00	5.770E-01	7.809E-03
1.300	1.733E 00	2.708E-02	1.760E 00	6.338E-01	8.353E-03

ELECTRONS IN BONE

ENERGY	STOPPING POWER			RANGE	RADIATION YIELD
	COLLISION	RADIATION	TOTAL		
MEV	MEV CM2/G	MEV CM2/G	MEV CM2/G	G/CM2	
1.400	1.734E 00	2.883E-02	1.762E 00	6.906E-01	8.890E-03
1.500	1.735E 00	3.059E-02	1.766E 00	7.473E-01	9.421E-03
1.600	1.737E 00	3.236E-02	1.770E 00	8.039E-01	9.945E-03
1.700	1.741E 00	3.400E-02	1.775E 00	8.603E-01	1.046E-02
1.800	1.744E 00	3.580E-02	1.780E 00	9.166E-01	1.097E-02
1.900	1.748E 00	3.761E-02	1.786E 00	9.727E-01	1.148E-02
2.000	1.752E 00	3.944E-02	1.792E 00	1.029E 00	1.198E-02
2.200	1.761E 00	4.317E-02	1.804E 00	1.140E 00	1.298E-02
2.400	1.770E 00	4.697E-02	1.817E 00	1.250E 00	1.397E-02
2.600	1.779E 00	5.084E-02	1.830E 00	1.360E 00	1.496E-02
2.800	1.788E 00	5.483E-02	1.843E 00	1.469E 00	1.594E-02
3.000	1.797E 00	5.883E-02	1.856E 00	1.577E 00	1.693E-02
3.500	1.819E 00	6.907E-02	1.888E 00	1.844E 00	1.939E-02
4.000	1.839E 00	7.963E-02	1.919E 00	2.107E 00	2.184E-02
4.500	1.858E 00	9.053E-02	1.948E 00	2.365E 00	2.430E-02
5.000	1.875E 00	1.016E-01	1.976E 00	2.620E 00	2.677E-02
5.500	1.890E 00	1.129E-01	2.003E 00	2.871E 00	2.923E-02
6.000	1.905E 00	1.243E-01	2.029E 00	3.119E 00	3.170E-02
6.500	1.919E 00	1.359E-01	2.055E 00	3.364E 00	3.416E-02
7.000	1.932E 00	1.477E-01	2.079E 00	3.606E 00	3.662E-02
7.500	1.943E 00	1.596E-01	2.103E 00	3.845E 00	3.908E-02
8.000	1.955E 00	1.716E-01	2.126E 00	4.082E 00	4.153E-02
8.500	1.965E 00	1.838E-01	2.149E 00	4.316E 00	4.397E-02
9.000	1.975E 00	1.969E-01	2.172E 00	4.547E 00	4.642E-02
9.500	1.985E 00	2.093E-01	2.194E 00	4.776E 00	4.888E-02
10.000	1.994E 00	2.218E-01	2.216E 00	5.003E 00	5.132E-02
20.000	2.116E 00	4.885E-01	2.604E 00	9.153E 00	9.812E-02
30.000	2.186E 00	7.718E-01	2.958E 00	1.275E 01	1.405E-01
40.000	2.234E 00	1.063E 00	3.297E 00	1.595E 01	1.785E-01
50.000	2.264E 00	1.360E 00	3.623E 00	1.884E 01	2.127E-01
60.000	2.287E 00	1.660E 00	3.947E 00	2.149E 01	2.437E-01
80.000	2.322E 00	2.267E 00	4.589E 00	2.618E 01	2.975E-01
100.000	2.347E 00	2.880E 00	5.227E 00	3.026E 01	3.427E-01
200.000	2.420E 00	5.994E 00	8.414E 00	4.520E 01	4.932E-01
300.000	2.459E 00	9.144E 00	1.160E 01	5.527E 01	5.802E-01
400.000	2.486E 00	1.231E 01	1.479E 01	6.289E 01	6.381E-01
500.000	2.506E 00	1.548E 01	1.798E 01	6.901E 01	6.799E-01
600.000	2.522E 00	1.865E 01	2.117E 01	7.413E 01	7.118E-01
800.000	2.547E 00	2.501E 01	2.756E 01	8.239E 01	7.577E-01
1000.000	2.566E 00	3.137E 01	3.394E 01	8.891E 01	7.895E-01

ELECTRONS IN AIR

ENERGY	STOPPING POWER			RANGE	RADIATION YIELD
	COLLISION	RADIATION	TOTAL		
MEV	MEV CM2/G	MEV CM2/G	MEV CM2/G	G/CM2	
0.010	1.970E 01	5.012E-03	1.971E 01	2.892E-04	1.463E-04
0.015	1.441E 01	4.909E-03	1.442E 01	5.901E-04	1.969E-04
0.020	1.155E 01	4.843E-03	1.155E 01	9.805E-04	2.428E-04
0.025	9.733E 00	4.797E-03	9.737E 00	1.454E-03	2.855E-04
0.030	8.475E 00	4.765E-03	8.479E 00	2.006E-03	3.259E-04
0.035	7.548E 00	4.735E-03	7.552E 00	2.632E-03	3.642E-04
0.040	6.835E 00	4.731E-03	6.840E 00	3.329E-03	4.011E-04
0.045	6.269E 00	4.738E-03	6.273E 00	4.093E-03	4.370E-04
0.050	5.808E 00	4.753E-03	5.812E 00	4.922E-03	4.719E-04
0.055	5.425E 00	4.775E-03	5.429E 00	5.813E-03	5.062E-04
0.060	5.101E 00	4.803E-03	5.106E 00	6.763E-03	5.398E-04
0.065	4.824E 00	4.834E-03	4.829E 00	7.771E-03	5.730E-04
0.070	4.585E 00	4.868E-03	4.590E 00	8.833E-03	6.057E-04
0.075	4.375E 00	4.906E-03	4.380E 00	9.949E-03	6.380E-04
0.080	4.190E 00	4.945E-03	4.195E 00	1.112E-02	6.700E-04
0.085	4.026E 00	4.973E-03	4.031E 00	1.233E-02	7.014E-04
0.090	3.879E 00	5.016E-03	3.884E 00	1.360E-02	7.326E-04
0.095	3.747E 00	5.062E-03	3.752E 00	1.491E-02	7.635E-04
0.100	3.627E 00	5.109E-03	3.632E 00	1.626E-02	7.943E-04
0.150	2.856E 00	5.637E-03	2.862E 00	3.197E-02	1.094E-03
0.200	2.466E 00	6.211E-03	2.472E 00	5.089E-02	1.380E-03
0.250	2.233E 00	6.834E-03	2.240E 00	7.221E-02	1.661E-03
0.300	2.081E 00	7.483E-03	2.088E 00	9.537E-02	1.937E-03
0.350	1.975E 00	8.161E-03	1.984E 00	1.200E-01	2.210E-03
0.400	1.899E 00	8.836E-03	1.908E 00	1.457E-01	2.480E-03
0.450	1.843E 00	9.527E-03	1.852E 00	1.723E-01	2.748E-03
0.500	1.800E 00	1.021E-02	1.810E 00	1.996E-01	3.012E-03
0.550	1.766E 00	1.090E-02	1.777E 00	2.275E-01	3.274E-03
0.600	1.740E 00	1.158E-02	1.752E 00	2.559E-01	3.532E-03
0.650	1.720E 00	1.227E-02	1.732E 00	2.846E-01	3.787E-03
0.700	1.704E 00	1.295E-02	1.717E 00	3.136E-01	4.039E-03
0.750	1.691E 00	1.364E-02	1.705E 00	3.428E-01	4.288E-03
0.800	1.681E 00	1.433E-02	1.696E 00	3.722E-01	4.534E-03
0.850	1.673E 00	1.498E-02	1.688E 00	4.018E-01	4.776E-03
0.900	1.667E 00	1.568E-02	1.683E 00	4.314E-01	5.016E-03
0.950	1.662E 00	1.637E-02	1.679E 00	4.612E-01	5.254E-03
1.000	1.659E 00	1.707E-02	1.676E 00	4.910E-01	5.490E-03
1.100	1.655E 00	1.848E-02	1.673E 00	5.507E-01	5.956E-03
1.200	1.653E 00	1.991E-02	1.673E 00	6.105E-01	6.415E-03
1.300	1.654E 00	2.134E-02	1.675E 00	6.702E-01	6.870E-03

ELECTRONS IN AIR

ENERGY	STOPPING POWER			RANGE	RADIATION YIELD
	COLLISION	RADIATION	TOTAL		
MEV	MEV CM2/G	MEV CM2/G	MEV CM2/G	G/CM2	
1.400	1.656E 00	2.279E-02	1.679E 00	7.298E-01	7.319E-03
1.500	1.659E 00	2.424E-02	1.683E 00	7.893E-01	7.763E-03
1.600	1.663E 00	2.571E-02	1.689E 00	8.487E-01	8.204E-03
1.700	1.667E 00	2.717E-02	1.695E 00	9.078E-01	8.640E-03
1.800	1.672E 00	2.866E-02	1.701E 00	9.667E-01	9.074E-03
1.900	1.677E 00	3.016E-02	1.708E 00	1.025E 00	9.505E-03
2.000	1.683E 00	3.168E-02	1.714E 00	1.084E 00	9.933E-03
2.200	1.694E 00	3.473E-02	1.729E 00	1.200E 00	1.078E-02
2.400	1.705E 00	3.783E-02	1.743E 00	1.315E 00	1.163E-02
2.600	1.716E 00	4.097E-02	1.757E 00	1.429E 00	1.246E-02
2.800	1.728E 00	4.394E-02	1.771E 00	1.543E 00	1.329E-02
3.000	1.738E 00	4.714E-02	1.786E 00	1.655E 00	1.412E-02
3.500	1.764E 00	5.538E-02	1.820E 00	1.933E 00	1.616E-02
4.000	1.789E 00	6.393E-02	1.852E 00	2.205E 00	1.820E-02
4.500	1.811E 00	7.282E-02	1.884E 00	2.473E 00	2.024E-02
5.000	1.831E 00	8.187E-02	1.913E 00	2.736E 00	2.229E-02
5.500	1.851E 00	9.108E-02	1.942E 00	2.995E 00	2.434E-02
6.000	1.868E 00	1.004E-01	1.969E 00	3.251E 00	2.639E-02
6.500	1.885E 00	1.099E-01	1.995E 00	3.503E 00	2.844E-02
7.000	1.901E 00	1.196E-01	2.020E 00	3.752E 00	3.049E-02
7.500	1.915E 00	1.294E-01	2.045E 00	3.998E 00	3.254E-02
8.000	1.929E 00	1.393E-01	2.068E 00	4.241E 00	3.459E-02
8.500	1.942E 00	1.493E-01	2.091E 00	4.482E 00	3.663E-02
9.000	1.955E 00	1.603E-01	2.115E 00	4.720E 00	3.868E-02
9.500	1.966E 00	1.705E-01	2.137E 00	4.955E 00	4.074E-02
10.000	1.978E 00	1.809E-01	2.159E 00	5.188E 00	4.280E-02
20.000	2.133E 00	4.008E-01	2.534E 00	9.447E 00	8.229E-02
30.000	2.225E 00	6.344E-01	2.859E 00	1.316E 01	1.185E-01
40.000	2.283E 00	8.745E-01	3.158E 00	1.648E 01	1.514E-01
50.000	2.324E 00	1.119E 00	3.443E 00	1.951E 01	1.814E-01
60.000	2.355E 00	1.366E 00	3.721E 00	2.231E 01	2.089E-01
80.000	2.400E 00	1.868E 00	4.268E 00	2.732E 01	2.576E-01
100.000	2.433E 00	2.374E 00	4.807E 00	3.173E 01	2.994E-01
200.000	2.520E 00	4.948E 00	7.468E 00	4.828E 01	4.445E-01
300.000	2.564E 00	7.552E 00	1.012E 01	5.974E 01	5.325E-01
400.000	2.593E 00	1.017E 01	1.276E 01	6.852E 01	5.928E-01
500.000	2.614E 00	1.279E 01	1.541E 01	7.564E 01	6.372E-01
600.000	2.630E 00	1.542E 01	1.805E 01	8.163E 01	6.714E-01
800.000	2.655E 00	2.068E 01	2.334E 01	9.135E 01	7.215E-01
1000.000	2.674E 00	2.595E 01	2.862E 01	9.907E 01	7.566E-01

ELECTRONS IN STANDARD EMULSION

ENERGY	STOPPING POWER			RANGE	RADIATION YIELD
	COLLISION	RADIATION	TOTAL		
MEV	MEV CM2/G	MEV CM2/G	MEV CM2/G	G/CM2	
0.010	1.315E 01	2.109E-02	1.317E 01	4.605E-04	9.478E-04
0.015	9.884E 00	2.110E-02	9.905E 00	9.038E-04	1.255E-03
0.020	8.050E 00	2.084E-02	8.071E 00	1.467E-03	1.532E-03
0.025	6.863E 00	2.113E-02	6.884E 00	2.140E-03	1.791E-03
0.030	6.028E 00	2.159E-02	6.049E 00	2.917E-03	2.045E-03
0.035	5.405E 00	2.224E-02	5.427E 00	3.791E-03	2.301E-03
0.040	4.922E 00	2.270E-02	4.945E 00	4.758E-03	2.557E-03
0.045	4.535E 00	2.311E-02	4.559E 00	5.812E-03	2.809E-03
0.050	4.219E 00	2.350E-02	4.242E 00	6.950E-03	3.059E-03
0.055	3.955E 00	2.386E-02	3.978E 00	8.168E-03	3.305E-03
0.060	3.730E 00	2.420E-02	3.755E 00	9.463E-03	3.548E-03
0.065	3.538E 00	2.452E-02	3.562E 00	1.083E-02	3.788E-03
0.070	3.370E 00	2.483E-02	3.395E 00	1.227E-02	4.025E-03
0.075	3.224E 00	2.513E-02	3.249E 00	1.378E-02	4.258E-03
0.080	3.094E 00	2.543E-02	3.119E 00	1.535E-02	4.488E-03
0.085	2.978E 00	2.559E-02	3.004E 00	1.698E-02	4.714E-03
0.090	2.875E 00	2.587E-02	2.901E 00	1.867E-02	4.936E-03
0.095	2.781E 00	2.615E-02	2.807E 00	2.043E-02	5.156E-03
0.100	2.697E 00	2.643E-02	2.723E 00	2.224E-02	5.374E-03
0.150	2.148E 00	2.910E-02	2.177E 00	4.303E-02	7.439E-03
0.200	1.869E 00	3.148E-02	1.900E 00	6.775E-02	9.329E-03
0.250	1.702E 00	3.421E-02	1.736E 00	9.537E-02	1.109E-02
0.300	1.593E 00	3.707E-02	1.630E 00	1.252E-01	1.278E-02
0.350	1.518E 00	4.009E-02	1.558E 00	1.566E-01	1.442E-02
0.400	1.464E 00	4.301E-02	1.507E 00	1.892E-01	1.601E-02
0.450	1.424E 00	4.593E-02	1.470E 00	2.229E-01	1.756E-02
0.500	1.394E 00	4.880E-02	1.442E 00	2.572E-01	1.905E-02
0.550	1.371E 00	5.164E-02	1.423E 00	2.921E-01	2.051E-02
0.600	1.353E 00	5.445E-02	1.408E 00	3.275E-01	2.193E-02
0.650	1.340E 00	5.724E-02	1.397E 00	3.631E-01	2.330E-02
0.700	1.329E 00	6.001E-02	1.389E 00	3.990E-01	2.465E-02
0.750	1.320E 00	6.277E-02	1.383E 00	4.351E-01	2.596E-02
0.800	1.314E 00	6.551E-02	1.379E 00	4.713E-01	2.724E-02
0.850	1.309E 00	6.731E-02	1.376E 00	5.076E-01	2.845E-02
0.900	1.305E 00	7.003E-02	1.375E 00	5.440E-01	2.965E-02
0.950	1.302E 00	7.278E-02	1.374E 00	5.803E-01	3.082E-02
1.000	1.299E 00	7.554E-02	1.375E 00	6.167E-01	3.198E-02
1.100	1.297E 00	8.112E-02	1.378E 00	6.894E-01	3.425E-02
1.200	1.296E 00	8.677E-02	1.383E 00	7.618E-01	3.646E-02
1.300	1.297E 00	9.248E-02	1.390E 00	8.340E-01	3.863E-02

ELECTRONS IN STANDARD EMULSION

ENERGY	STOPPING POWER			RANGE	RADIATION YIELD
	COLLISION	RADIATION	TOTAL		
MEV	MEV CM2/G	MEV CM2/G	MEV CM2/G	G/CM2	
1.400	1.299E 00	9.824E-02	1.397E 00	9.057E-01	4.076E-02
1.500	1.301E 00	1.041E-01	1.405E 00	9.771E-01	4.285E-02
1.600	1.304E 00	1.099E-01	1.414E 00	1.048E 00	4.492E-02
1.700	1.307E 00	1.161E-01	1.423E 00	1.119E 00	4.697E-02
1.800	1.311E 00	1.220E-01	1.433E 00	1.189E 00	4.899E-02
1.900	1.314E 00	1.280E-01	1.442E 00	1.258E 00	5.099E-02
2.000	1.318E 00	1.340E-01	1.452E 00	1.327E 00	5.296E-02
2.200	1.326E 00	1.460E-01	1.472E 00	1.464E 00	5.685E-02
2.400	1.333E 00	1.582E-01	1.491E 00	1.599E 00	6.067E-02
2.600	1.341E 00	1.704E-01	1.511E 00	1.732E 00	6.442E-02
2.800	1.348E 00	1.826E-01	1.531E 00	1.864E 00	6.811E-02
3.000	1.355E 00	1.949E-01	1.550E 00	1.994E 00	7.173E-02
3.500	1.372E 00	2.261E-01	1.598E 00	2.311E 00	8.058E-02
4.000	1.387E 00	2.577E-01	1.645E 00	2.620E 00	8.915E-02
4.500	1.401E 00	2.895E-01	1.690E 00	2.919E 00	9.747E-02
5.000	1.413E 00	3.218E-01	1.735E 00	3.211E 00	1.056E-01
5.500	1.424E 00	3.545E-01	1.779E 00	3.496E 00	1.135E-01
6.000	1.435E 00	3.876E-01	1.822E 00	3.774E 00	1.212E-01
6.500	1.444E 00	4.209E-01	1.865E 00	4.045E 00	1.287E-01
7.000	1.453E 00	4.546E-01	1.908E 00	4.310E 00	1.361E-01
7.500	1.461E 00	4.886E-01	1.950E 00	4.569E 00	1.433E-01
8.000	1.469E 00	5.229E-01	1.992E 00	4.823E 00	1.504E-01
8.500	1.476E 00	5.575E-01	2.033E 00	5.071E 00	1.573E-01
9.000	1.483E 00	5.945E-01	2.077E 00	5.315E 00	1.642E-01
9.500	1.489E 00	6.296E-01	2.118E 00	5.553E 00	1.709E-01
10.000	1.495E 00	6.650E-01	2.160E 00	5.787E 00	1.775E-01
20.000	1.571E 00	1.402E 00	2.972E 00	9.715E 00	2.871E-01
30.000	1.611E 00	2.187E 00	3.798E 00	1.269E 01	3.671E-01
40.000	1.638E 00	3.009E 00	4.647E 00	1.506E 01	4.288E-01
50.000	1.658E 00	3.839E 00	5.497E 00	1.704E 01	4.779E-01
60.000	1.674E 00	4.678E 00	6.352E 00	1.873E 01	5.180E-01
80.000	1.698E 00	6.372E 00	8.070E 00	2.152E 01	5.797E-01
100.000	1.716E 00	8.076E 00	9.792E 00	2.376E 01	6.254E-01
200.000	1.770E 00	1.671E 01	1.848E 01	3.108E 01	7.490E-01
300.000	1.799E 00	2.542E 01	2.722E 01	3.551E 01	8.063E-01
400.000	1.820E 00	3.415E 01	3.597E 01	3.869E 01	8.403E-01
500.000	1.836E 00	4.289E 01	4.473E 01	4.118E 01	8.631E-01
600.000	1.849E 00	5.165E 01	5.350E 01	4.322E 01	8.797E-01
800.000	1.869E 00	6.917E 01	7.104E 01	4.645E 01	9.022E-01
1000.000	1.885E 00	8.670E 01	8.858E 01	4.897E 01	9.171E-01

11. ATOMIC AND IONIC PARTIAL STOPPING POWERS[1]

Samuel K. Allison[2]

Abstract

The partial stopping power of a target material for an ion or an atom is the energy lost per target particle per cm^2 in all types of collisions in which the ion or the atom is the projectile, with the exception of those collisions in which the projectile leaves with its charge changed. Partial atomic stopping powers of target gases for atoms are measured by imposing a strong transverse magnetic field on the stopping cell. For partial ionic stopping-power measurements the ion beam is held in a circular orbit, closely defined by vanes and slits, as it traverses the stopping cell. The partial stopping powers ϵ_0 (for He^0 transvering H_2 gas), ϵ_1(for He^+), and ϵ_2(for He^{++}) have been measured in the kinetic energy range 40-460 kev, and new measurements of the ordinary, or total, stopping power of H_2 gas for helium from 40 to 22 kev have been made. Using the known charge composition of He beams in H_2, it is possible to deduce the fraction of the stopping-power losses due to charge-changing collisions, and this varies from 37 percent at 140 kev to 27 percent at 400 kev. At 120 kev, the total energy-loss in completing the charge-changing cycle $He^+ \rightarrow He^0 \rightarrow He^+$ is 95 ± 9 ev, rising to 117 ± 10 at 160 kev.

1. Introduction

Before the work of Henderson (1) and of Rutherford (2), the stopping of alpha particles from natural emitters was considered as due to the interaction of a moving electric point charge with the atoms or molecules encountered along its trajectory. In the theoretical treatments by Bohr (3) and by Bethe (4), the moving particle was assumed to be a bare nucleus, which, to a close approximation, acts as a point charge. However, Henderson, in examining the magnetic spectra of natural alpha particles, found that even at the highest velocities a detectable fraction of He^+ was always present, and at lower energies He^0 was indicated as a beam constituent. The presence of He^+ in the predominantly He^{++} beam shows that a moving He^{++} can undergo a type of inelastic impact in which an electron is captured from the target material. The He^+ ions and He^0 atoms can be involved in inelastic collisions in which occur electron capture and loss as well as other events more complicated than those experienced by nuclear projectiles.

---

[1] Supported in part by U. S. Atomic Energy Commission.

[2] The Enrico Fermi Institute for Nuclear Studies, The University of Chicago.

Allison, Cuevas, and Garcia-Munoz (5) have shown that it is possible in some projectile-target-velocity combinations to divide the energy losses into two measurable classes—the first consisting of all events that do not change the projectile's charge, the second consisting of those in which the projectile's charge is changed—and they have introduced the concept of partial stopping powers.

The partial stopping power ϵ_i of a target material for a projectile of charge $i|e|$ is the energy lost per target particle per cm^2 in all types of collisions except those in which the charge of the projectile is changed.

Depending on whether the moving particle is neutral or charged, we speak of an atomic or an ionic partial stopping power.

2. Energy Degradation of a Particle Beam Comprising Several Charge States

Consider a monoenergetic beam of particles impinging on matter at speeds at which electron capture and loss are probable. Let F_i be the fraction of the particles in the impinging beam in the charge-state $i|e|$. As will be discussed later, the beam, on traversing the matter rapidly comes to a state of charge equilibrium in which a set of numbers $F_{i\infty}$ represents the fractions present in each charge-state. The conventional stopping power ϵ of the material for the equilibrated beam, expressed in terms of the partial stopping powers, is

$$\epsilon = \Sigma\, \epsilon_i\, F_{i\infty} + \sum_{i,f} F_{i\infty}\, W_{if}\, \sigma_{if}\ ;\ (i \neq f)\ . \tag{1}$$

Here, W_{if} is the energy in electron volts lost by a beam particle in the charge-state i in a charge-changing collision $i \rightarrow f$, and σ_{if} is the corresponding charge-changing-collision cross-section.

At the present time, the only partial stopping powers that have been measured are those of hydrogen gas for hydrogen and helium projectiles, and the following discussion of the feasibility of their determination will apply to such light beams and targets. At the present time, no one has suggested a feasible method for the measurement of partial stopping powers in solids.

When particles having energies in the kilovolt region enter a new medium, the appropriate charge equilibrium is attained before significant energy losses have occurred. This phenomenon makes the experiment described in the report feasible. As an illustration we may consider the entrance of a pure proton beam ($F_1 = 1$) into a chamber containing hydrogen gas. The growth of the neutral fraction F_0 is described by

$$F_0 = F_{0\infty} \left\{ 1 - \exp \left[-\pi \left(\sigma_{01} + \sigma_{10} \right] \right] \right\}\ , \tag{2}$$

where π is the number of atoms of target gas per cm^2 that have been traversed by the beam. If $\bar{\pi}$ is the value at which $F_0 = 0.632\, F_{0\infty}$, then

$$\bar{\pi} = (\sigma_{01} + \sigma_{10})^{-1}\ . \tag{3}$$

As will become evident later, the experiment must be performed with very small, fractional energy-losses. Then, if $(E_p - E_p')$ is the energy lost by the composite beam from a beam whose original energy is E_p, we have $(E_p - E_p') = \pi\, \epsilon$, and the fractional loss is

$$(E_p - E_p')/E_p = \epsilon/E_p(\sigma_{01} + \sigma_{10}) \quad , \tag{4}$$

where ϵ is expressed in electron volts per target atom per cm^2 and E_p and E_p' are expressed in electron volts. Consider the range in which $15 < E_p < 150$ kev. In this range, ϵ varies from 4.6×10^{-15} through a maximum of 6.4×10^{-15} to 4.6×10^{-15}, and $(\sigma_{01} + \sigma_{10})$ decreases from 41 to 4.6×10^{-17} cm^2. Thus, the fractional loss in energy for this approach to charge equilibrium is less than 0.1 percent.[3]

Having thus rapidly attained charge equilibration, the beam proceeds with the effective charge $\bar{i}|e|$, where

$$\bar{i} = \sum_i i \, F_{i\infty} \quad . \tag{5}$$

3. Feasibility and Limitations of the Experimental Method

The experimental determination of a partial stopping power will be illustrated by a description of the measurement of ϵ_0 for a hydrogen beam traversing H_2 gas. The basic idea is to place the gas chamber in which the stopping power is being measured in a strong transverse magnetic field that sweeps out of the beam all entering protons, and also any regenerated protons formed from the loss of an electron from a moving neutral atom. The essential features of the experiment are shown in Figure 1. The proton beam, entering from the right, is first charge-equilibrated in

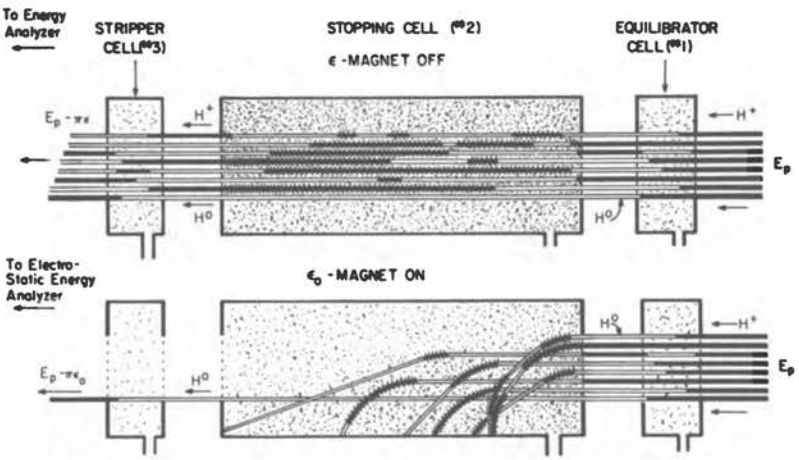

Figure 1. Schematic representation of the method of measuring the atomic partial stopping power of a hydrogen beam. The apertures in the cells are actually 0.091 cm in diameter, π is the number of target gas atoms/cm^2. With the magnet off, the conventional or total stopping power is measured; with the field on, only the statistically improbable cases of traversal without change of charge remain, but they may be detected and their energy loss determined.

[3] In this paper, the charge-changing cross sections are taken from Allison (6) and the stopping powers quoted are taken from Whaling (7).

Cell No. 1. It then passes into the stopping cell, No. 2, in which a transverse magnetic field may be applied. With the magnet off, the ordinary stopping power is measured. The stripper cell (No. 3) performs no essential function for the ordinary stopping-power measurements, and the pressure in it is left unchanged during "gas in" and "gas out" in Cell No. 2. The energy decrement is measured by electrostatic deflection[4] (not shown in Fig. 1) of the beam after leaving Cell No. 3. The lower part of Figure 2 shows the situation in the measurement of the atomic partial stopping power ϵ_0, which is performed in the presence of the field.

The most striking feature of the partial-stopping-power experiment is the very large attenuation of the beam where enough gas has been admitted to the stopping cell to produce a sufficient energy loss for accurate measurement. It follows that the experiment has an enhanced chance of success if the energy spread of the beam from the

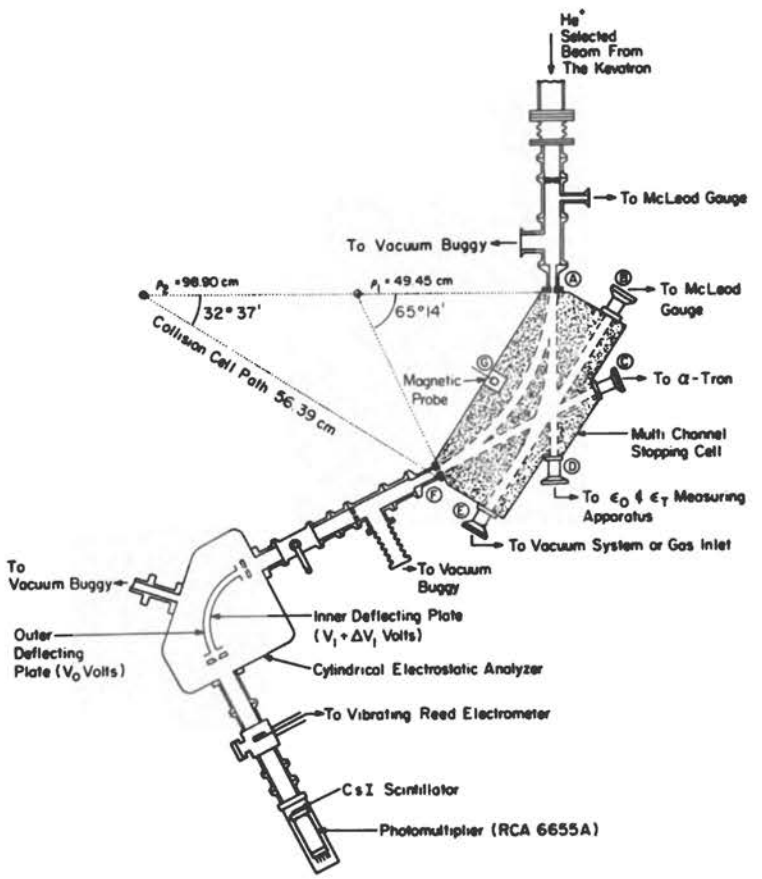

Figure 2. Equipment for measuring partial stopping powers. Vacuum "buggies" are movable vacuum-pumping systems. The channels for orbits in the magnetic field are cut into a brass block placed between the rectangular magnet pole faces.

[4]A suitable analyzer is described by Allison, Frankel, et al. (Ref. 8).

accelerator is minimized and if the resolving power of the energy analyzer is maximized in order to permit an accurate measurement of an energy loss $\pi\epsilon_0$ as small as possible. The feasibility of a determination of ϵ_0 may be discussed as follows. In the stopping cell, the intensity attenuation on admitting gas in the presence of the magnetic field will be $s \exp(-\pi\sigma_{10})$, where s is a factor less than unity due to loss through small-angle scattering. This scattering loss will depend on the size of the apertures through which the beam enters and leaves the stopping cell. With a cell 50 cm long and apertures 1 mm in diameter, the value of s for hydrogen or helium beams in hydrogen may be kept above 0.1. The fractional losses in cells 1 and 3 are $F_{1\infty}$ and $F_{0\infty}$, respectively.

Thus, the attenuation produced by a pressure corresponding to π atoms per cm^2 in Cell No. 2 must be expected to be

$$N/N_0 \sim sF_{0\infty}F_{1\infty} \exp(-\pi\sigma_{01}) \ . \tag{6}$$

N_0 is the beam current received by the detector with minimum pressure ("gas out") in all the three cells and with no magnetic field on the second cell.

Let $(E_p - E_p')_{min}$ be the smallest energy decrement, in ev, which can be measured to the desired accuracy (say 5 percent); then

$$\pi\epsilon_0 = (E_p - E_p')_{min}$$

and

$$N/N \sim sF_{0\infty}F_{1\infty} \exp\left[-(E_p - E_p')_{min}\,\sigma_{01}/\epsilon_0\right] \ . \tag{7}$$

For a 50-kev hydrogen beam in hydrogen gas, $F_{0\infty} = 0.525$ and $F_{1\infty} = 0.475$. For a feasibility calculation, ϵ_0 may be assumed to be half the total stopping power

$$(\tfrac{1}{2}\epsilon = 3.2 \times 10^{-15} \text{ ev cm}^2/\text{ atom}), \text{ and } \sigma_{01} \text{ is } 7.9 \times 10^{-17} \text{ cm}^2.$$

Let it be assumed that factors such as the stability of the accelerator and the deflecting voltages of the electrostatic analyzer, the resolving power of the analyzer, etc., will permit a 5-percent determination of ϵ_0 when $(E_p - E_p')_{min}$ is 1 percent of E_p, or 500 ev at 50 kev. The beam, then, according to Whaling (7) must be expected to attenuate by a factor of 10^{-7}. Whether this is tolerable depends on the beam current that can be passed through the cell apertures. With 10^{-10}A transmitted with vacuum throughout the system, there should be, with gas in and the field on, a final current of protons of 10^{-17}A, or 3750 protons per minute that may be counted with a particle detector.

With the feasibility of a measurement of ϵ_0 established, it is apparent that there probably are cases in which ionic partial stopping powers may be measured. For this purpose a curved stopping cell is used instead of the rectilinear one schematically shown in Figure 1, and only those particles for which the charge $i|e|$ remains unchanged during transit of the cell can pass through the exit slit. Figure 2 shows a multichannel stopping cell designed to fit between the rectangular pole faces of an electromagnet. ϵ_0 can be measured in the "straight through" channel from A to D or with a longer pathlength, from B to E, by allowing the beam to enter at B. The channels AE and AF allow measurements of ϵ_i at two different radii of curvature, i.e., at two different magnetic-field strengths. In contrast to the measurement of ϵ_0, where the magnetic field H may be varied within wide limits, and the independence of the result of H for large H (2000-3500 gauss in Fig. 2) demonstrated, the measurement of ϵ_i requires a highly precise and constant setting of H. It is well to try a measurement of ϵ_i for at least two values of H.

4. Experimental Values of Partial Stopping Powers

Table 1 shows experimental values of ϵ, ϵ_0, and ϵ_1, for hydrogen beams in molecular hydrogen gas. The first ionic partial stopping-power measurements were reported by Huberman (9) for proton kinetic energies from 42 to 93 kev in H_2 gas. More recently Huberman's measurements have been repeated by Cuevas, Garcia-Munoz, and Torres[5] and essentially confirmed, although in some cases slightly lower values were found. It is these later ϵ_1 measurements which are listed. The values of ϵ were measured with the partial-stopping-power apparatus by reducing the magnetic field to zero. Agreement of the ϵ values with those compiled by Whaling from the data of other observers indicates the absence of systematic errors in the procedure. The larger range of errors assigned to the new measurements arises from the fact that the values of $(E_p - E_p')/E_p$ used were only about 1 percent, whereas, in ordinary measurements of ϵ, energy decrements may be tenfold larger.

Table 2 shows experimental values of total and partial stopping powers for the components of a helium beam traversing hydrogen gas. In column 2, previously unpublished data (Allison), measured with the same equipment used to determine partial stopping powers, are given on ϵ down to 40 kev. The previous determinations, from 150 to 450 kev, are due to P. K. Weyl (11).

TABLE 1

Total and Partial Stopping Powers for Hydrogen Beams Traversing H_2 Gas; ϵ's Measured in Units of 10^{-15} ev x cm^2/Atom

(Values given, with the exception of those taken from Whaling and those indicated by asterisk are read from smooth curves through the data, the uncertainties in individual points of which are from ±10 to ±25 percent. Values indicated by asterisk are based on Huberman's results of 5.70 ± 0.6 at 75 kev and 5.07 ± 0.5 at 93 kev. Repetition of Huberman's work indicated that values at the lower limits designated by him are preferable.)

Kinetic Energy (kev)	ϵ		ϵ_0	ϵ_1
	New Measurements	Whaling's Collected Data		
20	5.2 ± 0.6	5.1 ± 0.2	3.8 ± 0.5	-
30	-	5.8	3.2	-
40	6.4	6.2	3.0	5.3 ± 0.5
50	-	6.4	2.7	5.4
60	6.7	6.4	2.4	5.1
70	-	6.4	2.2	5.1*
80	6.4	6.2	2.0	4.8*
90	-	6.0	1.9	4.6*
100	5.7	5.8	1.9	-
110	-	5.6	1.9	-
120	5.0	5.3	1.8	-
130	-	5.1	1.7	-
140	4.3	4.9	1.5	-
150	3.9 ± 0.5	4.7 ± 0.16	1.4 ± 0.4	-

[5] As reported by S. K. Allison (10).

TABLE 2

Total and Partial Stopping Powers for Helium Beams, Traversing Hydrogen Gas; ϵ's Measured in Units of 10^{-15} ev x cm^2/Atom

Kinetic Energy (kev)	ϵ (previous work) (Allison)	(Weyl)	ϵ_0	ϵ_1	ϵ_2
40	4.4 ± 0.4		3.3 ± 0.4	-	-
60	5.1		3.5	-	-
80	5.9		3.7	-	-
100	6.6		3.8	-	-
120	7.4		4.0	4.8 ± 0.3	-
140	8.1		4.2	5.6	-
160	8.9	9.0 ± 0.4	4.4	6.3	-
180	9.6	9.5	4.5	7.1	-
200	10.4	10.2	4.7 ± 0.6	7.8	-
220	10.7 ± 1.0	10.6	-	8.6 ± 0.4	-
250		11.0	-	-	-
275		11.2	-	-	-
300		11.4	-	-	12.2 ± 1.1
325		11.7	-	-	14.0
350		11.9	-	-	15.1
375		12.0	-	-	15.8
400		12.1	-	-	16.3
425		12.2	-	-	16.6
450		12.3 ± 0.6	-	-	16.8 ± 1.0

5. Energetics of the Charge-Changing Collisons

The experimental determination of the atomic and ionic stopping powers together with the known values of the total stopping power permit calculation of the energies involved in charge-changing collisions by Equation 1, using known values of the equilibrium fractions $F_{i\infty}$. Figures 3 and 4 show the percentage of the total energy losses involved in the charge-changing collisions as well as the percentages due to the charge-invariant collisions of the atoms and ions. It is seen that the charge-changing cycle may account for 39 percent of the total losses for hydrogen beams in hydrogen and 43 percent for helium beams.

Under certain circumstances, the sum in Equation 1 connected with charge-changing collisions may be simplified. In the traversal of hydrogen gas by hydrogen projectiles we are concerned, to the accuracy of the present stopping-power measurements, with a two-component system, H^+ and H^0. The fraction of H^- present is known, and it is too small to affect the results. Thus, for this case, Equation 1 becomes

$$\epsilon_H = \epsilon_0 F_{0\infty} + \epsilon_1 F_{1\infty} + F_{0\infty} W_{01} \sigma_{01} + F_{1\infty} W_{10} \sigma_{10} \quad . \tag{8}$$

The justification for omitting terms such as $F_{0\infty} W_{0\bar{1}} \sigma_{0\bar{1}}$ in the expansion of the charge-changing sum is given in detail in the paper of Huberman (9). Since

$$F_{0\infty} = 1 - F_{1\infty} = \sigma_{10}/(\sigma_{10} + \sigma_{01}) \quad , \tag{9}$$

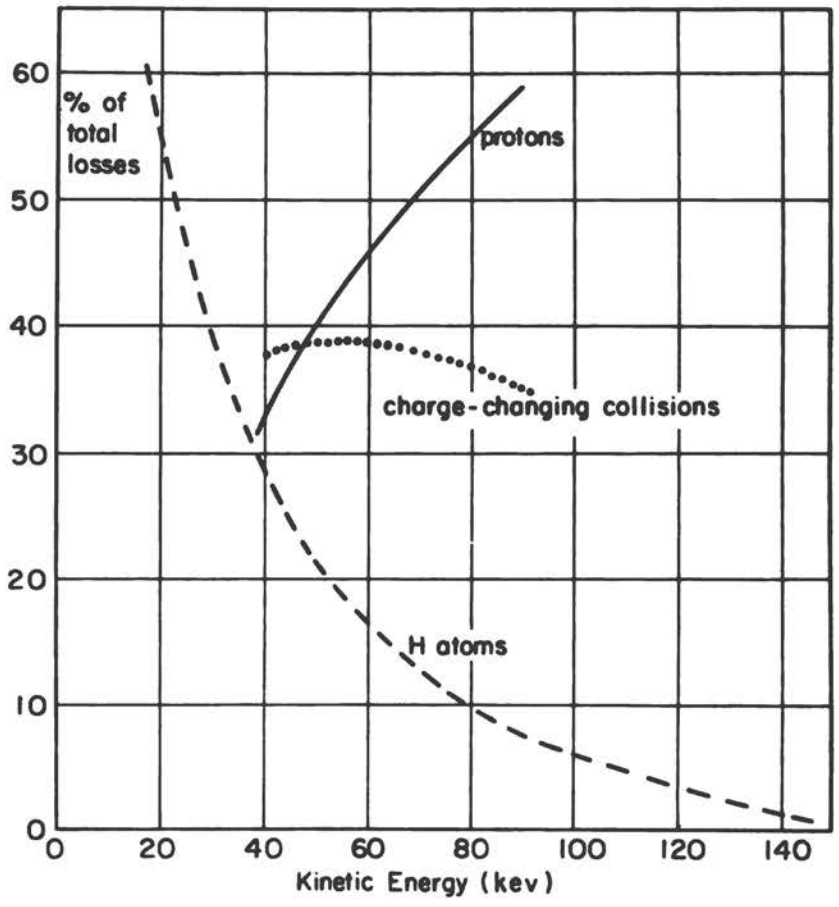

Figure 3. The fractions of the total energy-loss, expressed in percent, arising from the partial stopping power for H^0 and H^+ and from the charge-changing cycle. Hydrogen beams in H_2 gas.

the sum of the charge-changing terms of Equation 8 may be written

$$F_{0\infty}W_{01}\sigma_{01} + F_{1\infty}W_{10}\sigma_{10} = \sigma_c(W_{01} + W_{10}) \ , \tag{10}$$

where

$$\sigma_c = \sigma_{01}\sigma_{10}/(\sigma_{01} + \sigma_{10}) \ . \tag{11}$$

Since the σ's and the F's are all known (Ref. 6), values of $(W_{01} + W_{10})$ may be computed from the observed partial and total stopping powers. These values, given in Table 3, represent the sum of the energies lost in the two processes which initiate and terminate a charge-changing cycle, i.e., capture of an electron plus its subsequent loss.

In the case of helium projectiles, the expansion of the charge-changing sum in Equation 1 is, in general, more complex even after omitting terms involving He^-. We have

$$\sum_{if} F_{i\infty} W_{if} \sigma_{if} = F_{0\infty}(W_{01}\sigma_{01} + W_{02}\sigma_{02}) + F_{1\infty}(W_{10}\sigma_{10} + W_{12}\sigma_{12}) + F_{2\infty}(W_{20}\sigma_{20} + W_{21}\sigma_{21}) \ . \tag{12}$$

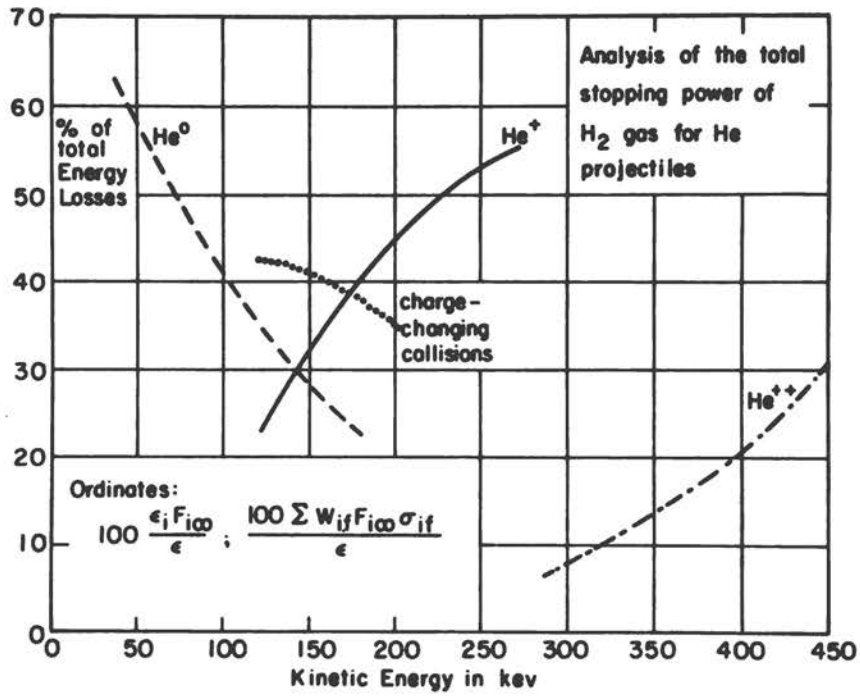

Figure 4. The fractions of the total energy-loss, expressed in percent, arising from the partial stopping power for He^0, He^+, and He^{++}, and from the charge-changing cycle $He^0 \rightarrow He^+ \rightarrow He^0$. Helium beams in H_2 gas.

TABLE 3

Sum of the Energy Decrements in the Electron Capture and Subsequent Loss Cycle for H^+ and He^+ Ions in Hydrogen Gas

Hydrogen Projectiles		Helium Projectiles	
Kinetic Energy (kev)	$(W_{01} + W_{10})$ (ev)	Kinetic Energy (kev)	$(W_{01} + W_{10})$ (ev)
43	40 ± 6	120	95 ± 9
54	54 ± 9	140	103 ± 10
75	86 ± 22	160	117 ± 10
93	118 ± 29	180	127 ± 12

In the kinetic energy region 120 - 180 kev the cross sections and equilibrium values are all known. The preponderant charge-changing process is $He^+ \rightleftarrows He^0$; the fraction $F_{2\infty}$ of He^{++} present is less than 0.01. Until the accuracy of measurement of partial stopping powers is greatly improved, Equation 12 reduces, for numerical evaluation, to the form of Equation 10, but applied, of course, to the $He^+ \rightleftarrows He^0$ interchange. The kinetic energy (in electron volts) lost in the $He^0 \rightarrow He^+ \rightarrow He^0$ cycle is shown in Table 3.

6. Theoretical Estimates of Partial Stopping Powers

There are no theoretical calculations of the partial stopping powers of molecular hydrogen gas for hydrogen or helium projectiles, but Dalgarno and Griffing (12) have calculated the cross sections and energy losses for many types of collisions of protons and hydrogen atoms with atomic hydrogen gas as the target. Excerpts from the Dalgarno and Griffing results are given in Table 4, and these include their numerical values for a beam kinetic energy of 56 kev. Since the experimental method distinguishes between projectile and target, in some cases only half the numerical value found by Dalgarno and Griffing should be used for a partial stopping power. For instance, single ionization by H^0 impact (Item I of Table 4) may ionize either of the two colliding atoms; the partial stopping power ϵ_0 will contain only half this loss, since a particular atom, namely the target, must be the one ionized.

References

1. G. H. Henderson, Proc. Roy. Soc. Lond. A102, 496 (1922).

2. E. Rutherford, Phil. Mag. 47, 277 (1924).

3. N. Bohr, Phil. Mag. 23, 449 (1912).

4. H. Bethe, Ann. der Physik 5, 325 (1930).

5. S. K. Allison, J. Cuevas, and M. Garcia-Munoz, Phys. Rev. 127, 792 (1962).

6. S. K. Allison, Rev. Mod. Phys. 30, 1137 (1958).

7. W. Whaling, in "Encyclopedia of Physics," 34 (S. Fluegge, ed., Springer-Verlag, Berlin, 1958).

8. Allison, Frankel, Hall, Montague, Morrish, and Warshaw, Rev. Sci. Instr. 20, 735 (1949).

9. M. Huberman, Phys. Rev. 127, 799 (1962).

10. S. K. Allison, in Proceedings of the Third International Conference on the Physics of Electronic and Atomic Collisions (North Holland Press, 1963).

11. P. K. Weyl, Phys. Rev. 91, 239 (1953).

12. A. Dalgarno and G. W. Griffing, Proc. Roy. Soc. Lond. A232, 423 (1955); also A. Dalgarno, Chap. 15, Atomic and Molecular Processes (D. R. Bates, ed., Academic Press, New York, 1962).

TABLE 4

Calculated Partial Stopping Powers (in Units of 10^{-15} ev x cm^2/atom)
Hydrogen Beams in Atomic Hydrogen Gas, Compared with Experimental Results in H_2 Gas
(From Dalgarno and Griffing, Ref. 12)

Term in Eq. 8	Type of Inelastic Collision	Numerical Value at 56 kev Calculated	Experimental Value in Molecular Hydrogen
ϵ_0	I. single ionization by H^0 impact $H^0(H^0;H^+,e)H^0$ or $H^0(H^0; H^0, e)H^+$	3.33/2 = 1.665	
	II. single excitation by H^0 impact $H^0(H^0;H^*)H^0$ or $H^0(H^0; H^0)H^*$	0.113	
	III. double excitation by H^0 impact $H^0(H^0; H^*)H^*$	0.161	
	IV. ionization and excitation by H^0 impact, $H^0(H^0; H^+, e)H^0$ or $H^0(H^0; H^*, e)H^+$	0.603/2 = 0.302	
		ϵ_0 = 2.241	2.6 ± 0.4
ϵ_1	V. ionization by H^+ impact $(H^0(H^+; H^+,e)H^+$	5.07	
	VI. excitation by H^+ impact $H^0(H^+; H^*)H^+$	1.82	
		ϵ_1 = 6.89	5.2 ± 0.5
$F_{i\infty}W_{if}\sigma_{if}$	VII. capture and excitation by H^+ impact, $H^0(H^+; H^+)H^*$	0.258 $F_{1\infty}$ = 0.133	
	VIII. H^+ momentum loss in capture $H^0(H^+; H^+)H^0$	1.76 $F_{1\infty}$ = 0.90	
	IX. single ionization by H^0 impact (cf. I)	3.33 $F_{0\infty}/2$ = 0.81	
	X. double ionization by H^0 impact, $H^0(H^0; H^+, 2e)H^+$	0.902 $F_{0\infty}$ = 0.44	
	XI. ionization and excitation by H^0 impact (cf. IV)	0.603 $F_{0\infty}/2$ = 0.146	
		Σ = 2.43	2.5 ± 0.4

12. A LIST OF CURRENTLY UNSOLVED PROBLEMS

U. Fano[1]

Abstract

The discussions within the Subcommittee on the Penetration of Charged Particles and the review work undertaken by the present author in the preparation of Appendix A of this volume have pointed up a number of unsolved problems. Some of these problems are of considerable importance and difficulty, so that their solution will require a major experimental or theoretical effort. Others are of lesser importance, and are easier to attack. It seems worthwhile to present here a list of such problems, with reference to sections of this volume or to other literature where their backgrounds are discussed in greater detail. The various papers of this volume will be referred to by number or letter (for the appendixes). The ordering of the problems in the following list relates only very loosely to their estimated importance and difficulty.

1. Improvements over the Born Approximation for the Slowing Down of Heavy Particles (Appendix A, Sec. 2.13)

Two major problems have arisen in this area in the last year or two. (a) A calculation by Tsytovich of radiative corrections (Appendix A, Ref. 129) has shown a decrease of stopping power at extreme relativistic velocity. Considerable difficulty has been met by Subcommittee members and by some of their colleagues in trying to understand the details of this work and to appreciate its significance. The experimental test of the effect shown by the Tsytovich calculation also is uncertain (Appendix A, p. 50). (b) Experiments by Barkas and coworkers on the comparative ranges of Σ^+ and Σ^- hyperons have yielded convincing evidence of a difference in stopping powers at equal velocities when these velocities are comparable to those of atomic electrons (Phys. Rev. Letters, vol. 11, p. 26, 1963). An effect of this kind is predicted qualitatively by second Born-approximation theory, but initial attempts to work out this theory quantitatively or to develop alternative approaches have met with substantial difficulties.

2. Theory of Slowing Down Near the End of the Range and for Ions Heavier Than Helium (Paper Nos. 1, 8, and 11, and Appendix B)

The accumulation of experimental evidence and the semiquantitative theoretical work by Lindhard have progressed to the point where some hope may be entertained

[1] National Bureau of Standards, Washington, D. C.

of accurate calculations of stopping power for this most difficult range of the velocity and ion-charge variables.

3. Relativistic Treatment of Inner-Shell Electrons (Appendix A, Section 2.6)

The stopping-power theory treats bound atomic electrons nonrelativistically, except in the high-Q approximation in which their initial motion within atoms is neglected altogether. This limitation of theory is rather serious for the inner electrons of medium and heavy elements, the more so because the basic sum rules on which the theory relies (in particular, Eq. 27) are not amenable to rigorous relativistic generalization. Overcoming this difficulty presents a probably very serious challenge, but a preliminary appraisal of the likely magnitude of errors and of possible ways of correcting them might prove comparatively easy and fruitful. Such a study appears highly desirable.

4. Inner-Shell Corrections (Appendix A, Section 4, and Paper No. 4)

Recent theoretical work has developed new points of view and some new results on this problem, but the work has not been pursued to its logical conclusion. Perhaps a fresh approach to the evaluation of the Bethe formula should be attempted along the line indicated at the end of Section 3 of Paper No. 4. On the experimental side, the analysis carried out in Paper No. 2 might be continued in order to assess more precisely the significance of the available information and to design new experiments that would be particularly informative.

5. Stopping-Power Theory for Low-Energy Electrons and Positrons

No opportunity exists within the first Born approximation to extend the theory of electron collisions down to incident velocities comparable to those of atomic electrons, that is, to proceed by analogy with the shell corrections in heavy-particle collision theory. No realistic suggestion is known to this writer concerning methods for a basic attack on the stopping power of slower electrons and positrons. Here again a survey study might be profitable—to assess the relevant aspects of the problem and their presumable influence on stopping power.

6. The Mean Excitation Energy I (Appendix A, Section 3, and Paper No. 6)

Several questions remain open here, in particular the following ones: (a) What is the quantitative theoretical interpretation of the smooth curve of I/Z vs. Z (Fig. 1, Paper No. 6)? (See the qualitative discussion in Paper No. 1.) (b) How large are the departures from this curve for low Z and what is their interpretation? (c) No substantial evidence of such departures exists for $Z > 20$, but verification that I/Z can be interpolated dependably would be useful. (d) Information on departures from the Bragg law is too scanty, and the apparent discrepancy for photographic emulsion remains puzzling. (e) Anchor points of the curve of I/Z vs. Z for medium Z, particularly at copper, still have too great an uncertainty (± 5 percent) owing to inconsistencies in experimental data (see following item).

7. Inconsistencies of Experimental Data (Paper No. 2)

The critical analysis in Paper No. 2 probably could be extended and sharpened further. In any event, discrepancies have already been pointed out, particularly in the high-energy experiments at Dubna and Berkeley, which probably should be reexamined experimentally.

8. Extension of Theory to the Extreme Relativistic Range (Appendix A, Section 2.12)

Apart from the problem mentioned in 1(a), above, the theory is incomplete above incident proton energies of the order of 1000 Mc^2. Inclusion of the effects of anomalous magnetic moment (which also causes neutrons to lose energy) and of particle form factors should be a rather straightforward task.

9. Nuclear Collision Effects (Paper No. 5)

Particle deflections stem primarily from their Coulomb interaction with nuclei, but they also stem from nuclear forces. The influence of non-Coulomb deflections, particularly of the smaller ones, on the penetration of protons in the Gev range does not appear to have been analyzed systematically. Extension of Paper No. 5 in this direction appears worthwhile.

10. Delta Ray Spectrum (Appendix A, p. 51)

The upper portion of this spectrum should be determined by high-Q collisions, but the theoretical prediction of the relevant approximation does not appear to have been tested critically over a wide range. In particular, the lower portion of the spectrum should contain additional electrons ejected from inner shells in lower-Q processes. The onset of this additional contribution and its position in the spectrum have not been detected.

11. Density Effect and Transverse Stopping Power (Appendix A, p. 21, note 18)

Curves that represent the contribution of transverse excitations to stopping power, inclusive of density effects, might profitably be constructed and discussed for various materials.

12. Straggling and Detour Effects

In Paper No. 5, an effort was undertaken to analyze the combined effects of energy straggling and track deflections upon the straggling of the projected range. This effort has not accounted fully for the experimental results and would be profitably continued, possibly in conjunction with item No. 9 above.

13. Energy-Loss Fluctuations at the Beginning of Penetration (Appendix A, p. 45)

These fluctuations produce characteristic transient effects at the threshold of nuclear reaction yield curves which are being studied experimentally (Ref. 135 of Appendix A and forthcoming publications). The correlation of experimental results with the analytic theory of loss fluctuations requires further analysis. New or improved experimental design or theories might result from such an analysis.

14. Shell Corrections to Straggling Parameters (Appendix A, p. 42)

The theory of energy straggling could be developed to evaluate accurately parameters analogous to the mean excitation energy and the shell corrections of the stopping-power theory. The methods of Paper No. 4 should be relevant for this purpose. Recent experiments have indicated a need for at least some progress in this direction, as shown by Bichsel and Uehling (Phys. Rev., vol. 119, p. 1670, 1960, particularly note 11).

APPENDIXES

APPENDIX A

PENETRATION OF PROTONS, ALPHA PARTICLES, AND MESONS[1,2]

By U. Fano

National Bureau of Standards, Washington, D. C.

[1] The survey of literature pertaining to this review was concluded in March 1963.

[2] This article is related to a "state of the art" survey being conducted by the National Research Council Committee on Nuclear Science, Subcommittee on Penetration of Charged Particles. The forthcoming final report of this survey (87) will contain considerably more detailed information than this article. Members of the Subcommittee are: S. K. Allison, Walter Barkas, Martin J. Berger, Hans Bethe, Hans Bichsel, U. Fano, R. L. Gluckstern, William P. Jesse, Jens Lindhard, L. C. Northcliffe, Robert L. Platzman, R. H. Ritchie, R. M. Sternheimer, J. E. Turner.

Dr. James E. Turner of the Health Physics Division, Oak Ridge National Laboratory, has been collaborating with the author in relevant research work and has helped him materially with the preparation of the article itself. His contribution and that of the Subcommittee members, particularly Dr. R. L. Platzman and Dr. H. Bichsel, are gratefully acknowledged.

1. INTRODUCTION

Since the early work of Rutherford and Bragg, the study of penetration of high energy radiation through matter has been important for nuclear physics, in connection with the analysis of experiments. The penetration also provides information on the properties of the materials traversed, but this important aspect of the phemomenon will be treated as secondary in the present article.

Protons, α particles, and mesons with energies up to the order of 1 GeV traverse matter, in great majority, on an approximately straight path, dissipating their energy gradually through a multitude of inelastic collision processes with atomic electrons. Therefore the penetration depends chiefly on the average energy loss resulting from these collisions (the "stopping power" of the material). Combination of experimental and theoretical results provides values of the stopping power with an accuracy which is currently approaching 1 percent for particle energies above 1 MeV. The total distance traveled by a particle in the course of its penetration ("range" of a particle) is obtained by integrating the reciprocal stopping power over the energy from its initial value down to rest.

At lower particle energies, i.e., at particle velocities comparable to those of outer atomic electrons, capture and loss of electrons by the penetrating particle complicate its energy loss process. Much experimental information on this energy range, within which the stopping power reaches its maximum value, has been developed and reviewed recently [Whaling (137), Allison & Garcia Munoz (87, 88)]. However, systematic analysis and comparison with theory have thus far been scarce in this range [see, e.g., Lindhard & Scharff (85), Lindhard (87)]. Accordingly, this part of our subject will not be treated in the present article. Notice that the stopping power below 1 MeV has little influence on the range of higher energy particles.

Above 1 GeV, the penetration of protons and other heavy particles (except μ mesons) is limited primarily by nuclear collisions. However, the stopping power along the tracks between these collisions remains important and is as well known as at lower energies, except for the disturbing influence of energy straggling.

Large-angle Rutherford scattering in the course of penetration is a rare event, not to be discussed here. Multiple small-angle Rutherford scattering introduces a gradual divergence in an initially parallel beam of heavy charged particles. This phenomenon is now well understood theoretically (11, 83, 112), and has been reviewed comprehensively by Scott (107). It will be considered here only insofar as it reduces the net penetration of the particles, by causing their tracks to depart from straight lines.

The penetration of electrons and positrons is closely related to that of protons with regard to the interaction with atomic electrons, but it is influenced to a much greater extent by Rutherford scattering and X-ray emission, with which we are not concerned. The penetration of ions heavier than the α particle involves electron capture and loss even far above 1 MeV, and is treated separately in an accompanying article (91). The stopping power of α particles (above several MeV), deuterons, and mesons is closely related to that of protons, as stated in Section 2.9.

Accordingly, the present article is concerned primarily with the stopping power for protons and secondarily with the minor effects of straggling and multiple scattering. The subject thus delimited has been covered in a previous article of this series (130), thus emphasis will be placed on developments after 1954. Among these, the principal ones are:†

(*a*) Additional measurements, particularly on proton beams up to 700 MeV and on high energy particle tracks in emulsions, have shown conclusively that the mean excitation energy I (the key parameter of stopping power theory) is close to 10 Z for medium and heavy elements, though larger for lighter elements. This result is explained approximately by theory.

(*b*) An apparent discrepancy between the interpretations of stopping powers at 10–20 MeV and above 200 MeV has been removed by the realization that shell corrections are more important than they were thought to be. This effect has also been accounted for theoretically.

(*c*) Understanding of the theory of stopping power in solids, particularly with regard to polarization effects, has improved appreciably.

(*d*) Analysis of multiple scattering effects has accounted for most, though not all, of the fluctuations in penetration of high energy protons.

Even though the basis of stopping power theory has remained unchanged

† *Note added in proof:* New results and points of view have been emerging rapidly since this article was planned. Some of them are not yet fully assimilated; others are still under development. Notice particularly the contributions by Barkas and Tsytovich outlined in Sec. 2.13 and by Lindhard on shell corrections (p. 35) and on the penetration of slower particles (87).

for a great many years, it appeared desirable to review it in some detail in the present article, in order to place in the proper context the recent progress and the questions that remain unexplored. A brief discussion of phenomena that occur along particle tracks and are incidental to penetration is given in Section 7.

2. The Theory of Energy Loss

The theory of the energy loss of fast charged particles caused by their inelastic collisions with atoms was established by Bohr (25) through a semiclassical procedure. In this procedure collisions are classified according to their impact parameter b, which is, roughly, the distance of closest approach of the incident particle to the center of an atom. The later quantum-mechanical formulation by Bethe (10) classified, instead, the collisions according to their momentum transfer q, which is *observable* in contrast to b. The vector q is a function of the energy transfer E_n and of the deflection θ experienced by the incident particle. (The uncertainty principle introduces a loose inverse correspondence between b and q, namely, $b \sim \hbar/q$.) The Bohr and Bethe theories apply to separate atoms, i.e., to gases. The influence of many atoms interacting simultaneously with an incident particle and with one another ("density effect") was first taken into account by Fermi (45), again through a semiclassical macroscopic procedure. The connection between the Bethe and Fermi theories was worked out more recently [Fano (43)].

The theory attained from the start an accuracy of the order of 10 percent through recognition of the dominant influence of certain simple circumstances. Further improvements depend, however, on numerous detailed factors.

2.1 *Initial formulas.*—The average energy loss per unit pathlength, $-dE/ds$, experienced by a particle traversing a material which consists of separate atoms (or molecules) is related to the cross section for all possible individual collisions by

$$-\frac{dE}{ds} = \Sigma_i N_i \Sigma_n E_{ni}\sigma_{ni} \qquad 1.$$

where σ_{ni} is the cross section for the inelastic collision which raises an atom of type i to an energy level E_{ni} above its ground state,[3] and where N_i is the density of atoms (or molecules) i. If N_i is expressed in atoms per unit volume, $-dE/ds$ is the energy loss per unit distance traveled; if N_i is in atoms per gram, dE/ds is the loss per g/cm² of material traversed. The treatment of a solid or liquid material as an aggregate of separate atoms embodies the approximate "additivity rule" of Bragg. Departures from this rule will be discussed in Sections 2.10, 2.11, and 3.1. In the following we shall normally refer to a single kind of atom and omit the index i and the summation over it for simplicity, but such a summation is implied wherever it is relevant. The Σ_n

[3] In plasmas or other systems, where many atoms are not in their electronic ground state, a collision may bring these atoms to a lower energy level, with negative E_{ni}.

includes both the discrete and the continuous spectrum of energy levels. The fluctuations of energy loss ("straggling"), i.e., the departures from the average $-dE/ds$, will be discussed in Section 5.

The cross section σ_n is taken initially, according to Bethe (10), in a form differential with respect to the final momentum p' of the incident particle (Fig. 1) and in lowest-order ("Born") approximation[4] in the electromagnetic interaction V between the incident particle and the atomic electrons

$$d\sigma_n = \frac{2\pi}{\hbar v} \left| (p', n \left| V \right| p, 0) \right|^2 \delta(E' + E_n - E) \frac{dp'}{h^3} \qquad 2.$$

Here p, E, and v are the initial momentum, kinetic energy, and velocity of the incident particle; p', E', and v' the corresponding values after the collision; and E_n the energy of the final stationary state of the atom (whose initial energy $E_0=0$). The δ function, which imposes energy conservation, yields 1 when integrated over dE'. This differential is contained in $dp' = p'^2(dp'/dE')dE'd(\cos\theta)d\varphi$, with $dp'/dE' = 1/v'$. Therefore Equation 2 is equivalent to

$$d\sigma_n = \frac{1}{4\pi^2\hbar^4 v v'} \left| (p', n \left| V \right| p, 0) \right|^2 p'^2 d(\cos\theta)d\varphi \qquad 3.$$

2.2 *Recoil variables; small recoil approximation.*—The momentum transfer

$$q = p - p' \qquad 4.$$

serves better than p' itself to classify the collisions because it represents the recoil of an atomic electron in each collision and it relates, at least statistically, to the energy transfer E_n. Even more closely related to E_n is the kinetic energy Q (see Footnote 5) of an unbound electron with momentum q, which is given by

$$Q(1 + Q/2mc^2) = q^2/2m \qquad 5.$$

$$Q \sim q^2/2m \qquad \text{(nonrelativistic)} \qquad 5a.$$

In the limit of large q, where the atomic electrons may be regarded as free and initially at rest, Q coincides with E_n.

Because we are dealing with incident particles of mass M much heavier than the electron mass m, we have normally

$$\left(\frac{q}{p}, \frac{p - p'}{p}, \frac{v - v'}{v}\right) \sim \frac{m}{M} \ll 1 \qquad 6.$$

In the following we shall normally disregard the quantities on the left-hand side of this equation. However, Equation 6 holds only under the condition

$$E \ll \frac{M}{m} Mc^2 \qquad 7.$$

[4] This approximation is discussed in Sec. 2.13.

[5] The definition of Q given here coincides with those of Bethe (10) or Uehling (130) only in the limiting cases of high Q and of low Q and low E_n.

which breaks down in the GeV range for muons and at higher energies for other particles.[6] This breakdown will be discussed briefly in Section 2.12.

Under the condition 6, the component of q parallel to p is fixed by the energy conservation (see Eq. 2 and Fig. 1) at

$$q\cdot\hat{p} = \frac{p^2 - p'^2}{2p} + \frac{q^2}{2p} \sim p - p' \sim \frac{dp}{dE}E_n = \frac{E_n}{v} \qquad 8.$$

and its perpendicular component may be indicated by $p\theta$, so that

$$q^2 = E_n^2/v^2 + p^2\theta^2 \qquad 9.$$

The differential on the right-hand side of Equation 3 can now be transformed in part, to yield

$$p'^2 d(\cos\theta) = p'^2\theta d\theta = qdq = m(1 + Q/mc^2)dQ \qquad 10.$$

and integrated in part ($\int d\varphi = 2\pi$) so that Equation 3 becomes

$$d\sigma_n = \frac{m}{2\pi\hbar^4 v^2}\,|\,(p', n\,|\,V\,|\,p, 0)\,|^2\left(1 + \frac{Q}{mc^2}\right)dQ \qquad 11.$$

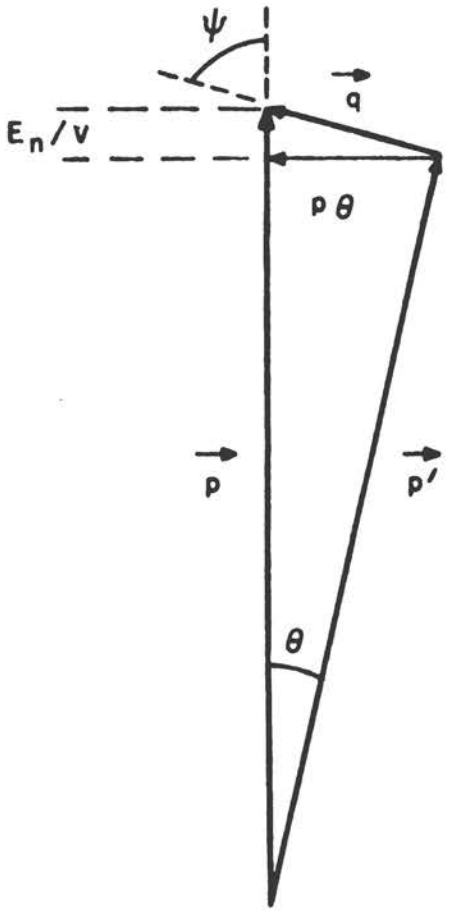

FIG. 1. Momentum transfer diagram in a heavy-particle inelastic collision.

2.3 *Longitudinal and transverse excitations.*—The electromagnetic interaction between the charge and spin, if any, of the incident particle and those of atomic electrons can be subdivided into two terms. One of these consists of the unretarded static Coulomb interaction and the other of the interaction through emission and reabsorption of virtual photons. (This subdivision is called the "Coulomb gauge" representation.) The Coulomb interaction between the incident particle of charge ze at the position r and an atomic electron at r_j can be represented as a Fourier integral $ze^2/|r - r_j| = (ze^2/2\pi^2)\int dk\, k^{-2}\exp[ik\cdot(r_j - r)]$. This representation is convenient because, as seen below, each Fourier component with wave vector k serves to transfer the momentum $\hbar k$ from the incident particle to the electron. Alternatively, the same momentum can be transmitted by emission and reabsorption of a photon with momentum $\pm\hbar k$. Emission of a photon of momentum $\hbar k$ by the incident particle is proportional to a matrix element of $\sec\alpha\cdot A_0\exp(-ik\cdot r)$,

[6] When Eq. 7 breaks down, the energies of an atomic electron and of the incident particle become comparable in their center-of-mass system.

where $zec\boldsymbol{\alpha}$ is the relativistic current operator of the particle and $\hat{\mathbf{A}}_s$ the unit polarization vector of the photon ($s=1$, 2 for two orthogonal directions). The absorption of the same photon by the jth electron is proportional to a matrix element of the corresponding operator $ec\boldsymbol{\alpha}_j\cdot\hat{\mathbf{A}}_s\exp(i\mathbf{k}\cdot\mathbf{r}_j)$. The transmission of the photon with momentum $\pm\hbar\mathbf{k}$ proceeds through an intermediate state whose energy differs from that of the initial and final states by $\hbar ck\pm E_n$. The sum of the contributions of these alternative channels yields the complete interaction matrix element in the form (42)

$$(\mathbf{p}',n\,|\,V\,|\,\mathbf{p},0)=\frac{ze^2}{2\pi^2}\int d\mathbf{k}\left\{\frac{(\mathbf{p}'\,|\,e^{-i\mathbf{k}\cdot\mathbf{r}}\,|\,\mathbf{p})(n\,|\,\Sigma_j e^{i\mathbf{k}\cdot\mathbf{r}_j}\,|\,0)}{k^2}\right.$$
$$\left.+\Sigma_s\frac{(\mathbf{p}'\,|\,\boldsymbol{\alpha}\cdot\hat{A}_s e^{-i\mathbf{k}\cdot\mathbf{r}}\,|\,\mathbf{p})(n\,|\,\Sigma_j\boldsymbol{\alpha}_j\cdot\hat{A}_s e^{i\mathbf{k}\cdot\mathbf{r}_j}\,|\,0)}{k^2-(E_n/\hbar c)^2}\right\} \qquad 12.$$

In Equation 12 the matrix elements between momentum eigenstates of the incident particle vanish except when $\hbar\mathbf{k}=(\mathbf{p}-\mathbf{p}')/\hbar=\mathbf{q}/\hbar$ (momentum conservation). These matrix elements depend also on spin and other relativistic variables of the particle states, but the square of expression 12 must be summed or averaged over these variables. Under the condition 7 which governs our approximation, this sum or average operation, combined with momentum conservation, is equivalent to setting, in Equation 12,

$$(\mathbf{p}'\,|\,e^{-i\mathbf{k}\cdot\mathbf{r}}\,|\,\mathbf{p})=(2\pi)^3\delta\left(\mathbf{k}+\frac{\mathbf{p}'}{\hbar}-\frac{\mathbf{p}}{\hbar}\right) \qquad 13.$$

$$(\mathbf{p}'\,|\,\boldsymbol{\alpha}\cdot\hat{A}_s e^{-i\mathbf{k}\cdot\mathbf{r}}\,|\,\mathbf{p})=\boldsymbol{\beta}\cdot\hat{A}_s(2\pi)^3\delta\left(\mathbf{k}+\frac{\mathbf{p}'}{\hbar}-\frac{\mathbf{p}}{\hbar}\right) \qquad 14.$$

where $\boldsymbol{\beta}=\mathbf{v}/c$. We also have

$$\Sigma_s\boldsymbol{\beta}\cdot\hat{A}_s\,\boldsymbol{\alpha}_j\cdot\hat{A}_s=\boldsymbol{\beta}_t\cdot\boldsymbol{\alpha}_j \qquad 15.$$

where $\boldsymbol{\beta}_t=\boldsymbol{\beta}-(\boldsymbol{\beta}\cdot\hat{q})\hat{q}$ is the component of $\boldsymbol{\beta}$ perpendicular to $\mathbf{q}$.

As seen in Equation 12, the Coulomb interaction exerts a force parallel to $\mathbf{q}$ and is accordingly called "longitudinal." The interaction through virtual photons is "transverse" because photon fields are perpendicular to $\mathbf{q}$. The Coulomb interaction induces no parity change with respect to reflection on any plane that contains $\mathbf{q}$ because its interaction operator is even under this reflection, whereas the transverse interaction transmits one unit of odd parity with respect to reflection on the plane through $\mathbf{q}$ perpendicular to the $(\mathbf{p},\mathbf{p}')$ plane. Therefore, any atomic system which is isotropic, i.e., invariant under space rotations and reflections, is excited to states n' and n'' of different parity by the longitudinal and transverse components of the interaction. We deal, then, with separate cross sections $\sigma_{n'}$ and $\sigma_{n''}$ for excitation to different sets of states, even though pairs of levels $E_{n'}$ and $E_{n''}$ often coincide for isolated atoms and molecules [Fano (42)].

In view of these considerations and of expressions 13, 14, 15, and 5, we can now enter Equation 12 into Equation 11 and find

$$d\sigma_n=\frac{2\pi z^2e^4}{mv^2}Z\left\{\frac{|\,F_n(q)\,|^2}{Q^2(1+Q/2mc^2)^2}+\frac{|\,\boldsymbol{\beta}_t\cdot\mathbf{G}_n(q)\,|^2}{[Q(1+Q/2mc^2)-E_n^2/2mc^2]^2}\right\}\left(1+\frac{Q}{mc^2}\right)dQ \qquad 16.$$

$$d\sigma_n\sim\frac{2\pi z^2e^4}{mv^2}\frac{dQ}{Q^2}Z\,|\,F_n(q)\,|^2 \qquad \text{(nonrelativistic)} \qquad 16a.$$

where Z is the number of electrons per atom (or molecule),

$$F_n(q) = Z^{-1/2}\Sigma_j(n \mid e^{2\pi i q \cdot r_j/\hbar} \mid 0),$$
$$G_n(q) = Z^{-1/2}\Sigma_j(n \mid \alpha_j e^{2\pi i q \cdot r_j/\hbar} \mid 0) \qquad 17.$$

and where n stands for either n' or n'' with the understanding that either F_n or G_n vanishes for any state of given parity. Notice that the transverse interaction becomes negligible as compared to the electrostatic one in the nonrelativistic limit 16a. The simple structure of Equation 16a is very important. It represents $d\sigma_n$ as the product of $(2\pi z^2e^4/mv^2)dQ/Q^2$, the Rutherford cross section for scattering on a free electron at rest with transfer of the recoil energy $E_n = Q$, of the number Z of atomic electrons, and of a factor (called the "inelastic form factor") which represents the probability of excitation of an atom to the level n if one of its atomic electrons has received a recoil momentum q.[7]

For the purpose of applying Equation 16 to the stopping power of isotropic materials, the matrix elements 17 may be regarded as functions only of the magnitude of q, i.e. of Q, and of the energy E_n of the final state n, even though they depend formally also on the direction of q and on any orientation characteristics of the states 0 and n. The ground state 0 of an isotropic material has, of course, no orientation characteristics, at least on an average basis. The orientation characteristics of n and of q average out at later stages of the calculation when a summation over the final states n is carried out with a weight function that depends only on E_n, because excited states of an isotropic system with different orientation are degenerate in energy.

[7] The classical derivation of the Rutherford formula for collisions with impact parameter b gives $Q = [(ze^2/b^2)(2b/v)]^2/2m = 2(z^2e^4/mv^2)/b^2$, where ze^2/b^2 is, in essence, the peak force between the charges and $2b/v$ the effective duration of the collision. The Bohr theory (25) was based, in effect, on Eq. 16a even though no method was available in 1913 to calculate $|F_n|^2$. In a sudden collision involving a classical system consisting of many particles, the energy absorbed by the system is the same as though the particles were free. Bohr surmised that this must remain true as a statistical average in a quantum system and, therefore, that the unknown $|F_n|^2$ must be such as to fulfill Equation 27. To calculate completely the nonrelativistic form of 38, Bohr required only the limits to the range of variation of Q. For the upper limit to Q, energy and momentum conservation gave him the correct value (Eq. 20). The lower limit was set by Bohr through the requirement that the collision be sudden, i.e., that its duration $\sim b/v$ remain shorter than the reaction time $\sim\hbar/E_n$ of atomic electrons, since slower ("adiabatic") collisions yield no energy loss. This consideration gives $Q_{\min} \sim z^2e^4/mv^2b_{\max}^2 \sim z^2e^4E_n^2/mv^4\hbar^2 = (ze^2/\hbar v)^2E_n^2/mv^2$, a limit which is less restrictive than the limit (Eq. 18) set by momentum and energy conservation whenever $ze^2/\hbar v < 1$. The limit (Eq. 18) becomes apparent when attention is focused on the momentum transfer rather than on the impact parameter. The stopping power formulas obtained by Bohr and the one obtained later by Bethe (10) are connected by the Bloch formula (18) which reduces to the other two in the limiting cases $ze^2/\hbar v \gg 1$ respectively. The Bohr limit becomes relevant only at low velocities (not considered in this article) at which atomic electrons are normally captured by the incident particle.

2.4 *Mapping on the* (Q, E_n) *plane.*—The inelastic collisions have been classified above in accordance with the energy transfer E_n and recoil parameter Q. The calculation of stopping power involves an integration over these variables. Let us consider the anticipated contribution to the integral from various regions of the (Q, E_n) plane, which are indicated in Figure 2 with logarithmic scales.

Equations 5 and 9 define Q as a monotonic function $Q(E_n, \theta)$. To the limitation $\theta \geq 0$ corresponds

$$Q \geq Q_{\min}(E_n) = Q(E_n, 0) = E_n^2/2mv^2 - \text{relativistic terms} \qquad 18.$$

The full line in Figure 2 represents the function $Q = Q(E_n, 0)$. The integration extends only over points above this line.

The other main relationship between Q and E_n results from the momentum balance in the collision. If an atomic electron were initially free and at rest, a collision with momentum transfer q would send it into the final state with momentum q and energy $E_n = Q$. Therefore, under this idealized, unrealistic circumstance, $F_n(q)$ and $G_n(q)$ would differ from zero only along the line $Q = E_n$ shown in dashes in Figure 2. In fact, the final state is not uniquely determined by the momentum transfer q from the incident particle to the electron because an atomic electron is subject to forces and thereby exchanges momentum with the rest of the atomic system to which it belongs. Therefore, $F_n(q)$ and $G_n(q)$ differ significantly from zero throughout a region of the (E_n, Q) plane, on either side of the line $Q = E_n$, which is indicated by the shaded area in Figure 2. The width of this region depends on the magnitude of the likely momentum exchanges between the electron and the rest of its atomic system. As an index of this magnitude we take the mean square momentum of the electron in its initial ground state, since momentum exchanges decrease after the electron moves away from nuclei following the collision. The mean square momentum is $2m\langle K\rangle_0$ in terms of the more familiar mean kinetic energy. It differs, of course, for electrons of different atomic shells, but an average $\langle K\rangle_0$ over all atomic electrons may be considered. More specific information on the statistical correlation between E_n and Q, which results from the values of $F_n(q)$ and $G_n(q)$, is afforded by inspection of the matrix elements $F_n(q)$ calculated for atomic hydrogen (10). From this inspection one obtains a parameter relevant to Figure 2, namely, the variance of the fractional departures of E_n from Q

$$\left\langle \left(\frac{E_n - Q}{E_n + Q} \right)^2 \right\rangle \sim \frac{2\langle K\rangle_0}{E_n + Q} \qquad 19$$

An analogous, more precise, result is given by Equation 69 in Section 5.

Significant values of the cross section $d\sigma_n$ are, therefore, expected to lie within a strip about the line $Q = E_n$ which is very narrow (on the logarithmic scale of Fig. 2) for large E_n and flares out rapidly as E_n decreases to the point of being comparable to $\langle K\rangle_0$.[8] This strip is indicated in Figure 2 by the shaded area.

[8] The flaring out is far more gradual in heavy than in light elements, because of the large spread in the values of $\langle K\rangle_0$ for different shells.

For large values of Q and E_n, the strip lies below the full line in Figure 2, that is, outside the range of integration over Q defined by Equation 18. Therefore, as a result of momentum and energy conservation, no collision occurs with energy loss E_n beyond the intersection of the strip and the full line (except as noted in Sec. 4). The intersection lies at the root of the equation $Q(E_n, 0) = E_n$, namely at $Q = E_n = Q_{max}$, where

$$Q_{max} = 2mv^2/(1 - v^2/c^2) \qquad 20.$$

under the condition 7. The exact value (10) is

$$Q_{max} = 2m(E^2 - M^2c^4)/[(M^2 + m^2)c^2 + 2mE] \qquad 20a.$$

For intermediate values of Q and E_n the strip lies entirely above the line, within the region consistent with Equation 18. Thus the theory need not

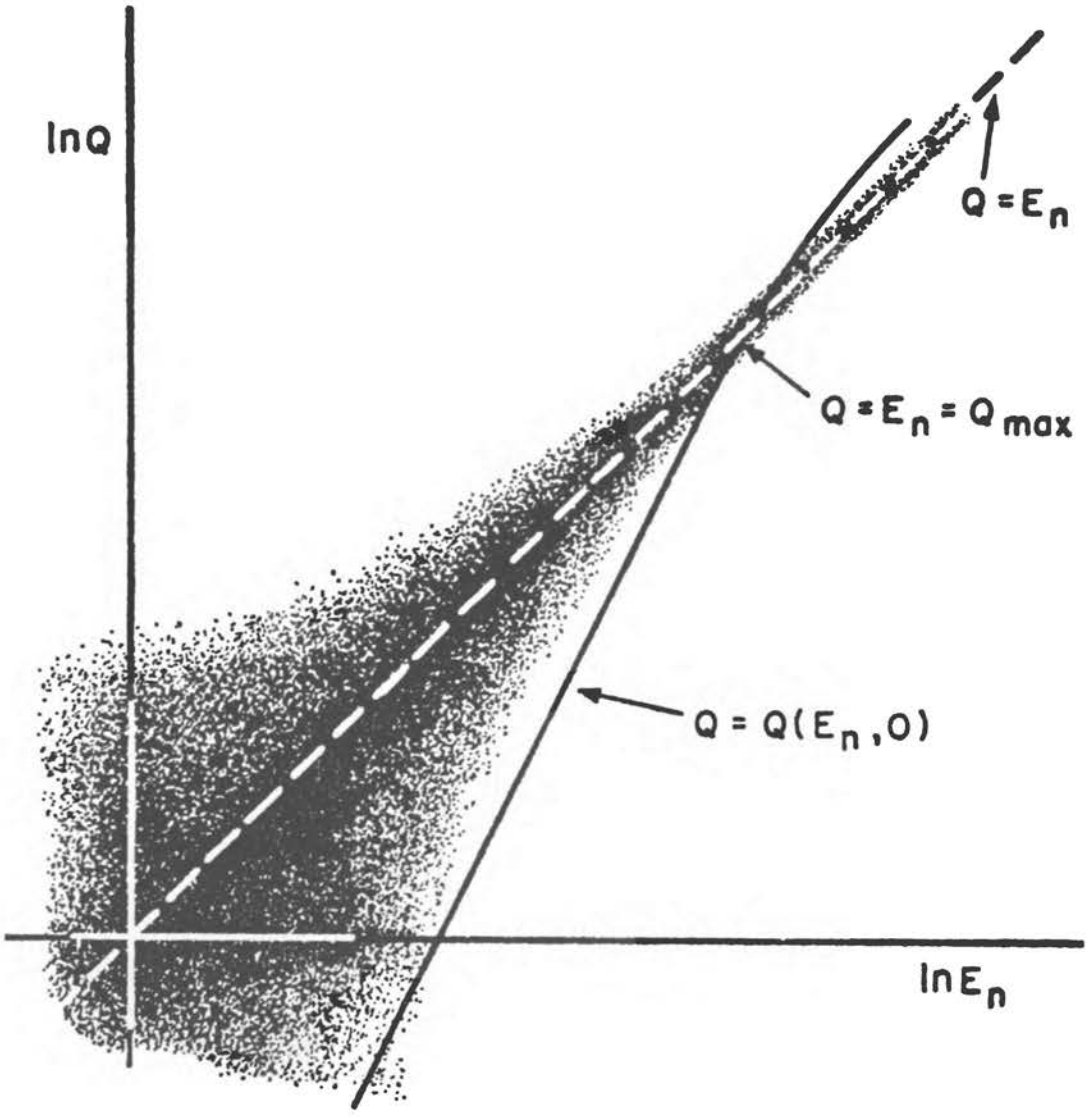

Fig. 2. Diagram of probability distribution of collisions with different values of Q and E_n.

consider the restriction imposed by Equation 18 explicitly in this range, and is thereby greatly simplified. The separation of the strip from the line is characterized graphically by the "empty crescent" between line and strip in Figure 2. The points of the chord of this crescent lie at values of E_n for which

$$\langle K\rangle_0 \ll E_n \ll 2mv^2 \qquad 21.$$

Therefore, the occurrence of the crescent and the simplification resulting from it depend on the condition $\langle K\rangle_0 \ll 2mv^2$, i.e., on the incident particle being much faster than the atomic electrons. Failure of condition 21 leads to a more difficult situation discussed in Section 4.

At low values of E_n the shaded strip reaches down to and below the full line of Figure 2.

Additional remarks can be made about the contribution of transverse excitations to Equation 16. In the first place, β_t and consequently the whole contribution vanish at the limit $\theta=0$, $Q=Q_{\min}$ (i.e., on the full line) because q is parallel to β at this limit. (A moving charge does not emit or absorb photons in its own direction.) Therefore, the limit $Q=Q_{\min}$ need not appear explicitly in the integrated contribution of transverse excitations to stopping power, as will be verified in Section 2.8. Secondly, the denominator of the second term in Equation 16 increases rapidly as Q increases, without any compensating increase of $G_n(q)$ in the numerator. As a result, values of $Q \gg Q_{\min}$ contribute little to transverse excitations. These excitations are thus confined to a narrow strip parallel to the full line in Figure 2 lying a little above it. This strip lies within the shaded strip only at low Q and again at high Q. The lack of points common to the two strips at intermediate Q means that transverse interactions can be disregarded here. This circumstance has facilitated the theory (10).

2.5 *Low-Q approximation.*—In the range of low Q, the matrix elements $F_n(q)$ and $G_n(q)$ can be evaluated by expanding the exponential within them into powers of q to the lowest nonvanishing order, namely, q^1 for F_n and q^0 for G_n. The expansion assumes that $\hbar/q$ is much larger than the linear dimension of the atomic system under consideration; it does not hold for macroscopic amounts of condensed matter that behave as a single atomic system and are treated separately in Section 2.10 and 2.11.

The matrix elements F_n and G_n reduce, in this approximation, to dipole and velocity matrix elements, respectively. Moreover, the velocity element equals the dipole element times $iE_n/\hbar$. One finds thus

$$|F_n(q)|^2 \sim Z^{-1}q^2 \left|(\Sigma_j x_j)_{n0}\right|^2/\hbar^2 = Qf_n/E_n \qquad 22.$$

$$|\beta_t \cdot G_n(q)|^2 \sim Z^{-1}\beta_t^2 E_n^2 \left|(\Sigma_j y_j)_{n0}\right|^2/\hbar^2c^2 = \beta_t^2 f_n E_n/2mc^2 \qquad 23.$$

where x_j, y_j are electron coordinates in the directions of q and β_t, respectively, and f_n is the optical dipole oscillator strength for excitation to the level n.[9]

[9] The oscillator strength is defined here with the normalization factor Z^{-1}, which leads to 33 instead of $\Sigma_n f_n = Z$.

Substitution of Equations 22 and 23 into the $d\sigma_n$ given by Equation 16 makes this expression easy to sum over n and integrate over Q. In the transverse excitation term, Q can be replaced by

$$\cos^2\psi = \frac{q_{\min}^2}{q^2} = \frac{Q_{\min}(Q_{\min} + 2mc^2)}{Q(Q + 2mc^2)} \qquad 24.$$

where ψ is the angle between $\mathbf{p}$ and $\mathbf{q}$. This yields

$$E_n d\sigma_n \sim \frac{2\pi z^2 e^4}{mv^2} Zf_n \left\{ \frac{dQ}{Q} + \beta^4 \frac{\sin^2\psi}{(1 - \beta^2\cos^2\psi)^2} d(\cos^2\psi) \right\} \qquad 25.$$

2.6 *Intermediate-Q range.*—This is the range in which the shaded area in Figure 2 is detached from the line $Q = Q_{\min}$ and in which the contribution of transverse excitations is assumed to be negligible. Detachment from the limit of integration over Q—which depends on E_n—enables one to calculate contributions to stopping power by carrying out the sum over the levels n for each value of Q. Dropping the transverse term in Equation 16 as well as relativistic corrections of order Q/mc^2, we obtain from Equation 16

$$\Sigma_n E_n d\sigma_n = \frac{2\pi z^2 e^4}{mv^2} Z \frac{dQ}{Q^2} \Sigma_n E_n \left| F_n(q) \right|^2 \qquad 26.$$

There is no need here to evaluate $\left| F_n(q) \right|^2$ itself, since a sum rule given by Bethe (10) (a generalization of $\Sigma_n f_n = 1$) yields

$$\Sigma_n E_n \left| F_n(q) \right|^2 = Q \qquad 27.$$

With reference to the interpretation of $\left| F_n \right|^2$ at the end of Section 2.3, the important result 27 means that, when atomic electrons receive a momentum q, they absorb on the average the same amount of energy Q as though they had been free and at rest, regardless of atomic binding and of the spectrum of energy levels E_n.[7]

Relativistic corrections Q/mc^2 have been dropped in the expectation that the high-Q approximation holds whenever $Q/mc^2 \ll 1$ fails. It has also been implied in Equation 27 that Q (or q) is sufficiently low to insure that relativistic values of E_n do not contribute appreciably to the sum. Indeed, Equation 27 rests on the assumed use of nonrelativistic wave functions in the matrix elements F_n. These assumptions break down, in fact, for the excitation of K-shell electrons in heavy elements, and are not very accurate for L electrons in heavy atoms or for the K electrons of medium-heavy elements. The errors incurred by the stopping power theory on account of this inaccuracy do not appear to have been studied extensively, but Perlman (94) found the stopping power of the mercury K electrons for incident 1-MeV electrons to be twice as large as predicted by a nonrelativistic calculation.[10] Even though Equation 26 introduces such a substantial error in the contri-

[10] According to Perlman, the ejection of K electrons by electron collisions shows relativistic effects of 10–20 percent even for incident energies ~50 keV and binding energies ~8 keV. Analysis of this calculation might be an initial step to a serious study of the upper limit of the intermediate-Q approximation.

bution of individual electrons to the stopping power, the total error may not exceed the order of 1 percent because the innermost shells contain only a small fraction of the electrons of heavy elements.

2.7 *High-Q approximation.*—When $Q \gg \langle K \rangle_0$, the mean kinetic energy that represents the effect of atomic binding in Equation 19, E_n cannot depart much from Q. One disregards, then, this departure, and the binding responsible for it, and evaluates the matrix elements $F_n(q)$ and $G_n(q)$ (Eq. 17) as though the initial and final electron states were free-particle momentum eigenstates, with momenta $p_0 = 0$ and $p_n = q$. This evaluation, carried out with Dirac relativistic wave functions and with appropriate averaging or sum over alternative spin orientations, yields

$$\begin{aligned} |F_n(q)|^2 &\sim \frac{1 + Q/2mc^2}{1 + Q/mc^2}\delta_{nq} \\ |\beta_t \cdot G_n(q)|^2 &\sim \beta_t^2 \frac{Q/2mc^2}{1 + Q/mc^2}\delta_{nq} \end{aligned} \qquad 28.$$

where the Kronecker δ indicates that the matrix elements vanish unless the state n is an eigenstate of momentum q. Substitution into Equation 16 gives

$$\Sigma_n E_n d\sigma_n = \frac{2\pi z^2 e^4}{mv^2} Z \left\{ \frac{1}{Q(1 + Q/2mc^2)} + \frac{\beta_t^2}{2mc^2} \right\} dQ \qquad 29.$$

Notice that this expression reduces to the "intermediate-Q" results (Eqs. 26, 27), in the nonrelativistic limit $Q \ll mc^2$. No separate high-Q approximation is, therefore, required for $\beta \ll 1$. On the other hand, the contribution of transverse interaction predominates in the opposite limit $Q \gg mc^2$. Part of the dependence of Equation 29 on Q is included in

$$\beta_t^2 = \beta^2(1 - q_{\min}^2/q^2) = (1 + Q/2mc^2)^{-1} - (1 - \beta^2) \qquad 30.$$

Substitution of Equation 30 into Equation 29 allows one to combine the longitudinal and transverse contributions[11] to yield

$$\Sigma_n E_n d\sigma_n = \frac{2\pi z^2 e^4}{mv^2} Z \left(\frac{1}{Q} - \frac{1 - \beta^2}{2mc^2} \right) dQ \qquad 31.$$

2.8 *The basic stopping power formula.*—The stopping power theory leans heavily on the possibility of piecing together the low-, intermediate- and high-Q approximations. For this purpose we assume that a value Q_1 of Q exists at which the results of both Sections 2.5 and 2.6 are applicable and another value Q_2 exists at which Sections 2.6 and 2.7 hold. Shortcomings of this assumption will be discussed below.

In the low-Q range we integrate Equation 25 from $Q_{\min}$, as given by Equation 18, to Q_1 and over $\cos^2 \psi$ from 0 to 1 and find

$$E_n \int_{Q\min}^{Q_1} d\sigma_n = \frac{2\pi z^2 e^4}{mv^2} Z f_n \left\{ \ln \frac{Q_1}{E_n^2/2mv^2} + \ln \frac{1}{-\beta^2} - \beta^2 \right\} \qquad 32.$$

[11] Heretofore, calculations have given 31 directly without prior separation of longitudinal and transverse contributions.

The remaining summation over n is trivial for the terms that contain only f_n, owing to the Thomas-Kuhn sum rule

$$\Sigma_n f_n = 1 \tag{33.}$$

The sum over the term with $\ln E_n$ is represented by means of an important atomic parameter, the mean excitation energy I, which is a logarithmic mean over the excitation energies E_n weighted according to the corresponding oscillator strengths f_n and is defined by[12]

$$\ln I = \Sigma_n f_n \ln E_n \tag{34.}$$

Equations 32, 33, and 34 yield, then,

$$\Sigma_n E_n \int_{Q_{\min}}^{Q_1} d\sigma_n = \frac{2\pi z^2 e^4}{mv^2} Z \left\{ \ln \frac{Q_1 2mv^2}{I^2} + \ln \frac{1}{1-\beta^2} - \beta^2 \right\} \tag{35.}$$

In the intermediate range, Equations 26 and 27 lead directly to

$$\int_{Q_1}^{Q_2} \Sigma_n E_n d\sigma_n = \frac{2\pi z^2 e^4}{mv^2} Z \ln \frac{Q_2}{Q_1} \tag{36.}$$

In the high-Q range, Equation 29 is to be integrated from Q_2 to the upper limit $Q_{\max}$[13] given by Equation 20. The expression 30 of β_i^2 is to be used and Q_2/mc^2 disregarded, in keeping with the intermediate-Q approximation. This yields

$$\int_{Q_2}^{Q_{\max}} \Sigma_n E_n d\sigma_n = \frac{2\pi z^2 e^4}{mv^2} Z \left\{ \ln \frac{2mv^2}{Q_2} + \ln \frac{1}{1-\beta^2} - \beta^2 \right\} \tag{37.}$$

where the last two terms in the braces arise from the transverse excitations[14] and are identical to the corresponding contribution to Equation 35.

The sum of Equations 35, 36, and 37, multiplied by N in accordance with Equation 1, gives the complete stopping power to within corrective factors indicated by C/Z and δ and discussed below. We write

$$\begin{aligned} -\frac{dE}{ds} &= N\Sigma_n E_n \int_{Q_{\min}}^{Q_{\max}} d\sigma_n \\ &= \frac{2\pi z^2 e^4}{mv^2} NZ \left\{ \ln \frac{(2mv^2)^2}{I^2} + 2 \ln \frac{1}{1-\beta^2} - 2\beta^2 - 2\frac{C}{Z} - \delta \right\} \qquad \text{38.} \\ &= \frac{4\pi z^2 e^4}{mv^2} NZ \left\{ \ln \frac{2mv^2}{I} + \ln \frac{1}{1-\beta^2} - \beta^2 - \frac{C}{Z} - \tfrac{1}{2}\delta \right\} \end{aligned}$$

[12] The energy I is often treated in the literature as an adjustable parameter of stopping power theory, which may depend on the velocity of the incident particle. Here, as in (10) and (130), it is treated as a property of each material defined by Eq. 34, regardless of the kind and speed of the incident particle, even though its numerical value may not be well known and is in practice commonly obtained by fitting the theory to experimental results.

[13] The integration would extend to $Q = \infty$ in principle, but the approximation introduced in Sec. 2.7 requires the introduction of a cutoff at $Q_{\max}$.

[14] Integration of Eq. 31 instead of Eq. 29 leads to a form of Eq. 37 with the first two terms in the braces combined to yield $\ln (Q_{\max}/Q_2)$.

and note that

$$4\pi z^2 e^4 NZ/mv^2 = 0.307\beta^{-2}z^2 Z/A \text{ MeV/g cm}^{-2} \qquad 38a.$$

where A is the chemical atomic weight.

Notice that Q_1 and Q_2, introduced to delimit the three approximation ranges, cancel out in the sum.

The stopping power formula 38 is the product of two factors. The first, in front of the braces, is a monotonically decreasing function of the incident particle's velocity. The second, in the braces, is a slowly (logarithmic) monotonically increasing function of the particle's energy. The second factor's influence predominates only at very low energies, below 1 MeV, where the logarithmic rise is comparatively fast, and at extremely high energies, where the first factor approaches its limiting value ($v^2 \sim c^2$). The stopping power increase at high energies stems from the transverse interaction and is called the "relativistic rise." This rise diverges logarithmically in the high energy limit, but the diverging term requires some modification and some reinterpretation, to be discussed in Sections 2.11 and 2.12. In the intermediate energy range, from less than 1 MeV to more than 1 GeV for protons, the first factor's influence predominates and causes the stopping power to decrease with increasing energy of the incident particle.

The principal nontrivial factor in the theoretical evaluation of the stopping power for each material thus becomes the determination of the average excitation energy I. This problem will be treated in Section 3. The remaining problems concern inaccuracies of the approximations utilized in the derivation of Equation 38. Of course, even sizable errors incurred at specific points of the calculation may have only a minor influence on the integral 38.

The chief inaccuracy lies often at the junction of the low-Q and intermediate-Q approximations. The existence of a Q_1, at which both approximations hold, depends on the validity of the low-Q formulas 22 and 23 all along the line $Q = Q_{\min}$, defined by expression 18, until it emerges from the strip defined by Equation 19. The low-Q formulas hold for $Q \ll \langle K \rangle_0$ and $Q \ll E_n$, conditions which are fulfilled by the relevant values of Q and E_n provided Equation 21 is satisfied, that is, provided the incident particle is much faster than the atomic electrons. This condition is actually satisfied for high energies of incidence and for the majority of atomic electrons, but it fails increasingly for inner electrons and at lower energies of incidence. The modifications required by this failure, called "inner shell corrections," are represented by C/Z in Equation 38 and are treated in Section 4.

Inaccuracies arising from inadequate overlapping of the intermediate and high-Q approximations at $Q = Q_2$ have not been studied, as noted in Section 2.6. They include the possible effect of transverse excitations in this range and result, like the inaccuracies at $Q = Q_1$, from the high speed of inner shell electrons in heavy atoms.

Other appreciable corrections stem from the "density effect," that is, from modifications to the low-Q formulas 22 and 23 which are required for application to condensed materials (see Sec. 2.10, 2.11). They involve a

more careful definition of the parameter I and the introduction of δ in Equation 38.

2.9 *Range formula.*—The range of a particle of given initial kinetic energy E_0 traversing a given material is variously defined as the mean pathlength covered by it before coming to rest or the mean distance traveled in its initial direction (depth of penetration). These two definitions differ somewhat on account of small deflections of the particle track, to be discussed in Section 6. In this article "range" means the mean pathlength, and the depth of penetration will be called "projected range." Normally it is sufficient to evaluate the mean pathlength in the continuous slowing down approximation (Sec. 5) which yields the result, to be called "c.s.d.a. range" in accordance with (87),

$$R(E_0) = \int_0^{E_0} \frac{dE}{-dE/ds} \qquad 39.$$

Poor knowledge of the stopping power at low energies, $E<1$ MeV, causes little uncertainty in $R(E_0)$ for $E_0 \gg 1$ MeV, since the interval $E<1$ MeV corresponds to large values of $-dE/ds$ and thus contributes little to the integral. In practice it is convenient to separate the interval of integration in Equation 39 into a small part, $0<E<E_1 \sim 1$ MeV, whose contribution is taken from experimental data, and a large one, $E_1<E<E_0$, which can be obtained from theory.

The stopping power, as given by Equation 38, depends on the particle's kinetic energy only through its velocity. Therefore it is a function of E/M, where M is the particle's mass. The stopping power is also proportional to the squared charge of the particle z^2e^2. These circumstances enable one to obtain the range functions of different particles from one another by a scaling operation, at least within the approximation 38. If we call $S_p(E)$ the stopping power (Eq. 38) of a given material for protons, the stopping power for another heavy particle of charge ze and of mass M, *in units of the proton mass*, is $z^2S_p(E/M)$ and its range will be

$$R(E_0) = \int_0^{E_0} \frac{dE}{z^2 S_p(E/M)} = \frac{M}{z^2}\int_0^{E_0/M} \frac{d(E/M)}{S_p(E/M)} = \frac{M}{z^2} R_p\left(\frac{E_0}{M}\right) \qquad 40.$$

This scaling operation does not apply to the onset of corrections for electron capture and loss at low particle energies. These corrections depend on the value of $ze^2/\hbar v$, the velocity ratio for a captured electron and the particle, and thus set in at higher velocity for α particles ($z=2$) than for protons. They can be applied by separating out the integration over the low energy interval as noted above (see also Sec. 8.3).

The current availability of range tables is discussed in Section 8. The c.s.d.a. range considered here coincides with the most probable pathlength only if the pathlength fluctuations, called "straggling," are symmetric about the mean. Departures from symmetry may be appreciable (see Sec. 5), especially when one deals with partial ranges, that is, with the mean path-

length $R(E_0)-R(E_1)$ traversed within a given small energy interval from E_0 to E_1.

2.10 *Low-Q longitudinal excitations in condensed materials.*—The basic low-Q approximation formula 22 for longitudinal excitations involves an expansion of exp $(i\mathbf{q}\cdot\mathbf{r}/\hbar)$ into powers of q. Practical use of this expansion implies that the positions $(\mathbf{r}_j, \mathbf{r}_k)$ of electron pairs of the atomic system of interest are correlated only over distances $|\mathbf{r}_j-\mathbf{r}_k| \ll \hbar/q$. This condition is met by low density gases which are properly regarded as assemblies of small independent molecules but is not met by denser materials whose electrons are correlated over distances $>\hbar/q$. It was believed until the 1950's that, at least, molecular or ionic solids and liquids could be treated on the same basis as gases, but this model proved to be of uncertain applicability owing to the influence of electric interaction between densely packed molecules or ions in their excited states.

In the application of stopping power theory to condensed materials, one can still utilize formally the low-Q approximation formula 22 provided that the oscillator strengths be defined by the double-limit procedure[15]

$$f_n = \lim_{Q=0} \lim_{Z=\infty} E_n |F_n(q)|^2/Q \qquad 41.$$

The limit $Z=\infty$ means that one includes larger and larger groups of atoms in the atomic system of interest. The f_n so defined still obey the sum rule 33, $\Sigma_n f_n = 1$. The energy levels E_n to be entered, together with the f_n, in the definition (Eq. 34) of I also must be understood to pertain to the limit $Z=\infty$.

Thus, longitudinal excitations in condensed materials may be included in the theory of stopping power merely by a more careful definition of f_n, E_n, and I. This redefinition has little consequence as long as the value of I for a condensed material is obtained from stopping power experiments. On the other hand, the problem of determining I for a condensed material by working out the f_n and E_n of the aggregate from the properties of its constituent atoms or molecules is difficult and, in the main, unsolved. Nevertheless, substantial understanding of this problem has been achieved, and is helped by relating the spectral levels and intensities observed under different conditions to a single macroscopic parameter, namely, the dielectric constant $\epsilon(\omega)$ of the material of interest. This parameter serves also to connect the quantum theory of stopping power with the classical one.

It is convenient for this purpose to consider three alternative expressions of ϵ, namely

$$\epsilon(\omega) = 1 + \alpha_l(\omega) \qquad 42a.$$

$$1/\epsilon(\omega) = 1 - \alpha_l(\omega) \qquad 42b.$$

$$\epsilon(\omega) = \frac{1 + \frac{2}{3}\alpha_m(\omega)}{1 - \frac{1}{3}\alpha_m(\omega)}, \qquad \frac{\epsilon(\omega) - 1}{\epsilon(\omega) + 2} = \frac{1}{3}\alpha_m(\omega) \qquad 42c.$$

[15] The symbol Z indicates, in this article, the number of electrons in the system (atom, molecule, aggregate) under consideration. It coincides with the atomic number, its usual meaning, only when the "system" consists of a single atom.

The quantities α on the right-hand side are different types of polarizability which manifestly coincide in the limit $|\epsilon-1| = |\alpha_t| \ll 1$. This limit is realized: (*a*) for a low density gas at all frequencies ω, and (*b*) at very high frequencies for all materials.

In case (*b*), intra-atomic forces are negligible as compared to the electrons' inertia so that the material behaves as a free electron gas, for which

$$\alpha(\omega) = -4\pi e^2 NZ/m\omega^2 = -\omega_p^2/\omega^2 \qquad 43.$$

where NZ is the electron density and ω_p is called the plasma frequency. Note that

$$\hbar\omega_p = (4\pi\hbar^2 e^2 NZ/m)^{1/2} = 29[(\rho)_{g/cm^3} Z/A]^{1/2}\ \text{eV} \qquad 43a.$$

where ρ is the density of the material and Z/A its number of electrons per unit atomic weight. In case (*a*) the polarizability is expressed in terms of the energy levels E_n of single molecules and of the corresponding oscillator strengths by the familiar expansion

$$\alpha(\omega) = \omega_p^2 \Sigma_n \frac{f_n}{E_n^2/\hbar^2 - \omega^2 - i\gamma\omega} \qquad 44.$$

where γ represents a very small damping constant. The essential effects of damping can be treated by considering, instead of Equation 44, its limiting form

$$\lim_{\gamma=0} \alpha(\omega) = \omega_p^2 \Sigma_n \frac{f_n}{E_n^2/\hbar^2 - \omega^2} + i\pi\omega_p^2 \Sigma_n f_n \delta(\omega^2 - E_n^2/\hbar^2) \qquad 44a.$$

In a condensed material, each of $\alpha_t(\omega)$, $\alpha_l(\omega)$, and $\alpha_m(\omega)$ possesses an expansion 44, but with different spectral parameters E_n and f_n, which are observed, as we shall see, under different conditions. The key point for us is that Equations 42a, b, and c establish a link between the different spectra. In particular, the function $\alpha(\omega)$ obtained by entering in Equation 44 the values of f_n defined by Equation 41 and the corresponding levels E_n of low-Q longitudinal excitation has been identified with $\alpha_l(\omega)$ [Fano (43), Sec. 5]. This set of levels and strengths is observed in the spectra of energy losses experienced by fast electrons traversing thin (~500 Å) films of material [see, e.g., Marton et al. (77)]. On the other hand, the f_n and E_n pertaining to the expansion of $\alpha_t(\omega)$ come under direct observation in the study of optical properties of a material, since $\epsilon(\omega) = 1 + \alpha_t(\omega)$ is the square of the refractive index. Finally, the Lorentz-Lorenz formula 42c is relevant to gases and to cubic lattices of molecules; provided the short-range molecular interactions in these materials are not too strong, the spectral characteristics of $\alpha_m(\omega)$ remain close to those of single molecules.

A striking manifestation of the link between the spectra observed in different circumstances is found in metals and semiconductors. The strong optical absorption of these materials in the infrared implies that the expansion of $\alpha_t(\omega)$ involves a continuum of levels with large strengths f_n in this range. It follows then from Equation 44a that the real part of

$\epsilon(\omega)=1+\alpha_t(\omega)$ is large and negative in the visible and near ultraviolet, as shown by metallic reflection. No energy levels E_n of longitudinal excitation, which correspond according to Equation 44a to peaks in the imaginary part of $1/\epsilon(\omega)=1-\alpha_t(\omega)=1-\alpha_t/(1+\alpha_t)$, can then occur in this range. These levels occur instead at higher frequencies where $|\alpha_t|$ has decreased to the point where $\mathrm{Re}(1+\alpha_t)$ vanishes and metallic reflection subsides. A characteristic energy level of intense longitudinal excitation by charged particles traversing a metal is indeed observed near the energy where a metal stops reflecting. This energy may be regarded as one quantum $\hbar\omega_p'$ of free oscillation of the plasma of conduction electrons, where $\omega_p'^2=4\pi e^2NZ'/m$ and NZ' is the density of electrons participating in the infrared optical absorption.

The upward shift of the main level of longitudinal excitation with respect to the levels of optical (transverse) excitation arises from the Coulomb repulsion of electrons over distances of the order of $\hbar/q$. Because of this strong interaction, the excitation involves a very large number of electrons and thus acquires a collective character which has been studied in some detail only for the model of free conduction electrons in metals [Bohm & Pines (22)]. The importance of the upward level shift for the stopping power of metals (where $\ln E_n$ would be $-\infty$ if the levels of the spectrum of α_t were relevant) was first appreciated by Kronig & Korringa (67), Kramers (66), and Bohr (23). A similar shift appears to occur, to a greater or smaller degree, in all condensed materials, but both theory [see, e.g., (1, 43, 44, 92)] and experimental evidence [see e.g. (77, 102)] are still fragmentary. Knowledge of $\epsilon(\omega)$, which embodies all spectral properties of long-wave excitations, throughout the range of interest into the far ultraviolet is quite scarce; and attempts at detailed verification of the consistency of longitudinal and transverse spectra, through Equations 42a and b, are just beginning [LaVilla & Mendlowitz (69)].

Our remaining task in this section is to express the energy loss of charged particles through longitudinal low-Q excitations in terms of $\epsilon(\omega)$. To this end one can multiply the right-hand side of the definition 34 of I by $2\int_0^\infty \omega d\omega\, \delta(\omega^2-E_n^2/\hbar^2)=1$ and rearrange the result by means of Equations 44a and 42b, to yield

$$\ln I=\frac{2}{\pi\omega_p^2}\int_0^\infty \omega d\omega\,\mathrm{Im}\left[\frac{-1}{\epsilon(\omega)}\right]\ln\hbar\omega \qquad 34a.$$

A similar adaptation of Equations 32 and 35 yields

$$N\Sigma_n E_n\int_{Q\min}^{Q_1}(d\sigma_n)_{\text{longit.}}=\frac{2\pi z^2e^4}{mv^2}NZ\Sigma_n f_n\ln\frac{2mv^2Q_1}{E_n^2}$$
$$=\frac{z^2e^2}{\pi v^2}\int_0^\infty \omega d\omega\,\mathrm{Im}\left[\frac{-1}{\epsilon(\omega)}\right]\ln\frac{2mv^2Q_1}{(\hbar\omega)^2} \qquad 45.$$

One also can obtain the same Equation 45 by macroscopic theory, considering the energy and momentum losses experienced by a charged particle as it traverses a medium characterized by $\epsilon(\omega)$ [Fröhlich & Pelzer (49), Hubbard (57)]. Notice, in Equations 34a and 45, that $\mathrm{Im}[-1/\epsilon(\omega)]=\mathrm{Im}[\epsilon(\omega)]/|\epsilon(\omega)|^2$;

thus the difference between the optical spectrum and that of longitudinal excitations is represented by the factor $1/|\epsilon(\omega)|^2$. This factor may be attributed to the dielectric screening of the squared electric field of the incident particle and reduces to 1 in the low density limit.

2.11 *Low-Q transverse excitations in condensed materials.*—The density of a material influences the nature of transverse excitations very substantially and, in particular, changes the trend of the stopping power versus energy curve in the high energy limit. This effect of strong interactions among atoms within the material may be described from different points of view. It was first studied by Fermi (45) and others [and reviewed by Uehling (130)] by treating the material as a macroscopic medium in which the field of an incident particle propagates and dissipates energy. Here we shall continue to utilize an atomistic point of view.

A main difference between longitudinal and transverse excitations lies in the occurrence, for transverse excitations of momentum q, of the energy cq which photons with this momentum have in empty space. Atomic electrons interact by emission and reabsorption of these photons not only with the incident particle but also with one another. This interaction is weak in a gas because of the small number of electrons perturbing each other; the derivation of the perturbation formula 12 may be said to assume that each excited state n of the material contains a small admixture of photon excitation. In condensed matter, perturbation theory no longer suffices to treat the coupling between electrons and photons. Neamtan (90) emphasized that the strength of this coupling is indicated by the departure from unity of the refractive index $n=[\epsilon(\omega)]^{1/2}$ which is proportional to the momentum-energy ratio for a photon.

In the presence of tight coupling, long-wave—i.e., low-q—transverse excitations are represented by superpositions of electronic excitations and of photons with comparable amplitudes. The properties of these excitations are represented in terms of the dielectric constant $\epsilon(\omega)$ of the material [Fano (43)]. Their energy levels $\hbar\omega$ are given by the roots ω of $c^2q^2-\omega^2\epsilon(\omega)=0$. The cross section for excitation of such a level, which corresponds to the second term of the atomic cross section (Eq. 25) multiplied by N, is

$$N\hbar\omega(d\sigma_\omega)_{\text{trans.}} = \frac{z^2e^2}{\pi v^2}\omega d\omega \,\mathrm{Im}\left[\frac{\beta^2\sin^2\psi}{1-\beta^2\epsilon(\omega)\cos^2\psi}\right]\frac{d(\cos^2\psi)}{\cos^2\psi}$$

$$= \frac{z^2e^2}{\pi v^2}\omega d\omega\,\beta^4\frac{\sin^2\psi\,\epsilon_2(\omega)}{[1-\beta^2\epsilon_1(\omega)\cos^2\psi]^2+\beta^4\epsilon_2^2(\omega)\cos^4\psi}d(\cos^2\psi) \qquad 46.$$

where $\epsilon_1=\mathrm{Re}\epsilon$, $\epsilon_2=\mathrm{Im}\epsilon$. Integration over $\cos^2\psi$ yields the analog of the second and third terms on the right-hand side of Equation 32

$$N\hbar\omega(d\sigma_\omega)_{\text{trans.}} = \frac{z^2e^2}{\pi v^2}\omega d\omega\,\mathrm{Im}\left\{\left[\beta^2-\frac{1}{\epsilon(\omega)}\right]\ln\frac{1}{1-\beta^2\epsilon(\omega)}\right\}$$

$$= \frac{z^2e^2}{\pi v^2}\omega d\omega\left\{\frac{\epsilon_2(\omega)}{|\epsilon(\omega)|^2}\ln\left[(1-\beta^2\epsilon_1)^2+\beta^4\epsilon_2^2\right]^{-1/2}\right.$$

$$\left.+\left[\beta^2-\frac{\epsilon_1(\omega)}{|\epsilon(\omega)|^2}\right]\arctan\frac{\beta^2\epsilon_2}{1-\beta^2\epsilon_1}\right\} \qquad 47.$$

In the low density limit ($\epsilon_2 \to 0$, $\epsilon_1 \to 1$), this formula reduces to the corresponding portion of (32).[16]

The logarithmic divergence of Equation 32 for $\beta \to 1$ stems from the fact that emission of a photon by a free incident particle is barely prevented by conservation of energy and momentum when β approaches 1 [Fano (42)]. When proper account is taken of the interaction between photons and atomic electrons, emission of radiation is seen to be possible indeed at frequencies for which $\epsilon_1(\omega) > 1/\beta^2 > 1$, more specifically, according to Equation 46, at $\cos^2 \psi = 1/\beta^2\epsilon(\omega) < 1$. This emission is the Cerenkov radiation which may be described as consisting of "dressed" photons, i.e., of photons accompanied by electron excitation; the coupling reduces the dressed photon's energy from cq to $cq(\epsilon_1)^{1/2}$. The integral over $\cos^2 \psi$ corresponding to this emission is now seen to be finite and to contribute the second term on the right-hand side of Equation 47, where the arctangent approaches π for $\beta^2\epsilon_1(\omega) > 1$.

The total energy loss through low-Q transverse excitations is obtained by integrating Equation 47 over ω from 0 to ∞. The integration succeeds best by complex variable techniques (45, 55, 118) summarized in App. B of (43). Its results are discussed in (130)[17] and have been represented by inserting in the braces of Equation 35 a "density effect correction" $-\delta$,[18] where

$$\delta = \frac{2}{\pi\omega_p^2}\left\{\int_0^\infty \omega d\omega \, \mathrm{Im}\left[\frac{-1}{\epsilon(\omega)}\right] \ln\left(1 + \frac{I^2}{\omega^2}\right) - \frac{\pi}{2} I^2(1-\beta^2)\right\}$$
$$= \Sigma_n f_n \ln\left(1 + \frac{\hbar^2 I^2}{E_n^2}\right) - I^2 \frac{1-\beta^2}{\omega_p^2} \qquad 48.$$

[16] The spectral distribution (Eq. 47) of transverse excitations produced by a charged particle differs from the distribution of excitations produced by incident white light because of different circumstances affecting the momentum transfer in the process.

[17] References (130, 55, 118, and 121) set out to treat simultaneously the effects of atomic interaction on longitudinal and transverse excitations. The oscillator strengths f_i and frequencies ν_i in these references pertain to isolated atoms or molecules; separate frequencies l_i are introduced which correspond to the E_n of the present treatment and are defined by $l_i = (\nu_i^2 + \omega_p^2 f_i)^{1/2}$ [Sternheimer (120)]. This relationship between the spectra of aggregates and of single atoms implies that $\hbar\omega_p f_n^{1/2} \ll |E_{n+1} - E_n|$, an assumption that would be inadequate to treat the spectra of optical electrons in condensed matter per se, but appears adequate for the calculation of δ. In fact, it is regarded as adequate to lump together into a single pair of parameters (f_i, l_i) the oscillator strengths and levels pertaining to the excitation of each atomic shell or subshell.

[18] Since δ modifies the contribution of low-Q transverse excitations in the braces in the middle of Eq. 38, namely $\ln[1/(1-\beta^2)] - \beta^2$, and since δ is in fact comparable to this contribution under all relevant conditions, one might cease treating δ separately as a "correction" and instead consider directly the correct contribution

$$\ln\frac{1}{1-\beta^2} - \beta^2 - \delta = \Sigma_n f_n \ln\frac{I^2}{(E_n^2 + \hbar^2 I^2)(1-\beta^2)} - \beta^2 + I^2\frac{1-\beta^2}{\omega_p^2}$$

This expression clearly reduces to $\ln[1/(1-\beta^2)] - \beta^2$ for $I^2 \ll (E_n, \hbar\omega_p)$ and to $2\ln(I/\hbar\omega_p)$ in the opposite limit $1-\beta^2 \ll 1$, $I^2(1-\beta^2) \to \omega_p^2$.

and l, an imaginary frequency, is the root of

$$1 - \beta^2\epsilon(il) = 0 \qquad 49.$$

that is,

$$\alpha_l(il) = \Sigma_n f_n \frac{\omega_p^2}{E_n^2/\hbar^2 + l^2} = 1 - \beta^2 \qquad 49a.$$

This root does not exist at low energies where $\beta < 1/\epsilon_1(0)$, in which case $\delta = 0$. As β^2 increases above $1/\epsilon_1(0)$ toward 1, l^2 increases from 0 towards infinity and eventually—at extremely high energies—it becomes proportional to $1/(1-\beta^2)$, so that the second term of Equation 47 equals unity and

$$\delta \to \ln \frac{\hbar^2\omega_p^2}{I^2(1-\beta^2)} - 1 \qquad 50.$$

Note that the f_n and E_n in Equations 48 and 49a pertain to the expansion of α_l, that is, are the same as appear in Equation 47. Note also that the density of electrons in the material has a determinant influence on the value of l, since ω_p^2 is proportional to NZ.

The numerical evaluation of l for any given material and value of β may appear difficult, because very little information is available on the function $\epsilon(\omega)$. However, this function behaves simply on the imaginary axis of ω, decreasing monotonically from $\epsilon(0)$ to 1 as shown by Equation 43. Therefore, crude information on the f_n and E_n suffices for an estimate of l. The most detailed studies and calculations of δ have been carried out by Sternheimer (118, 121)[17]; tabulations are described in Section 8.

2.12 *High-Q effects at extreme relativistic energies.*—The density effect removes the low-Q contribution to the $\ln[1/(1-\beta^2)]$ singularity of the stopping power formula 38, that is, one half of this singularity. The remaining part of the singularity, which arises from free recoil collisions with higher and higher Q, requires both reinterpretation and corrections at extremely high energies.

The probability, per unit track length, of collisions that produce recoils with energy in excess of any given large value E_n decreases almost as fast as E_n^{-1} for increasing E_n. Therefore, for sufficiently large E_n, the occurrence of such recoils becomes insignificant as compared to the occurrence of nuclear or bremsstrahlung processes. In other words, at extremely large incident energies, where very large E_n can in principle occur and contribute significantly to the stopping power (mean energy loss), the stopping power itself is no longer a relevant quantity because it is excessively influenced by unlikely extreme fluctuations. A relevant quantity is given in Section 7.1.

At extremely high energies of the incident particle, where condition 7 breaks down, corrections are required by the theory of stopping power. Some of these corrections allow for the failure of small recoil approximations like Equation 8, i.e., for the fact that the incident particle may lose an increas-

ingly large fraction of its energy in a single collision as E approaches and overtakes $(M/m)Mc^2$. Among these corrections is the replacement of the expression 20 of Q_{max} with 20a. Other corrections allow for the interaction between the spin of the incident particle and the atomic electrons. They are introduced as additional terms on the right of Equation 14, terms that depend on the spin and magnetic moment of the incident particle. Results based on simple assumptions on the magnetic moment for spin $\frac{1}{2}$ and 1 are given by Equations 3 and 4 of (130). Comparable results applicable to protons, with their anomalous moment, could be readily obtained but may never have been formulated as they would become important only for $E > 100$ GeV.

2.13 *Failures of the Born approximation and their correction.*—The basic cross-section formula 11 results from a calculation to the lowest non-vanishing order of approximation in the interaction between the incident particle and the atomic electrons. When the incident particle is much faster than the atomic electrons, Equation 16a can also be justified as the result of an impulse approximation, that is, as the product of the exact (Rutherford) cross section for collision with a free electron and of the probability that the electron recoil q yields an excitation of the atomic system to its level E_n. In the opposite limit, when the incident particle is much slower than the atomic electrons, its influence is much weaker than that of the nuclear charge, and the Born perturbation approach is also well justified[19] [see particularly the analysis by Henneberg (56)].

In the intermediate range of velocities, Equation 11 is not on firm foundations. Any error introduced by this equation has presumably been taken into account, together with others (shell corrections), through semiempirical procedures discussed in Section 4. Barkas points out, however (personal communication), that the next-higher-order correction to the Born approximation contributes to the stopping power in proportion to the cube of the incident particle's charge $(ze)^3$. Therefore, this correction is of opposite sign for negative and positive particle pairs, such as $\mu^{\pm}$, $\Sigma^{\pm}$, protons and antiprotons. It could thereby be separated from shell corrections at particle velocities comparable to those of inner electrons but still large enough to prevent the more obvious effect of electron capture by the positive particles. Indeed, evidence has been accumulating of a significant range excess of Σ^- over Σ^+ hyperons generated under comparable conditions. No evidence of comparable accuracy appears to exist for other particle pairs. The theory of this effect remains to be developed.

There are also radiative corrections to the basic theory which result from

[19] This statement applies, of course, only to incident heavy particles, whose motion remains nearly unperturbed, and not to electrons. For electron-atom collisions the Born approximation breaks down altogether unless the incident electron is much faster than the atomic electron.

the multiple virtual emission of photons by the incident particle. Recently, Tsytovich (129) has carried out a calculation of this effect to order e^4 and $e^4\ln^2(e^2)$. He emphasizes that the interaction of the virtual photons with the material magnifies the effect greatly for extremely high particle energy and high density of the material. The relevant condition is that the group velocity of virtual X-ray photons be smaller than the particle velocity. Tsytovich finds that the logarithmic factor in the "$e^4\ln^2(e^2)$" correction can become quite large so that the stopping power is reduced by 5–10 percent for densities $\sim$4 g/cm^3 and energies $E \gtrsim 200\ Mc^2$. Experimental evidence in agreement with this result has been presented [see Sec. 7.1 (93)].

3. The Mean Excitation Energy I

The mean excitation energy I, defined by Equation 34 or 34a (Sec. 2.10), is the main parameter of the stopping power formula 38. Its determination presents considerable difficulty because the most important excitation energies E_n lie in the range of 10 to 1000 eV where the oscillator strengths f_n are poorly known. On the other hand, I represents an average, and, further, only moderate accuracy of I itself is required for the determination of the stopping power, because an uncertainty ΔI causes a relative error on the stopping power approximately equal to $(\Delta I/I)/\ln(2mv^2/I)$, where the logarithm is of the order of 5 in the range of interest.

According to the Thomas-Fermi statistical model, atoms with different atomic numbers Z have spectral distributions of oscillator strengths, f_n versus E_n, with the same shape and differing only by a factor Z in the scale of frequencies ω or energy levels E_n.[20] Therefore, I itself is proportional to Z in the approximation of this model (17). Further considerations (Sec. 3.2) show the ratio I/Z to be approximately 10–15 eV and to be larger at lower than at higher Z. Beyond this fundamental information, provided by theory, the main reliance is placed on experimental data at this time.

The most significant data for this purpose have been obtained with protons of 300–700 MeV [Bakker & Segrè (3), Mather & Segrè (78), Zrelov & Stoletov (143), Barkas & von Friesen (6)], that is, in the energy range where the corrections C/Z and δ in expression 38 are hardly significant. Until very recently, these data appeared to be in disagreement with data obtained (36) from good measurements with 10–20 MeV protons. However, the values of the stopping power in medium and heavy elements at these lower energies are affected by substantial shell corrections. It has become progressively clear since 1958 [Brandt, Lindhard (85)] that these corrections had been underestimated (see Sec. 4) and that experimental results at the higher and lower energies are in fact consistent.

Table I presents a set of current estimates of I and of the ratio I/Z for

[20] Bloch (17) formulated the equation that governs this distribution, but the equation has apparently never been solved.

TABLE I

CURRENT ESTIMATES OF I[a]

	Substance	Z	I(eV)	I/Z	Reference (generally only latest published values cited)
	atomic	1	15.0 (theor.)	15.0	(32)
H	molecular		19 (theor.)	19	(96)
			18.3±2.6		(76)
	in compounds		15–18		(128)
He		2	42±3	21	(31)
			41.8 (theor.)		(82)
Li		3	40, 38	13	(23, 3)
			45, 38.8 (theor.)		(23, 37)
Be		4	64		(35)
			60, 66 (theor.)	16	(23, 37)
C	graphite	6	81	13.5	(128)
	in compounds		77–80		(128)
N	molecular	7	88	12.6	(128)
	in compounds		79–102		(128)
O	molecular	8	101		(128)
	in compounds		91–101	12.6	(128)
Al		13	163	12.6	(13)
Ar		18	190	10.6	(31, 76)
Fe		26	273	10.5	(143)
Cu		29	315	10.9	(143, 6)
Kr		36	360	10.0	(14)
Ag		47	471[b]	10.0	
Au		79	761[b]	9.6	
Pb		82	788[b]	9.6	(6)
U		92	872[b]	9.5	(6)
Emulsion		—	323	—	(6)
Air		—	85	—	(89)
CH_4		—	45	—	(31)

[a] In some cases values have been renormalized to $I_{Al}=163$ eV or $I_{Cu}=315$ eV.

[b] These values have been lowered to take into account the fact that shell corrections, as represented by C/Z in Equation 38, do not vanish at $v\to c$ (cf. Sec. 4.4). In the case of Pb, for example, the nonvanishing cf C/Z is equivalent to a lowering of I by approximately 32 eV; in the case of Ag, 7 eV.

a number of elements.[21] Interpolation in Z should be dependable to a few per cent of the value of I in the range $Z>20$ in which the great majority of atomic electrons belongs to closed shells, because the properties of closed

[21] In previous literature, I was determined by fitting Eq. 38 to stopping power data at high energy with the assumption that the shell correction C/Z vanishes in

shells are smooth functions of Z. Notice that I/Z decreases fairly regularly as Z increases, except for low Z. The high values of I/Z at low Z can be attributed to the "extra-stiffness" that results from the tighter binding of valence electrons as compared to the prediction of the Thomas-Fermi model. A slow decrease of I/Z throughout the periodic system results from exchange effects, which also stiffen the atoms but matter less and less as Z increases and the repulsion and exchange among inner shell electrons fade out as compared to nuclear attraction. A modified Thomas-Fermi treatment that includes exchange effects [Jensen (58), Brandt (29, 85)] leads to $I/Z = a + bZ^{-2/3}$ where a and b are constants, difficult to estimate dependably.

The information in Table I and in the preceding paragraph is incomplete and tentative in many respects. A more complete survey may be found in *NBS Handbook 79* (89). Even though the accuracy on the value of I for heavy metals now attains a few percent, the same cannot be said for other materials. For example, the same value $I = 190$ eV has been found for argon in two good experiments (31, 76), but its error range is stated to be ± 17 eV; on the other hand, interpolation on I/Z between aluminum and copper leads one to expect $I \sim 216$ eV for argon. A "low" value reported for neon (89) has been found to be erroneous (87). Thus one should not conclude that the I/Z values for the noble gases are systematically lower than for metals, and that this outer shell effect is felt very strongly for Z as high as 18 and appreciably for $Z = 36$ (Kr); note that one might have predicted the opposite effect on the basis of outer shell binding energies. This and other uncertainties make additional experimentation, particularly with Thompson's arrangement (128), desirable, especially now that the connection between measurements at high and low energies has been clarified.

3.1 *Chemical combination and aggregation effects.*—A material containing a density N_i of various elements of atomic number Z_i can be treated in first approximation, according to Bragg's additivity rule, as a combination of atoms which contribute separately to its stopping power. Equation 38 is then adapted to this material by setting in it

$$NZ = \Sigma_i N_i Z_i, \qquad NZ \ln I = \Sigma_i N_i Z_i \ln I_i \tag{51.}$$

An effective value of I is thereby defined for the material as a logarithmic average over the I_i for its constituent atoms, in keeping with Equation 34.

This approach proves remarkably accurate even though it disregards

---

the high energy limit. The data of Table I take into account that C/Z does not vanish in this limit because it depends on the velocity ratio of the atomic electrons and the incident particle. This ratio remains larger than zero and is not always very small because the incident particle's velocity does not exceed c. The difference between these points of view is barely significant at the current level of accuracy, because C/Z modifies the stopping power by less than 1 percent at high energies and I by a few percent at most (see Sec. 4, Eqs. 58 and 59).

chemical bonds and other aggregation properties of the material, which modify the stopping power through changes of the spectrum of excited levels E_n and through the density effect (Secs. 2.10 and 2.11). Several circumstances contribute to this accuracy, namely:

(*a*) Chemical bonds and other aggregation properties influence almost exclusively the contribution of valence electrons to the stopping power,[22] whereas this contribution constitutes a small fraction of the total for all but the lightest elements. Experimentally, an influence of chemical structure on stopping power, of the order of 1 percent, has been clearly demonstrated by Thompson (128) for light elements traversed by high energy protons.

(*b*) Valence electrons with particularly low binding in an isolated atom, which give a small contribution to the atomic I_i, are generally very active chemically and tend to form compounds with strong heteropolar bonds and higher contribution to I_i. Thus chemical binding in the common and stable substances tends to smooth out the variations of spectral levels and oscillator strengths of valence electrons along the periodic system. The effective I of a compound tends to be a smooth function of the logarithmically averaged Z of its constituent elements. Therefore application of Equation 51 with interpolated values of I_i (rather than realistic values applicable to isolated atoms) may yield a rather realistic value for the effective I.

(*c*) The electric interaction between distant particles in condensed matter, discussed in Section 2.10, also raises the spectral levels E_n of valence electrons just in those substances, like metals, where E_n would otherwise be particularly low. Here again aggregation has the effect of smoothing out the variations of f_n and E_n for valence electrons as functions of Z_i.

Some systematic effects of the chemical state of aggregation are nevertheless present. The presence of unsaturated bonds, which possess low-lying excitation levels, reduces I as shown by Thompson's comparison of the stopping powers of aromatic and aliphatic hydrocarbons (128). Alkali metals, with a single valence electron and low density, have a particularly low I inasmuch as the main E_n of the valence electrons lies at 5.3 eV for sodium as compared to 15 eV for aluminum.

An important example of a complex physicochemical system is photographic emulsion, where the track length of particles serves as a measure of their energies. Range-energy relations and other track properties in emulsions have been studied by many authors (130, p. 338), particularly in recent years by Barkas and his co-workers (4). The value of I determined by fitting the stopping power formula 38 to the observed range in Ilford G 5 emulsion has been reported to be 328 eV (6), whereas the corresponding value calculated by entering in expression 51 the known composition of this

[22] Inner shell electrons contribute very little to the zero-frequency dielectric constant, and their contribution to the density effect can accordingly be ignored except at extreme relativistic energies of incidence, as shown by Eqs. 49a and 48.

emulsion[23] and the values of I_i for the individual elements from Table I is 300 eV (4). It is not clear how this discrepancy should be solved.

3.2 *Calculations of* I.—Direct calculation of I has been carried out thus far only for a few light substances after sufficient information had been gathered on their spectral distribution of oscillator strengths f_n. The results are: H (atomic), 15.0 eV (10, 32); H_2 (gas), 19 eV (96, 100); He, 41.8 eV (82) or 41.5 eV (38); CH_4 (gas), 42.8 (100). Crude, but perhaps adequate, estimates of f for numerous substances might be feasible at this time; additional experimental and theoretical information on this subject will probably come forth in the next several years.

An interpolation method which relates I to other properties of the electronic ground state of atomic systems has been proposed by Dalgarno (37). The mean values $\langle E^r \rangle = \Sigma_n f_n E_n^r$ for various integers r between -8 and 2 can be obtained from observable optical properties or calculated from ground-state wave functions. If r is now regarded as a continuous variable, we have, owing to Equation 34,

$$\ln I = [d\langle E^r \rangle / dr]_{r=0} \qquad 52.$$

Applications of this procedure (37) yield $I = 14.8$ eV for H, 41.7 for He, 38.8 for Li, and 66.1 for Be.

Attempts at estimating the spectral properties of valence electrons from experimental polarizability data [Westermark (136), Brandt (28, 30)] appear unpromising inasmuch as they imply an estimation of the slope at $r=0$ in Equation 52 from a knowledge of only the two ordinates at $r=-2$ (polarizability) and at $r=0$ (sum rule 33).

Lindhard & Scharff (72) introduced an approach that emphasizes the approximate correspondence between the excitation levels E_n and the various atomic shells. They associate a characteristic frequency to each volume element of the atom, which depends on the local electron density as the plasma frequency does in a free-electron gas. Thereby a functional correspondence is established between the optical absorption spectrum $f(\omega)$ of an atom or molecule and the density distribution $\rho(r)$ of its electrons, with $\omega = [\chi 4\pi e^2 \rho(r)/m]^{1/2}$ and χ a proportionality constant of the order of 1 or 2. Information on the density $\rho(r)$ derived from Hartree-model calculations or from other models can then be utilized to calculate, in accordance with Equation 34, $\ln I = Z^{-1} \int d\tau \, \rho(r) \ln[\hbar\omega(r)]$. Results of remarkable accuracy are obtained. Brandt (30) has exploited this approach further. The tentative nature of the initial assumptions should, however, be borne in mind when dealing with detailed applications of the Lindhard-Scharff procedure.

Systematic studies of the small departures from Bragg's rule (Eq. 51) for different chemical combinations of elements would be interesting, but the

[23] In units of 10^{20} atoms/cm^3: $N_{Ag} = 101.01$, $N_{Br} = 100.41$, $N_I = 0.565$, $N_C = 138.30$, $N_N = 31.68$, $N_S = 1.353$, $N_H = 321.56$, $N_O = 94.97$.

Thompson experimental results (128) do not provide adequate guidance. An effort to extend Thompson's work would also be of interest as a problem of chemical physics. Brandt's extensive efforts in this direction (28, 30) rest on uncertain assumptions as indicated above.

4. Inner Shell Corrections

The stopping power theory, as presented in Section 2, rests on the assumption that the speed of the incident particle is much higher than that of the atomic electrons in their normal bound states. In fact, this approximation is often poor. Significant corrections are required at all energies in heavy elements, and substantial departures from the results of Section 2 occur in all but the lightest elements for protons below 100 MeV. As the velocity of the incident particle decreases, the full line in Figure 2, which limits the range of integration, moves up and leftward so as to wipe out the "empty crescent," which characterizes the all-important intermediate-Q range of approximation.

Even before this approximation breaks down altogether, corrections are required to carry the low-Q approximation of Section 2.5 beyond the first significant term and to improve the high-Q approximation of Section 2.7 in the range of $Q \sim Q_{max}$. Notice that the cutoff of the integration in Equation 37 at $Q = Q_{max}$ excludes incorrectly the region of integration indicated with horizontal hatching in Figure 3 and includes spuriously the region with vertical hatching. These two errors compensate each other to a large extent but their net effect vanishes only in the limit considered in Section 2.7, where the shaded area becomes infinitely narrow.

An example of directly observable collisions with E_n and Q larger than Q_{max} is afforded by the ejection of K electrons of medium and heavy elements by protons of a few MeV [Merzbacher & Lewis (80)]. For example, the cross section for ejection of K electrons in nickel by protons has a peak value of approximately 10^{-21} cm^2 near 20 MeV, at which energy Q_{max} is 5 times the minimum E_n for this process; a 10-fold reduction in proton energy, which brings Q_{max} well below the minimum E_n, reduces the cross section by only a factor of 10. [At still lower energies the cross section should eventually decrease as E^5 according to Henneberg's theory (56), but departures from this law have been observed by Messelt (81).]

As mentioned in Section 2.8, the departures from the results of that section due to insufficient velocity of the incident particle are represented by the corrective term C/Z in Equation 38.[24] Partial success has been obtained in estimating this term by a variety of empirical and theoretical approaches. Among the factors that influence the value of C/Z we shall not consider any

[24] Roughly speaking, one may say that the electrons of the inner shells, K, L, . . . cease to contribute to the stopping power in succession as the incident particle's velocity decreases. However, the cutoff of each shell is gradual.

effects of relativity on the motion of the atomic electrons or of the incident particle or any inaccuracies in the treatment of the effects of the transverse interaction. Thus, in the theoretical approach we shall regard C/Z as defined[25] in terms of the function

$$L(v, Z) = \ln \frac{2mv^2}{I} - \frac{C}{Z} = \tfrac{1}{2}\Sigma_n E_n \int_{E_n^2/2mv^2}^{\infty} |F_n(q)|^2 \frac{dQ}{Q^2} \qquad 53.$$

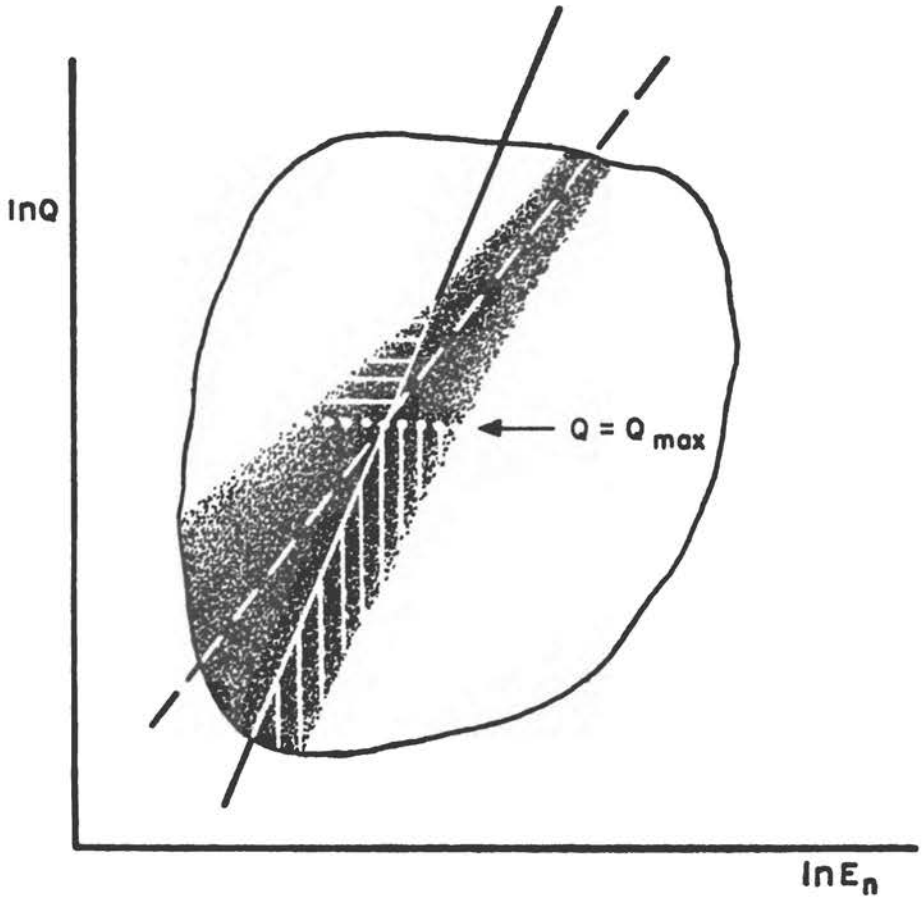

FIG. 3. Detail of Fig. 2 showing the region around Q_{max} for moderate velocity of incidence.

However, in the empirical approaches L or C/Z will be chosen by fitting Equation 38 to experimental results, i.e., by setting

$$L(v, Z) = \ln \frac{2mv^2}{I} - \frac{C}{Z} = \frac{mv^2}{4\pi z^2 e^4 NZ}\left(-\frac{dE}{ds}\right)_{exper.} - \ln \frac{1}{1-\beta^2} + \beta^2 + \tfrac{1}{2}\delta \qquad 53a.$$

[25] The correction C/Z is defined here as an average over the contributions of the several shells, with $C = C_K + C_L + \cdots$, where C_K, C_L are commonly used in the literature (130, 134). This interconnection requires the factor $\frac{1}{2}$ to appear on the right-hand side of 53.

regardless of the physical significance that is thereby attributed to L.[36]

The theoretical *nonrelativistic* definition of C/Z implied by Equation 53 can be cast into a form convenient for further analysis [Walske (134)]. To this end, we introduce the symbol $f_n(Q) = E_n |F_n(q)|^2/Q$—such that $f_n(0)$ coincides with the optical oscillator strength f_n—and recall the following facts from Section 2: (*a*) Equation 27 implies $\Sigma_n f_n(Q) = 1$ irrespective of Q; (*b*) $\ln(2mv^2/I)$ represents in effect $\frac{1}{2}\Sigma_n \int_{I^2/2mv^2}^{2mv^2} f_n(Q)dQ/Q$; (*c*) the integral $\Sigma_n \int_0^{I^2/2mv^2} [f_n(Q) - f_n(0)]dQ/Q$ vanishes because of (*a*) above; (*d*) the definition of I, Equation 34, is such that

$$\Sigma_n \int_{E_n^2/2mv^2}^{I^2/2mv^2} f_n(0)dQ/dQ = 0.$$

Thereby, Equation 53 is seen to be equivalent to

$$\frac{C}{Z} = \tfrac{1}{2}\Sigma_n \int_0^{E_n^2/2mv^2} [f_n(Q) - f_n(0)] \frac{dQ}{Q} - \int_{2mv^2}^{\infty} f_n(Q) \frac{dQ}{Q} \qquad 53b.$$

This expression has been evaluated numerically for atomic H by Walske (134)†; the result is shown in Figure 4 for purposes of orientation. The scale of abscissas, $\ln x = \ln(v/v_0)^2$, where $v_0 = c/137$ is the root mean square velocity of the electron in H, has been chosen so that the curve approaches the straight line

$$y = \ln(2mv^2/I) = \ln x + 1.29 \qquad 54.$$

at large x, where C/Z becomes negligible. Notice that the curve fails to depart much from the straight line except at excessively low energies even though the conditions that would lead to Equation 38 with $C/Z = 0$ fail completely at $x < 1$. For this reason C/Z is called a "correction" even though its definition by means of expression 53 abandons the method of Section 2.5–2.8 altogether. The initial drop of $L(v, Z = 1)$ below the straight line Equation 54, as v decreases, indicates reduced ability of the incident particle to excite the atomic electron; the tail of the curve toward low v indicates that some ability persists even after v has fallen below v_0.

[36] In setting up Eq. 38 one has dumped, by implication, into C/Z the influence of all inaccuracies of the theory of Sec. 2, because the other corrective term δ is fully defined by Eq. 48. To proceed consistently with the spirit of note 12, one should define C/Z firmly by means of Eq. 53 and insert a new corrective term $\mathfrak{C}$ in Eq. 38 to represent all other effects. This procedure appears premature because we have no adequate basis at present for estimating C and $\mathfrak{C}$ separately. (See, however, the comment in Sec. 2.13 on the stopping power for particles of negative charge.)

† However, the coefficient 19/6 in Equation 11, p. 1287 of *Phys. Rev.*, 88 (1952) is incorrect; its value is 25/6, namely, the same as that of the corresponding coefficient in the companion Equation 13.

4.1 *Calculations with hydrogenic wave functions.*—Because the innermost electrons are fastest, they might be expected to have a dominant influence on C/Z at higher energies of the incident particle.[27] Because their motion is controlled primarily by the nuclear attraction, their contribution to $L(v, Z)$

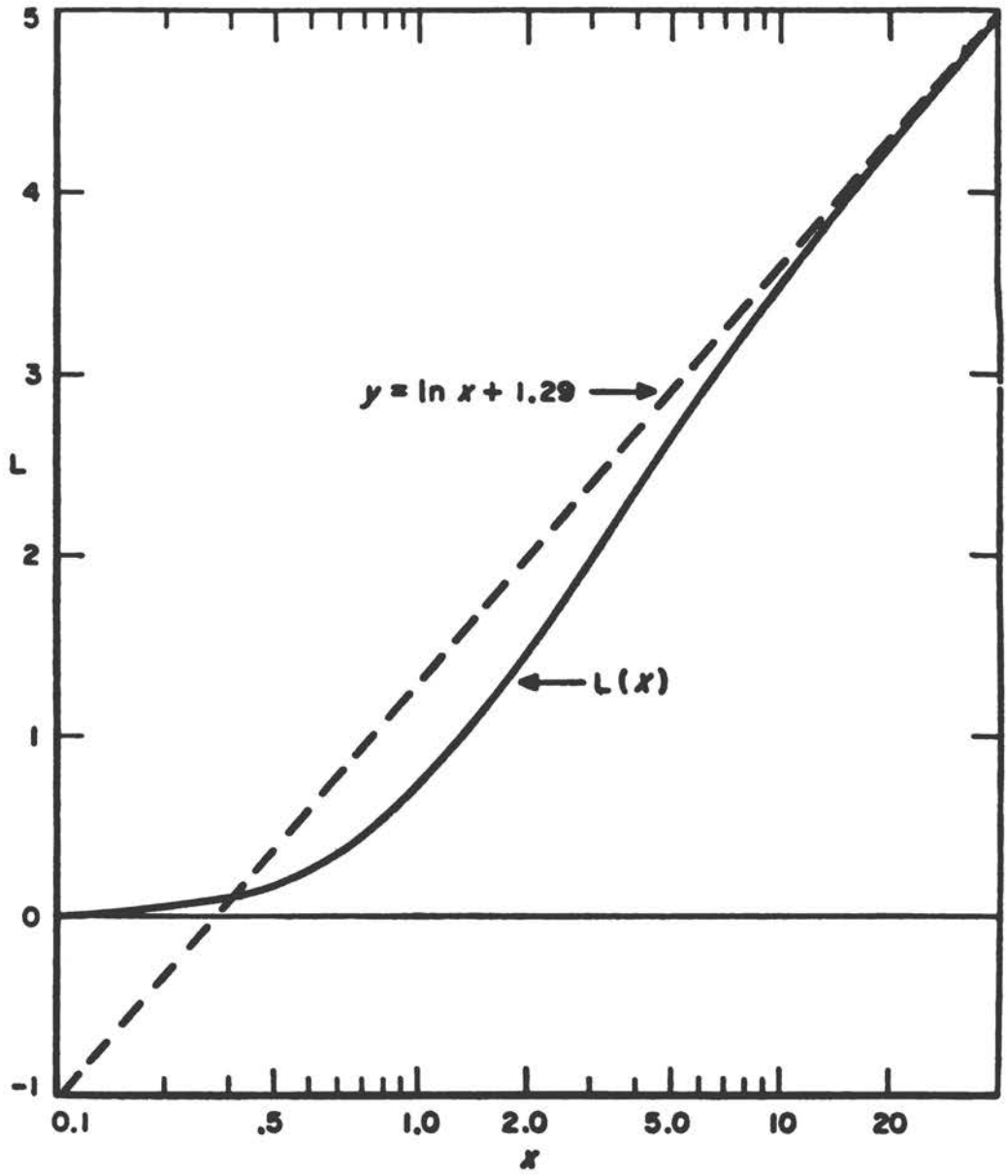

FIG. 4. L for atomic hydrogen as a function of $x = v^2/v_0^2 = E_{keV}/25$. (Courtesy J. E. Turner.)

may be calculated rather accurately by evaluating $F_n(q)$ with hydrogenic wave functions, with screening adjustments that make them applicable to all elements. Laborious calculations by this method have been carried out for K and L electrons (73, 134). Their results have been reviewed by Uehling

[27] This expectation is not really borne out, as shown in Sec. 4.4 below.

(130). These and analogous calculations account approximately for the probability of ejection of K and L electrons by protons of a few MeV (80, 81). Extension of this method to M electrons has been regarded as prohibitively laborious. On the other hand, M electrons are now known to contribute greatly to C/Z below 100 MeV in most materials (see Fig. 6).

4.2 *The statistical model.*—As noted in Section 3, the ratio I/Z should be the same for all atoms according to the Thomas-Fermi model. It may, then, be convenient to represent $\ln(2mv^2/I)$ in Equation 53 as $\ln(v^2/Zv_0^2)$ $+\ln(2mv_0^2Z/I)$, where $\ln(2mv_0^2Z/I)\sim 1.7$ is roughly equal for all materials and $v^2/v_0^2Z=x$ is the same as x in Equation 54 for $Z=1$. It was argued by Lindhard & Scharff (72) that the whole right-hand side of Equation 53 should depend on v and Z only in the combination v^2/Z, within the accuracy of the Thomas-Fermi model.[28] Accordingly, $L(v, Z)$ should be represented by a single curve for all elements when plotted against x as in Figure 4. In fact, Reference (72) defines L as $L(x)$.

Figure 5 shows that experimental estimates of L for different elements fall within a single strip when plotted against x, so that this type of plot proves useful. On the other hand, one cannot draw a single line that represents all results within much better than 10 percent. No better fit should have been expected in view of the variations of I/Z noted in Section 3.

By the procedure indicated on p. 28, Lindhard & Scharff (72) obtained an approximate theoretical evaluation of the entire curve $L(x)$. Their result has the same trend as the bundle of curves in Figure 5. In particular, for $x<5$, a good agreement was found between experimental results and the theoretical expression $L(x)=1.36x^{1/2}$.

4.3 *Extended application of hydrogenic calculations.*—In view of the difficulty of extending the calculations of Section 4.1 to the M and higher shells, Bichsel (14) has assumed that C_M, namely, the contribution of M electrons to C, depends on the particle's velocity in the same way as the C_L contribution calculated by Walske (134),[29] except for the scale factors. The same assumption was made for further shells. The scale factors were then determined, separately for the various M, $N\cdots$ subshells, by simultaneous least square fitting of Equation 38 to a large number of experimental stopping power and range data on each of various elements. The results appear reasonable in that, after the fitting, the contribution of each subshell is found to depend primarily on the ratio of the particle velocity to the root mean square velocity of the electrons in that subshell.

[28] More specifically, it is argued on p. 8 of (72) that $L(v, Z)$ should depend only on the ratio of $Q_{max}=2mv^2$ to the characteristic frequencies of the Thomas-Fermi atom which are proportional to Z. Notice, however, that L might also depend on the ratio of Q_{max} to the mean kinetic energy $\langle K\rangle_0$, which determines the width of the shaded strip in Fig. 2 and which is proportional to $Z^{4/3}$. An indication of relevance of $v^2/Z^{4/3}$ appears in Sec. 4.4.

[29] Notice, however, that the plots of the K- and L-shell contributions differ in shape somewhat.

The numerical work required by this approach is rather extensive in view of the limited accuracy and dependability of the data and procedures that are involved and tends to obscure the link between input and output. Nevertheless, this method has proved valuable for the purposes of correlating a large mass of data and of producing extensive numerical tables of stopping power (see Secs. 4.5 and 8).

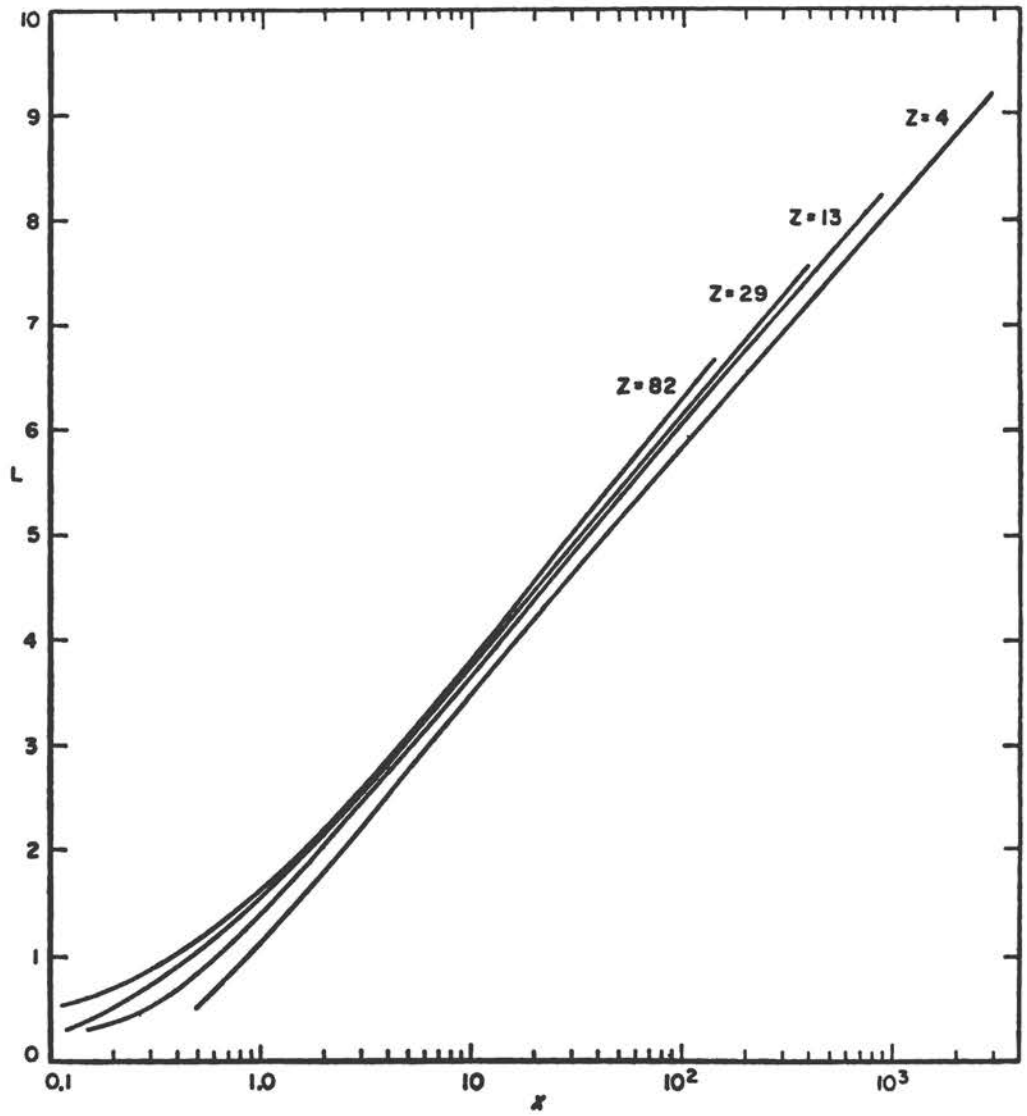

FIG. 5. L for various metals as a function of $x = v^2/v_0^2 Z$. (Courtesy J. E. Turner.)

4.4 *Expansion in powers of* $1/v^2$. Because the shell correction vanishes in the limit where the incident particle is infinitely faster than the atomic electrons, its behavior near this limit is studied appropriately by expanding the expression 53b into inverse powers of the incident particle's velocity. This study was initiated by Brown (32) and developed by Walske (134) for

atomic H and hydrogenlike atomic electrons and is being extended to other atoms by Fano & Turner (87). Analogous results on the stopping power of an electron gas emerge from recent work by Lindhard & Winther.* The significance of these developments remains limited by their nonrelativistic character.

Walske (134) pointed out that the Σ_n in the expression 53b is conveniently split into two parts corresponding, respectively, to energy transfers smaller and larger than $\sim mv^2$, the exact point of separation being irrelevant for calculations to order $(1/v^2)^2$. The values of the two partial sums will be called C_1 and C_2, respectively. The contribution to C_1 of the second integral in 53b arises from the region of Figure 2 with $Q > 2mv^2$, $E_n < mv^2$, which is unshaded; in fact this contribution is of order $(1/v^2)^5$ and will be disregarded here. The contribution to C_2 of the term with $f_n(0)$ consists only of canceling that of the term with $f_n(Q)$ at low Q and can be disregarded, to order $(1/v^2)^2$, if the integrations over Q are simultaneously limited to the range $mv^2 \lesssim Q \lesssim 4mv^2$ in the calculation of C_2.

To calculate C_1, one expands the remaining integrand[30]

$$f_n(Q) - f_n(0) = \Sigma_{r=1} \frac{1}{r!} \left(\frac{d^r f_n}{dQ^r}\right)_{Q=0} Q^r \qquad 55.$$

and then integrates over Q term by term. This yields

$$\frac{C_1}{Z} = \tfrac{1}{2}\Sigma_n^{(1)} \Sigma_{r=1} \frac{1}{r!r} \left(\frac{d^r f_n}{dQ^r}\right)_{Q=0} \left(\frac{E_n^2}{2mv^2}\right)^r \qquad 56.$$

The operations $\Sigma_n^{(1)}$ and $\Sigma_r (d^r/dQ^r)_{Q=0}$ can now be carried out in reverse order, so that C_1 is expressed in terms of the sums over states

$$\Sigma_n^{(1)} E_n^{2r} f_n(Q) = \Sigma_n^{(1)} E_n^{2r+1} \left| F_n(q) \right|^2 / Q \qquad 57.$$

Expressions such as 57 are evaluated by closure when the sum extends over a complete set of states. Thereby one obtains sum rules which express the sum in terms of the mean values of certain physical quantities (e.g., the electron kinetic energy) over the ground state of the atom.[31] In the present application $\Sigma_n^{(1)}$ excludes the states of highest excitation energy. This exclusion is of no consequence for $r = 1$ or 2, because in this case the states of highest excitation would contribute negligibly to $[(d/dQ)^r \Sigma_n E_n^{2r} f_n(Q)]_{Q=0}$; we replace then $\Sigma_n^{(1)}$ with Σ_n for $r = 1, 2$. For $r > 2$, the states of highest excitation contribute so heavily that the Σ_n would diverge whereas $\Sigma_n^{(1)}$ is finite; therefore, sum rules cannot be utilized to calculate $\Sigma_n^{(1)}$.

* Thanks are due to Prof. J. Lindhard for information on his unpublished work and for calling the author's attention to certain essential points.

[30] This expansion need not cause concern in itself, because F_n depends on q through an exponential whose convergence is assured.

[31] This procedure is similar to that used by Placzek (95) on neutron scattering.

Since, on the other hand, the separation of the contributions C_1 and C_2 is of practical relevance only up to expansion terms of order $(1/v^2)^2$, we limit the present treatment to the order of approximation $r \leq 2$ and set

$$\frac{C_1}{Z} \sim \frac{K_1}{2mv^2} + \frac{K_2}{(2mv^2)^2} \tag{58.}$$

where the coefficients are found, by sum rules, to be

$$K_1 = m\langle v^2 \rangle_0 + \text{correlation terms} \tag{58a.}$$

$$K_2 = m^2\langle v^4 \rangle_0 + \frac{10\pi}{3}\frac{\hbar^2 e^2}{m}\langle \rho(0) \rangle_0 + \text{correlation terms} \tag{58b.}$$

In these formulas $\langle v^2 \rangle_0$ and $\langle v^4 \rangle_0$ are the mean squared and mean fourth-power velocity of an atomic electron in the ground state of the atom, averaged over all electron shells, and $\langle \rho(0) \rangle_0$ is the mean electron density at the center of the atom. The "correlation terms," which depend on statistical pair-correlations of electrons, would vanish in the Hartree model and presumably yield a correction smaller than 10 percent; these terms will be disregarded here and treated further in (87).

Utilizing a current estimate (52) of the total binding energy of electrons (which is related to their kinetic energy by the virial theorem), we find

$$\frac{K_1}{2mv^2} \sim \frac{mv_0^2 Z^{1.4}}{2mv^2} = \frac{Z^{0.4}}{2x} \tag{59a.}$$

The Thomas-Fermi model yields $Z^{1/3}$ instead of $Z^{0.4}$ on the right-hand side of 59a.[28] In an independent electron approximation one can assess the contribution of the various inner shells to K_1, and one finds them approximately equal.[28] With regard to K_2, to which K electrons contribute most, $\langle v^4 \rangle_0$ and $\langle \rho(0) \rangle_0$ have been estimated crudely by hydrogenic nonrelativistic wave functions. This yields

$$\frac{K_2}{(2mv^2)^2} \sim \frac{bZ^3(2mv_0^2)^2}{(2mv^2)^2} + \frac{10\pi}{3}\frac{\hbar^2 e^2}{m(2mv^2)^2}\frac{Z^3}{\pi a^3}2.4 \sim \frac{b + 2.0}{x^2}Z \tag{59b.}$$

where b is a number of the order of 2 or 3 which increases slowly with Z. This result indicates that the second term of Equation 58 amounts to about 1/2 of the first one for protons of 700 MeV in uranium, and that this ratio is far smaller for lighter elements. On the other hand, the second term's importance increases rapidly as the proton energy decreases.

With regard to the evaluation of C_2/Z, the following situation exists at this time. Walske's calculation of C_2/Z for atomic H in its ground state, to

[28] If unscreened hydrogenic wave functions were used, the $\langle v^2 \rangle$ of each electron would be proportional to the inverse square of its principal quantum number, n^{-2}, a factor which is exactly balanced by the existence of $2n^2$ electrons in a complete shell. Screening makes the binding energy of successive shells decrease faster than n^{-2}, but it also makes $\langle mv^2/2 \rangle$ larger than the binding energy, in accordance with the modification of the virial theorem for a nonhydrogenic field; these two effects of screening cancel out approximately.

order $(1/v^2)^2$, yields exactly the same result as the corresponding calculation of C_1/Z (corrected as indicated in note† on p. 31); the same holds for his calculation of C_2/Z for atomic H in its $n=2$ state, which was carried out to order $1/v^2$ only (134). The same result, $C_2=C_1$ to order $(1/v^2)^2$, is again reported by Lindhard and Winther* for an electron gas. The discovery of this result for quite different systems suggests that it may have general validity. Accordingly, despite the absence of conclusive evidence on this point we proceed, in Section 4.5, on the *assumption* that $C_1=C_2$, i.e.,

$$\frac{C}{Z}\sim 2\left[\frac{K_1}{2mv^2}+\frac{K_2}{(2mv^2)^2}\right] \qquad \text{to order } \left(\frac{1}{v^2}\right)^2 \qquad 58c.$$

Notice that Equation 58 constitutes an expansion in inverse powers of the particle velocity rather than of its energy. Therefore, in the high energy limit, the shell correction C/Z approaches a nonzero value, corresponding to $v=c$, rather than zero. This result is implicit in the fact that Equation 53 depends on $v=dE/dp$ rather than on E, and is also borne out by the hydrogenic calculations (134).

4.5 *Summary of evidence.*—The experimental and theoretical evidence on shell corrections is represented conveniently either by a plot, analogous to Fig. 4, of $L(v, Z)$ versus $\ln x=\ln(v^2/v_0^2Z)$ (Fig. 5) or by plotting the departure of L from a straight line, namely, $C/Z=\ln x-L(v, Z)+\ln(2mv_0^2Z/I)$, also against $\ln x$ (Fig. 6). The "experimental" values of L are, of course, obtained from Equation 53a.

Figure 5 shows that L has for all elements the same general shape as that shown for atomic hydrogen in Figure 4, but departs from a straight line even less than in the case of hydrogen. The decrease in value of I/Z with increasing Z is reflected in the fact that the L curves lie above one another in order of increasing Z for large x, where C/Z becomes negligible. (Exceptions to this rule are expected for low-Z elements.) As x decreases, C/Z increases at first for all elements, as shown by Equations 58 and 59, but more rapidly for higher-Z ones, so that the L curves tend to draw nearer to one another. Figure 6 shows the same data in the more traditional form of shell correction curves. The sum of the theoretical K- and L-shell contributions for copper and lead, according to Walske (134), is indicated for purposes of orientation.

Because the curves for different elements do not lie far apart from one another and presumably do vary smoothly with Z for $Z>10$, it appears possible to estimate from Figure 5 or, better, from Figure 6 the value of L for each v and Z to within a very few percent.

Figures 5 and 6 may be described as an extract of experimental evidence on proton stopping power obtained by Bichsel (14) (see Sec. 4c) and by Whaling (137) at very low energies. If available results of individual measurements of stopping power for different elements were entered as points in the

* Thanks are due Professor J. Lindhard for information on his unpublished work and for calling the author's attention to certain essential points.

graphs, as in Figure 1 of (72), they would disperse over the region traversed by the curves and exhibit to visual inspection little systematic trend as functions of the atomic number. Each curve in the figures results, instead, from prior smoothing and interpolation of the data for one element. The elements chosen belong to a set of metals which have been studied extensively and whose atomic numbers span almost the whole periodic system.

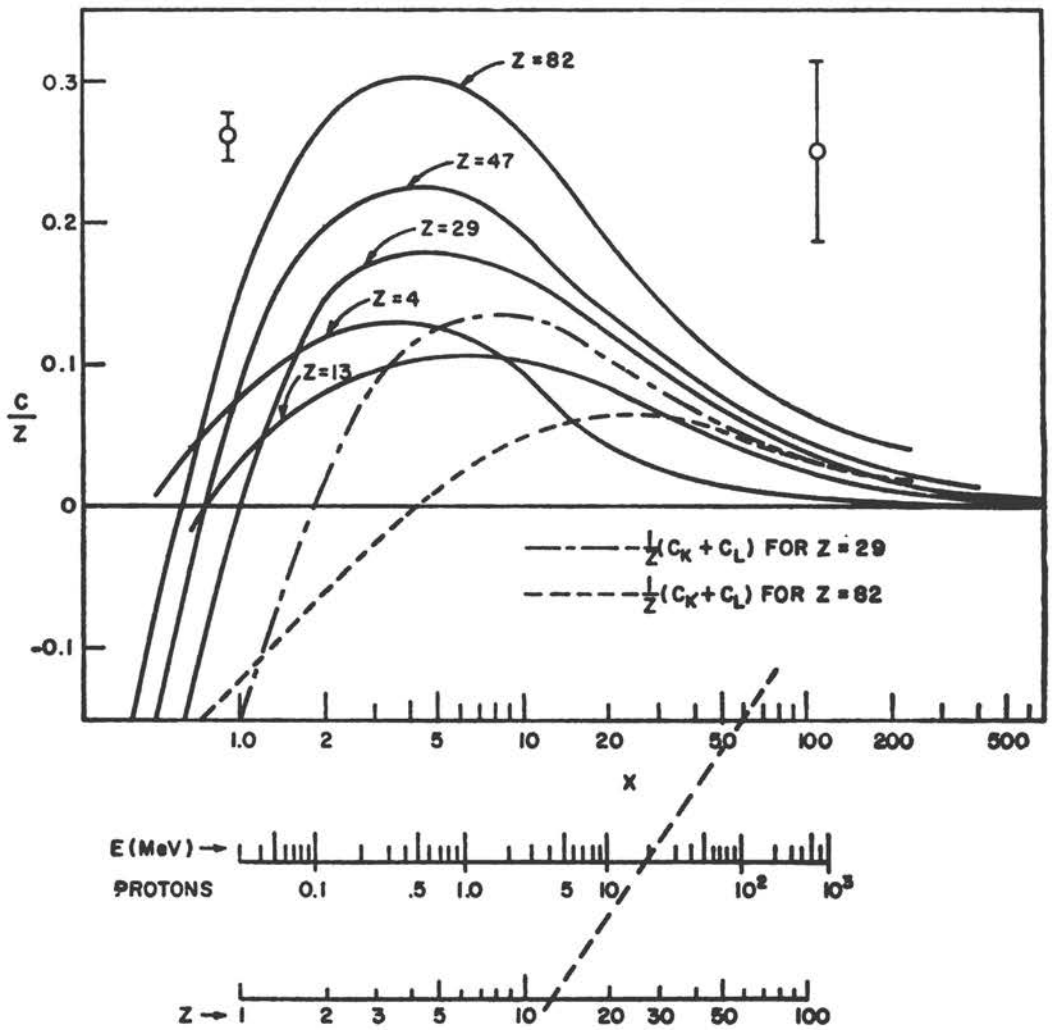

FIG. 6. C/Z for various metals as a function of $x = v^2/v_0^2 Z$. The error bars represent the approximate effect of 1 per cent error in the stopping power at the respective abscissas for all elements. The example of nomogram use shows that $x = 59$ for 20 MeV protons in aluminum. (Courtesy J. E. Turner.)

More specifically, the curves have been drawn through points taken from Bichsel's and Whaling's stopping power tables. Bichsel's tables, in turn, were obtained from a form of Equation 38 in which C/Z is represented as a specified function of the particle energy and of a number of free parameters.

These parameters, as well as the excitation energy I, were then adjusted to attain a best fit of Equations 38 and 39 to a large selection of stopping power and range data pertaining to each element under consideration. Bichsel states that a fit was obtained throughout to 1 percent or to the experimenter's estimate of his error, whichever is larger.

A small departure from Bichsel's results was introduced in Figures 5 and 6 at high energies, to allow for the fact that C/Z does not vanish at $\beta=1$ as assumed by Bichsel. Estimates of C/Z at $\beta=1$ were obtained from Equations 58 and 59, and each curve of Figure 6 was moved up or down to terminate at the correct value for $\beta=1$ (i.e. for $x=137^2/Z$). A corresponding correction was thereby made on I. These corrections are barley significant.

For purposes of orientation, some error bars corresponding to a ± 1 percent variation of the stopping power—roughly, the order of accuracy of the present state of the art—are shown in Figure 6. In view of the magnitude of this uncertainty in comparison to the rather small values of C/Z, only the major trends of the curves can be regarded as significant.

Despite this low level of significance and despite the lack of a direct recheck of the fitting to experimental data, independent of Bichsel's procedure, the curves in Figures 5 and 6 may afford a basis for a systematic study of C/Z throughout the periodic system. They show a rather clear, systematic, and plausible trend as functions of Z. They permit at least a tentative interpolation to obtain the value of C/Z or L for each material and each particle velocity. Incidentally, they also show, in comparison with the sample results of Walske (134), how unpromising the approach was through a theoretical shell-by-shell calculation of C/Z.

5. Energy Straggling

Statistical fluctuations of the number and kind of collisions along the track of a particle cause the effect of "straggling," i.e., of unequal energy loss along the tracks of particles that travel under identical conditions. Because of this effect, different particles starting under identical conditions have tracks of different lengths, and the range formulas of Section 2.9 represent only a mean value of these lengths; the formulas also require some correction indicated in Section 5.3.

Three closely related distributions result from straggling, namely: (*a*) the energy distribution

$$f(E, s)dE \tag{60a.}$$

of particles that have traveled a pathlength s under identical initial conditions; (*b*) the pathlength distribution

$$\frac{f(E, s)ds}{\int_0^\infty f(E, s)ds} \tag{60b.}$$

of particles whose energy has been reduced from an initial value E_0 to a given value E; (c) the distribution

$$\left[-\frac{d}{ds}\int_E^{E_0} f(E', s)dE'\right]ds \qquad 60c.$$

of the pathlength traveled by particles up to the collision at which their energy drops below the value E. Note that (b) and (c) differ because the energy of a particle drops in jumps and does not lie in turn at every level between E_0 and 0. [For additional discussion of these distributions, see Fano (40).] The distribution of total pathlength ("range straggling"), which is considered most frequently, is the limit of expression 60c for $E \to 0$. The distribution function $f(E, s)$ obeys the equation

$$\frac{\partial f(E, s)}{\partial s} = -N\Sigma_n\sigma_n(E)f(E, s) + N\Sigma_n\sigma_n(E + E_n)f(E + E_n, s) + \delta(E - E_0)\delta(s) \qquad 61.$$

where the last term represents the production of the particle at $s = 0$ with the source energy E_0.

The normalization integral in Equation 60b is of interest, because

$$y(E)dE = \left[\int_0^\infty f(E, s)ds\right]dE \qquad 62.$$

represents the mean value of the pathlength traveled by each particle while its energy lies between $E+dE$ and E in the course of its slowing down. This quantity serves to calculate the yield of reactions produced by a particle during its slowing down. For example, if protons penetrate a material containing $\mathfrak{N}$ nuclei per cm^3 with a cross section $\sigma(E-E_{res})$ for a (p, γ) resonance reaction, the reaction yield per proton is $\mathfrak{N}\int_0^{E_0} \sigma(E-E_{res})y(E)dE$. The differential pathlength $y(E)$ obeys the equation

$$N\Sigma_n\sigma_n(E)y(E) = N\Sigma_n\sigma_n(E + E_n)y(E + E_n) + \delta(E - E_0) \qquad 63.$$

which can be solved numerically (113). In the approximation that disregards straggling and was utilized in the range formulas of Section 2.9, one takes

$$y(E) \sim [N\Sigma_n E_n\sigma_n(E)]^{-1} = (-dE/ds)^{-1} \qquad 64.$$

This result follows from Equation 63 by expanding $\sigma_n(E+E_n)$ $y(E+E_n)$to first order in E_n and integrating over E.

As a heavy particle loses all or most of its energy, it experiences a great number of collisions in which all classes, including the less frequent ones with larger energy losses, are well represented. Therefore extreme fluctuations are quite unlikely over a long pathlength, and the straggling distributions are very nearly Gaussian. This result hinges on the circumstance that the maximum energy loss Q_{max} amounts normally to a very small fraction, $\sim 4m/M$, of the total energy of a heavy particle. The straggling distributions are far from being Gaussian when Q_{max} is comparatively large, i.e.: when condition 7 is violated at extremely high energies (Sec. 2.12), or when

one deals with short sections of path over which the energy loss is not much larger than Q_{max}, or for incident electrons under any condition.

As an index of the importance of unlikely fluctuations over a short pathlength s, one may consider the energy loss ξ' which is exceeded once, on the average, i.e., such that $Ns\Sigma_n^{(E_n>\xi')}\sigma_n = 1$. Under conditions of high-Q approximation (Sec. 2.7) we have

$$\xi' = \frac{2\pi z^2 e^4}{mv^2} NZs \left(1 - \frac{\xi'}{Q_{max}} - \xi' \frac{1-\beta^2}{mc^2} \ln \frac{Q_{max}}{\xi'}\right) \tag{65.}$$

Large fluctuations are prominent when $\xi' \ll Q_{max}$. The energy ξ' thus defined cannot exceed Q_{max}. It has been found convenient to consider, instead of ξ', the energy

$$\xi = \frac{2\pi z^2 e^4}{mv^2} NZs \tag{65a.}$$

which coincides with ξ' when $\xi' \ll Q_{max}$ but becomes $\gg Q_{max}$ when large fluctuations are unimportant. The numerical value of ξ is

$$(\xi)_{kev} = \frac{0.154}{\beta^2} z^2 \frac{Z}{A} (s)_{mg/cm^2} \tag{65b.}$$

Thus we have two main situations of interest, namely, that of long pathlengths, with $\xi/Q_{max} \gg 1$ and Gaussian fluctuations, and that of short pathlengths, with $\xi/Q_{max} < 1$ and prominent large fluctuations. In both cases simplifications arise from the fact that the collision cross sections vary by a negligible amount from one collision to the next, because Q_{max} is a small fraction of a heavy particle's energy. This derives in turn from the smallness of m/M, so that theoretical treatments rely in fact on expansions into powers of m/M.

5.1 *Long pathlengths; Gaussian straggling.*—This approximation is obtained by solving Equation 61 with $f(E+E_n, s)$ expanded into powers of E_n up to the second power only and with $\sigma_n(E+E_n) \sim \sigma_n(E)$. It is convenient to replace the pathlength s with the mean energy $\langle E \rangle$, which is related to s by[23]

$$s = \int_{\langle E \rangle}^{E_0} \frac{dE}{(-dE/ds)} \tag{66.}$$

This procedure yields

$$f(E, \langle E \rangle) = [2\pi \langle \Delta E^2 \rangle]^{-1/2} \exp\left[-\frac{(E - \langle E \rangle)^2}{2\langle \Delta E^2 \rangle}\right] \tag{67.}$$

where the mean square deviation $\langle \Delta E^2 \rangle$ results, according to Bohr (24), from the accumulated contributions of successive collisions

$$\langle \Delta E^2 \rangle = N \int_0^s \Sigma_n E_n^2 \sigma_n ds = \int_{\langle E \rangle}^{E_0} \frac{N\Sigma_n E_n^2 \sigma_n}{-dE/ds} dE = \int_{\langle E \rangle}^{E_0} \frac{\Sigma_n E_n^2 \sigma_n}{\Sigma_n E_n \sigma_n} dE \tag{68.}$$

[23] Notice that 66 coincides with the range formula Eq. 39 for $\langle E \rangle = 0$, $s = R$.

The calculation of $N\Sigma_n E_n^2\sigma_n$ proceeds analogously to that of the stopping power $N\Sigma_n E_n\sigma_n$ in Section 2. The basic sum rule 27 is replaced by

$$\Sigma_n E_n^2 \left| F_n(q) \right|^2 = Q^2 + \frac{4}{3} Q\langle K\rangle_0 + \text{correlation terms} \qquad 69.$$

where $\langle K\rangle_0$ indicates the mean kinetic energy of an atomic electron in the ground state of the atom, averaged over all electron shells, and where the "correlation terms"[34] are presumed to yield a correction smaller than 10 per cent. The low-Q limit of Equation 69, analogous to Equation 33, is

$$\Sigma_n E_n f_n = \frac{4}{3}\frac{1}{Z}\frac{\langle \left| \Sigma_j p_j \right|^2\rangle_0}{2m} = \frac{2}{3} m \left\langle \frac{\left| \Sigma_j v_j \right|^2}{Z} \right\rangle_0 \qquad 70.$$

inclusive of correlation terms. The analog of Equation 24 defines a mean excitation energy I_1 weighted differently from I, namely,

$$\ln I_1 = \Sigma_n E_n f_n \ln E_n / \Sigma_n E_n f_n \qquad 71.$$

The result is

$$N\Sigma_n E_n^2\sigma_n \sim 4\pi z^2 e^4 NZ \left\{ \frac{1 - \beta^2/2}{1-\beta^2} + \frac{2}{3}\frac{\langle \left| \Sigma_j v_j \right|^2\rangle_0}{Zv^2} \ln \frac{2mv^2}{I_1} \right\} \qquad 72.$$

The $\sim$ sign in this formula indicates that approximations have been made and corrective terms analogous to C/Z omitted. Relativistic corrections to the second term in the braces have been dropped because the second term is much smaller than the first one except when $\beta \ll 1$. In fact, the second term was disregarded altogether in Bohr's initial theory (24). Effects analogous to those represented by the shell correction C/Z to the stopping power formula do not appear to have been studied yet. Sternheimer (123) has carried out recently a rather accurate numerical evaluation of expression 72, including a modification to allow for the value (Eq. 20a) of $Q_{\max}$ at extremely high energies, where condition 7 breaks down.[35]

The pathlength distributions 60b and 60c, which coincide in the Gaussian approximation, are not conveniently obtained from Equation 67 where the pathlength s is represented indirectly by $\langle E\rangle$. Instead, one may return to solve Equation 61 in the same approximation used above, but replacing E with the mean pathlength $\langle s\rangle$ instead of replacing s with $\langle E\rangle$; the relationship of E and $\langle s\rangle$ is, however, the same as the relationship 66 of $\langle E\rangle$ and s. One finds, then,

$$f(\langle s\rangle, s) = [2\pi\langle \Delta s^2\rangle]^{-1/2} \exp\left[-\frac{(s - \langle s\rangle)^2}{2\langle \Delta s^2\rangle} \right] \qquad 73.$$

[34] The expression including electron correlations is

$$\Sigma_n E_n^2 \left| F_n(q) \right|^2 = \frac{Q}{2mZ} \left\langle \left| \sum_{j=1}^{Z} \left[\hat{q}\cdot p_j \exp(iq\cdot r_j/\hbar) + \exp(iq\cdot r_j/\hbar)\hat{q}\cdot p_j \right] \right|^2 \right\rangle_0$$

[35] Other effects mentioned in Sec. 2.12 also occur at these energies.

where (24)

$$\langle \Delta s^2 \rangle = \int_E^{E_0} \frac{N\Sigma_n E_n^2 \sigma_n}{(-dE/ds)^3} dE \qquad 74.$$

For the numerical calculation of $\langle \Delta s^2 \rangle$, which utilizes Equation 72, see (123).

5.2 *Short pathlengths; Landau-type approximations.*—When Equation 61 has to be integrated over a short interval of s, the expansion of $f(E+E_n, s)$ into powers of E_n cannot be utilized, because the spectrum of f is sharply peaked owing to the $\delta(E-E_0)$ factor in the source term. On the other hand, one can regard the cross sections $\sigma_n(E)$ and $\sigma_n(E+E_n)$ as equal to $\sigma_n(E_0)$ throughout the relevant range of integration. With this assumption, a Laplace transformation is applied conveniently by multiplying both sides of Equation 61 by $\exp[-p(E_0-E)]$ and integrating over E. Integration over s is then elementary and yields

$$\int_0^{E_0} dE \exp[-p(E_0-E)] f(E,s) = \exp\{-Ns\Sigma_n\sigma_n(E_0)[1-\exp(-pE_n)]\} \qquad 75.$$

Similarly one finds

$$\int_0^{E_0} dE \exp[-p(E_0-E)] y(E) = \{N\Sigma_n\sigma_n(E_0)[1-\exp(-pE_n)]\}^{-1} \qquad 76.$$

The problem resolves now into two separate parts: evaluation of the Σ_n and inversion of the transform, i.e., determination of $f(E, s)$ or $y(E)$ from a knowledge of the right-hand side of Equation 75 or 76.[36]

The calculation of the Σ_n in Equation 75 may begin by term-by-term summation over the expansion

$$1-\exp(-pE_n) = pE_n - (1/2)p^2E_n^2 + (1/6)p^3E_n^3 + \cdots.$$

The sum over the linear term is proportional to the stopping power and that over the second term is proportional to Equation 72. Since higher terms are weighted more heavily in favor of large E_n and, therefore, of large Q, they may be evaluted by means of the large-Q approximation 31 to σ_n. Use of this approximation yields an exponential integral without further resort to term-by-term summation. The result,

$$\begin{aligned} &Ns\Sigma_n\sigma_n(E)[1-\exp(-pE_n)] \\ &= p\xi\left\{\ln\frac{2mv^2}{\epsilon pI^2} + \ln\frac{1}{1-\beta^2} - \beta^2 - 2\frac{C}{Z} - \delta - \left(1+\frac{\beta^2}{pQ_{\max}}\right)\int_{pQ_{\max}}^{\infty} dt\,\frac{e^{-t}}{t}\right. \\ &\quad \left. - \frac{1-\exp(-pQ_{\max}) + \beta^2\ln(\gamma pQ_{\max})}{pQ_{\max}} - \frac{1}{3}pm\left\langle\frac{|\Sigma_i v_j|^2}{Z}\right\rangle_0 \ln\frac{2mv^2}{I_1}\right\} \end{aligned} \qquad 77.$$

with $\gamma = \exp C = 1.78107$ and $\epsilon = \gamma/e = \exp(C-1) = 0.6552$, has been given

[36] The inversion of the transform may be avoided for the purpose of experimental tests, since experimental data on $f(E, s)$ or $y(E)$ may be utilized to calculate the left-hand side of Eq. 75 or 76 numerically and compare the results directly with the right-hand side.

by Vavilov (133) except for the last term in the braces. This term, which is often small, corresponds to the last term of Equation 72 and to the Blunck-Leisegang (19) correction. Notice that the first five terms in the braces correspond to a stopping power formula from which the contribution of high-Q collisions with $Q > 1/p\epsilon$ has been eliminated. This group of terms was contained, in essence, in Landau's original theory (68), which regarded Q_{max} as infinitely large and thereby omitted the sixth and seventh terms. More accurately, the Landau result represents the limit of Equation 77 for $\xi/Q_{max} \ll 1$, with omission of the Blunck-Leisegang term.

Landau (68) first studied the inversion of the Laplace transform 75, within the approximation $\xi/Q_{max} \ll 1$ which yields

$$f(E, s) = \xi^{-1}F(\lambda) = (\xi 2\pi i)^{-1}\int_{-i\infty}^{i\infty} \exp(p\lambda + p \ln p)dp \qquad 78.$$

Here F is Landau's universal function of the single variable

$$\lambda(E, s) = \frac{E_0 - E}{\xi} - \left[\ln \frac{2mv^2\xi}{eI^2(1-\beta^2)} - \beta^2 - 2\frac{C}{Z} - \delta\right] \qquad 79.$$

which depends on s through ξ, and the path of integration in Equation 78 passes on the positive side of $p = 0$. The Landau function F peaks at $\lambda = 0.225$, drops off sharply on the negative side, and exhibits a λ^{-2} tail on the positive side. Numerical approximation methods that apply to intermediate values of ξ/Q_{max}, up to the large values of this ratio which yield a Gaussian curve, were developed by Symon (126) and described by Rossi (105). Vavilov (133) has also worked through the intermediate range quite successfully, obtaining $f(E, s)$ as function of λ and ξ/Q_{max}. He has shown that expansion of 77 into powers of p up to p^3 is adequate for $\xi/Q_{max} > 1$, in which case $f(E, s)$ is obtained analytically in terms of Airey's function (133, Eq. 13). Numerical curves obtained for $\xi/Q_{max} < 1$ reduce to the Landau curve at $\xi/Q_{max} \sim 0.01$. The remaining Blunck-Leisegang term in Equation 77, which was disregarded by Vavilov, can be taken into account as follows. If the energy distribution function calculated by Vavilov's method is called $\bar{f}(E, s)$, the corrected distribution is given by

$$(E, s) = \int_{-\infty}^{\infty} \frac{dE'}{\sqrt{\pi}\,\eta} \exp\left[-\frac{(E - E')^2}{\eta^2}\right] \bar{f}(E', s) \qquad 80.$$

where

$$\eta^2 = \frac{4}{3}\xi m \left\langle \frac{|\Sigma_i v_i|^2}{Z} \right\rangle_0 \ln \frac{2mv^2}{I_1} \qquad 80a.$$

A rapidly converging expansion for the differential pathlength $y(E)dE$ has been obtained from its transform 66 by Spencer & Fano (113), with the Landau approximation to Equation 77,

$$y(E) = \left[\frac{2\pi z^2 e^4 NZ}{mv^2}\right]^{-1}\left\{\frac{1}{\pi}\arctan\frac{\pi}{B} + \frac{\Gamma'(1)}{\pi^2 + B^2} + \frac{B\Gamma''(1)}{(\pi^2 + B^2)^2} + \cdots\right\} \qquad 81.$$

where the primes indicate derivatives of the gamma function and

$$B = \ln \frac{2mv^2(E_0 - E)}{\epsilon I^2(1 - \beta^2)} - \beta^2 - 2\frac{C}{Z} - \delta \qquad 81a.$$

For $B \gg \pi$, Equation 81 approaches the reciprocal stopping power formula 64, modified by removal of the contribution of collisions with $Q > (E_0 - E)/\epsilon$. For values of $E_0 - E \ll Q_{max}$, the quantity 81 becomes substantially larger than 64, showing that a particle travels an excess pathlength at the beginning of its penetration as though it had a small effective stopping power. This transient phase of penetration lasts until the particle has traveled a pathlength sufficient to render likely the occurrence of the less frequent larger energy losses. Once these losses have come into statistical equilibrium with the more numerous smaller ones, their full contribution to stopping power becomes effective and $y(E)$ drops to its normal value. The excess value of $y(E)$ at the beginning of penetration has been demonstrated by Walters et al. (135) as an excess yield of a (p, γ) resonance reaction when protons hit a target with an energy barely above the resonance.

5.3 *Corrections to long pathlength formulas.*—The range formula 39, the differential pathlength formula 64, and the Gaussian straggling formulas 67 and 73 involve errors of the order of $4m/M$ even for long pathlengths. Equation 64, which underlies the range formula, is derived under the assumptions that the cross sections σ_n for successive collisions differ negligibly from one another. Small variations of the cross section are taken into account by an expansion procedure (40) that replaces Equation 64 by

$$y(E) = \left(-\frac{dE}{ds}\right)^{-1} \left\{1 - \frac{1}{2}\frac{d}{dE}\frac{\Sigma_n E_n^2 \sigma_n(E)}{\Sigma_n E_n \sigma_n(E)} + \cdots\right\} \qquad 82.$$

(Localized sharp variations of $\sigma_n(E)$, if any, would give rise to transient disturbances of $y(E)$, akin to those represented by Equation 81 which stem from the sharpness of the initial energy spectrum.)

The correction in Equation 82 represents the fact that an unusually large energy loss exposes a particle to an unusually increased probability of further collisions. This effect reduces the total range, which is the integral of $y(E)$. However, it is overbalanced by the increase of $y(E)$ at the beginning of penetration which is large, even though limited to a narrow energy interval, as shown by Equation 81. There results a total net *increase* of the particle range which amounts to $\sim$1 percent for μ mesons. This increase was emphasized and calculated by Lewis (71) and discussed further by Fano (40).

Distortions of the Gaussian shape of straggling distributions may be expressed as departures of the various moments of the distributions, such as $\langle (E - \langle E \rangle)^n \rangle$, from the ratios prescribed by the Gaussian law. Each moment can be obtained, like $\langle \Delta E^2 \rangle$ in Equation 68, by summing the contributions of fluctuations in successive energy intervals. The gradual change of cross

sections introduces corrections to these contributions which are represented by perturbation formulas akin to Equation 82. For details of these calculations see (40) and (63). Lewis (71) has also given formulas that represent the distortion of the Gaussian range distribution corresponding to the corrected moments.

6. Multiple Scattering Effects on Penetration

The path of a heavy particle that penetrates a material is not quite straight. Therefore, the path's projection along its initial direction, i.e., the depth of penetration z, is a little shorter than the corresponding pathlength s. This difference is often of the order of 1 percent. It must accordingly be considered when data on the range (i.e., total pathlength) are obtained from observations of the thickness of material that is penetrated.

Determination of this correction requires a knowledge of the statistical distribution of $s-z$. A knowledge of the distribution of the angle θ between the path's directions at s and at $s=0$ is required for this purpose, since $dz=ds\cos\theta$ and[37]

$$\frac{d(s-z)}{ds}=1-\cos\theta\sim\tfrac{1}{2}\theta^2 \qquad 83.$$

The distribution in θ is also involved rather subtly in the analysis of penetration experiments, e.g., when the particles are detected by a flat ionization chamber whose response depends on the obliquity of traversal.

In principle, the fluctuations in energy (i.e., the straggling discussed in Sec. 5), in $s-z$, and in θ are related and are governed by a single equation. This equation has been considered but only partial aspects of it have been solved. In practice, for heavy particles the correlations between fluctuations of different variables are rather small. For example, the fluctuations in θ at the end of the range depend primarily on collisions in the last sections of the path, whereas fluctuations in $s-z$ have been building up in comparable amounts all along the path.

The mean value of $s-z$ is found by taking the mean of Equation 83 at each value of the pathlength s and integrating

$$\langle s-z\rangle_s=\int_0^s\langle 1-\cos\theta\rangle_{s'}ds'\sim\int_E^{E_0}\frac{\langle 1-\cos\theta\rangle_{E'}}{-dE'/ds'}dE' \qquad 84.$$

The mean value $\langle 1-\cos\theta\rangle_s$ is obtained with rather good accuracy from the theory of multiple elastic scattering (9, 70, 107). Sample data on $\langle s-z\rangle/s$ are given in Table II (see p. 48). The ratio

$$v=2\frac{s-z}{\langle s-z\rangle_s} \qquad 85.$$

is a natural variable for the distribution function of $s-z$.

[37] The small-angle approximation indicated on the right of Eq. 83 has been generally utilized for simplicity in studies of heavy-particle penetration. However, calculation of moments or other parameters of the distribution of $1-\cos\theta$ is actually more direct, is no more complicated, and avoids convergence difficulties.

Some useful qualitative remarks and approximate formulas for $\langle s-z\rangle$ are available. Recasting Equation 84 in the form

$$\langle s - z\rangle_s = \int_0^s \frac{d\langle 1 - \cos\theta\rangle_{s'}}{ds'} (s - s')ds' \qquad 84a.$$

shows that scattering at s', which is represented by $d\langle 1-\cos\theta\rangle_{s'}/ds'$, contributes to $\langle s-z\rangle_s$ in proportion to the remaining pathlength $s-s'$. [Similarly, the contribution of this scattering to higher moments $\langle(s-z)^n\rangle$ is proportional to $(s-s')^n$.] For this reason, scattering in the early portion of a track contributes appreciably to $\langle s-z\rangle_s$ even though it is weaker on account of the higher particle energy.

As seen from Equation 84, $\langle s-z\rangle$ is a function of the material and of the particle energy, which depends on the ratio of scattering to stopping power. Blanchard (15) emphasized that this ratio can be split into a material-dependent factor and an energy-dependent factor with greater accuracy than either the scattering or the stopping cross section alone. One finds for heavy particles

$$\langle 1 - \cos\theta\rangle_s \sim kZ\frac{m}{M} \ln\frac{E_0(E + 2Mc^2)}{E(E_0 + 2Mc^2)} \qquad 86.$$

where E_0 and E are the particle's kinetic energies at $s=0$ and at s, and k is a coefficient with a minor residual dependence on both material and energy, of which some values are given in Table II.[38] The material-dependent factor Zm/M results from the ratio of corresponding factors in the scattering and stopping power formulas. From Equation 86 follows

$$\langle s - z\rangle_s \sim Z\frac{m}{M}\langle l\rangle s \qquad 87.$$

where $\langle l\rangle$ is the approximate mean value of k times the logarithm in Equation 86 and lies generally between 0.3 and 0.6. Mather & Segrè (78) used, in essence, this formula with $k=1/2$ and with $\langle l\rangle=0.28$ for Cu.[39] Considerations analogous to those presented here have led Barkas (7) to a scaling procedure that relates the value of $\langle s-z\rangle$ in a material of interest to the value for photographic emulsions which can be measured.

Because the distribution of $s-z$ is very skew, one may wish to single out a value of $s-z$ nearer to the peak of the distribution than the mean. Bichsel & Uehling (13) achieved this end, in effect, by entering in Equation 84 a typical value of $1-\cos\theta$, for each s', somewhat lower than the mean

[38] The proton values of k differ systematically from the value for electrons, $k=0.3$, given by Blanchard (15). Note that Eq. 86 is the first term of an exponential series in powers of m/M, which would converge poorly for electrons.

[39] An early, often utilized, treatment by E. J. Williams leads to the nonrelativistic form of Eq. 86, with $(E+2Mc^2)/(E_0+2Mc^2)=1$, and to $k=\frac{1}{2}$. Further application of the approximate range-energy formula $R=aE_0^b$ yields then the mean value $1/b$ for the logarithm in Eq. 86 and thereby $\langle l\rangle=k/b$ in Eq. 87.

TABLE II

(Courtesy M. J. Berger)

MEAN SCATTERING CORRECTION ON PROTON PENETRATION

$100\langle s-z\rangle_{av}/R$

Figures in parentheses are values of $\langle l\rangle$ in Equation 87

Proton initial energy (MeV)	Be, $Z=4$ $I=64$ eV	Al, $Z=13$ $I=163$ eV	Cu, $Z=29$ $I=314$ eV	Sn, $Z=50$ $I=516$ eV	Pb, $Z=82$ $I=826$ eV
1000	0.070 (0.32)	0.247 (0.35)	0.580 (0.37)	1.04 (0.38)	1.75 (0.39)
500	0.075 (0.34)	0.266 (0.38)	0.628 (0.40)	1.13 (0.41)	1.90 (0.43)
200	0.081 (0.37)	0.288 (0.41)	0.683 (0.43)	1.23 (0.45)	2.09 (0.47)
100	0.085 (0.39)	0.306 (0.43)	0.724 (0.46)	1.32 (0.48)	2.25 (0.50)
50	0.090 (0.41)	0.327 (0.46)	0.779 (0.49)	1.41 (0.52)	2.44 (0.55)
20	0.096 (0.44)	0.347 (0.49)	0.831 (0.53)	1.51 (0.55)	2.62 (0.59)
		Values of k in Equation 86			
1000	0.65	0.67	0.70	0.72	0.74
100	0.70	0.76	0.80	0.83	0.85
10	0.86	0.94	0.99	1.03	1.08

$\langle 1-\cos\theta\rangle_{s'}$. The result of the integration, which they called ΔR_0 and tabulated for a set of initial energies and materials, represents the value of $s-z$ for a "smoothed out path" which has a specified typical obliquity θ at each pathlength s'. The lack of smoothness of actual paths was then taken into account by increasing ΔR_0 by 2/15.

Yang (139) developed a rather detailed theory of the distribution function of $s-z$, applicable to short pathlengths over which the cross sections are regarded as constant and utilizing a diffusion approximation to multiple scattering. This theory shows that the distribution function vanishes rapidly as v approaches zero, with a dominant factor $\exp(-1/v)$, that it peaks at $v\sim 1$, and that it decreases for large v according to $\exp(-\pi^2 v/16)$.

For longer pathlengths, over which the cross sections vary substantially, moments of the distribution of $s-z$ can be calculated by a procedure introduced by Lewis (70). Studies by Spencer (114, 115), using this method as well as a theoretical analysis of the distribution for very small v, show that the $\exp(-1/v)$ law remains applicable. This result is also borne out by extensive Monte Carlo calculations which have provided much of the current information on the distribution of $s-z$ near the end of heavy-particle ranges [Berger (9, 87, 88)].

This recent study by Berger (87) critically reviews current knowledge of the effects of scattering on penetration and applies it to an analysis of experimental curves (78, 143) of detector response versus thickness of particle absorber. The analysis accounts for the major part of the curves though not for their behavior in the direction of short penetration.

7. Phenomena Associated with Particle Tracks

The study of particle penetration in a material is traditionally associated with numerous effects, such as ionization or luminescence, which serve to detect the particle's passage and to provide information on its charge, mass, energy, etc. As the study of these processes progresses, it often bears increasingly on atomic properties of the material and less on the primary interaction of the particle. Thus this study develops into a number of separate chapters of physics, each of them of interest in its own right and with far-reaching ramifications, even while it remains relevant to particle penetration. In this section a number of associated effects will be mentioned, to give some indication of their present development and some reference to more detailed reports.

The effects of a particle that come under observation are, in general, rather remote from the initial particle collisions. The collection of ions affords plenty of time for their chemical transformation (e.g. $H_2^+ + H_2 \rightarrow H_3^+ + H$). Numerous processes—known and unknown—convert excitations into ionization. Light emission almost never proceeds from the levels of initial excitation. The often strikingly simple quantitative relationships between the energy lost by a particle and its observable effects, which emerge from experimental studies with moderate accuracy, may suggest, deceptively, a close link between these effects and the initial collisions, whereas the actual complexity of intervening events emerges only from more sophisticated tests.

7.1 *Energy deposition along particle tracks.*—Some of the energy lost by a fast charged particle is removed from the vicinity of its track within times $\lesssim 10^{-15}$ sec by fast secondary electrons or by Cerenkov radiation. To analyze the operation of detectors, one often wants to distinguish the energy left near the track ("restricted energy loss") from the total energy loss. The definition of restricted energy loss depends on the circumstances of interest. If often excludes the energy spent in producing secondary electrons with

initial energy in excess of a suitable limit T_0 and the Cerenkov radiation with frequency below that of the lowest absorption band of the material (higher frequency Cerenkov radiation is absorbed rapidly [Sternheimer (119), Budini & Taffara (34)]). Assuming that $Q=T_0$ lies in the range of the high-Q approximation, the theory excludes fast secondaries by replacing the integration limit Q_{max} with T_0 in Equation 37. To exclude the energy removed by Cerenkov radiation, one calculates separately the integral of the second term on the right-hand side of Equation 47 over the frequency band where ϵ_2 is negligible and the arctangent is near π. One finds then, instead of Equation 38,

$$\left(-\frac{dE}{ds}\right)_{restr.} = \frac{2\pi z^2 e^4}{mv^2} NZ\left\{\ln\frac{2mv^2T_0}{I^2} - \frac{1-\beta^2}{2mc^2}T_0 + \ln\frac{1}{1-\beta^2} - \beta^2 - 2\frac{C}{Z} - \delta - \Delta_C\right\} \quad 88.$$

where

$$\Delta_C = \frac{1}{\omega_p^2}\int_{Im\epsilon<0,\epsilon\beta^2>1} 2\omega d\omega\left[\beta^2 - \frac{1}{\epsilon(\omega)}\right] \quad 89.$$

remains below 1 in H_2 and He, below 0.1 in other gases and, $\sim$0.01 in solids [Sternheimer (140, pp. 8–10)].

The restricted energy loss has a finite limit at high energy, called the "Fermi plateau," which is, owing to Equation 50,

$$\left(-\frac{dE}{ds}\right)_{restr.,\beta=1} = \frac{2\pi z^2 e^4}{mv^2} NZ\left\{\ln\frac{2mc^2T_0}{(\hbar\omega_p)^2} - \left(2\frac{C}{Z}+\Delta_C\right)_{\beta=1}\right\}$$

$$= 0.154\frac{Z}{A}\left\{\ln\frac{1400(T_0)_{ev}}{(\rho)_{g\,cm^{-3}}Z/A} - \left(2\frac{C}{Z}+\Delta_C\right)_{\beta=1}\right\} \text{MeV g}^{-1}\text{ cm}^2 \quad 88a.$$

where $(2C/Z+\Delta_C)_{\beta=1} \ll 1$ in all materials but H and He.

Extensive experimental verification of this formula has been obtained [see, e.g., Sternheimer (140, pp. 20–40)]. However, doubts have been cast on it recently by experiments at $E>100\ Mc^2$ with nuclear emulsions [Alekseyeva et al. (2), Zhdanov et al. (141)] which show a decrease of $(-dE/ds)_{restr.}$ by 5–10 percent in this extreme relativistic range. Tsytovich's theoretical work [(129); see Sec. 2.13] accounts for this result in terms of radiative corrections. This matter remains unsettled at the moment as an attempt to reproduce the experiment has pointed to possible disturbing influences in the handling of the emulsions [Stiller (125)].†

† *Note added in proof.* Continued experimentation by Stiller and Herz (private communication) with various types of nuclear emulsion exposed and treated under strictly controlled conditions has failed to demonstrate a systematic uniform trend of the blob density count at $E>100\ Mc^2$. On the contrary, this work has emphasized differences in the behavior of different emulsions and thereby suggests that the blob density may not correlate with $(-dE/ds)_{restr.}$ to provide an adequate test of the theory.

7.2 *Delta rays.*—Delta rays are secondary electrons of energy sufficient to cause their track to fork out detectably from the heavy-particle track or to be otherwise noticeable. The minimum energy T_0 required for this classification depends of course on experimental criteria. If the high-Q approximation holds for $Q > T_0$, the number of δ rays of energy T produced per cm of track is given by a formula analogous to Equation 31

$$d\mathfrak{N}_T = \frac{2\pi z^2 e^4}{mv^2} NZ \left(\frac{1}{T^2} - \frac{1-\beta^2}{2mc^2 T} \right) dT \qquad 90.$$

This formula serves well to determine the z and v of a particle on the basis of its δ-ray production because all its elements are well defined. However, an excess of δ rays over the prediction of Equation 90 occurs at energies T that are not much larger than the binding energy of atomic electrons, because the high-Q approximation no longer holds. This increase, which is responsible for the second term of Equation 72, has not been studied quantitatively.

7.3 *Primary ionizations and excitations.*—Successive ionizing collisions occur far enough apart along the track of a fast particle for the particle to frequently traverse a low-pressure counter without causing any ionization and, therefore, any discharge. This circumstance offers an opportunity to measure the frequency of primary ionizations along a track [McClure (74)]. The great majority of collisions involve a small momentum transfer, even though high-Q collisions contribute about half of the total energy loss. Accordingly, measurements of the number $\mathfrak{N}_I$ of ionizing collisions per centimeter of track provide information on the parameters of the low-Q approximation, i.e., on the dipole strengths $|(\Sigma_j x_j)_{n0}|^2$ of Equations 22 and 23. The plot of $\beta^2 \mathfrak{N}_I$ versus the velocity function $\ln[\beta^2/(1-\beta^2)] - \beta^2$, which appears in Equation 35, is a straight line (within the limits of the Born approximation) whose slope measures the quantity

$$M_i^2 = \Sigma_{n \text{ ionized}} |(\Sigma_j x_j)_{n0}|^2 \qquad 91.$$

[Fano (41)].

Platzman (97) has emphasized that the set of ionized states over which the sum is performed in Equation 91 does not coincide with the set of all states whose energy E_n exceeds the ionization threshold E_i of the molecule in the collision. Final states of molecules with $E_n > E_i$ may be dissociated, for example, rather than ionized. On the other hand, excitation to states with $E_n < E_i$ may result in eventual ionization of another molecule with a lower E_i. In order to avoid classifying the states n according to their eventual properties, Platzman writes Equation 91 in the form

$$M_i^2 = \Sigma_n |(\Sigma_j x_j)_{n0}|^2 \eta_n \qquad 91a.$$

where η_n is the probability that the state n leads to ionization.

This method of analysis of collision cross sections has been applied to correlate the optical transition parameters $|(\Sigma_j x_j)_{n0}|^2$ and the cross sections

for excitation to specific levels n by electron collisions (82, 101). Figure 7 gives an example of this plot and provides, incidentally, a verification of the Born approximation collision theory over a large range of energies. The drop of the experimental points below the straight line at low energies represents the failing of the Born approximation. The shape of the curve in Fig. 7 is, of course, characteristic for optically allowed transitions from the ground

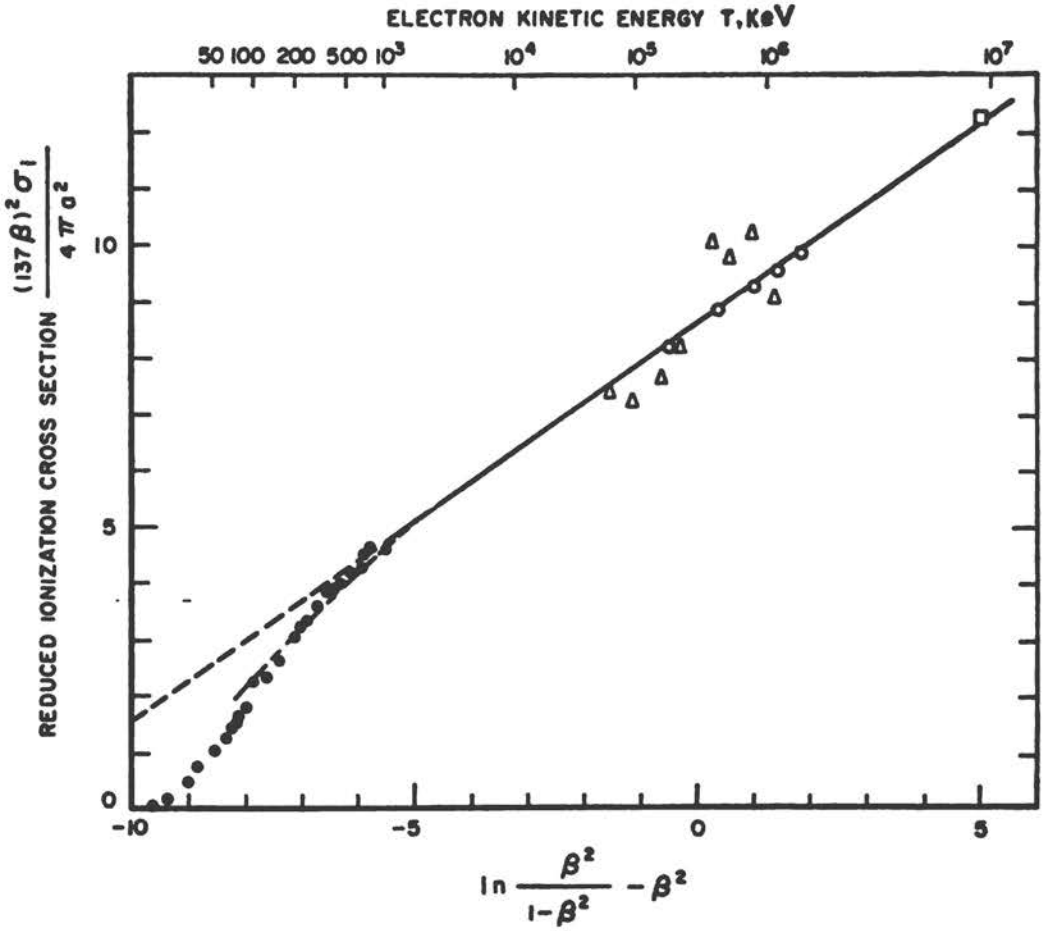

FIG. 7. Ionization of H_2 by electron bombardment. Experimental data: △ Williams & Terroux (1930), ● Tate & Smith (1932), □ Danforth & Ramsey (1936), ○ McClure (1953)

– – – —— Theoretical asymptotic law

$$(137\beta)^2\sigma_i/\pi a^2 = 0.711\ \{\ln[\beta^2/(1-\beta^2)]-\beta^2\}+8.63$$

—·—·— The same, corrected for exchange (100)

The coefficient 0.711, determined by fitting the theoretical law to experimental data, measures M_i^2 in units of the squared Bohr radius a^2. (Courtesy R. L. Platzman.)

state to the state n. The cross sections for forbidden transitions with $\Delta L \neq 1$ vanish in the low-Q approximation and therefore fail to rise linearly on the right of the figure but flatten out at a constant level.

7.4 *Ionization yield.*—The ionization chambers, which are the classic particle detectors, the proportional counters, which are ionization chambers with internal amplification, and the semiconductor counters respond to the passage of a heavy particle in proportion to the number of charge pairs separated in their sensitive volume. This number of charges is closely proportional to the energy dissipated, and the proportionality constant depends but little on the characteristics of the particle. The constant is usually expressed as the energy W dissipated per pair of ions produced. The quantity W is understood to represent a grand average over a large number of ionization processes produced by the incident particle, by secondary electrons, and by subsequent intermolecular processes.

Much effort has been devoted over the years to the study of W in gases. [See, e.g., the reviews by Boag (20), Valentine & Curran (131), Booz & Ebert (26), and Whyte (138).] The data shown in Table III pertain mostly to α particles and β rays. The values for 340-MeV protons are a little lower than those for α particles, but this difference is probably not significant. The data for electrons show values of W a few percent lower than those for α particles except in hydrogen and in the noble gases; achievement of accurate, absolute measurement of W for β rays (60) has represented considerable progress. The excess of W over the energy I_0 actually required to produce an ionization represents, of course, a diversion of energy to excitation and to other processes. For the monoatomic rare gases W/I_0 lies near 1.7 to 1.8; for the molecular gases, in which excitation is comparatively more likely and in which energy may go into molecular potential to yield dissociation or vibrational excitation, this ratio ranges from 2.1 to 2.6.

The remarkable stability of W against changes of velocity of the incident particles derives in part from the small influence of the velocity on the relative cross section for different types of excitation or ionization collisions. It is enhanced by the circumstance that excess energy imparted to fast secondary electrons can be utilized for the production of further ionization by these electrons; moreover, the energy distribution of these secondaries also depends weakly on the velocity of the incident particle. Other compensating factors which remain unidentified presumably operate. Platzman (87, 98) has achieved considerable progress in analyzing the distribution of the incident energy between ionization and other processes throughout the sequence of secondary phenomena. In the case of He, a theoretical calculation of the whole chain of events has been successfully completed (82, 98)[40] yielding $W=43$ eV, in very good agreement with experiments.

The study of W in gases has taken a new turn since the discovery of the

[40] This calculation requires a good knowledge of the collision cross sections for slow secondary electrons. The assembly of these data for helium (82) raised a major obstacle which has not yet been overcome for other gases except H_2. An earlier calculation by Erskine (39) utilized unrealistic cross sections.

TABLE III

VALUES OF W (eV/ion pair)

	Substance	α Rays	340-MeV protons	β Rays
Gases				
	He	42.7 (59) 46.0 (27)		42.3 (60)
	Ne	36.8 (59)		36.6 (60)
	Ar	26.4 (59, 27) 26.25 (53)		26.4 (60)
	Kr	24.1 (59)		24.2 (60)
	Xe	21.9 (59)		22.0 (60)
	H_2	36.3 (59) 37.0 (27) 36.0 (12)	36.5 (3)[a]	36.3 (60)
	N_2	36.38±0.07 (8) 36.39±0.07 (62) 36.50 (12)	34.7 (3)[a]	34.9 (61)
	O_2	32.5 (59) 32.2 (53) 32.2 (27)	32.6 (3)[a]	30.9 (60)
	Air	34.97±0.07 (8) 34.96±0.07 (62) 34.95 (12)	34.4 (3)[a]	33.8±0.2 (26) (>20-keV average)
	CO_2	34.04 (8) 34.3 (27) 34.3 (12)		32.9 (60)
	CH_4	29.0 (12) 29.2 (59) 29.4 (27)		27.3 (61)
Solids				
	Si	3.55 (86)		3.55 (65)
	Ge	2.9 (86, 79, 75)		
	Se	3.9 (79)		
	InSb	0.6 (127)		
	AgCl			7.6 (132)

Note—Experimental error estimates are indicated only where they are particularly low or otherwise significant.

[a] These values were adjusted to make $W_{Ar}=26.4$ eV.

Jesse effect, namely, of the extreme sensitivity of W in He to trace impurities which ionize upon collision with excited He atoms. The same effect occurs in Ne and, to a lesser extent, in Ar. The ionization yield has now become an indicator of the comparative probability of ionization and other molecular processes and of the energy exchanges among molecules in a gas. Following Platzman's observation that ionization in molecules is subject to competition with dissociation (97) and that the speed of dissociation is affected adversely by replacement of atoms with their heavier isotopes, Jesse has demonstrated that replacement of hydrogen with deuterium reduces the value of W [Jesse & Platzman (63)].

In semiconductor counters only $\sim$1 eV is required to lift an electron to the conduction band, as compared with the 10–20 eV required to ionize a gas molecule. Accordingly the ionization yield in semiconductors is much higher than in gases, and corresponds to a value of $W\sim3$ eV. This value has been accounted for remarkably well by a simple model of the mechanism through which the energy lost by a fast particle is converted to produce ionization in a solid [Chynoweth, Schweinler (86), Shockley (110)]. This model considers only the excitation of individual electrons to the conduction band by the passage of a fast particle and the subsequent chainwise excitation of other electrons if the one first excited had received sufficient energy. On the other hand, the evidence presented in Section 2.10 indicates that the main excitations in metals and semiconductors are of the collective ("plasma") type and have energy levels much higher than 1 eV. Thus the mechanism that controls the value of W in solid counters may require further clarification.

7.5 *Grain and bubble counts; luminescence.*—Other modern particle detectors, namely, photographic emulsions, bubble chambers, and scintillators, give a response that is closely related to the particle's energy loss but depends also appreciably on its velocity. The number of grains that appear along a particle track in an emulsion (after it has been developed), the number of bubbles in a bubble chamber, and the amount of light that emerges from a scintillator per centimeter of track depend, like gas ionization, on sequences of secondary processes. However, the circumstances for maintaining a stable response per unit energy loss are not quite as favorable here as for gas ionization.

Much effort has been devoted to studying the energy loss of heavy particles at relativistic velocities indirectly through grain or bubble counts and through the light output of scintillators. This effort was reviewed in considerable detail a few years ago (140, see particularly pp. 21–38 by Sternheimer). As an indication of order of magnitude, one "blob" (i.e., grain or group of grains) is observed per 10^3 eV of energy dissipation, one bubble per $3\text{–}5\times10^3$ eV in most of the relevant materials, and one scintillation photon per 10^2 eV.

Each grain or bubble may stem, at least for high-speed particles, from a single collision. Collisions involving different amounts of energy loss are not

equally effective in producing grains or bubbles. This fact alone would not spoil the proportionality of grain or bubble count to the energy loss if the relative frequency of different types of collision were independent of the particle's velocity. As can be seen from the theory of energy losses developed in Section 2, the relative frequency of collisions produced by the longitudinal interaction remains remarkably constant as the particle velocity varies, because it varies at most as the logarithm of the velocity. However, the rising contribution of the transverse interaction at relativistic energies introduces an appreciable change in the spectrum of energy losses because this interaction yields no intermediate-Q collisions (Sec. 2.4) and therefore very few δ rays of low or moderate energy.

This difference between the collisions produced by transverse and longitudinal interactions has a characteristic effect [Barkas (5)]. The production of a bubble appears to require a fair amount of energy, of the order of 300–1000 eV, and thus to depend particularly on the occurrence of low energy δ rays.[41] In hydrogen, which contains no inner-shell electrons, δ rays of this energy cannot arise from low-Q collisions. The frequency of these δ rays along the track is then given approximately by the first term of Equation 90 (since $T \ll mc^2$) and amounts to $25/\beta^2$ per centimeter for the total production of δ rays with $T > 400$ eV. Careful experimental studies [see e.g. Kenney (64), Sechi-Zorn (142)] have confirmed the β^{-2} law, and thus the absence of any relativistic rise of the bubble count in H_2, within the theoretical and experimental accuracy. (This bubble count amounts to $8.5/\beta^2$ cm^{-1}.) Other liquids, however, contain inner-shell electrons which can be ejected in low-Q collisions with $E_n > 300$ eV. Therefore, the frequency of these collisions should show a relativistic rise, arising from the contribution of the $\ln[1/(1-\beta^2)]$ term in Equation 32. A relativistic rise of 5 percent has actually been observed in propane [Blinov et al. (16)] and a much larger one of 30 percent has been reported for the heavier liquid $CBrF_3$ [Hahn & Hughentobler (54)].

Similar effects might also influence emulsion grain counts, but to a smaller extent because of the presumably lower threshold for grain development than for bubble formation. At any rate, the blob density along high energy particle tracks has been found to parallel closely the restricted energy loss (Eq. 88), with T_0 of the order of a few keV. The blob density exhibits a relativistic rise of the order of 15 percent from the minimum, at $E \sim 4\ Mc^2$, to the "plateau" at $E > 100\ Mc^2$ [see e.g. (140, p. 15), Shapiro (109), Patrick & Barkas (93)]. Notice, however, that the calculated magnitude of this rise is

[41] Dr. A. G. Tenner kindly points out that the amount of energy actually spent in bubble formation is only ~10 eV in hydrogen and helium, even though the transfer of a much larger amount of energy to a δ ray is probably necessary. He also points out that the interpretation given here of the absence of relativistic rise for the bubble count in liquid hydrogen implies the still unverified assumption that a rise should be observed for the restricted energy loss. Dr. Tenner has carried out a detailed study of the mechanism of bubble formation (145).

rather sensitive to the assumed values of I and T_0, because it is small as compared to the separate values of the minimum and the plateau. (See also the remarks on recent experiments at the end of Sec. 7.1.)

In the process of scintillation, the output of light is influenced greatly by the competing phenomena of dissociation, intermolecular energy exchanges, and radiationless de-excitation, wherein electrons return to lower states, transferring excess energy to molecular vibrations. The competition among alternative processes depends on the concentration of energy deposited along a particle track, particularly in organic scintillators. Light emission is least efficient along the tracks of slower particles where the energy concentration is highest. For example, along a proton track in anthracene the light output per kilo electron volt of energy dissipation decreases from 15 to 5 photons as the proton's energy drops from 100 to 1 MeV (140, p. 127). A disproportionately large fraction of the light emitted along heavy-particle tracks may be contributed by δ-ray branch tracks [Galanin (50), Murray & Meyer (84)].

In many scintillator materials the light is emitted by activator impurities (e.g., by Tl atoms in NaI crystals, by terphenyl in polystyrene), excited by transfer from molecules of the bulk material which have a somewhat higher excitation level. Whether these excitations of the bulk material ($\sim$5 eV in organic scintillators) are closely or remotely related to the collisions of charged particles is still unknown, even though substantial effort has been devoted to study of this question. It is of the essence, in this connection, that the majority of collisions lead to rather high (10–20 eV) excitations, whose study is barely getting under way [see e.g. Platzman (99)].

7.6 *Boundary effects.*—When a fast charged particle traverses the surface of a material (or, more generally, the boundary between any two media), it may experience energy losses that are not otherwise observed during its penetration of the homogeneous portions of the same material. These energy losses are small, of the order of 5 eV, and therefore contribute insignificantly to the overall slowing down of the particle. The formation of a thin oxide film on the surface has, of course, a substantial effect on the magnitude of such an energy loss and on the subsequent phenomena that derive from it.

Macroscopically, as a particle approaches a surface, it induces on it a charge distribution of opposite sign; the combination of the incident and induced charges constitutes a variable dipole which emits a "transition radiation" [Ginzburg & Frank (51)]. Microscopically, the separation of longitudinal and transverse excitations (Sec. 2 3), which hinges on the isotropy of a material, breaks down in the presence of a boundary. Levels of electronic excitation occur which are neither longitudinal nor transverse but are localized near boundaries and have a spectrum different from that of the collective excitations in bulk material discussed in Section 2.10 [Ritchie (103), Ferrell et al. (46); for experimental evidence see Powell (102)]. Thus one speaks of "surface plasmons" in opposition to "volume plasmons," both of them being low-q excitations of the outer atomic electrons influenced pro-

foundly by electrostatic interaction of electrons over distances of the order of 10^{-6} cm. The surface plasmons may decay through the emission of optical radiation from the surface [Ferrell (47)]. This emission has been discovered [Steinmann (116), Brown et al. (33)] and shown to coincide, at least in essence, with the macroscopic transition radiation [Silin & Fetisov (111), Stern (117)].

The surface effects are, of course, particularly accessible to observation when the volume effects are minimized by reducing the total thickness of material. In fact, they have generally been studied through experiments with thin films. However, the occurrence of two film boundaries at a short distance complicates the situation, and detailed understanding of the observations requires thorough experimental and theoretical analysis [Boersch et al. (21), Frank, Arakawa & Birkoff (48), Ritchie & Eldridge (104)].

8. Summary of Tabulations and Formulas

Interpretation of recent information on the stopping power and ranges of mesons, protons, deuterons, and α particles is based mostly on Equations 38 and 39, or on the related Equation 86 for the restricted energy loss, complemented by experimental data. Tabulations differ in general in the values assumed for I, C, and δ. Of these quantities, I has been discussed in Section 3 and C in Section 4; the practical evaluation of δ is described in Section 8.1. Suggested values of I and C/Z are given in Table I and Figure 6, respectively.

Because of the considerable uncertainties on the values of I and C in recent years, the trend is to allow the user maximum flexibility in the choice of these values. To this end, the user may be supplied either with only the raw Equation 38, or with tabulations of parts of this formula, or with more complete tabulations for specified values of I, rather than for specified materials. Evaluation of the formulas is discussed in Section 8.2, the main recent tables in Section 8.3.

The reader is reminded here that the stopping power at lower velocities, at which capture and loss of atomic electrons is frequent, has not been treated in this article. Some information on this subject is given in Section 8.4, and on the related stopping power of fast heavy ions in the companion article by Northcliffe (91).

Semiempirical range-energy formulas, usually of the type $R=aE^b$, have been frequently employed. Their connection with the theoretical formulas will be indicated in Section 8.5.

8.1 *Calculation of δ.*—The density effect correction δ is defined by Equation 48 as an integral in terms of the dielectric constant at all frequencies. The method of evaluation of this integral has been indicated in note 17. Sternheimer (118) has found it adequate and convenient to represent δ by the approximate analytical expressions

$$\begin{aligned}
\delta &= 0 && \text{for } X < X_0 \\
\delta &= 4.606X + C + a(X_1 - X)^m && \text{for } X_0 \leq X \leq X_1 \\
\delta &= 4.606X + C && \text{for } X > X_1 \\
X &= \log_{10}(p/Mc) = \tfrac{1}{2}\log_{10}[\beta^2/(1-\beta^2)] && 92.
\end{aligned}$$

where the parameters a, m, C, X_0, and X_1 have to be given for each material and depend on its dielectric constant.[42] This procedure has been in general use, with somewhat different values of the parameters, depending on the assumed value of I. Notice that the term 4.606 X merely cancels $\ln[\beta^2/(1-\beta^2)]$ in Equation 38 and that $-C=2\ln(I/\hbar\omega_p)+1$, owing to Equation 50. Current values of the parameters are given in Table IV.

8.2 *Evaluation of the stopping power formula.*—Bichsel (14) has cast expression 38 into the form

$$\begin{aligned}
-\frac{dE}{ds} &= z^2\frac{Z}{A}K(\beta)\left\{f(\beta) - \ln(I)_{ev} - \frac{C}{Z} - \tfrac{1}{2}\delta\right\} \text{MeV g}^{-1}\text{ cm}^2 \\
K(\beta) &= 0.307/\beta^2 \\
f(\beta) &= \ln[1.022\times 10^6\beta^2/(1-\beta^2)] - \beta^2 && 93.
\end{aligned}$$

and has given a table of K, f, and β as functions of a proton's kinetic energy. As elsewhere in this article, z is the incident particle's charge in units of e;

TABLE IV

PARAMETERS FOR STERNHEIMER'S EQUATION 92

(Courtesy S. Seltzer)

Z	I(eV)	$-C$	a	m	X_1	X_0
4	64	2.83	0.413	2.82	2.0	−0.10
13	164	4.21	0.0906	3.51	3.0	0.05
29	315	4.38	0.107	3.39	3.0	0.17
47	475	5.09	0.183	3.05	3.0	0.02
82	805	6.16	0.344	2.66	3.0	0.39
92	894	5.89	0.318	2.66	3.0	0.20

$v=\beta c$ represents its velocity; Z/A is the number of electrons per atomic weight unit of the material; I can be taken or interpolated from Table I; C/Z can be read or interpolated from Figure 6; and δ can be calculated from Equation 92 and Table IV. Equation 88 becomes, in a form analogous to Equation 93,

$$\begin{aligned}
\left(-\frac{dE}{ds}\right)_{restr.} &= z^2\frac{Z}{A}K(\beta)\left\{\frac{1}{2}f(\beta) - \ln(I)_{ev} + \frac{1}{2}\ln(T_0)_{ev}\right. \\
&\left. - 0.489\times 10^{-6}(1-\beta^2)(T_0)_{ev} - \frac{C}{Z} - \frac{1}{2}\delta - \frac{1}{2}\Delta_C\right\} \text{MeV g}^{-1}\text{ cm}^2 \quad 94.
\end{aligned}$$

[42] The parameter C in this paragraph is, of course, unrelated to the shell correction indicated by the same symbol.

Approximate analytical formulas to represent C have been given recently by Bichsel (14) and Barkas (7). In Bichsel's work (see Sec. 4.3) an analytical formula with adjusted parameters represents the contribution of each atomic shell or subshell to C. Barkas utilizes an empirical polynomial expression in two variables, $C=F(\eta^{-2}, I)$, which depends on the particle energy through $\eta^2=\beta^2/(1-\beta^2)$ and on the properties of the material through the mean excitation energy I. (This expression has been designed to yield an adequate fit for the total range, but not necessarily for the stopping power; it has been used for $\eta>0.13$ only.) Both the Bichsel and Barkas expressions of C are adjusted to vanish in the high energy limit, whereas C actually remains finite in this limit (see Sec. 4.4). However, this discrepancy is hardly significant at the current level of accuracy, because $(C/Z)_{\gamma=\infty}<0.05$ whereas $f(1)+\cdots$ in Equation 93 exceeds 5.

8.3 *Tables of stopping power and range.*—The most recent tables in regular publication channels appear to be those of Sternheimer (89, 122, 140). These tables provide a good coverage of the subject but two ingredients of their preparation have proved to be inaccurate,[43] namely, the "high" I values ($I/Z\sim13$ eV), akin to those of (36), and the assumption $C\sim C_K+C_L$, i.e., C_M, etc. ~0. Adaptation to improved I values was made possible in (124) by the development of interpolation procedures. These tables extend to a proton energy of 100 GeV.

Still in the "report" stage are two more recent tabulations by Bichsel (14) and Barkas (7), which rest on essentially the same input data and, therefore, differ only in format and in minor details. Bichsel's tables pertain to a set of specific materials and include both stopping power and ranges for proton energies up to 700 MeV.[44] Barkas' single main table gives ranges for proton energies up to 5 GeV. The density effect is not taken into account in this table, but can be corrected for by means of a subsidiary table. Barkas represents the proton range as a smooth universal function of two variables, the proton energy (or velocity) and the mean excitation energy I of the material, and has designed his table for interpolation in both variables. To achieve smoothness, Barkas' main table gives the range in "moles of electrons per cm^2," conversion to g/cm^2 being achieved by multiplication by A/Z (chemical atomic weight per electron). Another extensive table of ranges and stopping power has been prepared recently in report form by Williamson & Boujot (144); this table assumes $I=13.02\ Z$ eV for $Z>5$ and takes into account only the K-shell contribution to shell corrections.

All these range tables can be applied to mesons, hyperons, deuterons, and α particles in accordance with Equation 40; Barkas (7) gives a table of the scale parameter M/z^2. The effect upon the range of electron capture and loss

[43] Improved data on Cu and Pb have been calculated by Dr. Sternheimer [private communication and (122) "Errata"].

[44] Bichsel calls "pathlength" the quantity called "range" in this article and "range" the "projected range" (depth of penetration).

in the terminal section of the path is represented by Barkas as follows. He characterizes the main range data as pertaining to idealized particles with $M/z^2=1$ which do not capture electrons, and then represents the departure from the "idealized" particle range observed for protons or other heavy particles by an additional corrective term $(M/z^2)B_z$. The determination of B_z is an important goal of the studies of electron capture and loss (see Sec. 8.4).

Brandt's report (30) contains a very extensive table of stopping powers and ranges, with particular emphasis on organic compounds. The values of I underlying these tables are much lower than the currently accepted values for $Z>25$; for organic compounds the I values were obtained by theoretical procedures referred to in Section 3.2.

8.4 *Low energy effects of electron capture and loss.*—Empirical range-energy relations, usually in the form of power laws, have been used in the past at low energies where the stopping power theory described in this article breaks down. Recently the trend has emerged to provide the user with extensive range and stopping power tables derived by interpolation from experimental data. Extensive tables of this type for protons from .04 to 10 MeV and for α particles from 3 to 40 MeV have been prepared by Whaling (137).[45] A smaller table of proton ranges, based primarily on new measurements, has been given by Rybakov (106).[46]

For α particles, electron capture is already appreciable at several MeV and is very important at 800 keV. (However, rough data presented by Whaling (137) indicate no significant, ± 20 per cent, influence on stopping power above 1.6 MeV.) Spot comparison of Whaling's α-particle and proton ranges indicates departures from the scaling law 40 of the order of 10 per cent for α particles of energy as high as 8 MeV. The α-particle ranges show here an extension, due to reduced stopping power at lower energies when their charge is reduced by electron capture. Data by Heckman et al. (4) on the corresponding extension for heavier ions indicate, in agreement with Whaling's tables, that the range extension for α particles, B_2, has reached its maximum value at 4 MeV, i.e., that the stopping power theory should apply above this energy. [In emulsion B_z is found (4) to be $\sim z^{8/3}g(137\beta/z)$ where g increases almost linearly from $\beta=0$ to $\beta\sim 20z/137$ and thereafter remains constant at $\sim.2$ μ.] This problem is highly relevant to the accompanying article by Northcliffe (91).

8.5 *Semiempirical range formulas.*—Substitution of the stopping power expression 93 into the range formula 39 yields

[45] Caution is indicated in the use of these tables for protons in the 1–10 MeV range, because they are based largely on experimental data at lower energies and on extrapolation by means of a semitheoretical formula with no shell corrections.

[46] Rybakov's "ranges" represent depth of penetration; a correction (Sec. 6) is required to obtain pathlengths from them.

$$(R)_{g\ cm^{-2}} = 3.25 \frac{A}{z^2 Z} \int_0^{E_0} \frac{\beta^2}{\{f(\beta) + \cdots\}} d(E)_{MeV} \qquad 95.$$

By replacing the slowly varying function $f(\beta) + \cdots$ with a suitable average value, as a first approximation, one obtains

$$(R)_{g\ cm^{-2}} \sim 3.25 \frac{A}{z^2 Z} \frac{1}{\langle f(\beta) + \cdots \rangle} \left(\frac{E_0^2}{E_0 + Mc^2} \right)_{MeV} \qquad 95a.$$

namely, a quadratic dependence of R on the initial kinetic energy E_0 in the nonrelativistic range of energies and a linear dependence in the extreme relativistic range. The transition between these two laws of variation is gradual. This transition is made still smoother when one evaluates Equation 95 taking into account the variation of $f(\beta) + \cdots$, by the circumstance that $f(\beta) + \cdots$ actually increases faster at lower energies, where β^2 also increases, and more slowly at higher energies.

These considerations make it plausible that a plot of $\ln R$ versus $\ln E_0$ exhibits only a small curvature and that appreciable portions of it can be approximated rather accurately by straight lines

$$\ln R = \ln a + b \ln E_0 \qquad \text{(i.e., } R = aE_0^b\text{)} \qquad 96.$$

The slope b lies between 1 and 2 and decreases slowly as E_0 and R increase.

The value $b = 1.75$ has, for example, been utilized for an application to protons up to 300 MeV (78) (see p. 47). Recently Seb (108) has fitted proton ranges in photographic emulsions satisfactorily by means of Equation 96, taking $b = 1.74$ between 7 and 200 MeV and 1.52 between 200 and 1000 MeV. Seb also presents evidence that range-energy curves for different materials are fitted by Equation 96 with the same value of b and with a varying in proportion to I^{-b}. Thereby the range in all materials would be represented by a universal function of the ratio E_0/I. Inspection of the curves in Figure 5 shows that, first, the curves for different materials lie close to one another and, second, they would be pushed still closer over a broad range if the scale of abscissas were changed from $x = v^2/v_0^2 Z$ to $x' = 2mv^2/I$. This last scale would cause the curves to coincide for large x'. On the other hand, inspection of Figure 6, which provides an enlarged view of the differences among materials, shows that no really universal range-energy relation exists. Equation 95a emphasizes that the energy ratio E_0/Mc^2 is highly relevant, Seb emphasizes the relevance of E_0/I and Section 4.4 the relevance of the velocity ratio of the incident particle and atomic electrons, which differs somewhat from E_0/I. In view of these circumstances, a judicious exploitation of the gross simplifying features, of theoretical knowledge, and of empirical fitting of parameters to critical experimental data might well yield, in the next few years, stopping power and range formulas that meet all reasonable tests of simplicity, accuracy, and adherence to relevant physical circumstances.

LITERATURE CITED

1. Agranovich, V. M., *Fiz. Tverd. Tela*, **3**, 811 (1961) [Transl., *Soviet Phys.-Solid State*, **3**, 592 (1961)]
2. Alekseyeva, K. I., Zhdanov, G. B., Zamchalova, E. A., Novak, M., Tretyakova, M. I., and Shcherbakova, M. N., *Proc. III Intern. Conf. Nucl. Photography, Moscow, 1962*, 396; Alekseyeva, K. I., Zhdanov, G. B., Tretyakova, M. I., Tsytovich, V. N., and Shcherbakova, M. N. *IV, Intern. Koll. Korpuskularphot., München, 1963* (In press)
3. Bakker, C. J., and Segrè, E., *Phys. Rev.*, **81**, 489 (1951)
4. Barkas, W. H., *Nuovo Cimento*, **8**, 201 (1958); also Heckman, H. H., Perkins, B. L., Simon, W. G., Smith, F. M., and Barkas, W. H., *Phys. Rev.*, **117**, 544 (1960)
5. Barkas, W. H., *The Velocity Dependence of Bubble-Track Density, Univ. Calif. Radiation Lab. Rept. 9420* (1960)
6. Barkas, W. H., and von Friesen, S., *Nuovo Cimento, Suppl.*, **19**, 41 (1961)
7. Barkas, W. H., *The Range-Energy Function, Univ. Calif. Radiation Lab. Rept. 10292* (1962); to be superseded by ref. (87)
8. Bay, Z., Newman, P. E., and Seliger, H. H., *Radiation Res.*, **14**, 551 (1961)
9. Berger, M. J., *Methods in Computational Physics*, 1 (Alder, B., Fernback, S., and Rothenberg, M., Eds., Academic, New York, 1963)
10. Bethe, H. A., *Ann. Physik*, **5**, 325 (1930); *Handb. Physik*, **24/1**, 491 ff. (Springer, Berlin, 1933)
11. Bethe, H. A., *Phys. Rev.* **89**, 1256 (1953)
12. Biber, C., Huber P., and Müller, A., *Helv. Phys. Acta*, **28**, 503 (1955)
13. Bichsel, H., and Uehling, E. A., *Phys. Rev.*, **119**, 1670 (1960)
14. Bichsel, H., *Passage of Charged Particles through Matter, Univ. So. Calif. Rept. No. 2* (Contract AT(04-3)-136, 1961) (In press as Sec. 8c of *Handbook of Physics*, 2nd ed., McGraw-Hill, New York, 1963); *Higher Shell Corrections in Stopping Power, Univ. So. Calif. Rept. No. 3* (Contract AT(04-3)-136) (1961)
15. Blanchard, C. H., *Natl. Bur. Std. (U.S.), Circ. 527*, 9 (1954)
16. Blinov, G. A., Krestnikov, Iu. S., and Lomanov, M. F., *Soviet Phys. JETP (Engl. Transl.)*, **4**, 661 (1957)
17. Bloch, F., *Z. Physik*, **81**, 363 (1933)
18. Bloch, F., *Ann. Phys. (Leipzig)*, **16**, 285 (1933)
19. Blunck, O., and Leisegang, S., *Z. Physik*, **128**, 500 (1950)
20. Boag, J. W., *Quantities, Units and Measuring Methods of Ionizing Radiation* (Fossati, F., Ed., Hoepli, Milano, 1959)
21. Boersch, H., Radeloff, C. and Sauerbrey, G., *Phys. Rev. Letters*, **7**, 52 (1961)
22. Bohm, D., and Pines, D., *Phys. Rev.*, **92**, 609 (1953)
23. Bohr, A., *Kgl. Danske Videnskab. Selskab, Mat.-Fys. Medd.*, **24**, (19) (1948)
24. Bohr, N., *Phil. Mag.*, **30**, 581 (1915)
25. Bohr, N., *Phil. Mag.*, **25**, 10 (1913); *Kgl. Danske Videnskab. Selskab, Mat.-Fys. Medd.*, **18**, (8) (1948)
26. Booz, J., and Ebert, H. G., *Strahlentherapie*, **120**, 7 (1963)
27. Bortner, T. E., and Hurst, G. S., *Phys. Rev.*, **93**, 1236 (1954)
28. Brandt, W., *Phys. Rev.*, **104**, 691 (1956)
29. Brandt, W., *Phys. Rev.*, **111**, 1042 and **112**, 1624 (1958)
30. Brandt, W., *Phys. Rev.*, **112**, 1624 (1958); *Energy Loss and Range of Charged Particles in Matter* (du Pont Co. Rept., 1960)
31. Brolley, J. R., and Ribe, F. L., *Phys. Rev.*, **98**, 1112 (1955)
32. Brown, L. M., *Phys. Rev.*, **79**, 297 (1950)
33. Brown, R. W., Wessel P., and Trounson, E. P., *Phys. Rev. Letters*, **5**, 472 (1960)
34. Budini, P., and Taffara, L., *Nuovo Cimento*, **4**, 23 (1956)
35. Burkig, V. C., and MacKenzie, K. R., *Phys. Rev.*, **106**, 848 (1957)
36. Caldwell D. O., *Phys. Rev.*, **100**, 291 (1955)
37. Dalgarno, A., *Proc. Phys. Soc. (London)*, *A*, **76**, 422 (1960)
38. Dalgarno, A., *Atomic and Molecular Processes*, 627 (Bates, D. R., Ed., Academic, New York, 1962)
39. Erskine, G. A., *Proc. Phys. Soc. (London)*, *A* **67**, 640 (1954)
40. Fano, U., *Phys. Rev.*, **92**, 328 (1953)
41. Fano, U., *Phys. Rev.*, **95**, 1198 (1954)
42. Fano, U., *Phys. Rev.*, **102**, 385 (1956)
43. Fano, U., *Phys. Rev.*, **103**, 1202 (1956)
44. Fano, U., *Phys. Rev.*, **118**, 451 (1960)

45. Fermi, E., *Phys. Rev.*, **57**, 485 (1940); for a summary and later references see Uehling, E. A., *Ann. Rev. Nucl. Sci.*, **4**, 315 (1954)
46. Ferrell, R. A., *Phys. Rev.*, **107**, 450 (1957); Ferrell, R. A., and Quinn, J. J., *Phys. Rev.*, **108**, 570 (1957); Stern, E. A., and Ferrell, R. A., *Phys. Rev.*, **120**, 130 (1960)
47. Ferrell, R. A., *Phys. Rev.*, **111**, 1214 (1958)
48. Frank, A. L., Arakawa, E. T., and Birkhoff, R. D., *Phys. Rev.*, **126**, 1947 (1962)
49. Fröhlich, H., and Pelzer, H., *Proc. Phys. Soc.* (*London*), *A*, **68**, 525 (1955)
50. Galanin, M. D., *Opt. Spektroskopiya*, **4**, 758 (1958)
51. Ginzburg, V. L., and Frank, J. M., *Zh. Eksperim. Teor. Fiz.*, **16**, 15 (1946)
52. Gombás, P., *Encyclopedia of Physics*, **36/2**, 183 (Fluegge, S., Ed. Springer, Berlin, 1956)
53. Haeberli, W., Huber, P., and Baldinger, E., *Helv. Phys. Acta*, **26**, 145 (1953)
54. Hahn, B., and Hughentobler, E., *Nuovo Cimento*, **17**, 983 (1960)
55. Halpern, O., and Hall, H., *Phys. Rev.*, **73**, 477 (1948)
56. Henneberg, W., *Z. Physik*, **86**, 592 (1933)
57. Hubbard, J., *Proc. Phys. Soc.* (*London*), *A*, **68**, 976 (1955)
58. Jensen, H., *Z. Physik*, **106**, 620 (1937)
59. Jesse, W. P., and Sadauskis, J., *Phys. Rev.*, **90**, 1120 (1953)
60. Jesse, W. P., and Sadauskis, J., *Phys. Rev.*, **107**, 766 (1957)
61. Jesse, W. P., *Phys. Rev.*, **109**, 2002 (1958)
62. Jesse, W. P., *Radiation Res.*, **13**, 1 (1960)
63. Jesse, W. P., and Platzman, R. L., *Nature*, **195**, 790 (1962); also Jesse, W. P., *J. Chem. Phys.*, **3**, 2774 (1963); Platzman, R. L., *J. Chem. Phys.*, **38**, 2775 (1963)
64. Kenney, V. P., *Phys. Rev.*, **119**, 432 (1960)
65. Koch, L., Messier, J., and Valin, J., *IRE Trans. Nucl. Sci.*, **NS8** (1), 43 (1961)
66. Kramers, H. A., *Physica*, **13**, 401 (1947)
67. Kronig, R., and Korringa, J., *Physica*, **10**, 406 (1943); **15**, 667 (1949)
68. Landau, L., *J. Phys.* (*USSR*), **8**, 201 (1944)
69. LaVilla, R., and Mendlowitz, H., *Phys. Rev. Letters*, **9**, 149 (1962)
70. Lewis, H. W., *Phys. Rev.*, **78**, 526 (1950)
71. Lewis, H. W., *Phys. Rev.*, **85**, 20 (1952)
72. Lindhard, J., and Scharff, M., *Kgl. Danske Videnskab. Selskab., Mat.-Fys. Medd.*, **27** (15) (1953)
73. Livingston, M. S., and Bethe, H. A., *Rev. Mod. Phys.*, **9**, 282–83 (1937)
74. McClure, G. W., *Phys. Rev.*, **90**, 796 (1953)
75. McKenzie, J. M., and Bromley, D. A., *Proc. Inst. Elec. Engrs.* (*London*), *B*, **106**, Suppl. 16, 731 (1959)
76. Martin, F. W., and Northcliffe, L. C., *Phys. Rev.*, **128**, 1166 (1962)
77. Marton, L., Leder, L. B., and Mendlowitz, H., *Advan. Electron. Electron Phys.*, **7**, 183 (1955)
78. Mather, R., and Segrè, E., *Phys. Rev.*, **84**, 191 (1951)
79. Mayer, J. W., *J. Appl. Phys.*, **30**, 1937 (1959)
80. Merzbacher, E., and Lewis, H. W., *Encyclopedia of Physics*, **34/2**, 166 (Fluegge, S., Ed., Springer, Berlin, 1958)
81. Messelt, S., *Nucl. Phys.*, **5**, 435 (1958)
82. Miller, W. F., *A Theoretical Study of Excitation and Ionization by Electrons in Helium and of the Mean Energy Per Ion Pair* (Doctoral thesis, Purdue Univ., Lafayette, Ind., 1956)
83. Molière, G., *Z. Naturforsch.*, **3a**, 78 (1948)
84. Murray, R. B., and Meyer, A., *IRE Trans. Nucl. Sci.*, **NS9** (3), 33 (1962)
85. *Penetration of Charged Particles in Matter, Natl. Acad. Sci.—Natl. Res. Council Publ. 752* (1960)
86. *Semiconductor Nuclear Particle Detectors*, especially pp. 91–98, 3–5, *Natl. Acad. Sci.—Natl. Res. Council Publ. 871* (1961)
87. *Penetration of Charged Particles in Matter, Natl. Acad. Sci.—Natl. Res. Council. Publ. 1133* (In preparation)
88. *Penetration of Charged Particles in Matter, Prelim. Rept. Natl. Acad. Sci.—Natl. Res. Council* (1962)
89. *Natl. Bur. Std.* (*U. S.*) *Handbook 79, Stopping Powers for Use with Cavity Chambers* (1961)
90. Neamtan, S. M., *Phys. Rev.*, **92**, 1362 (1953)
91. Northcliffe, L. C., *Ann. Rev. Nucl. Sci.*, **13**, 67 (1963)
92. Nozières, P., and Pines, D., *Phys. Rev.*, **109**, 741, 762, 1062 (1958)

93. Patrick, J. W., and Barkas, W. H., *Nuovo Cimento, Suppl.*, 23, 1 (1962)
94. Perlman, H. S., *Proc. Phys. Soc. (London), A*, 76, 433, 623 (1960)
95. Placzek, G., *Phys. Rev.*, 86, 377 (1952), Secs. 3ff
96. Platzman, R. L., *Symp. Radiobiol., Oberlin Coll., 1950* (1952)
97. Platzman, R. L., *J. Phys. Radium*, 21, 853 (1960)
98. Platzman, R. L., *J. Appl. Radiation Isotopes*, 10, 116 (1961)
99. Platzman, R. L., *Radiation Res.*, 17, 419 (1962)
100. Platzman, R. L. (Private communication)
101. Platzman, R. L., and Miller, W. F. (To be published)
102. Powell, C. J., *Proc. Phys. Soc. (London), A*, 76, 593 (1960)
103. Ritchie, R. H., *Phys. Rev.*, 106, 874 (1957)
104. Ritchie, R. H., and Eldridge, H. B., *Phys. Rev.*, 126, 1935 (1962)
105. Rossi, B., *High Energy Particles*, 29 ff. (Prentice Hall, New York, 1952)
106. Rybakov, B. V., *Zh. Eksperim. Teor. Fiz.*, 28, 651 (1955) [Transl., *Soviet Phys. JETP*, 1, 435 (1955)]
107. Scott, W. T., *Rev. Mod. Phys.*, 35, 231 (1963)
108. Seb, Do In, *Zh. Eksper. Teor. Fiz.*, 43, 121 (1962) [Transl., *Soviet Phys. JETP*, 16, 87 (1963)]
109. Shapiro, M. M., *Encyclopedia of Physics*, 45,/2, 345 (Fluegge, S., Ed., Springer, Berlin, 1958)
110. Shockley, W., *Czech. J. Phys., B*, 11, 81 (1961)
111. Silin, V. P., and Fetisov, E. P., *Phys. Rev. Letters*, 7, 374 (1961)
112. Snyder, H. S., and Scott, W. T., *Phys. Rev.*, 76, 220 (1949)
113. Spencer, L. V., and Fano, U., *Phys. Rev.*, 93, 1172 (1954)
114. Spencer, L. V., *Phys. Rev.*, 98, 1597 (1955)
115. Spencer, L. V., and Coyne, J., *Phys. Rev.*, 128, 2230 (1962)
116. Steinmann, W., *Phys. Rev. Letters*, 5, 470 (1960)
117. Stern, E. A., *Phys. Rev. Letters*, 8, 7 (1962)
118. Sternheimer, R. M., *Phys. Rev.*, 88, 851 (1952)
119. Sternheimer, R. M., *Phys. Rev.*, 89, 1148 (1953); 91, 256 (1953); 93, 1434 (1954)
120. Sternheimer, R. M., *Phys. Rev.*, 93, 351 (1954)
121. Sternheimer, R. M., *Phys. Rev.*, 103, 511 (1956)
122. Sternheimer, R. M., *Phys. Rev.*, 115, 137 (1959) [Errata 124, 2051 (1961)]
123. Sternheimer, R. M., *Phys. Rev.*, 117, 485 (1960)
124. Sternheimer, R. M., *Phys. Rev.*, 118, 1045 (1960)
125. Stiller, B., *IV Intern. Kolloq. Korpuskularphot., München, 1963*
126. Symon, K. R., *Fluctuations in Energy Loss by High Energy Charged Particles in Passing Through Matter* (Doctoral thesis, Harvard Univ., Cambridge, Mass., 1948)
127. Tauc, J., *Phys. Chem. Solids*, 8, 219 (1959)
128. Thompson, T. J., *Effect of Chemical Structure on Stopping Power for High-Energy Protons, Univ. Calif. Radiation Lab. Rept. No. 1910* (1952)
129. Tsytovich, V. N., *Dokl. Akad. Nauk SSSR*, 144, 310 (1962) [Transl., *Soviet Phys. "Doklady,"* 7, 411 (1962)]; *Zh. Eksperim. Teor. Fiz.*, 43, 1782 (1962) [Transl., *Soviet Phys. JETP*, 16, 1260 (1963)]
130. Uehling, E. A., *Ann. Rev. Nucl. Sci.*, 4, 315 (1954)
131. Valentine, J. M., and Curran, S. C., *Rept. Progr. Phys.*, 21, 1 (1958)
132. van Heerden, P. J., *The Crystal Counter* (North-Holland, Amsterdam, 1945)
133. Vavilov, P. V., *Zh. Eksperim. Teor. Fiz.*, 32, 920 (1957) [Transl., *Soviet Phys. JETP*, 5, 749 (1957)]
134. Walske, M. C., *Phys. Rev.*, 88, 1283 (1952) and 101, 940 (1956); also *The Stopping Power of K and L Shell Electrons* (Doctoral thesis, Cornell Univ., Ithaca, N. Y., 1951)
135. Walters, W. L., Costello, D. G., Skofronick, J. G., Palmer, D. W., Kane, W. E., and Herb, R. G., *Phys. Rev. Letters*, 7, 284 (1961) and *Phys. Rev.*, 125, 2012 (1962); Palmer, D. W., Skofronick, J. G., Costello, D. G., Morsell, A. L., Kane, W. E., and Herb, R. G., *Phys. Rev.*, 130, 1153 (1963); see also theoretical discussion by Lewis, H. W., *Phys. Rev.*, 125, 937 (1962)
136. Westermark, T., *Phys. Rev.*, 93, 835 (1954)
137. Whaling, W., *Encyclopedia of Physics*, 34/2, 193 (Fluegge, S., Ed., Springer, Berlin, 1958)
138. Whyte, G. N., *Radiation Res.*, 18 265 (1963)

139. Yang, C. N., *Phys. Rev.*, **84**, 599 (1951)
140. Yuan, L. C., and Wu, C. S., Eds., *Methods Exptl. Phys.*, **5**, Pt. A (1955)
141. Zhdanov, G. B., Tretyakova, M. I., Tsytovich, V. N., and Shcherbakova, M. N., *Zh. Eksperim. Teor. Fiz.*, **43**, 342 (1962) [Transl., *Soviet Phys. JETP*, **16**, 245 (1963)]
142. Sechi-Zorn, B., and Zorn, G. T., *Bubble Density in a Hydrogen Bubble Chamber, Brookhaven Natl. Lab. Rept. 5866* (1962); *Nuovo Cimento, Suppl.* (In press)
143. Zrelov, V. P., and Stoletov, G. D., *Zh. Eksperim Teor. Fiz.*, **36**, 658 (1959) [Transl., *Soviet Phys. JETP*, **9**, 461 (1959)]
144. Williamson, C., and Boujot, J. P., *Tables of Range and Rate of Energy Loss of Charged Particles of Energy 0,5 to 150 MeV Rappt. CEA 2189* (Centre Études Nucl. Saclay, France, 1962)
145. Tenner, A. G., *Nucl. Instr. Methods*, **22**, 1 (1963)

APPENDIX B

PASSAGE OF HEAVY IONS THROUGH MATTER[1,2]

By Lee C. Northcliffe
Department of Physics, Yale University, New Haven, Connecticut

I. INTRODUCTION

The passage of charged atomic particles through matter continues to be a subject of interest and importance to atomic and nuclear physics even after half a century of active investigation. Much of the stimulus for this work has come from the practical demands of experimental nuclear physics, for example, the need for energy loss corrections when particles pass through foil windows, targets, etc., or the use of particle range or specific ionization as a means of energy measurement or of particle identification. It is not surprising that the theoretical and experimental description of alpha-particle and proton penetration phenomena is well advanced since these are the charged particles with which most experiments were performed before the discovery of nuclear fission. Now that accelerated ions of higher atomic number have become available and are used as bombarding particles in a growing variety of experiments, the passage of such ions through matter has become a subject of great practical importance.

It is common practice to call such ions "heavy ions" to distinguish them from protons and alpha particles. Fundamentally this distinction between "light" and "heavy" ions is arbitrary, at least so far as penetration phenomena are concerned, since there is no basic difference in the mechanisms by which protons and heavier ions lose energy while passing through matter. All of the phenomena observed with heavy ions are mirrored in the behavior of protons, and a complete theoretical description of the passage of heavy ions through matter would be valid and complete for protons as well. Conversely, much is to be gained by using the many theoretical and experimental results available for protons and alpha particles as a starting point and as a frame of reference for a discussion of heavy-ion stopping.

Although the distinction between light and heavy ions may be arbitrary it is nonetheless real from a practical viewpoint. The principal difference is that protons and alpha particles can be regarded as charge invariant over most of the energy region of concern to nuclear physics while ions of high

[1] The survey of literature for this review was concluded in March 1963.

[2] This article is related to a "state of the art" survey being conducted by the National Research Council Committee on Nuclear Science, Subcommittee on Penetration of Charged Particles. The forthcoming final report of this survey will contain considerably more detailed information than this article. Members of the Subcommittee are: S. K. Allison, Walter Barkas, Martin J. Berger, Hans Bethe, Hans Bichsel, U. Fano, R. L. Gluckstern, William P. Jesse, Jens Lindhard, L. C. Northcliffe, Robert L. Platzman, R. M. Sternheimer. This work was supported by the United States Atomic Energy Commission.

atomic number can not. As will become clear, with increasing atomic number of the ion there is an expansion of the velocity region in which charge variation is of importance. At velocities where charge variation can be ignored justifiably in the theory of proton energy loss, such variation may influence or even dominate the energy loss process for heavy ions. After recognizing the dominance of this difference it is appropriate to note also the tendency toward increased validity of a classical description of the energy loss process for ions of higher atomic number.

Our knowledge about the passage of protons and alpha particles through matter has been reviewed many times, most recently by Fano (1) in the preceding chapter of this volume. Earlier review articles by Whaling (2), Allison & Warshaw (3), and Bethe & Ashkin (4) contain fragmentary information on heavy ions. Theoretical and experimental knowledge about the penetration of fission fragments and reaction recoil atoms in matter has been surveyed by Bohr (5) and more recently by Harvey (6). The present article is primarily concerned with heavy ions of relatively low atomic number in the velocity region above 10^8 cm/sec. It includes a brief guide to the available theory pertaining to heavy-ion behavior, a survey of experimental data with emphasis on recent results obtained with beams of artificially accelerated ions, and a semiempirical correlation of a representative selection of these data. To some extent protons and alpha particles also are considered as heavy ions in the discussion although no attempt is made to review low energy proton and alpha-particle data comprehensively.

A. Notation and Units

For convenience of reference the symbols recurring throughout this paper and the units in which they are expressed are summarized here. The fundamental constants, $c,\hbar,e$, and m_e (velocity of light, Planck's constant $\div 2\pi$, charge and mass of the electron, respectively) are expressed in cgs esu. The rest mass of the ion [m] and that of an atom of the material medium [M] are in atomic mass units (physical scale); μ is the mass of one atomic mass unit in grams. The atomic number of the ion is z, and the atomic number of an atom of the medium is Z. The kinetic energy of the ion is E^* [ergs], or E [MeV], or $\mathcal{E}_m \equiv E/m$ [MeV/amu]. The integrated path length of the ion in the material medium is x [cm], or X [mg/cm^2]; the range of the ion is R [mg/cm^2]. The density of the material medium is ρ [gm/cm^3], and the number of atoms per unit volume is N [cm^{-3}]. When comparing the behavior of different ions in the same medium it is convenient to use the quantity $\mathfrak{X}_{zm} \equiv z^2X/m$ [mg/cm^2] as a measure of path length.

The instantaneous net charge of the ion is denoted by $\mathcal{Z} \equiv \gamma z$, the average charge at a given velocity by $\langle \mathcal{Z} \rangle \equiv \langle \gamma \rangle z$, the rms charge at a given velocity by $\langle \mathcal{Z}^2 \rangle^{1/2} \equiv \langle \gamma^2 \rangle^{1/2} z$ or $\mathcal{Z}_{rms} \equiv \gamma_{rms} z$, and the effective charge at a given velocity by $\mathcal{Z}_{eff} \equiv \gamma_{eff} z$, all in units of the electronic charge. The fraction of ions having charge $\mathcal{Z}$ in a charge-equilibrated monoenergetic beam is denoted by $\phi_{\mathcal{Z}}$, while the analogous fraction for a beam *not* at equilibrium with respect to

charge change is denoted by ϕ_Z*. The cross section $\sigma_{j,k}$ for change of ion charge from j to k is in units of square centimeters.

The ion velocity is sometimes symbolized by v (cm/sec) but more often is put in dimensionless form, either as $\beta \equiv v/c$, or as $\xi_0 \equiv \hbar v/e^2 = 137\,\beta$ (in units of the Bohr orbital velocity of the electron in the hydrogen atom), or as $\xi = \xi_0/z = 137\,\beta/z$ (in units of the Bohr orbital velocity of its own K electron). The quantity $B \equiv Z\mathfrak{L}$ is the stopping number of a medium for a given ion (dimensionless), while $\Delta B_r \equiv Z\Delta\mathfrak{L}_r$ is the relativistic part of B, and $C_K, C_L \cdots$ are the shell corrections to B. The quantity I is the mean excitation energy of the atomic electrons in ergs, and the Bloch "constant" $K \equiv I/Z$ therefore is in ergs unless otherwise specified.

II. DESCRIPTIVE AND THEORETICAL

If an atom or ion is given a velocity greatly in excess of the orbital velocities of its electrons and allowed to enter a material medium, these electrons will be quickly stripped from the atom and the bare nucleus will proceed through the medium, gradually losing energy because of the multitude of collisions it suffers with the electrons of the medium. (Collisions with the nuclei of the medium will be relatively rare at these high velocities and will play no significant role in the energy loss process.) At first there is a small but finite probability that the ion will capture an electron in one of these collisions and a large probability that the electron will be lost in the next collision, but as the ion slows down and approaches velocities comparable with the orbital velocity of a captured electron, the capture probability increases and the loss probability decreases. As the ion slows to velocities smaller than the orbital velocity of the first captured electron, the capture probability becomes very large and the loss probability approaches zero. Meanwhile the probability of capturing a second electron grows and the corresponding loss probability decreases so that with increasing probability the second electron is retained. As the velocity decrease continues, a third electron is "captured" in the same gradual way, and then a fourth, and so on. The major difference in the description of the capture process for successive electrons is the change in velocity scale necessary to match the progressive decrease of orbital velocity of these electrons within the ion.

Eventually the ion reaches velocities smaller than the orbital velocity of the least tightly bound electron and spends most of its time as a neutral atom. By this time its kinetic energy is being dissipated predominantly by the energy transfer arising from elastic collisions between the screened nuclear fields of the ion and atom, and a diminishing amount of energy is being transferred to the atomic electrons. The neutralized ion is said to be "stopped" when it either reaches thermal velocities or combines chemically with the atoms of the material.

A sketch of the theoretical description of various aspects of this complex process is presented in this section.

A. Electronic Stopping Power at High Energies

1. *The theoretical formula.*—It is well recognized that heavy charged particles lose energy while passing through matter predominantly through ionization and excitation of the atoms in the material. An essential aim of any theoretical description of this process is to predict the average energy loss per unit path length in the material, a quantity usually called the "stopping power" of the material of the ions.[3] There have been numerous theoretical treatments of this problem. Generally, these begin with different assumptions, have different regions of applicability, and give somewhat different formulas for the stopping power. It is convenient to collect the common features of these formulas into a universal term and confine the differences to a dimensionless multiplier B called the "stopping number." In this conventional form the theoretical formula for the "electronic" stopping power is

$$-\frac{dE^*}{dx}\left(\frac{\text{erg}}{\text{cm}}\right) = \frac{4\pi Z^2 e^4}{m_e v^2} NB = 7.341 \times 10^{-10}\left(\frac{Z^2 N}{v^2}\right) B = 4.921 \times 10^{-7}\left(\frac{Z^2 \rho}{\beta^2 M}\right) B \quad 1.$$

Alternative expressions in more convenient units are

$$-\frac{dE}{dx}\left(\frac{\text{MeV}}{\text{cm}}\right) = 0.3072\left(\frac{Z^2 \rho}{\beta^2 M}\right) B \quad 1a.$$

and

$$-\frac{dE}{dX}\left(\frac{\text{MeV}}{\text{mg/cm}^2}\right) = 3.072 \times 10^{-4}\left(\frac{Z^2}{\beta^2 M}\right) B \quad 1b.$$

A thorough discussion of the various formulas for B would go well beyond the scope of this article since it would include most of the content of stopping-power theory. [Several such discussions are available (1, 4, 5, 7), the most recent being that given by Fano (1) in the accompanying article.] Nevertheless, certain observations about B can best be made by considering briefly three of the most familiar theoretical treatments.

In the pioneering paper on the subject, Bohr (8) calculated the stopping power by means of nonrelativistic classical mechanics, assuming a Rutherford model of the atom, and obtained a result which can be expressed in the form[4]

$$B = \sum_i \ln \frac{1.123 m_e v^3}{Z e^2 \omega_i} = Z \ln \frac{1.123 m_e v^3}{Z e^2 \omega} \quad 2.$$

where $\omega_i/2\pi$ is the natural frequency for oscillation of the ith electron about its equilibrium position in the atom, the sum includes all atomic electrons,

[3] Often the rate of energy loss is given in terms of the "stopping cross section" ϵ related to the stopping power by the formula $\epsilon = N^{-1} dE/dx = \rho N^{-1}\, dE/dX$.

[4] More exactly, the mass in Eq. 2 should be the reduced mass $m_e \mu m\ (\mu m + m_e)^{-1}$ rather than the electron mass m_e, but for ions of mass $m \geq 1$ amu the simplification causes negligible change in the calculated stopping-power value.

and the effective frequency ω may be regarded as implicitly defined by the equation.

The first purely wave-mechanical solution to the problem was obtained by Bethe (9) through use of the Born approximation. For ions at nonrelativistic velocities, the stopping number given by Bethe's theory is

$$B = \sum_{i,k} f_{i,k} \ln \frac{2m_e v^2}{\hbar\omega_{i,k}} = Z \ln \frac{2m_e v^2}{I} \qquad 3.$$

in which $f_{i,k}$ is the atomic oscillator strength for the transition (i, k) with the frequency $\omega_{i,k}/2\pi$. The quantity I is the mean excitation energy of the atomic electrons and its definition in terms of the individual possible transitions is analogous to the definition of ω in terms of the possible ω_i values in Equation 2. Intuitively, it is tempting to associate the quantum-mechanical frequency equivalent of I with Bohr's effective vibrational frequency ω, implying the relationship $I = \hbar\omega$, and in fact a semi-quantum-mechanical theory developed by Gaunt (10) gives a formula for B which can be obtained from Bohr's formula using this substitution.

A more substantial bridge between the results of Bohr (Eq. 2) and Bethe (Eq. 3) was provided by Bloch (11) who took into account the perturbation of the wave functions of the atomic electrons caused by the presence of the incident particle. In Bloch's result the nonrelativistic stopping number is given by the formula

$$B = Z\left[\ln \frac{2m_e v^2}{I} + \psi\{1\} - \mathrm{Re}\psi\{1 + i(Z/\xi_0)\}\right] \qquad 4.$$

in which ψ is the logarithmic derivative of the gamma function and $\mathrm{Re}\psi$ is the real part of ψ. The interesting feature of this result is that it reduces to Equation 2 in the limit $Z/\xi_0 \gg 1$ and to Equation 3 in the limit $Z/\xi_0 \ll 1$, assuming that I can be replaced by

$$I = \hbar\omega \qquad 5.$$

Each of these authors extended his treatment to include a determination of the change in his stopping-power formula for ions at relativistic velocities (11, 12, 13). In all three cases the relativistic correction is the same; the quantity

$$\Delta B_r = Z\Delta\mathfrak{L}_r = Z[-\ln(1-\beta^2) - \beta^2] \qquad 6.$$

is added to the nonrelativistic stopping number. In addition, considerable attention has been devoted to the problem of determining corrections to Bethe's formula (the shell corrections C_K, C_L, $\cdots$) which become necessary when the tightly bound inner electrons of the atom fail to participate fully in the stopping process. This problem is discussed in detail by Walske (14), Bichsel (15), and Fano (1).

Bloch (16) provided another interesting insight by showing that in material media consisting of atoms adequately described by the Thomas-

Fermi atomic model (i.e., large Z) the mean excitation energy I is expected to be approximately proportional to Z,

$$I = KZ \qquad 7.$$

The empirically determined values of the "Bloch constant" K do turn out to be approximately the same [$\sim$10eV] for a wide range of Z values [Fano (1, Table I)].

It will be sufficient for present purposes first to make some general observations about the form and implications of the above results and then to consider some of the limitations of these theories when applied to the energy loss of heavy ions.

On the strength of these results it seems reasonable to suppose that the electronic stopping power is representable in general by a formula of the form

$$-\frac{dE}{dX} = k_1 \frac{(\gamma z)^2}{\beta^2} \frac{Z}{M} [\mathfrak{L}\{\beta, (\gamma z), Z\} + \Delta\mathfrak{L}_\tau\{\beta\}] \qquad 8.$$

where the function $\mathfrak{L}$ is the nonrelativistic stopping number per atomic electron, k_1 is the constant of Equation 1b, and the ion charge Z has been replaced by the equivalent term γz so as to separate the basic dependence on atomic number z of the ion from the influence of its temporary charge. The precise meaning of γ will be discussed more fully in Section II.B.3.

The exact dependence of $\mathfrak{L}$ on velocity is complicated and not entirely known but characteristically logarithmic; $\mathfrak{L}$ increases slowly with increasing ion velocity. The dependence of $\mathfrak{L}$ on Z arises indirectly, through the Z dependence of I [or ω] and of the shell corrections C_K, C_L, $\cdots$. Qualitatively $\mathfrak{L}$ is expected to decrease slowly with increasing Z. The possibility of a dependence on Z is indicated only parenthetically because Bethe's stopping number contains no such dependence even when shell corrections are considered. There is no reason to expect a dependence of $\mathfrak{L}$ on either M or m provided that the ion is heavy [$m \geq 1$ amu].

Considerations along these lines led Lindhard & Scharff (17) to an approach in which $\mathfrak{L}$ is regarded as a function of the dimensionless variable ξ_0^2/Z. The reasonability of this can be seen by substituting the Bloch relation [Eq. 7] into the Bethe stopping-number formula [Eq. 3] since the result, $\mathfrak{L} = \ln 2 m_e [(c/137)^2/K] + \ln(\xi_0^2/Z)$, implies a linear relationship between $\mathfrak{L}$ and $\ln \xi_0^2/Z$. Lindhard & Scharff chose to regard $\mathfrak{L}$ as an unknown universal function of ξ_0^2/Z, the form of which could be determined empirically by plotting the $\mathfrak{L}$ values calculated from experimental stopping-power data (using Eq. 8) vs. $\ln (\xi_0^2/Z)$. The result is a gratifyingly smooth curve (almost a straight line) with little dependence on Z [see Fig. 5 of (1) for a current version of this plot]. The slight dependence on Z corresponds to the slight inconstancy of K while the deviation from linearity reveals the departures from Bethe's formula in its uncorrected form (Eq. 3).

Were it not for the variable γ in Equation 8, it would be possible to calculate the stopping power of any material for any ion with reasonable accuracy through use of a Lindhard-Scharff plot and Equation 8, assuming

there is no dependence of $\mathfrak{L}$ on z.[5] Thus two questions assume importance: the dependence of $\mathfrak{L}$ on z, and the dependence of γ on Z, M, z, m, and v. It should be observed that the appropriate value of γ must be known before an empirical value of $\mathfrak{L}$ can be calculated, and thus the second question takes precedence over the first. Experimental data bearing on these questions will be considered in Section III. For the time being it is sufficient to note that the fractional charge γ is strongly dependent on v and z, somewhat dependent on Z and on the physical state and density of the medium, and probably not dependent on M and m.

2. *Relative stopping power.*—In terms of the viewpoint developed in the preceding section, the calculation of a theoretical value for the stopping power is reduced to the equivalent problems of calculating the values of $\mathfrak{L}$ and γ. Both of these are such formidable problems that their exact and general solution is probably unattainable. Even within the framework of Bethe's theory, for example, it is possible to calculate the value of I from first principles only in the simplest cases. Therefore I is normally regarded as an adjustable parameter characteristic of a given material medium but independent of v and z, and its value is determined empirically. In the same semiempirical spirit it is convenient to discuss the stopping powers for different ions or media in relative terms.

For both $\mathfrak{L}$ and γ the dependence on v is complicated and imperfectly known. It is best to eliminate it from the comparison of stopping powers for different ions or media by requiring that the ions have the same velocity. An equivalent requirement expressed in terms of energy is that the ions being compared have the same value of $E/m \equiv \mathcal{E}_m$. If $\mathcal{E}_m$ is introduced as the measure of ion energy it is advantageous to introduce the quantity $\mathfrak{X}_{zm} \equiv (z^2/m)X$ as the measure of path length. Then Equation 8 simplifies to the form

$$-\frac{d\mathcal{E}_m}{d\mathfrak{X}_{zm}} = -\frac{1}{z^2}\frac{dE}{dX} = \frac{k_1}{\beta^2}\frac{Z}{M}\gamma^2\{\beta, z, Z, \rho\}\left[\mathfrak{L}\{\beta, (\gamma z), Z\} + \Delta\mathfrak{L}_r\{\beta\}\right] \qquad 9.$$

All of the variables which seem likely to influence the functions γ, $\mathfrak{L}$, and $\Delta\mathfrak{L}_r$ are indicated. The relative stopping power of a given material medium for *different ions* moving with the same velocity is given by the ratio

$$\left(\frac{d\mathcal{E}_m}{d\mathfrak{X}_{zm}}\right)_2 \Big/ \left(\frac{d\mathcal{E}_m}{d\mathfrak{X}_{zm}}\right)_1 = \left(\frac{\gamma\{(z_2)\}}{\gamma\{(z_1)\}}\right)^2 \left[\frac{\mathfrak{L}\{(Z_2)\} + \Delta\mathfrak{L}_r}{\mathfrak{L}\{(Z_1)\} + \Delta\mathfrak{L}_r}\right]; \ (\mathcal{E}_m)_1 = (\mathcal{E}_m)_2 \qquad 10.$$

[5] Lindhard & Scharff used only proton and alpha-particle stopping-power data in their plot, presumably because of the uncertainty in the value of γ for heavier ions. Where charge distribution data are available and γ can be calculated (see Sec. II.B.3.), a Lindhard-Scharff plot could be made for heavy ions and compared with that for protons. To the extent that the calculation of γ is reliable, any difference in the plots would reveal the dependence of $\mathfrak{L}$ on z. While this approach has not been explored, it would seem to be worthwhile wherever heavy-ion charge distribution and stopping-power data of adequate accuracy are available.

It will be noted that the term in square brackets becomes unity when $\mathfrak{L}$ is independent of z, as it is in Bethe's theory, and Equation 10 then reduces to

$$\left(\frac{d\mathcal{E}_m}{d\mathfrak{X}_m}\right)_2 = \left(\frac{\gamma\{z_2\}}{\gamma\{z_1\}}\right)^2 \left(\frac{d\mathcal{E}_m}{d\mathfrak{X}_m}\right)_1 \qquad 10a.$$

Alternatively, the relative stopping power of two *different material media* for the same ions moving with the same velocity is given by the ratio

$$\frac{M'}{Z'}\left(\frac{dE}{dX}\right)' \Big/ \frac{M}{Z}\left(\frac{dE}{dX}\right) = \left(\frac{\gamma\{Z',\rho'\}}{\gamma\{Z,\rho\}}\right)^2 \left[\frac{\mathfrak{L}\{(Z'),Z'\} + \Delta\mathfrak{L}_r}{\mathfrak{L}\{(Z),Z\} + \Delta\mathfrak{L}_r}\right] \qquad 11.$$

It is also of practical value to consider the case when γ is independent of Z and ρ since the dependence often is negligibly small. In such cases Equation 11 reduces to

$$\frac{M'}{Z'}\left(\frac{dE}{dX}\right)' = \left[\frac{\mathfrak{L}\{Z'\} + \Delta\mathfrak{L}_r}{\mathfrak{L}\{Z\} + \Delta\mathfrak{L}_r}\right]\frac{M}{Z}\left(\frac{dE}{dX}\right) \qquad 11a.$$

3. *Limitations of the theories.*—The necessary conditions for the validity of the three stopping power formulas (Eqs. 2–4) have been discussed by many authors (1, 4, 5, 11, 18, 19). A brief summary and discussion of these requirements and their implications for heavy-ion stopping is in order. To begin with the classical formula (Eq. 2), the assumptions made by Bohr (8) in his original treatment can be represented by the two inequalities

$$Z \ll \xi_0 \qquad 12.$$

$$(Z^2Z)^{1/3} \ll \xi_0 \qquad 13.$$

Williams (18) gives two additional requirements for validity of a classical description, the condition

$$\frac{\hbar}{(\mu m)v} \ll \text{size of scattering field}, \qquad 14.$$

which is satisfied in all cases under consideration here, and the more restrictive condition

$$Z \gg \xi_0 \qquad 15.$$

By contrast, the use of the Born approximation in Bethe's quantum-mechanical treatment is associated with the restriction

$$Z \ll \xi_0 \qquad 16.$$

In addition Bethe's original derivation of Equation 3 also involved assumption of inequality 12, although this restricition is removed if the proper shell corrections C_K, C_L, $\cdots$ are included. Bloch (11) avoided the assumption of inequality 16 but only at the expense of requiring inequality 12 and the additional inequality

$$(ZZ)^{1/3} \ll \xi_0 \qquad 17.$$

The domains of validity implied by these various restrictions are shown in Figure 1, (p.76), a three-dimensional graph of Z vs. Z vs. $(\mathcal{E}_m)^{1/2}$, divided

into five regions by the five boundary surfaces corresponding to inequalities 12, 13, 15–17. Clearly these surfaces should be regarded only as approximate indications of the location of diffuse boundaries.[6] The implications of this diagram are largely self evident and will not be labored. The most important feature to be noted is the decreasing applicability of these theories with decreasing ion velocity.

The diffuseness of the boundaries of applicability in Figure 1 is not the only reservation to be borne in mind. Strictly speaking, the theories are valid only for a material medium consisting of isolated atoms (i.e., a rarefied gas). Also, the structure of the ion is ignored. On the other hand, some of the restrictions may be too harsh. For example, Mott (19) has shown that the Born approximation gives the right result independent of inequality 16 provided that $Z \ll Z$, thus considerably extending the domain of validity of Bethe's theory.

B. Fluctuation of Ion Charge

1. *Charge distributions and charge-change cross section.*—When an ion moves through matter with a velocity comparable with the orbital velocity of its own electrons, its net charge will fluctuate rapidly as electrons are captured or lost in the rapid succession of collisions with atoms of the material. Thus at any given instant a monoenergetic beam of otherwise identical ions will be characterized by a distribution of charge states. If ϕ_Z is the fraction of the ions which have charge Z, where Z can be any integer $0 \leq Z \leq z$, then the distribution is represented by the set of numbers $\phi_0, \phi_1, \cdots \phi_z$.[7] The average value of Z is

$$\langle z \rangle = \sum_{0}^{z} Z\phi_Z \qquad 18.$$

It is to be expected (and is verified experimentally) that the values of ϕ_Z become vanishingly small when Z differs greatly from $\langle Z \rangle$.

Since the energy loss of the ion in individual collisions is very small, a large number of collisions will occur while the ion velocity remains virtually unchanged, and an equilibrium with respect to electron capture and loss will be established. The set of probabilities ϕ_Z then describes the equilibrium distribution of charge states present in an otherwise homogeneous beam of the ions, and $\langle Z \rangle$ will be the equilibrium mean charge of the ions. However, such an equilibrium normally will not exist when the beam first enters the medium, and the set of probabilities ϕ_Z^* will describe the nonequilibrium distribution of charge states. The nonequilibrium mean charge $\langle Z^* \rangle$ can be defined by analogy with Equation 18. Both types of distribution are of interest, but for different reasons. The equilibrium distribution determines

[6] For example, Bohr (5) uses the inequality $2Z \ll \xi_0$ in place of inequality 16.

[7] In some circumstances there is a finite probability that $Z = -1$ but the probability is always small and the ϕ_{-1} term will be ignored.

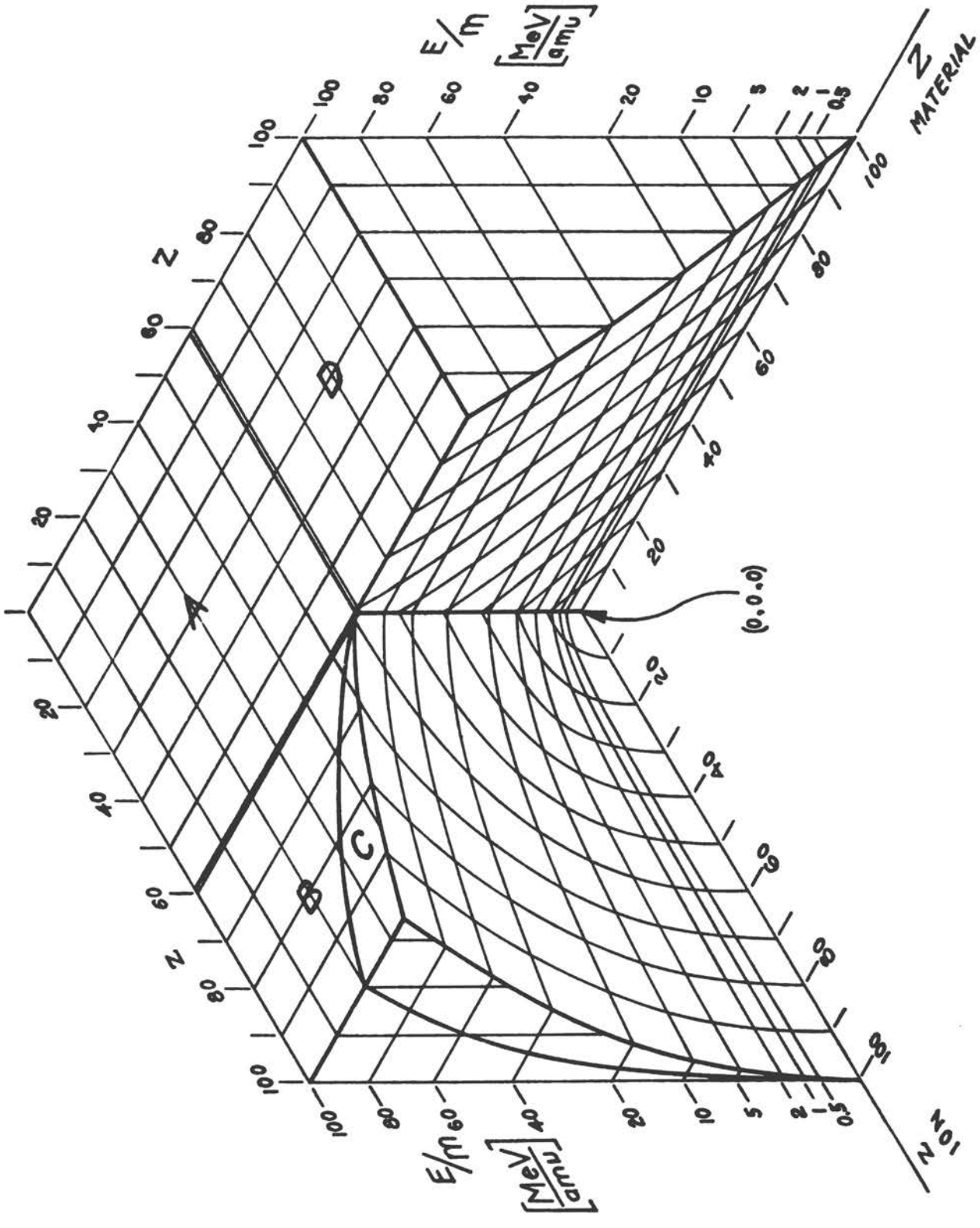
E/m [MeV/amu]
100
80
60
40
20
10
5
2
1
0.5
Z
MATERIAL
100
80
60
40
20
10
5
2
1
Z
A
B
C
D
(0,0,0)
E/m [MeV/amu]
Z

the rate of energy loss of the ions (through the quantity γ of Eqs. 8–11) while the transient behavior of the nonequilibrium distribution reveals the magnitude of the capture and loss cross sections (see Footnote 7).

The capture (or loss) cross section $\sigma_{j,k}$ is the quantitative measure of the probability that an ion of net charge j will capture (or lose) one or more electrons and become an ion of net charge k. It is defined by the formula $\sigma_{j,k}=dn_{j,k}/Ndx$, where $dn_{j,k}$ is the probability that the charge of the ion will change from j to k while the ion moves through the infinitesimal distance dx in a material containing N atoms per unit volume. If $j>k$, then $\sigma_{j,k}$ is a capture cross section, and if $j<k$, it is a loss cross section.

It is easily seen that the charge-change cross sections are related to the nonequilibrium charge distributions through the set of equations

$$\frac{d\phi_Z^*}{dx}=N\sum_{j=0}^{s}(\sigma_{j,Z}\phi_j^*-\sigma_{Z,j}\phi_Z^*);\ Z=0,1,\cdots s \qquad 19.$$

and to the equilibrium charge distributions through the set of equations

$$\frac{d\phi_Z}{dx}=0=\sum_{j=0}^{s}(\sigma_{j,Z}\phi_j-\sigma_{Z,j}\phi_Z);\ Z=0,1,\cdots s \qquad 20.$$

If the values of $\sigma_{j,k}$ are known, the values of both ϕ_Z and ϕ_Z^* can be calculated easily.[8]

2. *Theoretical treatments.*—A bibliography of theoretical papers concerned with the capture and loss of electrons by protons and alpha particles is contained in a recent review paper by Allison (20). While reasonable agreement can be obtained between theory and experiment in the simplest cases [e.g., protons in H_2 gas, see Jackson & Schiff (21)], the processes involved in the capture or loss of an electron by a moving heavy ion are in general so intricate as to defy precise and compact description. Various

[8] The converse calculation is more difficult since there are $s(s+1)$ values of $\sigma_{j,k}$ and only $(s+1)$ values of Z, and thus the set of Eqs. 20 is insufficient for the determination of $\sigma_{j,k}$. If multiple charge change is negligible, however (usually a reasonable assumption), it is easily seen that under equilibrium conditions $\sigma_{j,j+1}/\sigma_{j+1,j}=\phi_{j+1}/\phi_j$. Thus loss to capture cross-section ratios are given by the equilibrium charge-fraction ratios. In order to determine individual $\sigma_{j,k}$ values, it is necessary to investigate the nonequilibrium charge distribution as a function of penetration depth. In practice the initial beam is usually in a single charge state k so that $\phi_k^*=1$ and $\phi_{j\neq k}^*=0$ at $x=0$. Then Eqs. 19 evaluated at $x=0$ become $(d\phi_Z^*/dx)_{x=0}=N\sigma_{k,Z}$ for $Z\neq k$, and $(d\phi_k^*/dx)_{x=0}=-N\sum_{j=0}^{s}\sigma_{k,j}$.

Fig. 1. Regions of applicability of various stopping-power formulas; Bethe theory (Eq. 3)—region *A;* Bohr theory (Eq. 2)—region *B;* Bloch theory (Eq. 4)—regions *A*, *B*, and *C;* Bethe theory with shell corrections—regions *A* and *D*. Each of the regions is wedge shaped and approaches zero in width as the ion velocity approaches zero. The boundaries are diffuse and their locations are somewhat uncertain.

theoretical treatments of this problem have been based on simplified or even crude models. Usually they can claim only approximate validity and are applicable only in restricted regions of Z, z, and v.

The earliest theoretical discussions of the charge variation of ions heavier than the α particle arose in attempts to account for the range of fission fragments in matter. Bohr (22) based an estimate of the fragment charge on the assumption that an electron was permanently captured by the fragment when its orbital velocity in the fragment (crudely estimated) exceeded the velocity of the fragment. Lamb (23) made the essentially equivalent assumption that an electron of the medium would be permanently captured when its kinetic energy in the coordinate system of the fragment was less then the binding energy of the lowest unfilled bound state of the fragment. Knipp & Teller (24) followed Bohr's approach but used a Thomas-Fermi model to obtain more accurate estimates of orbital electron velocities and regarded the velocity ratio v_e/v_c (electron orbital velocity to critical ion velocity at which the electron is attached) as an unspecified parameter, to be determined empirically. This approach was explored still further by Brunings, Knipp & Teller (25) who extracted the electron velocity v_e from the Thomas-Fermi model on the extreme alternative assumptions that v_e is (a) the velocity of the least tightly bound electron, or (b) the velocity of the outermost electron. The velocities given by assumptions (a) and (b) might be regarded as upper and lower limits of v_e respectively and, not surprisingly, the authors found the empirically indicated values of v_e/v_c to be >1 on assumption (a) (increasing from ~ 1.2 for $z=10$ to ~ 1.8 for $z \sim 55$), and <1 on assumption (b) (decreasing from ~ 0.6 for $z=6$ to ~ 0.35 for $z \sim 55$).

It was realized by all of these authors, of course, that electron capture is a much more complex phenomenon than the one-step irreversible process assumed and that a proper description would involve an equilibrium distribution of charge states ϕ_Z given by the capture and loss cross sections $\sigma_{j,k}$, as in Equation 20. The simplified picture is qualitatively correct because the values of ϕ_Z are appreciable only for charge states Z in which the least tightly bound electrons have velocities of the order of the ion velocity. An interesting phenomenological method of predicting these charge distributions was developed by Dmitriev (26), again on the assumption that the relative velocity v/v_e is the key parameter. Representing the probability that the ith electron is attached to the ion by the function P_i, he assumed that P_i is the same smoothly varying universal function of the relative velocity v/v_{ei} for all electrons of the ion and for all ions in a given medium, and in particular that the value of P_i is uninfluenced by the presence or absence of other electrons in the ion. He applied this model to ions of moderately low z [$2 \leq z \leq 9$], and assumed the value of v_{ei} to be the velocity $(2I_i/\mu m)^{1/2}$ corresponding to the empirical ionization potential I_i of the ith electron. The dependence of the universal function P on v/v_e was assumed to be the same as the observed variation of the proton fraction ϕ_1 of a hydrogen beam with velocity v. On these assumptions the values of P_i are

determined, and then the charge fractions ϕ_Z are obtained by appropriate summations. A variant of this method was used by Heckman, Hubbard & Simon (27) in the analysis of their experimental equilibrium charge distribution data for heavy ions in Zapon. They achieved good fits by deriving the universal function P from their own data rather than proton charge fraction data, and by assuming different universal functions for the K and L electrons.

In his comprehensive treatise on the penetration of charged particles in matter, Bohr (5) derived estimates of the capture and loss cross sections on the assumptions (among others) that the electron velocities in the ion and atom are given by a simplified Thomas-Fermi model and that the ion returns to its ground state between collisions. The latter assumption severely restricts the usefulness of these estimates since it is fulfilled only in the case of very rarefied gaseous media. Bell (28) and Gluckstern (29), using more sophisticated versions of the Thomas-Fermi model and more detailed descriptions of the charge exchange collisions, calculated capture and loss cross sections for some representative heavy ions in rarefied gases by numerical methods.

In order to eliminate the restriction to rarefied gases and to account for the observed dependence of the charge of a fission fragment of a given velocity on the density and state of condensation of the material medium, Bohr & Lindhard (30) reconsidered the problem, taking the effect of residual excitation of the ion on the charge-change mechanism into account, and derived revised estimates of the capture and loss cross sections. On the other hand, Neufeld, working alone (31) and with Snyder (32), showed that the process of "autoionization" (field emission of electrons from the moving ion, caused by polarization of the medium in its wake) is partly responsible for the difference in charge of a fission fragment in solids and in gases.

3. *Effective charge.*—As defined in connection with Equation 8, the quantity γ is the ratio of the instantaneous charge of an ion to its nuclear charge. Thus Equation 8 gives the instantaneous rate of energy loss while the ion has charge Z. However, the ion charge will fluctuate and consequently the rate of energy loss will fluctuate. Since the instantaneous stopping power varies approximately as Z^2 and the ion spends the fraction ϕ_Z of its time in charge state Z, it is to be expected that the average stopping power will be approximately proportional to the mean squared charge of the ion, given by $\langle Z^2 \rangle = \langle \gamma^2 \rangle z^2$ where

$$\langle \gamma^2 \rangle = \gamma_{rms}^2 = \sum_{Z=1}^{z} \phi_Z (Z/z)^2 \qquad 21.$$

Since this average stopping power usually is the quantity of practical interest, the values of γ used in Equations 8–11 should be the root mean square values defined by Equation 21.

An alternative approach is suggested by the approximate expression (Eq. 10a) for the relative stopping power of a given medium for two dif-

ferent ions. Since both γ_{rms} and $d\mathcal{E}_m/d\mathcal{X}_{zm}$ are rather well known for protons, it is useful to regard the proton as a reference ion associated with the subscript "1" in Equation 10a. Then the measured value of $d\mathcal{E}_m/d\mathcal{X}_{zm}$ for any other ion (subscript "2") can be characterized by an effective charge $Z_{eff}=\gamma_{eff}Z$ defined purely in terms of empirical measurements by the equation

$$(\gamma_{eff})_2 = (\gamma_{rms})_1 \left[\frac{(d\mathcal{E}_m/d\mathcal{X}_{zm})_2}{(d\mathcal{E}_m/d\mathcal{X}_{zm})_1}\right]^{1/2} \qquad 22.$$

If Equation 10a is valid (i.e., if Eq. 8 is valid and $\mathcal{L}$ is independent of Z), then of course $(\gamma_{rms})_2$ and $(\gamma_{eff})_2$ are equal. Conversely, nonequality of $(\gamma_{rms})_2$ and $(\gamma_{eff})_2$ indicates either a dependence of $\mathcal{L}$ on Z or, more fundamentally, some inadequacy of the theoretical descriptions leading to Equation 8.

Indeed, such inadequacy would be expected when the ion velocity decreases to the point where the energy loss from "nuclear" collisions becomes important. Moreover, at low velocities the implicit assumption that an ion may be treated as a moving point charge of magnitude $\gamma_{rms}z$ may no longer be good since atomic electrons penetrating the ionic charge cloud during collisions would see a higher effective charge than that given by the equilibrium charge of the ion. While Bohr (5) at first estimated that the effect of finite ion dimensions would be negligible, a revised estimate by Bohr & Lindhard (30) indicated that such an assumption may not be justified for very heavy ions.

C. Electronic Stopping Power at Low Energies

At high ion velocities ($\xi_0 \gg z$) the stopping power increases with decreasing velocity roughly as β^{-2}, but at intermediate velocities ($\xi_0 \sim z^{2/3}$) the gradual neutralization begins to dominate this dependence, and the stopping power goes through a maximum. As the decrease in ion velocity continues, the electronic stopping power decreases, eventually falling to zero. In the limit of very low velocities ($\xi_0 < 1$), a theory developed by Fermi & Teller (33) to describe the stopping power for μ mesons and adapted by Warshaw (34) to apply to protons predicts a stopping power which is proportional to β. The same dependence was found theoretically by Lindhard (35) and semiempirically by Lindhard & Scharff (17). In a later paper, Lindhard & Scharff (36) used the Thomas-Fermi model to find the dependence of electronic stopping power on z and Z in the velocity region below $\xi_0 \sim z^{2/3}$ and found it to be given approximately by the formula

$$\left(-\frac{dE^*}{dx}\right)_e = \kappa_e 8\pi e^2 N a_0 \frac{zZ}{(z^{2/3}+Z^{2/3})^{1/2}}\xi_0 \qquad 23.$$

in which a_0 is the Bohr radius of the hydrogen atom and κ_e is a numerical factor of the order of $z^{1/6}$.

D. Nuclear Stopping Power

A heavy ion at high velocities ($\xi_0 \gg 1$) loses very little energy through collisions with nuclei of the medium, but this is no longer true when the

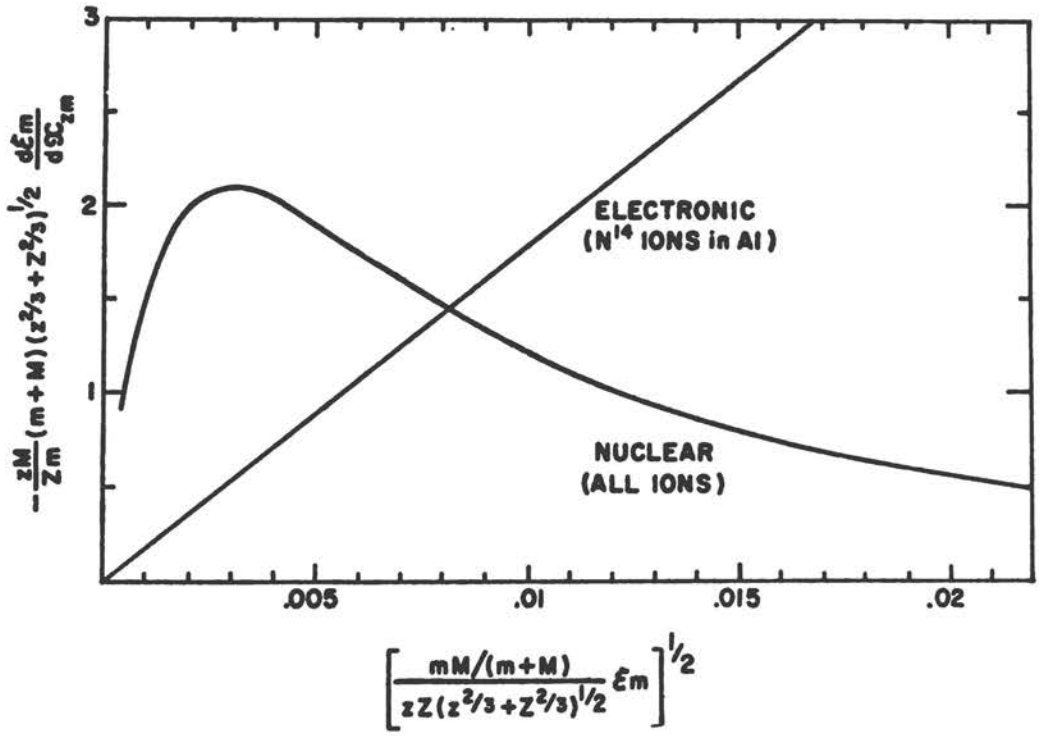

FIG. 2. Universal nuclear stopping-power curve for heavy ions at low velocities. A typical electronic stopping-power curve given by Eq. 23 also is shown.

ion is moving so slowly ($\xi_0 \sim 1$) that its average net charge approaches zero. While the electronic stopping power is declining to zero with decreasing ion velocity, the average energy loss per unit path length from elastic nuclear collisions (i.e., the "nuclear" stopping power) is increasing rapidly (approximately as β^{-2}). Below a certain critical velocity ($137\,\beta_c \ll 1$) the nuclear stopping power exceeds the electronic stopping power. Eventually, as screening of the nuclear fields of the ion and atom becomes the dominant factor, the nuclear stopping power goes through a maximum and then also declines to zero.

The role of nuclear collisions in the penetration process was discussed extensively by Bohr (5). More recently Bohr's ideas have been developed and refined by Nielsen (37), Lindhard & Scharff (36), and Lindhard, Scharff & Schiøtt (38). The latter authors have derived a universal curve for the nuclear stopping power, using the Thomas-Fermi model to determine the effects of screening. This curve is shown in Figure 2 along with a typical electronic stopping power curve given by Equation 23.

E. Statistical Fluctuations

Because of the statistical nature of the energy loss process, individual particles starting with the same velocity and direction at the same point will follow somewhat different paths and at any given depth of penetration will be distributed in energy, in direction of motion, and in lateral displacement from the projection of their common initial path. Similarly, they will

come to rest at positions distributed both in depth of penetration and in lateral displacement from the projected initial path. This spreading of the initial particle beam is slight at high energies but increases rapidly when the "nuclear" energy loss mechanism becomes significant. While these distributions cannot be discussed here in detail [see Bohr (5), or Lindhard, Scharff & Schiøtt (38)], their significance in connection with the precise definition of range, the relationship between stopping power and range, and the interpretation of experimental data is considered briefly in the following paragraph.

F. Range, Range Difference, Straggling

Loosely speaking, the range of a particle is the distance it penetrates into a material before coming to rest. If the lateral deflections and the statistical fluctuations are disregarded, the range is simply given by integration of the reciprocal of the stopping power

$$R = \int_0^E \left(-\frac{dE}{dX}\right)^{-1} dE \qquad 24.$$

and the depth of penetration corresponding to a decrease of energy from E_0 to E is given by the range difference

$$X = R(E_0) - R(E) = \int_E^{E_0} \left(-\frac{dE}{dX}\right)^{-1} dE \qquad 25.$$

where $-dE/dX$ is the sum of the "nuclear" and the "electronic" stopping power. Because of the small lateral deflections suffered by the ion, the integrated path length in the material, given by Equation 24, will be somewhat larger than the depth of penetration along the initial direction. In general the deflections are associated with nuclear collisions, and the difference between path length and depth of penetration may become large whenever elastic nuclear collisions account for much of the energy loss. The quantity given by integration of the theoretical stopping-power formulas is the path length and it is directly observable in nuclear emulsions or cloud chamber photographs. In most other experimental situations, however, it is the depth of penetration which is observable. Thus either quantity might be called the range under appropriate circumstances.

A further ambiguity in the meaning of range arises from the statistical fluctuations of the energy loss process, since a beam of monoenergetic incident ions is spread in energy by these fluctuations, giving rise to "range straggling," i.e., to a distribution of path lengths or penetration depths in the material. This distribution may be almost symmetric (Gaussian) or very asymmetric, the amount of asymmetry being associated with the relative importance of elastic nuclear collisions in the energy loss process [see Bohr (5)]. Thus the mean and the most probable penetration depths often are different. Each of these can be used as a definition of range, and various other measures such as the maximum penetration depth also have been used. It is natural to identify the mean path length with R of Equation 24 since

$-dE/dX$ is defined as the average energy loss per unit of path length, but this identification is only approximately correct.

III. EXPERIMENTAL AND SEMIEMPIRICAL

A. Equilibrium Charge Distributions

Uncertainty about the net charge of a heavy ion is probably the major cause of uncertainty in the theoretical calculation of dE/dX for the ion. Although experimental data on the equilibrium charge distributions of heavy-ion beams are not abundant, they are sufficient to reveal significant relationships which can be of considerable help in dE/dX calculations, particularly in the high energy region.

At energies above 1 MeV/amu, equilibrium charge distributions have been measured for C, N, O, and Ne ions in Zapon by Heckman, Hubbard & Simon (27), and for B, C, N, O, F, and Ne ions in aluminum by Northcliffe (39).[9] These results are displayed in Figure 3 plotted as functions of the velocity ratio $\xi=\beta/\beta_k=\xi_0/z$, where $\beta_k=z/137$ is the velocity of an electron in the innermost Bohr orbit of the ion. This is consistent with the usual assumption that the probability of attachment of an electron to an ion is a function only of the relative magnitudes of the ion velocity and the orbital velocity of the electron when bound to the ion. The data are plotted in this way, of course, in the hope of finding a universal relationship between ϕ_Z and ion velocity. The choice of β_k rather than the Thomas-Fermi velocity $\beta_{TF}=\xi_0/z^{2/3}$ as a reference velocity is suggested by the fact that the capture and loss of the two K electrons dominate the charge exchange process throughout most of this velocity region, as can be seen from the smallness of the ϕ_Z values for $Z\leq z-2$.

The charge distribution data for a given material seem to be represented reasonably well by a single universal curve for each value of $z-Z$. Furthermore, the universal curves for the two materials are not very different.[10]

[9] Only the O^{16} data were published in (39) but the unpublished data included here for other ions were obtained in the same manner as the O^{16} data.

[10] It may be noted on close inspection that the Zapon data deviate systematically from a universal curve, and in fact Heckman et al. (27) find that a better universal curve is obtained if the data are plotted vs. the velocity parameter $\xi_0/(Z-0.62)^{0.7}$ rather than $\xi=\xi_0/z$. These deviations are small, however, and for present purposes can be ignored. The data for aluminum are less precise than the Zapon data but sufficiently accurate to indicate that the systematic deviations are less than $\Delta\phi\sim0.02$ in the region $1.5<\xi<2.5$. When the relative accuracy of individual points for Al is taken into account, it is found that the points which deviate noticeably from the universal curve are also those marked by the greatest uncertainty. On the whole the Al data are satisfactorily described by the universal curve of Fig. 3. It will be noted that the universal curve for Al does not fit the Zapon data. That this difference is real is corroborated by Heckman et al. who find, in unpublished measurements with O^{16} ions of velocity $\beta=0.148$ (i.e., $\xi=2.54$), that ϕ_8 and ϕ_7 are respectively 0.979 and 0.021 in Zapon, 0.956 and 0.044 in Al, 0.930 and 0.069 in Ag, and 0.919 and 0.079 in Au.

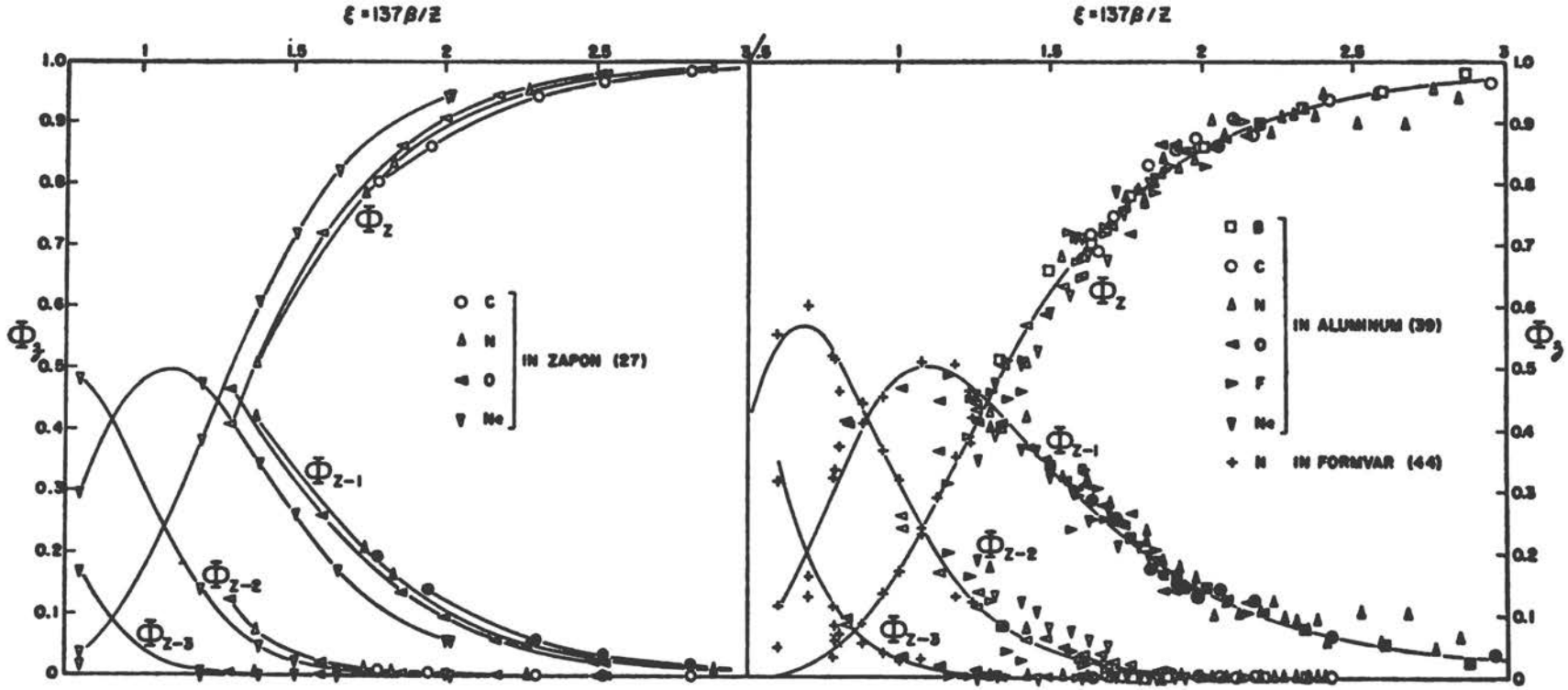

FIG. 3. Experimental equilibrium charge distribution data for heavy ions at high velocities. The charge fractions ϕ_Z are plotted vs. 137 β/z in order to demonstrate an approximately universal relationship.

At lower energies several sets of equilibrium charge distribution measurements are available. The most extensive are reported in a series of papers by Nikolaev, Dmitriev, Fateeva & Teplova (40–43), including data for He, Li, B, N, O, Ne, Na, Mg, Al, P, Ar, and Kr ions of velocities in the region $1<\xi_0<5$ passing through celluloid, H_2, He, N_2, Ar, Kr, and air, and also for N ions in Be, Ni, and Au. Other available measurements include those of Reynolds et al. (44) for N ions in Al and Formvar; of Almqvist et al. (45) and Litherland et al. (46) for F, Cl, Br, and I ions in C and O_2; of Stephens & Walker (47) for N, O, and F ions in Zapon; of Hubbard & Lauer (48) for O and Ne ions in Ar; of Tombrello et al. (49) for Be ions in Be; and of Kavanagh & Seeger (50) for C ions in vanadium nitride. In addition, Stier et al. (51), Leviant et al. (52), Allison et al. (53), and Steiger (54) have measured equilibrium charge distributions for heavy ions at very low velocities.

It is difficult to display these results in compact form not only because of the considerable scatter resulting from experimental uncertainties but also because real differences must occur for different ion beams and probably occur for different material media as well. Still, it would be of interest to extend the universal charge distribution curves for Figure 3 to somewhat lower velocities. For this purpose the data of Reynolds et al. (44) for N^{14} ions in Formvar have been chosen. The justification for combining the data for Al and Formvar lies in the observation by Reynolds et al. that the charge distributions at $\mathcal{E}_m = 1.86$ MeV/amu are the same in both materials. Other charge data in this region are omitted from the plot to avoid confusion. An extension of this plot to still lower velocities would not be advisable since K electron capture and loss no longer would dominate the charge-change process there.

It is advantageous to display charge distribution data in another way. If charge change takes place predominantly by capture or loss of a single electron [normally this is the case, see Nikolaev et al. (57)], it can be seen that $\sigma_{Z,Z-1}/\sigma_{Z-1,Z} \cong \phi_{Z-1}/\phi_Z$ (see Footnote 8). It was predicted theoretically by Bohr (5) that σ_c/σ_l should be an almost constant power of the velocity. Thus a plot of log (ϕ_Z/ϕ_{Z-1}) vs. log ξ should be approximately a straight line. Such a plot is shown in Figure 4 for the ϕ_s/ϕ_{s-1} and ϕ_{s-1}/ϕ_{s-2} charge-fraction ratios of the data displayed in Figure 3. (The plot for ϕ_{s-2}/ϕ_{s-3} is similar.) For purposes of comparison the proton charge-fraction ratio ϕ_1/ϕ_0 measured by Phillips (55) also is shown. It will be noted that the aluminum data do not show the systematic dependence on s that appears in the Zapon data. Thus it is plausible to draw universal curves (the solid lines of Fig. 4) for Al. The formulas for these curves are: $\phi_s/\phi_{s-1} = 0.365\ \xi^4$ for $\xi \lesssim 2$; $\phi_s/\phi_{s-1} = 0.3\xi^{4.35}$ for $\xi \gtrsim 2$; $\phi_{s-1}/\phi_{s-2} = 1.6\xi^4$; $\phi_{s-2}/\phi_{s-3} = 12\xi^4$. [This fourth-power dependence of ϕ_Z/ϕ_{Z-1} on ion velocity also was found for heavy ions at lower velocities in celluloid by Nikolaev et al. (40, 42).] The universal curves of Figure 3 were constructed using the above formulas.

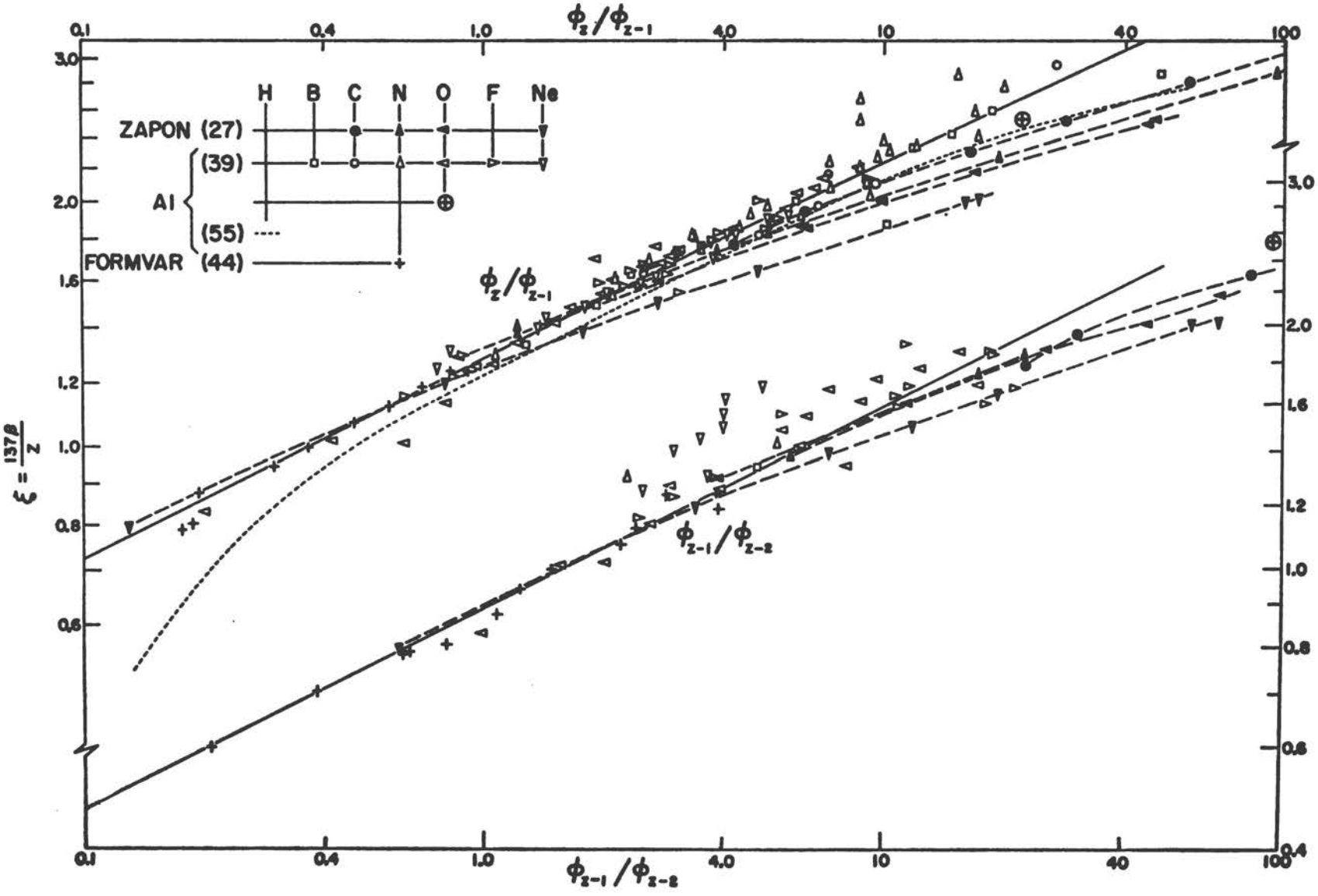

FIG. 4. Equilibrium charge-fraction ratios for heavy ions at high velocities. The unidentified points for O ions in Al are taken from Footnote 10.

B. Nonequilibrium Charge Distributions and Charge-Change Cross Sections

Experimental measurements have been reported by Hubbard & Lauer (48), Heckman et al. (27), Nikolaev et al. (56–59), Reynolds et al. (60), and Stephens & Walker (61). Because of space limitations no discussion of these results will be attempted.

C. Electronic Stopping-Power Curves

The most direct determination of stopping power is achieved by passing ions of known initial energy E through a thin layer of the material and measuring the energy loss $-\Delta E$. The thickness ΔX of the material layer should not be so small that surface effects and the approach to charge equilibrium are important but should be small enough to permit the equating of $-\Delta E/\Delta X$ with the stopping power $-dE/dX$ (at energy $E-\frac{1}{2}\Delta E$). The practical difficulty with this method is that the thickness often must be so small (especially with heavier ions) that the uniformity of the thin layer and the precision with which ΔX can be measured limit the accuracy of the determination.

The experimental difficulties associated with very thin layers can be avoided with some sacrifice of directness by using the derivative approach in which the stopping power is determined from the slope of the smoothed experimental range-energy curve or its mirror image, the plot of ΔE vs. ΔX for ions of fixed initial energy. The relationship between this slope and the stopping power already has been discussed in Section II.F. A third method of deriving stopping powers is considerably less direct and has less solid theoretical justification but deserves consideration because it utilizes a different body of experimental data. In this method Equation 21 is used to calculate the root mean square fractional charge of the ions from the observed equilibrium charge distributions, and the result is used together with the known proton stopping power and equilibrium charge to calculate the heavy-ion stopping power by means of Equation 22.

When the stopping-power data obtained by direct measurement are supplemented by the values derived from energy loss or range data and from equilibrium charge distribution measurements, the result is a substantial body of information. In fact, it is not practical to display and discuss all such information for all ions and material media in this paper. It seems preferable to concentrate attention on the most thoroughly studied ion-absorber combinations in the hope of gaining insight which may be used as the basis for generalization. For this purpose the data for B, C, N, O, F, and Ne ions in C, Al, Ni, Ag, and Au seem particularly well suited. A display of most of the available electronic stopping-power values derived from experimental data by all three methods for these ions and materials is presented in Figures 6 and 7. The aim has been to present all available data for aluminum in each

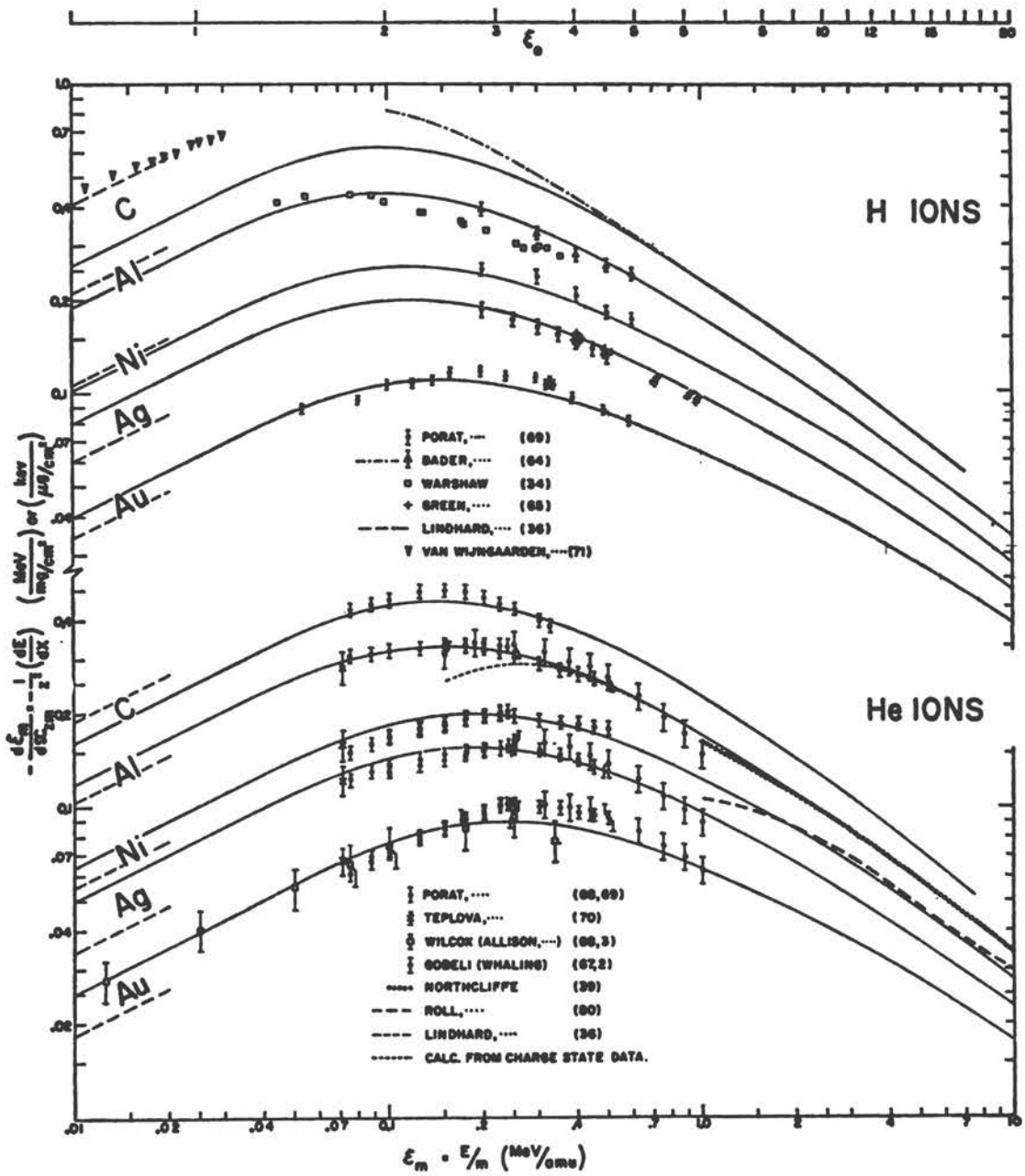

FIG. 5. Stopping power for H and He ions in C, Al, Ni, Ag, and Au.

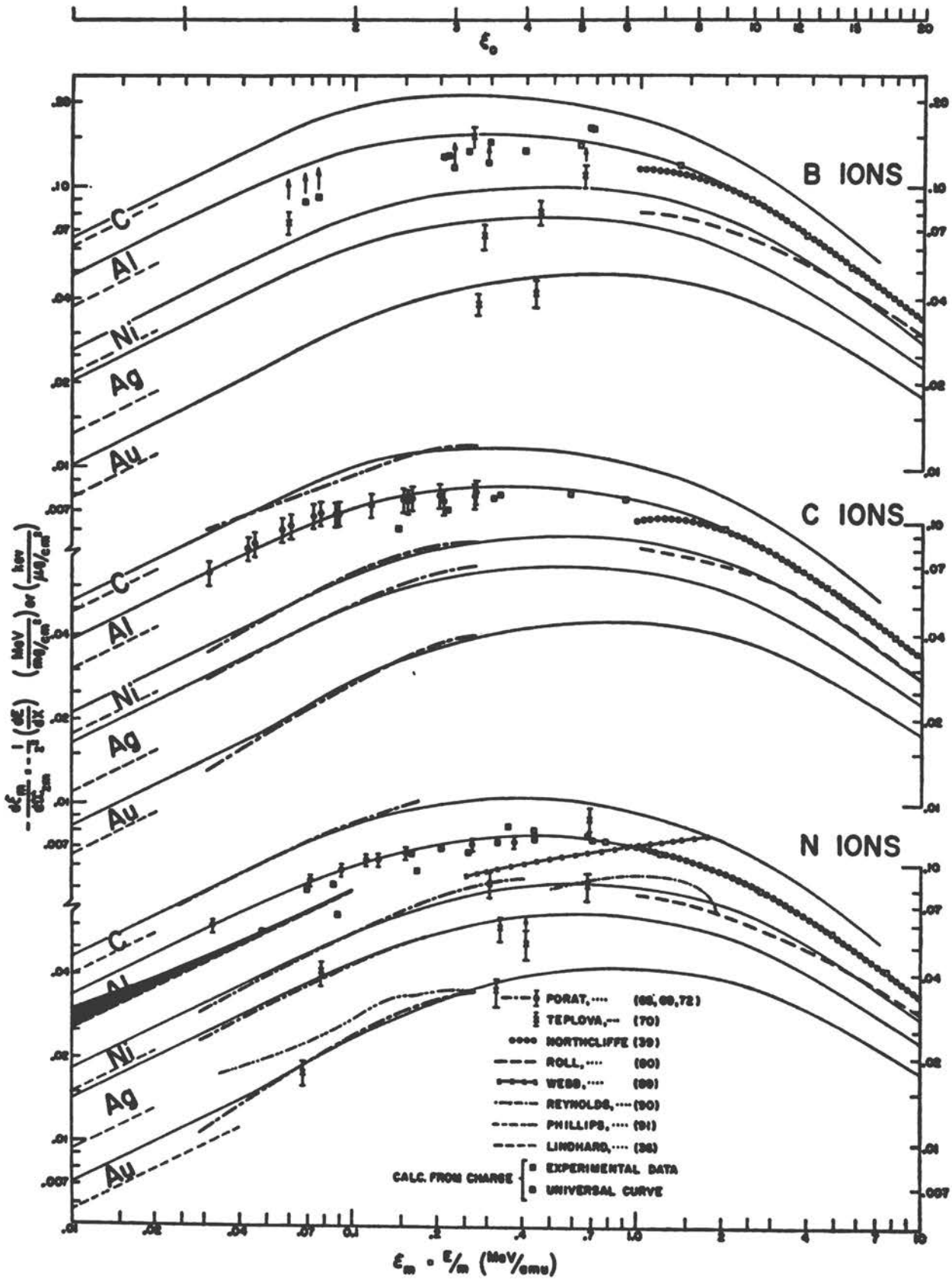

FIG. 6. Stopping power for B, C, and N ions in C, Al, Ni, Ag, and Au.

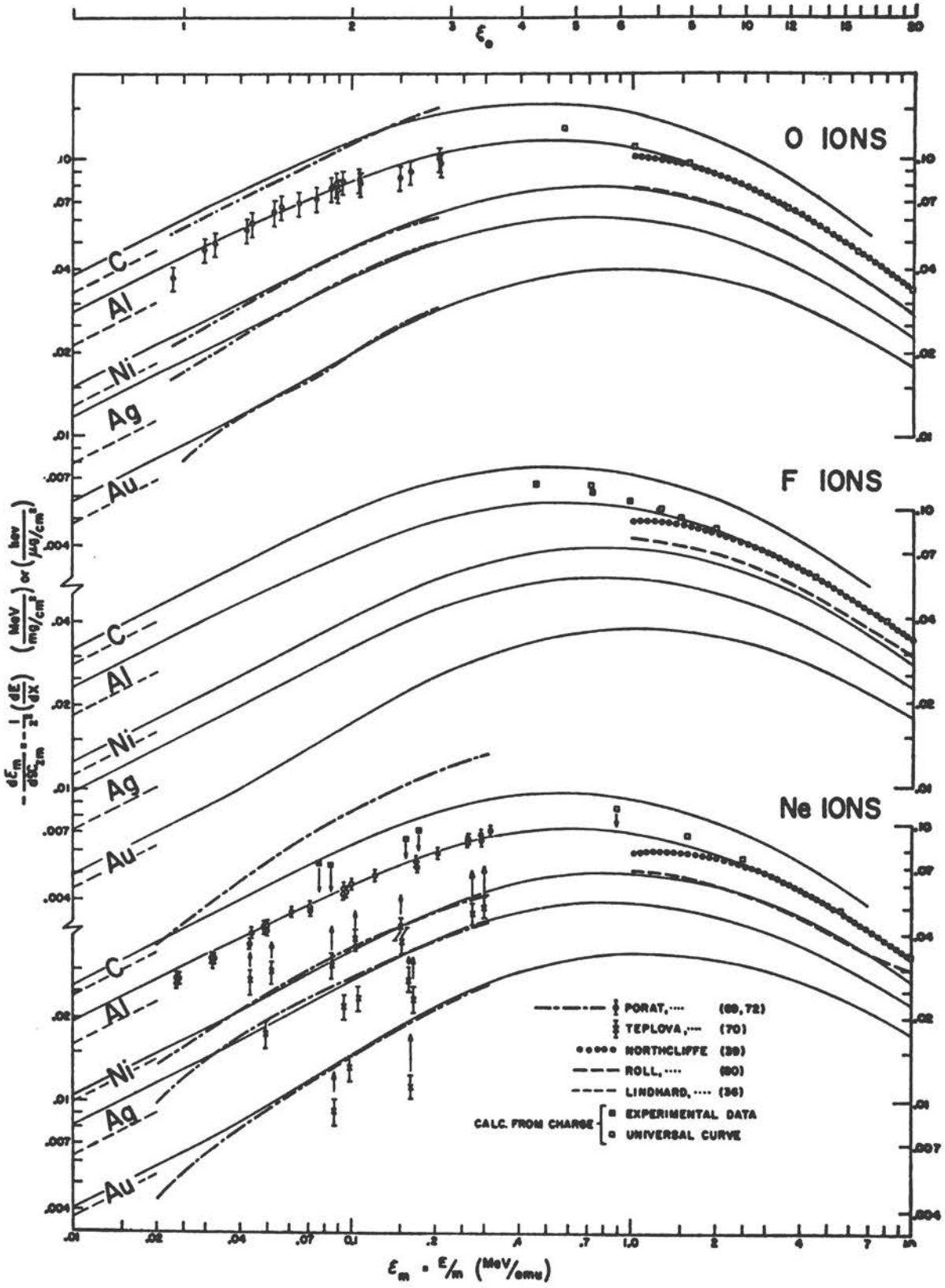

FIG. 7. Stopping power for O, F, and Ne ions in C, Al, Ni, Ag, and Au.

case and to include as much information on other materials as could be shown without undue confusion.

For purposes of comparison a set of stopping-power curves for H and He ions in the same materials is shown in Figure 5. Above 1 MeV/amu the curves are essentially those given by Bichsel (62) and by Demirlioglu & Whaling (63) except in the case of silver where the curve is slightly higher ($\sim$2%; $1 < \mathcal{E}_m < 3$) than that given by those authors. Below 1 MeV/amu all of the curves differ somewhat from those of (62) and (63). (The reason for these differences will be indicated presently.) In the region where the curves here are different, some of the data upon which the curves of (62) and (63) were based are shown to indicate the plausibility of the present curves. These include the measurements of Bader et al. (64), Green et al. (65), Warshaw (34), Wilcox (66) [as corrected by Allison & Warshaw (3)], and Gobeli (67) [as interpreted by Whaling (2)]. New measurements reported by Porat & Ramavataram (68, 69), Teplova et al. (70), and Van Wijngaarden & Duckworth (71) also are shown.[11] It may be noted that much of the difference between the stopping power for H and He ions (and the heavier ions, Figs. 6 and 7) has been removed, as predicted by Equation 10a, by plotting $-d\mathcal{E}_m/d\mathcal{X}_m$ vs. $\mathcal{E}_m$ rather than $-dE/dX$ vs. E.

The only direct stopping-power measurements shown in Figures 6 and 7 are those in the velocity region $1 \leq \xi_0 \leq 4\frac{1}{2}$ by Porat & Ramavataram (68, 69, 72), and Teplova et al. (70). The actual measurements of Porat & Ramavataram are displayed for Al, but only the smoothed curves given by those authors are shown for C, Ni, Ag, and Au. According to the authors the absolute uncertainty of these measurements is 5 percent or less in general, but in certain cases (e.g., C and O ions in Al) it seems that a 10 percent uncertainty has been assigned. (It is not clear whether or not the 10% uncertainty also should be assigned to data for other ions in Al or for C and O ions in carbon.) The uncertainties shown for the data of Teplova et al. are their estimates of the maximum errors. It will be noted that the agreement of the two groups is good for He and N ions but poor for Ne ions. Teplova et al. also have measured stopping powers for other ions (Li, Be, Na, Mg, Al, P, Cl, K, Br, and Kr) and in other materials (celluloid, H_2, He, Ar, CH_4, air, and benzene). There is also a measurement by Braid & Detenbeck (73) of the velocity loss of C ions in Al, Au, and polystyrene at $\mathcal{E}_m = 0.307$ MeV/amu which has been omitted from Figure 6, and a few other direct

[11] Error bars are not drawn for the data of Warshaw (34) because the error estimate of 4½% of this experiment apparently was unreliable [see Whaling (2)]. They are not drawn for the carbon data of Bader et al. (64) because those results were obtained by a subtraction process from stopping-power data for gaseous carbon compounds, while the present curves are meant to be for solids. The data of (71) were not used in the analysis being described. If they had been appreciated earlier, the form taken for the stopping-power curve of carbon would have been somewhat different at low energy. However, the effect on the range-energy curves for carbon would be small.

stopping power measurements for ions, materials, or velocity regions not included in Figures 6 and 7. Among these are measurements by Wilcox (66) for Li ions in Au and Al; by Allison & Littlejohn (74) for Li ions in H_2, He, Ar, and air; by Weyl (75) for N and Ne ions in H_2, He, Ar, and air; by Segrè & Wiegand (76) and Lassen (77) for fission fragments in various materials; and by Tel'kovskii & Pistunovich (78) and Ormrod & Duckworth (79) for various ions at very low velocities.

Stopping-power values derived from the slopes of range or energy loss curves do much to fill out the picture, especially at higher velocities. In the energy region $1 < \mathcal{E}_m < 10$ MeV/amu such values can be derived from the measurements of Northcliffe (39) for various ions in Al; of Roll & Steigert (80) for various ions in Ni and O_2; of Walton & Hubbard (81) for C ions in Be, Al, Ni, Ag, and Au; of Gilmore (82) for Ne ions in Al; of Sikkeland (83) for N and O ions in Al; of Schambra et al. (84) for C, O, and Ne ions in plastics; of Roll & Steigert (85), Heckman et al. (86), and Parfanovich et al. (87) for various ions in nuclear emulsion; and of Martin & Northcliffe (88) for various ions in H_2, He, N_2, Ar, and CH_4. Some of these derived values are shown in Figures 5, 6, and 7. These values are not very accurate below about 2 MeV/amu. At lower ion velocities the range measurements for N ions in Al by Webb et al. (89), in Ni by Reynolds et al. (90), and in Au by Phillips & Read (91) provide additional values which are shown in Figure 6. There are few other data of sufficient accuracy for this purpose.

It is of considerable interest to explore the extent to which stopping-power values derived from equilibrium charge distribution measurements through use of Equations 21 and 22 agree with the more direct stopping-power measurements. Such values have been calculated for the various ions in Al in two ways: the open square symbols of Figures 6 and 7 were calculated from the universal curves of Figure 3, while the filled squares were calculated using experimental charge data. The charge distribution data used were those of Phillips (55) for H ions; of Dissanaike (92), Nikolaev et al. (42), and Briggs (93) for He ions; of Nikolaev et al. (41, 42, 43) for B, N, and Ne ions; of Kavanagh & Seeger (50) for C ions; and of Almqvist et al. (45) for F ions. It may be noticed that most of these measurements were for solid materials other than aluminum. This should not give rise to appreciable error, however, since the charge distributions at low velocities in solid materials appear to be independent of material, within the experimental accuracy of present data.

The agreement between stopping-power values derived from charge state data and those obtained more directly is extremely good at high energies ($\mathcal{E}_m \geq 2$ MeV/amu) where both charge distribution and energy loss data are relatively accurate. At lower velocities the agreement is less impressive, but the experimental charge and energy loss data also are less accurate. The uncertainty of the charge state data can be judged from the scatter of the solid square symbols in Figures 6 and 7. This scatter is seen to be of the same order of magnitude as the difference from stopping-power values determined more directly. Considering the uncertainties of the latter, it is possible that much

of the difference actually arises from experimental errors in both types of measurement, and that γ_{eff} is equal to γ_{rms} not only at high energies but also in the region of the stopping-power maximum. Even if this is not precisely true and γ_{eff} does differ from γ_{rms} at low velocities, the difference is not much larger than the experimental uncertainties in energy loss and charge state data. Thus stopping values calculated from charge state data apparently are not much less reliable than those obtained in typical direct measurements, at least in the cases examined here.

It also is of interest to compare the experimental stopping-power data with the theoretical predictions of Equation 23. According to Lindhard & Scharff (36) this formula should be valid for velocities below $\xi_0 \sim z^{2/3}$ and for z and Z values greater than ten. The predictions are indicated by the straight dashed lines of slope equal to $\frac{1}{2}$ at the left-hand edge in Figures 5, 6, and 7. The predicted energy dependence seems to be approximately correct below $\xi_0 \sim 1$ but not all the way up to $\xi_0 \sim z^{2/3}$. The relative magnitude of the stopping power also seems to be predicted with qualitative correctness although the predicted values consistently are lower than the measured values. A similar systematic deviation from the predictions of Equation 23 was seen at much lower velocities by Ormrod & Duckworth (79) who further observed that the departure from Equation 23 varies with z with a periodicity apparently associated with the chemical valence of the neutralized ion.[13] Such discrepancies might be expected since the restriction $z > 10$ is violated for these data and the theory of Lindhard & Scharff does not take shell effects into account. All in all, the formula works remarkably well, even giving plausible stopping-power values for H and He ions.

When all of this stopping-power information is put together, the influence of deviant individual results is reduced and it is possible to construct a set of stopping-power curves having smooth and plausible variations with z, Z, and $\mathcal{E}_m$. The obvious virtue of this approach is that such curves provide a reasonable basis for prediction of stopping powers where they have not been measured. The thin solid lines of Figures 5, 6, and 7 represent such a set of smoothed curves constructed in accordance with the following assumptions:

(*a*) The relative stopping power of two materials for the same ion at a given velocity is independent of z, and its velocity dependence is the smoothly varying function shown in Figure 8. At high energies [$\mathcal{E}_m > 1$ MeV/amu] this function is given by proton stopping-power data, in the limit of low energies it is assumed to be independent of energy (consistent with the energy dependence of Eq. 23), and in between it is an estimated best fit to available data for all ions subject to the requirement that the velocity dependence be smooth and monotonic.

[13] Teplova et al. (70) have observed a similar periodicity in the z dependence of ion range at low velocities, also apparently related to the shell structure of the neutralized ion.

(*b*) The stopping-power curves for various ions in aluminum are the smoothly varying set shown in Figure 9.

The smooth unbroken curves of Figures 5, 6, and 7 are given uniquely by these assumptions. However, all of the curves for a given Z [or z] could be altered simultaneously by a suitable change of the appropriate curve in Figure 8 (or Fig. 9). The generation of similar semiempirical stopping-power curves for other solid materials would require only the addition of the corresponding relative stopping-power curves to Figure 8. Since the relative stopping power is given by proton data at the high energy end and can be estimated with the aid of Equation 23 at the low energy end, such curves can be generated for many materials with reasonable ease and confidence.

On the whole, the fit of these semiempirical stopping-power curves to the wide variety of data displayed in Figures 5, 6, and 7 is remarkably good considering the simplicity of the above assumptions. It is likely that an even better fit could be obtained with some revision of Figures 8 and 9, especially if the data of Van Wijngaarden & Duckworth (71) were taken into account (see Footnote 12). For present purposes, however, these curves are satisfactory.[13]

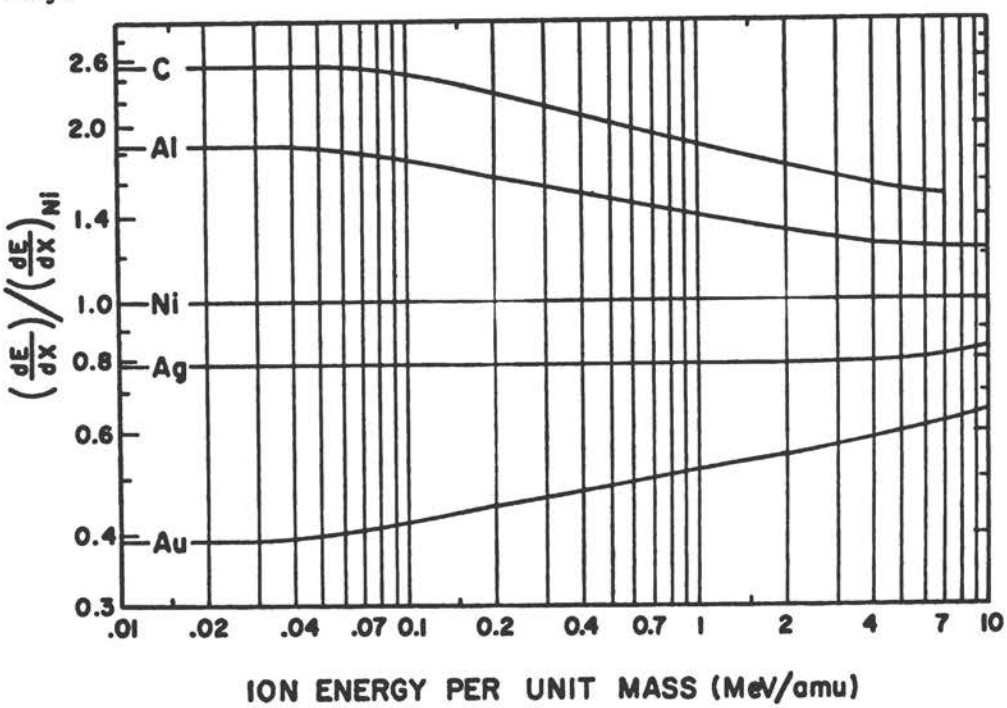

FIG. 8. Smoothed relative stopping-power curves for a given ion in different materials. The curves are assumed to be the same for all ions.

[13] The smoothed curves were strongly influenced at low energies by the abundant data of Porat & Ramavataram. Therefore the fact that these data fit the curves so well cannot prove their correctness since a systematic error in the data would be duplicated in the curves. However, it does show that the data have a high degree of internal consistency.

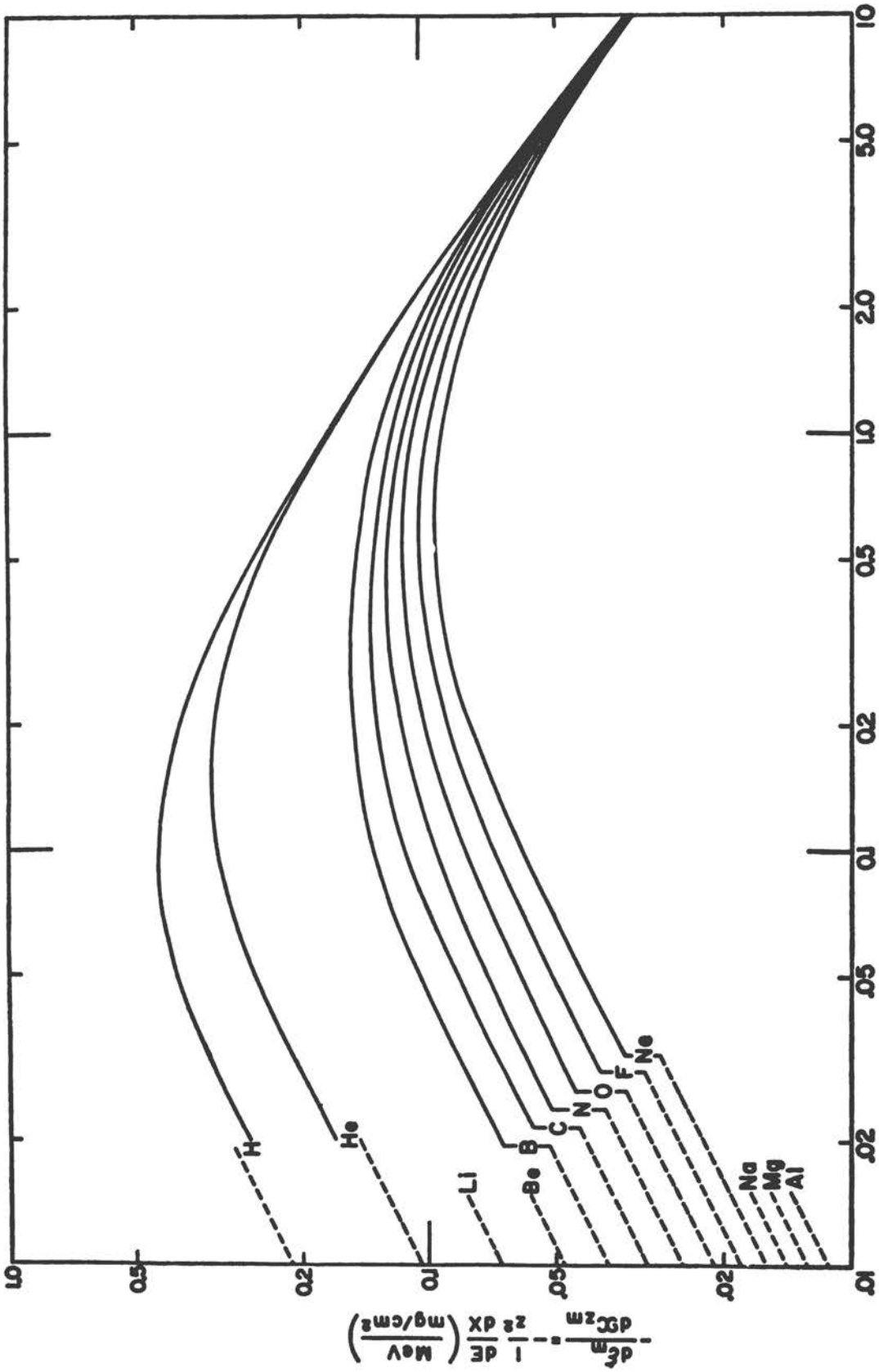

FIG. 9. Smoothed stopping-power curves for various ions in Al.

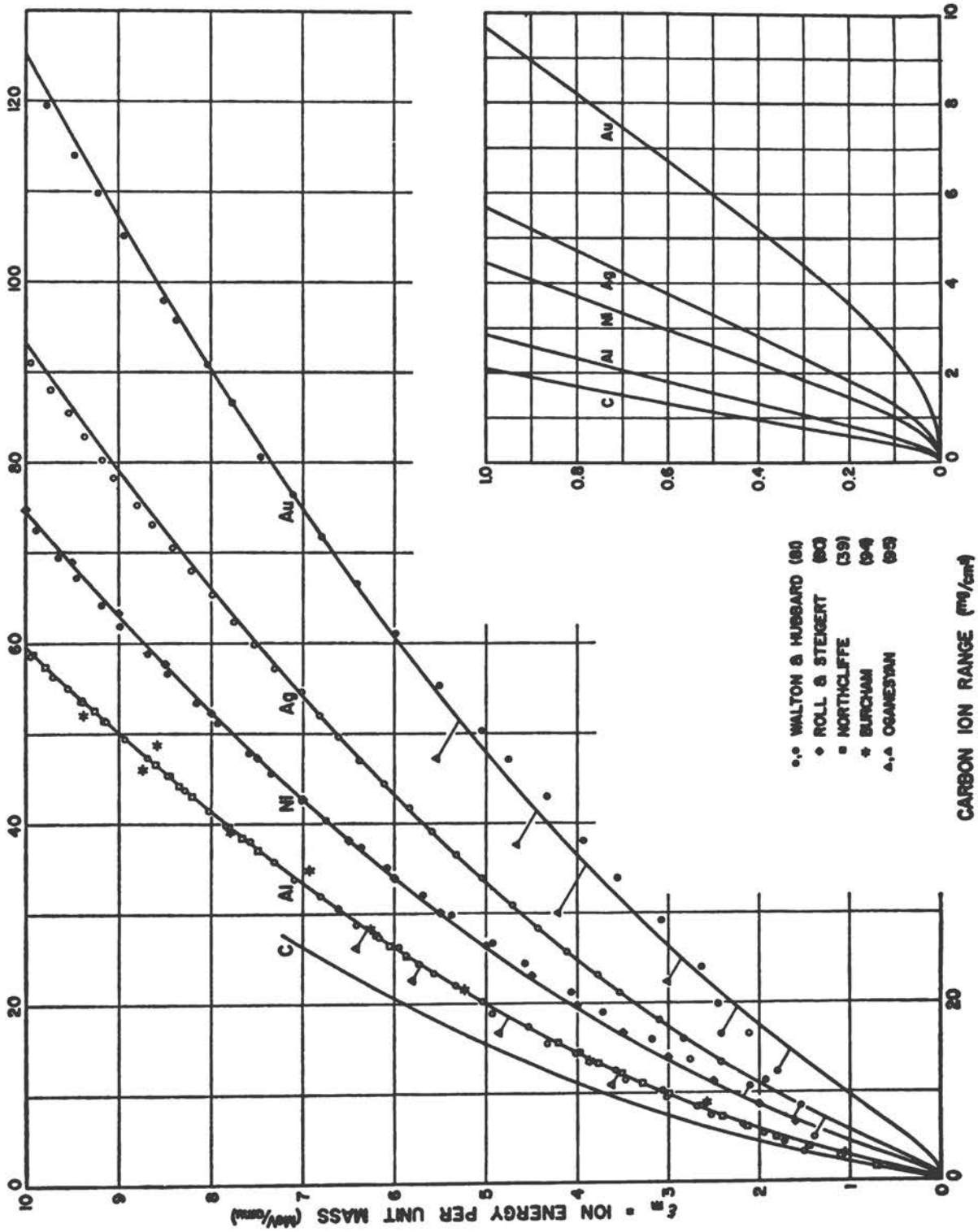
Au
Ag
Ni
Al
C
0
20
40
60
80
100
120
1
2
3
4
5
6
7
8
9
10
E_3 = ION ENERGY PER UNIT MASS (MeV/amu)
CARBON ION RANGE (mg/cm²)
•,• WALTON & HUBBARD (61)
◆ ROLL & STEIGERT (60)
▪ NORTHCLIFFE (39)
★ BURCHAM (94)
▲,▲ OGANESYAN (95)
0.2
0.4
0.6
0.8
1.0
2
4
6
8
10

The effect of screened elastic "nuclear" collisions on the stopping power is illustrated in Figure 6 for the case of N ions in Al, where the shaded area shows the increase in stopping power from this effect as given by the theory of Lindhard et al. (38) (see Fig. 2).

D. Range-Energy Relations

1. *Integration of the stopping-power curves.*—Equation 24 can be used to calculate range-energy curves by numerical integration from the smoothed stopping-power curves of Figures 5, 6, and 7. The results of such a calculation from the smoothed carbon ion curves of Figure 6 are shown in Figure 10 along with all available experimental range and energy loss data for C ions in Al, Ni, Ag, and Au (there are no published data for C ions in C). The data of Walton & Hubbard (81), Roll & Steigert (80), Northcliffe (39), and Burcham (94) are energy loss measurements. These have been converted to ranges using Equation 25 with values of the constant $R(E_0)$ arbitrarily chosen so as to give range values which fit the calculated curves at $\mathcal{E}_m \sim 7$ MeV/amu. The measurements of Oganesyan (95) are direct range measurements and the published values are shown. The fit of Oganesyan's data to the calculated curves would be much better if a suitable constant were added to his range values for each material (as it was, in effect, in the fitting of the energy loss data). All in all, however, the agreement between the calculated curve and the measured ranges is remarkably good.

The effect of nuclear stopping was ignored in the numerical integration leading to the curves of Figure 10. The error caused by this neglect is small on the scale used in the plot but not negligible. When nuclear stopping is taken into account by the method of Lindhard et al. (38), the calculated C ion ranges are decreased by 0.57 mg/cm² in Au, 0.36 mg/cm² in Ag, 0.23 mg/cm² in Ni, 0.13 mg/cm² in Al, and 0.07 mg/cm² in C. It should also be noted that the range values calculated by Equation 24 are integrated path lengths rather than penetration depths. However, the difference between these distances is negligibly small on the scale of Figure 10.

It is not possible to present similar sets of curves for all ions in this article. (As might be expected, such curves generally are in agreement with existing experimental data.) However, it is practical and informative to compare the range-energy curves for different ions in a representative material. If Equation 10a is valid, the plot of $\mathcal{E}_m$ vs. $\mathfrak{X}_{sm}$ should differ for different ions only when the fractional charge of the ions is not the same. With this in mind, Northcliffe (39) displays his experimental energy loss curves for various heavy ions in Al as plots of $\mathcal{E}_m$ vs. $\mathfrak{X}_{sm}$ in Figure 11, along with a similar

---

FIG. 10. Range-energy relations for C^{12} ions. The solid lines were obtained by numerical integration from the smoothed stopping-power curves of Fig. 6. The points show experimental values, mostly derived from energy loss measurements.

curve for H ions in Al adapted from the proton range measurements of Bichsel (96). These experimental curves are closely reproduced by integrating the stopping-power curves of Figure 9.

2. *Semiempirical relations.*—The curve shown in Figure 10 for C^{12} ions in C is an example of a semiempirical range-energy curve, just as the curves for F ions in Figure 7 are examples of semiempirical stopping-power curves. Since it is unrealistic to contemplate experimental measurements for all ion-absorber combinations, heavy reliance must be placed on semiempirical methods of determining ion ranges and energy losses. The present article is largely an exploration of semiempirical relationships between the ranges, stopping powers, and equilibrium charge distributions for heavy ions. There have been numerous earlier attempts to develop and utilize such relationships, often with an approach somewhat different from that used here. A partial list of references would include papers by Barkas (97), Lonchamp (98), Papineau (99), Livesey (100), Grinberg & Lemberg (101), and Roll & Steigert (102) as well as several references cited earlier (22–27, 39, 86, 88, 91) and an unpublished report by Hubbard (103). In addition, useful summaries

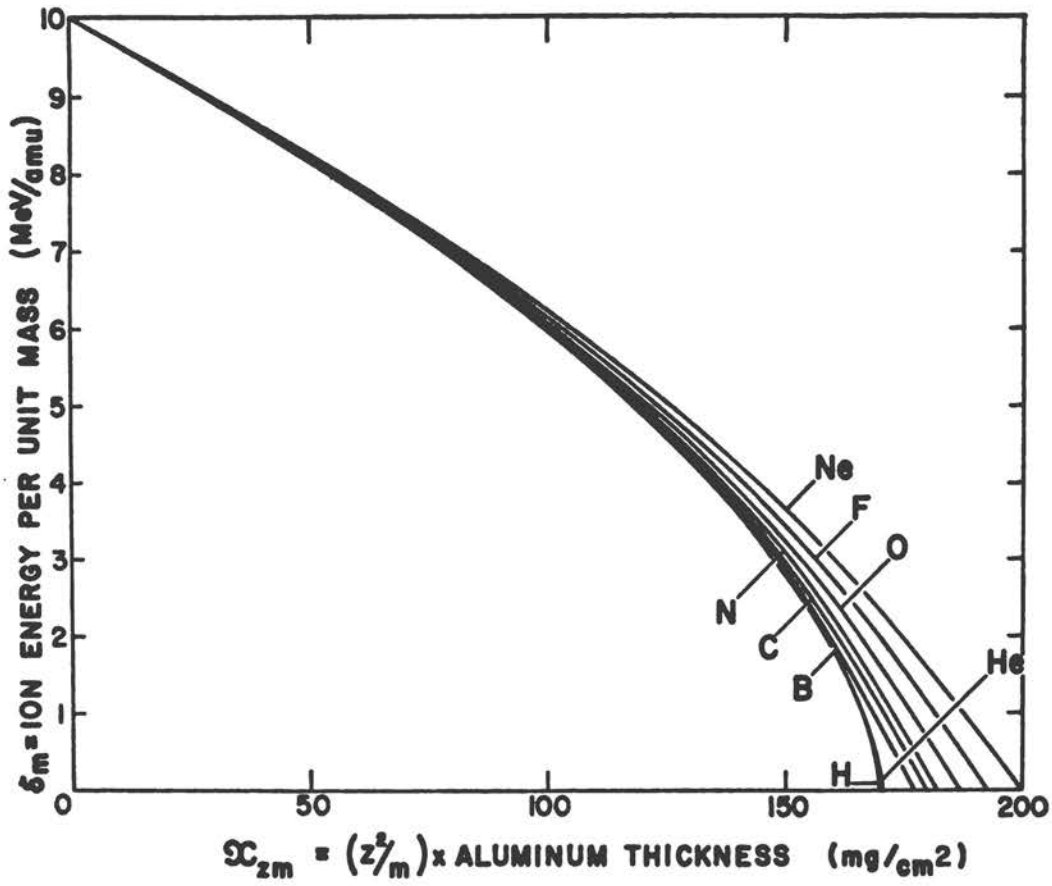

FIG. 11. Energy loss curves for various heavy ions in aluminum. The near-universality in shape is emphasized by plotting E/m vs. $(z^2/m)\ X$.

of heavy-ion penetration data have been assembled by Wallace (104) and Allison & Garcia-Munoz (105).

3. *Experimental measurements.*—In the region of higher energies ($2 \leq \mathcal{E}_m \leq 10\frac{1}{2}$ MeV/amu), several recent investigations already cited (39, 80–88) have provided range or energy loss data of considerable accuracy for B, C, N, O, F, Ne, and Ar ions in various metals, gases, plastics, and nuclear emulsion. These are supplemented by older measurements of Burcham (94), Oganesyan (95), Chaminade et al. (106), Lonchamp (107), Parfanovich et al. (108), and Miller (109).

Some of the measurements cited above extend down to energies below $\mathcal{E}_m = 1$ MeV/amu but unfortunately their accuracy is not as great at these energies. The only other experimental measurements in the region $\frac{1}{2} < \mathcal{E}_m < 2$ MeV/amu are those of Webb et al. (89), Reynolds et al. (90, 110), and Hower & Fairhall (111) for N and Be ions in Al, Ni, Au, and nuclear emulsion. At somewhat lower energies the measurements of Phillips & Read (91), Teplova et al. (70, 112), Maikov (113), Devons & Towle (114), Lillie (115), Vorob'ev (116), Cüer & Lonchamp (117), Neuendorffer et al. (118), Feather (119), Blackett & Lees (120), Clerc et al. (121), Evans et al. (122), and Powers & Whaling (123) provide range data for a variety of ions in both solids and gases. No attempt will be made to list the numerous range measurements for fission fragments and for heavy ions in the kiloelectronvolt region [see Harvey (6), and Lindhard et al. (38)].

IV. CONCLUSION

A gratifying pattern of consistency and regularity emerges from this appraisal of heavy-ion penetration phenomena. The equilibrium charge distribution of a heavy-ion beam appears to be reasonably well approximated by a universal function of $\xi = 137\,\beta/z$ at high velocities, and the root mean square charge given by this distribution is the same as the effective charge within the experimental uncertainties. Even in the region of the stopping-power maximum the root mean square charge and the effective charge are not found to be distinctly different. At very low velocities, the theory of Lindhard et al. appears to be in reasonable agreement with the few available stopping-power measurements. By assuming a smooth dependence of the relative stopping power on z, Z, and $\mathcal{E}_m$, it is possible to generate semiempirical stopping-power curves which fit the available data remarkably well, and the range-energy relations calculated from these curves by numerical integration are in good agreement with the available range data. These generalizations are based on experimental data of limited accuracy and it is unlikely that they are precisely true. Furthermore, it is not certain that they would hold equally well for very heavy ions or for very different material media. Nevertheless they should provide a reasonable basis for semiempirical predictions in a wide variety of situations.

LITERATURE CITED

1. Fano, U., *Ann Rev. Nucl. Sci.*, 13, 1 (1963)
2. Whaling, W., *Encyclopedia of Physics*, 34, 193 (Fluegge, S., Ed., Springer-Verlag, Berlin, 1958)
3. Allison, S. K., and Warshaw, S. D., *Rev. Mod. Phys.*, 25, 779 (1953)
4. Bethe, H. A., and Ashkin, J., *Experimental Nuclear Physics*, 1, Chap. 2 (Segrè, E., Ed., Wiley, New York, 1953)
5. Bohr, N., *Kgl. Danske Videnskab. Selskab, Mat.-Fys. Medd.*, 18, 8 (1948)
6. Harvey, B. G., *Ann. Rev. Nucl. Sci.*, 10, 235 (1960)
7. Uehling, E. A., *Ann. Rev. Nucl. Sci.*, 4, 315 (1954)
8. Bohr, N., *Phil. Mag.*, 25, 10 (1913)
9. Bethe, H. A., *Ann. Physik*, 5, 325 (1930)
10. Gaunt, J. A. *Proc. Cambridge Phil. Soc.*, 23, 732 (1927)
11. Bloch, F., *Ann. Physik*, 16, 285 (1933)
12. Bohr, N., *Phil. Mag.*, 30, 581 (1915)
13. Bethe, H., *Z. Physik*, 76, 293 (1932)
14. Walske, M. C., *Phys. Rev.*, 88, 1283 (1952); 101, 940 (1956)
15. Bichsel, H., *Higher Shell Corrections in Stopping Power, Univ. Southern Calif., Linear Accelerator Group Tech. Rept. No. 3* (1961); *Bull. Am. Phys. Soc.*, 6, 46 (1961)
16. Bloch, F., *Z. Physik*, 81, 363 (1933)
17. Lindhard, J., and Scharff, M., *Kgl. Danske Videnskab. Selskab, Mat.-Fys. Medd.*, 27, 15 (1953)
18. Williams, E. J., *Rev. Mod. Phys.*, 17, 217 (1945)
19. Mott, N. F., *Proc. Cambridge Phil. Soc.*, 27, 553 (1931)
20. Allison, S. K., *Rev. Mod. Phys.*, 30, 1137 (1958)
21. Jackson, J. D., and Schiff, H., *Phys. Rev.*, 89, 359 (1953)
22. Bohr, N., *Phys. Rev.*, 58, 654 (1940); 59, 270 (1941)
23. Lamb, W. E., Jr., *Phys. Rev.*, 58, 696 (1940)
24. Knipp, J., and Teller, E., *Phys. Rev.*, 59, 659 (1941)
25. Brunings, J. H. M., Knipp, J. K., and Teller, E., *Phys. Rev.*, 60, 657 (1941)
26. Dmitriev, I. S., *J. Exptl. Theoret. Phys.* (*USSR*), 32, 570 (1957) [Transl.: *Soviet Phys. JETP*, 5, 473 (1957)]
27. Heckman, H. H., Hubbard, E. L., and Simon, W. G., *Phys. Rev.*, 129, 1240 (1963)
28. Bell, G. I., *Phys. Rev.*, 90, 548 (1953)
29. Gluckstern, R. L., *Phys. Rev.*, 98, 1817 (1955)
30. Bohr, N., and Lindhard, J., *Kgl. Danske Videnskab. Selskab, Mat.-Fys. Medd.*, 28, 7 (1954)
31. Neufeld, J., *Phys. Rev.*, 96, 1470 (1954)
32. Neufeld, J., and Snyder, W. S., *Phys. Rev.*, 107, 96 (1957)
33. Fermi, E., and Teller, E., *Phys. Rev.*, 72, 399 (1947)
34. Warshaw, S. D., *Phys. Rev.*, 76, 1759 (1949)
35. Lindhard, J., *Kgl. Danske Videnskab. Selskab, Mat.-Fys. Medd.*, 28, 8 (1954)
36. Lindhard, J., and Scharff, M., *Phys. Rev.*, 124, 128 (1961)
37. Nielsen, K. O., *Electromagnetically Enriched Isotopes and Mass Spectrometry*, 68 (Smith, M. L., Ed., Butterworths, London, 1956)
38. Lindhard, J., Scharff, M., and Schiøtt, H. E., *Kgl. Danske Videnskab. Selskab, Mat.-Fys. Medd.* (To be published); Lindhard, J., Nielsen, V., Scharff, M., and Thomsen, P. V., *Kgl. Danske Videnskab. Selskab, Mat.-Fys. Medd.*, 33, 10 (1963)
39. Northcliffe, L. C., *Phys. Rev.*, 120, 1744 (1960)
40. Nikolaev, V. S., Fateeva, L. N., Dmitriev, I. S., and Teplova, Ya. A., *J. Exptl. Theoret. Phys.* (*USSR*), 32, 965 (1957) [Transl.: *Soviet Phys. JETP*, 5, 789 (1957)]
41. Teplova, Ya. A., Dmitriev, I. S., Nikolaev, V. S., and Fateeva, L. N., *J. Exptl. Theoret. Phys.* (*USSR*), 32, 974 (1957) [Transl.: *Soviet Phys. JETP*, 5, 797 (1957)]
42. Nikolaev, V. S., Dmitriev, I. S., Fateeva, L. N., and Teplova, Ya. A., *J. Exptl. Theoret. Phys.* (*USSR*), 33, 1325 (1957) [Transl.: *Soviet Phys. JETP*, 6, 1019 (1958)]
43. Nikolaev, V. S., Dmitriev, I. S., Fateeva, L. N., and Teplova, Ya. A., *J. Exptl. Theoret. Phys.* (*USSR*), 39, 905 (1960) [Transl.: *Soviet Phys. JETP*, 12, 627 (1961)]
44. Reynolds, H. L., Wyly, L. D., and Zucker, A., *Phys. Rev.*, 98, 474 (1955); Reynolds, H. L., and Zucker, A., *Phys. Rev.*, 95, 1353L (1954)

45. Almqvist, E., Broude, C., Clark, M. A., Kuehner, J. A., and Litherland, A. E., *Can. J. Phys.*, **40**, 954 (1962)
46. Litherland, A. E., Almqvist, E., Andrews, R. H., Broude, C., and Kuehner, J. A., *Bull. Am. Phys. Soc.*, **8**, 75 (1963); (Also private communication)
47. Stephens, K. G., and Walker, D., *Phil. Mag.*, **45**, 543 (1954); *Proc. Roy. Soc. (London), A*, **229**, 376 (1955)
48. Hubbard, E. L., and Lauer, E. J., *Phys. Rev.*, **98**, 1814 (1955)
49. Tombrello, T. A., Parker, P. D. M., and Bacher, A. D. (Private communication)
50. Kavanagh, R. W., and Seeger, P. A. (Private communication)
51. Stier, P. M., Barnett, C. F., and Evans, G. E., *Phys, Rev.*, **96**, 973 (1954)
52. Leviant, Kh. L., Korsunsky, M. I., Pivovar, L. I., and Podgornyi, I. M., *Dokl. Akad. Nauk. SSSR*, **103**, 403 (1955)
53. Allison, S. K., Cuevas, J., and Garcia-Munoz, M., *Phys. Rev.*, **120**, 1266 (1960)
54. Steiger, N. H., *Conf. Reactions Between Complex Nuclei, 3rd, Asilomar, Calif., April 14–18, 1963*, Paper G.2; (Also private communication)
55. Phillips, J. A., *Phys. Rev.*, **97**, 404 (1955)
56. Dmitriev, I. S., Nikolaev, V. S., Fateeva, L. N., and Teplova, Ya. A., *J. Exptl. Theoret. Phys. (USSR)*, **42**, 16 (1962) [Transl.: *Soviet Phys. JETP*, **15**, 11 (1962)]
57. Nikolaev, V. S., Fateeva, L. N., Dmitriev, I. S., and Teplova, Ya. A., *J. Exptl. Theoret. Phys. (USSR)*, **41**, 89 (1961) [Transl.: *Soviet Phys. JETP*, **14**, 67 (1962)]
58. Nikolaev, V. S., Dmitriev, I. S., Fateeva, L. N., and Teplova, Ya. A., *J. Exptl. Theoret. Phys. (USSR)*, **40**, 989 (1961) [Transl.: *Soviet Phys. JETP*, **13**, 695 (1961)]
59. Nikolaev, V. S., Fateeva, L. N., Dmitriev, I. S., and Teplova, Ya. A., *J. Exptl. Theoret. Phys. (USSR)*, **33**, 306L (1957) [Transl.: *Soviet Phys. JETP*, **6**, 239L (1958)]
60. Reynolds. H. L., Wyly, L. D., and Zucker, A., *Phys. Rev.*, **98**, 1825 (1955)
61. Stephens, K. G., and Walker, D., *Phil. Mag.*, **46**, 563L (1955)
62. Bichsel, H., *Passage of Charged Particles through Matter*, Sec. 8c of *Am. Inst. Phys. Handbook*, 2nd ed. (McGraw, New York, 1963)
63. Demirlioglu, D., and Whaling, W. (Private communication)
64. Bader, M., Pixley, R. E., Mozer, F. S., and Whaling, W., *Phys. Rev.*, **103**, 32 (1956)
65. Green, D. W., Cooper, J. N., and Harris, J., *Phys. Rev.*, **98**, 466 (1955)
66. Wilcox, H. A., *Phys. Rev.*, **74**, 1743 (1948)
67. Gobeli, G. W., *Phys. Rev.*, **103**, 275 (1956)
68. Porat, D. I., and Ramavataram, K., *Proc. Roy. Soc. (London)., A*, **252**, 394 (1959)
69. Porat, D. I., and Ramavataram, K., *Proc. Phys. Soc. (London)*, **78**, 1135 (1961)
70. Teplova, Ya. A., Nikolaev, V. S., Dmitriev, I. S., and Fateeva, L. N., *J. Exptl. Theoret. Phys. (USSR)*, **42**, 44 (1962) [Transl.: *Soviet Phys. JETP*, **15**, 31 (1962)]
71. Van Wijngaarden, A., and Duckworth, H. E., *Can. J. Phys.*, **40**, 1749 (1962)
72. Porat, D. I., and Ramavataram, K., *Proc. Phys. Soc. (London)*, **77**, 97 (1961)
73. Braid, T. H., and Detenbeck, R. W., *Bull. Am. Phys. Soc.*, **2**, 225 (1957)
74. Allison, S. K., and Littlejohn, C. S., *Phys. Rev.*, **104**, 959 (1956)
75. Weyl, P. K., *Phys. Rev.*, **91**, 289 (1953)
76. Segrè, E., and Wiegand, C., *Phys. Rev.*, **70**, 808 (1946)
77. Lassen, N. O., *Kgl. Danske Videnskab. Selskab, Mat.-Fys. Medd.*, **25**, 11 (1949)
78. Tel'kovskii, V. G., and Pistunovich, V. I., *Dokl. Akad. Nauk SSSR*, **112**, 1035 (1957) [Transl.: *Soviet Phys. "Doklady,"* **2**, 184 (1957)]
79. Ormrod, J. H., and Duckworth, H. E. (Private communication; to be published)
80. Roll, P. G., and Steigert, F. E., *Nucl. Phys.*, **17**, 54 (1960)
81. Walton, J. R., and Hubbard, E. L. (Private communication); also Hubbard, E. L., *Univ. Calif. Radiation Lab. Rept. UCRL-9053* (1960)
82. Gilmore, J., *Univ. Calif. Radiation Lab. Rept. UCRL-9304* (1960)
83. Sikkeland, T. [Unpublished measurement quoted in Hubbard, E. L., *Univ. Calif. Radiation Lab. Rept. UCRL-9053* (1960)]

84. Schambra, P. E., Rauth, A. M., and Northcliffe, L. C., *Phys. Rev.*, **120**, 1758 (1960)
85. Roll, P. G., and Steigert, F. E., *Nucl. Phys.*, **16**, 534 (1960)
86. Heckman, H. H., Perkins, B. L., Simon, W. G., Smith, F. M., and Barkas, W. H., *Phys. Rev.*, **117**, 544 (1960)
87. Parfanovich, D. M., Semchinova, A. M., and Flerov, G. N., *J. Exptl. Theoret. Phys.* (*USSR*), **33**, 343 (1957) [Transl.: *Soviet Phys. JETP*, **6**, 266 (1958)]
88. Martin, F. W., and Northcliffe, L. C., *Phys. Rev.*, **128**, 1166 (1962)
89. Webb, W. H., Reynolds, H. L., and Zucker, A., *Phys. Rev.*, **102**, 749 (1956)
90. Reynolds, H. L., Scott, D. W., and Zucker, A., *Phys. Rev.*, **95**, 671 (1954)
91. Phillips, W. R., and Read, F. H., *Proc. Phys. Soc.* (*London*), **81**, 1 (1963)
92. Dissanaike, G., *Phil. Mag.*, **44**, 1051 (1953)
93. Briggs, G. H., *Proc. Roy. Soc.* (*London*), *A*, **114**, 341 (1927)
94. Burcham, W. E., *Proc. Phys. Soc.* (*London*), *A*, **70**, 309 (1957)
95. Oganesyan, Yu. Ts., *J. Exptl. Theoret. Phys.* (*USSR*), **36**, 936L (1959) [Transl.: *Soviet Phys. JETP*, **9**, 661L (1959)]
96. Bichsel, H., *Phys. Rev.*, **112**, 1089 (1958)
97. Barkas, W. H., *Phys. Rev.*, **89**, 1019 (1953)
98. Lonchamp, J. P., *J. Phys. Radium*, **14**, 89 (1953); *Ann. Phys.*, **10**, 201 (1955)
99. Papineau, A., *Compt. Rend.*, **242**, 2933 (1956); *J. Phys. Radium*, **17**, 566 (1956); *Comm. Energie At.* (France) *Rappt. CEA-543* (1956) (Unpublished)
100. Livesey, D. L., *Can J. Phys.*, **34**, 203 (1956)
101. Grinberg, A. P., and Lemberg, I. Kh., *Izvest. Akad. Nauk SSSR* (*Ser. Fis.*), **23**, 887 (1959)
102. Roll, P. G., and Steigert, F. E., *Phys. Rev.*, **120**, 470 (1960)
103. Hubbard, E. L., *Univ. Calif. Radiation Lab. Rept. UCRL-9053* (1960)
104. Wallace, R., *Univ. Calif. Radiation Lab. Rept. UCRL-9518* (1961)
105. Allison, S. K., and Garcia-Munoz, M., *Univ. Chicago, Enrico Fermi Inst. Nucl. Studies Rept. EFINS 61-68* (1961)
106. Chaminade, R., Crut, M., Faraggi, H., Garin-Bonnet, A., Olkowsky, J., and Papineau, A., *Compt. Rend.*, **242**, 105 (1956)
107. Lonchamp, J. P., *Compt. Rend.*, **244**, 1486 (1957); **239**, 877 (1954)
108. Parfanovich, D. M., Rabin N. V., and Semchinova, A. M., *J. Exptl. Theoret. Phys.* (*USSR*), **31**, 188 (1956) [Transl.: *Soviet Phys. JETP*, **4**, 99 (1957)]
109. Miller, J. F., *Univ. Calif. Radiation Lab. Rept. UCRL-1902* (1952)
110. Reynolds, H. L., and Zucker, A., *Phys. Rev.*, **96**, 393 (1954)
111. Hower, C., and Fairhall, A., *Phys. Rev.*, **128**, 1163 (1962)
112. Teplova, Ya. A., Nikolaev, V. S., Dmitriev, I. S., and Fateeva, L. N., *J. Exptl. Theoret. Phys.* (*USSR*), **34**, 559 (1958) [Transl.: *Soviet Phys. JETP*, **7**, 387 (1958)]; *Izvest. Akad. Nauk SSSR* (*Ser. Fis.*), **23**, 894 (1959)
113. Maikov, V. N., *Pribory Tekh. Eksperimen.*, No. 1, 50 (Jan.–Feb. 1959) [Transl.: *Instr. Exptl. Tech.*, No. 1, 55 (1959)]
114. Devons, S., and Towle, J. H., *Proc. Phys. Soc.* (*London*), *A*, **69**, 345 (1950)
115. Lillie, A. B., *Phys. Rev.*, **87**, 716 (1952)
116. Vorob'ev, Yu. A., *J. Exptl. Theoret. Phys.* (*USSR*), **35**, 1306L (1958) [Transl.: *Soviet Phys. JETP*, **8**, 912L (1959)]
117. Cüer, P., and Lonchamp, J. P., *Compt. Rend.*, **232**, 1824 (1951)
118. Neuendorffer, J. A., Inglis, D. R., and Hanna, S. S., *Phys. Rev.*, **82**, 75 (1951)
119. Feather, N., *Proc. Roy. Soc.* (*London*), *A*, **141**, 194 (1933)
120. Blackett, P. M. S., and Lees, D. S., *Proc. Roy. Soc.* (*London*), *A*, **134**, 658 (1932)
121. Clerc, H. G., Wäffler, H., and Berthold, F., *Z. Naturforsch.*, **16a**, 149 (1961)
122. Evans, G. E., Stier, P. M., and Barnett, C. F., *Phys. Rev.*, **90**, 825 (1953)
123. Powers, D., and Whaling, W., *Phys. Rev.*, **126**, 61 (1962)

The National Academy of Sciences—National Research Council is a private, non-profit organization of scientists, dedicated to the furtherance of science and to its use for the general welfare.

The Academy itself was established in 1863 under a Congressional charter signed by President Lincoln, Empowered to provide for all activities appropriate to academies of science, it was also required by its charter to act as an adviser to the Federal Government in scientific matters. This provision accounts for the close ties that have always existed between the Academy and the Government, although the Academy is not a governmental agency.

The National Research Council was established by the Academy in 1916, at the request of President Wilson, to enable scientists generally to associate their efforts with those of the limited membership of the Academy in service to the nation, to society, and to science at home and abroad. Members of the National Research Council receive their appointments from the President of the Academy. They include representatives nominated by the major scientific and technical societies, representatives of the Federal Government, and a number of members-at-large. In addition, several thousand scientists and engineers take part in the activities of the Research Council through membership on its various boards and committees.

Receiving funds from both public and private sources, by contributions, grant, or contract, the Academy and its Research Council thus work to stimulate research and its applications, to survey the broad possibilities of science, to promote effective utilization of the scientific and technical resources of the country, to serve the Government, and to further the general interests of science.

The Committee on Nuclear Science, within the Division of Physical Sciences of the National Academy of Sciences—National Research Council, was established in 1947 on the recommendation of a representative group of nuclear scientists that included physicists, geophysicists, chemists and biologists. It was envisaged that the Committee would serve as a channel of communication through which the advances in this field would be made available to a wide range of related endeavor, in addition to stimulating new research in nuclear science itself.

With its initial financial support provided by the Office of Naval Research, the coordinated work of the Committee began under the direction of Dr. R. C. Gibbs, then chairman of the Division of Physical Sciences, and Dr. L. F. Curtiss, who was chairman of the Committee from its establishment to 1962. The work became concerned with many diverse aspects of nuclear science, such as heavy ionizing particles, beta and gamma ray measurements and standards, neutron measurements and standards, nuclear constants, disintegration schemes, instruments and techniques, units, shipment of radioactive substances, radiochemistry, radiobiology, and nuclear geophysics. A list of currently available publications issued under the Committee's auspices is included in this volume.